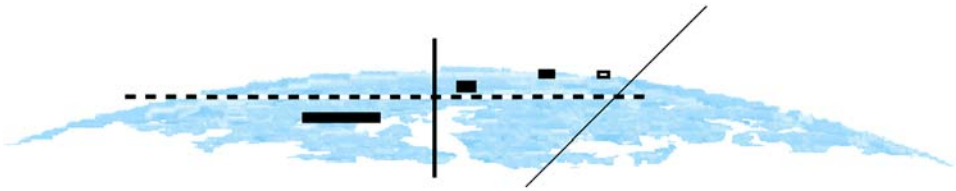

GeoForschungsZentrum Potsdam

STIFTUNG DES ÖFFENTLICHEN RECHTS

Scientific Technical Report

ISSN 1610-0956

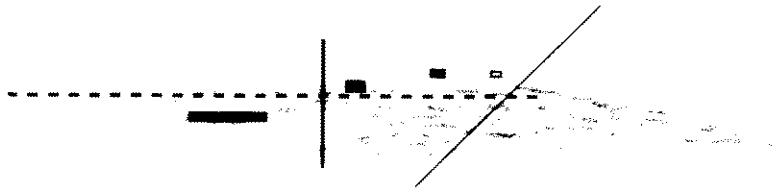

GeoForschungsZentrum Potsdam
STIFTUNG DES ÖFFENTLICHEN RECHTS

P. Bormann

Regional International Training Course 1995 on

Seismology and Seismic Hazard Assessment

Lecture and exercise notes

Volume I

Interner Bericht

Scientific Technical Report STR 95/TK
DOI: 10.2312/GFZ.b103-95tk7

Imprint

Edited by:

Peter Bormann
GeoForschungZentrum Potsdam
Telegrafenberg A 34
D-14473 Potsdam, Germany

Printed in Potsdam, Germany
December 1995

The regional international training course on "Seismology and Seismic Hazard Assessment" was held in Managua, from October 22 to December 2, 1995.

It was sponsored by:

- GeoForschungsZentrum Potsdam (GFZ)
- Instituto Nicaragüense de Estudios Territoriales (INETER), Managua
- Federal Ministry for Economical Co-operation and Development (BMZ), Bonn
- Federal Foreign Office (AA), Bonn
- Carl Duisberg Gesellschaft (CDG), Regional Office in the State of Brandenburg
- Swedish International Development Agency (SIDA)
- United Nations Educational, Scientific and Cultural Organization (UNESCO), Paris

P. Bormann
Editor

Lecture and exercise notes, Volume I

Regional International Training Course 1995 on

Seismology and Seismic Hazard Assessment

Managua, Nicaragua, October 22 to December 2, 1995

---

jointly organized by
GeoForschungsZentrum Potsdam (GFZ)
Instituto Nicaragüense de Estudios Territoriales (INETER)

in co-operation with
Carl Duisberg Gesellschaft (CDG)

co-sponsored by
AA (Bonn), BMZ (Bonn), SIDA (Stockholm) and UNESCO (Paris)

Scientific Technical Report STR 95/TK
DOI: 10.2312/GFZ.b103-95tk7

CONTENTS OF VOLUME I

8. Earthquake damages and earthquake engineering

Foreword of the editor

I welcome wholeheartedly all the participants and lecturers in the regional international training course on "Seismology and Seismic Hazard Assessment". The course has been jointly organized by the Instituto Nicaragüense de Estudios Territoriales (INETER) of Nicaragua, the GeoForschungsZentrum Potsdam (GFZ) and the Carl Duisberg Gesellschaft (CDG), Regional Office in the State of Brandenburg (both Federal Republic of Germany).

Despite of the significant contributions made to the course by the three organizers in personnel, cash and kind, the course would not have been possible without additional funds made available by the Federal Foreign Office (AA) in Bonn, by the Federal Ministry for Economic Co-operation and Development (BMZ) in Bonn, by the Swedish International Development Agency (SIDA) in Stockholm, and by the United Nations Educational, Scientific and Cultural Organization (UNESCO) in Paris. This allowed us to cover the cost of education, bed and boarding, excursion fees, textbooks, software, etc. for 18 participants and to grant air tickets to most of them.

Additionally, we have compiled as many as possible available lecture notes and exercise materials. They were copied and loose-bound by INETER for dissemination amongst all participants and lecturers. Unfortunately, the course-related negotiations and communication between Europe, Latin America and Asia and the tedious struggle until the last moment to secure the funding of the course turned out to be much more difficult and time-consuming then originally thought. Besides this, unexpected events such as strong earthquakes and volcanic eruptions, e.g. in Chile, Nicaragua and elsewhere, forced several lecturers to go on extended field missions and to reconsider their work priorities. The regrettable consequence is that several lecture notes reproduced in this volumes are still older versions which do not yet represent the up-to-date contents of the lectures as they will be presented during the course, while some other lectures scheduled in the programm are not yet contained in the lecture and exercise material at all. A few more lecture notes were handed out to me at the opening of the course only. They will be copied for you in loose-leaf form and integrated into the final printed course material as published in the series of Scientific Technical Reports of the GeoForschungsZentrum Potsdam. Nevertheless, this year's course volumes will contain, as compared to last year's ones, in total about 282 pages of new lecture and exercise material. My special thanks go to Ms Katrin Weiße who has taken the trouble of uniformly formatting and correcting all these new manuscripts.
On the other hand, we are providing you in chapter 8 with some additional information related to a proper earthquake engineering and land-use planning philosophy which - although not lectured in this year's course because of time and monetary constraints - should be the final goal of long-term activities aimed at disaster preparedness, mitigation and prevention.

Since 1980, together with you, 382 participants from 70 developing countries from all over the globe have participated in the Potsdam seismology training courses. Many of these fellows still keep contact with us, have meanwhile successfully completed some post-gradual research or graduation, are serving now as professors or lecturers at universities and

thus as "multipliers" of the knowledge and expertise acquired in these courses or even as heads of or senior scientists at relevant research institutions or at seismic monitoring systems in their home countries. I sincerely hope that also you will gain a lot from your participation in this course, both scientifically and spiritually, and that you will successfully bring to bear the enthusiasm, the knowledge and the skills acquired during this 6-weeks training, to the benefit of your disaster stricken countries and their people.

Potsdam, 30 September 1995

Prof. Dr. Peter Bormann
Chairman of the Potsdam training courses

INTRODUCTION TO NATURAL DISASTERS AND DISASTER MITIGATION AND TO THE POTSDAM TRAINING COURSES AS A GERMAN CONTIBUTION TO THE IDNDR

Peter Bormann

GeoForschungsZentrum Potsdam, Department of Disaster Research,
Telegrafenberg A 34, D - 14473 Potsdam

1. DEFINITION OF TERMS

Disaster aid organizations speak frequently of a **disaster** as soon as an event kills more then 10 people or injures more than 100. But in a wider sense an event becomes a disaster only if it seriously disrupts the functioning of an affected community due to widespread human, material or environmental losses that exceed the community's capability to cope without external relief.

If the latter definition holds then events such as the San Francisco earthquake in 1989 or the winter storms in Central Europe in 1990 could not be considered as real disasters although the damages ranked in the order of 6 and 15 billions US$, respectively. On the other hand already smaller damages can be terrible disasters to many developing countries because they strip these people of their already meager resources, often disrupt their economies and distroy their limited potential for reconstruction. So, the 1972 Managua earthquake, which killed about 5000 people and left 300 000 homeless, caused estimated economic losses of "only" about 1.3 billion US$. But this corresponded to roughly 1 year's GNP at that time and Nicaragua was unable till now to rebuild the center of its capital.

One differentiates between **sudden disasters** and **creeping disasters**. Sudden events hit man unexpectedly or more or less prepared in an instant of seconds or minutes such as earthquakes and avalanches, during hours or days such as storms and storm surges and days or weeks at the most such as violent volcanic eruptions or floods. These sudden events are rare. There may be years, decades, centuries or even millennia before another event of the same kind and magnitude strikes the same area or locality again. Contrary to this, creeping disasters, such as desertification, soil erosion and salinization, drought, famine and epidemics develop slowly over month, years or even decades and may last comparably long. Although man has a much larger lead-time to prepare for them and often also possibilities to avoid them at all they have caused most of the disaster victims during this century. More then 8 million, probably more then 10 million people died since 1900 because of drought and famine as compared to about 4 million people being killed by sudden disasters of natural origin.

Man-made disasters are directly related to human activities, sometimes deliberate, sometimes unwanted in their detrimental effects, such as wars, explosions, mining collapses, traffic accidents, failure of major technical systems, air, soil and water pollution, uncontrolled deforestation, overgrazing or improper irrigation resulting in soil erosion, desertification etc.

Natural disasters are related to natural phenomena and processes such as earthquakes, tsunamis, avalanches, rock falls, land slides, floods, storms, volcanic eruptions, desert locust infections etc. Often they give rise to **chains of disasters** with consequences which may go far beyond that of the primary cause of disaster. Thus, earthquakes may trigger rock falls, the outbreak of fire, the generation of tsunamis with related flooding, polution of potable water and epidemics. The 1970 Peru off-shore earthquake (M = 7.8), e.g., generated a tsunami

which killed many people and caused heavy damages in the coastal area. It also triggered a rock and mud avalanche in the Andes about 100 km inland at an epicentral distance of some 130 km which swept away the towns of Yungay and Ranrahirca in an instant, burying another 25 000 to 30 000 people. This debris avalance also caused the damming of the Rio Santa. When this dam broke a few days later many people were drawn downstream and the flush of water and debris devastated villages and crops in the flood plains along the river course over a distance of about 160 km down to the Pacific coast. Only about the half of a total of some 70 000 people lost their lifes due to the primary cause, namely the collapse of their mostly adobe houses under the strong Earth's shaking. About 800 000 people were left homeless. A special issue of BSSA was dedicated to the detailed evaluation of this horrible event and disaster chain (e.g. Cluff 1971). In 1923 the majority of the 143 000 casualties in the Tokyo earthquake were not killed by their collapsing houses but by the outbreak of large areal fires in the densily populated city as a consequence of electric shorts, broken fire places and gas pipes. Also, in conjunction with tropical storms, an average of 90 to 95 % of the people is not killed by the strong winds but rather by the a accompanying sturm surges flooding the coastal lowlands.

Due to the ever growing impact of human activities on natural cycles and equilibriums there is an increasing tendency of coupling between man-made and natural disasters. These **mixed disasters** often develop feedback mechanisms of mutual reinforcement (e.g. increased hazard of flooding due to large scale deforestation and soil erosion or aggravation and prolongation of periods of drought due to large scale overgrazing and related regional changes of Earth's albedo).

But rigerously speaking, **the term natural disaster is misleading.** According to the above definition the term disaster has a meaning only with respect to men and human activities. Nature itself does not know about disasters at all. There is nothing but a great variety of natural phenomena and processes of different time, spatial and intensity scale. They all bear wittness of our still living planet Earth. Some of them may have an impact on men with disastrous consequences. This may be due to:

- **lacking awareness** of the natural hazard, human vulnerability and related economic and social risks;

- **settlement in risky areas** (e.g. along active faults, in low level coastal areas, near steep slopes or cliffs, in flood plains or avalanche corridors, on unstable grounds etc.;

- **unknown or ignored** natural **conditions** such as ecosystems stability, soil liquifaction potential, sub-soil amplification characteristics, attenuation laws of seismic waves etc.;

- **improper use, design or execution** of building material, houses, industrial facilities, infrastructure and life-lines not in accordance with the actual hazard and risk;

- **missing or not appropriate** land-use **regulations**, safety and preparedness measures **and lacking control** of proper execution and **inforcement** of regulations by law, taxes, insurance etc.;

- **ignorance** of human safety interests and long-term needs for sustainable development;

- **lack of** well **trained** and motivated **man-power** to tackle with the above shortcomings.

Consequently, **all disasters are finally man-made.** This neccessitates to investigate, first and foremost, the natural hazard, the vulnerability of human lifes and structures and the risk of impact of a natural phenomena with disaster potential. Taking recommedations by an UNDRO Expert Meeting on Vulnerability Analysis in July 1979 into account, these terms can be defined as follows:

Hazard H: Probability of occurrence of an event with disaster potential within a defined area and interval of time;

Vulnerability V: Expected degree of loss ($0 < V < 1$) due to a disaster event; 0 - no loss/damage, 1 - total loss/damage;

Specific Risk SR: Expected degree of loss due to a particular event i with the probability of occurrence H_i, i.e. $SR_i = V * H_i$;

Elements of Risk RE: Endangered elements RE_j ($j = 1 \ldots m$) within a defined area, e.g. number of persons, value of property, level of economic activity etc. which constitute the elements of an "exposure model";

Risk R: Expected total loss due to a specific type of event i, e.g. earthquakes, i.e.:

$$R_i = H_i \sum_{j=1}^{m} RE_j * V_j ;$$

Cumulative Risk CR: Expected cumulative loss as a consequence of n different potential disaster events, i.e.:

$$CR = \sum_{i=1}^{n} \sum_{j=1}^{m} RE_{ji} * V_{ji} * H_i$$

From this follows: **high hazard does not necessitate high risk**. This will only be the case when people, structures and values are exposed to hazard (**exposure model**) and if their vulnerability is significant. Low density of population, proper land use, safe constructions, good developed preparedness etc. will result in low risk even in high hazard areas. Consequently, the prime task is to develop, on the basis of a scientifically based deeper understanding of causes and effects, strategies, methods and technologies for the reduction of vulnerability. This can be achieved by:

1.) **Prediction** of the location, time of occurence and strength/magnitude of an event with disaster potential with a view to take prophylactic measures:

2.) **Warning** of the population and/or of governmental, private or public institutions aimed at (in case of early warning systems automatic) switching-off of critical facilities such as lifeline and transport systems, at mobilizing the civil defense, activating emergency and rescue teams or even ordering the evacuation of the population if the prediction is sufficiently accurate and reliable with respect to location, time and magnitude of the forthcoming event;

3.) **Prevention** or **mitigation** of the negative impact of pending disasters particularly by means of proper land use regulations and physical planning (United Nations 1978), building codes and other disaster related legislation (United Nations 1980; IAEE 1984) based on **long-term predictions**, hazard, vulnerability and risk analyses. Here one has to differentiate between **corrective measures** with respect to already existing settlements and industrial facilities by means of strengthening and retrofitting on the one hand and **prophylactic measures** based on comprehensive interdisciplinary planning and execution in connection with the development of new areas (United Nations 1976 b);

4.) **Preparedness** in taking effective countermeasures for the prevention or limitation of damages or injury/death of people in case of unavoidable disaster events. This requires a developed information/communication system (United Nations 1979 b), public awareness, conscious and trained personel at all social and regional levels, availability of contingency plans and resources, evacuation schemes etc. (United Nations 1984) taking also social and sociological aspects into account (United Nations 1986);

5.) Quick and realistic **assessment** of the extent of a disaster and the kind of damages/injuries as a precondition for a quick **emergency response** and the effective execution and co-ordination of national und international **rescue and relief** activities.

2. STATUS OF DISASTER PREDICTION AND HAZARD ASSESSMENT

While most of the above mentioned points are essentially of political, administrative and organizational nature supported by logistic-technical means the successful realization of 1.) and 3.) requires extensive basic and applied geoscientific and civil engineering research, data and skills. The current status may be characterized as follows:

2.1 Deterministic prediction and early warning

Prediction of future events is at the very heart of science. The reliability of predictions is an effective yardstick to assess the achieved state of knowledge, theory development and their practical handling. One discriminates between **deterministic prediction** of the precise location, time and magnitude of a given event and **probabilistic prediction** that an event of a given magnitude or magnitude range will occur within a given time window in a considered area (cf. definition of hazard H above). The former necessitates the availability of a reliable **deterministic parameter model** of the causing physical processes or related phenomena, an **operational monitoring system** which provides the needed multiparameter input data for the model calculations in the required quantity, quality and representativeness in near real time as well as powerful computers which are able to carry out the calculations within the lead-time required for the practical use of a prediction of a forthcoming event in terms of **warning** of the population and the realization of short-term prevention or mitigation measures such as evacuation, mobilization of civil defense etc. Even when the prediction problem is solved sufficiently good in academic terms its beneficial practical applicability is not yet assured. The latter does not only necessitate the availability of a well developed communication system for rapid dissemination and assured receipt of warnings by the population at risk but also the availability of well developed and trained response schemes at all administrative levels down to the affected communities. Besides this, public awareness and rational response to such emergency messages and measures are precondition for avoiding panics or other detrimental social misbehaviour in the wake of published predictions, issued warnings, ordered evacuations or related measures.

Prediction and warning schemes for tropical cyclones are currently most advanced. These storms develop over warm oceans only. They can be detected in time by operational weather satellites and their track, velocity of migration and power (maximum wind speeds) be determined sufficiently accurate, also by means of complementary ground-based techniques. This allows to issue and regularly up-date early warnings with days to hours lead-time through established channels of the World Meteorological Organization's World Weather Watch and Global Telecommunications System as well as other national services (e.g. of the USA). The number of casualties due to such tropical storms could, therefore, already drastically be reduced although the material losses are still dramatic and increasing.

Also rather well developed are operational predictions and warnings of tsunamis by the International Tsunami Warning Center (ITWC) at Honolulu, Hawaii, but only for coastal areas which are sufficiently far away (several 1000 kms) from the epicentre of the causing earthquake. The ITWC avails of more than a dozen on-line recorded seismic stations on Oáhu and other Hawaiian islands and on-line access to 9 USA stations on the Aleutian islands, in Alaska and on the USA mainland. It is connected via satellite communications both with the US National Earthquake Informations Centre (NEIC) at Boulder and other important centres in Japan (Matsushiro), Alaska, Sachalin, Kamchatka, Hong Kong, Soul, Manila, Port Moresby and Tahiti (French GEOSCOPE network). NEIC reports to the ITWC within 10-15 minutes after a Pacific earthquake with body wave magnitudes $m_b > 6$ the their location. It may be improved by consulting the recordings of the ITWC stations. Via satellite further parameter data can be requested and received in an instant from the other centers mentioned

above in order to check and refine the location and magnitude of the event. Additionally, via satellite, actual sea level data from more than 100 tidal stations around the Pacific can be acquired. Then, for the given earthquake location, the travel times of the expected tsunami wave front travelling through the whole Pacific Basin are calculated and plotted (Fig. 1a and b). These results are transmitted on request, or in case of M > 7.5 at once, to all countries in the Pacific region.

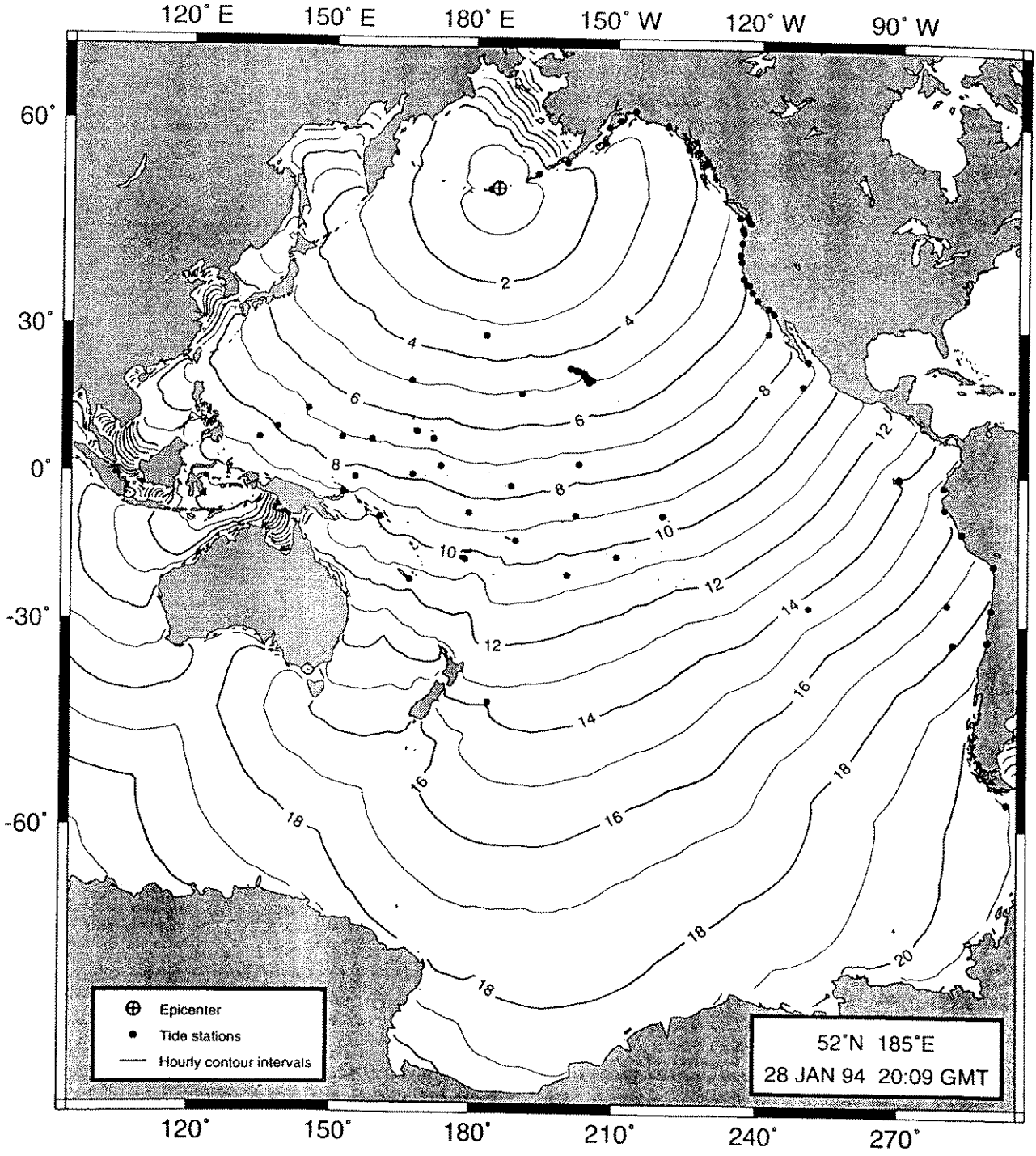

Fig. 1: Calculated travel times through the Pacific of tsunami waves generated by earthquakes a) in the central Aleutian Islands and b) off-shore of Chile (courtesy of the Pacific Tsunami Warning Center, Honolulu, Hawaii, 1994)

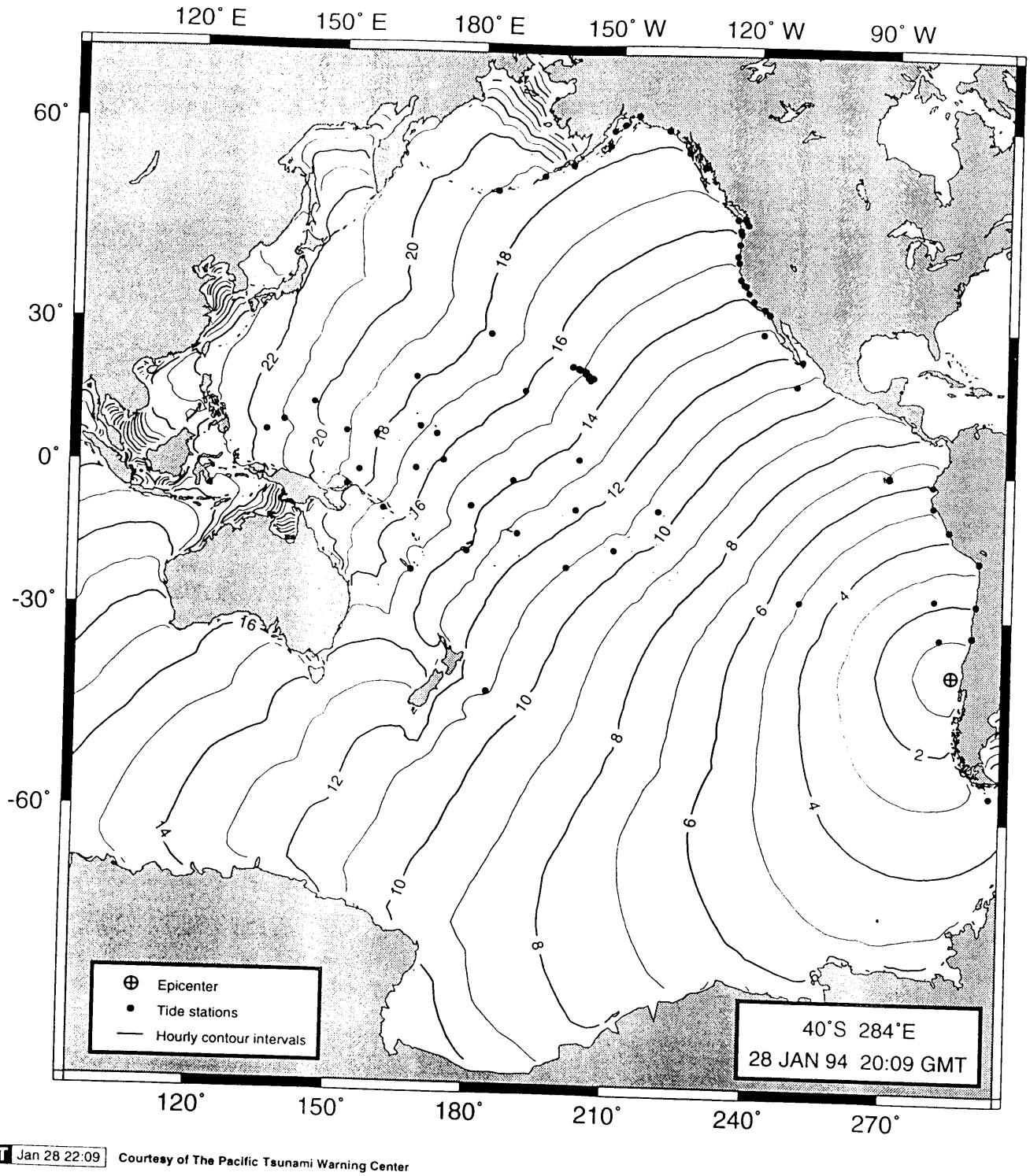

Fig. 1b (cf. Fig. 1)

This kind of prediction is possible due to the fact that the tsunami wave generated in the ocean by a submarine earthquake is a simple gravity wave. It travels with the speed $v = \sqrt{g\,h}$ (in m/s) with g - gravity and h - water depth in meters, e.g. with v = 200 m/s in case of 4000 m water depth and v = 100 m/s in case of 1000 m water depth. This is about 100 times slower than the apparent velocity of teleseismic P-waves. Therefore, the seismic event can first be located, its magnitude be determined and its tsunami potential be assessed with a sufficient lead-time, in case of distant events about 10 to 20 hours ahead of the arrival of the tsunami wave on far away shores (cf. Figs. 1a and b).

But this system fails to provide sufficiently early tsunami warnings for earthquakes off ones country's own shores although some of the national tsunami warning centres in Alaska, Kamtschatka, Japan and Tahiti struggle currently with the development of some suitable kind of rapid early warning systems also for that case. Unfortunately, also reliable operational predictions of the expected height of a tsunami wave are not yet possible at the ITWC since the controlling parameters such as earthquake magnitude and source mechanism, ocean bottom relief, coastal profil and shoreline configuration vary too much, are not readily available with sufficient precision or not yet well enough known on a larger scale as to consider them in regional prediction and warning procedures. But local solutions of tsunami heights for particularly tsunami prone risky shores by detailed tsunami modelling are already practized in Japan, Russia and the USA and may become more widespread in future .

The relative successful and to a certain extent already operational prediction and early warning systems in case of tsunamis and tropical storms are mainly due to a number of beneficial circumstances. In both cases the source develops out in the sea. It does then, in most cases, not yet constitute an immediate disaster threat to densily populated areas on land. It can be localized with high precision by available operational global monitoring systems (weather satellites or seismographic stations) shortly after its generation with a sufficient lead-time so as to allow ahead warnings. The propagation direction and velocity of the phenomena with disaster potential can either be continuously or in short time-intervalls be monitored or, as in the case of the tsunami waves, be calculated on the basis of relatively simple deterministic physical relationships with sufficient precision.

On principally the same grounds earthquake early warning systems are designed, namely, a group of sensors is placed along a fault or around a potential source area at a sufficiently large distance from objects or sites at risk. The sensors will record strong ground motions, may additionally determine the location and size of the causing event and/or the direction of propagation of the fault rupture and will trigger the immediate automatic switching-off of critical lifeline systems, power stations, electricity and gas supplies, will stop trains or road traffic etc. This may drastically reduce electric shorts and the related outbreak of fires, the derailing of trains, the crashing of cars when driving over collapsing bridges and similar earthquake effects. But since the lead-time before the arrival of the strong ground motions at some 10 to 100 km from the earthquake epicentre is only in the order of a few seconds to about a minute at the most no deliberate human decision and response is possible any more. Such systems are operational already for many years in Japan along the National Railway system. Others are currently installed, tested or operated along the San Andreas fault in California, in Mexico, in Taiwan or at special high-risk sites such as nuclear power plants (United States Department of the Interior 1990; Toksöz et al. 1990; National Research Council 1991; Espinoza-Aranda et al. 1992; Nanometrics 1994).

This is generally not the case with sudden geological events such as earthquakes and volcanic eruptions. They occur in the lithosphere which presents a hierarchy of solid volumes or blocks which move relative to each other (Sadovsky and Pisarenko, 1990; Fig. 2), underlain by the less rigid, partially molten asthenospere which interacts with the lithosphere. But any such complex multi-parameter system consisting of interacting elements has the tendency of developing into an instable **non-linear chaotic dynamic system of self-organized criticality** (Bak et al. 1988). Earthquakes, volcanic eruptions, rock avalanches etc. are expressions of the "catastrophic" collapse/destabilization of **fractal geological systems** (e.g. Bak and Tang 1989; Ito and Matsuzaki, 1990; Korvin 1992, Turcotte 1992). Such events cannot precisely be described in deterministic terms but they are somehow conditioned by the scale-independent selfsimilar internal structuring, the phase composition of the medium as well as by the external acting forces. Consequently, they develop certain characteristic stochastic patterns of forms, spatial dimensions, frequency of occurrence and energy release. They follow a power law distribution, i.e. a logarithmic decay of the frequency of events with increasing size (so-called 1/f or "flicker noise" relationship). This aplies in the same way to the relationship, e.g., between number and size of trunk, branches and twigs of a tree as to the branching of tectonic faults and fractures at various scales. But the accurate size, time and location of the occurrence of the next "avalanche" or branching/bifurcation/fracture/collapse

event is generally not deterministically predictable. If at all, prediction can be made only in a probabilistic sense despite of certain typical, conditioned stochastic patterns that may develop prior to a pending major event (e.g. "quiescence" and/or clustering of micro-earthquakes prior to a main shock).

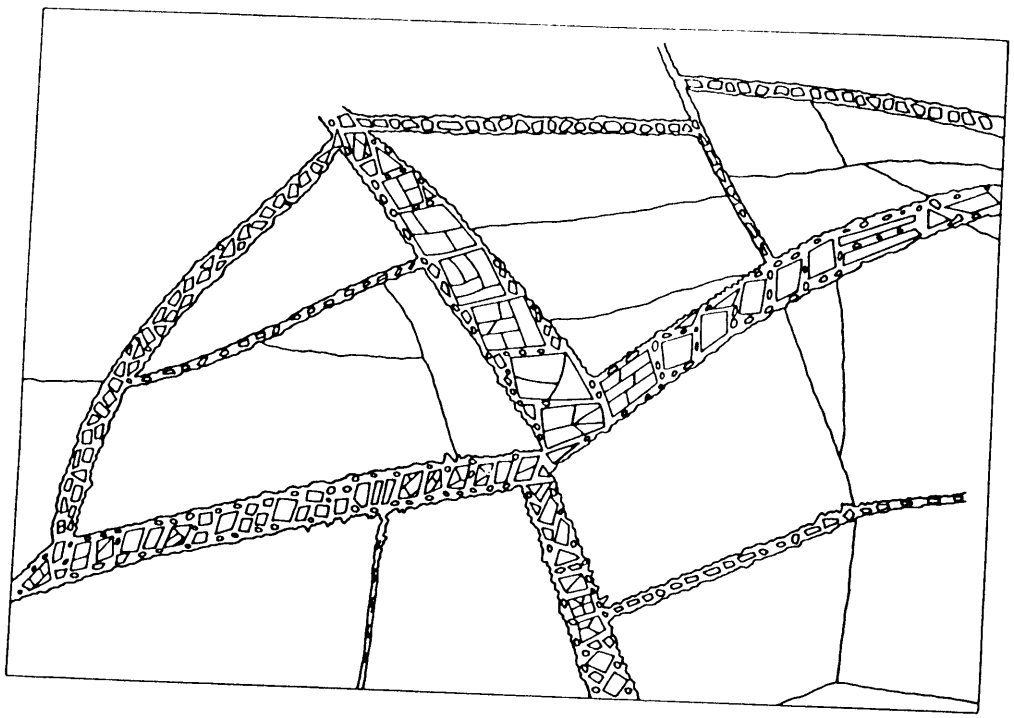

Fig.2: Schematic depiction of the lithosphere as a hierarchy of volumes or blocks which can move relatively to one another (taken from Keilis-Borok 1990)

Earthquakes occur along the less rigid boundaries of block structures as shown in Fig. 2. Such fault zones are typically about 10 - 100 times smaller than the adjacent blocks. The same applies to the internal structuring within such fault zones. They constitute, according to Keilis-Borok (1990), boundary zones which hold the blocks together by forces of friction and cohesion. These forces are controlled by internal processes which are confined mainly to the boundary zones, e.g. by interaction with fluids, phase and petrochemical transformations, fracturing etc. These processes can **rapidly and unobtrusively change the friction and cohesion and thus the effective strength** within fault zones **by a factor up to 10^5 - 10^6** (Keilis-Borok 1990). This makes earthquake prediction so difficult a task.

In this context we have to be aware that despite of the existence of some common first order features which allow to classify an object as a "tree" or an event as an "earthquake", there exists a great variety of "species" of trees, earthquakes etc. The latter, e.g., vary drastically in their relevant parameters such as seismic moment-release, stress drop, depth distribution, magnitude-frequency relationship, average return periods etc. They depend on the given seismotectonic environment (plate boundary or intraplate situation; continent-continent collision, subduction or rifting zones), magnitude and orientation of stresses (compressional, extensional or shearing regime), rock type, crustal rheology etc.. This makes it principally impossible to apply - with the hope for success - certain systematic precursory patterns or quantified "prediction criteria" as derived from investigations in one earthquake zone to another earthquake area belonging to a different seismotectonic regime. Even within a given area no future earthquake with all its related inter-, pre-, co- and post-event features will ever be a precise copy of any previous event there, as there is never any oak, birch or pine tree

a precise copy of any individual member of its species. Each earthquake somehow changes the conditions and fine structure of a fault zone. Accordingly, subsequent processes of stress redistibution and reloading, recrystallization and fracture healing etc. will vary with time and never be the same again.

But despite of these remarks, which should make us sober in our expectations and critical against unjustified claims to have already found the key to succesful earthquake prediction (e.g. Varotsos and Alexopoulos 1984 a and b) the problem is still thought to be not completely hopeless by many researchers. Both earthquakes and volcanic eruptions are connected with preparatory, co- and post-event deformational and fracturing processes. They are accompanied by plenty of more or less subtle and noisy long-, medium- and short-term changes in related phenomena or geophysical field parameters (e.g. Mogi 1985, Rikitake 1987 and 1988; Ma Zongjin et al.; Boschi and Dragoni 1992; Gasparini et al. 1992). Their comprehensive complex monitoring with sufficiently dense and precise networks of sensors capable also of recording disturbing influences from other sources (e.g. meteorological, hydrogeological and other effects), which might cause similar anamolies or parameter changes, is an indispensable precondition for any kind of prediction research aimed at physical modelling of parameter changes related to pending earthquakes or volcanic eruptions. But only if the assumed or derived model does indeed, and independent with time, correctly reflect the complex controlling processes and their quantitative interrelationship and provided that the 3-D starting conditions can indeed precisely enough be determined from (in most cases spatially scarce point-like) surface measurements an effort of deterministic **prediction of future events** (and not retrospective as usual) could have a chance at all.

In the case of volcanoes such an approach seems to be, at a first glance, to be most promising. A volcano is a structurally complex 3-phase system with solid, liquid and gaseous phases interacting. Modelling of its active states requires to consider non-linear flows of a two-phase compressible liquid. But at least the location of the "trouble maker" is known. This enables us to focus the complex monitoring of precursory phenomena on a small area with rather dense networks of sensors. This may be the main reason for several successful predictions of pending eruptions which allowed to issue early warnings and to evacuate the population at risk out of the endangered zones (e.g. in case of Mt. Pinatubo in the Philippines). In other cases it made possible a full-scale geoscientific monitoring and documentations of the eruptions in all phases as in the case of Mt. St. Helens in 1980 and of several eruptions in Kamchatka, e.g. of the volcano Tolbatschik in 1977. None the less, also for volcanoes, there is no fixed patterns of precursory phenomena which signal a pending eruption. Each volcanoe has its own life and his signals must be studied individually. Also, there is no assurance that different eruption episodes, often with decades, hundreds or even thousands of years of quiescence in between, will be ushered by the same set and intensity of precursory features since the state of activity of a volcano may change significantly with time.

There have been, therefore, several false alarms, and evacuations of thousands of people in vain as well, when strong signs of seismic "unrest" or even initial volcanic activity were not followed by larger dangerous eruptions. Examples are the volcano La Soufrière on the island Guadalupe in 1975 (Schick 1991) and the volcano Mihara Yama on Izu-Oshima in the Bay of Tokyo in 1986/87 (Shimozuru 1988; Schick 1991). In other cases, completely unexpected strong eruptions of well monitored volcanoes occurred practically without any seismic precursory signals (failure to predict). Examples are the eruptions of the volcano Avachinsky on Kamchatka on 13 January 1991 and of the volcano Galeras in Colombia on 14 January 1993 (Schick 1994).

With reference to earthquakes the situation is still much more complex, especially because of the much more extended and heterogeneous seismogenic zones. The monitoring of the preparatory zones of large earthquakes would require to run permanently dense networks of costly multiparameter sensors covering vast areas of about 10^5 to several 10^6 km^2. But even then we could not expect to gain from them more reliable and consistent precursory patterns or better ratios for successful predictions against false alarms and failures than in the case of well monitored volcanoes. That is why leading seismologists nowadays share the view that a **deterministic earthquake prediction is not possible** (e.g. Aki 1989; Geller 1991).

There have been several "academic" (e.g. Morgan et al. 1988) and at least one spectacular practical success(es) in earthquake prediction. The latter refers to the prediction of the Haicheng earthquake in 1975 in China (e.g. in Ma Zongjin et al. 1990). Besides this there have been plenty of failures to predict (e.g. Tangshan earthquake 1976, all recent strong Californian and Japanease events) as well as false alarms, e.g. in case of the expected Parkfield earthquake in California (Bakun et al. 1986; Hellweg 1994)(see also Bormann 1994, vol.2, p. 324-327 of the course material). False predictions published in 1978 and 1981, related to strong events to be expected in the Oaxaca province of Mexico and in Peru, respectively, had detrimental economic and social consequences. They upset the local population, caused many people to abandon their home and land and triggered large-scale speculative business transactions. Tourist rates and related income dropped significantly. The overall losses were estimated to be in the order of several 100 Mio US$, i.e. larger than the real losses due to the earthquakes which followed indeed in these areas with several month of delay and smaller magnitudes than predicted. This should make us aware that even in case of correct predictions they may contribute to the mitigation of disaster losses only if they are sufficiently reliable in space, time and magnitude, if they are issued not earlier then a few days and not later then several hours before the event and if they meet a well aware and trained population which will consciously and disciplined follow the instructions given by the authorities without panic or riots. Otherwise, even successful predictions may turn out to be worse than no predictions at all.

Nevertheless, there are still strong endeavours in some countries, Germany with the GFZ included, in the area of earthquake prediction research. They are first of all aimed at a better understanding of the complexity and interrelationship of the inter-, pre-, co- and post-event phenomena, their causing physical and geochemical processes and their modelling. But globally, spendings on earthquake prediction have - as compared to the seventies and early eighties - been more and more reoriented towards seismic hazard, vulnerability and risk assessments, microzoning of local underground response to strong earthquake shaking and into the development of codes and practices of earthquake resistant design and construction, i.e. into practical preparedness and preventive measures based on statistical medium- and long-term predictions of the probability of occurrence of strong earthquake ground motions or underground failures. Therefore, the practice-oriented Potsdam seismology training course, will focus on these topics.

2.2 Probabilistic prediction and hazard assessment

According to Aki (1989) the ideal prediction in probabilistic terms could be defined as follows: "100 years before a target earthquake with a given magnitude and location we would tell people that the probability of the occurrence of this eartquake is one per 100 years. Then, 1 year before the earthquake, the probability rate goes up to one per year, and 1 minute before ... (it) reaches one per minute". Fig. 3 shows this relation betwenn the probability rate and the time before the target earthquake in a log-log plot. For the ideal probabilistic prediction we would get a staight line with the slope of 45°. For comparison, several realistic prediction curves are shown which are based on different kind of data and analysis procedures. The horizontal line at the bottom corresponds to the long-term average rate of occurrence as determined from earthquake catalogs or paleoseismological data. Its level of probability is typically rather low. It also differs from region to region according to the level of seismic activity and related mean return periods for events of a given magnitude class. The broken line "gap theory" in Fig. 3 indicates that a probability increase of about one order of magnitude can be achieved when the long-term averages can be related to identified gaps along a given plate boundary. The gap concept was originally proposed by Kelleher et al. (1973) and McCann et al. (1979). It allowed already several successful long-term predictions and has since then further be refined by including information on rates of plate motion, average repeat times, estimates of earthquake size in a probabilistic manner for specific segments of relatively simple major plate boundaries. A comprehensive review of the development of this concept since its introduction, its current state as well as criticism together with many suitable references is given by Nishenko and Sykes (1993).

According to Fig. 3 the achieved prediction probabilities in the intermediate-term range (a few weeks to years) are until now about one to three orders of magnitude below the ideal

probabilistic prediction while, partially by chance, the actual short-term prediction probability in the Haicheng case came rather close to that of an ideal prediction. Aki (1989) concluded from this that precursory signals may be significantly stronger immediately prior to an earthquake than at a longer time before. This is also plausible from a physical point of view when considering both the necessary "nucleation" around the starting point of an earthquake rupture and the non-linear accelleration of many related phenomena when approaching the critical state. But the apparently rather high short-term probability in the Parkfield case was a false-alarm. The prediction window is over without the expected event. The vertical line SCAN in Fig. 3 stands for "Seismic Computerized Alert Networks" such as the ones discussed above. But they are no true prediction but rather early warning systems. They are suitable only for sites at some distance from the event and based on the detection of ground motions of an already ongoing earthquake.

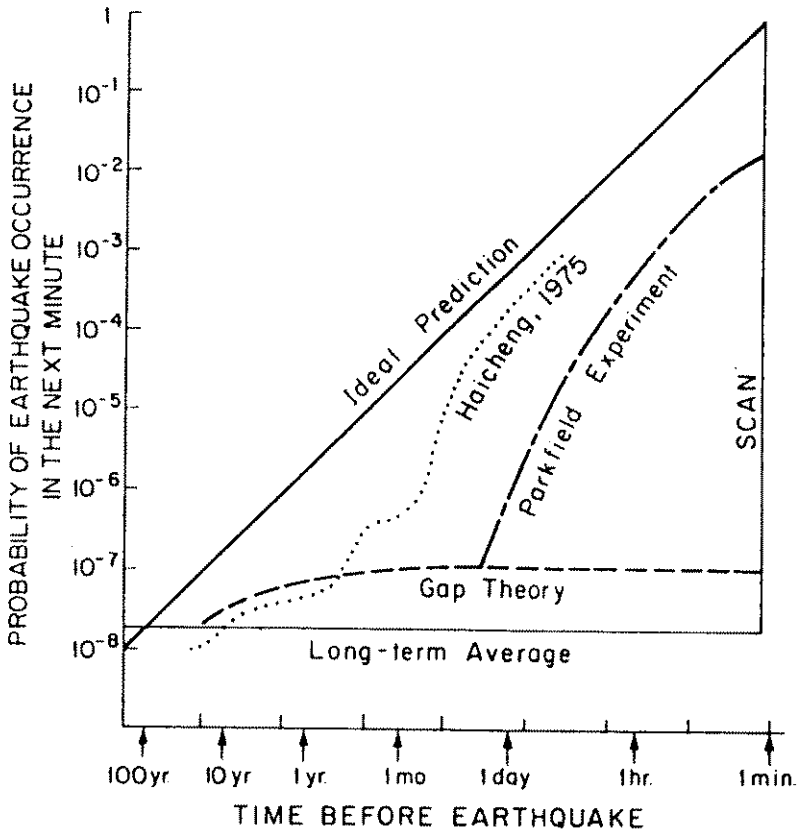

Fig. 3: Probability of earthquake occurrence in the next minute (from Aki 1989)

Also probability predictions are not free from assumptions. In case of long-term predictions it is mostly assumed that the data on which it is based are complete for the considered intervall of time, that they include the strongest "characteristic" event in that area or that the strongest possible earthquake can be inferred sufficiently accurate from seismotectonic considerations or paleoseismological data. Besides this, it is mostly assumed that the recurrence intervals between consecutive strong events follow a "normal", i.e. Gaussian distribution and that the frequency of earthquake occurrence is a stationary process which follows a Poissonian distribution. But in reality these assumptions are often not fulfilled. Although Fig. 4 may be debatable in detail it clearly shows that the potential time span for which earthquake catalogues may be complete for events with magnitudes $M > 6$, i.e. for potentially seriously damaging earthquakes, differs significantly from region to region. For most areas these catalogues can be complete for less then 200 years only due to various reasons such as sparse population and settlements or only rather recent inhabitation by population groups capable of and practising careful written reports of unusual events. Only for Japan, parts of China, Europe and the Near East earthquake catalogues are available which cover more than 800 years. If we consider this in the context of Fig. 5 which shows the differences in strain rates of the lithosphere in different tectonic environments as well as the related variability of the duration of seismic cycles we can draw the following conclusions:

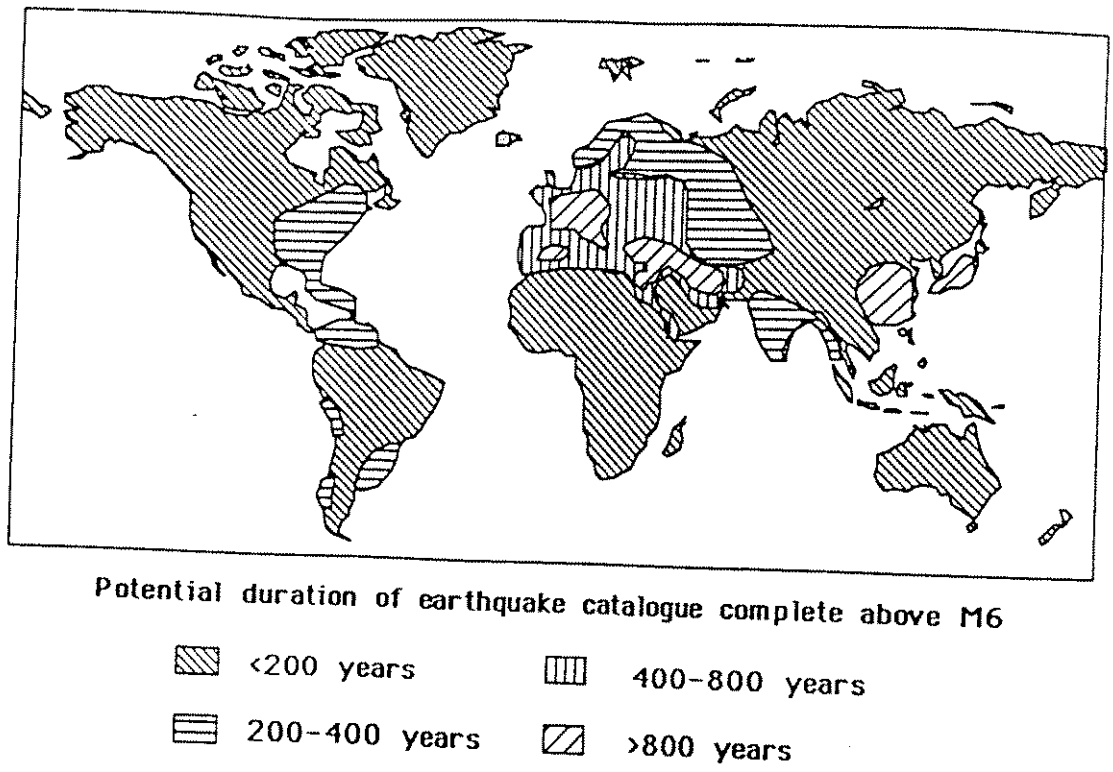

Fig. 4: Worldwide completeness of earthquake catalogues (after Muir-Wood 1993)

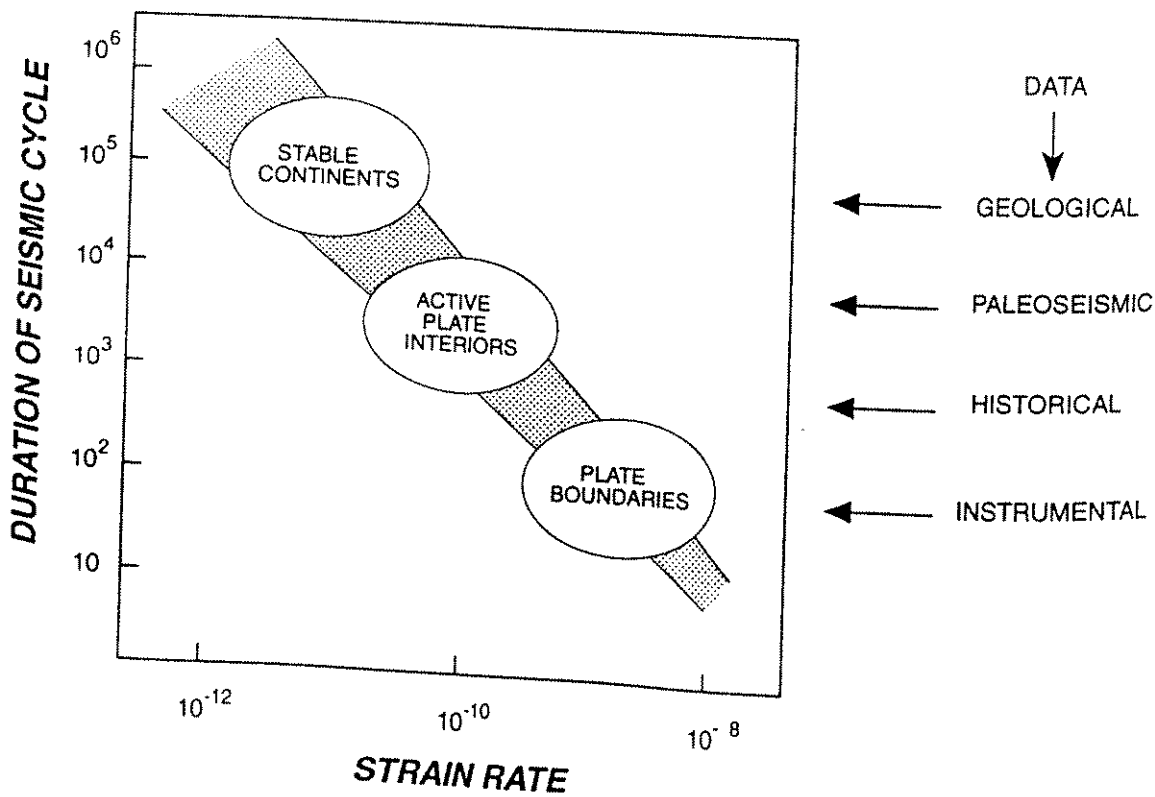

Fig. 5: The duration of seismic cycle (in years) as a function of strain rate (courtesy of D. Giardini 1994)

- Earthquake catalogues solely based on instrumental records do generally not cover a sufficient time period (< 50 - 100 years) as to cover at least one full seismic cycle but they have the advantage of being more complete for lower magnitudes;
- Along active plate plate boundaries strain rates are large enough as to cover one or more seismic cycles with complete catalogues dating back for more than one or a few hundred years;
- In active intraplate environments the historical records of only the oldest cultural nations date sufficiently far back (> 800 years) so as to assure the coverage of one or more seismic cycle(s) containing also the strongest "characteristic" events;
- On stable continental platforms even the longest catalogues or historical records do not reach back sufficiently far in the past as to assure the coverage of at least one seismic cycle and the strongest possible earthquake in such areas.

The last conclusion was dramatically confirmed by the most devastating Haicheng (1975, Ms = 7.3, Imax = 9° MSK) and Tangshan earthquakes (1976, Ms = 7.8, Imax = 11° MSK) in China. Both events occured in regions for which the former Chinese seismic zoning map, based on data of an about 3000 year old earthquake catalogue, assumed only a maximum intensity of ground shaking Imax = 6° MSK. Later paleoseismological investigations in the Tangshan area revealed that two prehistoric events of about the same magnitude as the 1976 event had occured in this region with an estimated return period of about 3000 years (Wang 1987). The importance and methodology of using both historical and paleoseismological investigations for the extension of the time window of earthquake catalogues as an indispensable precondition for more reliable long-term hazard assessments are well summarized, with many suitable references for further readings, in papers by Vittori et al. (1991), Guidoboni and Stucchi (1993) and Pantosi and Yeats (1993).

But even if we have covered one or more seismic cycles containing also the strongest possible or at least the "characteristically" strongest events probable in the considered region we still have to base our statistical calculations for seismic hazard assessment on other assumptions, e.g. with respect to the statistical distribution of the data. The return period of strong events may follow a normal (i.e. Gaussian) or another, e.g. a log-normal distibution. In practice, we have for most regions not enough realizations of strong events in order to derive the most appropriate or "true" distibution model from the data itself. Also, our current understanding of the underlying physical processes that control the recurrence times is not yet good enough as to give us any assurance on whether they distibute normally or log-normally or different from both. But different assumptions on their distribution may have dramatic consequences on the hazard assessment, This was demonstrated by Jacob (1984) who calculated for the critical gaps along the Aleutian Islands' arc a two to three times lower conditional probability of occurrence of strong events with seismic moment magnitudes Mw >7.8 within the 20 years' intervall 1983 - 2003 when assuming a log-normal instead of a normal distribution of the respective recurrence times (Fig. 6). As long as these basic uncertainties remain the long-term probabilities for great earthquakes have to be taken with great caution. This is especially true when considering the possible social impact of such "predictions" as well as the risk assessments based on these probabilities.

Another important finding from old catalogues is that over periods of several hundred or thousand years the seismic activity within a given area varies. Ben-Menahem (1981) derived from the catalogue of earthquakes in North and Central Israel, which dates back for about 4000 years, activity maxima with events up to M = 7 - 7.5 every 760 +- 40 years while in time intervals between these "peaks" the maximum magnitudes of events reached only values of M = 6.5 +- 0.1. Ambrasseys (1980) could show that phases of higher and reduced earthquake activity may occur alternatingly in neighboring seismotectonic zones such as the North Anatolian and the East Anatolian or Border Zone (Fig. 7). This behaviour resembles the oscillations of a coupled pendulum with a week connecting spring.

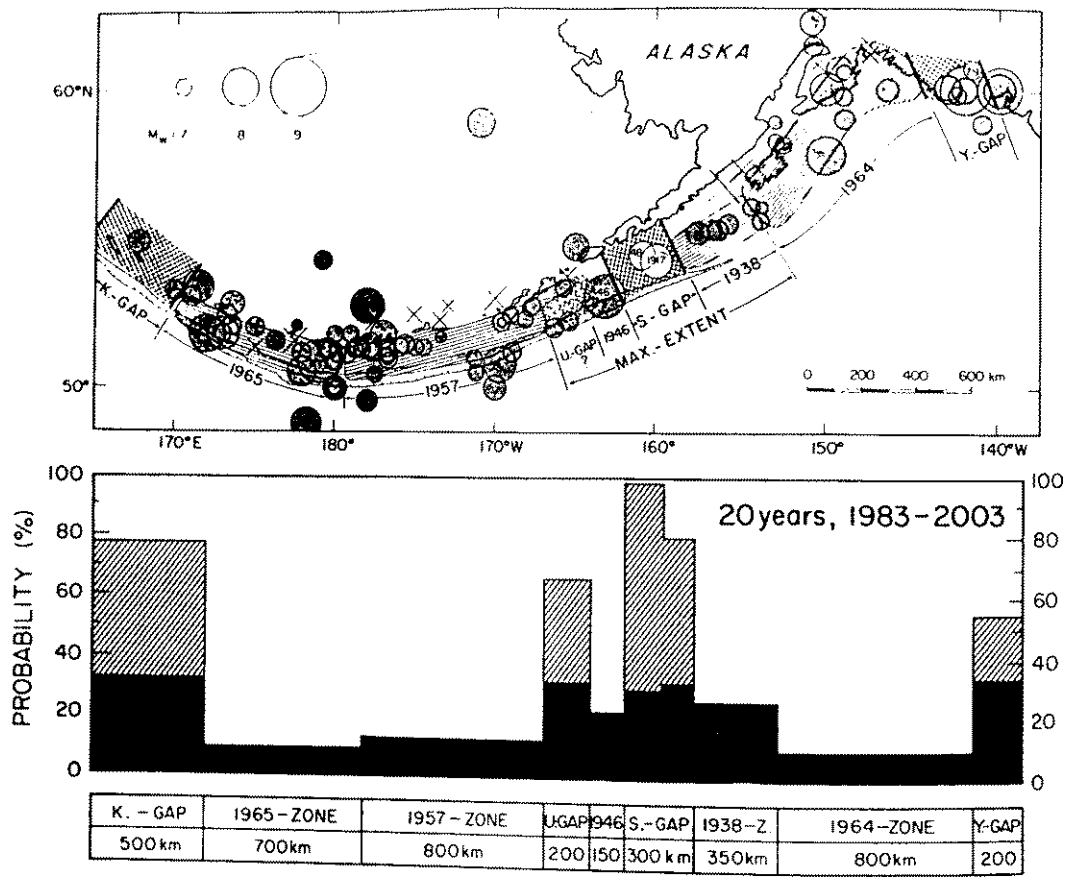

K. – GAP	1965 – ZONE	1957 – ZONE	U-GAP	1946	S.-GAP	1938 – Z.	1964 – ZONE	Y-GAP
500 km	700 km	800 km	200	150	300 km	350 km	800 km	200

Fig. 6: Top: Instumental seismicity since 1898 for Mw > 7.0 and segmentation into major zones of recent ruptures with Mw > 8 as well as seismic gaps. Bottom: Conditional probabilities for great earthquakes with Mw > 7.8 in all major segments of the Aleutian arc for the time window 1983 - 2003 based on normal distribution (hatched columns) or log-normal distribution of recurrence times (solid columns) (after Jacob 1984)

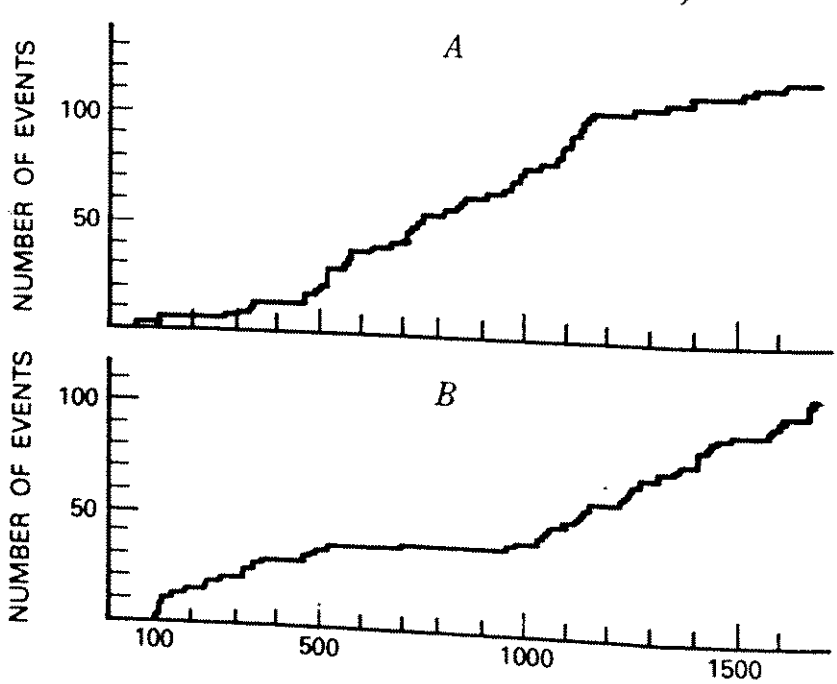

Fig. 7: Cumulative number of damaging earthquakes for the Border zone (A) and North Anatolian zone (B) between 0 and 1700 AD (after Ambraseys 1980)

The fundamental precondition for the applicability of the Poisson model in earthquake hazard assessment, namely, that the earthquake generating process is a stationary one, is under such circumstances not strictly applicable. Time-dependent Markov models, considering both the temporal and magnitude dependence of earthquake recurrence, would then, in principle, better describe the probability distribution of events. But in the case that the instrumental or even the historical record is shorter than the duration of major episodes of increased or reduced activity we will not recognize this variability and cannot evaluate its possible influence on the long-term hazard assessment. Consequently, the latter might turn out to be either too high or too low, i.e. conservative or unconservative. But for more short-term hazard assessments as being relevant for many engineering applications with typical time windows of about 50 to 100 years and magnitude levels with annual exceedance probabilities of 10^{-3} or less (i.e. considering very strong and rare earthquakes) this is in most cases not critical. According to Cornell and Winterstein (1988) Poisson estimates are insufficient in practice only in cases where the hazard is controlled by single features for which the elapse time since the last significant event exceeds the average time between such events. But the Poisson estimate "will generally be adequate if the mean interevent time between significant events exceeds the ... elapsed time since the last such event or the length of the historical record, which ever is less". Consequently, "... a gap with higher than Poissonian hazard may be rather unusual in engineering design practice." This may also be due to the reasonable assumption that the sum of several non-Poissonian processes may be appropriately Poissonian again. Since, in practice, two or more factors will control the hazard at a particular site the combined hazard is, according to Cornell and Winterstein (1988), better estimated by the Poisson model than by a single feature non-Poissonian one. On the other hand, Muir-Wood (1993) gave a striking example for how strong also short-term hazard assessments may depend on our knowledge of the hazard generating process, i.e., whether such assessments are based on probabilities derived from historical data only or on seismotectonically constraint or time-dependent probabilistic models (Fig. 8).

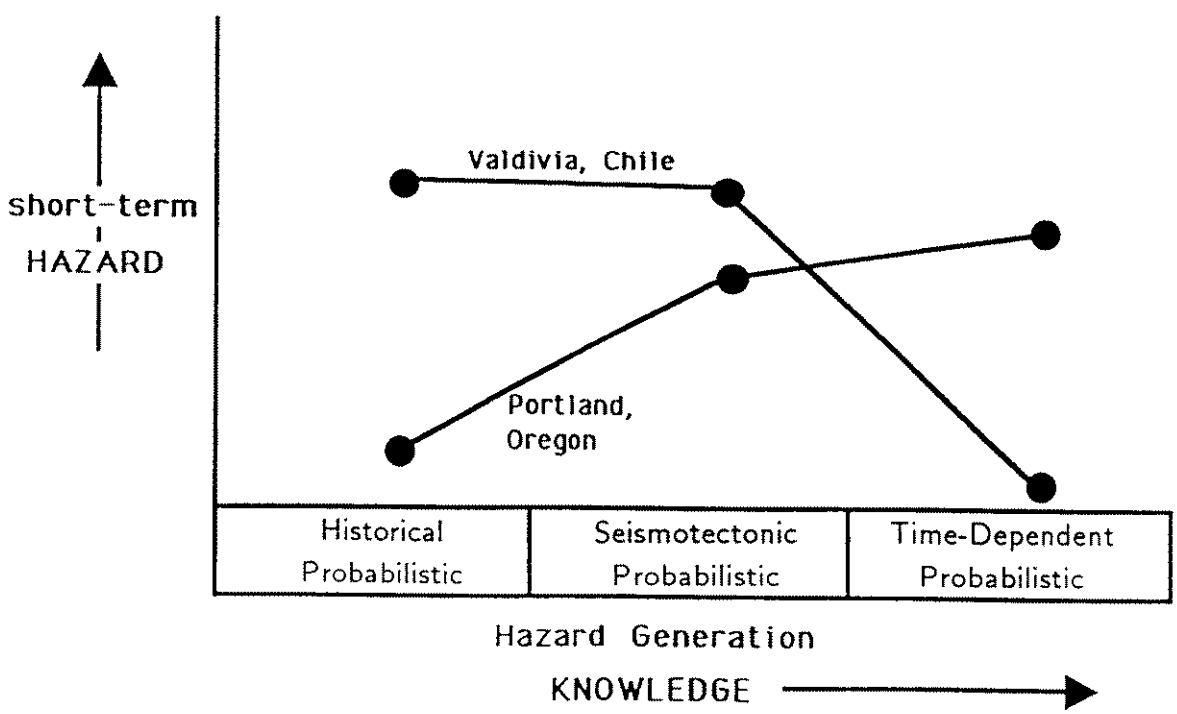

Fig. 8: Dependence of the short-term hazard assessment for the towns of Valdivia, Chile and Portland, Oregon, on the applied probabilistic model (after Muir-Wood 1993)

But in general, available methodologies for the calculation of seismic hazard are well established. According to McGuire (1993) uncertainties in interpretation can be accounted for by applying multiple hypotheses resulting in uncertainties in the hazard assessment. Being aware of them leads to the most informed decisions for risk mitigations. The training course will, therefore, strongly focus on the fundamentals, data to be used, chief steps to be considered and methods to be applied in seismic hazard assessment (Grünthal 1994, volume II of the course material, p. 376 - 490). According to Rhoades and Evison (1989) comprehensive and reliable precursory observations may additionall provide a basis for the quantification of time-variable hazard models. But the precondition is that the precursor data are sufficient to allow the derivation of intermediate quantities such as probability distributions for location, magnitude and time of occurrence of events as well as valid false alarm and failure rates. But this is, in the authors opinion, not yet available anywhere in the world for practical applications. Other crucial interdisciplinary questions such as vulnerability (e.g. Petrovski 1991) and risk assessments, which have to be tackled mainly by engineers, economists, sociologists et al., go beyond the scope of the training course and cannot be considered here.

3. A REVIEW OF NATURAL DISASTERS IN THE 20TH CENTURY

Fig. 9 shows the probably most complete compilation of casualties due to natural disasters between 1900 and 1988 (Science Council of Japan 1989). Respectives shares given for various kinds of disasters as well as regions differ slightly from source to source, also depending on the time interval considered. Not considered are in Fig. 9 casualties due to drought and famine. They are by far the largest (> 8 to 10 Mio) but at the same time also least reliable figures. Also not shown in Fig. 9 is the fact that generally the number of people being injured is typically 3 to 10 times and that of those being left homeless about 10 to several 100 times larger. Accordingly, in the preamble of a related resolution of the United Nations General Assembly of December 1987 it is stated, that during the last two decades natural disasters claimed world-wide more than 3 million human lifes and affected the life of at least 800 million people. Consequently, the human suffering and tragedy is immense, not to speak of the material losses.

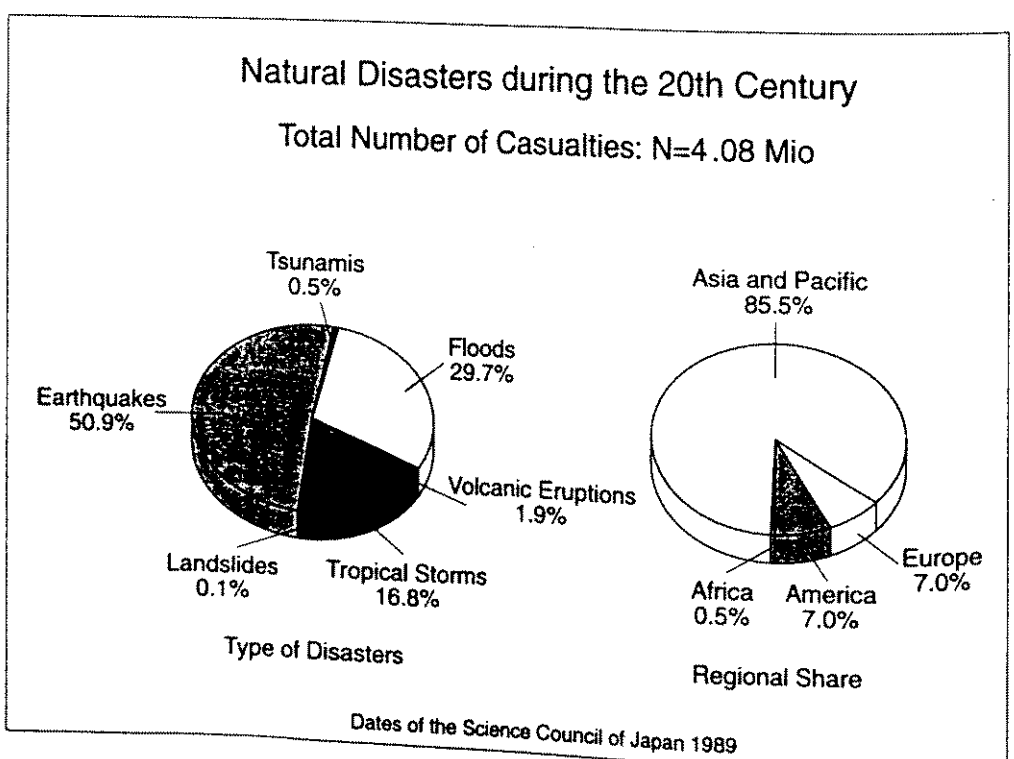

Fig. 9:

On the basis of still incomplete data published by the German IDNDR-Committee (1994) for disaster events with more than 1000 casualties and complemented by data published in Hurtig and Stiller (1984) for earthquakes and for other types of events by data from another German IDNDR publication (1991), the author compiled Tab. 1. It gives the country-wise percentage of casualties during this century for different kinds of major natural disasters. According to it India/Bangladesh and China are by far the most disaster stricken countries.

Tab. 1: Natural Disasters 1900 - 1993: Relative death toll due to various types of disasters for the most the affected countries

Type of disaster	Country	% of disaster type total
Drought/Famine	India/Bangladesh	75
	USSR	14.6
	Sahel countries	>10
Floods	China	98.1
Tropical Storms	India/Bangladesh	92.7
	Hong Kong	1.6
	USA	1.5
	Honduras	1.3
	Philippines	1.0
Earthquakes	China, Taiwan	40.2
	USSR	10.9
	Japan	10.4
	Italy	8.0
	Iran	7.2
	Peru	4.4
	Pakistan	4.2
	Turkey	3.7
	Central America & Mexico	2.8
	India	2.6
	Chile	2.2
	Morocco	0.9
	Ecuador	0.5
	Argentina	0.3
	Philippines	0.3
	Algeria	0.2
	Indonesia	0.2
	Yemen	0.2
	Romania	0.2
	Papua New Guinea	0.1
	USA	0.1
	Yugoslavia	0.1
Volcanic Eruptions	Martinique	39.0
	Colombia	30.9
	Indonesia	14.0
	Guatemala	8.1
	Papua New Guinea	3.9
	Cameroon	2.3
	Philippine	1.7

From the various consulted data sources the following conclusions can be drawn:
- Earthquakes have a significant share in the total deaths toll of over 10 Mio. due to natural disasters during this century;
- The frequency of casualties is not uniformly distributed over the various decades (cf. also Fig. 12);

- Within a given decade one or two disaster events may account for over 80 per cent of the total losses due to this type of event.

A more detailed account of loss of life due to earthquakes between 1900 and 1979 is depicted in Fig. 10 and compared in Fig. 11 with the changes in seismic moment and seismic energy release. Shown are both the respective values for strong individual events and the moving annual averages over intervals of 5-years (according to Kanamori, 1980). The comparison reveals that there is no direct correlation between the number of earthquake casualties and the global seismic activity and energy release. A single giant events such as the Chile earthquake 1960 released roughly as much seismic energy as the long-term global cumulative average over 25 years corresponding to about 20 percent of the total annual energy of lithospheric plate motion. It killed about 3000 people while hitting a sparsely populated area. Contrary to this, the about 300 times weaker event which struck the populated area around the Chinese town of Tangshan in 1976 caused officially quoted 242,000 casualties. Not confirmed earlier estimates spoke even of more than 600,000 deaths (still depicted in Fig. 10).

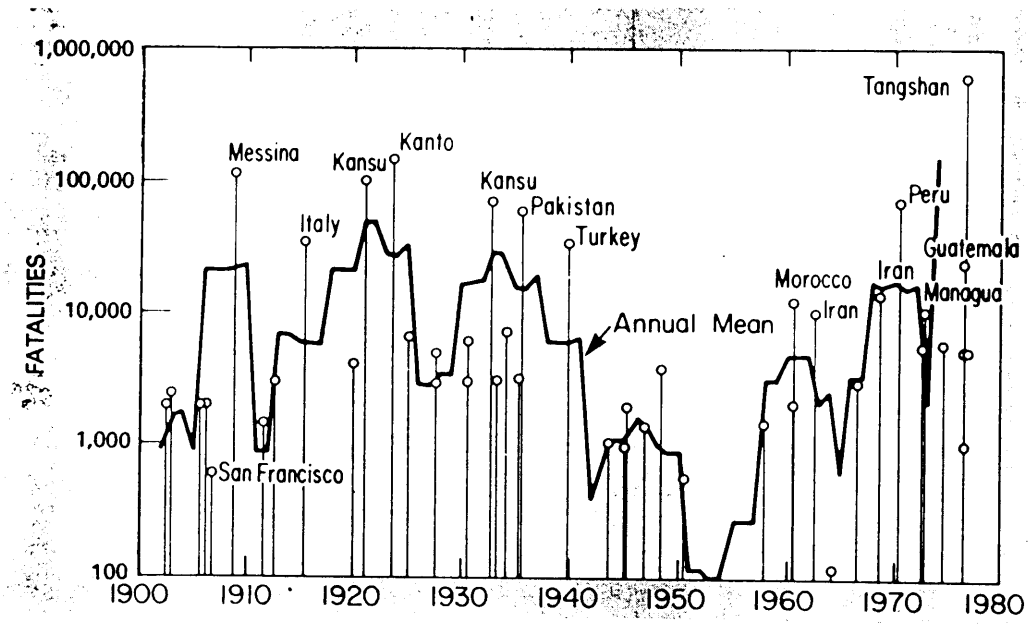

Fig. 10: Loss of life caused by major earthquakes since 1900. Individual events are marked with thin vertical lines and open circle. The solid line is the annual average taken over 5 years at a time (according to Kanamori 1980).

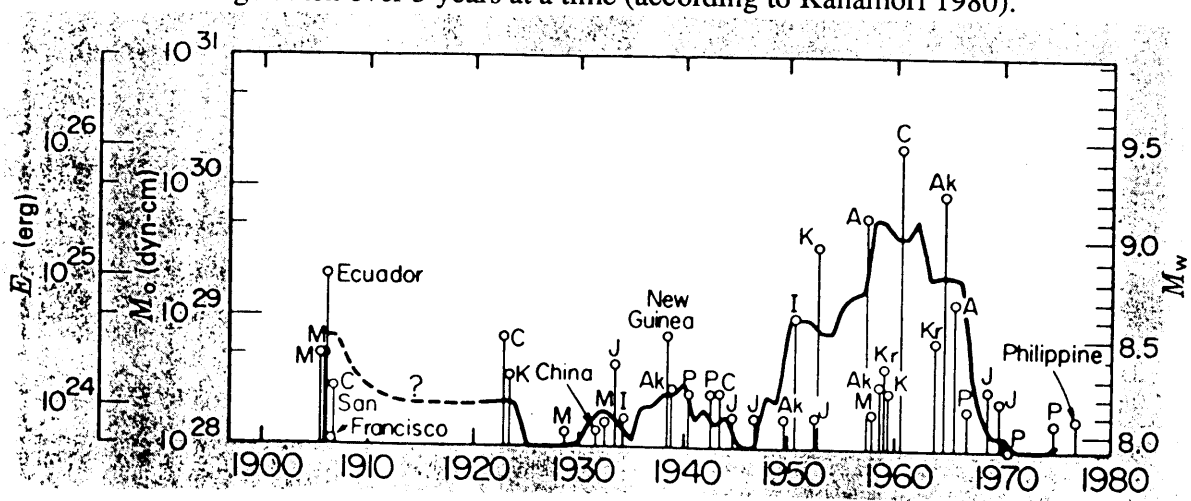

Fig. 11: Seismic moment M_0, seismic energy E, and moment magnitude Mw for large earthquakes together with the 5-year running annual average of E (solid line). Abbreviations are: A - Aleutian, Ak - Alaska, C - Chile, I - India, J -Japan; K - Kamchatka, Kr - Kuriles, M - Mongolia, P - Peru (from Kanamori 1980).

Figs. 10 and 11 do discard speculation of an escalation of global seismic and volcanic activity due to the underground nuclear testing (UNT) by military superpowers. As large as these explosions are in human terms and as devastating they would be in a targetted military application as small they are still when compared with the energies by global lithospheric plate motions and those released to major earthquakes. UNT reached its climax between 1967 and 1976 with many yields ranging between about 1 and 6 megatons of TNT equivalent. But just during this time window the global curve of seismic energy release shows a dramatic decline. The following increase again coincides with the prohibition of testing of devices with more than 0.150 Mt TNT equivalent. Seismologists should know that even the strongest UNT had a body wave magnitude of about 7 only . Every year there occur about 10 earthquakes of this magnitude and stronger. And the Chile earthquake was about 3,000 times stronger then the strongest UNT and about 200,000 times stronger than the largest tests after 1976. About half of these later tests had even yields between about 1 and 20 kt TNT only (magnitudes between 2 and 5.5). Every year there are thousands to hundreds of thousand of natural events in this magnitude range. Although very strong UNTs may trigger hundreds of tectonic aftershocks in an area up to about 20 km radius around the source along pre-existing faults they can neither trigger nor cause earthquakes at significantly larger distances. Beyond 30 to 100 km distance the quasi-static deformations of the Earth's crust after a Mt-UNT do fall already below the periodic deformations due to the gravitational forces of the sun and moon (solid earth tides) which have no proven significant effect on the triggering of earthquakes (cf. Bormann 1990).

Fig. 12 depicts the economic losses due to natural disasters for the time span 1960 to 1991 on the basis of data published by the Munich Reinsurance Company. One recognizes, despite of significant annual fluctuations, a striking trend of steadily increasing decade averages. The total economic losses per decade (in terms of 1991 values) were about 40 billion US$ between 1960 and 1969, 70 billion US$ between 1970 and 1979 and 120 billion US$ between 1980 and 1989. For Europe (with Turkey included), the respective values increased from about 0.6 billion US$ for 1960 - 69 to about 11 billion US$ for 1980 - 89. Since then the total losses within less than 5 years amount to already more than 140 billion US$. Hurrican "Andrew" in 1993 and the Northridge earthquake in January 1994 (California) accounted alone for damages of about US$ 30 billion and 15-20 billion, respectively.

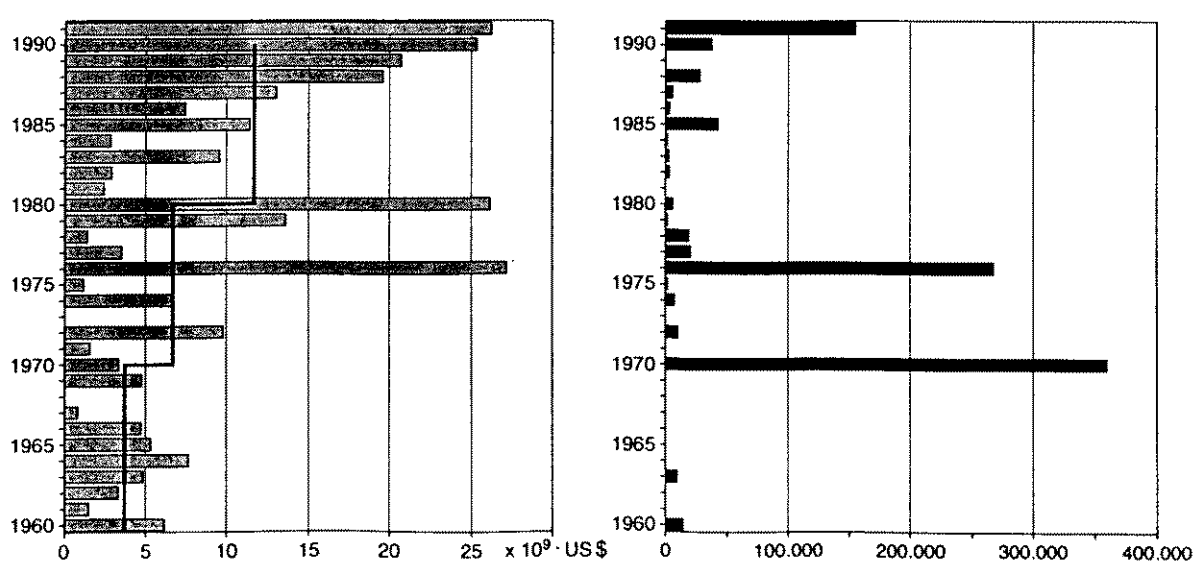

Fig. 12: Losses due to large natural disasters between 1960 and 1991 (without drought and famine) according to Munich Reinsurance 1992. Left: Economic losses in billion US$ (1991 values) per year (bars) and annual mean losses per decade (solid line); right: number of death per year.

This speaks of a rapidly increasing vulnerability of human society due to population growth, expanding settlements into more and more risky areas and poverty related inappropriate building materials and techniques in developing countries on the one hand and more and more dense and costly settlements, industries, equipments, infrastructure and life-line systems on the other hand in highly industrialized countries. In the first case the losses are mostly human lives, in the latter case material values. The United States Agency for International Development (US-AID) estimates for the next decade disaster losses of about 400 billion US$. It states at the same time that damages of about 280 billion US$ could be avoided when immediate prophylactic measures were taken. They would cost about 40 billion US$, i.e. one seventh only of the expected losses. On the other hand, in a 1989 report, the Tokai Bank of Japan predicted that another earthquake in the Tokyo area comparable with the size of that in 1923 could cause US$ 650 billion in damage alone. Losses of this order to Tokyo as one of the leading world financial centres are expected to have a detrimental effect on the economies of other countries as well.

Although as much as three fourth of the global material disaster losses occur in the industrialized countries, the proportional losses in terms of percentage of GNP are much higher in developing countries. The damage caused exceeds by far the total amount of economic assistance which disaster-prone developing countries receive from abroad and cancel out in many of these countries any real economic growth. And their share in human losses is about 95 % of the disaster total. The United Nations Conference on Human Settlement cited in its conference background paper A/Conf. 70/B/7 of 24 February 1976 the result of a case study of the office of the United Nations Economic Commission for Latin America (ECLA). According to this, the estimated disaster damage in the five countries of the Central American Common Market has averaged 2.3 per cent of the gross domestic product in the 15-years period 1960 - 74, even without taking indirect disaster effects such as disruption of economic activities, soil degradation etc. into account which are in most cases higher than the direct material losses. Considering too, that the countries concerned have an average population growth rate of about 3 per cent a year an economic growth rate of at least 5.3 per cent would be necessary in order to remain at a static level of development. Since only a few of these countries achieve this rate most are falling back in relative terms, to a large extent because of the detrimental impact of natural disasters.

These facts demonstrate that disaster prevention or at least the mitigation of their destructive effects must be viewed as a problem of economic and social development, too. Vulnerability studies, hazard and risk assessments and mapping, cost-benefit analyses of various alternative preventive or mitigation measures and pre-disaster planning must be considered, therefore, integral part of any national development strategy and planning in disaster-prone countries. This the more so if one considers that most developing countries are still at the initial stages of urbanization and industrialization and that, according to the United Nations Habitat Conference in Vancouver 1976, "... as many human settlements will have to be made available during the next 25 years as during the whole of man's previous history." To cope with these challenging problems a major joint effort of scientists and educators, development planners, decision makers and community officials is needed. The newly established Global Seismic Hazard assessment project (GSHAP) (Giardini and Basham 1993), proposed by the International Lithosphere Program (ILP) and sponsored by the International Council of Scientific Unions (ICSU), strives to make a major contribution towards these goals and to foster the interdisciplinary co-operation amongst the concerned scientific disciplines (Fig. 13).

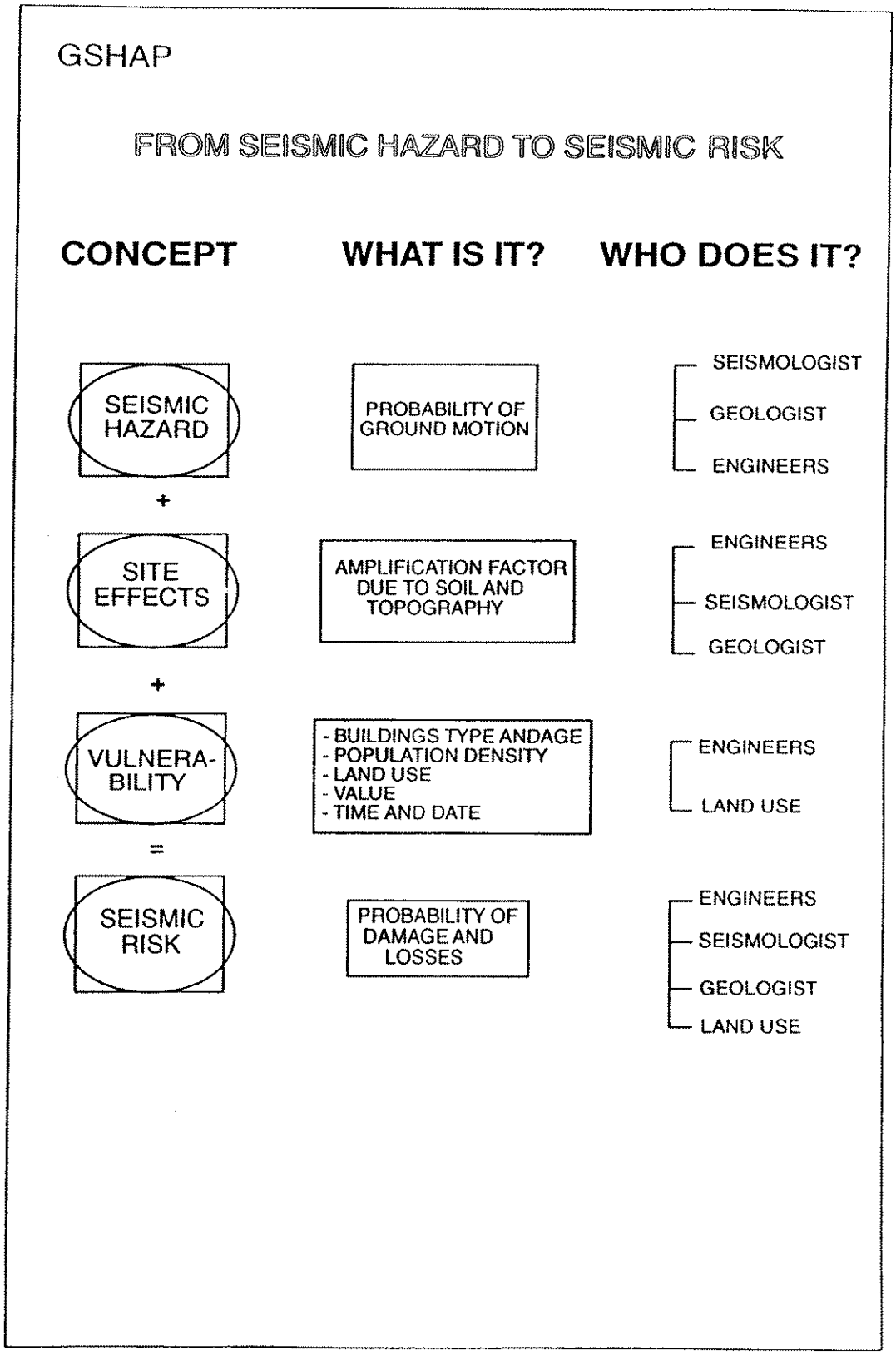

Fig. 13: The GSHAP concept from seismic hazard to seismic risk (courtesy of D. Giardini 1994)

4. THE INTERNATIONAL DECADE FOR NATURAL DISASTER REDUCTION (IDNDR)

The situation described above induced the renown seismologist and president of the U.S. National Academy of Sciences, Dr. Frank Press, to propose in a keynote address to the Eighth World Conference on Earthquake Engineering in 1984 the establishment of an International Decade for Natural Hazard Reduction, beginning in 1990. This initiative resulted, after various international expert meetings and preparatory reports, in the Resolution 44/236 of the United Nations General Assembly. It was adopted on 22 December 1989 and proclaimed the **International Decade for Natural Disaster Reduction (IDNDR)**, beginning on 1 January 1990. The International Framework of Action annexed to this resolution outlines the following objectives and goals of the IDNDR:

1. To reduce through **concerted international action**, especially in developing countries, the loss of life, property damage and social and economic disruption caused by natural disasters;

2. To improve the capacity of each country to mitigate the effects of natural disasters expeditiously and effectively, paying special attention to **assisting developing countries** in the **assessment of disaster damage potential** and in the **establishment of early warning systems** and disaster-resistant structures when and where needed;

3. To **devise** appropriate **guidelines** and strategies for applying existing scientific and technical knowledge, taking into account the cultural and economic diversity among nations;

4. To **foster scientific and engineering endevours** aimed at closing critical gaps in knowledge in order to reduce loss of life and property;

5. To **disseminate** existing and new technical **information** related to measures for the assessment, prediction and mitigation of natural disasters;

6. To develop measures for the assessment, prediction, prevention and mitigation of natural disasters through programmes of **technical assistance** and **technology transfer**, demonstration projects, and **education and training**, tailored to specific disasters and locations, and to evaluate the effectiveness of those programmes.

The Scientific and Technical Committee of the United Nations for the IDNDR has specified as targets for the decade that by the year 2000, all countries, some trough regional arrangements, should have in place, as part of their plans to achieve sustainable development:

National assessments of risks:
- Overall identification of those natural hazards which pose a disaster threat;
- For each type of **hazard** threat, an **evaluation** of the geographic distribution of the threat, usually in the form of maps, and estimates of its **recurrence interval** and impacts;
- **Assessment of vulnerability** of the most important concentrations of population and resources.

National and/or local prevention and preparedness plans:
- Adoption of **land-use and construction practices** to resist or avoid hazards;
- Adoption of **emergency-response plans** that identify responsible organizations, hazard scenarios and essential actions;
- Awareness programmes to **educate people** on the nature of the threat, including a **training** component **for responsible personnel**;
- Concrete measures to mitigate damages and to increase resilience to hazards.

Global, regional, national and local warning systems:
- **Monitoring** and, if possible, prediction **systems** capable of forecasting and detecting threatening phenomena in time to initiate actions to avert or reduce impacts;
- **Communication systems** to disseminate warnings;
- Enhancement of the perception of hazards by responsible authorities.

5. THE POTSDAM TRAINING COURSES ON "SEISMOLOGY AND SEISMIC HAZARD ASSESSMENT": A GERMAN CONTRIBUTION TO THE IDNDR

Along the lines of the key requirements and goals of the IDNDR post-graduate international training courses on "Seismology and Seismic Hazard Assessment" are arranged every year by the GeoForschungsZentrum Potsdam (GFZ) in close co-operation with the Carl Duisberg Society e.V. (CDG), a non-profit organization for international advanced professional training and human resources development. These courses are a contribution of the Federal Republic of Germany to the educational program of UNESCO in the field of Earth Sciences (Bormann 1992) and at the same time one of the international co-operative projects of the German IDNDR-Committee (1994) to the United Nations International Decade for Natural Disaster Reduction (IDNDR). The course program and concept has been devised in 1980 and permanently updated on the basis of a thorough analysis of internationally available training courses, identified gaps and urgent requirements (Bormann 1993).

The courses are financially supported by the GFZ, by the Division for Humanitarian Aid of the Federal Foreign Office, by the Ministry of Higher Education, Research and Culture of the Land of Brandenburg (through the CDG), by the Federal Ministry for Economic Co-Operation and Development (BMZ), by the German Society for Technical Cooperation (GTZ), by international organizations such as UNESCO, UNDP, and DHA (former UNDRO), and, in case of courses outside of Germany, also by the concerned ministries and organizations of the hosting country as well as by the respective regional offices of UNESCO and/or UNDP. These financial contributions are used to provide annually about 20 to 25 cost-covering fellowships and travel grants to participants from earthquake-prone developing countries. Since 1980 327 participants from 64 countries have received training in these courses (Fig. 14 and Tab. 2). The number of course participants is, in the interest of effective training and student-teacher interaction, limited to about 25.

The courses have the character of highly intensive **"crash courses"**. They are tailored to provide interdisciplinary problem understanding and thorough **applicable knowledge and skills** to preferably young post-graduate students and research workers but also to "multipliers" such as university lecturers, planners and decision makers in the fields of applied seismology, geosciences, earthquake engineering and disaster management.

The course duration is **5 weeks**. Two weeks are reserved for introductory lectures, two weeks (interspersed) for practical exercises and one week is spent for workshop discussions with papers and case studies presented by participants, for field excursions to seismotectonic outcrops and for visits of seismological observatories, monitoring networks and other facilities. Successful participation in the courses is acknowledged by a course certificate.

While former courses were globally open and held in Germany only emphasis is now increasingly laid on providing "on-the-site" and "on-the-job" training in developing countries according to their special needs and potentials. The first two regional courses of this kind took place in 1993 in Iran (short course) and India (regular course). In future the courses will be run alternatingly at Potsdam and, on invitation from earthquake prone developing countries, as regional courses. The course 1995 is scheduled to be held in Nicaragua for participants from Latin America. Kenia has extended an invitation for 1997.

The course program covers all fundamental topics of applied seismology. It comprises both basic introductory lectures with related practical exercises and complementary state-of-the-art lectures. The latter are to deepen the theoretical insight and interdisciplinary problem understanding or do address specific problems relevant for the hosting country or region.

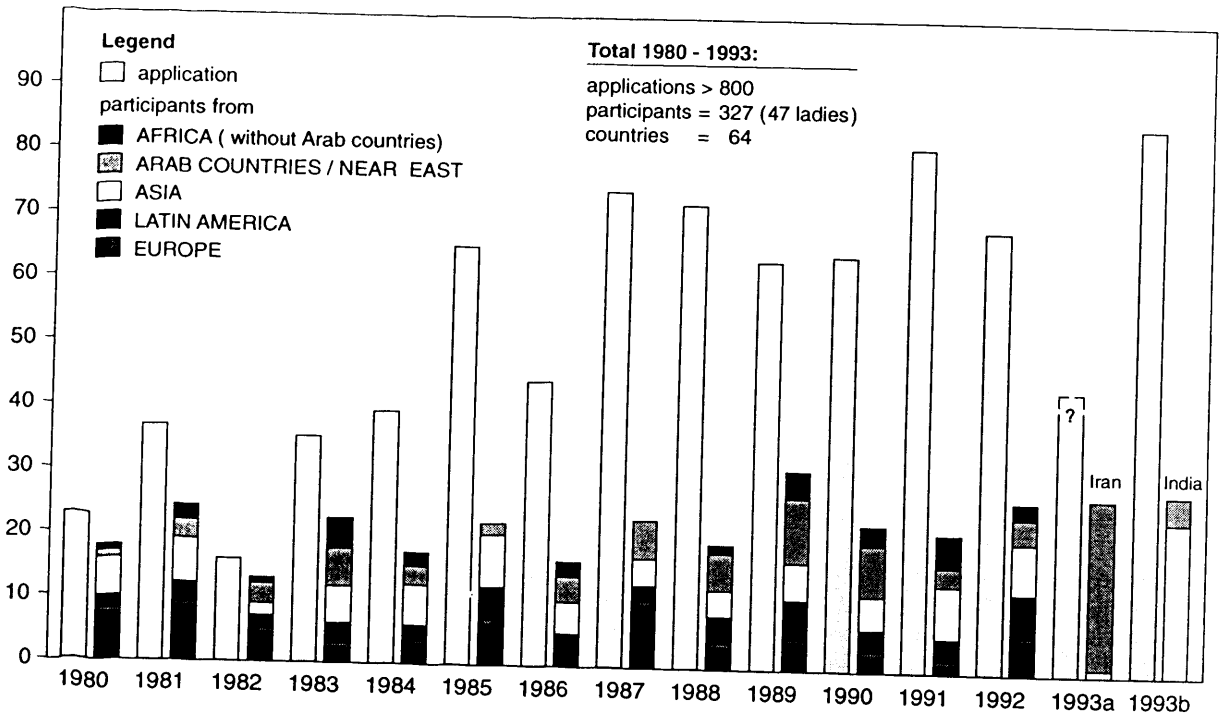

Fig. 14: Statistics of applications and participants in the international post-graduate Potsdam training courses on "Seismology and Seismic Hazard Assessment"

Afghanistan	9	Croatia	1	Kuwait	1	Romania	6
Albania	1	ČSFR	5	Kyrghyzstan	1	Portugal	1
Algeria	11	Cuba	8	Malaysia	2	Sierra Leone	1
Argentinia	3	Egypt	16	Mali	1	Sudan	4
Armenia	1	Ethiopia	4	Mexico	4	Syria	5
Bangladesh	1	Germany	30	Mongolia	2	Thailand	2
Bhutan	1	Ghana	5	Morocco	1	Tunesia	1
Boliva	2	Greece	3	Mozambique	3	Turkey	8
Brazil	4	Guyana	1	Nepal	1	Uganda	2
Bulgaria	7	Hungary	1	Nicaragua	4	U.S.S.R.	2
Burma/Myanmar	2	India	33	Nigeria	3	Venezuela	3
Cameroon	1	Indonesia	1	Pakistan	1	Vietnam	12
Chile	1	Iran	40	Papua New Guinea	1	Yemen	6
China	23	Iraq	5	Peru	1	Yugoslavia	3
Colombia	5	Jordan	2	Philippines	4	Zaire	1
Costa Rica	5	Kenya	4	Poland	2	Zimbabwe	1

Tab. 2: Participating countries and number of participants in the Potsdam training courses on "Seismology and Seismic Hazard Assessment" between 1980 - 93

The fundamental topics form the **core of the course**. They remain widely unchanged (although permanently up-dated) from year to year. For them a printed course material will be made available to each participant. The lectures and exercises of the core course will mainly be presented by lecturers of the GFZ who are involved in the course for many years already. Supplementary lectures will be handled more flexible and presented mostly by international experts from other institutions, in case of courses abroad also from the hosting country or region. Printed versions of these complementary lectures are distributed individually.

Fundamental course topics are:

- Fundamentals of seismology;
- Introduction into seismometry, instrument deployment, calibration and parameter determination with emphasis on broadband seismology;
- Site selection, station equipment and network optimization;
- Theory of wave propagation and practice of structural analysis (foreward and inverse problem);
- Seismic monitoring and routine analysis of analog records from three-component stations;
- Digital data acquisition and PC assisted data analysis;
- Event location and determination of source parameters (magnitude, fault plane solution, seismic moment, stress drop, source radius etc.);
- Macroseismic and engineering seismological parameters and their determination;
- Earthquake statistics and seismic hazard assessment;
- Direct and indirect effects of strong earthquake ground motions and microzonation;

Supplementary course topics are:

- Global and regional seismicity and seismotectonics;
- Causes and influence of crustal rheology on earthquake occurrence and energy release in space and time;
- Fundamentals, methodology and prospects of earthquake prediction and prediction research;
- Tsunami and volcanoe monitoring and warning;
- Earthquake engineering and resistance of non-engineered structures (rural housing);
- Vulnerability and risk assessments;
- Sociological and educational aspects of earthquake preparedness and disaster management.

A peculiarity of the courses are the "regional evenings" arranged by participants themselves as relaxing get-togethers aimed at introducing their fellow participants into the geography, history, people, culture, customs and current situation in their home countries/regions. These evenings contribute significantly to a better mutual understanding and respect and help to develop a spirit of solidarity and co-operation.

The courses started originally with an even wider scope (geophysics, tectonics and seismology) and 2 weeks time only. This allowed for lecturing only but not for extensive interaction between instructors and students, for practical training and skill development. But since the early years participants of each course are requested to submit at the end their answers to a questionnaire which is disseminated at the beginning. It invites their ratings and comments on the following questions:

1. Which exercises/lectures were for your work
   a) most useful, b) useful, c) less useful?

2. Was the time allocated for lectures, exercises, discussions, workshops, excursions and general exchange of views
   a) properly chosen, b) too much or c) insufficient?

3. Was the balance between lectures dedicated to basic knowledge, applicable knowledge and latest results and methods
   a) properly chosen, b) too much or c) insufficient?

4. Which topics should be
   a) expanded, b) shortened, c) deleted or d) added?

5. Were the facilities (boarding, class room arrangements) and services provided (food, access to PCs, exercise assistance, weekend excursions, social gatherings, others)
   a) good, b) satisfactory or c) needed improvement?

6. Any other comments or suggestions.

The replies are statistically evaluated and jointly discussed with the participants at the end of each course. As a consequence of this permanent feed-back and assessment of course acceptance its content and didactic approach have been changed over the years and adopted to the changing needs and potentials in developing countries (Fig. 15):

- the course duration was expanded to 5 weeks;
- the course subject was focussed on applied seismology;
- the interdisciplinary approach was kept;
- the time sharing between lectures, exercises and workshops/excursions was changed over many years on the expense of formal lectures and to the benefit of more exercises/workshops and field excursions. The latter has now stabilized at a ratio of about 40%/40%/20%;
- the courses are held at premises where all facilities are nearby (accommodation, meals, lecture rooms, social facilities) and where students and key lecturers stay together for most of the time of the course.

6. CONCLUDING REMARKS

During the last few years course structure, contents, approach and acceptance level have been rather stable. With this concept we hope to be able to make a valuable contribution to the development of needed expertise and self-reliance in disaster-prone developing countries and to lay a solid and stimulating foundation, both in scientific and human terms, for closer regional and global co-operation. Because, we should always be aware that natural phenomena causing disaster to man do not observe political borders. They also completely ignore our religious, social or other quarrels and misconceptions. To understand our living planet Earth deeply enough and to respond appropriately requires the pooling of all human intellectual, scientific, spiritual and economic-technical resources on both regional and global scale. Consequently, we have only one choice: either to live in harmony and co-operatively with nature and each other, or to perish.

What is applicable between nations is valid on a smaller scale within nations and communities as well. Often we forget that our own contribution to the tackling of pressing problems can be only very limited even when it is based on the best motivations and specialized expertise. Problems of disasters prevention and mitigation, as most other problems affecting a whole society, are much to complex as to be handled successfully by specialists alone. And also the most honorable decisions taken by politicians and other generalists will be in vain or even counterproductive if they are not based on solid scientific-technical and sociological expertise and social responsibility.

You as scientists, specialized in applied seismology, seismotectonics, engineering seismology or earthquake engineering are only one target group which has to be addressed and trained in order to achieve the challenging goals of the IDNDR. Our training course will try, therefore, to develop a mutual problem understanding amongst yourselves but also to develop a sensitive "interface" towards other disciplines. This will help you in critically assessing the limits of your knowledge with respect to the problems to be tackled, to better

Scientific Technical Report STR 95/TK
DOI: 10.2312/GFZ.b103-95tk7

GeoForschungsZentrum Potsdam

Development of course duration, methodology and topics with IDNDR revelance

Course title: "GEOPHYSICS, SEISMOLOGY & TECTONICS"
Year: 1981
Duration: 2 weeks

Topics:

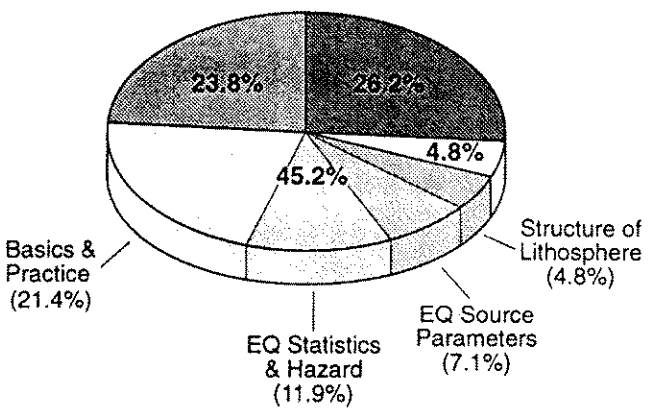

"SEISMOLOGY AND SEISMIC HAZARD ASSESSMENT"
1992
5 weeks

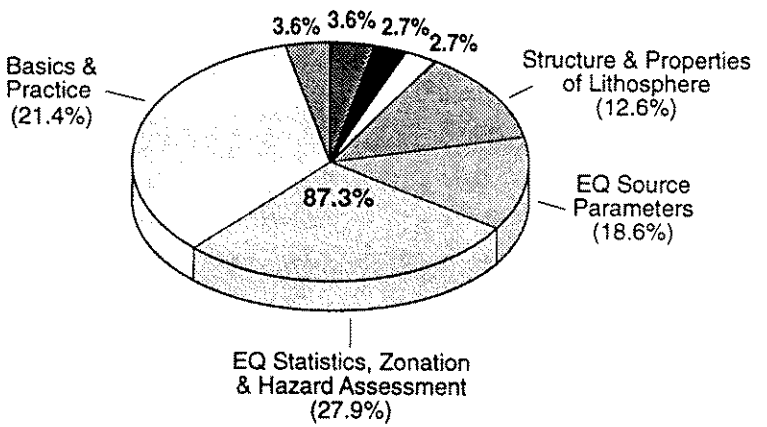

Geology & Tectonics | Geophysics & Remote Sensing | Seismology | Earthquake Engineering | Social & Educational Aspects of Disaster Reduction

Ways of instruction:

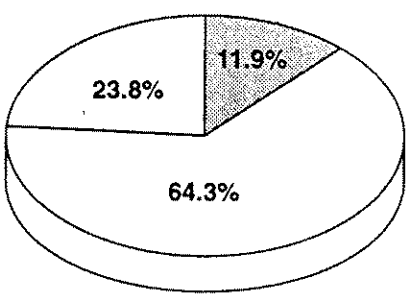

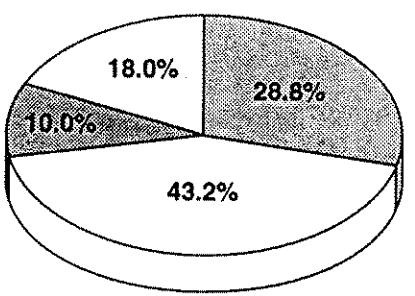

Lectures | Excursions | Exercises | Workshops

Fig. 15

judge whom you have to consult, with whom you have to co-operate and where you have more courageously to interfere in order to bring your specialized knowledge better into play to the benefit of your country and community (Fig. 13). This also requires to develop a mutually understandable language, to be able to translate our expert "slang" into words which make sense to other people as well, especially to those who have to make use of our results in their own fields of activities but also to the ordinary public. The Potsdam seismology training courses strives to make a contribution also into this direction. Therefore, be inquisitive, do question any term, notion, fact, formula or idea which you do not understand!

We will focus on introducing you to the very fundamentals of seismological practice, hopefully to an extent which will either enable you to set up a respective program in your country, if not yet available, or to do the respective jobs yourself straight away when coming home or, at least, to motivate you to follow the items up by consulting more thoroughly the specialized literature on the related topic. More fancy subjects such as earthquake prediction research, which are still far from being operational and yet forefront science, also from a sociological point of view (Kitazawa 1982), will be touched only in order to make you both curious and sober in your own decisions when setting priorities why, when and where to spent the limited human, financial and technical resources at your disposal in investigating and combating your own disasters.

REFERENCES

Aki, K. (1989). Ideal probabilistic earthquake prediction. Tectonophysics, 169, 197-198.

Ambraseys, N. (1980). Studies in historical seismicity and tectonics. Earthquake Information Bulletin, vol. 12, No. 1, 26-35

Bak, P., Tang. Ch. and Wiesenfeld, K. (1988). Self-organized criticality. Physical Review A, Vol. 38, No. 1, July 1, 364-374

Bak, P. and Tang, Ch. (1989). Earthquakes as self-organized critical phenomenon. JGR, Vol. 94, No. B11, 15635-15637

Bakun, W.H., Bredehoeft, J., Burford, R.O., Ellsworth, W.L., Johnson, M.J.S., Jones, L., Lindh, A.G., Mortensen, C., Roeloffs, E., Shulz, S., Segall, P. and Thatcher, W. (1986). Parkfield earthquake prediction scenarios and responses plans. U.S. Geol. Surv., Open-File rep., 86-365

Berry, M.J. (Ed.) (1989). Earthquake hazard assessment and prediction. Special issue of Tectonophysics, Vol. 167, No. 2-4, 81-364 pp.

Berz, G. (1992). Versicherungswirtschaft und IDNDR - Gemeinsame Aspekte und Aufgaben. Schriftenreihe der DGEB, Heft 2, 159-172.

Bormann, P. (1987). Disaster prediction, prevention and mitigation - its scientific, social, economic and organizational aspects. Veröff. Zentralinstituts Physik der Erde, Potsdam, 8th International Training Course on "Seismology, Tectonics and Seismic Risk Assessment", Lectures and Exercises, Vol. II, 302-312

Bormann, P. (1990). Können unterirdische Kernwaffentests Erdbeben auslösen? Wissenschaft und Fortschritt,40, 10, 283-286.

Bormann, P. (1992). UNESCO-Trainingskurse zur Seismologie in Potsdam: Ein deutsches Fortbildungsangebot für Geowissenschaftler aus Entwicklungsländern. UNESCO heute, 39/3, 242-247.

Bormann, P. (1993). Seminare und Kurse für Training und Weiterbildung. In: E. Plate et al. (Eds.): Naturkatastrophen und Katastrophenvorbeugung. Report of the Deutsche Forschungsgemeinschaft. VCH Verlagsgesellschaft, Weinheim, 323-342.

Boschi, E. and Dragoni, M. (Eds.). (1992). Earthquake prediction. Il Cigno Galileo Galilei di Arte e Sciencia, Roma, 610 pp.

Cluff, J.S. (1971). Peru earthquake of May 31, 1970: Engineering geology observations, Bull. Seis. Soc. Am., 61, 3, 511-534.

Cornell, C.A. and Weinstein, St.R. (1988). Temporal and magnitude dependence in earthquake recurrence models. BSSA, Vol. 78, No. 4, 1522-1437

Espinoza-Aranda, J.M., Jimenez, A.O.C., Ibarrola, G. and Ortega, R. (1992). Mexico City seismic alert system. Proc. Intern. Symp. Earthquake Disaster Prev., Mexico D.F., 315-324

Gasparini, P., Scarpa, R. and Aki, K. (Eds.) (1992). Volcanic Seismology. Springer Verlag Berlin-Heidelberg, 572 pp.

Geller, R.J. (1991). Shake-up for earthquake prediction. Nature, Vol. 352, 275-276

German IDNDR-Committee (1994). Projects for the understanding and mitigation of natural disasters. International Decade for Natural Disaster Reduction; published by Grube & Speck, Karlsruhe, 307 pp.

Giardini, D. and Basham, P. (Eds) (1993). Global Seismic Hazard Assessment Program for the UN/IDNDR. Annali di Geofisica, Vol. XXXVI, N0. 3-4, 257 pp.

Giardini, D. (1994). Personal communication

Gu G. & Ma X. (Eds.) (1984). On continental seismicity and earthquake prediction. Proceedings of an international conference, Seismological Press, Beijing, 867 pp.

Guidoboni, E. and Stucchi, M. (1993). The contribution of historical records of earthquakes to the evaluation of seismic hazard. Annali di Geofisica, Vol. XXXVI, No. 3-4, 201-216

Hellweg, P. (1994). Das Parkfield-Experiment zur Erdbebenvorhersage - Erfolg oder Mißerfolg?. Lecture at the GeoForschungsZentrum Potsdam, 13.10.1994

Hurtig, E. and Stiller, H. (1984). Erdbeben und Erdbebengefährdung. Akademie-Verlag Berlin, 328 pp.

International Decade for Natural Disaster Reduction (1991). Organization and tasks of the German Committee to the IDNDR, 35 pp.

IAEE (International Association for Earthquake Engineering) (1984). Earthquake resistant regulations: A world list - 1984. Tokyo, 904 pp.

Ito, K. and Matsuzaki, M. (1990). Earthquakes as self-organized critical phenomena. JGR, 95, B5, 6853-6860.

Jacob, K. (1984). Estimates of long-term probabilities for future great earthquakes in the Aleutians. Geophysical Research Letters, Vol. 11, No. 4, 295-298

Kanamori, H. (1980). The size of earthquakes. Earthquake Information Bulletin, Jan.-Febr. 1980, Vol. 12, No. 1, 10-15

Keilis-Borok, V.I. (1990). Introduction: Non-linear systems in the problem of earthquake prediction. Physics Earth Planet. Inter., 61, 1-7.

Kelleher, J., Sykes, L.R. and Oliver, J. (1973). Possible criteria for predicting earthquake locations and their application to major plate boundaries of the Pacific and the Caribbean. J. Geophys. Res., Vol 78, 2547-2585
Korvin, G. (1992). Fractal Models in the Earth Sciences. Elsevier, Amsterdam, 396 pp.

Kitazawa, K. (1982). Earthquake prediction and public response. Impact of Science on Society, 32, 29-37.

Mark, R.K. and Stuart-Alexander, D.E. (1977). Disasters as a necessary part of benefit-cost analysis. Science, 197, 1160-1162

Ma Zongjin, Fu Zhengxiang, Zhang Yingzhan, Wang Chengmin, Zhang Guomin, Liu Defu (1990). Earthquake prediction - nine major earthquakes in China. Seismological Press Beijing and Springer Verlag Berlin Heidelberg, 332 pp.

McGuire, R.K. (1993). Computations of seismic hazard. Annali di Geofisica, Vol. XXXVI, No. 3-4, 181-200

Mogi, K. (1985). Earthquake prediction. Academic Press, Tokyo, 355 pp.

Morgan, F.D., Wadge, G., Latchman, J., Aspinall, W.P., Hudson, D. and Samstag, F. (1988). The earthquake hazard alert of September 1982 in Southern Tobago. BSSA, Vol. 78, No. 4, 1550-1562

Muir-Wood, R. (1993). From global seismotectonics to global seismic hazard. Annali di Geofisica, Vol. XXXVI, 3-4, 153-168

Nanometrics (1994). Early warning system for Taiwan. Nanometrics News, March 31, Vol. 1

National Research Council (1991). Real-time earthquake monitoring, early warning and rapid response. National Academy Press, Washington D.C., 1-52

Nishenko, St.P. and Sykes, L.R. (1993). Comment on "Seismic gap hypothesis: Ten years after" by Y.Y. Kagan and D.D. Jackson. JGR, Vol. 98, No. B6, 9909-9916

Petrovski, J. (1991). Modelling and assessment of seismic vulnerability and risk for earthquake disaster management. Proc. 1st Intern. Conf. on "Seismology and Earthquake Engineering", May 27-29, 1991, Tehran, Vol. II, 1209-1225

Reiter, L. (1990). Earthquake hazard analysis. Columbia University Express, New York, 254 pp.

Rhoades, D.A. and Evison, F.F. (1989). Time-variable factors in earthquake hazard. Tectonophysics, 167, 201-210

Rikitake, T. (1987). Earthquake precursors in Japan: precursors time and detectibility. Tectonophysics 136, 265-282

Rikitake, T. (1988). Earthquake prediction: an empirical approach. Tectonophysics 148, 195-210

Sadovsky, M.A. and Pisarenko, V.F. (1990). Seismic process in block medium, Nauka, Moscow.

Science Council of Japan (1989). In: Information Bulletin of the Pacific Science Association, Honolulu, Vol. 42, No. 1, p. 21

Shimozuru, D. (1988). Role of the Co-ordinating Committee Hazard Mitigation and the evacuation. In: The 1986-87 eruption of Izu-Oshima volcano. Earthquake Research Institute, Univ. of Tokyo, 61 pp.

Tilling, R.I. (Ed.) (1989). Volcanic Hazard. American Geophysiscal Union, Washington, Shourt Course in Geology: Vol. 1, 123 pp.

Toksöz, M.N., Dainty, A.M. and Bullit, T. (199=). A prototype earthquake warning system for strike-slip earthquakes. PAGEOPH, Vol. 133, No. 3, 145-187

Turcotte, D.L. (1992). Fractals and chaos in geology and geophysics. Cambridge University Press, 221 pp.

UNDRO (1979). UNDRO Expert Group Meeting on Vulnerability Analysis, 9 - 12 July 1979, Geneva.

United Nations (1976 a). Disaster prevention and mitigation: A compendium of current knowledge. Vol. 1 - Volcanological Aspects. Geneva, 38 pp.

United Nations (1976 b). Guidelines for disaster prevention. Vol. 1: Pre-disaster physical planning of human settlements. Geneva, 93 pp.

United Nations (1976 c). Conference on Human Settlements, Vancouver, Canada, Conference background paper A/Conf. 70/B/7, 24 February 1976.

United Nations (1978). Disaster prevention and mitigation: A compendium of current knowledge, Vol. 5 - Land use aspects. New York, 61 pp.

United Nations (1979 a). Disaster prevention and mitigation: A compendium of current knowledge, Vol. 7 - Economic aspects, 48 pp.

United Nations (1979 b). Disaster prevention and mitigation: A compendium of current knowledge, Vol. 10 - Public informnation aspects, 142 pp.

United Nations (1980). Disaster prevention and mitigation: A compendium of current knowledge, Vol. 9 - Legal aspects. New York, 67 pp.

United Nations (1984). Disaster prevention and mitigation: A compendium of current knowledge, Vol. 11 - Preparedness aspects, 218 pp.

United Nations (1986). Disaster prevention and mitigation: A compendium of current knowledge, Vol. 12 - Social and sociological aspects, 48 pp.

United Nations (1990). Resolution A/RES/44/236 on the International Decade for Natural Disaster Reduction, 20 March 1990.

United States Department of the Interior (1990). Early warning alert system. Geological Survey, Western Region, Menlo Park, California 94025, Release of the public Affairs Office, 3 pp.

Varatsos, P. and Alexopoulos, K. (1984 a). Physical properties of the variations of the electric field of the Earth preceding earthquakes. Part I. Tectonophysics, Vol. 110, 73-98

Varatsos, P. and Alexopoulos, K. (1984b). Physical properties of the variations of the electric field of the Earth preceding earthquakes. Part II: Dertermination of epicentre and magnitude. Tectonophysics, Vol. 110, 99-125

Vittori, E., Labini, St.S. and Sera, L. (1991). Palaeoseismology: Review of the state-of-the-art. Tectonophysics, 193, 9-32

Wang, T. (1987): English abstract in Geology and Seismology, Beijing

Wyss, M. (Ed.) (1991). Earthquake prediction. Special issue of Tectonophysics, Vol. 193, No. 4, 253 - 412

SEISMICITY, SEISMOTECTONICS AND SEISMIC HAZARD ASSESSMENT IN MEXICO, CENTRAL AMERICA AND THE CARIBBEAN

David A. Novelo-Casanova

Instituto de Geofísica
Universidad Nacional Autónoma de México
México, D.F., México 04510

1. INTRODUCTION

The seismotectonics of the Mexico, Central America and the Caribbean region is dominated by the interaction of six major tectonic plates (Fig. 1). The area contains the three main types of plate boundaries: divergence, convergence and transform-fault. Seismicity is concentrated in the plate-boundary regions.

Many crustal earthquakes occur as slip on the principal interfaces between plates and have slip vectors that are parallel to directions of relative plate motion (Dewey and Suárez, 1991). Also, substantial crustal seismicity occurs in plate interiors within 100 to 200 km of some interfaces. Mantle earthquakes define subducted lithosphere to depths of more than 150 km in the major Middle American subduction zones (Fig. 2). As in other places of the world, some important plate-boundary elements appear to be aseismic.

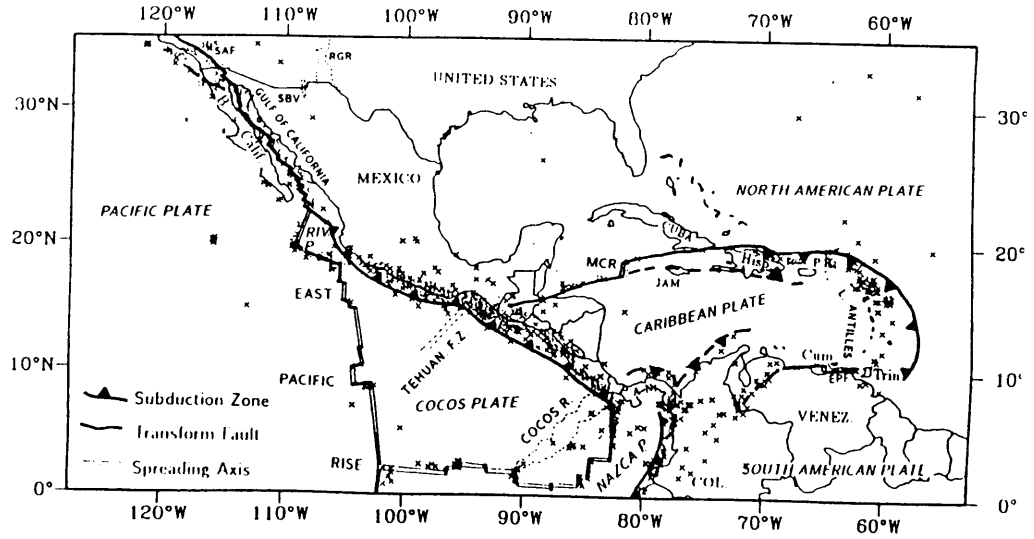

Fig. 1: Plate tectonics and shallow earthquakes of Middle America. Cumm: Cumana; EPF: El Pilar fault; MCR: Mid-Cayman Rise; RGR: Rio Grande Rift; SAF: San Andreas fault; SBV: San Bernardino Valley (from Dewey and Suárez, 1991).

Although many countries of this region have made important efforts to know their geological hazards, cooperative work is needed for research on seismic risk and prediction, on instrumentation as well as on strategies for earthquake mitigation efforts.

2. MEXICO

Most earthquakes in the northern part of Mexico occur beneath the Gulf of California (Fig. 1) where the transform plate boundary is located along which the Pacific plate is moving northwest with respect to the North American plate at a velocity of about 5 cm/year (Fig. 2). In this region strike-slip earthquakes occur on the transform faults, and both normal-faulting and strike-slip earthquakes occur in diffuse right-stepping offsets of the transform faults (Reichle and Reid, 1977; Goff and others, 1987).

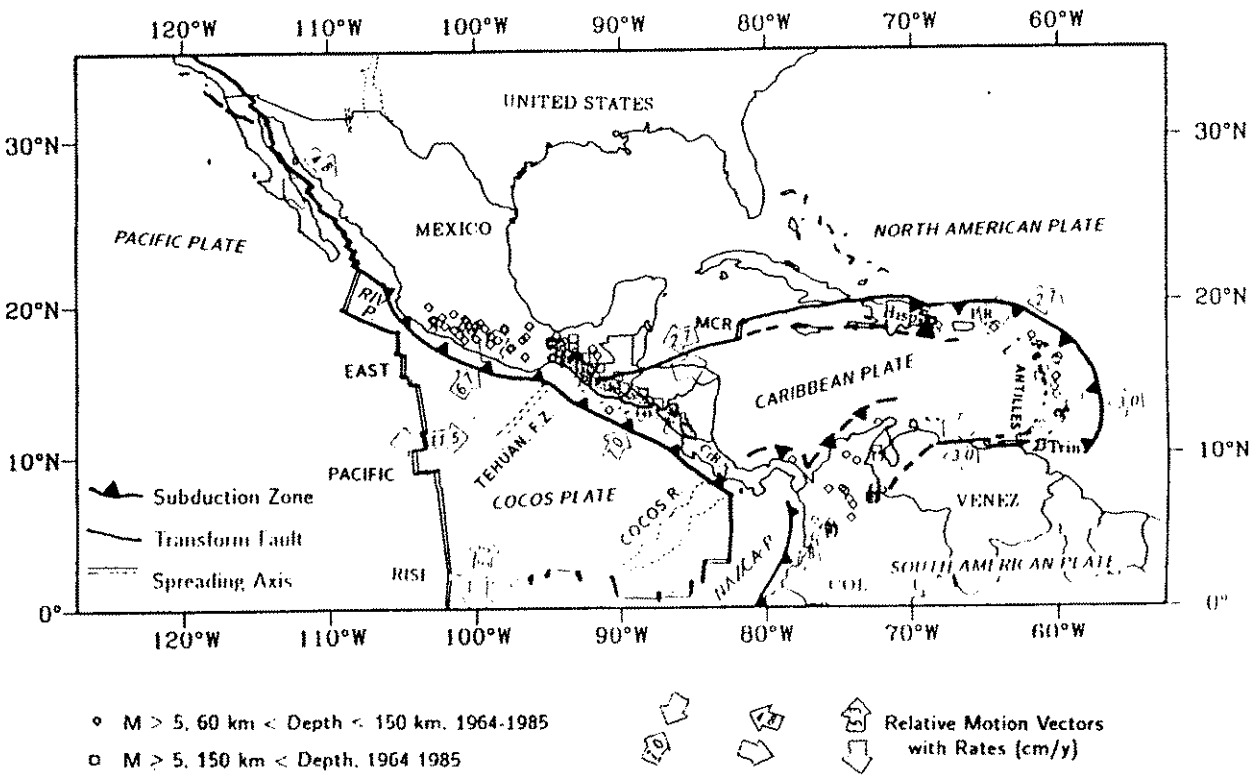

Fig. 2: Plate velocities and zones of mantle earthquakes in Middle America. Most motion vectors are determined with a variation of model AM1-2 of Minster and Jordan (1978). The relative velocity between the North American and Pacific plates in northwest Mexico is based on NUVEL-1 of Demets and others (1987). From Dewey and Suárez (1991).

Seismicity on the East Pacific Rise is typical of a fast-spreading oceanic rise system (Isacks and others, 1968). Earthquakes are concentrated in the transform fault zones, with only a few microearthquakes possibly emanating from the spreading centers. The Rivera lithosphere (Fig. 1) consumed at the trench is of late Miocene age and is one of the youngest lithosphere being subducted anywhere in the world (Klitgord and Mammerickx, 1982). Although the slow rate of convergence and the high temperatures of a young oceanic plate might have been thought

conducive to aseismic subduction, in this area occurred the largest thrust-fault earthquake along the Middle American trench in this century, the earthquake of 3 June 1932 (M = 8.4). The epicenter was located near the diffuse Rivera-Cocos-North American triple junction and ruptured predominantly along the Rivera-North American boundary (Singh and others, 1985).

The tectonic regime of central Mexico is dominated by the subduction of the Cocos plate beneath the western margin of the North American plate (Fig. 1). The subducted Cocos plate dips at about 15°. Thrust-fault events occurring on the gently dipping subduction zone have repeatedly damaged coastal cities and towns and, farther inland, Mexico City and other large populations centers.

Many segments of the subduction zone have recurrence times of 30 to 40 years for earthquakes of magnitude 7.5 or larger. Fig. 3 shows the epicenters of events with Ms > 7.0 occurred in Mexico during this century and Fig. 4 displays the space-time diagram of historic and recent great earthquakes along the Pacific subduction zone of Mexico. Most earthquakes within the subducted Cocos plate have normal-fault focal mechanisms, with axes of maximum extensional strain (T-axes) that are approximately parallel to the dip of the sinking lithosphere (LeFevre and McNally, 1985; McNally and others, 1986; González-Ruiz and McNally, 1988).

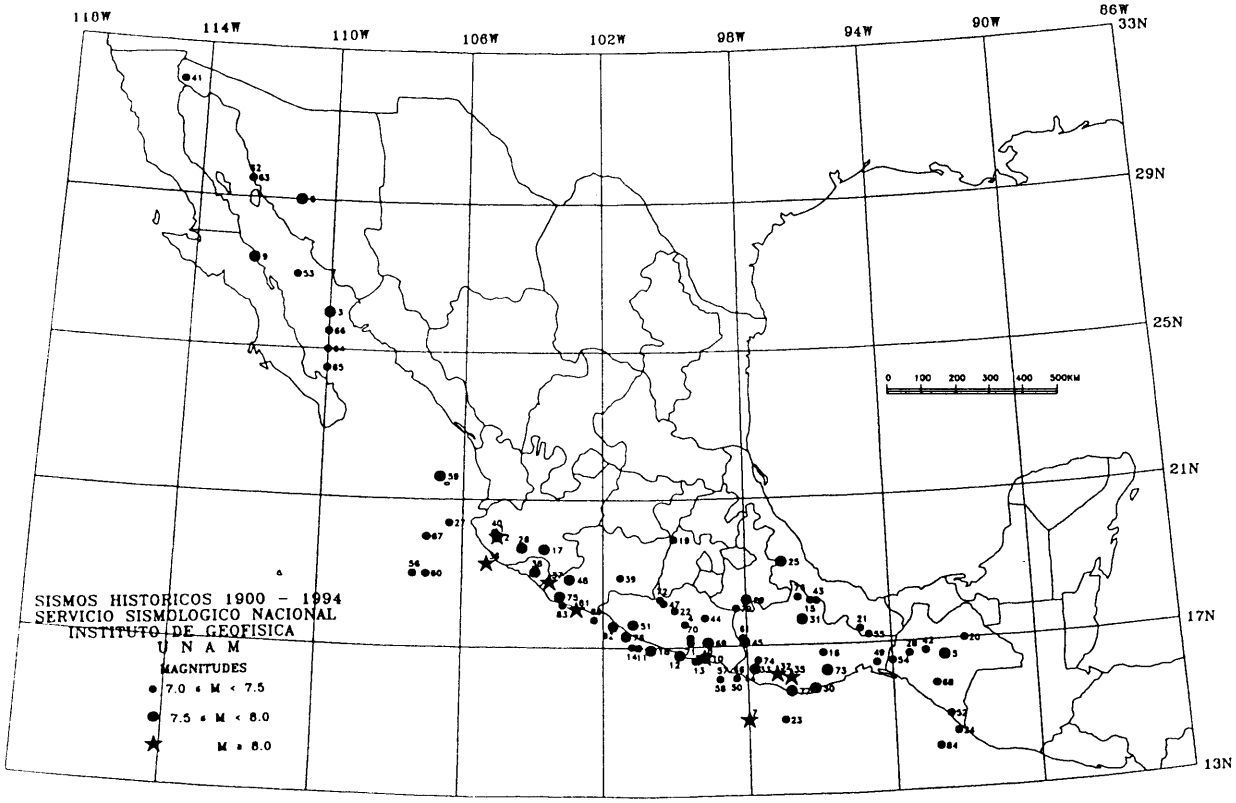

Fig. 3: Earthquakes of Ms > 7.0 which occurred in Mexico during this century. The numbers indicate the earthquake sequence.

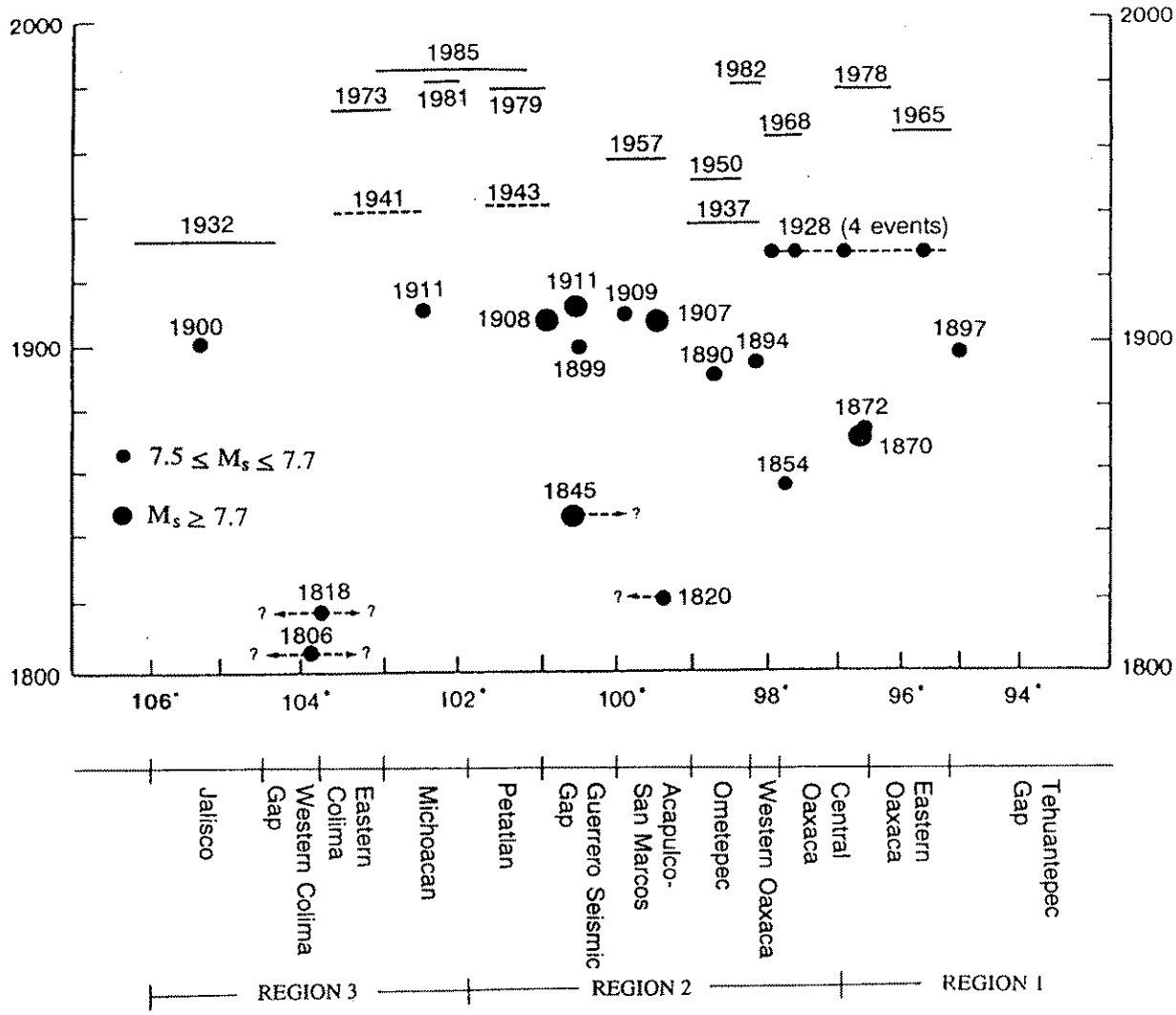

Fig. 4: Space-time diagram of historic and recent great earthquakes along the subduction zone of Mexico. Dashed lines with questions marks representing locations before 1850. Horizontal lines indicate the lateral extent of rupture zones based on aftershock studies and are dashed where less will determined (after Nishenko and Singh, 1987).

A belt of shallow-focus earthquakes in continental Mexico extends several hundred kilometers inland from the Middle American trench (Fig. 1). Because of their shallow focal depths, shocks within the overriding North American plate, such as the 1912 and 1920 earthquakes in central Mexico, have been extremely destructive.

3. CENTRAL AMERICA

A zone of intermediate-depth earthquakes extends from south-easternmost Mexico to northern Costa Rica (Bevis and Isacks, 1984; Burbach and others, 1984; Fig. 2). This Central American Wadati-Benioff zone is generally much steeper than the Mexican Wadati-Benioff zone, and

seismicity in many segments extends to depths of approximately 200 km (Burbach and others, 1984). The steeper dip of the Central American Wadati-Benioff zone is probably, in part, a consequence of the greater age, and hence greater density, of the oceanic lithosphere south of the Tehuantepec Fracture Zone (Couch and Woodcock, 1981). The dip of the Central American Wadati-Benioff zone becomes shallower at its southern end, and the zone disappears several hundred kilometers north of the Cocos-Nazca-Caribbean triple junction (Burbach and others, 1984; Guendel and McNally, 1986; Fig. 2).

The largest instrumentally recorded earthquakes on or near the Central American thrust interface have magnitudes of about 8 (McNally and Minster, 1981). In much of Central America, the most destructive historical earthquakes have been shallow intraplate shocks of moderate magnitude (5 to 6.5.) that occur in the densely populated regions surrounding the Quaternary volcanoes (White, 1991). The earthquakes typically occur as strike-slip faulting but also as left-lateral faults striking at a large angle to the trend of the Middle American arc, and right-lateral faults approximately parallel to the arc (Carr and Stoiber, 1977).

Dip-slip movements within the Guatemala City Rift were documented during the 1976 Motagua earthquakes and appear responsible for several large historical earthquakes. Aftershocks to the southwest of the 1976 Motagua earthquake (M = 7.5) occurred near the Guatemala City Rift as well as along three lineaments suggestive of recent faulting (Langer and Bollinger, 1979). Composite focal mechanism solutions of aftershocks indicate normal faulting on planes at a high angle to the westernmost extension of the Motagua Fault Zone (Langer and Bollinger, 1979; cf. Fig. 7).

Active faults, volcanoes, and rifts in Central America are shown in Fig. 5. Thirteen active Quaternary rifts have been identified; eight of these occur within a north trending zone of discontinuous grabens and faults known as the Honduras Depression (Mann and Burke, 1984); two occur in the 30-km-wide zone bounded by the Motagua and Jocotan strike-slip fault zones; and three rifts occur in the triangular wedge defined by the Middle America volcanic arc to the southwest, the Honduras Depression to the east, and the Motagua strike-slip zone to the north (Plafker, 1976). The Honduras Depression is well defined by shallow earthquakes. Although rifts occur near curved strike-slip faults (Motagua and Jocotan), no rifts are closely associated with the relatively straight Polochic Fault Zone (cf. Fig. 7). North trending faults including some bordering rifts have served as conduits for the Quaternary volcanic eruptions that extend northward from the Middle America volcanic front to the Motagua Fault Zone (Mann and Burke, 1984).

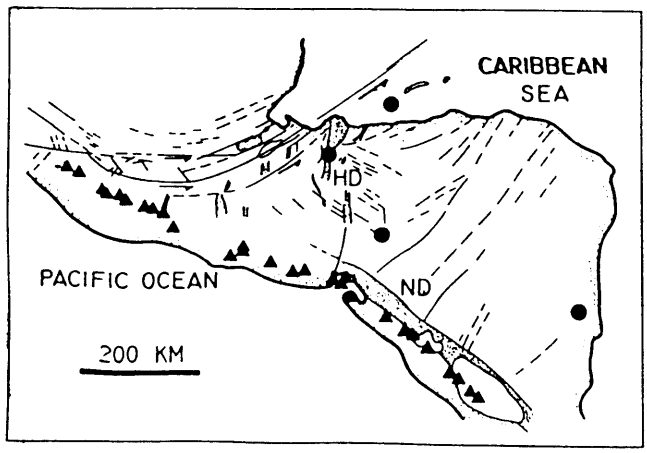

Fig. 5: Active faults, volcanoes (black triangles), and rifts in Central America. HD: Honduras Depression; ND: Nicaragua Depression (from Mann and Burke, 1984).

Instrumentally recorded shallow-focus earthquakes have occurred over a wide area both north and south of the Isthmus of Panama, however, many have involved reverse faulting rather than strike-slip faulting (Wolters, 1986; Adamek and others, 1988). South-directed underthrusting of the Caribbean lithosphere along the northern coast of the Isthmus is implied by a deformed accretionary wedge north of the Isthmus (Bowin, 1976) and by the occurrence of mantle earthquakes landward of the accretionary wedge (Wolters, 1986; Adamek and others, 1988). These observations suggest that the Nazca and Caribbean plates are separated by microplates or by a zone of distributed deformation rather than by a simple boundary (Bowin, 1976; Adamek and others, 1988).

4. THE CARIBBEAN

Central America, northernmost South America, and the West Indies are on the margins of the Caribbean plate (Fig. 1), and the seismotectonics of these regions are therefore determined by the velocity of the Caribbean plate. The interior of the Caribbean plate is relatively aseismic with the exception of a single poorly defined band of intraplate seismic activity extending along the east coast of Central America near 82° W (Sykes and others, 1982).

For the coast of northern Venezuela between 68° W and 63° W, an east-west transform boundary between the two plates accounts for the historical and instrumental seismicity (Molnar and Sykes, 1969). The presence of an easterly or southeasterly dipping Wadati-Benioff zone in northern Colombia and western Venezuela (Schneider and others, 1987) is consistent with the hypothesis that subduction occurs along the Caribbean coast of Colombia (Kellogg and Bonini, 1982).

The Boconó fault zone (Schubert, 1982; Fig. 6) is commonly postulated to accommodate a significant fraction of transform displacement between the undeformed interiors of the Caribbean and South American Plates. The last great rupture in the Boconó fault zone was probably during the earthquake of 26 March 1812 (Fig. 6).

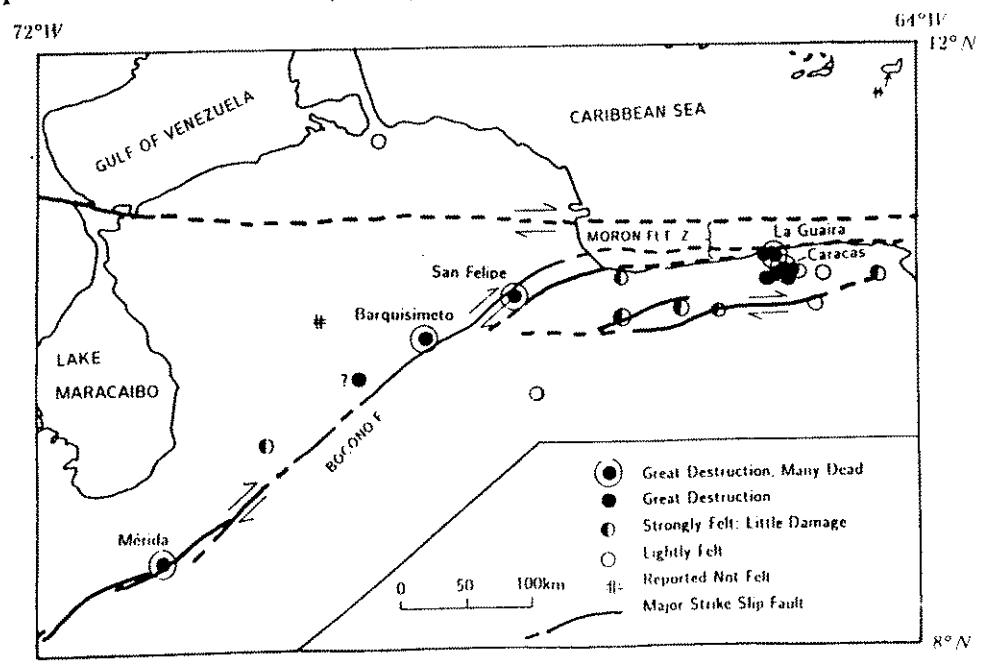

Fig. 6: Damage distribution of the Venezuelan earthquake of 26 March 1812 (from Dewey and Suárez, 1991).

Between 62.8° W and about 60° W, the boundary between the South American and Caribbean plates changes from an east-west transform to the north-south Lesser Antilles subduction zone. The historic and instrumental seismicity of this region has been too low to determine how the change in boundary orientation is accomplished at shallow depth. At upper-mantle depths, earthquakes near the south end of the Antilles Wadati-Benioff zone at 10.9° N, 62.8° W (Fig. 2) exhibit focal mechanisms consistent with the subducting American lithosphere detaching from the surface lithosphere along an east-west hinge fault (Molnar and Sykes, 1969).

The Antilles arc, from Trinidad to eastern Hispaniola, reflects the subduction of the relatively old oceanic lithosphere of one or both of the American plates. Wadati-Benioff zones extend to depths of about 200 km beneath the Antilles arc (Molnar and Sykes, 1969; Dorel 1981; Fig. 2). At shallow depths within the Lesser Antilles arc, seismicity has been substantially higher north of 14° N than to the south.

Earthquakes of magnitude about 8 occurred in the northern Lesser Antilles in 1843 and, probably, in 1690 (Robson, 1964; Dorel, 1981). South of 14° N, the largest historical shallow-focus earthquakes had magnitudes of about 7 (Dorel, 1981). During the instrumental era, most moderate and large shocks have been shallow intraplate shocks near the plate boundary, occurring in both the overriding Caribbean and the subducting American plates (McCann and others, 1982; Morgan and others, 1988).

Although the trend of the plate boundary north of Puerto Rico is nearly parallel to the direction of relative plate motion, a Wadati-Benioff zone dips south from the Puerto Rico trench (Fisher and McCann, 1984). Focal mechanisms suggest that the approximately easterly motion of the Caribbean with respect to North America is accommodated by strike-slip motion on the gently south-dipping interface between the Caribbean plate and the subducting North American plate (Molnar and Sykes, 1969).

Eastern Hispaniola has subduction zones along both its northern and southern coasts. At the north, the North American plate is being subducted toward the south. The northern subduction zone has a mantle seismic zone and has experienced great earthquakes in the instrumental era (McCann and Sykes, 1984).

Between Hispaniola and the Middle American trench, the plate boundary is predominantly a transform boundary. The distribution of historical seismicity (Sykes and others, 1982) and Neogene tectonism (Burke and others, 1980) suggest that the boundary between Hispaniola and the Mid-Cayman Rise comprises two branches - one, probably the principal branch, passing through northern Hispaniola and just south of Cuba, and the other passing through southern Hispaniola and near Jamaica (Fig. 1).

The North American-Caribbean plate boundary in Guatemala includes the Polochic and Motagua faults (Burkart, 1983; cf. Fig. 7). The Guatemala earthquake of 4 February 1976 (M = 7.5) involved 270 km of strike-slip rupture on the Motagua fault (Kanamori and Stewart, 1978) and some of the normal faults were reactivated (Langer and Bollinger, 1979, Fig. 7).

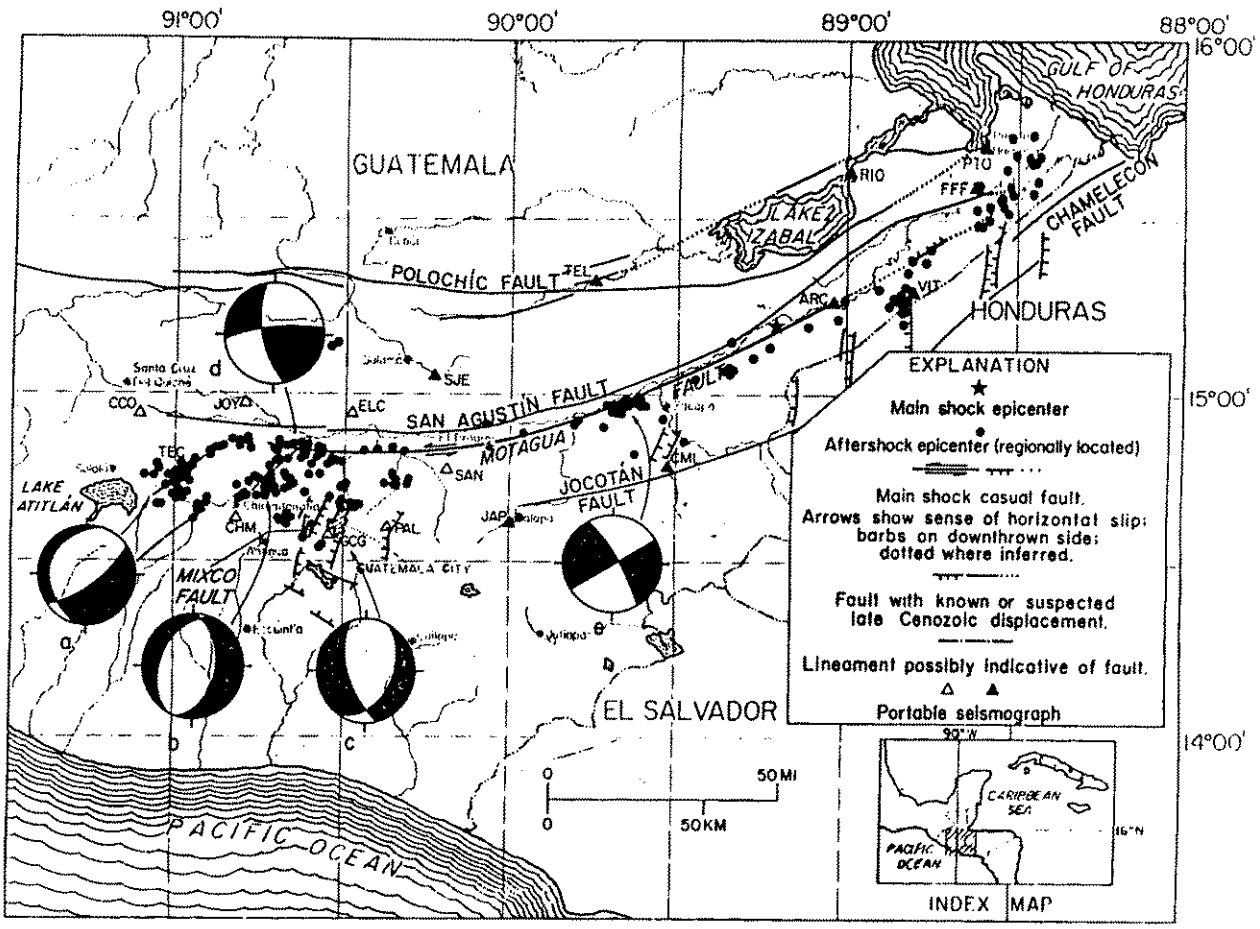

Fig. 7: Aftershocks and focal mechanisms of the Guatemala earthquake of 4 February 1976 (from Langer and Bollinger, 1979).

5. SEISMIC HAZARD ASSESSMENT

Seismic hazard assessment including long-term, mid-term (to 1 year), short-term (to 1 month) and operative hazard assessment differs fundamentally from earthquake prediction. As it is generally considered, earthquake prediction involves confining the place, the time and the intensity of an earthquake. This makes the set task rigidly determined.

Seismic hazard assessment allows us to undertake adequate precautionary measures on seismic risk reduction in order to protect people against possible strong earthquakes. The methods for seismic hazard assessment depend on the concrete physical and geological as well as technical conditions of a seismically active region.

The basis for long-term assessment of seismic hazard (more than several years) are detailed studies on active faults, tectonics and seismic activity, types of crustal movements and their intensity, properties of the geological medium and other structural and geological factors. Studies

of active faults are carried out along with geological and geophysical investigations of focal zones of historically large earthquakes and current seismic activity of the most active faults.

The regions with high seismic hazard are those with the following features:

1. prolonged seismic quiescence, especially in areas with known sources of past and large earthquakes;
2. high seismic potential based on the recurrence-period of past large earthquakes;
3. sudden activation of seismicity;
4. a combination of a part or all of the above mentioned features (maximal seismic hazard).

A major problem in assessing seismic risk in the Middle America region is that the short historical and instrumental record does not allow determination of the long-term seismic behavior. In such a situation, the method of identifying seismic gaps (areas which have not experienced a large shock over an arbitrary time span, usually a few decades) is unlikely to reveal as much information on the sites of future large shocks as it is the case in areas where the historical record is longer. However, the Middle America region favors a broader seismic research and instrumentation cooperation, particularly, because we share a common geological framework. Some steps to perform this task are:

1. cataloging of pre-instrumental seismicity;
2. magnitude estimation of pre-instrumental earthquakes using regionally derived intensity-attenuation laws;
3. increase of the number of permanent seismographic networks and improvement of their configuration and resolution so as to be able to locate earthquakes to within 5-to-10 km;
4. improvement of the regional and global seismographic network so as to allow the determination of focal mechanisms even of small earthquakes;
5. identification of areas of high seismic potential;
6. identification of areas of seismic wave amplification within the region (seismic microzonation);
7. analytical evaluation of the degree of vulnerability of buildings with respect to seismic given levels of seismic hazard;
8. expansion of techno-scientific cooperation for monitoring seismic phenomena;
9. construction of earthquake-resistant structures;
10. establishment of other urbanistic instruments aiming at the reduction and hopefully prevention of seismic risk.

Another avenue of earthquake research are geologic studies aimed at characterizing long-term fault behavior by studying: (1) uplifted marine terraces, (2) fault-scarp morphology, (3) physiographic features offset along faults, and (4) faulted or otherwise deformed young sediments (Sieh, 1981; Mann and Burke, 1984).

REFERENCES

Adamek, S., Frohlich, C., and Pennington, W. D. (1988). Seismicity of the Caribbean-Nazca boundary: Constraints on microplate tectonics of the Panama region. J. Geophys. Res., 93, 2053-2075.

Bevis, M., and Isacks, B.L. (1984). Hypocentral trend surface analysis; Probing the geometry of Benioff zones. J. Geophys. Res., 89, 6153-6170.

Bowin, C. (1976). The Caribbean; Gravity field and plate tectonics. Geol. Soc. Amer. Special Paper, 169, 79 p.

Burbach, G. V., Frohlich, C., Pennington, W.D., and Matumoto, T. (1984). Seismicity and tectonics of the subducted Cocos plate. J. Geophys. Res., 89, 7719-7735.

Burkart, B. (1983). Neogene North American-Carribbean plate boundary across northern Central America; Offset along the Polochic fault. Tectonophysics, 99, 251-270.

Burke, K., Grippi, J., and Sengor, A.M. (1980). Neogene structures in Jamaica and the tectonic style of the northern Caribbean plate boundary zone. J. Geol., 88, 375-386.

Carr, M. J., and Stoiber, R.E. (1977). Geologic setting of some destructive earthquakes in Central America. Bull. Geol. Soc. Amer., 88, 151-156.

Couch, R., and Woodcock, S. (1981). Gravity and structure of the continental margins of southwestern Mexico and northwestern Guatemala. J. Geophys. Res., 86, 1829-1840.

Demets, C., Gordon, R. G, Stein, S., and Argus, D. F. (1987). A revised estimate of Pacific-North American plate motion and implications for western North American plate boundary zone tectonics. Geophys. Res. Lett, 14, 911-914.

Dewey, J. W., and Suárez, G. (1991). Seismotectonics of Middle America. The Geology of North America, Decade Map, 1, 309-321.

Dorel, J. (1981). Seismicity and seismic gaps in the Lesser Antilles arc and earthquake hazard in Guadeloupe. Geophys. J. Royal Astron. Soc., 67, 679-695.

Fisher, K. M. and McCann, W.R. (1984). Velocity modeling and earthquake relocation in the northeast Caribbean. Bull. Seism. Soc. Amer., 74, 1249-1262.

Goff, J.A., Bergman, E. A., and Solomon, S.C. (1987). Earthquake source mechanisms and transform fault tectonics in the Gulf of California. J. Geophys. Res., 92, 10485-10510.

González-Ruiz, J.R., and McNally, K.C. (1988). Stress accumulation and release since 1882 in Ometepec, Guerrero, Mexico; Implications for failure mechanisms and risk assessment of a seismic gap. J. Geophys. Res., 93, 6297-6317.

Guendel, F., and McNally, K. C. (1986). High resolution evidence of smooth Benioff zone gradations approaching the southern terminus of the Middle American trench [abs.]. EOS Trans. Amer. Geophys. Union, 67, 1114.

Isacks, B., Oliver, J., and Sykes, L.R. (1968). Seismology and the new global tectonics. J. Geophys. Res., 73, 5855-5899.

Kanamori, H., and Stewart, G.S. (1978). Seismological aspects of the Guatemala earthquake of

February 4, 1976. J. Geophys. Res., 83, 3427-3434.

Kellogg, J. N., and Bonini, W.E. (1982). Subduction of the Caribbean plate and basement uplifts in the overriding South American plate. Tectonics, 1, 251-276.

Klitgord, K. D., and Mammerickx, J. (1982). Northern East Pacific Rise; Magnetic anomaly and bathymetric framework. J. Geophys. Res., 87, 6725-6750.

Langer, C. J., and Bollinger, G. A. (1979). Secondary faulting near the terminus of a seismogenic strike-slip fault; Aftershocks of the 1976 Guatemala earthquake. Bull. Seism. Soc. Amer., 69, 427-444.

Lefevre, L. V., and McNally, K. C. (1985). Stress distribution and subduction of aseismic ridges in the Middle America subduction zone. J. Geophys. Res., 90, 4495-4510.

McCann, W. R., and Sykes, L. R. (1984). Subduction of aseismic ridges beneath the Caribbean plate; Implications for the tectonics and seismic potential of the northeastern Caribbean. J. Geophys. Res., 89, 4493-4519.

McCann, W. R., Dewey, J. W., Murphy, A. J., and Harding, S. T. (1982). A large normal-fault earthquake in the overriding wedge of the Lesser Antilles subduction zone; The earthquake of 8 October, 1974. Bull. Seism. Soc. Amer., 72, 2267-2283.

Mann, P., and Burke, K. (1984). Neotectonics of the Caribbean, Rev. Geophys. Sp. Phys., 22, 309-362.

McNally, K. C., and Minster, J. B. (1981). Nonuniform seismic slip rates along the Middle America trench. J. Geophys. Res., 86, 4949-4959.

McNally, K. C., González-Ruiz, J. R., and Stolte, C. (1986). Seismogenesis of the 1985 great (Ms = 8.1) Michoacan, Mexico, earthquake. Geophys. Res. Lett., 13, 585-588.

Minster, J. B., and Jordan, T. H. (1978). Present-day plate motions. J. Geophys. Res., 83, 5331-5354.

Molnar, P., and Sykes, L. R. (1969). Tectonics of the Caribbean and Middle American regions from focal mechanisms and seismicity. Bull. Geol. Soc. Amer., 80, 1639-1684.

Morgan, F. D., Wadge, G., Latchman, J., Aspinall, W. P., Hudson, D., and Samstag F. (1988). The earthquake hazard alert of September 1982 in southern Tobago. Bull. Seism. Soc. Amer., 78, 1550-1562.

Nishenko, S. P., and Singh, S. K. (1987). Conditional probabilities for the recurrence of large and great interplate earthquake along the Mexican subduction zone; 1986-2006. Bull. Seism. Soc. Amer., 77, 1094-2114.

Plafker, G. (1986). Tectonic aspects of the Guatemala earthquake of 4 February, 1976. Science, 193, 1201-1208.

Reichle, M., and Reid, I. (1977). Detailed study of earthquake swarms from the Gulf of California. Bull. Seism. Soc. Amer., 67, 159-171.

Robson, G. R. (1964). An earthquake catalogue for the eastern Caribbean. Bull. Seism. Soc. Amer., 54, 785-832.

Schneider, J. F., Pennington, W. D., and Meyer, R. P. (1987). Microseismicity and focal mechanisms of the intermediate-depth Bucaramanga nest. J. Geophys. Res., 92, 13913-13926.

Schubert, C. (1982). Neotectonics of Boconó fault, western Venezuela. Tectonophysics, 85, 205-220.

Sieh, K. E. (1981).A review of geological evidence for recurrence of large earthquakes, in Earthquake Prediction-An International Review, Maurice Ewing Ser., vol. 4, edited by D. W. Simpson and P. G. Richards, 181-207, AGU, Washington, D. C.

Singh, S. K. Ponce, L.,and Nishenko, S. P. (1985). The great Jalisco, Mexico, earthquakes of 1932; Subduction of the Rivera plate. Bull. Seism. Soc. Amer., 75, 1301-1313.

Sykes, L. R., McCann, W. R., and Kafka, A. L. (1982). Motion of Caribbean plate during last 7 million years and implications for earlier Cenozoic movements. J. Geophys. Res., 87, 10656-10676.

White, R. A. (1991). Tectonic implications of upper-crustal seismicity in Central America. The Geology of North America, Decade Map, 1, 323-338.

Wolters, B. (1986). Seismicity and tectonics of southern Central America and adjacent regions with special attention to the surroundings of Panama. Tectonophysics, 128, 21-46.

SEISMIC MONITORING, DATA ANALYSIS AND COMMUNICATION IN MEXICO AND THE CONTRIBUTION OF MEXICO TO REGIONAL SEISMOLOGICAL CO-OPERATION IN LATIN AMERICA

David A. Novelo-Casanova

Instituto de Geofísica
Universidad Nacional Autónoma de México
México, D.F., México, 04510

1. INTRODUCTION

On April 1st, 1904, 18 countries, Mexico among them, met in Strasbourg, France, with the purpose of integrating an international Seismological Association. To meet its responsibilities, the Mexican government founded the National Seismological Service (SSN) on September 5, 1910. This event was part of the celebration of the first centenary of the National Independence. At that time, the SSN was under the direction of the National Geological Institute which was part of the Mining and Resources Secretariat.

Between 1910 and 1923, nine mechanical autonomous stations were deployed. The central station was installed in Tacubaya, Mexico City. The other stations were located in Oaxaca, Mazatlan, Merida, Chihuahua, Veracruz, Guadalajara, Monterrey and Zacatecas. The last three observatories were installed during the mexican revolution. The selected seismographs were "Wiechert" manufactured in Germany. Seven of these stations are still operating and they are probably one of the oldest scientific systems still working since its installation at the beginning of this century.

The SSN has been part of the National Autonomous University of Mexico (UNAM) since 1929 and in 1948 was assigned to the Institute of Geophysics (IGF) of this institution. At the beginning, the SSN had the most modern stations but new instruments were not added until 1960 when the installation of electromagnetic seismographs was initiated. In 1985, the National Seismographic Network had about 20 stations, however, the instruments were operating discontinuously and without telemetry and the signals were recorded on smoked and photographic paper.

The deployment of the Continental Seismic Network (RESMAC) was initiated at UNAM in the mid-seventies with the purpose of installing telemetric digital stations in all the country. The signals were transmitted via microwave links and the system had computerized automatic detection of events. In 1986, RESMAC was integrated into the SSN. This integration improved the seismic monitoring in Mexico although the national coverage was still insufficient.

In 1988, the SSN initiated the modernization of the telemetric network. A total of 20 stations started to send their signal to the central station at UNAM where the information is processed and

analyzed. The data are automatically digitized and stored by a seismic detection system implemented in a PC/AT.

In 1992, the Ministry of the Government approved the project of installing a National Broadband Seismic Network. The new broadband stations will replace strategic sites of the present network, although the mechanical stations will continue operating. The purpose of the new network is to provide good quality data for seismic research and civil seismic protection.

2. THE NATIONAL SEISMOGRAPHIC NETWORK

Until 1991, due to technical and financial limitations in the development of the Mexican National Seismographic Network (MNSN), it was difficult to meet the needs of the country in all aspects of hazard mitigation, seismic risk, design of seismic-resistant structures, and basic research in seismicity.

In 1992, with financial support from the Ministry of Government, the National Council of Science and Technology (CONACYT) and the National Autonomous University of Mexico, the modernization of the MNSN was initiated. Between 15 and 20 seismological observatories will be installed throughout the country. These stations will complement the efforts of governmental institutions. With the new system of observatories it will be possible to inform interested institutions within a few minutes after a great earthquake, about the sites where maximum intensities and accelerations were recorded. This information will be useful for civil protection measures and earthquake mitigation.

The MNSN will include approximately 15 broadband stations, about 15 short-period instruments and the 5 mechanical stations which have been operating since the beginning of this century. Fig. 1 shows the locations of the nine broadband observatories now operating.

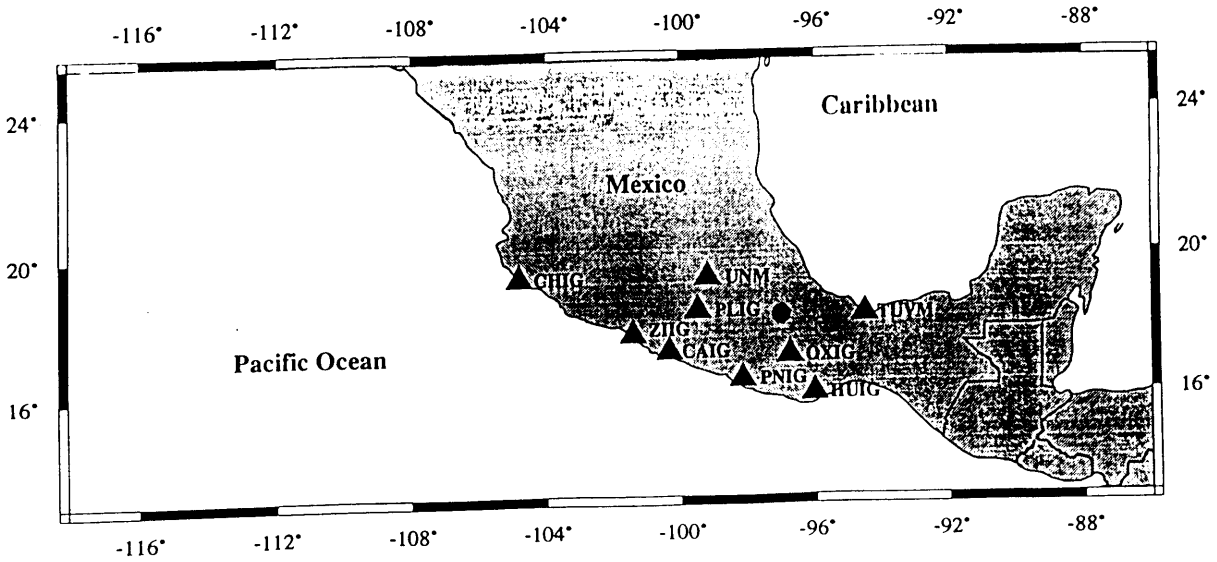

Fig. 1: Broadband observatories in operation. The solid circle indicates the epicenter of an event of magnitude 5.4 recorded by the network.

Each broadband observatory is equipped with STS-2-BB seismometer, FBA-23 accelerometer and Quanterra Processor Q680/LT-G of 24 bits. Data from selected sites will be telemetered via satellite. At all stations continuous and triggered data are stored in the field in "mini-SEED" format. All information will be concentrated at the central data acquisition and processing center located at UNAM. The central station will be able to receive, process, store and distribute seismic data in real time. The characteristics of the central station are shown in Fig. 2.

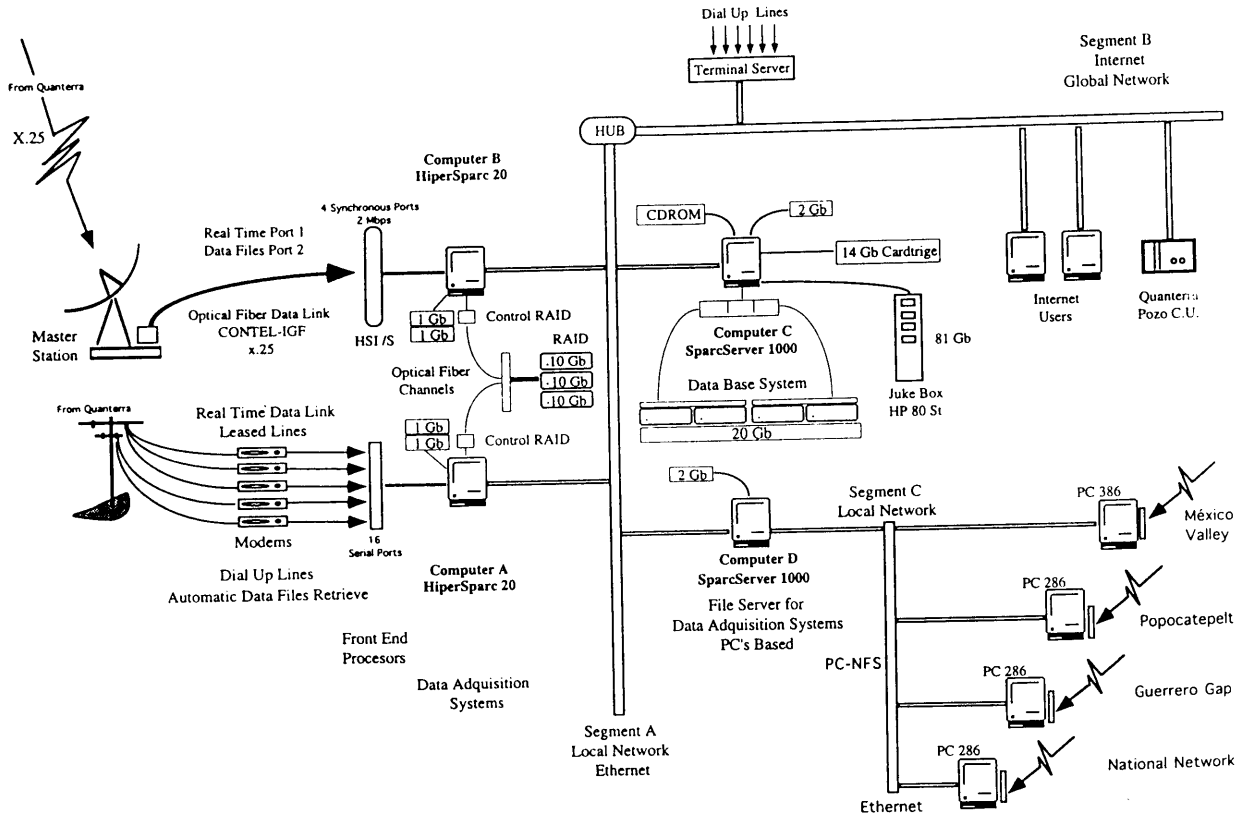

Fig. 2: Diagram of the central station of the Mexican National Seismic Network.

In cooperation with the GEOSCOPE program, a very broadband station with STS-1 sensor has been operating since 1990 at UNAM (UNM). In collaboration with IRIS a GSN site installation will be completed this year.

Fig. 3 shows seismograms of a local event of Ms = 6.2 recorded by some stations of the broadband network. Note the quality of the records. These data have already been used for research in seismic risk, seismic source and crustal structure studies. Also, some routines have been developed to determine the magnitude of moderate and large earthquakes in about 30 minutes.

The main objectives of the network are :

1. study of Mexican earthquakes in unprecedented detail;
2. collection of accelerograms and estimation of intensities anywhere in the country within a few minutes;
3. preliminary information within a few minutes on maximum acceleration from several sites to evaluate potential regions of damage;
4. preliminary estimation of seismic moment, magnitude, hypocentral parameters, and source properties within a few minutes;
5. collection of high-quality data base for the evaluation of seismic risk, potential, and studies of earthquake prediction in Mexico;
6. automatic transmission of seismic parameters to governmental institutions responsible for disaster prevention measures;
7. collection of data base for assessment of seismic hazard and earthquake-resistant design.

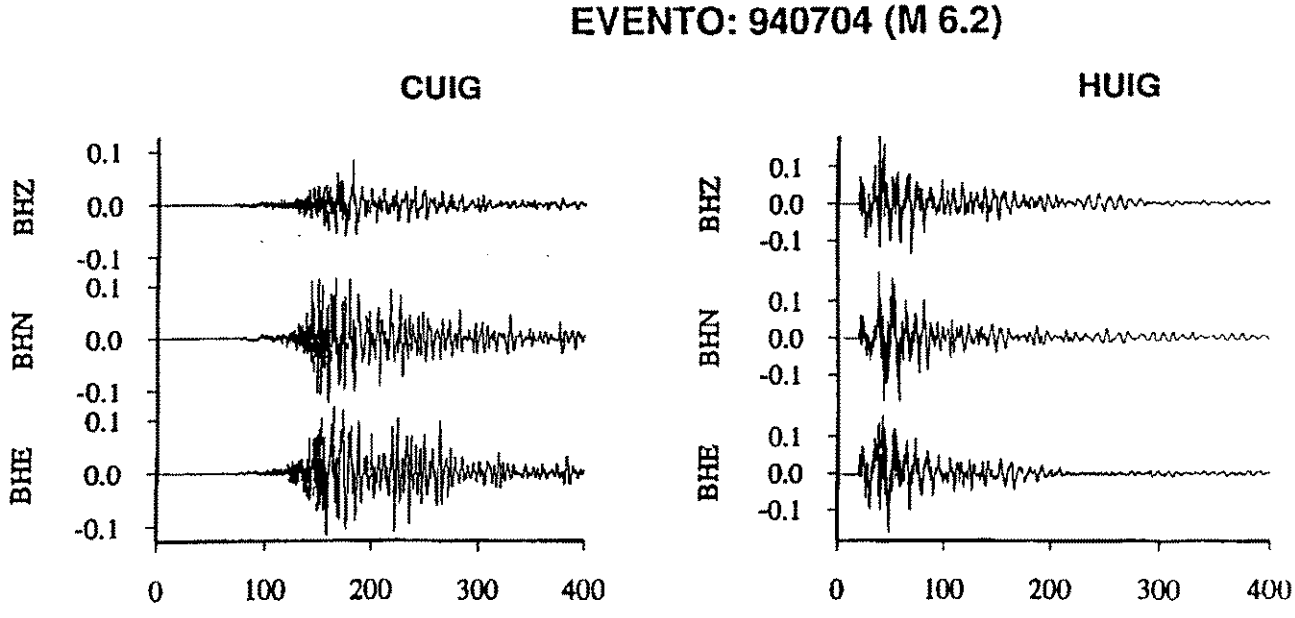

Fig. 3: 3-component STS-2 seismograms of an earthquake of Ms = 6.2 which occurred on July 4, 1994 (15.2° N, 97.3°W), recorded at the stations CUIG (epicentral distance D = 490 km) and HUIG (D = 150 km).

3. OTHER SEISMIC NETWORKS OPERATED BY IGF-UNAM

3.1 The Mexico City Network

With the purpose of monitoring the local seismicity in the Mexico City area, a total of nine stations were installed by the Institute of Geophysics (IGF) during 1994 and 1995. The locations of these stations are shown in Fig. 4. The sensors are of short period and data are transmitted by radio to the central station at UNAM.

This network is able to locate local events of magnitude 3.0 and above. The signals are automatically digitalized. Some of the goals of the network are: (1) to determine the origin of the micro-earthquakes that occur within the Mexican Valley and to identify active faults; (2) to complement the data base for the construction of seismic-resistant structures and the analysis of amplification/attenuation of seismic waves; and (3) to complement the information recorded by the accelerographs installed in the City.

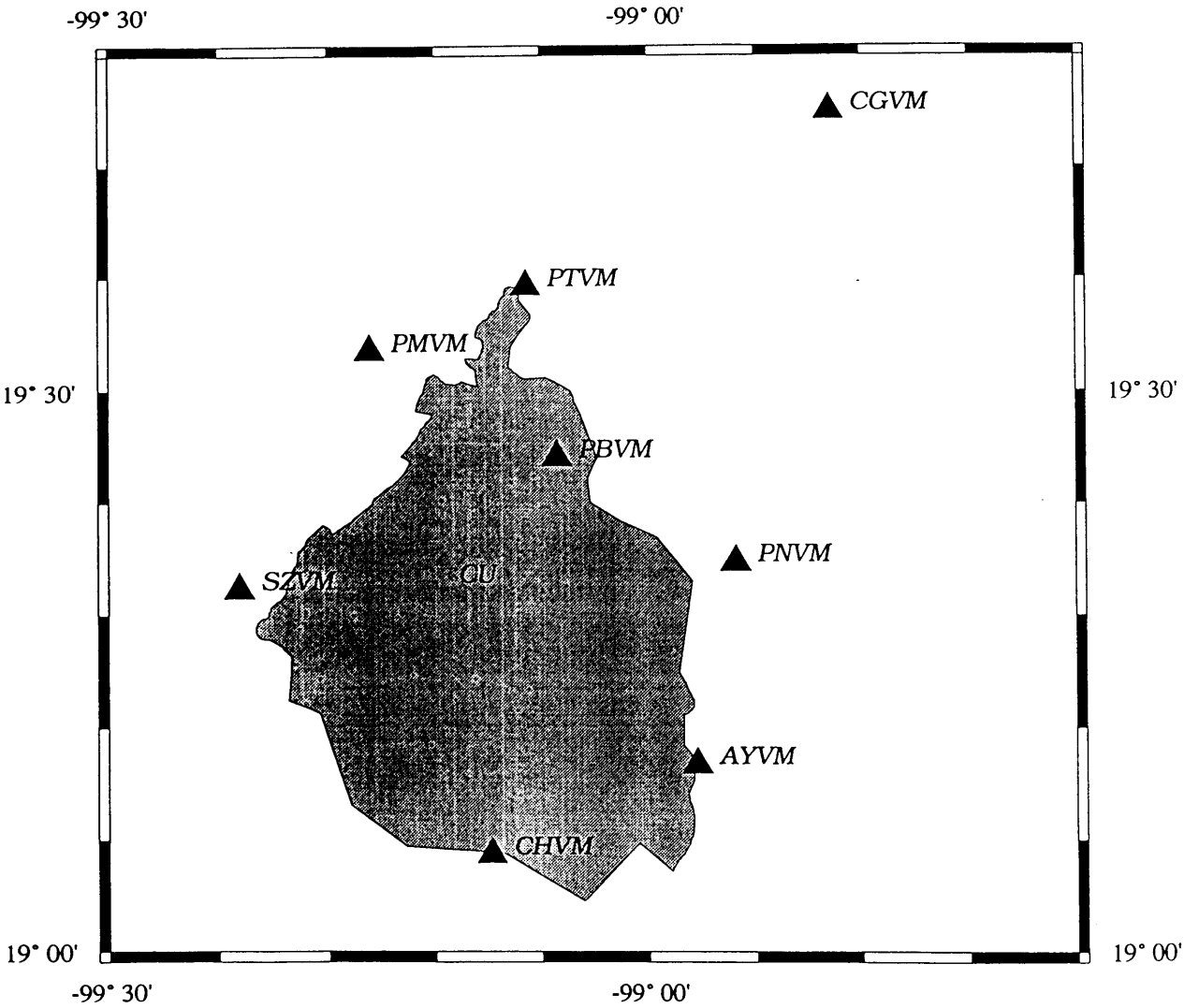

Fig. 4: Locations of the seismic stations of the Mexico City network. The border of the city is indicated.

3.2 The Popocatepetl Network

This network was implemented to monitor the microseismicity associated to the Popocatepetl volcano located about 40 km from Mexico City. This is the most recent telemetered network installed in the country.

The stations were deployed during the months of December, 1994, and January, 1995, after the increase of activity of this volcano. Fig. 5 shows the location of the seven stations of the network. Some broadband portable instruments will be deployed in the near future to complement the information.

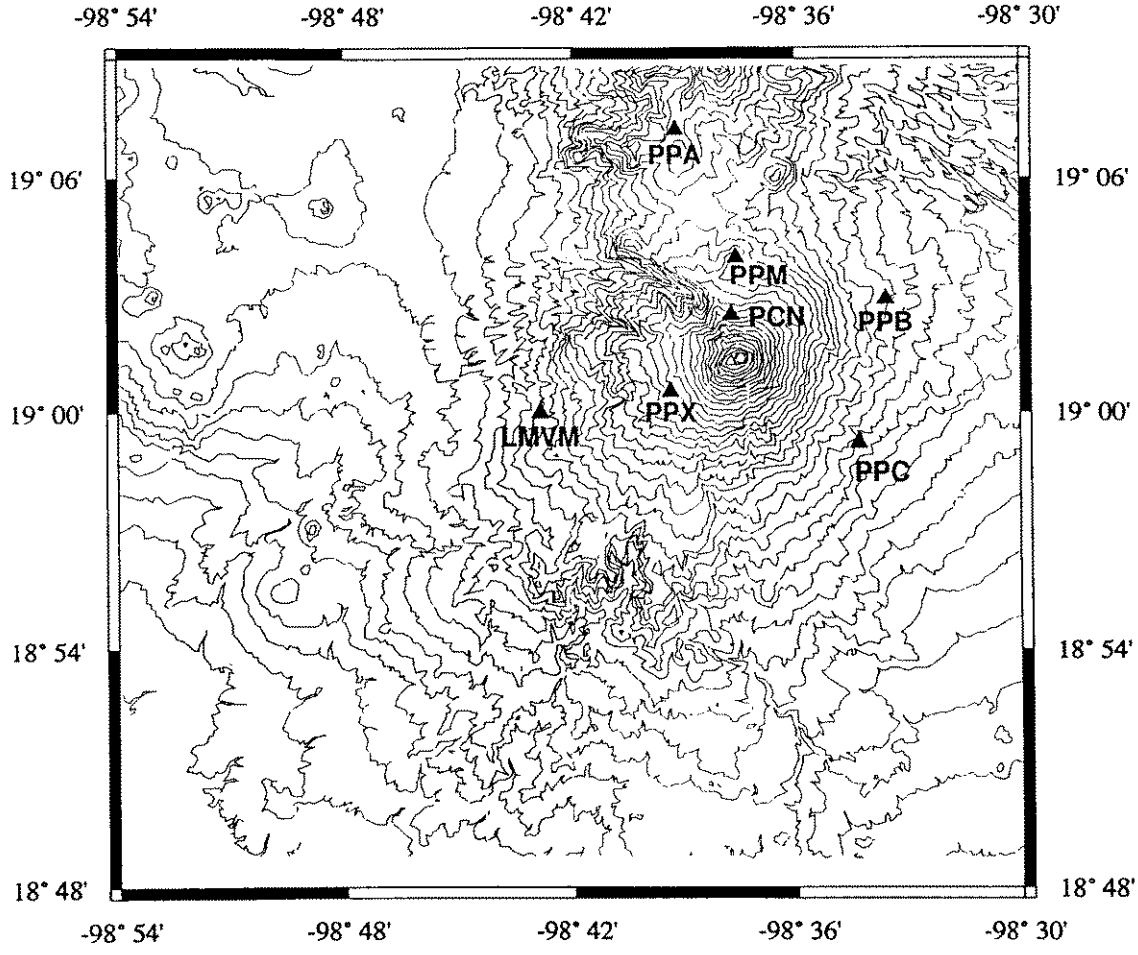

Fig. 5: Locations of the seismic stations of the Popocatépetl network.

3.3 The Guerrero Network

This network has been operating for about ten years with the purpose of monitoring the seismic activity of the Guerrero seismic gap (Fig. 6). The region has been identified as an area with a high probability for an earthquake of magnitude 7.0 or above to take place in the near future (in less than ten years).

The data have provided information about the characteristics of the Benioff zone and the subduction of the Cocos Plate in the area. Also, about the properties of the seismicity that will precede the eventual large earthquake.

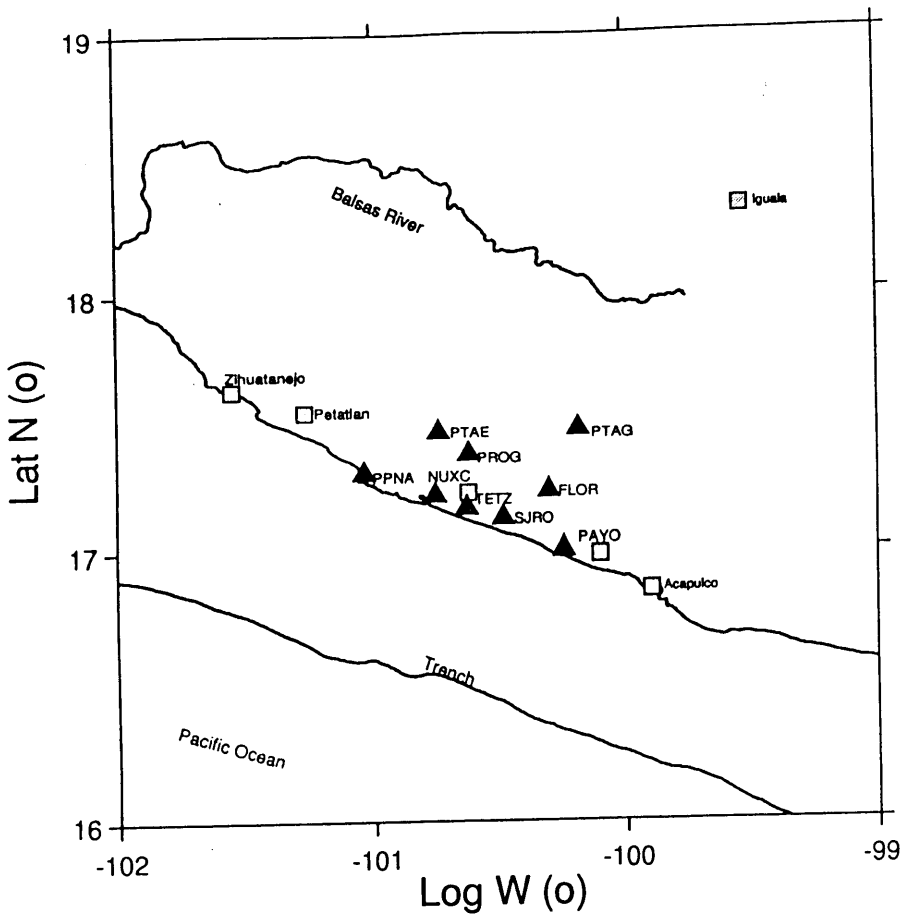

Fig. 6. Locations of the seismic stations of the Guerrero network.

4. SEISMIC NETWORKS OPERATED BY OTHER INSTITUTIONS

The SISMEX network is operated by the Engineering Institute of UNAM and covers the region outside Mexico City and the central part of the country. The RESNOR network covers the northwestern part of Mexico to monitor the fault system of the San Andreas Fault that continues through Mexico up to the Gulf of California. This network is operated by the Center for Scientific Research and Superior Education of Ensenada, Baja California, (CICESE).

Other local networks are operated mainly by the Mexican Power Company to monitor the microseismic activity of the areas where dams are located.

5. CONTRIBUTION OF MEXICO TO REGIONAL SEISMOLOGICAL CO-OPERATION IN LATIN AMERICA

Very often UNAM has cooperative activities with different institutions in Latin America. These activities include exchange of technical information, exchange visits, and cooperative research between scientists engaged in research disciplines of mutual interest.

Also, Mexico, through the Institute of Geophysics, has had an important participation in

promoting and organizing the Middle American Digital Seismic (MIDAS) project. The main purpose of this project is the development and use of broadband instrumentation in the Middle America region.

5.1 The "MIDAS" Project

On January 11-12, 1990, representatives from several countries met in Barbados to discuss the need for a co-ordinated effort to address seismological issues relevant to the Caribbean and Middle America region. Participants at the meeting agreed to form an international consortium of seismological institutions from the Middle America region, including: Belize, Cayman Island, Costa Rica, Cuba, Colombia, El Salvador, Guatemala, Haiti, Honduras, Jamaica, Mexico, Nicaragua, Panama, Puerto Rico, Trinidad & Tobago, the Bahamas, the Dominican Republic, the Dutch, French & British Antilles, the United States of America, and Venezuela. Recently, Ecuador was incorporated as a member.

The Consortium shall provide an international framework for scientific and technical cooperation between seismological institutions in Middle America and the Caribbean. Seismological institutions are considered those geophysical institutes and observatories engaged in the recording, transmission, and/or analysis of ground motion information produced by earthquake sources.

The principal objective of the Consortium is to promote scientific interaction between participating institutions and to facilitate the rapid, efficient, and widespread utilization of earthquake data by Middle American and Caribbean countries in routine observatory operations and in more advanced seismological research. To this end, the Consortium shall pursue the following specific objectives:

1. Improve the quality of the recorded earthquake data by promoting the increase in seismograph station coverage throughout the region, particularly through the advancement of broadband instrumentation and high dynamic range digital recording.

2. Coordinate the exchange of earthquake information including, but not limited to, arrival-time, amplitude, and full-waveform data throughout the region by using existing telecommunication channels and by incorporating new techniques for rapid data transmittal as they become available.

3. Increase the technical and scientific capabilities of personnel from the member institutions through the coordination of regional courses and/or workshops.

The second Assembly of the MIDAS Consortium was held on April, 1993, in Ixtapa-Guerrero, Mexico, during the 88 General Assembly of the American Seismological Society. The third Assembly was held on August, 1994, at Brasilia, Brazil, during the Regional Seismological Assembly in South America.

During the Assemblies, members have discussed the status of the seismographic networks in Middle America and the Caribbean. There is a clear need for broadband instruments in the region. However, in Latin America, some of these instruments are now operating in Costa Rica, Colombia, Mexico and Venezuela.

Fig. 7 shows the general location of the projected stations of the MIDAS network. At present, nine stations in Mexico are operating as indicated before. An observatory, similar to those in Mexico, will be installed in 1995 in Panama. This broadband instrument was financed jointly by the National Autonomous University of Mexico and the United States Geological Survey. The Center of Coordination for Natural Hazards Prevention of Central America (CEPREDENAC) will finance another broadband station as counter part to the Panama station. Possible sites for this new observatory are central Guatemala and the northern regions of Honduras and Nicaragua (Fig. 7).

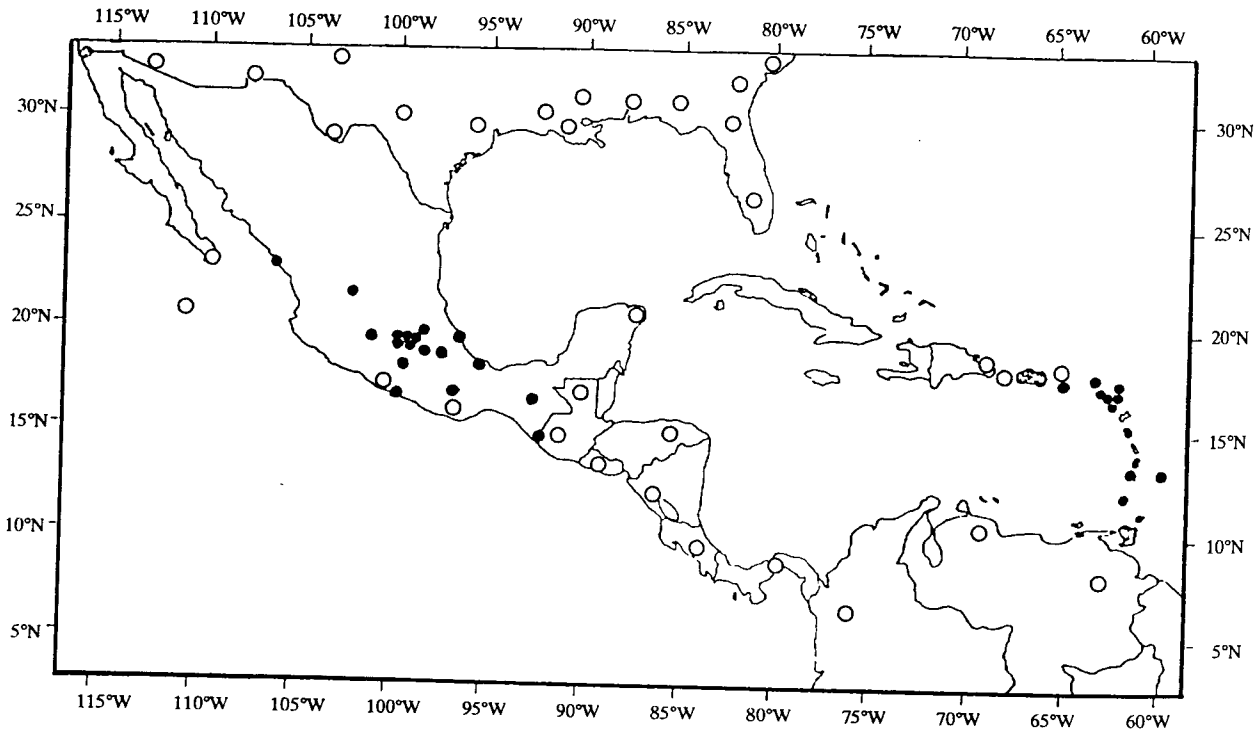

Fig. 7: The MIDAS network. The large open circles show the locations of the projected stations, the small, full circles show the short-period stations complementing the broad-band seismic network.

ACTIVIDAD VOLCANICA Y AMENAZAS EN AMERICA CENTRAL Y DEL SUR

LOS OBSERVATORIOS VULCANOLOGICOS SON ESENCIALES EN LA ESTRATEGIA DE REDUCCION DE LA VULNERABILIDAD EN LA REGION DEL MUNDO EN QUE VIVIMOS, TIENEN CARACTERISTICAS MUY ESPECIALES QUE SE DEBEN DE FOMENTAR EN SU ORGANIZACION Y PUEDEN TENER OPORTUNIDAD DE OBTENER FONDOS POR MEDIO DEL APOYO A PROYECTOS DE PLANIFICACION INTEGRAL EN UN FUTURO MEDIATO

Eduardo Malavassi Rojas Ph.D.

Observatorio Vulcanológico y Sismológico de Costa Rica
Universidad Nacional
OVSICORI-UNA
Aptdo. 86-3000, Heredia, Costa Rica

1. INTRODUCCION

Existen unos 120 volcanes potencialmente activos en la América Central y México que forman parte del Cinturón de Fuego del Pacífico. De ellos unos 90 se encuentran ubicados en los países de la América Central y unos 30 se encuentran ubicados en México. Si tomamos en cuenta solo los volcanes que han hecho erupción desde 1800 o que tienen un corta periodicidad eruptiva, los números se reducen un poco más, teniendo 39 volcánes históricamente activos de los cuales 28 se encuentran en la América Central y 11 se encuentran en México (OEA,1991).

La distribución dentro de la región de los volcanes que tienen actividad histórica desde 1800 o que tienen una corta periodicidad eruptiva, no es homogénea, según podemos deducir de la tabla siguiente:

País	Número de Volcanes Activos desde 1800 o de corta periodicidad eruptiva
México	11
Guatemala	8
El Salvador	7
Honduras	0
Nicaragua	8
Costa Rica	5
Panamá	1
Total	39

Scientific Technical Report STR 95/TK
DOI: 10.2312/GFZ.b103-95tk7

El índice de explosividad indica la relación entre el volumen de material piroclástico (eruptado por el aire) respecto al volumen total de material eruptado por un volcán. Los volcanes del arco mesoamericano tienen uno de los más altos indices de explosividad a nivel mundial. Ello significa que un porcentaje muy alto del volumen eruptado por los volcanes de la América Central se convierten en ceniza volcánica.

La combinación de vivir en un área muy activa desde el punto de vista volcánico y en la cual el índice de explosividad es muy alto, sugiere la necesidad de tratar de reducir la vulnerabilidad con el fin de mitigar los efectos de las erupciones volcánicas.

2. LA RAZON DE SER DE LOS OBSERVATORIOS VULCANOLOGICOS

Debemos de tener muy presente que el costo de monitorear los volcanes y de la planificación pre-desastre es muy bajo comparado con las pérdidas potenciales. Sin embargo, en todos los países de la región el financiamiento de las instituciones responsables del monitoreo volcánico y de aquellas encargadas de la planificación pre-desastre es insuficiente. El resultado es que los institutos responsables del monitoreo volcánico dependen de los dineros que brinda la cooperación internacional para comprar equipo, repuestos y hasta para cubrir algunos gastos de operación.

La combinación de una alerta oportuna y planes pre-desastre que posibiliten la evacuación de los vecinos de los volcanes es la única alternativa para poder disminuir la vulnerabilidad asociada a la presencia de los peligros volcánicos.

3. METAS DE UN OBSERVATORIO VULCANOLOGICO

La organización de un observatorio vulcanológico para el monitoreo de la actividad de los volcanes es condición previa para el establecimiento de sistemas de pronósticos y de alerta de erupciones volcánicas.

Los volcanes no hacen erupciones mayores en forma expontánea, sino que los cambios asociados al ascenso del magma se van presentando gradualmente. Estos cambios se presentan en forma de cambios en el número de eventos sísmicos, cambios en la actividad hidrotermal del volcán, cambios en la deformación del suelo volcánico, y cambios en la geoquímica de los gases y aguas volcánicas. No existe mejor alternativa que la vigilancia o monitoreo volcánico. Ella consiste en realizar mediciones sistemáticas y periódicas en los volcanes activos para establecer líneas base de comportamiento volcánico. El científico no puede ser llamado a evaluar el estado de actividad de un volcán sin tener a mano una línea base que indique su comportamiento anterior. La función del observatorio es la de compilar datos sobre los volcanes, ordenarlos sistemáticamente y utilizarlos para ofrecer valoraciones sobre el estado de actividad de un volcán.

Al iniciar un programa de estudio de los volcanes, lo prioritario es iniciar la vigilancia con los métodos que se tenga disponibles y luego cambiarlos gradualmente conforme se tenga a disposición mayores recursos. La construcción de líneas base del comportamiento de un volcán debe iniciarse siempre a la mayor brevedad posible. Otras actividades como el cartografiado

Scientific Technical Report STR 95/TK
DOI: 10.2312/GFZ.b103-95tk7

geológico tienen una segunda prioridad, ya que pueden ser realizadas en cualquier otro momento. En contraposición, no es posible evaluar el estado de actividad de un volcán si no se tienen líneas base de comportamiento. Debemos saber qué es normal para aprender luego qué es anormal.

4. CARACTERISTICAS DEL GRUPO DE TRABAJO

El grupo que labora para un observatorio debe ser multidisciplinario e interdisciplinnario con el fin de incorporar diversas visiones del mundo profesional en el trabajo. En un laboratorio vulcanológico caben químicos, físicos, geólogos, geógrafos, geofísicos, geodestas, técnicos en computación, técnicos electrónicos, y muchos más. Se trata de estudiar el fenómeno volcánico desde muchos puntos de vista. Se debe garantizar una integración y colectivización contínua de la información recogida por todos y que permita desarrollar una visión de conjunto del fenómeno volcánico.

Los observatorios deben mantener su personal en el campo gran parte del tiempo vigilando los volcanes, describiendo los procesos que observan, y tomando datos que permitan hacer diagnósticos periódicos del estado de actividad del volcán y para ello necesitan contar con un sistema estable de transporte, de gastos de viaje y de apoyo para salir al campo. Si los observatorios tienen problemas de financiamiento se ven forzados a abandonar la continuidad de las mediciones y luego es más difícil volver a empezar de nuevo.

Los observatorios deben de tratar de aprovechar la ayuda internacional recibiendo instrumental y equipo, sin embargo, uno de los papeles principales de la ayuda internacional, que no se ha explotado como corresponde en la región consiste en becar a los funcionarios para que vayan a estudiar al extranjero y luego regresen a laborar en vulcanología. El tener personas con una amplia formación académica permite a los científicos locales establecer intercambios con instituciones extranjeras para conseguir ayuda económica y además que el trabajo científico que el grupo produzca sea de gran excelencia académica.

Los países que más éxito han tenido en el desarrollo de observatorios vulcanológicos en la última década, han mantenido un crecimiento acelerado, pero sostenido cuando invirtieron en educación para sus funcionarios en el extranjero.

Los observatorios necesitan contar con una ágil política de becas que le permita abrir oportunidades a los funcionarios y que a su vez los deje comprometidos para que sirvan con un contrato por un cierto período de tiempo para la institución.

5. LA POLITICA DE INFORMACION

Los observatorios vulcanológicos están obligados a retroalimentar a los planificadores de emergencias y al público en general sobre el estado de actividad del volcán. Tienen que estar difundiendo los cambios observados en la evolución de la actividad volcánica y comunicarlo de tal forma que el gran público entienda lo que está sucediendo.

Scientific Technical Report STR 95/TK
DOI: 10.2312/GFZ.b103-95tk7

Dado que los observatorios tratan día a día con periodistas, deben promover talleres sobre el tratamiento periodístico de los volcanes en los diferentes géneros comunicacionales. Eso tiende a mejorar las relaciones con los periodistas y reduce el tono amarillista de aquellos que les gusta este tipo de cobertura en las noticias.

Todo observatorio tiene dos formas de comunicación que les son propias. Ellas incluyen los diagnósticos sobre el estado de actividad de un volcán preparados como síntesis del grupo que realiza la observación y la comunicación educativa que pretende realizar transferencia del conocimiento general sobre los volcanes para que sea incorporado en la cultura popular y cambien las actitudes de las personas hacia los volcanes, y su percepción de los peligros involucrados.

6. LA PRODUCCION CIENTIFICA

Los observatorios pueden ser lugares en donde se realice buena ciencia. Por ello deben mantener y alimentar bases de datos para uso de su personal científico. Además, es conveniente que realicen investigación con los datos volcánicos colectados por la comunidad y que establezcan proyectos específicos de investigación. Como parte de estos proyectos se puede realizar la cartografía geológica y la evaluación de peligros volcánicos. También, los observatorios vulcanológicos están llamados a realizar aportes importantes en la caracterización de los materiales de construcción de origen volcánico y en la búsqueda de posibles fuentes de material. Pueden cumplir con la función de asesores y prestadores de servicios a la comunidad que les necesita para proyectos en donde estén involucrados rocas volcánicas o aspectos asociados al vulcanismo.

7. EL ENTRENAMIENTO EN EL TRABAJO

Para una institución científica dedicada a la investigación es fundamental que su personal tenga la capacidad de procesar grandes cantidades de datos en forma eficiente y confiable. Por ello es necesario la realizacion de cursos de capacitación y entrenamiento en el trabajo, así como contar con buena tecnología en el campo del almacenamiento de datos.

8. LA COMUNICACION CON OTROS CIENTIFICOS

Todo observatorio tiene que tener canales de comunicación expeditos con otros científicos y debe de estimular a su propio personal para que escriba y para que publique. La realización de seminarios talleres sobre los modos comunicacionales utilizados en ciencias son de gran importancia para promover un ambiente estimulante para los científicos.

9. El PAPEL DE LA AYUDA INTERNACIONAL

La ayuda internacional ha hecho aportes muy generosos y relativamente poco condicionados en la región. El resultado ha sido un nivel de desarrollo institucional de los observatorios, por

Scientific Technical Report STR 95/TK
DOI: 10.2312/GFZ.b103-95tk7 GeoForschungsZentrum Potsdam

debajo de las expectarivas y por lo tanto se han perdido oportunidades muy valiosas para robustecerlos. Algunos supuestos de la ayuda internacional que recibíamos en 1991 indicaban que para el año de 1995 nuestros países deberían asumir la obligación de ser autorsuficientes, de no depender de la ayuda internacional para la compra de repuestos, sin embargo eso no se ha logrado a la fecha.

Existen en al actualidad algunos proyectos de cooperación que desean realizar transferencia tecnológica, sesiones de entrenamiento en el manejo y utilización del software involucrado y que parecieran interesados en darle seguimiento a la inversión de la ayuda internacional en el tiempo. Estos proyectos pueden dar un aporte importante en la consolidación de los observatorios.

10. EL PAPEL DE LA PLANIFICACION DEL DESARROLLO NACIONAL Y REGIONAL

Si el tema de la reducción de la vulnerabilidad se incorporara en el proceso de planificación nacional y regional, es posible que muchos proyectos de inversión vayan a requerir que se les preste servicios de información y asesoría en la preparación de sus informes de factibilidad. El resultado de este proceso es que de pronto una gran cantidad de proyectos de desarrollo económico tendrían recursos para comprar servicios a los obsevatorios vulcanológicos, y por ende, por medio de la incorporación de la reducción de vulnerabilidad a los peligros volcánicos se pueda lograr recursos por servicios a muchos proyectos de inversión.

De la misma manera, es necesario plantearse formas de cooperación horizontal entre países o instituciones. Compartir más experiencias y utilizar mejor las ventajas comparativas que pueda tener la región. El OVSICORI pondrá en operación un observatorio movil que podrá desplazarse a Centro América en caso de crisis volcánicas. Dado que las crisis volcánicas pueden durar muchas semanas es probable que el obseratorio movil deba verse más como un recurso que se pone al servicio de la región y que tendríamos que atender entre los científicos de la misma. Ello nos permitirá interaccionar con frecuencia y nos permitirá establecer procedimientos estandar en muchas de nuestras acciones.

De la misma manera en que los proyectos de desarrollo integral de cada país tienen la posibilidad de entrar a comprar servicios de los observatorio, es posible que proyectos regionales de desarrollo tengan la misma necesidad.

11. CONCLUSION

A pesar de la significativa ayuda internacional recibida por los observatorios vulcanológicos de la región, aún no reciben la contrapartida nacional correspondiente a la ayuda internacional recibida. Los observatorios vulcanológicos no reciben todos los recursos que deberían de recibir de parte de los gobiernos para desarrollarse y producir la reducción de la vulnerabiliad. Por sus metas, formas de organización y de interacción con el público los observatorios vulcanológicos son instituciones muy particulares que deberían estar siendo estimuladas por los estados. A pesar de que esa no parece ser la tendencia principal actualmente, existen la posibilidad de

Scientific Technical Report STR 95/TK
DOI: 10.2312/GFZ.b103-95tk7

incorporación del tema de la reducción de la vulnerabilidad en los proyectos nacionales y regionales de desarrollo y que a través de ellos puedan financiarse los observatorios. Existen además otras oportunidades en el fortalecimiento de la ayuda horizontal que nos permitiría compartir experiencias enriquecedoras y profundizar la comunicación entre científicos de la región.

Bibliografía

OEA, 1991, Desastres, Planificación y Desarrollo: Manejo de Amenazas Naturales para Reducir Daños, Washington D.C., 80 p.

Scientific Technical Report STR 95/TK
DOI: 10.2312/GFZ.b103-95tk7

VULNERABILIDAD Y EVALUACION DE RIESGOS RELACIONADOS CON AMENAZAS SISMICAS Y VOLCANICAS, ASI COMO LAS RESPECTIVAS ACCIONES EN REGULACIONES DEL USO DEL SUELO, PLANIFICACION DEL DESARROLLO, CODIGOS DE CONSTRUCCION, DEFENSA CIVIL, ETC., EN UNA ESCALA NACIONAL Y REGIONAL

Eduardo Malavassi Rojas Ph.D.

Observatorio Vulcanológico y Sismológico de Costa Rica
Universidad Nacional
Aptdo. 86-3000, Heredia, Costa Rica

1. INTRODUCCION

El tema de esta charla es muy amplio y muchas cosas se podrían decir acerca de las amenazas sísmicas o volcánicas y de las acciones que como sociedad podemos tomar para vivir una mejor calidad de vida, avanzar a estadios superiores de desarrollo económico y sobre todo garantizar la seguridad de vidas y bienes ante la presencia de esas amenazas.

Iniciaremos nuestra charla hablando de los conceptos de amenaza, riesgo y vulnerabilidad en terminos generales y referidos a todo tipo de desastres. Hablaremos luego sobre la evaluación de peligros y la respuesta, sobre la evaluación y percepción del riesgo y sobre los ajustes posibles a la existencia del peligro con que cuenta la sociedad. Una vez establecido este marco de referencia pasaremos a revisar los ajustes posibles a la existencia de los peligros volcánicos y sísmicos.

2. CONCEPTOS GENERALES DE AMENAZA, RIESGO Y VULNERABILIDAD

Para efectos de esta charla vamos a hablar de **Peligro o Amenaza** como una amenaza potencial para la vida o las pertenencias de las personas, y nos referiremos al **riesgo** como la probabilidad de la ocurrencia de un peligro o amenaza.

Un ejemplo puede servirnos para clarificar la diferencia entre ambas definiciones tal como fue ilustrado por Okrent (1984): Dos personas cruzando un mar tormentoso, uno en un barco, otro en una improvisada balsa. El peligro de ahogamiento es el mismo en los dos casos, sin embargo, el riesgo o sea la probabilidad de ahogarse en ambos casos es muy diferente. La persona que cruza el mar en un barco tiene menor probabilidad de ahogarse que la persona que cruza en una balsa improvisada.

Scientific Technical Report STR 95/TK
DOI: 10.2312/GFZ.b103-95tk7

La **vulnerabilidad** implica una medida de riesgo combinada con la habilidad del sistema social o económico de enfrentarse al evento resultante para resistir la alteración de las funciones o de pérdidas según Timmerman (1981). La vulnerabilidad puede ser definida también como el grado a que un sistema, o parte de un sistema, puede reaccionar para compensar la ocurrencia de un evento peligroso.

3. EVALUACION DE PELIGROS Y RESPUESTA

Para reducir los peligros debemos seguir una serie de pasos:

1. Debemos identificar el peligro y estimar el riesgo basándose en qué tan amenudo el evento ocurre y las consecuencias que puede tener. Desgraciadamente, ello implica que tienen que ocurrir eventos antes de que pueda estimarse su riesgo.

2. Identificado un peligro es posible adoptar una estrategia de respuesta en cualquier sociedad que tiene un rango de opciones, desde aceptar en forma pasiva la presencia del peligro, hasta tratar de controlar el proceso generador de peligro. Ello, en la mayoría de los casos, implica la adopción de una estrategia de reducción del peligro que adopta un grupo social.

El **manejo comprensivo del peligro o del riesgo** incluye la evaluación y la respuesta, y contiene cuatro pasos cronológicos, que usualmente se traslapan. Estos pasos son un ciclo cerrado que pretende aprender de la experiencia y la retroalimentación. Los cuatro pasos son los siguientes:

1. Planificación Pre-Desastre: Envuelve una amplica variedad de acciones que van desde el reforzamiento de obras de ingeniería, planificación del uso del suelo, la formulación, diseminación y mantenimiento de planes de evacuación.

2. Preparación para Desastre: Refleja un grado de alerta inmediatamente antes del desencadenamiento de un peligro. Este es el caso de los simulacros o la difusión de información sobre sistemas de alarma.

3. Respuesta ante Desastre: Implica la respuesta inmediatamente antes y después de que ocurren, incluyendo la respuesta a alarmas y a actividades de atención de emergencias.

4. Recuperación y reconstrucción: Estas actividades son de largo plazo. Pretenden llevar al área a la normalidad después de un proceso de devastación.

4. EVALUACION DE RIESGOS Y PERCEPCION

Como el riesgo no puede ser completamente eliminado, la única opción posible es la de aprender a manejarlo o a administrarlo.

La **Evaluación del Riesgo** implica realizar una medida cuantitativa y confiable del riesgo. El análisis de riesgo es basado en las teorías matemáticas de probabilidad y métodos científicos para

Scientific Technical Report STR 95/TK
DOI: 10.2312/GFZ.b103-95tk7 GeoForschungsZentrum Potsdam

la identificación de relaciones causales entre diferentes tipos de actividades peligrosas y las consecuencias adversas resultantes.

La evaluación de riesgo comprende tres diferentes pasos:

1. La identificación de un peligro con potencial de producir un desastre. ¿Cuáles eventos peligrosos pueden ocurrir?
2. La estimación de los riesgos de esos eventos. ¿Cuál es la probabilidad de cada evento?
3. Una evaluación de las consecuencias sociales derivadas del riesgo. ¿Cuáles son las pérdidas creadas por cada evento?

En síntesis, un conocimiento de la magnitud y frecuencia probable de ocurrencia de eventos que produzcan daños es un elemento vital en el manejo del riesgo.

La **Administración o Manejo de Riesgos** significa reducción de las amenazas para la vida, propiedad y el ambiente causados por los peligros en tanto maximizamos simultáneamente cualquier beneficio asociado. Es el proceso de decidir qué hacer para mitigar los problemas, una vez que han sido evaluados. Sin embargo, el manejo o administración de los riesgos no solo depende de la valoración estadística del riesgo que es una medida objetiva, pero depende de la percepción del riesgo por parte de individuos de la misma comunidad y de la gama de alteranativas de respuesta que ellos visualicen como viables. Esta es la parte subjetiva del manejo de riesgo asociada a la percepción individual del riesgo.

5. AJUSTES A LA EXISTENCIA DEL PELIGRO

Los ajustes a la existencia del peligro pueden dividirse en tres categorías:

1. **Modificación del peso de las pérdidas**: Consiste en tratar de modificar el peso de las pérdidas, distribuyendo el peso financiero de las mismas, lo más lejos posible de las víctimas inmediatas por medio de programas de alivio para las víctimas y programas de seguros.

2. **Modificación de los eventos peligrosos**: Se trata de medidas tomadas para reducir las pérdidas ajustando los eventos destructivos a la gente. Esta alternativa puede ser más viable para desastres antropogénicos o tecnológicos. Sin embargo, la mayoría de los desastres naturales son muy poco conocidos en su física como para poder modificarlos o suprimirlos en su fuente por medio de alguna alternativa en manos del hombre.
   Para reducir las pérdidas se recurre a dos métodos principales: modificar el evento peligroso o reducir su impacto humano. Como es imposible modificar los eventos peligrosos que resultan en desastres naturales, o al menos desconocemos sus resultados por cuanto pueden tener efectos laterales inciertos, la reducción de pérdidas se reduce al patrocinio de diseños resistentes a los peligros. El diseño resistente a los peligros es algo más que la pura ciencia de la ingeniería, es operado a través de los códigos de construcción y de otras regulaciones que implican un alto grado de aceptación y respaldo comunitario.

3. **Modificación de la vulnerabilidad humana a los peligros**: Incluye todas las medidas que

Scientific Technical Report STR 95/TK
DOI: 10.2312/GFZ.b103-95tk7 GeoForschungsZentrum Potsdam

pretenden reducir las pérdidas por peligros por medio del ajuste de la gente a los eventos destructivos. Esto se obtiene por medio de programas de preparación orientados a cambiar el comportamiento humano, por medio de la instalación de esquemas de pronóstico y alarma y mediante el patrocinio, por medio de la planificación de medidas más apropiadas en lo que a uso de la tierra se refiere.

La modificación de la vulnerabilidad humana implica la creación de un cambio en actitudes humanas y de comportamiento hacia los desastres naturales. Este es el grupo de respuestas más práctico. Cubre todo de la preparación de programas de respuestta comunal, hasta pronóstico y alertas, hasta medidas financieras o legales designadas para promover mejor manejo del uso del suelo.
Con la posible excepción del pronóstico y sistemas de alarmas, mucho menos investigación y desarrollo ha sido invertida en la mitigación de peligros que lo que se ha invertido en modificaciones de eventos.

Para los peligros sísmicos o volcánicos no existen métodos de supresión positiva o de control.

6. SISMICIDAD

Correspondería realizar un análisis de la distribución, frecuencia, magnitud y otras características generales de los sismos a nivel mundial. Sin embargo, por tratarse de un curso cuyo tema principal es la sismología, omito esa discusión que ha de haber sido el tema de las charlas introductorias.

6.1 Ajustes para compartir las perdidas

Ayuda para desastre:

Después de las guerras y los conflictos armados civiles los sismos son los que le siguen en importancia en la atracción de fondos de ayuda para desastre debido a la pérdida catastrófica de vidas. Sin embargo, falta mucho para lograr optimizar la ayuda en caso de desastre sísmico. En algunos casos la ayuda no llega a tiempo, en otros el tipo de ayuda no es el apropiado, en otros no llega del todo y el resultado es un perído muy largo en que personas evacuadas continúan teniendo arreglos de vivienda provisionales.

Seguros:

El seguro sísmico se puede comprar en muchos países del mundo, sin embargo, la capacidad de las compañías privadas para asumir las pérdidas potenciales es limitada. La gran mayoría del riesgo expuesto de los sismos no tiene seguros, aún en aquellos países que tienen esquemas de seguros con aporte del Estado. En adición, la mayoría de las pólizas están en propiedades industriales y comerciales, y no cubren usualmente la propiedad residencial. En la mayoría de los casos, el ciudadano promedio que paga sus impuestos es el que asume mucho del peso de la carga financiera de un sismo.

Scientific Technical Report STR 95/TK
DOI: 10.2312/GFZ.b103-95tk7

Otro aspecto que inhibe la compra de seguros en algunos lugares es que tienen un deducible de un 5 % del valor de la casa y por lo tanto empiezan a pagar los daños después de que la residencia se haya dañado un 5 %. Ello implica que los dueños de casas de madera que sufrirán poco en caso de sismo, se inclinarían por no tomar seguro, ya que es razonable esperar que las compañías paguen solo después de que se presente un daño considerable.

6.2 Ajustes que modifican el evento

Control ambiental:

En el presente parecen existir pocas posibilidades de que los humanos podamos llegar a suprimir o a modificar la magnitud y frecuencia de los sismos. Por ahora, una de las opciones más sonadas en este sentido, sería la inducción de sismicidad en pequeña escala como forma de evitar la acumulación de energía sísmica. Una forma de realizar esto sería el manejo de las aguas superficiales o subterráneas cerca de una falla peligrosa. Se conoce que el llenado de grandes presas ha podido inducir eventos pequeños en fallas superficiales, sin embargo esto ha ocurrido solo en ciertos ambientes tectónicos y en fallas muy pequeñas. En contraparte, una gran presión de agua, asociada a un levantamiento de la tabla de agua superficial, podría incrementar la presión de poro entre las rocas saturadas de tal forma que se reduzca la resistencia a la fricción a lo largo del plano de falla. Esto converiría a las fallas en planos de resbalamiento asísmico que potencialmente liberen gradualmente la energía sísmica.

Diseño Sismo Resistente:

Una gran mayoría de las muertes y de las pérdidas económicas asociadas a los sismos, se debe al colapso estructural de casas y otros edificios. El impacto es altamente influenciado por los materiales y métodos utilizados para hacer los edificios. El estilo arquitectónico puede contribuir al desastre si muchas de los formas arquitectónicas como chimeneas, balcones, decorados, etc. no están aseguradas adecuadamentte.

Todas las estructuras sin refuerzo estructural se encuentran bajo riesgo pero los edificios más vulnerables son los construidos utilizando adobe o ladrillos de arcilla secados al sol. El adobe utiliza materiales locales en zonas áridas y semiáridas, y es barato, fácilmente trabajable y abundante cuando otros materiales son escasos. El barro mezclado con materiales que le ayudan a darle cohesión como boñiga o paja, absorbe humedad, es resitente al fuego y produce ambientes interiores frescos. Desafortunadamente, el adobe tiene poca resistencia a las sacudidas de los sismos y usualmente tiene techos de materiales muy pesados como tejas que tiende a colapsarse cuando son sacudidos.

En muchos países pobres, aproximadamente dos tercios de las casas rurales y un tercio de las casas urbanas son hechas de adobe. Ello explica la alta morbilidad registrada en diversos eventos sísmicos. Por ejemplo, en el Perú en mayo de 1970 unas 60.000 casas de adobe collapsaron, matando a unas 50.000 personas e hiriendo a otras 150.000 más.

La solución es adoptar métodos de construcción resistentes a los sismos. Muchas sociedades

Scientific Technical Report STR 95/TK
DOI: 10.2312/GFZ.b103-95tk7 GeoForschungsZentrum Potsdam

parecen haber desarrollado históricamene sistemas de construcción que dan respuesta a esta necesidad construyendo casas con paredes y cielo rasos livianos capaces de resistir las sacudidas sísmicas, sin embargo esto no es cierto para los incendios que pueden acompañar los sismos.

Una de las estrategias que se está explorando es la de producir estructuras más fuertes con materiales débiles, lo que para los países pobres sería de gran utilidad. Se investiga en mejorar el amarre entre las paredes hechas de adobe utilizando bambú que es un material abundante en los trópicos, demostrándose que puede producir estructuras hasta un 40 % más fuertes como resultado de la flexibilidad del bambú. Esta línea de investigación toma muy en cuenta que los países pobres tienen que estar en capacidad de poder financiar las nuevas tecnologías de construcción que resulten.

Una línea de trabajo ha sido la investigación de la respuesta a las cargas de los diversos materiales de construcción, bajo la premisa de que si se conoce cómo se comportan y cómo se deforman será posible optimizar sus características para aplicarlas en la construcción resistente a los sismos. En este contexto se prefieren materiales fuertes, flexibles y dúctiles para la construcción de los elementos estructurales que hacen la construcción resistente al movimiento horizontal, y otros materiales para elementos no estructurales. Además, la experiencia acumulada a través de la observación de muchos eventos sísmicos ha permitido a los ingenieros establecer lineamientos que permiten el diseño y la construcción de casas y edificios resistentes a los sismos, así como poder comprender mejor la razón de las fallas en las estructuras viejas, ya construidas, lo que permite el reforzamiento de las mismas.

Otra línea de trabajo que tiene prioridad es la del diseño y construcción de edificios que deben de seguir funcionando despúes de un sismo, en especial aquellos que garantizan los servicios de salud y las líneas de energía. Las líneas vitales que deben recibir una atención especial en cuanto a diseño sismoresistente son el transporte, la comunicación, la electricidad, el agua, el alcantarillado y la transmisión de combustibles por medio de ductos.

No es posible demoler todos los edificios que no fueron diseñados para resistir las sacudidas sísmicas, por lo tanto ha sido necesario reforzar estructuras préviamente construidas para mejorar su comportamiento sismoresistente. En California existen unos 60 mil edificios de ladrillo sin reforzar que están siendo usados diariamente y existe un amplio programa para patrocinar su reforzamiento estructural. Sin embargo, mientras esto no ocurra deben de tomarse otras medidas que garanticen que la comunidad conozca su ubicación, que se establezcan límites en cuanto al número de ocupantes diarios y que los inquilinos conozcan del riesgo a que están expuestos.

El establecimiento de códigos de construcción que se actualicen en el tiempo y su cumplimiento es una de las mejores alternativas para garantizar un bajo nivel de daños en una comunidad. En el caso del sismo de Loma Prita en California (M:6.9) el número de muertos fue muy bajo y localizado en aquellas estructuras construidas antes de la puesta en vigencia de los códigos de construcción mejorados. Si comparamos el sismo de Loma Prieta con el de Armenia (1988) que tuvo una magnitud similar, encontramos que en Armenia murieron 25.000 personas, en contraste en el sismo de Loma Prieta murieron tan solo unas decenas de personas.

Scientific Technical Report STR 95/TK
DOI: 10.2312/GFZ.b103-95tk7

6.3 Ajustes que modifican la vulnerabilidad

El factor clave en la mitigación del impacto de los sismos es la preparación de la población y la planificación de la recuperación de las funciones normales de la sociedad. Las autoridades políticas de una ciudad no van a establecer planes de preparación si no reciben un estímulo para que lo hagan. Este estímulo en muchas ocasiones proviene de experimentar un sismo destructivo y en otros casos del patrocinio de estas actividades a nivel regional desde un gobierno central.

La preparación de la comunidad se desarrolla mejor al nivel local dentro del marco de soporte y organización del esfuerzo que puede ser regional o nacional.

La respuesta a las emergencias es más eficiente cuando se ha pre-establecido los trabajos priorizados que deben realizarse y se ha establecido de antemano quién es responsable de cada trabajo a realizar. Las acciones expontáneas no pueden substituir a las acciones pre-planificadas y asesoradas profesionalmente.

Pronóstico y Alarma Sísmica:

La predicción sísmica y el desarrollo de sistemas de alarma sísmica es una medida de mitigación que ha atraído recientemente mucha investigación por el potencial que representa el poder evacuar en poco tiempo los ocupantes de edificios sin reforzar. Sin embargo, a pesar de ello predicciones totalmente creíbles o mejor dicho con capacidad de aplicación universal no han sido desarrolladas y posiblemente no lo serán en mucho tiempo.

En casos en donde existen datos históricos, es posible aplicarles estadística a pesar de las limitaciones inherentes a estos juegos de datos. El resultado ha sido el reconocimiento de tendencias de comportamiento sísmico que tienen aplicación por lo general para el establecimiento de planes de preparación de la comunidad o en planes de mitigación que conlleven al reforzamiento de líneas vitales de tal forma que los esfuerzos para disminuir la vulnerabilidad a los sismos no sean hechos en forma generalizada, sino en los sitos que se consideren más susceptibles de sufrir sus efectos en los próximos años.

En contraste al peligro sísmico primario causado por la sacudida del suelo, el peligro secundario causado por los tsunamis ha cosechado importantes éxitos en el campo de la predicción y los sistemas de alerta. El sistema de alerta de tsunamis del Pacífico se organizó en 1948 con sede en Hawai y porteriormente se organizó otro sistema de alerta local para Alaska y el Pacífico noreste. Estos sistemas reciben información de 30 estaciones sismográficas y 70 mareógrafos alrededor de la Cuenca del Pacífico. Las alertas de tsunami actualmente se realizan a dos niveles en la Cuenca del Pacífico. El primer nivel da alarmas a todos los países de la Cuenca para tsunamis que pueden abarcar todo el Pacífico. Inmediatamente después de un sismo de magnitud 7.0 o mayor, se establece un monitoreo de las mareas cerca del epicentro. Si se detacta alguna alteración se establece una alarma de tsunami. El propósito de la alerta es que dentro de un período de una hora, todas las comunidades costeras que se encuentran bajo riesgo más allá de los 750 Km de distancia de la fuente puedan ser notificadas y se pueda pronosticar la llegada de la primera onda del tsunami con una exactitud de 10 minutos. Para eventos que afectan toda la Cuenca del Pacífico toma de 10-12 horas para las ondas atravesarla. Ello implica que existe

Scientific Technical Report STR 95/TK
DOI: 10.2312/GFZ.b103-95tk7

tiempo para anunciar la alarma y para tomar medidas de evacuación.

El segundo nivel da alarmas es regional y se utiliza en regiones que generan tsunamis. El propósito de estos sistemas es emitir una alarma en minutos para áreas que se encuentran entre 100 y 750 Km de la fuente. Una medida del éxito de este servicios de alerta de tsunamis en Japón lo sugienten las estadísticas, ya que antes de establecerse el servicio regional en 1952 unas 6000 personas habían muerto en 14 tsunamis, en tanto desde 1952, solo 215 personas han muerto en unos 20 tsunamis en que este sistema regional ha producido alarmas.

A pesar de todo, muchas costas continúan sin protección local en especial en los países más pobres que no pueden pagar por sistemas sofisticados. Recientemente se ha instalado en Chile un sistema local que tiene la capacidad de detectar un tsunami y difundir la alarma en unos tres minutos para proteger áreas costeras muy cercanas a la fuente. Este sistema tiene un costo relativamente bajo, similar al de una estación sismográfica, por lo tanto es una opción real para muchos países.

Planificación del Uso del Suelo:

El mejor ajuste del uso del suelo en áreas de alto riesgo sísmico consiste en evitar su utilización para construir obras de ingenierría. La microzonificación de áreas ya construidas con el propósito de transformarlas en áreas abiertas, con parques o bosques, o usos similares, así como la prevención de más desarrollo en áreas de alto riesgo, debe convertirse en una prioridad social. Esta política puede tener problemas por falta de disponibilidad de información en las manos del público y en asegurar una respuesta positiva del público. En algunos países el comprador de una casa debe recibir información sobre los peligros a que está expuesta la propiedad con el fin de patrocinar cambios en el uso del suelo.

Rezonificación en zonas costeras expuestas al riesgo de tsunamis puede ser una efectiva defensa contra tsunamis, que patrocine con el tiempo, el establecimiento de una zona de abierta cercana a la playa que se utilice en actividades de recreación y la reubicación de los edificios hacia zonas más altas.

7. VULCANISMO

Existen a nivel mundial unos 500 volcanes activos, de los cuales existen en la América Central unos 28 volcanes que han tenido actividad en tiempos históricos. Todo volcán que no haya estado activo en los últimos 25.000 años debe ser considerado como un volcán potencialmente activo. En promedio un 5 % de las erupciones volcánicas produce pérdidas de vidas.

Los volcanes se encuentran en tres ambientes tectónicos distintos. Existen volcanes en el límite de placas convergentes o se en las zonas de subducción, así como volcanes en el límite de placas divergentes o sea en las dorsales medioceánicas, como en el caso de Islandia. Un tercer tipo de volcán ocurre dentro de las placas en relación a puntos calientes en el manto superior que inducen la producción y ascenso del magma hacia la superficie produciendo volcanes como los de Hawai.

Scientific Technical Report STR 95/TK
DOI: 10.2312/GFZ.b103-95tk7

Un 80 % de los volcanes se encuentra en zonas de subducción y por lo general son estratovolcanes cuyos conos consisten de capas alternas de lavas y materiales piroclásticos. Estos volcanes tienen un caracter explosivo y pueden generar tan grandes explosiones que acaban por destruir el cono volcánico dejando atrás una depresión central conocida con el nombre de caldera. Estas explosiones volcánicas son las más destructivas, sin embargo, ocurren con muy poca frecuencia a nivel mundial.

Una mezcla de silicatos fundidos asciende hacia la superficie por contraste de densidad con las rocas de la corteza terrestre, desde profundidades superiores a los 60 Km. El ascenso es gradual y es común que el **magma** pueda ser almacenado en grandes volúmenes a diferentes profundidades debajo de los volcanes. Allí, el magma evoluciona se enfriá y cristaliza una fracción importante de su masa. A medida que los magmas cristalizan se enriquecen en componentes volátiles, como agua, dióxido de carbono, dióxido de azufre, que se mantienen en solución dentro del magma. El resultado es una disminución de la densidad del magma y un incremento en su viscosidad. Es común que los magmas al entrar en contacto con los mantos acuíferos en profundidad, absorban agua incrementando así potencialmente su contenido de volátiles. Estudios experimentales han llegado a establecer que contenidos de 3-4 % por volúmen de volátiles no son imposibles a presiones propias de los primeros 15 kilómetros bajo la superficie.

A medida que asciende un magma hacia la superficie, los volátiles que se encuentran en disolución dentro del magma tienden a escapar y ello resulta en la formación de burbujas a partir de una cierta profundidad o presión litostática determinada. A medida que las burbujas crecen el magma disminuye en densidad y tiende a asecender aún más rápido. Una vez que las burbujas llegan a un tamaño crítico empiezan a coalescer y a forman burbujas más grandes, hasta que escapan violentamente del magma produciendo las explosiones que conocemos muy cerca del fondo del cráter de los volcanes. El volumen de magma involucrado en una erupción, la cantidad de volátiles que contiene, su velocidad de ascenso hacia la superficie y sus características físicas (temperatura, viscosidad, cantidad de cristales presentes, etc.) que determinan su reología son variables que definen si el magma produce erupciones explosivas o en contraposición si produce erupciones en donde el magma fluye hacia la superficie de la tierra sin ningún problema, y con relativa calma.

Los fenómenos volcánicos pueden ser clasificados en primarios y secundarios. Los primarios son **coladas de lava, tefras de caída y flujos piroclásticos.** Los secundarios son **gases volcánicos, lahares, deslizamientos y tsunamis**.

Si el magma pierde los gases sin producir explosiones, y existiendo un ascenso de suficiente volumen de magma hacia la superficie, los volcanes producen coladas de lava. Las **coladas de lava** son corrientes de roca parcialmente fundida que inicialmente llena los cráteres volcánicos y posteriormente fluye por las laderas volcánicas a muy poca velocidad, por lo general muchos metros por día en el caso de los magmas más viscosos y lentos, hasta varios kilómetros por hora en el caso de los magmas más fluídos y veloces, como los magmas de Hawai. Dada la baja velocidad a que se mueven las coladas de lava, por lo general no ponen en peligro la vida, pero dado que siguen las depresiones topográficas pueden inundar aldeas en las laderas volcánicas.

Scientific Technical Report STR 95/TK
DOI: 10.2312/GFZ.b103-95tk7 GeoForschungsZentrum Potsdam

Si el magma pierde los gases de manera violenta generará como resultado de la explosión materiales de diferente tamaño que pueden estar hechos del mismo magma o de rocas pre-existentes arrancadas de las paredes del volcán por la explosión. Los materiales así generados reciben el nombre de tefras de caída. El rango de diámetro de partículas generado oscila entre varios micrones para el caso de los aerosoles de origen volánico, hasta varios metros para los bloques balísticos lanzados a varios kilómetros de distancia por los volcanes. A medida que aumenta el diámetro de las partículas las llamamos polvos, cenizas, piedrecillas o lapilli, bombas o bloques. El viento se encarga de dispersar las partículas de granulometría más fina, en tanto las partículas más gruesas caen sobre la superficie de la parte superior de cono volcánico. Las cenizas volcánicas tienen caracter abrasivo, son químicamente y eléctricamente activas, si se mojan adquieren una densidad elevada y flotan en el aire fácilmente. Por ello son capaces de producir una gran cantidad de problemas en el desarrollo normal de las funciones de una sociedad moderna.

En algunos casos, materiales muy calientes que tienen todavía algunos volátiles en solución son lanzados al aire violentamente y continúan expandiéndose y descendiendo por las laderas volcánicas por gravedad. En otro casos se produce un deslizamiento de parte de un domo o cono volcánico teniendo como resultado la caída por gravedad de materiales incandescentes que también se expanden a medida que descienden por las laderas volcánicas. Estos flujos de partículas incandescentes y bloques involucran grandes cantidades de aire a altas temperaturas, varios cientos de grados y se trasladan a velocidades típicas de unos 100-200 Km por hora, lo que hace imposible la evacución oportuna de los habitantes de las laderas volcánicas. Genera incendios a su paso y depósitos de bloques y cenizas de forma elongada al pie de las laderas volcánicas. Genéricamente a todas las erupciones en donde están involucrados rocas incandescentes que descienden por gravedad en medio de un flujo turbulento y caótico de gases calientes, ceniza y bloques se les llama **flujos piroclásticos**.

Los **gases volcánicos** emitidos como resultado de la degasificación del magma, aunque son en su gran mayoría agua y dióxido de carbono, contienen cantidades significativas de gases altamente venenosos y químicamente activos, que al mezclarse con el agua generan ácidos fuertes. De ser respirados cuando los gases todavía no se han diluido en el aire, pueden ser venenosos y representan un peligro para la vida. Los gases volcánicos generan acidificación del medio y ello conlleva daños a la ecología, pero también a la salud de los seres humanos y a la infraestructura. En Camerun, dos volcanes han dejado escapar en forma pasiva grandes cantidades de gases ricos en dióxido de carbono. El dióxido de carbono es muy peligroso en alta concentración por cuanto no tiene color, ni olor característico y por ser más denso que el aire, lo desplaza hacia arriba, provocando muerte por falta de oxígeno en la pesonas que lo respiran, sin que las personas siquiera lo noten.

Cuando se producen grandes emisiones de partículas como resultado de las erupciones y a la vez, se producen grandes precipitaciones de lluvia, el resultado más común es la ocurrencia de avalanchas de barro ricas en ceniza volcánica, conocidas también como **lahares**. En algunos casos, el vaciado violento de un lago cratérico y subsecuente flujo del agua pendiente abajo o la fusión rápida de la nieve, al producirse una erupción de cenizas calientes ha producido lahares gigantescos de gran poder destructivo.

Scientific Technical Report STR 95/TK
DOI: 10.2312/GFZ.b103-95tk7

Otro aspecto bastante desconocido de los volcanes es su capacidad de generar grandes **deslizamientos**. Estos deslizamientos pueden ocurrir en conjunción con actidad volcánica o sin ella, y producen avalanchas frías capaces de viajar muchos kilómetros desde su origen. Estos deslizamientos se desplazan por gravedad a partir del colapso de una ladera del volcán cuyo ángulo de reposo, después de ser alterada por la acción hidrotermal, resulta inadecuado. En otros casos, cuando está involucrada la actividad volcánica en forma inmediatamente anterior al deslizamiento, es posible que la fuerza de la erupción provea la energía inicial que genere el deslizamiento.

Los **tsunamis** pueden ser generados por sismos y por grandes explosiones volcánicas. Uno de los tsunamis más destructivos que se conoce estuvo asociado a la explosión del volcán Krakatoa, volcán con un cono volcánico que se levantaba muchos cientos de metros por encima del nivel del mar. Su cono fue destruido por la explosión, dejando tan solo un arreglo semicircular de islas definiendo la ubicación del borde de la caldera submarina.

7.1 Ajustes para compartir las perdidas

Ayuda por desastre:

Las erupciones volcánicas han atraído la ayuda internacional en forma de ayuda financiera, o también en especie, y ayuda técnica por muchos años hacia los países afectados.

Hay que hacer notar que cuando ocurre una erupción volcánica de grandes proporciones es común que la ayuda internacional provea grandes cantidades de cosas que no se necesitan y que otras necesidades más apremiantes no sean cubiertas. Por ejemplo, durante la erupción del volcán Galuggung de Indonesia en 1972 se albergaron alrededor de 70 mil personas evacuadas en tiendas de campaña que colapsaban al caerles ceniza, o ardían con facilidad cuando, en sitios más cercanos al volcán, les caía encima algunas piederecillas calientes. Durante la crisis de Camerún en 1986 el gobierno recibió cinco frazadas para cada habitante evacuado y miles de libras de comidas congeladas que necesitaban un sistema de transporte dotados de congeladores para poder hacerlos llegar a los evacuados, algo que no existía en el país.

Una de las características de los emergencias volcánicas es que se pueden extender durante muchos meses si las erupciones continúan, lo que implica que la ayuda debe tratar de satisfacer las necesidades de vivienda y cuido por períodos mucho más largos que para víctimas de otros desastres. El período de rehabilitación y reconstrucción muchas veces no se inicia hasta que las erupciones volcánicas terminen y ello trae como consecuencia largos períodos en que la ayuda es necesaria. La explosión de Galunggung ocurrieron 29 fases eruptivas en un período de seis meses. Durante los primeros meses los evacuados recibieron comida y ayuda en forma irregular, pero luego la Cruz Roja tuvo que establecer un programa regular de alimentación en virtud del prolongado estado eruptivo.

Seguros:

A nivel mundial, los seguros específicos contra los efectos de las erupciones volcánicas están

Scientific Technical Report STR 95/TK
DOI: 10.2312/GFZ.b103-95tk7 GeoForschungsZentrum Potsdam

menos desarrollados que los seguros contra terremotos. En algunos casos los seguros de cosechas cubren las pérdidas causadas por cenizas volcánicas. Algunas obras de infraestructura de gran tamaño son aseguradas por las transnacionales de seguros.

7.2 Ajustes que modifican el evento

Control ambiental:

Las erupciones volcánicas no se pueden prevenir. No se conoce, además, ninguna defensa posible contra los flujos piroclásticos. Las caídas de piroclastos, especialmente de ceniza, pocas veces ponen en peligro la vida de las personas, pero causan grandes daños económicos y no se puede hacer mucho por proteger las cosechas y los reservorios de agua para consumo.

Las coladas de lava junto con los lahares son los únicos peligros volcánicos sobre los que se puede hacer un control físico. Se ha tratado de desviar el rumbo de las coladas de lava por mucho tiempo, con resultados parciales. En Hawai se ha utilizado el bombardeo de los túneles o canales de lava que alimentan coladas con explosivos en la parte superior del volcán. Alternativamente, en Italia se han construido barreras topográficas para tratar de desviar el curso de la colada. Este mismo método puede utilizarse para desviar el curso de los lahares. En Islandia las coladas de lava se rociaron con millones de metros cúbicos de agua para enfriarlas deteniendo con éxito su avance sobre una ciudad.

En el volcán Kelur de Java, su lago cráter producía explosiones freáticas que vaciaban el lago periódicamente, produciéndose numerosos lahares sobre las pobladas laderas volcánicas. Fué así como en los años 20 se contruyó un tunel que redujo el lago a un 5 % de su volumen original, disminuyendo drásticamente el riesgo de lahares.

Diseño Vulcano Resistente:

Uno de los problemas asociados a las erupciones volcánicas es el colapso de edificios, especialmente aquellos de techo plano como consecuencia del peso de la ceniza mojada. Para solucionar este problema se pueden reforzar edificios que de otra manera sufrirían colapso estructural o mejor aún, construirles techos con un gran ángulo de gradiente.

7.3 Ajustes que modifican la vulnerabilidad

Preparación de la comunidad:

El costo de monitorear la actividad de los volcanes y de la planificación pre-desastre es muy bajo comparado con las pérdidas potenciales. La mayoría de las comunidades expuestas a los peligros volcánicos tienen consciencia del peligro.

Cuando existe vigilancia de la actividad volcánica y una efectiva preparación, es posible establecer advertencias que permitan la evacuación de la población de los sitios más peligrosos

antes de que la erupción ocurra.

La planificación de emergencias en zonas de peligro volcánico está muy bien desarrollada y contienen elementos secuenciales muy bien definidos.

La ceniza volcánica puede producir impactos severos en la actividad económica a cientos de kilómetros de distancia del volcán y también afectar severamente el tránsito aéreo de una región, afectando a personas para las que no sea tan obvio estar expuestos a un peligro volcánico.

Predicciones y alarmas:

Las erupciones volcanicas mayores no ocurren expontáneamente, sino que son precedidas por una serie de cambios que acompañan el ascenso del magma hacia la superficie. El seguimiento y la medición de estos cambios en forma sistemática y contínua es la mejor esperanza de llegar a diseñar sistemas de predicción y alarma confiables. Desafortunadamente, tan solo unos 10-20 volcanes a nivel mundial se encuentran hoy día suficientemente instrumentados como para tratar de realizar predicción científica.

Los precursosres que ocurren en un volcán antes de que entre en erupción son: Cambios en los patrones de actividad sísmica, deformación del suelo, fenómenos hidrotermales como la aparición de fumarolas o el incremento en la temperatura, y finalmente cambios en la composición química de los gases y aguas superficiales.

En el presente no existe una metodología completamente confiable para realizar pronósticos de las erupciones volcánicas. Sin embargo, es posible reconocer cuando un volcán se encuentra más activo y comunicarlo a la población a tiempo para que respondan a los planes de emergencia pre-establecidos. Sin embargo, esto no es siempre tan sencillo según lo indica la experiencia debido a que una crisis volcánica puede durar muchas semanas y existen preguntas sobre el comportamiento futuro del volcán que no siempre pueden responder los científicos.
Cuando científicos de experiencia han tenido un volcán suficientemente instrumentado, ha sido posible realizar valoraciones del potencial eruptivo que han conducido a salvar vidas y pérdida innecesaria de recursos.

Planificación del uso del Suelo:

La planificación del uso del suelo tiene un papel muy importante que jugar en la reducción de los desastres volcánicos, en la forma de restringir el desarrollo en áreas peligrosas y en la preparación de planes de evacuación de emergencia. La zonificación del suelo y la selección de lugares seguros depende de los pronósticos a largo plazo de la probabilidad de erupción volcánica y en la identificación de areas de riesgo potencial.

Mapas de amenaza volcánica pueden ser contruídos con base en la evidencia geológica de eventos pasados para definir el área posible de extensión de los fenómenos volcánicos. Las limitaciones más obvias de estos mapas provienen del desconocimiento del tamaño de las erupciones futuras.

Scientific Technical Report STR 95/TK
DOI: 10.2312/GFZ.b103-95tk7

Otra limitación práctica, especialmente en países pobres, proviene de la ausencia de recursos para realizar estudios de campo a profundidad o para realizar pruebas de laboratorio, como dataciones que son necesarias para valorar periódos de recurrencia y valorar con precisión el riesgo en un sitio dado. Otra limitación proviene de que las condiciones ambientales durante la erupción pueden controlar las características del peligro y es imposible pronosticarlas, por ejemplo, la cantidad de nieve que puede transformarse en agua para alimentar lahares o la dirección y fuerza del viento que puede distribuir la ceniza a lugares lejanos. Las variables ambientales obligan en muchos casos a trabajar varios escenarios como variables posibles de la una erupción, complicando aún más la situación.

ACCIONES EN LA PLANIFICACION DEL DESARROLLO NACIONAL Y REGIONAL

El manejo de amenazas debe ser incorporado a la planificación del desarrollo nacional y regional por las siguientes razones:

1. Es más factible y realista la reducción de la vulnerabilidad cuando aparece dentro de los proyectos de desarrollo económico, que cuando aparece como propuestas de mitigación en sí mismas.

2. Es más barato reducir la vulnerabilidad cuando las medidas de reducción se han incorporado dentro de la formulación de los proyectos de intervención y no cuando se las incorpora a posteriori como resultado de haber encontrado problemas inesperados en las etapas avanzadas de preparación de un proyecto.

3. Las prioridades fijadas para responder a las necesidades de los proyectos de intervención como parte del proceso de planificación obligan a los científicos e ingenieros a producir conocimiento de aplicación inmediata en la mitigación de los desastres y de gran impacto social.

4. Las medidas de reducción de la vulnerabilidad dentro de los proyectos de desarrollo benefician a los sectores más pobres de la sociedad.

La planificación integral del desarrollo requiere de un conocimiento y evaluación del riesgo que es costosa si se considera en sí misma, pero relativamente barata si se le considera como parte de un análisis económico obligado de los factores negativos que determinado proyecto puede encontrar en su desarrollo. De la misma manera, muchos proyectos de intervención van a requerir información similar, lo que permite dividir mejor los costos de los estudios o valoraciones necesarias entre muchos proyectos como parte del proceso de planificación. Además, otros sectores de la sociedad que no pueden pagar por realizar los estudios específicos de riesgos pueden requerir de la información generada de tal forma que indirectamente produzcan un impacto social muy amplio. Por ejemplo, un proyecto de intervención que pretenda la construcción de casas populares no puede pagar por estudios de riesgo, sin embargo puede utilizar información generada para la justificación de otros proyectos de construcción de grandes obras de infraestructura, cuyo costo ha sido plenamente justificado.

Scientific Technical Report STR 95/TK
DOI: 10.2312/GFZ.b103-95tk7

Bibliografía

OEA, 1991, Desastres, Planificación y Desarrollo: Manejo de Amenazas Naturales para Reducir Daños, Washington D.C., 80 p.

Smith K, 1992, Environmental Hazards: Assessing Risk and Reducing Disaster, Rouledge, London and New York, 323 p.

Okrent D, 1980, Comment on Societal Risk, Science, 208: 372-375.

Timmerman P, 1981, Vulnerability, Resilence and the Collapse of Society, Environmental Monograph #1, Institute for Environmental Studies, University of Toronto, Toronto.

Scientific Technical Report STR 95/TK
DOI: 10.2312/GFZ.b103-95tk7

SEISMICITY, SEISMOTECTONICS AND SEISMIC HAZARD ASSESSMENT IN SOUTH AMERICA

Hansjürgen Meyer

Observatorio Sismológico del SurOccidente - OSSO,
Universidad del Valle
Cali - Colombia

1. INTRODUCTION

South America (SA) is among the continents which most often suffers disasters caused by earthquakes. It also features some of the "records" of seismicity related phenomena for modern times: the largest earthquake (Chile 1960); the deepest ever recorded earthquake (Colombia, 1970), the biggest of the very deep earthquakes (Bolivia 1994), the largest and most disastrous Pacific-wide tsunami (Chile 1960). Seismicity and seismic hazards in SA are concentrated in its Andean countries, close to the Nazca-SA and Caribbean-SA active margins, but intraplate regions such as Brazil and Paraguay also register occasional damaging earthquakes.

The history of observation and efforts to understand earthquake phenomena in SA is about as long as anywhere else. All major traits and many details of SA seismicity are known and this regional and local knowledge has certainly been having social impact, but it is still a long way before the seismological scientific community in SA reaches a critical mass, sufficiently large, autonomous, integrated, self-conscious and visibly delivering in all countries.

This short overview is not very detailed and certainly not very complete; also, faults and important omissions may have occurred. It was not possible to tap all relevant sources of information and the references included may not be representative; much - if not most - of the seismological and seismic hazards information on SA has not been published in indexed scientific journals. Frequent mention of details pertaining to Colombia have but one reason, the author's acquaintance. It is hoped that these illustrations, at least often, exemplify circumstances, achievements and problems typical in the region.

This paper is related to another one, which presents an overview of earthquake and volcanic risk mitigation in South America (Meyer, this volume).

For some topics, reference is also made to the neighboring countries Panamá and Trinidad - Tobago, which share seismic hazard sources with some areas in SA.

2. SEISMOLOGY IN SOUTH AMERICA

An attempt to give an overview of a discipline and its results and social impact would not be complete without a brief mention of the human context in which the knowledge evolved and came to bear. This paper was written for a regional training course addressing those who will be advancing Seismology and its application to risk mitigation in South America. Thus, a short look at historical aspects might help to better decide on goals and strategies for the future.

2.1 Education and training

Although there are strong academic programs in Seismology in SA (Chile, Brazil), most of those who work in the field have been graduated elsewhere, or came from other disciplines to postgraduate studies in Geophysics/Seismology, or were trained on the job. Probably the number of professionals working in Seismology today in SA is less than the number of trained people; opportunities in the oil industry and other fields have drawn many. Also, many outstanding seismologist from South America have settled in other countries, seeking better

Scientific Technical Report STR 95/TK
DOI: 10.2312/GFZ.b103-95tk7

opportunities for scientific work. In this regard it might be interesting to mention a new approach taken by the Colombian Science Foundation: rather than sustaining efforts to attract those who are abroad (with paid travel, bonuses, etc), they took advantage of modern means of communication (Internet) and established a web between Colombian scientists abroad and those working in the country. This program, now three years old, has shown substantial achievements in overcoming the relative isolation of the national community.

International training programs, like those organized by GFZ-Potsdam and its predecessor, have had a very important role in this field, where human resources have never been enough. To mention a few examples: more than 50 participants from SA have graduated during the last 35 years from the 1-year seismology courses held at the Int. Institute of Seismology and Earthquake Engineering, Japan (IISEE, 1994). CERESIS and IPGH - Comisión de Geofísica have sponsored a good number of workshops and seminars on seismological observation and practice and seismic hazard assessment. The International Institute of Mathematical Earthquake Prediction Theory and Mathematical Geophysics (Russian Academy of Sciences) has held two courses on intermediate-term earthquake prediction and reduction of seismic risk in South America (Lima, Perú; Caracas, Venezuela), with a strong emphasis an data analysis. Several students of South America have been attending IIEPT&MG workshops at the International Centre for Theoretical Physics (Trieste, Italy).

2.2 The regional community

It is difficult to assess, how many people are working in Seismology in SA. Two available figures might give an approximate idea: the membership list of the American Geophysical Union includes 256 from SA. The recent Regional Seismological Assembly in Brasilia was attended by 94 participants from Latin American countries (CERESIS, IASPEI, 1994). Although efforts from organizations such as CERESIS and the Comisión de Geofísica (Instituto Panamericano de Geografía e Historia - IPGH, OAS) have been fundamental to the integration of the regional community, much remains to be done. New ways of communication such as bulletin boards in Internet, for instance the "Onda Latina" coordinated at the Departamento de Geofísica, Univ. de Chile (*onda-latina@dgf.uchile.cl*), may contribute significantly to integrating the community. It should also be mentioned that regular publications such as the Revista de Geofísica (IPGH), Revista Brasileira de Geofísica and Interciencia (Venezuela) have been contributing to foster communication and interaction among South American seismologists. If and how the still marginal position of science in South America (Gibbs, 1995) has affected the international visibility of its seismological research cannot be evaluated easily.

2.3 Institutions

Activities related to seismicity and seismic hazards evaluation in South America have been based at very diverse institutions, from private organisms and universities to state and military organisms. Strong academic and scientific programs are rather recent, contemporary with the development of research capacity at universities and the strengthening of Basic Sciences as a national strategy. Today, most of the strong programs in seismological observation and research are based at universities. As elsewhere too, many institutions for Seismology and Seismic Hazard Assessment, specially at state level, have been created in the aftermath of major disasters. This is the case in Venezuela (FUNVISIS-Fundación Venezolana de Investigaciones Sismológicas), in Argentina (INPRES-Instituto de Prevención Sísmica) and Colombia; its advanced digital, satellite-based national seismic network traces its origins back to the Volcán Nevado del Ruiz disaster.

2.4 Regional and international cooperation

As the most important regional organizations for coordination and/or promotion one must mention CERESIS - Centro Regional de Sismología para América del Sur (Lima), IPGH - Instituto Panamericano de Geografía e Historia (OAS-Organization of American States) and its Comisión de Geofísica (México), and ORCYT - Organización Regional de Ciencia y Tecnología, UNESCO's regional office (Montevideo) and its program for earth sciences and natural hazards.

CERESIS, a regional intergovernmental organization based in Lima, was created in 1966. Its members are all SA countries except the three Guayanas, and Trinidad-Tobago and Spain. Its initial funding was from UNESCO. One could argue that most seismologist in SA have known their colleagues in the region at some CERESIS meeting. Its programs and activities include the first regional hazard evaluation (SISRA), organization of the 1973 IASPEI General Assembly (Lima), many courses and seminars, promotion of projects for new organisms or networks (SA Seismic Array, Brasilia; Instituto Geofísico, Ecuador), post-earthquake missions, publications, etc. CERESIS has also integrated seismological data in several projects (SISAN, SISRA), but it does not perform as a routine regional data center.

The list of other countries, organizations and projects which have been contributing in one or another way to the strengthening of Seismology in SA would be quite long. Just to mention a few examples: the US Geological Survey and its advanced instrumentation (WWSSN, SRO, IRIS) and data services through NEIC; the Instituto Geográfico Nacional of Spain and its continued support to CERESIS; UNDRO/DHA and its seed projects for seismic hazard evaluations in Colombia and Ecuador; the Swiss Disaster Relief (startup projects for regional observatories in Colombia and Ecuador). Probably most of the foreign participation has gone into infrastructure, specially equipment.

New international programs such as GSHAP, ISOP and SALSA (which aims also at setting up a regional data center at the Univ. de Chile) hold much promise.

2.5 Seismological observation

The origins of modern seismological observation in SA can be traced back nearly a century. It has not yet been established, which was the first seismic station in the region (Giesecke, 1995), but Caracas, La Paz, La Plata, Lima, Bogotá, Rio de Janeiro and Quito are among the candidates. A station in Quito recorded the "Great Colombia Earthquake" of 31 Jan. 1906 (Rudolph & Szirtes, 1911).

One of the first organizations operating seismic stations was the Jesuit Seismological Association; their observatories at La Paz (Observatorio San Calixto; station LPZ since 1912) and Bogotá (Instituto Geofísico - Univ. Javeriana) still operate. The most important station on the continent has been La Paz, for its long and reliable operation and for its excellent location. About this station B. Gutenberg once said that it is "the single most important station in the world".

While the era of World War II somehow delayed development of seismic observation in SA (Ramírez, 1977), the Cold War entailed benefits, as it did for seismic observation worldwide. The project Vela-Uniform (World-Wide Standardized Seismic Network) installed 16 stations on the continent (plus one each in Panamá and Trinidad - Tobago).

Broadband Seismology began in SA less than 20 years ago, with the installation of the first SRO stations. Now stations of various global networks and types are operating in Chile, Brazil, Bolivia, French Guayana, Venezuela and Colombia and the region is represented in the Federation of Broadband Digital Seismograph Networks (Berrocal, 1995).

Non-permanent seismic networks have also been an important source of seismic data and knowledge in SA, for instance in studying induced and intraplate seismicity in Brazil (Pearce, 1995), in studying the Andean Bend, the Altiplano (Projects BANJO and SEDAS) and the N-Chilean seismic gap (Rivera, 1995).

Although these usually do not exchange their data routinely, in most countries seismotectonic research has certainly also had benefits from many temporal local seismic networks, most often operated by state or private organizations for the purposes of seismic hazard evaluations for critical facilities. Seismological research has also gained from active seismic experiments, of crucial importance in heterogeneous crust such as western SA. Among these are some of the first seismic refraction experiments across leading edges, in international projects led by the Carnegie Institution of Washington (Ramírez & Aldrich, 1978).

The number of seismic stations in SA which have been reporting their readings continuously is quite below the total of installed stations. For example, while in a typical month 2.000

stations worldwide supply data to ISC-International Seismological Centre, in June 1992 only 92 stations in South America (with a relative concentration in Central Chile and neighboring W-Argentina) reported data to the Centre, while 433 stations were reported as being open in 1993 in the region. The NEIC station list contains presently 255 stations in SA (Presgrave, 1995). This agency points to poor E-W control in locations, due to lack of sufficient stations to the E of the Andes, and to large gaps in observation along the Andean region (N-Perú; S-Chile/Argentina) and the lack of a regional crustal model as limitations. According to the ISC, the study of seismicity in SA has been hindered (Adams & Richardson, 1994) by the very uneven distribution of stations, the uneven reporting in time and the lack of communication between observatories, thus contributing to uncertainty in estimation of seismic hazard. Perhaps its is fair to hint in this regard, too, to the often almost heroic struggles for support and continuity.

Another type of seismic instrument which is crucial to hazard evaluations are strong motion recorders. Their distribution in the region is much more difficult to assess, but many of the instruments have been installed during large engineering projects; their data does not flow routinely into international bases. Colombia, where accelerometry began some 30 years ago with 6 stations operated by the Instituto Geofísico de los Andes, is now developing a national strong motion network (35 already operational) as part of the Red Sísmica Nacional (Pulido, 1995).

Today there are all types of seismic instruments in operation in SA, from old Wiecherts to advanced digital broadband stations such as GEOSCOPE and IRIS. A list of South American seismic observatories and networks in SA should include the following:

Argentina: The National Meteorological Service installed in 1987 two Milne seismographs in Córdoba, cooperating with the British Association for the Advancement of Science (Gershanik, 1995). Between 1912 and 1922 Milne and Bosch-Omori seismographs were installed in Prov. Catamarca, Mendoza, Buenos Aires, Jujuy, Prov. Rio Negro. INPRES-Instituto Nacional de Prevención Sísmica (San Juan), established by a law in 1972 (Aguirre, 1976), operates a network in W-Argentina. The Observatorio Astronómico (Univ. Nal. de La Plata) and the Instituto Sismológico (Univ. de San Juan) also have seismic observation facilities. Most stations are located in NW-Argentina.

Bolivia: The first seismograph operated by the Observatorio de San Calixto was installed in 1912. Further stations were installed after 1960.

Brazil: Today, most seismic stations in Brazil are being operated by the national seismological service (Univ. Brasilia) and the Observatorio Astronómico y Geofísico (Univ. Sao Paulo). They are concentrated in E-Brazil.

Chile: The Servicio Sismológico was created shortly after the 1906 Valparaiso earthquake (Univ. de Chile, 1995). Today, the Depto. de Geofísica of the Univ. de Chile operates a dense network of seismic stations and strong motion instruments, mainly in Central Chile. Four WWSSN stations are operating in Chile.

Colombia: The history of the first 65 years of instrumental seismological observation in Colombia (Ramírez, 1971) belongs to members of the Jesuit Seismological Association. The first seismograph to record in the country (1918) was built in Bogotá following an Omori design, after a series of strong earthquakes there. The first continuously operating station was set up in 1921 at the Jesuit school San Bartolomé in Bogotá; two years later a still operating Wiechert instrument was commissioned. In 1941 the Jesuits founded the Instituto Geofísico de los Andes Colombianos (Now Instituto Geofísico, Universidad Javeriana). After 1945, they expanded their network to 7 stations in Andean Colombia. Among the instruments and stations the Instituto operates presently are a horizontal Wiechert, Colombia's WWSSN station and the first broadband station in this country, near Bogotá (IRIS, following a SRO installed in 1977).

Since 1987 the Observatorio Sismológico del SurOccidente - OSSO (Universidad del Valle, Cali) operates a short period telemetered network in SW-Colombia, installed with support from the Colombian Research Foundation and Swiss organizations (Swiss Disaster Relief, ETH Zürich). OSSO also operates a 15-station PASSCAL net in E-Colombia.

Following the Ruiz disaster, the national geological survey - Ingeominas - in cooperation with

Canadian agencies and UNDP, installed the Red Sismológica Nacional, with presently 15 stations (SPZ, digital, satellite telemetry) in Andean Colombia, in regular operation since June 1993, monitoring tectonic and volcanic activity. Ingeominas also operates a network of presently 35 strong motion recorders.

Ecuador: The first seismograph may have been operating since before 1906 at the Observatorio Astronómico in Quito. The Instituto Geofísico (Escuela Politécnica Nacional, Quito) began installation of a telemetered network in the late '70, for tectonic and volcanic observation; it covers now most of the country.

Perú: From 1971 on the state organization Instituto Geofísico del Perú has been in charge of the national seismic net. The Instituto Geofísico at Universidad de Arequipa is now also attending several stations in the South.

Venezuela: The Observatorio de Cajigal (Navy, Caracas) began instrumental observation with a Wiechert, in 1931 (Grases G., 1994). However, documents related to the 1900 Caracas earthquake allow to infer that there was some sort of instrumental recording at that time. The disastrous Caracas earthquake of July 1967 led to the establishment of the FUNVISIS - Fundación Venezolana de Investigaciones Sismológicas, which years later initiated the installation of a seismic network, mainly in N-Venezuela. At the Universidad de los Andes (Mérida), the Laboratorio de Geofísica began operating a telemetered network in W-Venezuela in the late '70.

Panamá: The first station was set up during the construction of the Canal. A station of the WWSS network was operational in Balboa Heights for many years. The Instituto de Geociencias of the Universidad de Panamá operates now a telemetered seismic network.

Trinidad - Tobago: The Seismic Research Unit (Univ. of the West Indies, Trinidad) operates a telemetered network covering more than a dozen islands of the eastern Caribbean and exchanges data with Venezuela.

3. SEISMICITY AND SEISMOTECTONICS

3.1 The regional tectonic frame

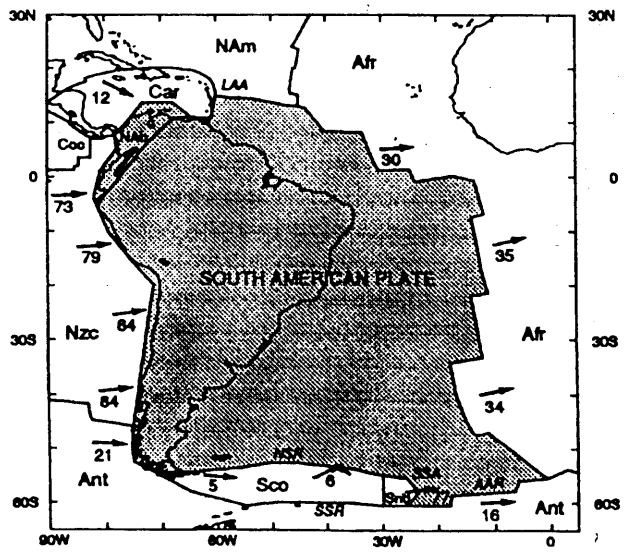

Fig. 1. Boundaries of the South American plate

(Meijer & Wortel, 1992)

SA is part of one of the major plates. As seen in Fig. 1, the South American plate, to which also belongs the area of the Southwest Atlantic Ocean, is bounded (clockwise from right) by the Mid Atlantic Ridge, the American-Antarctic Ridge, the South Sandwich Arc, the North

Scotia Ridge, the Antarctic plate, the Nazca plate and the Caribbean plate.

The subduction zone, which contacts the Nazca and South America plates and spans almost all of the Pacific coast from N-Colombia to S-Chile, is SA's prime active tectonic feature. Two mayor zones can be discerned on the continent, the stable Precambrian platform (Brazil, Paraguay, Uruguay, Guayanas and parts of neighboring countries) and the active belt along the western and northern rims. Here, along the western rim, the Nazca-SA subduction zone causes the Andean orogeny, all of the continent´s volcanism and most of the seismicity of the region. To the N, the oblique convergence with the Caribbean plate builds up the Venezuelan Andes and generates a complex pattern of shallow active tectonics, the Boconó system.

In the shield region, two main types of units can be distinguished: the exposed platform and major basins, Amazon, Paraná and Parnaiba, whose sediment loads may be contributing to the patterns of intraplate seismicity(Assumpçao, 1992),. In the active belt, with the Andes as one of the world´s longest orogens, segmentation is evident at various scales, correlating with subduction parameters such as slab dip, age and velocity, and seismicity parameters (Jarrard, 1989).

According to Assumpçao (1992), the direction of maximum horizontal stress in western SA is uniformly E-W and not affected by changes in strike of the Andean orogen. In the high Andes of central SA dominates N-S extension (Mercier et al., 1992)

Probably the most complex and as yet not well understood area on the continental part of the South America plate is the NW corner. Here a part of the continent - the North Andes Block parts of Ecuador, Colombia and Venezuela - is detached from the plate and moves independently, pushed by the South America, Nazca and Caribbean plates, and possibly a microplate, the E-Panama block. In this context a rather new technology deserves to be mentioned, the satellite-based geodesy and its great contribution to unraveling the kinematics of complex plate motion patterns (Freymueller et al., 1993).

The tectonic setting and seismicity in South America has many outstanding features, which have been attracting a lot of research initiatives at the national, regional and international levels, certainly to the benefit of the understanding of hazards too. Among these features are the following:

- the world´s most extended single subduction zone (more than 50º of latitude);
- the worlds deepest Wadati-Benioff zone, with large earthquakes right down to the 650 km discontinuity;
- a complex continental triple junction, in NW-Colombia (Freymueller et al., 1994);
- possibly the world´s most active deep seismicity nest, in Bucaramanga, Colombia (Schneider et al., 1987);
- outstanding and well studied examples of intraplate and induced seismicity, in NE-Brazil Joao Camara; Aço).

3.2 Regional seismicity

Epicenters from one of the global catalogs, the PDE (USGS/NEIC, 1994), have been included in Fig. 2. The left map shows foci with depth 0-33 km, the right shows the deeper activity, from 34 km on. Several features can be identified at this scale: the Nazca-South America convergence as the main source of seismicity in the region; segment of high shallow seismicity in the Andes; clusters of deep Wadati-Benioff activity; segments of low activity along the shallow subduction zone, such as in N-Chile; clusters of seismicity which may be attributed to dense networks and efficient international reporting, etc.

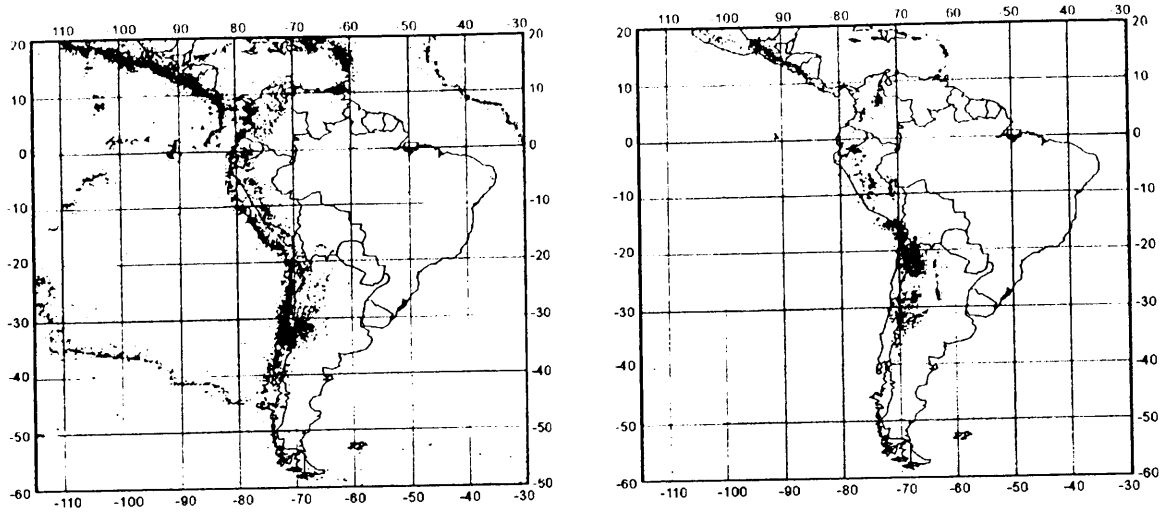

Fig. 2. Seismicity of South America. (USGS/NEIC, 1994), PDE cataloge. Left: 0-33 km. Right: depths > 33 km.

3.3 Tectonic traits

The first regional hazard assessment (CERESIS, 1985) includes a neotectonic map (1:5´000.000) of the region, with most of its data from 1:2'000.000 mapping. Now most countries seem to have their fault traces mapped at larger scales.

4. HAZARD EVALUATIONS

Presently, all countries with historical seismicity in South America have earthquake hazard evaluations at some level, either national or regional, such as achieved through a major regional project, SISRA, promoted and coordinated by CERESIS (CERESIS, 1985), with support from the Office of Foreign Disaster Assistance - OFDA (USAID). Between 1979 and 1985, a group of about 200 brought together and analyzed the available information and generated databases, maps, models and descriptions on regional seismicity, neotectonics, liquefaction, landslides and economic effects of earthquakes. On the other hand, if the more detailed seismic hazard maps at the national level are being compared, one can still find misfits at the borders (Grases G., 1995). It should be annotated that many national seismic hazard evaluations were done under the leadership of a most concerned group: civil engineers (García et al., 1984).

Presently CERESIS is updating the regional seismic catalogue (Giesecke, 1995). The results will be merged with another ongoing regional assessment project (Shepherd & Tanner, 1994), supported by the Canadian IDRC-International Development Research Centre.

4.1 Ground motion

A recent global compilation of seismic hazard evaluations at the national level (IASPEI/ESC, 1993), which includes asssessments from 58 countries, includes six examples from South America (Argentina, Bolivia, Brasil, Chile, Colombia, Ecuador). It must be added in this regard that other countries of the region, like Perú and Venezuela (Grases G., 1994) have had national hazard assessments and updatings for quite some time.

Among the generalized problems that ground motion estimation have to face in South America are rather short historical catalogues (less than 500 years) on recurrence estimation, the lack of data for modeling of regional or local attenuation laws, and the limitations in source zoning, in areas of complex and dense shallow tectonics and seismic catalogs with high magnitude thresholds and large location errors.

Here, again, one must mention the contribution for some areas which stem from specific local studies for critical facilities (Page, 1986).

4.2 Local effects and microzonation

In South America too, superficial geology has been very important in the toll taken by earthquakes. Conditions such as pronounced topography, climate and vegetation have led in many areas to thick and poorly consolidated soil deposits. Many of the larger cities in SA have now microzonation maps. An international pilot project in Quito recently brought advanced geotechnical and computer resources to the regional practice (Yepes et al., 1994). UNDRO-DHA has started pilot projects in several places, mainly in Colombia and Ecuador (Cardona & Meyer, 1991). There are even examples of "validated" microzonations, such as those for urban areas in the Mendoza - San Juan region (Argentina), which sustained strong shocks several times in recent decades, with evaluation and mitigation measures in between. The updated version of the seismic building code of Colombia, presently afore the Congress, will mandate microzonations for cities with more than 100.000 inhabitants in the zones with highest hazard levels.

4.3 Associated phenomena - landslides

In this case, as for local effects on ground motion, topography and climate conspire with the earthquake phenomenon to increase the hazards. Earthquake-induced landslides account for some of the worst seismic disasters in South American history, such as the May 1970 Ancash (Perú) event, with 67.000 deaths. The March 1987 earthquake in Ecuador (Lago Agrio) triggered landslides which paralyzed the country's oil industry (60% of its exports) for a long time. The June 1994 Páez (Colombia) earthquake destabilized hundreds of km^2 of agricultural land in the Central Cordillera. The October 1992 Urabá earthquakes (NW-Colombia) also destroyed a large area of tropical forest in a hilly region. In general, earthquakes seem to be one of the major factors of disturbance in areas with rain forests of NW-South America and parts of Central America (Garwood et al., 1979).

The first regional assessment (1:5'000.000) of landslide potential was done in CERESIS' SISRA project. Most geologic maps had been done with mining interests in mind, rather than environmental geology, thus leaving information on superficial layers out (Hermelin, 1995). But now the efforts towards mapping of soils are becoming more common. Using available geologic, hydrologic and topographic information and modern instruments such as computer processing of spatial information, landslide potential maps at regional scales for most of Colombia's mountainous areas were made recently (OSSO, 1995).

4.4 Associated phenomena - liquefaction

The vibration-induced loss of strength in granular, saturated soils and the ensuing damaging effects (lateral spreading of soils, subsidence of structures, etc.) has been a major factor of damage in many places in South America, and not only along the coasts. The climatic and topographic conditions found here in many areas, leading to thick unconsolidated sand/sandy deposits, favour the occurrence of this secondary seismic phenomena. This type of hazard was also included in the evaluations during the SISRA project (CERESIS, 1985), at 1:5'000.000.

4.5 Associated phenomena - tsunami

The most frequent and damaging tsunami are generated by shallow earthquakes in subduction zones. Many disastrous tsunami caused by the Nazca-SA subduction zone have occurred on the coasts of Chile, Perú, Ecuador and Colombia (Soloviev & Go, 1984; Soloviev et al., 1992), among these the most disastrous Pacific-wide tsunami of this century (May 1960), caused by an earthquake which as such also holds a record (M = 9.6). One of the early detailed scientific descriptions of a major earthquake and tsunami - by Ch. Darwin - was due to observations during the 1835 Concepción event (Central Chile).

Although the awareness (and mitigation measures) of tsunami hazards during the last decades was focused mainly on the Pacific, the Caribbean coast also had disastrous tsunami during historical times (Grases G., 1994), with damaging effects on the coasts of Venezuela. One of the major seismic disasters of the Caribbean, the destruction of Port Royal (Jamaica, 1692), was partly due to a tsunami.

The occurrence of tsunami is, in practice, less amenable to probabilistic modeling than the earthquake occurrence itself, due to other intervening factors, such as source depth and mechanical properties of the subduction zone. This is even more the case in South America, where the historical record is shorter than five centuries. The impact of tsunami, i. e. the likely terminal wave heights and runup distances at coastal sites, yields even less to modeling, because of independent variables such as tide levels, the high amplitude of tides on the Pacific coast and the lack of sufficient tidegage observations of tsunami (for calibration).

Whereas the site and size of future tsunami are difficult to forecast, the short-term prediction in time is feasible, the waves being a secondary phenomena, caused by a nowadays well observable and quantifiable phenomenon, large earthquakes. In South America´s Pacific coast, where most of the tsunami hazard comes from near sources, such a forecast window is of the order of tens of minutes. This relative advantage, the time predictability, compensates partly the relatively limited feasibility of structural mitigation measures (such as building reinforcement).

After several large Pacific-wide tsunami in the early '60 attracted much of the international efforts and research and mitigation resources, the last decade saw important fundamental and technical achievements towards detection and warning capability for near-source tsunami (IOC, 1995). In the mid '80, a NOAA/USAID project (Bernard et al., 1988) developed a near-source detection and warning system for Chile (Project THRUST), based on real time analysis of strong motion and tidal data. In the mean time, new concepts such as the "Mantle Magnitude" (Okal & Talandier, 1987) led to the development of a method for real-time assessment of the most tsunamigenic earthquake parameter, the seismic moment. This new technique, tested at the Centre Polinésien de Prévention des Tsunamis (Tahiti) for nearly a decade, has now been extended to local events (Schindele et al., 1995). This system is in the process of installation in Chile and will soon be implemented for Colombia´s Pacific coast too (IOC, 1995).

Other components which are crucial in the assessment of tsunami hazards, such as the forecasting of wave heights (a function of the perturbation at the source and the water depths on the path, mainly) and inundation areas, are now also subject of quite realistic hydrodynamic computer modeling (Shuto, 1989 and Caristan, 1995) and are in the process of being applied in SA. So far, all major areas of tsunami risk in Chile, Perú, Ecuador and Colombia have been subject of inundation modeling, either with numerical simulation or with empirical relations.

4.6 Earthquake prediction

The ultimate goal of seismic hazard analysis, the space-time prediction of specific events, which has been a goal of major research projects in different countries for the last two decades, has also been pursued for regions in South America. The prediction of a devastating earthquake off-shore the Lima region for mid-1985, by scientists from U.S. Bureau of Mines and U.S. Geological Survey, ended with a failure and severe socioeconomic disruption (Olson, 1989).

Nishenko (1989) published an analysis of occurrence probabilities in the decade 1989-1999 for the whole Pacific Rim, based on a modified model of the Immamura-Kelleher seismic gap theory. This model and its specific results have been reevaluated recently (Kagan & Jackson, 1995). Scientists in SA have also done research on seismic gaps in the region (Comte & Suárez,1993).

Several groups are studying the N-Chile gap, where a truly large earthquake is expected (Delouis et al., 1994; Comte & Suárez, 1993), with means such as dense local seismic networks and GPS deformation measurements. An M=8.2 event occurred in the observed segment on August 30, 1995.
A different approach to the seismic prediction problem, developed at the Int. Institute of Earthquake Prediction Theory and Mathematical Geophysics in Moscow (Keilis-Borok, 1990; Healy et al., 1992), has also been applied on data for South America. This methodology uses instrumental seismic catalogues to identify precursory patterns and to calculate space-time windows of increased probability of occurrence (TIPs, Times of Increased Probability); several of these are active in SA presently. This type of prediction has already shown some positive impacts (Meyer, 1995b), perhaps mostly due to the fact that the length of the

windows leave a sense of relative urgency, thus allowing for countermeasures.

CONCLUDING REMARKS

Perhaps this - rather "inventory"- type - presentation might leave the impression that the problem, understanding of seismicity in the region and assessment of seismic hazards, is being solved with sufficient resources and results. However, the wish for more colleagues is an everyday experience. There can be no doubt that South America has come a long way on its pursue for knowledge about these dangerous phenomena, but much remains to be achieved: more scientists and research groups, more interaction and integration, more and better tools to map the seismic sources, more and more continuous support from governments and funding agencies, more efforts from scientists to reach beyond descriptive work, more interaction between seismologists and other societal sectors .....

ACKNOWLEDGEMENTS

This paper would not have been possible without contacts and assistance from many colleagues in other South American countries, too many to be named. I also owe sincerest thanks to my colleagues Andrés Velásquez and Jorge Mendoza for their generous help.

REFERENCES

Adams, R.D., W.P. Richardson (1994). A view of Latin America from the International Seismological Centre. Proceedings, Regional Seismological Assembly in South America, Brasilia.

Aguirre, J. (1976). El terremoto de San Juan - República Argentina - del 15 de enero de 1944 y su influencia en la conciencia sísmica nacional. Revista Geofísica, no. 5, 135-144, IPGH, México,

Assumpçao, M. (1992). The Regional Intraplate Stress Field in South America. J. Geophys. Res. 97, B8, 11.889-11.903.

Bernard, E.N., R.R. Behn, G.T. Hebenstreit, F.I. Gonzalez, P. Krumpe, J.F. Lander, E. Loca, P.M. McManamon, H.B. Milburn (1988). On mitigating rapid onset natural disastres: Project THRUST. EOS, 69, no. 24.

Berrocal G., J. (1995). Personal communication, Instituto Astronomico e Geofisico, Univ. Sao Paulo.

Cardona, O.D., Hj. Meyer (1991). Integrated urban seismic risk mitigation project. Proceedings, IV Int. Conference on Seismic Zonation, vol. III, p. 139-147, EERI, Stanford, CA.

Caristan, Y (1995). Personal communication, EC Project GITEC-Genesis and Impact of Tsunami on European Coasts, Laboratoire de Geophysique, Bruyeres-le-Chatel.

Cabré, R. (1976). Conocimientos sobre el riesgo sísmico en Bolivia. Revista Geofísica, no. 5, 157-160, PAIGH, México.

CERESIS (1989). Riesgo volcánico-Evaluación y mitigación en América Latina. Lima, 298 pp.

CERESIS (1985). Earthquake Mitigation Program in the Andean Region (Proyecto SISRA), vols. 1-14, Centro Regional de Sismología para América del Sur, Lima.

CERESIS, IASPEI, (1994). Meeting Report, Regional Seismological Assembly in South America, Brasilia.

Comte, D., G. Suárez (1993). Spatio-temporal Variations of Seismicity in the Southern Perú and Northern Chile Seismic Gaps. PAGEOPH, 140, no. 2 and in Shallow Subduction Zones: Seismicity, Mechanics and Seismic Potential Part I, edit. R. Dmowska & G. Ekström, Birkhäuser, 317-330.

Delouis, B., A. Cisternas, L. Dorbath, L. Rivera, E. Kausel (1994). Chronicle of an announced earthquake (Northern Chile). Abstracts, Regional Seismological Assembly in South America, Brasilia.

Freymueller, J.T., J.N. Kellogg, V. Vega (1993). Plate Motions in the North Andean Region. J. Geophys. Res. 98, B12, 21.853-21.863.

García, L.E., A. Sarria, A. Espinosa, C.E. Bernal, M. Puccini (1984). Estudio general de riesgo sísmico de Colombia. Asociación Colombiana de Ingeniería Sísmica y Departamento Nacional de Planeación, 243 pp., Bogotá.

Garwood, N.C., D.P. Janosh, N. Brokaw (1979). Earthquake-caused Landslides: A Major Disturbance to Tropical Forests. Science, 205, 7 September, pp. 997-999.

Gershanik, S. (1995). Sismología en Argentina. Buenos Aires

Giesecke M., A. (1995). Personal commmunication. CERESIS, Lima.

Gibbs, W.W. (1995). Lost Science in the Third World. Scientific American, August, 76-83.

Grases G., J. (1995). Comunicacion personal.

Grases G., J. (1994). Venezuela / Amenazas naturales, terremotos - maremotos - huracanes. Academia de Ciencias Físicas, Matemáticas y Naturales de Venezuela, Cámara de Aseguradores de Venezuela, Caracas, 162 p.

Grases G., J. (1994). Terremotos destructores del Caribe 1502 - 1990. Oficina Regional de Ciencia y Tecnología de la UNESCO para América Latina y el Caribe - ORCYT, Montevideo, 132 p.

Healy, J.H., V.G. Kossobokov, J.W. Dewey (1992). A Test to Evaluate the Earthquake Prediction Algorithm, M8. U.S. Geol. Survey Open-File Report 92-401, 222 pp. and 5 App.

IASPEI - Int. Assoc. of Seismology and Physics of the Earth's Interior, ESC - European Seismological Commission (1993).The Practice of Earthquake Hazard Assessment. R.K. McGuire edit.. 284 pp.

IISEE - Int. Institute of Seismology and Earthquake Engineering (1994). Year Book, Vol. 23. Building Research Intitute, Ministry of Construction, Ibaraki, Japan.

IOC- Intergovernmental Oceanographic Commission of UNESCO (1995). Proceedings, XV Int. Coordination Meeting of the Tsunami Warning System in the Pacific, Papeete. UNESCO, Paris.

Jarrard, R.D. (1986). Relations among subduction parameters. Reviews of Geophysics 24, no. 2, 217-284.

Kagan, Y.Y., D.D. Jackson (1995). New seismic gap hypothesis: Five years after. J. Geophys. Res. 100, B3, 3943-3959.

Keilis-Borok, V.I. (1990). Introduction: Non-linear systems in the problem of earthquake prediction. Physics of the Earth and Planetary Interiors, Special Issue on Intermediate-Term Earthquake Prediction: Models, Algorithms, Worldwide Tests.

Kossobokov, V.G., V.I. Keilis-Borok (1990). Localization of Intermediate-Term Earthquake Prediction. J. Geophys. Res. 95, B12, 19.763-19.772.

Meijer, P.Th., M.J.R. Wortel (1992). The Dynamics of Motion of the South American Plate. J. Geophys. Res. 97, B8, 11.915-11.931.

Mercier, J.L., M. Sebrier, A. Lavenu, J. Cabrera, O. Bellier, J.-F. Dumont, J. Machare (1992). Changes in the Tectonic Regime Above a Subduction Zone of Andean Type: The Andes of Peru and Bolivia During the Pliocene-Pleistocene. J. Geophys. Res. 97, B8, 11.945-11.982.

Meyer, Hj. (1994). Prevención de tsunami en Colombia. Memorias, Conferencia Interamericana sobre Reducción de los Desastres Naturales, vol. I, A-04, Cartagena de Indias.

Montessus de Ballore, F. (1906). La Géographie Séismologique, Cap. XX, Les Andes. Lib. Armand Colin, Paris, 356-372.

Nishenko, S.P. (1989). Circum-Pacific Seismic Potential 1989-1999. U.S. Geological Survey Open-File Report 89-86.

Okal, E.A., J. Talandier (1987). M_m: Theory of a variable-period mantle magnitude. Geophys. Res. Letts. 14, 836-839.

OSSO (1995). Evaluación de amenazas, vulnerabilidades y riesgos naturales para las redes de transporte del Sistema Nacional de Masificación de Gas. Informe final a Empresa Colombiana de Petróleos, Observatorio Sismológico del Suroccidente - OSSO, Universidad del Valle, Cali.

OAS - Organization of American States (1991). Primer on Natural Hazard Management in Integrated Regional Development Planning. Dept. of Regional Development and Environment. Washington, D.C.

Olson, R.S. (1989). The Politics of Earthquake Prediction. With Bruno Podesta and Joanne M. Nigg. Princeton University Press, 187 pp.

Paz, M. (1994). International Handbook of Earthquake Engineering - Codes, Programs and Examples. Chapman & Hall.

Pearce, R.G. (1995). Personal communication, Dept.òf Geology and Geophysics, University of Edinburgh.

Ponce, L., E. Bacigalupo, E. Kausel (1994). Spatio-temporal variations of b-value before and after the March 3, 1985 (Mw=8.0) Chilean earthquake: evidence of a precursory anomaly. Abstracts, Regional Seismological Assembly in South America, Brasilia.

Pulido, N. (1995).La Red Nacional de Acelerógrafos. Memorias, Seminario Sismotectónica de Colombia, Sociedad Colombiana de Geotecnia & Ingeominas, Bogotá.

Page, W.D. (1986). Geología sísmica y sismicidad del Noroeste de Colombia. ISA, Integral y Woodward-Clyde Consultants, 281 pp., Bogotá.

Presgrave, B. (1995). Personal communication, NEIC-National Earthquake Information Center, US Geol. Survey.

Ramírez, J.E., L.T. Aldrich (1977). The ocean-continent transition in SW-Colombia. Instituto Geofísico-Universidad Javeriana, Bogotá.

Rivera, L.A. (1995). Personal communication, Inst. de Physique du Globe, Univ. de Strasbourg.

Ramírez, J.E. (1977). Historia del Instituto Geofísico al conmemorar sus 35 años. Instituto Geofísico - Univesidad Javeriana, Vol. I, II. Bogotá.

Ramírez, J.E. (1971). Historia de la Sismología en Colombia. Geofísica Panamericana, I, no. 1, 179-195, PAIGH, La Paz.

Ramírez, J.E., T. Aldrich (1978). Nariño Project. Instituto Geofísico de los Andes Colombianos, Bogotá.

Rudolph, E., S. Szirtes (1911). Das kolumbianische Erdbeben am 31. Januar 1906. Gerland's Beiträge zur Geophysik, XI, 1, p. 132-275, Leipzig.

Shepherd, J.B., J.G. Tanner (1994). Revised Earthquake Catalogue for Latin America and the Caribbean. Proceedings, Regional Seismological Assembly in South America, Brasilia.

Schindele, F., D. Reymond, E. Gaucher, E.A. Okal (1995). Analysis and Automatic Processing in Near Field of Eight 1992-1994 Tsunamigenic Earthquakes: Improvements Towards Real-Time Tsunami Warning. Submitted to PAGEOPH.

Schneider, J.F., W.D. Pennington, R.P. Meyer (1987). Microseismicity and focal mechanisms of the intermediate-depth Bucaramanga nest. J. Geophys. Res. 92, B13, 13.913-13.926.

Shuto, N. (1989). Numerical Simulation of Tsunamis - Its Present and Near Future. Natural Hazards, 4, 171-191.

Smithsonian Institution (1989). Global Volcanism 1975-1985. Edit. McClelland, L., T. Simkin, M. Summers, E. Nielsen, T. Stein. Prentice Hall and American Geophysical Union, 655 pp.

Smithsonian Institution (1981). Volcanoes of the World. Edit. T. Simkin. Hutchinson Ross, Stroudsburg, 240 pp..

Soloviev, S.L., Ch.N. Go (1984). Catalogue of Tsunamis on the Eastern Shore of the Pacific Ocean. Canadian Translation of Fisheries and Aquatic Sciences 5078, S.O. Wigen compiler, Institute of Ocean Sciences, 285 p., Sidney, B.C., Canada.

Soloviev, S.L., Ch.N. Go, Kh.S. Kim (1992). Catalog of Tsunamis in the Pacific 1969- 1982. Academy of Sciences of the USSR, Soviet Geophysical Committee, Results of Researches on the International Geophysical Projects, 208 p., Moskow.

Universidad de Chile (1995). WWW homepage, Internet.

USGS/NEIC (1994). PDE Catalogue, Global Hypocenter Data Base, Version 3.0

Velásques, A. (1990). Estudios históricos de desastres y medidas de prevención en América Latina. Informe manuscrito, Proyecto UNDRO/ACDI/ONAD "Mitigación de Riesgos en Colombia", OSSO, Universidad del Valle, Cali.

Veloso, J.A.V., J.E.P. Soares, J.C. Velásquez (1994). Earthquakes in Paraguay: an appraisal. Abstract, Regional Seismological Assembly in South America, Brasilia.

Yepes, H., J. Fernández, J. Valverde, J.L. Chatelaine, B. Tucker, G. Hoefer, C. Villacis, T. Yamada, F. Kaneko, G. Bustamante (1994). An example in Quito, Ecuador, of the use of seismic microzoning for risk reduction in developing countries. Abstracts, Regional Seismological Assembly in South America, Brasilia.

VULNERABILITY AND RISK ASSESSMENTS RELATED TO EARTHQUAKE AND VOLCANIC THREATS IN SOUTH AMERICA AND RESPECTIVE ACTIONS IN LANDUSE REGULATIONS, DEVELOPMENT PLANNING, BUILDING CODES, CIVIL DEFENSE ETC. ON A NATIONAL AND REGIONAL SCALE

Hansjürgen Meyer

Observatorio Sismológico del SurOccidente - OSSO,
Universidad del Valle
Cali - Colombia

1. INTRODUCTION

Of the two main factors which determine the level of risk due to natural phenomena - hazard and vulnerability - the latter is far more controllable. The power of earthquakes cannot be reduced, but we can identify and reduce the exposure and susceptibility of our habitats and lives to these powers, dwelling far enough from their influence, giving our buildings and systems enough strength, being prepared to escape their impacts, or just being prepared to attend and manage the consequences of their occurrence. While the first is certainly the safest approach, the last was until not long ago the most common, if not the only. Meanwhile, the enforcement of strength of structures - via building codes - became the most used means to reduce seismic risk. Nowadays many cities in South America's (SA) earthquake prone regions have significant proportions of their buildings designed under such provisions. This reduction of risk is mostly an achievement of the last 2-3 decades.

However, all available figures and scenarios show that the potential for disasters in SA is growing, due to increasing amount of elements at risk and their vulnerability and, more specifically, due to the still dominating development models (Declaración de Cartagena, 1994); high population growth rates, accelerated urbanization processes, landuse tendencies, impoverishment of large segments of the population and obsolete schemes of social organization have been increasing the vulnerability to all kinds of dangerous natural phenomena. Disasters due to natural phenomena in SA in present times should largely be considered as an unresolved problem of the development process (Maskrey, 1994).

So, being exposed to high levels of seismic hazards in most of its densely populated areas, SA sustains apparently outrunning risk problems, due to generic problems of developing regions. Many of the now multi-million cities in SA's seismically active rim have sustained devastating earthquakes during their pre-modern times (Silgado, 1985) and their present behavior under earthquake stresses can only be imagined.

Research on vulnerability and risk problems has probably been much less than on hazards. Moreover, research and actions on vulnerability and risk have been focusing primarily physical and technical aspects, rather than those of cultural, social and economical order (Maskrey, 1994).

This status and tendencies of earthquake risk in SA could face those striving for more and better knowledge on seismicity and seismic hazards with questions like: Is it worth the effort? Can and should seismologists contribute to enhance the social impact of their expertise and information? Should seismologist spend efforts on direct interaction with other social sectors and groups for the purposes of mitigation?

This paper is a brief attempt to sample some interesting and hopefully representative traits and tendencies - historical, socioeconomical, technical, institutional, legal, etc. - of earthquake and volcanic risk assessment and mitigation in SA. It is a complement to one on earthquake hazards in South America (Meyer, this volume). As it was the case in that paper, rather frequent references to Colombia do not imply anything but the author's relative level of

acquaintance. Hopefully these details on one country may partly exemplify developments in a region whose countries have very much in common in its historic development, cultures and present socioeconomical conditions, and in their geologic hazards too.

2. ASSESSMENT AND MITIGATION OF RISK - SOME HISTORICAL, CULTURAL, SOCIOECONOMICAL AND INSTITUTIONAL ASPECTS

2.1 Historical development of vulnerability

Not much is known about how pre-hispanic cultures in SA acted and reacted with respect to Nature's adverse phenomena. Many facts await their interpretation: still intact structures from the Inca culture on steep slopes; height-seeking dwellings of ancient cultures on Colombia's and Ecuador's Pacific coast, and many others. During Spanish and early Republican times, earthquake disasters occurred frequently and are, in most cases, well documented. Attempts to regulate construction are known from the XVIII century. But, in general, building types did not change substantially during four centuries. Adobe construction, for instance, was still common by the turn of the century.

Most countries in SA began their turn towards modern societies and emerging industrialization about a century ago. Complex and often rapidly changing social, political and economical processes led to vulnerability-boosting processes such as accelerated growth of population, even higher growth rates of urban population, urban expansion to lesser quality terrain such as slopes and soft soils, rupture of social organization, improvised housing built by untrained people, impoverishment of former rural population, desperate striving for survival which suppressed caring for any long-term concerns, incursion of rather unfamiliar building technologies, etc.

One of the risk-increasing effects entailed by the explosive growth of urban centers is the progressive occupation of lesser quality terrain. The city of Cali (Colombia) could be an example for many others: until about half a century ago (Velásquez & Meyer, 1994) the city, with a population of about a quarter of a million, occupied only rather flat areas and firm soils. Further development, to now about 2 million inhabitants, extended with mostly illegal and uncontrolled settling to steep slopes and rather unconsolidated alluvial soils. The first landslide, destructive indeed, in Cali's more than 450-year history occurred just a few decades ago.

Recently two strong earthquakes in Colombia (Murindó, 1992:10:18 and 19; Páez, 1994:04:06) have drawn attention to a specific kind of vulnerability which had not been noted before; it could be called "ethnic vulnerability". Remaining indigenous groups tend to be rather endemic, living in small and often mountainous areas. The Páez earthquake (M=6.4, h_0=10 km) affected a large portion of the habitat of the Páez group, an estimated 100.000 community living largely on agriculture on mostly steep terrain. The earthquake caused extensive landsliding, a large mudflow, destroyed most of the important roads and bridges and grounded entire villages, leaving more than 1000 people dead and about 35.000 homeless. The event was a major impact and rupture to a socially very organized group; it may have left deep and irreversible negative social and even cultural consequences. The national government established an institution to deal with the consequences and coordinate reconstruction. The earthquake occurred in one of the major active tectonic systems, but in an area without known historic large earthquakes nor seismicity above background. Something similar, although with less dramatic impact, occurred (18 and 19 Oct. 1992) in NW-Colombia when two shallow earthquakes with magnitudes about 7 hit a region - largely rainforest covered - were groups of the Emberá-Katio group settled. These events also caused extensive landsliding and displaced an unknown number of indigenous groups.

The development process and the tendency to use more modern building materials and techniques can also lead to an increase of vulnerability. Large segments of the mostly low-income population in SA lived in traditional housings which have significant levels of resistance to shaking and do not require much understanding of earthquake-related behavior and design, such as "quincha" (wood+earth) in Perú, wood in Colombia's Pacific coast and "bahareque" (bamboo+earth) in Colombia. These dwellings are now being replaced by more modern and wealth-reflecting materials, mostly rigid and brittle, which impose certain

measures to withstand strong shaking, not generally known or considered as expensive and not entirely necessary.

With respect to volcanic hazards, the roots of the present levels of exposure and vulnerability are much older: the fertile soils and good irrigation they generate have always been a strong attraction.

2.2 Education and training

While earthquake hazard evaluation has been fostered and done mostly by individuals and organisations from the government and academic sectors, the actors in the process of evaluating and mitigating risks are from a much more diverse social base, actually spanning the whole community.

While the education and training of those professionals prepared for earthquake and seismic hazard studies is still limited to a few programs and components in affine careers, engineering programs which include earthquake risk reduction techniques or specialize in earthquake engineering are much more common. However, non-engineering knowledge and programs related to earthquake risk evaluation and control, be it in fields like architecture, economics, political sciences, history, psychology, sociology, etc., is still exceptional. Some universities are beginning to offer now graduate courses focusing on medical, social and organizational aspects of risk and disaster management (Muñoz, 1994).

More than 120 professionals from South American countries have been graduated since 1960 from the 1-year Earthquake Engineering courses held at the Int. Institute of Seismology and Earthquake Engineering, in Japan (IISEE, 1994).

Regarding the international training courses on Earthquake Engineering held at the University of Skopje (Macedonia,Yugoslavia) it should be pointed out, at least for students from Colombia, that they provided the concepts and techniques of seismic vulnerability assessment, which proved a very necessary complement, for a country with cities where pre-code building and non-engineered structures still outnumber by far those with earthquake resistant designs.

Many professionals from South American countries have been trained since 1989 in the yearly 3-week international seminars held at the CISMID - Centro Peruano-Japonés de Investigaciones Sísmicas y Mitigación de Desastres (Universidad Nacional de Ingeniería, Lima). Participants from diverse fields of activity (government, engineering, social sciences, academia, etc.) present and discuss their achievements and projects in areas such as microzonation, mitigation through urban planning, seismic safety for lifelines and critical facilities, health care centers in seismic areas, etc., and interact with international experts. Since information on earthquake risk and mitigation is less represented in the available literature than topics related to hazards, this kind of seminars also fill an important gap in regional communication and interaction.

With respect to training, one must also include the manuals and guides issued by international agencies, such as OAS (1991), which have fostered application of concepts like development planning with risk and, integrated risk mitigation.

2.3 Institutions

Until now, probably the single most important institution - social group, rather - in the process of technologically based earthquake mitigation in SA are the civil engineers and their professional associations (Grases, 1995). They have been, in many countries, the power behind the process of developing and raising earthquake-resistant design and construction measures to the status of law or professional code. Moreover, their impact at the regional level has been increased through networks (see below).

Probably much more than in the field of hazards evaluation, done primarily at academic and state research institutions, NGOs have a very significant and increasing participation in mitigation efforts, predominantly with educational and technical advice projects for social groups of lower income. It is interesting to note that in some cases (see below) even

governments have chosen to create or join NGOs to channel their policies and resources for risk and disaster mitigation.

One could mention many other groups and institutions which are representative of different sectors and approaches in the mitigation effort, and have been making socially relevant and innovative contributions:

The Centro Peruano-Japonés de Investigaciones Sísmicas y Mitigación de Desastres-CISMID, a research and academic center established with cooperation from Japan in 1986 at the Universidad Nacional de Ingeniería in Lima, is a good example of efficient contribution of the university sector to the mitigation problem. CISMID integrates good technical and scientific resources (including one of SA's few dynamical testing facilities), vigorous training, educational and publishing programs, international support, many socially relevant projects, permanent interaction with other sectors and institutions addressing mitigation problems, thus probably representing a good approximation to how a single organism can make quite integral contributions to the complex risk evaluation and mitigation problem.

While CISMID is a case of a multidisciplinary center working for earthquake risk mitigation, the Fundación para la Prevención de Riesgos Sísmicos-FUNDAPRIS in Mérida, Venezuela, is an interesting case of a coordination and promotion unit and network, which itself does not execute any projects, but rather links and instills many diverse sectors and organisms towards a common aim. FUNDAPRIS was established in 1979 by the provincial government of the state of Mérida (then as a commission, later converted to an autonomous NGO). with strong initiative and commitment from the Laboratorio de Geofísica, Universidad de los Andes (Estévez, 1992), which by that time was establishing a seismic network for the region. FUNDAPRIS now coordinates its members to provide training, advice, specific solutions and public education and information for hazard zonations, risk assessments, earthquake-safe urban development and building and capability for emergency management, as well as support for the regional seismic network. FUNDAPRIS was one of the pioneers of seismic vulnerability assessments in SA. It is also an interesting example of coordination and promotion of mitigation efforts at the provincial level.

Following an initiative from the Grupo de Tecnología Intermedia para el Desarrollo-ITDG (Lima), and considering the rapid increase of vulnerability to diverse natural phenomena of the Latin American population, as well as the fact that strategies and actions towards this risk were still dominated by natural sciences and engineering approaches, members of ten institutions or groups with emphasis on socially-oriented risk and disaster studies founded (1992) the Red Latinoamericana de Estudios Sociales de Desastres - LA RED, thus beginning to fill a severe gap in risk assessment and mitigation previously only addresses by few individuals. LA RED has already held a good number of seminars and workshops in different countries and distributes its publications all over the continent in bookstores.

2.4 International and regional cooperation

While the early stages of earthquake risk mitigation in South America through building codes were largely processes at the national level, initiated and led by individuals or professional associations and their increasing interactions across borders, the influence of regional and international organisms and programs has been playing an expansive and important role in recent decades. Here stands out, again, the regional organization CERESIS - Centro Regional de Sismología para América del Sur, established with initial support from UNESCO and Spain. One could point out here their regional study SISRA (CERESIS, 1985), which included also a section on evaluation of economical effects of earthquakes, and the first regional symposium on earthquake and volcanic hazard and risk, in 1984 (CERESIS, 1985).

International and regional cooperation has been an important factor in training and education, led by institutions such as CERESIS, CISMID and IISEE.

With initial support from UNESCO's regional office, earthquake engineers created (Grases, 1995) the Red Latinoamericana de Centros de Ingeniería Sísmica - RELACIS. Among the activities which have been fostering the communication and interaction between centers and professionals working in seismic engineering are a series of seminars and workshops held in different Latin American countries.

The Organization of American States has also had a strong influence on the unfolding of capabilities for risk evaluation and mitigation in the region, mostly through their Dept. of Regional Development and Environment, with manuals for development planners (OAS, 1991) and support for many specific projects.

UNDHA (former UNDRO) has been playing an increasingly important role, since the inception of the International Decade. Mainly in northern countries (Colombia, Ecuador and Perú) this organism has been financing projects and seeding processes in which the integration of scientific, technical, government, community and NGOs and the assessment of vulnerabilities are crucial components. Recently UNDHA established a regional office in Quito.

In 1992 a Pan-american group initiated by the Central United States Earthquake Consortium-CUSEC began to foster interaction between institutions and professionals in Latin America, with seminars, newsletters and individual projects.

There are also interesting examples of international integrated earthquake risk assessment and mitigation projects in which the private sector has a leading participation (Yepes et al., 1994).

These are but a few examples of regional and international cooperation, but it must be mentioned here too that many institutions and projects started and made their way with only local resources (Estévez. 1992); in other projects the foreign resources were sought to complement and strengthen local efforts (Cardona & Meyer, 1991).

3. ASSESSMENT OF RISKS

The distribution of earthquake and volcanic hazards is probably much better known in SA than the distribution of vulnerability and risk. Certainly the assessment of vulnerabilities is a much newer concept in the region. And, while it has been accepted - and applied - for quite some time that certain components of hazards can be quantified a priori, the non-aleatoric factor in risk - human-made vulnerability - has only very recently been acknowledged by governments as such (see below).

3.1 Historical record

Many publications deal with the historical aspects of earthquake risks (Montessus de Ballore, 1906; Silgado, 1985; Grases, 1994; Velásquez, 1992), although in most cases for the purpose of establishing the catalogue of occurrences. Attempts to identify such aspects as patterns of evolution in risk mitigation strategies or long-term costs are less frequent (Velásquez, 1990).

3.2 Earthquake risks

Many local studies of earthquake risk now go quite beyond the shaking microzonation problem, integrating also such aspects as distribution of vulnerabilities and recommendations for mitigation (Yepes et al., 1994; Cardona & Meyer, 1991).

One of the aspects of earthquake risk which have only recently been receiving strong attention are the secondary losses, which quite often are the really heavier ones, as in the case of the Lago Agrio, Ecuador, event (Schuster, 1991). Only few cases of earthquake disasters have been followed with respect to their long-term effects, such as the 1983 earthquake in Popayán (Colombia).

Most of the data and models on likely direct losses have probably been developed inside the insurance sector. In Colombia, after a series of damaging earthquakes in the last 3 years, the national insurers federation has recently contracted updated loss models, supported with local data.

3.3 Risks from associated hazards - liquefaction, landslides, tsunami

While resistant design and construction is, in most cases, an appropriate and efficient measure for the mitigation of risks induced by strong shaking, secondary hazards such as landslides, liquefaction and tsunami require other types of mitigation strategies, such as reduction of exposure, preparedness for evacuation and even hazard control.

All SA countries which are exposed to tsunami from near sources (Chile, Perú, Ecuador and Colombia) have now ready or in development more or less sophisticated instruments for mitigation of the ensuing risks: detection and warning systems (Chile, Colombia), mapping of most exposed and vulnerable areas (Espinoza, 1992), relocation programs and evacuation plans (Meyer, 1994). In Perú, Ecuador and Colombia UNDHA (former UNDRO) contributed the initial funding for these projects.

The liquefaction potential at regional scales has also been assessed in most countries (CERESIS, 1985; OSSO, 1994) and in some cases it has led to landuse planning and even relocation projects (Castano & Giuliano, 1994; Meyer, 1994). The distribution of potential for induced landslides is also known at different scales (CERESIS, 1985; OSSO, 1985), but the extension of susceptible terrain is too large, at least in tropical and Andean SA, as to allow radical and really covering countermeasures in the foreseeable future. Yet, in some cases (OSSO, 1994) the state has provided legal instruments and resources to relocate population in areas identified as most prone to such phenomena (see below).

3. 4 Volcanic hazards in Southamerica

A comprehensive and detailed account of volcanic activity and hazards in South America is included elsewhere in this volume (Malavassi-Rojas). This section only recalls a few basic facts about volcanoes in the region.

The Smithsonian catalogue (Simkin et al., 1981) lists six countries in South America with active volcanoes: Argentina (3), Bolivia (15), Chile (62), Colombia (13), Ecuador (10, + 13 on Galápagos Islands) and Perú (10). All these foci are linked to the subduction zone and have dominantly explosive activity. 21 of these had activity in the decade 1975-1985 (Smithsonian Institution, 1989); among them was the tragic eruption and lahar of volcano Nevado del Ruiz, the northernmost of the active Southamerican volcanoes, in Colombia. All these volcanoes are located in the high Andes; many are ice-clad and drain to extended basins. The volcanoes in Colombia and Ecuador are also in areas with high pluviosity and extensively covered with thick soils. Thus, associated phenomena such as mudflows are very often the principal hazard factors.

Although systematic studies of the region's volcanoes have been made since long ago (Stübel & Wolf, 1906; Hantke & Parodi, 1966), analysis - mapping, monitoring - of their hazards are much more recent. Yet, once again, the Spanish past reveals noteworthy examples of interest for natural phenomena and rigorous documentation: during recent studies (Velásquez, 1992) at the Archivo General de Indias (Sevilla, Spain) colored views of a Ecuadorian volcano (Tungurahua) were found, depicting in detail the type of phenomena and affected areas, for an eruption on 23 April 1773.

Modern hazard assessments date back to the last 15-20 years. For example, volcanoes in Ecuador are being monitored (Hall, 1988) since the early '80; hazard maps were made for all historically active volcanoes. In Colombia the monitoring of volcanoes began shortly before the 1985 Nevado del Ruiz eruption; now all active volcanoes are monitored continuously - at least with seismic stations - by the national geological survey (Ingeominas).

Several cities in SA are known to be within the radius of likely severe effects of volcanic eruptions, for example Perú's second largest city, Arequipa, on the slopes of El Misti (DHA/Ginebra-INDECI, 1995) or Pasto (SW-Colombia, 300.000 inhab.), beside volcano Galeras.

Almost all volcanoes with historic activity in SA have now hazard maps, predominantly based on type and extent of known deposits. Some lack information on long-term recurrence of eruptive activity.

4. MITIGATION

4.1 Programs

A list of programs for mitigation of earthquake and volcanic risk in SA would be very long. Most of these programs are probably of educational character. Among the numerous interesting ones, a program which stands for many others, is an adobe improvement project (CERESIS and Univ. Católica, Lima; GTZ); it addresses one of the still very common traditional building types in SA, which usually have no elements to resist lateral forces.

Another type of innovative mitigation program are those which integrate steps from hazard evaluation to mitigation planning, involving diverse sectors and institutions. In Colombia such projects have been in progress in Medellín (González, 1995), with UNDP-support, and in Cali (Cardona & Meyer, 1991), with UNDHA-support. The project in Cali, started in 1989, has already induced to such activities as retrofitting of official buildings, landuse regulations (Velásquez & Meyer, 1994) and relocation programs.

4.2 Legislation and risk control - Colombia as an example

Laws and codes for risk and disaster control have been developing in response to various processes and events, but the factors which most strongly induced their development could be quite similar in most countries. Legislation for risk control is typically "after the fact", and the most powerful in this case are disasters.

Until recently, the problem of risk and disasters was left to NGOs which traditionally took charge of it worldwide, and to Civil Defense. Major disasters were managed directly from high-level government authorities, such as the President's office or the Ministry of the Interior. In 1979 (Ley 9) preparedness and disaster management was placed under the coordination of the Ministry of Health and its regional and local dependencies, with the Red Cross and the Civil Defense as main operational organisms.

When an earthquake hit in 1983 hard the city of Popayán, releasing a wave of awareness and sensibility at all levels, the Asociación Colombiana de Ingeniería Sísmica was ready with a code which had been developed during the previous years and already applied by many structural engineers; it became a national law soon (Ley 1400, 1984).

The Nevado del Ruiz volcano tragedy (Nov. 1985) set off a radical change in policy. A permanent coordination office for mitigation and management was established at the President's office and Law # 46 (1988) created the Sistema Nacional para la Prevención y Atención de Desastres, with startup funds from UN organisms. It is decentralized and distributes responsibilities among the three levels of government. For the first time risk evaluation, mitigation and management got a permanent state budget (Fondo Nacional de Calamidades) and also for the first time mitigation was declared a priority and vulnerability acknowledged as the prime factor of risk, thus officially accepting that disasters from natural phenomena are not only occurrences in the realm of uncontrollable chance. This law and its regulatory decrees mandated vulnerability and risk evaluations for all municipalities and infrastructure projects and created a set of national hazard monitoring and evaluation systems.

The drive for risk mitigation was such that some regulations had to be revised (Ley 2, 1992), such as a part of the Urban Reform law (# 9, 1989), which threatened local authorities considered as acting too slow or not at all with respect to risk problems with penal suits and sentences up to jail. Majors are now allowed prudential times for risk mitigating actions.

Through the Ministry of Development and its dependency in charge of urban development and housing - INURBE - the State instituted a system of subventions for the relocation of population in areas of high risk.

Further government support for risk mitigation, mainly at the local level, came through recently established national funds which promote with partial funding infrastructure projects which aim at or include risk mitigation.

However, in a country where more than 75% of the population live in areas prone to strong

earthquakes and landslides, among other phenomena, all these innovative legal and financial instruments for risk mitigation have to be adjusted, priorities have to be set, etc.

4.3 Landuse regulations

Probably most difficult to enforce among the different approaches to risk mitigation is the landuse planning (except siting of state-owned infrastructure), due to its competition against the market value of land and probably other factors such as the accelerated rural immigration. However, there are examples of successful regulation and control. In Colombia these cases are more common in areas where several types of hazards come together, such as on sloping terrain.

The exposed areas and elements at risk for volcanic hazards are much more confined and thus easier to assess. Even so, there are few cases of successful landuse regulation, perhaps also due to the fact that disastrous volcanic events have been much less frequent than big earthquakes in recent times in SA.

4.4 Earthquake risk and infrastructure

Modern societies and cities are characterized also by complex and highly interactive systems and functions. The entailing high levels of secondary risks have already shown strong impacts in SA. For instance, the economical and social impact of the Lago Agrio earthquake in Ecuador, 1987 (Schuster, 1991), which set off landslides that destroyed a critical part of the country's oil exporting infrastructure, is still detectable.

In many SA countries the first compulsory measures for earthquake-mitigating siting and design in modern times were probably those imposed by international lenders for development projects, such as the Interamerican Development Bank for hydroelectric projects in Colombia. In hindsight one could say that these regulations had a wider impact, on the awareness and expertise of the local engineering community and as transfer of hazard evaluation capabilities. Presently, also due to recent legislation for risk mitigation and environmental protection, almost all infrastructure projects require evaluation of hazards including earthquakes. To mention one example: the design of a nationwide gas transport system in Colombia has been based on a previous regional evaluation of hazards and vulnerabilities (OSSO, 1995) and the planning authority for W-Colombia ordered a study (OSSO, 1994) which provided the government offices and development institutions in the region for the first time with a comprehensive set of maps and a manual, for first-order evaluations of the levels of exposure to natural hazards and for decisions on further studies and mitigation strategies.

4.5 Building codes

Although modern seismic building codes have been developed and enforced, as elsewhere, during recent times, there are some surprising historical facts. For instance, Colombia's first newspaper, the "Aviso del Terremoto", issued (1785) after a strong earthquake which struck a few days before the capital, Santafé de Bogotá, contains recommendations and rules which reflect remarkable insight to seismic vulnerability (mixing of building materials, use of adobe walls in multi-story buildings). Another example of early mitigation policies and measures can be found in E-Argentina's seismic zone (Castano & Giuliani, 1994), where the first landuse regulations and building codes for seismic safety were issued and enforced since 1861.

A recent worldwide review of seismic resistant building codes (Paz, 1994) includes eight countries from SA. Most seismic countries in the region have their seismic codes now at the level of national laws; in some (Ecuador, for instance) the code is being held and enforced at the level of professional associations.

In most countries, if not all, large segments of the population are not covered by seismic building codes or not reached by the enforcement mechanisms. Some of these are being taken care of by building loan organisms, which require earthquake insurance (in turn demanding evidence of seismic resistance design). Others, mostly non-engineered structures in low income groups, have been subject of many projects aiming at voluntary action, through training

programs and manuals (CERESIS, CISMID, SENA in Colombia, and others).

While building codes have been the most traditional, feasible and efficient mitigation measure for earthquakes (except their associated phenomena landslides and tsunami), for volcanic hazards the general tendency is to instill or mandate more radical measures, such as landuse regulation and relocation of exposed population.

4.6 Preparedness and disaster management

The most traditional institutions in disaster preparedness and management - Red Cross and Civil Defence - are on the scene in all SA countries and may have taken most of the burden of disaster management in modern times. Pérez (1994) gives a presentation, from the view of the Panamerican Health Organization, of the state of preparedness in 10 SA countries, including training and educational programs at university level.

In some countries, at least in Colombia, it has been a practice of the central government to create temporary organisms, even under private law, to manage the aftermath and the reconstruction process. This was the case for the 1983 Popayán earthquake (Corporación para la Reconstrucción del Cauca), for the 1985 Ruiz disaster (the now extinct Resurgir), and for the 1994 Páez earthquake (Corporación Nasa Kiwe).

4.7 Response to earthquake predictions

Earthquake predictions originated from scientific bodies or individuals have had an impact on risk mitigation in South American countries too. The case which generated most resonance (and possibly social impact too) was the "Brady-Spence prediction", published in the mid '70 in scientific journals. The most detailed available account of this prediction - although not with a seismological nor risk mitigation scope - is probably in Olson (1989). This prediction announced a large event in proximity of Perú's capital for mid-1981 (similar to one which struck the city disastrously in the XVIII century); it was issued by members of well known and renowned institutions (U.S. Bureau of Mines and U.S. Geol. Survey) and it was stated in terms of a rather narrow time window. The phenomena did not occur and the consequences of the prediction, which became public in Perú about a year ahead of the announced dates - were profound and very damaging.

The hazard evaluation aspects of the Colombian tsunami mitigation program (UNDHA & DNPAD, 1995) work with a multiple-window strategy (Meyer, 1994), using available concepts such as the traditional seismological tsunami potential estimation techniques, intermediate-term earthquake prediction and recurrence evaluation with historical data, in order to have some level of knowledge about the proximity of large (tsunamigenic) earthquakes. The first results of a intermediate-term earthquake occurrence analysis, obtained in cooperation with the Int. Institute of Earthquake Prediction Theory and Mathematical Geophysics (Russian Academy of Sciences), which diagnosed a window (5 years) of increased probability of occurrence in SW-Colombia, were presented by OSSO to the national disaster prevention authority in May 1991. Among the mitigation measures which this communication entailed was a resettlement program for the 3500 most exposed families in the port of Tumaco (SW-Colombia), now under way, with partial support (about US 10 million) from the European Union.

One could dare to identify a pattern in how it is being reacted to earthquake predictions: while long-term forecastings (Nishenko, 1989), although widely communicated, go by relatively unnoticed and short-term predictions (Olson, 1989) cause more or less chaotic and adverse reactions, intermediate-term forecasts (Meyer, 1994) tend to induce rather controlled and beneficial actions.

CONCLUDING REMARKS

While the social processes which have been causing accelerated increase of risk due to earthquake hazards (and other natural phenomena too) began long ago, the processes which aim at characterizing risks and mitigating them began just a few decades ago and their

priorities have to compete with many others, more recurrent and more perceived. What is important for now is that much has been created in recent decades - concepts, human resources, programs, institutions - and that these innovations have ensued ongoing processes, including increasing awareness, policy changes at government levels and a rapidly growing amount of exposed elements with reduced vulnerability. For those working in the sciences of hazards evaluation it is probably most important - besides continuous efforts to improve their expertise, tools and results - to reach for an efficient communication and interaction with other disciplines and social sectors with responsibilities in risk mitigation.

REFERENCES

Aviso del Terremoto (1785). No. 1-3, Bogotá, Facsimile published by COLCULTURA, Bogotá.

Campos, A. (1994). Evaluación de la vulnerabilidad sísmica de líneas vitales y estrategias para la mitigación del riesgo en Cali, Colombia. Memorias, Conferencia Interamericana sobre Reducción de los Desastres Naturales, vol. I, A-12, Cartagena de Indias.

Cardona, O.D., Hj. Meyer (1991). Integrated urban seismic risk mitigation project. Proceedings, IV Int. Conference on Seismic Zonation, vol. III, p. 139-147, EERI, Stanford, CA.

Castano, J.C., A.P. Giuliano (1994). La prevención sísmica en la República Argentina. Memorias, Conferencia Interamericana sobre Reducción de los Desastres Naturales. vol. III, D-07, Cartagena de Indias.

CERESIS - Centro Regional de Sismología para América del Sur(1989). Riesgo volcánico-Evaluación y mitigación en América Latina. Lima. 298 p.

CERESIS (1985). Earthquake Mitigation Program in the Andean Region (Proyecto SISRA), vols. 1-14, Lima.

Declaración de Cartagena (1994). Memorias, Conferencia Interamericana sobre Reducción de los Desastres Naturales, vol. III, Cartagena.

DHA/Ginebra - INDECI (1995). Programa de Mitigación de Desastres en el Perú. Informe de Proyecto, Departamento de Asuntos Humanitarios de las Naciones Unidas, Ginebra, e Instituto Nacional de Defensa Civil del Perú, 22 p.

Espinoza, J. (1992). Efectos potenciales de un tsunami en la costa norte de la Provincia de Esmeraldas - Ecuador, Proyecto UNDRO/ECU/91/004. INOCAR-Instituto Oceanográfico de la Armada del Ecuador, Guayaquil, 52 p.

Estévez, R. (1992). Personal communication. Laboratorio de Geofísica, Universidad de los Andes, Mérida, Venezuela.

Giesecke, A. (1995). Personal communication. CERESIS, Lima.

González, L.F. (1995). Personal communication. Proyecto Alcaldía-UNDP Prevención de Riesgos, Medellín.

Grases G., J. (1995). Comunicacion personal.

Grases G., J. (1994). Venezuela / Amenazas naturales, terremotos - marEmotos - huracanes. Academia de Ciencias Físicas, Matemáticas y Naturales de Venezuela, Cámara de Aseguradores de Venezuela, Caracas, 162 p.

Grases G., J. (1994). Terremotos destructores del Caribe 1502 - 1990. Oficina Regional de Ciencia y Tecnología de la UNESCO para América Latina y el Caribe - ORCYT, Montevideo, 132 p.

Hall, M.L., B. Beate, C.G. Hillebrandt (1988). Mapa de los peligros volcánicos potenciales asociados con el volcán Tungurahua, Provincia de Tungurahua. Instituto Geofísico. Escuela Politécnica Nacional. Impresión Instituto Geográfico Militar, Quito. Escala 1:50.000.

Hantke, G., I. Parodi (1966). Catalogue of the Active Volcanoes of the World including Solfatara Fields. Part XIX, Colombia, Ecuador and Perú. Int. Assoc. Volc. Chem Earth's Interior, Rome.

IHA (1990). Instrucciones Generales sobre el Sistema Nacional de Alarma de Maremotos. Instituto Hidrográfico de la Armada de Chile, 3a Edición, 35 p., Valparaiso.

IISEE - Int. Institute of Seismology and Earthquake Engineering (1994). Year Book, Vol. 23. Building Research Intitute, Ministry of Construction, Ibaraki, Japan.

LA RED (1992). Agenda de investigaciones y constitución orgánica. ITDG/COMECSO, editores, Lima, ITDG, 60 p.

Lavell, A., compiler (1994). Viviendo en riesgo: comunidades vulnerables y prevención de desastres en América Latina. LA RED/FLACSO/CEPREDENAC, Talleres de Tercer Mundo Editores, Bogotá, 386 pp.

Lavell, A., R. Pérez (1994). Desastre y Sociedad en América Latina: Directorio de investigadores, instituciones y proyectos. LA RED/FLACSO/Centro de Documentación de Desastres - OPS/CEPREDENAC, San José, Costa Rica, 246 pp.

Maskrey, A. (1994). Comunidad y desastres en América Latina: estrategias de intervención. Memorias, Conferencia Interamericana sobre Reducción de los Desastres Naturales, vol. II, 2-04, Cartagena de Indias.

Meyer, Hj. (1994). Prevención de tsunami en Colombia. Memorias, Conferencia Interamericana sobre Reducción de los Desastres Naturales, vol. I, A-04, Cartagena de Indias.

Montessus de Ballore, F. (1906). La Géographie Seismologique, Cap. XX, Les Andes. Librairie Armand Colin, Paris, 356-372.

Nishenko, S.P. (1989). Circum-Pacific Seismic Potential 1989-19999. US Geol. Survey Open-File Report 89-86.

OAS (1991). Primer on Natural Hazard Management in Integrated Regional Development Planning. Organization of American States - OAS, Dept. of Regional Development and Environment. Washington, D.C.

Olson, R.S. (1989). The Politics of Earthquake Prediction. With Bruno Podesta and Joanne M. Nigg. Princeton University Press, 187 pp.

OSSO (1994). Atlas Regional de amenazas, vulnerabilidades y riesgos en el Occidente Colombiano. Informe final a Consejo Regional de Política Económica y Social - CORPES, Observatorio Sismológico de Suroccidente - OSSO, Universidad del Valle, Cali.

OSSO (1995). Evaluación de amenazas, vulnerabilidades y riesgos naturales para el sistema de transporte del Plan Nacional de Masificación de Gas. Informe final a Empresa Colombiana de Petróleos-Gerencia de Gas, Observatorio Sismológico del Suroccidente - OSSO, Universidad del Valle, Cali.

Paz, M. (1994). International Handbook of Earthquake Engineering - Codes, Programs and Examples. Chapman & Hall.

Pérez, L.J. (1994). Informe sobre preparativos, prevención y atención de emergencias en América del Sur. Memorias, Conferencia Interamericana sobre Reducción de los Desastres Naturales, vol. I, 1-01, Cartagena de Indias.

Schuster, R.L. edit. (1991). The March 5, 1987, Ecuador Earthquakes - Mass Wasting and Socioeconomic Effects. Natural Disaster Studies, vol. 5, Committee on Natural Disasters, National Research Council, National Academy Press, Washington D.C., 163 p.

Silgado, E. (1985). Destructive earthquakes of South America 1530-1894. Earthquake Mitigation Program in the Andean Region (Proyecto SISRA), Vol. 10, CERESIS - Centro Regional de Sismología para América del Sur, Lima.

Smithsonian Institution (1989). Global Volcanism 1975-1985. Edit. McClelland, L., T. Simkin, M. Summers, E. Nielsen, T. Stein. Prentice Hall and American Geophysical Union, 655 pp.

Smithsonian Institution (1981). Volcanoes of the World. Edit. T. Simkin. Hutchinson Ross, Stroudsburg, 240 pp.

Stübel, A., T. Wolf (1906). Die Vulkanberge von Colombia. Verlag Wilhelm Baensch, Dresden.

UNDHA (1994). Tsunamis - Evacuación de la población y planes de uso del suelo para mitigar sus efectos - Localidades estudiadas en el Perú entre 1981 y 1994. Publ. Instituto Nacional de Defensa Civil - INDECI y Marina de Guerra del Perú, Lima, 30 p and annex.

UNDHA, DNPAD (1995). Programa de Mitigación de Riesgos en Colombia. Informe de proyecto 1988-1994, Departamento de Asuntos Humanitarios de las Naciones Unidas, Ginebra y Dirección Nacional para la Prevención y Atención de Desastres, in press.

UNDRO (1990). Proyecto para la prevención y preparación para desastres en el Ecuador u países vecinos. Informe Técnico, Quito, 19 p.

Velásquez, A. (1995). Personal communication. OSSO, Universidad del Valle.

Velásquez, A. (1992). Informe de misión sobre estudios en el AGI a UNDRO. Observatorio Sismológico del SurOccidente - OSSO, Universidad del Valle, ?? p., Cali.

Velásquez, A., Hj. Meyer (1994). Ofertas y amenazas ambientales en Cali. Serie Publicaciones Ocasionales del OSSO, No. 3, Observatorio Sismológico del Suroccidente - OSSO, Universidad del Valle, Cali.

Velásquez, A., Hj. Meyer, W. Marín, A. David, A. Campos, M. Hermelin, S. O. Bender, M. Arango (1994). Planificación regional del Occidente Colombiano bajo consideración de las restricciones por amenaza. Memorias, Conferencia Interamericana sobre Reducción de los Desastres Naturales, vol. III, Cartagena de Indias.

Yepes, H., J. Fernández, J. Valverde, J.L. Chatelaine, B. Tucker, G. Hoefer, C. Villacis, T. Yamada, F. Kaneko, G. Bustamante (1994). An example in Quito, Ecuador, of the use of seismic microzoning for risk reduction in developing countries. Abstracts, Regional Seismological Assembly in South America, Brasilia.

FUNDAMENTALS OF SEISMOMETRY

Christian Teupser †
Central Institute for Physics of the Earth, Branch Jena, Burgweg 11, D-6900 Jena

1. The mechanical receiver

The most common procedure of measuring the ground motion is to suspend a mass with a minimum of attachment to the earth and depend upon its inertia to keep it fixed in position as the earth moves. The simplest type of seismometer uses a pendulum having only one degree of freedom. It is usually designed to measure one component of ground motion especially the translation in N-S, E-W or Z direction. Due to the gravity different constructions are necesarry for the horizontal and the vertical component.

The horizontal component consists in principle of a pendulum swinging around a nearly vertical axis (Fig. 1). If the inclination of the axis is the angle ν to the vertical, the natural period will be

$$(1) \quad T_s = 2\pi \sqrt{\frac{l}{g \sin \nu}}$$

where l is the reduced pendulum length and g the acceleration due to gravity [TEUPSER and ULLMANN, 1964]. The motion of such a pendulum can be described by the following linear differential equation [TEUPSER, 1962]

$$(2) \quad \frac{d^2\eta}{dt^2} + 2D_{so}\omega_s \frac{d\eta}{dt} + \omega_s^2\eta = \frac{1}{l}\left(\frac{d^2x}{dt^2} + g\zeta\right) - \frac{G_s}{K_s} i_s$$

where D_{so} is the open damping, $\omega_s = 2\pi/T_s$ the natural angular frequency, G_s the electrodynamic constant of the magnet and coil assembly, K_s the inertial moment, and η the angular deflection of the centre of mass. x is the ground displacement in the direction of the free motion of pendulum, ζ a small tilt against an axis perpendicular to the axis of rotation through the centre of mass, and i_s the current in the coil.

The vertical motion can be detected by a pendulum swinging about a horizontal axis. The pendulum is supported against gravity by a helical spring fixed at the frame in A and at the boom in B (Fig. 2). In order to obtain a long-period seismograph with neglegible non-linear effects, the principle of LaCOSTE [1934] is the best solution using a so-called 'zero-length' spring. As the centre of mass is not generally situated in the horizontal plan through the axis of rotation ($\varepsilon \neq 0$), the natural period of a pendulum will be

$$(3) \quad T_s = 2\pi \sqrt{\frac{l \sin\gamma}{g \cos(\gamma+\varepsilon)}}$$

where ist the angle between the ends of the spring [TEUPSER, UNTERREITMEIER, 1977]. The equation of motion is

$$(4)\quad \frac{d^2\eta}{dt^2} + 2D_{so}\omega_s \frac{d\eta}{dt} + \omega_s^2\eta = -\frac{1}{l}\left(\frac{d^2y}{dt^2} + g\beta\sin\varepsilon\right) - \frac{G_s}{K_s} i_s$$

where β is a small tilt about the axis of rotation. y is the ground displacement in a direction inclined against the vertical by the angle ε. If $\varepsilon = 0$, the pendulum is sensitive about vertical motions only. This is the condition for an exact vertical seismograph [MALISCHEWSKY et al., 1970]. If $\varepsilon = 54.7°$, a homogeneous triaxial equipment can be constructed using three such inclined vertical pendulums.

2. The response of mechanical receiver

A pendulum with low damping responds to a forced oscillation with an oscillation of the same period superposed by the free oscillation of the pendulum with his own period T_s. The unwanted free oscillation distorts the wanted forced one. To make satisfactory use of pendulums in seismometry, it is necessary to diminish the effects of the transient free oscillations. This will be obtained by introducing sufficient damping, by which we mean any force opposing the pendulum motion and increasing with its velocity. The ideal equipment for this purpose is a magnet and coil assembly. As the boom motion induces the voltage $e_s = G_s d\vartheta/dt$ in the coil, the current i_s will be

$$(5)\quad i_s = \frac{G_s}{R_s + R_{as}} \frac{d\vartheta}{dt}$$

when the coil with the resistance R_s is terminated by R_{as}. Neglecting tilts, the differential equation of a vertical or horizontal seismograph is

$$(6)\quad \frac{d^2\vartheta}{dt^2} + 2D_s\omega_s \frac{d\vartheta}{dt} + \omega_s^2\vartheta = -\frac{1}{l}\frac{d^2x}{dt^2}$$

where D_s is the total damping

$$(7)\quad D_s = D_{so} + \frac{G_s^2}{2\omega_s K_s (R_s + R_{as})} .$$

The differential equation (6) can be solved using the Laplace transform

$$(8) \quad F(s) = \int_0^\infty f(t)e^{-st}dt$$

where $f(t) = 0$ for $t < 0$. The inverse transform is given by

$$(9) \quad f(t) = \frac{1}{2\pi j}\int_{-j\infty}^{+j\infty} F(s)e^{st}ds \ .$$

As the Laplace transform of the derivate $f^{(n)}(t)$ equals $s^n F(s)$, the differential equation (6) becomes an algebraical equation

$$(10) \quad (s^2 + 2D_s\omega_s s + \omega_s^2)\,\theta(s) = -\frac{s^2 X(s)}{l}$$

where $X(s)$ is the Laplace transform of the ground displacement. If the deflection of the centre of intertia $l\,\vartheta(t)$ is linearly magnified by mechanical, optical, or electronic devices with the factor V_o, the recorded amplitude $a(t)$ is obtained using (6)

$$(11) \quad a(t) = V_o l\vartheta(t) = \frac{V_o}{2\pi j}\int_{-j\infty}^{+j\infty} U_s(s)X(s)e^{st}ds \ .$$

The transfer function function of the mechanical receiver $U(s)$ included in (11) is

$$(12) \quad U_s(s) = \frac{s^2}{s^2 + 2D_s\omega_s s + \omega_s^2} \ .$$

Let $s = j\omega$ with denoting ω angular frequency, the Laplace transform changes into the Fourier transform and the transfer function (12) can be written

$$(13) \quad U_s(j\omega) = V_s(\omega)e^{j\varphi_s(\omega)}$$

where $V_s(\omega)$ is the amplitude and $\varphi_s(\omega)$ the phase response of the mechanical receiver

$$(14) \quad V_s(\omega) = \frac{\omega^2}{\sqrt{(\omega^2 - \omega_s^2)^2 + 4D_s^2\omega_s^2\omega^2}} \ ,$$

$$(15) \quad \tan\varphi_s(\omega) = \frac{2D_s\omega_s\omega}{\omega^2 - \omega_s^2} \ .$$

Amplitude and phase responses for different dampings are given in Fig. 3 and 4. If at $t = 0$ a harmonic ground motion suddenly starts, the formulas (8) and (11) yield

$$(16) \quad X(s) = \frac{\omega x_o}{s^2 + \omega^2}$$

and $a(t) =$

$$(17) \quad = -V_o x_o U_s(\omega)\left[\sin(\omega t + \varphi_s) - \frac{\omega_s}{\omega\beta_s} e^{-D_s\omega_s t} \sin(\beta_s\omega_s t + \zeta_s)\right]$$

where $\beta_s = \sqrt{1 - D_s^2}$ and $\sin\zeta_s = 2D_s\beta_s V_s(\omega)$.

As mentioned above the recorded motion consists of two terms, a steady state one with the frequency of the forced motion and negative exponential one, the so-called transient response, with the frequency of the pendulum. The steady state part is associated with the poles and zeros of $U_s(s)$ and the transient one is obtained from the poles and zeros of $X(s)$.

The amplitude and the phase angle of the forced motion is given by the responses (14) and (15), respectively. Neglecting the transient response, the mechanical receiver can record the displacement, the velocity, and the acceleration of ground motion in certain frequency intervals. These three special cases are:

1. For $\omega \geqq \omega_s$ and $0.4 < D_s < 0.7$ is $V_s(\omega) \approx 1$.
   The response of the seismograph is proportional to the displacement of the ground motion.

2. A heavy damping $D_s \gg 1$ gives $V_s(\omega) \approx \omega/2D_s\omega_s$ in the range $\omega_s/2D_s < \omega < 2D_s\omega_s$. The response is proportional to the velocity of the ground motion.

3. For $\omega \leqq \omega_s$ and $0.4 < D_s < 0.7$ is $V_s(\omega) \approx \omega^2/\omega_s^2$.
   The response is proportional to the acceleration of the ground motion.

3. The electromagnetic seismographs

In these instruments the coil of the mechanical receiver is connected to a galvanometer through a network of resistances (Fig. 5). The equation of motion of the galvanometer is

$$(18) \quad \frac{d^2\psi}{dt^2} + 2D_{go}\omega_g \frac{d\psi}{dt} + \omega_g^2\psi = \frac{G_g}{K_g} i_g$$

where ψ is the angular deflection of the galvanometer. The other values are defined like those of the mechanical receiver. As in the receiver coil a voltage $e_g = -G_g\, d\psi/dt$ will be induced in the galvanometer coil opposite to the galvanometer motion. In the theory of electromagnetic seismographs the transference factor k_g and the coupling factor σ are defined as

$$(19) \quad k_g = \frac{G_s G_g R_3}{K_g[(R_s+R_1)(R_g+R_2) + R_3(R_s+R_g+R_1+R_2)]} ,$$

$$(20) \quad \sigma = \frac{k_g}{2}\sqrt{\frac{K_g}{D_s\omega_s D_g\omega_g K_s}} .$$

It can be shown that the coupling factor describing the galvanometer reaction lies between the limits $0 < \sigma < 1$. [EATON, 1957 and TEUPSER, 1958]

Applying Kirchhoff's laws for the coupling network (Fig. 5) and the Laplace transform for eq. (6) and (18), the transfer function of the elektromagnetic seismograph becomes

$$(21) \quad T(s) = \frac{2D_m\omega_m s^3}{(s^2+2D_s\omega_s s+\omega_s^2)(s^2+2D_g\omega_g s+\omega_g^2) - 4D_s D_g\omega_s\omega_g\sigma^2 s^2}$$

where D_g is defined like D_s (eq. 7) and

$$(22) \quad D_m\omega_m = \mathrm{Max}(D_s\omega_s,\ D_g\omega_g) .$$

If L_g is the optical lever arm of the galvanometer the magnification factor will be defined as

$$(23) \quad V_o = \frac{L_g\, k_g}{D_m\omega_m l} .$$

Neglecting the galvanometer reaction ($\sigma = 0$), the amplitude response $W(\omega)$ and the phase angle $\varphi(\omega)$ are

$$(24) \quad W(\omega) = \frac{2D_m\omega_m U_s U_g}{\omega} ,$$

$$(25) \quad \varphi = \varphi_s + \varphi_g - \frac{\pi}{2} .$$

Special tuning of the 4 parameters of the electromagnetic seismograph, the two natural frequencies and the two dampings, enables the registration of the integral, the displacement, the velocity, the acceleration, and the third derivate of ground motion. The conditions for this tuning and the operating range is shown in Table 1. $V_n \approx V_o W(\omega)/\omega^n$ is the magnification of the n^{th} derivate of the ground motion in the operating range. The schematic response curve are shown in Fig. 6. Detailed theoretical treatment shows that any response characteristic which includes the galvanometer can be produced by the so-called equivalent parameters of the mechanical receiver and the galvanometer [GRENET, COULOMB, 1935].

4. The electronic seismographs

The possibility to built up long-life electronic amplifiers enables the installation of a new generation of seismological instruments. The output of such a seismograph with conventional moving-coil transducer or displacement transducer delivers a high-level electronic signal suitable for registration on magnetic tape or electronic data processing.

The signals of the transducers are led to combinations of low-, band-, and high-pass filters. The transfer functions of second-order low-pass are given by

$$(26) \quad U_L = \frac{\omega_L^2}{s^2 + 2D_L\omega_L s + \omega_L^2} ,$$

those of band-pass filters by

$$(27) \quad U_B = \frac{2D_B\omega_B s}{s^2 + 2D_B\omega_B s + \omega_B^2}$$

and those of high-pass filters by

$$(28) \quad U_H = \frac{s^2}{s^2 + 2D_H\omega_H s + \omega_H^2} .$$

Such second-order filters can be easily built up using operational amplifiers. Therefore, the transfer function of such a seismograph is given by

$$(29) \quad T(s) = \frac{N(s)}{D(s)} .$$

This function is described by the roots of the numerator, the zeros of T(s), and the roots of the denominator D(s), the poles of T(s).

Important new classes of seismograph can be constructed by feeding the output signal into an auxiliary transducer attached to the pendulum. In this way, the output signal generates a force acting on the mass. If this feedback is negative, the relativ motion between the seismometer boom and the frame is reduced. This invokes the well-known general properties of negative feedback systems, which are to improve stability, linearity, and dynamic range as compared with open-loop systems using components of similar quality.

The schematic diagram of such a feedback seismograph shows Fig. 7. The Laplace transform of the transfer function is

$$(30) \quad T_f(s) = \frac{s^2 Q(s)}{s^2 + 2D_S\omega_S s + \omega_S^2 + kG(s)Q(s)}$$

where Q(s) and G(s) are the transfer functions of the transducer or the filter in the feedback loop, respectively. Using different filters in the feedback loop one can modify the transfer function. In general, the feedback is negative

and the loop consists of a parallel connection of a low-pass, a direct way, a one-stage high-pass, and a two-stage high-pass [PLESINGER, 1973]

$$(31) \quad G(s) = \frac{\beta_0 \omega_0}{s + \omega_0} + \beta_1 + \frac{\beta_2 \omega_h s}{s + \omega_h} + \frac{\beta_3 \omega_H^2 s^2}{s^2 + 2\alpha_H \omega_H s + \omega_H^2} .$$

If there is only the direct way, the natural frequency will be increased to

$$(32) \quad \omega_s' = \sqrt{\omega_s^2 + k\beta_1} .$$

Such devices measure the acceleration for frequencies $\omega < \omega_s'$ and are called force-balance accelerometers [MELTON, 1976]. These in modern seismometry often mentioned force-balance systems, therefore, sense the ground motion after the same inertial principle explained above, but provide an additional restoring force. The electric signal generating this force is nearly proportional to ground acceleration and is used as output signal. The precision to which the ground motion can be measured is rised as in well-known potentiometric meters.

Using a low-pass the same effect will be obtained but only for long periods. The co-called centering factor is [SUTTON and LATHAM, 1969]

$$(33) \quad F = \frac{\omega_s^2 + k\beta_0}{\omega_s^2} .$$

A high-pass in the feedback loop increases the apparent damping of the pendulum. As shown above the seismograph acts as a velocity meter. A more subtile benefit is that the elimination of dissipative elements from the electromechanical system removes the primary source of Brownian motion of the seismometer mass, and therefore opens the door to the development of very small seismometers. A least, the second-stage high-pass simulates an increasing of the inertial moment. This lengthen the period and the range in which the seismograph measure the displacement. Such a feedback must be combined with velocity feedback because the increased inertia requires more damping.

Looking again at the response of the feedback seismograph one can see that it is controlled entirely by the feedback network if the last term in the denominator dominates the other ones. In this case the response is independent of the parameters of the mechanical receiver. Using a proportional, integral and differential feedback (PID) [WIELANDT and STRECKEISEN, 1982]

$$(34) \quad G(s) = a + \frac{b}{s} + cs ,$$

a conventional electromagnetic seismograph can be simulated. With a displacement transducer the response will be

$$(35)\quad T_f(s) = \frac{s^3}{s^3 + (2D_s\omega_s + kc)s^2 + (\omega_s^2 + ka)s + kb}$$

Apart from the term with s^3 in the denominator this equation represents the transfer function of an electromagnetic seismograph. As the natural period of this system can be chosen much greater than the period of the mechanical receiver, a velocity response can be obtained in broad frequency band. Such seismographs are called Very-Broad-Band (VBB) seismographs [STEIM, 1986]. They will be recommanded as a new standard in global seismic networks. With high resolution A/D converters such broad-band seismographs are able to record the whole spectrum and dynamic range of seismic signals.

5. The strainseismographs

The seismographs discussed up till now uses the inertia of a suspended mass. Therefore, they are called inertia seismographs contrary to the strainseismographs which measure the variation of the distance between two points during the passage of seismic waves [BENIOFF, 1935 and AGNEW, 1986]. In other words, these instruments are excited by the phase difference of the propagating wave. They also measure as so-called extensometers the ground deformation caused by earth tides, meteorological influences, and tectonic processes. Their main field of application is the recording of long-period events reaching from seismic waves to secular variations.

The terminals of the strainseismograph are usually piers inbedded in the soil. For measuring the variation of the distance three methods are mainly used (Fig. 8). In the first suitable instrument one pier was lengthened by a rigid rod, so that a transducer can be fixed between its free end and the second pier. Instead of the rod an invar wire can be used as length normal, too. The third possibility is the light beam strainseismograph constructed by the aid of lasers. As the strainseismographs using rods or wire are not longer than 30 m, laser strainseismographs of 1000 m length have been developed.

References

AGNEW, D.C.: Strainmeters and tiltmeters. Rev. of Geophysics 24 (1986) 3, 579-624.

ARANOVICH, Z.I.; D.P. KIRNOS; V.M. FREMD: Apparatura in metodika sejsmometriceskich nabljudenij v SSSR. NAUKA, Moskva 1974.

BENIOFF, H.: A linear strain seismograph. Bull. Seism. Soc. Am. 25 (1935), 283-309.

BORMANN, P.: Registrierung und Auswertung seismischer Ereignisse. Veroeff. Inst. Geodyn. (1966) 1, 158 S.

EATON, J.P.: Theory of the electromagnetic seismograph. Bull. Seism. Soc. Am. 47 (1957), 37-75.

GRENET, G.; J. COULOMB: Nouveaux principes de construction des seismographes electromagnetiques. Annales de Physique, Paris, 11. serie, 3 (1935), 321-369.

LACOSTE, L.J.B.: A new type long period vertical seismograph. Physics 5 (1934), 178-180.

MALISCHEWSKY, P.; CH. TEUPSER; W. ULLMANN: Der Vertikalseismograph unter besonderer Beruecksichtigung des Typs VSJ-I. Veroeff. des Inst. f. Geodynamik Jena (1970) 15, 77 S.

MELTON, B.S.: The sensitivity and dynamic range of inertial seismographs. Rev. Geophys. and Space Physics 14 (1976) 1, 93-116.

PLESINGER, A.: Synthesis of feedback controlled broadband modifications of conventional seismograph systems. Zeitschr. Geophys. 39 (1973) 4, 573-596.

SAWARENSKI, E.F.; D.P. KIRNOS: Elemente der Seismologie und Seismometrie. Berlin: Akademie-Verlag, 1960. 512 S.

STEIM, J.M.: The very-broad-band seismograph. Harvard University Cambridge, Massachusetts, Doctoral Thesis, 1986.

SUTTON, G.H.; G.V. LATHAM: Analysis of a feedback-controlled seismometer. Journ. Geophys. Res. 69 (1969) 18, 3865-3882.

TEUPSER, CH.: Der Rueckwirkungsfaktor bei elektrodynamischen Erschuetterungsmessern. Freiberger Forschungshefte C 51 (1958), 64 S.

TEUPSER, CH.: Die Eichung und Pruefung von elektrodynamischen Seismographen. Freiberger Forschungshefte C 130 (1962), 103 S.

TEUPSER, Ch.; W. ULLMANN: Der neue Jenaer Horizontalseismograph HSJ-I. Veroeff. Inst. fuer Bodendynamik und Erdbebenf. (1964) 76, 147 S.

TEUPSER, CH.; E. UNTERREITMEIER: Der elektronische Dreikomponentenseismograph EDS-1, Theorie, Aufbau, Wirkungsweise. Veroeff. Zentralinst. Physik d. Erde (1977) 51, 114 S.

WIELANDT, E.; G. STRECKEISEN: The leaf-spring seismometer: Design and performance. Bull. Seism. Soc. Am. 72 (1982), 2349-2367.

WILLMORE, P.L.: Manual of seismological observatory practice. World Data Center A for Solid Earth Geophysics, Report SE-20 (1979) Boulder, Colorado USA.

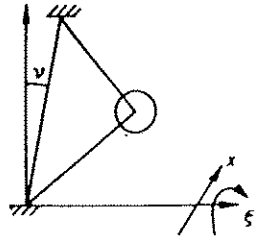

Fig. 1 Horizontal seismograph

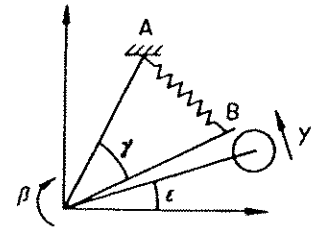

Fig. 2 Vertical seismograph

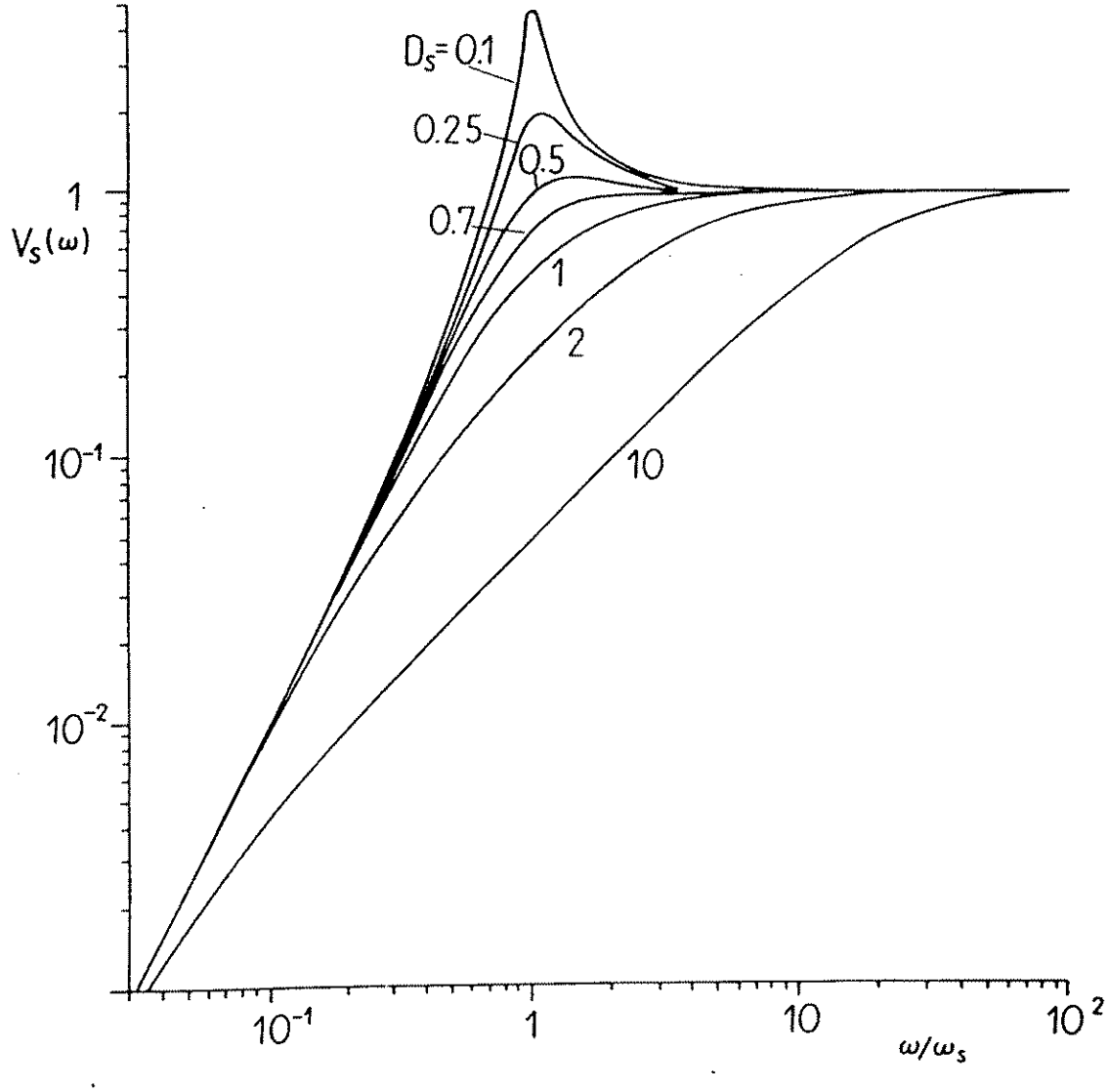

Fig. 3 Amplitude response

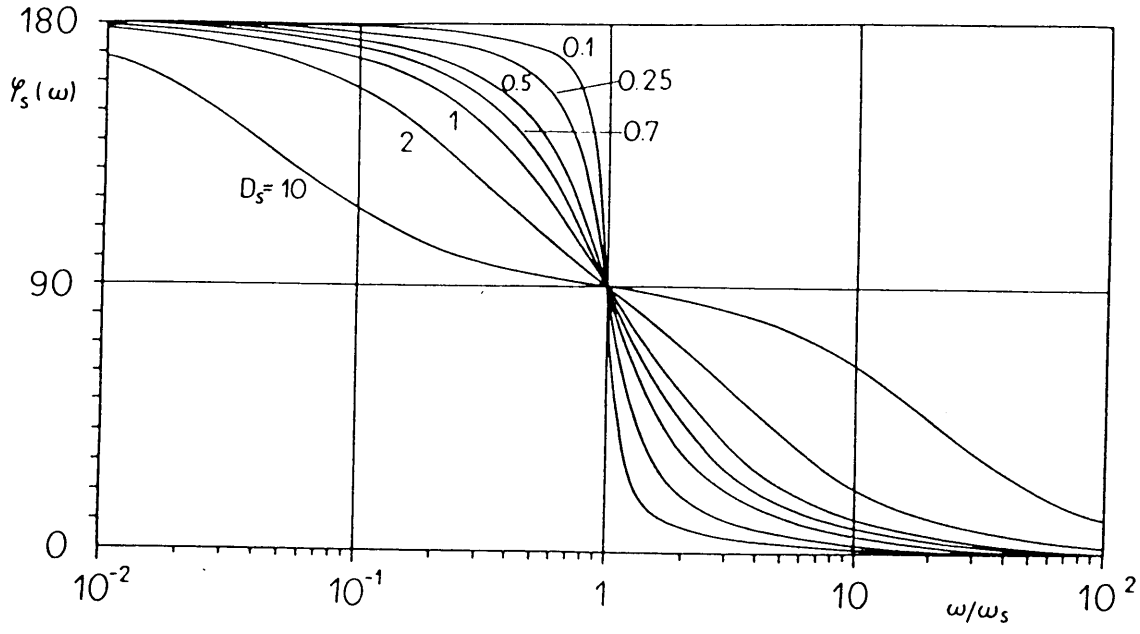

Fig. 4 Phase response

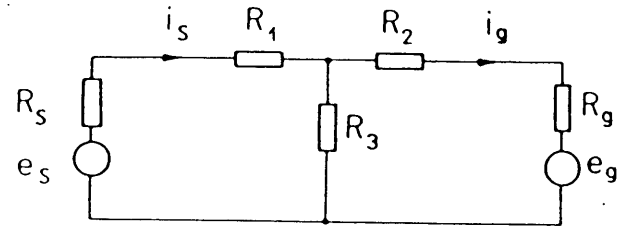

Fig. 5 Circuit diagram of electromagnetic seismograph

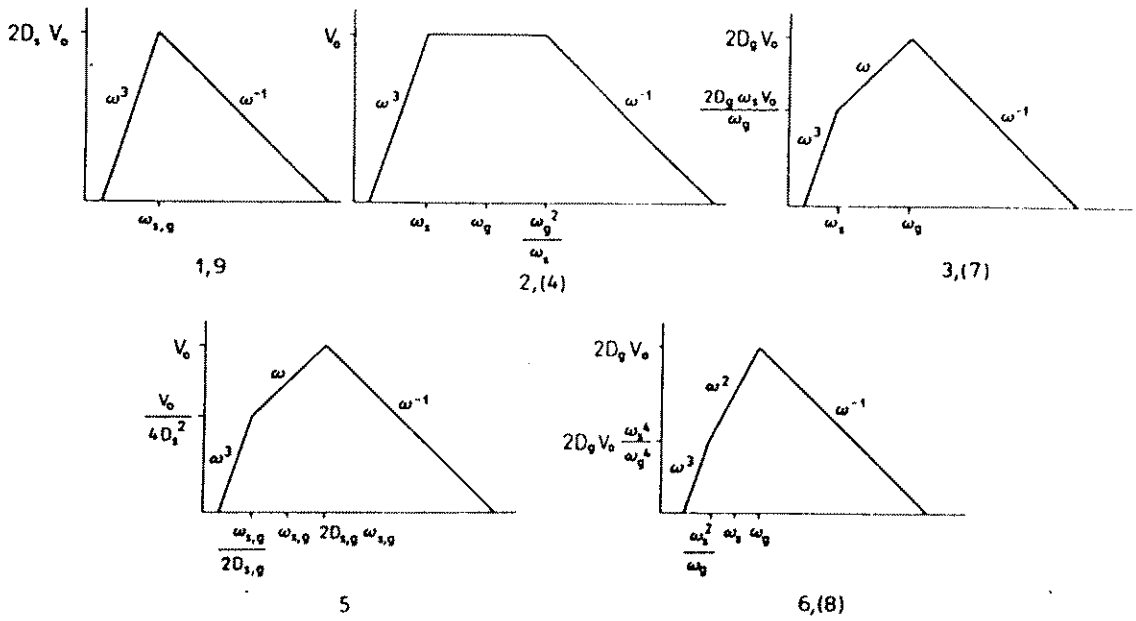

Fig. 6 Schematic responses of electromagnetic seismograph

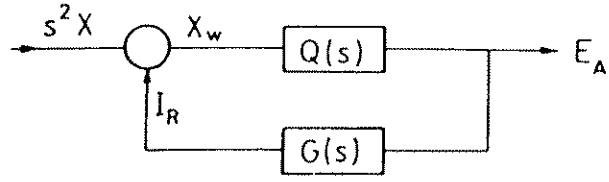

Fig.7 Circuit diagram of electronic seismograph

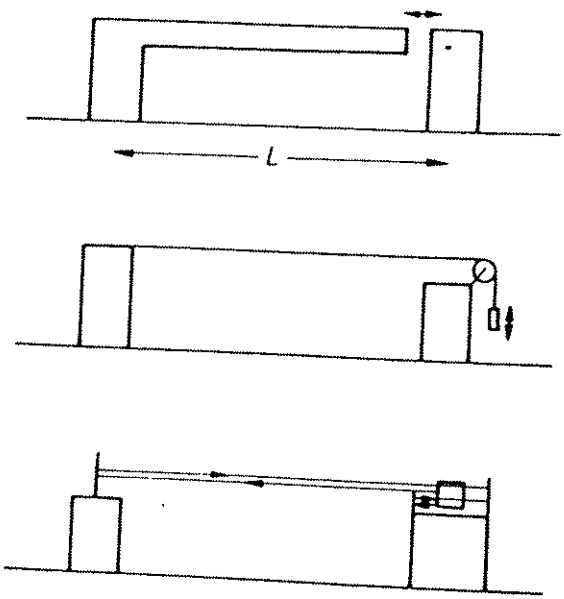

Fig. 8 Principles of strainseismograph

Table 1

case	tuning	$\frac{\omega_g}{\omega_s}$	D_s	D_g	operational range	V_n
1	integral	≈ 1	$0.47 \leq D_{s,g} \leq 0.6$		$\omega \geq \omega_{s,g}$	$\frac{2L_g k_g}{1}$
2	displacement I	< 1	0.5	$\frac{\omega_g}{2\omega_s}$	$\omega_s \leq \omega \leq \frac{\omega_g^2}{\omega_s}$	$\frac{L_g k_g}{D_g \omega_g 1}$
3	velocity I	< 1	$0.4 \leq D_{s,g} \leq 0.7$		$\omega_s \leq \omega \leq \omega_g$	$\frac{2L_g k_g}{\omega_g^2 1}$
4	displacement II	> 1	$\frac{\omega_s}{2\omega_g}$	0.5	$\omega_g \leq \omega \leq \frac{\omega_s^2}{\omega_g}$	$\frac{L_g k_g}{D_s \omega_s 1}$
5	velocity II	≈ 1	$D_{s,g} > 1$		$\frac{\omega_s}{1.3D_s} \leq \omega \leq 1.3D_s\omega_s$	$\frac{L_g k_g}{2D_s^2\omega_s^2 1}$
6	acceleration I	< 1	$\frac{\omega_g}{2\omega_s}$	0.5	$\frac{\omega_s^2}{\omega_g} \leq \omega \leq \omega_g$	$\frac{2L_g k_g}{\omega_g^3 1}$
7	velocity III	> 1	$0.4 \leq D_{s,g} \leq 0.7$		$\omega_g \leq \omega \leq \omega_s$	$\frac{2L_g k_g}{\omega_s^2 1}$
8	acceleration II	> 1	0.5	$\frac{\omega_s}{2\omega_g}$	$\frac{\omega_g^2}{\omega_s} \leq \omega \leq \omega_s$	$\frac{2L_g k_g}{\omega_s^3}$
9	3rd derivate	≈ 1	$0.47 \leq D_{s,g} \leq 0.6$		$\omega \leq \omega_{s,g}$	$\frac{2L_g k_g}{\omega_g^4 1}$

INSTRUMENT CALIBRATION AND PARAMETER DETERMINATION OF SEISMOMETERS AND SEISMIC MEASURING SYSTEMS

Manfred Schmidt

Central Institute for Physics of the Earth, Branch Jena
Burgweg 11, D-6900 Jena

1. General background

Recent developments in sensor technology (feedback seismometers) and in digital broad-band seismometry have provided the technological capability to record and analyze ground motion with high fidelity over a broad frequency and amplitude range. In a frequency band spanning several orders of magnitude (from periods of thousands of seconds to frequencies of hundrets of Hertz) there are no longer any technical limitations in detecting and recording ground motion ranging in amplitude from background noise at the quitest sites to the strong motions produced in the near-field by large earthquakes.

The utilization of such sophisticated seismometers and data acquisition systems suppose, that the system parameter are stable and can be rechecked from time to time to guarantee the reliability of data. The knowledge of system parameters is also the basis for restoration of seismograms (SEIDL, STAMMLER 1984) in order to determine the true earth movement.

Parameter determination and calibration of seismometers are complex problems in seismometry and of vital importance for observatory practice.

It is necessary to distinguish between different procedures:

- the initial parameter determination immediately after the production of the seismometer. The parameters measured in this process are documented by the producer in a data sheet for user. This procedure is out of the scope of this paper.

- the adjustment and measurement of the parameters planned during installation at observatories and the rechecking of parameters having been adjusted from time to time, respectively. This paper deals only with these procedures.

- in situ measurement of seismometer parameters without disturbation of measuring mode of the system. This will be mentioned in an advanced lecture.

More detailed descriptions on parameter determination and instrument calibration are given by WILLMORE (1979), TEUPSER (1962), KISSLINGER (1967), for example.

Scientific Technical Report STR 95/TK
DOI: 10.2312/GFZ.b103-95tk7

2. Instrument parameters for seismological observatory practice

A seismometer system is a linear or quasi-linear measuring system. It can be described, therefore, by terms of linear system theory. The transfer function describes the amplitude and phase response of the system in the frequency range of interest.

The combination of subsystems like seismic sensor, displacement transducer, filter amplifier etc. to the total system is analytically to explain by multiplication of the subsystems transfer functions in the Laplace domain or by convolution in the time domain. Because of this fact the determination of the transfer function (e. g. in its graphical form as the so-called BODE-plot for amplitude and phase response) is very important in seismometry as well as for deconvolution/restoration of recorded signals.

In order to calibrate the whole system, the over-all transfer coefficient, which gives the relation between mechanical input (e. g. earth acceleration) and electrical output, is of importance. The transfer function may be normalized to one at its amplitude plateau.

Despite of the fact that highly sophisticated instruments are available, physically determined limitations must be considered especially in broad-band seismometer systems: The capability of seismometer to resolve very small input signals is ultimately limited by its noise. This instrumental noise is combined mainly of mechanical noise, transducer and quantization noise. Noise figure in terms of power spectral density describes the sensitivity or resolution of the seismometer systems.

Real seismometer systems may be considered as quasi-linear systems. The remaining nonlinearities cause nonlinear distortions, if more or less large input signals are to measure. They produce spurious signals in the output spectrum. Nonlinearities must be kept so small by design and adjustment, that those spurious signals does not disturb seriously the output (in digital systems: they have to be less than the least significant bit).

Whereas in traditional "small-band" systems a linearisation procedure was carried out only for vertical sensors (seismometers) itself, this procedure must be qualified and extented for broad-band and high-fidelity systems. The result of adjustment must be described qualitatively by a special parameter which is easy to interprete.

Generally spoken, for modern observatory practice are only some parameters of interest, which describe the measuring system in a sufficient manner: the transfer function (in its analytical or graphical form), the transfer coefficient, a parameter for instrumental noise and a parameter (or at least a plot) describing nonlinearities.

In the following selected methods to measure or to estimate these parameters are compiled.

3. Determination of transfer function of seismometers by "classical" method (parameter determination)

The transfer characteristic of the seismometer itself (that means the mass spring system as seismic sensor) of an accelerometer is given by

$$(1) \quad H_{s,a}(s) = \frac{s^2}{s^2 + 2D_s\omega_s s + \omega_s^2}$$

[see TEUPSER (1989) eq. 12] with $s = j\omega$, $\omega_s = 2\pi f_s$, D_s = damping of seismometer. Because of the well-known relations the transfer function may be written respect to velocity or displacement input:

$$(2) \quad H_{s,v}(s) = \frac{s}{s^2 + 2D_s\omega_s s + \omega_s^2}$$

$$(3) \quad H_{s,d}(s) = \frac{1}{s^2 + 2D_s\omega_s s + \omega_s^2}$$

By measuring the mechanical parameters 'natural frequency' and damping of the seismometer its transfer function can be calculated. This is the very simple way to determine this function.

If the damping of the seismometer is switched off or removed, the difference of two sequential zero crossings of pendulum gives the natural period T_s'. The influence of a natural damping (zero damping) D_{so} of the mass spring system can be corrected by

$$(4) \quad T_s = T_s' \sqrt{1 - D_{so}^2}$$

The natural damping D_{so} of the seismometer is measured by recording the free oscillations after exciting and picking up the peak-to-peak values of recorded amplitudes. Using the ratio of two amplitudes (see also Fig. 1)

$$(5a) \quad k = \frac{|A_n| + |A_{n+1}|}{|A_{n+2}| + |A_{n+3}|}$$

or

$$(5b) \quad k' = \frac{|A_n| + |A_{n+1}|}{|A_{n+1}| + |A_{n+2}|}$$

with the relation

$$(6) \quad k' = \sqrt{k}$$

the logarithmic decrement can be calculated by

$$(7) \quad \Lambda = \ln k = 2.303 \log k$$

and, finally, the damping (factor) is given by

$$(8) \quad D_s = \frac{1}{\sqrt{1 + \left(\frac{2\pi}{\Lambda}\right)^2}} = \frac{1}{\sqrt{1 + \frac{2{,}45}{(\log k)^2}}} .$$

The values of k' and D_s are listed in tables [e. g. TEUPSER (1962), p. 31] or as diagram [Geo Space, Technical Information No 100-6, see Appendix], which may be used for convenience. In this diagram the overswing ratio A/B = k' is used as input value to read out the damping .

The seismometer damping D_s may be determined in a similar manner, if $D_s < 0{,}6$, for determination of larger seismometer damping see TEUPSER (1962).

The following equation gives the relation between damping, natural damping, resistance of coil R_s. electrodynamic constant G_s, and external resistor for damping R_d

$$(9) \quad D_s = D_{so} + \frac{G_s^2}{2m\omega_s (R_s + R_d)}$$

(This expression stands for linear oscillators. The inertial mass m must be substituded by the moment of inertia in the case of rotational oscillators.) In order to adjust a special damping by external resistor across the coil of coil magnet assembly of the seismometer, it is necessary to determine the electrodynamic constant. This constant gives the relation between electrical and mechanical units or related units. Note, that at least the following units are possible: force/current (N/A = Vs/m), torque/current (Nm/A = Vs), in the case of seismometers with feedback in which the coil is need as forcer the unit acceleration/voltage in also in use.

The electrodynamic constant is measured by a zero compensation method (Fig. 2). In the case of vertical and inclined vertical seismometers, the pendulum is deflected from its zero position by loading with a small additional mass. The resulting deflection is then compensated by a current through the coil. Then, for vertical seismometers is

$$(10) \quad G_{s,\,vertical} = \frac{m_{add} \cdot g \cdot d}{I_{compensation}}$$

The deflection from the zero position is produced by tilting in the case of horizontal seismometers.

$$(11) \quad G_{s,\,horizontal} = \frac{K_s \cdot g \cdot \zeta}{l \cdot I_{compensation}}$$

DOI: 10.2312/GFZ.b103-95tk7

(m_{add} - additional mass, g - earth acceleration, d - distance, lever arm for m_{add}, I_{comp} - current for compensation, Ks moment of inertia, ζ - angle of inclination, l - reduced pendulum length).
In the case of feedback seismometer the coil magnet assembly is used to feed back the output signal partially to generate new properties of seismometer. In these cases the electrodynamic constant is also called forcer constant. There is not any physical difference between the two terms.

After determining these parameters and substituting them into equation (1) the transfer characteristic may be calculated in its algebraic form.

This mathematical expression covers all the information of response of the seismometer. The complex transfer function may be brought in a graphical expression by substituting $s = j\omega$, multiplying with its conjugate complex expression and splitting in two diagramm for amplitude characteristic ($|U_s|$ vs. frequency) and phase characteristic (φ vs. frequency).

Because of the fact that, in general, the transfer function is the quotient of complex denominator and complex numerator

$$(12) \qquad G(s) = \frac{N(s)}{D(s)}$$

the roots of N(s) give the zeros of G(s) and the roots of D(s) form the poles of G(s), respectively. The list of poles and zeros (pole zero notation) is also a quite common form of presentation of the transfer characteristics.

Only the transfer function of the mechanical sensor (the seismometer itself) was taken into account so far. An equivalent procedure must be carried out for the other parts of the system and the transfer functions of all subsystems must be combined to the transfer function of the total system.

Of course, a seismometer in the version mentioned above (without filters, amplifiers and other signal processing units) is used seldom. More complex systems have a total transfer function

$$(13) \qquad G(s) = G_s(s) \cdot G_1(s) \cdot G_2(s)$$

in which $G_i(s)$ represents the transfer function of the several subsystems. It is also possible to calculate the transfer function in such cases theoretically, but for practice there is an urgent need to check the theoretical results by experiments. This is especially important in observatory practice for rechecking the parameters planned. Using more complex systems it should be of practical interest to have other procedures for testing the seismometer system. Methods for carrying out such measurements are described in the following part.

4. Harmonic drive method

The system theory offers several tools to describe the behaviour of a system by graphical means derived from analytical expression of the transfer function. BODE has chosen logarithmic scales for graphical demonstration of amplitude and phase response

$$(14)\quad \lg G(j\omega) = \lg |G(j\omega)| e^{j\varphi(\omega)}$$
$$= \lg |G(j\omega)| + j\,\varphi(\omega)$$

with the amplitude response

(15) $\lg |G(j\omega)|$ as a function of $\lg \omega$

and the phase response

(16) $\varphi(\omega) = \arg G(j\omega)$ as a function of $\lg \omega$

Both curves are also called BODE diagram. It is a very helpful mean to describe the behaviour of a system at different frequencies.

In order to determine the BODE diagram of a system under test experimentally, it is necessary to excite the seismometer by a stationary sinusoidal signal (decay of transients) and to measure its output signal. This procedure must be carried out at different frequencies.

There are two possibilities for exitation: the input signal is fed into the coil of coil magnet assembly of the seismometer under test or a shaking table is used, respectively. Note, that the current through the coil has the same effect as an (earth) acceleration. The equivalent displacement of pendulum can be calculated by

$$(17)\quad x = \frac{G_s \cdot 1}{\omega^2 K_S} I = \frac{G_s \cdot 1}{\omega^2 K_S} \cdot \frac{U_{sign}}{R_{coil}}$$

This procedure can be used only at frequencies less than about 1 Hz. If the coil for exciting and the coil for damping in the case of electrodynamic seismometers are wound on the same carrier. The mutual inductivity of the two coils may cause resonances at higher frequencies. Therefore, it may be of advantage to use an additional coil magnet assembly for testing or an (additional) displacement transducer. If only one coil is available, the current must be fed in by means of an MAXWELL bridge.

The exciting signal and the seismometer output signal must be recorded by a two-channel recorder. The analysis of signal recordings (amplitude and phase) yields the response curve in form of BODE diagram in accordance to (15) and (16). Fig. 3 shows both the amplitude and phase curves of a seismometer (T_s = 10s) with a displacement transducer.

For the analytical interpretation of the seismograms or seismic data, respectively, the seismometer system must be calibrated. The calibration procedure is carried out to determine the transfer coefficient of the seismometer system at a single or at few different frequencies. For all other frequencies of interest the absolut value of transfer coeffecient is given or may be estimated via the amplitude response. (For direct recording of signals the transfer coefficient may be substituted by magnification). Note, that the transfer coefficient has the dimensions of voltage/acceleration, voltage/velocity, voltage/displacement, respectively, while the magnification is dimensionless.) The calibration is based on the exact knowledge of electrodynamic constant (exciting signal via coil) or using a calibrated shaking table.

The harmonic drive method may be modified by different excitation forms as well as by the appropriate analysis of response signals for practical purposes. This method may also be upgraded by digital data acquisition and analysis. Nevertheless, this method in its original form is time-consuming and the system is "out of order" during this intervall, it is not in its measuring mode. To shorten this interruption for checking, other non-sinusoidal signal forms can be applied, e. g. sweep signals or random signals. These procedure will be mentioned in an advanced lecture.

5. Linearity adjustment and comprehensive test of working order

The real seismometer may be considered as a quasi-linear system. Remaining nonlinearities will act especially in the case of large input signals and produce undesired spurious signals at output. Therefore, it is of importance to minimize the nonlinearities by design and for (inclined) vertical seismometers of LaCOSTE type by adjustment of the zero length spring. To carry out this procedure, there are two test criteria: the constancy of natural period of seismometer at different zero positions of pendulum and the constancy of natural period at different amplitude of oscillations, respectively. The approach to these requirements by adjustment is equivalent to minimizing the third order terms in the according differential equation.

$$\omega_s^2\ (\eta,\varphi) \sim \left(\frac{\partial M(0,0)}{\partial \eta} + \frac{\partial^2 M(0,0)}{\partial \eta^2}\,\eta + \frac{\partial^2 M(0,0)}{\partial \eta\ \partial \varphi}\,\varphi\right)$$

with ω_s-natural frequency, η deflection angle of pendulum, φ tiltings of pendulum against its theoretical zero position. Both methods are well known (MELTON 1971, MALISCHEWSKY et al. 1970). But they are very time-wasting and are inconvenient in application.

A new-developed iterative linearisation method with high sensitivity (UNTERREITMEIER et al. 1983 and 1988) offers some advantages, but need a (auxiliary) displacement transducer. This method allows to adjust linearity in three steps and to retest linearity later only by using the last step. Additionally, the last step of this procedure can be carried out automatically.

In the first step only the transducer linearity is adjusted statically, and the transducer itself is calibrated by external reference. In this connection, the advantageous fact is used that all measurements are relative measurements in relation to the theoretical zero position of the boom, defined by the seismometer theory and construction.

The second step involves mostly checking of mechanical properties of flexible bearings and hinges and checking the operating accuracy of the coil magnet damping and forcing system, respectively. To do this, a variable current (sine-wave, triangle) is fed into the forcer coil and simultaneously to the X-input of an X-Y-recorder. The response of the seismometer is recorded in Y-direction by using the transducer voltage output signal, see Exercises.

Of course, this step should be carried out as a matter of principle without the seismometer spring, but this cannot be made practically. Therefore, the spring is unloaded partly by adjusting the position of the boom upward.

The recorded result is expected to be a straight line, but a "hysteresis loop", often disturbed by jumps (Fig. 4), results. Causes for deviations which occurred are: faulty

leaf springs in the hinges ("cracked" leaf springs), badly adjusted hinges and/or coils, dust in the air gap, torsion in the main spring.

These mistakes or faults must be found, eliminated, and then the second step must be carried out repeatedly to obtain a sufficient linearity.

The third step is carried out to check and to adjust the linearity of the complete seismometer in the measuring mode. We use the same configuration as in step 2, but with loaded spring. It is necessary to emphasize that the driving current (sinewave or triangle) should have a period at least 100 times greater than natural period of the seismometer under test to avoid influences of its phase response to the result.

Of course, the resulting curve should be a straight line, but even mechanical imperfections of real materials and construction do prevent this. In most cases a bent hystereses loop (Fig. 5) will occur.

Summarizing, in the step-by-step procedure the operator has to readjust the leaf spring hinges, to relax torsion in the main spring, and last but not least, to adjust its zero length. This procedure seems to be very complicated, but in reality a trained lab assistent is able to do this work quickly and efficiently. This differs clearly from the well-known troublesome and time-consuming procedure to measure, to calculate, and to draw the plot of the natural period of the seismometer as a function of the boom's zero position.

The following examples may demonstrate the efficiency of the new procedure (EDS-2, $\pm$ 2.5 mm, $T_s \approx$ 5 s).

Fig. 6 shows a relatively large drift caused by a bad spring (not aged or bad temperature coefficient), and Fig. 7 indicates a nearly final state of adjustment.

Note, that the new method can be carried out very easily, it is applicable to all types of mass spring systems and pendulums, it yields even more hints of imperfect materials or not exactly adjusted parts of the seismometer under test.

6. Instrumental noise and dynamic range

Since the seismologists have focused their interest on broadband seismometry and instrumentation questions of instrumental noise and dynamic range of seismometer systems have become more and more important.

The instrumental noise, covering white mechanical noise of the mechanical oscillator, the 1/f-noise of electronics, and the quantization noise, cause a physical determined limitation of seismometer resolution. Therefore, the total instrumental noise level must be minimized at least down to or better beyond the level of seismic noise by system design, highly sophisticated instrumentation, and installation.

Noise is a random process, noise values are measured in terms of power spectral density, that means a power or a squared value related to bandwidth [e. g. in V^2/Hz or in seismometry the mechanical equivalents like $(m/s^2)^2/Hz = m^2 s^{-3}$].

Measuring instrumental noise is a difficult process because the seismic measuring system must be in operation and the instrumental noise is in general overlaid by larger seismic noise and microseism.

Correlation methods must be applied for separating both noise contributions from each other, a spectral analyzer is necessary to measure and to analyze the signals.

Only rough - but not sufficient - estimations may be carried out with clamped seismometers. But the operator must keep in mind, that
- than the mechanical noise of sensor itself will be dropped
- that any form of clamping is uncomplete and
- that the seismometer is not really in its operating or measuring mode.

While instrumental noise limits the resolution of seismometer system at very small signals, a limitation exists for very strong signals on the other hand: Nonlinearities of the seismometer produce spurious signals, which appear in the output spectra. Nonlinearities will remain still after a appropriate linearisation adjustment (of mechanical parts) of the seismometer system. They limit the values of input signals which the seismometer is capable of processing.

The input signal range between instrumental noise and large signals which does not produce disturbing signal components in the output is called dynamic range of seismometer. It is given in the most cases as a logarithmic measure, requirements of 120 dB dynamic range are quite common nowadays.

The direct measurement of dynamic range by special so-called two-tone signals known from radio communication measurement is possible.

Measuring instrumental noise and dynamic range need a well-developed measuring technique and equipment. An advanced lecture will deal with these problems more in detail.

7. Literature

KISSLINGER, K.; Lecture notes on seismological instrumentation. International Institute of Seismology and Earthquake Engineering, Tokyo 1967

MALISCHEWSKY, P.; TEUPSER, Ch.; ULLMANN, W.: Der Vertikalseismograph unter besonderer Beruecksichtigung des Typs VSJ-1. Veroeffentlichungen des Instituts fuer Geodynamik, Reihe A, Heft 15, Berlin 1970

MELTON, B.S.; The LaCoste suspension - Principles and practice. Geophys. J. R. Astron. Soc. 22 (1971) 521-543

MITRONOVAS, W., WIELANDT, E.: High precision phase calibration of long-period electromagnetic seismographs. BSSA 65 (1975) 2, 411-424

SEIDL, D., STAMMLER, W.: Restoration broad-band seismograms. J. Geophys. 54 (1984) 114-122

TEUPSER, Ch.: Die Eichung und Pruefung von elektrodynamischen Seismographen. Freiberger Forschungshefte C 130, Berlin 1962

TEUPSER, Ch.: Fundamentals of Seismometry. This volume

UNTERREITMEIER, E., SCHMIDT, M., BOHL, W.: Patent DD 216 332, 1983

UNTERREITMEIER, E., SCHMIDT, M., KRACKE, D.: A new portable homogeneous triaxial seismometer: design and performance, test and calibration, direct signal analysis. Gerlands Beitr. Geophysik 97 (1988) 3, 218-228

WILLMORE, P.L. (ed.): Manual of seismological observatory practice. World Data Center A for Solid Earth Geophysics Report SE-20, Boulder, Col., 1979

CONSTRUCTING RESPONSE CURVES - AN INTRODUCTION TO THE BODE DIAGRAM

Jens Bribach

Dept. of Structure of the Earth
GeoForschungsZentrum Potsdam, Telegrafenberg A 17, D-14473 Potsdam

1. THE BODE DIAGRAM

True Ground Motion is of main interest in seismology. On the other hand any measuring device will alter the incoming signal as well as any amplifier, and as any output device. Working in the frequency domain, the quotient of input signal and output signal is called RESPONSE. This response is complex, and to get a more handy result it can be split into two terms: Amplitude Response and Phase Response (see FOURIER Transform). Amplitude Response means the output amplitude divided by the input amplitude at a given frequenc. Phase Response is the difference between output phase and input phase, or the phase shift. A graphical expression of this splitting is known as BODE Diagram. One part shows the logarithm of amplitude A versus the logarithm of frequency f (or angular frequency ω, or period T, see Fig. 1a). The other part depicts the (linear) phase ϕ versus the logarithm of frequency f (or ω, or T, see Fig. 1b). For A also the terms AMPLIFICATION and MAGNIFICATION are used.

1.1 The signal chain

The signal passes a chain of devices. Any single element of this chain can be described by its response. It is useful to split any response into elements of first or second order. At the end the Overall Amplitude Response of the complete chain can be constructed by multiplying all single amplitude responses, and the Overall Phase Response by adding all single phase shifts.

1.2 First and second order elements

For the amplitude response the double logarithmic scale of the amplitude diagram facilitates an easy and fast construction. Any element can be approximated by two straight lines. One horizontal line leads to the element corner frequency, and one line dropping from that point with a slope depending on the order of this element.
A first order element is completely described by its amplification A and by its corner frequency fc. The slope beyond fc is one decade in amplitude per decade in frequency. The real amplitude value at fc is dropped to 0.707 of maximum amplitude (see Fig. 2, dotted line), for our fast construction we don't take this line into account.
A second order element inhibits the slope of two decades in amplitude per amplitude in frequency. Additionally it needs another parameter called Damping D, describing the amplitude behaviour at frequencies near fc (compare Fig. 3).

2. THE SEISMOLOGICAL SIGNAL CHAIN

The seismological signal passes the chain
- mechanical receiver
- transducer
- preamplifier
- filter
- recording unit (to be recognized separately)

Note! The following chapters (Mech. Receiver and Transducer) construct responses related to ground displacement. Thus the BODE Diagram axis of ordinates (amplitude A) for the mechanical receiver owns no unit (or the unit [m/m]), and for the transducer the unit is [V/m]. Changes to other movement types, as proportional to ground velocity or to ground acceleration, will be described in chapter 3.

2.1 The Mechanical Receiver

The mechanical receiver is a second order system. It describes the relative movement of the pendulum (the seismic mass attached to the frame by a spring) with respect to the frame. Damping D is set mostly to 0.707 . Only at this damping value the amplitude value at fc is also 0.707 (Fig. 3, dotted curve). For higher values of damping one obtains a more flat curve (dashed). For lower values the dash-dot curve overtops the amplification level at fc, signalizing low damped oscillations of the pendulum, which are triggered by any signal.
The amplification of the mechanical receiver is $A = 1$. That means for frequencies $f > fc$ the amplitude of the pendulum movement related to the frame is similar to the ground amplitude. For the phase shift see at HIGH Pass 2 (fig. 7b).

2.2 The Transducer

The transducer transforms the relative movement of the pendulum into an electrical signal, finally a voltage. The Transducer Constant G gives the value of the Output Voltage U depending on the relative pendulum movement z.
There are three main types of transducers, distinguished by their proportion to ground motion and its derivatives:

- Displacement $U \sim z$ $Gd[V/m]$
  (Capacitive or Inductive Bridges)

- Velocity $U \sim dz/dt$ $Gv[Vs/m]$
  (Magnet-Coil Systems)

- Acceleration $U \sim d^2z/dt^2$ $Ga[Vs^2/m]$
  (Pieco-electric Systems, $U \sim F = m \bullet a$)

A proportion to ground motion is, of course, only given for frequencies $f > fc$, or the horizontal line of the mechanical receiver response.
All transducer Amplitude Responses can be drawn as straight lines all over the frequency range (fig. 4), differing in their slope only.
The Phase Responses appear as a constant phase shift all over the frequency range, drawn as horizontal lines at the values of $0°$ (displacement), or $90°$ (velocity), or $180°$ (acceleration).

2.3 The Preamplifier

The preamplifier is a first order LOW Pass. Its corner frequency is beyond the signal range of seismology - at up to several *10 kHz* . So only the amplification is of interest (fig. 5), and the response is a horizontal line drawn at the amplification level *A*.
The phase shift is $\phi = 0°$, but one should keep in mind that, if using the inverting input, the phase shift will be $\phi = -180°$ all over the frequency range.

2.4 First and second order LOW Passes

LOW Passes have constant amplifications *A* for all frequencies lower than their corner frequency *fc* . For frequencies higher than fc the amplification drops with a slope depending on their order (fig. 6a). It cuts the high frequencies, so the term High Cut is also in use.
The phase shift for $f < fc$ is about *0°*, and for $f > fc$ it turns to *-90°* (first order, LP1) respectively *-180°* (second order, LP2; see fig. 6b), passing half of the phase shift exactly at *fc*.
Of course, the given amplitude and phase values are approximations. In reality we would obtain $\phi = 0°$ only if inserting a frequency of *0 Hz*, and $\phi = -90°$ (*-180°*) for infinite frequency values. But the accuracy is sufficient for our fast construction.

2.5 First and second order HIGH Passes

HIGH Passes have constant amplifications *A* for all frequencies higher than their corner frequency *fc* . For frequencies lower than fc the amplification drops with a slope depending on their order (fig. 7a). It cuts the low frequencies, so You can find also the term Low Cut.
The phase shift for $f > fc$ is about *0°*, and for $f < fc$ it turns to *+90°* (first order, HP1) respectively *+180°* (second order, HP2; see fig. 7b), passing half of the phase shift exactly at *fc*.
Comparable to the description of LOW Passes the given amplitude and phase values are an approximation.

2.6 Second order BAND Pass

The second order BAND Pass (BP2) can be explained as a combination of a first order LOW Pass and a first order HIGH Pass. It suppresses all frequencies except fc with a slope of one decade in amplitude per decade in frequency (fig. 8a). The top at *fc* can be turned into a horizontal line (symmetrical to *fc*) by increasing damping to values $D > 1$. For those *D* it is also possible to construct this BAND Pass by one HIGH Pass and one LOW Pass.
The phase shift for $f < fc$ is about *+90°*, and for f > fc it turns to *-90°* (see fig. 8b), passing half of the phase shift at *fc*.

3. THE OVERALL RESPONSE

The construction of the Overall Response shoult be divided into two steps:
- from mechanical receiver to the final filter stage
- adding the recorder response

The first result, the electrical output, is useful for fitting the signal to the recorder input. It has to be fix, that means changes in magnification (or signal resolution) should be done by setting up the recorder only.

3.1 From the Mechanical Receiver to the final Filter

As defined in chapter 2., the Amplitude Response is constructed related to ground displacement. Multiplying all the units of our signal chain, we get the unit *[V/m]* for the axis of ordinates. All elements, mechanical receiver, transducer, and filter stages can be implemented into the same sheet of a double logarithmic grid, each element with its magnification and its corner

frequency.
Then the resulting amplitude response has to be constructed point by point at certain frequencies. Either by multiplying the amplitudes of all elements at these frequencies. That's the more secure method. Or by adding the distances (eg. in centimetres) of all element amplitudes to the amplitude level line of $A = 1$, positive distances if above this line, negative ones if below. This method is faster. A linear adding is, in this logarithmic scale, a multiplication of the amplitude values.
The final amplitude response curve can be drawn at the same sheet, together with the single elements.

3.2 Adding the Recorder

At the real end of our signal chain we will find a commercially available recorder, transforming the obtained voltage back into movement (drum recorder) or into computable digital values (Analog-to-Digital Converter ADC). Their main parameter is the Input Sensitivity, lets call it H:

- Drum Recorder, H in *[m/V]* is the pen deflection per Volt
- ADC, H in *[digit/V]* is the digital count per Volt

Thus the Overall Amplitude Response needs a separate BODE Diagram for each recorder type. Multiplying the units we obtain the units *[m/m]* for the drum recorder, and *[digit/m]* for the ADC. You will find also derivatives of this unit, like *[digit/nm]* or *[counts/nm]*.

3.3 Introducing Ground Velocity and Ground Acceleration

If the amplitude response curve has to be constructed related to Ground Velocity (or Ground Acceleration), it is sufficient to redraw either the response of the mechanical receiver or this of the transducer. The more simple method is to change the transducer response. Each slope will change one order if turning from displacement to velocity, or from velocity to acceleration. The unit of the ordinate turns from *[V/m]* (displacement) via *[Vs/m]* (velocity) to *[Vs²/m]* (acceleration). These units will also be the units of the amplitude response from the mechanical receiver to the final filter stage. Beyond this the construction of the overall amplitude response is similar to chapter 3.1.
The units of the recorder amplitude response will alter to *[m•s/m]* (velocity) or *[m•s²/m]* (acceleration) for the drum recorder. For the ADC we obtain *[digit•s/m]* (velocity) or *[digit•s²/m]* (acceleration).

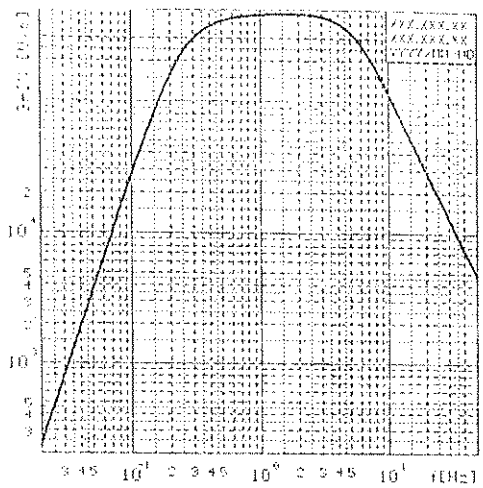

Fig. 1a: Amplitude Response

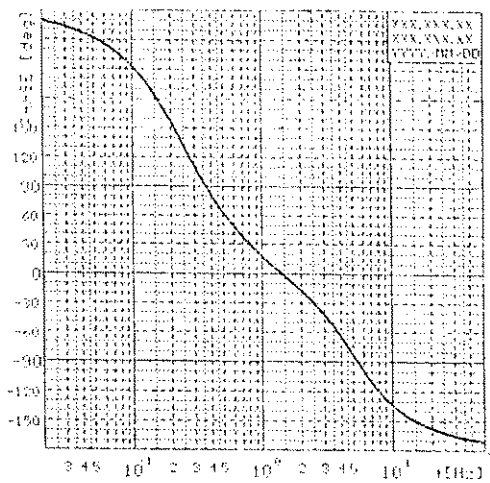

Fig. 1b: Phase Response

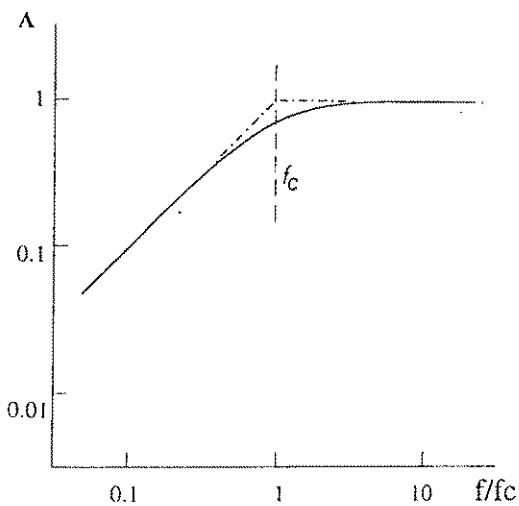

Fig. 2: First order HIGH Pass (HP1)

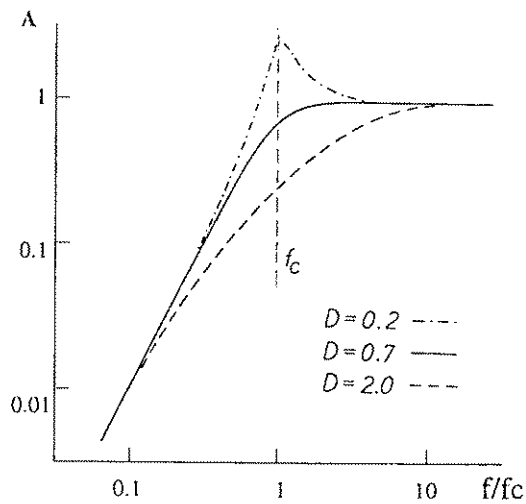

Fig. 3: Second order HIGH Pass (HP2) or Mechanical Receiver

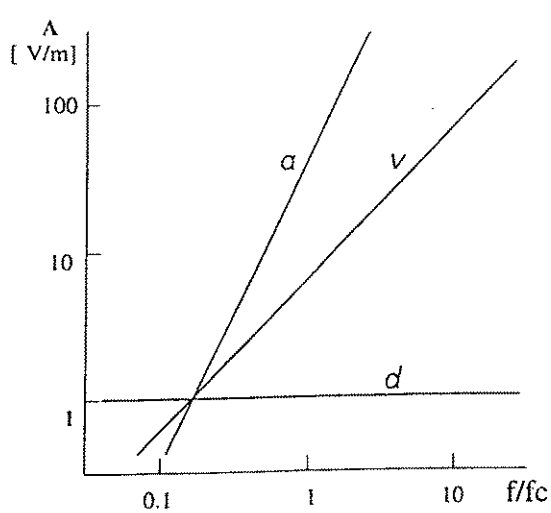

Fig. 4: Transducer Amplitude Response

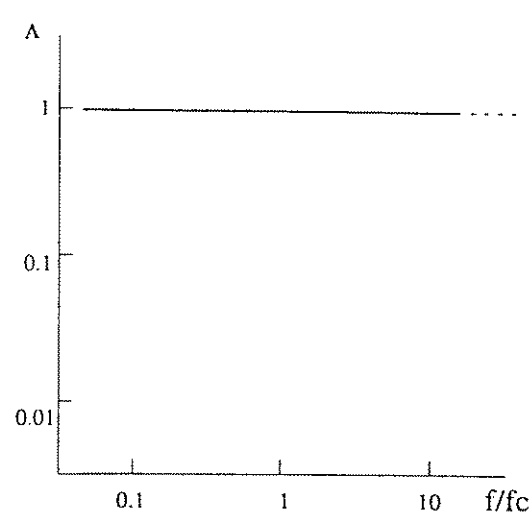

Fig 5: Preamplifier Amplitude Response

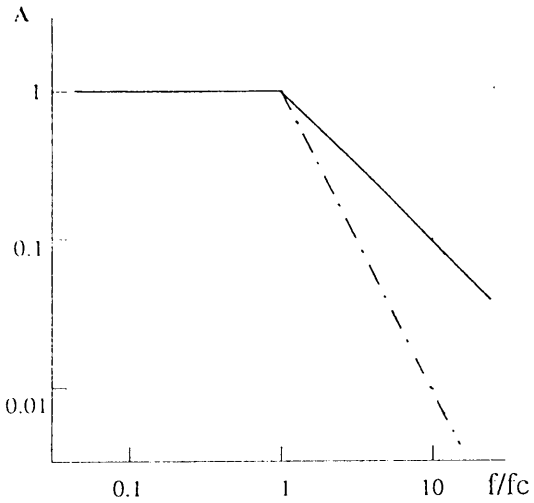

Fig. 6a: LOW Pass Amplitude Response

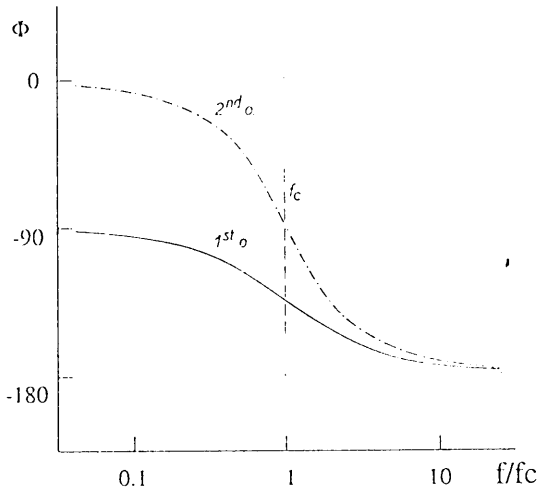

Fig. 6b: LOW Pass Phase Response

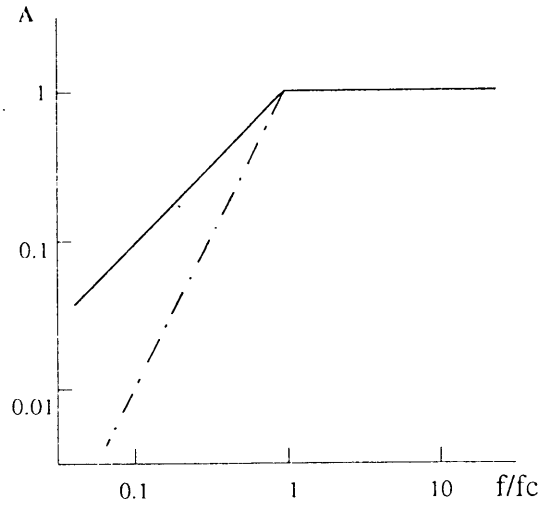

Fig. 7a: HIGH Pass Amplitude Response

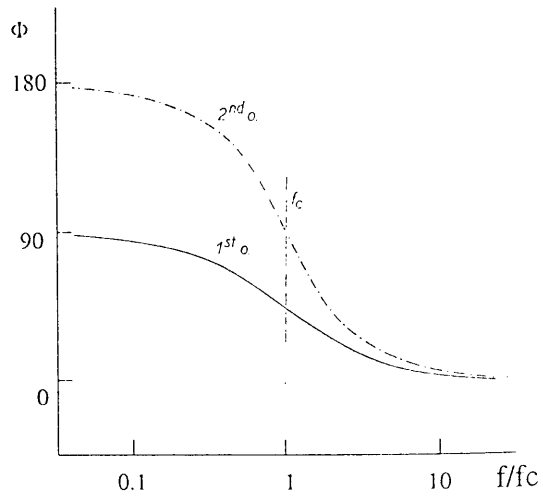

Fig. 7b: HIGH Pass Phase Response

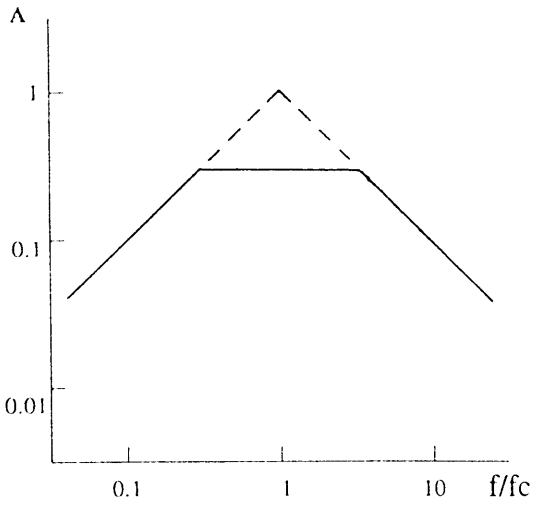

Fig. 8a: BAND Pass Amplitude Response

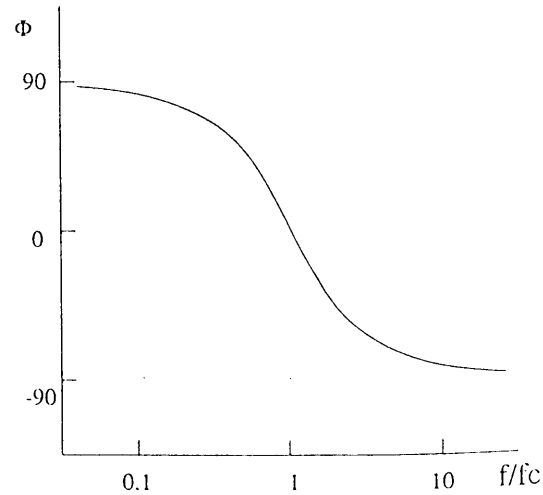

Fig 8b: BAND Pass Phase Response

Remarks on Exercise 1

Plotting Seismograph Response (BODE-Diagram)

by Jens Bribach

The Bode-Diagram displays the Transfer Funktion of a given device as a plot of logarithmic amplitude A and of linear phase shift ϕ versus logarithmic frequency f (or period $1/f$) scales. Its main advantage consists of an easy constructing of response curves which can be approximated by straight lines:
So any Pole generates an amplitude decay proportional to frequency f (20 dB per decade or 6 dB per octave) and a phase shift ϕ of $+90^o$; any Zero causes a slope of 1:1 also and a phase shift of -90^o. Corner frequencies (f. e. filters) occur as the point of interception of two straight lines.
All stages of a signal transfer chain can be constructed component by component (it is recommended to split all functions into parts of 1^{st} or 2^{nd} order). One gets the complete transfer function by multiplying the above named single functions. In the logarithmic amplitude scale as well as in the linear phase scale this is done by adding up these single curves.

Exercise 1 :

1) Plot the Bode-Diagrams (amplitude only) of the following devices:

Seismometer

Transducer Constant	$G_S = 15.915\ Vs/m$
Natural Period	$T_S = 5\ s$
Damping	$D_S = 0.707$

HIGH Pass HP1

magnification	$A_{H1} = 1$
Corner Frequency	$f_{H1} = 0.01\ Hz$

LOW Pass LP1

magnification	$A_{L1} = 5$
Corner Frequency	$f_{L1} = 0.2\ Hz$

LOW Pass LP2

magnification	$A_{L2} = 2$
Corner Frequency	$f_{L2} = 10\ Hz$
Damping	$D_{L2} = 0.707$

2) Plot the system overall response (amplitude, approximated by straight lines)

Remarks on Exercise 2

Estimating Seismometer Parameters by STEP Transition

by Jens Bribach

1. General Terms

Transition Function means the response of a system versus time caused by a STEP Function input. Applying a step in any way to a seismometer You will be able to evaluate the main seismometer parameters via the generated time series. The absence of expensive calibration equipment (shaking table) or the problem of just sealed seismometers can ask for this simple method also usable under field conditions.

2. STEP Transition

2.1. Applying STEPs to the Seismometer

Applying steps is the oldest calibration method in seismology. TEUPSER (1962) schedules three main types

a) pulling a thin block of max. 0.01 *mm* off the seismometer bottom

b) applying a heavy weight upon the seismometer platform

c) applying a constant current to the coil of an electrodynamical system (if available; driving current see EXERCISE 3)

Because *a*) is the most rough method one should use it for field or for portable seismometers only and never for sensitive station types.
In *a*) and *b*) the seimometer mass will return to the former position after deflection, in c) to a offset position depending on the current. Due to linearity the mass deflection - or the seismometer displacement - should not exceed several 100 micrometers.

2.2. Evaluating STEP Transition Time Series

2.2.1. All Types of Seismometers ($D_S < 0.5$)

Figure 1 shows the time series of a low damped seismometer ($D_S = 0.1$). Section A represents the moment of step input up to the transition to a real harmonic movement of the mass. The moment of step causes odd signals. Mechanical application generates additional vibrations because of hitting effects. Electrical one can induce an electrical pulse if calibration coil and signal coil are mounted to the same core (the so-called transformer effect). So evaluation should start beyond Section A.

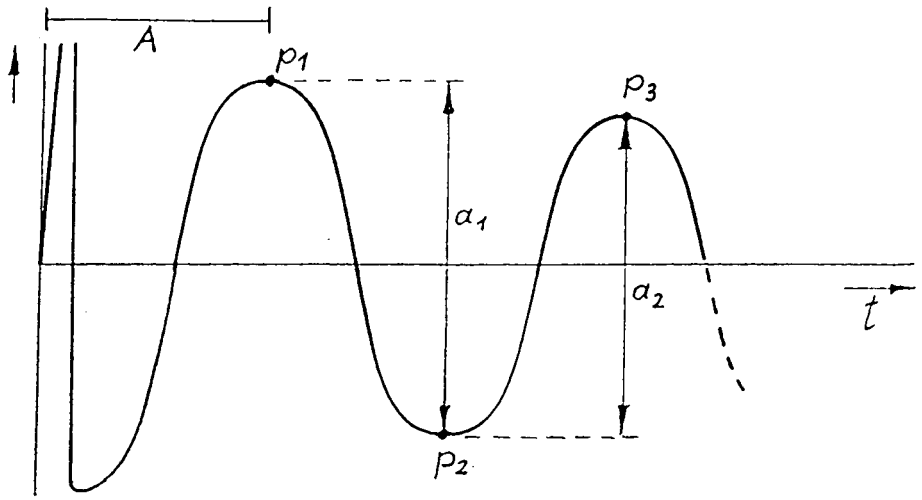

Figure 2.2.1: Low damped seismometer

First step: Measuring of Time Series Period and Damping

Period T should be measured over a maximal amount of periods (10 or more) to get an accuracy better then 99% .

Note: The measured period is larger than the natural period because of the seismometer damping.

Damping D is calculated by

$$D = \frac{1}{\sqrt{\left(\frac{(N-1)\ \pi}{\ln(a_1/a_N)}\right)^2 + 1}} \tag{1}$$

with a_1 as amplitude difference of the first couple of maxima (p_1 and p_2) and a_N as another couple (p_N and p_{N+1}). N should be selected in a way to get an $a_N \approx 0.2 \ldots 0.4\ a_1$.

Second step: Estimation of Seismometer Natural Period T_S

If possible switch off all external attenuators (f.e. resistors) to decrease the measuring error. For example: with a damping $D = 0.2$ the measured period is $T = 1.02\ T_S$. Seismometer Natural Period is calculated by

$$T_S = T\ \sqrt{1 - D^2} \tag{2}$$

2.2.2. Electro-dynamical System (moving coil)

The electro-dynamical constant (or generator constant) G_S of moving coil systems can also be estimated by step transition via its relation to damping D. Here the complete seismometer damping D_S consists of

$$D_S = D_{S0} + D_G \tag{3}$$

with D_{S0} as Seismometer Natural Damping (mechanical effects mostly), and with D_G as the moving coil damping, caused by an external resistor R_a shorting the coil (electro-magnetical force)

$$D_G = \frac{G_S^2\ T_S}{4\ \pi\ m_S(R_a + R_S)} \tag{4}$$

Except R_a and T_S all further parameters are documented by the manufacturer and will not change over time

- K_S $[kg\ m^2]$ — inertial moment
- l_0 $[m]$ — reduced pendulum length

Geophone systems note instead of the two above the seismic mass m_S

- m_S $[kg]$ ($= K_S\ l_0^{-2}$) — seismic mass
- R_S $[\Omega]$ — coil resistance

Note: If measuring coil resistance don't forget to lock the seismometer.

So evaluation again starts with

First step: Measuring of Time Series Period and Damping

Second step: Estimation of Seismometer Natural Period T_S

as given above.

Third step: Estimation of Seismometer Natural Damping D_{S0}

The external damping resistor must be removed (open circuit). So we get similar to (1)

$$D_{S0} = \frac{1}{\sqrt{\left(\frac{(N-1)\pi}{\ln(a_1/a_N)}\right)^2 + 1}} \tag{5}$$

Scientific Technical Report STR 95/TK
DOI: 10.2312/GFZ.b103-95tk7

Fourth step: External Damping

The external resistor must be set to a value that causes a damping downto 20 ... 50% per period.
Now we measure the neighbouring amplitudes a_1 (p_1 and p_2) and a_2 (p_2 and p_3; p_2 is used twice to reduce measuring error) and get

$$G_S\ [Vs/m] = \sqrt{(D_S - D_{S0})\frac{4\ \pi}{T_S} m_S (R_a + R_S)} \tag{6}$$

This constant You also can use if You calibrate a system by harmonic drive.

Note: For pendulum seismometers there are different notations

1) force/current $[N/A] = [Vs/m]$ and

2) torque/current $[Nm/A] = [Vs]$

of this constant, transferable via reduced pendulum length l_0 as

$$G_{S_{1)}}\ [Vs] = G_{S_{2)}}\ [Vs/m]\ *\ l_0\ [m] \tag{7}$$

Exercise 2

Calculating Seismometer Parameters

by Jens Bribach

Below You find a typical parameter list.

1) Mark the seismometer parameters absolutely necessary for calculating the seismometer response curve (Bode-diagram)

2) Complete the list by help of the related time series plot

3) Calculate the current (through calibration coil) necessary to deflect the seismometer mass for 1 μm at a frequency $f = 1\ Hz$ (see Remarks on Exercise 3)

SEISMOMETER

Mechanical Constants

Natural Period	T_S	..... s
Open Damping (Attenuation)	D_{S0}	.....
Reduced Pendulum Length	l_0	0.0785 m
Inertial Moment	K_S	0.0201 $kg\ m^2$
(Seismic Mass	m_S	..... kg)

Transducer Constants 1 (Signal Coil)

Coil Resistance	R_{S1}	6030 Ω
Electrodynamical Constant	G_{S1}	..... Vs/m

Transducer Constants 2 (Calibration Coil)

Coil Resistance	R_{S2}	835 Ω
Electrodynamical Constant	G_{S2}	..... Vs/m

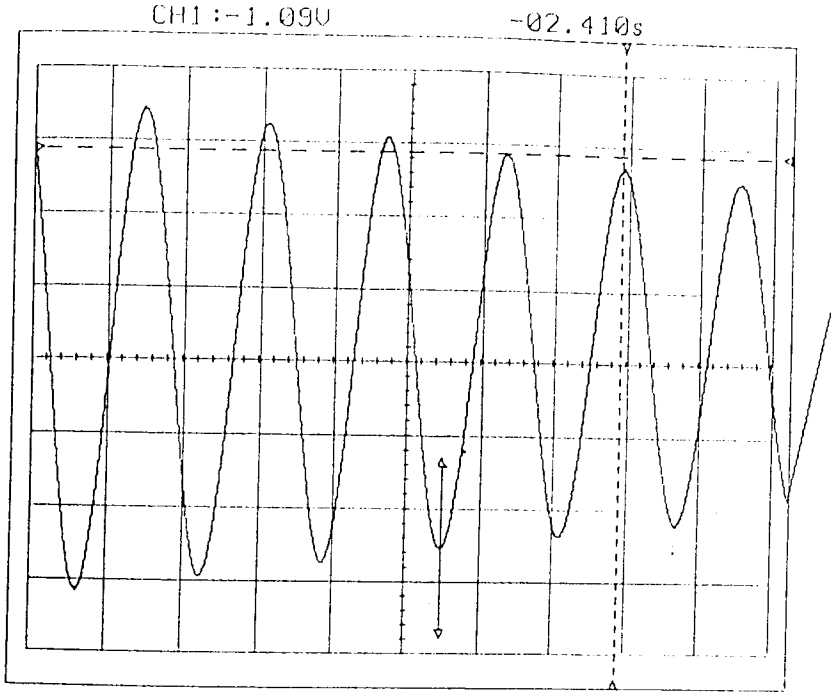

DATE:Nov 12/90
TIME:14:51:32

CH1: 0.20V :1s

open circuit

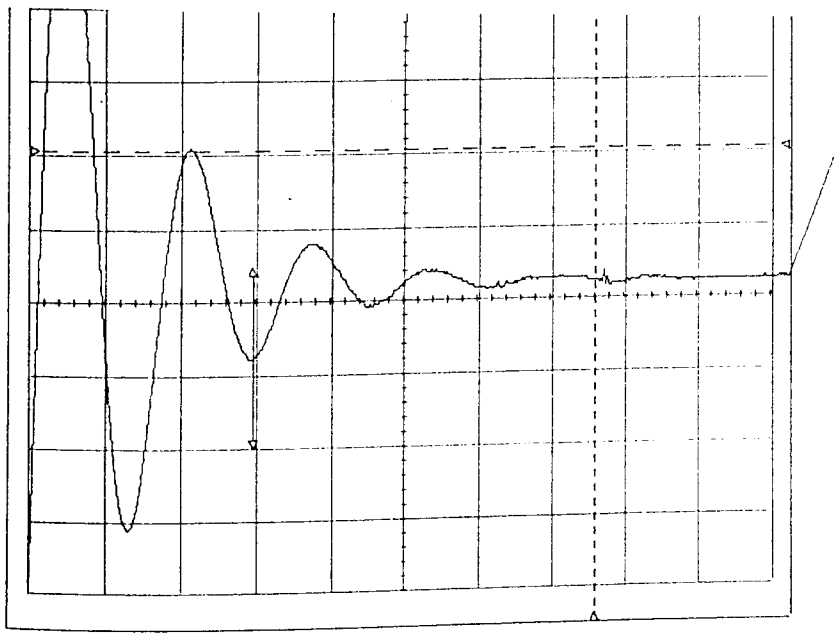

CH1: 0.50V :1s

signal coil

extern. resistor

$R_a = 67\ k\Omega$

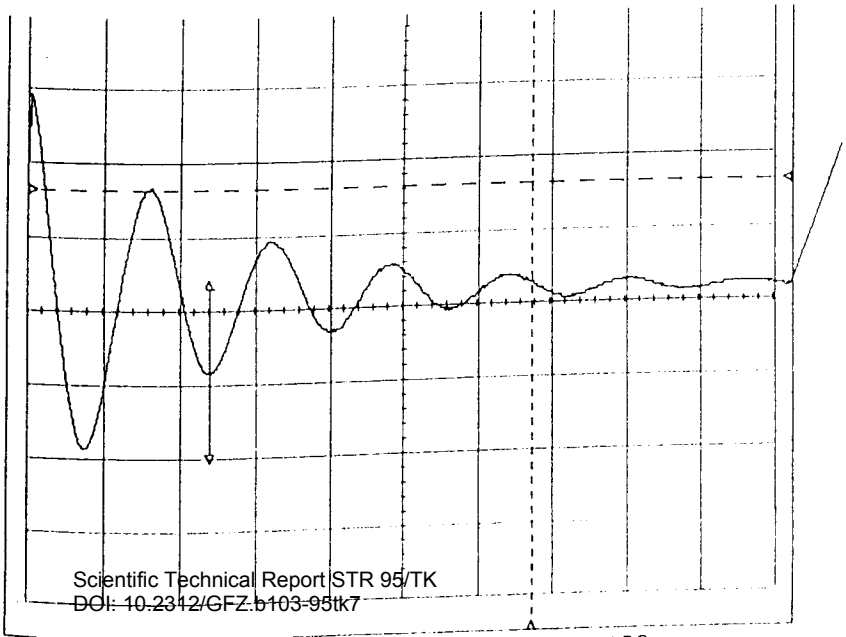

CH1: 0.20V :1s

calibration coil

extern. resistor

$R_a = 1\ k\Omega$

Remarks on Exercise 3

Calibration by Harmonic Drive

after a manuscript by Christian Teupser

If the seismometer possesses an auxiliary magnet and coil assembly, the calibration can be carried out by the aid of an electric current. The equation of motion (see Fundamentals equ.(2)) shows that a current i_S acts as a ground acceleration

$$\frac{d^2x_e}{dt^2} = \frac{G_{S2}\ l_0}{K_S}\ i_S \tag{1}$$

where G_{S2} is the electrodynamic constant of the auxiliary coil (given in $[Vs/m]$; other constants see Remarks on Exercise 2). It corresponds for a harmonic drive of frequency f with an equivalent ground displacement

$$x_e = \frac{G_{S2}\ l_0}{4\pi^2\ f^2\ K_S}\ i_S \tag{2}$$

For a translational seismometer, for example a geophone, with the seismic mass m_S the equivalent ground displacement is

$$x_e = \frac{G_{S2}}{4\pi^2\ f^2\ m_S}\ i_S \tag{3}$$

As the output voltage of a geophone with electromagnetic transducer is

$$E_S = G_{S1}\ \frac{dz}{dt} \tag{4}$$

where z is the displacement of the seismic mass, G_{S1} is the electrodynamic constant of the signal coil, and f_S the natural frequency, one obtains for a harmonic excitation

$$E_S = \frac{G_{S1}\ G_{S2}\ f}{2\pi\ m_S\ \sqrt{(f^2 - f_S^2)^2\ +\ 4D_S^2\ f^2\ f_S^2}} \tag{5}$$

Changing the frequency of the exciting current the output voltage attains a maximum at $f = f_S$. This can be used to determine the natural frequency and the damping using an oscilloscope.

INFLUENCE OF THE FREQUENCY CHARACTERISTICS OF THE SEISMOGRAPH ON ITS SEISMIC RECORDINGS

Peter Bormann

GeoForschungsZentrum Potsdam, Telegraphenberg A 34, D-14473 Potsdam

1. Introduction

Quantifyable instrumental recordings of the ground motion are a precondition for deriving quantitative scientific information from the analysis of seismic data. Seismologically relevant ground motions cover a wide range of periods (0,03 s < T < 3200 s). Within this range the frequency characteristic of the seismographs, i. e. the frequency dependence of their magnification is normally designed such as to ensure the best possible signal - to-noise ratio. This requires to consider the selection of frequency characteristics in the context of predominating spectra of seismic signals as well as noise. On the other hand misconceptions are widespread as to the proper meaning and use of the frequency characteristics or instrumental response curves derived from the calibration of seismographs. From this a number of systematic errors result when standard procedures of deriving the so-called "true ground motion" from instrumental recordings are applied. This will be illustrated both from a theoretical as well as a phenomenological point of view.

2. Frequency and phase characteristics of electrodynamic seismographs

A mechanical seismic receiver with galvanometric recording forms a coupled vibration system. Assuming small deflections of the pendulum and the galvanometer mirror the magnification of this system results from the solution of a linear differential equation of the 4th order. The solution consists of a time-dependent negative exponential term describing the transient response and of a time-independent stationary term. In case of a stationary harmonic ground oscillation the frequency and phase characteristics of the system ($\overline{U}(\omega)$ and $\varphi(\omega)$, respectively) are unambiguously defined by the eigenperiods T_s and T_g of seismometer and galvanometer, respectively, their damping factors D_s and D_g, the coupling factor σ^2 between seismometer and galvanometer and the magnification factor V_o. These parameters can be determined by various calibration methods. The resonance factor $\overline{U}$ results as the product of the individual resonance factors of seismometer (fig. 1) and galvanometer (fig. 2), i. e. $\overline{U} = U_s \cdot U_g / \omega$ with $\omega = 2\pi/T$ and T - period of ground motion. The amplitude-magnification characteristic of the coupled system is $V(\omega) = V_o \cdot \overline{U}$. In case of galvanometric recordings and under the conditions $T_s > T_g$ and $D_s < D_g$, V_o and $\overline{U}$ can be determined from the following formulas /1/:

$$(1) \qquad V_o = \frac{2 l_L}{l_{red}} \sqrt{\sigma^2 \frac{D_s T_g K_s}{D_g T_s K_g}} \qquad \text{and}$$

$$(2) \qquad \overline{U} = \frac{2 D_g}{T_g} \frac{1}{\sqrt{T^{-2} + a + b T^2 + c T^4 + d T^6}}$$

with l_L-length of the light indicator, l_{red} - reduced length of the pendulum, K_s and K_g - moments of invertia of the seismic pendulum and galvanometer, respectively,

and

$$(3)\quad \begin{cases} a = m^2 - 2p\,, \quad b = p^2 - 2mq + 2s\,, \quad c = q^2 - 2ps\,, \quad d = s^2\,, \\ m = 2\left(\frac{D_s}{T_s} + \frac{D_g}{T_g}\right)\,, \quad p = \frac{1}{T_s^2} + \frac{1}{T_g^2} + \frac{4 D_s D_g}{T_s T_g}(1 - \sigma^2)\,, \\ q = \frac{2 D_s}{T_s} \cdot \frac{1}{T_g^2} + \frac{2 D_g}{T_g} \cdot \frac{1}{T_s^2}\,, \quad s = \frac{1}{T_s^2 T_g^2} \end{cases}$$

Because of the symmetry of these formulas one obtains identical frequency characteristics when permuting the respective parameters of the seismometer and galvanometer and observing the conditions $T_s < T_g$ and $D_s > D_g$. This option is very important for the recording of very long-period seismic waves since it is relatively easy to operate galvanometers even at periods $T_g > 100$ s while seismometers with $T_s > 30$ s tend to be unstable. In this case the recorded ground motion is displacement proportional when the conditions $T_s \approx T < T_g$, $D_g < 1$ and $D_s \gg 1$ are observed.

The recorded harmonic motion $y(t) = Y \sin(\omega t + \varphi)$ shows a phase shift φ when compared with a harmonic ground motion $x(t) = X \sin\omega t$. The phase characteristic $\varphi = \varphi(\omega)$ can be determined from the relationship

$$(4)\qquad \tan\varphi = \frac{p T^2 - s T^4 - 1}{m T - q T^3}$$

when taking the relations given under (3) into account.
The amplitude X of the true ground motion could be determined from the recorded amplitude Y if V_o and $\overline{U}(\omega)$ are known and the presupposition of stationary harmonic oscillations holds true:

$$(5)\qquad X = \frac{Y}{V_o\,\overline{U}(\omega)}\,.$$

3. Influence of the seismograph's transient response

But seismic waves are more complicated. In particular body wave onsets cannot be described by a stationary harmonic oscillation but rather by wavelets with modulated amplitudes corresponding to a generalized BERLAGE function

$$(6)\qquad x(t) = \begin{cases} 0 & \text{for } t < 0 \\ t^a e^{-b\omega t} \sin\omega t & \text{for } t \geq 0 \end{cases}$$

with a and b - wavelet parameters, t - time (cf. /2/).

In this case the transient response of the seismograph has to be taken into account. Its duration and character depend on the duration and form of the seismic signal as well as on the vibration parameters of the seismograph. The transient response results in a systematic distortion of the amplitude and period of the recorded signal, i. e. the effective magnification $\overline{U}_i^B(\omega, a, b)$ is different from the frequency characteristic $\overline{U}(\omega)$ for stationary harmonic oscillations. This difference is largest for the first half-cycle. While in this case the distortion shows no strong dependence on the wave form the latter has a significant influence on the effective magnification of later half-cycles. The period of the incoming wave - particularly that of the first cycle - is also distorted due to the seismograph's phase shift. On the other hand the true and recorded onset time as well as the direction of first motion are always identical as long as the condition $x(t) = 0$ for

DOI: 10.2312/GFZ.b103-95tk7

$t < 0$ is fulfilled (i. e. if there is no movement of the seismograph prior to the onset-time due to noise or any preceding ground motion.

The transient response is largest for narrow-band peak - like frequency characteristics. This resonance type of frequency response is realized if for $T_s \approx T_g$, D_s and $D_g \ll 1$ and $\sigma^2 \gg 0{,}1$. In this case the seismograph reacts strongly only to ground periods close to the eigenperiod of the system. But the maximum amplification is only reached after the system has absorbed the energy of many ground oszillation, i. e. the transient response will take a long time. At the same time owing to its small attenuation the system will respond rather unspecifically with a long mono-frequency wave train to any kind of ground motion containing frequencies identical or close to the resonance frequency. In case of zero attenuation this wave train - once excited - would be of infinite duration. On the other hand a broad-band characteristic with a flat top is originated by combining a seismometer and galvanometer with very different eigenperiods and highly overcritical damping of at least on component of this coupled system, normally that with the shorter eigenperiod. This means that the resonance peak has to be truncated at the expense of the system's magnification. The strong damping of the individual reaction of the seismograph results in a small phase shift between ground motion and seismograph response for ground periods T between T_s and T_g and consequently in a very short transient response. The seismograph thus follows the ground motion very closely with minimum distortion. A seismograph with infinite attenuation would be equivalent to a rigid body that follows exactly the ground motion for all frequencies without magnification or distortion and thus, without transient response.
Besides this physical explanation there is a very illustrative one from the point of view of FOURIER-transformation. A needle impulse in the time-domain is equivalent to an infinite spectrum in the frequency domain while a single spectral line in the frequency domain corresponds to an infinite wave train of one definite period in the time domain. Therefore a ground deformation in form of a needle impulse can only be reproduced properly on the record if the frequency characteristic of the seismograph corresponds to a filter of infinite band-width. If, on the contrary, the band-width of the frequency characteristic is infinitesimal small the seismograph picks up only one of the infinite number of endless mono-frequent wavetrains that form the needle impulse. Its reaction, therefore, will be an undamped wave train of that given filter frequency.

But natural phenomena as well as technical possibilities for constructing real seismographs lie between these extremes of mathematical and physical abstraction. For illustration fig. 3, shows various short-period frequency characteristics used at Moxa station of the Central Institute for Physics of the Earth as well as examples of their recordings (figs.4, 5 and 6). Although the narrow-band characteristic A' is the optimal fit to the inverse short-period noise spectrum observed at Moxa station with a maximum magnification at T = 1 s 4times that of the standard type A the amplitude of the recorded first motions is not larger than in records of type A. Even the maximum ground motion of body wave onsets as calculated by using formula (5) is still generally lower when records of type A' are used (fig. 7). This partly explains the systematically lower magnitude estimates from records of narrow-band peak characteristics such as the ones installed at WWNSS stations as compared with the medium - to broad - band records typical for basic stations in most socialist countries. Geophones used in exploration geophysics and deep seismic sounding normally have narrow-band resonance characteristics, too, resulting in limited frequency content of the recorded signals and significant distortion of their character with respect to the true ground motion. The longer wavelets in narrow-band records make the discrimination and exact determination of onset-times of closely spaced successive onsets generally more difficult and sometimes impossible. These effects are detrimental for both quantitative amplitude studies as well as detailed travel-time

analyses of later arrivals (depth phases of shallow events, intersections and triplications of travel-time curves).

4. Deconvolution of seismograms

Seismological interpretation methods leading to physically more informative results require in most cases the knowledge of true ground motion and/or high-resolution travel-time data. The true ground motion can be restored by deconvolving the seismogramme.

In principle the deconvolution of the seismographic record means its transformation to the record of a seismograph with the band width $(2T_0, \infty)$ by means of calculation. This can be accomplished in the frequency domain by a two-fold Fourier transformation or in the time domain by applying the exact or the approximate inverse filter operator of the seismograph (cf. NEUGEBAUER /9/). But the exact restoration of the true ground movement is possible only in case of perfect unbiased seismogramms.

The presence of noise as well as random and truncation errors can falsify the result to uselessness. Another independent approximate method was proposed by NEUNHÖFER /10/ who accomplished the deconvolution by repeated convolution of suitable wavelets using a generalized Monte-Carlo-technique and trial and error until the residuals between the recorded seismogramme and the seismogramme for the synthesized approximate ground movement become smaller than a given figure. This method allows the recognition and elimination of disturbing drifts and jumps and cannot be applied on a routine basis. KORČAGINA and MOSKVINA /8/ outline in their paper, too, the difficulties and uncertainties involved in practical attempts to restore the true ground motion from classical analog recordings. Therefore, to avoid all these problems, the easiest and best way of deconvolution is to avoid convolution. But this means that one should give preference to broad-band seismographs, to guarantee that the primary information has been recorded with minimum distortion. This is all the more so if one has facilities for analog or digital recording on magnetic tape which, by means of computers, will later allow the application of desirable operations such as the determination of other derivatives of the ground displacement (ground velocity and acceleration), spectral analysis, band-pass, multi-channel and noise prediction filtering.

The only significant problem when recording teleseismic signals of both very week as well as strong seismic events with an extremely broad displacement proportional frequency characteristic is the very large dynamic range to be coped with (some 120 dB). It can be reduced by some 20 dB when using a pass-band magnification proportional to ground acceleration. At the same time such a characteristic fits best the overall trend of the inverse noise spectrum thus ensuring a good signal-to-noise ratio with a minimum dynamic range. Frequency characteristics of this type have for the first time been recommended for world-wide use by BERCKHEMER /4/. In case of digital recordings ground displacement and velocity can easily be derived from these data by one- or two-fold integration, very stable records presupposed.

5. Conclusions

Broad-band frequency characteristics give a better picture of the true ground motion than small-band ones. The expected gain in magnification when fitting a frequency characteristic into a small noise window might be lost completely in case of short wavelets owing to the reduced effective magnification during the transient response. This fact also explains partly the discrepancy between so-called "Eastern" and "Western" body wave magnitudes.

Broad-band characteristics are particularly suitable for the determination of the direction of first motion and the identification and onset-time determination of successive body wave groups, e. g. in connection with a multiple rupture process in

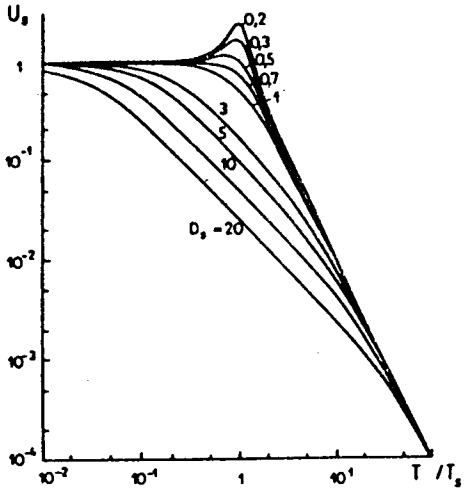

Fig. 1 Resonance factor U_s of the seismometer as a function of the ratio T/T_s for different values of the seismometer damping D_s (after /6/)

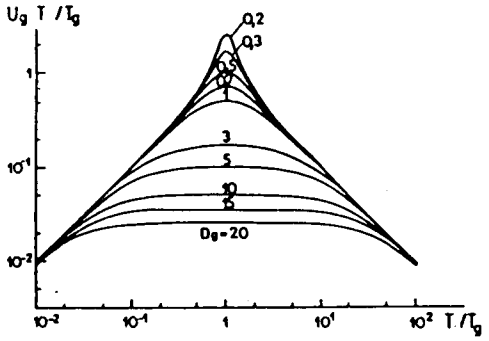

Fig. 2 Normalized resonance factor $U_g \cdot T/T_g$ of the galvanometer as a function of the ratio T/T_g for different values of the galvanometer damping D_g (after /6/)

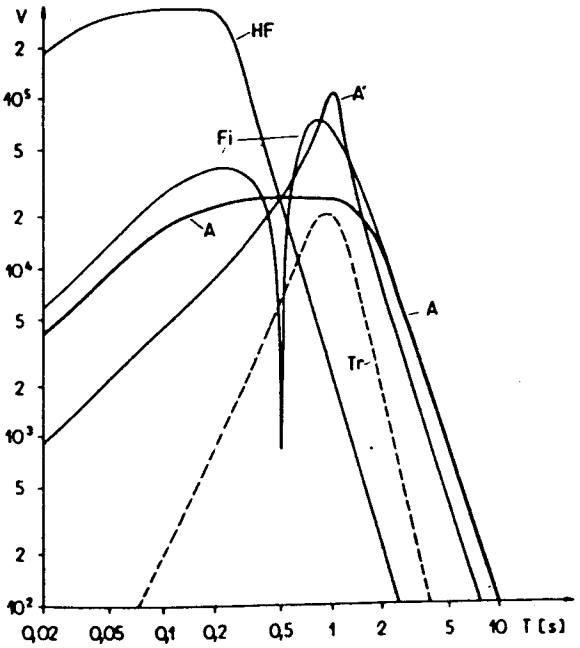

Fig. 3 Frequency characteristics of various short-period seismographs at Moxa station

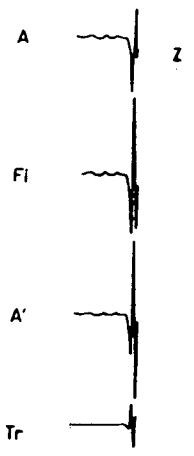

Fig. 4 Vertical records of types A, Fi, A' and Tr from a deep earthquake under the Sea of Okhotsk (29 Jan 1971, D=72.3°, h=544 km, MPV=6.1)

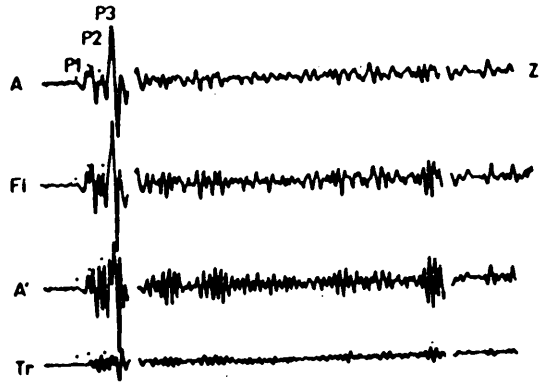

Fig. 5 Vertical records of types A, Fi, A' and Tr from an earthquake in Honshu, Japan (7 Oct 1970, D = 68.0°, h = 179 km, MP1V = 5,8, MP3V = 6.4)

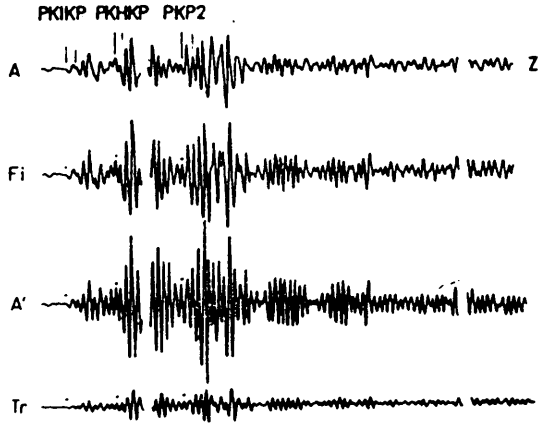

Fig. 6 Vertical records of types A, Fi, A' and Tr from a deep earthquake in the Fiji Island region (D = 152.6°, h = 584 km, MPV = 5.7)

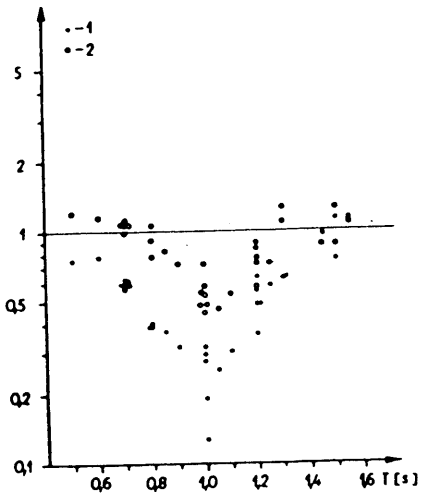

Fig. 7 Amplitude ratio of the first onsets and of the maximum amplitude of P, respectively, in records of type A' and A, normalized to the same magnification for stationary harmonic oscillations. 1 - first onsets, 2 - maximum amplitude of P

the focal region or with closely spaced travel-time curves in case of triplications, depth phases of shallow events etc.

While narrow-band frequency characteristics distort strongly the character of true ground motion extreme broad-band characteristics show minimum convolution. In case of velocity or acceleration proportional characteristics a good fit with the general trend of the inverse noise spectrum is achieved thus insuring a good signal-to-noise ratio over the whole period range and a dynamic range still managable with modern digital records.

Selected references

/1/ ARCHANGEL'SKIJ, V.T. et al.: Apparatura i methodika nabljudenij na sejsmiceskich stancijach SSSR.
Izdat. Akad. Nauk SSSR, Moskva (1962).

/2/ ARONOVIC, Z.I.; VIL'KOVIC, E.V.; DOLGOPOLOV, D.V.: Amplitudnye charakteristiki sejsmografa pri nestacionarnych vchodnych signalach i ocenka pogresnostej, svjazannych s primeneniem amplitudnych charakteristik dlja stacionarnych garmoniceskich kolebanij. Analiz seismiceskich nabljudenij na elektronnych mašinach.
Vyčislitel'naja sejsmologija, Vypusk 1, Izdatel'stvo "Nauka", Moskva (1966), p. 73 - 91.

/3/ BANERJA, K.N.: Response characteristics of electrodynamic seismographs.
Proc. nat. Inst. Sci. India 26 (1960) 4, Part A, Phys. Sci., p. 348 - 354.

/4/ BERCKHEMER, H.: The concept of wide-band seismometry.
Proc. XII Ass. Gén. CSE, Obs. Roy. Belg. Comm. Sér A, 13, Sér Geophys., 101, Bruxelles (1971).

/5/ BORMANN, P.: Standardization and optimization of frequency characteristics at Moxa station (GDR).
Proc. XIIIth General Ass. European Seismological Comm., Technical and Economical Studies, D. Series, No. 10, Bucharest (1974), p. 133 - 145.

/6/ DUCLAUX, F.: Seismoetric théorique.
Gauthier-Villar, Paris (1960), 129 pp.

/7/ KONDORSKAJA,N.V.; ARANOVIC, Z.I.: Metodiceskie osnovy optimizacii sistemy sejsmiceskich nabljudenij.
Izv. AN USSR, Fiz. Zemli (1971) 7.

/8/ KORČAGINA, O.A.; MOSKVINA, A.G.: O vosstanovlenii istinnogo dvizenija pocvy po sejsmogramme.
Izv. Akademija Nauk, Fiziki Zemli (1975) 7, p. 27 - 42.

/9/ NEUGEBAUER, H.-J.: Aplication of elastic network theory in seismometry.
Proc. XII. Ass. Gén CSE, Obs. Roy. Belg. Comm. Sér A, 13, Sér Geophys., 101, Bruxelles (1971), p. 224 - 238.

/10/ NEUNHÖFER, H.: Deconvolution by reiterated convolution.
Zeitschrift für Geophysik, Würzburg 39 (1973) 4, p. 513 - 514.

/11/ SAWARENSKI, E.F.; KIRNOS, D.P.: Elemente der Seismologie und Seismometrie.
Akademie-Verlag Berlin (1960), 512 pp.

/12/ TEUPSER, Ch.: Die Eichung und Prüfung von elektrodynamischen Seismographen.
Freiberger Forschungshefte C 130, Akademie—Verlag Berlin (1962), 103 pp.

/13/ TEUPSER, Ch.: Verallgemeinerung der Theorie elektrodynamischer Seismographen durch frequenzabhängige Koppelung.
Veröff. des Inst. für Geodynamik der DAW zu Berlin, Nr. 2, Akademie-Verlag (1965), 127 pp.

/14/ TEUPSER, Ch.: Die kurzperiodischen Seismographen Typ VSJ-II und HSJ-II.
Veröff. des Zentralinstituts für Physik der Erde Nr. 12 (1971), 59 pp.

/15/ TEUPSER, Ch.; UNTERREITMEIER, E.: Der elektronische Dreikomponenten-seismograph EDS-1. Theorie, Aufbau und Wirkungsweise.
Veröff. des Zentralinstituts für Physik der Erde Nr. 51 (1977), 144 p.

/16/ ULLMANN, W.: Analytische Seismometrie.
Veröff. des Inst. für Geodynamik Jena, Akademie-Verlag Berlin (1971), 339 pp.

/17/ UNTERREITMEIER, E.: Zur Erhöhung der Störfreiheit langperiodischer Seismographensysteme.
Veröff. des Zentralinstituts für Physik der Erde Nr. 12 (1971), 199 pp.

/18/ WILLMORE, P.L. (Editor): Manual of seismological observatory practice.
World Data Centre A for Solid Earth Geophysics. Report SE-20, Sept. 1979.

Mitteilung des Zentralinstituts für Physik der Erde Nr. 1046

FUNDAMENTALS ON SIGNAL AND NOISE SPECTRA

Peter Bormann

GeoForschungsZentrum Potsdam, Department of Disaster Research,
Telegrafenberg A17, D-14473 Potsdam, Federal Republic of Germany

1. SIGNAL AND NOISE SPECTRA AND THEIR UNITS

Traditionally, spectra of seimic noise were determined from *analogue* seismic records by determining the *peak or average* amplitudes within a given time window, e.g. of several minutes duration, for visually recognizable dominating periods. Fig. 1 shows microseismic spectra of this kind as derived by Brune and Oliver (1959) from an averaging compilation of global noise observations.

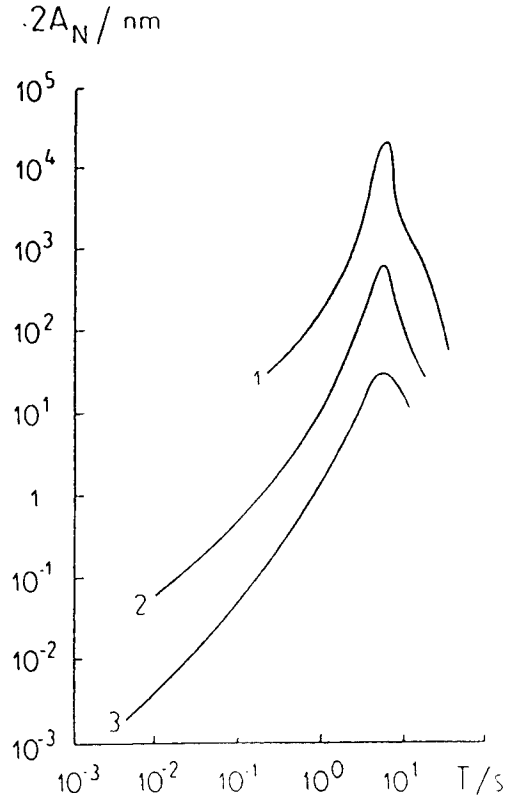

Fig. 1:Peak-to-peak (double) amplitudes of microseismic noise as a function of period for 1 - very noisy, 2 - normal and 3 - very quiet areas (after Brune and Oliver 1959)

Nowadays, digital seismic records allow proper computational spectral analysis. But contrary to *coherent transient seismic signals* f(t) of finite length such as seismograms from explosions or earthquakes irradiated by a defined localized source *ambient seismic noise* can be considered as a more or less *stationary stochastic process*.

While for a transient signal f(t) the Fourier transform f(ω) exists with

$$f(\omega) = \int_{-\infty}^{\infty} f(t)\, \exp(i\omega t)\, dt = |f(\omega t)|\, \exp^{i\phi(\omega)} \qquad \text{and} \tag{1}$$

$$f(\omega) = (2\pi)^{-1} \int_{-\infty}^{\infty} f(t)\, \exp(-i\omega t)\, d\omega, \tag{2}$$

with $|f(\omega)|$ as the *amplitude spectral density* with the unit m/Hz and $\phi(\omega)$ as the *phase-delay spectrum* with the units deg, rad or 2πrad,

Seismic noise cannot properly be expressed by (1) for non-coherent stochastic noise has no defined phase-delay spectrum. Therefore, a more suitable spectral presentation of seismic noise is the *power spectral density* P(ω). It is the Fourier transform of the autocorrelation function $P(\tau) = < f(t)\, f(t + \tau) >$, i.e.

$$P(\omega) = \int_{-\infty}^{\infty} P(\tau)\ \exp(i\omega\tau)\, d\tau \tag{3}$$

with the unit m^2/Hz. The symbol < > indicates averaging over the time t. P(ω) does not contain information about the phase.

Despite of the above said both signal and noise spectra are often jointly calculated on the basis of (2), e.g. for a presentation of the spectral *signal-to-noise ratio* (SNR) which provides a good orientation on the most suitable ranges for signal filtering and noise suppression. Fig. 2 shows respective examples based on teleseismic recordings of an Iran earthquake (D ≈ 40°) with digital braodband STS-2 seismometers at the two nearby stations Hamburg (HAM) and Bad Segeberg (BSB) which have very different noise conditions. While the high-pass filtering (f = 0.2 - 5 Hz) of the broadband record (f = 0.008 - 40 Hz) shows clear short-period P-wave arrivals at BSG but not at HAM the latter has an even better record than BSG after low-pass filtering with a corner frequency $f_c < 0.1$ Hz (Fig. 3).

Fig.4 shows, as an example, the displacement power spectrum of ambient noise in the frequency range $0{,}3 < f < 50$ Hz in units of nm^2/Hz (1nm = 10^{-9}m) for a site in Iran. In case of ground velocity or acceleration power spectral densities the respective units would be $(m/s)^2$/Hz and $(m/s^2)^2$/Hz, respectively (e.g. Figs. 5 and 6). But when transforming displacements $a = a_o \sin\omega t$ into the respective velocities or accelerations one has to consider that the amplitudes of these higher derivatives are $a_o = a_o\omega$ and $a_o = a_o\omega^2$, respectively.

Often the noise displacement power density spectra are given in units of decibel = 10 log m^2/Hz = 20 log m/Hz referred to $1m^2$/Hz or as 10 log(m^2/s^4)/Hz = 20 log(m/s^2)/Hz referred to $1(m/s^2)^2$/Hz. Fig. 6 is an example for the latter, presenting both the original (O) and the new (N) global *high-noise models* (HNM) and *low-noise models* (LNM) according to Peterson (1991).

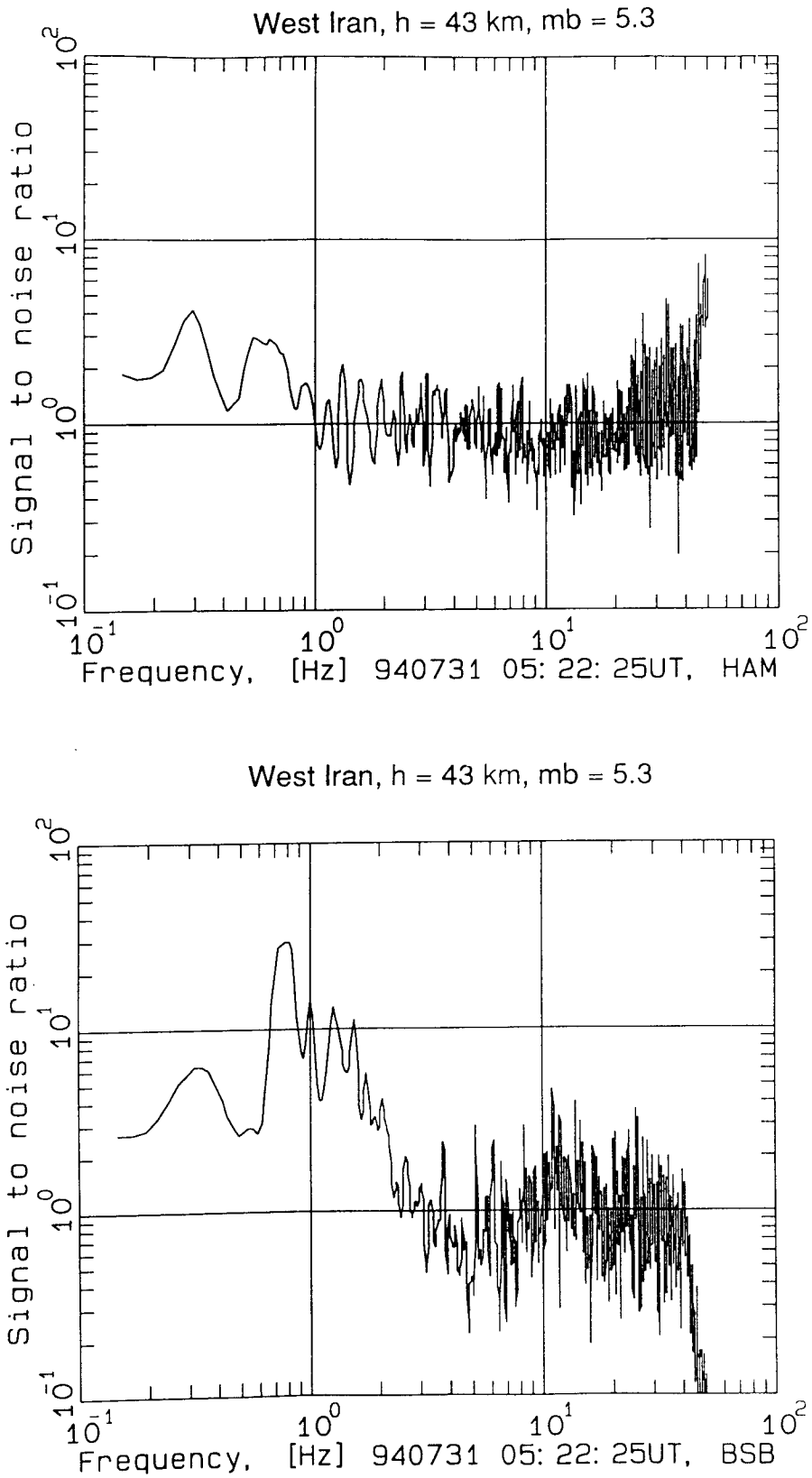

Fig. 2: Signal-to-noise ratios of a seismic event in West Iran (epicentral distance about 40°) as calculated from records of broadband seismometers STS-1 at the station HAM and BSG in northern Germany

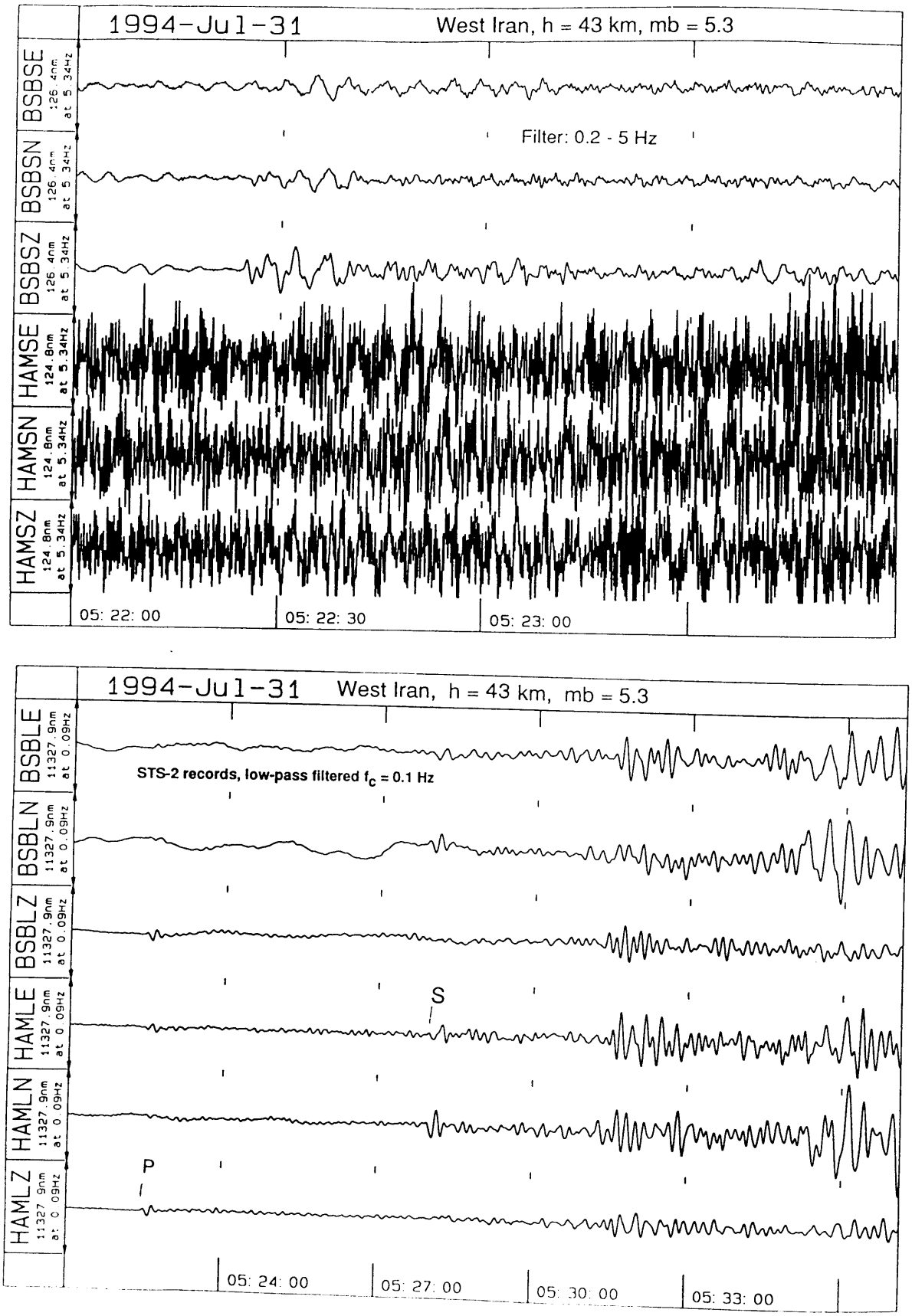

Fig. 3: High-pass (above) and low-pass (below) filtered records of the Iran event at HAM and BSB

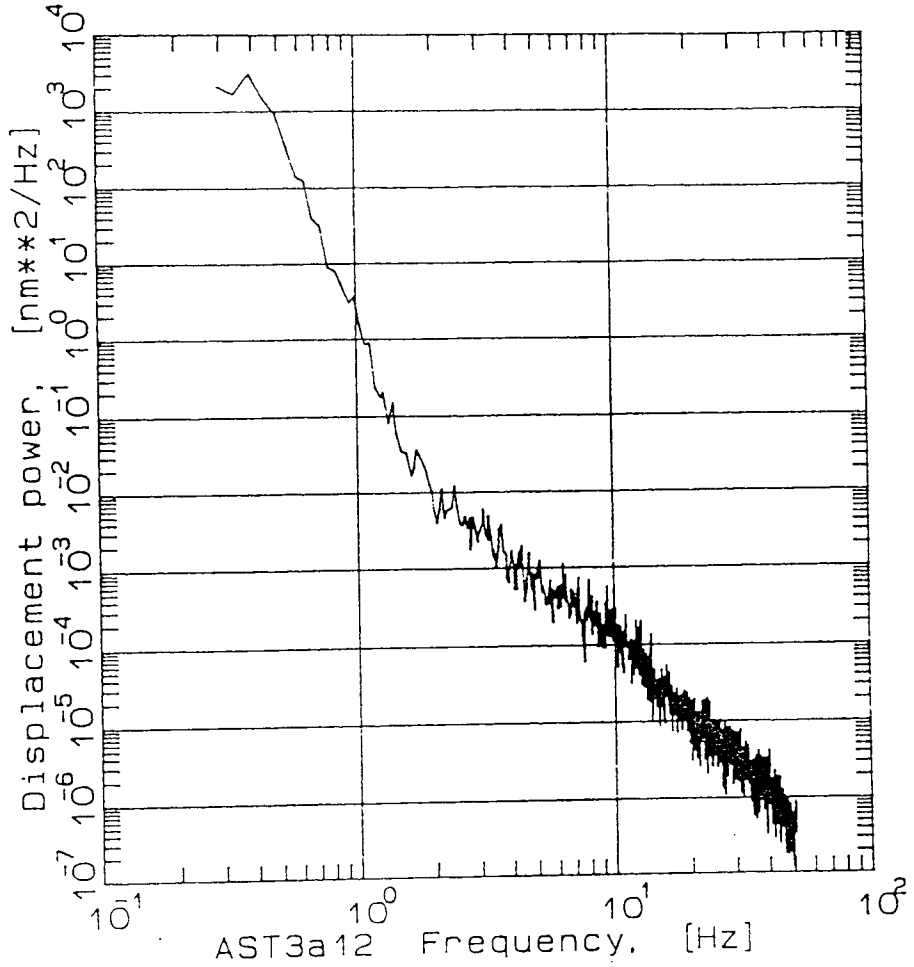

Fig.4: Spectrum of displacement power density recorded at a very quiet remote site in Iran

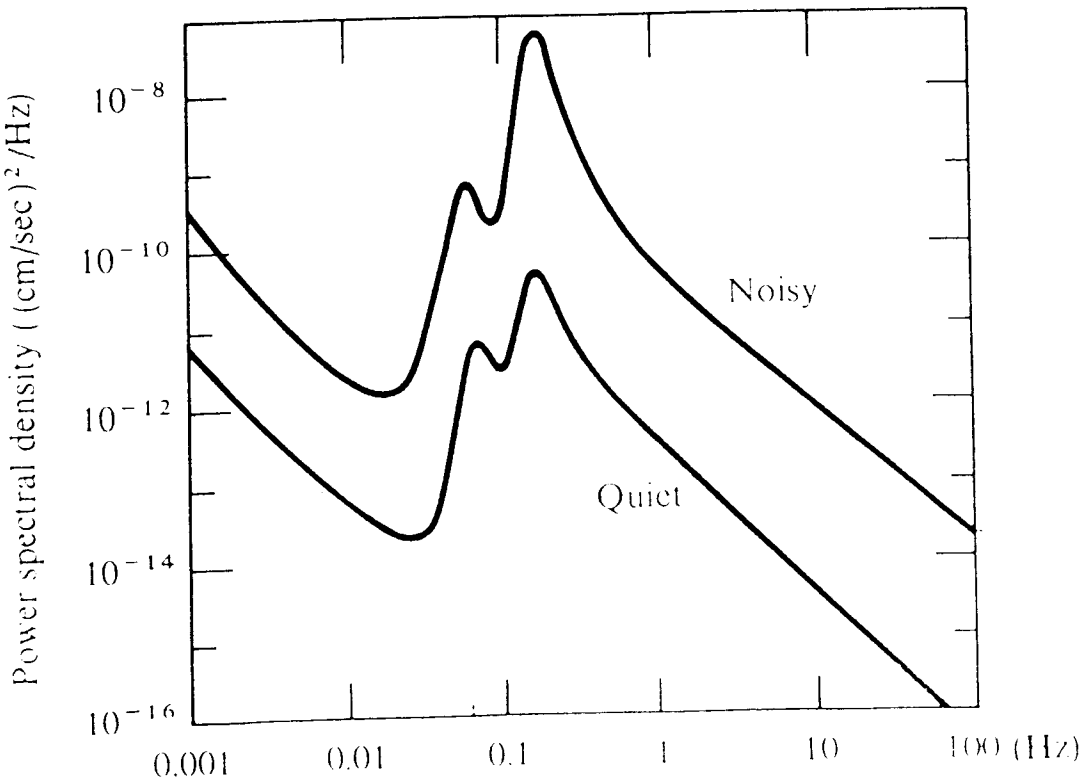

Fig. 5: Velocity power spectra of ambient seismic noise at noisy and quiet conditions for a typical station on hard basement rock (taken from Aki and Richards 1980)

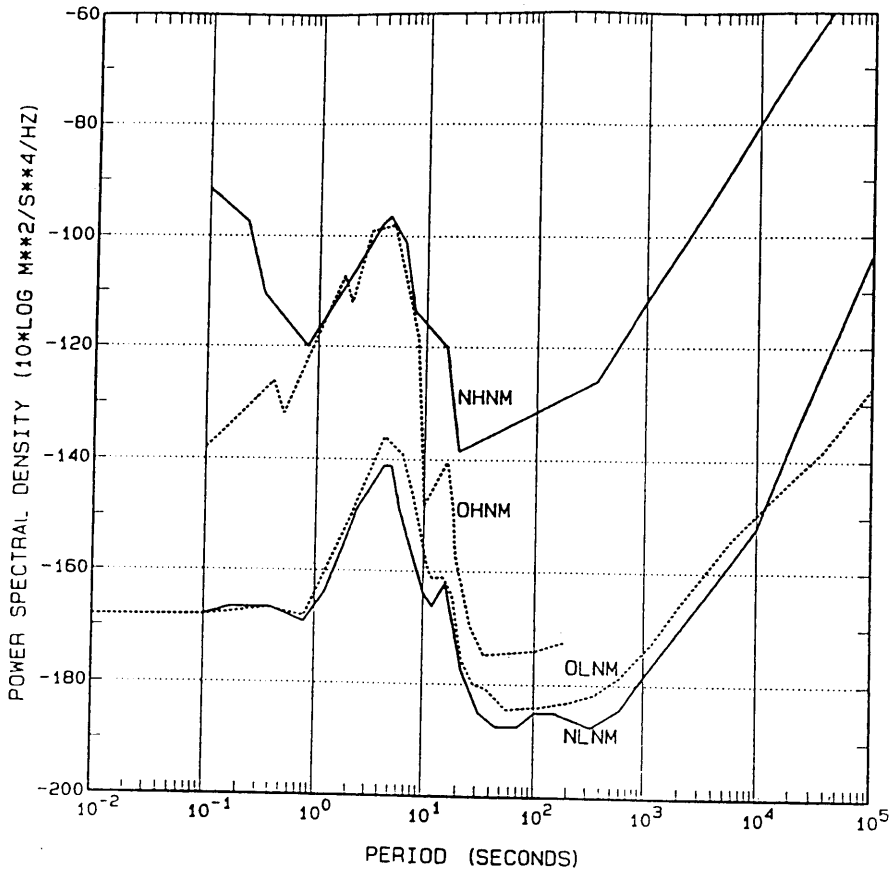

Fig. 6: Comparison of the new (N) and original (O) noise models according to Peterson (1993). HNM stands for high-noise model and LNM for low-noise model. The OHNM was based on SRO data which were recorded in boreholes at about 100 m depth. This explains the large difference between the OHNM and NHNM at long periods

2. Transformation of spectral amplitude densities into recording amplitudes

According to Aki and Richards (1980) the maximum amplitude of a wavelet f(t) can be **roughly approximated** by the product of the amplitude spectral density and bandwidth of the wavelet, i.e.

$$f(t)_{max} = |f(\omega)|\ 2\ (f_u - f_l) \qquad (4)$$

with f_u and f_l as the upper and lower corner frequencies of the frequency band of the wavelet. Fig. 7 depicts the ranges of amplitude spectral densities for surface waves, teleseismic P-waves and short-period S-waves from microearthquakes within different magnitude ranges according to Aki and Richards (1980, p. 496). Assuming an earthquake with mb = 8 at an epicentral distance $\Delta = 90°$ and relatively narrowband 2-octave short-period and medium-period recordings (f_u = 2Hz, f_l = 0.5 Hz and f_u = 0.2 Hz, f_l = 0.05 Hz, respectively), then, according to (4) and Fig. 7, the expected maximum "true ground amplitude" of the recorded P-wave wavelets with dominating "center frequencies" around 1Hz and 0.1 Hz would be roughly 6×10^{-3} mm and 1.5×10^{-1} mm, respectively. For surface waves, Ms = 8.5, $\Delta = 90°$ and center-period of about 20s (f_o = 0.05 Hz) $f(t)_{max}$ becomes roughly 5 mm.

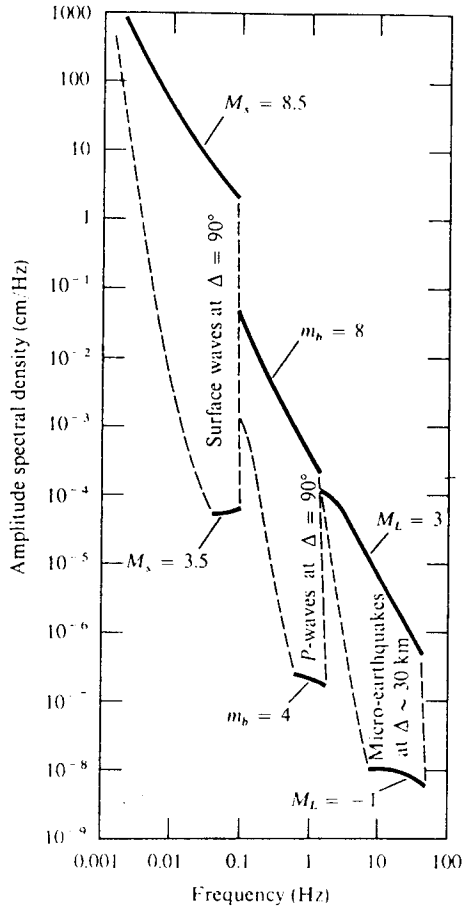

Fig. 7: Ranges of amplitude spectral densities for seismic waves according to Aki and Richards (1980, p. 496)

Likewise, if the power spectral density defined for noise is $P(\omega) = P$ within the frequency band $f_u < |f| < f_l$ and $P(\omega) = 0$ otherwise, then

$$< f^2(t) > = 2P\,(f_u - f_l), \tag{5}$$

i.e., knowing the bandwidth of the noise signal we can approximately relate its power *spectral density* (PSD) to the *mean square amplitude*.

Proper determination and intercomparison of spectral densities in different frequency ranges require octave filtering. Increasing the frequency of a signal by one octave means doubling its frequency. Accordingly, a signal (or filter) with n octaves of bandwith has corner frequencies

$$f_u = 2^n f_l \qquad \text{and } \textit{a geometric center frequency } f_o \text{ of} \tag{6}$$

$$f_o = (f_u \times f_l)^{1/2} = f_l \times 2^{n/2}. \tag{7}$$

From this follows for the *relative bandwidth*

$$(f_u - f_l)/f_o = (2^n - 1)/2^{n/2}, \tag{8}$$

i.e. the relative bandwith for a 2-octave filter is 1.5 and for a 2/3-octave filter 0.466 ≈ **0.5.**

Thus, when putting the bandwith half the considered center frequency, i.e. $f_u - f_l = 0.5 f_o$ as recommended by Aki and Richards (1980) on p. 498 of their vol. 1, then this would correspond to the assumption of a bandwidth of 2/3 octaves. According to (5) the estimated *root mean square* (RMS) amplitudes would then be simply $(< f^2(t) >)^{1/2} = (P\ f_o)^{1/2}$. Signals recorded by typical classical narrowband seismographs, e.g. of WWSSN type, have bandwith of about 1 to 2 octaves.

But several other authors (e.g. Fix 1972; Melton 1978) have used an integration bandwith of 1/3-octave only for computing RMS amplitudes from PSD, reasoning that this is nearly ±10% about the center period in width and that this is close to the tolerance with which an analyst can measure the period on an analog seismogram. Therefore, using a 1/3-octave bandwidth seems to be a reasonable convention for calculating RMS amplitudes from PSDs. The differences as compared to RMS values based on 1/4- or 1/2-octave bandwiths are less than 20% but 1/3-octave RMS amplitudes will be only about 50% or 30% of the respective RMS amplitudes as calculated for 1- or 2/3-octave bandwith, respectively.

ACKNOWLEDGEMENT

My thanks go to Dr. Kurt Wylegalla for kindly providing the Figs. 2 and 3

REFERENCES

Aki, K. and Richards, P.G. (1980). Quantitative seismology - theory and methods. W.H. Freeman and Company, San Francisco, Vol.1, chapter 10: principles of seismometry, 477-524

Brune, J.N. and Oliver, J. (1959). The seismic noise of the Earth´s surface. BSSA 49, 349-353

Fix, J.E. (1972). Ambient Earth motion in the period range from 0.1 to 2560 sec. BSSA, 62, 1753-1760

Melton, B.S. (1978). The sensitivity and dynamic range of inertial seismographs. Rev. Geophys. Space Phys., 14, 93-116

Peterson, J. (1980). Preliminary observations of noise spectra at the SRO and ASRO stations. U.S. Geol. Survey Open-File Report 80-992, 25p.

Peterson, J. (1993). Observations and modeling of seismic background noise. U.S. Geol. Survey Open-File Report 93-322, 95p

Exercise on bandwidth calculations and the transformation of power spectral densities in root mean square amplitudes

Peter Bormann

GeoForschungsZentrum Potsdam, Division of Disaster Research,
Telegrafenberg A34, D-14473 Potsdam, Federal Republic of Germany

1. Determine the *relative bandwidth* of an:

a) 1-octave filter
b) 1/2-octave filter
c) 1/3 octave filter
d) 1/4-0ctave filter

using equation (8).

2. Calculate for the noise maximum in Fig. 5 the corresponding RMS (root mean square) particle velocity and displacement:

a) Estimate the velocity power maximum from Fig. 5

b) Give this value also in units of $(m/s)^2/Hz$

c) Estimate the frequency related to this maximum

d) Calculate the RMS particle velocity by considereing eq. (5) and a bandwidth of 2/3 octaves

e) Transform this RMS particle velocity determined under d) into the corresponding RMS particle displacement

f) Give the *amplitude spectral density* for the displacement amplitude determined under e) considering eq. (4)

g) Compare the value calculated under f) with Fig. 7 and discuss the reason for the "notch"-shaped lower boundary of the seismic signals´amplitude spectral density range

3. Transform the displacement power values of Fig. 4 at f = 1 Hz and f = 10 Hz in:

   a) units of m^2/Hz

   b) acceleration power values with units $(m/s^2)^2/Hz$

   c) the value determined under b) in units of dB and compare the result with the respective values in Fig. 6 for the New Low Noise Model (NLNM)

4. Determine from Fig. 6 the NHNM-values in units of $(nm/s^2)/Hz$ for:

   a) f = 1 Hz

   b) f = 0.1 Hz

   c) f = 10 Hz

5. Transform the values determined under 4. into the corresponding RMS displacement amplitudes considering a signal of 1/3 octave bandwidth and compare the result with the respective amplitudes in Fig. 1. Discuss possible discrepancies.

6. Transform the *peak noise* amplitudes in Fig.1 for curve 1 ($2 A_N \approx 2 \times 10^4$ nm at $T \approx 6$ s, i.e. $f \approx 0.17$ Hz into the respective acceleration power spectral density in units of $(nm/s^2)^2/Hz$ assuming a bandwidth of the signal of 1/3 octave.

7. Express the result of 6. in dB referred to 1 $(m/s^2)^2/Hz$.

8. Compare the result of 7. with the respective value for the NHNM in Fig. 6 and discuss possible discrepancies.

Station selection, instrument operation, maintenance and control

by

P. Bormann and K.D. Klinge

1. Types of stations

The present network of seismographic stations in the world, consisting of more than thousand stations is very unequally spaced. While the U.S.A. has about 700 /1/ and Japan 120 /2/ active stations, there are almost none in large areas, especially in the great oceans and in the southern hemisphere. In recent year, much effort has been devoted to improvement of the station networks, partly by standardizing instruments, partly by extending observations to new areas. The latter item includes installation of unmanned stations in remote parts of the continents and of stations on the sea bottom. Several experiments with the operation of ocean-bottom seismographs have been made, particularly by the Soviet Union and the U.S.A. But still very much remains to be done, before the earth is covered by an equally spaced station network.

Among instrumental improvements, we mention the array stations in different countries and such networks like WWSSN (World Wide Standard Seismic Networks), SRO (Seismic Research Observatories), ASRO (Abbreviated-SRO) and HGLP (High-Gain Long Period) with their standards for seismographs and/or their frequency characteristics, with recordings on magnetic tape and the use of big computers such stations offer a quicker and more complete analysis of the recorded waves then traditional ones. However, special research has shown that even more traditional station networks can be treated as great array stations, as long as the signals on the different stations are good enough correlated so that array techniques can be applied.

By placing seismometers into bore holes disturbing surface background noise can sometimesbe suppressed significantly. The improvement of the signal-to-noise ratio (SNR) is sometimes even better than the one accomplished by considerably more expensive multi-seismometer arraysat the surface or near to it /2/.

In the following we will discuss the main types of seismographic stations.

1.1 First-Order Stations

The first-order stations provide the main coverage of the earth surface for the observation of long-period and short-period earthquake waves over teleseismic distances $D > 1000$ km. As the sources of the seismic waves are distributed over the whole earth, the interest in the data is also world-wide. A first-order station is not primarily a research tool of the institution which operates it. Instead, it is an element in the world network, and should be operated for the benefit of seismology as a whole /3/. The international exchange of data can only be effective if these data fulfil certain basic requirements and if they are acquired and/or disseminated in a standard form. Three main demands are (after /3/):

1. The stations of the first-order network should be within 1000 km of each other in all parts of the world. Europe, most of Asia and North America are already covered to an appropriate density. The areas which have much less than optimum cover are, most notably, the oceans followed on land by South America and Africa.

2. First order stations should be equiped to record the components N-S, E-W and vertical of short-period and long-period ground motion. Equipment, operation, recording and reporting procedure should conform with world standards.

3. First order stations should provide a continuous record of all seismic signals that are observable above the threshold set by local noise conditions. In highly seismic areas additional equipment for recording at lower sensitivity should be provided. At stations where destructive earthquakes are to be expected, accelerographs and seismocopes may be appropriate. New developments over the past decade are improved methods for recording the analogous earthquake signals - after conversion into a computer-compatible digital format - on magnetic tape. This allows to use high-speed-computers for spectral analysis and other types of signal processing. First-order stations are for instance all WWSSN-stations, the station Moxa in the GDR and other stations in many countries.

1.2 Second-Order Stations

Second-order stations are usually established for short-range observations ($D < 1000$ km) and for this purpose are frequently grouped into regional networks, reporting to a single interpretation centre. Problem-oriented regional interest dominate over those of global data exchange. This frequently results in a lower degree of standardization as compared to the requirements for the first-order network. Nevertheless, the importance of international co-operation in the observation of small events is steadily increasing since respective data are an important complement to some world-wide observations. Record format and operating procedures for second-order stations should therefore follow first-order standards.

1.3 Temporary Stations

The erection of temporary or mobile stations has been quite common practice. It has obvious advantages in the investigation of local noise conditions, crustal structures, microearthquakes and aftershock sequences. Long-period and short-period seismographs and even extensive arrays can be operated using transportable seismometers and recording equipment.

1.4 Array Stations

An array consists of a number of seismometers spaced out on the ground and connected by cable or radio links to a central recording system. The aim is to increase the sensitivity with regard to a particular seismic signal in comparison with other signals or random noise. In the simplest type of array, the seismometers are distributed over an area which extends over a fairly small fraction of a wavelength of the useful seismic signal. The desired signal, therefore, arrives approximately in phase at all the detectors. The outputs of all the seismometers are added together and the sum - which is approximately the arithmetic sum of the individual elements - is recorded on a single information channel. In contrast to the coherent seismic signals, noise which originates from small incoherent sources near the detectors will produce a sum which is more nearly proportional to $\sqrt{n}$ (n is the number of instruments). Thus the signal-to-noise ratio increases approximately by a factor $\sqrt{n}$. Besides this other more sophisticated computer assisted array techniques are applied for SNR improvement, signal detection, source localization, event identification etc. Examples for major seismic arrays are the NORSAR array in Norway, the Hagfors array in Sweden, arrays in the U.S.A. (Montana and Alaska) and in a number of other countries.

1,5 Special Stations

Special stations working as first-order stations or station networks are, e. g. the Seismic Research Observatories (SRO). Long-period borehole seismometershave been developed for these observations. They are sensitive enough to resolve long-period earth displacements measured in Å (10^{-8}cm).
To accomodate a large range of signal amplitude, a digital recording system on magnetic tape with a dynamic range of 126 dB is used. In contrast most conventional seismographs with drum recording on photographic paper have a recording range of only 44 dB, or little over two orders of magnitude.

Other special stations are the HGLP and the ASRO systems.

2. Station Selection

The site for a station must fulfil several conditions according to the type of station, and these demands are continually increasing with the steady development of seismometry and the growing requirements of basic and application oriented research. The following factors are important /3/:

1. Remoteness from local disturbances like traffic, heavy machinery, wind action on buildings and trees, large lakes, waterfalls.
2. Accessibility for personal and power supply.
3. Stable underground. Hard bedrock, preferably crystalline, within reach of the surface.
4. Low relief. Broken country scatter seismic waves, and passes through mountain ranges can act as channels for hith winds. When stations have to be built in rough country, they should be sited as low down in the valleys as other conditions permit.

Obviously, the first two items are not usually compatible, and the selection of the site should therefore be governed by the aim of the station and by the range of options open to the particular institution. The following table /4/ gives the minimum recommended distances between seismograph stations and potential sources of disturbance.

Sources of disturbance	Minimum distance
1. Oceans	200 km
2. Inland seas	100 km
3. High waterfalls, small lakes	15 km
4. Heavy machinery	15 km
5. Rapids of a large river	10 km
6. Railways	10 km
7. Balanced industrial machinery	5 km
8. Highways with continuous traffic	2 km
9. Big roads and high buildings	1 km
10. Low buildings and high treas	100 m

Seismic noise in the range of period from 0.01 to more than 10 seconds has been observed. Seismic noise with periods 0.1 s is mainly of local origin, and of limited extent. It is caused by wind, traffic, machinery, etc. Seismic noise having periods between 0.2 and 2.0 s belongs to a second characteristic group with a most prominent component around T = 0.5 sec in Europe, the USSR and the USA. The third group of seismic noise is in the period range from 3 to 10 s. It is most widely recorded. Microseisms of this sort are caused by cyclonic storms over oceans.
High noise levels occur in towns, particularly at short periods.

The seismological station MOXA, which we will visit, fulfils most of the recommendations set forth in the above table.

The quality of the site will be determined not only by noise, but by the amplitude response to a given earthquake signal. At some quite sites a low noise level coincides with generally poor transmittion of waves from the earth interior. This can be investigated by inspecting records of distant earthquakes of known magnitude. It often happens that the noise curve contains 'windows' of relatively low noise level. In this case we can construct a special frequency response curve by plotting the inverse noise amplitudes as function of period. The noise window at the station Moxa is near 1 s and therefore we have constructed a sharp frequency response curve with its maximum at 1 s suitable for the detection of weak P-wave signals of distant earthquakes.

3. Basic requirements for seismological observatories

A first-order routine station should be spacious enough to accomodate a full set of seismographs. At least three long-period and three short-period instruments are to be used. For best results the seismometers should be placed in a vault separated from the recording and control area and - if possible - be directly installed on a solid floor on hard rock. The construction of a special pier surrounded by a vertical slot is a common method of insulation against mechanical disturbances. But the slot should not be to deep and the pier should not rise to high above its point of attachement to the ground. Such a structure would, in itself, be unsatisfactory. Examples of vaults are given in the Manual of Seismological Observatory Practice /3/.

Some basic requirements for facilities of a first-rate station are demonstrated by way of example at the seismological station Moxa.

The temperature in the seismometer rooms must be kept constant. The importance of temperature control in the vault arises from the fact that a seismograph is capable of detecting extremely small movements of the ground. Temperature changes cause the pier and the rigid parts of the seismograph to expand or contract slightly and - even much more important - change the elastic constants of the seismometer springs. The latter may result in relatively large displacements of the seismometer pendulum, especially for vertical seismometers. Seismometers used to detect short-period waves are much less sensitive to temperature variations than those used for long-period waves. Long-period seismometers, however, need protection even against the body heat of an operator entering the vault. They are always covered with insulating material, and all practical methods of stabilising the surrounding temperature must be adopted. Usually, two covers are used to protect long-period seismometers. Much effort is needed to reduce temperature variations and thermal disturbances arising inside the vault. For instance heating elements should be high up in the vault, to minimize air convection.

Humidity,too, is a serious problem in seismometer rooms. Condensation on the instruments can give rise to corrosion, the generation of electrochemical processes and leakage in the electronic circuit. The humidity in the vault should therefore be monitored continuously, and held between limits of 20 % and 80 % of saturation. The use of chemical dehumidifiers inside the instruments has some advantages.

Cleaness is indispensible for all seismometer rooms. The generation of dust in the vault should be kept to a minimum.
Many other types of disturbances can be caused by electric induction, by leakage currents and by thermal electromotoric forces. It is important to avoid loops in

power circuits and to minimize switching. The wiring between seismometers and galvanometers should be of high quality shielded cable. Connections should be as short as possible and contacts of different alloys should be avoided. A next possible source of noise is the movement of water round the vault. This can disturb the temperature and cause movements of the ground.

Air pressure and wind variations cause serious disturbances of long-period seismometers. These disturbances are recorded as long-period waves (with T between 20 s and several minutes) which may mask ordinary surface waves of comparable periods but small amplitudes. The influence of pressure variations can be minimized by using rigid covers. To avoid wind generated noise the seismometer would have to be placed about 100 m deep into boreholes. In vaults near the surface this noise cannot be avoided.
To avoid disturbances due to breaks in electrical power supply it is necessary to use sets of batteries and to have a standby power generator.

4. Instruments, their characteristics and recordings at seismological observatories

4.1 Frequency characteristics

For a first-order-observatory it is necessary to use at least 3 components each of short-period and long-period seismometers. Their response curves are different and typical for each class of seismic records (e. g. short-period, medium-period and long-period). The Committee for the Standardization of Seismographs of the International Association of Seismology and Physics of the Earth (IASPEI) recognized five main classes of galvanometric seismographs. In the socialist countries the so-called characteristics of class A, B and C are standardized. Class A for short-period instruments has maximum sensitivity in the period range 0.1-1.6 s. The magnification depends on the actual noise level and its value amounts between one thousand and one million. In the medium period range (class B) the frequency characteristic is flat between about 0.1 to 20 s with the magnification ranging between 100 and 3000. In the long-period range (class C) the response curve is nearly flat between 10 and 100 s with a magnification between about one hundred and a few thousands.
At the station Moxa a complete 3-component set of all three classes of frequency characteristics is at our disposal. Furthermore, one vertical seismograph works in the range of 4 to 20 Hz with a magnification of 300 000 and a second one with a characteristic adapted to the noise spectrum at Moxa has a peak magnification of 100 000 at 1 s. These two instruments make it possible to detect weak signals and to distinguish between local and remote events.

All mentioned seismometers are recorded photographically on drum recorders and on paper for fast interpretation of seismic events.

New developments of broad-band seismometers like the electronic seismometer TSJ 1 developed at the Jena branch of our institute provide frequency-modulated signals and can be used for seismic signal transmission over telephone lines up to distances of several hundred kilometers. Signals from many seismometers can thus be transmitted to and recorded at a central recording site, e. g. at the headquarters of our institute in Potsdam. The following table shows the magnification V required to detect earthquakes of magnitude M_L (local Richter magnitude) at distance D (km):

D (km)	M_L		
	4,5	3,5	2,5
100	56	560	5600
200	175	1750	17500
400	1750	17500	175000
600	4500	45000	450000

From the table it is obvious that the larger V the larger is the area within which an event of a given magnitude can be detected.

4.2 Recording methods

Of the various recording methods, the photographic one has dominated ever since Galitzin's days. This is still the case. In general, this method is very reliable in operation, but its major drawback is that the records have to be developed before they can be read. Instead of recording on photographic paper, sometimes film recording is applied. In order to eliminate the photographic work, as well as the need for darkrooms for recordings and developing, instruments with visible recording have been introduced in recent year. They have the further advantage of permitting an immediate inspection of the records. There are different types on the market, such as ink-writing recorders, hot-stylus recorders etc. In order to operate these, an amplifier has to be installed between the seismometer and the recorder. Therefore, the operation may be more expensive and less dependendable than the photographic one.

For drum recording their are several standards /3/:

1. Records should be made on sheets having approximately a 3 : 1 ratio of length to width.
2. Short-period instruments should be recorded with the drum rotating 4 revolutions/hour. For long-period instruments the speed should be 1 or 2 revolutions/hour.
3. The intervall between minute marks is 60 mm for short-period records and 15 mm or 30 mm for long-period records.
4. Time should increase from left to right.
5. Galvanometers should be connected so that N, E and upward motion of the ground moves the trace towards the top of the page.
6. The following information should be written on the front face of each sheet:
   Name of station
   Name of instrument
   Date and time on
   Date and time off — UTC (Co-ordinated Universal Time)
   Direction of motion
   Time correction at beginning and end of the trace

The dynamic range of such a photographic record covers an amplitude ratio of about 1 : 100, whereas the ratio between an earthquake of magnitude 5 at a distance of 10 000 km and one of magnitude 8 at 100 km is about 1 : 10^6. It follows that stations which shall record large, nearby earthquakes as well as small distant ones must be equiped with seismographs and records of both high and low magnification. In case of the GDR without large earthquakes on its own and neighbouring territories two different magnification levels with a dynamic range of 40 dB each are normally sufficient.

There is a rapid development of magnetic tape recordings for seismic events. In modern research large electronic computers are constantly used. The advantage of this medium is the ease with which the data can be processed after recording, and the high dynamic range. A dynamic range of 120 dB can be obtained by digitising the seismometer output before it is recorded on tape or read-in the computer. By applying such techniques the number of seismographs with specialized response characteristics can be drastically reduced. Only one 3-component broad-band seismometersystem is necessary for recording the wohle seismic spectrum. The signals recorded on magnetic tape are up to now not uniform. Different seismological stations have different formats of the stored seismic data. But for data exchange it is essential to have a uniform format. Special data formats are used for the network day tape of SRO and DWWSSN, for GRF and NORSAR: At the Seismological Observatory Moxa/Jena we use a format similar to the network day tape of the United States Geological Survey (USGS) and of the seismic array of Gräfenberg (GRF):

4.3 Timing system

When a record of an earthquake has been obtained, the first task is to determine the arrival times of various phases with an accuracy up to 0.1 sec. Today, quartz crystal clocks are generally used at seismological stations. Such a clock can keep its time accurate within 0.1 s to UTC for several weeks without any need for correction.
Such crystall clocks perform the following operations:

1. Deliver minute and hour marks to the recording apparatus.
2. Deliver electric voltage with well controlled frequency to the motors driving the recording drums.

In order to check the crystall clock it is necessary to compare its internal time with the time of a radio receiver, at least once per day.

5. Duties of staff

The placing of seismic stations and networks into relatively inaccessible regions raises staffing and maintenance problems and calls for a trade-off between optimal site conditions and living conditions for the staff. Current trend, especially for second-order stations and station networks, are towards maintenance of remote stations by part-time staff or the establishment of fully automatic stations with data transmission via telephone or radio links. But most of the first-order stations are staffed and have a seismologist on duty. Their tasks are the following:

1. Keeping the station in good order. Cleanness is one of the first suppositions for excellent working and measuring conditions.
2. Exchange of recording paper, time control and annotation of records.
3. Photographic processing.
4. Preliminary interpretation of all recorded events, differentiation between near explosions and earthquakes, sending results of interpretation to the world data centres and central stations interested in the data.
5. Control of all instruments at the observatory, reporting of interruption in recording, or disorderly operation due to changes in period or damping, sticking of coils, shifts in zero position, problems with electrical contacts especially in wet rooms irregularities of drum speed etc.
6. Control of frequency characteristics by means of calibration pulses. If the routine check indicates that the instrumental response has drifted outside acceptable limits, a recalibration is necessary.

The most likely faults in operation are that the natural period of either the seismometer or the galvanometer has altered or that a bad connection has changed the resistance of part of the circuit. A decrease in magnification can be caused by dirt on the coil, or spider's web between coil and magnet in electromagnetic transducers. Sometimes there is a change in the damping constants and the recorded trace seems to be underdamped. The reason for this may be a fault contact in the wiring, or a break in the coil itself. If overdamped, there is probably a short circuit in the wiring or in one of the coils. In case of electromagnetic seismograph the operator can adjust the period of the seismometer and the resistors in the coupling network which determine the magnification and the damping constants of the seismometer and galvanometer. The eigenperiod of the galvanometer and the dynamic constants of the galvanometer and seismometer are usually not at the disposal of the operator.

At a big first-order station like the station Moxa, where besides the whole complex of routine operations a number of special seismometers and new developed instruments are frequently tested a highly qualified staff with the minimum number of 6 is needed.

References

/1/ Report US(GSE/12 (1981), A summary of U.S. and international seismic facilities

/2/ Bath, M., Introduction to Seismologc, Birkhäuser Verlag Basel and Stuttgart (1973)

/3/ Willmore, P. L., Manual of seismological observatory practice, World Data Center A for Solid Earth Geophysics, Report SE-20 (1979) Boulder, Colorado

/4/ Corder, Vesiac report (1963)

Mitteilung des Zentralinstituts für Physik der Erde Nr. 1220

Selection and construction of seismological stations

by Jens Bribach

1. Selection of station sites within given areas

According to source situation a former chapter dealed with station site selection from the geometrical point of view. But an ultimate decision has to depend on the signal conditions of the very near surrounding of the measuring point.

1.1. Planning on maps

Before starting outside measuring campaigns one should recognice the area by help of plane table sheets (resolution < 100 m).

Geological maps

give a first idea of the station underground. Here the first ten meters are of interest. Don't You find bedrock in this depth Your choose should take into account the distance to nearby noise sources. Are there only layers of sediments You should look for salt domes reaching the surface.
A change of the choosen location in the range of some kilometers can increase the Signal-to-Noise Ratio SNR efficiently.

Source type	Distance
ocean	200 km
large lakes	100 km
large water falls, small lakes	15 km
large immobile engines	15 km
fast rivers	10 km
railway lines	10 km
engines	5 km
highway	2 km
streets, high buildings	1 km
high trees, small buildings	0.1 km

Tab. 1: Required distances to noise sources (from Carder 1963)

According to former schedule the choosen location should be far from human and natural noise up to distances of several kilometers.

Surface maps

show all kinds of traffic lines. Also keep off lakes which are shipped. Mostly marshy ground in their border region causes ideal coupling to wind or to human generated surface waves. If You can't leave this area try to find a strip of more than a kilometer width of consolidated layer shore. For example test measurements near lakes within Rugen Island in northern Germany brought noise lowering up to 40 dB by putting up a station on the opposite shore 500 m from its former situation.
On the other hand You need power and information links.

Plane table sheets

give a rough estimation of radio wave propagation in this area. Receiving time signal is vital to a single station. And centralized networks linked by transmitter demand direct (that means visible) contact to the related receiving stations.
Surface plan table sheets also contain information on open air power lines. The neighbourship of industry is connected with dense information networks as telephone or data links. Additional to public lines also dams, chemical plants or power stations are surrounded by control cables and supervising technique. Power companies use high voltage lines for information exchange via carrier frequencies, and they run their own telephone networks.

Cable plans

You get in offices responsible for power and for telephone companies. Try to get underground cable for both power and information to protect Your station from lightening. The cables should reach next transformator station or next post office directly.
After choosing the final point look again for

- no marshy ground
- no high voltage lines crossing the station area (lightening; induced voltages into sensitive devices)
- power and information links available

1.2. Noise and signal measurements

Noise is generated by nature, by weather and by industry. Its alternating behaviour demands a measuring campaign covering all different activities around the year. Either You run a temporary station around the clock, or You pick up typical dates by time controlled measuring periods.

The measurements ought to include

- **several times of day** as rush-hour, week and weekend (don't forget tourism) and the main changes within a year as frozen soil or high humidity after raining periods
- **several points** of some hundred meters distance: The bedrock You found can belong to a broken block, also small caves can influence the signal
- **several methods:** Evaluating digital broadband recordings in the interesting frequency range the changing noise levels allow qualitative comparisions to other stations. Planning accurately You will find that the main noise spectral lines are generated by sources several kilometers away.

But the behaviour of the station underground and the coupling to the ground (good to the basement, and bad to the surrounding surface) You get by near sources only. So set pulses very near to the ground ($1 \ldots 10\ m$) where the seismometer is placed. For that reason a jump of a person in distances less than ten meters can give a hint to resonances of bad coupled or of broken blocks under the station. Here the record shows monofrequent vibrations. The same method can be used for evaluating the surface coupling and the propagation of surface near noise.
Stronger stimulations can be generated by heavy engines as lorries driven around the measuring ground, and by their immediate breaking (breaking pulse) towards the recorder.

Noise measurements can lead to a low noise level or to a window of low noise. But low noise also can include low signal. A comparision with other stations or measuring points is to be based on the signal-to-noise ratio. This comparision demands recordings of same events.
But the SNR also depends on source direction and on source distance. So signal measurements should cover a couple of several events from different but interesting areas.

2. Foundation of the measuring platform

Bedrock foundation

needs a few preparations only: Scraping the first centimeters of weathered surface and putting the platform concret direktly on.

Salt dome platforms

have to be founded in rock salt if available. After scraping the first 10 centimeters (down to $1\ m$) a plane pit will build the platform. There is no necessity of concret.

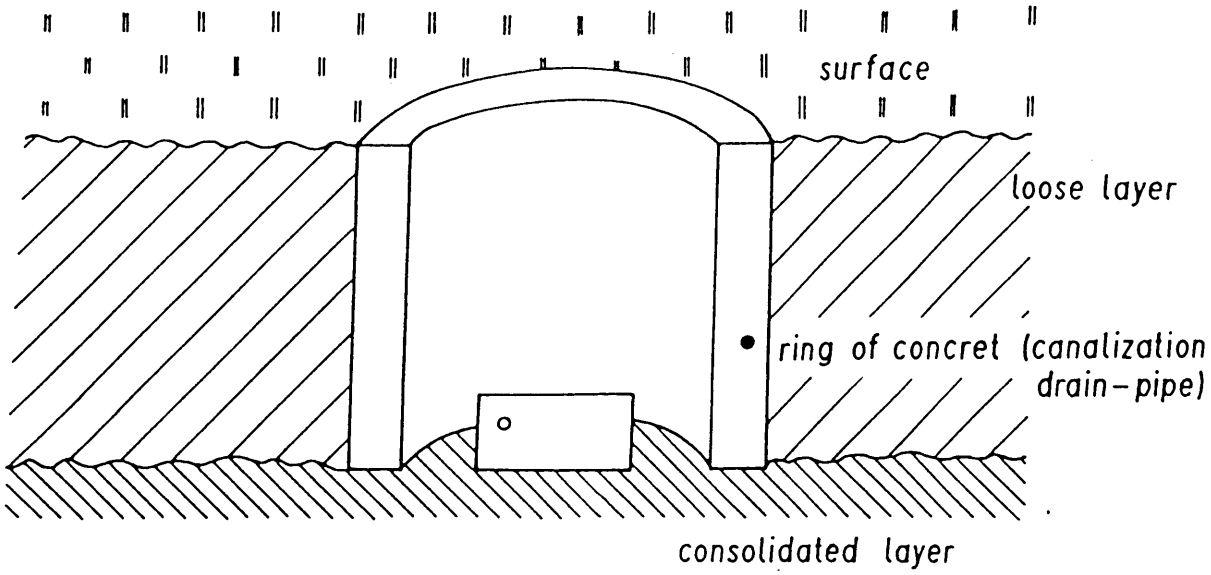

Fig. 1: Inverse foundation

Sediment platforms

need additional examinations because compact plates of several 10 meters diameter can resonate under certain stimulations.

Sandy grounds

require digging of some meters of loose sediments. Don't place small pedestals on a sandy surface: Mainly you will receive natural vibrations of the pedestal itself. Better You put the seismometer directly on the plane pit if no expensive foundation is available.

Lowering noise especially in nonrocky areas uses the following effects: Human and natural noise (here: traffic and wind) doesn't penetrate deeply into the ground. Additionally some components of this special noise are lead within the upper layer only.

In sandy soil You can improve noise conditions by an inverse foundation. It shields near surface noise that is lead in the loose layer. But don't forget canalization drain-pipes.

Another improvement can be obtained by putting a borehole pillar within the pit. The pillar should be of a diameter greater than 50 *cm* and reach more consolidated layers down to 10 meters.
To get good coupling to the soil the pillar concret must be pressed into the hole

- immediately after pulling the auger
- from the ground by pipe
- under additional vibrations for consolidating

The pillar shouldn't overtop the fastened layer for more than its diameter. Otherwise the pillar would build a pendulum itself, and it would amplify ground motions.

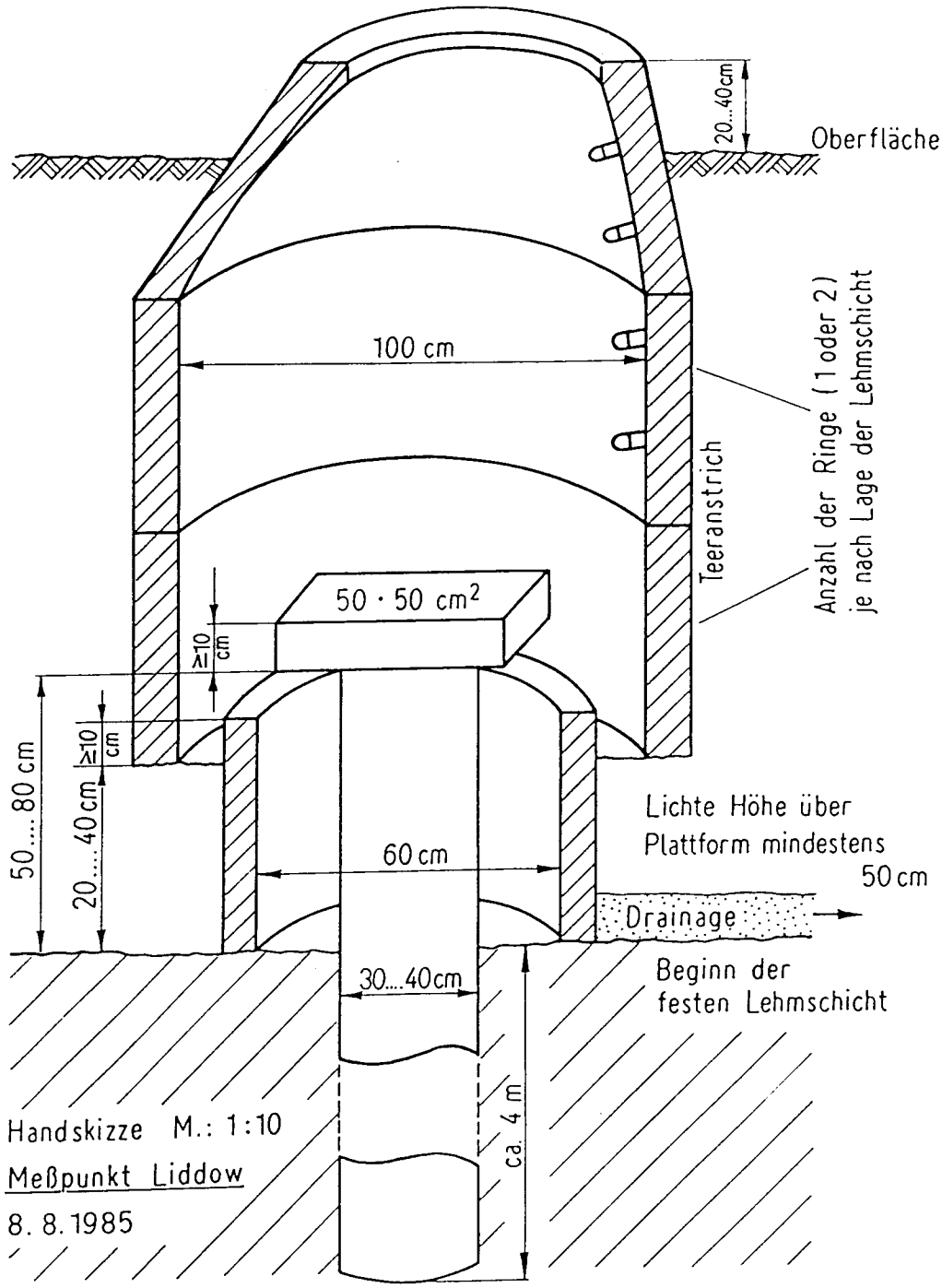

Fig. 2: Borehole pillar platform

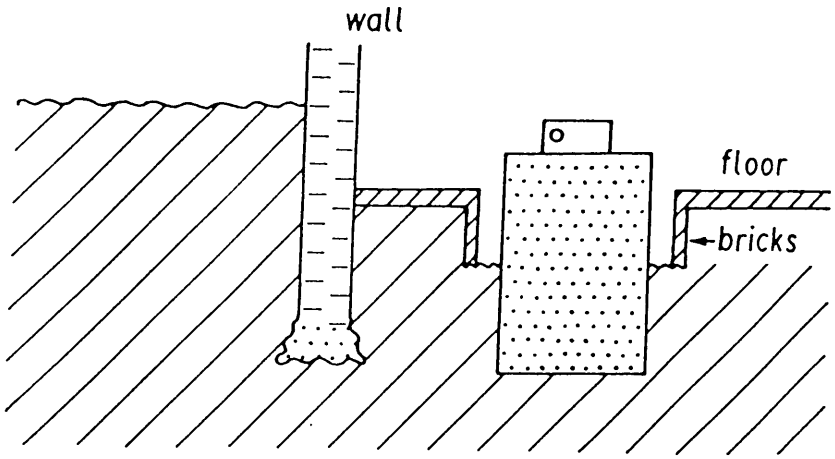

Fig. 3: A housed platform

If the platform is housed by a special building their foundations should be independend of each other.

Foundations on sands should enclose pedestals of several cubic meters of solid material. If available You also can use large coherent masses of flat and compact buildings. Thus favour conditions are given within concret dams, at the foundation of closed underground water reservoirs, or in old shelters.

Most favour but most expensive solutions are given by boreholes. Putting the seismometer deeper than 40 m prevents it from streets surface noise, 100 m can exclude noise of heavy engines, and from 400 m downwards also breakers noise coming from the coast line can be damped efficiently.
Same conditions can be obtained by installing the station within a mine. But You have to count with two odd effects. Near caves will change Your signal. And events from distances less than 100 km can generate low signal amplitudes.

3. Climate notes

Depending on measuring tasks the platform housing should suffer the following climate conditions.

Temperature changes
around the year shouldn't exceed

40^o	for	short	period	instruments	SP	(T_S <	2 s)
5^o	"	long	"	"	LP	(T_S <	20 s)
1^o	"	long	"	"	LP	(T_S <	100 s)
0.1^o	"	very long	"	"	VLP	(T_S >	300 s)

with T_S as seismometer natural period.

The first measure is air conditioning but this technics (including air channels) is to be installed far from platform and seismometers. The air conditioning effort can be decreased by building double walls with air channels between, or by small cabins built within the house.
Against daily temperature changes the very old method of greened roofs can be used. The natural behaviour of the plants generates a self-controlling temperature regime.

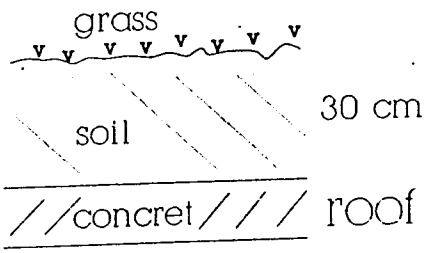

Fig. 4: Greened roof

The same effect You get by putting the platform under the surface soil. A dept of about 2 m keeps daily temperature changes less than 1^o.
An installation in mines, especially in excaved salt mines, can guarantee changes less than 1^o around the year.

Humidity
can destroy Your whole apparatus. Inside rooms demoisturer are sufficient which are running under the refrigerator principle.
Outside You need drains, and for temperatures less than 0^oC a small heating. That inquires a power supply of about 1 kW . Additionally You need several Watts to keep sensitive parts of the device warmer than their surroundings because of the dew point. This heating is to be placed within the apparatus in a way that prevents air convection (use the ceiling of the case!).

Pressure influences
have to be avoided for very long period records only. This problem is to be solved by vacuized cases which are part of the sensor case nowadays.

References

Carder, D.S.; *The requirements of a high-sensitive seismograph station.* VESIAC State-of-the-Art Report 4410-63-x (1963)

Principles of acquisition, handling and storage of digital seismological data

by Jens Bribach

This lesson deals with terms of signal acquisition related to technical realisations. It covers the signal path from the seismic sensor to the computer final memory.

1. Signal terms

Generally a signal can be described by its dynamic range and its bandwidth. Dynamic range means the relation between available resolution and (estimated) maximum amplitudes in the logarithmic form of

$$20\ lg\ \frac{max.\ amplitude}{resolution}\ [dB]; \quad dB = deciBel \tag{1}$$

But any technical solution will limit both resolution and processable amplitudes. Analog records on paper, on film or on magnetic tape are of a dynamic range less than 45 dB.

Example: Direct writing paper record

$$\left.\frac{max.\ pen\ deflection \quad 20mm}{resolution \quad 0.2mm}\right\} 40\ dB \tag{2}$$

Digital records obtain higher ranges (... 140 dB, see 2.3.4.). Estimating the resolution one should keep in mind the Signal-to-Noise Ratio (SNR). The smallest signal to be processed ought to be of $SNR = 5 \ldots 10$.

Bandwidth means the frequency range $B = f_{CH} - f_{CL}$. Technical solutions necessarily limit it by the whole acquisition unit (sensor, filters).
Corner frequency is defined as that point the amplitude drops to $-3\ dB$ ($= 0.707$). Under real conditions f_{min} and f_{max} are different from the related corner frequencies because technical filters can't perform infinit slope (in literature You often find $B = f_{max} - f_{min}$).

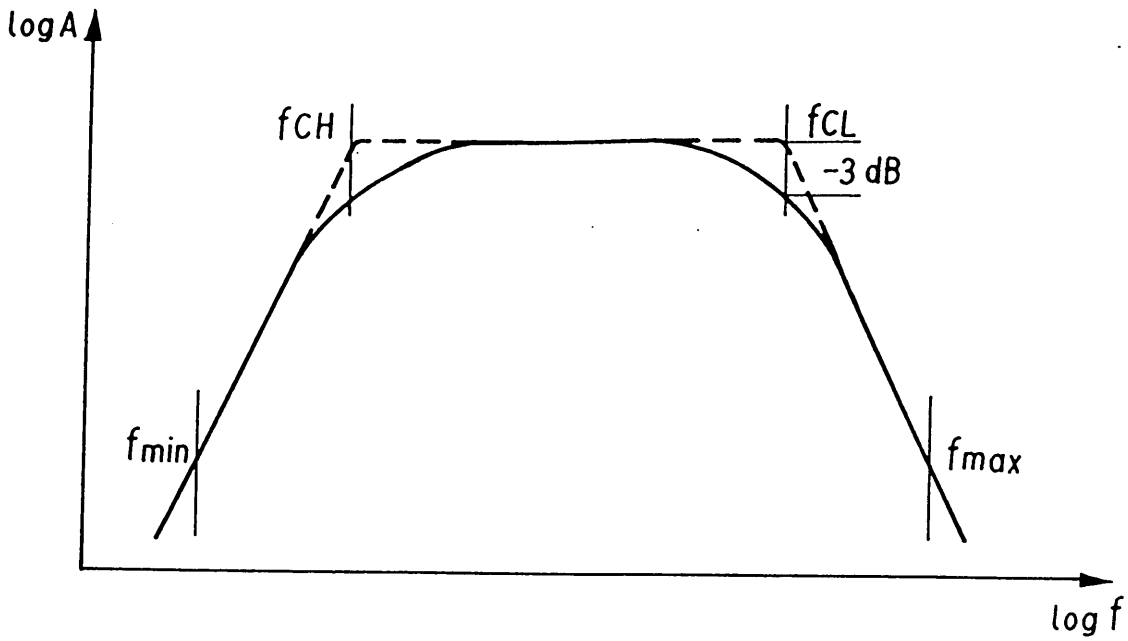

Fig. 1: Passband filter; amplitude A related to frequency f
f_C: Corner frequency; index H: Highpass, L: Lowpass

Another note to signal resolution: The noise power density is proportional to the square of bandwidth. That means the signal-to-noise ratio SNR can be improved by bandpass filtering before processing.

2. The seismic signal

The bandwidth of the seismic signal covers the frequency range from about 1 mHz to 1 kHz ($>$ 6 decades). On the lower end You find strain measurements (0.01 Hz downwards), on the upper end seismoacoustics from about 200 Hz to several 10 kHz. A rough estimation of the possible maximum frequencies of the received signal can be made in dependence on source distance.

Distance	Corner frequency	
0.1 km	...	1000 Hz
10 km	...	100 Hz
100 km	...	10 Hz
1000 km	...	5 Hz
10000 km	...	1 Hz

Tab. 1: Possible maximum corner frequencies f_C

The dynamic range of seismic noise as of seismic signalis a function of bandwidth firstly. But secondly amplitudes of noise as of signal are variing more than 3 decades in a comparable dependence on frequency.

Narrow band short period measurements ($f > 1\ Hz$) on favour places show noise amplitudes less than 1 nm (nanometer). This leads to a demanded resolution of 0.1 nm in this frequency range.

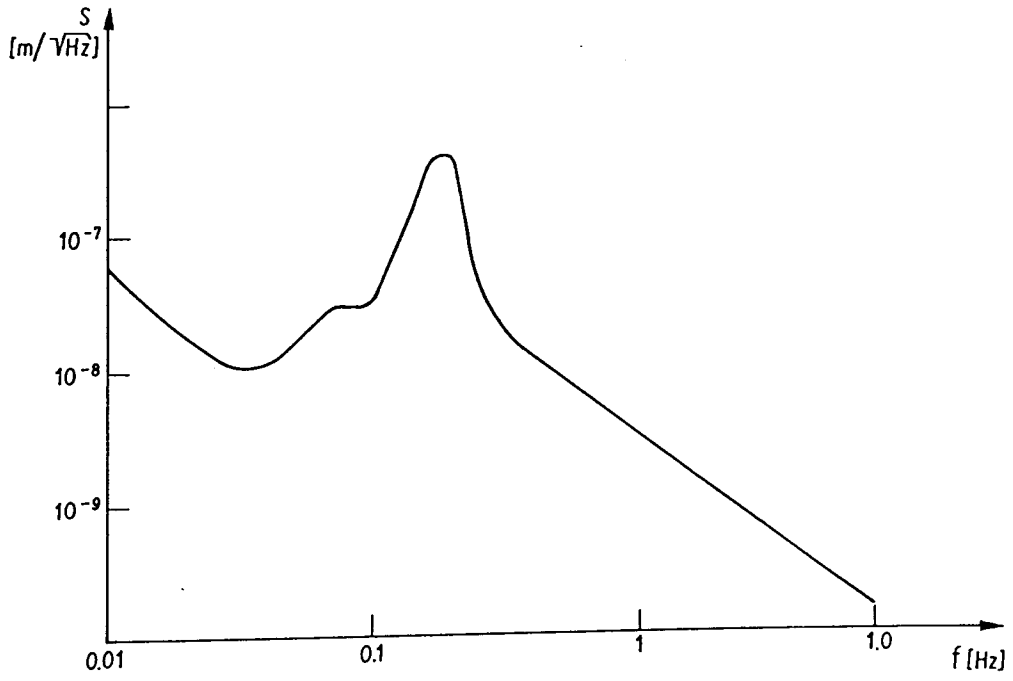

Fig. 2: Amplitude spectra of noise
Worldwide favour conditions by Peterson (1976)

On the other end events of magnitude

$$M = 6 \quad \text{in } \Delta = \quad 10 \text{ km(at } f < \quad 1Hz) \text{ Hz}$$
$$M = 7.5 \quad \text{in } \Delta = 10000 \text{ km(at } f < \quad 0.1Hz) \text{ Hz}$$

generate maximum amplitudes of some 10 mm . That's a dynamic range of $3 * 10^8$ or 170 dB .

Scientific Technical Report STR 95/TK
DOI: 10.2312/GFZ.b103-95tk7

3. Instrument response

Mechanical seismic sensors (spring-mass-system) follow the earth displacement for signal frequencies higher than sensor natural frequency. Their bandwidth is situated in a range of about 2 decades between their natural frequency (lower end) and spurious resonances (f. e. spring natural frequency) on the upper end.

Sensor		Natural frequency			max. clean freq.	
geophone	(g.)	2.	...	20. Hz	300 ...	3000 Hz
short period seismometer	(SP)	0.2	...	2. Hz	50 ...	200 Hz
long period seismometer	(LP)	0.01	...	0.1 Hz	1 ...	20 Hz
broad band seismometer	(BB)	(0.003)	...	0.1 Hz	10 ...	50 Hz

Tab. 2: Bandwidth of seismic sensors

The transducer transforms the mechanical movement of the sensor into an electrical signal.

Transducer	Sensor type	Output prop. to	
piecoelectrical	g.; SP	acceleration	a
electrodynamical	g.; SP; LP	velocity	v
capacitive/inductive	SP; LP; BB	displacement	d

Tab. 3: Types of transducers

Because of the frequency dependence of noise amplitudes as signal amplitudes (proportional to f^{-1} upto f^{-2}) the use of a velocity proportional output reduces the necessary dynamic range from 170 dB to 130 dB .

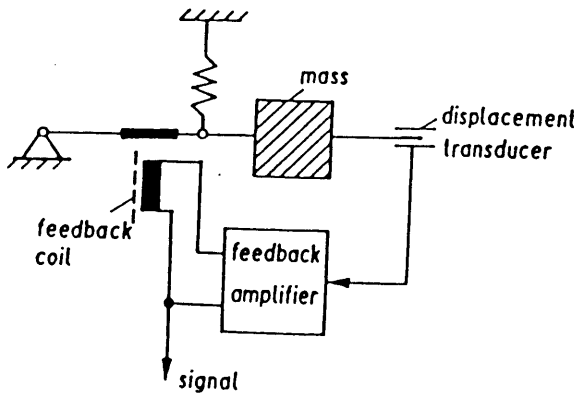

Fig. 3: Scheme of a force-balance feedback system

But common mechanical systems as transducers can perform either high linearity or high dynamics. This problem was solved by feedback systems which force zero position of the

mechanical sensor. On this way high linearity of both sensor and transducer can be guaranteed combined with high resolution of the transducer, and independend on dynamic range.
The system output is proportional to acceleration (down to $f \rightarrow 0$). Here an additional integration can generate a velocity proportional response within certain limits. (Wielandt 1986: 3 mHz ... 10 Hz).

The high slope of all response curves for $f > f_C$ is necessary to prevent digitizing errors.

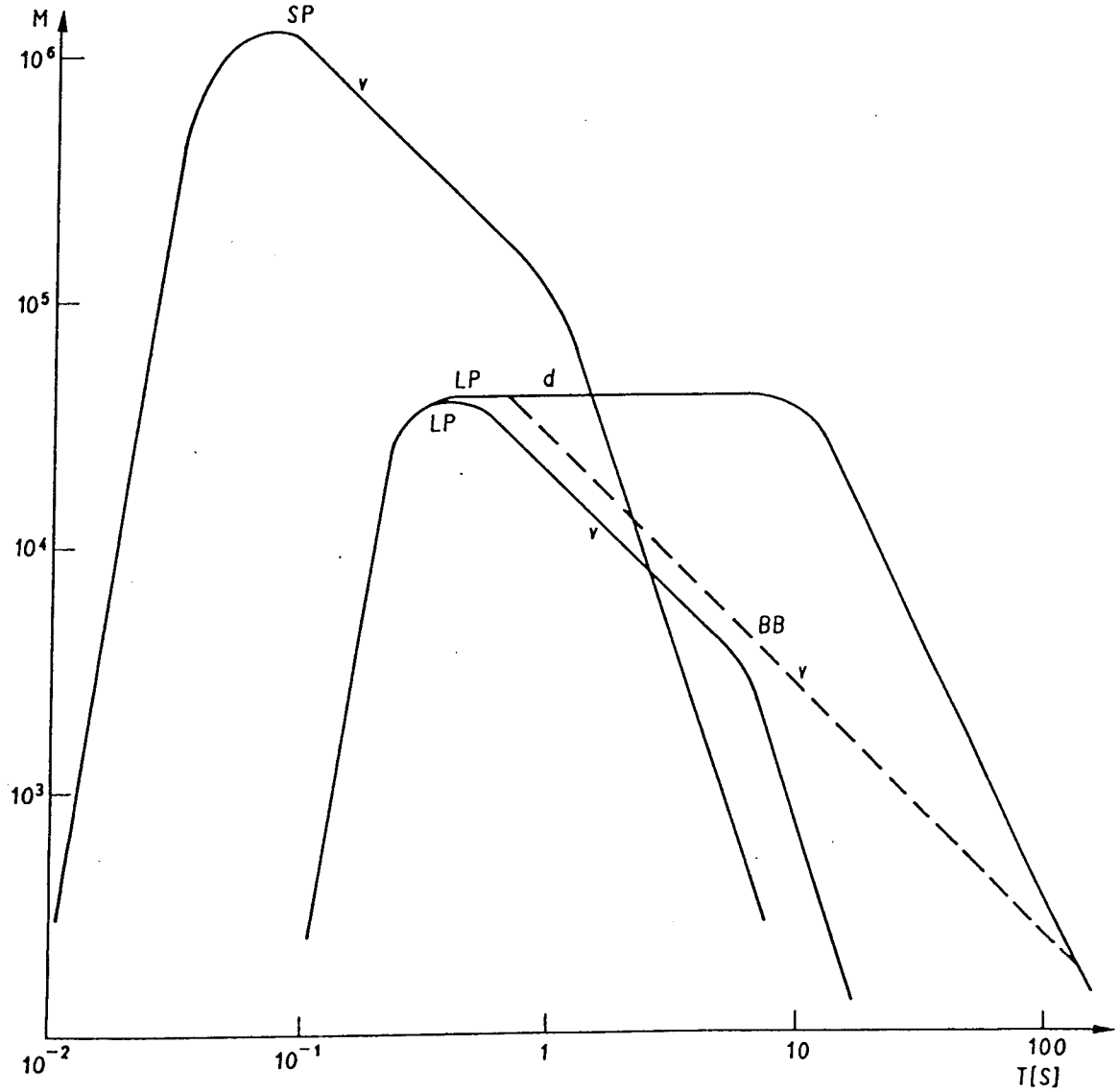

Fig. 4: Typical response curves

4. Digitizing analog signals

4.1. Sampling

Sampling means to get probes of the analog signal. The sampling time T_S is limited by the speed of possible signal changes to

$$T_S < \frac{resolution}{2\pi\, f_{max} * max.\ amplitude} \tag{3}$$

T_S has to be much shorter than the period T of the maximum given frequency f_{max} to prevent the first digitizing error ($T_S \ll T$). On the other hand the Analog-to-Digital Converter (ADC) needs time as much as available for digitizing the probe. This is performed by a Sample-and-Hold Circuit ($S\&H$; see fig. 2.3.5): To get probes an electronic button S is closed for T_S only. The input voltage U remains on capacitor C.

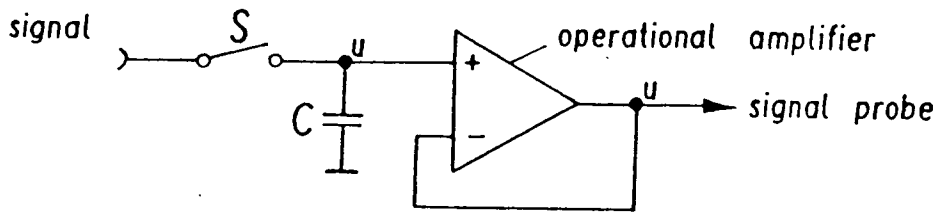

Fig. 5: Sample-and-hold circuit

The necessary sampling density (sampling rate) f_D is defined by Shannon's sampling theorem

$$f_D = 2\, f_{max}\ ; \qquad f_{max}\ :\ occuring\ max.\ frequency \tag{4}$$

Often f_{max} is named as Nyquist rate ($f_{Ny} = 0.5\, f_D$). Here the second digitizing error occurs: Aliasing. Because of real filter structures any analog signal will contain components of $f > f_{Ny}$. But spectral lines of those frequencies then will be presented as spectral lines of $f < f_{Ny}$ (periodical repeat of the spectra). The quantity of the aliasing effect is in the same range as the signal is damped for frequencies $f < f_{Ny}$ related to its main level. But You only know the error range, and You don't get real amplitude and real phase information of the aliasing.

In seismology the anti-aliasing LOW PASS mostly was set to a corner frequency $f_C = 0.5\, f_{max} = 0.5\, f_{Ny}$. In this case a 6^{th} or a 7^{th} order low pass is sufficient for visual utilisation only (amplitude decay 6 or 7 octaves per one frequency octave; $2^6 = 64 \triangleq 36\ dB$).

By use of digital acquisition and digital evaluation the damping at f_{Ny} has to cover the size of the Analog-to-Digital-Converter (ADC) dynamic range. But analoque filter constructions shouldn't exceed 8^{th} order ($48\ dB/oct.$).

This problem is solved by OVERSAMPLING:

- The input sampling rate f_i is set to more than 10 times faster than the wanted sampling - or acquisition - rate f_D.
- The analog input low pass is set to $f_C = 0.5 \ldots 0.1\ f_D$.

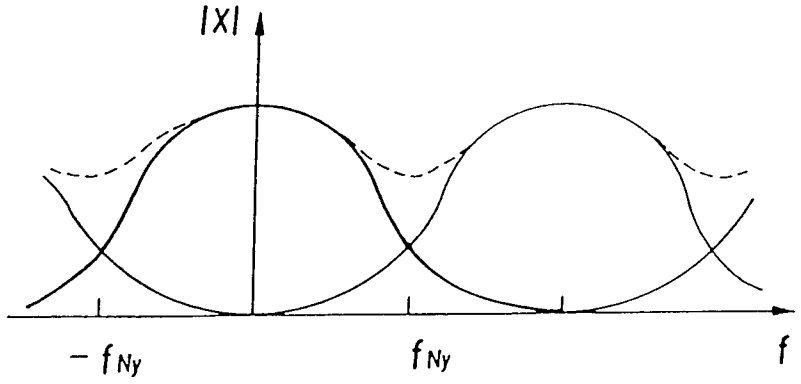

Fig. 6: Spectral aliasing

Origin spectrum ——————
Periodic repetition ——————
Aliasing effects - - - - -

Thus - for example - with a given oversampling of $f_i = 20\ f_D$
and with a 6^{th} order low pass of $f_C = 0.5\ f_D = 0.025\ f_i$

the signal at $f_{Ny}(f_i) = 0.5\ f_i$ is damped to $-156\ dB$, sufficient for a (still theoretical) 27-bit-ADC.

The final filtering to reduce the sampling rate to f_D is done digitally, mostly by special signal processors fast enough to process real time filtering up to 64^{th} order. This large slope allows low pass corner frequencies closer to the originally wanted sampling rate f_D, commonly up to $f_{Cdig} = 0.8\ f_{Ny}(f_D)$.
For the given example (64^{th} order, $0.08\ f_{Ny}$) the low pass performs a damping of $-124\ dB$ at $f_{Ny} = 0.5\ f_D$.

But using such high slope low passes one should process frequencies up to f_{Cdig} only. Re-calculating the filter influence for $f_{Cdig} > f > f_{Ny}$ would increase digital noise, and also it would remagnify the just damped aliasing effects.

4.2. Analog-to-Digital Conversion

The Analog-to-Digital Converter (*ADC*) turns the values of given probes into a number of quantized values. The smallest digitization step is called *digit* or *count*. The ADC counts in steps of powers of 2 (2^n). Every cipher is called *bit* as an abbreviation of *bi*nary digi*t*.

Example: The 4 bit number H H L H ; H $\longrightarrow$ High or present
L $\longrightarrow$ Low or absent

binary number	H		H		L		H		
binary values	2^3		2^2		2^1		2^0		
decimal value	8	+	4	+	0	+	1	=	13

The smallest unit of a digital value or word is *Byte* (= 8 bit).

bits (incl. sign)	digits	dyn. range
12	2,048	66 dB
16	32,768	90 dB
24	8,338,608	140 dB

Tab. 4: Common ADC dynamic ranges

12 bit and 16 bit *ADC* are sold as personal computer plug-in boards including *S&H* interface and multiplexor for 8 or 16 input channels. Their insufficient for some problems dynamic range can be extended by switchable amplification levels depending on signal level (so called *gain ranging*). A wide spread solution uses a 12-bit-ADC in the form of

mantissa	11 bit	16 bit = 2 Byte
sign	1 bit	
exponent	4 bit	

The exponent represents the gain level in powers of 2 or 4 or 8.

5. Signal transmission

Analog transmission is used for short or nonexpensive connections.

Signal	Link	Distance
direct connection	wire	some 100 m
amplitude modulation	wire	some 10 km
	telephone line	direct conn. 40 .. 100 km
frequency modulation	radio link	via relais > 1000 km

Tab. 5: Distances for analog transmission lines

The most used analog method is frequency modulation. The instrument analog output controls a Voltage Controlled Oscillator (VCO). Instrument voltage changes cause frequency changes in the range of the speech band of 300 ... 3400 Hz . You have only to take into account the modulation condition: $carrier\ frequency > 3\ f_{max}$.

The VCO output can be switched immediately to commercial transmitters.

Transmitter	Carrier [Hz]	Dyn. range [dB]	Power supply
telephone	300 ... 3400	60 ... 90	... 10 mW
walkie-talkie	300 ... 3400	40 ... 60	... 10 W

Tab. 6: Available commercial transmitters

For a larger number of channels You should hire whole carrier groups. A carrier group of 24 telephone channels can be switched via one galvanic coupled telephone wire, e. g. in local networks.

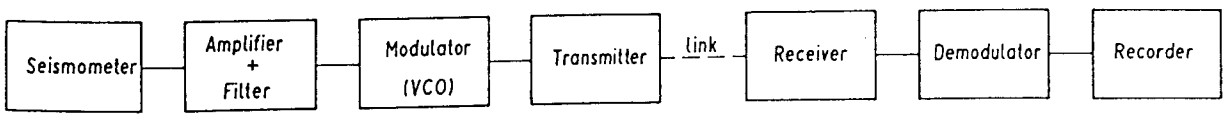

Fig. 7: Analog transmission

The same links are available for digital transmission. The digital information is converted bit by bit into frequency or phase jumps of the carrier frequency by help of a $MODEM$ (MOdulator/DEModulator).

Digital transmission allows connections in both directions via one line in the same moment (full duplex) or alternating (half duplex).

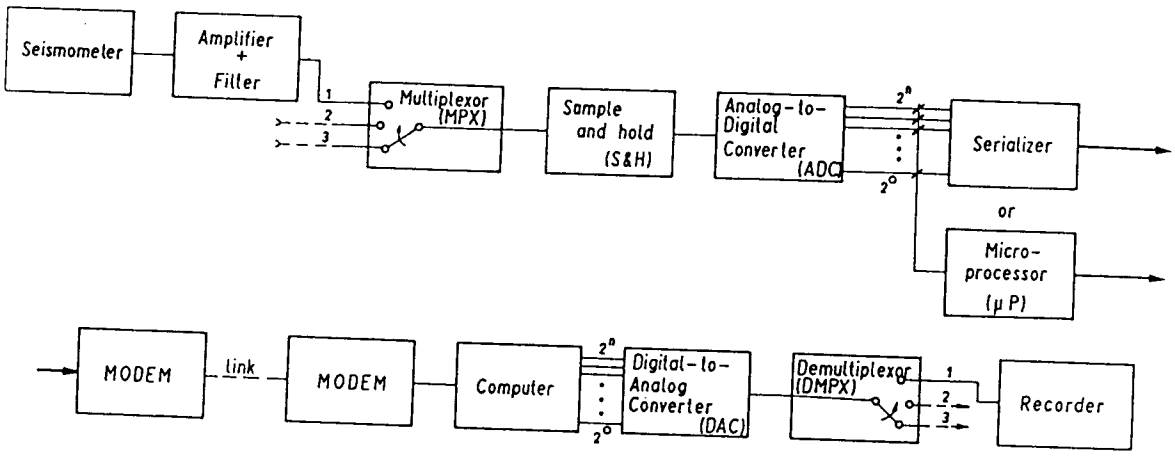

Fig. 8: Digital transmission

6. Data transmission

Data rates depend on sampling rates. In the following explanations we count on the base of a 16-bit-word (= 2-Byte-word) per sample. The sampling rate is the number of samples per second (*sps*). Seismology commonly uses sampling rates f_D of

$$f_D = 2.5 \ \ldots \ 4 \ f_C \tag{5}$$

with f_C as filter upper corner frequency. For evaluating the signal slope f_C should be up to two times higher than the expected signal corner frequency.

Problem	Sampling rate [sps]	Components per station	Data rate [bit/s]
near field investig.	1000	1	16,000
local networks	200	1 (3)	3,200 (9,600)
territ. monitoring SP	20	3	960
global monitoring LP	1 (20)	3	48
one station	1 * 200	vertical	3200
	3 * 20	vert.; N-S; E-W	960
	3 * 1	vert.; N-S; E-W	48
sum (example)	263	3-component	4208

Tab. 7: Common sampling rates

Alas sampling rates generally are a compromise related to transmission and to storage capacity.

Transmission rate	Telephone	Data network	Radio
65,000 Bd		ISDN narrow band	
9,600 Bd		Datex	
4,800 Bd		Datex	
2400 or 1200 Bd	leased lines		walkie-talkie
300 Bd	acoust. coupling		

Tab. 8: Transmission rates (brutto)

Line or channel transmission rates (capacity) are given in *Baud* (1 Bd = 1 bit/s). Transmission procedures reduce this values to 90 ... 80% . On the other hand the statistical behaviour of the information allows bit coding to run 4800 and 9600 bit/s on 2400 Bd lines. This coding is part of the MODEM transmission procedure, and it doesn't touch computer input or output routines
(MNP5-protocol: compression factor 2; V42: factor 4).

7. Data storage

According to transmission rates storage capacity forms the second limitation.

Medium	Capacity [Byte]	Storage of 263 sps for	Access time
Tapes			
- tape 1/2"	25 ... 200 M	13 ... 100 h	several min.
- video*)	13 G	280 d	"
- R-DAT	3 G	65 d	"
- EXABYTE/video8	5 G	110 d	"
Discs			
- floppy disc	0.6 ... 3 M	0.5 ... 2.5 h	some 10 ms
- hard disc	20 ... 1200 M	10 ... 600 h	"
- optical disc	0.5 ... 5 G	10 ... 100 d	some 100 ms
Solid state			
- 1-Mbit-chips	4 MByte/board	2 h/board	some 100 ns
- 4-Mbit-chips (C-MOS-SRAM)	16 MByte/board	8 h/board	

Tab. 9: Storage media ; Storage duration is based on
1 * 200 sps + 3 * 20 sps + 3 * 1 sps
*) for data no commercial solution available

Storage of triggered records only will reduce data amount down to 10 ... 5% . The same effects but nearly without false alarms (or vice versa: nondetection cases) will be obtained by dayly or weekly review and selection based on the whole time series.

In field measurements solid state memories (Integrated Circuits IC) have pushed away audio tape cassetta technique. But also there are floppy disc drives usable under rough field conditions.
Data processing demands quick access and will run within the computer main solid state memory supported by discs.
In archiving the trend tends from high density tape to optical disc (MOD) and to compact disk (CD).

Before storing data their formats should be standardized in sampled data as in guiding information. But there is no dominating international standard. That's why some remarks on necessary statements:
Data of time series should be stored in dual form (that's powers of 2). A group of data (file, data set) is to open with a guiding information named 'header'.

The header should contain at least

- time	beginning of the record
	length
	time correction if no absolute time base
- order	of channels
	stations
	station components (vertical, N-S, E-W ...)
- station information	station coordinates
	states(absence of station/component)
	sampling rates
	response curves
- event information	location
	onset times
	magnitude
	comments

The multiplex structure defines the order or the arrangement of data from different sources within a data file. Sampling of different components generates

time multiplex:	first	sample	of	component	1
	"	"	"	"	2
	"	"	"	"	3
	...	...	...	...	...
	second	sample	of	component	1
	"	"	"	"	2
	"	"	"	"	3
	...	...	...	...	...

In this structural form also transmission and immediate storage are done.

But before processing and archiving the data file should be converted into

channel multiplex:	first	sample	of	component	1
	second	"	"	"	1
	third	"	"	"	1
	...	...	...	...	...
	first	sample	of	component	2
	second	"	"	"	2
	third	"	"	"	2
	...	...	...	...	...

because transforms and filtering take place channel by channel.

Inside the processing system the following scheme runs:

1) $Sampling\ Unit \overset{Time\ Multiplex}{\longrightarrow} Disc \overset{Channel\ Multiplex}{\longrightarrow} Tape$

2) $Tape \overset{Channel\ Multiplex}{\longrightarrow} Disc \overset{Channel\ Multiplex}{\longrightarrow} Processing$

8. Time signal

The time signal is the main guiding information of time series. Its accuracy should be better than $t = 0.1\ s$ for global and better than $t = 0.01\ s$ for local evaluations. For digital data acquisition a rough estimation can be made in relation to sampling rate f_D

$$t = \frac{1}{10\ f_D} \tag{6}$$

Cristal clocks run with an error of 10^{-6} to 10^{-8} for temperature compensated cristals ($TCXO$). That's about $0.1\ \ldots\ 0.001\ s$ per day.
Radio time signal errors occur on receiver side only. The first main component of the travel time error depends on station distance ($300\ km \Rightarrow 1\ ms$; weather induced components are not relevant for seismological purposes). The second one occurs within the receiver (filters). Its about $1\ ms$ up to several $10\ ms$ dependend on receiver type. Because of different receiving conditions a radio controlled cristal clock is the most used device. Advanced solutions use computer controlled compensation of the cristal behaviour (aging, temperature) derived from average time signal differences.

The time signal is distributed by national as by worldwide services.
National time service signals are transmitted by radio stations (hourly pulse groups), time transmitters (pulse coded signal: *year ... sec*) and by television transmitters: On several defined times the start time of a (picture) frame synchronizing pulse is controlled by the national time service nuclear clock.
Worldwide time signals are available from satellite positioning systems. The United States Global Positioning System GPS is receivable around the world for 24 hours per day. Limitations for nonmilitary users don't touch seismological time signal requirements. In 1988 also the former Soviet Union opened its system for civil use.
Sufficient results one can get also by worldwide long wave transmission systems as Omega time service. Meanwhile here tecnical effort and receiver costs are higher than by use of the satellite systems

The coordination of the time signal to the recorded time series should be placed at two points:

- The header contains year, month, down to minute or second to find archived data.
- Within the time series additional time pulses (f. e. 1 bit per word) will help either synchronizing or correlating and finding one's way in long data blocks

The synchronizing effect is a necessary one for blockwise digital transmission. Firstly outside sampling happens at a time different from centralized storage time. Secondly transmission procedures change the length of a data block dependend on information structure.

Figure 9 shows variations of the acquisitioning system. The solution drawn in the upper part (seismometer to paper record) is the cheapest one (if you don't use special papers) but expensive in evaluation. In the middle You find one-way transmission of frequency modulated analog or hardware coded digital signal. In the lower part computer based acquisition allows transmission in both directions for additionally automatic

checking and controlling of the outside station. That's to be used for clock correction, seismometer and amplifier calibration, and for changing of station parameters.

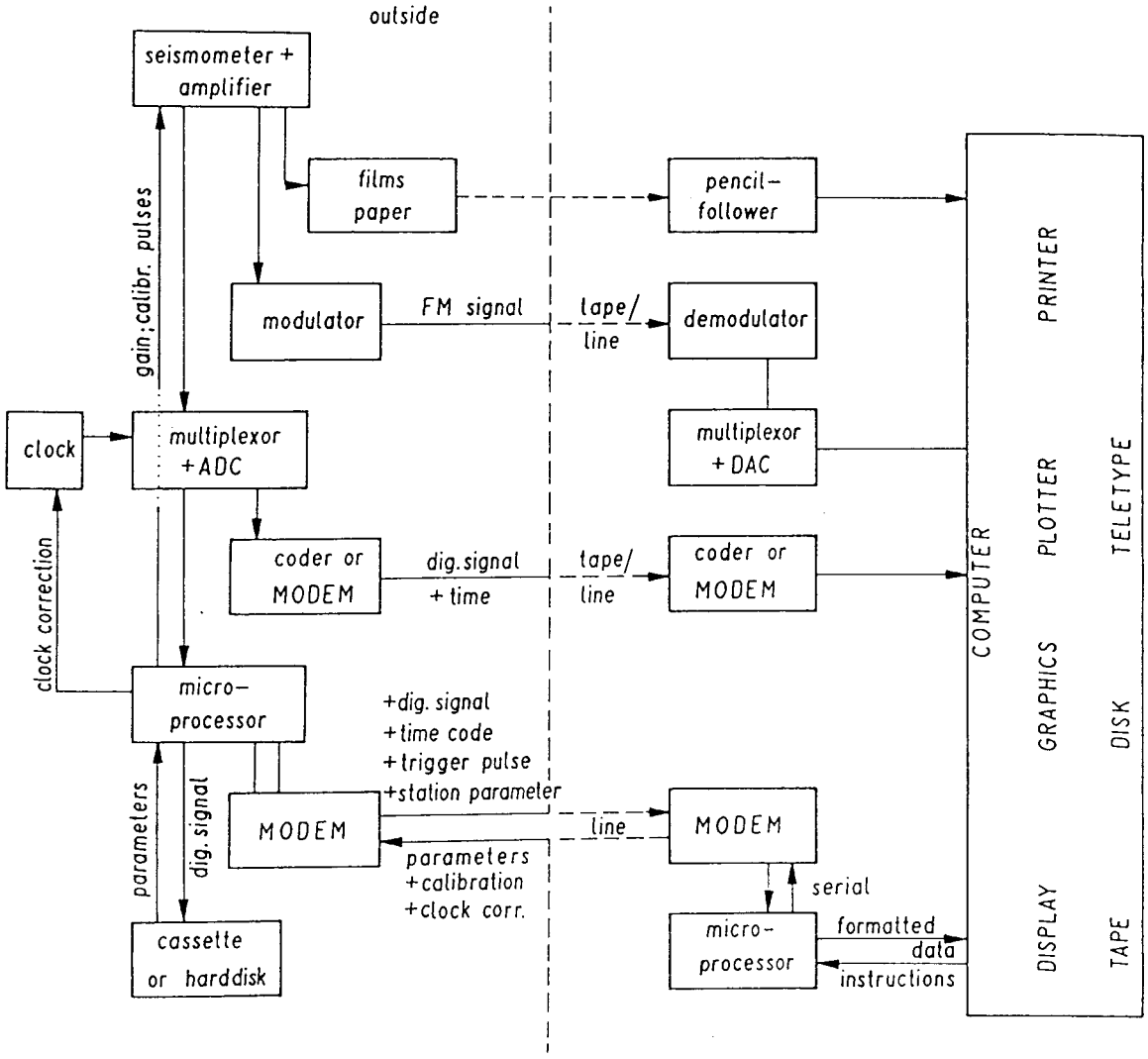

Fig. 9: Components from seismometer to computer

9. Trigger criteria

Amplitude criteria are nonexpensive in analog hardware or in computer software realisation. The most simple one consists of a treshold level fixed at 3 ... 5 times of maximum noise amplitudes. But noise level is proportional to bandwidth. This problem can be solved by passband filtering at the expected maximum of the signal-to-noise ratio SNR:

local events	higher than 5 Hz
territorial events	2 ... 5 Hz
global events	lower than 1 Hz

Additionally the treshold level can be related to current noise. Long time noise changes as natural noise (weather) or human noise (traffic) are compared with short time changes (STA/LTA: Short Term Average / Long Term Average).

$$\tau_{STA} = 2 \cdot \pi \cdot R_1 \cdot C_1 = 0.1 \ldots 1s$$

$$\tau_{LTA} = 2 \cdot \pi \cdot R_2 \cdot C_2 = 10 \ldots 100s$$

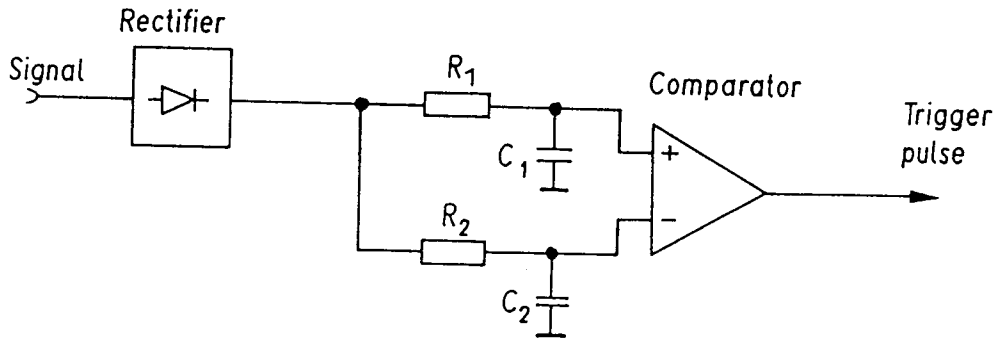

Fig. 10: Analog STA/LTA

The signal is rectified, and its absolute values are integrated by first order low passes of different integration times:

STA	$\approx$	0.1 s ...	1 s
LTA	$\approx$	10 s ...	100 s

Commonly the amplitude tresholt level is set to $STA/LTA = 3 \ldots 5$. A digital software solution needs first order recursive low passes only, and it can run on-line in background processing of any PC.

Frequency criteria are more sensitive and they cover a broad signal band simultaneously. Here the less expensive one consists of periodogram analysis to watch some main spectral lines via STA/LTA.

Fourier transform of a given time window is also used for identification. To reduce calculation expense often Walsh transform is applied. It needs addition and subtraction procedures only, but calculated Walsh spectral lines are different from signal frequencies. Thus evaluation becomes more difficult. Spectral analysis can't run on-line without additional signal processors.
Error predicting filters use the difference between the (predicted) model and the signal. Models can be Fourier or Walsh spectra or the statistical behaviour of random variables. The trigger compares model coefficients with signal coefficients or model generated time series with origin time series.

Lowering the treshold level will increase the false alarm rate exponentially. Checking criteria will reduce this effect. The most widespread criteria are *postdetector* and *voting*. The postdetector checks the signal behaviour after triggering, e. g. the signal enveloppe. For short period measurements the signal duration should be longer than 3 seconds to exclude pulses generated by disturbances within the device.
Voting means that an event must be triggered by 3 ... 5 stations of a network within given time windows depending on signal travel times.

References

Bath, M.; *Spectral Analysis in Geophysics*, Elsevier Sci. Publ. Comp., Amsterdam-Oxford-New-York 1974

IASPEI/CCSS; *Proceedings of the workshop on portable digital seismograph development*, 30.Nov.- 2. Dec. 1983, Los Altos, California

Lee, W.H.K.; Stewart, S.W.; *Principles and applications of microearthquake networks*, Academic Press New York-London-Toronto-San Francisco Sidney, 1981

Peterson, J.; Hutt, C.R.; Holcomb, L.G.; *Test and Calibration of the Seismic Research Observatory*, Open-File Report 80-187, Albuquerque, New Mexico 1980

Stearns, Samuel D.: *Digital Signal Analysis*

Wielandt, E.; *Design Principles of Electronic Inertial Seismometers*, Inst. of Geophysics, Publ. No. 384, Zurich 1986

Introduction into the theory of seismic wave propagation

by A. SCHULZE

Wave propagation plays an important role in many fields of physics. This process is involved in electrodynamics, decay of atoms,oceanography etc. Most of the observed phenomena of seismology and seismics (at least out of the vicinity of the source (focal region and shot, respectively,)) are connected with propagation of elastic waves. Therefore we shall confine ourselves in the following to the process of wave propagation in elastic media, i. e. we concerned to a mechanical problem. The goal of this lecture is to give a brief summary of phenomena ocurring in the field of seismic (i. e. elastic) wave propagation.

In this lecture is emphasized the influence of the assumptions on the results. After the opinion and the experience of the author this is essential interpreting seismological observations. We should take into account always the theoretical background which is based on our observations. (For instance interpreting P- and S-waves means we are concerned to pure elastic homogenous and isotropic medium.) The reader who is more interested in throughout mathematical treatment of the problems of wave propagation should use one of the standard text books cited below.

1. Equation of motion

Seismic waves are generated by forces acting only for a short time as for instance an earthquake or an explosion. They can propagate through the medium, if this has at least some elastic properties. It is a heuristic definition of elasticity that the medium returns in its initial state after the influence of the force. The basic equation of motion for all mechanical processes is the second law of NEWTON. In case of the theory of elasticity it has the following form:

$$\varrho \frac{\partial^2 u_i}{\partial t^2} = \frac{\partial}{\partial x_K} \sigma_{iK}$$

$i,K = 1,2,3$ ϱ = *density*; u_i = *component of displacement*

$\sigma_{iK} = \sigma_{Ki}$ = *stress tensor*

It is essential to remark that the stress tensor is symmetric.

2. stress- strain relations

In case of elasticity the medium is completly described by a relationship which connects the tensor of strain (deformation) with the stress tensor. This means that strain rates (derivatives of the strain with respect to time) are excluded. Strain rates occur in creep processes which are nonelastic.
The stress- strain relations have the following form:

$$\sigma_{ik} = c_{iklm} \cdot \varepsilon_{lm} \qquad (2.1)$$

$i,k,l,m = 1,2,3$ $\quad c$ = tensor of elasticity

$\varepsilon_{lm} = \varepsilon_{ml}$ = tensor of strain

$$\varepsilon_{lm} = \frac{1}{2}\left(\frac{\partial u_l}{\partial x_m} + \frac{\partial u_m}{\partial x_l}\right)$$

$$\sigma_i = c_{ij}\,\varepsilon_j$$

$i,j = 1 \ldots 6$ with: $11 = 1$, $12 = 2$, $13 = 3$, $22 = 4$, $23 = 5$, $33 = 6$

The srain tensor is symmetric too. This reduces the theoretical 81 components of the tensor of elasticity (tensor of 4th order) to maximal 21 independent components. (The tensor of elasticity is also symmetric) The strain tensor in the given form is an approximation to the first order. This means we deal only wirh a linear material law excluding all nonlinear effects.

2.1 the isotropic case

Let us now investigate the most simple case of the stress-strain relations the so called law of HOOKE. This law describes a pure elastic, homogenous amd isotropic medium. In this (high symmetric) case the tensor of elasticity reduces to only two independent components:

$$\begin{aligned}
\sigma_{11} &= (\lambda+2\mu)\varepsilon_{11} + \lambda\varepsilon_{22} + \lambda\varepsilon_{33} \\
\sigma_{12} &= 2\mu\varepsilon_{12} \\
\sigma_{13} &= 2\mu\varepsilon_{13} \\
\sigma_{22} &= \lambda\varepsilon_{11} + (\lambda+2\mu)\varepsilon_{22} + \lambda\varepsilon_{33} \\
\sigma_{23} &= 2\mu\varepsilon_{33} \\
\sigma_{33} &= \lambda\varepsilon_{11} + \lambda\varepsilon_{22} + (\lambda+2\mu)\varepsilon_{33}
\end{aligned}$$

Putting this special stress-strain relation in the equation of motion we obtain:

$$\varrho \frac{\partial^2 \vec{u}}{\partial t^2} = (\lambda+\mu)\,\mathrm{grad}\,\mathrm{div}\,\vec{u} + \mu\,\mathrm{div}\,\mathrm{grad}\,\vec{u}$$

$$\varrho \frac{\partial^2 \Theta}{\partial t^2} = (\lambda+2\mu)\,\mathrm{div}\,\mathrm{grad}\,\Theta \equiv (\lambda+2\mu)\,\nabla^2\Theta$$

$$\Theta = \mathrm{div}\,\vec{u}$$

$$\varrho \frac{\partial^2 \mathrm{rot}\,\vec{u}}{\partial t^2} = \mu\,\mathrm{div}\,\mathrm{grad}\,\mathrm{rot}\,\vec{u} \equiv \mu\nabla^2\,\mathrm{rot}\,\vec{u}$$

Now we can split up an abitrary displacement into a dilational and a rotational part:

$$\vec{u} = \mathrm{grad}\,\Phi + \mathrm{rot}\,\Psi :$$

Thus we obtain: $\varrho \frac{\partial^2 \Phi}{\partial t^2} = (\lambda + 2\mu) \nabla^2 \Phi$; $\varrho \frac{\partial^2 \psi}{\partial t^2} = \mu \nabla^2 \psi$

with:

$$v_p = \sqrt{\frac{\lambda + 2\mu}{\varrho}} \qquad v_s = \sqrt{\frac{\mu}{\varrho}}$$

The both equations above are wave equations indicating that the quantities Φ and ψ propagate through time and space. Thus we see that in an elastic, homogenous and isotropic medium there are two different types of waves propagating with differnt velocities. Two solutions of the wave equqtions which play an important role are:

1. *spherical wave* : $\Phi = \Phi_0 \cdot \frac{1}{r} \exp i\,(|\vec{k}||\vec{r}| - \omega t)$
2. *plane wave* : $\Phi = \Phi_0 \exp i\,(\vec{k} \cdot \vec{r} - \omega t)$

The plane wave is a good approximation for all cases far from the source. The vector of propagation has the following properties:

$$\vec{k} = 2\pi \left(\frac{k_1}{\lambda}, \frac{k_2}{\lambda}, \frac{k_3}{\lambda} \right)$$

$$= 2\pi \left(\frac{\sin \vartheta_1}{\lambda}, 0, \frac{\cos \vartheta_1}{\lambda} \right)$$

now: $\vec{k}/\omega = \left(\frac{k_1}{c}, \frac{k_2}{c}, \frac{k_3}{c} \right) = \vec{s}$ = slowness

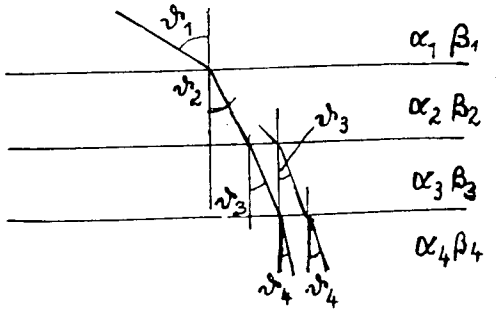

$$\frac{\sin \vartheta_1}{\alpha_1} = \frac{\sin \vartheta_2}{\alpha_2} = \frac{\sin \vartheta_3}{\alpha_3}$$

$$= \frac{\sin \vartheta_2}{\beta_2} = \ldots. \text{ const.} = p$$

p = ray parameter $\hat{=}$ horizontal component of slowness

If we now put the expression of a plane wave via the stress-strain relations in the equation of motion, we obtain:

$$\begin{pmatrix} A_{11} - \varrho c^2 & A_{12} & A_{13} \\ A_{21} & A_{22} - \varrho c^2 & A_{23} \\ A_{31} & A_{32} & A_{33} \end{pmatrix} \begin{pmatrix} \tilde{u}_1 \\ \tilde{u}_2 \\ \tilde{u}_3 \end{pmatrix} = 0$$

$(A_{ij}) = (A_{ji})$ $\qquad A_{il} = c_{iklm} \cdot k_k \cdot k_m$

isotrop: $A_{il} = (\lambda + \mu)\, k_i k_l + \mu\, \delta_{il}$

$\hookrightarrow$ EW: $c_1 = \left(\frac{\lambda + 2\mu}{\varrho} \right)^{1/2}$ $\qquad c_2 = c_3 = \left(\frac{\mu}{\varrho} \right)^{1/2}$

EV: $\tilde{u}_1 = (k_1, k_2, k_3)$; $\tilde{u}_2 = (-k_3, 0, k_1)$; $\tilde{u}_3 = (-k_2, k_1, 0)$

$\hookrightarrow$ $\tilde{u}_1 \parallel k$; $\tilde{u}_2 \perp k$; $\tilde{u}_3 \perp k$; $\tilde{u}_2 \not\perp \tilde{u}_3$

This means that in isotropic media the amplitude vector of a P-wave is parallel to the direction of the vector of propagation while that of a S- wave is perpendicular to the direction of propagation. Therefore the P- waves are called longitudinal waves and the S- waves are transverse waves. This means the P- waves and S- waves differ with regard to their polarization.

2.2 the quasi anisotropic case

The quasi anisotropic case is charactrized by the fact that the elastic components differ in the vertical direction compared with the horizontal ones. This is a model which describes well the observations made in geology. In this case the stress-strain relations are more complicated:

$$
\begin{aligned}
\delta_{11} &= (\lambda_{\parallel}+2\mu_{\parallel})\varepsilon_{11}+\lambda_{\parallel}\varepsilon_{22}+\lambda_{\perp}\varepsilon_{33}\\
\delta_{12} &= 2\mu_{\parallel}\varepsilon_{12}\\
\delta_{13} &= 2\nu\,\varepsilon_{13}\\
\delta_{22} &= \lambda_{\parallel}\varepsilon_{11}+(\lambda_{\parallel}+2\mu_{\parallel})\varepsilon_{22}+\lambda_{\perp}\varepsilon_{33}\\
\delta_{23} &= 2\nu\,\varepsilon_{23}\\
\delta_{33} &= \lambda_{\perp}\varepsilon_{11}+\lambda_{\perp}\varepsilon_{22}+(\lambda_{\perp}+2\mu_{\perp})\varepsilon_{33}
\end{aligned}
$$

If we put this stress-strain relation in equation (3), we obtain:

$$\varrho\frac{\partial^2 u_1}{\partial t^2} = (\lambda_{\parallel}+2\mu_{\parallel})\frac{\partial^2 u_1}{\partial x^2}+\nu\frac{\partial^2 u_1}{\partial x^2}+(\lambda_{\perp}+\nu)\frac{\partial^2 u_3}{\partial z\,\partial x}$$

$$\varrho\frac{\partial^2 u_3}{\partial t^2} = (\lambda_{\perp}+\nu)\frac{\partial^2 u_1}{\partial z\,\partial x}+\nu\frac{\partial^2 u_3}{\partial x^2}+(\lambda_{\perp}+2\mu_{\perp})\frac{\partial^2 u_3}{\partial z^2}$$

$$\Phi = \Phi_0\, exp\; ik\,(lx+nz-ct) \qquad l = sin\,\vartheta$$

$$\Psi = \Psi_0\, exp\; ik\,(lx+nz-ct) \qquad n = cos\,\vartheta$$

$$2\varrho c^2 = \left[(\lambda_{\parallel}+2\mu_{\parallel})\,l^2+(\lambda_{\perp}+2\mu_{\perp})\,n^2+\nu\right] \pm\left\{\left[(\lambda_{\parallel}+2\mu_{\parallel})-\nu\right)l^2-(\lambda_{\perp}+2\mu_{\perp}-\nu)n^2\right]^2+4(\lambda_{\perp}+\nu)^2 l^2 n^2\Big\}^{1/2}$$

This result shows that in quasi anisotropic media the velocity depends on direction of the wave propagation. If we would check the polarization behaviour of seismic waves in anisotropic media we would remark that the amplitude vector of P- waves is not longer parallel to the direction of propagation. Therefore these waves are called quasi P- waves. The same holds true for S- waves. Thus we see, if we speak in terms of P- and S- waves, respecticely we cannot interprete a medium in terms of anisotropy.

2.3 the inhomogenous (isotropic) case

Now we consider the case where the elastic parameters depend on the coordinates. This is a realistic assumption keeping in mind how often and abrupt the rocks change in the nature. Now we have:

$$\lambda=\lambda(x,y,z),\quad \mu=\mu(x,y,z),\quad \varrho=\varrho(x,y,z)$$

$$\varrho\frac{\partial^2\vec{u}}{\partial t^2} = (\lambda+\mu)\nabla(\nabla\vec{u})+\mu\nabla^2\vec{u}+\nabla\lambda(\nabla\vec{u})+\nabla\mu\times\nabla(\nabla\times\vec{u})$$

This equation cannot be solved analytically. Thus we must try an approximation:

$$\vec{u} = \sum_{K=0}^{\infty} \vec{u}_K \cdot F_K \left(c_0 t - w(x,y,z) \right)$$

Let us now investigate only the phase term w describing the propagation of the wave. Putting the approximation into the wave equation we obtain:

$K = 0$ *(first approximation)*:

$$0 = -\varrho\, c_0^2\, \vec{u}_0 + (\lambda+\mu)\, \nabla w\, (\vec{u}_0 \nabla w) + \mu\, (\nabla w)^2 u_0$$

$$(\nabla w)^2 = \frac{c_0^2}{c^2}$$

$$\frac{c_0^2}{c^2} = \left(\frac{\partial w}{\partial x}\right)^2 + \left(\frac{\partial w}{\partial y}\right)^2 + \left(\frac{\partial w}{\partial z}\right)^2 \quad \textit{(Eikonal-equation)}$$

This expression is a differential equation of first order (in contrast to the wave equation). Now we have to look for the condition of application of the eikonal equation:

$$\Phi = A(x,y,z)\, \exp i\omega \left(w(x,y,z)/c_0 - t \right)$$

$$\left(\frac{\partial w}{\partial x}\right)^2 + \left(\frac{\partial w}{\partial y}\right)^2 + \left(\frac{\partial w}{\partial z}\right)^2 - \left(\frac{c_0}{c}\right)^2 - \left(\frac{c_0}{\omega}\right)^2 \left[\frac{1}{A} \left(\frac{\partial^2 A}{\partial x^2} + \frac{\partial^2 A}{\partial y^2} + \frac{\partial^2 A}{\partial z^2} \right) \right] = 0$$

$$\frac{c_0}{\omega} \to 0 \hookrightarrow \omega \to \infty\,; \quad \lambda_0 = \frac{2\pi c_0}{\omega} \to 0\,; \quad \lambda \frac{\delta c}{c} \ll 1$$

$\hookrightarrow$ *concept of rays*

Example: $\lambda = \lambda(z)$, $\mu = \mu(z)$, $\varrho = \varrho(z) \hookrightarrow v = v(z)$

$$x = 2p \int_0^z \frac{v}{\sqrt{1-p^2v^2}}\, dz \qquad t = 2 \int_0^z \frac{dz}{v\sqrt{1-p^2v^2}}$$

We state that in cases where the condition for the application of the eikonal equation is satisfied we can work with seismic rays instead of the complete wavefield. This means in that cases we can solve the kinematical aspects (i. e. calculating of travel time curves) of the direct (forward) problem. The remaining question is how many energy propagates in which direction.

3. the partition of seismic energy at plane interfaces

If a seismic ray (which is the normal to the wavefront) intersects a plane interface the following boundary conditions must be fullfilled:

$$u_1^{(1)} = u_1^{(2)}$$
$$u_3^{(1)} = u_3^{(2)}$$
$$\partial_{13}^{(1)} = \partial_{13}^{(2)}$$
$$\partial_{33}^{(1)} = \partial_{33}^{(2)}$$

These boundary conditions state that the interfaces are welded in contact. Due to the fact that at each interface a reflection and a transmission can take place, we have to expect for an incident wave four waves generated at this interface; namely:

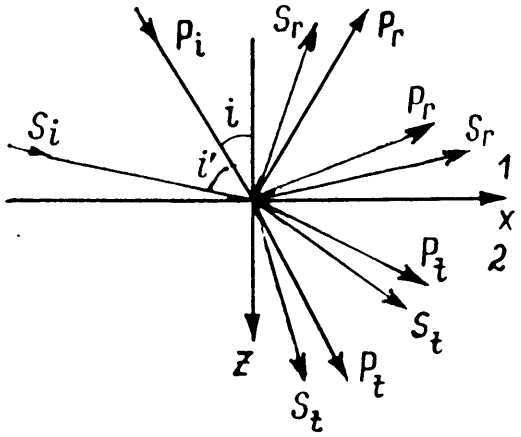

The potentials for this case have the following form:

$$\Phi = A_1 \exp i\left(k(ct - x - az)\right) + A_2 \exp ik(ct - x + az) = \Phi\downarrow + \Phi\uparrow$$
$$\psi = B_1 \exp ik(ct - x - bz) + B_2 \exp ik(ct - x + bz) = \psi\downarrow + \psi\uparrow$$
$$\varphi = A' \exp ik(ct - x - a'z);\ \tilde{\psi} = B' \exp ik(ct - x - b'z)$$
$$a = \sqrt{\frac{c^2}{\alpha^2} - 1} = \cot i \qquad b = \sqrt{\frac{c^2}{\beta^2} - 1} = \cot i'$$
$$a' = \sqrt{\frac{c^2}{\alpha'^2} - 1} \qquad b' = \sqrt{\frac{c^2}{\beta'^2} - 1}$$

A1 and B1 stand for the amplitudes of the incident potential (A for P- wave, B for S- wave), while A2 and B2 describe the reflected energy (P- and S- wave, respectively). A' and B' are the amplitudes of the transmitted energy.
Let us consider the case where two halfspaces are separated by an interface. If we now take into account an incident P-wave, so B1 equals zero.

For convinience let be A1 equal unity. Thus we have to solve four equations with four unknowns. The solutions are often called the ZOEPPRITZ equations. Instead of the formulas here are shown two diagrams for an incident P- wave propagating from higher to lower velocity (above) and vice versa (below).(From PILANT.)

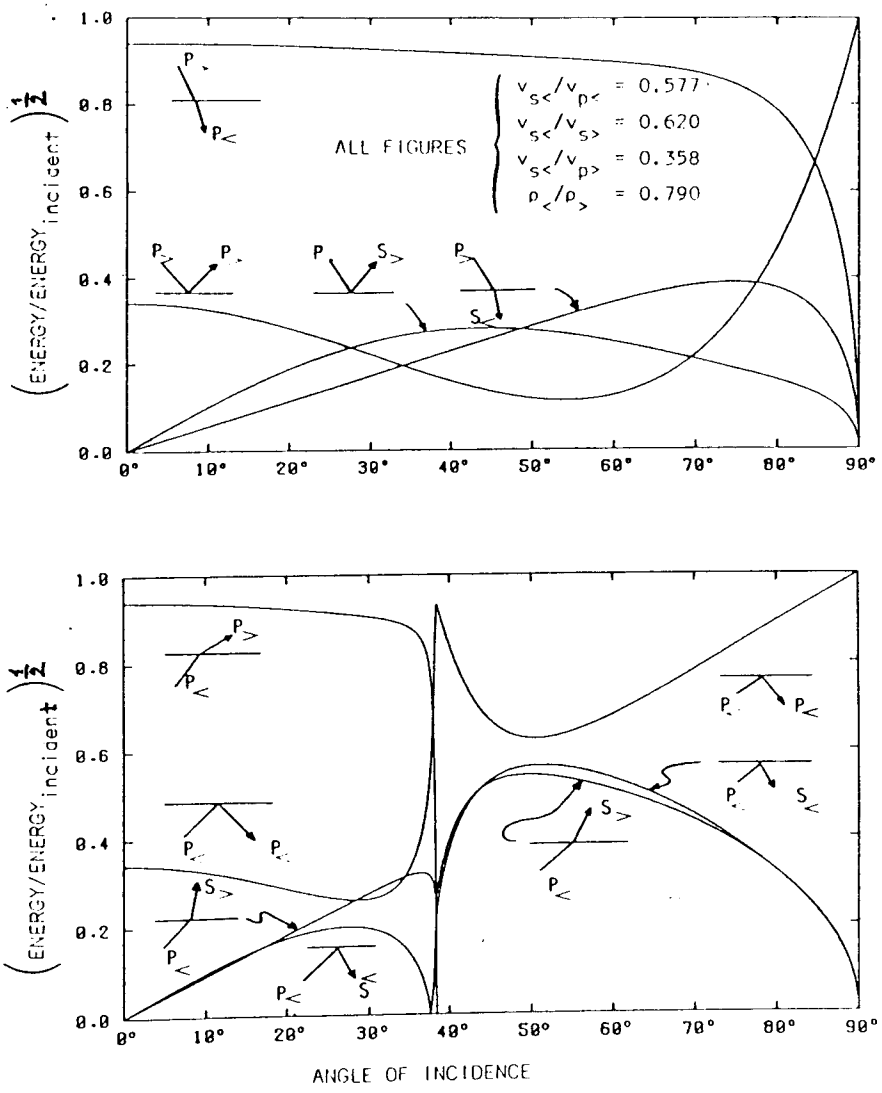

It is obvious that the amount of reflected and transmitted energy depends very sensitively on the angle of incidence. There are also critical angles (see below) which are connected with the generation of inhomogenous waves. For such details the reader is referred to textbooks.
We want now to investigate what happens, if there are more than one interface. In this case at each interface occur the same process described above .Because this process becomes very complicate it is convinient to systemize it. This can be easily done using matrices and vectors. We introduce a vector P which contains the up- and downgoing potential of the P- and S- waves, respectively. This vector has four components. On the other hand let be the vector S containing the two components of displacement and the two components of the stress tensor which are relevant in the boundary conditions. Both these vectors are related by

a 4x4- matrix which contains the parameters of the layer under consideration as well as the operators by which the quantities of S and P are related. Let be this matrix T.
We consider the following situation:

$$\begin{pmatrix} u_1 \\ u_3 \\ \delta_{13} \\ \delta_{33} \end{pmatrix} = T \begin{pmatrix} \Phi_\uparrow \\ \psi_\uparrow \\ \Phi_\downarrow \\ \psi_\downarrow \end{pmatrix} \equiv S = T \cdot P \; ; \quad P = T^{-1} S$$
$$T = (4 \times 4)\ matrix$$

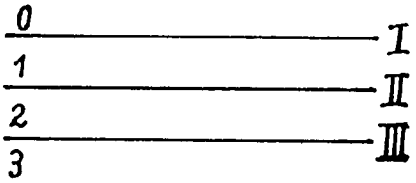

$$\begin{aligned}
I^u: &\quad S_0 = T_0 \cdot P_0 \\
I^L: &\quad P_1^u = T_1^{-1} \cdot S_0 &&= T_1^{-1} \cdot T_0 \cdot P_0 \\
II^u: &\quad P_1^L = D_1 \cdot P_1^u &&= D_1 \cdot T_1^{-1} \cdot T_0 \cdot P_0 \\
&\quad S_1 = T_1 \cdot P_1^L &&= T_1 \cdot D_1 \cdot T_1^{-1} \cdot T_0 \cdot P_0 \\
II^L: &\quad P_2^u = T_2^{-1} \cdot S_1 &&= T_2^{-1} T_1 \cdot D_1 T_1^{-1} \cdot T_0 \cdot P_0 \\
III^u: &\quad P_2^L = D_2 \cdot P_2^u &&= D_2 T_2^{-1} T_1 \cdot D_1 \cdot T_1^{-1} \cdot T_0 \cdot P_0 \\
&\quad S_2 = T_2 P_2^L &&= T_2 \cdot D_2 \cdot T_2^{-1} \cdot T_1 D_1 \cdot T_1^{-1} \cdot T_0 P_0 \\
III^L: &\quad P_3 = T_3^{-1} S_2 &&= T_3^{-1} \cdot G_2 \cdot G_1 \cdot T_0 P_0 \; ; \quad G_i = T_i D_i T_i^{-1}
\end{aligned}$$

$$\begin{pmatrix} 0 \\ 0 \\ T_{pp} \\ T_{ps} \end{pmatrix} = M \begin{pmatrix} R_{pp} \\ R_{ps} \\ 1 \\ 0 \end{pmatrix} ; \quad \begin{pmatrix} T_{sp} \\ T_{ss} \\ 0 \\ 0 \end{pmatrix} = M \begin{pmatrix} 0 \\ 1 \\ R_{sp} \\ R_{ss} \end{pmatrix} ; \quad M = T_n^{-1} \prod_{i=1}^{n-1} G_i T_0$$

The matrix D depends essentially on the thickness of the layer and produces the time delays which are needed by the wave to travel from the upper to the lower boundary (or vice versa). We see that the procedure can systematically expanded. Each layer is described by a specific layer matrix. The result of a reflection or transmission of some layers imbedded into two halfspaces is essentially a product of the layer matrices.

The following figure illustrates the reflectivity of a so called sandwich structure for several ratios of the velocity and different frequencies.

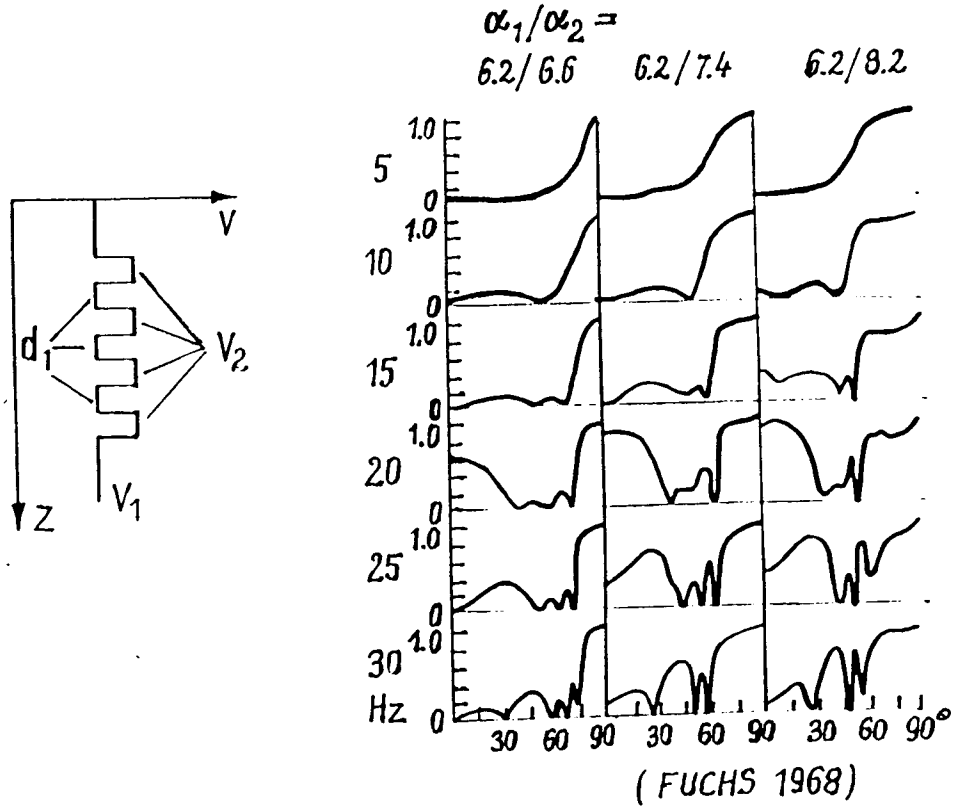

$d_2 = 82m \quad 88m \quad 102m$

$d_1 = 77m \quad 77m \quad 77m$

4. horizontal propagation

Very shortly the basic features of surface waves are mentioned. Here we deal with potentials propagating parallel to the x- axis. Thus the potential can be written:

$$\Phi = f(z) \cdot \exp i\,(kx - \omega t); \quad \Psi = g(z) \exp i\,(kx - \omega t)$$

$$\hookrightarrow f(z) = A_1 \exp ikaz + D \exp ikaz \quad a = \sqrt{\frac{c^2}{\alpha^2} - 1}$$

$$g(z) = B \exp ikbz + E \exp ikbz \quad b = \sqrt{\frac{c^2}{\beta^2} - 1}$$

free boundary ($\partial_{13} = \partial_{33} \equiv 0$):

$$(2\beta^2 - c^2)^2 = -4\beta^4 ab$$

$\hookrightarrow c < \beta < \alpha \quad \hookrightarrow a, b$ imaginary!

$$u_1 = A \cdot k \left(\exp + ikaz - \left(1 - \frac{c^2}{2\beta^2}\right) \exp + ikbz\right) \sin kx = \tilde{A}(z) \sin kx$$

$$u_3 = -Ak|a| \left(\exp + ikaz + \left(1 - \frac{c^2}{2\beta^2}\right) \exp + ikbz\right) \cos kx = -\tilde{B}(z) \cos kx$$

with

$$\exp ikaz = \exp ik\sqrt{\frac{c^2}{\alpha^2} - 1}\cdot z = \exp -\frac{\omega}{c}\sqrt{1-\frac{c^2}{\alpha^2}}\cdot z$$

The wave which is characterized by the above potential is called RAYLEIGH wave. Typical for this waves is the elliptical polarization described by the terms for the components of displacement. The velocity of propagation for a RAYLEIGH wave is less than the S- wave velocity (about 90 %). Furthermore we remark a frequency dependent amplitude. This means that lower frequencies penetrate deeper into the subsurface than higher do. The depth dependence of the components of displacement differ, so we have the following behaviour:

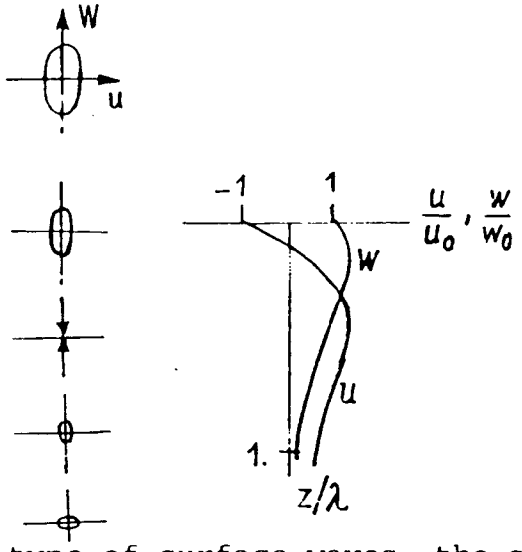

Another type of surface waves, the so called LOVE waves, are connected with the layering of the Earth. Here we consider for simplicity the waveguide effect of a fluid between two rigid bodies. This has the advantage of simple boundary conditions and showing the essential features

$$\Phi = A \exp ik(x+az) + D \exp ik(x-az)$$

boundaries:

$$\left.\begin{array}{rl} A\exp ikah + D\exp -ikah &= 0 \\ A \quad - D &= 0 \end{array}\right\} \cos kah = 0$$

$$kah = (n+\tfrac{1}{2})\,\pi = \frac{\omega}{c}\sqrt{\frac{c^2}{\alpha^2}-1}\cdot h$$

$$c(\omega) = \left[\frac{1}{\alpha^2} - \frac{[(n+\tfrac{1}{2})\cdot\pi]^2}{\omega^2 h^2}\right]^{-1/2};\quad k = \frac{\omega}{c(\omega)} = k(\omega)$$

c, k *show dispersion!*

An important result is the dispersion of the velocity. This means that different frequencies propagate with different velocities. Another characteristic of surface waves are the modes. The equation for the velocity depends on the number n. For each value there is a special state which can propagate with its velocity.

This state is called mode. The main part of energy is distributed on low modes (zero and first mode). Due to the dispersion we must ditinguish two different velocities. We look for the constant value of the phase term:

$$K(\omega)x - \omega t = const.$$

$$\frac{d}{d\omega}\left[K(\omega)x - \omega t\right] = 0$$

$$\Rightarrow \quad u = \frac{x}{t} = c(\omega)\Big/\left(1 - \frac{\omega}{c(\omega)}\,\frac{dc}{d\omega}\right)$$

u = group velocity

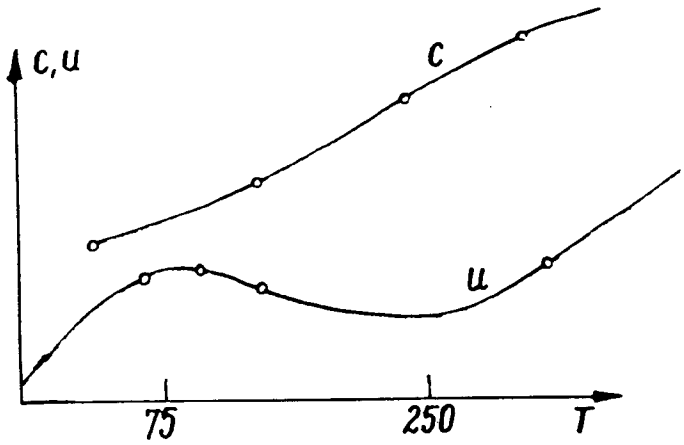

Due to the dispersion we obtain the group velocity u (which describes the propagation of energy) and the phase velocity c which gives the velocity of a single frequency. Generally the phase velocity is higher than the group velocity.

5. literature

AKI, K., RICHARDS, P. G. : Quantative Seismology
W. H. Freeman and Co., San Francisco (1980)

BULLEN, K. E. An introduction to the theory of seismology
2nd ed. Cambridge University Press, London 1953

EWING, W. M., JARDETZKY, W.S., PRESS, F.: Elastic waves in layered media. Mc Graw- Hill Book Company NY, Toronto, London

GRANT, F. S., WEST, G.F., Interpretation theory in applied geophysics. Mc Graw- Hill Book Company 1965

PILANT, W. L. Elastic waves in the Earth
Elsevier Amsterdam, Oxford, NY 1979

Seismic methods for investigation of the lithosphere by means of body waves

by

A. Schulze

1. Introduction

Seismic mrthods are the most powerful tool to investigate the lithosphere i. e. the uppermost 100 km of the Earth. Reasons for this are the use of controlled sources of seismic signals,a broad frequency range which gives a resolution power from some 10 meters up to several kilometers and a very sophisticated recording and processing technique.
The first kilometers of the lithosphere attract the main interest of the geopysicists and geologists because of the importance of accumulations of mineral deposits within the reach for economic and social use.
Seismic waves are generated by explosions (in boreholes or in shallow water) or by gas exploders and vibrators,respectively. These waves are elastic ones and propagate according to their respective physical laws. In the following we restrict ourselves to the consideration of wave propagation through the solid Earth. The aim of this paper is to give some hints as to the application of seismic data for the interpretation and estimation of a structural-geological model of the subsurface under investigation, and not to present a comprehensive mathematical treatment of interpretation theory.

2. Data aquisition

Here we deal only with investigations along profiles i.e. linearly shaped observation schemes. The interpretation of such measurements results in models revealing the deep structure of the underground beneath this profile.
Depending on the special target of the investigation different observation schemes are applied.

2.1 Surveying the whole crust (depth about 25-50 km)

If a first overlook is desired, a relatively sparse spacing of receivers (1-5 km) is sufficient. The most common observation scheme is a single shot profile.

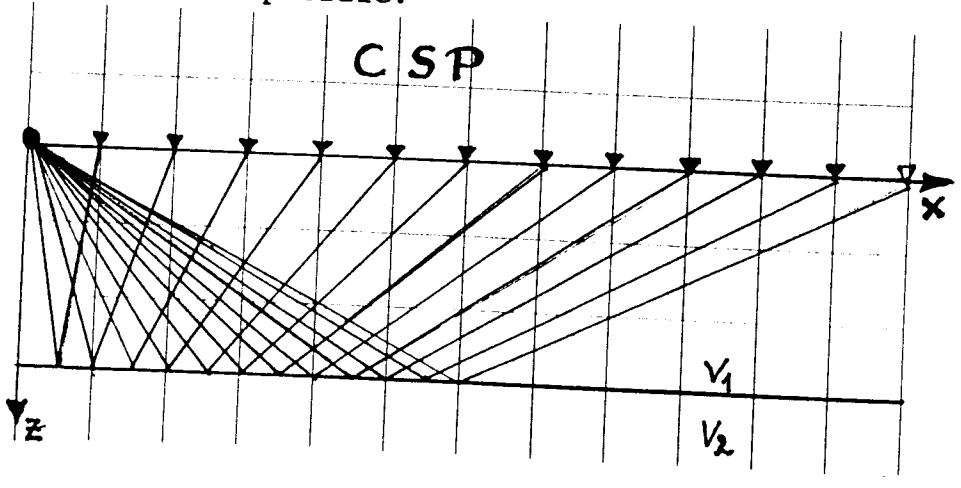

The waves mainly used are diving (or head) waves and wide angle (supercritically reflected) waves,respectively.
These measurements demand due tu the great observation distances (>150 km) large charges up to some hundred kg of explosives which are detonated in old quarries, bore holes or lakes. The single shot profiles are also called CSP (common shot point) profiles.

2.2 Performing special investigations

If special structures in the underground are the tagets a more sophisticated method is necessary. The applied observation scheme contains a lot of shotpoints and a dense spacing of receivers (50-100 m). To obtain a high horizontal resolution near vertical (subcritical) reflections are used. This means the observation distances are small (5-15 km) thus only small charges (1-10 kg) are necessary. The most applied observation scheme is the the common midpoint (CMP) method. A CMP gather results from sorting a lot of CSP's in such a way that a given point in the subsurface is hit by different rays, the number by which this point is hit is called the coverage (ranging from about 50-200).

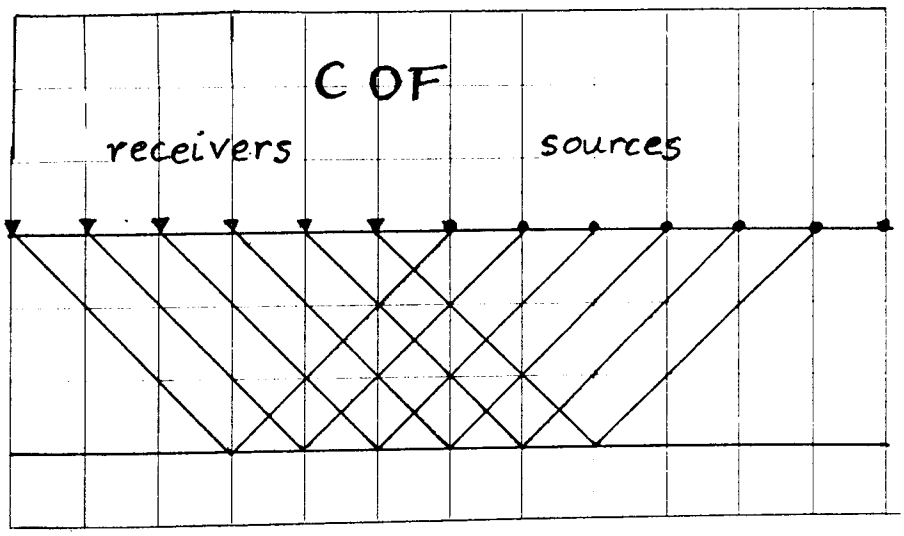

Two further cases should be mentioned:

2.3 Constant offset measurements (COF)

If one wants to trace a special interface (to determine variations in depth) this method can be applied. Using source receiver-pairs with a fixed offset (for instance the critical distance) and adjust them corresponding its midpoint distance one obtains a seismogram section in which the desired interface is emphazised. This is due to the fact that reflected waves at this distance are characterized by strong amplitudes. The COF observations need, of course, a lot of sources. COF sections can be derived by a special sorting parallel to CMP sorting.

2.4 Constant receiver observations (CRP)

If ther is a moving source for instance a ship or the shotpoints of a CMP profile and the shots are recorded by one station (one land station or one fixed station on a profile) a scheme results equivalent to a CSP.

In each case the result of a seismic measurement is a seismogram section adopted to the special task of investigation (see fig. 1-3).
The main task for a geophysicist working in the field of seismics is to draw conclusions concerning the structure and composition of the underground i.e. to interpret the seismic data.

3. Two basic schemes of interpretation: the direct and the inverse problem

3.1 General remarks

To interprete geophysical data two principally different methods are known. They are called the direct and the inverse problem, respectively.
The solution of the direct problem starts with an assumption concerning the physical model. The next step is to calculate the effect of this model. In the field of seismics we start with a (one or two dimensional) velocity-depth model and determine the travel times (i.e. the kinematic solution of the direct problem) or the amplitudes (i.e. the dynamical solution of the direct problem). This is done by computation of synthetic seismograms by different methods. After the calculation we have to compare the calculated results with observed data. By a stepwise improvement of the start model this procedure is repeated as long as the calculated data fit the measured ones sufficiently. The solution of the direct problem belongs to the so called trial and error methods.
To solve the inverse problem we start with the observed data and try to derive that model which is the cause of those data. In dependence of the quantities from which we draw the conclusions one speaks about the kinematic inverse problem (using travel times) or the dynamical inverse problem (using amplitude data).
Generally inverse methods are not unique. This is induced by the fact that the model contains more degrees of freedom than can be extracred from the data. (for instance in seismics we observe traveltimes, amplitudes and apperent velocities.) Besides this we are faced with the situation that the measured data set is commonly not complete.

3.2 Some important formulas for seismic interpretation

In this section important formulas both to solve the kinematic direkt problem and the kinematic inverse problem are given. Here only the most simple cases are considered.

3.2.1 Basic formulas for the direct problem

- constant velocity:

$$\sin i_1 / V_1 = \sin i_2 / V_2 = p = \text{const.}$$

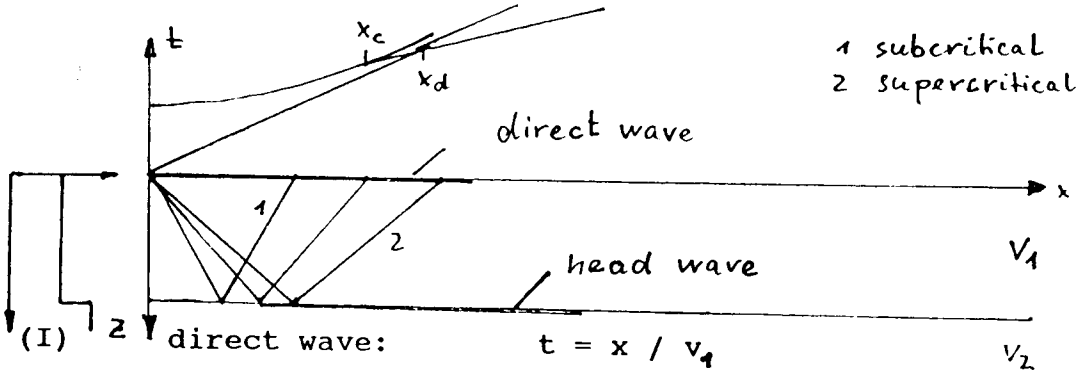

(I) direct wave: $t = x / v_1$

(II) reflected wave: $(x/2)2 + h2 = (t*v/2)2$

$t = SQRT(x2+4h2)/v_1$

(III) head wave: $i_c = \sin^{-1}(v_1/v_2)$

$(t-t_0)/(x-x_0) = 1/v_2 = p$

with $x_0 = 2*h*\tan i_c$; $t_0 = 2*h/(v*\cos i_c)$ leads to

$$t = x/v_2 + 2*h*\cos i_0 / v_1 \qquad (0)$$

-depth depending velocity:

Suppose the velocity depends only on the depth: v = v(z) (one dimensional model). In this case an infinitesimal part of the ray is defined by:

$$dx/dz = \tan i\,(z)$$

and an infinitesimal time increment is given by

$$dt = ds/v(z) = dz/(\cos i * v(z))$$

i = angle between the ray and the z-axis, ds = infinitesimal ray path segment. Then we obtain from the above equations:

$$dx = \{p*v(z)/SQRT(1-(p*v(z))2)\}dz$$

$$x = 2\int_0^{z_m} \{p*v(z)/SQRT(1-(p*v(z))2)\}dz \qquad (1)$$

and

$$dt = \{1/(v(z)*SQRT(1-(p*v(z))2))\}dz$$

$$t = 2\int_0^{z_m} \{1/(v(z)*SQRT(1-(p*v(z))2))\}dz \qquad (2)$$

p = ray parameter. We further assume a special velocity depth dependence

$$v = v_0 + \gamma z.$$

Integrating (1) and (2), respectively, one obtains using the angle i as parameter:

$$x = v_0*(\cos i_0 - \cos i)/(\gamma * \sin i_0) \qquad (3)$$

$$z = v_o*(\sin i - \sin i_o)/(\gamma*\sin i_o) \quad (4)$$

$$t = \ln(\tan(i/2)/\tan(i_o/2))/ \quad (5)$$

γ =velocity gradient, i_o =take off angle, v_o =start velocity, f = free parameter. Equations (3) and (4) are parametric formulas of a circle. This means for a linear dependent velocity depth function seismic energy propagates along parts of a circle with a radius v /(*sin i).

3.2.2 Basic formulas for the inverse problem

- constant velocities

Referring to eq. (0) we look for that time of a head wave which correspond to the sourcepoint (x = 0). This means the head wave is continued backward until it intersects the time axis. The time for x = 0 is called intercept time. From eq. (0) follows:

$$\tau = 2*h*\cos i_c/v_1 \qquad \text{with } i_c = \sin^{-1}(v_1/v_2).$$

Thus we find in this formula only measured quantities with exception of the thickness h which can be calculated easily:

$$h = \tau*v_1/(2*\cos i_c).$$

Are there more than one interfaces

$$\tau = \sum_{k=1}^{n} 2*h_k*\cos i^{(k)}/v_k \qquad \text{with } i^{(k)} = \sin^{-1}(v_k/v_{k+1}).$$

- depth depending velocity

Eq. (1) can be transformed after some steps into the following form:

$$z(v) = 1/\pi \int_0^{x_o} \cosh^{-1}(v(x_o)/v(x))dx,$$

the well-known WIECHERT-HERGLOTZ integral. It belongs to the classical inversion formulas in geophysics. On the right hand side only observed quantities occur and the result is the depth of the maximum penetration depth of the ray under investigation. It should be noted that the integrand contains apparent velocities. It is obvious that the WIECHERT-HERGLOTZ integral can be applied only if the following restrictions are fulfilled:

-the velocity depends only on the depth v=v(z) (one dimensional model) and

- the integrand must be greater than unity; oherwise the function cosh is not defined.

4. Refraction seismics

After compiling a seismogram section for a CSP gather the correlation has do be done. Correlation means the connection of arrivals in neighboured seismograms under the assumption that they belong to the same wave. The complete system of correlated arrivals is called travel time curve. The determination of the travel time curve is one of the most important steps in the interpretation process. The correlation depends strongly on the experience of the interpretator. Restricting ourselves to direct and head waves, respectively, the slope of the correlated travel time

branch is the inverse of the apparent velocity. The inverse of the apparent velocity is the ray parameter p = sin i/v =1/v'.

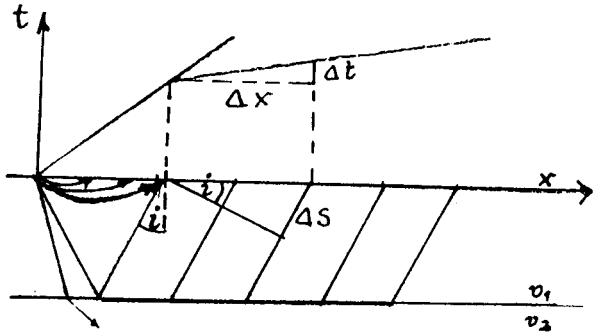

$$V_a = \frac{\Delta x}{\Delta t}\ ;$$

$$V = \frac{\Delta s}{\Delta t}\ ; \qquad V_a = \frac{V}{\sin i}$$

$$\frac{\Delta s}{\Delta x} = \sin i\ ;$$

In practice we determine from travel time curves the value of p by measurements of the arrival times in at least two points on the seismogram section. Keeping in mind that p is constant along a ray it follows that the determination of p is equivalent with the determination of the true velocity at maximum depth of the ray. (At maximum depth the ray propagates horizontaly, thus the angle between the ray and the z-axis is 90°;the corresponding sinus equals unity.) The remaining problem is the unknown depth. It can be calculated just by the WIECHERT-HERGLOTZ integral.

In case of an inclined interface we have the following situation:

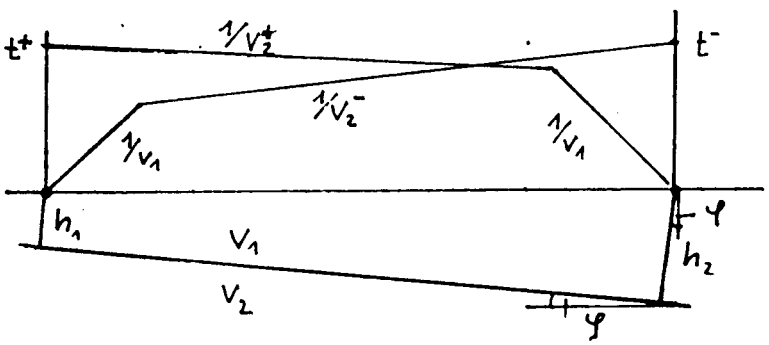

$t^+ = t^-$

Now the apparent velocity is also influenced by the dip of the layer:

observing updip: $v_2^+ = v_2 / (\sin(i-\varphi))$

observing downdip: $v_2^- = v_2 / (\sin(i+\varphi))$

thus the dipping angle can be determined:

$$\varphi = (\sin^{-1} v_1 / v_2^- - \sin^{-1} v_1 / v_2^+)/2$$

and

$$v_2 = 2 * \cos\varphi * v_2^+ * v_2^- / (v_2^+ + v_2^-)$$

$$t_0^- = 2 * h_1 * \mathrm{SQRT}(v_2^2 - v_1^2) / (v_2 * v_1)\ .$$

It is an essential feature also for dipping interfaces that the reversed time t and t are equal. So it is easy to check, if the correlation is correct. From the above is clear that at least two schots are needed to check, if there is an inclined layer in the subsurface. From only one shotpoint we cannot draw any conclusion with respect to dipping.
In the case of a varying velocity gradient the radius of the ray

path is changed. If there is a layer with a relatively strong gradient, the radius is decreased. By this we can observe a loop in the travel time curve:

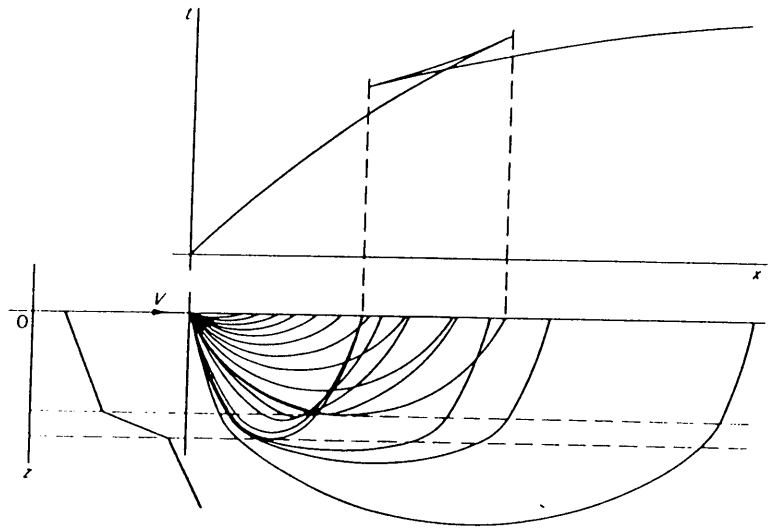

If exists a so called low velocity zone the travel time curve is characterized by two features. There is a shadow zone, because the ray is bent more vertically by the transition to the lower velocity. Besides in this layer the seismic ray needs more time, thus a time jump occurs in the travel time curve. It is difficult to estimate the thickness and velocity inside the low velocity zone using diving waves alone. But in practice, of course, there are also reflected waves from the upper and lower edge of the low velocity zone.

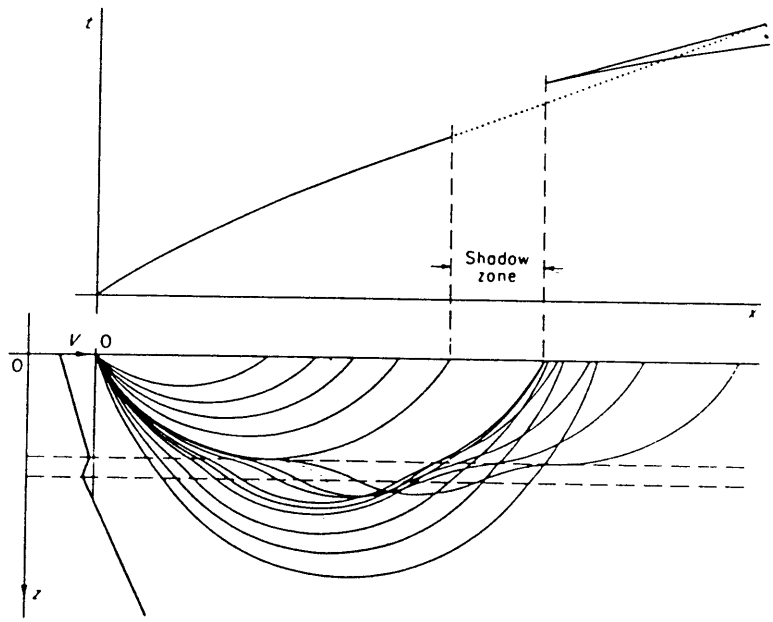

literature

GIESE, P., PRODEHL, C., STEIN, A.: Explosion seismology in Europe
Springer Verlag Berlin, Heidelberg, NY 1976
GRANT, F.S., WEST, G. F. Interpretation in applied geophysics
Mc Graw- Hill Book Company NY, Toronto, Tokio 1965
SHERIFF, R. E., GELDART, L. P. Exploration seismology
Cambridge university press; Cambridge, NY, Sydney 1982
WATERS, K. H. Reflection seismology
John Wiley and sons, NY 1978

PROCESSING OF NEAR VERTICAL REFLECTION DATA

Albrecht Schulze

GeoForschungsZentrum, Telegrafenberg, D-14473 Potsdam

1. General remarks

Reflection data are commonly recorded as CMP-data. Their processing is provided mainly by comercial processing systems, which consist of different modules (subroutines) performing the single steps of the processing.
Although the processing is done by a computer the subjective influence of the interpreter is significant. The final results depend strongly on the decisions of the interpreter when parameters for filtering, static corrections etc. are to be chosen.
In the following a principal scheme by STILLER and THOMAS (see: The German Continental Deep Drilling Program (KTB), 1989 Springer) is discussed more in detail.

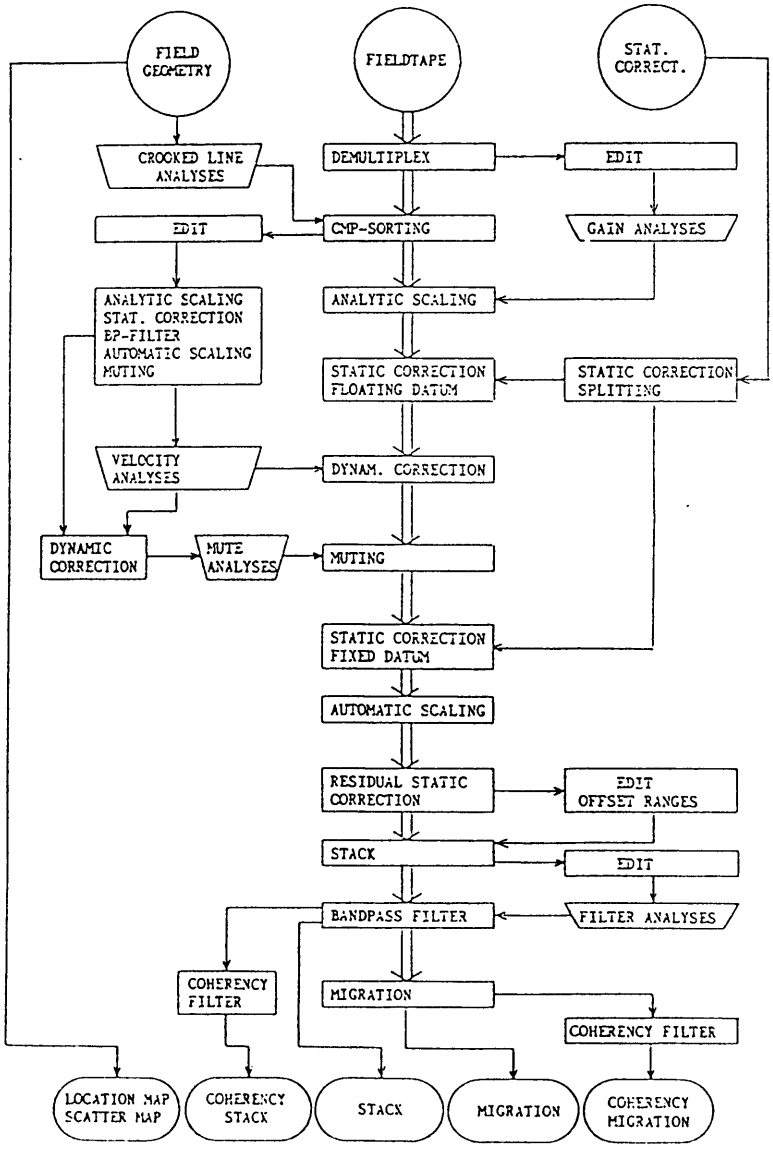

Fig. 2. Generalized flowchart for deep-seismic vibroseis processing

1. **DEMUX** The data are recorded in the field as CSP gather in a time sorted manner. This is done by the multiplexer. The first step of processing is to demultiplex the data which correspond to a resorting to the seismic input channels (eg. geophones): The following transformation is performed:

field (multiplexed) data:

$[N_1(t_1), N_2(t_1), \ldots\ldots N_m(t_1), N_1(t_2)\ldots.]$ --->DEMUX--->

$[N_1(t_1), N_1(t_2), \ldots\ldots N_1(t_T), N_2(t_1)\ldots.]$

trace sorted (demultiplexed data)

N_1, N_m first and last channel (trace), respectively

$t_1 \ldots t_T$ first and last time sample, resp.

2. Sorting

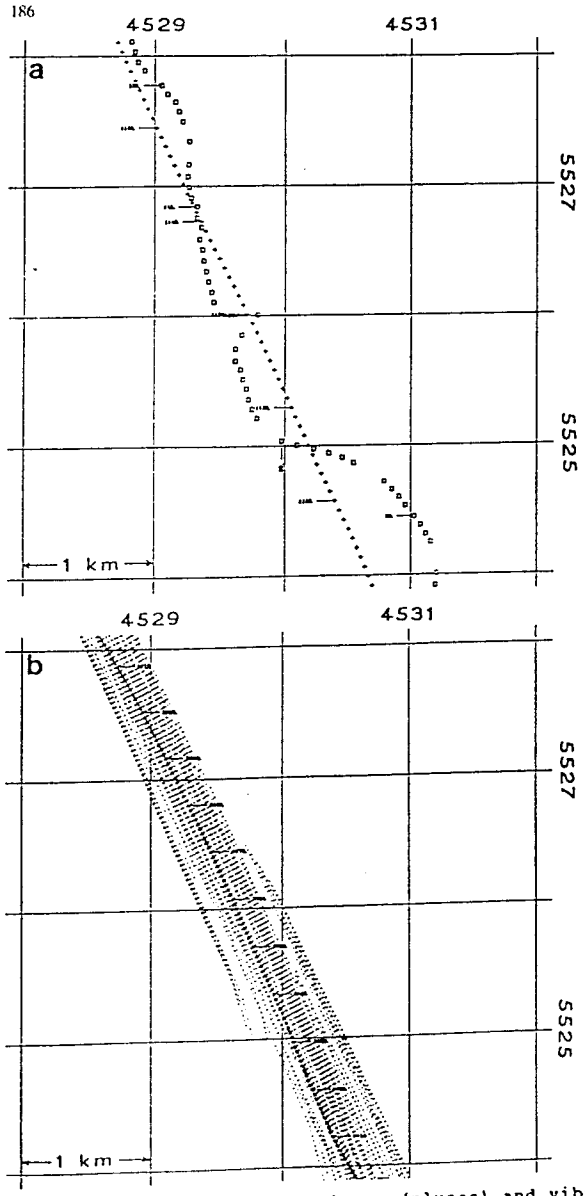

Fig. 4.a Positions of geophones (pluses) and vibrators (squares), segment of Oberpfalz line KTB 8506 (km 8.2-12.7)

Fig. 4.b Scattergram for subsurface points of surface layout in Fig. 4a; line of crosses is CMP processing line

The data initially recorded as CSP- data are sorted in such a way that CMP gather result. Because under realistic conditions a remarkable scattering of the source- and geophone- points exits, an approximation of the true CMP-line must be calculated. This process is called crooked line approximation.

3.Analytical scaling

Seismic amplitudes are attenuated mainly by two processes:

- spherical divergence, e.g. the amplitudes decrease proportionaly to 1/R (R = length of travel path). Is the velocity +/- constant, it holds true also for 1/T (T = traveltime).
- absorption (irreversible processes) e.g. the amplitudes decrease according exp(- αT). $\alpha$is the coefficient of absorption.

To compensate both processes, the seismogram is multiplied by a term:

$$R = k*T*\exp(\alpha T).$$

The quantities k and α have to be determined seperately.

4. static corrections

The sampling intervals of near vertical seismic investigations are commonly 2 or 4 ms. Thus one sample corresponds a distance between about 6 to 24 m. All deviations of this order of the source points (elevation, depth of drilling, velocity of weathering layer) as well as of the receiving points (elevation) must be corrected. The result of this correction is a unified level of all source and receiver points. In cases of a stongly varying topography the static corrections are calculated for different levels (floating datum).

5 dynamical corrections

The analytical expression for the travel time curve of a CMP gather is:

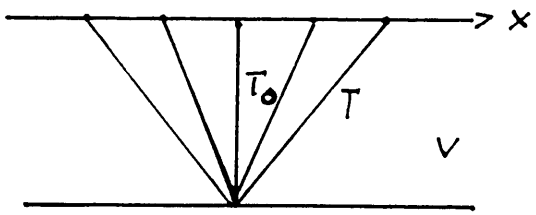

$$T = \mathrm{SQRT}(T^2_0 + (x/v)^2) \quad (1)$$

Each seismogramm is corrected in such a way that all arrivals of one CMP gather have an identical onset time after applying this correction.

$$\Delta t(x) = T - T_0 = \mathrm{SQRT}(T^2_0 + (x/v)^2) - T_0$$

This correction is called NMO (normal move out)- correction. To apply the NMO- correction the velocity is needed.
If there is a sufficient large spread length, one gets the velocity from the asymptots of the hyperbola:

$$t = x/v.$$

Another method is the $x^2 - t^2$ method. From (1) follows:

$$T^2 = T^2_0 + (x/v)^2.$$

From this the velocity corresponds to the slope of this curve.
A further method is the determination of so called velocity spectra. For a chosen set of velocities the sum along the corresponding hyperbolas is calculated and the maximum of the sum corresponds to the most appropriate velocity.
Up to now all considerations hold true for a single layer case. In this case the used velocity equals the layer velocity.
If there are more than one layer the travel time curve consists of different parts of hyperbola branches. Generally holds true:

$$x = \sum_{k=1}^{n} \frac{p V_k}{(1-p^2 V_k^2)^{1/2}} \Delta z_k \qquad (2)$$

$$t = \sum_{k=1}^{n} \frac{}{V_k (1-p^2 V_k^2)^{1/2}} \Delta z_k \qquad (3)$$

v_k = intervall or layer velocity.
We introduce now the so called rms- velocity:

$$V_{rms} = \frac{1}{\tau} \left\{ \sum_{k=1}^{n} V_k^2 \Delta \tau_k \right\}^{1/2}$$

$\Delta\tau_k$ and τ, respectively, are the vertical travel times in the k^{th} layer (or the complete vertical travel time).
In case of more layers all layers above the reflecting interface of interest are replaced by **one** layer, which is represented by the **rms- or stacking or effective- velocity.** This means multi- layer cases are reduced to an one layer case. It can be shown that the rms- velocity leads to less deviations with respect to the the exact travel time than the average velocity.

6. Muting

Muting means the cutoff of undesired parts of the seismograms (e.g.first arrivals, surface waves etc.).

7. Automatic gain control (AGC)

AGC is a nonlinear scaling of the amplitudes to achieve more or less comparable amplitudes before stacking. AGC is the division of single seismogram values by a sum which corresponds to a chosen time window. Using a too long time window leads to a constant scaling (like a multiplcation by a constant factor). Applying very short time windows leads to strong distortions of the seismogram.

8.Stacking

Stacking means the summations of all reflector amplitudes which occur due to the NMO- correction to the same time. Is the degree of coverage to N, so equals the (theoretical) improvement of the signal/noise ratio SQRT(N). Practical used coverages range from 80 to 200. Stacking reduces the amount of data significantly. Due to the summation the amplitudes of a stacked seismogram cannot be used for true amplitude investigations. A stacked seismogram is apriori a vertical seismogram.

9. Migration

Are there in stacked sections inclined reflection elements they cannot have the true position, because stacked seismograms are vertical. The process which leads to the right position is called migration. If we look at a given seismogram on the position x_0 the energy at a abitrary time can result from subsurface points which are distributed on a part of circle with the radius v*t/2.

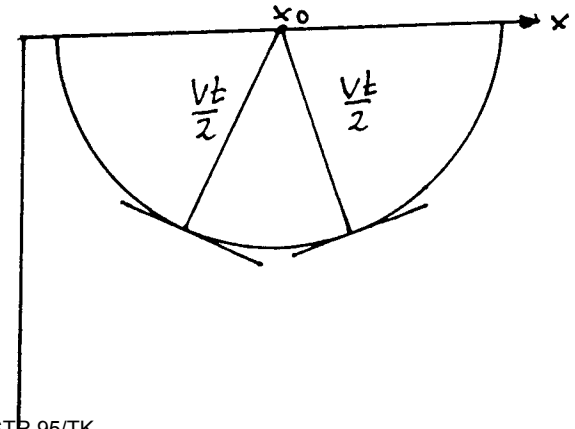

Thus we have: $(x-x_0)^2+z^2 = (V*t/2)^2$ (5)
Here x_0 and t are fixed.
Now we assume the inclined element lies at a fixed position x and z (we look for a special point in the underground). x_0 is variable (we take various seismograms into account). (5) changes now to:

$$(v*t/2)^2-(x-x_0)^2 = z^2. \quad (6)$$

(6) corresponds to a hyperbola. If we sum up the energy (amplitudes) along the hyperbola for different x_0 (seismograms) and times we obtain the output which belongs to z and x (the point in the subsurface). This procedure, of course, depends still on the velocity.

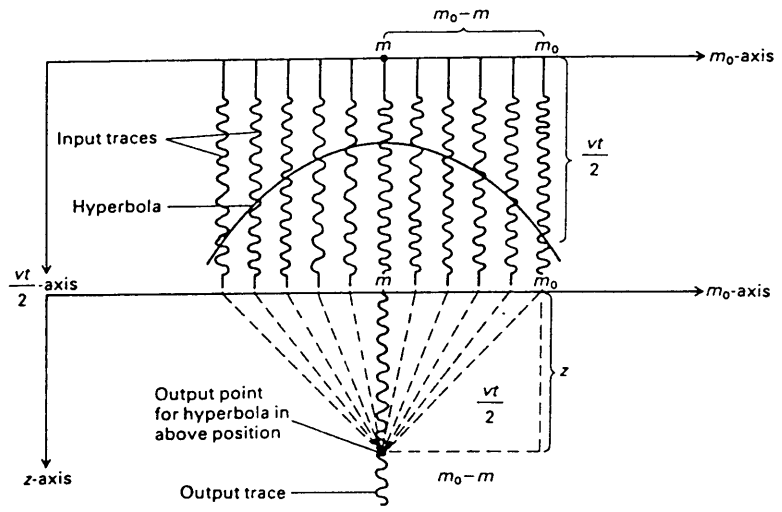

Figure 1.14 Output trace on bottom diagram is produced from input traces on top diagram. Vertical scale on top diagram has been converted to units of one-way distance *vt*/2. Each output amplitude is obtained by summing input amplitudes along the hyperbola.

References: Interpretation Theory in Applied Geophysics, by F. S. Grant and G. F. West. Mc Graw-Hill Book Company N. Y. 1965

The German Deep Drilling Program (KTB) edited by R. Emmermann and J. Wohlenberg. Springer Berlin and Heidelberg, 1989

Filter methods for improving phase detection with a special view on crustal investigations

by A. Schulze

1 General remarks

Filtering of seismic data has two goals:

- the enhancement of the signal/noise ratio to improve the seismic events. What is a desired seismic event depends stongly on the problem which has to be solved. While in reflection seismics the first arrivals are noise and are therefore suppressed, they are the essential parts of the wavefield in refraction seismics.
- to get a better insight in the medium under investigation using special physical properties of the wavefield. Also here depends the definition of signal and noise on the problem to be solved.

2. Frequency filtering

Each seismogram is a superposition of different processes. Some of them can be regarded as useful while other are noise. If the frequencies of the signal and the noise are different (e.g. oscillating trees and waves due to an explosion) both processes can be seperated. The mathematical procedure achieving this is the FOURIER analysis. Nearly each time series can be decomposed with regard its frequencies by means of this transformation:

$$F(w) = \int_{-\infty}^{\infty} f(t)\exp(-iwt)\,dt \qquad (1)$$

where w = circular frequency and i = imaginary unit.
F(w) is the FOURIER transform of f(t). This is a complex function which can be written:

$$F(w) = |F(w)|\exp(i\varphi) \qquad (2)$$

$|F(w)|$ is the amplitude spectrum. It indicates how strong each frequency is involved in analyzed process.
φ is the phase spectrum which shows the phase delays of each frequency.
There is a inverse transformation which reconstructs the original time series from its spectra:

$$f(t) = 1/2\pi \int_{-\infty}^{\infty} F(w)\exp(iwt) \qquad (3)$$

The basic scheme of frequency filtering is as follows:

1. Apply the FOURIER analysis (1)
2. Multiply the spectrum by a function which supresses the undesired frequencies
3. Apply the FOURIER synthesis (3).

There are very efficient subroutines which carry out the FOURIER-transformation.
There is a essential relationship between time series and their FOURIER transforms:

$$F(w)G(w) \;<\!-\!-\!>\; f(t)*g(t). \qquad (4)$$

The "*" stands for the convolution: $f(t)*g(t) = \sum_{i=0}^{n-1} f(i)g(t-i)$.
The meaning of (4) is the following: To apply a filtering in the frequency domain by multiplying the spectrum of the input time

series by the filter function it can be done by convolution of the time series with the FOURIER synthesis of the filter function.

2.Optimum filtering

Problem of optimum filtering: We have a input signal x_t and we look for a filter function f_t which influences the input in such a way that the result is "an optimum approximation" to a desired signal d_t.
"Optimum approximation" means in the sense of least squares.

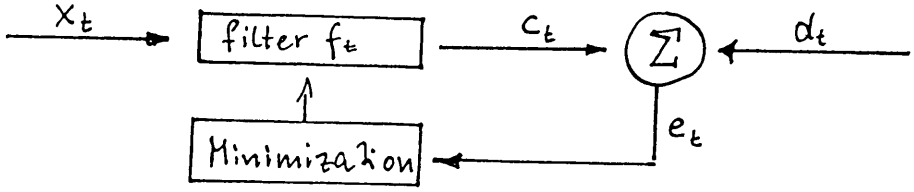

To find the optimum filter:

Let be $$c_t = \sum_{s=0}^{n-1} f_s x_{t-s} \qquad (t=0,1,2..) \qquad (5)$$

$\{f_s\}$ is to evaluate that $e_t = d_t - c_t$ is minimal. This leads to:

$$J_n = E[e_t^2] = E[(d_t - c_t)^2] = \min$$
$$= E\left[\left(d_t - \sum_{s=0}^{n-1} f_s x_{t-s}\right)^2\right] = \min$$

$$\hookrightarrow \quad \frac{\partial J_n}{\partial f_k} = E\left[2e_t \cdot \frac{\partial e_t}{\partial f_k}\right] = 0 \qquad k = 0, 1, \ldots n-1$$

This leads to the following system of linear equations:

$$R_{xx} f = r_{xd} \qquad (6)$$

or

$$\begin{pmatrix} R_{xx}(0) & R_{xx}(1) & \ldots & R_{xx}(n-1) \\ R_{xx}(1) & R_{xx}(0) & \ldots & R_{xx}(n-2) \\ \cdot & \cdot & \cdots & \cdot \\ \cdot & \cdot & \cdots & \cdot \\ \cdot & \cdot & \cdots & \cdot \\ R_{xx}(n-1) & R_{xx}(n-2) & \ldots & R_{xx}(0) \end{pmatrix} \begin{pmatrix} f(0) \\ f(1) \\ \cdot \\ \cdot \\ \cdot \\ f(n-1) \end{pmatrix} = \begin{pmatrix} r_{xd}(0) \\ r_{xd}(1) \\ \cdot \\ \cdot \\ \cdot \\ r_{xd}(n-1) \end{pmatrix}$$

R is called TOEPLITZ matrix
(6) is called WIENER- HOPF equation where $r_{xx}(k) = \sum_{i=0}^{n-1} x_i x_{i+k}$ = auto-correlation and $r_{xd}(k) = \sum_{i=0} x_i d_{i+k}$ = cross- correlation.
(6) is a basic equation for many problems of optimum filtering.
Now we look more in detail for a special application the *prediction filtering:*
let be $$\hat{x}_{t+1} = \sum_{p=0}^{n-1} f_p x_{t-p} \qquad (7)$$
problem: $\hat{x}_{t+1}$ should as good as possible approximate x_{t+1}.
With very similiar considerations as previous shown we obtain the following equation:

$$Rf = g \qquad (8)$$

Here R is again the TOEPLITZ matrix, $f^T = [1, -f_0, -f_1, \ldots, -f_{n-1}]$ and $g^T = [J_n(min), 0, \ldots, 0]$.
The application for seismic event detection is as follows: Step by step one value is predicted (using the equation(8)) and compared with the corresponding observed value. Is there a periodic noise in the time series under investigation the predicted value will be a good approximation to the observed one. If a seismic event occurs it cannot be predicted from the previous values of the time series. Thus the difference between the predicted value and observed will be rather large. This is used as an indication of a seismic event.

3. Polarization filtering

To distinguish between P- and S- waves is of special importance. Often it is essential to know the velocities of both types of waves, to obtain more information concerning the composition of the medium. Due to the less velocity of S- waves it is general difficult to detect them. Thus the possibility to determine S- waves using their polarization properties seems to be an adequate approach.
To look for the polarization properties of seismic waves we need 3- component seismograms to record the complete vector of displacement. To evaluate the polarization characteristics we take into account N points of the digitized 3- coponent seismogram where N is so chosen that more or less a closed trajectory of the vector of displacement is represented. Is Δt the sample interval and T the dominating period, we have for N:

$$N = T/\Delta t.$$

Now this (3- dimensional) trajectory is appoximated by a straight line, because we expect a linear polarization for body waves. Thus we minimize the differences between the trajectory and the desired straight line:

$$S = \sum_{i=1}^{N} \frac{(\vec{x_i} \times \vec{a})}{a^2} = min \qquad (9)$$

where $a = (\cos\alpha\sin\vartheta; \sin\alpha\sin\vartheta; \cos\vartheta)$ and $x_i = (x_i - x; y_i - y; z_i - z)$.
Now we look for the minimum of $S(\alpha, \vartheta)$:

$$\frac{\partial S}{\partial \alpha} = \frac{\partial S}{\partial \vartheta} = 0$$

This leads to the expression

$$0 = \begin{pmatrix} a_1 \\ a_2 \\ a_3 \end{pmatrix} \begin{pmatrix} -(T_{22}+T_{33}) - \gamma & T_{12} & T_{13} \\ T_{12} & -(T_{11}+T_{33}) - \gamma & T_{23} \\ T_{13} & T_{23} & -(T_{11}+T_{22}) - \gamma \end{pmatrix} \qquad (10)$$

This is an equation of 3rd order where the values of correspond to the length of the three axes in space (which are a measure for the energy polarized in the threee directions) and the eigenvectors a give the direction of polarization.

To check the degree of linear polarization we can construct functions of the type:

$$F(i) = \max(\lambda_1, \lambda_2, \lambda_3)/(\lambda_1+\lambda_2+\lambda_3)$$

Similiar we can determine from which direction the wave actually comes to the receiver. Calculating the dot product between the theoretical directions and the observed ones we can determine which part of the seismogram is propagated directly from the source to the receiver and which part is scatterd in the vicinity of the seismometer.

References: Geophysical Signal Processing by E. A. Robinson and T. S. Durrani, Prentice/Hall Int. London 1986

Time Series Analysis and Applications by E. A. Robinson, Reidel Publishing Co. Boston and Dordrecht 1981

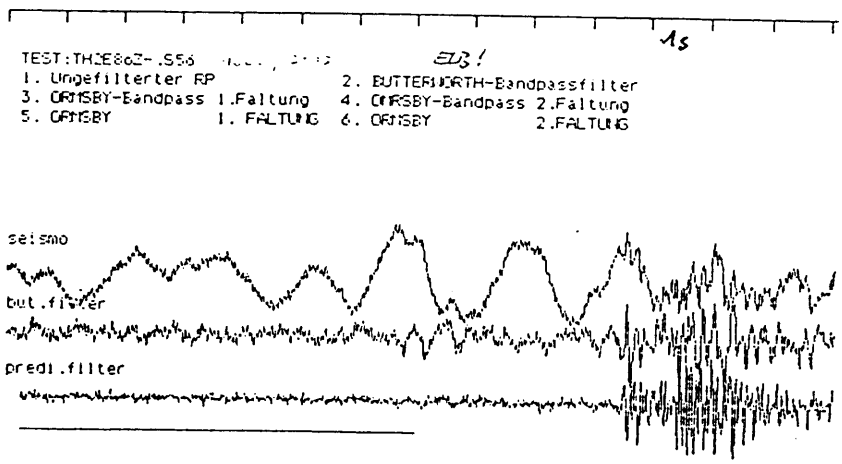

fig.1 upper seismogram: original data with a predominant low frequency noise. middle: freyuency filtered seismic trace (bandpass 2-15 Hz) below: same data as above but prediction filtered (best noise suppression)

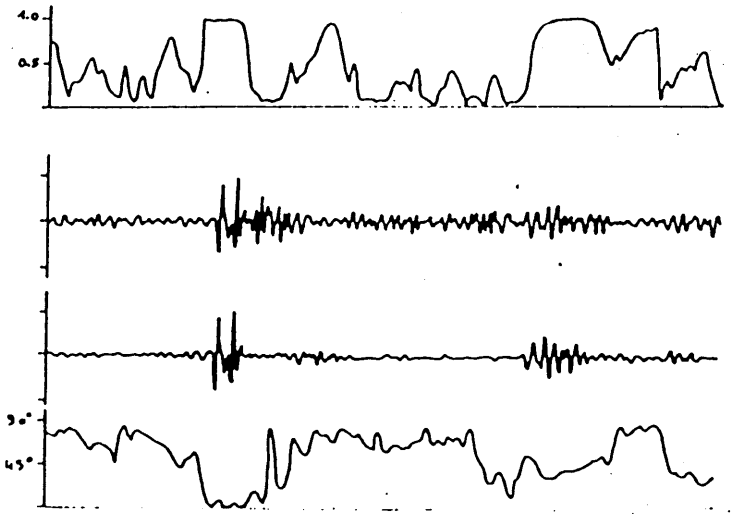

fig.2 application of a polarisation filter. Above: calculated rectlinearity function of the seismogram shown below (here only vertical component); net trace: filtered trace by multiplcation of the original data with the rectlinearity function; below calculated angle of incidence. Compare the coincidence of high values of the rectlinearity and low values of angle of incidence (corresp. wave comes nearly verical to the receiver e.g. P-wave)

4 The Tau - P - Transformation

The Tau - P - Transformation (slant stack) transforms the wavefield (a common shot section) into a representation depending on the velocities and the different values of the layer thickness. This means using this transformation we obtain immediately geological parameters of the subsurface. The Tau - P - Transformation belongs to the class of integral transformations which are closely connected to the two- dimensional FOURIER transformations. It is defined as:

$$S(p,\tau) = \int s(T,X)\,dx$$

$T = \tau + p\,X$, T= travel time, τ= intercept time
p = ray parameter

$$S(p,\tau) = \int s(\tau + pX, X)\,dx$$

This equation states that for all couples τ,p the amplitudes of the seismograms summed up and allocated to the corresponding point in the τ- p field.
The expression $T = \tau + p\,X$ can be interpreted as travel time of a head wave. Thus the meaning of this procedure is a stacking of the amplitudes for different values of p (or equivalent for different velocities) coreesponding a decomposition of the wavefield with respect to its constituting velocities.
For τ is related to the depth the different values of τ correspond to different depths.

Main properties of the Tau - P - Transformation:

1. a straight line in the (X,T) domain is represented as a point in the (τ,p) domain
2. a hyperbola in the (X,T) domain is represented as a ellipse in the (τ,p) domain

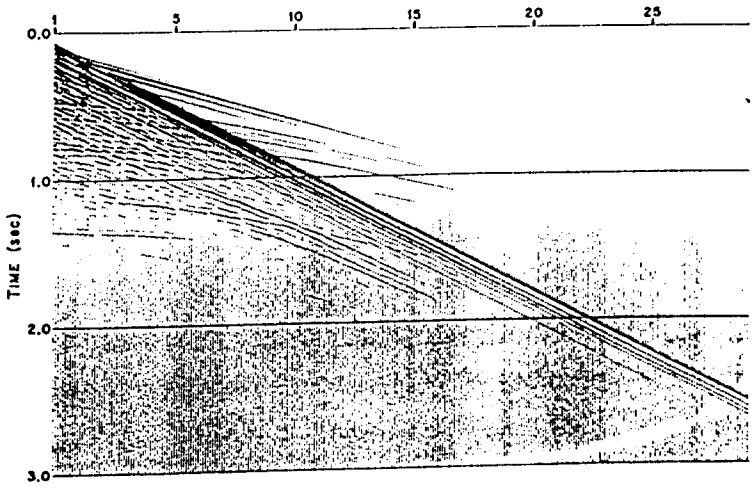

fig. 3: common shot point data with a narrow spacing of 100 ft.

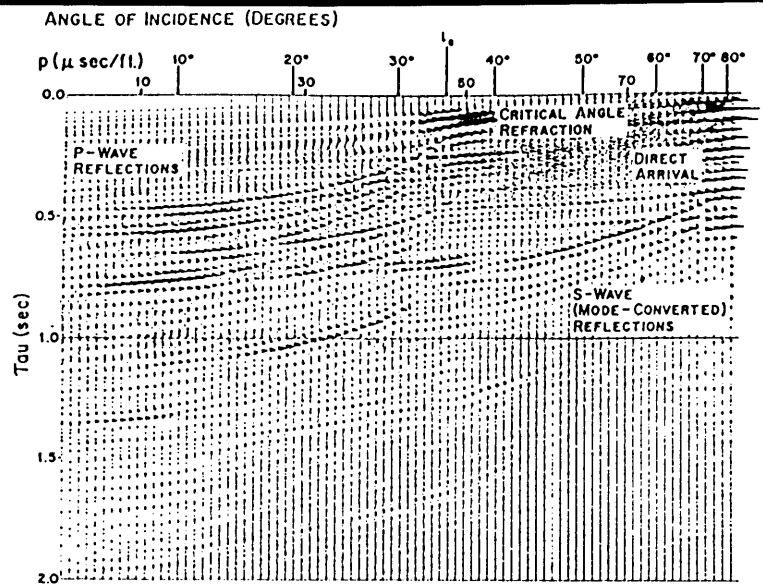

fig. 4: Tau - P - Transformation of the data shown in fig. 3

The Use of Surface Waves for Structural Investigations

by

P. MALISCHEWSKY and H. NEUNHÖFER

Everything should be made as simple as possible, but not simpler.
(Albert Einstein)

1. Introduction

The surface waves represent the most significant contribution of the recorded ground displacement of natural and artificial earthquakes. On the other hand, in most regions of the Earth the local seismicity and the station density is not high enough to provide enough depth resolution into the lithosphere or upper part of the mantle with methods of body-wave tomography. So it is logical to try to use surface waves for structural investigations. Such an action should, however, consider the specific peculiarities of surface wave motion. By doing so, anomalies in the propagation of surface waves from distant earthquakes can reveal at least the gross features of regional lithospheric and upper mantle structure.

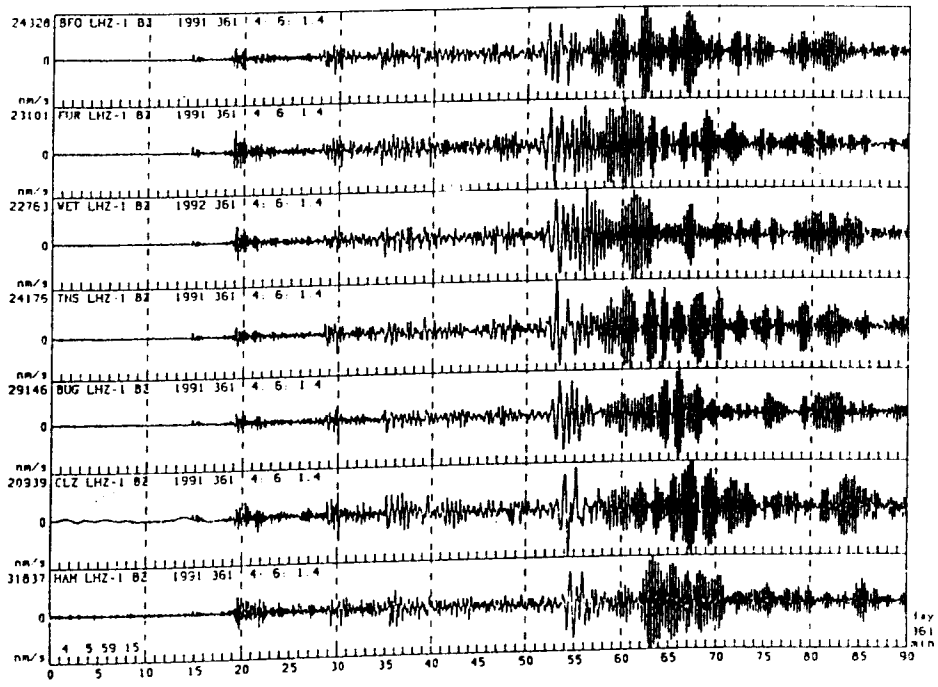

Fig. 1: Seismograms (sampling rate: 1 Hz) of a seismic event in the South Sandwich Islands region recorded at broadband GRN stations (German Regional Network)

By examining a seismogram we easily establish (see Fig. 1) a partition in body waves and surface waves.

The geographic location of the source and the great circle wave paths belonging to it are represented in Fig. 2.

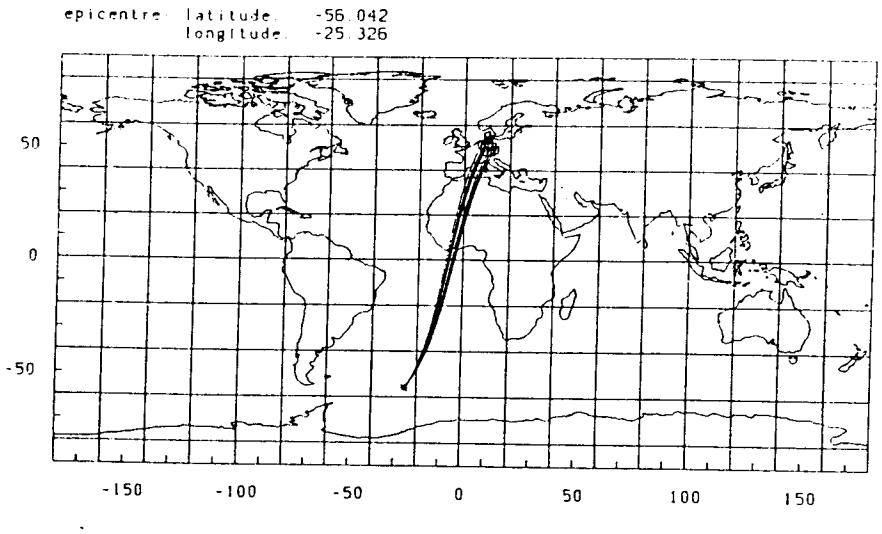

Fig. 2: Geography corresponding to Fig. 1

The body waves, which occur at shorter periods, propagate across the bulk of the Earth, following, as a first approximation, the laws of geometrical ray theory. The body wave seismogram is characterized by various arrivals being due to reflections and refraction of the waves at boundaries in the Earth. The surface wave seismogram has a structure too (see Fig. 1). However, at this wave groups with longer periods without sharp arrivals dominate. The most prominent feature of the surface wave seismogram is **dispersion**, that means the dependence of the wave velocity on the frequency or period. By analyzing the arrivals of body waves it is possible to obtain information such as concerning the horizontal stratification in the Earth. The interpretation of the dispersion of surface waves also gives such information. On the other hand, by clarifying the structure of the surface wave seismogram, i. e., how it splits into different wave groups, important information concerning lateral inhomogeneities can be obtained. Such an information is interesting from geological and geophysical point of view as well. By using surface waves in this way, the range of problems, solvable with seismological and seismic methods, is greatly extended.

It is expected that surface waves, with their complicated structure, are sensitive to lateral inhomogeneities. They may therefore be useful at the search for and localization of

tectonic faults and other geological formations which distinguish from the surrounding medium by their seismic properties. The dispersive nature of surface waves requires a special kind of data processing which is quite different from that in body wave analysis. A basic requirement for the application of surface waves for structural investigations is a network of seismic broadband stations. These should record the vertical and both horizontal components as well.

2. Theoretical background

In theory the phrase **surface wave** denotes a certain term in the expansion of the total wave motion. The starting-point of any kind of seismic analysis is the equation of motion of the elastic continuum

$$L_{ij}\, u_j = F_i \; ; \qquad i, j = 1, 2, 3,$$

where u_j are the components of the displacement vector, L_{ij} is a certain differential operator and F_i is a source term. The theoretical response of a layered half-space to a seismic source traditionally has been studied from two different approaches:

- Using geometric ray theory one can compute the amplitude and travel times of individual signals which propagate as direct, reflected or refracted body waves. Ray theory predicts a series of impulsive responses for an impulsive source excitation and is most useful for interpreting the early arriving phases of the seismogram.

- A complementary approach is the modal analysis, where the crucial point is the formulation as an eigenvalue problem by neglecting the source term. In the case of a layered half-space, the response can be physically understood as an interference phenomenon due to the superposition of multiply reflected body waves totally trapped in the wave-guide. This leads to an oscillatory response for an impulsive excitation. Mode theory is mainly concerned with interpretation of the later arriving portion of the earthquake record; e. g., surface waves.

We assume the displacement vector u_r in the plane wave form as

$$u_r = U_r(x_3)\, e^{i(kx_1 - \omega t)},$$

where $U_r(x_3)$ is an **amplitude-depth function** whose occurrence is typical for surface waves. The corresponding eigenvalue equation for an anisotropic but laterally homogeneous medium becomes

$$\mathcal{L}_{pr} U_r = \lambda_{pr} U_r ,$$

where the eigenvalue matrix λ_{pr} is a quadratic function of the eigenvalue k, the wave number. The surface is assumed to be stress-free and, as a condition of surface waves, the motion has to vanish for $x_3 \longrightarrow \infty$. For an isotropic medium, the eigenvalue equation decouples into Rayleigh-type motion with a radial component U_1 and a vertical component U_3 and Love-type motion with a transverse component U_2 only. For a given radian frequency, a finite number of Rayleigh and Love modes, characterized by their wave numbers, exists. Following MALISCHEWSKY (1987) they can be combined to form a homogeneous eigenfunction system in such a way:

$$\text{wave number } \overset{\alpha}{k} \text{ with } \quad \alpha = 1 , \ldots , M \quad \textbf{Rayleigh modes,}$$

$$\alpha = M+1 , \ldots , N \quad \textbf{Love modes.}$$

Of these two principal types of surface waves, the most commonly studied are the Rayleigh waves which appear on the vertical component (as well as on the horizontal radial component - along the direction of propagation). The Love waves are seen only on the horizontal transverse component (perpendicular to the direction of propagation). To reconstruct Love waves in any given observatory where horizontal components are conventionally oriented towards North and East, one thus needs observations on **both** horizontal components.

The dispersion of surface waves appears as the functional dependence of the wave number on the frequency or period:

$$k = k(\omega) ; \qquad \alpha = 1, \ldots N .$$

From this function, the so called **dispersion curves** of the **phase velocity** $c(\omega)$ and the **group velocity** $U(\omega)$ can be derived as

$$c(\omega) = \omega / k(\omega)$$

and

$$1/U(\omega) = 1/c + \omega \frac{d}{d\omega} (1/c) , \textit{ respectively.}$$

That is, group velocity can be calculated from phase velocity but not conversely. Strictly speaking, a group velocity curve does not provide additional information on the medium compared with that given by phase velocity. Both are, however,

extensively used in geophysical interpretation analyses. Among other things, this is due to the fact that, not infrequently, group velocity alone can be measured. The following Fig. 3 shows typical dispersion curves for the phase and group velocity, respectively.

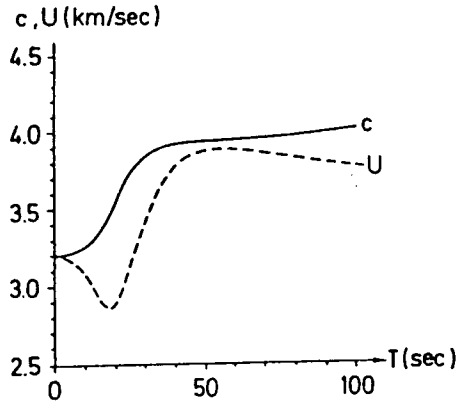

Fig. 3: Phase and group velocity of the Rayleigh fundamental mode for a four-layer model, T is period

3. Processing of seismic records concerning surface waves

The treatment of seismic surface waves has two different aspects:

- Extraction of individual dispersion curves of surface waves from seismograms,
- Inversion of the observed curves into models of the Earth's crust and upper mantle and interpretation in geologic terms.

The basic ideas of both steps are totally different. Let us begin with the first one. It should be mentioned that two well-pronounced types of surface wave polarization typical for laterally homogeneous isotropic media (Love and Rayleigh waves) occur in seismograms. In Fig. 4, it is demonstrated how a Love wave can be extracted from the usually recorded horizontal components N and E by rotating them into the components parallel to the direction of propagation (R) and transverse (T) to it. We observe a pure transverse motion, indicating the Love wave, at about 45 min.

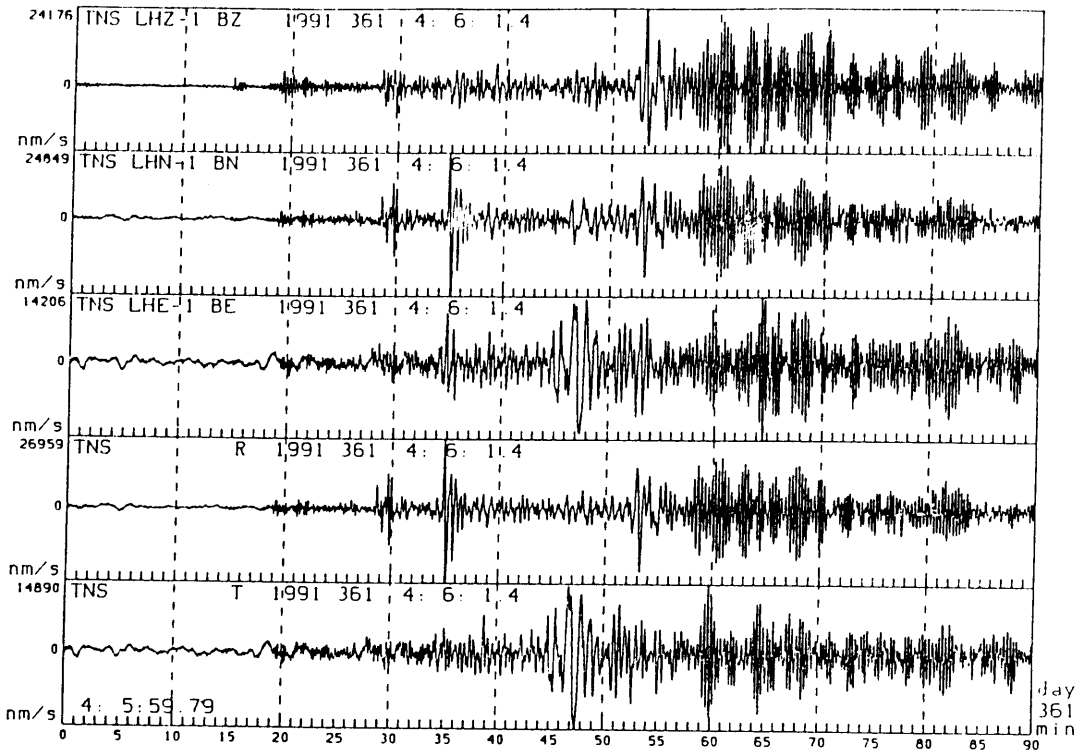

Fig. 4: Z-, N-, E-, R-, and T-components for the earthquake in Fig. 1 recorded at the Taunus station

Nowadays, several methods exist to extract dispersion curves from real seismograms. The older ones work either in the time domain like the classical **peak and trough method** or in the frequency domain like the **phase difference method.**

On the other hand, we have to distinguish between the **group** and the **phase velocity method** depending on the kind of velocity to be investigated. The group velocity method can be recommended if the seismic source is located within the area under investigation. The record of only *one station* is required, and the information involved is valid for the whole wave path between source and receiver. Otherwise, with the phase velocity method, phase velocity dispersion is determined between *two stations* or within a *station triangle* [see e. g. PLEŠINGER et al. (1991)]. By this method information obtained is valid for the great circle between the two stations or for the station triangle. The phase velocity method is currently the most used one. On the other hand, the determination of the group velocity dispersion from seismograms is simpler.

The theoretical starting-point of further analysis is always the representation of the observable wave $f(x_1,t)$ in the form

$$f(x_1, t) = \frac{1}{2\pi} \int | f(x_1, \omega) | \exp[-i\omega(t - \frac{x_1}{c(\omega)}) + i\phi(\omega)] d\omega ,$$

where t is time, x_1 is here the distance between source and receiver, $\Phi(\omega)$ is the phase which characterizes the source and $|f(x_1,\omega)|$ is the amplitude spectrum. A basic requirement for the application of this formula is that the wave train consists of one mode only. The classical methods fail when the signal consists not only of the direct wave but also of secondary waves. In this general case, it is necessary to apply the modern methods which are characterized by a **common analysis in both the time and frequency domain.** The basic concept is to build up the time signal by "elementary signals" in frequency and time. The amplitudes of the complex signal powers of these elementary signals are represented in the so-called **Gabor matrix** as a function of frequency and time. The dispersion curve of the group velocity appears as a mountain ridge in the frequency-time plane or period-time plane, respectively, see Fig. 5. The crests belonging to the fundamental mode of the Rayleigh wave are connected by a broken line.

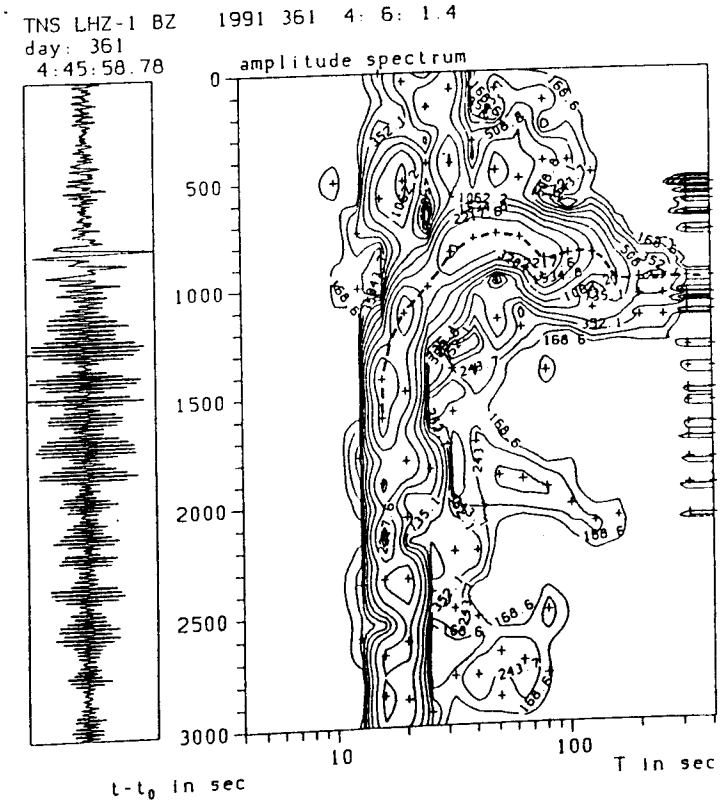

Fig. 5: Representation of the Gabor matrix for the Z-component in the period-time plane for the earthquake under consideration recorded at the Taunus station

Essentially, there are two different methods to carry out this procedure practically:

- Multiple filter technique,
- Mowing-window analysis.

Both methods require the processing of digital data. A version of the first method was applied at the Seismological Observatory at Moxa [see NEUNHÖFER (1985)].

4. Inversion of dispersion curves into Earth models-generalization of dispersion results

Between the dispersion of surface waves and the structure of crust and mantle, a rather complicated connection exists. If the investigated medium consists of m layers, the last one being the half-space, then the dispersion relations are

$$F_L\ (h_i, \beta_i, \rho_i, c, \omega) \ = \ 0 \quad \textit{for Love waves,}$$

$$F_R\ (h_i, \alpha_i, \beta_i, \rho_i, c, \omega) \ = \ 0 \quad \textit{for Rayleigh waves,} \quad i = 1, \ \ldots \ , m \ ,$$

where h_i, α_i, β_i, and ϱ_i denote the thickness, velocity of longitudinal and shear waves and density of the i-th layer, and c is phase velocity. The dominating elastic parameter in these relations is β_i. The problem of inversion can be handled in such a way that the parameters of the model layers are varied as long as the theoretical dispersion curve fits the observation. If the fitting is good enough the model for which the theoretical curve was calculated is defined to be the crust and mantle model of the investigated region. This procedure is not unique, but the ambiguity can be essentially diminished by restriction to geophysically suggestive models and by taking into account more than one mode. The variation of the parameters can be realized by using the **Monte Carlo method** which is a time consuming procedure. This is the reason why the parametrization should be reduced to a suitable degree.

A useful tool in interpreting changes of the dispersion curve is the so-called **partial derivatives.** Fig. 6 takes as a basis the partial derivative of the phase velocity to the shear wave velocity in a certain depth.

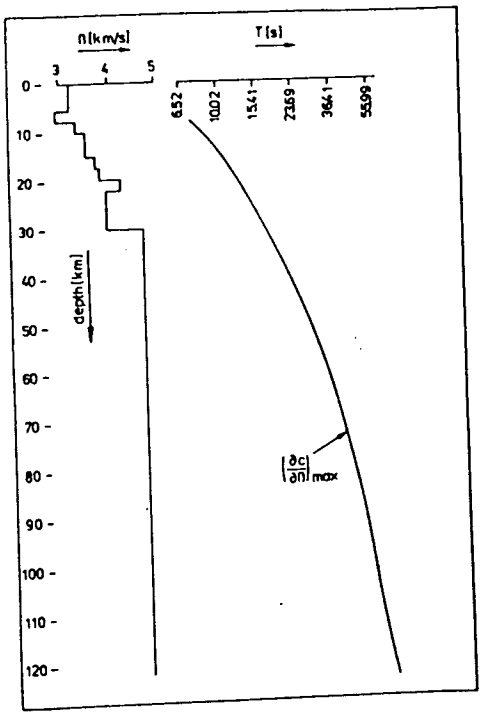

Fig. 6: Depth dependence of the partial derivative of c to ß as a function of period T (right hand side) for a given ß-depth model (left hand side)

The represented curve can be utilized in such a way: it connects the maximum change of the dispersion curve, or any other effect on Rayleigh waves at the period T, with the depth of the source of this change.

A dispersion curve of seismic surface waves comprises the integral information about an entire wave path. The current method is to assign this information to the path from focus to station if group velocity was determined or to the path between two stations in the phase velocity case. If, in a given region a sufficiently large number of different dispersion curves is known, then the local resolving power of surface waves can be better exhausted by applying two methods:

- Transformation of numerous observed dispersion curves into a reduced number where each of them is characteristic for a geologically meaningful subregion.
- Calculation of **isotaches** for different periods by using the observed dispersion curves.

The so-called **phase velocity splitting** proposed e. g. by NEUNHÖFER and GÜTH (1975) is an example for the first method. Two phase velocity curves which describe geologically homogeneous regions were calculated from many mixed-path curves (see Fig. 7).

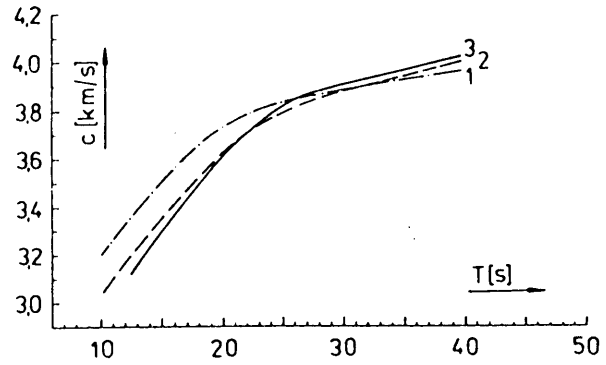

Fig. 7: Mean dispersion curves for southern (1) and northern (3) part of the former GDR and for mixed propagation paths (2)

An extensive splitting of group velocity curves was carried out by FENG (1982) for the Eurasian continent. On the other hand, NEUNHÖFER (1985) has calculated isotaches for the territory of the former GDR (see Fig. 8) by applying a method proposed by YANOVSKAYA (1982).

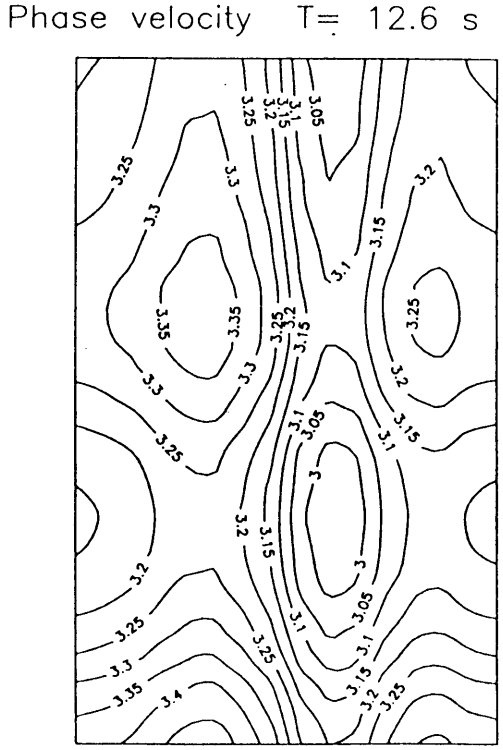

Fig. 8: Isotaches of phase velocity for the period T = 12.6 s

A different procedure was created by PANZA et al. (1980) and applied to the construction of phase velocity isotaches for the European Mediterranian region.

It should be mentioned that the range of applicability of surface waves for structural investigations reaches from very short period channel waves ($T < 0.1$ s) used for the detection of discontinuities in coal seams, up to ultralong-period waves with $T \leq 160$ s which yield us information about the global structure of the Earth's mantle.

5. Attenuation of seismic surface waves

Each seismic wave is attenuated in a real medium. We have to distinguish between the geometrical attenuation and the intrinsic attenuation. The latter is an important material parameter which refers to the inelastic properties of the medium and can be inferred from body and surface waves. However, the observations are disturbed by many effects, e. g. multipathing, scattering, focal mechanism and the basement of the seismic station. Some of these effects can be eliminated under suitable conditions. Nevertheless, the observation yields an apparent attenuation only.
The observations of attenuation are carried out on global scale, on continental and on regional scale. Global investigation requires only one station, the other two or more stations. If we apply the so-called **two-station method**, the focal and the station effect can be eliminated by using complementary azimuths.

6. Anisotropy inferred from surface waves

From body wave investigations it is well known that in the uppermost mantle anisotropic behaviour can occur. The propagation of surface waves gives an independent possibility to study anisotropy in the lithosphere or asthenosphere. So, an azimuthal dependence of the phase velocity exhibits the existence of anisotropy. The velocity differences are in most cases too small to prove anisotropy in such a manner. Another, more significant way is the search for anomalous polarization of Love and Rayleigh waves. These two families of surface waves degenerate in a slightly anisotropic medium into pseudomodes, that means the polarization is no more SH-like or elliptical in the sagittal plane. From the frequency dependence of the found anomalous polarization one can conclude on the source via Fig. 6.

7. Lateral inhomogeneities

As mentioned above, lateral inhomogeneities in the Earth's crust and upper mantle have a large influence on the propagation of seismic surface waves, where we have to distinguish between weak and strong discontinuities. In heterogeneous media, surface waves no longer propagate along great circles with the consequence that discrepancies in travel times between the great circle path and the exact ray path cannot be neglected in some cases. Also, there are many observations of **amplitude anomalies** for surface waves [e. g., LAY and KANAMORI (1984)] which are partly caused by **horizontal refraction.** Since most of the Earth is strongly stratified horizontally and the lateral variations are fairly smooth, we can develop a special kind of ray theory for surface waves. The crucial point is the different treatment of wavefields between vertical and horizontal directions. Vertically, the wavefield is expressed by normal mode theory while surface waves are considered to propagate horizontally in a similar way to ray theory [see, e. g., YOMOGIDA (1987)]. When such 'surface wave rays' meet a sharp vertical discontinuity then we have a similar situation as for body waves at a discontinuity. However, an incoming surface wave mode produces a whole set of reflected and transmitted modes including **converted waves Rayleigh to Love** and vice versa in addition to body waves. The determination of the corresponding **surface wave reflection and transmission** coefficients requires a very complicated theory [see MALISCHEWSKY (1987)]. The coefficients depend on the angle of incidence, however, contrary to body waves, they are also frequency dependent. It is this property which allows us to draw conclusions concerning the depth extension of the discontinuities.

Obviously, the reflected wave groups overlay the directly propagating modes and so it is necessary to extract them by a suitable processing which includes

- Investigation of the spectra of surface waves,
- Autocorrelation function,
- Detection of different group velocity curves by multiple bandpass filtering,
- Extraction of pure wave groups by spatial filtering.

The geophysical interpretation includes the determination of **time delay of the reflected wave group** and the **amplitude ratio $\bar{R}$ of reflected to direct wave,** especially its dependence on frequency. If the delay is known for different stations, the reflector can be constructed by using a comparatively simple procedure. The depth of the reflector can be estimated from the frequency dependence of $\bar{R}$. Reflectors are found in practice in the lithosphere and the asthenosphere as well.

Recently, we have started to investigate the famous Tornquist-Tesseyre Fault Zone in Eastern Europe by using reflected surface waves, see Fig. 9. Reflected wave portions should be searched in

the Gabor-matrix representation of Fig. 5 as later arrivals in the region just below the broken line.

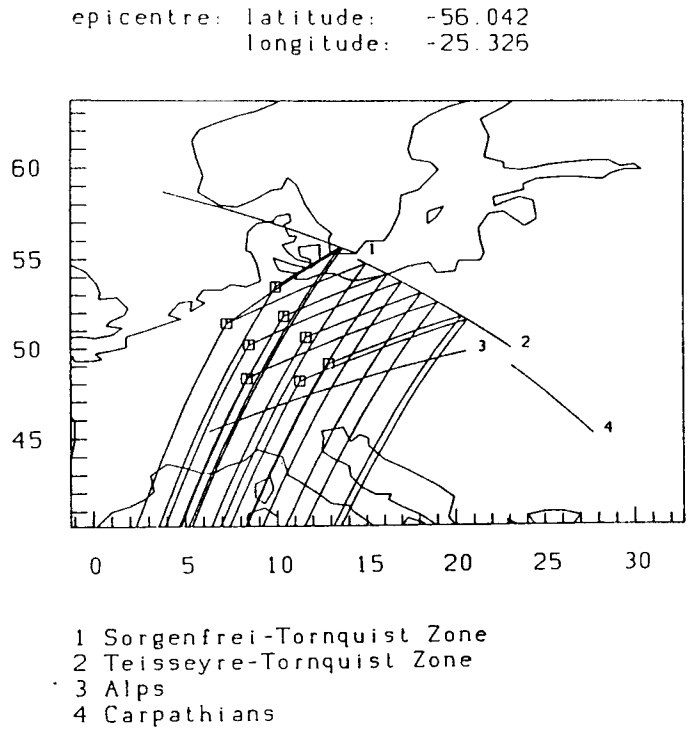

Fig. 9: Direct and reflected wave paths for the earthquake under consideration [MEIER (1992)]

For details concerning surface waves in general and in laterally inhomogeneous media in particular, the monographies of MALISCHEWSKY (1987) and KEILIS-BOROK (1989) are recommended.

8. Surface wave tomography

Finally, we should mention that tomography is a very modern field of research in seismology, in which surface waves can also be included. While delay times play an important role in solving the tomographic problem for body waves, they are replaced by **local perturbations of phase velocity** for surface waves. The crucial difference is that the tomographic problem for body waves in 3-D while the analogous problem for surface waves is 2-D but frequency dependent. It is this frequency dependence which yields the additional information concerning the third dimension.

The inversion of surface wave waveforms is possible, and with sufficient data, scattered and diffracted surface waves can be imaged [for details concerning tomography see NOLET (1987)].

9. Literature

FENG, Chi-Chin: A surface wave study of crustal and upper mantle structure of Eurasia. Ph. D. thesis, University of Southern California, Los Angeles 1982.

KEILIS-BOROK, V.I. (Ed.): Seismic surface waves in a laterally inhomogeneous Earth. Kluwer Academic Publishers, Dordrecht 1989.

LAY, T., KANAMORI, H.: Geometric effects of global lateral heterogeneity on long period surface waves propagation. J. Geophys. Res. 90 (1985), 605-621.

MALISCHEWSKY, P.: Surface waves and discontinuities. Developments in Solid Earth Geophysics, 16. Elsevier, Amsterdam 1987.

MEIER, T.: Personal communication, 1992.

NEUNHÖFER, H. Primary and secondary effects of surface wave propagation and their geophysical causes (In German). Veröff. Zentlnst. Phys. Erde No. 85, Potsdam 1985.

NEUNHÖFER, H., GÜTH, D.: Dispersion of Rayleigh waves in Middle Europe and phase velocity splitting.
The XIIIth General Assembly of the ESC (Part III), Brasov, 223-227, Bukarest 1975.

NOLET, G. (Ed.): Seismic tomography. D. Reidel Publishing Company, Dordrecht 1987.

PANZA, G.F., MÜLLER, St., CALCAGNILE, G.: The gross features of the lithosphere-asthenosphere system in Europe from seismic surface waves and body waves. Pure Appl. Geophys. 118 (1980), 1209-1213.

PLEŠINGER, A., NEUNHÖFER, H., WIELANDT, E.: Crust and upper mantle structure of the Bohemian Massif from the dispersion of seismic surface waves. Studia Geoph. et Geod. 35 (1991), 184-195.

YANOVSKAYA, T.B.: The surface wave group velocity pattern in the Northern Atlantic (In Russian). Izv. Akad. Nauk SSSR, Fiz. Zemli (1982) 2, 3-11.

YOMOGIDA, K.: Surface waves in weakly heterogeneous media, In: Mathematical Geophysics, 53-75. D. Reidel Publishing Company, Dordrecht 1988.

Practical exercises in seismic methods for structural investigations by means of body waves

part I

Correlation of wave groups in measured seismogram sections

Scientific Technical Report STR 95/TK
DOI: 10.2312/GFZ.b103-95tk7

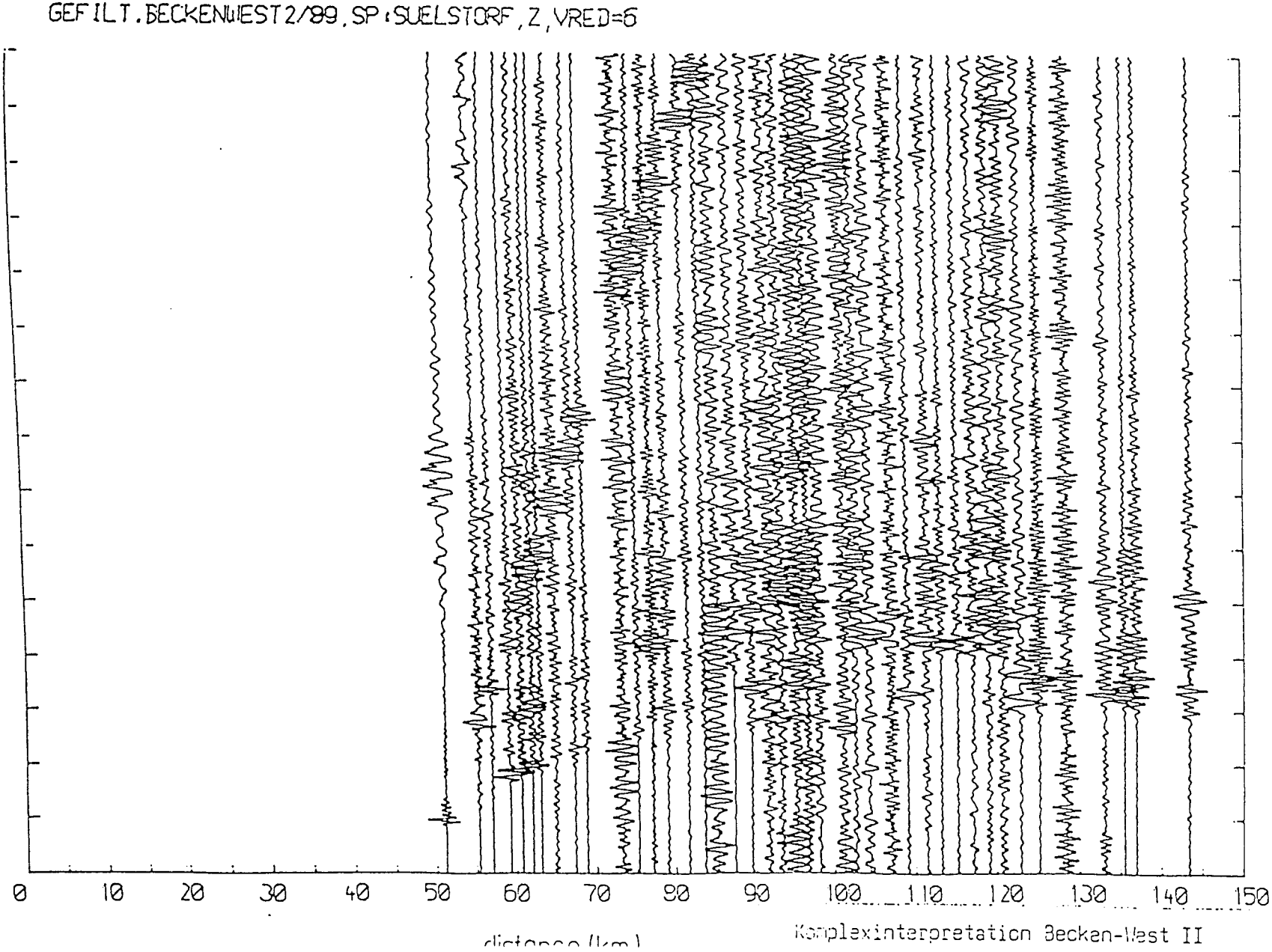

Scientific Technical Report STR 95/17
DOI: 10.2312/GFZ.b103-95tk7

THUYGRK2/86, SP FILE, Z.FILTER 5-15HZ, VRED=6
0
10
20
30
40
50
60
70
80
90
100
110
120
130
140
150
160
170
180
190
200
6
5
4
3
2
1
0
-1

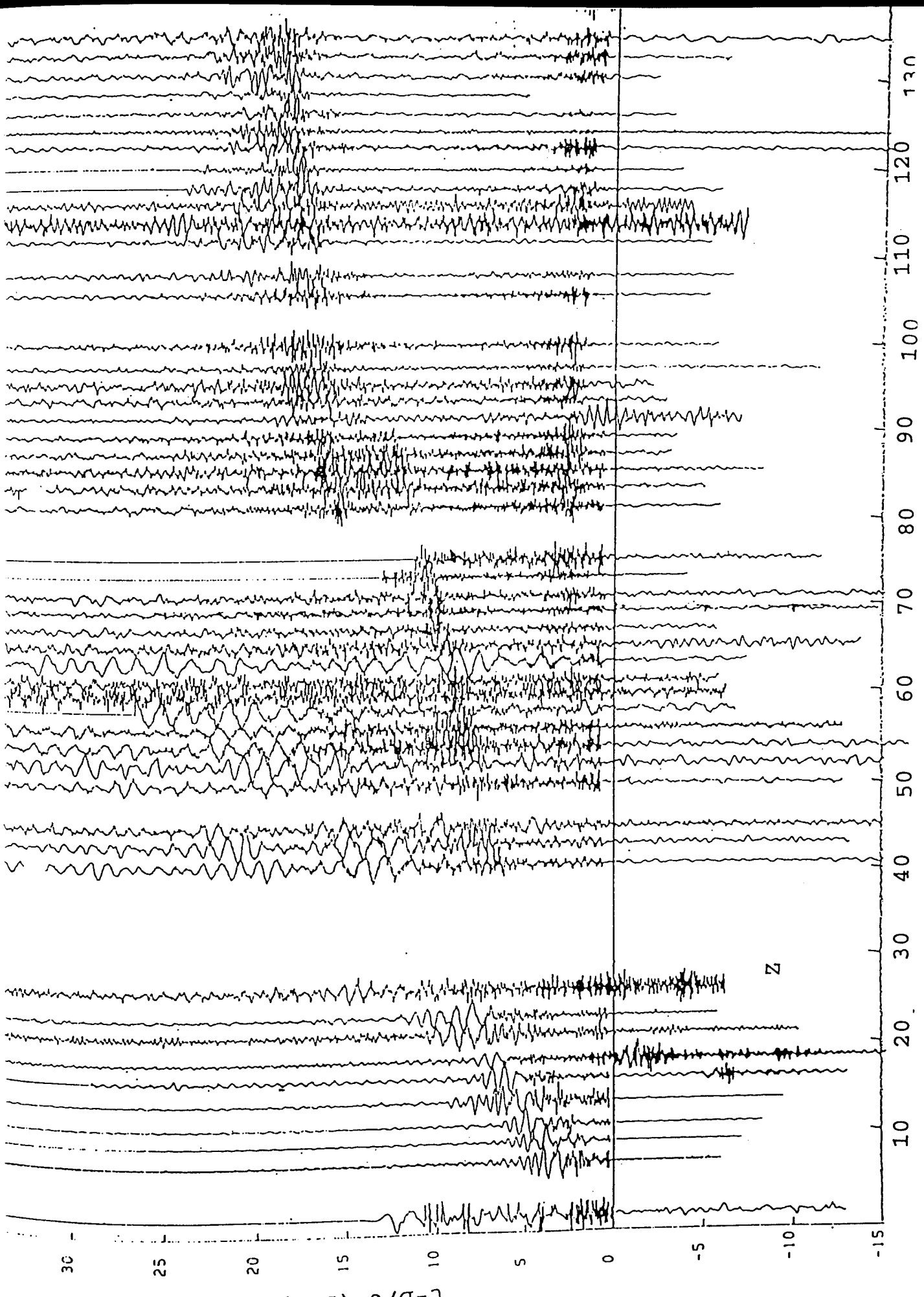
Z
t-D/6 (sec)

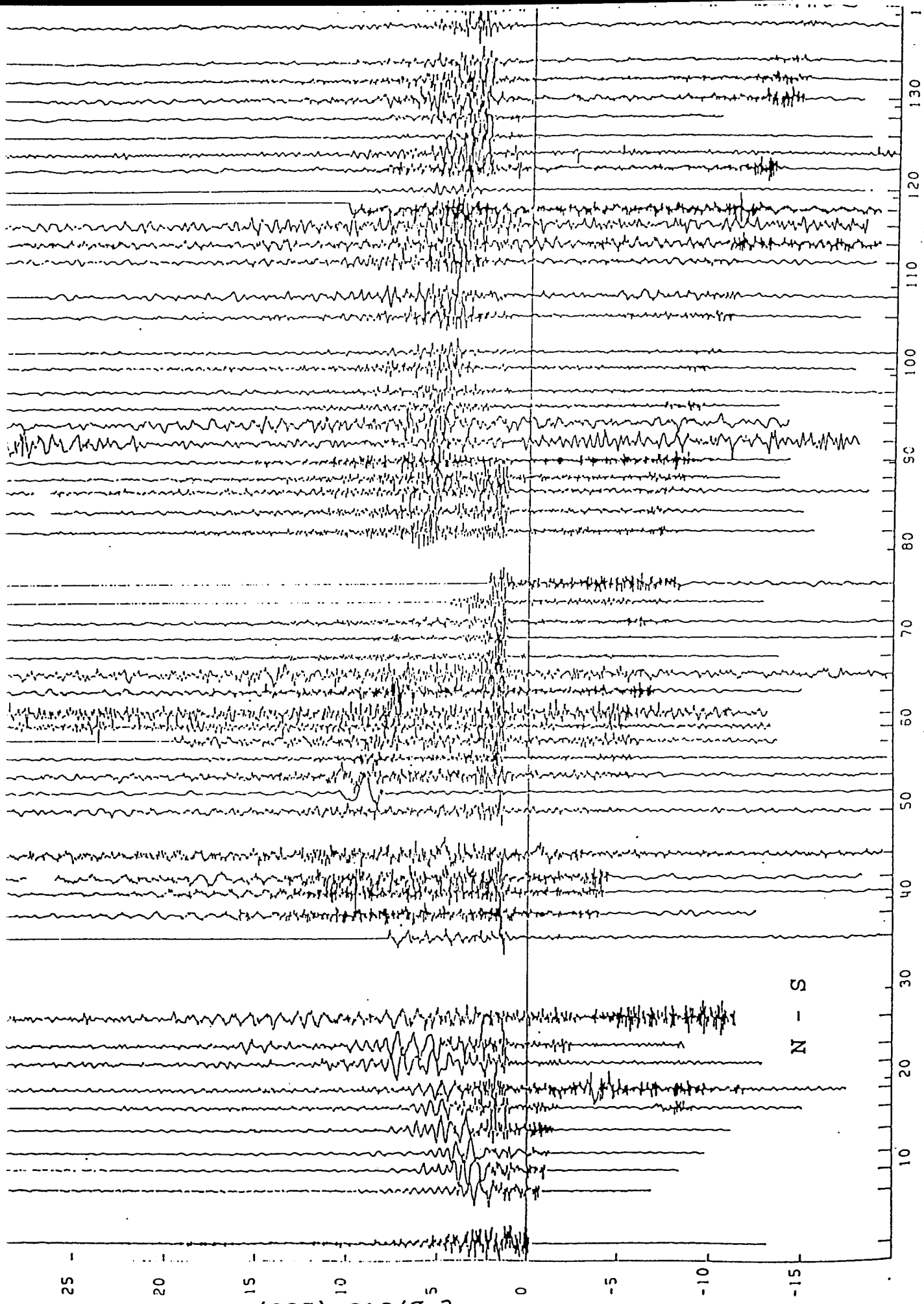
N - S
t-D/3.5 (sec)
25
20
15
10
5
0
-5
-10
-15
10
20
30
40
50
60
70
80
90
100
110
120
130

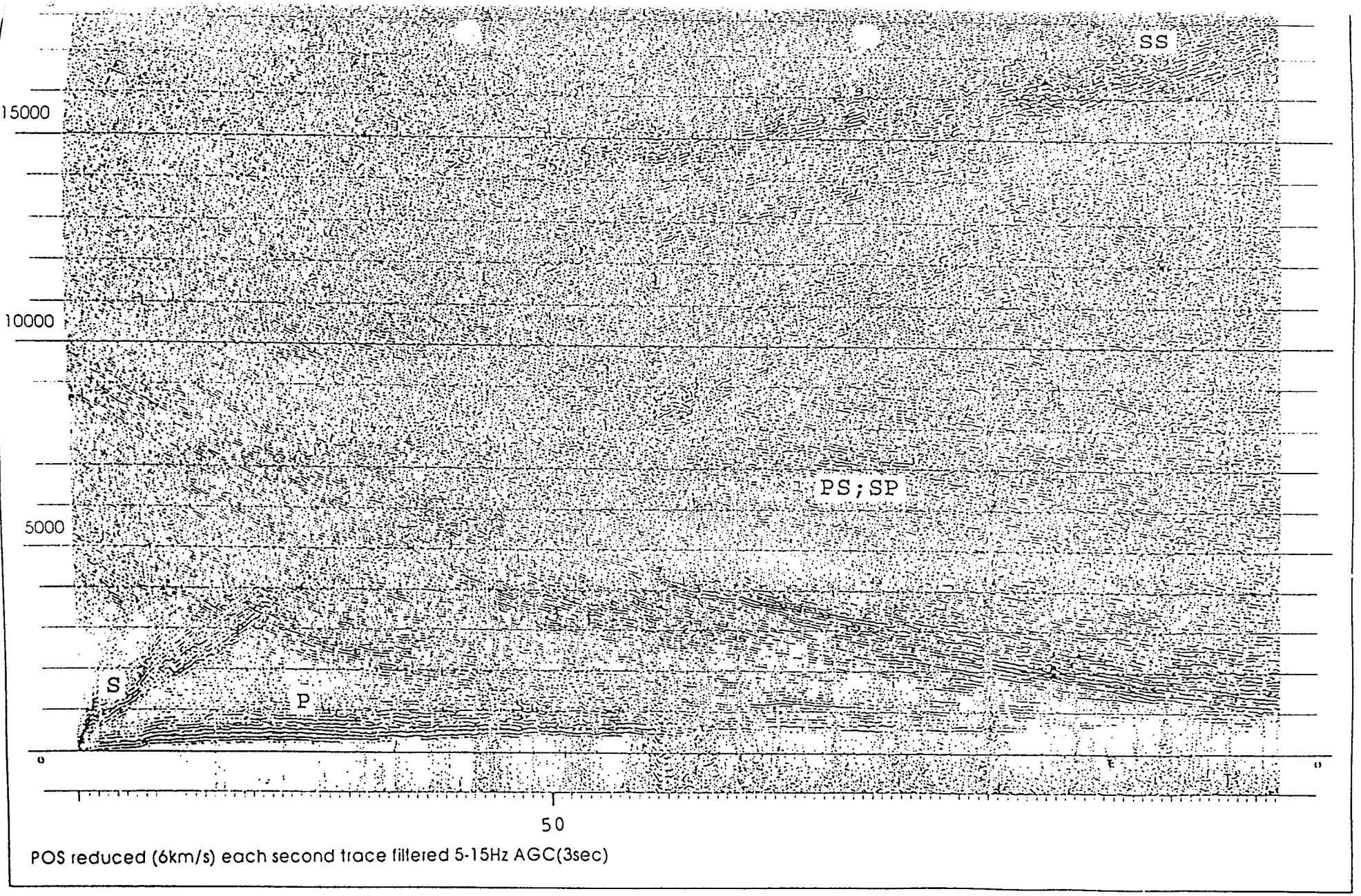

POS reduced (6km/s) each second trace filtered 5-15Hz AGC(3sec)

Scientific Technical Report STR 95/TK
DOI: 10.2312/GFZ.b103-95tk7

GeoForschungsZentrum Potsdam

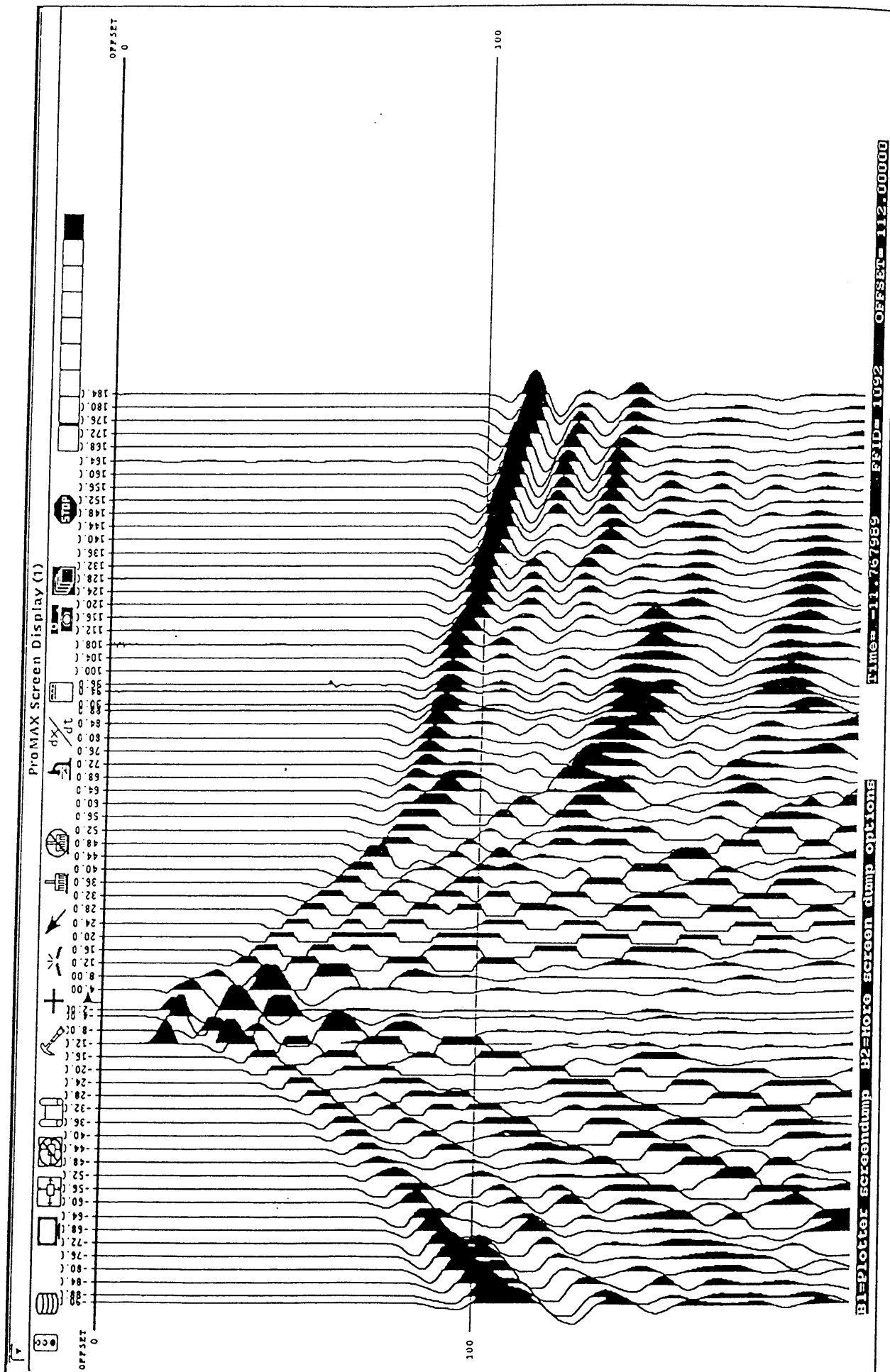
ProMAX Screen Display (1)
OFFSET
0
100
B1=Plotter screendump B2=Hoke screen dump options
Time= -11.757989 FID= 1092 OFFSET= 1112.000000

ProMAX Screen Display (1)
OFFSET
0
100
STOP
dx/dt
F1=plotter screendump F2=hard screen dump options
Time= -12.023815 SHID= 1151 OFFSET= 43.000000

Practical exercises in seismic methods for structural investigations by means of body waves

part II

Modeling

Scientific Technical Report STR 95/TK
DOI: 10.2312/GFZ.b103-95tk7

GeoForschungsZentrum Potsdam

Practical exercises in seismic methods for structural investigations by means of body waves

Exercise 1: Calculation of a structural model from a seismogram section (Fig. 1a)

Fig. 1a shows a synthetical seismogram section for a simple crustal model (calculated with the reflectivity method). The model contains two discontinuities which are responsible for several types of body waves. The strongest of them are reflected P- and S-waves. Additional converted waves and headwaves occur.
The main task of *exercise 1* is to determine P- and S-wave velocities for both crustal layers and to calculate their layer thicknesses.

1.1 Identify the following waves in Fig. 1a!

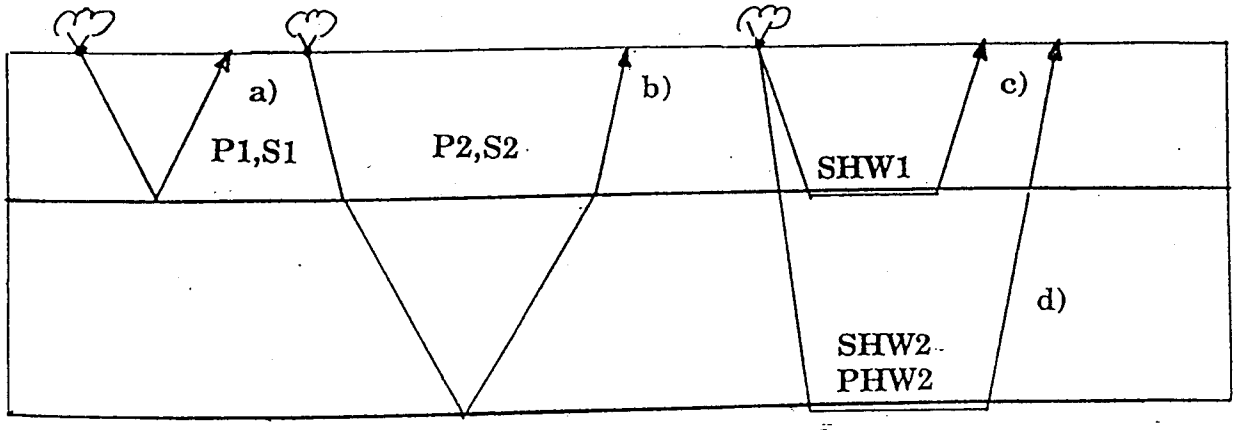

a) reflected P-wave and reflected S-wave at the upper boundary
b) reflected P-wave and reflected S-wave at the deeper boundary
c) S-headwave for the upper boundary
d) S-headwave and P-headwave for the deeper boundary

1.2 Compare your results with Fig. 1b!

1.3 Determine the velocities for the marked travel time branches in Fig. 1b!

The asymptotic slope of the reflected travel time branches from the first boundary corresponds to the slowness of the upper layer whereas the slope of the haedwave branches provides the slowness of the layer below the interface.
For the whole model a v_p/v_s-ratio of $\sqrt{3}$ was assumed.

a) v_{p1} = v_{s1} =
b) v_{shw1} = $v_{phw1} = \sqrt{3}\, v_{shw1}$ =
c) v_{shw2} = v_{phw2} =

crustal layer 1 : v_p = v_s =
crustal layer 2 : v_p = v_s =
upper mantle : v_p = v_s =

1.4 Calculate the thickness for both crustal layers. For this you should measure the intercept-times for each headwave.

intercept time for the upper S-headwave: τ_1^s = τ_1^p =
intercept time for the lower headwaves : τ_2^s = τ_2^p =

Scientific Technical Report STR 95/TK
DOI: 10.2312/GFZ.b103-95tk7

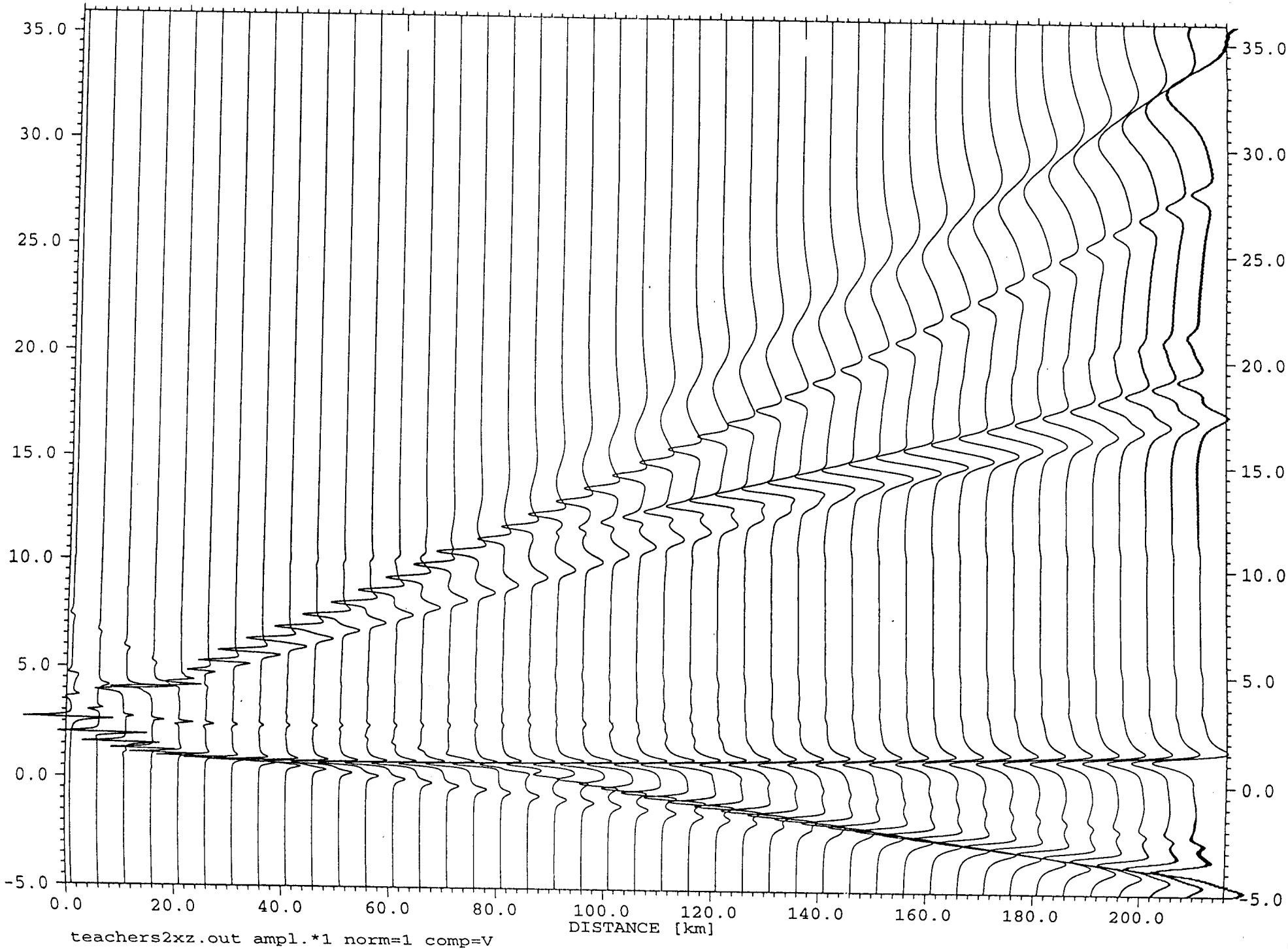

GeoForschungsZentrum Potsdam

Scientific Technical Report STR 95/7[Ks] DOI: 10.2312/GFZ.b103-95tk7

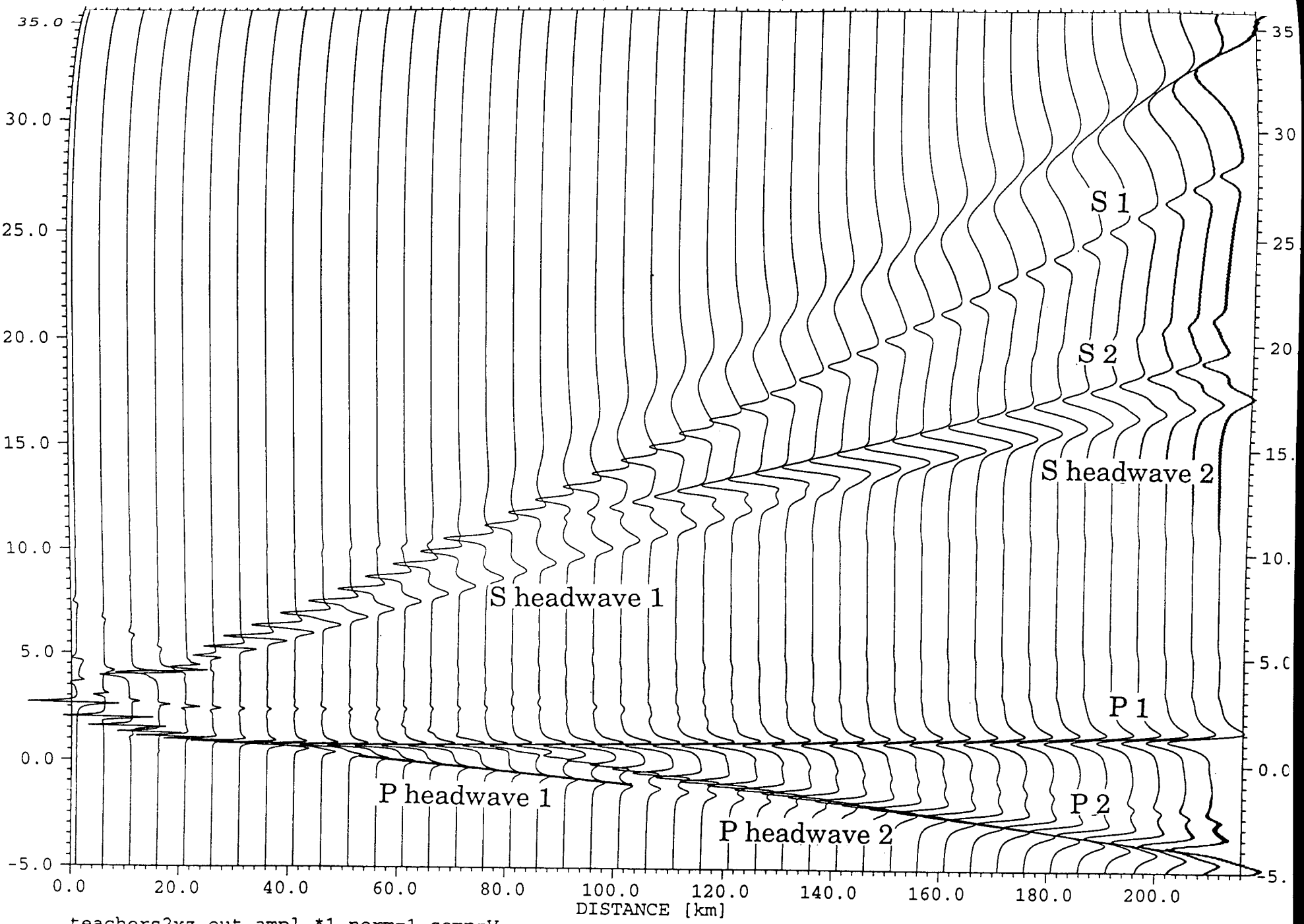

Fig. 1b

GeoForschungsZentrum Potsdam

1.5 Now please calculate the layer thicknesses h_1 and h_2 with the help of the following equation:

$$\tau_i = \sum_{j=1}^{i} 2h_j \cos(\Theta_{j,i+1})/v_j$$

The critical angle $\Theta_{j,i+1}$ follows from *Snells law*:

$$\sin(\Theta_{n,m}) = v_n/v_m.$$

1.6 As the final result please draw the velocity depth function for P- and S-waves into Fig. 2.

1.7 For an illustration of exercise 1 please have a look again on the measured seismogram sections and try to estimate simple models.

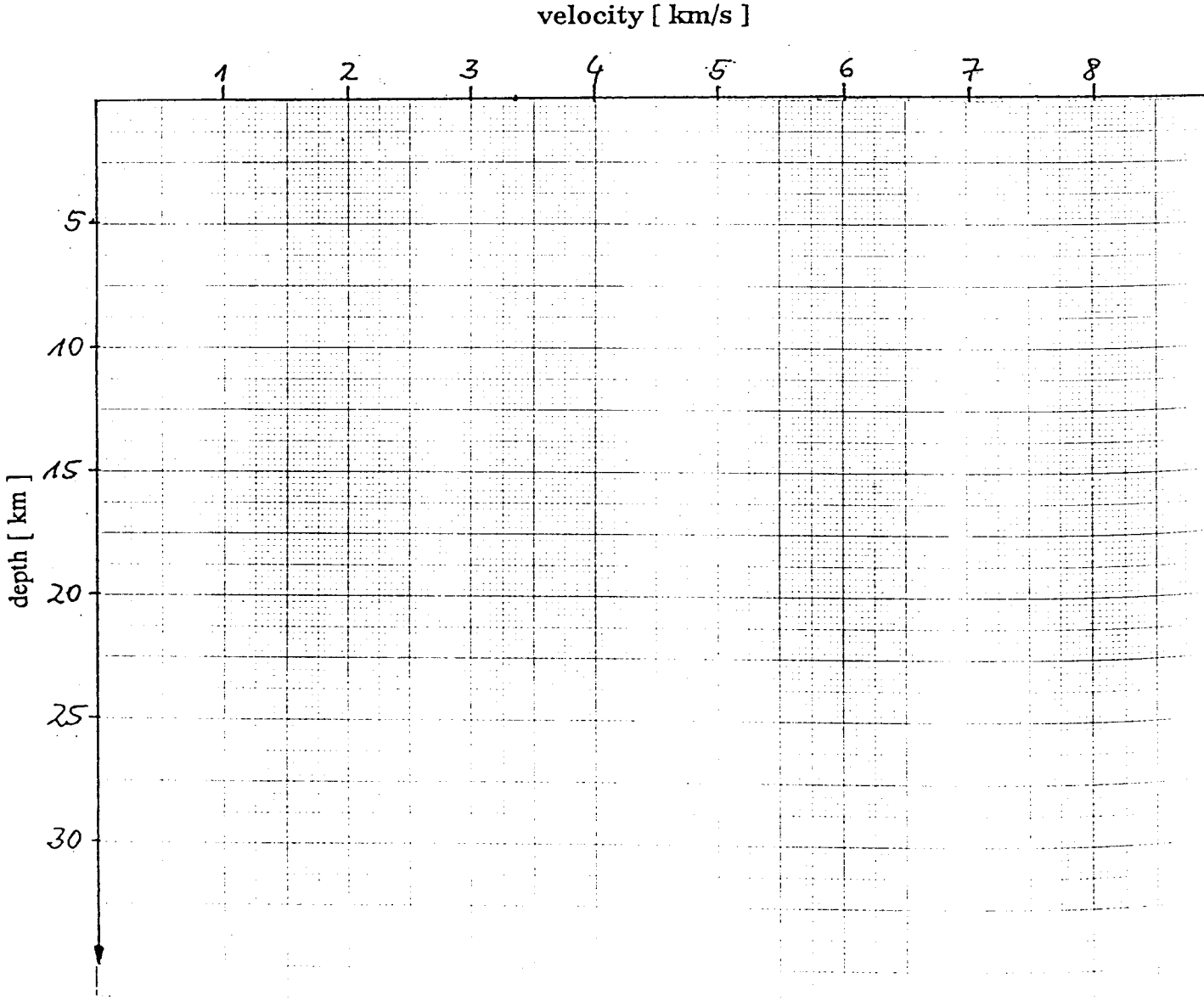

Fig. 2

Practical exercises in seismic methods for structural investigations by means of body waves

Exercise 2: Wiechert-Herglotz-Integral

The *Wiechert- Herglotz- Integral* is a classical method to interprete traveltime curves which correspond with the propagation of diving waves in media with continuous increasing velocity.
Please have a look on a typical traveltime branch and corresponding ray paths:

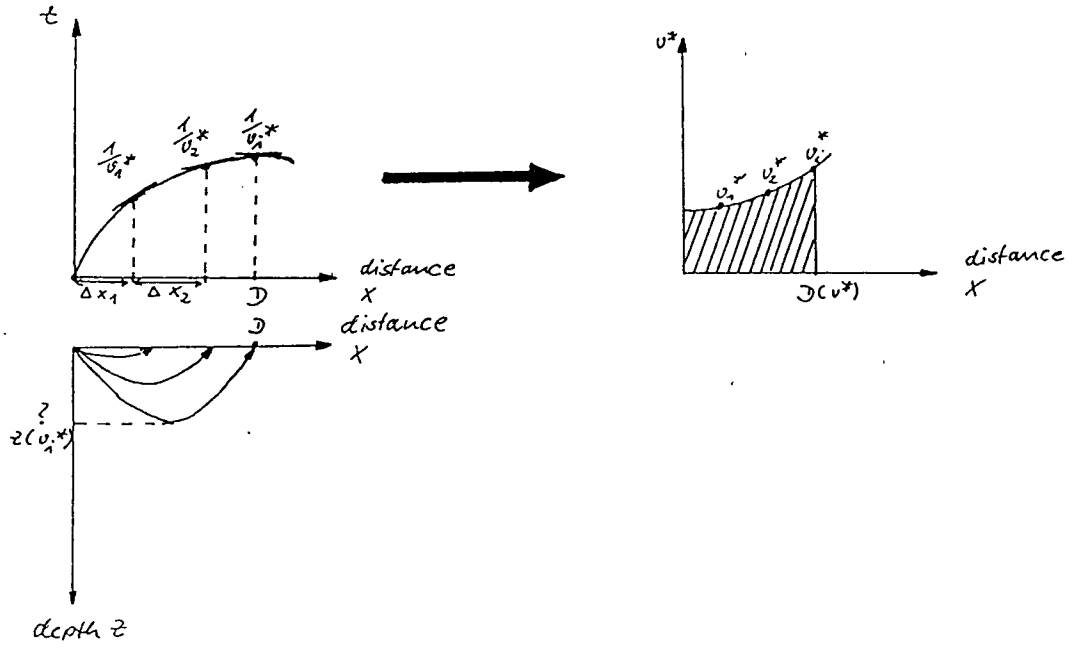

The slope of the traveltime curve has the value $1/v^*_i$ where v^*_i is the apparent velocity at the distance x_i. Representing the apparent velocity in dependence on x one gets the *Wiechert- Herglotz- Integral* as the area under the $v^*(x)$-curve.
The physical meaning of the *Wiechert- Herglotz- Integral* is the depth $z(v=v^*)$ at which the velocity just equals to the apparent velocity v^*_i:

$$z(v=v^*) = 1/\pi \int_0^D \cosh^{-1}(p(x)/p(D))\, dx \qquad \text{with } p = \sin(i)/v\ .$$

For practical application the following approximation is sufficient:

$$z(v=v^*) = 1/\pi \sum_{j=1}^{i} \Delta x_j \underbrace{\ln\{ v^*_i(D)/v^*(x_j) + \sqrt{[v^*_i(D)/v^*(x_j)]^2 - 1}\}}_{A_j}$$

Calculate for two velocities the corresponding depths z(v).
The curve v*(x) is given in the table below:

2.1 *D = 3 km and v*(D) = 2.5 km / s*

x_j[km]	v^*_j[km/s]	Δx_j	A_j
0	2.000		
1	2.060		
2	2.236		

$z(v = 2.5\ km/s) =$

2.2 *D = 7 km and v*(D) = 4.03 km / s*

x_j[km]	v^*_j[km/s]	Δx_j	A_j
0	2.000		
1	2.060		
2	2.236		
3	2.500		
4	2.828		
5	3.202		
6	3.606		

$z(v = 4.03 km/s) =$

Practical exercises in seismic methods for structural investigations by means of body waves

Exercise 3: Calculation of the traveltime curve from the velocity-depth-function of a model consisting of homogeneous layers

Use the following equations:

$x_i = h_i \tan\Theta_i$

$t_i = h_i / (v_i \cos\Theta_i)$

$x_{tot} = 2\sum_i x_i$

$t_{tot} = 2\sum_i t_i$

$t_{red} = t_{tot} - (x_{tot} / v_{red})$

$\sin\Theta_{i+1} = v_{i+1} \sin\Theta_i / v_i$

$v_{red} = 6$ km/s

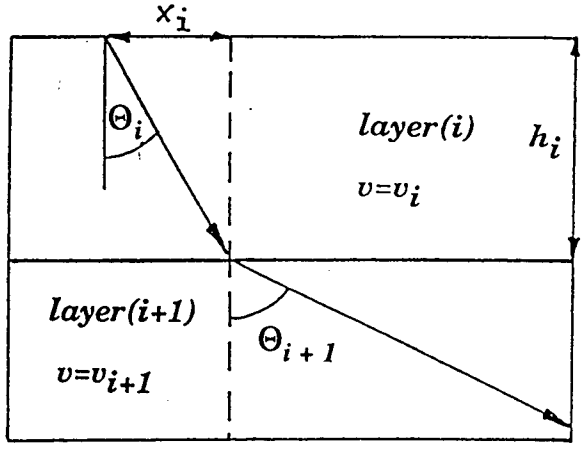

3.1 Calculate the critical points for all P- and S-headwaves for the velocity-depth-function from Fig. 2 (exercise 1)!

boundary 1

$\Theta_1 = \Theta_{crit} =$
$x_1 =$
$x_{tot} =$

boundary 2

$\Theta_1 =$
$x_1 =$

$\Theta_2 = \Theta_{crit} =$
$x_2 =$
$x_{tot} =$

boundary 1

$t_1 =$
$t_{tot} =$
$t_{red} =$

boundary 2

$t_1 =$
$t_2 =$
$t_{tot} =$
$t_{red} =$

3.2 Calculate the travel time curve of the P-wave reflected at the crust-mantle-boundary!

take off angle Θ_1	0^o	20^o	40^o	50^o
Θ_2				
x_1				
x_2				
x_{tot}				
t_1				
t_2				
t_{tot}				
t_{red}				

Please compare your results with the travel time branches in Fig. 1 (exercise 1).

Practical exercises in seismic methods for structural investigations by means of body waves

Exercise 4: Calculation of the traveltime curve for a model consisting of inhomogeneous layers

Let us consider layers with increasing velocity:

$v_i = v_{oi} + \gamma_i z$,

v_{oi} ... velocity at the top of layer i
γ_i ... velocity gradient of layer i
z ... distance from the top of the layer.

The corresponding travel time curve follows from the following equations:

$x_i = v_{oi} (\cos\Theta_o - \cos\Theta)/(\gamma_i \sin\Theta o)$

$t_i = 1/\gamma_i \ \ln[\tan(\Theta/2)/\tan(\Theta_o/2)]$

Looking on the sketch we distinguish two cases

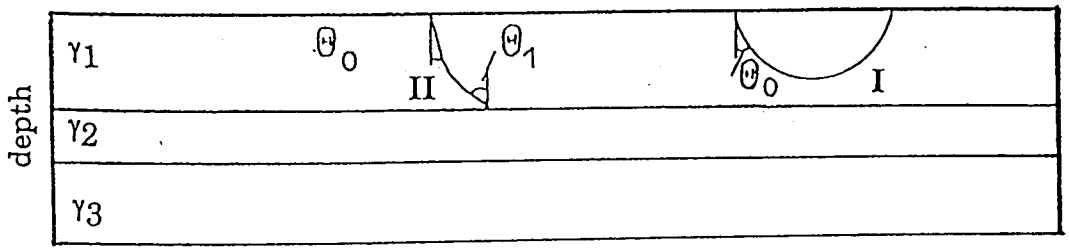

case I : There is a turning point in layer i ($v \sin\Theta_o / v_o > 1$)

$x_i = 2v_{oi} \cot\Theta_o/\gamma_i$

$t_i = 2 \ln[\cot(\Theta_o/2)]/\gamma_i$,

case II : There is no turning point in layer i ($v \sin\Theta_o / v_o < 1$)

$x_i = v_{oi} (\cos\Theta_o - \cos\Theta_1)/(\gamma_i \sin\Theta o)$

$t_i = 1/\gamma_i \ \ln[\tan(\Theta_1/2)/\tan(\Theta_o/2)]$

Please calculate the traveltime curve for the following model and book the results into the table on the following page!

depth [km]	*velocity [km / s]*	*velocity gradient* $[s^{-1}]$
0	2	
2	4	γ_1 =
5	6	γ_2 =
10	7	γ_3 =

				horizontal increment in layer				*time increment in layer*					
Θ_0	Θ_1	Θ_2	Θ_3	$^1x_1$	$^2x_2$	$^3x_3$	x_{tot}	$^1t_1$	$^2t_2$	$^3t_3$	t_{tot}	$x_{tot}/6$	t_{red}
40°													
35°													
30°													
25°													
20°													
19°													
18°													
17°													

QUANTIFICATION OF EARTHQUAKES[1)]

by

Severyn J. Duda

University of Hamburg
Geophysical Institute

EARTHQUAKES: MAGNITUDE, ENERGY, AND INTENSITY

Development of the Concepts

Preliminaries. The focus of an earthquake radiates mechanical energy in the form of seismic waves. The radiation of seismic energy during the event continues from a fraction of a second to several tens of seconds. The duration of seismic wave radiation is identical with that of the instantaneous faulting.

The time between two radiation events from a given focus is substantially larger than the radiation duration of a given event. Thus, earthquakes are transient radiation phenomena, and the methods for the determination of the strength of sources radiating transient signals are correspondingly applicable. On this basis the earthquake magnitude scale was introduced. A steady development of the magnitude concept is necessitated by ongoing improvements in seismological instrumentation and in the theories of the focal process and of seismic wave propagation.

A comprehensive review of the magnitude problem was given by Båth (1981), together with an extensive bibliography on the topic. Reference is made to this paper, as far as pre-1981 findings are concerned. In the following, only essential information is repeated; otherwise the development since 1981 stressed.

Basic Principles of Seismic Rating. The seismic energy radiated from the focus F is sensed at the earth surface. Figure 1 shows the basic geometry of the problem. At short epicentral distance Δ the ground motion can be strong enough to cause specific sensations to human beings and/or to inflict damage to them and to objects. Sensation and damage are usable to rate the macroscopic strength of ground motion at a given place. In order to quantify the strength of shaking, the noninstrumental seismic intensity scale is available, first introduced more than 100 years ago (i.e., prior to seismographs), and thus prior to the definition of the earthquake magnitude. Usually, a suit of strengths will correspond to a given earthquake, the strengths generally decreasing with

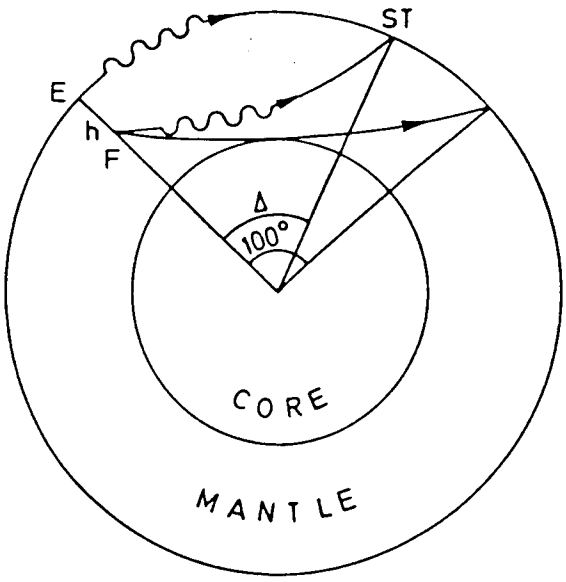

FIGURE 1. Propagation of body waves and surface waves radiated from focus F with focal depth h and arriving at station ST with epicentral distance Δ.

the distance from the epicenter of the earthquake. The seismic intensity reflects the total effect of the ground motion generated by the earthquake at the point of observation (see the last section, "Seismic Intensity").

The seismic energy arrives at the point of observation ST in the form of seismic phases, notably of body waves (P waves and S waves) and of surface waves (Love and Rayleigh waves). The seismographic recordings of the waves constitute the basis of an instrumental rating of the strength of the radiation from the seismic source F.

The foci F can have depths h below the earth surface ranging from 0 km (surface events, explosions) to 700–800 km (deepest earthquakes so far observed). For a given focal depth the amplitude of the seismic phase varies with epicentral distance. In order to arrive at a quantity independent of the epicentral distance and characterizing the radiation strength of the seismic source only, the amplitude measured at a particular epicentral distance Δ must be compensated for this variation. Thus, the amplitude variation curve is essential for the definition of any magnitude scale. Examples of amplitude variation curves are shown in Fig. 2. Here and in the following, it is assumed that with respect to the amplitude and the frequency content of the signal, the radiation from the focus is the same in all directions.

Because the shadow of the Earth core prevents the observation of body waves at greater distances, the amplitude variation curves for P and S waves are obtained only up to epicentral distances of about 100°. The application of reflected and diffracted P

[1)] The paper has been copied from "The Encyclopedia of Solid Earth Geophysics", edited by David E. James (Chapman & Hall, 1989)

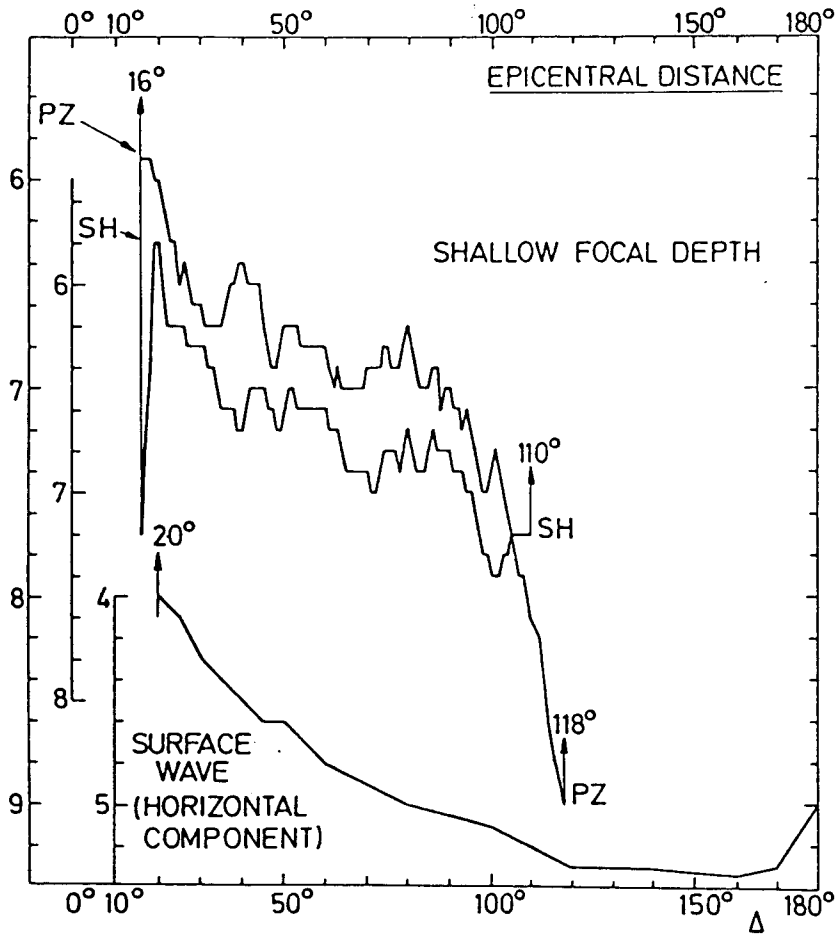

FIGURE 2. Amplitude variation of body waves and surface waves as function of epicentral distance. The ordinates are of σ_b (6), as given in Fig. 3 for the PZ and SH waves, and σ_s (3), as given in Table 2 for the surface waves.

and S waves, as well as that of body waves that are refracted through the core and arriving at greater distances, is inopportune for magnitude determinations, notwithstanding some attempts to utilize such waves correspondingly. Surface wave amplitude variation curves, on the other hand, are obtained out to epicentral distances of 180°.

With the knowledge of the amplitude variation curve, the magnitude scale for the corresponding seismic phase can be defined, if two further conditions are specified: (1) when to consider two earthquakes with the same focal depth to have magnitudes 0 and 1, respectively, and (2) when to consider two earthquakes with different focal depths to have identical magnitudes. As in any analogous definition of a physical quantity, the answer can only be arbitrary.

All magnitude scales employ decadic logarithms. Thus, the increase by one magnitude unit entails a tenfold increase of the measured quantity (seismogram trace amplitude, ground displacement amplitude, ground velocity amplitude, etc.). The zero-magnitude event is taken small enough to assure that most magnitudes are numerically positive.

According to the intention of Gutenberg and Richter (1956), two events are assigned the same body wave magnitude if the seismic energies released in the events are identical. The seismic energy is thus intended to link with each other events having different focal depths. This implies that a unique relation exists between the body wave magnitude and the seismic energy released. It also implies that it is possible to determine the seismic energy independently and with sufficient accuracy so as to make it applicable as a standard quantity entering the definition of the magnitude.

Magnitude Calibrating Functions.

The Local Magnitude M_L. The first magnitude scale was defined by Richter (1935) for earthquakes in California:

$$M_L = \log A(\Delta) + \sigma_L(\Delta)$$

$A(\Delta)$ is the vectorial sum of the maximum trace amplitudes on the horizontal seismograms of a given earthquake, in millimeters, as obtained on a particular seismometer located at the epicentral distance Δ (Wood-Anderson seismometer, $T_0 = 0.8$ s, $V_{max} = 2800$, $\eta = 0.8$, where $T\sigma$, V_{max} and η are the free period of oscillation, the maximum magnification, and the damping ratio, respectively).

The calibrating function is

TABLE 1. Calibrating the Function Equation 1 for Local Magnitude M_l

Δ (km)	$\sigma_l(\Delta)$	Δ (km)	$\sigma_l(\Delta)$	Δ (km)	$\sigma_l(\Delta)$	Δ (km)	$\sigma_l(\Delta)$
0	1.4	90	3.0	260	3.8	440	4.6
10	1.5	100	3.0	280	3.9	460	4.6
20	1.7	120	3.1	300	4.0	480	4.7
30	2.1	140	3.2	320	4.1	500	4.7
40	2.4	160	3.3	340	4.2	520	4.8
50	2.6	180	3.4	360	4.3	540	4.8
60	2.8	200	3.5	380	4.4	560	4.9
70	2.8	220	3.65	400	4.5	580	4.9
80	2.9	240	3.7	420	4.5	600	4.9

Source: From Richter, 1958.

$$\sigma_L(\Delta) = -\log A(\Delta; M_L = 0) \qquad (1)$$

where $A(\Delta; M_L = 0)$ is the maximum trace amplitude, in millimeters, for a magnitude-zero event at the distance Δ.

The calibrating function $\sigma_L(\Delta)$ does not depend on the focal depth, as the earthquakes in California were assumed to occur at common depths.

Table 1 gives the calibrating function (Eq. 1), defined up to an epicentral distance of 600 km. As seen from the table, a magnitude-zero event is one that would record at a distance of 100 km with a maximum trace amplitude of 1 μm.

In the strict sense the local magnitude, as defined here, is applicable in a region outside of California only if in both regions the maximum trace amplitudes on the Wood-Anderson seismograph vary in the same way and if the focal depths of earthquakes are the same.

The difficulties in verifying the conditions have led to the development of numerous independent local magnitude scales (Båth, 1981).

The Surface Wave Magnitude M_s. In order to extend the magnitude scale to larger epicentral distances, the surface wave magnitude, applicable to shallow events, was introduced. Here use is being made of the observation that surface waves with a period of about 20 s are persistently recorded for a large portion of earthquakes (Airy phase in the dispersion curve of the surface wave train).

The magnitude M_s is defined as

$$M_s = \log A(\Delta) + \sigma_s(\Delta) \qquad (2)$$

where $A(\Delta)$ denotes the ground displacement amplitude, in micrometer, of the horizontal components of the surface waves combined vectorially, with a period of 20 s ± 3 s. Table 2 gives the calibrating function

$$\sigma_s(\Delta) = -\log A(\Delta; M_s = 0) \qquad (3)$$

for epicentral distances Δ ranging from 20° to 180° (Richter, 1958).

Accordingly, a magnitude-zero event is defined as one producing at an epicentral distance of 20° a horizontal ground displacement with an amplitude of 10^{-4} μm at a period of about 20 s. The particular amplitude value was chosen in an attempt to obtain surface wave magnitudes M_s numerically identical to local magnitudes M_L. The problem of relating the surface wave magnitude to the local magnitude, however, was never solved satisfactorily, and both scales have to be considered as largely independent of each other.

In order to utilize surface waves with periods diverging from 20 s ± 3 s, the surface wave magnitude was redefined as

$$M_s' = \log \frac{A(\Delta)}{T} + \sigma_s'(\Delta) \qquad (4)$$

TABLE 2. Calibrating the Functions in Equations 3 and 5 for Surface Wave Magnitude

Δ (degs)	$\sigma_s(\Delta)$	$\sigma_s'(\Delta)$	$\sigma_s'(\Delta)$ for T = 20 s	Δ (degs)	$\sigma_s(\Delta)$	$\sigma_s'(\Delta)$	$\sigma_s'(\Delta)$ for T = 20 s
20	4.0	5.46	4.16	90	5.05	6.54	5.24
25	4.1	5.62	4.32	100	5.1	6.62	5.32
30	4.3	5.75	4.45	110	5.2	6.69	5.39
40	4.5	5.96	4.66	120	5.3	6.75	5.45
50	4.6	6.12	4.82	140	5.3	6.86	5.56
60	4.8	6.25	4.95	160	5.35	6.96	5.66
70	4.9	6.36	5.06	170	5.3		
80	5.0	6.46	5.16	180	5.0		

where

$$\sigma_s'(\Delta) = -\log \frac{A(\Delta;\, M_s' = 0)}{T}$$

$$= 1.66 \log \Delta^\circ + 3.3 \qquad (5)$$

(Vanek et al., 1962). $A(\Delta)$ is the amplitude of the horizontal component of the ground displacement of the Rayleigh wave, in micrometers, and the period T ranges from 10 to 30 s.

To be consistent with Eq. 2, the ground displacement amplitude $A(\Delta)$ for any Δ is required for all earthquakes to increase linearly with period from 10 to 30 s. Equation 4, known as the Moscow-Prague formula, applies for earthquakes with focal depths smaller than 50 km and observed in the distance range 20°–160°. It was adopted and recommended for general use during the 1967 Zürich General Assembly of the International Union of Geodesy and Geophysics (IUGG) (Båth, 1973). The calibrating function $\sigma_s'(\Delta)$ is given in Table 2. It can be seen that $\sigma_s'(\Delta)$ for 20 s exceeds, on the average, $\sigma_s(\Delta)$ by 0.2; i.e., Eq. 5 yields surface wave magnitudes numerically larger by 0.2 than the original calibrating function (Eq. 3).

The Body Wave Magnitude m_b. An extension of the magnitude scale to events with arbitrary focal depths became possible by employing body waves:

$$m_b = \log \frac{A(\Delta)}{T} + \sigma_b(\Delta, h) \qquad (6)$$

This scale is based on the maximum ground velocity $(A(\Delta)/T)$ observed at the epicentral distance Δ, whereby $A(\Delta)$ denotes the maximum ground displacement amplitude in the respective phase (P or S), in micrometers, and T is the corresponding period in seconds.

Figure 3 gives the calibrating functions σ_b for the vertical and horizontal components of the P wave and the horizontal component of the S wave (Gutenberg and Richter, 1956). A magnitude-zero event occurring at the Earth surface is seen from the figure to produce at 90° epicentral distance maximum ground velocities of 10^{-7}, $10^{-7.3}$, and $10^{-6.85}$ $\mu m \cdot s^{-1}$ associated with the PZ, PH, and SH phase, respectively.

The definition of the body wave magnitude implies that one and the same magnitude figure can be obtained for a given earthquake regardless of whether the P phase or the S phase is employed. It further implies that the magnitude figure will be the same regardless of the period of the phase utilized. The general use of the calibrating functions in Fig. 3 for the determination of body wave magnitudes was recommended by the 1967 Zürich General Assembly of IUGG (Båth, 1973).

Based on observations of shallow focus earthquakes, several conversion formulas were developed for the body wave and surface wave magnitudes.

The use of the following formula was recommended by the 1967 Zürich General Assembly:

$$m_b = 0.56M_s + 2.9 \qquad (7)$$

equivalent to

$$M_s = 1.79m_b - 5.18$$

Relation between Magnitude, Energy and Intensity. If the earthquakes would occur at only one, say shallow, focal depth, the maximum seismic intensity at the surface could serve as a rating of the strength of the given earthquake, provided the ground conditions were similar at all observational sites. Because focal depths vary and ground conditions are largely different at various points of observations, the maximum intensity shows generally only a weak correlation with the strength of the earthquake as expressed by the magnitude.

Numerous efforts have been undertaken to find whether seismic intensities do correlate with instrumentally measurable quantities, such as, e.g., the maximum ground acceleration or the maximum ground velocity occurring in the course of the earthquake. Table 3 shows the relation, as published by Bolt (1978). However, the acceleration and velocity values for the wave motion are for firm ground only. They vary greatly depending on surface conditions and on the type of earthquake source.

Richter (1958) gives a relation between the ground acceleration a $(cm \cdot s^{-2})$ and the intensity I expressed in the M.M. scale (see the last section):

$$\log a = \frac{I}{3} - \frac{1}{2}$$

which is valid for California. Båth (1973) cites a relation between the maximum intensity I_0 and the corresponding acceleration $a_0 (cm \cdot s^{-2})$:

$$I_0 = 3 \log a_0 + 1.5$$

which is valid for Southern California.

The same author gives the interrelation between the seismic energy released E (in ergs), the surface and body wave magnitudes M_s and m_b, the maximum intensity I_0, and the maximum ground acceleration a_0, as shown in Table 4. Thereby, he utilizes the empirical formulas

$$\log E = 12.24 + 1.44M_s$$

and Eq. 7 to obtain

$$\log E = 4.78 + 2.57m_b$$

$$M_s = 1 + \frac{2I_0}{3}$$

$$I_0 = 3 \log a_0 + 1.5$$

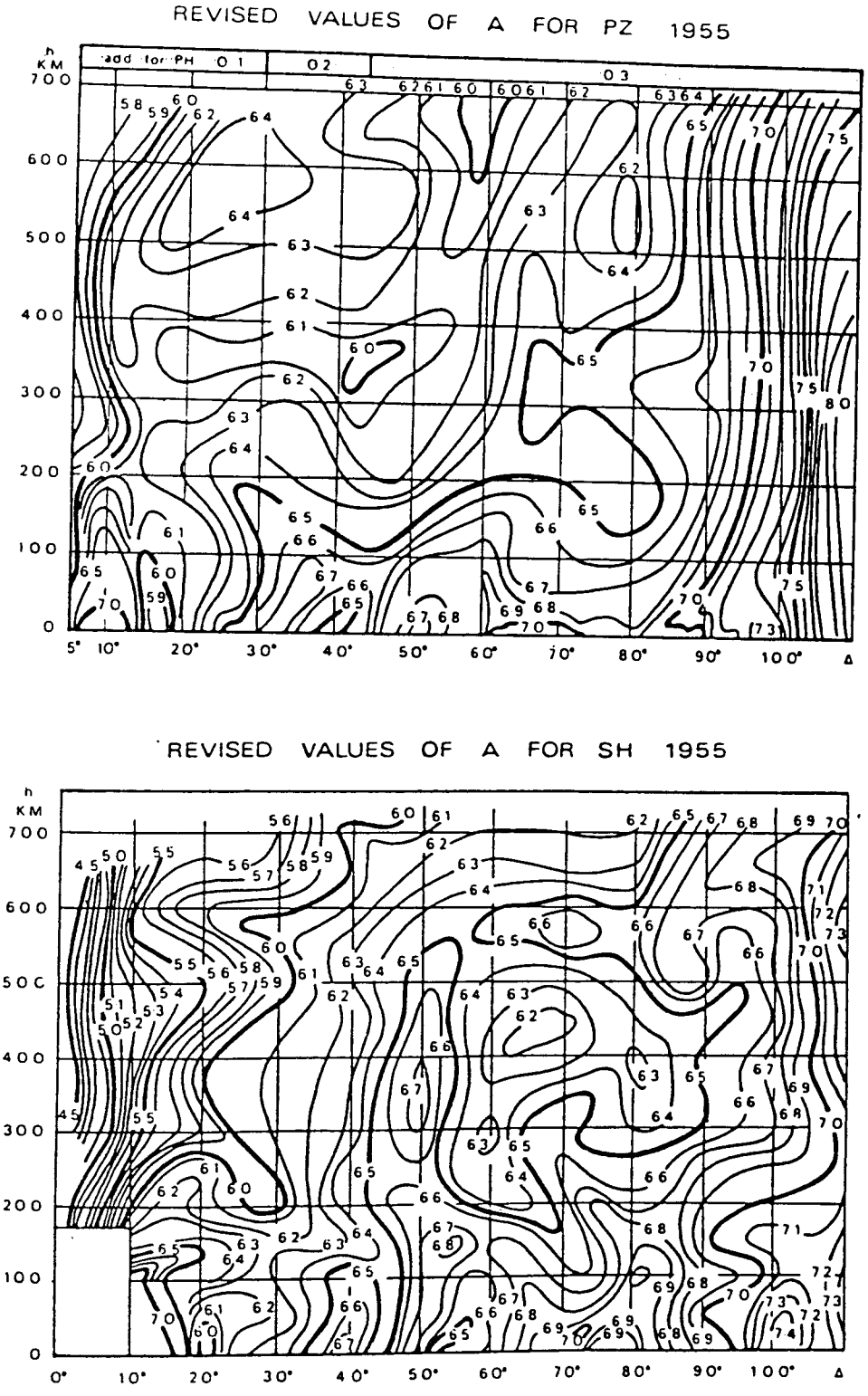

FIGURE 3. Magnitude calibrating functions for PZ, PH, and SH waves (Richter, 1958). The functions are generally used for the determination of m_b.

TABLE 3. Relation between Seismic Intensity, Maximum Ground Velocity and Maximum Ground Acceleration

Maximum Velocity (average; $cm \cdot s^{-1}$)	Seismic Intensity (according to the abridged modified Mercalli intensity scale)	Maximum Acceleration (average; $g = 980\ cm \cdot s^{-2}$)
1–2	IV	$0.015g$–$0.02g$
2–5	V	$0.03g$–$0.04g$
5–8	VI	$0.06g$–$0.07g$
8–12	VII	$0.10g$–$0.15g$
20–30	VIII	$0.25g$–$0.30g$
45–55	IX	$0.50g$–$0.55g$
>60	X	$>0.6g$

Source: From Bolt, 1978.

The figures in Table 4 have to be considered with care. They are gaining significance, however, if only incomplete information on the earthquake is available, as, e.g., historical earthquakes. Here, the description of damage inflicted, as eventually found in historical records at large, may lead to an estimate of the maximum intensity of shaking and subsequently to at least a rough estimate of the magnitude of the earthquake.

Earthquake Magnitude and Energy

Present Practice of Determination and Publication. Magnitudes are being determined from observations at individual stations or as averages from observations at a network of stations. The present practice of magnitude determination at the agencies publishing annually the largest number of magnitudes is given below.

National Earthquake Information Service (NEIS), U.S.A. The surface wave magnitude is computed from Eq. 4, whereby the vertical component of the surface wave must have a period ranging from 18 to 22 s, and the epicentral distances range from 20° to 160°. No depth correction is applied. The magnitude is determined for earthquakes with focal depth not greater than 50 km, making allowance for uncertainties in the depth determination. The M_s value published is the average of individual magnitudes computed from reported amplitude and period data.

The body-wave (P-wave) magnitudes are computed from Eq. 6. The period though is restricted to the range 0.1–3.0 s, and the amplitude is not necessarily the maximum in the P group. The epicentral distance must be larger than 5°. All NEIS magnitudes obtained as averages are computed by a 25% trimmed mean (Preliminary Determination of Epicenters, Monthly Listing, U.S. Department of the Interior/Geological Survey, National Earthquake Information Center).

United Services for Earthquake Research (ESSN), USSR. In the routine work of ESSN (Edinaya slushba seismicheskich nabludenii) one surface wave and two body wave magnitudes are being determined. Each of the magnitudes is the arithmetic average of a possibly large number of individual determinations. According to Vanek et al. (1980), the surface wave magnitude is found from the maximum ground velocity associated with the Rayleigh wave having periods in the range 10–20 s. Thereby the recordings made on medium-period seismographs located at epicentral distances larger than 25° and the calibrating function (Eq. 5) are utilized.

The two body wave magnitudes are based on recordings in the distance range 20°–100° of the vertical component of the P wave obtained on short-period (SKM-3) and medium-period (SK, SKD) seismographs, respectively. In some cases also the horizontal component of P, PP, and S waves is used. The body wave magnitude of a deep-focus earthquake is based exclusively on the vertical component of the P wave. In all cases the calibrating functions of Gutenberg and Richter (1956), shown in Fig. 3 for P and S waves, are used.

Since 1976, for a selection of major earthquakes, body wave magnitudes are determined based on an experimental setup at the Obninsk station. Here, a broadband seismograph (SKD) with a flat velocity response in the frequency range 2–20 s is connected to eight galvanometers. The transfer functions of the seismometer-galvanometer systems are given in Fig.

TABLE 4. Relation between Seismic Energy E, Surface Wave Magnitude M_s, Body Wave Magnitude m_b, Maximum Intensity I_0, and Maximum Ground Acceleration

E (erg)	M_s	m_b	I_0	a_0^a ($cm \cdot s^{-2}$)
10^{20}	5.4	5.9	VI–VII	40
10^{21}	6.1	6.3	VII–VIII	100
10^{22}	6.8	6.7	VIII–IX	200
10^{23}	7.5	7.1	IX–X	400
10^{24}	8.2	7.5	X–XI	1,000
10^{25}	8.9	7.9	XII	2,000

Source: From Båth, 1973.

[a]Refers to periods of ground motion ranging from 0.1 to 0.5 s.

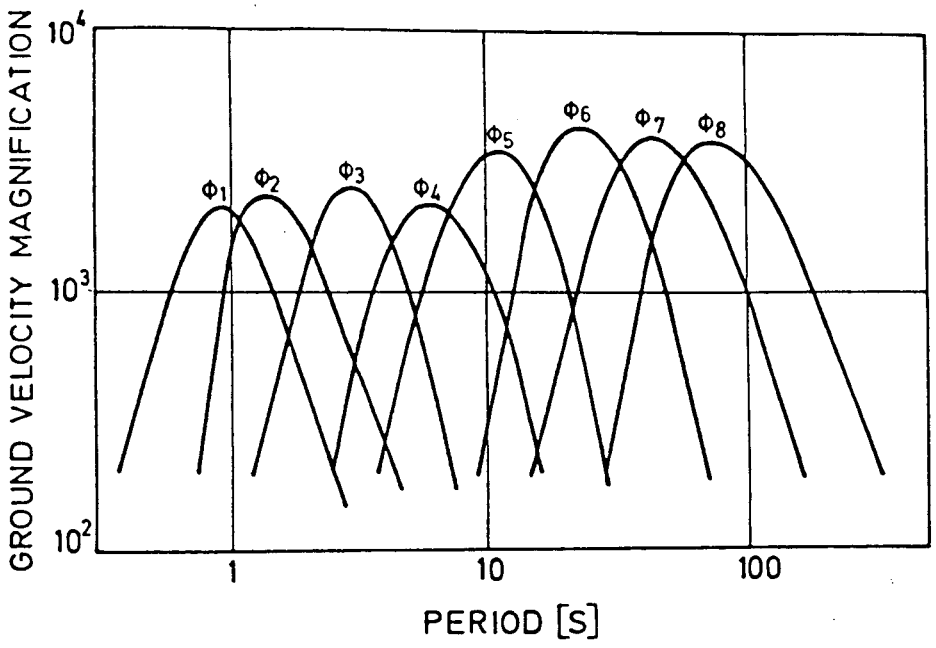

FIGURE 4. Ground velocity magnification for the system of one broadband seismograph and eight galvanometers attached. The system is operational at Obninsk (USSR).

4. Eight analog recordings are obtained at one time. Amplitude and period measurements are made for the P wave, and up to eight P-wave magnitudes are obtained. The maximum P-wave magnitude, together with its period, is published in addition to the surface wave and the two conventional body wave magnitudes of the selected earthquakes.

International Seismological Centre (ISC), U.K. The surface wave magnitude is determined from Eq. 4 by using the vertical or the resultant horizontal amplitudes with periods ranging from 10 to 60 s in the distance range 5° to 160°.

The body wave magnitude is based on Eq. 6, assuming the amplitude to be observed on a short-period vertical instrument. No station corrections are applied, and the epicentral distances must be more than 20° and less than 101°. The two magnitudes are published as averages (Bulletin of the International Seismological Centre, vol. 21, July 1984). It is estimated that generally the magnitudes published by ISC are based on a larger number of individual observations than any other magnitude figures.

Physical Significance of the Earthquake Magnitude.

Amplitude Spectral Density and Bandwidth of the Wavelet. The ground motion at the point of observation ST (Fig. 1) is a time function with finite duration. Its Fourier transform will thus have an infinite duration. The significant frequency range can be defined as the one within which the amplitude density lies not more than 3 dB below its maximum value (ANS, 1966). The bandwidth B of the signal is then obtained as the difference of the band-edge frequencies.

On the other hand, each seismograph system constitutes a bandpass filter for the ground motion. Usually the bandwidth of the seismograph system is narrower than that of the arriving signal. Table 5

TABLE 5. Bandwidth Characteristics, and Bandwidth Correction b for Determination of Spectral Magnitude (11)

Seismograph Type	Midband Period (s)	Passband (s)	Passband (Hz)	Bandwidth B(Hz)	Bandwidth Octaves	$b = \log B$
WWSSN-SP	0.66	0.37–1.19	0.84–2.70	1.86	1.69	−0.27
WWSSN-LP	14.2	6.03–33.6	0.03–0.17	0.14	2.48	+0.87
SRO-SP	0.71	0.34–1.48	0.68–2.94	2.26	2.12	−0.35
SRO-LP	28.2	18.5–43.0	0.02–0.05	0.03	1.22	+1.51
Wielandt/Streckeisen (broadband velocity output)	2.00	0.20–19.9	0.05–5.00	4.95	6.64	−0.69

shows the bandwidths for a selection of seismographic instruments currently in use. Whereas a broadband wavelet generally has a complex form, narrowband wavelets tend to have an approximately sinusoidal form.

The maximum amplitude a_{max} of the wavelet is, approximately, the product of the spectral density F within the bandwidth Δf of the wavelet and the bandwidth:

$$a_{max} = 2F\Delta f \tag{8}$$

Here, $\Delta f = f_2 - f_1$, where f_1, f_2 are the band-edge frequencies of the wavelet, a_{max} corresponds to the displacement, the velocity, or the acceleration of the ground at a frequency within the range $f_1 - f_2$, and F is assumed to be constant in the range (Aki and Richards, 1980).

The ground amplitude measured for the purpose of the surface wave magnitude determination corresponds to a nearly monochromatic wave with a period of 20 s ± 3 s, and the bandwith is constant. Thus, the amplitude is an estimate of the amplitude spectral density of the ground displacement $A(\Delta)$ (in Eq. 2) or the ground velocity $A(\Delta)/T$ (in Eq. 4). For a constant focal depth, the surface wave magnitude is, consequently, a rating of the spectral density of the radiation from the seismic source at a period of about 20 s.

The situation is less favorable with the body wave magnitude. From Eqs. 6 and 8 it is seen that this magnitude is an estimate of the amplitude spectral density of the ground velocity multiplied by the bandwidth of the seismograph system. Only body wave magnitudes determined from seismograph systems with the same bandwidth are eventually free from the bias due to variable bandwidths.

For example, the 1-s body wave magnitudes of a given earthquake will differ from each other if they are obtained on the basis of records from instruments with different bandwidths. This was clearly demonstrated by Båth (1977): Operating on one and the same pier two seismographs with a period of oscillation of 1 s (Benioff and Grenet-Coulomb seismographs), he found a systematic difference of body wave magnitudes amounting, on the average, to as much as 0.43, the larger magnitudes being obtained from the Grenet-Coulomb system, featuring the larger bandwidth.

In general, the body wave magnitude, as usually published, is thus a rating of the radiation at variable periods and is based on observations from seismographs systems having unknown bandwidths. The deficiencies in the definition of the body wave magnitude certainly contribute to the numerical instability of this magnitude, if determined for a given earthquake at several stations. It appears that the potential of the body-wave magnitude is not yet fully exploited (see the subsection "Spectral Magnitudes and Magnitude Spectra").

Far-Field Spectrum of Body Waves. A minimum of assumptions about the focal process is required when rating the source strength by way of the magnitude or the seismic energy. If, on the other hand, a specific source model is assumed, additional parameters, independent of each other, for the source strength can be defined and eventually determined. For example, consider the model of unidirectional faulting along a rectangular fault plane. Assuming a homogeneous, isotropic, unbounded elastic medium, the displacement waveform of P or S waves at the point x in the far field is

$$\Omega(\mathbf{x}, t) = \int\int_{\Sigma} \Delta\dot{\mu}\left(\xi, t - \frac{r}{c}\right) d\Sigma$$

Δu is the source function, which describes the time history of the motion at the point ξ located in the fault plane Σ, and c is either α, the P-wave, or β, the S-wave velocity. The amplitudes of the waves decrease inversely proportional to r, the distance from $d\Sigma$ to the point of observation x (Aki and Richards, 1980).

For a source model having the form of a ramp with rise time τ and final slip D, and for a rupture along a fault plane with length L and width W, the far-field spectrum of the displacement waveform is

$$\Omega(\mathbf{x}, \omega)\Big| = WLD\,\frac{\sin X}{X}\left|\frac{1 - e^{i\omega\tau}}{\omega\tau}\right| \tag{9}$$

Here

$$X = \frac{\omega L}{2}\left[\frac{1}{v} - \frac{\cos\Psi}{c}\right]$$

with v the rupture velocity and Ψ the angle between the rupture direction and the direction to the point of observation. For $\omega \to 0$ the spectrum becomes flat and proportional to WLD, which in turn is related to the moment of an equivalent double-couple point source:

$$M_0 = \mu WLD$$

with μ the shear modulus of the medium.

Figure 5*a* shows the envelopes of Eq. 9 for the choice of fault parameters indicated. The corner frequency is generally seen to decrease with the increase of the strength of the earthquake. For an earthquake with a given seismic moment the corner frequency changes with the stress drop of the earthquake (Sarkar and Duda, 1985).

In Fig. 5*b* the velocity density spectra are given. Here the significance of the body wave magnitude can be clearly seen: The body wave magnitude based on the ground velocity $A(\Delta)/T$ (in Eq. 6) samples the spectrum in Fig 5*b* at the frequency corresponding to the period T. The broader the bandwidth

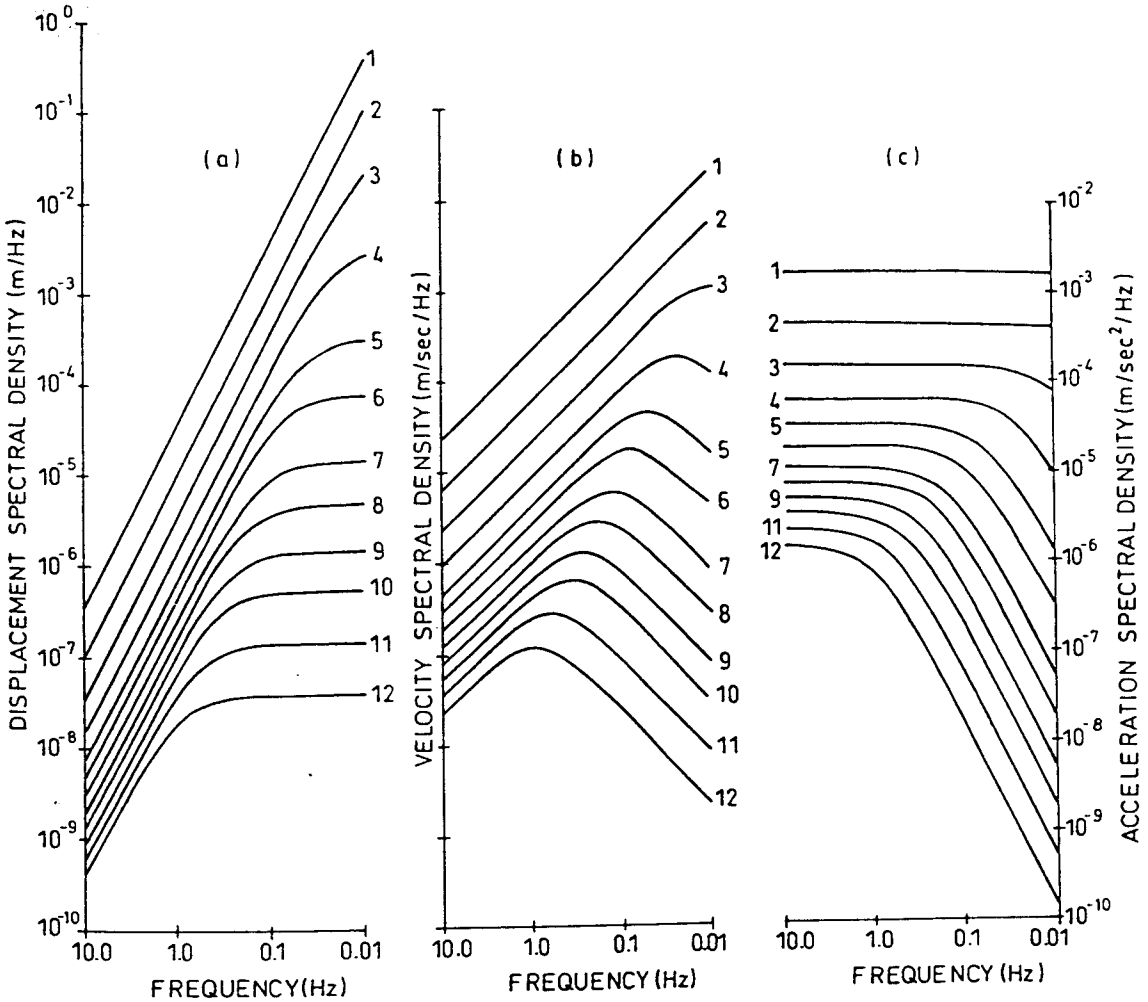

FIGURE 5. Spectral densities at a distance of 1 km from the point source complying with the ω-square model. For a stress drop of p bars the ordinate has to be multiplied by p.

of the seismograph is, the more blurred is the sampling of the velocity density, as the assumption about the constancy of F in Eq. 8 is progressively violated. The narrower the bandwidth is, the better the assumption in Eq. 8 is satisfied, and the sampling of the velocity density is more precise. Thereby the body wave magnitude is, as a rule, a function of the period T. The maximum body wave magnitude is thereby attained for the corner period (frequency).

Figure 5*c* presents the ground acceleration density spectra for the source model considered.

Quantification. The spectra in Fig. 5 range in frequency over ten octaves. A conventional seismogram, however, covers only part of the spectrum radiated from the focus. For example, from Fig. 6 it is seen that the short-period WWSSN seismograph passes only the spectrum around 1 s, and the body wave magnitude based on the record is thus a rating of the velocity spectral density at about this period. The period of this seismograph, however, was chosen because of a relatively low ground noise, not because of the particular relevance of the period for source processes. Thus, the rating of the source strength at this period is largely incidental.

On this background it is evident that a single magnitude figure cannot suffice to fully describe the strength of the source. Rather, a suit of figures sampling the radiated spectrum over a range of frequencies will yield an adequate rating of the source strength.

The practice to independently determine and publish more than one magnitude figure for a given earthquake is a step in this direction (compare with the previous section).

New Developments of the Magnitude Concept.

Synthetic Magnitude Calibrating Functions. The calibrating function projects the far-field surface motion at the epicentral distance Δ to a common distance near the source. Changes of the signal along the Earth's surface are due primarily to the radial heterogeneity of the Earth structure and, to a lesser degree, to lateral heterogeneities.

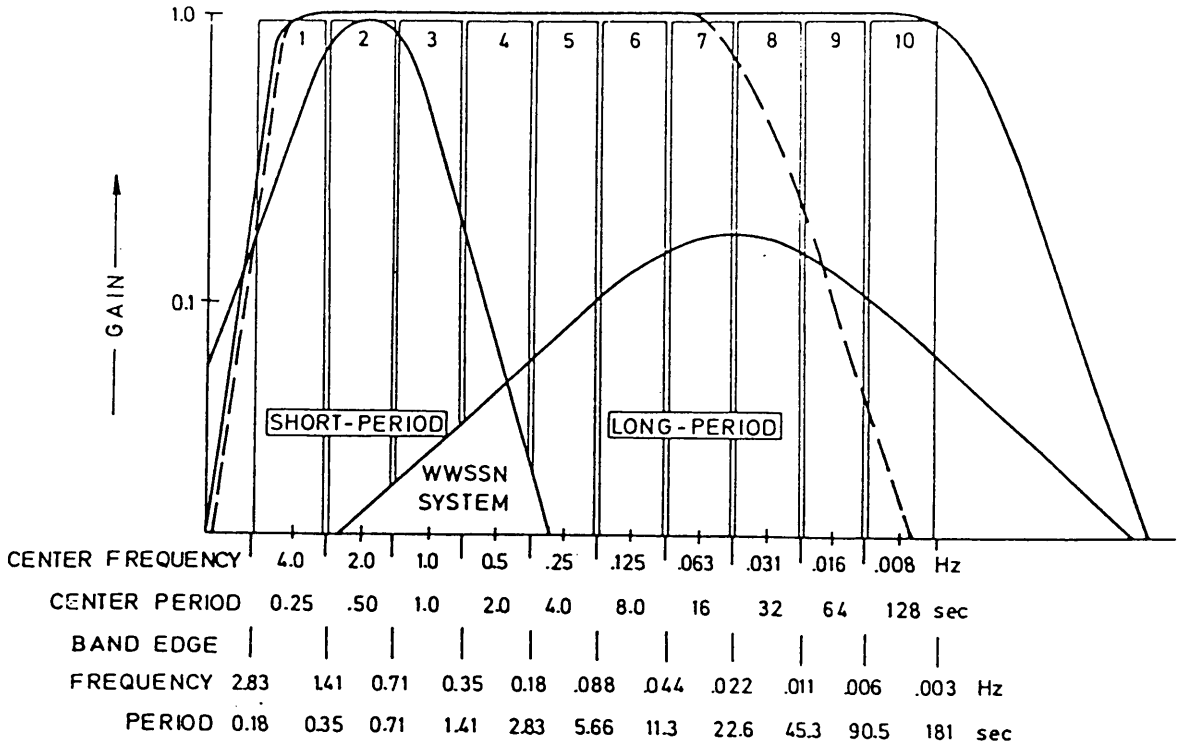

FIGURE 6. Magnification of short-period and long-period seismograph systems of the World Wide Standardized Seismograph Network. Magnification of Wielandt-Streckeisen seismograph (dashed curve). Applying inverse filtering, we obtain a seismogram with a flat magnification over nearly ten octaves. Superimposed is a system of ten one-octave filters (compare Fig. 8*a*).

The dependence on lateral heterogeneities is summarized in the "regional" and "station" corrections that are added in some cases to magnitude determinations at a given station. The calibrating functions in Eqs. 1, 3, and 5 and the ones in Fig. 3 were obtained prior to standardization of seismographs. They are based on amplitude observations on older instruments and, thus, possibly degrade magnitude measurements made on modern seismographs. For this reason, attempts are undertaken to arrive at new calibrating functions. Reliable functions have been obtained on the basis of amplitude variation curves for large explosions. They apply though to surface events only. Much effort has been expended on homogenizing the magnitudes determined from a selection of Eurasian stations (Vanek et al., 1980). In an involved iterative procedure, calibrating functions for P wave were calculated together with station corrections.

In a global scale, calibrating functions may be derived from global velocity and anelasticity models. The amplitude variation of body waves along the Earth's surface for a radially heterogeneous Earth is expressed by the so-called geometric spreading function:

$$G(\Delta, h) = \frac{1}{r_0} \left| \frac{\rho_h}{\rho_0} \frac{v_h}{v_0} \frac{\sin i_h}{\sin \Delta \cos i_0} \frac{di_h}{d\Delta} \right|^{1/2}$$

where ρ and v are the density and velocity and the subscripts h and 0 refer to the focal depth and to the Earth surface, respectively. The remaining symbols are defined in Fig. 1. In case of an anelastic medium the factor $\exp(-\pi t^*/T)$ has to be superimposed with

$$t^* = \int_S \frac{ds}{Q(T, s)v(s)}$$

where T is the period of the wave, $Q(T, s)$ and $v(s)$ are the intrinsic quality factor and the seismic velocity of the medium, respectively, at the distance s along the ray path with a total length S (Båth, 1974).

In addition to the epicentral distance and focal depth, the amplitude variation is seen to depend on the period of the wave.

Numerical computations have been performed by Nortmann and Duda (1982). Figure 7*a*,*b* shows $g(\Delta, h)$ and $a(\Delta, h)$ for the two kinds of body waves and corresponding to the radial velocity heterogeneity and to the anelasticity, respectively. The two functions are utilized in the definition of the spectral magnitudes (see the section after the next).

Broadband, Digital Recording of Seismic Body Waves. The dynamic range of conventional seismographic observations amounts to 60–80 dB. The range can be increased to more than 130 dB by digital

(Text continues on page 286.)

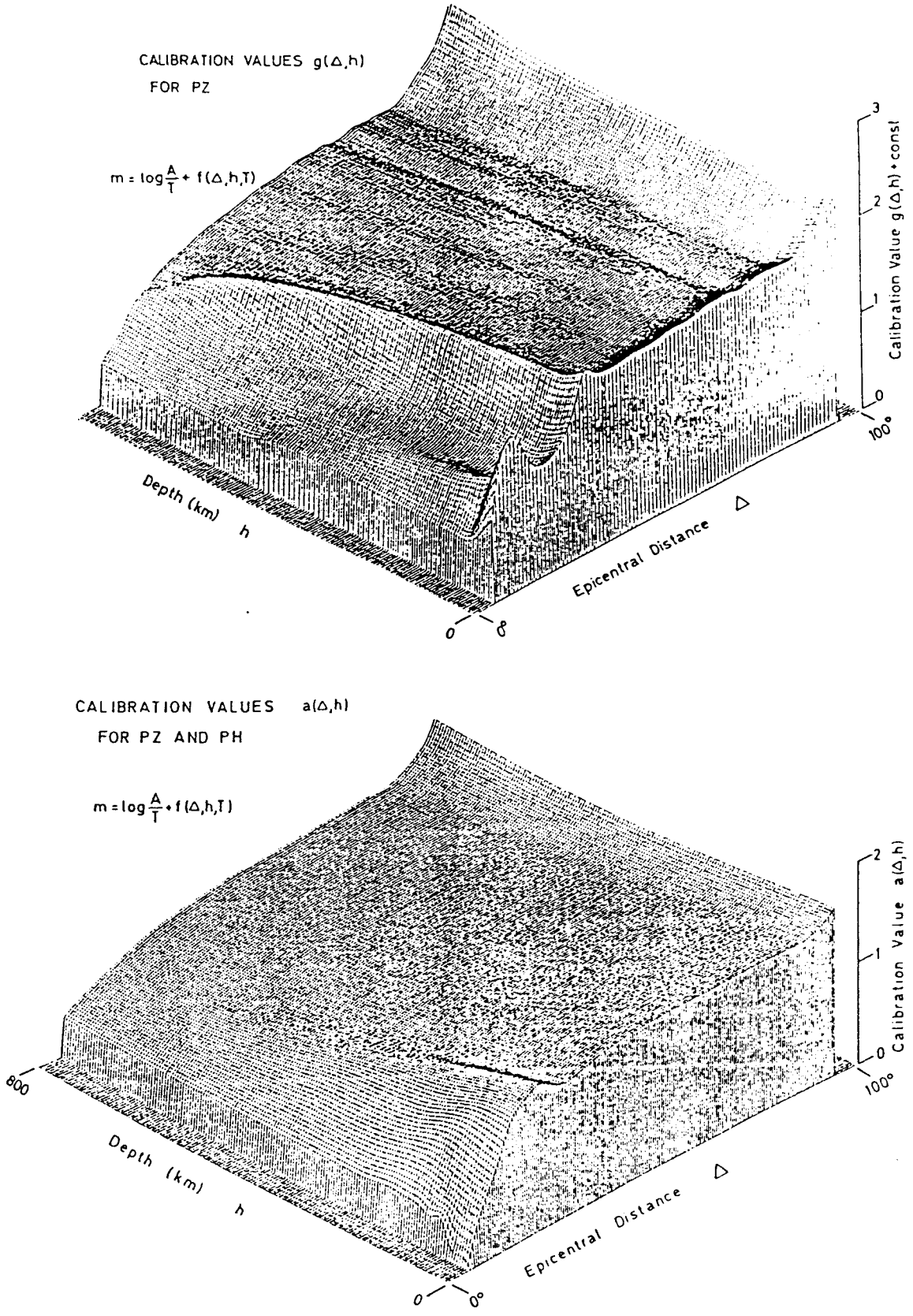

FIGURE 7. Synthetic magnitude calibrating functions. The functions $g(h, \Delta)$ and $a(h, \Delta)$ enter Eq. 11: (*left*) PZ and PH waves; (*right*) SH wave.

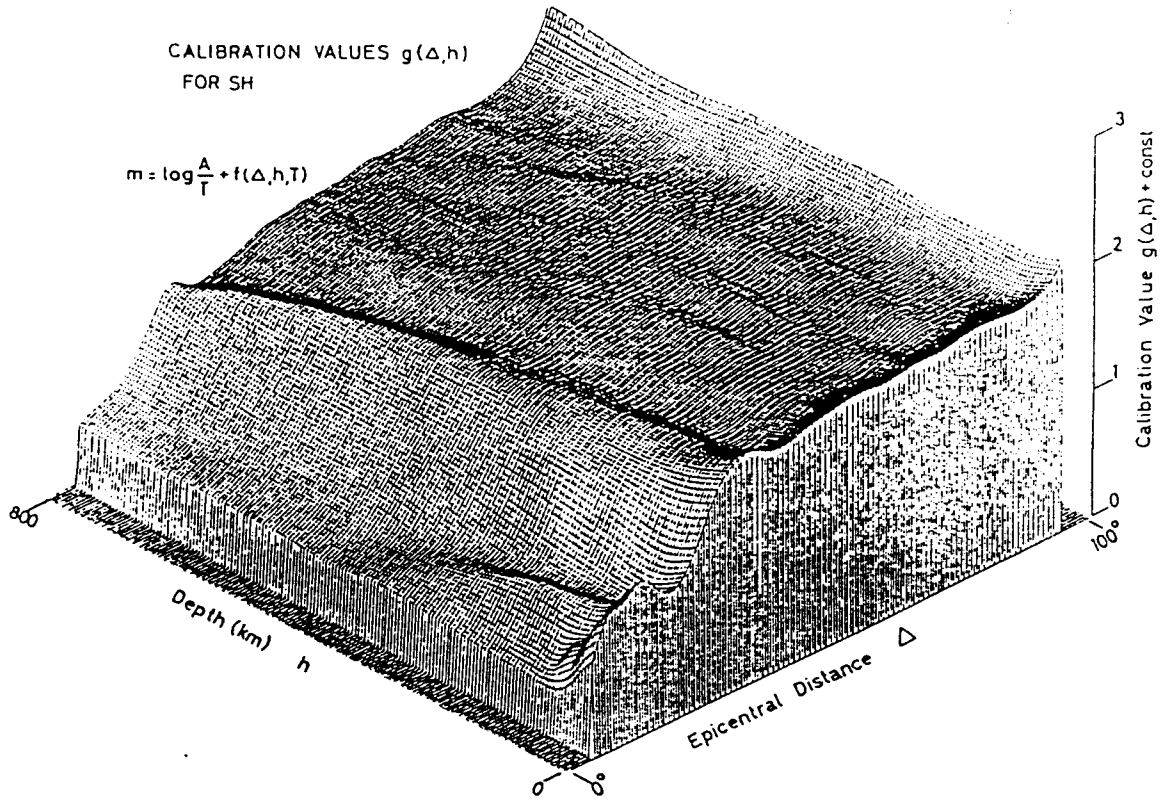

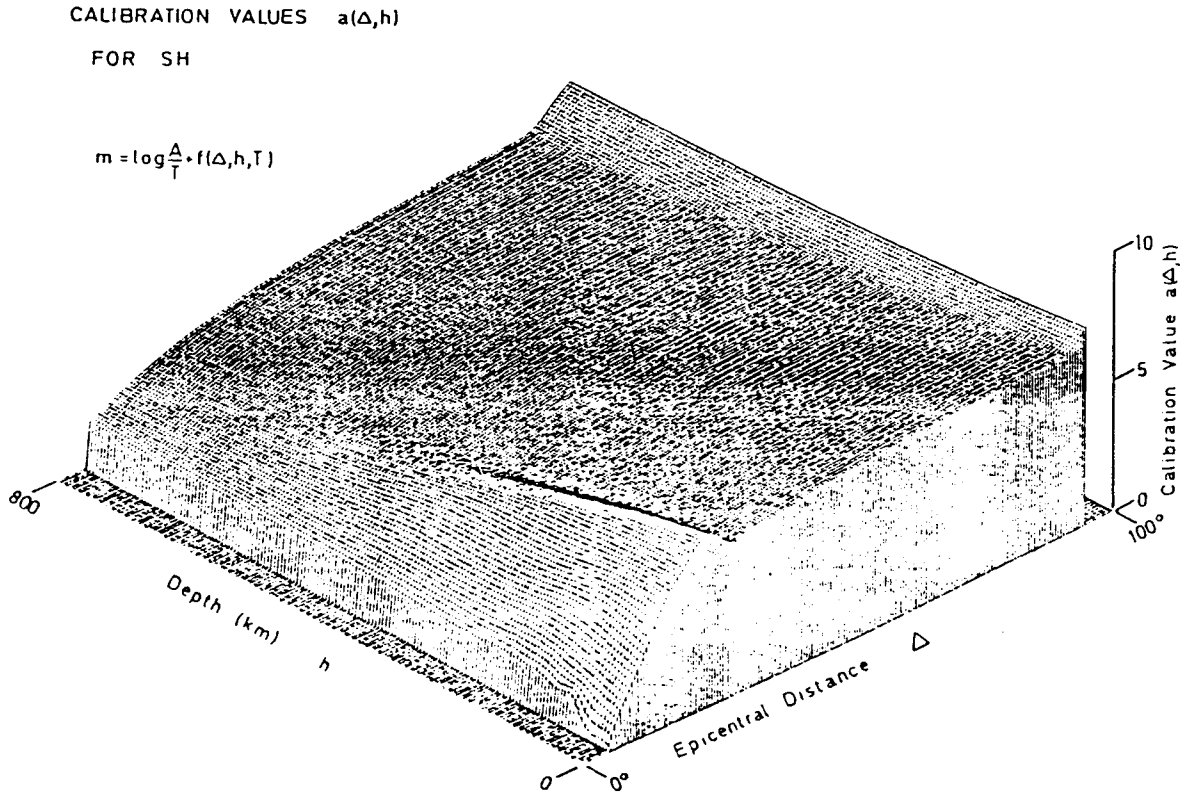

FIGURE 7. (*Continued*)

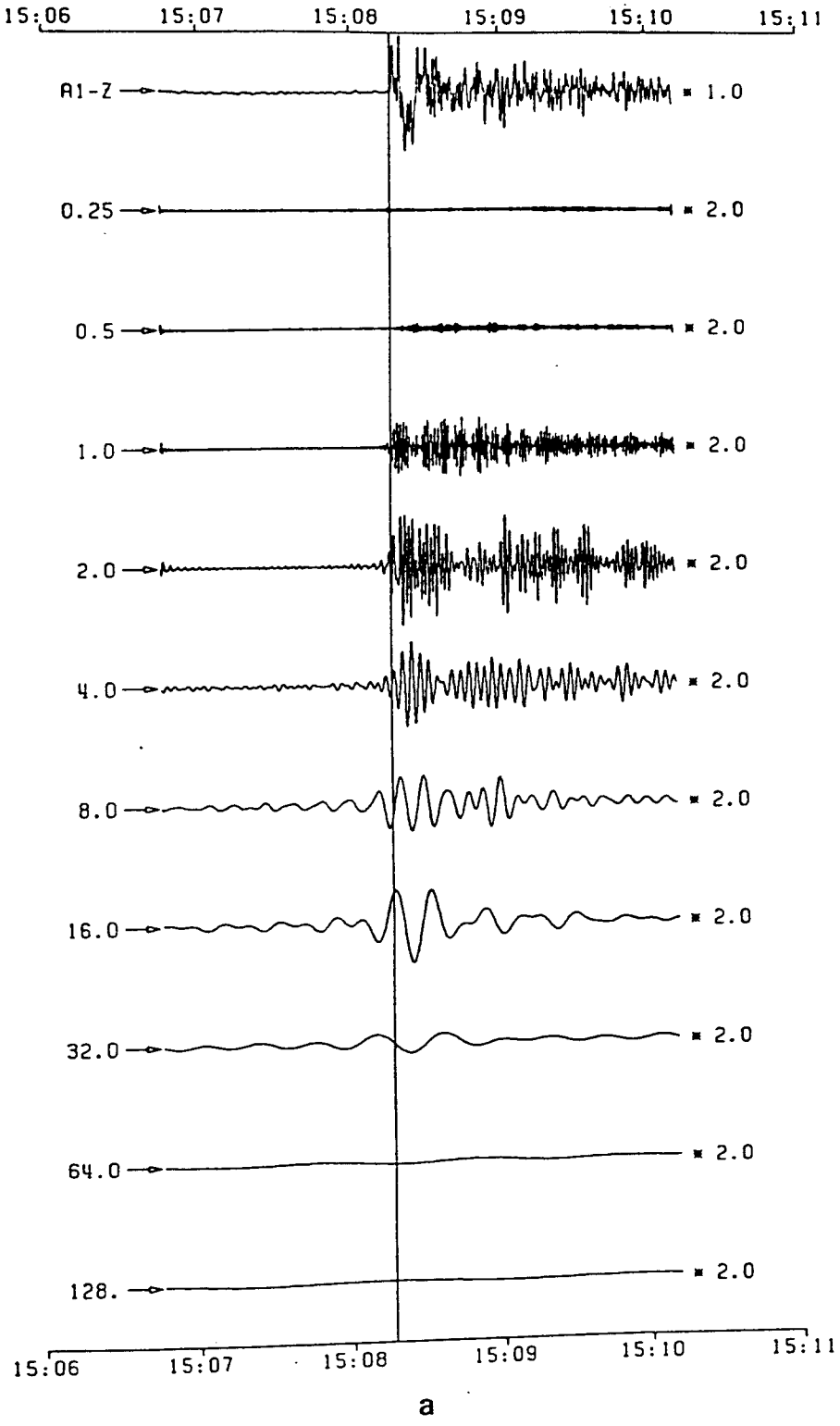

FIGURE 8. Record of Nepal earthquake (29.07.1980; 14:58:40.8; 29.60N, 81.09E; 18 km according to NEIS) as obtained at the Central Seismological Observatory of the Federal Republic of Germany at Erlangen (GRF): (*a*) Broadband (top line) and ten bandpass seismograms of vertical component of P wave. The bandpass characteristics are shown in Fig. 6. (*b*) P-wave signal and P-wave magnitude spectrum for four time windows as indicated. Only the longest window yields a stable estimate of the low-frequency component of the signal.

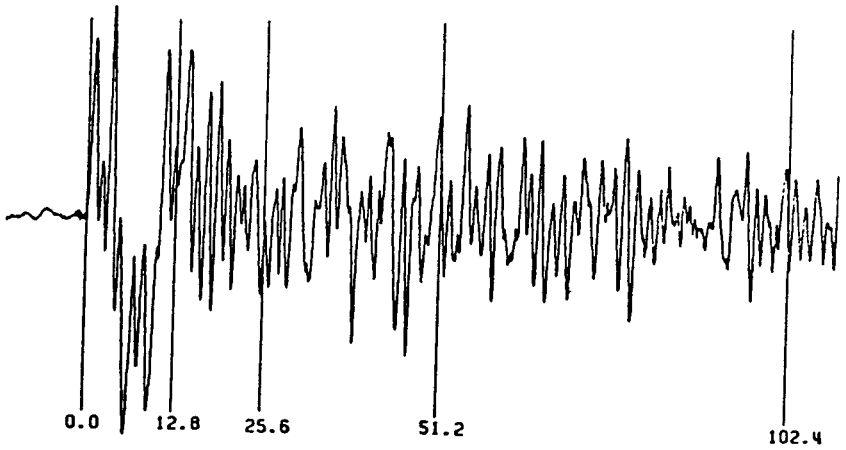

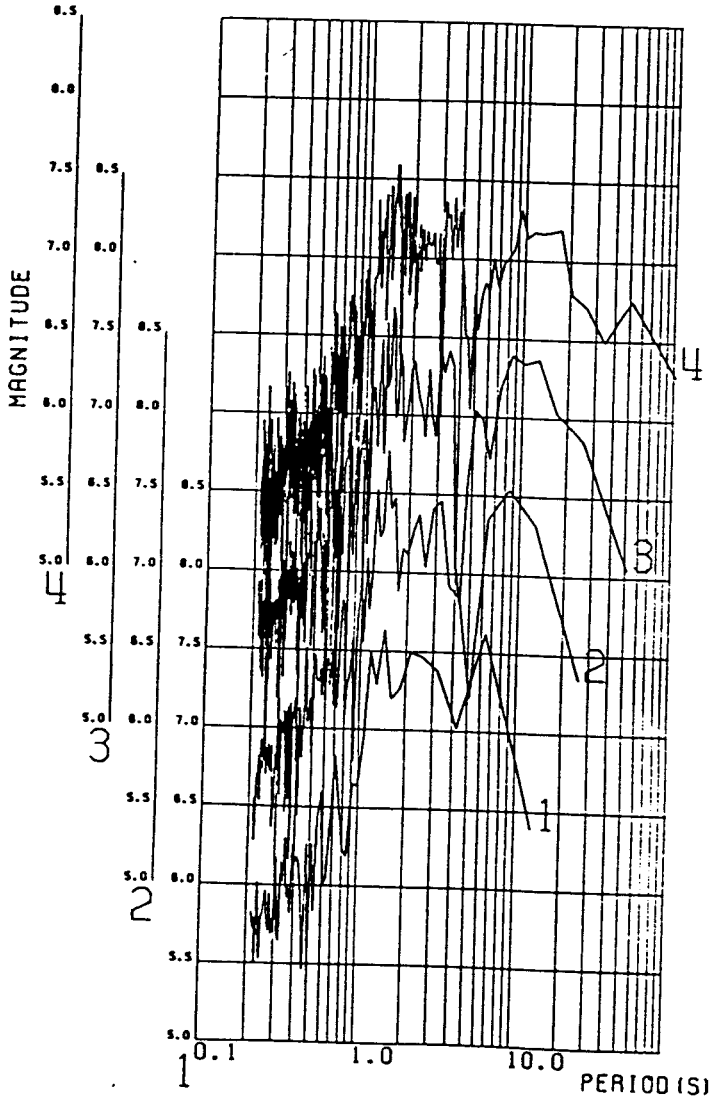

b

FIGURE 8. (*Continued*)

recording and by utilization of new seismographs (Harjes and Seidl, 1978).

Figure 6 shows the velocity magnification of the broadband, wide dynamic range seismograph (Wielandt-Strecheisen seismograph) operational at the Central Seismological Observatory of the Federal Republic of Germany at Erlangen (GRF) (dashed curve). Superimposed is the magnification of a virtual seismograph, simulated by inverse filtering of the actual record. An example of the corresponding broadband recording of the P wave (vertical component) is shown in Fig. 8*a* (top line). Applying to the recording ten one-octave bandpass filters, as defined in Fig. 6, ten bandpass seismograms are obtained as shown in Fig. 8*a*. From the bandpass seismograms body wave magnitudes can be determined as functions of the center period of the respective filter.

Spectral Magnitudes and Magnitude Spectra. On the bases of bandpass seismograms and of the new calibrating functions, the body wave magnitude is redefined:

$$m_{P,S}(T) = \log \frac{A_{P,S}(\Delta)}{T} + f_{P,S}(\Delta, h, T) + b \tag{10}$$

with the calibrating function

$$f_{P,S}(\Delta, h, T) = g_{P,S}(\Delta, h) + \frac{a_{P,S}(\Delta, h)}{T^*} + b \tag{11}$$

Equation 10 defines spectral magnitudes separately for P and S waves. T^* in Eq. 11 is a function of T, the period measured, and takes into account the period dependence of Q; b is the bandwidth correction, as given, e.g., in Table 5. For further details see Nortmann and Duda (1983).

The spectral magnitude yields estimates of the radiation strength of the seismic source at the given period. The bandwidth correction ensures that spectral magnitudes are not biased by instrumental characteristics. Thus, a spectral magnitude can be determined from conventional recordings if the bandwidth of the seismometer-galvanometer system is known.

Digital recordings permit the bandwidth of the bandpass seismograms to be varied. The narrower the filter will be, the more details of the radiated spectrum are reflected. Ultimately, the bandwidth may be reduced to the Nyquist frequency. The set of spectral magnitudes yields in this case a sampling of the velocity density spectrum radiated at the frequencies within the given range. The set is the velocity density spectrum rated in magnitude units. It is called the P-wave or S-wave magnitude spectrum.

As an example, Fig. 8*b* shows the P-wave magnitude spectrum of the same earthquake as in Fig. 8*a*. Four time windows are applied to the broadband record of the P wave. The windows range in length from 12.8 sec (spectrum 1) to 102.4 sec (spectrum 4).

All four windows yield the maximum of the spectrum at about 1.5 sec, the corner period of the P wave. The location of a secondary maximum changes from about 6 sec (spectrum 1) to about 9 sec (spectrum 4). It is concluded that only the longest window (102.4 sec) can yield a stable estimate of the longperiodic radiation intensity. However, as it is usually the case in the magnitude problem the likely contamination of the signal by later arrivals is not taken into account.

Earthquake Magnitude and Other Focal Parameters. Undoubtedly, the best single quantity characterizing the strength of the seismic source is the total seismic energy released. To determine the energy, we must integrate the velocity density spectrum of the given earthquake (see Fig. 5*b*). Thus, no unique relation can exist between the magnitude, sampling the spectrum at some period, and the energy. Though for some class of earthquakes the semilogarithmic relation

$$\log E = a + bM$$

(E is the seismic energy, M is the magnitude in general, and a,b are constants) was found to hold, the relation cannot apply in all cases.

An analogous conclusion holds for parameters such as the seismic moment M_0, fault length L, final slip D on the fault plane, stress drop $\Delta\sigma$, each parameter being an a priori independent characteristic of the strength of the source.

According to Aki (1967), the fault length is related to the corner frequency f_0 by

$$L\ (\text{km}) = \frac{C_1}{f_0}$$

The constant C_1 ranges from 0.65 to 4.47 $\text{km}\cdot\text{s}^{-1}$ (Hanks and Wyss, 1972). The maximum spectral magnitude $m(f)_{\max}$ is related to the product of the seismic moment M_0 and the corner frequency by

$$m(f)_{\max} = C_2 + \log(M_0 f_0) \tag{12}$$

A good control is given of the constant C_2 (Sarkar and Duda, 1985), and, based on Eq. 12, the seismic moment can be conveniently found. For a circular fault with radius r_0, the seismic moment is also expressed as

$$M_0 = \tfrac{16}{7}\,\Delta\sigma\, r_0^3$$

with $\Delta\sigma$ the stress drop along the fault plane (Keilis-

Borok, 1959). Thus, from the seismic moment and the fault dimension the stress drop can be calculated.

Finally, with the energy spectral density $E(f)$ related to the spectral magnitude of the given body wave by

$$E(f) = 10^{2m(f)-1.4} \quad \mathrm{J \cdot Hz^{-1}}$$

the seismic energy E in the frequency band f_1-f_2 is

$$E = \int_{f_1}^{f_2} E(f)\, df$$

The total energy is composed of that radiated in the form of P waves and S waves. In each case the principal part of the energy is reflected by the maximum spectral magnitude.

Seismic Intensity

The effects of the earthquake at near epicentral distances need to be quantified, primarily for engineering purposes. Although there is an increasing number of instruments in earthquake-prone areas capable of recording strong motions during the event, an adequately dense distribution of instruments proves to be too costly. For this and other reasons, noninstrumental observations continue to play an important role in assessing the intensity of shaking during an event as well as in predicting the intensities to be expected in future earthquakes. The noninstrumental intensity scale eventually establishes a connection between places in which the ground acceleration, velocity displacement, and the duration of shaking are instrumentally determined. Thereby it must be borne in mind that the frequency content of the signal recorded changes with epicentral distance, and the relation between the intensity and the respective element of ground motion needs to take into account the period of the signal (Hurtig and Stiller, 1984).

The seismic intensity reflects the integral effect of all elements of ground motion. The intensity scales presently in use have 12°. The scales differ from each other slightly, due to the variation of building standards in different parts of the world. Table 6 gives the abridged modified Mercalli intensity scale, as it was developed for California (and most of the United States) from the Mercalli scale introduced in Italy around the turn of the century (Bolt, 1978).

Concentric stripes at the Earth's surface experiencing the same seismic intensity are separated from

TABLE 6. Abridged Modified Mercalli Intensity Scale

Value	Description of Sensation to Human Beings and Damage to Objects
I.	Not felt except by a very few under especially favorable circumstances.
II.	Felt only by a few persons at rest, especially on upper floors of buildings. Delicately suspended objects may swing.
III.	Felt quite noticeably indoors, especially on upper floors of buildings, but many people do not recognize it as an earthquake. Standing motorcars may rock slightly. Vibration like passing of truck. Duration estimated.
IV.	During the day felt indoors by many, outdoors by few. At night some awakened. Dishes, windows, doors disturbed; walls make creaking sound. Sensation like heavy truck striking building. Standing motorcars rocked noticeably.
V.	Felt by nearly everyone, many awakened. Some dishes, windows, and so on broken; cracked plaster in a few places; unstable objects overturned. Disturbances of trees, poles, and other tall objects sometimes noticed. Pendulum clocks may stop.
VI.	Felt by all, many frightened and run outdoors. Some heavy furniture moved; a few instances of fallen plaster and damaged chimneys. Damage slight.
VII.	Everybody runs outdoors. Damage negligible in buildings of good design and construction, slight to moderate in well-built ordinary structures, considerable in poorly built or badly designed structures; some chimneys broken. Noticed by persons driving cars.
VIII.	Damage slight in specially designed structures, considerable in ordinary substantial buildings with partial collapse, great in poorly built structures. Panel walls thrown out of frame structures. Fall of chimneys, factory stacks, columns, monuments, walls. Heavy furniture overturned. Sand and mud ejected in small amounts. Changes in well water. Persons driving cars disturbed.
IX.	Damage considerable in specially designed structures; well-designed frame structures thrown out of plumb; great in substantial buildings, with partial collapse. Buildings shifted off foundations. Ground cracked conspicuously. Underground pipes broken.
X.	Some well-built wooden structures destroyed; most masonry and frame structures destroyed with foundations; ground badly cracked. Rails bent. Landslides considerable from river banks and steep slopes. Shifted sand and mud. Water splashed, slopped over banks.
XI.	Few, if any, (masonry) structures remain standing. Bridges destroyed. Broad fissures in ground. Underground pipelines completely out of service. Earth slumps and land slips in soft ground. Rails bent greatly.
XII.	Damage total. Waves seen on ground surface. Lines of sight and level distorted. Objects thrown into the air.

each other by lines called *isoseismals*. They are usually elongated in the direction of the fault that is activated during the earthquake. The distance between isoseismals increases with the focal depth of the earthquake. Respective empirical relations show a pronounced regional variability.

The distribution of isoseismals for a multitude of earthquakes in a region is of basic importance for estimating the distribution of shakability in the region. The latter, in turn, enters the problem of seismic zoning, together with parameters like the maximum magnitude of the earthquakes to be expected, their frequency distribution, the frequency content of the radiation from the source, and others.

SEWERYN J. DUDA

References

Aki, K., 1967. Scaling law of seismic spectrum. *Jour. Geophys. Research* **72**, 1217–1231.

Aki, K., and P. G. Richards, 1980. *Quantitative Seismology—Theory and Methods*, vols. I and II. San Francisco: W. H. Freeman, 932 p.

ANS, 1966. *American National Standard, specification for octave, half-octave, and third-octave band filter sets*. New York: American National Standards Institute, Inc., 26 p.

Båth, M., 1973. *Introduction to Seismology*. Basel and Stuttgart: Birkhäuser Verlag, 395 p.

Båth, M., 1974. *Spectral Analysis in Geophysics*. Amsterdam-Oxford-New York: Elsevier, 563 p.

Båth, M., 1977. Teleseismic magnitude relations. *Annali di Geofis.* **30**, 299–327.

Båth, M., 1981. Earthquake Magnitude—Recent Research and Current Trends. *Earth-Sci. Rev.* **17**, 315–398.

Bolt, B. A., 1978. *Earthquakes—A Primer*. San Francisco: W. H. Freeman, 241 p.

Gutenberg, B., and C. F. Richter, 1956. Magnitude and Energy of Earthquakes. *Annali Geofisica* **9**, 1–15.

Hanks, T. C., and M. Wyss, 1972. The use of body wave spectra in the determination of seismic source parameters. *Seismol. Soc. America Bull.* **62**, 561–589.

Harjes, H.-P., and D. Seidl, 1978. Digital recording and analysis of broad-band seismic data at the Graefenberg (GRF)-array. *Jour. Geophys.* **44**, 511–523.

Hurtig, E., and H. Stiller, 1984. *Erdbeben und Erdbebengefährdung*. Berlin: Akademie-Verlag, 328 p.

Keilis-Borok, V., 1959. On estimation of the displacement in an earthquake source and of source dimensions. *Annali di Geofis.* **12**, 205–214.

Nortmann, R., and S. J. Duda, 1982. The amplitude spectra of P- and S-waves and the body-wave magnitude of earthquakes. *Tectonophysics* **84**, 251–275.

Nortmann, R., and S. J. Duda, 1983. Determination of spectral properties of earthquakes from their magnitudes. *Tectonophysics* **93**, 251–275.

Richter, C. F., 1935. An instrumental earthquake scale. *Seismol. Soc. America Bull.* **25**, 1–32.

Richter, C. F., *Elementary Seismology*. San Francisco and London: W. H. Freeman, 768 p.

Sarkar, D., and S. J. Duda, 1985. Spectral P-wave magnitudes, Aki's ω-square model and source parameters of earthquakes. *Tectonophysics* **118**, 175–193.

Vanek, J., A. Zatopek, V. Karnik, N. V. Kondorskaya, Yu. V. Riznichenko, E. F. Savarensky, S. L. Solov'yov, and N. V. Shebalin, 1962. Standardization of magnitude scales (in Russian). *Akad. Nauk CCCP, Izv. Ser. Geofiz.* 2, 153–158.

Vanek, J., N. V. Kondorskaya, and L. V. Christoskow, 1980. *The Earthquake Magnitude in Seismological Practice - PV- and PV$_z$- Waves* (in Russian). Sofia: Bulgarian Academy of Sciences, 263 p.

Cross-references: *Earthquake Mechanisms; Earthquakes: Hazards and Prediction; Earthquakes and Crustal Deformation; Earthquake Seismology; Earthquakes and Seismicity; Seismic Instrumentation; Seismic Instrumentation: History; Seismicity and Plate Tectonics; Strong Motion Seismology.*

Scientific Technical Report STR 95/TK
DOI: 10.2312/GFZ.b103-95tk7

Introduction into methods of seimological routine practice

by

P. Bormann and W. Strauch

The basic tasks of a seismological observatory are to maintain equipment in continous operation, with complete 3-component sets of basic types of seismographs (short-, medium- and long-period), calibrated and adjusted to conform with agreed standards, to produce records which conform with necessary standards for research purposes, internal use and international exchange, to undertake preliminary readings needed to meet the immediate requirements of data reporting to local, regional and global, national or international agencies for scientific, commercial or other use. Observatories should be sited on hard rock remote from local disturbances (traffic, heavy machines, large lakes etc.) but with access to personnel and power supply. Before installing new stations measurements of signal to noise ratio at possible sites should be made in order to avoid unsuitable locations.

Seismological networks contain a number of individual recording stations controlled from a central office. Until today most of the stations are of conventional type equiped to record at least a vertical but frequently also two horizontal components (N-S, E-W) of short period and in many cases also long-period earth motion on photographic paper or, after electronic amplification, on direct writing systems. The routine of an ordinary station can be regarded the work for one to two men permanent staff. They have to maintain the facilities and instrumentation, to exchange the recording paper, to develope the photographic film and to carry out instrument calibration and time control. Good mechanical or quartz clocks manually or automatically controlled by radiotime or directly recorded radio-time are used as time basis. An accuracy of time measurements on the records of 0.1 sec must be guaranteed. Quality of recording traces (sharp, without irregular jumps or light changes; spacing of time marks; direction, shape and amplitudes of calibration impulses) must be controlled daily. Breaks or irregularities in recordings have to be noticed and reported. The staff should be able to make preliminary readings of the seismogrammes. The quality of the records depends to a high degree on the qualification, disciplin and engagement of the station personnel and to a lesser extent on technical facilities available.

Sometimes the seismic readings are not routinely done at the stations but the records (often undeveloped) are sent to the central office, where a more qualified staff with better facilities for processing, handling and evaluation of seismic recordings is operating. More advanced equipment and methods such as low-power magnetic tape recordings and automatic data transmission (wireless or by telephon-line) require less or no personnel at the stations. The routine work is then almost exclusively concentrated at the central station or office. Planning a new seismic network a trade-off has to be made to find the optimum between the availability and cost of station facilities (local and/or central), instrumentation, infrastructure (communication, lifelines), qualified manpower and the requirements for data quality and availability under the conditions of the given country.

The evaluation of seismic records should be carried out by a scientist himself or by good technicians under his guidance and control. The basic requirement is to recognise the occurrence of an earthquake in the record, to identify the nature of

clearly recognizable groups of waves (phases), to describe them in terms of internationally agreed symbols and to determine the time of their occurrence (onset-time). Experience helps to discriminate between real earthquakes and disturbances and to carry out these readings efficiently and with high quality. Often it is sufficient to read only the first phase of each earthquake though many other phases may be discernable. Proper identification and indication of the direction of first motion (FM) (+ for compression, - for dilatation) provides a very useful information for the determination of the focal mechanism of the seismic event and should be done where ever possible. Besides the onset-time the amplitude A and dominant period T of P-, S- and surface waves (at least) should be measured since they are the basic data for magnitude determinations (cf. below). The amplitude A of the ground motion can be obtained in a first approximation by dividing the trace amplitude B by the magnification of the seismograph for the respective period T as given by its frequency characteristic for a stationary vibration (fig. 1). The time of the zero crossing between the points of maximum deflection from which the phase amplitude is determined may also be measured.

The character of a seismogramme is strongly influenced by distance, depth of focus, source mechanism and size of the event. Near earthquakes have short total duration and a large high-frequency content (up to 10 Hz). With increasing distance the record becomes more widespread, in different distance ranges the picture is more or less complex. The predominant periods of teleseismic events ($\Delta > 10^{\circ}$) are about 1 sec for P-waves (in short-period recordings), 5 - 10 sec for S-waves and 10 - 30 sec for surface waves (in medium- and long-period records, respectively).

The phases can be identified by their time difference to the first arriving wave (P or PKP) using travel-time tables or curves. Simultaneously the best fit of properly identified phases with the travel-time curve provides a rather good estimate of the epicentral distance Δ ($\delta\Delta$ generally $< \pm 2^{\circ}$) and sometimes also allows to determine the depth of the focus (especially if so-called depth-phases could reliably be identified). Besides the travel-time differences the occurrence, polarization as well as the relative amplitudes and periods of seismic phases in short- and long-period records, respectively, are important additional identification criteria. The azimuth from the station to the epicentre can also be obtained from the polarization of the first arrival as determined by means of 3-component records. Thus a preliminary location of seismic events can be obtained by using records of a single station only.

The magnitude of an earthquake is a kind of instrumental measure of its size or energy. It is routinely determined from seismic waves adjusted by a calibrating function taking the energy decay depending on epicentral distance and focal depth into account. For reliable local and regional magnitude determinations calibration functions must be derived from special investigations for the given region. Maximum trace amplitude, as well as amplitude of a distinct phase (eventually divided by the corresponding period) or duration of the recorded event are used as typical measures. For teleseismic earthquakes global calibrating functions (after GUTENBERG and RICHTER, 1956 for P-waves and KARNIK et. al., 1962 for surface waves) are used in world wide practice. Here magnitude is determined mostly from amplitude to period ratio of P-waves in short period records or of surface waves on long period records, both horizontal and vertical (fig. 2).

If records of several stations are available localizations of near as well as distant

earthquakes can be carried out using phase arrival times. For first preliminary localizations simple graphical methods are very usefull. Different algorithms are available for finding the focus numerically. The most simple algorithms can already be run on programmable pocket calculators. More sophisticated programmes need larger computers. The accuracy of localization is influenced by geometrical configuration of the network, size of the event, experience of operators, accuracy of onset time determination, number of stations, used earth model and algorithm.
In case of dense networks commonly only first P-arrivals are used (Pg, Pn for near events). For small networks also onset-times of later phases must be included, especially in the case of foci outside the station network. In very modern local networks microprocessor controlled automatic localization is used. The determination of source parameters of teleseismic earthquakes by means of local or regional nets is principally possible but recommended for preliminary purpose only because of low accuracy. In modern systems with centralized digital registration so-called array techniques can be used. Apparent velocity and azimuth of incident seismic waves are determined by means of sophisticated computer programmes(beam forming, correlation, adaptive processing).
The readings from single observatories or from networks are exchanged with other mainly neighbouring stations and transferred to national, regional or global centres for further processing. Reports are given by telegram, air letter, machine readable forms or printed bulletins. Often telegrams or telex reports in standard formats are used for fast data transmission to other agencies. The most important centres are the World data centres in Moscow (Soviet Union), Golden (USA) for relatively fast global localization.
Using the output of these and of other agencies the stations check their first evaluations and give their data to the International Seismological Centre in Newbury (Great Britain) for final processing. The bulletins of this agency are the most complete in a global sense.
In GDR there are three conventional first rate seismological observatories, a centralized network with digital registration (s. example of a record, fig. 3), a microarray and a computer controlled broadband station in operation. For special purposes portable seismic stations with autonomous digital data recording on magnetic tape or with data transmission by radio-link to a centre are used. The data of these different systems are either routinely processed or used for special scientific studies.

Selected references

Manual of seismological observatory practice.
World Data Centre A, Sept. 1979.

ADAMS, R.D.: Survey of practice in determining magnitudes of near earthquakes. Part 2: Europe, Asia, Africa, Australasia, the Pacific.
World Data Centre A, Report SE-8, 1977.

BORMANN, P.: Statistische Untersuchungen zur Ortung teleseismischer Ereignisse aus Raumwellenuntersuchungen der Station Moxa.
Veröffentl. Zentralinstitut Physik der Erde, Nr. 9, 1971.

BORMANN, P.: Travel time and azimuth residuals of body waves at Moxa station (GDR) and their possible causes.
XIIIth General Assembly of ESC (Part I), Bukarest, 1974.

CHRISTOSKOV, L.; KONDORSKAYA, N.; VANEK, J.: Homogeneous magnitude system of the eurasian continent: P-waves.
World Data Centre A, Report SE-18, 1979.

DOUGLAS, A.; LILWALL, R.C.; YOUNG, J.B.: Computer programs for epicentre determination.
AWRE Report No. 028/74, 1974.

GUTENBERG, B.; RICHTER, C.F.: Magnitude and energy of earthquakes.
Annali di Geofisica 9 (1956).

HURTIG, E. et. al.: Das seismologische Stationsnetz der DDR.
Gerlands Beiträge Geophysik 89 (1980) 3/4.

KARNIK, V. et. al.: Standardization of the earthquake magnitude scale.
Stud. geophys. et geod., Prag, 6 (1962).

LEE, W.H.K.; LAHR, J.C.: HYPO 71 (Revised): A computer program for determining hypocenter, magnitude and first motion pattern of local earthquakes.
USGS Open file report 75-311, 1975.

LEE, W.H.K.; WETMILLER, R.J.: Survey of practice in determining magnitudes of near earthquakes. Part 1: North, Central and South America.
World Data Centre A, Report SE-9, 1978.

LEHMANN, I.: Characteristic earthquake records.
Mem. Geod. Inst. Denmark, Ser. 3, 18 (1954).

Mitteilung des Zentralinstituts für Physik der Erde Nr. 1048

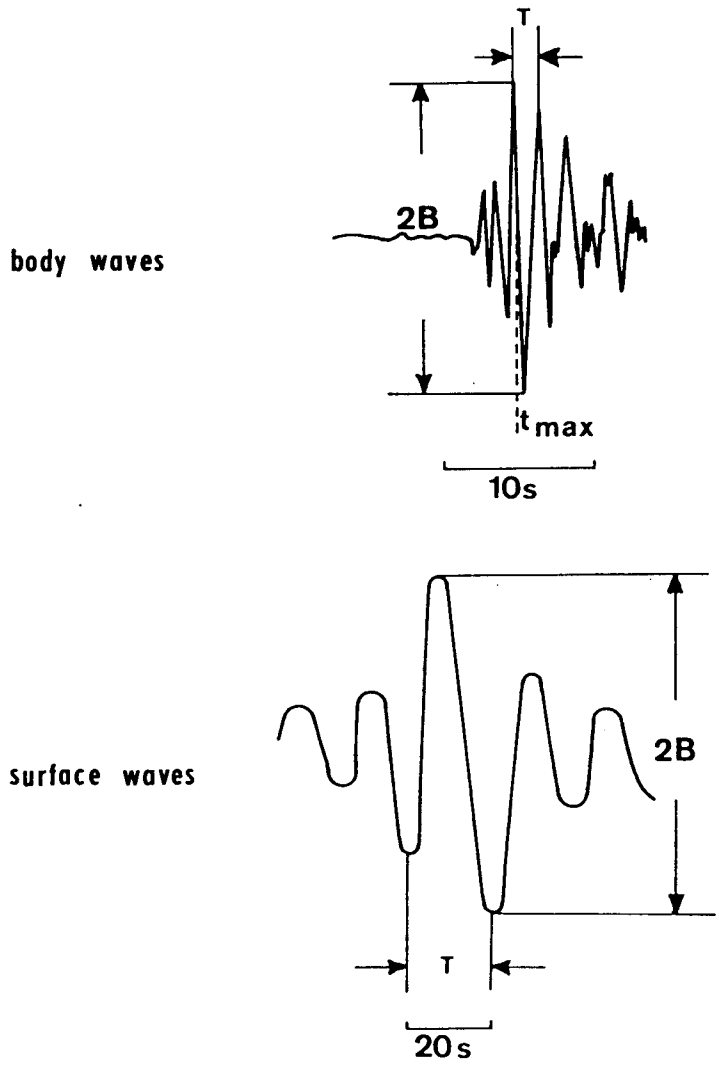

Fig. 1
Amplitude and period measurement

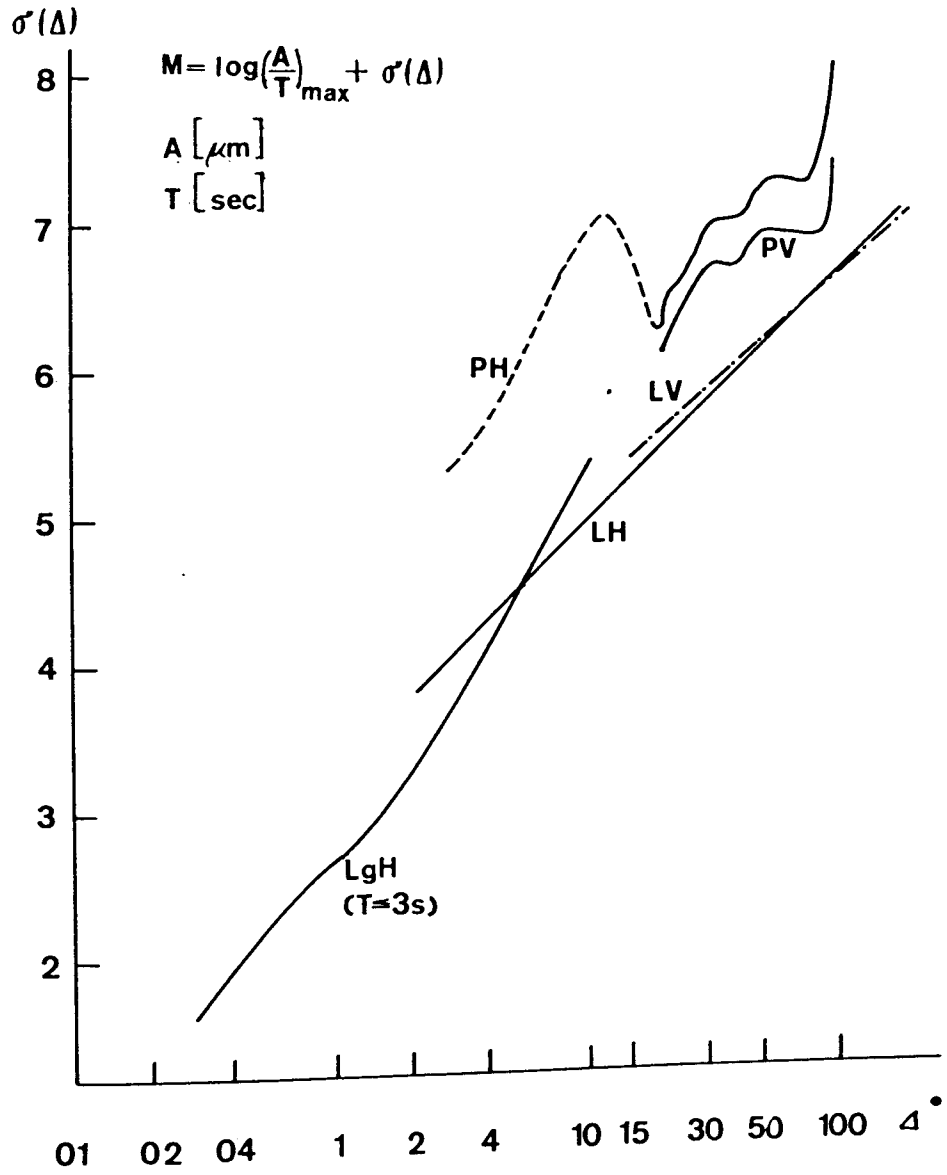

Fig. 2
Calibrating functions for magnitude determination from P and surface (L) waves, vertical (V) or horizontal (H)

Scientific Technical Report STR 95/TK
DOI: 10.2312/GFZ.b103-95tk7

GeoForschungsZentrum Potsdam

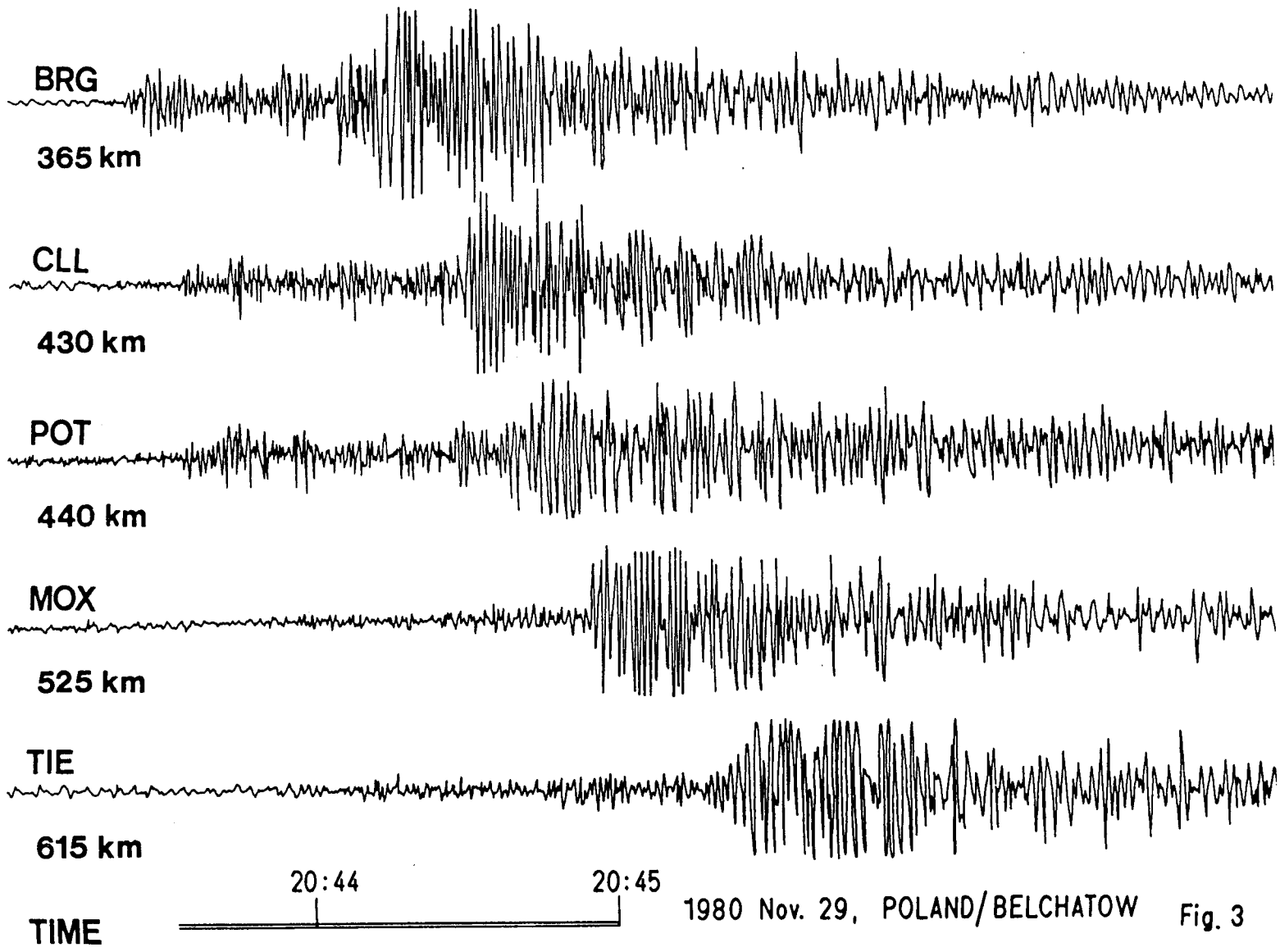

Fig. 3

Appendix: Instruction for Measuring and Reporting Amplitudes and Periods for Magnitude Determination from Observations at Regional and Teleseismic Distances

(Recommendation by IASPEI Commission on Practice, Canberra 1979)

The determination of earthquake magnitude is based on observations of amplitude A and period T of seismic waves. It is essential for subsequent earthquake studies to report the time that an observation of A and T is made.

The amplitude of a seismic signal on a record is defined as its deflection from the base-line. It is important that A, T, and the time of the observation should be measured for P, S. and surface waves.

For many phases, and particularly in surface waves, the record is symmetrical about the base-line and amplitude may be determined either by direct measurement from the base-line or by halving the peak-to-trough deflection. For phases that are strongly asymmetrical the amplitude should be measured as the maximum deflection from the base-line.

The amplitude and period from the vertical component is the most important. If horizontal components are available, readings from these should be also reported. When such readings are reported, they should be measured at the same time on the record so that the amplitudes can be combined vectorially.

The period T corresponding to amplitude A is measured in seconds between two neighbouring peaks, or two neighbouring troughs, or from trace crossings of the base-line.

P WAVES

The P wave amplitude measured should be that of the maximum trace deflection, usually within the first 25 seconds of the first onset or before the arrival of the next clear phase, but this interval may be extended up to 60 seconds for large earthquakes recorded on broad-band instruments. When more than one component is available, the amplitude from each should be reported separately.

The observation time should always be measured as the time to the first peak or trough of the trace cycle being measured. This need only be estimated to the nearest 1 to 2 seconds. The amplitude measured on the record should be converted to ground motion in nanometres or some other stated SI unit, using the amplitude-period response curve of the instrument. When several instruments of different frequency response are available, the amplitude and period from each should be reported separately.

S WAVES

The measurement of amplitudes and periods on the seismogram is performed as described above. It is recommended that the beginning of the S wave is checked against travel-time tables. The amplitude and period should be selected in the interval up to 40-60 seconds after the beginning of S waves.

SURFACE WAVES

For surface waves the measurement of amplitudes, period and times of observation on records is performed as described above for the maximum deflection from the base-line. If the maximum deflection does not occur in the period range 17-23 seconds, then the largest deflection within this range should also be reported for teleseismic distances ($\triangleq > 25^{o}$).

For large earthquake when mantle waves are often recorded, amplitudes and periods of the vertical and horizontal components with the period in the neighbourhood of 200 seconds should also be measured.

The observations of A and T for all waves mentioned above should be included in station report. It is essential in reporting such observations that the type of instrument used is clearly stated. For this, the classification given in the manual of Seismological Observatory Practice may be used. Broad-band instruments are preferred for all measurements of amplitude and period.

NOTE: Seismograms can be very complicated and, ultimately, the selection of a particular measurement must be left to the observer's experience.

Additional considerations for local earthquakes

TRACE AMPLITUDE MEASUREMENT

On some types of short-period instruments it is not possible to measure the period of seismic waves recorded from close events, and thus to convert trace deflection to ground motion. In such cases magnitude scales may be used which depend on measurement of trace amplitude.

DURATION MEASUREMENT

For local earthquakes, stations should report the signal duration defined as: the time in seconds between the first onset and the time the trace never again exceeds twice the noise level which existed immediately prior to the first onset. Very often local earthquake recordings will cause high-gain, short-period instruments to saturate, thereby making an amplitude reading impossible even for small seismic disturbances. Therefore, to provide data from which to derive relations between magnitudes based on duration and those based on signal amplitude, both types of observations should be made of as many of the same earthquakes as possible.

Preliminary notes for the interpretation of seismograms

In the Bulletin the international code is used:

1. Phase interpretation

Pg — direct longitudinal wave in near epicentral distances ($D < 10°$)

Pb, Pn — guided longitudinal head waves along the CONRAD- or MOHOROVIČIĆ-discontinuity ($D < 10°$)

P — direct longitudinal wave travelled through the earth mantle

P diff — direct longitudinal wave diffracted around the core boundary

PKIKP — direct longitudinal wave travelled through the inner core (travel-time branch DF)

PKHKP — direct longitudinal wave refracted in the intermediary zone between inner and outer core. Phase symbol according to BOLT [1] (travel-time branch GH)

PKP2 — direct longitudinal wave travelled through the outer core only (travel-time branch AB)

PKP — first noticeable onset of longitudinal core phase not identified

PP, PPP — waves reflected at the earth surface with permanent longitudinal character

PKKP — core phase reflected once within the core at the outer core boundary

PKPPKP — longitudinal core phase reflected at the earth surface

Sg — direct transversal wave in near epicentral distances ($D < 10°$)

Sb, Sn — guided transversal head waves along the CONRAD- or MOHOROVIČIĆ-discontinuity ($D < 10°$)

S — direct transversal wave travelled through the earth mantle

SKS — direct wave travelled transversal through the mantle and longitudinal through the core

SS, SSS — waves reflected at the earth surface with permanent transversal character

SKKS — wave travelled transversal through the mantle, longitudinal through the core and reflected within the core at the outer core boundary

PcP, ScS, PcS, ScP — longitudinal and transversal waves with steady or changing character reflected at the outer core

PS, SP, PPS — longitudinal and transversal waves with changing character reflected at the surface of the earth

pP, sP. pPP, sPP, pPKIKP, sPKP2, pS — phases of deep-focus earthquakes of longitudinal or transversal waves with steady or changing character. p;s — reflected near the epicentre

pPKP, sPKP — phases of deep focus earthquakes of longitudinal core waves not exactly to be coordinated

SKP, PKS — core phases with different character before and after the direct transit of the core

SKSP — SKS wave with longitudinal character after the reflection at the surface of the earth

P1, P2, P3, . . , S1, S2, . . . — multiple onsets of body waves

Pn, Sn — teleseismic Pn and Sn waves in the epicentral distances $23° < D < 40°$ after BÅTH [2]

Pa, Sa — waves probably guided in the astenosphere channel or higher modes of surface waves

PL leaking modes, normal dispersed train of waves of periods greater than about 10 s, beginning at or near the time of initial P-wave

X, Y, Z — remarkable phases of body waves, not to be identified

LmV, LmH — maximum of the vertical and horizontal component respectively of longperiodical surface waves. If there are several maxima with comparable proportions in A/T; the numeration was carried out in a temporal sequence e.g. Lm1H, Lm2H

The phase symbol is followed by the designation of the type of seismometer from which the time of onsets is taken.

A — seismograph with amplitude characteristic of type A (short-period)

B — seismograph with amplitude characteristic of type B (middle-period)
C — seismograph with amplitude characteristic of type C (long-period)

2. Measurements of amplitudes and calculation of magnitudes

All data of amplitudes and periods printed in the column "remarks" are always taken from the records of the same instruments, from which are taken the onset-times of the corresponding phases. The symbol of phase and component is followed by the symbol of the type of instruments e.g.: PV A, PV B, LmH B, LmV C.

Data of amplitudes obtained from records of instruments of type A are given in units of length of nm (1 nm = 1 nanometre = 10^{-6} millimetre). Data of amplitudes obtained from instruments of type B and such obtained from instruments of type C are given in units of length μm (1 μm = 1 micrometre = 10^{-3} millimetre) e. g.: PVA 1.3 s 38.6 nm, SHB 10 s 3.2 μm, LmH B 22 s 15 μm.

Magnitudes are determined from all those phases, for which calibrating functions are known and internationally used, i. e.

for maxima of body waves P(PH, PV), PP(PPH, PPV), and S(SH)-Q-functions from GUTENBERG and RICHTER [3] — and

for maxima of surface waves (h < 100 km) LmH, LmV — calibrating functions from Prague σ [4] —.

The station correction S was not yet taken into consideration.

MB — magnitude of vertical component V of the first onset of P-waves given by NEIS
MS — magnitude of horizontal component H of the maximum surface wave given by NEIS
M — magnitude calculated from given data of station Moxa. Notice the wave type and the type of instruments written on the same line

3. Direction of body-wave onsets

If the direction of motion at the beginning of a wave onset is clearly to be recognized, the sign + or — is placed before the phase symbol. It means:

in the Z component	+	ground motion upwards, compression
	—	ground motion downwards, dilatation
in the N component	+	ground motion to the north
	—	ground motion to the south
in the E component	+	ground motion to the east
	—	ground motion to the west

4. Further abbreviations

i — sharp beginning of phase motion (impetus)
e — gradual beginning of phase motion (emersio)

Scientific Technical Report STR 95/TK
DOI: 10.2312/GFZ.b103-95tk7

D — epicentral distances in degree (°), calculated according to geocentric coordinates, the maximum error of the own calculations amounts to $\pm 0{,}1°$

Az — azimuth: clockwise measured angle between north direction in epicentre and the connecting line from epicentre to station Moxa

h — depth of focus in km. In case of own depth determinations on the basis of identified depth phases the travel-time curves for deep focus earthquakes after GUTENBERG and RICHTER (5) are used.

H — origin time in UTC (Universal Time)

NEIS — National Earthquake Information Service, Denver, Colorado, USA

BCIS — Bureau Central International de Seismologie, Strasbourg, France

ANUSSR — Akademia Nauk USSR, Moscow, USSR

AEC — United States Atomic Energy Commission, Washington, D.

ISC — International Seismological Centre, Newbury, UK

NORSAR — Norwegian Seismic Array, Kjeller, Norway

All source data given in ehe column "Remarks" which are not the result of Moxa data evaluations are followed in brackets by the abbreviation of the reporting agency or station, repsectively (e. g. NEIS, ISC, PRU). For abbreviations of seismological stations and other agencies in the international three letter code see the introductions to the Regional Catalogue of Earthquakes, Newbury and the Bulletin of the International Seismological Centre, Newbury. In all other instances round brackets indicate uncertainties in interpretation of phases, time depth of focus or epicentral distances, respectively.

[1] BOLT, A., The velocity of seismic waves near the earth's center. Bull. Seism. Soc. Am. 54 (1964) 1, 191—208.

[2] BÅTH, M., Propagation of Sn and Pn teleseismic distances. Pure and Applied Geophysics 65 (1966/II) 19—30.

[3] GUTENBERG, B. and RICHTER, C. F., Magnitude and energy of earthquakes. Annali di Geofisica 9 (1956) 1, 1—15.

[4] KÁRNÍK, V., KONDORSKAJA, N. V. u. a., Standardization of the earthquake magnitude scale. Stud. Geophys. et Geodet., Prague 6 (1962) 41—48.

[5] GUTENBERG, B. and RICHTER, C. F., Materials for the study of deep-focus earthquakes. Bull. Seism. Soc. Am. 26 (1936) 4, 341—390.

Zentralinstitut fuer Physik der Erde - Seismischer Dienst
O - 6900 Jena, Burgweg 11, Postfach 106
Bundesrepublik Deutschland

Preliminary seismogram readings at MOXA (MOX) JUL91

```
910701 149.0 DEG DEPTH 33
EPKIKP          13 13 19.5
IPKP1           13 13 23.8
       SZ  1.4s      28nm
EPKP2           13 13 30
-----------------------------
910701  99.92DEG DEPTH47
IP      U  SL   13 46 27
E               13 49 45
EPP        L    13 50 30
ISKS       L    13 57 10
EPS        L    13 59 20
ESS     Z  L    14 04 42
ESSS    Z  L    14 08 36
ELR     Z  L    14 20 00
LMV        L    14 34 00
       LZ 19.0s     3.5my 5.9
LMH        L    14 37 19
       LN 19.0s     2.6my
       LE  0.0s     0.0my 5.8
(NEIS):  15.794S     74.982W
NEAR COAST OF PERU
13h 32m 44.60s        REG 115
5.3mb          5.9Msz
-----------------------------
910701
EP              13 53 57.5
-----------------------------
910701
EP              17 01 22.5
-----------------------------
910701
  LUBIN
ESG             17 23 43
-----------------------------
910701
E(P)            22 27 23.5
-----------------------------
910702
E(PG)           01 04 35.5
ESG             01 04 44
-----------------------------
910702
  LUBIN
ISG             03 30 36.5
-----------------------------
910702 148.5 DEG DEPTH 33
EPKIKP          04 09 37.3
IPKP1           04 09 40.5
       SZ  1.7s      29nm
-----------------------------
910702
EP              04 51 13.1
       SZ  1.6s      15nm
-----------------------------
910702
LMV     Z  L    05 24 50
-----------------------------
910702  89.78DEG DEPTH33
EP      U  SL   05 27 24.5
       SZ  2.0s     130nm 5.9
I               05 27 41
EPP        SL   05 30 51
ESKS    E  L    05 37 48
ES      ZH L    05 38 12
ESP     Z  L    05 39 10
E       Z  L    05 45 05
ELR     Z  L    05 56 30
LMH        L    06 11 30
       LN  0.0s     0.0my
       LE 26.0s     3.9my 5.7
LMV     Z  L    06 11 40
       LZ 27.0s     5.0my 5.8
(NEIS):   1.136S     99.901E
S.W. OF SUMATERA
05h 14m 28.00s        REG 273
6.1mb          6.2Msz
-----------------------------
910702 151.12DEG DEPTH424
EPKIKP          06 27 07.5
IPKP1           06 27 14.1
       SZ  1.2s     140nm
IPKP2           06 27 24
IpPKP           06 28 57
EPP             06 30 52
(NEIS):  22.984S    179.231W
S.OF FIJI
06h 08m 09.40s        REG 171
5.6mb
-----------------------------
910702
EP         SL   20 07 09
LMV     Z  L    20 44 35
-----------------------------
910702
ESG             21 07 38
-----------------------------
910702
LMV     Z  L    21 11 00
-----------------------------
910702  22.42DEG DEPTH10
IP      C  SL   21 29 03
       SZ  1.6s     320nm 5.5
ES      N  L    21 33 13
ESS     E  L    21 33 37
E       ZN L    21 38 30
LMH        L    21 40 58
       LN 15.0s     0.8my
       LE  0.0s     0.0my 4.3
LMV        L    21 42 43
       LZ 14.0s     1.1my 4.6
```


DOI: 10.2312/GFZ.b103-95tk7

Day	Phase		h m s	Remarks
24.	e(P)	A	12 08 36	Iceland 65.0 N 20.0 W H = 12 03 39 h = 33 km D = 21.80 Az = 116 (ISC) (P)V A 1.5s 20.1nm M = 4.3
24.	eP	A	17 32 32	Kurile Islands 44.33 N 149.61 E H = 17 20 32.1 h = 36.2 km MB = 4.7 (NEIS) D = 78.5
24.	eP	A	19 24 44	Kurile Islands 44.55 N 149.20 E H = 19 12 46.6 h = 48 km MB = 5.1 D = 78.29 Az = 334 (NEIS) h = 41 km LmH C 20s 1.6/um M = 5.4 LmV C 17 0.7/um 5.1
	epP	A	24 55	
	LmH	C	57.6	
	LmV	C	58.5	
24.	+eiPKIKP	AB	22 08 12.5	Kermadec Islands Region 28.64 S 177.59 W H = 21 48 25.8 h = 78.2 km MB = 6.2 D = 156.94 Az = 345 (NEIS) PKIKPV A 2.0s 265.0nm PKIKPV B 7.0 2.4/um PKHKPV A 2.1 201.3nm PKP2V A 1.5 356.8nm PPV A 2.2 185.4nm M = 5.8 PPV B 8 2.2/um 6.3 LmH B 25 3.1/um LmV B 24 2.7/um
	ePKHKP	A	08 23.5	
	ePKP2	AB	08 43	
	ePP	AB	12 19	
	eSKSP	C	22 45	
	ePPS	C	25 30	
	eSS	C	33 30	
	LmV	E	23 13.5	
	LmH	B	15.7	
24.	eP	A	22 51 02	Kurile Islands 44.50 N 149.18 E H = 22 39 05.0 h = 47 km MB=5.2 MS=5.6 D = 78.32 Az = 334 (NEIS) h = 52 km PV A traces
	epP	A	51 16	
24.	eP	A	23 34 38	Kurile Islands 44.51 N 149.08 E H = 23 22 41.6 h = 47 km MB = 5.0 D = 78.28 Az = 334 (NEIS) h = 37 km
	epP	A	34 48	

Day	Phase		h m s	Remarks
3.	iP	A	10 50 19	Kurile Islands 45.37 N 150.44 E
	LmH	B	11 28.0	H = 10 38 23.4 h = 33 km MB = 5.5 (NEIS)
	LmV	B	28.0	D = 77.9
				PV A 1.2s 34.6nm M = 5.3
				LmH B 20 0.6/um 4.9
				LmV B 20 0.8/um 5.1
3.	eP	A	16 06 03	Ionian Sea 37.81 N 19.87 E
				H = 16 02 33.5 (CSEM)
				D = 14.22
3.	e	A	20 32 08	Loyalty Islands Region 21.52 S 169.50 E
				H = 20 12 19.8 h = 33 km MB = 4.7 (NEIS)
				D = 146.2
4.	+iP	AB	07 59 21.5	Salta Province, Argentina
	epP	AB	08 01 26.5	24.69 S 63.36 W
	esP	AB	02 22	H = 07 46 33.8 h = 549 MB = 6.0 (NEIS)
	iPP	AB	03 28	D = 99.8 h = 566 km
	ipPP	B	05 24	PV A 1.3s 135.5nm M = 6.2
	esPP	B	06 21	PV B 9 1.9/um 6.5
	iSKS	B	09 08	PPV B 8 3.6/um 6.7
	eS	B	10 09	LmH B 17 3.3/um
	eSP	C	11 40	LmV B 23 4.4/um
	ePS	C	13 10	
	esS	C	13 50	
	isSP	C	15 20	
	e(PKKP)	A	16 06	
	eSS	C	17 15	
	eSKKP	A	18 11	
	esSS	C	20 35	
	eSSS	C	21 00	
	LmH	B	25.3	
	LmV	B	28.4	
4.	ePn	A	20 58 18	Austria 46.19 N 13.22 E
	ePg	A	58 40	H = 20 57 10.2 h = 33 km (NEIS)
	eSn	A	59 08.5	D = 4.6
	iSg	A	59 30.5	

Scientific Technical Report STR 95/TK
DOI: 10.2312/GFZ.b103-95tk7

Principles locating earthquakes

by

W. STRAUCH[1)]

1. Introduction

The location of earthquakes is a basic problem in seismological observation and research. It is strongly connected with the investigation of the structure of the Earth and especially of the Earth crust.

An earthquake occurring at hypocentre and origin time (x, y, z, t) generates waves which are recorded at seismic stations. Parameters t_i of different wave groups can be measured at the stations and serve as input data for the location process. These parameters are currently arrival times of wavelets but also azimuth or other informations can be used.

The measured data t_i can be expressed as functions f_i of the focal coordinates and the origin time:

$$t_i = f_i(x, y, z, t). \qquad (1)$$

The functions are generally nonlinear in the coordinates x, y, z and represent the geometrical conditions and the Earth model.

Location means to find the unknown hypocentre coordinates and the origin time by solving a set of nonlinear equations (1) with given t_i.

The main strategy to overcome this problem is to linearize (1) and to use thereafter the well practicable tools of linear algebra.
A simple case for illustration: Assume x, y, z as Cartesian Coordinates, the Earth model is represented by a halfspace, arrival times t_i of waves propagating with the constant velocity v were measured.
The nonlinear equations are

$$t_i = f_i(x, y, z, t)$$

$$= t + \frac{\sqrt{(x_i-x)^2 + (y_i-y)^2 + (z_i-z)^2}}{v}$$

x_i, y_i, z_i - station coordinates

or

$$v^2(t_i-t)^2 = (x_i-x)^2 + (y_i-y)^2 + (z_i-z)^2 \quad , \qquad (2)$$

respectively.

By subtracting one "reference" equation in (2) from the others a set of simple equations linear in x, y, z, t will be found.
(Carry out this step explicitly as exercise!)

1) Dipl.-Phys. Wilfried Strauch, Academy of Sciences of the GDR, Central Institute for Physics of the Earth, DDR-1500 Potsdam, Telegrafenberg.

The arrival times t_i at 5 stations have to be used for the hypocentre determination with this simple method, when $z_i = z = \text{const}$ 4 stations are sufficient.

2. The Geiger-algorithm

The commonly used method to solve the location problem was suggested by Geiger (1910). It is based on the Gauß-Newton-iteration scheme for the solution of systems of nonlinear equations.

The procedure needs starting values (x_s, y_s, z_s, t_s) for focus and origin time near the true solution (x_0, y_0, z_0, t_0).

For each arrival t_i the nonlinear functional

$$F_i = t_i - f_i\,(x_i, y_i, z_i, x, y, z, t) \equiv 0$$

can be written for the realizations

$$F_i^s = t_i - f_i(x_i, y_i, z_i, x, y, z, t) \Big|_{x=x_s, y=y_s, z=z_s, t=t_s}$$

at the starting point, and

$$F_i^0 = t_i - f_i(x_i, y_i, z_i, x, y, z, t) \Big|_{x=x_0, y=y_0, z=z_0, t=t_0}$$

for the final solution.

The realization F_i^0 has to fulfill certain conditions which define the solution. Obviously, only a small step ($dx = x_0 - x_s$, $dy = y_0 - y_s$, $dz = z_0 - z_s$, $dt = t_0 - t_s$) in the parameter space is necessary to come from F_i^s to F_i^0 because the starting point is near the final solution.

Therefore F_i^0 can be expressed by the Taylor development of F_i at the point (x_s, y_s, z_s, t_s) taking only the linear terms in dx, dy, dz, dt:

$$\begin{aligned} F_i^0 &= F_i(x_s + dx, y_s + dy, z_s + dz, t_s + dt) \\ &= F_i(x_s, y_s, z_s, t_s) + \frac{\partial F_i^s}{\partial x} dx + \frac{\partial F_i^s}{\partial y} dy + \frac{\partial F_i^s}{\partial z} dz + \frac{\partial F_i^s}{\partial t} dt + e_i \qquad (3) \\ &= t_i - f_i^s - \frac{f_i^s}{x} dx - \frac{f_i^s}{y} dy - \frac{f_i^s}{z} dz - \frac{f_i^s}{t} dt + e_i = 0 \end{aligned}$$

(e_i contains the error by neglecting the higher derivatives and the measuring error.)

So with (3) a set of equations linear in the unknown steps dx, dy, dz, dt is found. If there are more than the necessary 4 informations t_i the solution is found applying the principle of least squares, demanding

$$Q = \sum_i e_i^2 = \sum_i (t_i - f_i^s - \frac{\partial f_i^s}{\partial x} dx \ \ldots - \frac{\partial f_i^s}{\partial t} dt)^2 \longrightarrow \text{MIN} \,. \qquad (4)$$

The necessary condition to fulfill these demands is

$$\frac{\partial Q}{\partial (dx)} = 0 \ \ldots \ \frac{\partial Q}{\partial (dt)} = 0 \quad .$$

There are several methods to solve (4). Well known is the use of the system of normal equations (Establish the system of normal equations as exercise.). Better suited are more modern methods like the QR-algorithm overcoming some numerical problems outlined by Buland (1976).

The result of solving (4) is the vector of correction step (dx, dy, dz, dt) leading from the starting point towards the final solution.

Adding the correction vector to the starting point the true location is not yet reached because the e_i in (3) are not exactly considered. But the new point should be nearer to the focus than the starting point and can serve as a starting point itself in a next iteration. This process is repeated until the correction vector becomes neglectable.

The Geiger-algorithm is not too complicated but any computations have to be done repeatedly depending on the convergence speed.

Therefore the method became important only since computers were available.
Nowadays the algorithm can be implemented already on low cost personal computers with success.

As starting point the location at the station nearest to the focus that means with the first arrival time can be chosen.
In complicated cases (danger of divergence or false solutions) searching the position of the minimal Q in a coordinate grid containing the hypocentre can give a better starting point. But such a procedure is more time consuming.
Problems that may arise applying the Geiger-algorithm as

- no convergence or even divergence occurs in the iteration process,
- the convergence leads to a relative minimum of Q and the location result is wrong

can be avoided practically considering the hints given in the next remarks.

3. Remarks

It is not too hard to locate seismic events with a dense network of seismic stations surrounding the source region. The problems can arise when only few stations are available, and the earthquakes occure outside the system or at its periphery. Buland (1976) gives some hints which are supported and added by own experience of the author of this paper as follows:

1. Use, if possible, not only first P-arrivals but also later onsets, especially S-waves.
2. Use modern methods for solving eq. (4), e.g. QR-algorithm and step length damping if necessary (bad convergence).
3. Locate first with a fixed depth (z = const), take the found location as starting point for the location with free depth.
4. Check the location with different starting points.
5. Check the location by repeating with different datasets (taking away or adding some information).

Taking these remarks into account a location programme will give reliable results also in complicated cases.

Mitteilung des Zentralinstituts für Physik der Erde Nr. 1264

4. A special case - location of distant earthquakes with a local network

The Geiger-method described above works satisfying if the event occured inside the station net or not too far away from its periphery. It can also be applied for the location with global networks - the use of geographical coordinates provided instead of a Cartesian system.

For some purposes it might be interesting to locate distant earthquakes with a local network as it is done by the wellknown seismic arrays (LASA, NORSAR). This problem can be solved by a simple algorithm. Only arrival times of the P-wave recorded at the stations are neccessary for the procedure. Due to the far distance to the focus p (and other waves too) can be assumed as a plane wave travelling with a constant velocity through the net.

The apparent velocity v of this plane wave can be expressed in terms of polar coordinates of the stations r_i, α_i as:

$$v = \frac{r_i \cdot \cos(az - \alpha_i)}{t_i - t_o}$$

t_i - arrival time at station i
t_o - (unknown) arrival time at coordinate origin
az - azimuth

Because $\cos(az - \alpha_i) = \sin az \cdot \cos \alpha_i + \cos az \cdot \sin \alpha_i$

and $x_i - x_o = r_i \cos \alpha_i$; $y_i - y_o = r_i \sin \alpha_i$

(x_i; y_i - coordinates in a Cartesian system)

we get $t_i - t_o = \frac{\sin az}{v}(x_i - x_o) + \frac{\cos az}{v}(y_i - y_o)$

Defining the slowness vektor $\bar{s}$ with its coordinates

$$s_x = \frac{\sin az}{v} \quad ; \quad s_y = \frac{\cos az}{v} \qquad \left(|\bar{s}| = \frac{1}{v} \right)$$

an equation can be established for each station having measured an arrival time:

$$t_i = t_o + s_x x_i + s_y y_i \qquad (x_o = y_o = 0)$$

The unknowns t_o, s_x, s_y can be computed if 3 or more informations t_i are given solving a set of linear equations.

From $s = \sqrt{s_x^2 + s_y^2}$ the distanced can be calculated if a dependence $s = f(d)$ exists. The azimuth is available from $az = \arctan(-s_y/-s_x)$. The function $s = f(d^o)$ is given in the Jeffreys-Bullen-Tables.

For regional events the method can only be applied using arrival times of crustal phases (Pn, Pg) if $D \ll d$; D - the diameter of the net. In this case the azimuth can be calculated but the distance must be taken from S - P because the apparent velocity of crustal phases depends not or only weak on the distance (shallow focus assumed).

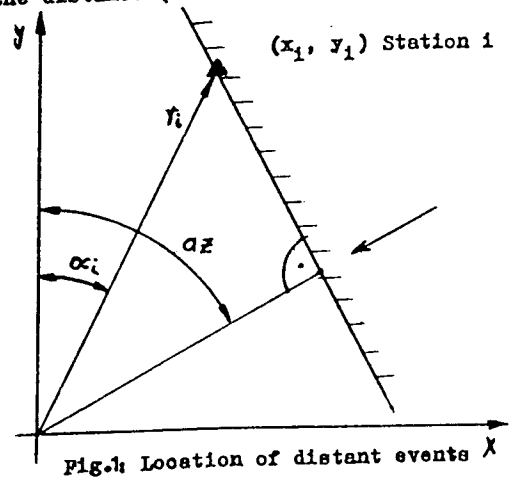

Fig.1: Location of distant events

References

GEIGER: Herdbestimmungen bei Erdbeben aus den Ankunftszeiten. Kgl.Ges.Wiss.Gött. 4 (1910), 331-349.

BULAND: The mechanics of locating earthquakes, BSSA 66 (1976) 1, 173-187.

LEE& STEWART: Principles and Applications of Microearthquake Networks, Academic Press

Exercise on local event localisation by means of seismic network recordings: Graphical and PC assisted methods

P. Bormann, M. Baumbach and K. Wylegalla

GeoForschungsZentrum Potsdam,
Telegrafenberg, D-14473 Potsdam

1. Identify the local phases (Pn, Pg, Sn and Sg only) in the records of the Potsdam seismic network shown in Figs. 1 and 2 using the travel-time difference curve shown in Fig. 3 and provided as transparent overlay. Mark the onset-times and annotate them with the respective phase symbols (by weak pencil only!).

2. Write the distance, corresponding to your phase interpretation, on each record and mark also the origin time according to your interpretation with a vertical line on each trace. Determine the average origin time.

3. Use a) the circle and b) the chord method on the map (Fig. 4) to determine the epicenter co-ordinates for both events. As epicenter take the center of gravity of your circle- or chord-crossings, respectively.

4. Carry out the phase interpretation and event localization of several digitally recorded local events by using the PC program **seis89**.

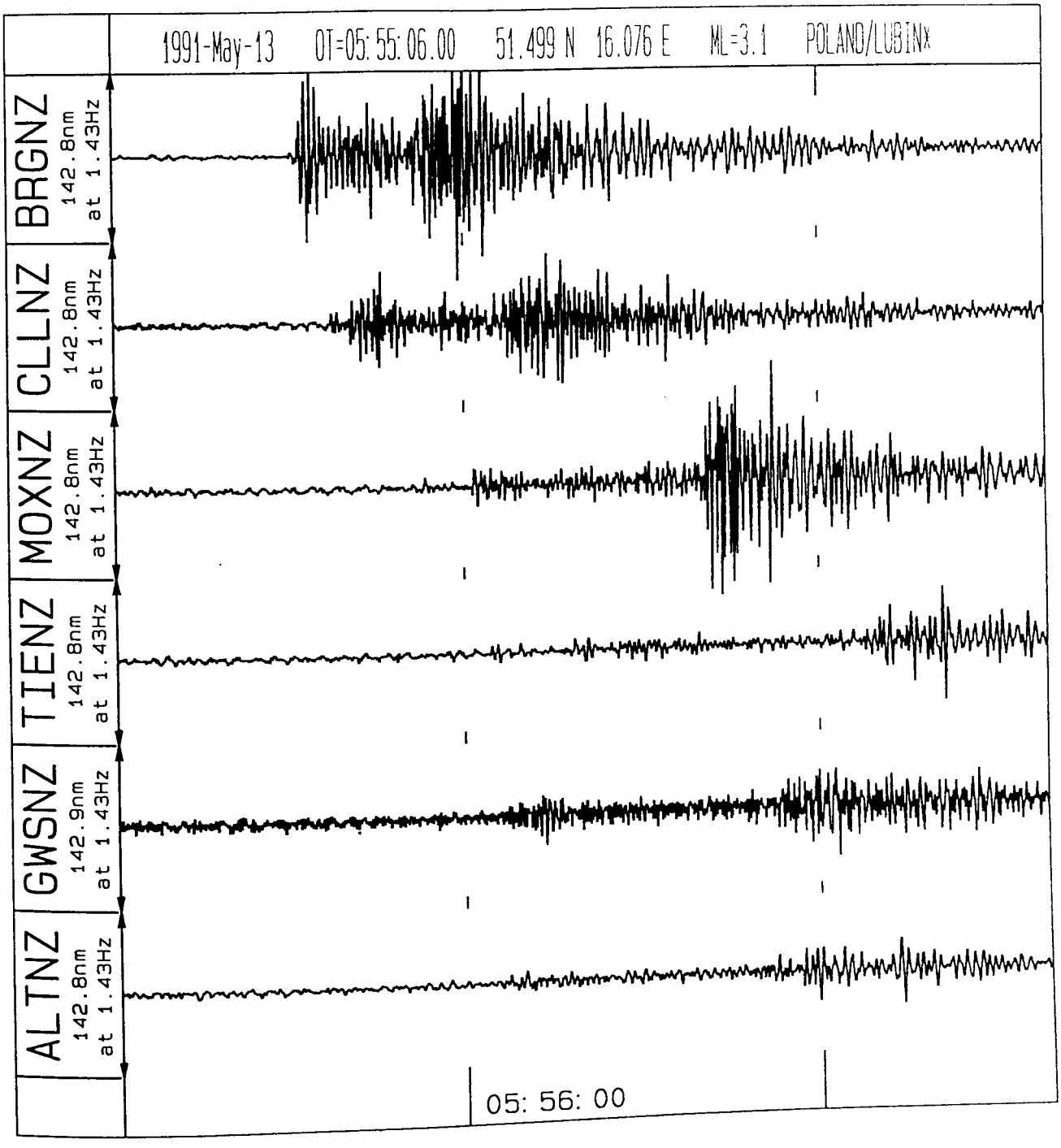
1991-May-13 OT=05:55:06.00 51.499 N 16.076 E ML=3.1 POLAND/LUBIN
BRGNZ
142.8nm
at 1.43Hz
CLLNZ
142.8nm
at 1.43Hz
MOXNZ
142.8nm
at 1.43Hz
TIENZ
142.8nm
at 1.43Hz
GWSNZ
142.9nm
at 1.43Hz
ALTNZ
142.8nm
at 1.43Hz
05: 56: 00

Fig. 1

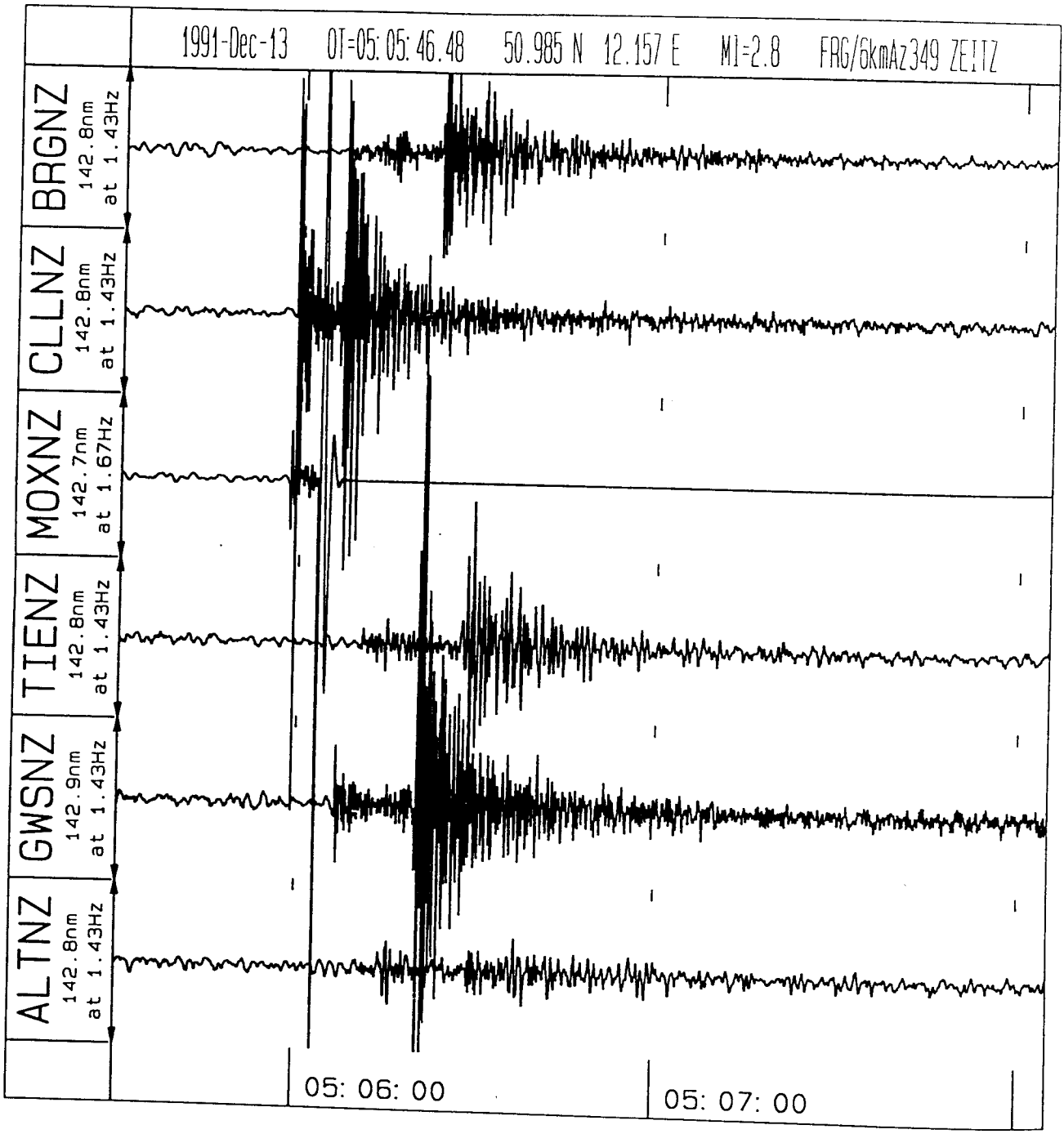
1991-Dec-13 OT=05:05:46.48 50.985 N 12.157 E M1=2.8 FRG/6kmAz349 ZEITZ
BRGNZ 142.8nm at 1.43Hz
CLLNZ 142.8nm at 1.43Hz
MOXNZ 142.7nm at 1.67Hz
TIENZ 142.8nm at 1.43Hz
GWSNZ 142.9nm at 1.43Hz
ALTNZ 142.8nm at 1.43Hz
05:06:00
05:07:00

Fig. 2

Scientific Technical Report STR 95/TK
DOI: 10.2312/GFZ.b103-95tk7

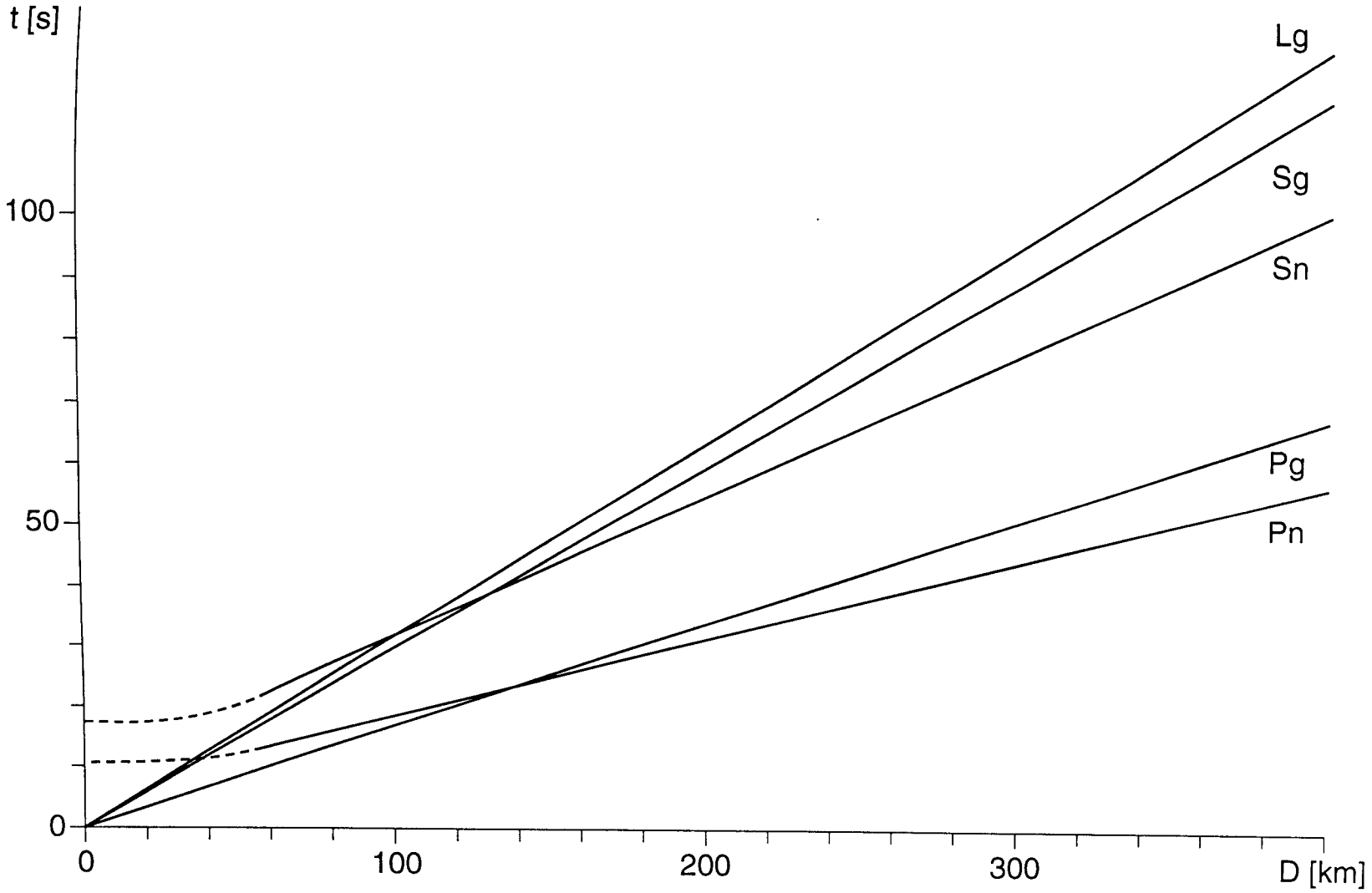

Fig. 3: Local travel-time curves for SE Germany

Scientific Technical Report STR 95/TK
DOI: 10.2312/GFZ.b103-95tk7

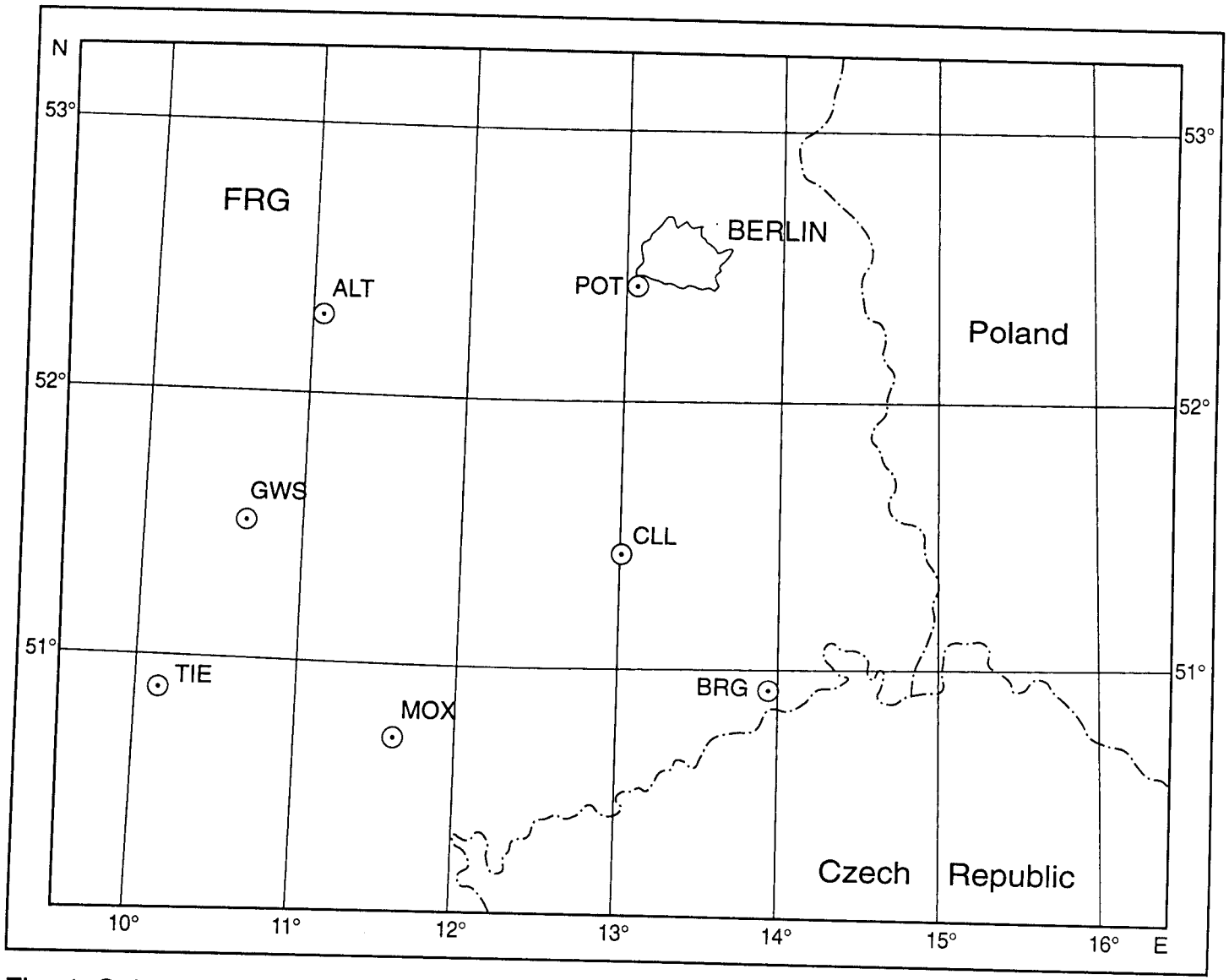

Fig. 4: Seismic stations of Potsdam - network

Exercise on 3-component seismogram interpretation

P. Bormann and K. Wylegalla

GeoForschungsZentrum Potsdam,
Telegrafenberg, D-14473 Potsdam

1. Analyse Fig. 1, i.e.:

1.1 Decide whether the earthquake shown is shallow or deep taking into account also Tab. 1 which gives the travel-time difference between the first P-wave onset and the surface Rayleigh-wave maximum R_{max}.

Tab. 1

Δ°	$t_{Rmax} - t_p$ minutes	Δ°	$t_{Rmax} - t_p$ minutes	Δ°	$t_{Rmax} - t_p$ minutes
10	4-6	55	26	100	45-46
15	6-8	60	28-29	105	47-48
20	9-10	65	31	110	48-50
25	10-12	70	33	115	53
30	13-14	75	35	120	55
35	15-16	80	37	125	57
40	18-19	85	39-40	130	60
45	21	90	42	140	64
50	24	95	43	150	70

1.2 Identify the first onset and the largest secondary onset.

1.3 Determine the epicentral distance Δ from the S - P times:
a) using the "rule of thumb" $\Delta\,[^\circ] = [t\,(S\text{-}P)_{[min]} - 2] \times 10$;
b) using the Jeffreys-Bullen travel-time difference graph for shallow events shown in Fig. 2 and provided as transparent overlay.

1.4 In case you had decided under 1.1 that the event was a deeper one, please try to identify the onset of depth phases (pP and/or sP, respectively) and calculate the focal depth h using Tab. 2 and/or 3.

1.5 Calculate the back-azimuth of the event using the following relationship **Az** = arctan (A_E/A_N). Be careful in deciding about the proper quadrant in which the azimuth is situated by comparing the polarities in all three components.

1.6 Determine the epicentral coordinates and source region of the event shown in Fig. 1 on the global map (Fig. 3).

2. Interprete along the lines outlined under 1. at least one more analog 3-component record given to you. Additionally try to identify as many as possible phases in the record and improve the distance determination by best possible fit of your identified onsets with the detailed travel-time difference graphs available from the exercise assistants.

Note! Please mark and annotate onsets in the seismograms only with weak pencil so as to be erasable.

3. Carry out the phase interpretation, distance and depth determination, polarization analysis and back-azimuth determination as well as event localization for several teleseismic events by using the PC program **seis89** and the global map in Fig. 3.

Scientific Technical Report STR 95/TK
DOI: 10.2312/GFZ.b103-95tk7

GeoForschungsZentrum Potsdam

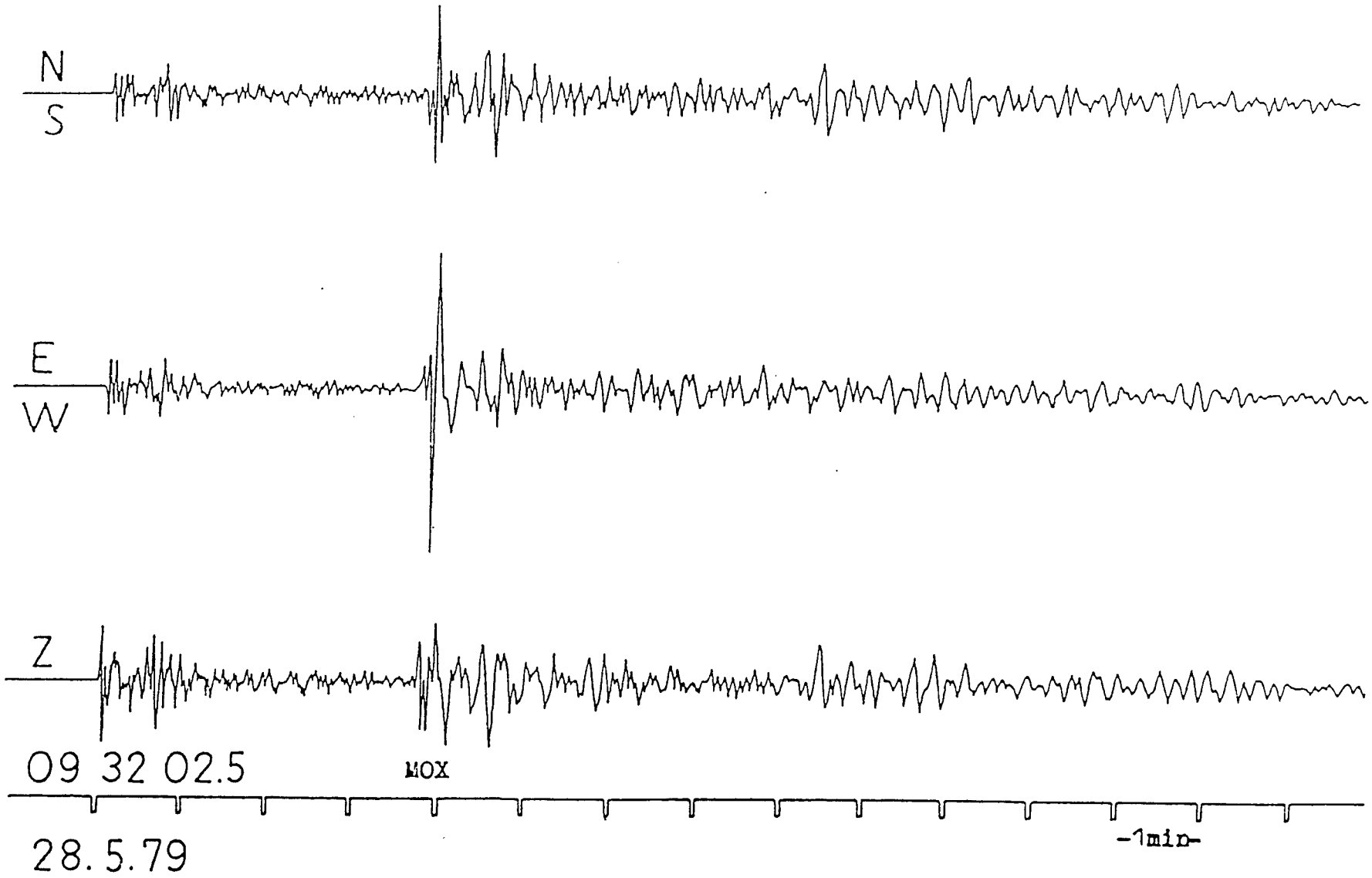

Fig.1

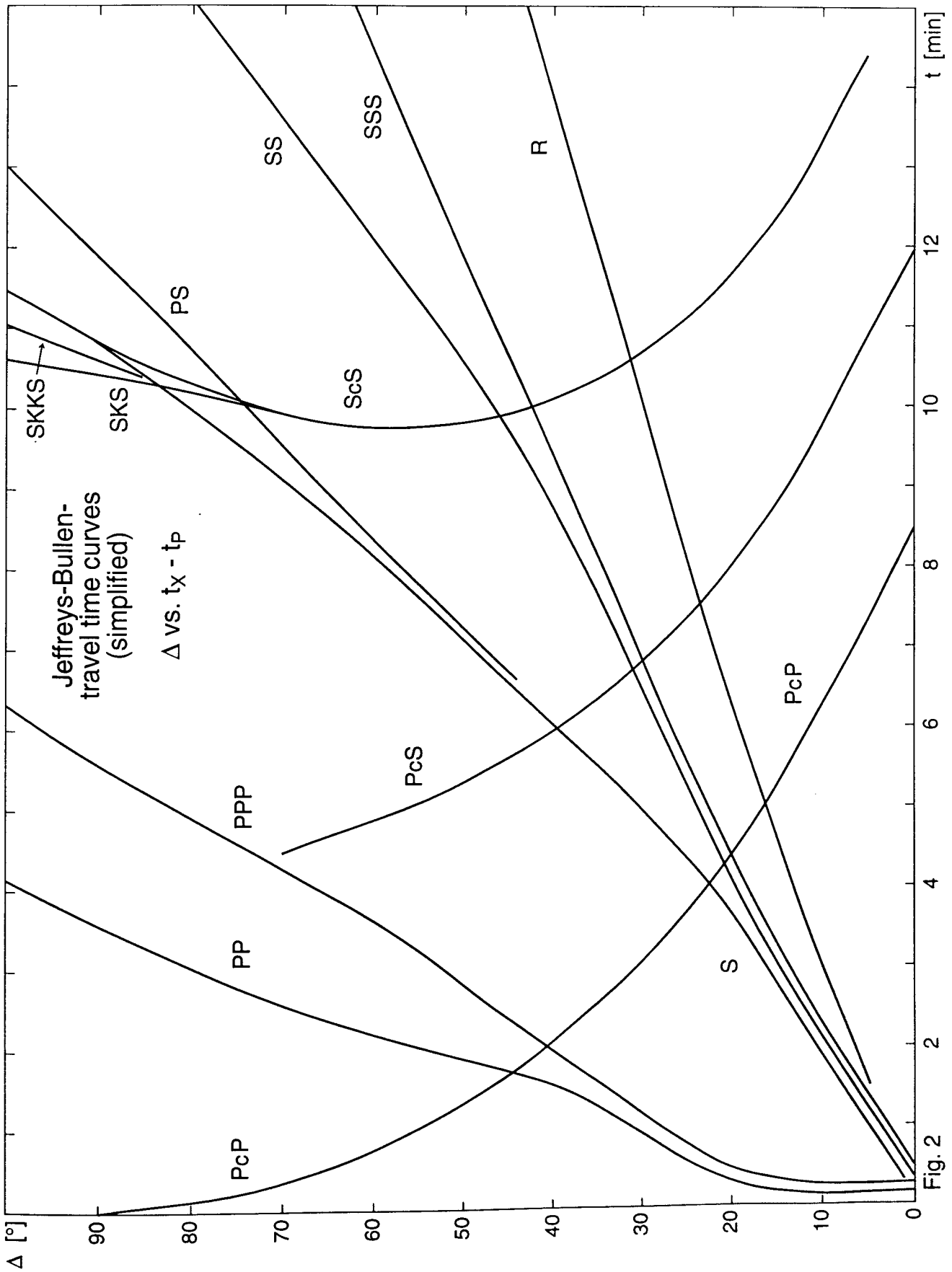
Jeffreys-Bullen-
travel time curves
(simplified)
Δ vs. t_X - t_P
SKKS
SKS
PS
SS
SSS
R
ScS
PcS
PPP
PP
PcP
S
PcP
Δ [°]
t [min]
0
10
20
30
40
50
60
70
80
90
2
4
6
8
10
12

Fig. 2

Scientific Technical Report STR 95/TK
DOI: 10.2312/GFZ.b103-95tk7

Tab. 2

pP-P

Δ	Depth of source [km] 15.	35.	50.	100.	150.	200.	250.	300.	400.	500.	600.	700.
	s	s	s	s	s	s	s	s	s	s	s	s
2	3.6	7.5										
4	3.6	7.5										
6	3.6	7.5										
8	3.6	7.5										
10	3.6	7.6										
12	3.6	7.6	7.9									
14	3.6	7.6	8.0									
16	3.8	8.1	9.3	20.1	26.2							
18	4.0	8.5	10.1	16.2	25.9	32.6	38.8					
20	4.3	9.2	11.5	19.0	25.6	33.2	39.6	45.4				
22	4.3	9.3	11.7	19.4	26.9	34.4	41.7	48.4	59.9			
24	4.5	10.0	12.7	21.4	29.8	37.8	45.3	52.2	64.1	82.7		
26	4.6	10.0	12.8	22.1	31.3	40.2	48.7	55.8	68.2	83.4	93.4	
28	4.6	10.0	12.9	22.3	31.5	40.5	49.1	57.2	72.2	84.3	94.4	
30	4.6	10.1	12.9	22.4	31.7	40.8	49.4	57.7	72.9	85.2	95.6	
32	4.6	10.1	13.0	22.5	31.9	41.0	49.8	58.1	73.5	86.1	96.8	
34	4.6	10.1	13.0	22.6	32.1	41.3	50.1	58.5	74.1	87.0	98.1	
36	4.6	10.2	13.1	22.8	32.3	41.6	50.5	59.1	74.9	88.0	99.4	
38	4.6	10.2	13.1	22.9	32.6	42.0	51.0	59.6	75.6	89.1	100.8	109.7
40	4.7	10.2	13.2	23.1	32.8	42.3	51.4	60.2	76.5	90.2	102.2	111.6
42	4.7	10.3	13.3	23.2	33.1	42.7	51.9	60.8	77.3	91.3	103.7	113.5
44	4.7	10.3	13.4	23.4	33.4	43.0	52.4	61.3	78.1	92.4	105.1	115.4
46	4.7	10.4	13.4	23.6	33.6	43.4	52.8	61.9	78.9	93.5	106.6	117.3
48	4.7	10.4	13.5	23.7	33.9	43.7	53.3	62.5	79.7	94.6	108.0	119.1
50	4.7	10.5	13.6	23.9	34.1	44.1	53.7	63.0	80.5	95.6	109.3	120.9
52	4.8	10.5	13.6	24.0	34.4	44.4	54.2	63.5	81.3	96.7	110.7	122.7
54	4.8	10.5	13.7	24.2	34.6	44.8	54.6	64.1	82.0	97.7	112.0	124.3
56	4.8	10.6	13.8	24.3	34.8	45.1	55.0	64.6	82.7	98.6	113.2	125.9
58	4.8	10.6	13.8	24.5	35.1	45.4	55.4	65.1	83.4	99.6	114.5	127.5
60	4.8	10.7	13.9	24.6	35.3	45.7	55.8	65.6	84.1	100.5	115.6	129.0
62	4.8	10.7	13.9	24.8	35.5	46.0	56.2	66.0	84.8	101.4	116.8	130.4
64	4.9	10.7	14.0	24.9	35.7	46.3	56.5	66.5	85.4	102.2	117.9	131.8
66	4.9	10.8	14.1	25.0	35.9	46.5	56.9	66.9	86.0	103.1	119.0	133.2
68	4.9	10.8	14.1	25.1	36.1	46.8	57.2	67.4	86.6	103.9	120.0	134.5
70	4.9	10.8	14.2	25.3	36.3	47.1	57.6	67.8	87.2	104.7	121.0	135.8
72	4.9	10.9	14.2	25.4	36.5	47.3	57.9	68.2	87.8	105.4	122.0	137.0
74	4.9	10.9	14.3	25.5	36.7	47.6	58.2	68.6	88.4	106.2	122.9	138.2
76	4.9	10.9	14.3	25.6	36.8	47.8	58.6	69.0	88.9	106.9	123.9	139.3
78	4.9	11.0	14.4	25.7	37.0	48.1	58.9	69.3	89.4	107.6	124.8	140.5
80	5.0	11.0	14.4	25.8	37.2	48.3	59.2	69.7	90.0	108.3	125.7	141.5
82	5.0	11.0	14.5	25.9	37.4	48.5	59.5	70.1	90.5	109.0	126.5	142.6
84	5.0	11.1	14.5	26.1	37.5	48.8	59.8	70.4	91.0	109.7	127.4	143.7
86	5.0	11.1	14.6	26.1	37.7	49.0	60.0	70.8	91.4	110.3	128.2	144.7
88	5.0	11.1	14.6	26.3	37.9	49.2	60.4	71.2	92.0	111.0	129.0	145.6
90	5.0	11.1	14.6	26.3	37.9	49.3	60.5	71.4	92.3	111.4	129.5	146.3
92	5.0	11.1	14.7	26.3	38.0	49.4	60.6	71.5	92.4	111.6	129.8	146.6
94	5.0	11.1	14.7	26.4	38.0	49.5	60.6	71.5	92.5	111.7	130.0	146.9
96	5.0	11.2	14.7	26.4	38.1	49.5	60.7	71.6	92.7	111.9	130.2	147.2
98	5.0	11.2	14.7	26.4	38.1	49.6	60.8	71.8	92.8	112.1	130.5	147.5
100	5.0	11.2	14.7	26.5	38.1	49.6	60.9	71.8	92.9	112.2	130.6	147.6

Tab. 3

sP-P

Δ	Depth of source [km] 15.	35.	50.	100.	150.	200.	250.	300.	400.	500.	600.	700.
	s	s	s	s	s	s	s	s	s	s	s	s
2	5.9	12.7	15.4	22.8	27.0	35.7						
4	5.9	12.7	15.5	24.4	32.4	40.0	46.9	53.1	63.7			
6	5.9	12.7	15.6	24.8	33.5	42.0	50.1	57.5	70.6	81.2	89.2	
8	5.9	12.7	15.6	25.0	34.3	43.5	52.4	60.8	75.8	88.6	98.5	106.0
10	5.9	12.7	15.7	25.3	35.1	45.0	54.6	63.7	80.6	95.1	106.6	115.9
12	5.9	12.8	15.7	25.7	36.3	46.7	57.0	66.7	86.0	101.4	114.0	125.3
14	5.9	12.8	15.8	26.8	38.0	49.0	59.8	70.5	91.4	107.7	121.3	134.6
16	6.0	13.1	16.7	28.6	40.4	52.4	64.4	75.9	97.2	114.1	130.3	143.9
18	6.1	13.4	17.2	30.5	43.6	56.5	69.0	80.9	103.0	121.7	139.3	153.3
20	6.3	13.9	18.1	31.9	45.5	58.9	72.0	84.6	108.5	129.6	148.2	162.8
22	6.4	14.0	18.2	32.2	46.0	59.9	73.8	87.3	113.0	135.2	155.5	171.4
24	6.6	14.5	19.0	34.0	48.6	63.0	77.1	90.7	116.5	139.1	159.6	177.1
26	6.6	14.5	19.0	34.1	49.0	63.7	78.1	92.1	118.8	142.4	163.5	181.3
28	6.6	14.6	19.1	34.2	49.2	64.0	78.5	92.5	119.3	143.0	164.9	184.0
30	6.6	14.6	19.1	34.3	49.3	64.1	78.7	92.8	119.7	143.6	165.7	185.1
32	6.6	14.6	19.2	34.4	49.4	64.3	78.9	93.1	120.2	144.2	166.5	186.2
34	6.6	14.6	19.2	34.5	49.6	64.5	79.2	93.4	120.7	144.9	167.4	187.3
36	6.6	14.7	19.3	34.6	49.8	64.8	79.5	93.8	121.2	145.6	168.3	188.5
38	6.6	14.7	19.3	34.7	49.9	65.0	79.8	94.2	121.8	146.4	169.3	189.8
40	6.7	14.7	19.4	34.8	50.1	65.3	80.2	94.6	122.4	147.2	170.3	191.1
42	6.7	14.8	19.4	34.9	50.3	65.6	80.5	95.1	122.9	148.0	171.3	192.3
44	6.7	14.8	19.5	35.0	50.5	65.8	80.8	95.5	123.5	148.7	172.3	193.6
46	6.7	14.8	19.5	35.2	50.7	66.1	81.2	95.9	124.1	149.5	173.3	194.8
48	6.7	14.9	19.6	35.3	50.9	66.3	81.5	96.3	124.7	150.3	174.3	196.0
50	6.7	14.9	19.6	35.4	51.1	66.6	81.8	96.7	125.2	151.0	175.2	197.2
52	6.7	14.9	19.7	35.5	51.3	66.8	82.2	97.1	125.8	151.8	176.1	198.3
54	6.7	15.0	19.7	35.6	51.4	67.1	82.5	97.5	126.3	152.5	177.0	199.5
56	6.8	15.0	19.8	35.7	51.6	67.3	82.8	97.8	126.8	153.2	177.9	200.6
58	6.8	15.0	19.8	35.8	51.8	67.6	83.1	98.2	127.4	153.8	178.8	201.6
60	6.8	15.0	19.9	36.0	51.9	67.8	83.4	98.6	127.8	154.5	179.6	202.6
62	6.8	15.1	19.9	36.1	52.1	68.0	83.6	98.9	128.3	155.1	180.4	203.6
64	6.8	15.1	20.0	36.2	52.3	68.2	83.9	99.2	128.8	155.7	181.2	204.6
66	6.8	15.1	20.0	36.3	52.4	68.4	84.2	99.6	129.3	156.3	182.0	205.5
68	6.8	15.2	20.1	36.3	52.6	68.6	84.4	99.9	129.7	156.9	182.7	206.5
70	6.8	15.2	20.1	36.4	52.7	68.8	84.7	100.2	130.1	157.5	183.4	207.4
72	6.8	15.2	20.1	36.5	52.8	69.0	84.9	100.5	130.6	158.1	184.1	208.2
74	6.9	15.2	20.2	36.6	53.0	69.2	85.2	100.8	131.0	158.6	184.8	209.1
76	6.9	15.3	20.2	36.7	53.1	69.4	85.4	101.1	131.4	159.1	185.5	209.9
78	6.9	15.3	20.3	36.8	53.3	69.6	85.7	101.4	131.8	159.7	186.2	210.7
80	6.9	15.3	20.3	36.9	53.4	69.8	85.9	101.7	132.2	160.2	186.8	211.5
82	6.9	15.3	20.3	37.0	53.5	69.9	86.1	101.9	132.6	160.7	187.4	212.3
84	6.9	15.3	20.4	37.0	53.6	70.1	86.3	102.2	132.9	161.2	188.0	213.0
86	6.9	15.4	20.4	37.1	53.8	70.3	86.5	102.5	133.3	161.7	188.7	213.8
88	6.9	15.4	20.4	37.2	53.9	70.5	86.8	102.8	133.7	162.2	189.2	214.5
90	6.9	15.4	20.5	37.2	54.0	70.5	86.9	102.9	133.9	162.4	189.5	214.8
92	6.9	15.4	20.5	37.3	54.0	70.6	86.9	103.0	134.0	162.5	189.7	215.0
94	6.9	15.4	20.5	37.3	54.0	70.6	87.0	103.0	134.0	162.6	189.9	215.3
96	6.9	15.4	20.5	37.3	54.1	70.7	87.1	103.1	134.2	162.8	190.1	215.5
98	6.9	15.4	20.5	37.3	54.1	70.7	87.1	103.2	134.3	162.9	190.2	215.7
100	6.9	15.4	20.5	37.3	54.1	70.7	87.2	103.2	134.3	163.0	190.3	215.7

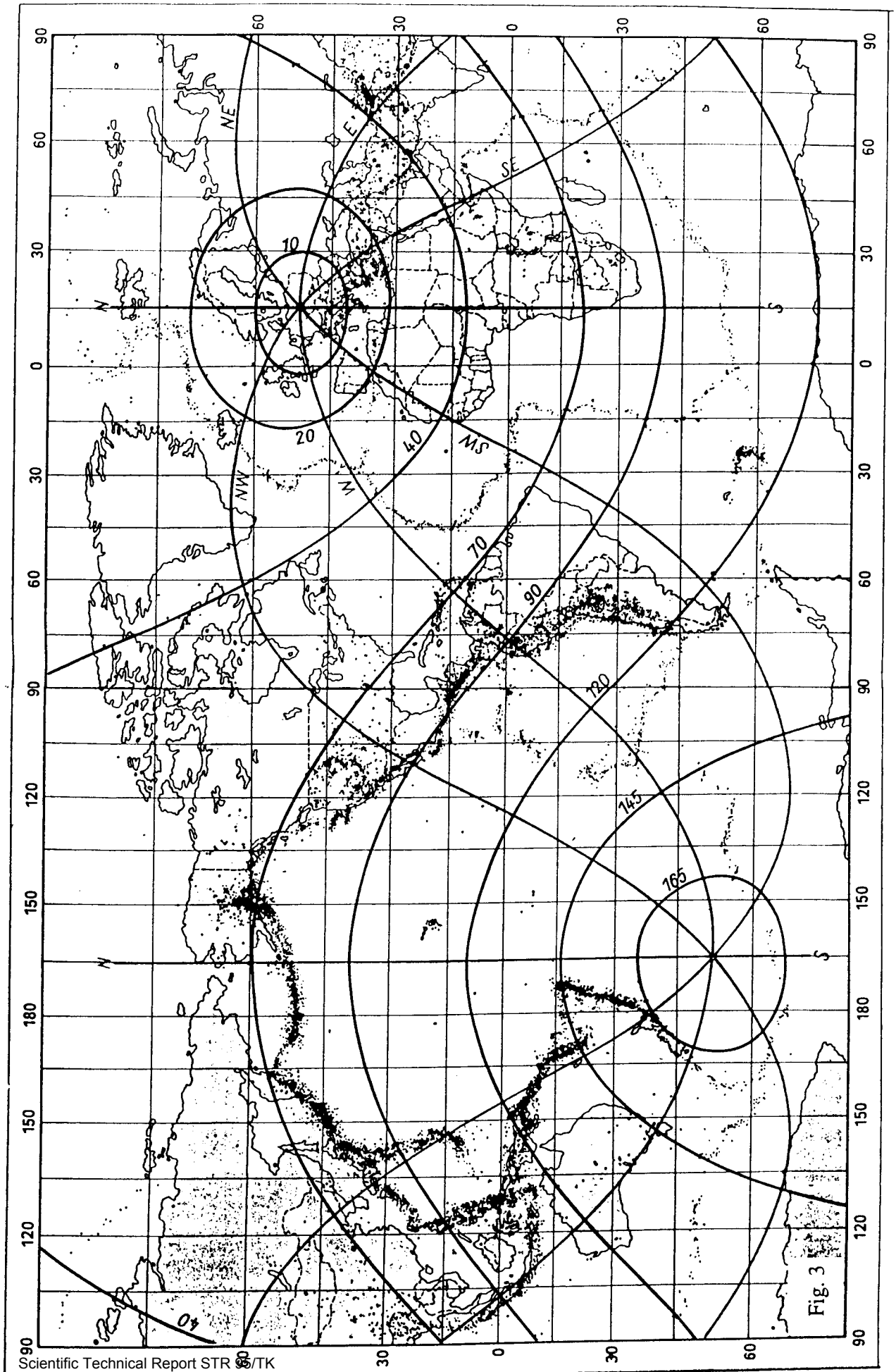
NE
E
SE
S
SW
W
NW
N
10
20
40
70
90
120
145
165
180
60
30
0
30
60
90
120
150
180

Fig. 3

Exercise on magnitude determination

P. Bormann and K. Wylegalla

GeoForschungsZentrum Potsdam,
Telegrafenberg, D-14473 Potsdam

1. Determine the surface wave magnitude $M_S = \log (A/T)_{max} + \sigma (\Delta)$ both from the maximum amplitudes of the vertical (MLV) and horizontal components (MLH) of surface waves in the record given in Fig. 1. Use Tab. 1 for the calibration functions and the epicentral distance Δ and depth h as given on the record. The frequency response of all three seismometer components is identical. The respective magnifications V as a function of the period T are given in the table inserted in Fig. 1.

2. Determine the body wave magnitude $m_b = (A/T)_{max} + \sigma (\Delta)$ for the intermediate deep earthquake shown in Fig. 1 of the exercise on 3-component seismogram interpretation both for the vertical component of P (MPV) and the horizontal component (vector sum!) of S (MSH). As calibration functions use the graphs shown in Fig. 2. As epicentral distance use $\Delta = 20.2°$ and as focal depth h = 111 km.

3. Determine the local magnitude ML using the Potsdam magnitude formula developed by WAHLSTROEM and STRAUCH (1984):

$$ML_{POT} = \log \mathbf{A} - \log \mathbf{V}_{net}(\mathbf{T}) + \log \mathbf{V}_{WA}(\mathbf{T}) + 0.83 \log \mathbf{D} + (0.0017/\mathbf{T}) \times (\mathbf{D} - 100) + 1.41$$

with
- **A** - measured seismogram amplitude of Sg wave in mm
- $\mathbf{V}_{net}$ - amplification of the network seismographs
- $\mathbf{V}_{WA}$ - amplification of a standard Wood-Anderson seismograph
- **D** - epicentral distance in km
- **T** - measured period in s

Note! This formula is applicable for distances between 100 km < **D** < 700 km only.

Determine ML for at least two stations of the Potsdam-network given in Fig. 1 of the exercise on local event localization. Use the maximum amplitude of Sg waves taking into account the event distance **D** as determined from these records. Use the period dependent magnifications $\mathbf{V}_{net}(\mathbf{T})$ and $\mathbf{V}_{WA}(\mathbf{T})$ as given below.

T [s]	$\mathbf{V}_{net}$	$\mathbf{V}_{WA}$	T [s]	$\mathbf{V}_{net}$	$\mathbf{V}_{WA}$
0.1	35000	2800	1.1	190000	1100
0.2	92000	2700	1.2	180000	950
0.3	125000	2600	1.3	170000	850
0.4	150000	2400	1.4	155000	750
0.5	170000	2200	1.5	140000	700
0.6	190000	2000	1.6	120000	
0.7	200000	1800	1.7	90000	
0.8	201000	1600	1.8	80000	
0.9	201000	1400	1.9	70000	
1.0	200000	1200	2.0	60000	

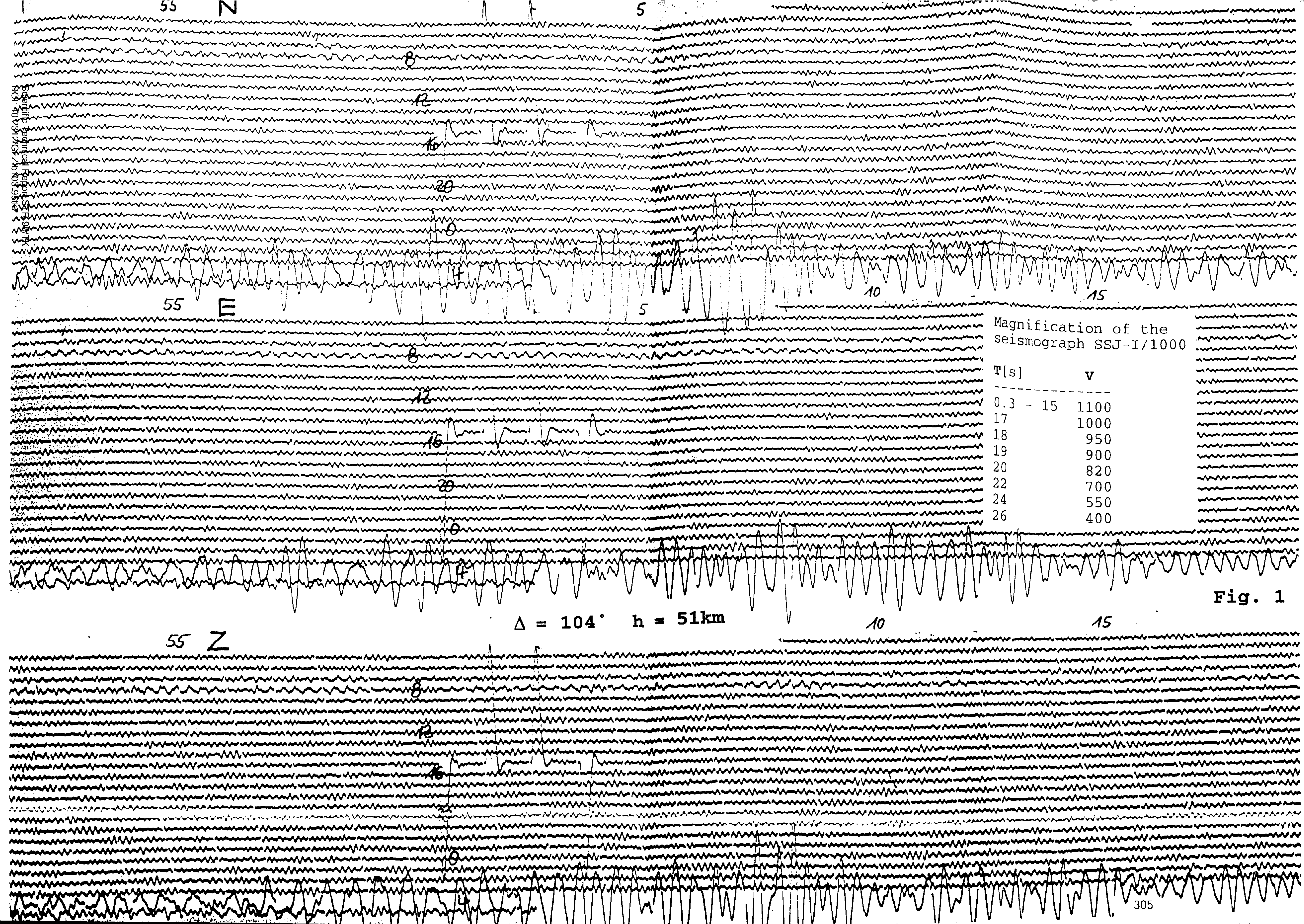

Magnification of the seismograph SSJ-I/1000

T[s]	V
0.3 - 15	1100
17	1000
18	950
19	900
20	820
22	700
24	550
26	400

$\Delta = 104^{\circ}$ $h = 51km$

Fig. 1

Scientific Technical Report STR 98/TK
DOI: 10.2312/GFZ.b103-98tk7

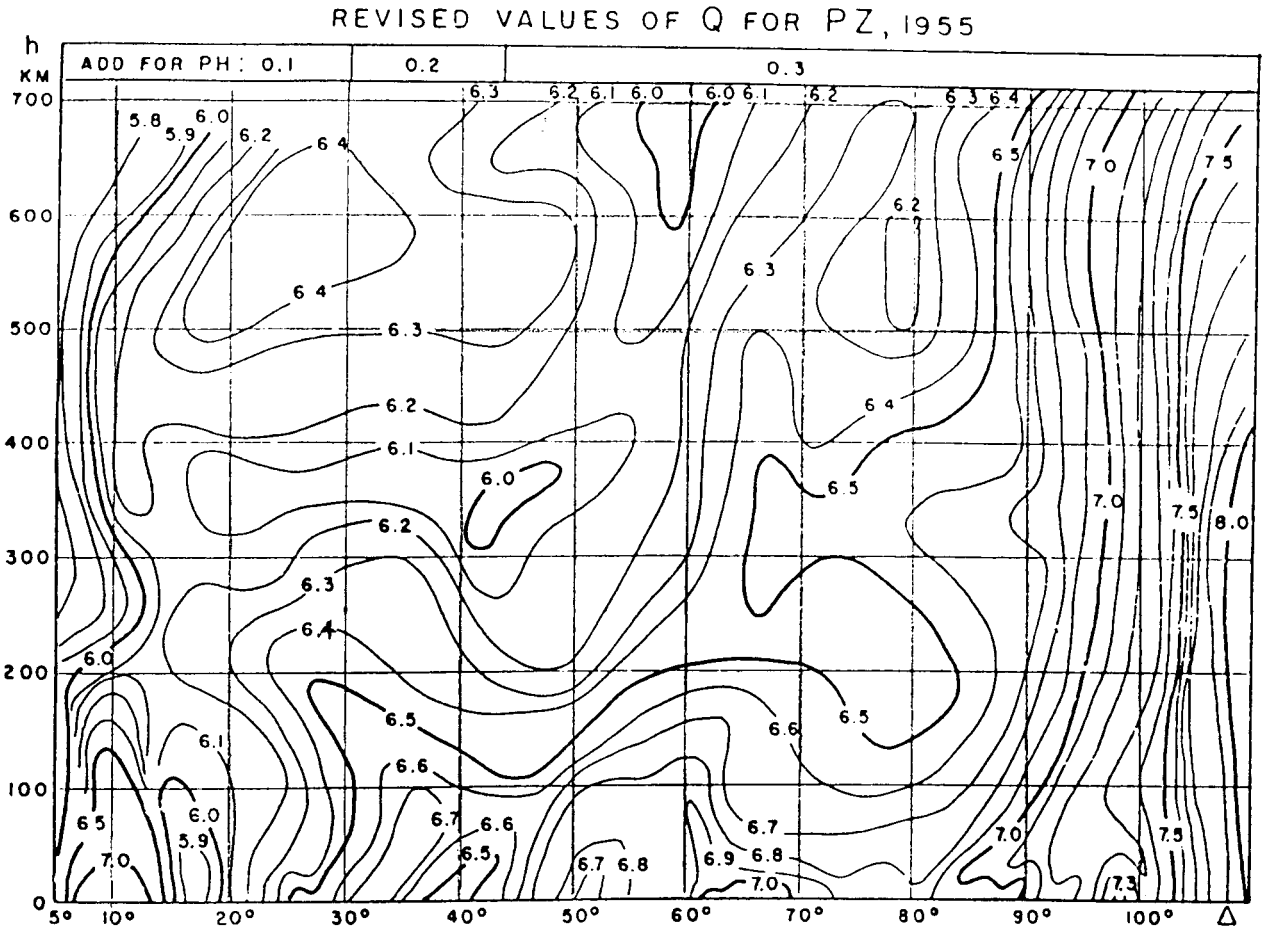

GUTENBERG - RICHTER MAGNITUDE, ETC 3 1955

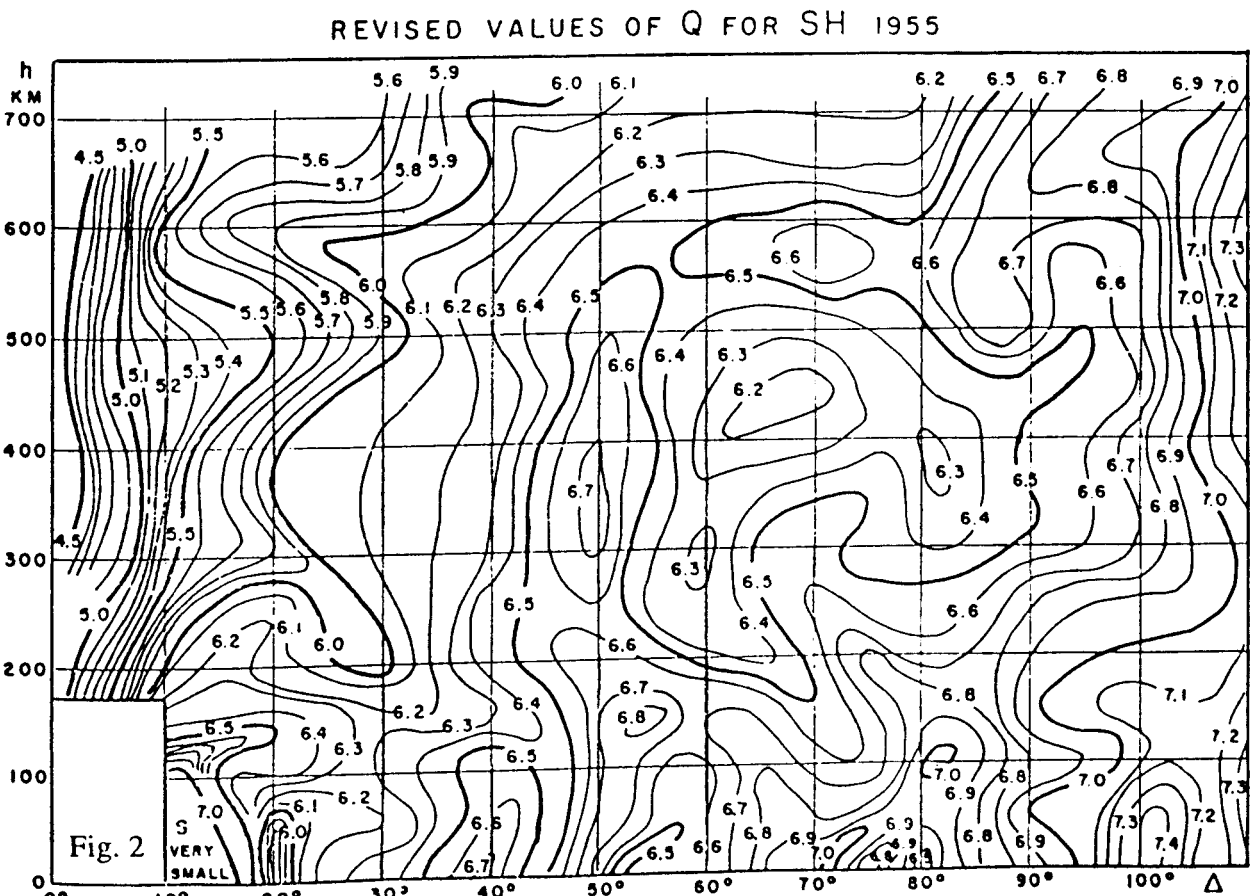

Fig. 2

Δ°	0°		1°		2°		3°		4°		5°		6°		7°		8°		9°		Δ°
	H	V	H	V	H	V	H	V	H	V	H	V	H	V	H	V	H	V	H	V	
0°			3.30		3.80		4.09		4.30		4.46		4.59		4.70		4.80		4.88		0°
10°	4.96		5.03		5.09		5.15		5.20		5.25	5.43	5.29	5.47	5.34	5.50	5.38	5.54	5.42	5.58	10°
20°	5.46	5.61	5.50	5.64	5.53	5.67	5.56	5.70	5.59	5.72	5.62	5.75	5.65	5.78	5.68	5.80	5.71	5.82	5.73	5.85	20°
30°	5.75	5.87	5.78	5.89	5.80	5.91	5.82	5.93	5.84	5.95	5.86	5.97	5.88	5.98	5.90	6.00	5.92	6.02	5.94	6.03	30°
40°	5.96	6.05	5.98	6.07	5.99	6.08	6.01	6.10	6.03	6.11	6.04	6.13	6.06	6.14	6.07	6.15	6.09	6.17	6.10	6.18	40°
50°	6.12	6.19	6.13	6.21	6.14	6.22	6.16	6.23	6.17	6.24	6.18	6.25	6.20	6.26	6.21	6.28	6.22	6.29	6.24	6.30	50°
60°	6.25	6.31	6.26	6.32	6.27	6.33	6.28	6.34	6.30	6.35	6.31	6.36	6.32	6.37	6.33	6.38	6.34	6.39	6.35	6.40	60°
70°	6.36	6.41	6.37	6.42	6.38	6.42	6.39	6.43	6.40	6.44	6.41	6.45	6.42	6.46	6.43	6.47	6.44	6.48	6.45	6.48	70°
80°	6.46	6.49	6.47	6.50	6.48	6.51	6.49	6.52	6.49	6.52	6.50	6.53	6.51	6.54	6.52	6.55	6.53	6.55	6.54	6.56	80°
90°	6.55	6.57	6.55	6.57	6.56	6.58	6.57	6.59	6.58	6.59	6.58	6.60	6.59	6.61	6.60	6.62	6.61	6.62	6.61	6.63	90°
100°	6.62	6.63	6.63	6.64	6.64	6.65	6.64	6.65	6.65	6.65	6.66	6.67	6.66	6.67	6.67	6.68	6.68	6.68	6.69	6.69	100°
110°	6.69	6.69	6.70	6.70	6.70	6.71	6.71	6.71	6.72	6.72	6.72	6.72	6.73	6.73	6.74	6.73	6.74	6.74	6.75	6.75	110°
120°	6.75	6.75	6.76	6.76	6.76	6.76	6.76	6.77	6.77	6.77	6.77	6.78	6.78	6.78	6.78	6.79	6.78	6.79	6.79	6.80	120°
130°	6.79	6.80	6.79	6.81	6.80	6.81	6.80	6.82	6.80	6.82	6.81	6.83	6.81	6.83	6.81	6.84	6.81	6.84	6.81	6.84	130°
140°	6.82	6.85	6.82	6.85	6.82	6.86	6.82	6.86	6.83	6.87	6.83	6.87	6.83	6.88	6.83	6.88	6.83	6.88	6.83	6.89	140°
150°	6.84	6.89	6.84	6.90	6.84	6.90	6.84	6.91	6.84	6.91	6.84	6.91	6.84	6.92	6.84	6.92	6.84	6.93	6.84	6.93	150°
160°	6.84	6.93	6.84	6.94	6.83	6.94	6.83	6.95	6.83	6.95	6.82	6.95	6.82	6.96	6.82	6.96	6.82	6.96	6.82	6.97	160°
170°	6.81	6.97	6.81	6.98	6.80	6.98	6.79	6.98	6.77	6.99	6.74	6.99	6.71	7.00	6.69	7.00	6.64	7.00	6.59	7.01	170°
180°	6.49	7.01																			180°

Table 1. Magnitude calibration values $d(\Delta)$ for surface-waves ($h \leq 50$ km)

REFERENCES

Wahlstroem, R. and Strauch, W. (1984). A regional magnitude scale for Central Europe based on crustal wave attenuation. University of Uppsala, Seismol. Dept., Report No. 5-79, 21 p.

Source parameters and source mechanism of earthquakes

by

E. HURTIG

1. General

Faults and fractures are representing ruptural deformations in geological media. From geological and tectonic investigations the deformation process can be obtained as an integral effect for a given geological formation or time interval.
Furthermore, from geological data one can obtain information on recent active faults and fault zones. Satellite data and processing of aerocosmic images are an outstanding tool for locating and analyzing active faults.
But, the dynamics and the process of fracturing cannot be investigated simply by using geological methods.
Fracturing of rocks is the source for earthquakes and for radiating seismic waves. Thus, interpreting seismic records one can obtain information about the seismic source and the rupture process.
Determination of source parameters and source mechanism studies belong to the main aimes of seismological research work and are essential for assessing earthquake hazard and seismic risk.
Any fracturing of rocks is connected with a dislocation (or slippage) along the fault plane. In his classical work, REID studied the dislocation along the San Andreas fault system during the San Francisco earthquake of 1906 and derived the elastic rebound theory.
In the 60-ies of this century, HASKELL, BURRIDGE & KNOPOFF and others developed the dislocation theory as a theoretical basis for explaining the radiated wave pattern in terms of a given dislocation along the fault.
The basic idea is the equivalence of a finite dislocation and a single couple or double couple force system (see fig. 1).
In general, seismic source studies are to be performed using seismic records from stations the epicentral distance of which is greater than the source dimensions. For this far field case strong limitations must be taken into account when studying the source mechanism because information about the source is lost during the propagation of seismic waves (e. g. by attenuation of the higher frequencies). Therefore, one is restricted to determine some source parameters for describing the seismic source.
The classical HASKELL uniform dislocation model as a kinematic model can be described by 5 parameters: the fault dimension (fault length L, fault width W), the final dislocation D, the rupture velocity v and the rise time τ which equals approx. the rupture time.
On the other hand, dynamic models try to include the physical processes at the fault, the physical properties of the material to be fractured, and the time-space distribution of the stress.

2. Determination of source parameters

From seismic records information about the source can be obtained either using data directly read from the records (amplitude and period) or using parameters derived

from spectral analysis of the records (fig. 2).

2.1. Fault plane solution

In an early stage of seismogram interpretation it was recognized that the polarity of the first motion of the P- and S-waves showsa characteristic pattern.
The basic idea for understanding this pattern is the assumption of a double couple force system representing the earthquake focus. For practical fault plane solutions the polarity of the first motion for stations is determined from different azimuths and epicentral distances. Around the focus a focal sphere is assumed with constant velocity of the seismic waves. The stations for which the polarity is obtained are marked in a polar co-ordinate grid by their azimuths and their angles of incidence (length of the radius vector).
The areas with positive and negative polarities (for P-waves: compression and dilatation) can be seperated by great circles which are representing the course of two nodal planes, one being the fault plane the other one being the auxiliary plane.
Additional geological or other information is needed to decide which of both nodal planes is the fault plane or the auxiliary plane.
The details of fault plane solutions are discussed in practical exercises.
For seismotectonic studies the results of fault plane solutions are of great importance. Fig. 3 gives some characteristic examples of fault plane solutions for strike slipe, dip slip, and overthrust cases.

2.2. Spectral source parameters

Spectral analysis of seismic records is a very important tool for determining source parameters.
Fig. 4 shows the typical form of the amplitude spectrum of the ground motion.
Three characteristic parameters can be obtained:

- The level of the long period asymptote ($\Omega(0)$).
  From this the seismic moment is calculated using the relation

$$M_0 = 4\pi \varrho\, Rc^3\, \Omega(0)/R_{\theta\varphi}$$

  $\Omega(0)$: long period spectral amplitude level of P or S wave
  $R_{\theta\varphi}$: radiation pattern of P or S wave
  ϱ : density near the source
  R : hypocentral distance
  c : P or S wave velocity

- The corner frequency f_c.
  The frequency at the intersection point of the long period and of the high frequency asymptotes is called the corner frequency.
  The following relations are used for calculating the source dimensions from the corner frequency.

$$r(W \text{ or } L) = \frac{c_p v_p}{2\pi f_{c_p}} \qquad \text{for P-waves}$$

$$r(W \text{ or } L) = \frac{C_s v_s}{2 \pi f_{C_s}} \qquad \text{for S-waves}$$

C_p and C_s are constants depending on the model used. They are differing slightly for determination of r, W or L.

Using the seismic moment and the source dimensions (or the source radius) additional parameters can be calculated

$$\text{Dislocation } D = M_o / \mu L W$$
$$= M_o / \mu r^2$$

Stress Drop $\Delta\sigma$: This is the difference between the initial stress σ_0 (before fractioning) and the final stress σ_1

$$\Delta\sigma = \sigma_0 - \sigma_1$$

The radiated seismic energy E_s is

$$E_s = \eta L W D \bar{\sigma}$$
$$= \eta M_o \bar{\sigma} / \mu$$

$\bar{\sigma}$: average stress $(\sigma_0 + \sigma_1)/2$
η : seismic efficiency
$\eta\bar{\sigma}$: apparent stress

η depends on the ratio v/v_s and σ_0 / σ_f; σ_f is the sliding frictional stress. As a first approximation the following expression for E_s is valid (after YAMASHITA, 1979):

$$E_s \approx 0{,}23 \Delta\sigma^2 L W^2 / \mu$$

It must be stressed that the described source parameters are depending on the used theoretical model of the dislocation. They are to be regarded as a measure of the real source parameters, only. Table 1 gives some typical results (after GELLER, 1976).

2.3. Scaling Laws

The relations between the different source parameters are called scaling laws. Generally, these relations are empirical ones, the physical basis of the scaling laws is studied by KANAMORI and ANDERSON (1975). The investigation of scaling laws gives important information about the general relation between the single source parameters, and they are the basis for deriving one source parameter from another. The scaling laws show regional variations depending on the characteristics of the single seismotectonic regions.

3. Exercises

3.1. Practical exercises in fault plane solution

3.2. Practical exercises in determining spectral source parameters

4. Further Readings

AKI, K.; RICHARDS, P.: Quantitative Seismology. Theory and Methods. Freeman and Comp., San Francisco, 1980.

AKI, K.: Earthquake mechanism. In: RITSEMA, A. R. (Edit.): The Upper Mantle. Tectonophysics 13 (1972), 423 - 446.

KANAMORI, H.; ANDERSON, D.L.: Theoretical basis of some empirical relations in seismology. Bull. Seismol. Soc. Am. 65 (1975), 1073 - 1095.

GELLER, R.J.: Scaling laws for earthquake source parameters and magnitudes. Bull. Seismol. Soc. Am. 66 (1976), 1501 - 1523.

BRUNE, J.N.: Tectonic stress and the spectra of seismic shear waves from earthquakes. J. Geophys. Res. 75 (1970), 4997 - 5009.

YAMASHITA, T.: Energy balance of fault motions, and radiated seismic energy and seismic efficiency of shallow earthquakes. J. Phys. Earth 27 (1979), 171 - 187.

Mitteilung des Zentralinstituts für Physik der Erde Nr. 1049

Table 1 Earthquake Source Parameters

Event	Date	M_s	m_b	M_0 $\times 10^{27}$ dyne-cm	L (km)	W (km)	$\bar{D}$ (m)	t (sec)	t* (sec)	V_R (km/sec)	Δa (bars)
1. Kanto	1 Sep. 1923	8.2	-	7.6	130	70	2.1	7	10	-	21
2. Tango	27 Mar. 1927	7.75	-	0.46	35	13	3	6	2.5	2.3	115
3. North Izu	25 Nov. 1930	7.1	-	0.2	20	11	3	-	1.7	-	150
4. Saitama	21 Sep. 1933	6.75	-	0.068	20	10	1	2	1.6	2.3	59
5. Sanriku	2 Mar. 1933	8.3	-	43	185	100	3.3	7	12	3.2	42
6. Long Beach	11 Mar. 1933	6.25	-	0.028	30	15	0.2	2	2.5	2.3	7
7. Imperial Valley	19 May 1940	7.1	-	0.48	70	11	2	-	3.2	-	55
8. Tottori	10 Sep. 1943	7.4	-	0.36	33	13	2.5	3	4.0	2.3	99
9. Tonankai	7 Dec. 1944	8.2	-	15	120	80	3.1	-	9.2	-	39
10. Mikawa	12 Jan. 1945	7.1	-	0.087	12	11	2.2	-	1.3	-	140
11. Nankaido	20 Dec. 1946	8.2	-	15	120	80	3.1	-	9.2	-	39
12. Fukui	28 Jun. 1948	7.3	-	0.33	30	13	2	2	1.9	2.3	100
13. Tokachi-Oki	4 Mar. 1952	8.3	-	17	180	100	1.9	-	14	-	17
14. Kern County	21 Jul. 1952	7.7	-	2	60	18	4.6	1	3.6	-	140
15. Fairview	16 Dec. 1954	7.1	-	0.13	36	6	2	-	1.7	-	100
16. Chile	22 May 1960	8.3	-	240	800	200	21	-	36	3.5	91
17. Kitamino	19 Aug. 1961	7.0	-	0.09	12	10	2.5	2	1.3	3.0	170
18. Wasaka Bay	27 Mar. 1963	6.9	-	0.033	20	8	0.6	2	1.5	2.3	40
19. North Atlantic I	3 Aug. 1963	6.7	6.1	0.12	32	11	1	-	2.2	-	44
20. Kurile Islands	13 Oct. 1963	8.2	5.7	75	250	140	3	-	17	3.5	28
21. North Atlantic II	17 Nov. 1963	6.5	5.9	0.038	27	9	0.48	-	1.8	-	24
22. Spain	15 Mar. 1964	7.1	6.2	0.13	95	10	0.42	-	3.6	1.4	11
23. Alaska	28 Mar. 1964	8.5	6.2	520	500	300	7	-	35	3.5	22
24. Niigata	16 Jun. 1964	7.4	6.1	3.2	80	30	3.3	-	5.3	-	66
25. Rat Island I	4 Feb. 1965	7.9	6.0	140	500	150	2.5	-	25	4.0	17
26. Rat IslandII	30 Mar. 1965	7.5	5.7	3.4	50	80	1.2	-	5.8	-	33
27. Parkfield	28 Jun. 1966	6.4	5.3	0.032	26	7	0.6	0.7	1.6	2.7	32
28. Aleutian	4 Jul. 1966	7.2	6.2	0.226	35	12	1.6	-	2.4	-	64
29. Truckee	12 Sep. 1966	5.9	5.4	0.0083	10	10	0.3	-	1.2	-	20
30. Peru	17 Oct. 1966	7.5	6.3	20	80	140	2.6	-	9.6	-	41
31. Borrego	9 Apr. 1968	6.7	6.1	0.063	33	11	0.58	-	2.2	-	22
32. Tokachi-Oki	16 May 1968	8.0	5.9	28	150	100	4.1	-	12	3.5	37
33. Saitama	1 Jul. 1968	5.8	5.9	0.019	10	6	0.92	1	0.9	3.4	100
34. Portuguese	28 Feb. 1969	8.0	7.3	5.5	80	50	2.5	-	6.1	-	53
35. Kurile Islands	11 Aug. 1969	7.8	7.1	22	180	85	2.9	-	12	3.5	28
36. Gifu	9 Sep. 1969	6.6	5.5	0.035	18	10	0.6	1	1.7	2.5	35
37. Peru	31 May 1970	7.8	6.6	10	130	70	1.6	-	8.7	2.5	28
38. San Fernando	9 Feb. 1971	6.6	6.2	0.12	20	14	1.4	1	2.0	2.4	62
39. Nemuro-Oki	17 Jun. 1973	7.7	6.5	6.7	60	100	1.6	-	7.5	-	35
40. Turkey	22 Jul. 1967	7.1	6.0	0.83	80	20	1.7	-	4.7	-	32
41. Iran	31 Aug. 1968	7.3	5.9	1	80	20	2.1	-	4.7	-	38

Scientific Technical Report STR 95/TK
DOI: 10.2312/GFZ.b103-95tk7

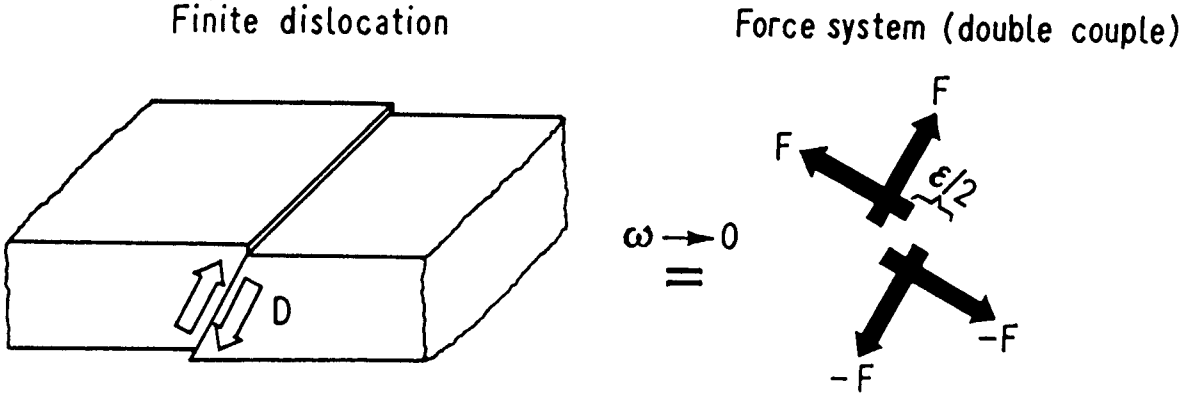

Fig. 1

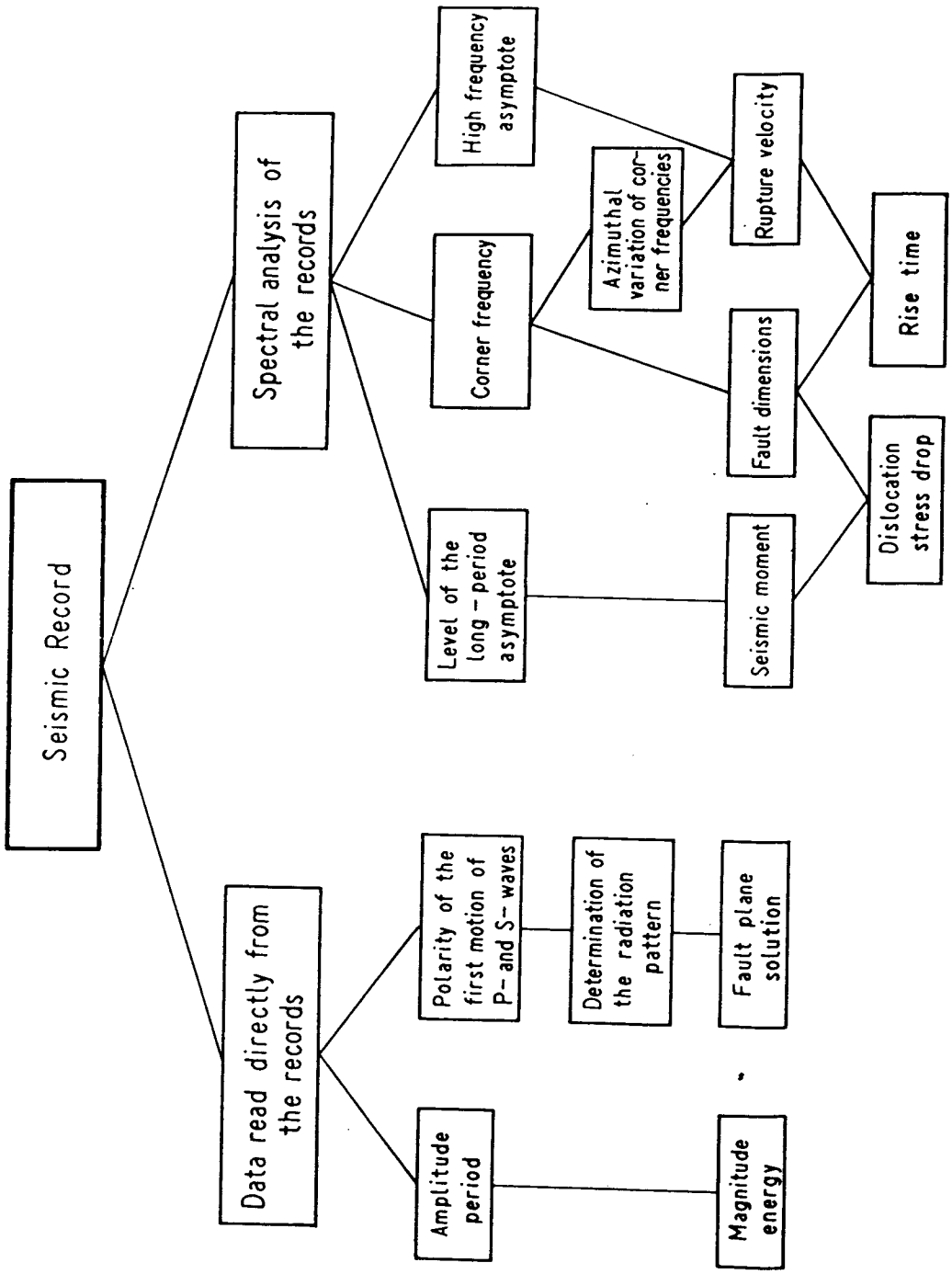
Seismic Record
Spectral analysis of the records
Data read directly from the records
High frequency asymptote
Corner frequency
Level of the long – period asymptote
Azimuthal variation of corner frequencies
Rupture velocity
Fault dimensions
Seismic moment
Rise time
Dislocation stress drop
Polarity of the first motion of P- and S- waves
Determination of the radiation pattern
Fault plane solution
Amplitude period
Magnitude energy

Fig. 2

Scientific Technical Report STR 95/TK
DOI: 10.2312/GFZ.b103-95tk7

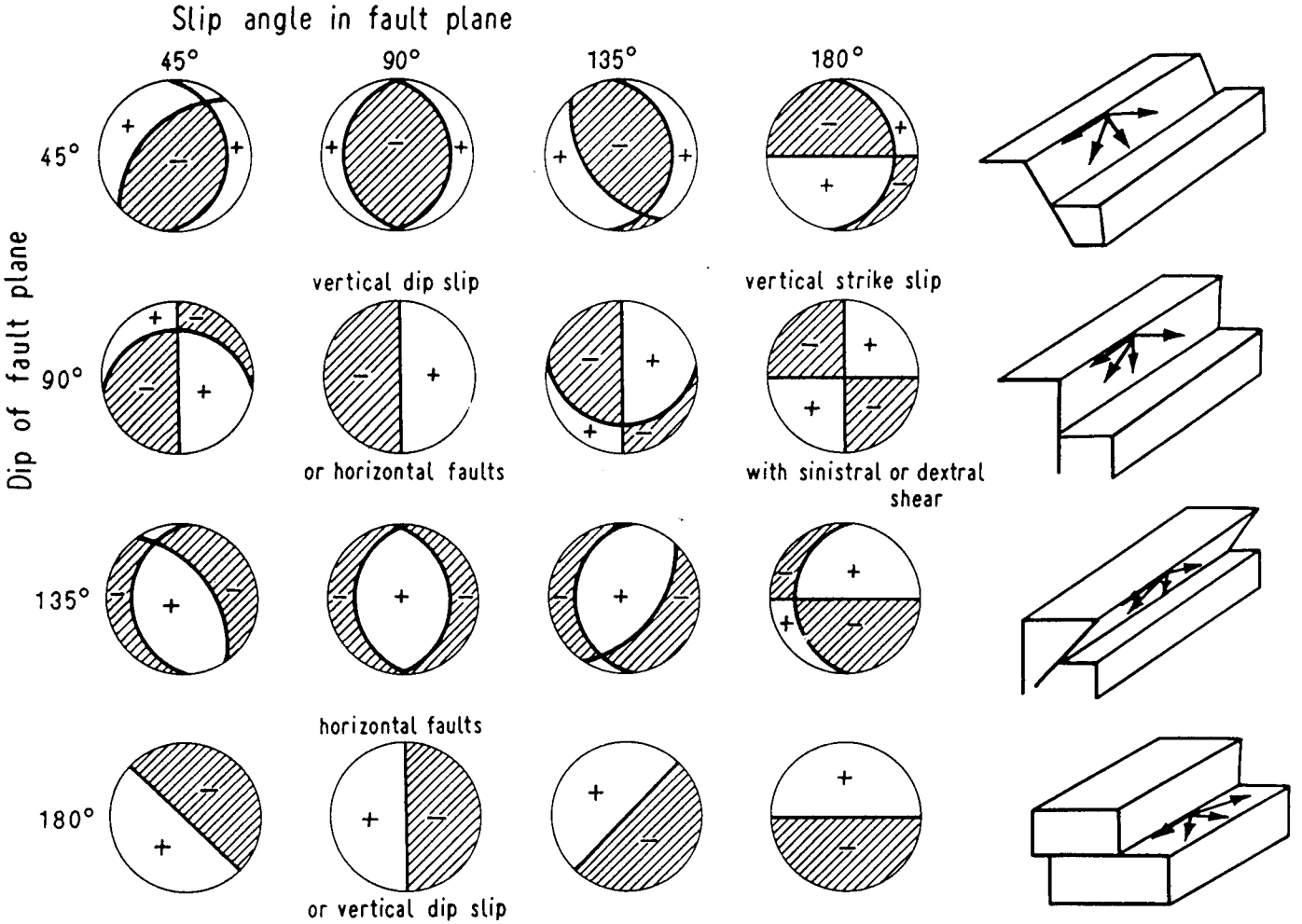

Fig. 3 Fault plane orientations for different cases of the dip and the slip angle of the fault plane. Hatched quadrants are negative (dilatation)

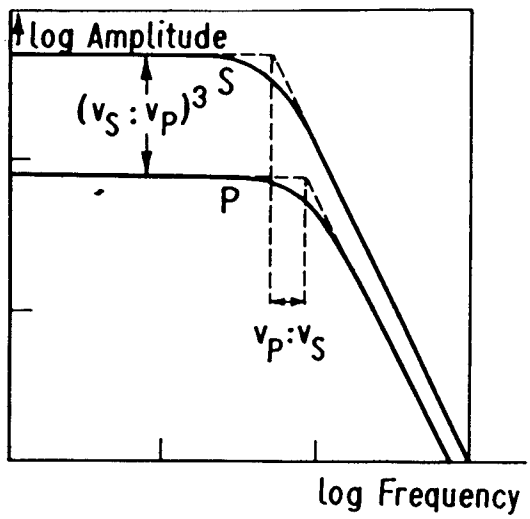
log Amplitude
$(v_S : v_P)^3$
S
P
$v_P : v_S$
log Frequency

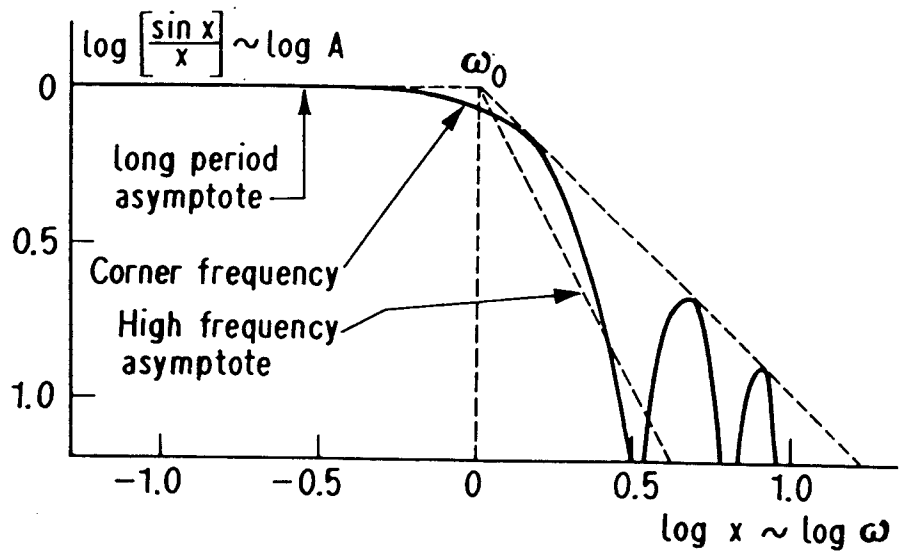
$\log\left[\frac{\sin x}{x}\right] \sim \log A$
ω_0
0
0.5
1.0
long period asymptote
Corner frequency
High frequency asymptote
−1.0
−0.5
0
0.5
1.0
log x ~ log ω

Fig. 4

Practical Exercises in Source Parameter Estimation

by

H. GROSSER

This exercise deals with problems of estimating focal parameters by means of real seismograms. In the lectures interpretation methods for seismic registration are given. Following topics which are to train will be:
fault plane solution, estimation of corner frequency,
seismic moment and static stress drop. In the following are given foundations for these problems by means of the distribution of the polarity of an earthquake of Nov. 7, 1969, Southern Persia / Western Asia and by the amplitude spectra of theoretical and recorded seismograms, respectively.

Fault plane solution

Foundations

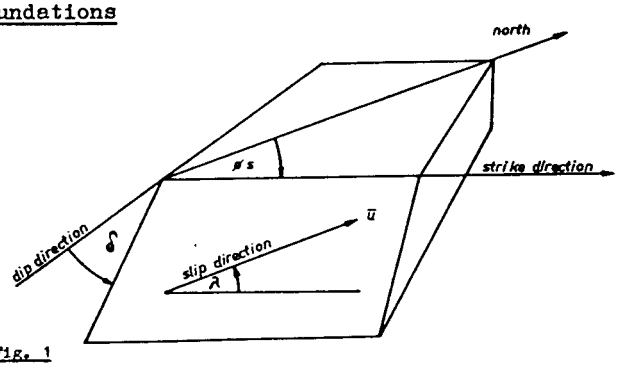

Fig. 1

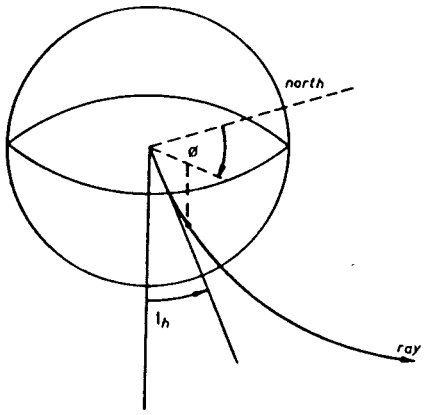

Fig. 2

Fig. 1 Definition of the fault-orientation parameters (strike Φ_S, dip δ), and slip-direction. Φ_S is measured clockwise round from north, with the fault dipping down to the right of the strike direction: $0 \leq \Phi_S < 2\pi$. δ is measured down from the horizontal: $0 \leq \delta < \pi/2$. Rake λ is the angle between strike direction and slip direction: $-\pi < \lambda \leq \pi$.

Fig. 2 The focal sphere for a seismic point source is a sphere centred in the source and having arbitrarily small radius. It is a convenient device for displaying radiation patterns, since information recorded by seismometers (distributed over the Earth's surface) may be transfered to the focal sphere; this involves tracing the ray back from receiver to source and seeing where it intersects the focal sphere. Equivalently, one may specify a point on the focal sphere by angular ray coordinates (I_h, Φ), used now in a spherical polar system centred in the source. $I_h = 0$ is the downward vertical; Φ is azimuth round from North.

Fig. 3 The stereographic projection of the focal sphere maps point P to the point P' as shown in the equatorial plane of the focal sphere. (a) Shown here is a vertical plane through the centre of the focal sphere and the point P. (b) A plan view of the horizontal plane viewed on edge in (a). This is the plane of the projection, and point P' is at distance $\tan \frac{1}{2} I_h$ from the point O.
The figure shows projection only of the lower half of the focal sphere, but by projecting from B instead of A, the upper half of the focal sphere can also be mapped inside a circle of unit radius.
The stereographic projection is used in association with a Wulff net, which provides a template for drawing in (b) the possible curves that in (a) represent the intersection of the focal sphere with fault planes of arbitrary orientation.

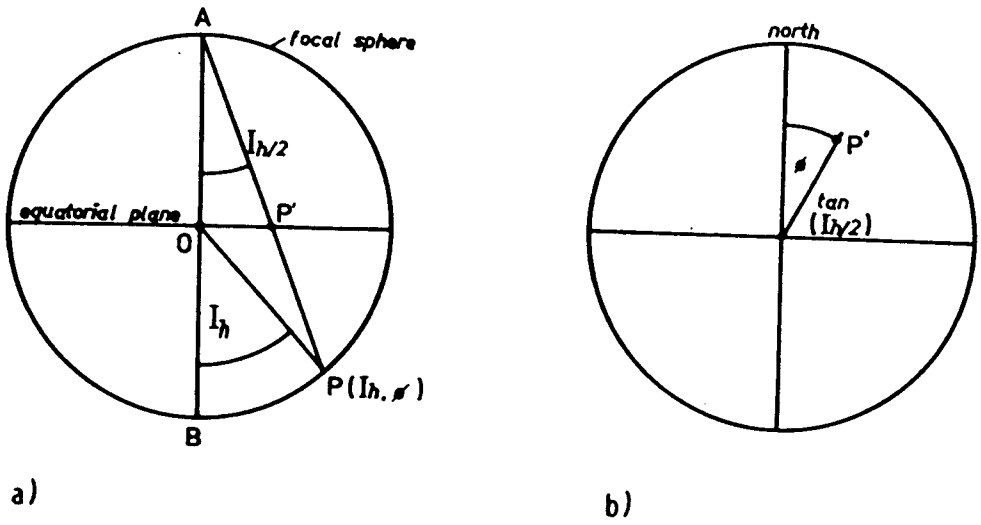

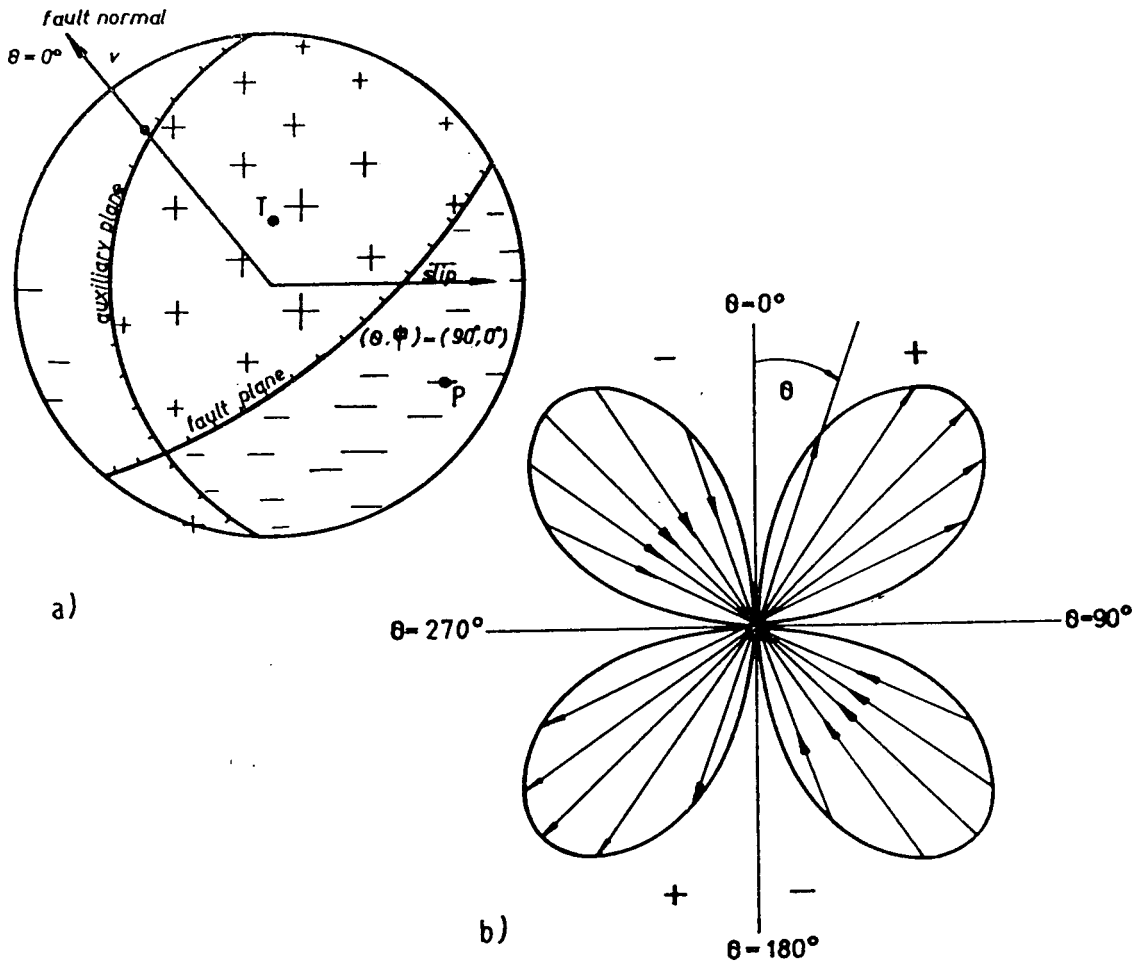

Fig. 4 Diagrams for the radiation pattern of the radial component of displacement due to double couple or an equivalent shear dislocation, i.e., $\sin 2\theta \cos\phi$. (a) The lobes are a locus of points having a distance from the origin that is proportional to $\sin 2\theta$. The diagram is for a plane of constant azimuth, and the pair of arrows at the centre denotes the shear dislocation. Note the alternating quadrants of inward and outward directions. In terms of far-field P-wave displacement, plus signs denote outward displacement, and minus signs denote inward displacement. (b) View of the radiation pattern over a sphere centred in the origin. Plus and minus signs of various sizes denote variation (with θ, ϕ) of outward and inward motions. The fault plane and the auxiliary plane are nodal lines (on which $\sin 2\theta \cos\phi = 0$). An equal-angle projection has been used (see Fig. 3). Point P marks the pressure axis, and T the tension axis. The pressure axis is located in the centre of the dilational quadrant, and the tension axis in the centre of the compressional quadrant.

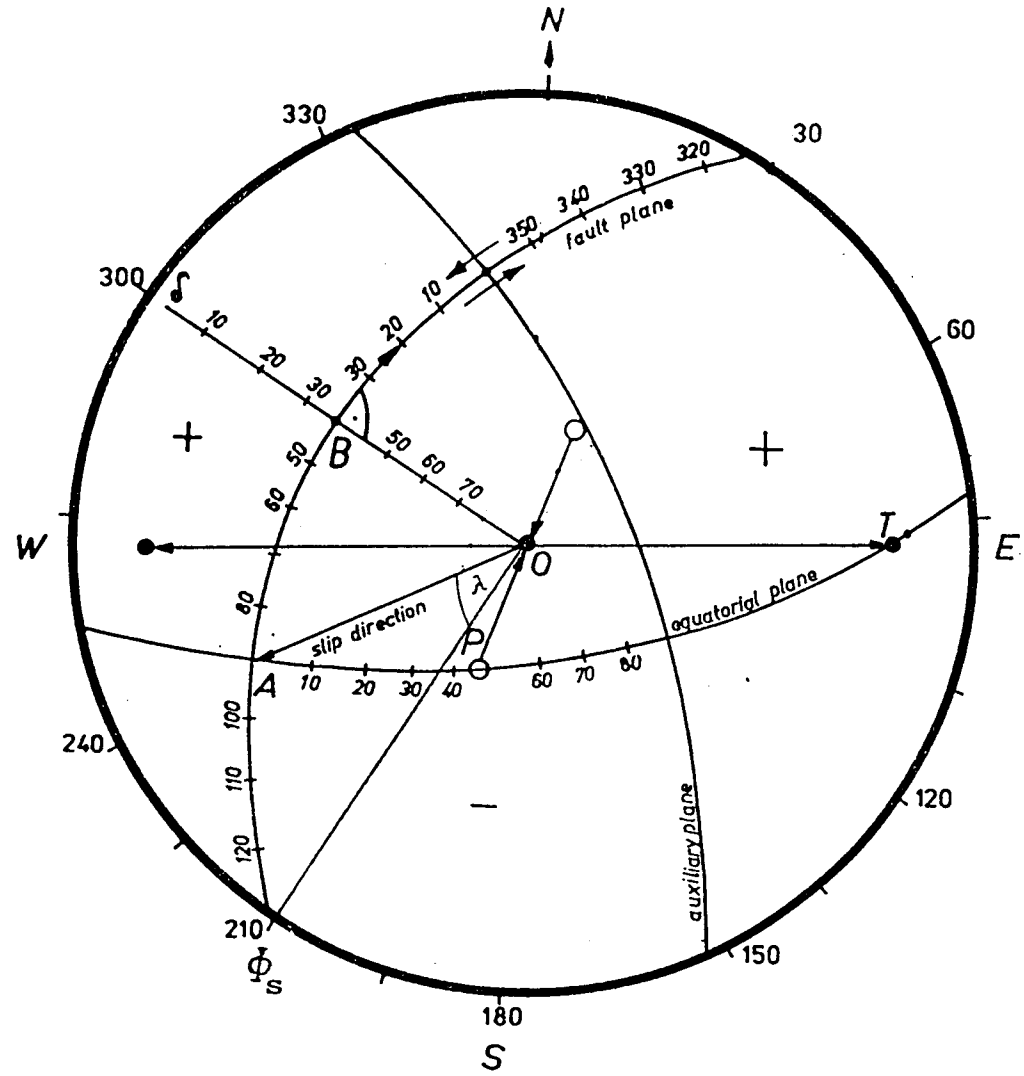

Fig. 5 Determination of the fault plane parameters Φ_S, δ and λ in the lower focal sphere. After drawing the distribution of first motion sign, the fault plane and the auxilary plane there is the problem to determinate the parameters of the fault plane Φ_S and δ and the rake λ of the slip direction. The strike angle Φ_S is measured from north. The dip angle is measured down from the horizontal. In a stereographic projection (Wulff net) point B is at distance $\tan\left[\left(\frac{\pi}{2} - \delta\right)/2\right]$ from point O (the radius of the net is unit). The slip direction is given by the vector $\overrightarrow{OA}$ where A is determined by the intersection of the fault plane, the equatorial plane and the surface of the focal sphere.

In fig. 5 the following parameters are obtained:

$\Phi_S = 210^\circ$
$\delta = 40^\circ$
$\lambda = -40^\circ$

Locations of pressure axis P and tension axis T

P : 30°S, 10°W
T : 5°N, 75°E

P r o b l e m

Determine the parameters of the fault plane (strike direction Φ_S, dip direction δ, slip direction λ of the earthquake on Nov. 7, 1969, Southern Persia/Western Asia. The stations, their distances Δ from the epicentre, the azimuth Φ measured clockwise round from north, the polarity and the take-off angle I_h are given in table I. In the stereographic projection (Wulff net) the value for $R_{WN} \cdot \tan(I_h/2)$ is necessary, too (R_{WN} - radius of the Wulff net).
Perform the following steps:

a) Marke positive and negative signs with full and open circles, respectively. The distance of every point from the centre of the Wulff net is $R_{WN} \cdot \tan(I_h/2)$ and the azimuth is the angle between North and the great circle path through the epicentre and the station (Fig. 1 - Fig. 5).

b) If you can recognize quadrants with different first motion sign, separate them by means of two perpendicular great circles. These curves represent the intersection of the focal sphere with the fault and auxiliary plane, respectively.

c) Choose from the two nodal planes the focal one. Draw the equatorial plane which is perpendicular to the fault and to the auxiliary planes. The intersection line between the fault plane and the equatorial plane marks the slip direction. The so-called pressure axis (P) is located in the centre of the dilatational quadrant and a tension axis (T) is to be found in the centre of the compressional quadrant. These are the principal axes of the moment tensor, and simultaneously they are also the principal stress axes if the fault plane is a plane of maximum shear.

d) Determine the parameters Φ_S and δ of the fault plane and the slip direction λ according to Fig. 5.

Corner frequency and fault dimension, seismic moment and stress drop

F o u n d a t i o n s

The corner frequency ω_c of a spectrum is determined by the intersection of the low-frequency level and the high-frequency asymptote. It is reciprocaly related to the fault dimension L.

$$\omega_c = K\ v/L$$

v - wave propagation velocity

The factor K strongly depends on the fault geometry and on the wave type (P or S) used. In the table II some formulas from different authors are given.

Table II

	P-wave	S-wave
Madariaga (1977)		
rectangular fault	$\omega_c = 1.8 \cdot v_S/L$	$\omega_c = 1.25\ v_S/L$
circular fault	$\omega_c = 2 \cdot v_S/R_0$	$\omega_c = 1.3\ v_S/R_0$
Hanks, Wyss (1972)	$\omega_c = 2.34 \cdot v_P/R_0$	$\omega_c = 2.3\ v_S/R_0$

v_S - shear velocity
v_P - compressional velocity
R_0 - radius of a circular fault

The seismic moment of a double couple point source is a measure for acting momentum of forces. On the base of the equivalence of dislocation and force models for a seismic source a seismic moment can be defined for a dislocation also. In general the seismic moment is a symmetrical tensor with six components. Assuming a shear dislocation (the mostly used model for an earthquake) this tensor is essentially determined by the scalar moment M_0 defined by

$$M_0 = \mu \cdot A \cdot D$$

with μ - shear modulus, A - area of source plane, D - static dislocation.

From the registrations M_0 can be estimated in the far-field from the low-frequency level of the amplitude spectra of P-waves, S-waves and others. For instance, M_0 is given by

$$M_0 = 4\pi\varrho\ u_0(P,S)\ v^3_{P/S}\ r/R_{\theta\phi}\ (P,S)$$

with ϱ - density in the focal region, $v_{P/S}$ - wave velocities of P- or S-waves in the focal regions, $u_0(P,S)$ - low-frequency level of the amplitude spectrum of P- or S-wave, $R_{\theta\phi}\ (P,S)$ - radiation pattern of P- or S-wave, r - epicentral distance.

A seismic source can be described in two ways: in terms of dislocation (kinematic model) or in terms of stress changes (dynamic model).

The stress change is marked by the stress drop $\Delta\sigma_i$. In the case of a shear fault $\Delta\sigma_i$ can be described by a scalar. Keilis-Borok (1959) gives the mostly used relationship for the estimation of the static stress drop supposing a circular shear crack.

$$\Delta\sigma = \frac{7}{16} \frac{M_0}{R_0^3}$$

Problems

1. Determine the corner frequency and calculate the fault dimension for the theoretical spectra in fig. 6 by the three formulas given in table II!
   The shear and compressional velocities are 4.5 and 7.5 km/sec, respectively.

2. Determine the corner frequency, the fault dimension, the seismic moment M_0 and the static stress drop $\Delta\sigma$ of an earthquake (M_L = 3.5) occurred on Febr. 20, 1982 near Leipzig. P-wave spectra are given in Fig. 7.(v_p = 6.0 km/sec, v_s = 3.5 km/sec).

References:

AKI, K.; RICHARDS, P. G.: Quantitative seismology. Theory and Methods. - Volume I and II; W. H. Freeman and Company, San Francisco 1980.

GUTENBERG, B.; RICHTER, C. F.: Magnitude and energy of earthquakes. - Ann. Geofis. 9 (1956), 1 - 15.

HANKS, T. C.; WYSS, M.: The use of body wave spectra in the determination of seismic source parameters. - Bull. Seism. Soc. Am. 62 (1972), 561 - 589.

KEILIS-BOROK, V. I.: On the estimation of the displacement in an earthquake source and source dimensions. - Ann. Geofis. 12 (1959), 205 - 214.

MADARIAGA, R.: High frequency radiation from crack (stress drop) models of earthquake faulting. - Geophys. J. Royal. astron. Soc. 51 (1977), 625 - 651.

Scientific Technical Report STR 95/TK
DOI: 10.2312/GFZ.b103-95tk7

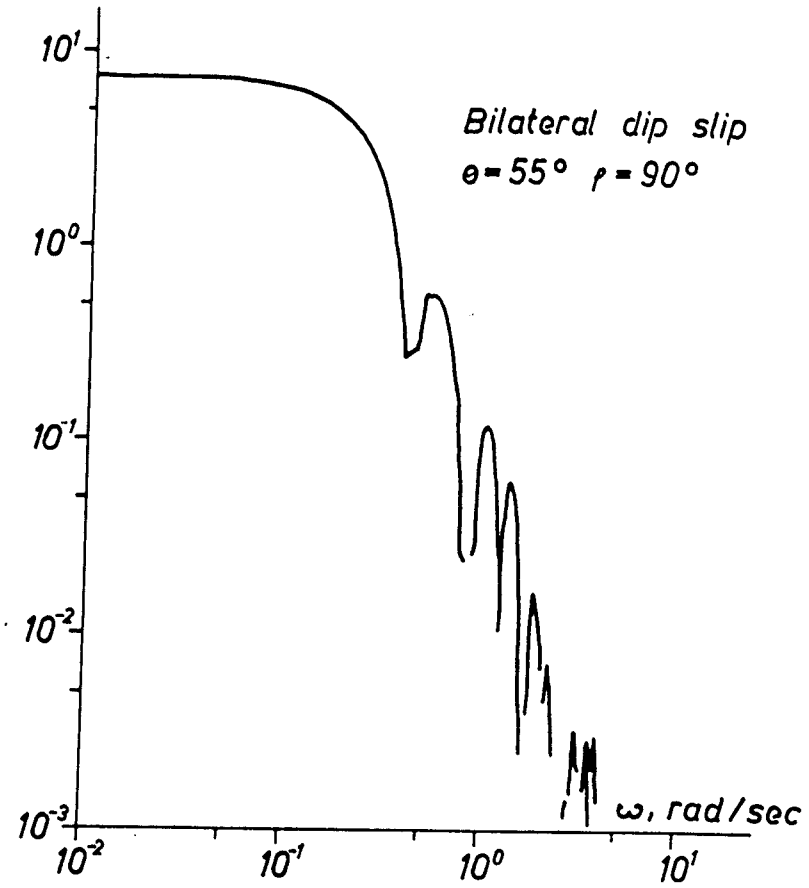

Fig. 6 SV-wave, spectrum of true ground motion source time function: ramp-function, to = 15s

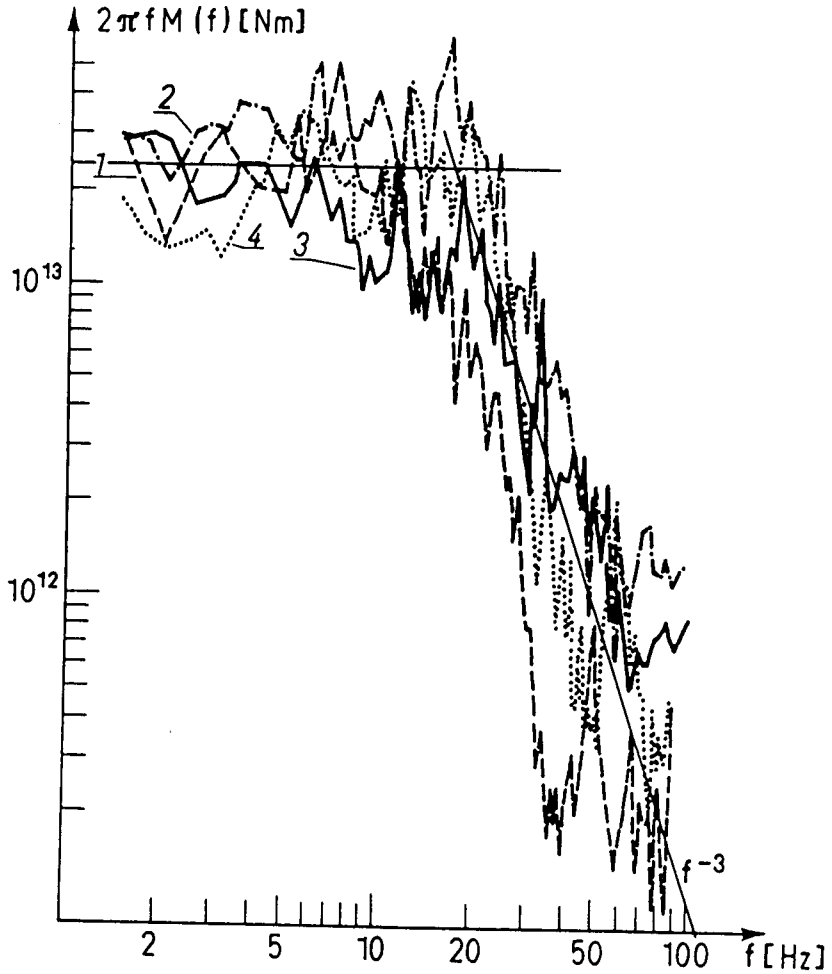

Fig. 7 Corrected P-wave spectra of the Leipzig earthquake of February 20, 1982

Table I Distribution of the first motion of the earthquake of 7. Nov. 1969, 27.9N 60.1E, depth 35 km, m = 6.1, Southern Persia/Western Asia (Bulletin of the International Seismological Centre, 1969 November)

Station Code	Δ (°)	Φ (°)	Polarity	I_h (°)*	$8 \cdot \tan \frac{I_h}{2}$
1	2	3	4	5	6
SVE	29.00	1	+	40.4	3.0
INK	83.67	5	+	21.8	1.5
PJD	85.03	11	+	21.2	1.5
GLN	85.09	11	+	21.2	1.5
MCB	85.36	11	+	21.1	1.5
SCM	87.99	13	-	20.4	1.4
TNN	84.01	13	+	21.6	1.5
BIG	88.38	17	-	20.3	1.4
TAS	15.59	27	+	70.0	5.6
YAK	56.35	32	+	31.2	2.2
FRU	19.11	34	+	56.1	4.2
KUL	12.97	37	+	77.5	6.4
PET	73.18	39	+	25.5	1.8
KMU	66.95	53	+	27.4	1.9
WRS	11.64	54	-	79.5	6.7
VLA	58.82	54	+	30.3	2.2
MAT	65.10	60	+	28.4	2.0
OIS	63.55	64	+	28.9	2.1
LAH	12.99	70	-	77.5	6.4
ANP	54.60	78	+	31.9	2.3
NDI	15.19	83	+	71.2	5.8
HKC	49.04	84	-	33.8	2.4
SHL	28.52	87	-	40.5	3.0
PLV	42.85	89	-	36.1	2.6
RAB	93.83	93	-	19.8	1.4
CHG	36.76	96	-	38.2	2.8
ESA	95.17	98	-	19.7	1.4
WAB	86.99	98	-	20.6	1.4
PMG	91.81	100	-	19.9	1.4
CTA	95.95	109	-	19.7	1.4
FUR	42.63	112	+	36.1	2.6
WRA	86.12	115	-	20.9	1.4
HYB	19.96	117	-	53.4	4.0
POO	15.70	123	+	70.0	5.6
MEK	78.03	129	+	23.9	1.7
KLG	82.63	130	-	22.2	1.6
KOD	23.97	133	-	44.0	3.2
MUN	79.95	134	-	23.1	1.6
MAW	95.13	179	-	19.7	1.4
TAN	47.98	196	-	34.2	2.5
CNG	60.07	209	-	30.0	2.2
CLK	49.57	212	-	33.6	2.4
CIR	55.78	213	-	31.4	2.2
BUL	56.52	216	-	31.2	2.2
KRR	53.27	217	-	32.5	2.3
NAI	36.52	221	-	38.4	2.8

1	2	3	4	5	6
MFP	54.61	253	-	31.9	2.3
EIL	22.06	281	-	48.3	3.6
HLW	25.18	282	-	42.6	3.1
BAB	53.88	288	+	32.0	2.3
AVE	57.44	293	+	30.8	2.2
IFR	55.53	293	+	31.5	2.2
REA	56.81	294	+	31.0	2.2
ACM	52.74	297	+	32.6	2.3
ATH	31.95	298	+	39.8	2.9
LIS	57.63	300	-	30.8	2.2
EHR	49.98	301	-	33.5	2.4
TOL	53.53	301	+	32.2	2.3
KER	12.85	304	+	78.0	6.5
ISK	28.60	306	-	40.5	3.0
PAV	43.65	307	+	35.9	2.6
ZAG	39.01	309	+	37.7	2.7
BEO	35.71	309	-	38.7	2.8
LJU	40.05	309	+	37.1	2.7
BUH	44.72	312	+	35.4	2.6
WLS	45.26	312	+	35.2	2.6
KRL	44.65	313	+	35.5	2.6
STU	44.10	313	+	35.6	2.6
VIE	39.34	313	-	37.3	2.7
KHC	41.34	314	+	36.6	2.6
GRF	42.97	314	+	36.1	2.6
WRM	46.72	314	+	34.7	2.5
DOU	47.26	314	+	34.5	2.5
BNS	45.75	315	+	35.0	2.5
GIP	46.45	315	+	34.8	2.5
PRU	40.95	315	+	36.8	2.6
TAB	15.38	315	+	70.0	5.6
VAL	56.66	316	-	31.1	2.2
SRI	12.67	317	+	78.5	6.6
SIM	26.81	317	+	41.0	3.0
KIS	31.01	317	-	40.1	2.9
KRA	37.67	317	+	38.0	2.7
CLL	42.25	317	+	36.3	2.6
TEH	10.79	319	+	80.5	6.7
GRS	16.29	319	+	67.7	5.4
DUR	51.52	319	+	32.9	2.4
BKR	19.37	320	+	55.1	4.2
COP	43.88	323	+	35.7	2.6
GWC	89.69	327	+	20.0	1.4
SIC	89.17	329	+	20.1	1.4
ARG	103.25	329	-	19.6	1.4
UPP	43.06	330	+	36.0	2.6
SCM	85.92	332	+	21.0	1.5
NUR	40.48	334	+	37.0	2.6
MOS	32.24	336	+	39.7	2.9
PUL	37.86	336	+	37.8	2.7
UME	44.13	336	+	35.6	2.6

1	2	3	4	5	6
KTG	61.40	338	+	29.5	2.1
FBC	80.20	339	+	23.0	1.6
OUL	43.04	340	+	36.0	2.6
KIR	46.51	341	+	34.8	2.5
TRO	48.06	342	+	34.2	2.5
JOD	44.44	342	+	35.5	2.6
APA	42.92	345	+	36.1	2.6
KEV	46.09	345	+	35.0	2.5
FCC	91.11	347	+	19.9	1.4
FFC	96.36	350	+	19.7	1.4
BLC	86.28	350	+	20.8	1.4
NOR	60.74	351	+	29.7	2.2
ALE	66.59	353	+	27.9	2.0
RES	76.47	353	+	24.4	1.8
EDM	99.12	356	+	19.6	1.4
SES	101.75	356	+	19.6	1.4
CMC	84.59	358	+	21.4	1.5
MSH	8.49	358	+	82.2	7.0
MBC	76.21	360	+	25.5	1.8

Physical source models and their geologic-tectonic reality

by

H. Grosser, D. Stromeyer, P. Bankwitz

1. Fundamentals of the fracture process in geological materials

The internal structure of rocks is frequently disturbed by features of primary origin (as bedding, flow planes etc.) or by features which are created by tectonic processes: folds, faults, joints. Rocks are fractured at low ductility. Fracture planes once formed are planes of loss of cohesion, weakening the rock body, frequently they become the place of mineral veins dykes, intrusions, in some cases even lineaments. Near the surface the faults or joints (= fractures) influence slope stabilities, the occurrence of rock bursts etc.

External forces produce a stress state within the rock body. If the deformation is large enough a rock will fracture in a ductile or brittle manner. Dependent on the stress characteristics we distinguish between tension and shear fractures (= faults, with a displacement between both flanks). Sometimes extension fractures are characterized by $\sigma_1 > \sigma_2 > 0 > \sigma_3$, but geological indications make it possible to speak of extension fractures also in cases where $\sigma_3 > 0$.

Because the fracture process in rocks is governed by dislocations, microflakes, cleavange planes, groin boundaries, older cracks, temperature, fluid pressure, confining pressure, velocity mode of faulting etc. the fracture origin is a complicated process. Its development is difficult to reconstruct because the megascopic effects of loading, geometry of the geological bodies are of additional influence.

Stress conditions of fractures

According MOHR a special curve tau = f (sigma) expresses the failure criterion of material. Ninety years back MOHR found the relationship between normal stress and shear stress which act on a fracture plane. The criterion means that shear failure will happen along a plane if the shear stress is large enough to overcome the cohesive strength and the frictional resistance. This resistance equals the stress normal to the shear surface multiplied by the internal friction.

Stress fields which cause fractures appear in the crust when the stress state loses its equilibrium. At the Earth's surface the shear stress is zero and one of the axes of principal stress is vertical. The two other axes are horizontal. There are only three possible positions for the principal compressive stress (conjugate shear planes or faults). The validity is restricted to brittle shear failure of intact rocks, whereas under conditions of middle and lower crust quasi-plastic behaviour causes different faulting events with mylonites and blastocataclasites. Using the Coulomb criterion and other theories faults and joints can be used for palaeo-stress field reconstructions (GZOVSKY, ANGELIER, GUSHCHENKO).

The special case of fractures, the joints, were formed during tectogenetic movements, but mostly later, when the geological structures rise to shallower levels in the crust.

Distance between faults

Of importance for fault tectonic investigations is the distance between individual faults: if a fault is formed the amount of tectonic stress is lowered. As a rough approximation we can suppose that the stress is lowered for 30 % of the primary amount in a distance which equals the vertical extension. This leads to a tendency of equal distances. A lowering of 5 % of stress drop can inhibit the origin of a new parallel fault.

Temperature and fault activity

Significant rise of temperature depends on a high velocity of fault planes (only velocities of more than 10 cm/a cause rise of 50 - 60°). Melting along faults is therefore seldom, only if the ciameter of the fault is small enough to avoid rapid dissipation of energy. But then it is sometimes difficult to distinguish between real rock melting or intense occurrence of dislocations in the crystal lattices.
If the temperature rises under brittle conditions the frequency of microcracks grows, at ductile conditions mylonitic features originate.

2. Seismological description of an earthquake process

The physical-mathemadical description of such a complicated geologic-tectonic process like an earthquake requires some necessary simplifications.
In seismology the physics of an earthquake process is essentially restricted to the mechanics of the rupture and of the generation of seismic waves. An earthquake and the radiated seismic signals are time and spatial dependent motions in the solid Earth. In general the source volume behaves as a nonelastical, noncompatible and nonlinear medium. Outside the source an elastic or low-attenuating (quasielastic) behaviour is assumed.
An elegant general framework can be constructed for the representation of the elastic field generated by an earthquake based on classical elastodynamics.
The effect of a seismic source on its surroundings is described by the linearezid elastic equation of motion and by given boundary values on a surface enclosing the source. The modelling of a seismic source means: fixing, estimating or calculating the stress and/or the displacement on the surface of the source volume and solving the equation of motion outside the source. For a realistic but seismologically sufficient calculation of this motion something has to be known about the material behaviour and about the processes inside the source volume. These informations can be derived from geologic-tectonic studies, crack experiments and from the theoretical fracture mechanics.
Probably, the seismic moment density distribution serves as the simplest description of inelastic processes in terms of results of the classical continuum mechanics. No specific fracture criterion is necessary and the seismic moment density, also called stress glut, describes the inelastic processes as function of time and space. Being a symmetric tensor of rank 2 it has all properties of a stress tensor. It measures the inelastic deformation at the source during the earthquake and its value at the end of the rupture process measures the permanent inelastic strain produced by this event (Madariaga, 1983). The seismological problem consists in finding the distribution of forces or moments which are equivalent to the inelastic deformation associated with an earthquake.
The seismic-source representation theory enables to describe a source by different ways. These "different" methods developed by seismologists in the past few decades are in many points equivalent. Here we start with the generalized body force f_i representing the source. Mostly a seismic source is of internal origin and, therefore, it may not be represented by a single point force. The traditional way of building an adequate source in seismology was to use couples, double couples and vector dipols without moment (Hasegawa, 1930). This is a special case of the above introduced inelastic-stress distribution. Its equivalent bode force is given by

$$f_i = -m_{ij,j} \qquad (1)$$

where to comma indicates the differentiation with respect to the spatial variables.

In the most frequently used earthquake models the inelastic processes are limited to a narrow fault zone. This fault zone is usually idealized to a plane, i. e. its thickness is supposed to be narrower rhan its length and width as well as than any wavelength of interest in seismology.

A well known description of a seismic source is the creation of displacement discontinuity (dislocation), or a slip between the walls of the fault. The source is considered as an internal surface on which the displacement as a boundary value at both sides is given (kinematic model). The time and spatial dependent slip u_i is related to the m_{ij} by

$$m_{ij} = c_{ijkl}\ \Delta u_l n_k\ \delta_D(S) \tag{2}$$

where $\delta_D(S)$ is the surface Dirac function converting any volume integral over a region intersected by some part of S to a surface integral over that part of S, c_{ijkl} is the modulus tensor satisfying $c_{ojkl} = c_{jikl} = c_{ijlk} = c_{klij}$ and n_k is the unit normal of the surface S. The equivalent body force can be written as (Burridge, Knopoff, 1964)

$$f_i(x_m,t) = -\int_S dS(x_n')n_k\ \Delta u_l(x_n',t)c_{ijkl}\ \frac{\partial}{\partial x_j}\ \delta(x_n-x_n') \tag{3}$$

where $\delta(x_n-x_n')$ is the volume Dirac function. The seismic moment tensor M_{ij} is defined by

$$M_{ij}(t) = \int_V dV(x')m_{ij}\ (x',t) \tag{4}$$

where V is the source volume. Inserting (2) in (4) we find

$$M_{ij}(t) = \int_S dS(x')c_{ijkl}\ \Delta u_k(x',t)n_l\ . \tag{5}$$

For an isotropic material with the elastic constants and (5) is reduced to

$$M_{ij}(t) = \int_S dS(x')\ \lambda\,\delta_{ij}n_k\Delta u_k + \mu\,(\Delta u_i n_j + \Delta u_j n_i)\ . \tag{6}$$

If λ, μ and n_k are constant on the source plane M_{ij} can be expressed by an average dislocation D(t) defined by

$$D(t)\,\nu_i = \frac{1}{S}\int_S dS(x')\,\Delta u_i(x',t) \tag{7}$$

(ν_i - unit vector in the direction of the slip)
as follows

$$M_{ij}(t) = \left[\ \lambda\,\delta_{ij}\,\nu_k n_k + \mu\,(\nu_i n_j + \nu_j n_i)\right]\ D(t)S\ . \tag{8}$$

For a pure shear slip ($\nu_k n_k = 0$) we get

$$M_{ij}(t) = M(t)\ (\nu_i n_j + \nu_j n_i)\ , \tag{9}$$

where

$$M(t) = \mu\,D(t)S. \tag{10}$$

An important focal parameter in the seismological practice is the static value of the seismic moment which is connected with the static slip. In the following the static value of any function is zero indexed, e. g.

$$M^0_{ij} = \lim_{t\to\infty} M_{ij}(t) = \int_S dS(x') \left[\lambda \delta_{ij} \Delta u^0_k(x'_n) n_k + \mu (\Delta u^0_i(x'_n) n_j + \Delta u^0_j(x'_n) n_i) \right] . \qquad (11)$$

From (10) the conventional expression for the so called seismic moment M_0 is written as

$$M_0 = \lim_{t\to\infty} M(t) = \lim_{\omega\to 0} i\omega M(\omega) = \mu D_0 S \qquad (12)$$

where $M(\omega)$ is the Fourier-transform of $M(t)$ defined by

$$M(\omega) = \int_{-\infty}^{\infty} dt\, e^{-i\omega t} M(t). \qquad (13)$$

It can be shown that the displacement in the medium due to a slip can be calculated without knowledge of the stress on the source plane if no stress discontinuities of the components $n_j \sigma_{ij}$ appear. Generally in a boundary value problem both the stress and the displacement on the boundary have to be known but only one of them can be chosen indepedently. Therefore, the boundary values outside the fractured part of the source plane has in practice to be taken into consideration, if the temporal stress change on an increasing but finite surface is used to describe the source process (dynamical model). For calculation of the displacement field in the dynamical case it is necessary to solve an integral equation (with mixed boundary conditions), whereas in the kinematical model only an integral has to be calculated.

Dynamical problems are difficult to solve and simple relationships between the stress change (stress drop) and other source parameters (slip, moment) do not exist. The widely known and often used special case (e. g. Rice, 1980) is a deeply buried circular shear fault of radius R_0 that sustains a uniform shear stress drop $\Delta\sigma$ ($\Delta\sigma$ is one of the two shear components of the vector $\Delta\sigma_i = n_j \Delta\sigma_{ij}$ where $\Delta\sigma_{ij}$ is the difference between the initial stress and the final stress on the fault). The static elasticity solution for the displacement discontinuity in an isotropic medium is given by

$$\Delta u^0(r) = \frac{8(\lambda+2\mu)}{\pi\mu(3\lambda+4\mu)} \Delta\sigma \, (R_0^2 - r^2)^{1/2} \qquad (14)$$

where r is the radial co-ordinate on the source plane. In (14) the direction of slip is parallel to the direction of $\Delta\sigma$.

For $\lambda = \mu$ the long term seismic moment (12) is connected with the stress drop in the following form (Keilis-Borok, 1959)

$$M_0 = \frac{16}{7} \Delta\sigma \, R_0^3 . \qquad (15)$$

In general the relation between a nonuniform traction drops $\Delta\sigma_i$ and the static seismic moment tensor is written as

$$M^0_{ij} = \int_S dS(x') \, \Delta\sigma_k(x'_n) \, E_{kij}(x'_n) , \qquad (16)$$

where $E_{kij}(x'_n)$ is the static slip due to a uniform stress drop equal $n_l c_{klij}$.

Formula (14) can be also applied to complex and multiple faults, e. g. juxtaposed faults,

en échelon shear faults, fault planes with barriers or asperities.
In terms of the source parameters $\Delta\sigma$, D_0, S and M_0 the radiated seismic energy E_S is

$$E_S = 1/2\ \Delta\sigma\, D_0 S = \frac{1}{2\mu}\Delta\sigma\, M_0 \qquad (17)$$

assuming the fracture energy on the fault is small compared with E_S and can be neglected (Madariaga, 1983).

The lecture "Source parameters and source mechanics of earthquakes" and in "Practical exercises in source parameter estimation" shows how the source area S (or the radius R_0) and the seismic moment can be read off from a seismic recording. Applying (12), (15) and (17) $\Delta\sigma$, D_0 and E_S can be calculated but it is to note that the given relations depend more or less on the used model.

References

BURRIDGE, R.; KNOPOFF, L.: Body force equivalents for seismic dislocation.- Bull. Seism. Soc. Am., 54 (1964), 1787 - 1888.

HASEGAWA, M.: Die erste Bewegung bei einem Erdbeben.- Gerlands Beitr. Geophysik, 27 (1930), 102 - 125.

KEILIS-BOROK, V.I.: On the estimation of the displacement in an earthquake source and of source dimensions.- Ann. Geofis., 12 (1959), 205 - 214.

MADARIAGA, P.: Earthquake Source Theory: A Review. in: Earthquakes: Observation, Theory and Interpretation, 1983, LXXXV Corso Soc. Italiana di Fisica, Bologna, Italy.

RICE, J.R.: The Mechanics of Earthquake Rupture. in: Physics of the Earth's Interior (Proceedings of the International School of Physics "Enrico Fermi", Course 78, 1979), edited by A.M. Dziewonski and E. Boschi, Italian Physical Society (printed by North Holland Publ. Co.), 1980, pp 555 - 649.

Mitteilung des Zentralinstituts für Physik der Erde Nr. 1513

THE DETERMINATION OF THE SEISMIC MOMENT TENSOR FROM BROAD-BAND SEISMOGRAMS

Frank Krüger

Bundesanstalt für Geowissenschaften und Rohstoffe,
Zentralobservatorium Gräfenberg, Krankenhausstraße 1,
D-91054 Erlangen

ABSTRACT

The lecture gives an overview with respect to the theory of the seismic moment tensor, starting with the formulation of Backus and Mulcahy for the "equivalent volume force" description of the nonlinear source process. Then the first three terms of the multipole expansion of the moment tensor (i.e. monopole, dipole and quadrupole term) are discussed with respect to the question what can be learned about the source process by observation and identification of these terms. Finally the two methods routinely used by the Harvard group (centroid moment tensor solutions – CMT) and by the USGS (Multichannel signal enhancement algorithm – MSE) are briefly summarized .

Scientific Technical Report STR 95/TK
DOI: 10.2312/GFZ.b103-95tk7

Conventions

Throughout the whole lesson the following conventions will be used for the coordinate system (modified after Aki and Richards 1980 in Jost and Herrmann (1989)):

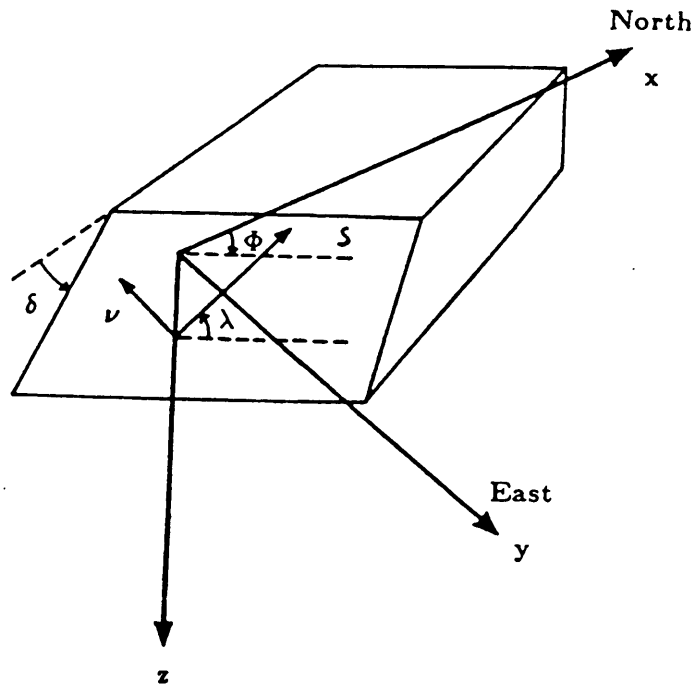

Fig. 1. Cartesian coordinate system (x,y,z). The origin is at the epicenter. Strike (Φ) is measured clockwise from north, dip (δ) from horizontal down, and slip (λ) counterclockwise from horizontal. s and ν are the slip vector and fault normal, respectively.

and

u_i is displacement in direction i

M_{ij} is the moment tensor

G_{ij} is the Greens tensor

f_i denotes a body force

and the Einstein summation convention is used (i.e. repeated indices are summed: $G_{ik}f_k = \sum_k G_{ik}f_k$) .

Backus and Mulcahy theory

First a brief review of Backus and Mulcahys (1976; BM) derivation of the seismic moment tensor is given. The propagation of elastic waves is expressed by the linear elastodynamic equation, and the eventual failure of the elastic stress–strain relation occurs in the source region. BM write the exact equation of motion of the Earth, describing both the elastic–wave propagation and the source dynamics as

$$\rho a_j = \partial_i S_{ij} - \rho \partial_j \psi + f_j^V \tag{1}$$

where V is the volume occupied by the Earth, $\rho(x,t)$ is the density, $a_j(x,t)$ is particle accelleration, $S_{ij}(x,t)$ is the stress field, ψ is the self–gravitational potential of the Earth's mass and f_j^V is the force from an external body.

In the Backus and Mulcahy phenomenological representation theory of Earthquake sources, the failure of the elastic stress–strain relation involved in the source process is transferred into an equivalent "volume force". They replaced the true stress S_{ij} by a model stress given by the elastic stress-strain relation $S'_{ij} = E_{ijkl}\partial_k u_l$ with the true displacement field u_i. They obtain

$$\rho a_j = \partial_i S' - \rho \partial_j \psi + m_j^V + f_j^V \tag{2}$$

where m_j^V is an equivalent volume force defined as

$$m_j^V = \partial_i \Gamma_{ij} = \partial_i (S_{ij} - S'_{ij}) \tag{3}$$

Γ_{ij} is called the stress glut.

BM linearized equation 2 by subtracting the initial equilibrium state and neglecting the nonlinear terms of ρ, a and ψ. The real $\rho(x,t)$ is approximated by the undisturbed density ρ_0 and the particle accelleration $a_j(x,t)$ is approximated by $\partial_t^2 u_j$ (i.e. the partial derivative with respect to time at a fixed point in space), whereas $\rho\partial_j\psi$ was taken to first order in u. The linearized equation can be solved by using the Greens tensor G_{ij} for a completely elastic Earth. The displacement field is then (with $f_j^V = 0$):

$$u_i(X,t) = \int\int m_j^V(x,\tau) G_{ij}(X,t,x,\tau) dV d\tau \tag{4}$$

The m_j^V is all what can be determined uniquely from observations of the elastic wavefield. BM expressed $m_j^V(x)$ by a series of polynomial moments located at one particular point ξ_0 as

$$m_j^V(x) = M_j^0 \delta(x-\xi_0) + M_{ji}^1 \partial_i \delta(x-\xi_0) + M_{jik}^2 \partial_i \partial_k \delta(x-\xi_0) + \ldots \tag{5}$$

where

$$M_{jk1\ldots kn}^n = \int_V m_j^V(x)(x_{k1} - \xi_{k10} \cdots (x_{kn} - \xi_{kn0}) dV \tag{6}$$

The displacement field can now be rewritten in terms of the polynomial moments as

$$u_i(X,t) = \sum_{n=0}^{\infty} \frac{1}{n!} G_{ij;k1\ldots kn}(X,t,x,\tau) M^n_{jk1\ldots kn}(x,\tau) \tag{7}$$

The zeroth order moment M^0_j is

$$M^0_j = \int_V m^V_j(x) dV \tag{8}$$

and by substituting eq. (3) into eq. (7) the vanishing of this component is confirmed, because the stress glut (and the equivalent body forces)are zero outside the source volume.

$$M^0_j = \int_V \Gamma_{ij,i}(x) dV = \int_{\partial V} \Gamma_{ij}(x) n_i dS = 0 \tag{9}$$

The same way of argumentation leads to the vanishing of the simple torque in the BM representation of the moment tensor.

BM state "that the vanishing of the total force and torque exerted by the equivalent forces is to be expected, since an indigenous source cannot change the total linear or angular momentum of the Earth".

Takei and Kumazawa (1994; TK) showed that the single force and the torque do not vanish, if the effect of mass advection is taken into account.

$n = 0$

The $n = 0$ term corresponds to sources, which do not conserve the momentum of the Earth or have its origin in a redistribution of the density structure of the source volume. Examples are meteorite impacts, volcanic explosions, caldera collapses, landslides etc.

Neglecting the external force term Takei and Kumazawa (1994) wrote the equation of motion as

$$\rho^t D^2_t u_j = \partial_i S ij - \rho^t \partial_j \psi^t \tag{10}$$

with an explicit expression for the true density field $\rho^t(x,t)$, a function of both space and time, and also with the explicit expression for the real accelleration $D^2_t u_j$, where

$$D_t = \partial_t + v_k \partial_k \tag{11}$$

Eq. 10 at the initial static equilibrium state is written as

$$0 = \partial_i S^0_{ij} - \rho^{t0} \partial \psi^{t0} \tag{12}$$

where the superscript 0 represents the initial undisturbed quantity. The governing equation for the incremental quantities is obtained by subtracting eq. 12 from eq. 11. Using ∂S_{ij} as incremental stress $(S_{ij} - S^0_{ij})$ the equation of motion for the incremental quantities is obtained as:

$$\rho^t D^2_t u_j = \partial_i S_{ij} - (\rho^t \partial_j \psi^{t0}) \tag{13}$$

The equation of motion for the linear elastodynamic model is given for incremental quantities as

$$\rho^m \partial_t^2 u_j = \partial_i S'_{ij} - (\rho^{ml} \partial_j \psi^m + \rho^m \partial_j \psi^{ml}) \tag{14}$$

where ρ^m is a model density structure approximated by the undisturbed state and ψ^m is a model gravitational potential approximated by the undisturbed gravitational potential field. The equivalent volume force is defined by the difference of the actual equation of motion (eq. 13) from the linear elastodynamic model (eq. 14). The linear elastodynamic equation for everywhere in the Earth, including the source region, is constructed as

$$\rho^m \partial_t^2 u_j = \partial_i S'_{ij} - (\rho^{ml} \partial_j \psi^m + \rho^m \partial_j \psi^{ml}) + m_j^V \tag{15}$$

where an apparent indigeneous body force m_j^V consists of three factors:

$m_j^V = m_j^S + m_j^D + m_j^G$

with

$m_j^S = \partial_i \Gamma_{ij} = \partial_i (S_{ij} - S'_{ij})$

$m_j^D = -(\rho^t D_t^2 u_j - \rho^m \partial_t^2 u_j)$

$m_j^G = -[(\rho^t \partial_j \psi^t - \rho^{t0} \partial_j \psi^{t0}) - (\rho^{ml} \partial_j \psi^m + \rho^m \partial_j \psi^{ml})]$

where each of the three factors represents a nonlinear source process with different physics.

The first term m_j^S is the contribution from the stress glut as in the BM formulation. The second term m_j^D is the difference of the inertial forces in the real Earth and in the model, i.e. they originate from the difference of the density structure of the prescribed model from the actual value in the source region before the event and from a temporal change of the density structure in the source region caused by finite displacement of mass during the event (mass advection) Unlike m_j^S defined as a gradient of the symmetric stress tensor, $m^{0(D)}$ and the corresponding torque component do not always vanish. The third term m_j^G is essentially a glut of gravitational force compared with that expected in the model, which originates from the movement of the centre of gravity of the source with respect to the centre of gravity of the Earth.

TK give the following example for a force with nonvanishing single force component (Fig. 2). Another example is the salt mine collapse near the german town of Völkershausen (13.3.89 13:02:16.8 m_b=5.6 50.8N 10.0E), which can be modelled with a detached mass model (see Fig. 3).

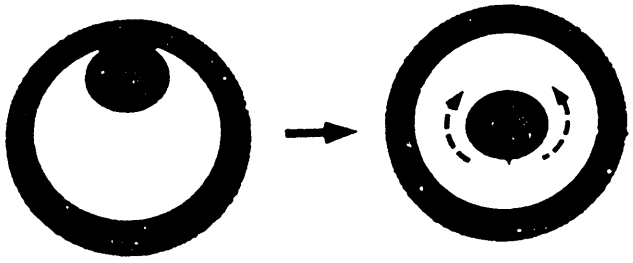

Fig. 2. Detachment of a dense body in a magma chamber. Example for a seismic source process describable with a single force (Fig. 1 in TK).

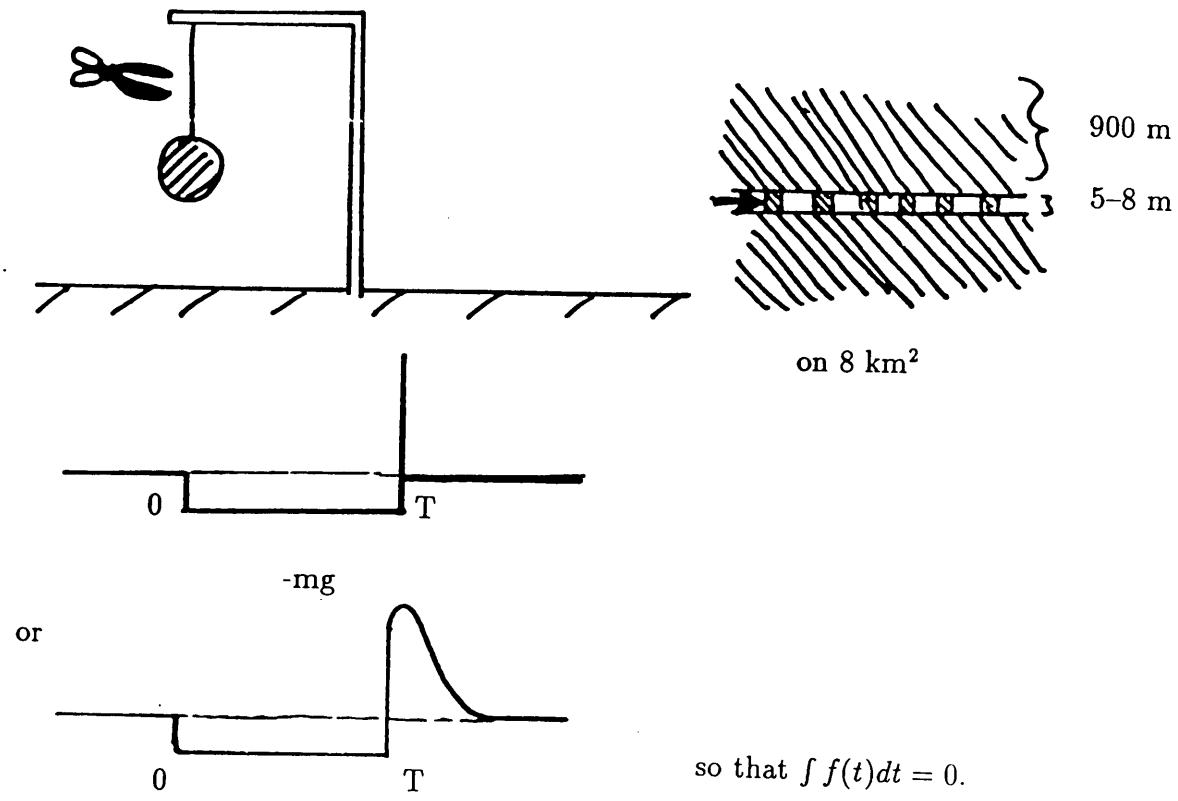

Fig. 3a. Example for a source with nonvanishing single force component: The salt mine collapse at Völkershausen (13.3.89 13:02:16.8 $m_b = 5.6$ 50.8N 10.0E). This event is describable with a "gallow" model. When the rope is cut, the ground moves up, while the mass is falling freely. The impact of the mass shows up by a positive impulse (modified after G. Müller (1989)).

Scientific Technical Report STR 95/TK
DOI: 10.2312/GFZ.b103-95tk7

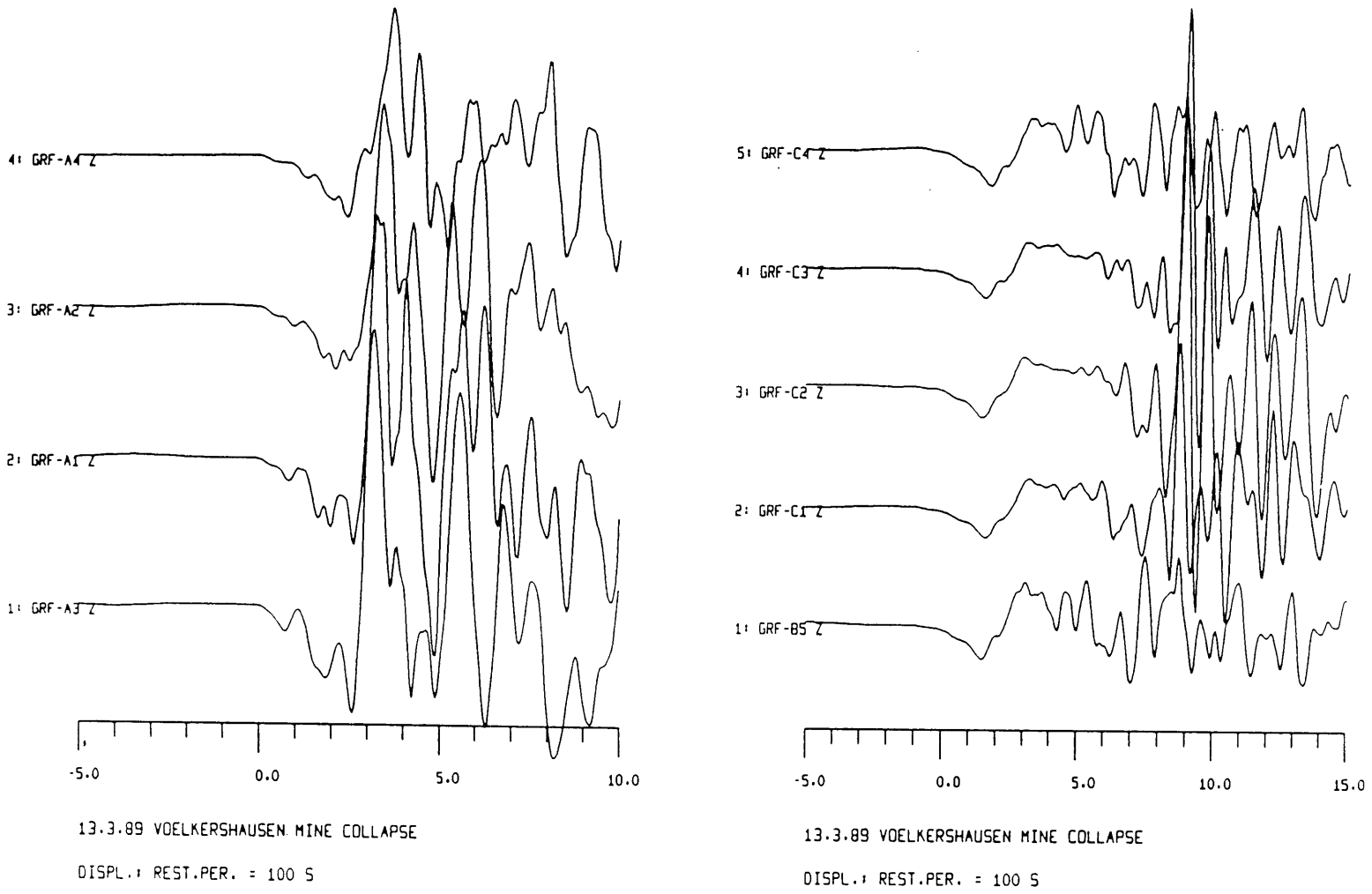

Fig. 3b. Gräfenberg array recordings of the salt mine collapse at Völkershausen. Shown is the ground displacement (rest. period 100 sec) for the northern A-subarray stations (north, Δ = 150 km) and the C-subarray stations (south, Δ = 228 km). The negative onset is followed by an impulsive positive onset.

$n = 1$

Under the assumption of a source acting synchronous for all components describable with a single source time function $s(t)$ the $n = 1$ term can be written as follows:

$$u_i(X,t) = M_{kj} G_{ik,j} d(t) \tag{16}$$

M_{kj} represents the quantity usually termed **the** moment tensor. If the source time function $d(t)$ is a delta function, the only term left in the brackets is $G_{ik,j}$ describing nine generalized couples (The derivative of a Greens function component with respect to the source coordinate x_j is equivalent to a single couple with arm in the x_j direction (see Fig. 4).

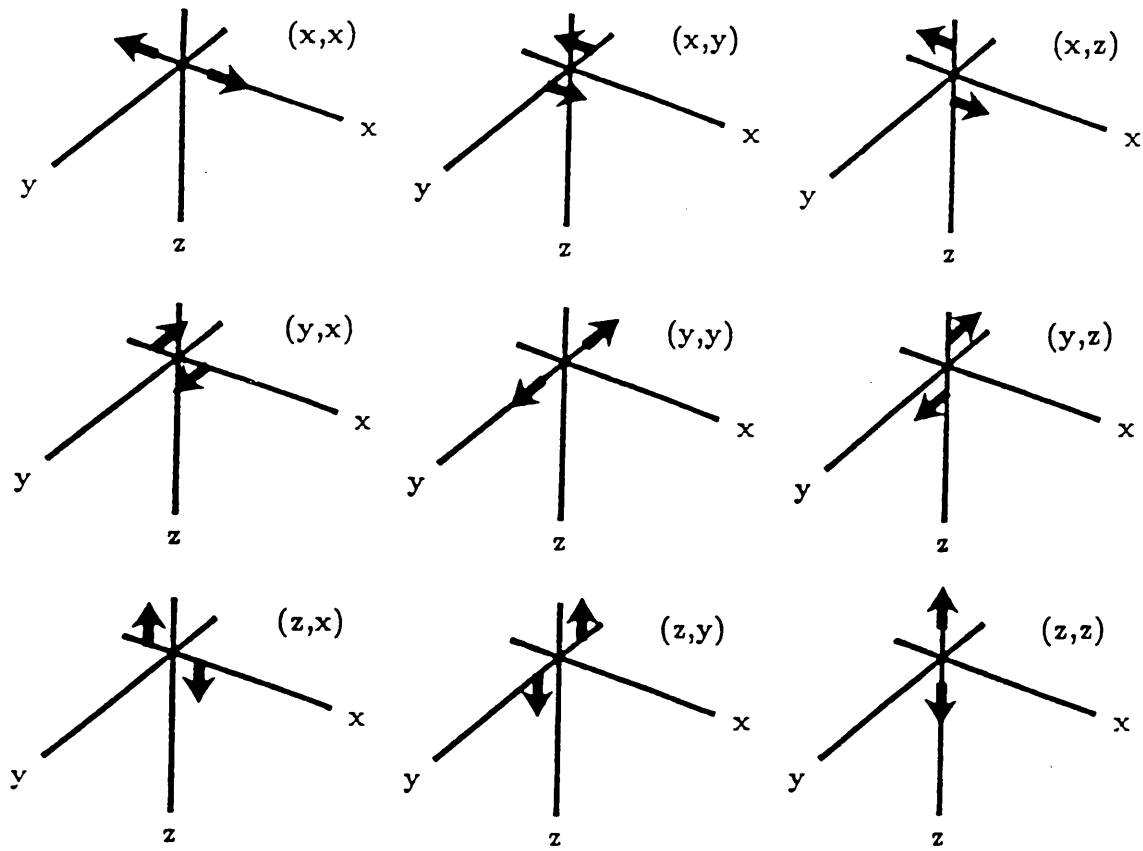

Fig. 4. The nine couples by which the first order moment tensor can be represented.

For an isotropic medium eq. (16) becomes:

$$M_{kj} = \Lambda \nu_k s_j \delta_{kj} + \mu A(s_k \nu_j + s_j \nu_k) \tag{17}$$

and if the slip is parallel to the fault the scalar product $\nu \cdot s$ is zero (shear fault)

$$M_{kj} = \mu A(s_k \nu_j + s_j \nu_k) \tag{18}$$

where

Λ = compression modulus
μ = shear modulus
A = area of fault surface
s = slip vector on the fault surface
ν = normal to the fault plane

The term $s_k \nu_j + s_j \nu_k$ forms a tensor D describing a double couple. This tensor is real and symmetric, giving real eigenvalues and orthogonal eigenvectors. The eigenvalues are proportional to (1,0,-1). Hence, the characteristic properties of a moment tensor representing a double couple are

(i) one eigenvalue vanishes
(ii) the sum of the eigenvalues vanishes

The tensor D can be diagonalized, where the eigenvectors

$$t = \frac{1}{\sqrt{2}}(\nu + s) \tag{19}$$

$$b = \nu \times s \tag{20}$$

$$p = \frac{1}{\sqrt{2}}(\nu - u) \tag{21}$$

give the direction of the principal axes. The eigenvector b corresponding to the eigenvalue zero gives the null axis, the eigenvector t corresponding to the positive eigenvalue gives the tension axis and the eigenvector p (corresponding to the negative eigenvalue) gives the pressure axis. Note that the p and t axis inferred from the motion on the fault are not necessarily identical to the axes of maximum tectonic stress, since the motion can happen to be on a preexisting plane of weakness. From the symmetry of M it should be noted that the roles of the vectors u and ν could be interchanged without affecting the displacement field leading to the wellknown fault plane – auxiliary plane ambiguity. The relation between tension and pressure axes and slip vector and fault normal is:

$$s = \frac{1}{\sqrt{2}}(t + p) \tag{22}$$

$$\nu = \frac{1}{\sqrt{2}}(t - p) \tag{23}$$

The other nodal plane is defined by

$$s = \frac{1}{\sqrt{2}}(t - p) \tag{24}$$

$$\nu = \frac{1}{\sqrt{2}}(t + p) \tag{25}$$

In terms of strike Φ, dip δ, and slip λ the slip vector s and the fault normal ν are given by (Aki and Richards 1980)

$$s = |s|(\cos\lambda\cos\Phi + \cos\delta\sin\lambda\sin\Phi)e_x + |s|(\cos\lambda\sin\Phi - \cos\delta\sin\lambda\cos\Phi)e_y - |s|\sin\delta\sin\lambda e_z \tag{26}$$

The fault normal ν is

$$\nu = -\sin\delta\sin\Phi e_x + \sin\delta\cos\Phi e_y - \cos\delta e_z \tag{27}$$

The range of the fault orientation parameters are $0 \leq \Phi \leq 2\pi$, $0 \leq \delta \leq \frac{\pi}{2}$, $-\pi \leq \lambda \leq \pi$. The scalar seismic moment is

$$M_0 = \mu A|s| \tag{28}$$

Eq. 16 together with eqs (26), (27) and (28) lead to the cartesian components of the symmetric moment tensor in terms of strike, dip, and slip angles.

$M_{xx} = -M_0(\sin\delta\cos\lambda\sin 2\Phi + \sin 2\delta\sin\lambda\sin^2\Phi)$
$M_{yy} = M_0(\sin\delta\cos\lambda\sin 2\Phi - \sin 2\delta\sin\lambda\cos^2\Phi)$
$M_{zz} = M_0(\sin 2\delta\sin\lambda)$
$M_{xy} = M_0(\sin\delta\cos\lambda\cos 2\Phi + 0.5\sin 2\delta\sin\lambda\sin 2\Phi)$
$M_{xz} = -M_0(\cos\delta cos\lambda\cos\Phi + \cos 2\delta\sin\lambda\sin\Phi)$

$$M_{yz} = -M_0(\cos\delta\cos\lambda\sin\Phi - \cos 2\delta\sin\lambda\cos\Phi) \tag{29}$$

Eq. 16 is still complicate, because the partial derivatives of the Greens tensor form a tensor of degree 3. Writing formally

$G_{ij} = G_{ij}(X(x), t(x))$

the derivative with respect to the source coordinate x is

$$G_{ij;k} = \frac{\partial G_{ij}}{\partial X_l}\frac{\partial X_l}{\partial x_k} + \frac{\partial G_{ij}}{\partial t}\frac{\partial t}{\partial x_k} \tag{30}$$

where $\frac{\partial X_l}{\partial x_k}$ are the direction cosines and $\frac{\partial t}{\partial x_k} = \zeta_k$ can be identified as the slowness. The first term is the nearfield term and is usually neglected.

$$u_i = M_{jk} * G_{ij}\zeta_k = M_{jk} * G_{ij}\zeta_k \tag{31}$$

In a cylindrically medium we get finally for the Z- and R-component (in the frequency domain):

$$u_z(X,\omega) = (-0.5(M_{yy} - M_{xx})\cos 2\Phi + M_{xy}\sin 2\Phi)I_z^2 + (M_{xz}\cos\Phi + M_{yz}\sin\Phi)I_z^1 \tag{32}$$

$$+\frac{1}{3}(0.5(M_{yy}+M_{xx})-M_{zz})(I_z^2-2I_z^0)+\frac{1}{3}(M_{xx}+M_{yy}+M_{zz})(I_z^0+I_z^2)$$

where the I correspond to elementary sources ($I_i^0=\omega G_z^i\zeta_z$, $I_i^1=\omega(G_r^i\zeta_z+G_z^i\zeta_r)$, $I_i^2=\omega G_r^i\zeta_r$, $i=z,r,\phi$).

n=2

In order to investigate the relative importance of higher–degree moment tensors, one must express the source of interest in terms of its equivalent body forces. For purposes of illustration, a longitudinal shear fault where the displacement is parallel to the direction of rupture propagation was analysed by Stump and Johnson (1982). A pictorial representation of the model is given in the next figure (Fig. 5).

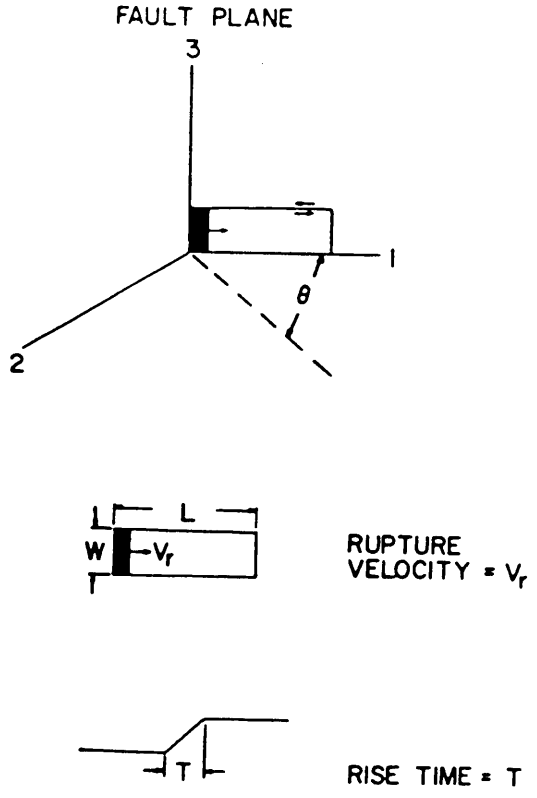

Fig. 5. Model for a longitudinal left–lateral shear fault used for modelling finite source effects. The entire width of the fault, W, breaks simultaneously and propagates in the 1 direction with rupture velocity V_r. The time function for each point on the fault is illustrated in the bottom of the figure (Fig. 1 from Stump and Johnson (1982)).

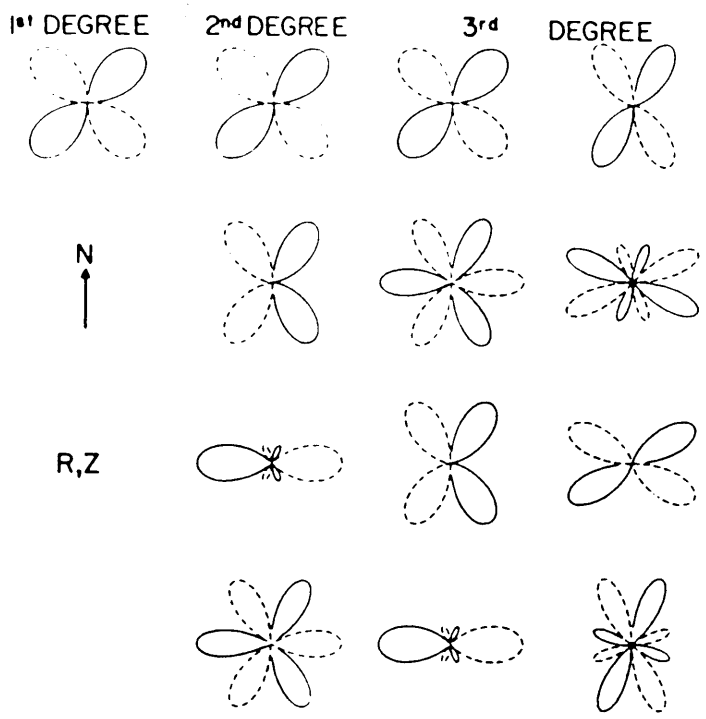

Fig. 6. $P \quad -SV$ radiation pattern for components of the first–, second– and third–degree moment tensors for the fault model shown in Fig. 5. North is the 1 direction in Fig. 5. Solid lines indicate areas of compression and dashed lines represent dilatation. (Fig. 2 from Stump and Johnson (1982)).

Figure 6 shows the radiation patterns of various moment tensor components for the P–SV case. The first degree ($n = 1$) moment is represented by the standard quadrupole radiation pattern for a point source shear fault. The fault lies in the north–south plane. As the degree of the moment tensor increases, the complexity of the radiation pattern also increases and more lobes are introduced into the radiation patterns. Note that the radiation patterns of each higher–degree moment tensor includes all the various radiation patterns of the lower–degree tensors in addition to new ones. Once any of the higher–degree moments are included, one of the nodal planes vanishes. The disappearance of the nodal plane at 90° from the strike of the fault in the P–SV problem can be explained physically in terms of the receiver at 90° being able to see the ends of the fault.

In the next figure (Fig. 7) synthetic seismograms are shown using the multipole expansion for the moment tensor and synthetics calculated for a propagating source (i.e. by proper summation of point sources distributed over the fault surface). In this case the moment tensor series is converging rapidly and the point source approximation (first–degree only) works well. The figure on the right side (azimuth 210°) shows that for such azimuths the effects of source finiteness and rupture propagation are only small. If the configuration shown in Figure 8 is used the observation point is not always at 90° for the entire fault. The first degree term is zero as expected. It is the second term that matches the contribution of the propagating

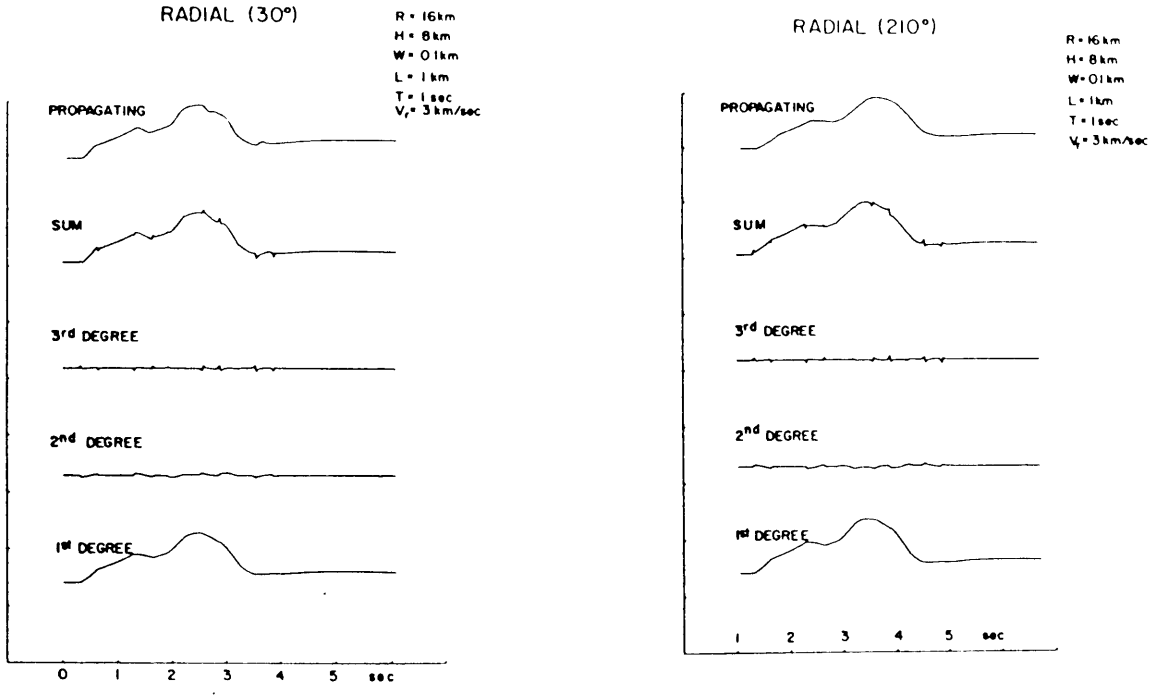

Fig. 7. The contributions to the seismogram due to the first–, second–, and third degree moment tensors are plotted along with the sum of these components. Also plotted is the seismogram computed by summing point sources distributed over the fault surface. The observation points are at 30° from the strike of the fault (*left side*; i.e. the source is propagating towards the receiver) and 210° (*right side*; i.e. the source is propagating away from the receiver). (Fig. 7 and 8 from Stump and Johnson (1982)).

seismogram. The physical interpretation of the waveforms is that since the fault is always propagating away from the observer the direction is radial towards the source and vertically down. Note that these synthetic motions are a factor of ten smaller than those observed at azimuths of 30° or 210°. To see the effects of higher degree moments more clear the following much extremer case was calculated (Fig. 9):

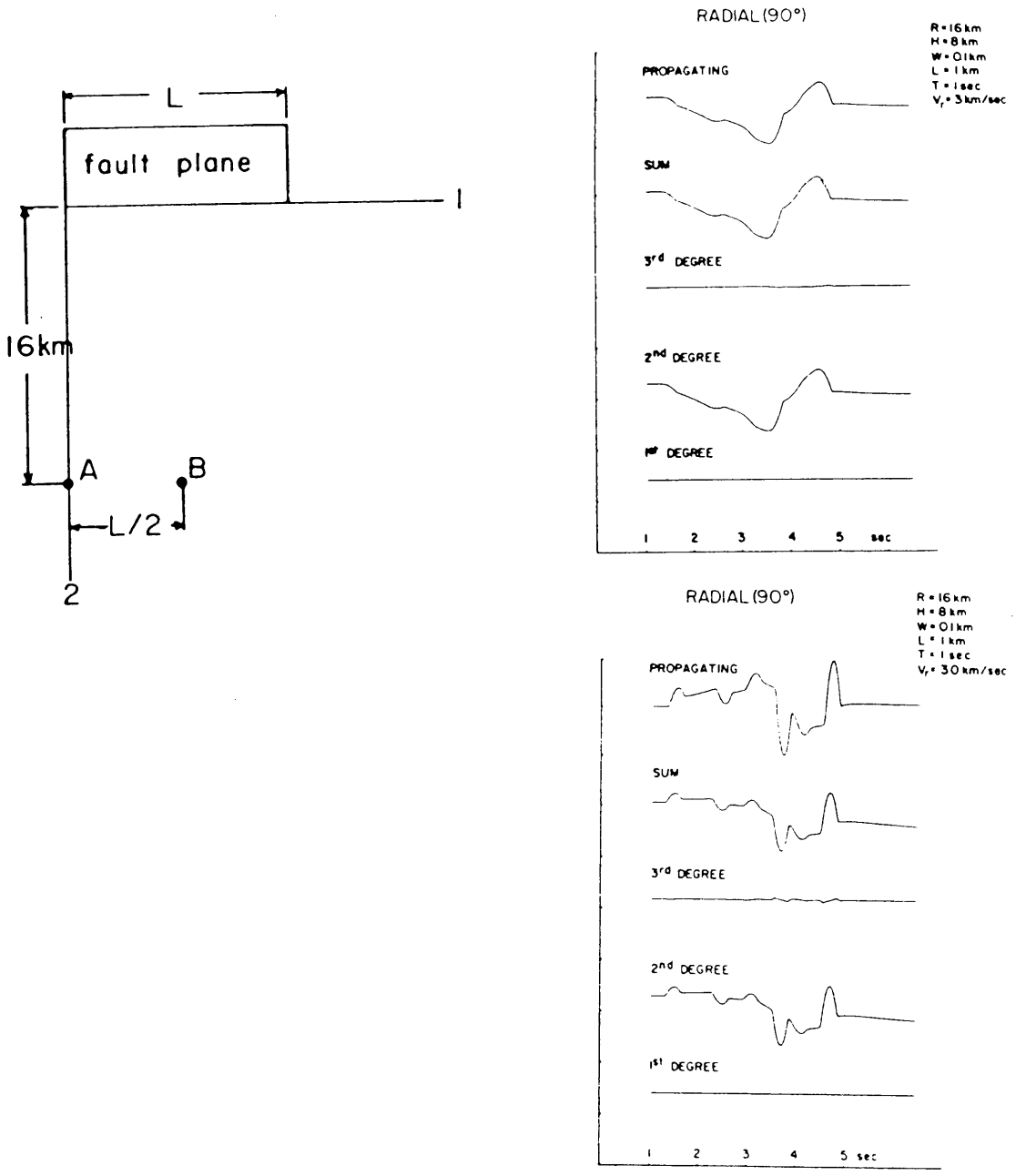

Fig. 8. *Left:* The location of two receiver points at right angles to the fault plane. Point A ia at right angles to the end of the fault and point B is at right angles to the center of the fault. *Right:* Seismograms observed at point A (top) and point B (bottom). Amplitudes are scaled by a factor of 10 (top) and 100 (bottom). (Figs. 9, 10 and 11 from Stump and Johnson (1982)).

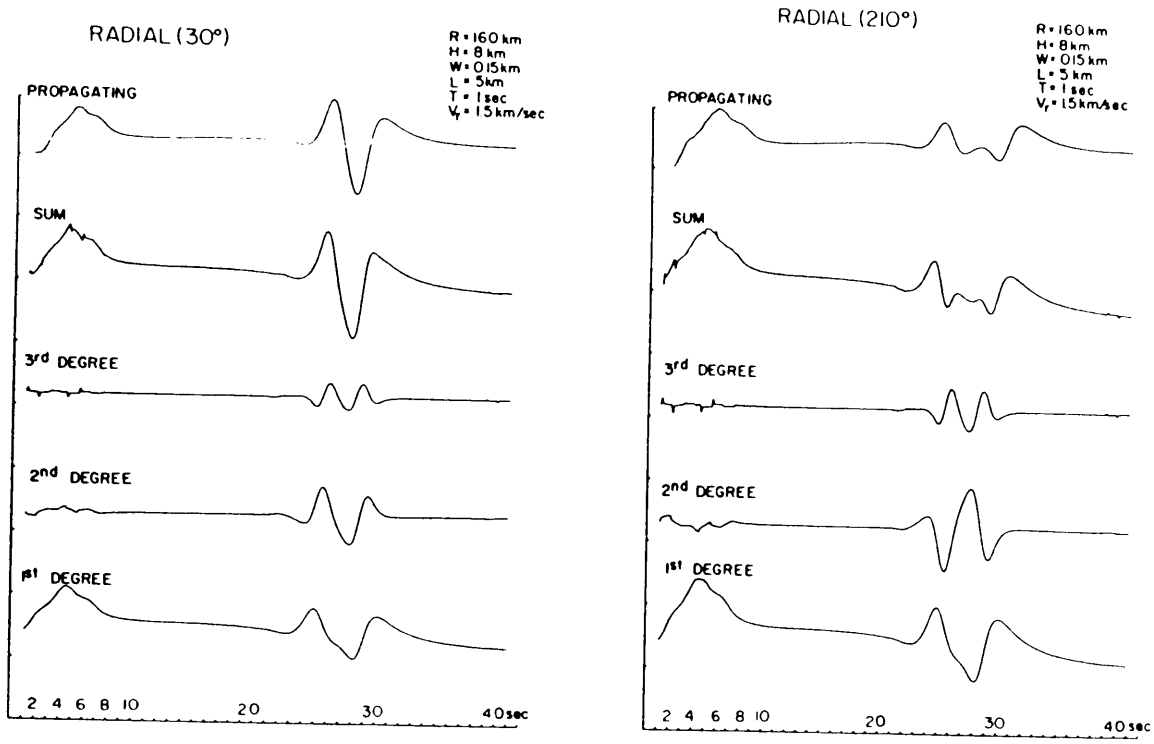

Fig. 9. Seismograms for a model with changed source parameters (i.e. slower rupture velocity). *Left:* Observation point at 30° from the fault strike. *Right:* Observation point at 210°. (Figs. 12 and 13 from Stump and Johnson (1982)).

Inversion

All inversion methods solve the inversion of eq. (16). For further reference on inversion methods see Jost and Herrmann (1989).

CMT method (Harvard solutions)

The epicenter locations derived using shortperiod body waves are supposed to represent the initiation point of rupture. Dziewonski et al. (1981) use a perturbaton method with respect to the inversion of the seismic moment tensor. They use eq. (16) in the form

$u_i = \sum_{l=1}^{6} \psi_{ik}(r, r_s, t) * f_l(t)$

where the *psi* represent excitation kernels calculated by the summation of normal modes. After making an initial estimate with the epicenter given by body waves by the inclusion of small perturbations into this equation (i.e. partial derivatives of the excitation kernels with respect to the source coordinates and the momentum tensor. The whole seismogram is inverted using effectively body waves in the period

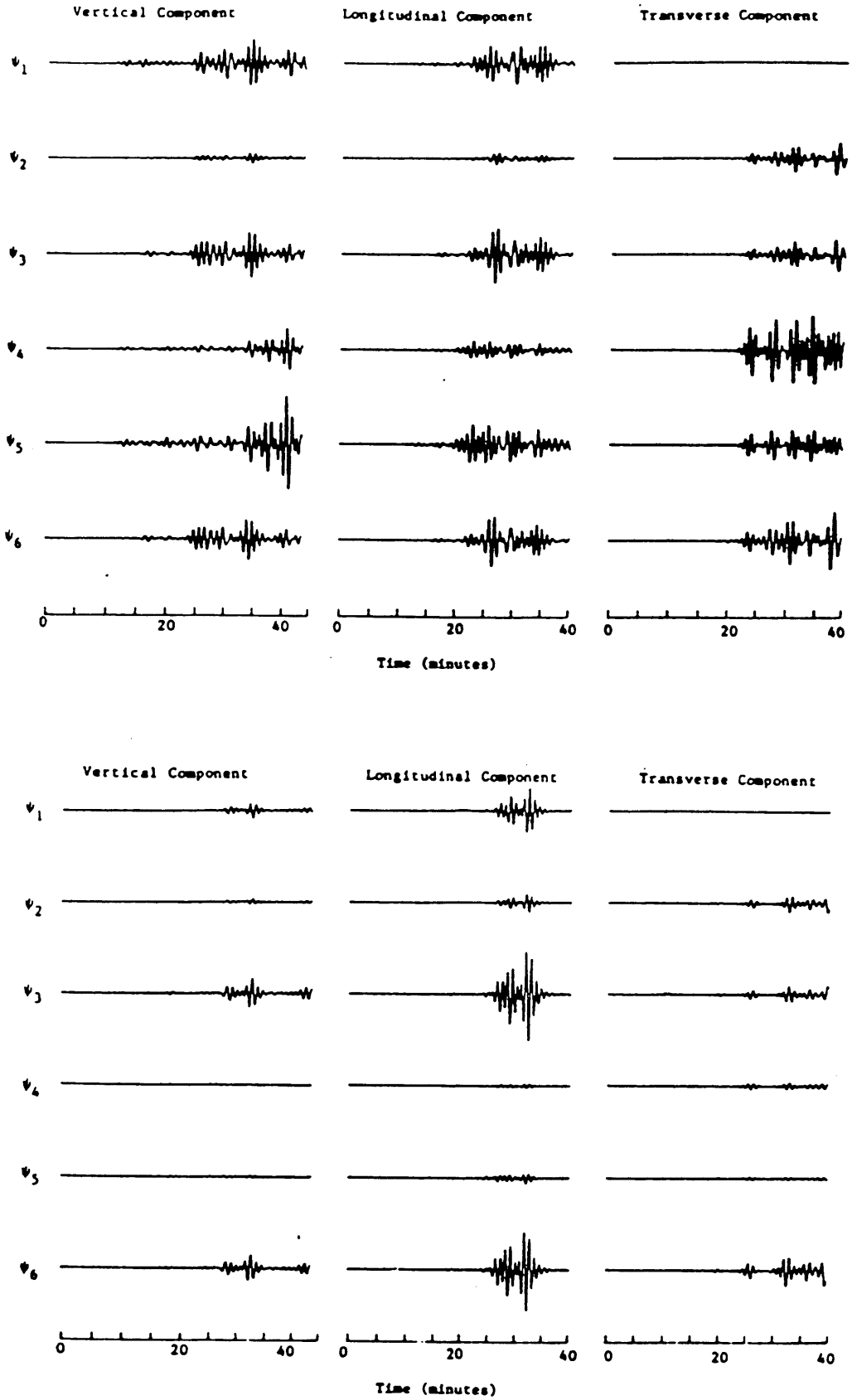

Fig. 10. *Top:* Excitation kernels for a deep earthquake (580 km) computed for the three components of ground motion for a point on t earth's surface at a distance of 98.8° and azimuth 294.1° from the epicenter. The scale is common for all traces. Notice that there is a gre diversity of shapes among the kernel functions. Intuitively this indicates that for deep earthquakes, good resolution of the source properti could be achieved with relatively few recordings. *Bottom:* Excitation kernels for a source at 3 km depth. Notice that the ground moti is relatively insensitive to the components f_4 and f_5. Also, for a given component of the ground motion the shapes of all synthetic trac are nearly identical. This means that inversion with respect to f_4 and f_5 (M_{xy} and M_{xx}; vertical dip–slip) may be very unstable and mo extensive coverage is necessary to obtain resolution for the remaining elements of the moment tensor. (Fig. 2 from Dziewonski *et al.* (1981

Inversion for the Moment Tensor and Location of a Set of Synthetic Seismograms Computed for a Network of 12 Three-Component Stations

	Interation				
	0	1	2	3	4
		Location			
Origin time, s	0.00	5.53	6.93	7.47	7.50
Latitude	20.84°S	21.10°S	21.40°S	21.51°S	21.50°S
Longitude	178.64°W	178.04°W	178.23°W	177.98°W	178.00°W
Depth, km	600.00	584.27	587.31	579.75	580.00
		Moment Tensor			
f_1	0.69844	0.71056	0.99344	1.00006	1.00000
f_2	0.33230	0.35757	0.97671	0.99992	1.00000
f_3	0.47704	0.51578	0.98099	1.00022	0.99998
f_4	−0.13696	−0.15316	−0.01460	0.00048	−0.00003
f_5	−0.02306	−0.09278	−0.00845	0.00034	−0.00001
f_6	0.14698	0.14584	0.93683	0.99946	1.00000
		Principal Axes			
Axis I					
Moment	0.76273	0.83205	1.91597	1.99995	2.00000
Plunge/azimuth	63/145	55/133	1/135	0/135	0/135
Axis II					
Moment	0.52791	0.49440	0.99317	1.00006	1.00000
Plunge/azimuth	24/293	32/287	89/300	90/	90/
Axis III					
Moment	0.21714	0.25246	0.04200	0.00061	−0.00001
Plunge/azimuth	13/28	12/25	0/45	0/45	0/45
Relative rms	0.84706	0.74561	0.16420	0.00175	0.00000

The parameters used in construction of the synthetic seismograms were origin time, 7.5 s; latitude, 21.5°S; longitude, 178°W; depth, 580 km; moment tensor, $f_1 = f_2 = f_3 = 1$, $f_4 = f_5 = 0$, $f_6 = 1$. The starting source location parameters are given in the column for iteration 0 (only the moment tensor is derived in the starting iteration); in the subsequent columns all entries correspond to the results obtained in a particular iteration.

Table 1. Inversion for the moment tensor and location of a set of synthtetic seismograms computed for a network of 12 3–component stations (SRO + ASRO).

range 40 to 70 sec and additionally mantle waves with periods larger than 100 sec. Fig. 10 shows the excitation kernels for a source at a depth of 3 km and one at a depth of 580 km showing one of the problems of moment tensor inversion, because the excitation kernels ψ_4 and ψ_5 become very small. In the table the results of an iterative inversion with synthetic data is shown. Clearly the algorithm works. What is the benefit of it? The deviation of the centroid time from the origin time measured with shortperiod body waves should correspond to the rupture length. Using the proportionality of M_0 and fault length ($M_0 \propto L^3$; Kanamori and Anderson 1975) one gets under the assumption of a constant rupture velocity ($v_{rup} = 3.3$ km/s) the relation $DT = 1.3 + 1.55 \times 10^{-8} M_0^{\frac{1}{3}}$, which is shown in Fig. 11. Three isolated events show much longer centroid times than the rest of the events and are therefore candidates for slow earthquakes.

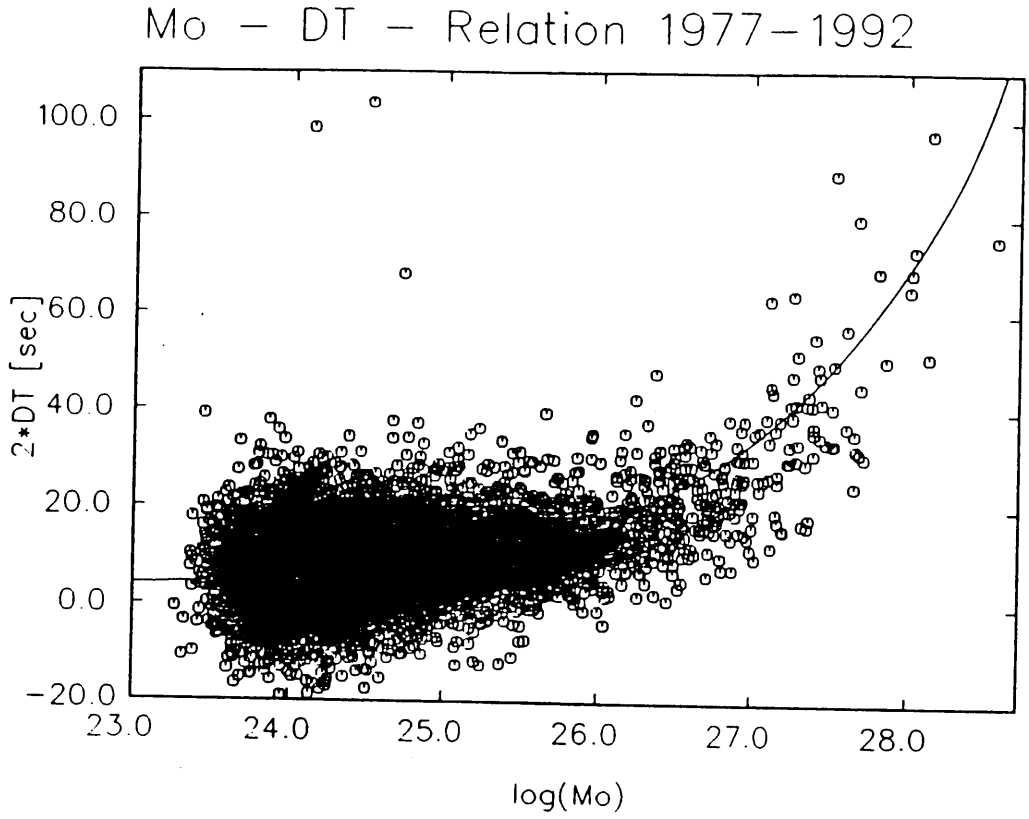

Fig. 11. Relation between the scalar moment (M_0) and the difference between the centroid time and the PDE onset time (assuming unilateral rupture propagation). The line corresponds to a fit assuming a cube root relation between scalar moment and rupture time (rupture length).

MSE method (USGS solutions)

S. Sipkin (1982) uses a time domain approach from the theory of optimal filter design. The moment tensor is regarded as an unknown multichannel filter whose input is a set of Greens functions and whose output is a set of theoretical seismograms. The input Greens functions are taken as known, and the algorithm determines the filter (moment tensor) that makes the output agree as well as possible, in a least squares sense, with the observed seismograms. Features of the seismograms that are not included in the Greens functions are regarded as noise and have little effect on the solution. Used for the inversion are only the SRO P–wave data. The moment tensor is automatically calculated as a function of time. Fig. 12 shows examples for two events with large non double couple components from Sipkin (1986).

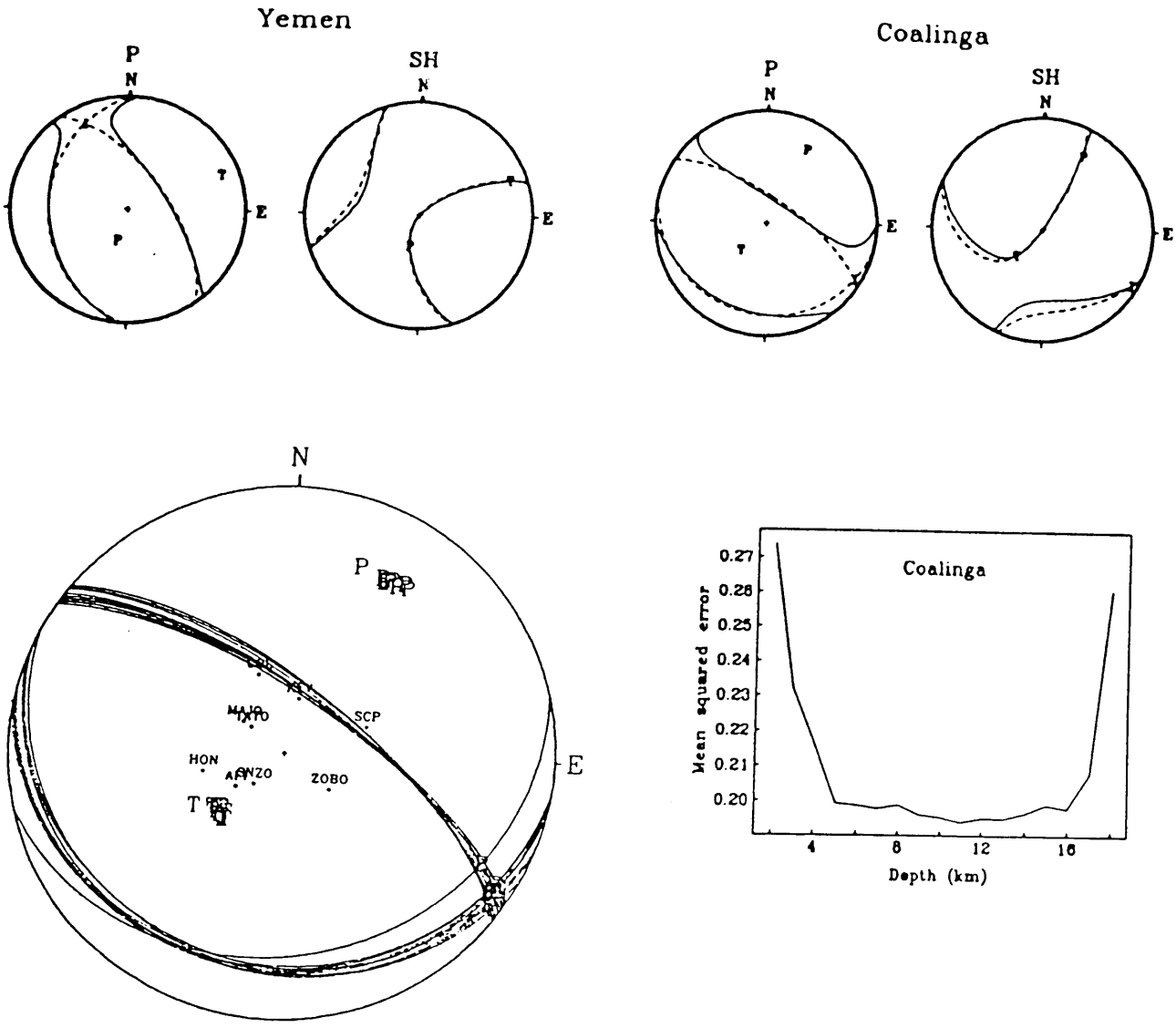

Fig. 12a. *Top:* P–wave solutions found using the MSE algorithm for a Yemen event (13-Dec-1982 09:12:48.0 14.701N 44.379E $h = 5$ $m_b = 6.0$) and a Coalinga event (2-May-1983 23:42:37.7 36.219N 120.317W $h = 10$ $m_b = 6.2$). Solid curves are the nodal surfaces of the moment tensors; dashed lines are the nodal planes of the best double couples. *Bottom, left:* Best double couples for the Coalinga event determined for source depths from 5 to 16 km at 1 km intervall showing the robustness of the fault plane determination with respect to small errors in the depth. *Bottom, right:* Mean squared error versus depth for the Coalinga event. (Modified after Figs. 6, 7 and 8 from Sipkin (1986)).

Scientific Technical Report STR 95/TK
DOI: 10.2312/GFZ.b103-95tk7

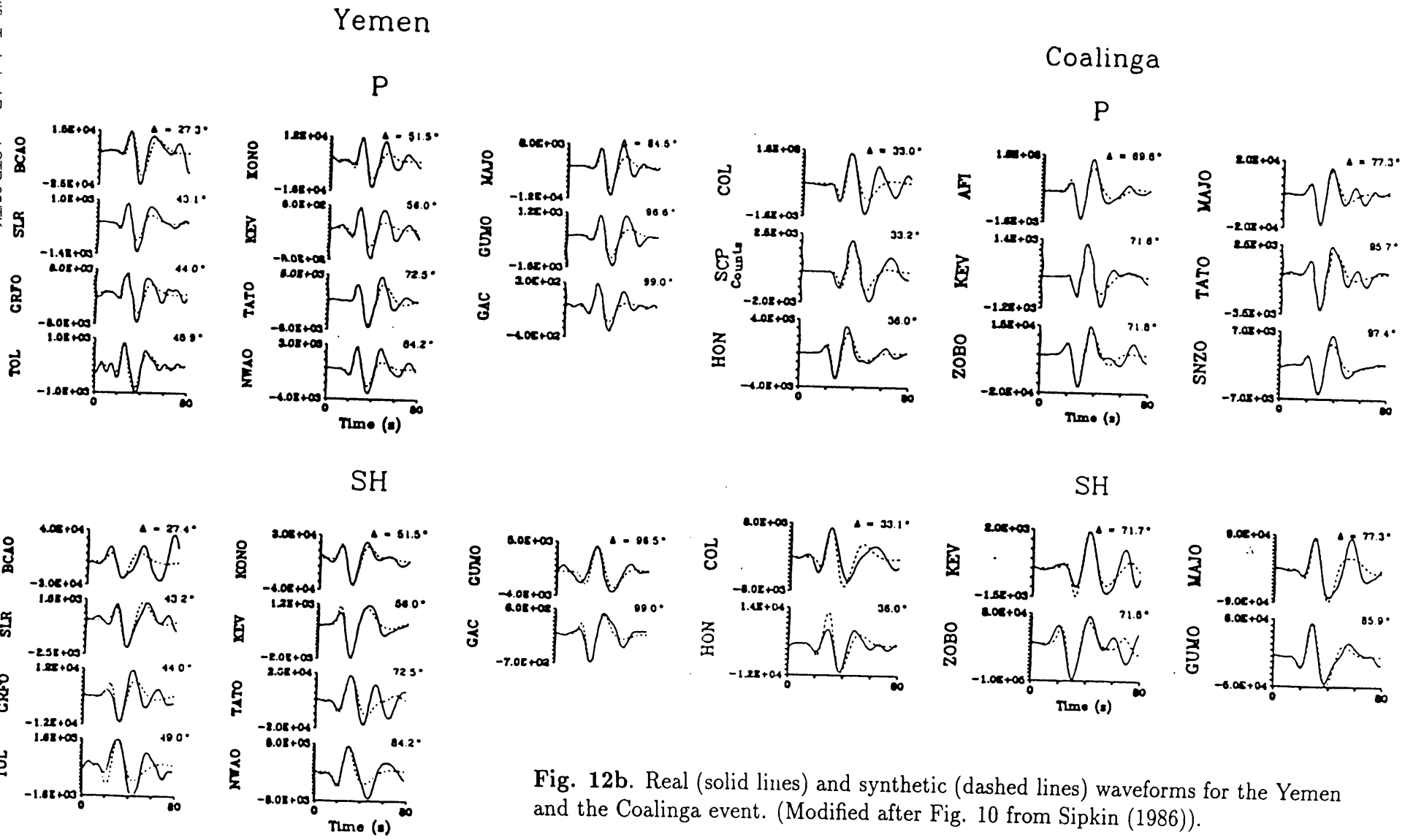

Fig. 12b. Real (solid lines) and synthetic (dashed lines) waveforms for the Yemen and the Coalinga event. (Modified after Fig. 10 from Sipkin (1986)).

GeoForschungsZentrum Potsdam

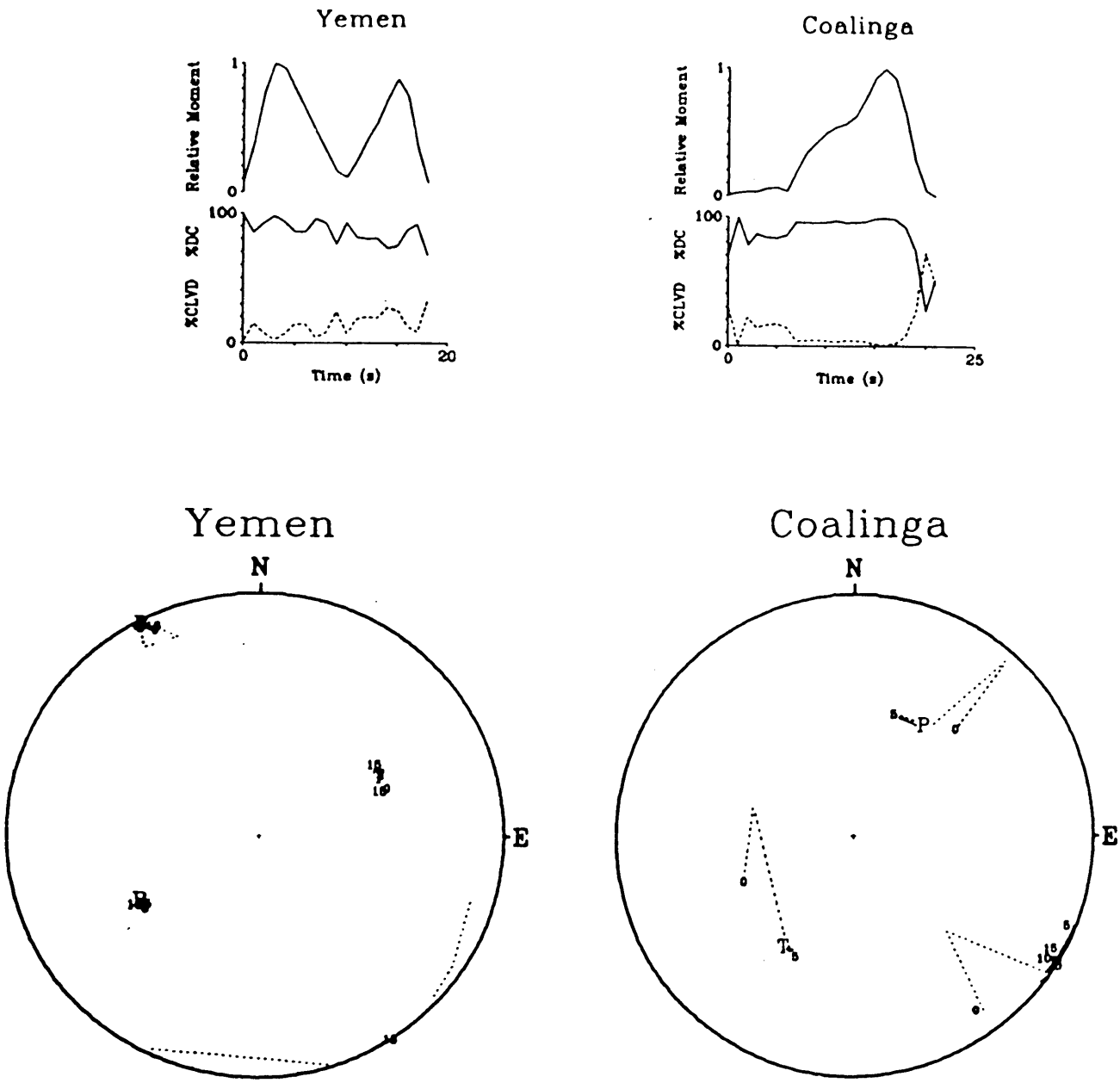

Fig. 12c. *Top:* Relative moment versus time (top panels) and percent double couple (solid lines) and CLVD (dashed lines) versus time (bottom panels) for the Yemen and the Coalinga events. *Bottom:* Principal axis positions on the focal sphere as functions of time for the Yemen and the Coalinga event. Numbers correspond to number of seconds after the origin time. Dashed lines correspond to times during which the moment is less than 0.25 M_{max}. (Modified after Figs. 12 and 13 from Sipkin (1986)).

References and suggestions for further reading

Aki, K., and P.G. Richards, 1980. Quantitative seismology: Theory and methods, W.H. Freeman and Co., New York, San Francisco.

Backus, G. and Mulcahy, M., 1976. Moment tensors and other phenomenological descriptions of seismic sources, 1, Continous displacements, *Geophys. J. R. astr. Soc.*, **46**, 341–361.

Dziewonski, A.M., Chou, T.A., and Woodhouse, J.H., 1981. Determination of earthquake source parameters from waveform data for studies of global and regional seismicity, *J. geophys. Res.*, **86**, 2825–2852.

Jost, M.L. and Herrmann, R.B., 1989. A students guide to and review of moment tensors, *Seis. Res. Letters*, **60**, 37–57.

Müller, G., 1989. Herdvorgang des Gebirgsschlags Völkershausen. Abstract, Arbeitsgruppe Gräfenberg des FKPE.

Sipkin, S., 1982. Estimation of earthquake source parameters by the inversion of waveform data: synthetic waveforms, *PEPI*, **30**, 242–259.

Sipkin, S., 1986. Interpretation of non double couple earthquake mechanisms derived from moment tensor inversion, sl J. geophys. Res, **91**, 531–547.

Stump, B.W. and Johnson, L.R., 1982. Higher degree moment tensors – the importance of source finiteness and rupture propagation on seismograms, *Geophys. J. R. astr. Soc.*, **69**, 721–743.

Takei, Y. and Kumazawa, M., 1994. Why have the single force and torque been excluded from seismic source models?, *Geophys. J. Int.*, **118**, 20–30.

For many further references see the review article of Jost and Herrmann.

Exercises

1. Determine the cartesian moment tensors for an underground nuclear explosion, a focal mechanism with strike $(\Phi) = 0^o$, $(\text{dip})\delta = 90^o$, and slip $(\lambda) = 0^o$, a focal mechanism with strike $(\Phi) = 0^o$, $(\text{dip})\delta = 45^o$, and slip $(\lambda) = 90^o$, a focal mechanism with strike $(\Phi) = 0^o$, $(\text{dip})\delta = 90^o$, and slip $(\lambda) = 90^o$. Use eqs. (17) and (29).

Solution:

$$M = M_0 \begin{pmatrix} 1 & 0 & 0 \\ 0 & 1 & 0 \\ 0 & 0 & 1 \end{pmatrix}$$

$$M = M_0 \begin{pmatrix} 0 & 1 & 0 \\ 1 & 0 & 0 \\ 0 & 0 & 0 \end{pmatrix}$$

$$M = M_0 \begin{pmatrix} 0 & 0 & 0 \\ 0 & -1 & 0 \\ 0 & 0 & 1 \end{pmatrix}$$

$$M = M_0 \begin{pmatrix} 0 & 0 & 0 \\ 0 & 0 & -1 \\ 0 & -1 & 0 \end{pmatrix}$$

2. Determine the moment tensor for a tension crack in the direction normal to the fault plane in an homogenous isotropic medium. Use eq. (17).

Solution:

$$M = \begin{pmatrix} \Lambda s_3 & 0 & 0 \\ 0 & \Lambda s_3 & 0 \\ 0 & 0 & (\Lambda + 2\mu)s_3 \end{pmatrix}$$

3. Suppose you have a program that calculates synthetic seismograms for double couples and explosions. How can you generate the Greens functions needed to invert equation 16 ? Which source orientations do you have to use? Use eq. (31).

Solution

$$I_0 = \begin{pmatrix} 0 & 0 & 0 \\ 0 & -1 & 0 \\ 0 & 0 & 1 \end{pmatrix}$$

or $\Phi = 0$, $\delta = 45^o$, $\lambda = 90^o$.

$$I_1 = \begin{pmatrix} 0 & 0 & 1 \\ 0 & 0 & 0 \\ 0 & 0 & 0 \end{pmatrix}$$

or $\Phi = 0$, $\delta = 0^o$, $\lambda = 180^o$.

$$I_2 = \begin{pmatrix} 1 & 0 & 0 \\ 0 & -1 & 0 \\ 0 & 0 & 0 \end{pmatrix}$$

or $\Phi = 45$, $\delta = 90^o$, $\lambda = 180^o$.

GeoForschungsZentrum Potsdam
STIFTUNG DES ÖFFENTLICHEN RECHTS

P. Bormann

Regional International Training Course 1995 on

Seismology and Seismic Hazard Assessment

Lecture and exercise notes

Volume II

Interner Bericht

Scientific Technical Report STR 95/TK
DOI: 10.2312/GFZ.b103-95tk7

Imprint

Edited by:

Peter Bormann
GeoForschungZentrum Potsdam
Telegrafenberg A 34
D-14473 Potsdam, Germany

Printed in Potsdam, Germany
December 1995

The regional international training course on "Seismology and Seismic Hazard Assessment" was held in Managua, from October 22 to December 2, 1995.

It was sponsored by:

- GeoForschungsZentrum Potsdam (GFZ)
- Instituto Nicaragüense de Estudios Territoriales (INETER), Managua
- Federal Ministry for Economical Co-operation and Development (BMZ), Bonn
- Federal Foreign Office (AA), Bonn
- Carl Duisberg Gesellschaft (CDG), Regional Office in the State of Brandenburg
- Swedish International Development Agency (SIDA)
- United Nations Educational, Scientific and Cultural Organization (UNESCO), Paris

P. Bormann
Editor

Lecture and exercise notes, Volume II

Regional International Training Course 1995 on

Seismology and Seismic Hazard Assessment

Managua, Nicaragua, October 22 to December 2, 1995

---

jointly organized by
GeoForschungsZentrum Potsdam (GFZ)
Instituto Nicaragüense de Estudios Territoriales (INETER)

in co-operation with
Carl Duisberg Gesellschaft (CDG)

co-sponsored by
AA (Bonn), BMZ (Bonn), SIDA (Stockholm) and UNESCO (Paris)

Scientific Technical Report STR 95/TK
DOI: 10.2312/GFZ.b103-95tk7

CONTENTS OF VOLUME I

8. Earthquake damages and earthquake engineering

VOLCANIC MONITORING AND WARNING SYSTEMS IN LATIN AMERICA AND CASE STUDIES FROM COSTA RICA

Guillermo E. Alvarado

Observatorio Sismológico y Vulcanológico de Arenal y
Miravalles (OSIVAM), ICE, Apdo. 10032 1000, Costa Rica

1. INTRODUCTION

Eruptions vary widely in character, magnitude and duration, not only from one volcano to another but even at the same volcano in short or long periods of time. The frequency of eruptions also varies, from volcanoes which are in almost continuous eruption to those which erupt only at intervals of hundreds or even thousands of years. Most eruptions are preceded by premonitory signs which, if recognized and heeded, can give timely warning of the impending events. Thus, forecasting the time, place, and character of volcanic eruption is one of the major goals in volcanology. However, these signs may be subtle or complex, and may demand careful and detailed study before they can be interpreted correctly, according to the knowledge of the volcanological setting at one specific volcano.

In the past years, substantial progress has been made in the field of volcanology in Latin America. Interest in volcanology was recently renewed by spectacular and/or catastrophic eruptions (El Chichón, Mexico 1982; Nevado del Ruiz 1985 and Galeras 1990-91, Colombia; Hudson, Chile 1991; and Cerro Negro, Nicaragua 1992) as well as significant volcanic crises or alerts (Irazú 1991, Costa Rica; Popocatépetl, México 1995; etc.).

The purpose of this short paper is to provide the international community with a general review of existing monitoring systems in Latin America, and with some examples of existing knowledge of the characteristics of volcanic crises and premonitory phenomena, that can be taken to understand better the volcanic behaviour, and to minimize or eliminate its disastrous impact on human society.

2. VOLCANIC SETTING IN LATIN AMERICA

More than 200 stratovolcanoes are known to have erupted during the past 11,000 years in Latin America (see Simkin and Siebert, 1994). In Middle America there are two major belts of active volcanoes, an east-west trending one through Mexico and another with northwest-southeast trend from Guatemala to Costa Rica, with a volcanic gap of 175 km between Turrialba, Costa Rica, and Barú or Chiriquí, Panama (Fig. 1). The Quaternary volcanic front of Central America extends for 1,100 km from the Mexico-Guatemala border to central Costa Rica and comprises 40 major volcanic centers (large andesitic shield volcanoes, compound volcanoes, and twin stratovolcanoes). These centers are regularly spaced along narrow discrete lineaments. The close spacing, approximately 26 km, provides one of the highest densities of active volcanic centers along any convergent plate margin (Carr and Stoiber, 1988). Twenty two active volcanoes in Mexico made

a total of about 100 eruptions since 1500 A.D. In contrast, the Central American belt of 57 historically active volcanoes had a total of more than 400 eruptions during the same time span. Volcanoes which were dormant for quite some time are often the most dangerous ones.

The 600-km-long active arc of the Lesser Antilles had at least 15 active volcanoes during the Holocene. During the last 300 years, at least 14 phreatic/phreatomagmatic events, 10 magmatic eruptions, 9 submarine eruptions, and 6 volcanic crises have occurred (Roobol and Smith, 1989).

These two active volcanic belts mark the eastern and western margins of the Caribbean plate. The Lesser Antilles on the east form a classic island arc, but Central America in the west is a continental volcanic belt and not particularly arcuate. The Central American volcanic range is slightly longer than that of the Lesser Antilles, 1,100 km versus 750 km, but Central America has 69 Quaternary volcanic centers as compared to only 15 for the Lesser Antilles (after Carr and Stoiber, 1988). Central American volcanoes have produced 16 km^3 of volcanic products since 1680, whereas the Antillean volcanoes have produced only 1 km^3 in the same period (Wadge, 1984).

The Andean range, extending for about 7500 km, resulted from the subduction of the Pacific oceanic plate beneath the western margin of the continental South American plate, generating three principal zones of active volcanism (de Silva and Francis, 1991): the Northern Zone (in Ecuador and Colombia), the Central Zone (southern Peru, northern Chile, southwestern Bolivia, and northwestern Argentina), and the Southern Zone (southern Chile and southern Argentina) (cf. Fig. 1).

3. VOLCANIC MONITORING IN LATIN AMERICA

From a list of the world's 101 most notorious volcanoes cited by Decker and Decker (1981), 23 volcanoes are from Latin America and the Caribbean Sea (about 23%) and only 11 from Central America (about 11%). However, it seems that the list of Holocene active volcanoes in Latin America is much longer, comprising at least 210 volcanoes. From the total of volcanoes active during the Holocene time, only 27 stratovolcanoes (13%) have at least one permanent seismic station and only a few stratovolcanoes are relatively well known in all the different aspects of volcanology (geology, tephrastratigraphy, petrology, precursor signals, etc.), including a more or less complete monitoring system composed of 3 or more seismic stations (6%), and periodically also geochemical, geophysical and visual monitoring (see Tab. 1a, 1b, 2, 3 and 4). Tab. 2 does not include several Quaternary cinder cones, maars and calderas. The information included in these tables is based on Cheminée et al. (1993), Barquero et al. (1994), Simkin and Siebert (1994), WOVO (1994), and correspondence with several Latin American volcanologists (up to August 31, 1995).

Scientific Technical Report STR 95/TK
DOI: 10.2312/GFZ.b103-95tk7

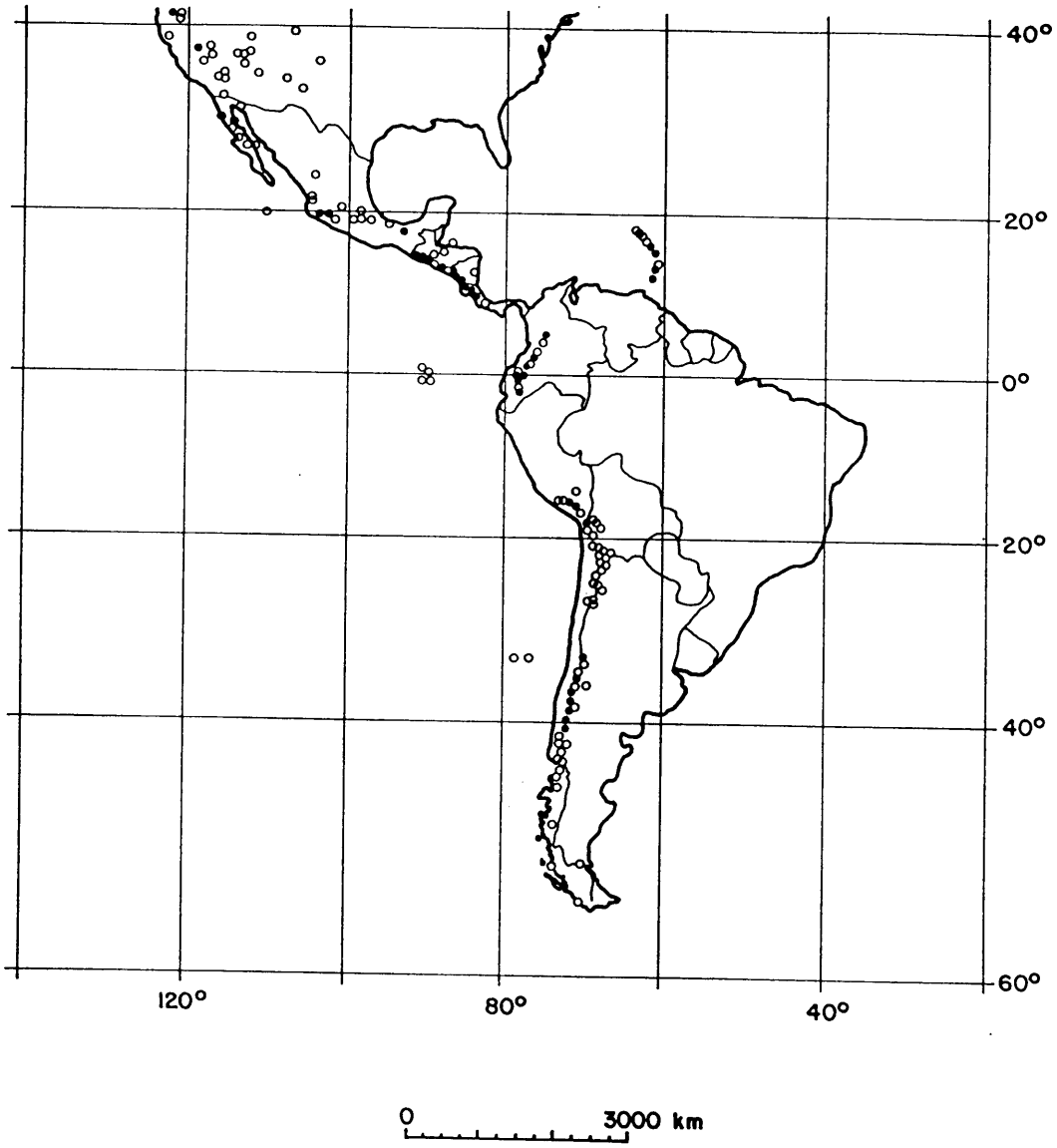

Fig. 1: Active volcanoes during the last 10,000 years. Full circles: recently active; open circles: active during the Holocene. Simplified after MacClelland *et al.*, 1989.

Thus, at the moment only 12 volcanoes have enough monitoring systems to control the normal activity: Nevado de Colima and Popocatépetl and proximally Tacaná (México); Fuego Acatenango volcanic complex (Guatemala); Miravalles and Arenal volcanoes (Costa Rica); Nevado del Ruiz Galeras and Puracé (Colombia); Cotopaxi Guagua Pichincha and Tungurahua (Ecuador). Nevado de Sabancaya (Perú) has only seismic stations but no other specific volcano monitoring system and the Deception Island (Antarctica) is monitored by the Argentine and Spanish group in summer time only.

Table 1a: Type of monitoring systems operating on Mexican and Central American volcanoes.

Volcano	Seismic stations	Ground deformation	Geo-chemical	CO-SPEC*
Colima, Mexico	5 (t,a,d)	yes	yes	yes
Popocatépetl, Mexico	8 (t,a,d)	yes	yes	yes
Tacaná, Mexico	-	yes	yes	-
El Chichón, Mexico	-	-	yes	-
Santiaguito, Guatemala	1 (a)	-	yes	-
Fuego-Acatenango, Guat.	4 (a,t)	-	-	-
Pacaya, Guatemala	1 (a,t)	yes	-	-
San Miguel, El Salvador	1 ?	-	yes	-
Masaya, Nicaragua	1	-	-	-
Monotombo, Nicaragua	1	-	yes	-
Telica, Nicaragua	2 (a,t)	yes	-	-
Rincón de la Vieja, Costa Rica	1 (a,t)	yes	yes	-
Miravalles, Costa Rica	6 (d,t)	yes	yes	-
Arenal, Costa Rica	6 (d,t)	yes	yes	-
Poás, Costa Rica	2 (d,t)	yes	yes	-
Irazú, Costa Rica	2 (d,t)	yes	yes	-
Turrialba, Costa Rica	1 (d,t)	yes	yes	-

a: analogic, t: telemetric, d: digital.

*COSPEC: The abbreviation stands for COrrelation SPECtrometer which is widely used to measure remotely the SO_2 discharge.

Table 1b: Type of monitoring systems on South American volcanoes

Volcano	Seismic stations	Ground deformation	Geochemical	CO-SPEC
Nevado del Ruiz, Colombia	8 (d,a,t)	yes	yes	yes
Galeras, Colombia	9 (d,a,t)	yes	yes	yes
Puracé, Colombia	5 (d,a,t)	yes	yes	-
Cerro Bravo, Colombia	1	-	-	-
Nevado Santa Isabel, Colombia	1	-	-	-
Nevado de Tolima, Colombia	1	-	-	-
Cerro Machín, Colombia	1	-	-	-
Nevado del Huila, Colombia	1	-	-	-
Santará, Colombia	1	-	-	-
Cumbal, Colombia	1	-	-	-
Cotopaxi, Ecuador	4 (t)	yes	yes	yes
Guagua Pichincha, Ecuador	10 (d,t)	yes	yes	-
Tungurahua, Ecuador	5 (t)	yes	yes	-
Quilotoa, Ecuador	1 (t)	yes	yes	-
Cuicocha, Ecuador	1 (t)	yes	yes	-
Chimborazo, Ecuador	1 (t)	yes	-	-
Antisana, Ecuador	1 (t)	-	-	-
Imbabura, Ecuador	-	yes	-	-
Cayambe, Ecuador	1 (t)	-	-	-
C. Negro de Mayasquer, Ec.	1 (t)	-	-	-
Nevado Sabancaya, Perú	3 (t)	-	-	-
Villarrica, Chile	1 (t)	yes	-	-
Llaima, Chile	-	yes	-	-
Deception Island, Antartic	5* (temporaly)	yes	yes	-

a: analogic, t: telemetric, d: digital.

Table 2: Monitored stratovolcanoes which had been active during the last 10,000 years in Latin America.

Country	Number of active strato-volcanoes	Volcanoes with monitoring system				
		≥3 seismic stations	≤2 seismic stations	Ground deformation	Geo-chemical control	COSPEC
Mexico	22	2	-	3	4	2
Guatemala	20	1	2	2	-	-
El Salvador	17	-	1	-	3	-
Honduras	4	-	-	-	-	-
Nicaragua	14	-	3 ?	-	-	-
Costa Rica	12	2	4	6	6	-
Panama	2	-	1	-	-	-
Colombia	13	3	8	5	10	2
Ecuador	18	3	7	7	5	1
Peru	13	1	-	-	-	-
Bolivia	15	-	-	-	-	-
Chile	47	-	1	2	-	-
Argentina	13	1*	-	-	1	-
Total	210	13	27	25	29	5

* Considering Deception Island as Argentinian without any political border preference.

Table 3: Type of monitoring systems on Caribbean (West Indies) volcanoes.

Volcano	Seismic stations	Ground deformation	Geochemical	CO-SPEC
Soufrière, St. Vincent	11 (t)	yes	yes	-
Mt. Misery, St. Kitts	1	-	-	-
Soufrière Hills, Montserrat	1	-	-	-
Dominica	1	-	-	-
Mt. St. Catherine, Grenada	1	-	-	-
Mont. Pelée, Martinique	7	yes	yes	-

Table 4: Number of active volcanoes in the West Indies with monitoring system.

Number of active stratovolcanoes	Volcanoes with monitoring system				
	≥ 3 seismic stations	≤ 2 seismic stations	Ground deformation	Geochemical	COSPEC
15	3	4	3	3	-

Although several volcano observatories and research centers have been established in Latin America promoting volcanological investigations, hazard evaluations and improving monitoring systems, many high risk dormant and active volcanoes remain poorly known, and many of them are located very close to cities, and energetic and industrial complexes. In fact, much of the Latin American countries lack the necessary resources to carry out a well equipped observatory and basic volcanological research (geology, radiometric dating, geochemical and isotopical analysis, etc.). Besides, several financial problems do not allow to maintain the permanent monitoring networks and its appropriate stock working. Additionally, the transport, training of personnel, and changing activities of volcanologists which are looking for another job in other fields, are daily problems at all observatories.

Thus, some of history's greatest catastrophes have been caused by eruptions whose early signs unrecognized, remained misunderstood or ignored. On the other hand, the great explosions of Cosigüina (Nicaragua) in 1835, Santa María (Guatemala) in 1902, and Arenal (Costa Rica) in 1968, all took place at volcanoes that had no historic record of previous eruptions.

4. CASE STUDIES: PREMONITORING SIGNALS OF COSTA RICAN VOLCANOES

4.1 Seismicity

Harlow (1971) compiled a list of 71 studies of earthquakes and volcanic eruptions: in 58% there was an increase in the number of earthquakes before an eruption; in 38% there was an increase in earthquakes without an eruption; and in 4% there was an eruption without any increase in earthquakes. Another serious problem in volcanic forecasting is the lack of reliable criteria for distinguishing between the precursory pattern of a pending eruption and of other phenomena such as magma intrusion or hydrothermal effect; the latter type of activity is called aborted eruptions *sensu* Walker (1982). Recent volcanic crises in Costa Rica correspond to this type (Alvarado et al., 1992). Some cases of the link between seismic activity and volcanic eruption or unrest are shown in Tab. 5 for illustration.

4.1.1 Arenal volcano

Arenal, located in the northern part of Costa Rica, is one of the most active volcanoes in the world. The height of the volcano is 1633 m above sea level (a.s.l.) and 1100 above the surrounding area. Arenal volcanic activity has been continuous over the last 27 years and is characterized by frequent Strombolian explosions and lava flows, gas emission, fumarolic activity,

a permanent lava pool since 1974, and sometimes there are small pyroclastic flows. For volcanoes with Strombolian activity such as Arenal, the observation of acoustic and visual phenomena at the eruptive center is helpful for interpreting the seismic records, providing the opportunity for volcanologists to obtain very valuable data in short time intervals to develop knowledge of explosive and effusive volcanic processes and related seismicity. Seismic activity at Arenal volcano has been the subject of several recent studies (e.g., Alvarado and Barquero, 1987; Barquero et al., 1992; Alvarado et al., 1995). Since 1984, a continuous seismological and visual monitoring has been carried out.

Seismic phenomena previous to the paroxysmic explosion of July 29, 1968, started as early as May 1968. On July 28, beginning at approximately 23:00 (local time), the inhabitants of Tabacón and Pueblo Nuevo towns at the base of the volcano reported numerous earthquakes. The small earthquakes gradually increased in magnitude and number. The intensity was great enough to awake people who, fearing the possible collapse of their houses, fled outdoors (see Barquero et al., 1992).

A period of explosive volcanic activity occurred in June 1975. "A-type" earthquakes occurred between the end of January and February, before the reactivation of the volcano. A new moderate increment in the explosive activity was recorded in June 1984, whose strombolian explosions were preceded several weeks before by an increase in the frequency and amplitude of tremor, suggesting movement and resonance of the magma column (see Alvarado and Barquero, 1987; Barquero et al., 1992).

Studies of the seismicity at Arenal volcano during recent eruptive phases reveal several features. "A-type" earthquakes show systematic patterns associated with the moderate explosive phases (1968, 1975, 1984, 1987, and 1993). Also, an inverse relation between tremor activity and the number of discrete volcanic events has been observed (Barquero et al., 1992).

For example, a new high-frequency earthquake swarm (at least 55 "A-type" earthquakes magnitude <2) was recorded in the seismic station Fortuna (FOR, 3.5 km east of the active vent) between May 11 and June 3, 1993 (4 months before an unusual eruption). The nature of seismic signals was variable, suggesting a complex source. Unfortunately, no seismic locations were possible, although the time delay P and S waves suggested a local source whose focus decreased in distance (and/or depth) with time. Focal depths were calculated empirically between 20 km beneath the volcano edifice for the very first events and less than 1 km for later ones attributed as sources near or within the volcano edifice. Alvarado and Soto (in prep.) point out that the seismic behaviour of the volcano changed after the eruption due to an open vent which permitted an almost continuous lava effusion, with few explosions. This status of activity corresponded with a period of seismic recordings which showed a predominance of tremor.

The volcanic activity studied during 1994 95 consists mainly of Strombolian explosions, basaltic andesite blocky lava flow effusion, a permanent lava pool, gas ejections, fumarolic activity, and small blocky slides. Several types of volcanic signals are distinguishable according to their waveform, their spectral content, and their correlation with field observations. In the order of their frequency these are: volcanic tremor (T), explosive earthquakes ("E-type"), low frequency (LFE or "B-type"), and surface high-frequency events, the last ones associated with lava slides.

Preliminary locations of "E-type" events suggest that the source of the Strombolian explosions is located within the volcano edifice and slightly northward of the active crater. The tremor varied

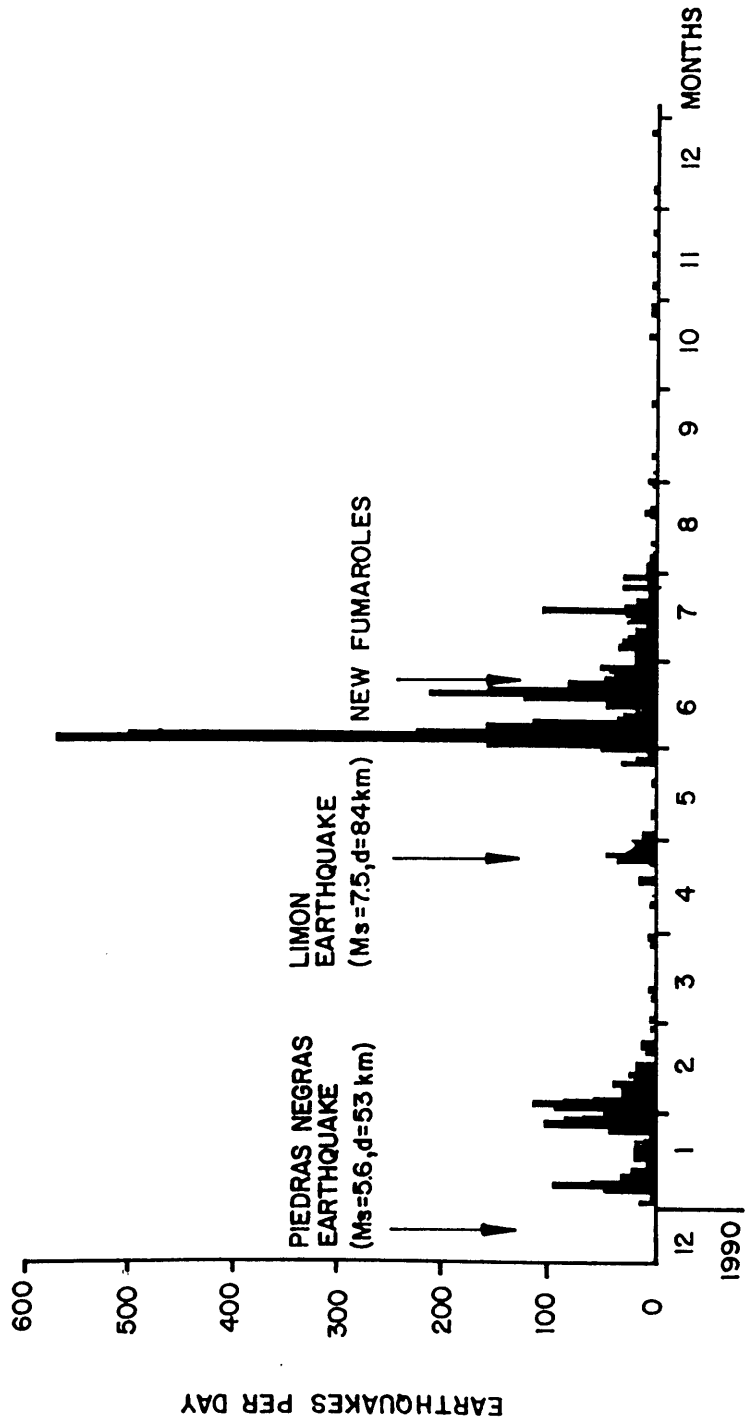

Fig. 2: Earthquakes in 1991 at Irazú volcano triggered by regional intraplate earthquakes (After Barquero *et al.*, 1992).

between a type that has a broad spectrum (spasmodic tremor) to a more frequent type with a sharply peaked spectrum (harmonic or single-resonator tremor). Very energetic tremor and explosions have been recorded at distances of 80 km from the volcano. Frequency variations with time of some spectral frequency peaks have been compared with volcanic activity and, on the basis of these results, a new schematic diagram for the feeding system of the summit vent is proposed. The source of the harmonic tremor at Arenal could be modeled as a resonator with a frequency of 1.4-2.5 Hz, although other tremor frequencies have been observed as well.

The main seismic-producing resonator is likely to contain gas-rich magma which is located in the upper 200-300 m of the eruptive conduit within the volcano, slightly shallower or near to the focus of the Strombolian explosions. Gas-piston events could be present at the lava pool, especially after strong degassing and explosive events. Some very high-frequency events are associated with lava slides recorded at distances as far as 4 km. The volcanic seismicity at Arenal is thus a train of different manifestations of the same basic process of unsteady magma-gas transport (Alvarado et al., 1995).

4.1.2 Irazú volcano

During 1991, earthquake swarms were recorded at Irazú volcano. Since May 1991, numerous fumaroles and hot springs were discharging on the floor of the main crater, forming the subaerial expression of a long-lived hydrothermal system related to a deeper magmatic system in the volcano. A local digital seismic network around the summit of the Irazú volcano was set up in June 1991 to monitor microearthquake activity. The maximum duration magnitude of the earthquakes (M_D = 4.3) is equivalent to an energy release of >15 x 10^{16} erg, and one of the smaller earthquakes (5 s duration) had a magnitude M_D = 0.3, equivalent to an energy of 2.1 x 10^9 erg. The total energy released from January 1991 to February 1992 was 4.5 x 10^{18} erg, with ca. 3 x 10^{17} erg released during June 1991 (Barquero et al., 1992; Barquero and Rojas, 1994). The two series of seismic swarms were triggered after the Piedras Negras earthquake (December 22, 1990, M_S = 5.6) and the Limón earthquake (April 22, 1991, M_S = 7.5), respectively. Both earthquakes (located 53 and 84 km WSW and ESE of Irazú, respectively) triggered more than 6000 "A-type" earthquakes (M_D < 4.3, h < 10 km) at Irazú), many low-frequency events and new intracrater fumaroles (Fig. 2).

4.1.3 Miravalles volcano

Another example of seismic swarm triggered by a local earthquake occurred at Miravalles volcano. On March 25, 1995, a local earthquake that occurred at the same hypocentral locality as during another seismic crisis in 1985, triggered a seismic swarm in a nearby geothermal field (see 4.3.2).

4.2 Ground deformation

Precursors of volcanic activity involve changes in the pressure and volume of magma reservoirs at depth which, in turn, deform the ground surface overlying the changing magma chambers and conduits. There are, however, other processes that can generate measurable ground deformation. Below we give two examples from Costa Rica.

4.2.1 Irazú volcano

During the last eruption of Irazú (1962-65), surveyors of the Instituto Geográfico de Costa Rica ran a line of precise leveling along the highway to the summit during mid-May 1964. Compared with previous elevations obtained for the same set of benchmarks in 1949, no significant change in elevation was found from Cartago up to the crossing of Canada creek (8.7 km in direct line southwest from the summit). Above this point, the new determinations became progressively larger. A maximum difference of +10 to +11 cm above the 1949 levels at the highest stations occurred within 2 to 3 km of the summit. Using the principles of Mogi (1958), the pressure source (magma chamber) was located 4 to 5 km directly beneath the summit (Murata et al., 1966). New precise leveling in 1966 revealed a backward position of the benchmarks to similar levels as in 1949. Thus, it is likely that the conspicuous ground deformation measured was due to the uprising magma which caused the eruption.

4.2.2 Arenal volcano

At Arenal the deformation studies were carried out by different groups in 1969, 1974-78 and 1982 to present (Alvarado et al., 1988; Soto, 1991). In the same way, all data sets show a continuous subsidence at the volcano with small episodes of uplifting in the order of 10 microradians. The subsidence seems to be related to the ground loading due to the lava flows erupted since 1968 up to present (ca. 0.5 km^3), while the small inflation episodes could be an effect of natural noise, geological conditions and some periods of higher magma moving along the conduit. The rate of downtilt observed at Arenal is in close agreement with those observed at Etna and Sakurajima volcanoes in similar lava fields (Soto, 1991).

The most accurated ground deformation has been recorded at the station C, located 1.8 km westward from the active vent, which downtilted toward azimuth 78° almost constantly at a rate of 1.7-2.5 μ/month between 1986 and 1990 (Soto, 1991). A similar deformation pattern was observed until April 1992. Since then, a relatively anomalous deformation was recorded up to January 1993. Between January and July 1993, the volcano inflated with a downtilt outward the edifice of 44 μrad recorded at station C (Alvarado and Soto, in prep.). Since the measurements were not continuous but separated by 184 days from each other, it is difficult to know when exactly this inflation occurred. But anyhow, it averages 7.2 μ/rad/month). Other reports by Observatorio Vulcanológico y Sismológico de Costa Rica (OVSICORI UNA) account also for an inflation of the west flank of the volcano, figuring out 15 μrad during the period October 1992 to July 1993, but they did not specify the location of the calculated inflation (GVN Bulletin, 1993). Unfortunately, during the volcanic event of August 28, 1993, the station C was destroyed by a pyroclastic avalanche event. However, reports from OVSICORI UNA (GVN Bulletin, 1993) account for a post eruptive deflation of 24 μrad of the SW quadrant of the volcano. Once again, the observed pre-eruption inflation and post-eruptive deflation show unequivocally an increase of magma pressure over the known background, which positively related to an impending eruption.

4.3 Temperature and geochemical monitoring

Changes in the temperature, volume and gas composition discharges of fumaroles and hot springs are often associated with changes in volcanic activity, preceding or not an eruption. Some cases in Costa Rica are:

4.3.1 Poás volcano

In Poás the temperature rose from 100°C (December 1980) to 875°C (February 1981) and 1020°C (March 1981). It remained high until November 1981 and started a gradual decrease which has continued to the present. It is likely that the July 1980 seismic crisis (M < 5.2), located in the NW Pacific (200 km from Poás), triggered "A-type" events that fractured the upper cap of a magmatic mass cooling inside the volcanic conduit of the 1952-55 eruption. Therefore, a large volume of phreatic water opened its way close to the magma body, was heated up and reached the surface five months later (Casertano et al., 1983). There were no clues pointing at a magma intrusion or any impending eruption. This interpretation also justified the absence of phreatic activity during a long period (1980 to 1986).

4.3.2 Miravalles volcano

In December 1985, several geothermal exploration wells at the foot of Miravalles volcano (actually the Miravalles Geothermal Plant), sited into a Quaternary caldera, showed an increase of up to 17°C after several earthquakes (M < 4.6, April - November 1985) on the northern flank of the volcano. This was another example of a crisis which did not result in a volcanic eruption.

4.3.3 Arenal volcano

Starting in 1965 pending volcanic activity was preceded by the following phenomena:

(a) colorless gas (CO and/or CO_2?) on the NE flank of the volcano, affecting animals and vegetation;
(b) water level of Cedeño lake on the north flank dropped completely and therefore the fishes died;
(c) hot springs at Tabacón river that drains the volcano on the northwest, increased their discharge temperature in 1967 and
(d) cows were seen moving down from the middle upper slopes of the volcano two weeks prior to the July 29-31, 1968 eruption (Alvarado and Barquero, 1987; Barquero et al., 1992).

Arenal has several moderately high-temperature springs (about 37-61°C) at the NNW-NW and NNE-NE slopes. During the past years, a large number of chemical analyses of the water of the warm springs at Arenal volcano have been carried out. They provide a unique data set that allows to study the spatial and transient variations in chemical composition and discharge temperature happening in these springs. According to the conclusions of a recent paper by Soto et al. (1995), two sources of heat and chemical species could be generating the thermal waters of Arenal. One is the external source formed by the recent hot lava flows and the plume of the volcano that can contribute with heat and chemical species to the infiltrating rain water. The other source is the magmatic chamber that releases heat and gases to the groundwater system. Also, they concluded that earth tides seem to trigger seismic activity in this volcano, and at the same time, earth tides are correlated with variations in monthly rainfall, and with the chemistry and temperature of the springs discharging at the slopes of Arenal volcano.

5. CONCLUSIONS

The aims of this work were, firstly, to identify the existing volcanic monitoring systems in Latin America, and secondly, to provide some examples of volcanic crises and premonitory signals with

Table 5: Some examples of unrest at Costa Rican volcanoes.

Volcano	Date	Type of volcanic unrest			Eruption
		Seismic	Thermal	Ground deformation	
Rincón de la Vieja	1991	Low-frequency events several hours before (May 6-8)	Uncertain	?	May 8: phreato-magmatic eruption and lahars
Miravalles	1985	April-November 1985 tectonic swarm	Increased temperature in some wells	?	None
Arenal	1968	3 months before eruption A-type swarm	Moffetes and increase of temperature at one hot spring	?	July 29-31, 1968 phreato-magmatic events
	1975	4 months before eruption A-type swarm and B-type events	?	?	June 17-21, 1975 pyroclastic avalanches
	1993	2.5 months before eruption A-type swarm	Several new fumaroles on the summit	7.2 μrad/ month, since January	August 28, 1993 pyroclastic avalanche
Platanar	1980 , 1986	Seismic swarm	None	?	None
Poás	198 0-81	Seismic swarms	100 °C in July 1980 to 1020 °C in March 1981	?	None
	1989	High-and low-frequency events	High-temperature fumaroles	yes	1989 phreatic eruptions
Irazú	1991	Two seismic swarms and low-frequency events	Fumaroles and hot springs in May	yes	None
	1994	Tectonic swarm in November (3 weeks before)	Uncertain	?	Phreatic explosion and landslide

emphasis on case studies from Costa Rica. Knowledge of the complete volcanological framework of a specific volcano is of great importance in estimating the danger of future eruptions. However, in Latin America only a few volcanoes are relatively well known (e.g., Nevado de Colima, Popocatépetl, Santa María, Cerro Negro, Turrialba, Irazú, Arenal, Mt. Pelée, Nevado del Ruiz, Galeras, Puracé, Cotopaxi, Guagua Pichincha, Villarrica, Lascar, etc.).

Volcanic eruptions along crustal plate boundaries from Mexico to Chile represent a significant hazard to many rapidly growing population centers. For example, the three destructive eruptions in 1902 (Mont Pelée, Soufriére and Santa María) and the 1985 eruption of Ruíz alone account for about 75% of the total deaths from volcanic activity in the twentieth century (Tilling, 1989). An eruption similar to the great volcanic explosion of Cosigüina volcano, Nicaragua, in 1835 and Santa María volcano, Guatemala, in 1902 would cause catastrophic loss of life and property today. The losses from such disasters gravely impact the social, economic, and political systems of an entire country.

Several new volcano observatories and research centers have been established in Latin America (i.e., México, Guatemala, Costa Rica, Colombia, Ecuador, Chile, Argentina, etc.) during the last few years promoting volcanological investigations, hazard evaluation and improving monitoring systems. However, many dangerous volcanoes remain poorly understood, are virtually unmonitored, and represent a potential hazard of future eruptions. Most of the world's highest-risk volcanoes are found near to densely populated Latin American cities that lack sufficient economic and scientific resources to study them adequately *(more than 6 stratovolcanoes per each Latin American volcanologist...)*. A sense of urgency is required to ensure that, at the beginning of the next century, we have a better knowledge of the potential for volcanic disasters and avail of more adequate monitoring systems, at least at the dangerous volcanoes located very close to population centers.

Worldwide experience shows that short-term eruption forecasting is best achieved by integrating results from a wide variety of approaches. The lack of reliable criteria for distinguishing between the precursory pattern of an eruption and that of a magma intrusion and/or hydrothermal unrest remain a serious problem. Magma intrusions can cause volcanic crises, but often result in "abortive" eruptions (Walker, 1982). For example, in Costa Rica, regional earthquakes ($M > 4$, distance from the volcano <200 km) often trigger local "volcano-tectonic earthquakes" under the volcano, and also affect the stability of geothermal reservoirs producing increases in the temperature of fumaroles or drilled wells, new fumarolic activity, and seismic volcanic signals, as the examples of Poás in 1980, Miravalles in 1985, and Irazú in 1991 (Alvarado et al., 1992). Thus, previously accumulated tectonic stresses within the volcanic system can be released by regional earthquakes and thus trigger local "A-type" events which affect the stability of the geothermal reservoir causing: (1) ascents of hydrothermal fluids to the surface, (2) new fumaroles and hot springs, and (3) low-frequency and tremor events.

In addition, when a volcano begins to show unrest, particularly after a long period without eruptions, the culmination of the course of events is almost always uncertain. Volcanologists can rarely make definitive predictions. In general, there is a broad range of possibilities depending on the characteristics of the volcano and on the scope of previous investigations, but also require a considerably mutual agreement between scientists and public authorities, and a positive collaboration from the public and journalists.

ACKNOWLEDGEMENTS

The critical review of this manuscript by Gerardo J. Soto and Rafael Barquero is gratefully appreciated. To Luis Madrigal, Mahrbin Rodríguez and G.J.S.B. for their collaboration during the edition. To Servando de la Cruz (Mexico), Héctor Cepeda and Alvaro Nieto (Colombia), and Hugo Yepes and Renán Herrera (Ecuador), for their valuable information.

REFERENCES

Alvarado, G.E. and Barquero, R. (1987). Las señales sísmicas del volcán Arenal (Costa Rica) y su relación con las fases eruptivas (1968-1986). Ciencia y Tecnología, 11 (1), 15-35.

Alvarado, G.E. and Soto, G.J. (in prep). The pyroclastic avalanche associated to crater-wall collapse and outpouring of a lava pool, Arenal volcano (Costa Rica), August 28, 1993.

Alvarado, G.E., Argueta, S. and Cordero, C. (1988). Interpretación preliminar de las deformaciones asociadas al volcán Arenal. Bol. Obs. Vulc. Arenal, 1 (2), 26-43.

Alvarado, G.E., Fernández, M., Barquero, R., Flores, H. (1992). Aborted eruptions triggered by earthquakes?: Costa Rica. Eos Trans. Spring Meeting Suppl., AGU, 73(14), 194.

Alvarado, G.E., Taylor, W.D., Ohrnberger, M.M., Soto, G.J. and Madrigal, L.A. (1995). First observations of volcanic seismicity at Arenal volcano (Costa Rica) using a new three-component seismic digital network. Open file report, OSV 95.8 ICE, 41 pp.

Barquero, R. And Rojas, W. (1994). Sismicidad inducida por el terremoto de Limón. Rev. Geol. Amér. Central, Esp. Vol. Terremoto de Limón, 111-120.

Barquero, R., Alvarado, G.E. and Matumoto, T. (1992). Arenal volcano (Costa Rica) premonitory seismicity. In: P. Gasparini, R. Scarpa and K. Aki (eds.): Volcanic Seismology, IAVCEI Proceedings in Volcanology, 3, 84-96.

Barquero, R., Soto, G. and Lesage, P. (1992). Volcán Irazú: Informe Vulcanológico, periodo enero 1991-mayo 1992. Open file report (ICE, UCR, Saboya Francia); San José, 65 pp.

Barquero, R., Barrantes, J.M., Boschini, I., Taylor, W., Alvarado, G. and Climent, A. (1994). Nueva red sismológica digital Arenal-Miravalles. Tecnología-ICE: Energía y Telecomunicaciones, 5 (2), 13-22.

Carr, M.J. and Stoiber, R.E. (1988). Volcanism. In: G. Dengo and J.E. Case (eds.): The Geology of North America, vol. H, The Caribbean region, Boulder, Colorado, Geol. Soc. America.

Casertano, L. Borgia, A. and Cigolini, C. (1983). El Volcán Poás, Costa Rica: Cronología y características de la actividad. Geof. Inter., 22-23, 215-236.

Cheminée, J.L., Dubois, J., Le Mouël, J. L. and Grappin, C. (1993). Les Observatoires Volcanologiques Francais. Institut de Physique du Globe de Paris, Institut National des Sciences de L'Univers, 45 pp.

de Silva, S.L. and Francis, P.W. (1991). Volcanoes of the Central Andes. Springer Verlag, 216 pp.

Decker, R. and Decker, D. (1981). Volcanoes. W.H Freeman and Co., New York, ix + 244.

Harlow, D.H. (1971). Volcanic earthquakes. M.A. Thesis, Dartmouth College, Hannover, N.H.

Global Volcanism Network Bulletin (1993). Smithsonian Institution, Vol. 18 (5- 8, 12); Washington D.C..

MacClelland, L., Simkim, T., Summers, M., Nielsen, E. and Stein, T.C. (1989). Global Volcanism 1975-1985. Smithsonian Institution Scientific Event Alert Network (SEAN), Prentice Hall, Inc. and American Geophysical Union, Washington, D.C., 657 pp.

Mogi, K. (1958). Relation between the eruptions of various volcanoes and deformation of the ground surface around them. Bull. Earthquake Res. Inst., Tokyo Univ., 36 (2), 99-134.

Murata, K. J, Dóndoli, C. and Sáenz, R. (1966). The 1963 65 eruption of Irazú volcano Costa Rica (The period of March 1963 to October 1964). Bull. Volcanol., 29, 765-796.

Roobol, M.J. and Smith, A.L. (1989). Volcanic and associated hazards in the Lesser Antilles. In: J.H. Latter (ed.): Volcanic Hazards: Assessment and monitoring. Springer-Verlag, 57-85.

Simkin, T. and Siebert, L. (1994). Volcanoes of the World. Geoscience Press, Smithsonian Inst., x + 349 pp.

Soto, G.J. (1991). Análisis de inclinometría seca en el volcán Arenal, 1988-90. Bol. Obs. Vulc. Arenal, 4 (7), 33-61.

Soto, G.J., López, D.L., Fernández, J.F. and Alvarado, G.E. (1995). Caracterización geoquímica de las aguas termales del volcán Arenal (Costa Rica) dentro de su marco geovulcanológico. Submitted to V Congreso Nacional de Recursos Hídricos, San José, Costa Rica, September 1995.

Tilling, R.I. (1989). Volcanic hazards and their mitigation: Progress and problems. Reviews of Geophysics, 27 (2), 237-269.

Wadge, G. (1984). Comparison of volcanic producting rates and subduction rates in the Lesser Antilles and Central America. Geology, 12, 555-558.

Walker, G.P.L. (1982). Volcanic hazards. ISR interdiscip. Sci. Rev., 7, 148-157.

WOVO, 1994. Directory of volcano observatories 1993-1994. WOVO/IAVCEI/UNESCO, Paris, 1991.

VOLCANO SEISMOLOGY

Rolf Schick

Institut für Geophysik, Richard-Wagner-Str. 44, D-70184 Stuttgart
FAX: +49 711 236 1218 e-mail: rs@zeus.geologie.uni-stuttgart.de

1. INTRODUCTION

Volcano seismology is in many parts different from earthquake seismology. In earthquake seismology, we have to deal with only one kind of source mechanism: it is the stress drop caused by a transient shear dislocation which presents the source of seismic wave radiation. No question, the temporal and spatial function of this source might be very complex but the point source, or the elementary source, has a known character.
In volcano seismology we wish to study dynamical processes associated with eruptive volcanic activity on the basis of observed seismic waves. The waves can be radiated by a variety of different sources inside the volcano. They include:

1. Mechanical instabilities within the solid part of the volcano. This category contains tectonic earthquakes. Landslides, lahars or rockfalls are other typical mechanical failures generating seismic waves.
2. Following the law of Bernoulli, non-stationary fluid flows are associated with pressure changes and induce vibrations. Magmatic melt is not the only liquid flowing inside a volcano. The flow of water or gasjets may as well present effective radiators of seismic waves. In an eruptive volcano, all these sources can act simultaneously, thus creating very complex source conditions.

It is the aim of the volcano seismologist to assign phases in the recorded seismograms with the relevant source mechanisms. When this first step can be achieved, the next step is the approach to a quantitative, or semi-quantitative correlation between the physics of the source mechanisms and the corresponding seismic phases. However, there are many restrictions in finding a 'true source model'. Even a striking similarity between the calculated seismograms of an assumed source model and the observed seismograms must not necessarily reveal a true physical source model.

2. INSTRUMENTATION

In principle, the seismic instrumentation set up on a volcano is comparable to the one which is used to record 'tectonic earthquakes'. However, there exist some differences. The spectral composition of the wave excitation with the fluid-dynamical sources is different from fracture sources, i.e. from earthquakes. From experience we know that the fluid-flow sources on a volcano show a high spectral amplitude variation in a wide frequency range. There is no distinct 'corner frequency' as we know it from fracture sources. These factors demand high quality seismometers with linear transfer functions in a wide amplitude range from tens of Hertz and down to frequencies as low as it is instrumentally possible. The lower frequency limit which can be achieved on a volcano follows essentially the instrumental protection against variations in environmental conditions, mainly temperature and atmospheric pressure. With a good insulation,

volcano seismic signals down to less than 0.01 Hz may successfully be recorded and analyzed.

3. SHOCKS AND TREMOR

In a first, although rough classification, seismic motions recorded on a volcano may be separated into three categories:

- seismograms which resemble the typical characteristics of tectonic earthquakes;
- seismograms which still have a transient character but without a sharp first onset; thus phases are difficult to discriminate and the spectrum often shows a narrow bandwidth;
- seismograms where wavetrains show durations of many minutes or hours, or where the seismic signals are 'ever present'.

Typical examples are shown in Figs. 1 to 3. The first category we call 'tectonic or fracture shocks', the second one 'volcanic shocks' and the third one 'volcanic tremor'. Unfortunately, the nomenclature for identifying and describing seismograms on a volcano is not consistent. The source mechanism of a 'volcanic shock' can be identical to a 'tectonic earthquake'. The setting of the earthquake in heterogenous volcanic terrain with low shear rigidity and high signal scattering can disturb the traditionally known signal character. On the other hand, waves with seismogram forms similar to 'volcanic shocks' may actually have their origin in fluid flow or hydraulic transients. From that point they would belong better to the group of 'volcanic tremor'. Instead of the name 'volcanic tremor', other expressions are used (harmonic tremor, volcanic unrest, volcanic microseism and others).

4. TECTONIC AND VOLCANIC SHOCKS

Although by no means it is guaranteed that seismogram patterns resembling those of tectonic shocks actually have their origin in shear failure source mechanisms, in many cases an analysis of these events with the proved methods of traditional earthquake seismology gives useful results. Clustering of earthquakes is typical and sheds light on the fracturing level of rock. Aseismic zones may indicate a region of low shear rigidity and might be interpreted as 'hot spots' or magma chambers. Focal mechanism studies give us information about the stress state at the time and location of the rupture. As with higher volcanic activity levels earthquakes on volcano es are numerous and often occur in swarms, stress- and pressure fields may be studied using the known methods of fault-plane solutions. Of special interest are temporal variations where, e.g., an increase of pressure is associated with an intrusion of magma. As mentioned, there must be no principal difference in the mechanism of a 'volcanic shock' and a 'tectonic earthquake'. But the values of the source parameters are often numerically quite different. Volcanic shocks commonly show low values of stress drop and a low velocity of fracture propagation. The magnitude-frequency relations show high b-values, indicating that the events occur in highly pre-fractured rock.

Investigations of 'volcanic shocks' result in successful modeling of magma and fissure systems and their evolution in time on a number of volcanoes. Special good outcomes were obtained in studies of the Hawaiian rift systems, with the Mount St. Helens volcano complex and with the South Italian volcanoes Mt. Etna and Vulcano. Fig. 4 shows the spatial seismicity beneath Mt. Etna (Sicily) for the year 1986.

5. VOLCANIC TREMOR

The knowledge of the movement of magma inside a volcano is of prime importance. The volcanic shocks which occur in the shear-rigid part of the volcano can only indirectly serve as a tracer for the magma flow. Volcanic tremor is in general the generation of sound, or in our case of seismic waves, by flows. Thus the study of volcanic tremor belongs to the field of flow acoustics. Steady flows do not produce sound, only unsteady flows do. High pressure variations, and therefore efficient generators of volcanic tremor, are especially found with the pressure instabilities of multi-phase flows. Within an eruptive volcanic vent the liquid magma and the dissolved gases comprise at least a two-phase flow system. The major problem in the interpretation of volcanic tremor using the laws of flow acoustics is that flows are governed by highly nonlinear equations. Only with care and caution, characteristic and fundamental processes may be isolated which allow us to study some aspects of the processes involved and give us a deeper insight into the underlying physical mechanisms which may lead to the working of the volcano.

In recording volcanic tremor, there exists the possibility of studying pressure variations directly at the source. Fig. 5 (upper trace) shows a fine example of a fluid-flow transient which leads to a 'Strombolian eruption'. Strombolian eruptions (named after Stromboli volcano where they persistently occur) are events in which gas, ash, spatters of incandescent lava and rock fragments are ejected in explosions. The seismogram was recorded with a 'Broadband Seismometer' of the type Wielandt-Streckeisen STS-2. The instrument records the ground motion between 100 s and 50 Hz. In Fig. 5, frequencies above 0.1 Hz were filtered out and the seismogram contains only the lower frequencies between about 0.01 Hz and 0.1 Hz. This low frequency band is of great advantage in studying and discriminating the mechanisms of different sources since, as with many observations on a volcano, the wavelengths belonging to these frequencies are much longer than the distances from receiver to source. Such a near-field observation reflects the displacement at the source much better as disturbances by the wave path or soil resonances beneath the recording station play a negligible role.The eruptive system seems to be governed by an aperiodic loading-deloading process. The lower trace in Fig. 5 simulates a seismogram as it would be recorded by the traditionally used short-period instruments with 1 Hz eigenfrequency. It is obvious that the long-period and often neglected part of the seismic spectrum contains frequencies which are essential when the source process is studied.

For long, volcanologists believe to recognize rhythms and periodicities in the strength and material outflow of volcanic eruptions. The observation of volcanic tremor provides a powerful tool to parameterize these processes and search for patterns which might be correlated to a characteristic behaviour of the eruptive activity.

Fig. 6 illustrates significant periodicities which can be found when the intensity of volcanic tremor signals observed at Mt. Merapi (Central Java, Indonesia) is analyzed. The observed rhythms range from a few minutes to hours. Diurnal (24 hours) and semi-diurnal (12 hours) periods suggest that processes in the volcano occur which are triggered by external forces, e.g. by meteorological temperature or barometric pressure variations. The origin of this oscillatory character is still poorly understood. Because of the viscosity of the fluid, friction is present. For the magma to remain in motion, the fluid system must be subject to internal (mainly thermal) or external (mainly gravitational) driving forces. However, we have to assume that in comparison to the fast and more or less chaotic (random) pressure fluctuations of the magma flow, the driving forces vary in time much slower and in a more systematic manner.

This mentioned effect is only one special case of the much wider problem we face when we try to get an insight into the dynamical processes which occur in the transition from low (or non-) eruptive activity to high eruptive activity. What is the cause that slowly varying, quasi-static pressure variations in a magma reservoir undergo a transition to fast pressure variations? In other

words, we must seek for a device which transforms potential energy into kinetic energy. The study of stability problems in fluid flow and the transition from one type of state to another one, for instance from steady laminar flow to random turbulent flow is of prime importance. The underlying equations are governed by non-linear terms and it is this effect which gives even the simplest non-linear dynamical system a wide range of possible behaviors. Numerous in stabilities in two-phase (gas/liquid silicate melt) flow may lead to fast flow velocity and pressure fluctuations. Boundary conditions from the material properties of the fluid flow (density, compressibility, viscosity) and from the geometrical dimensions of the feeding conduit determine, together with the driving forces, the spatial and temporal patterns of the resulting flow. The resulting temporal behavior can be periodic, quasi-periodic, intermittent or random. These transition processes can be seen and studied in the observation of volcanic tremor.

The working of a volcano might in a way be comparable to the function of a steam engine. Potential heat energy is transformed into kinetic energy. A non-linearly working device is needed to perform this transformation. With the steam engine, this is the slida valve. With the eruptive volcano, non-linear terms in the flow equations may be the responsible factor for the conversion of slow temporal energy variations into fast energy variations. A volcano may physically be represented as a pulse power amplifier. The block diagram of Fig. 7 gives an illustration of this concept.

6. POSSIBLE TREMOR SOURCE MODELS

From the mentioned remarks it is understandable that it requires great efforts to build even a qualitative model which may reliably explain the generation of volcanic tremor. The information content in the volcanic tremor signals is far too low to establish a unique source mechanism. Estimates of source models thus relate only to particular experimental effects.
Fig. 8a,b shows an experiment in which the introduction of a constriction in a linear pipe connected to a vapour emitting reservoir, leads from continuous to rhythmic steaming. An acoustical or seismic sensor attached to the configuration of Fig. 8b would show distinct pressure bursts.
A major instability in fluid flow represents the transition from subsonic to supersonic flow. The velocity of sound in a homogeneous two-phase mixture can be far less than the sound velocity of the components alone. Even a small percentage of gas in a liquid increases the compressibility by orders of magnitude while the density of the mixture is nearly kept constant. Thus the velocity of sound in a gas-silicate melt mixture can decrease to a few meters per second, a value which may come close to the velocity of the flow. The occurrence of prominent pressure shocks may be the result. An example is illustrated in Fig. 9. The system leads to a feedback subsonic-supersonic-subsonic. It might be one cause for the observed rhythmic degassing.

7. PREDICTING VOLCANIC ERUPTIONS

The ultimate aim of volcano monitoring should lead to the estimation of future activity. However, the problem is physically, technically and socially too complex to be described here in detail. Quite a few volcanic events could be claimed as 'successfully predicted' only due to not clearly defined terminology in use.
A general approach to the question is illustrated in Fig. 10. An active volcano represents physically a high-order system, i.e. a system with many degrees of freedom. Any useful

mathematical quantification of this dynamical system must reduce the amount of recorded data. Different signal processing methods can be applied to convert the continuous stream of high sampled seismic data into a low sampled data stream. In a simple case, the number of shocks per minute, hour or day is calculated. The next step could include a classification of the shocks due to spectral composition, duration and character of first onset. More sophisticated methods may use wavelet transformation, neural analysis or fractal dimensions. The aim is finding numbers, which are related to the visible eruptive activity of the volcano. We call these numbers 'Volcanic Activity Parameters (VAP). Quantitative meteorology is based on similar concepts. Like volcano dynamics, weather is a process of high order. Nevertheless, few parameters are sufficient to describe the weather conditions. They are temperature, barometric pressure, wind velocity and direction, humidity, and others.
Many more parameters determine the volcano process and they vary significantly from region to region. Therefore, it may take a long observation time to obtain, at least to a certain degree, a statistically significant relationship between the VAP and the eruptive activity of a given volcano. After this relations hip has been achieved, an extrapolation of the VAP time series can lead to an estimation of the future dynamic state of that volcano but it cannot be extrapolated to other volcanoes in different environments.

8. DISCUSSION

It is very suggestive that instabilities in the fluid flow of the magma-gas mixture play an important if not a crucial role in the origin of high pressure pulses. These pressure pulses are possibly the ultimate cause for explosive volcanic activity. The pressure fluctuations in the magma conduits lead to vibrations on the surface of the volcano. An analysis of these vibrations can give the volcanologist an indication of different patterns in the flow regime. The transitions between different patterns (periodic or random in the simplest cases) may eventually lead to an estimation of the actual volcanic hazard. This means that considerable time and expense are justified to obtain the necessary data. On an erupting volcano, however, many and for a quantitative analysis necessary data are simply unobtainable. Nevertheless, there is optimism about the utility of volcanic tremor for a better understanding of the internal dynamics of an eruptive volcano.

FURTHER READING

"How Volcanoes Work": A collection of multidisciplinary papers of modern studies of volcanic phenomena. Three special sections in: J. Geophys. Res., Part 1: Vol. 92, B13, Dec 1987, Part 2: Vol. 93, B5, May 1988, Part 3: Vol. 93, B12, Dec 1988.

Modeling of volcanic processes. Chi-Yu King, R. Scarpa (eds.), Vieweg-Verlag, Braunschweig-Wiesbaden, 206 p., 1988.

Volcanic Seismology. P. Gasparini, R. Scarpa, K. Aki (eds.), IAVCEI Proceedings in Volcanology 3, Springer-Verlag, Berlin-NY-Ldn, 572 p., 1992.

D. Chester: Volcanoes and Society. Edward Arnold, London-Melbourne-Auckland, 351 p., 1994.

Volcanic Tremor and Magma Flow. R. Schick, R. Mugiono (eds.), Sc. Series Int. Bureau, Forschungszentrum Jülich, Vol. 4, 200 p., 1991.
Moran, S.C.: Seismicity at Mt. St. Helens, 1987-1992: Evidence for repressurization of an active magmatic system. J. Geophys. Res., Vol. 99, B3, 4341-4354, 1994.

M. Ukawa, M. Ohtake: A monochromatic earthquake suggesting deep-seated magmatic activity beneath the Izu-Ooshima Volcano, Japan.

J. Geophys. Res., Vol. 92, B12, 12649-12663, 1987.

M. Takeo, H. Yamasato, I. Furuya, M. Seino: Analysis of long period seismic waves excited by the November 1987 eruption of Izu-Oshima volcano. J. Geophys. Res., Vol. 95, B12, 19377-19393, 1990.

J.J. Dvorak, A.T. Okamura: Variations in tilt rate and harmonic tremor amplitude during the January-August 1983 East Rift eruptions of Kilauea volcano, Hawaii. J. Volc. Geotherm. Res., Vol. 25, 249-258, 1985.

M. Cosentino, G. Lombardo, E. Privitera: A model for internal dynamical processes on Mt. Etna. Geophysical J., Vol. 97, 367-379, 1989.

D. Seidl, R. Schick, M. Riuscetti: Volcanic tremors at Etna: a model for hydraulic origin. Bull. Volcanol., Vol. 44-1, 43-56, 1981.

F. Dobran, P. Papale: Magma-Water interaction in closed systems and application to lava tunnels and volcanic conduits. J. Geophys. Res., Vol. 98, B8, 14041-14058, 1993.

A. Toramaru: Formation of propagation pattern in two-phase flow systems with application to volcanic eruptions. Geophys. J., Vol. 95, 613-623, 1988.

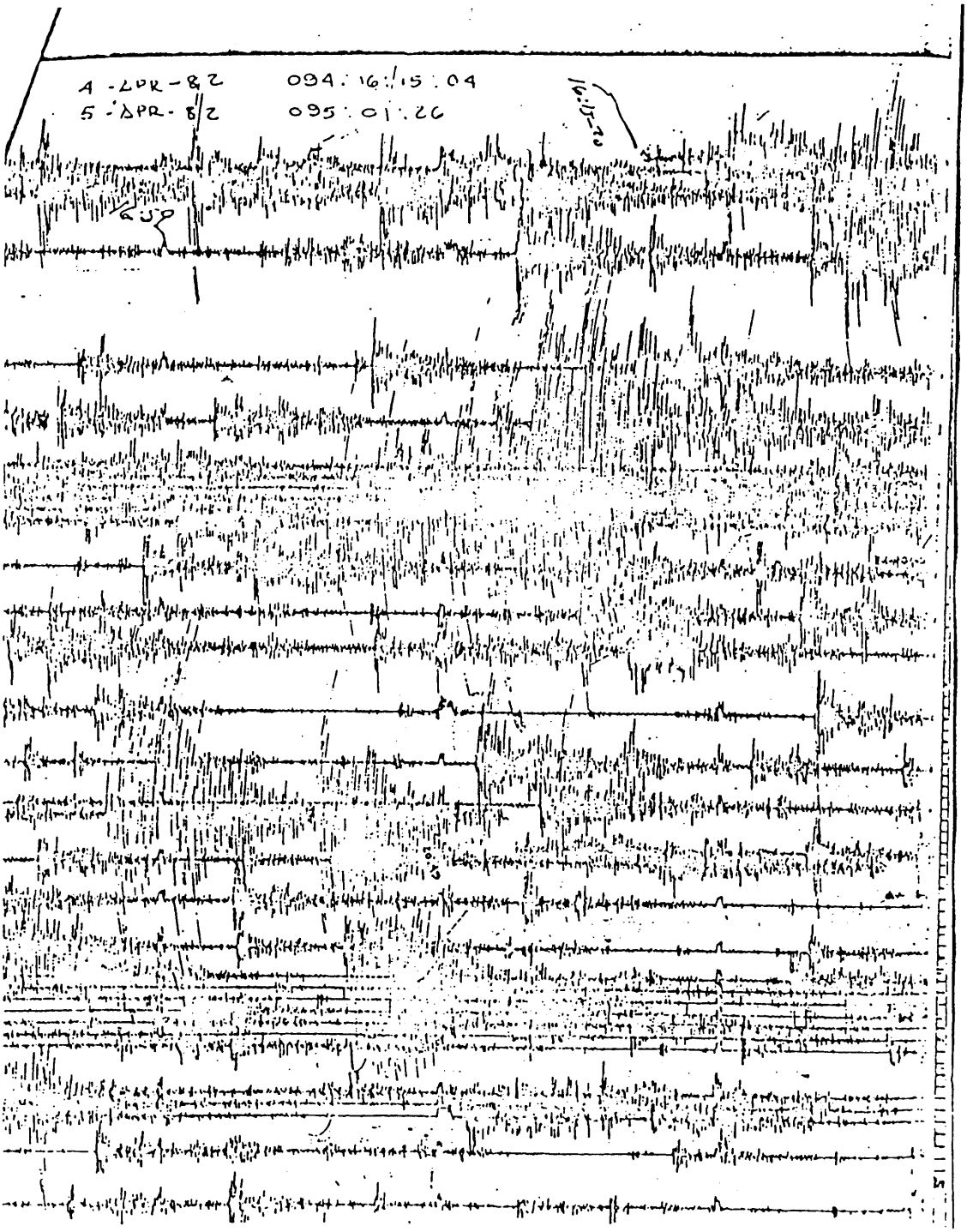

Fig. 1: Series of shocks following the El Chichon (Mexico) eruption of March-April 1982. The shocks show a sharp first onset. They are possibly caused by shear-failures associated with the crater collapse and caldera formation.

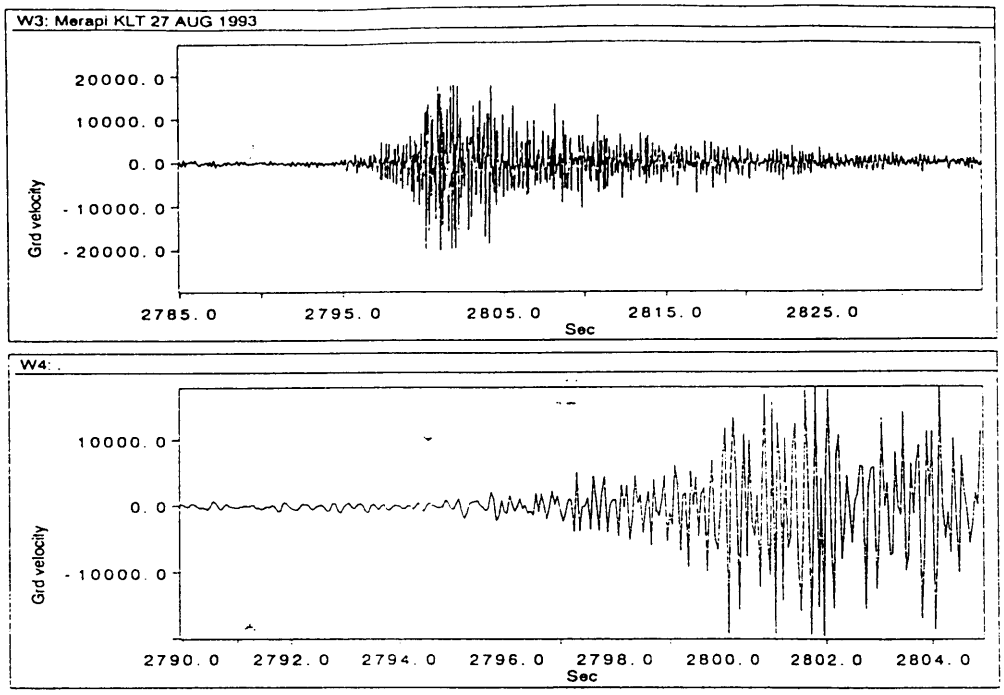

Fig. 2: Typical seismogram of a 'volcanic shock' recorded on Merapi volcano (Indonesia). The upper trace shows the full seismogram, the lower trace is a zoom of the starting phase. The onset of the seismogram is very emergent. Thus it is impossible to read first arrival times with sufficient accuracy for epicenter or hypocenter calculations. Other methods, like the determination of the angles of incoming wavefronts, must be used.

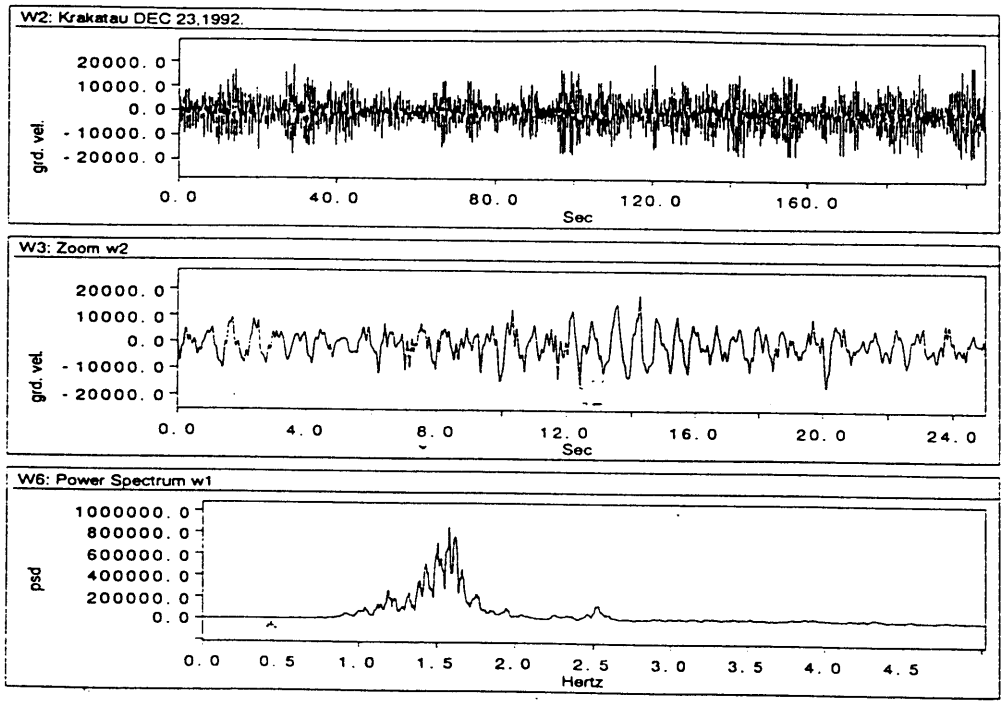

Fig. 3: Seismogram and power spectrum of 'volcanic tremor' showing a 'persistent' character. Recording was performed with the activity of 'Anak Krakatau'-volcano (Indonesia) in December 1992.

Upper trace: Typical seismogram. The envelope of the seismogram shows a rather stationary character when an average over about 100 s of the seismogram is performed.

Middle trace: Zoom of the first 25 s.

Lower trace: Power spectrum of the seismogram shown in the upper trace. The power is limited to a small frequency band, with a peak at around 1.6 Hz.

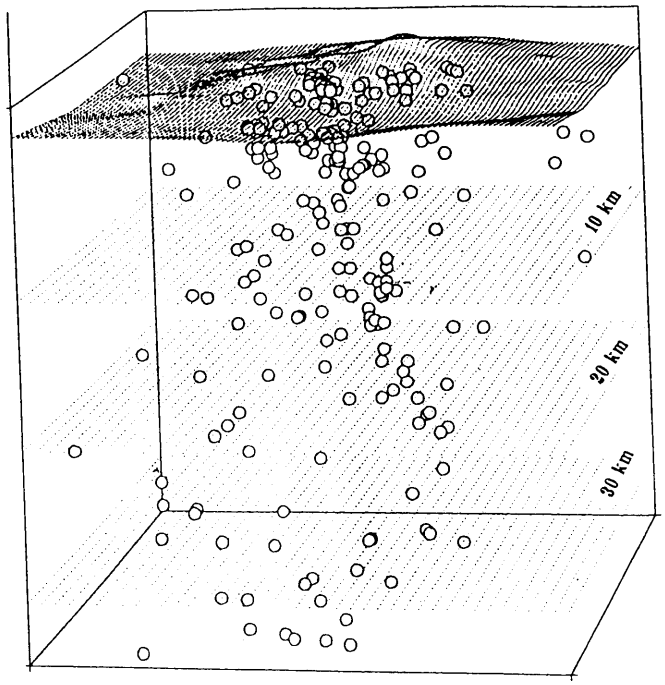

Fig. 4: The spatial distribution of shocks beneath Mt. Etna volcano (Sicily) in the year 1986. Following the seismograms from which the locations were calculated it is suggestive that the shocks correspond to fracture events. No clear aseismic zone can be found as one would assume with the existence of a large volume magma chamber.

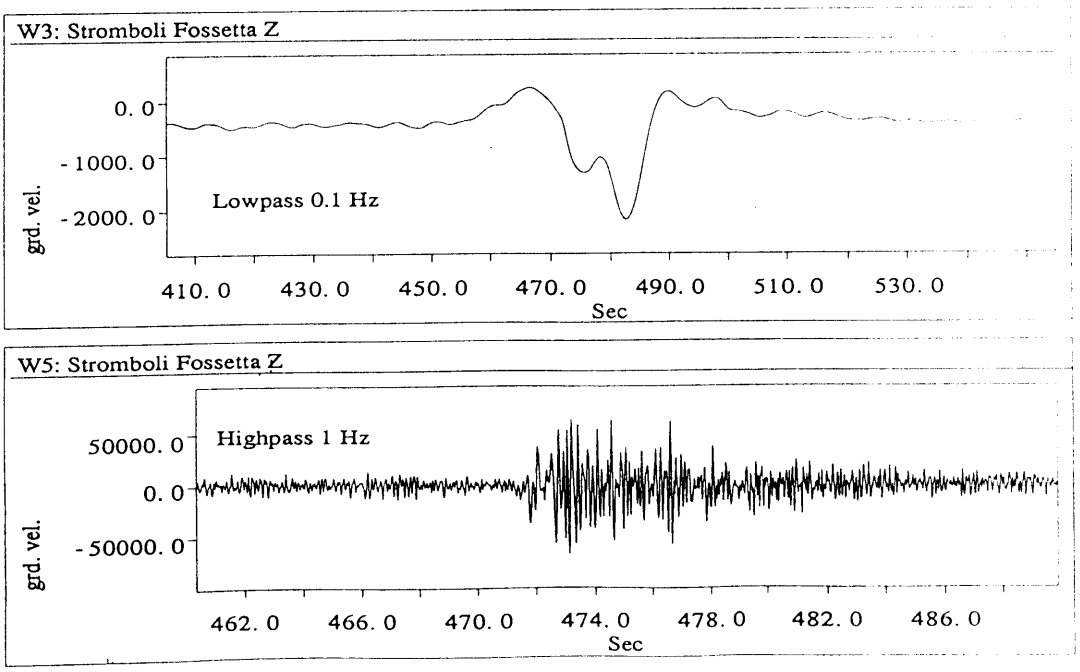

Fig. 5: Seismogram with origin of a Strombolian explosion, recorded with a broadband STS-2 seismometer.
above: lowpass filtering with 0.1 Hz cut-off frequency, below: highpass filtering with 1 Hz cut-off frequency.
The lower trace simulates the seismogram as it is recorded with the traditionally used short-period seismometers of 1 Hz eigenperiod. It can be seen clearly that frequencies below 1 Hz are essential for modeling the source process.

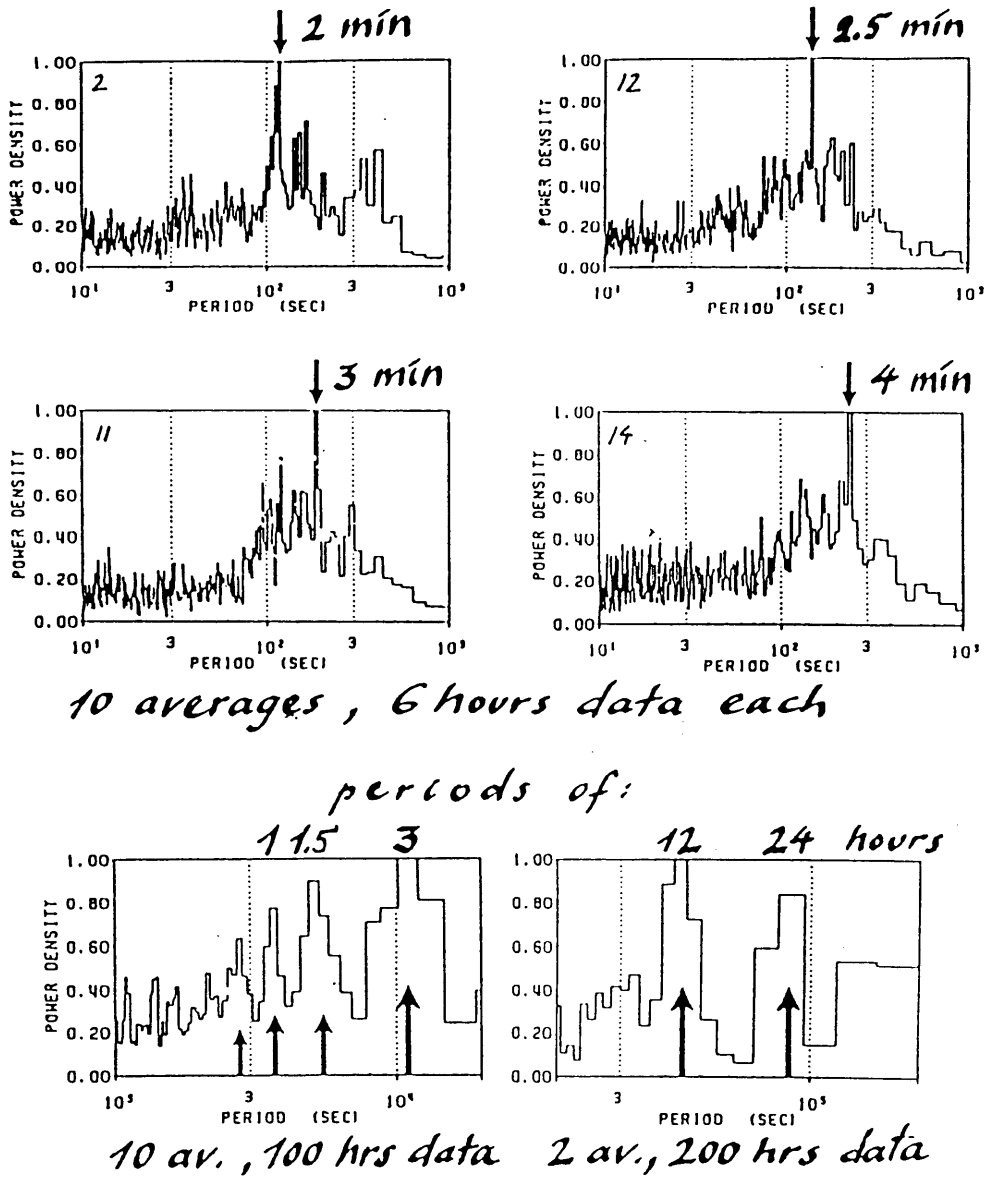

Fig. 6: Power spectra of the envelope of seismograms associated with the volcanic activity at Merapi volcano (Indonesia). The spectra show significant spectral peaks, ranging from minutes to hours. The peaks at 12 hours and 24 hours have their origin in trigger effects by barometric pressure variations and/or temperature induced stress.
(Plot: courtesy of W. Brüstle)

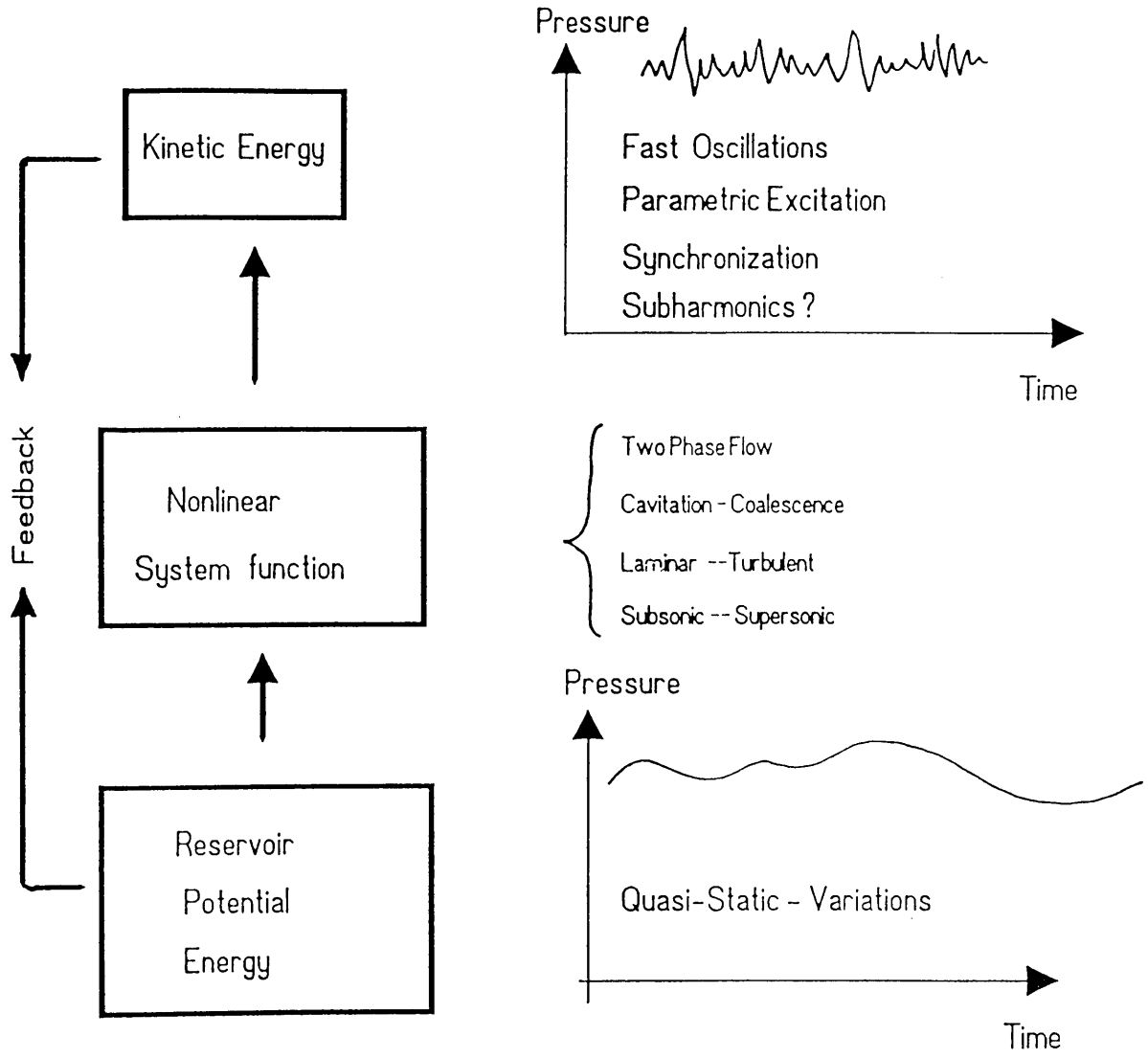

Fig. 7: Conversion of potential thermal energy into kinetic energy. The process is associated with the generation of fast pressure variations. The key to transformation are non-linear terms in the equations controlling the fluid flow.

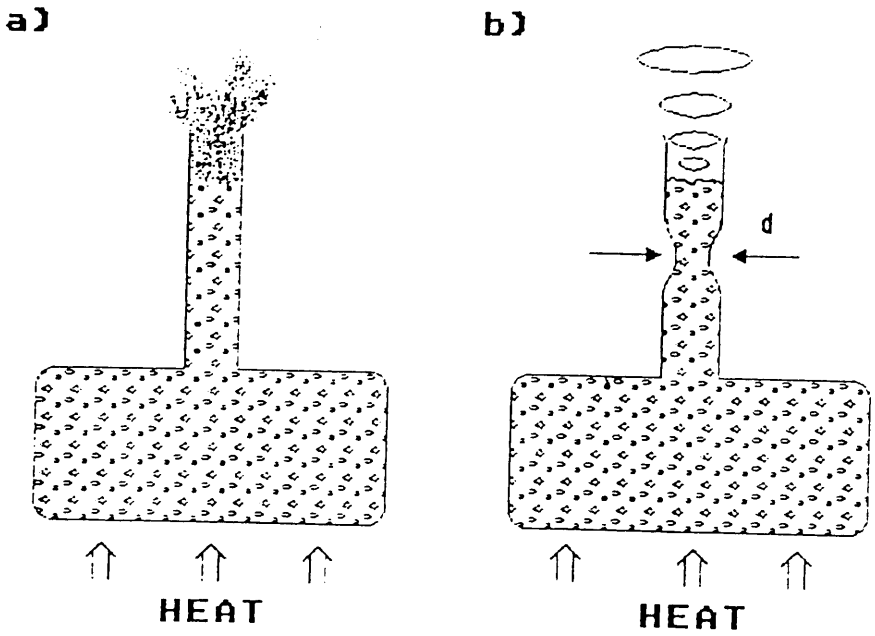

Fig. 8: A 'volcano-experiment': a) continuous steaming; b) occurrence of discrete steam bursts with constriction in pipe.

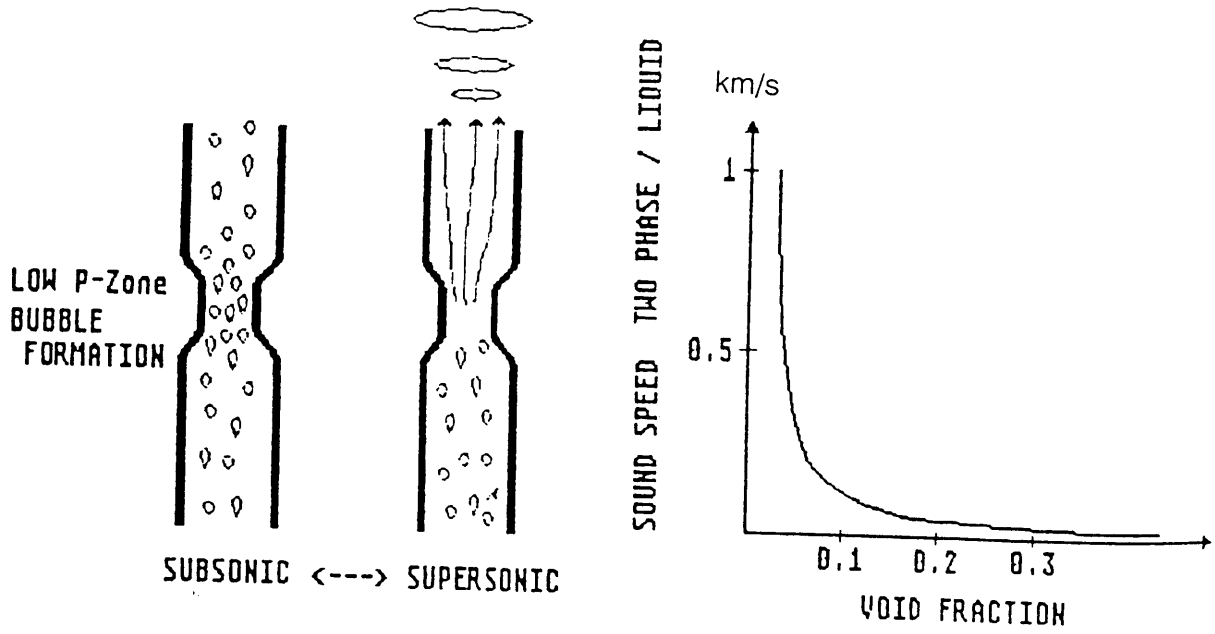

Fig. 9: left: Pressure pulses induced by transitions from subsonic to supersonic flow.
right: Sound velocity of liquid-gas mixture versus void fraction.

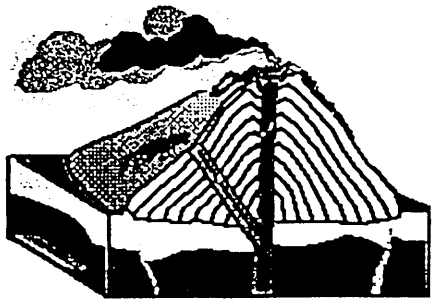

High Order System

Data Acquisition

Data Processing

Volcanic Activity Parameters

Time Series Analyses
Stability Criteria

Modeling
Low Order System
Fluid Dynamical Source

Observation Results
Visible Eruptive Activity

Prediction

Fig. 10: Block diagram illustration the quantification of volcano dynamics.

Exercise in Volcano Seismology

Rolf Schick
Institut für Geophysik, Richard-Wagner-Str. 44, D-70184 Stuttgart, FRG

Introduction

The training is based on a time series which was recorded on Stromboli Volcano in July 1995. Stromboli is a small island located in the Tyrrhenian Sea, part of the Mediterranean Sea. It belongs to Sicily (Italy). The summit height of the volcano is 923 m. Stromboli is famous for its persistent eruptive activity ('Strombolian Activity'). In times of average activity, several explosions with ejecta of incandescent lava, ash, gas and steam can be observed within one hour. The recording was performed with a Wielandt-Streckeisen STS-2 ('broadband') seismometer at the location 'Fossetta'. The output of the seismometer is proportional to ground velocity in the frequency range from 0.00833 Hz to 50 Hz. The time series covers one hour. Sampling frequency is 62.5 Hz giving a total of 225000 data points for each component. The time series consists of the 3 components vertical (Z, plus up). North-South (NS, plus N) and East-West (E-W, plus E). One count corresponds to about 1 nm/s. Fig. 1 illustrates the summit area of Stromboli, marking the craters and the station site. Fig. 2 shows the seismograms of Z, N, E. The start of the series is July 8, 1995, 22:00:00 UT. The persistent background signals are volcanic tremor. Several shocks can be identified in the series. They are associated with Strombolian explosions. The volcano Arenal in Costa Rica is another famous volcano of Strombolian type.

Problem 1:
Determine the seismic energy release induced by the volcanic activity. What is the share of energy released by shocks as compared to that released by tremors?

Problem 2:
Determine the amplitude spectrum of the time series (N-component).
a) Is it useful to calculate the spectrum for the total length?
b) Do you have to modify the time series before the spectral calculation?
c) Can you use the spectrum as it comes out of the Fourier calculation? What is the statistical error of the spectral amplitudes? What is the frequency resolution?
d) Scaling of amplitude and frequency axis: Which criteria influence the amplitude scale, which the frequency scale? When do you use linear and when logarithmic scales?
e) What is the lowest frequency for which the wave field can still be approximated by far-field solutions?

Problem 3:
Extract the event which follows after the second 1940.
a) Filter the pulses for Z, N, E with a lowpass filter of 1 Hz corner frequency. Discuss the

filtered pulses. Was the application of lowpass filtering useful?

b) Simulate numerically the pulses as they would have been recorded by a traditionally used 1 Hz seismometer. Compare the pulses with the broadband recordings. What do you think is more useful for studying source mechanisms?

Problem 4:

Determine the ground displacement for the lowpass filtered pulses. Is it sufficient to apply a simple process of integration? Discuss and compare the displacement pulses with the velocity pulses.

Problem 5:

Calculate the orbital motions for the velocity components of the lowpass filtered time series and for the extracted event. Discuss the results in relation to body waves, surface waves and to the azimuthal angle craters-station site (neglecting influence from free surface).

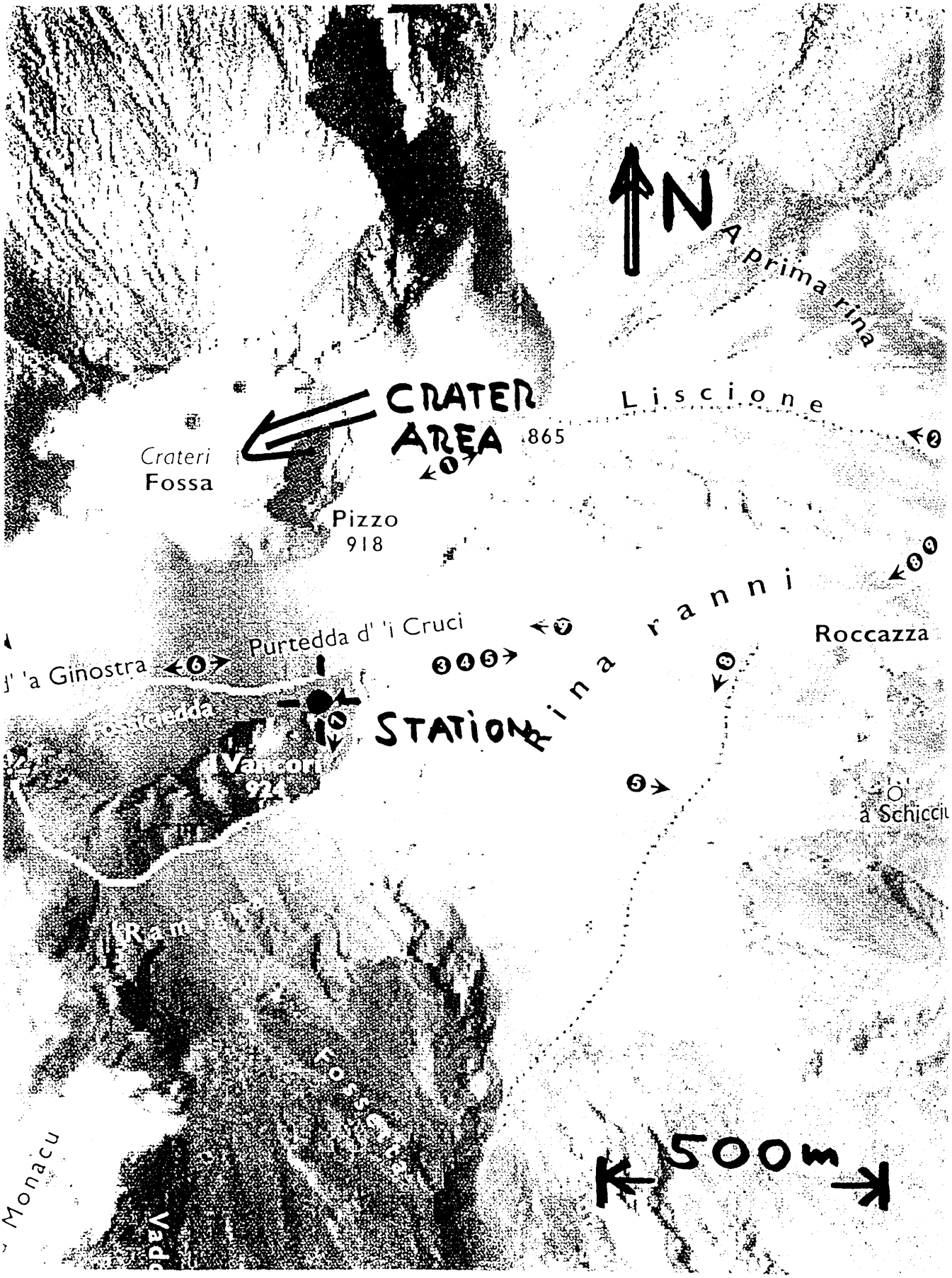

Fig. 1: Map of summit of Stromboli showing location of crater area and recording station.

Scientific Technical Report STR 95/TK
DOI: 10.2312/GFZ.b103-95tk7

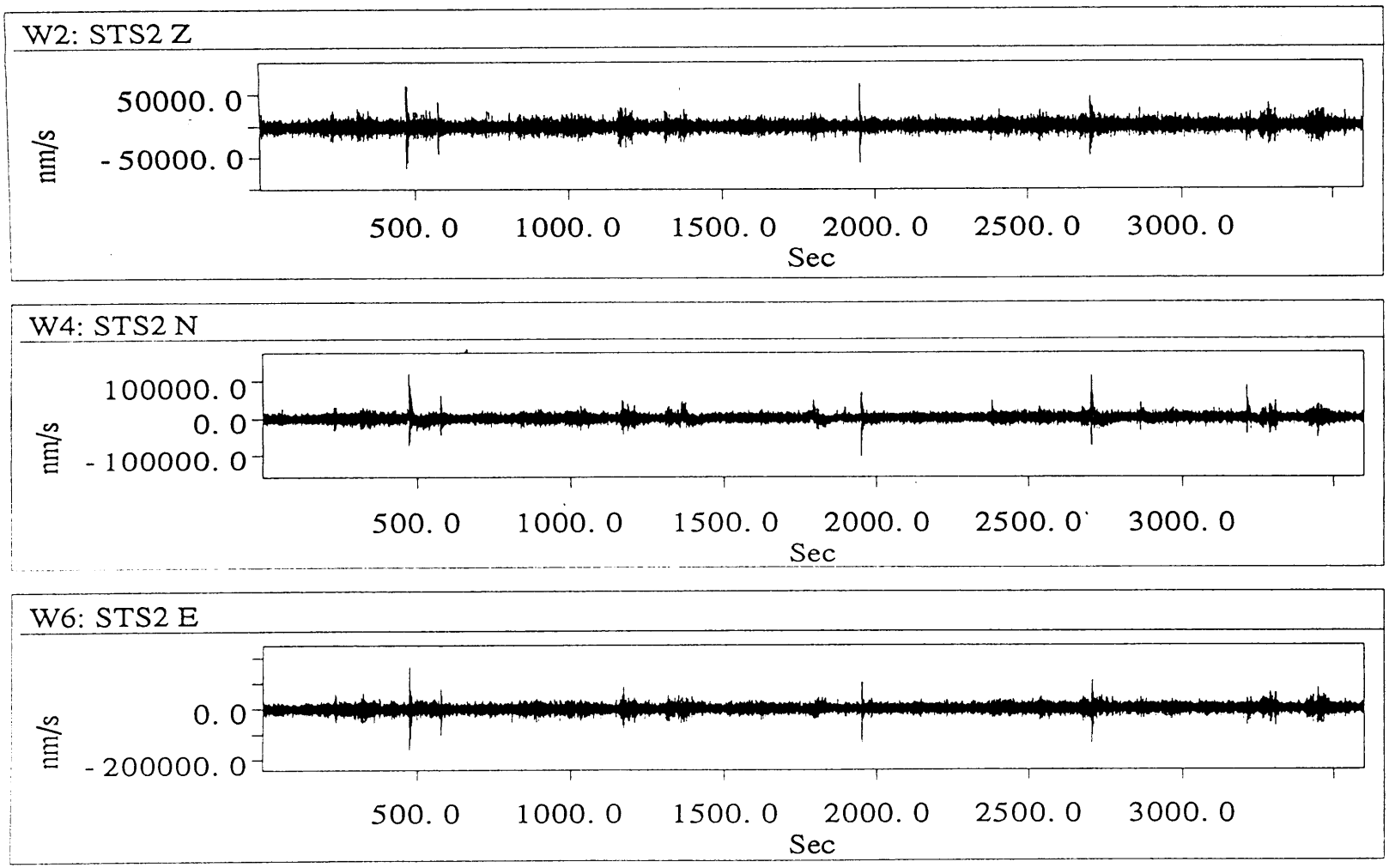

Fig. 2: Seismogram of the components Z,N,E used for the exercise.

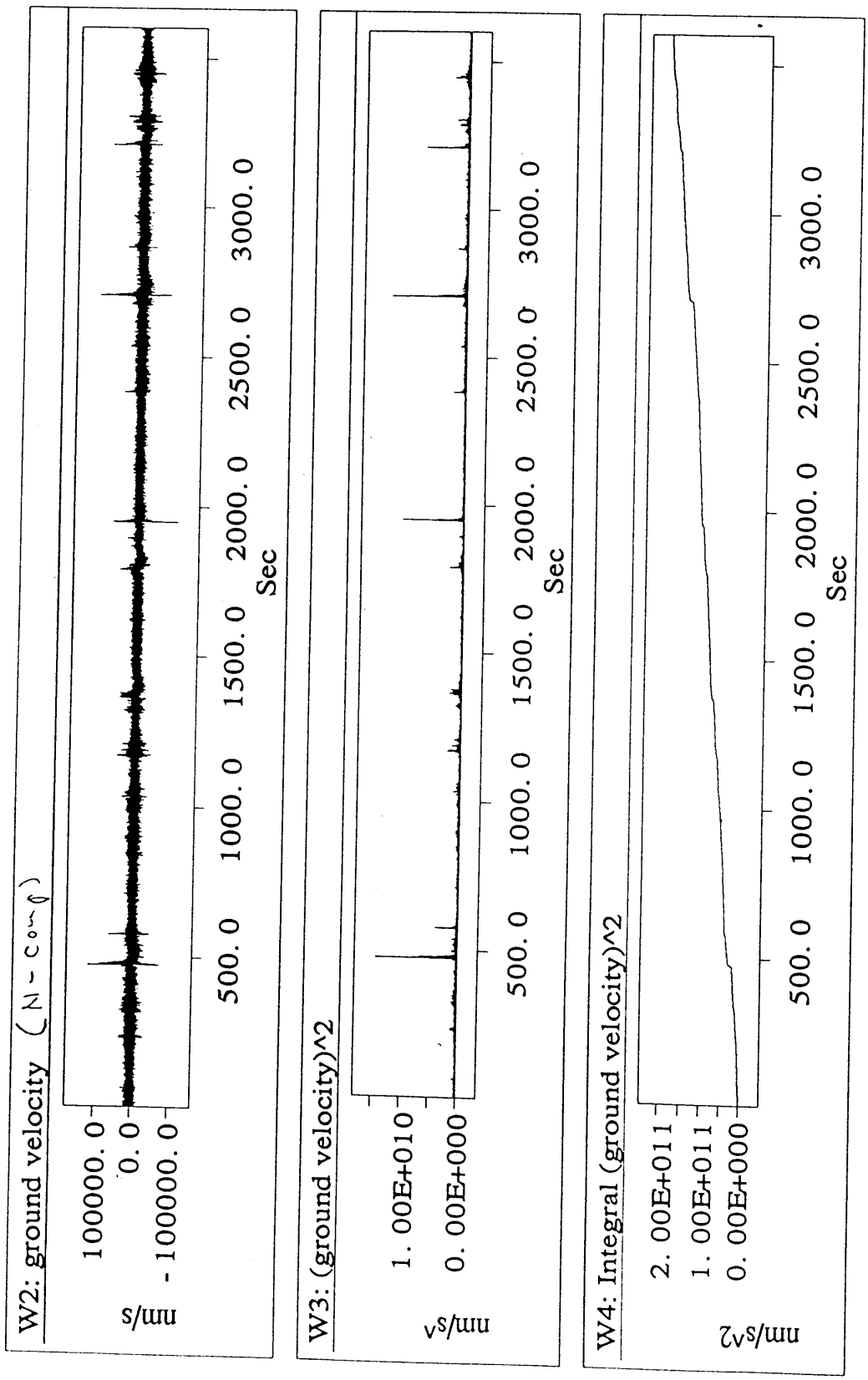

Fig. 3: Seismogram, energy and integrated energy (top to bottom), N-component.

Scientific Technical Report STR 95/TK
DOI: 10.2312/GFZ.b103-95tk7

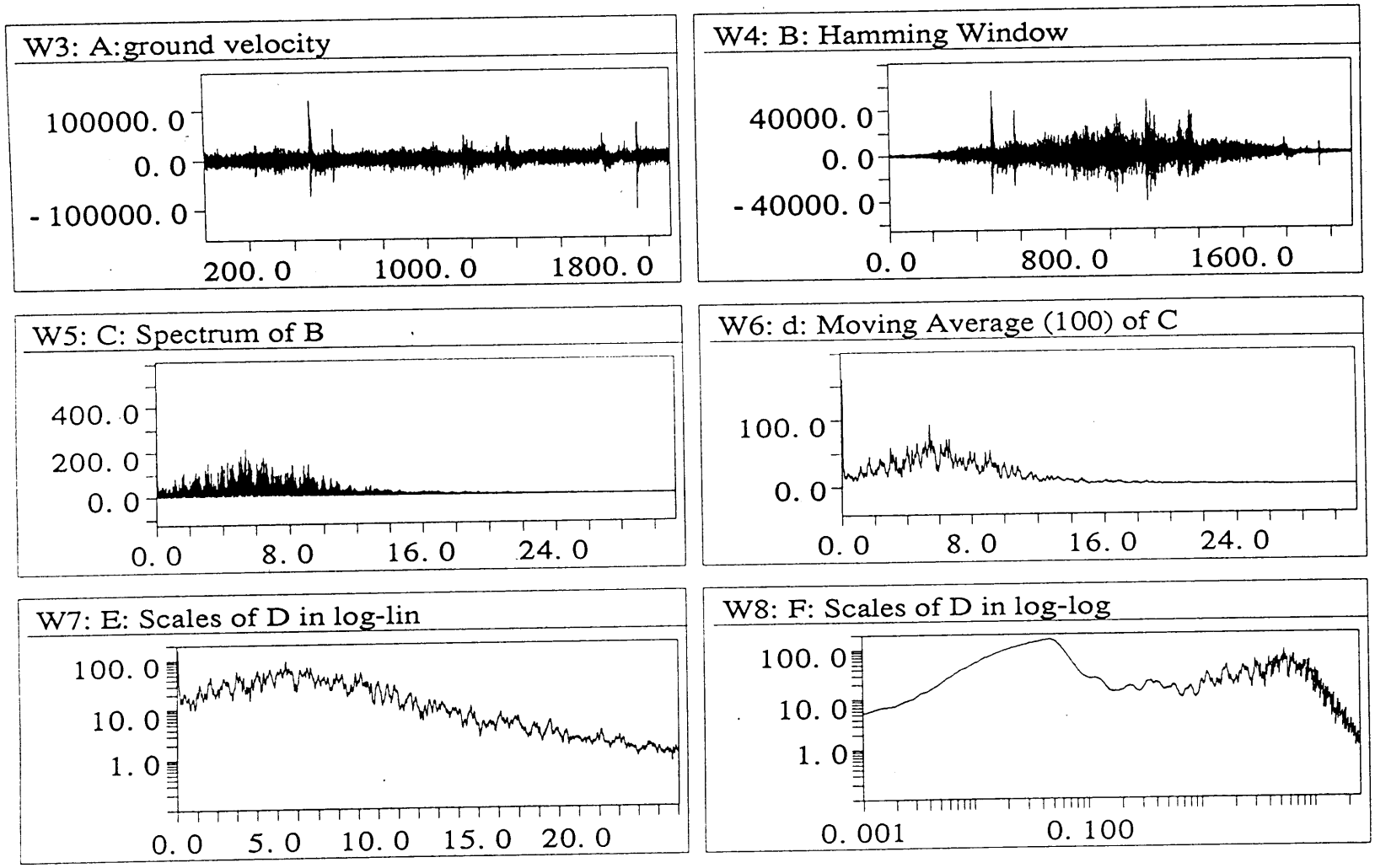

Fig. 4: Calculation of amplitude spectra, N-component

Scientific Technical Report STR 95/TK
DOI: 10.2312/GFZ.b103-95tk7

GeoForschungsZentrum Potsdam

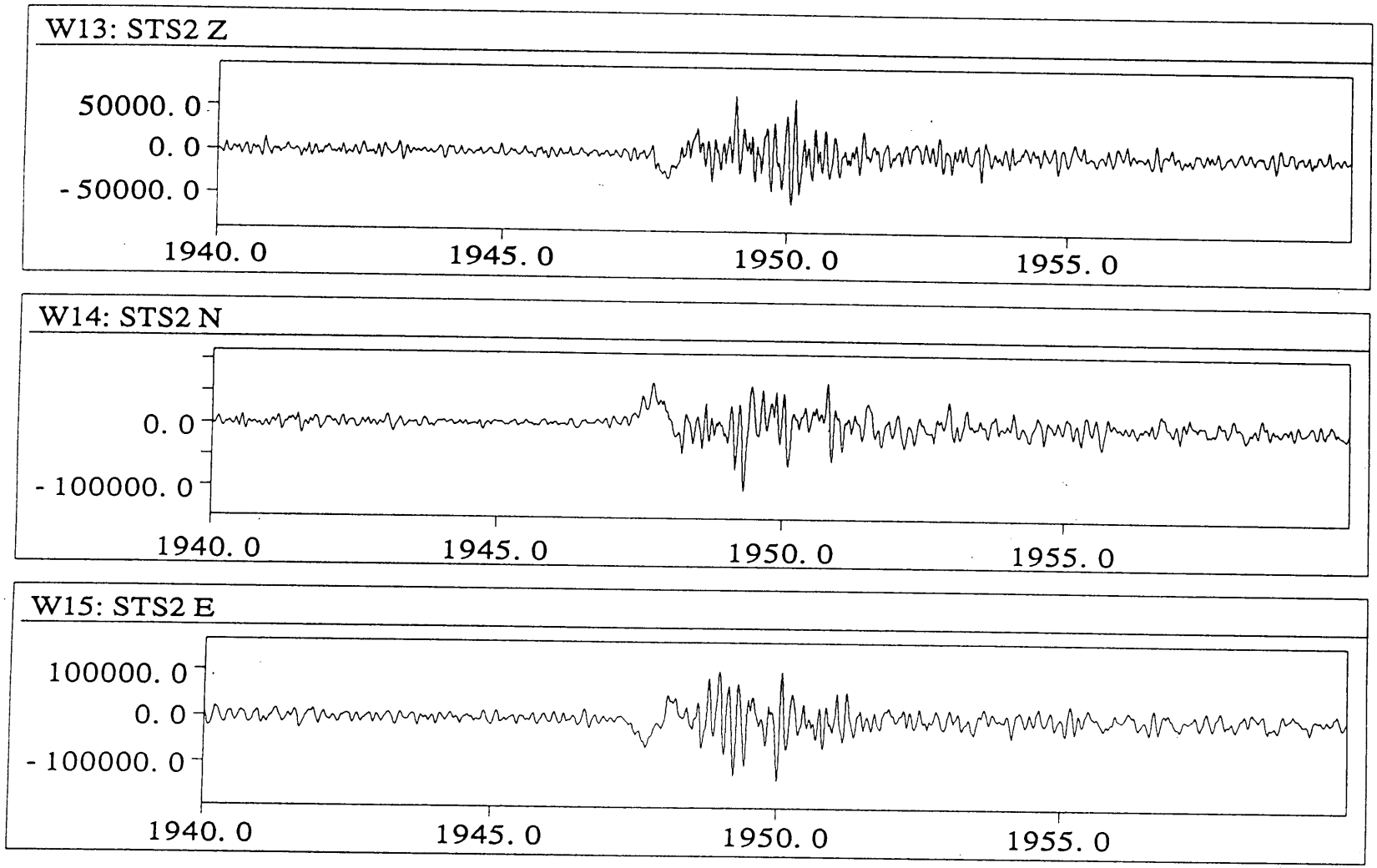

Fig. 5: Seismogram of shock (Z,N,E), unfiltered. Time on abscissae in seconds, corresponding to fig. 2

Scientific Technical Report STR 95/TK
DOI: 10.2312/GFZ.b103-95tk7

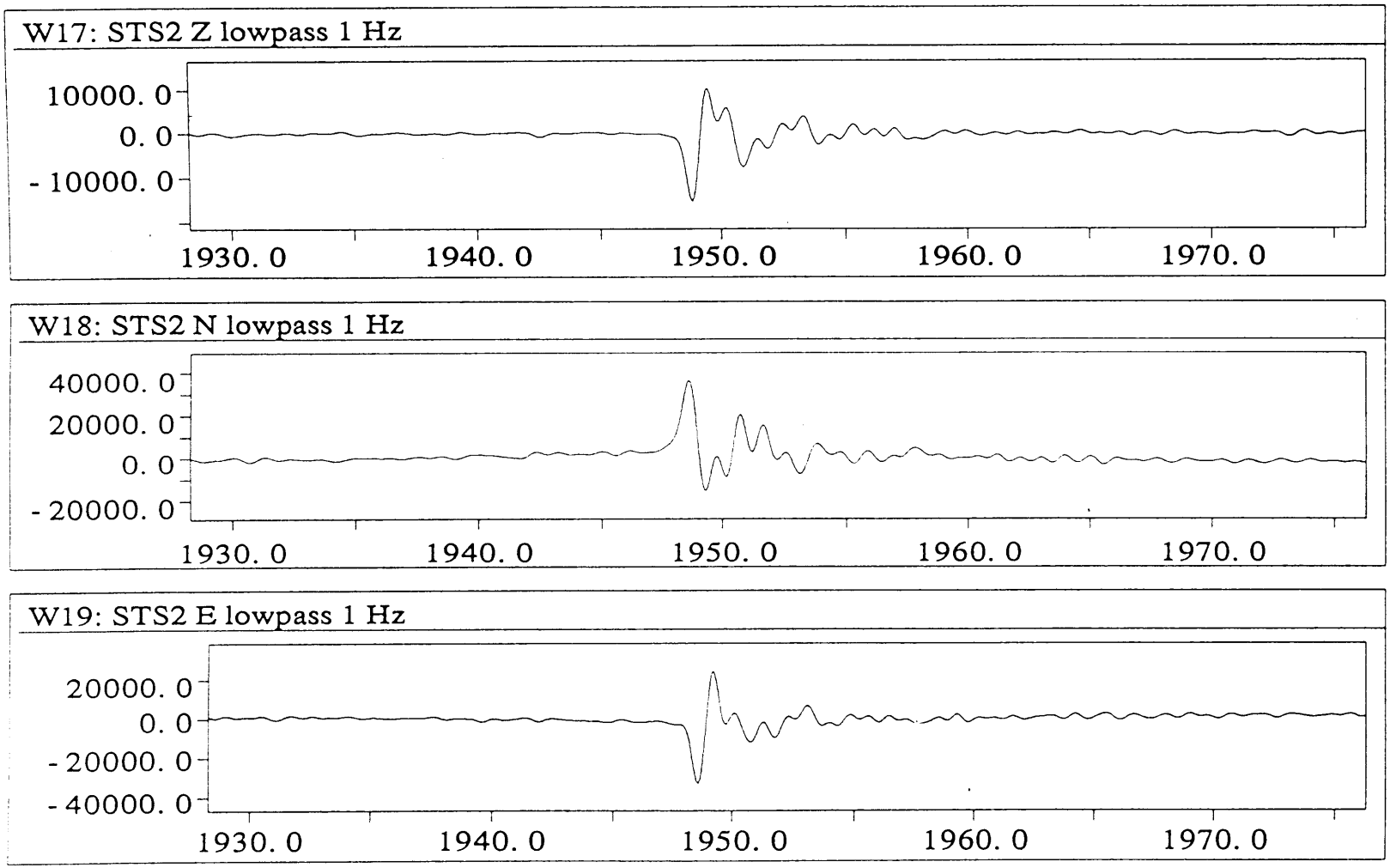

Fig. 6: Corresponding to fig. 5, but lowpass filtered at 1 Hz cut-off.

GeoForschungsZentrum Potsdam

Scientific Technical Report STR 95/TK
DOI: 10.2312/GFZ.b103-95tk7

GeoForschungsZentrum Potsdam

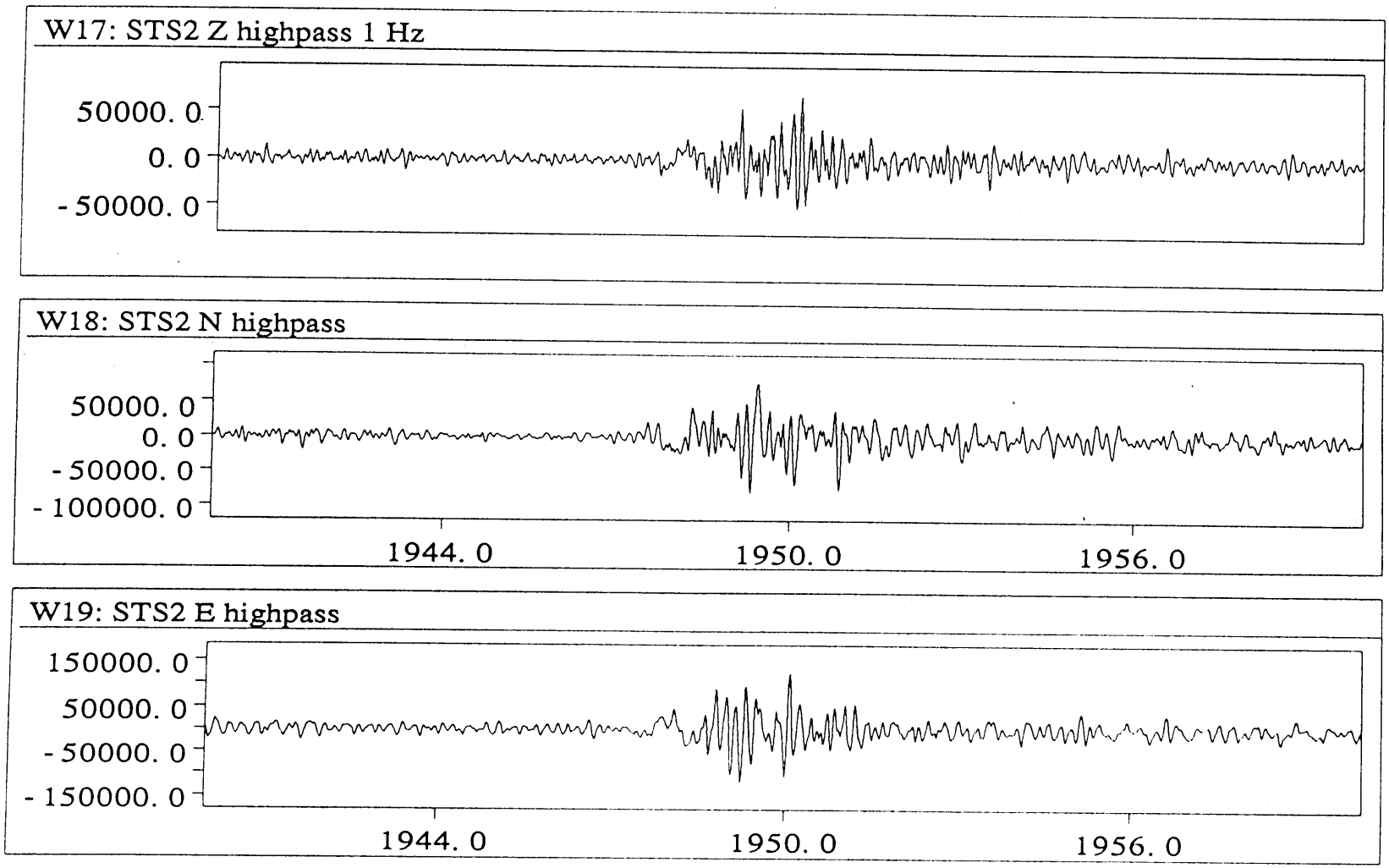

Fig. 7: Corresponding to fig. 5, but highpass filtered at 1 Hz cut-off.

Scientific Technical Report STR 95/TK
DOI: 10.2312/GFZ.b103-95tk7

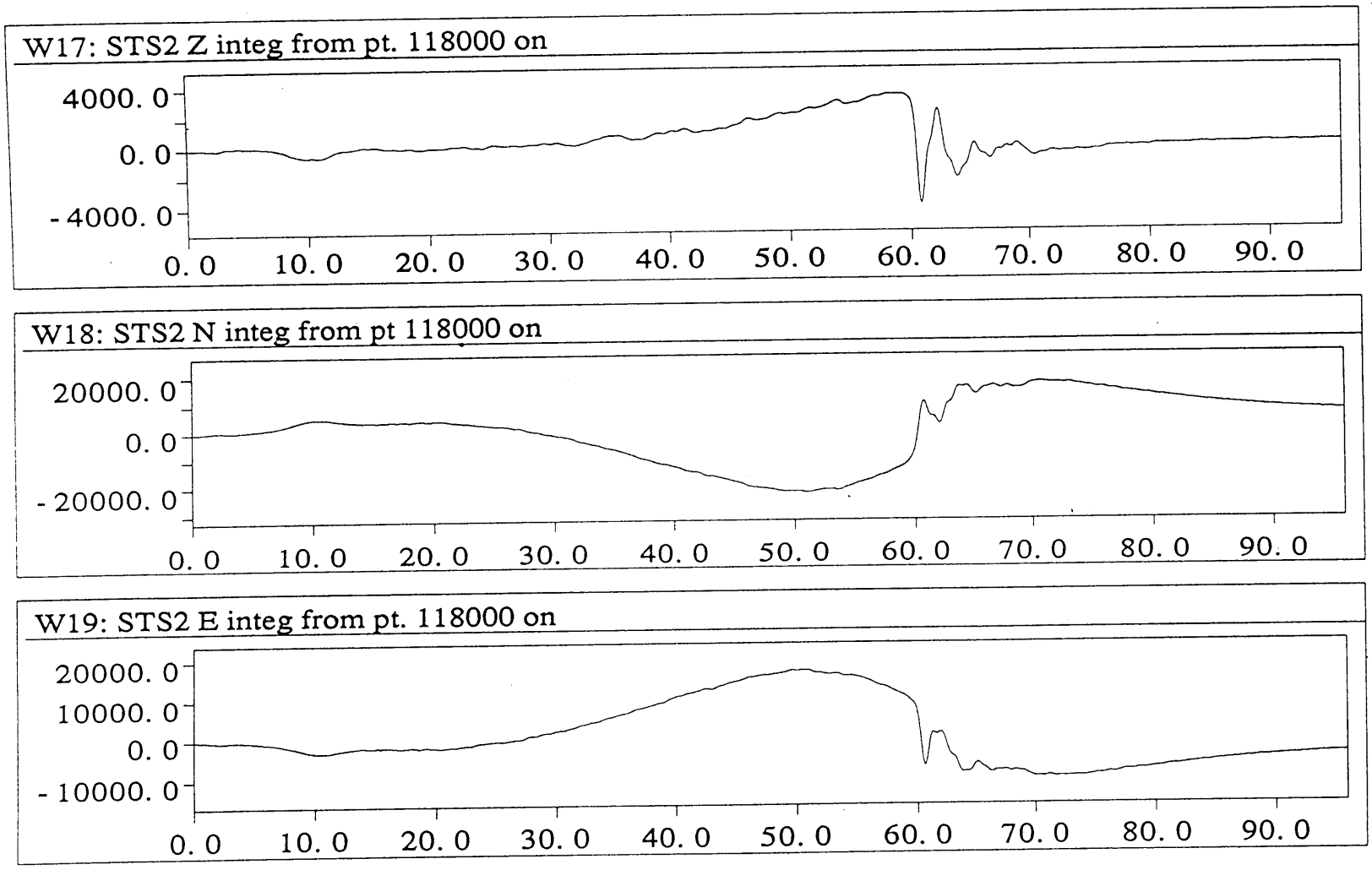

Fig. 8: Seismogram of fig. 6 integrated to ground displacement.

Scientific Technical Report STR 95/TK
DOI: 10.2312/GFZ.b103-95tk7

GeoForschungsZentrum Potsdam

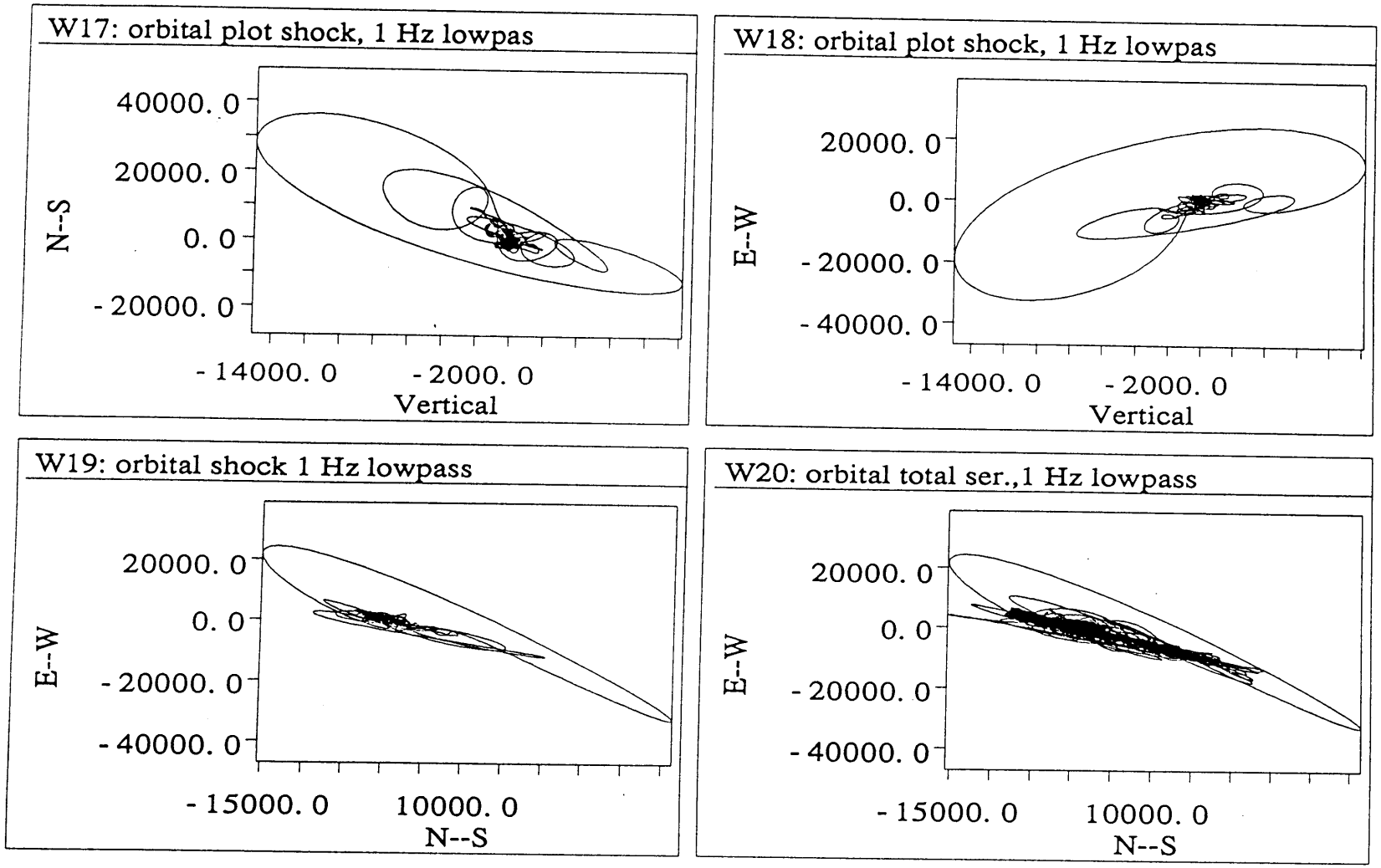

Fig. 9: Orbital motions

Answers (not complete!) to

Exercise in Volcano Seismology

Rolf Schick

Institut für Geophysik, Richard-Wagner-Str. 44, D-70184 Stuttgart, FRG

The demonstrated analysis including plots was performed using the computer program DADISP (Data Analysis and Display Software). It is supplied both for PC and workstations, DOS and WINDOWS. The program is especially helpful for volcanic tremor analysis as long time series can be scrolled easily on the screen for visual display, searching for 'unusual effects'. The program is obtainable through software distributors or from the company: DSP Development Corporation, One Kendall Square, Cambridge, MA 02139, USA. Tel: (617) 577 1133, FAX (617) 577 8211.
Other programs, like PITSA or MATLAB, may be used as well.

Problem 1:
The seismic energy release can be illustrated by squaring and integrating the velocity output. Fig. 3 shows the procedure for the N-component. It can be seen that the shocks provide high energy bursts (W3), but due to the short duration their energy contribution to the total amount of seismic energy release is small (W4).

Problem 2:
Results are illustrated in Fig. 4 (for N-component).

a) For the application of FFT, the number of data points in the series has to be equal to an integer power function of two. For fast computation, the series was cut at 2E17 data points.
b) Yes. Mean value of the series must be removed. Furthermore, the series must be multiplied with a 'window' (Hamming window was used in Fig. 4).
c) The statistical error with the spectral amplitudes depends on the frequency resolution (Principle of Uncertainty). Averaging spectral amplitude values of adjacent time windows reduces the statistical uncertainty of the amplitudes but increases bandwidth (an averaging of n lines reduces the error to sqrt(n) but increases spectral resolution by a factor of n). A moving average of 100 was used in the spectra calculation of Fig. 4. This reduces the statistical amplitude error from 100 % with no averaging to 10 %, increasing the frequency resolution at the same time by a factor of 100.
d) The amplitude range of the plot must be in concordance with the dynamic range of the recording equipment. With 16 bit per data, the amplitude range is 96 db, or 1 to +/- 32768. In a logarithmic plot, it is therefore not appropiate to use more than 5 decades. With the frequency scale, the minimum frequency is determined by the length of the time series, the maximum frequency by the Nyquist-frequency which is half the sampling frequency. In

practice and due to non ideal anti alias filters, it is advantageous to use an upper frequency limit which is, say 80 % of the Nyquist frequency. (25 Hz in W6..W8 in Fig.4)

Problem 3:

a) Fig. 5 shows the unfiltered traces of the shock, Fig. 6 the 1 Hz lowpass filtered traces. The filtered pulses show a simple pulse shape with very clear first motions. Apparently the source mechanism generating these pulses is associated with a decompression, as the vertical component shows a motion downwards and the horizontal components are directed toward the source (N and W).

b) Fig. 7 illustrates the simulation corresponding to the output of a 1 Hz seismometer. It simply can be approximated by filtering the original time series with a two-pole Butterworth high-pass filter of 1 Hz. It can be seen clearly that with the use of a 1 Hz seismometer neither simple pulse shapes nor clear first motions would have been obtained.

Problem 4:

Integrating from ground velocity to ground displacement is generally difficult as small offsets and trends (due to non volcanic disturbances like temperature effects, barometric pressure changes, wind and others) in the time series may accumulate to large errors in the integration process. Before integration, the time series must be 'stabilized' by removing DC offsets, as well as non-periodic trends. Of course, also interesting information which has its origin in the volcano dynamics can suffer from this process. Which methods are used is rather subjective. Before integrating the shock of Fig. 6, DC offsets at the beginning and end of the series were removed with a hamming-filter. Highpass filtering would have been an alternative, the integration shows a feature which is worth to be discussed. The shock is preceded by a long, nearly aperiodic motion. This motion is opposite to the motion in the velocity component. It could be caused by a pressure increase in the volcano preceding the explosion. As a result, one can assume such an upward motion, and on the horizontal components a motion away from the crater, which is S and E on the seismogram. The demonstration illustrates the importance of longperiod recording in volcano seismology.

However, recording signals on a volcano with frequencies below about 0.1 Hz requires not only appropiate instruments but also great care and experience in the installation and operation of the station.

Problem 5:

Fig. 9 presents orbital motions for the shock (W17..W19), and for the total time series (all 1 Hz lowpass filtered) (W18). Comparing the polarization angle with the azimuth from station to crater area it is suggestive that a radial motion is dominant (Rayleigh waves or P-waves with large incidence angle or small emergence angle, respectively). However, as the station is located in the near field it might be more justified to speak of pure motions, without an association to waves.

TSUNAMI WARNING SYSTEMS: AN AMERICAN PERSPECTIVE

Michael E. Blackford

United States National Weather Service
Pacific Tsunami Warning Center
91-270 Fort Weaver Road, Ewa Beach, Hawaii 96706

1. ABSTRACT

Following the April 1, 1946, destructive tsunami in the Hawaiian Islands, the United States established a tsunami warning center for the Islands in 1948. Its services were extended to United States Pacific coast and to Alaska in 1953. As a result of the 1960 great Chilean earthquake, the warning center in Hawaii, in 1965, became the operational center for an international warning system. The great Alaska earthquake in 1964 demonstrated the need for a regional tsunami warning center for that area and such a center was established in 1967. In 1975 a destructive local tsunami in the Hawaiian Islands resulted in modifications to procedures at the Pacific Tsunami Warning Center, making it a Hawaii regional tsunami warning center in addition to its responsibilities for earthquakes and tsunamis elsewhere in the Pacific. In the late 1970's and 1980's both the Pacific and Alaska tsunami warning centers automated the processing of earthquake and water level data and their dissemination of information and warning messages following the installation of computers in their facilities. Also in the 1980's, and continuing into the 1990's, the Pacific tsunami warning center has incorporated near real-time telemetered water level data from remote sites throughout the Pacific into its operations. In the next few years to come, the United States tsunami warning system will be working to develop new instrumentation and methodologies to improve the characterization of tsunamis. It will also seek the support of other countries operating regional tsunami warning centers to foster the development of additional regional warning centers in other areas of the Pacific that are susceptible to locally generated tsunamis.

1.1 Key Words:

automation; earthquake; inundation; regional tsunami warning center; tsunami; runup.

2. INTRODUCTION

Lander (1986) pointed out that ninety-nine percent of the world's destructive tsunamis travel less than thirty minutes from their place of origin to the area where they inflict loss of life and significant property damage. In a practical sense, the Pacific Tsunami Warning Center (PTWC), the designated operational center for the International Coordinating Group for the Tsunami Warning System of the Pacific (ITSU), cannot provide timely warnings for many areas of the Pacific because the speed of the seismic waves, the time necessary to process the data, and the

Scientific Technical Report STR 95/TK
DOI: 10.2312/GFZ.b103-95tk7

time required to disseminate a warning are such that areas an hour's travel time of the source of the tsunami would most likely not receive a PTWC warning. Given these two observations, one could question the purpose of PTWC, if it cannot provide warnings to those areas most likely to experience tsunami destruction. The answer to this question is simply that PTWC cannot and should not be expected to act as a regional warning center for those areas in the Pacific basin where these centers do not exist. PTWC can and should act as a coordinator, making certain that accurate information developed by itself, or provided by regional warning centers, is disseminated to ITSU member states and others in a timely fashion to keep them apprised of the potential for a Pacific-wide tsunami. The ITSU members who have developed effective regional warning centers for their areas should be assisting, in whatever ways they can, with the development of regional centers elsewhere in the Pacific basin.

This paper will examine the origins of the United States of America's Tsunami Warning System and changes it has undergone up to the present. It will also touch on directions along which it is expected to proceed over the next few years.

3. TSUNAMI WARNING SYSTEM ORIGINS

During the first century of written history or descriptions of the Hawaiian Islands there exist at least six instances where tsunamis of remote origin caused some damage in the islands. The relationship between these tsunamis and their causative earthquakes was largely unknown at the time of the tsunamis and was established only after subsequent analysis sometimes many years later. By the end of the nineteenth century the relationship between destructive earthquakes in the Hawaiian Islands and large earthquakes elsewhere in the Pacific basin was fairly well established. This set the stage for the initial efforts made to predict the arrival of remotely-generated tsunamis in Hawaii and to provide some warning to its populace.

Using data from seismographs recently installed in the Islands, in 1923, and again in 1933, successful predictions of destructive tsunamis were made prior to their arrival from sources off the coasts of Kamchatka and northern Japan respectively. But, for a number of these predictions, there was no destructive tsunami and the public began to disregard the announcements. By 1946 several of those involved in these early warnings were no longer in Hawaii and interest in providing the predictions had waned.

Shortly after 2:00 A.M. Hawaiian time, April 1, 1946, seismic waves from a moderately large earthquake (MS7.4, Kanamori and Kikuchi (1993)), originating in the Aleutian trench off of Alaska, reached the seismographs of the U.S. Coast and Geodetic Survey on Oahu Island and the Hawaiian Volcano Observatory on Hawaii Island. Unfortunately, the arrival of these waves was unnoticed and four and a half hours later the first tsunami waves resulting from the earthquake struck Hawaii without warning eventually taking 159 lives and causing property damage totaling about $26 million. Near the epicenter, on the southwest tip of Unimak Island in the Aleutians, a reinforced concrete lighthouse whose base was nearly 15 meters above sea level was swept away, together with five lighthouse keepers, by a thirty meter tsunami wave. On the central California coast near Santa Cruz a fisherman was swept off a rock to his death by a wave of over three meters. Elsewhere in the Pacific, although the tsunami was broadly recorded on tide gauges, it apparently did little or no damage.

Scientific Technical Report STR 95/TK
DOI: 10.2312/GFZ.b103-95tk7
GeoForschungsZentrum Potsdam

In the aftermath of this disaster in Hawaii there was much discussion as to whether or not the public could have been warned of the approach of this destructive tsunami in sufficient time for them to evacuate to places of safety from areas of inundation. The elements thought necessary at the time to provide such a warning consisted of a seismic alarm to alert warning system operators at any time of a potentially tsunamigenic earthquake, seismographs with visible recorders to enable a quick determination of the nature of the event triggering the alarm, a network of similar seismic stations and water level stations linked to the central station through a highly reliable, rapid two-way communications system and a set of tsunami travel time charts for each of the water level stations in the network.

Operators, alerted to the occurrence of a large earthquake by the alarm, would send messages to other stations in the network requesting phase arrivals from their stations so that the epicenter and origin time of the earthquake could be determined. Using this information and the tsunami travel time charts, operators would then send messages to the network of tide observers requesting water level information at the times when the tsunami was expected to have passed by their particular stations. If significant tsunami wave action is reported back by the tide observers, a warning would be disseminated to appropriate civil and military authorities.
This approach received initial approval on August 12, 1948, and an official tsunami warning system, operating under the auspices of the U.S. Coast and Geodetic Survey, was established soon thereafter. Figures 1, 2, and 3 illustrate the current, 1995, status of seismic and water level stations used by the warning system. The system initially provided warnings only to the Hawaiian Islands, however, following two great earthquakes in the northwest Pacific in 1952, one of which produced a maximum tide gauge amplitude of 1.4 meters in California, dissemination's of the warnings were extended to the west coast of the conterminous United States. The fact that no lives were lost as a direct result of the tsunami that followed the March 9, 1957, Andreanof Islands earthquake, even though $5 million damage was done in the Hawaiian Islands, demonstrates that the system functioned well.

4. SIGNIFICANT MODIFICATIONS TO THE TSUNAMI WARNING SYSTEM

The Tsunami Warning System, or Seismic Sea Wave Warning System as it was originally called, was initially established to provide warnings to United States' possessions and other areas where the United States had vested interests subject to coastal hazards. The great Chilean Earthquake of May 22, 1960, changed that purpose. Following the earthquake, which devastated nearly the entire coast of Chile, a tsunami spread across the Pacific basin causing additional damage in the millions of dollars to many countries throughout the Pacific basin. Sixty-one lives were lost in Hawaii, mainly through foolish disregard for the warnings issued, and nearly a day after its origin, the tsunami reached Japan where between 180 and 190 people perished.

The magnitude of the losses throughout the Pacific basin from the Chilean earthquake, and the additional losses resulting from the 1964 Alaskan earthquake, convinced many countries of the need to establish an international tsunami warning system. In 1965 the United States extended an offer to UNESCO to expand the responsibilities of the Tsunami Warning Center in Hawaii to include the issuance of warnings of Pacific-wide tsunamis to all countries of the Pacific basin interested in such warnings. The offer was accepted and subsequently the International Coordinating Group for the Tsunami Warning System of the Pacific (ITSU), comprised of over two dozen countries throughout the Pacific, was formed to provide feedback and suggestions on

Scientific Technical Report STR 95/TK
DOI: 10.2312/GFZ.b103-95tk7
GeoForschungsZentrum Potsdam

ways to improve the quality of Pacific-wide tsunami warnings on a continuing basis.

The 1964 Alaskan earthquake also had a significant impact on the Tsunami Warning System of the United States. At the time of the Alaskan earthquake communications with the state were almost entirely cut off. Critical information on whether or not the earthquake had generated a tsunami was not forthcoming from Alaska. Nearly three hours went by before communications was reestablished and the tsunami devastation at Kodiak was reported to the Tsunami Warning Center in Hawaii. A Pacific-wide warning was immediately issued but preparation time for many emergency managers on the Canadian and United States west coasts was severely curtailed. There was virtually no warning other than the earthquake strong ground motion for many Alaska coastal communities in the Gulf of Alaska and along the Pacific coast of the Alaska peninsula. The tsunami struck the village of Chenega in Prince William Sound almost immediately after the onset of strong shaking from the earthquake and it took 23 lives, a significant portion of the village population. About one half an hour after the earthquake origin time the tsunami swept into Kodiak and Kodiak Naval Station causing massive destruction and taking eight lives. Local tsunamis caused by submarine landslides, in turn triggered by the prolonged strong shaking of the earthquake, struck Seward, Whittier, and Valdez where greatest loss of life, 31 persons, in a single community occurred. Overall in the Gulf of Alaska and Kodiak Island vicinity 107 lives were lost and about $80 million damage occurred. Valdez and Chenega accounted for nearly half the lives lost and Kodiak and its naval station accounted for half of the cost of the damage done. Elsewhere in Oregon four children, camping with their parents on a beach, drowned and in Crescent City, California 11 persons lost their lives and damages were estimated to cost $7.5 million.

As a result of this shortcoming in the United States Tsunami Warning System, a regional warning center, the Alaska Tsunami Warning Center (ATWC), was established in 1967 at Palmer, Alaska. Because of the need to have seismic and water level data available very quickly in order to provide timely responses to local and regional earthquakes, the Center was established with full, real-time telemetry to stations ranging from the westernmost reaches of the United States in the Aleutian Islands to Sitka in southeast Alaska, a span of over 4000 kilometers. The Center can warn some areas within its region that are less than thirty minutes travel time from the tsunami source and most, if not all, areas within its region that are less than an hour's travel time from the source. The Center augments its active warning system with an extensive public education program reaching out to the coastal communities in its region.

The need for a regional warning system was made evident to the Tsunami Warning Center in Hawaii in 1975. On November 29 a strong local earthquake, magnitude 7.2, struck the southeast coast of the Island of Hawaii early in the morning. Two persons who were camping on the coast in the epicentral in the epicentral area, where coseismic subsidence reached three meters and local tsunami runup was about eight meters, lost there lives. Figure 4 illustrates how quickly a local tsunami can effect the populated islands of Hawaii. Property damage, restricted to the Island of Hawaii, totaled $4 million. The Warning Center did not get out a timely warning and the Hawaii State Civil Defense sounded its sirens well after the tsunami had done its destruction. A real-time network of stations, established by the University of Hawaii in the late sixties and early seventies under contract to the Warning Center, was in operation but definitive procedures on how to respond to a tsunamigenic local earthquake had not yet been firmly established, much less tested. Procedures were established to issue a local warning on an earthquake magnitude threshold basis, without waiting for confirmatory water level changes. In this way the Center can probably get

Scientific Technical Report STR 95/TK
DOI: 10.2312/GFZ.b103-95tk7

information to the Hawaii State Civil Defense in time to provide some degree of warning to those beyond about ten minutes tsunami travel time from the source area and most likely to those beyond twenty minutes travel time. The currently operating PTWC seismic and water level networks are shown in Figure 5.

In the late seventies earthquake location and message generation processes were automated at the United States Warning Centers with the installation of computers at both sites. At ATWC, where the reliance on a real-time large aperture seismic network for earthquake locations was well established, arrangements were made with NEIC to exchange data between Alaska and the contiguous States in real time over a dedicated telephone circuit. This enlarged ATWC's network aperture to sixty degrees, more than adequate to locate moderate to large earthquakes located nearly anywhere in the world. PTWC established a similar arrangement with NEIC about five years later.

During the eighties PTWC expanded its capability to monitor water level throughout the Pacific basin by establishing a number of tide stations that transmit their data to the Center via geostationary earth satellites. PTWC maintains a network of about twenty-five of these stations and it also receives data from a like number of stations that are maintained by the University of Hawaii. In addition, data from a network of about fifty stations maintained by the U.S. National Ocean Survey are also acquired. The availability of these data have obviated the need to send out requests to tide observers for water level data, a practice no longer done.

In the early eighties ATWC developed an automatic earthquake detection and location system that digitized the incoming seismic data from its own network as well as that provided by NEIC, picked the arrival times of seismic waves at the various stations, and attempted an automatic earthquake location when sufficient data had been acquired. The system performs remarkably well for earthquakes located both within the ATWC network and elsewhere in the world. NEIC has put a similar system into operation in the early nineties using data from its National Seismic Network, which receives real time data from well over one hundred seismic stations. PTWC, utilizing a portion of its direct link with NEIC, transfers the location parametric data to its computers and relocates the earthquake augmented with data received from various Asian and Australian sources. In addition, PTWC is now making extensive use of the Internet system to exchange information on earthquakes and their tsunami potential with other interested parties throughout the Pacific basin. This information exchange is in addition to, and augments, the dissemination systems formally used by the Warning System. Details of the augmented system and information flow through the Warning Center are depicted in Figures 6 through 9. Also the Center is now transmitting graphical representations of the earthquake location and, when appropriate, tsunami travel time plots centered on the earthquake epicenter.

5. THE TSUNAMI WARNING SYSTEM - FUTURE DIRECTIONS

The Tsunami Warning System should proceed in a proactive manner in three areas over the next few years. The first of these efforts should be to develop the means to determine seismic moment and mechanism information in a timely fashion sufficient for warning purposes. A second effort would be to develop instrumentation that can better characterize tsunamis, again in a timely fashion, than is currently available. Finally, the United States Tsunami Warning System, together with other nations in the Pacific who have effective regional warning centers, should be

Scientific Technical Report STR 95/TK
DOI: 10.2312/GFZ.b103-95tk7
GeoForschungsZentrum Potsdam

promoting and assisting with the development of additional regional warning centers, especially in areas that are vulnerable to local tsunamis.

Over the last decade seismologists have developed procedures that allow them to automatically determine centroid moment tensor (CMT) solutions on a routine basis. These solutions include as products a set of nodal planes and a moment that characterizes the best double couple displacement on these planes. This information provides critical input to the determination of whether or not sufficient tectonic displacement of the seafloor has occurred that could, in turn, give rise to the generation of a tsunami. Currently a CMT solution can be determined within about three hours after the origin time of an earthquake. Efforts to shorten the determination time down to one half hour or even less and to apply these procedures to earthquakes relatively close to the instruments used for CMT solutions are beginning to approach operational status. These data will allow a more realistic assessment of the tsunami generation potential of a given strong earthquake.

One area where considerable effort should be expended over the next few years is the development of instrumentation that can provide warning centers with a relatively true picture of the tsunami situation close to its source and in the region within a few hundred kilometers of the source. The traditional instrument used for tsunami determination is the tide gauge. This instrument, while capable of recording tsunamis, is not designed to do so and has filters, both physical and electronic, that enhance the quality of the tide signal to the detriment of the tsunami signal. The dynamic range of these instruments also can be limited by the height of the stilling well, if they employ such a device. High dynamic range pressure transducers with relatively high sample rates (about 1sps) telemetered to a warning center in real time, or at least near real time, can more accurately track the water level changes associated with a tsunami. Warning centers should be installing instruments of this type in critical locations that can enhance the centers' knowledge of the magnitude of the tsunami.

One type of instrument that has received scant attention is a device that could sense the presence of tsunami runup in real time. Typically runup is a tsunami characteristic that is determined after the fact by field examination of inundation effects. This is of little or no value to a warning system because the information is not timely in a warning sense. A device that could detect the presence, and perhaps the depth, of sea water at a land site within the inundation zone and telemeter that information back to a warning center would provide positive evidence of a significant tsunami. A conceptual drawing of such a device is shown in Figure 10. If such devices could be manufactured and installed relatively cheaply compared to the more traditional water level measurement systems, then a much greater number could be deployed along vulnerable coastlines enabling warning centers to have a clearer picture of the extent of the tsunami inundation. Some care would have to be taken to ensure that the instruments are placed in sites that will receive significant flooding. These instruments could also be subject to flooding from other causes such as stream overflow or storm surge. This signal would normally be distinguishable from that caused by a tsunami because of the lack of an earthquake. which would most likely trigger the tsunami. Such a signal would, of course, be useful to emergency managers because flooding, no matter the cause, is a hazardous situation.

Perhaps the most important path existing warning systems should pursue over the next few years is to foster the development of additional warning centers. Only regional warning centers can provide the type of coverage necessary to be able to warn populations close to epicenters of major

Scientific Technical Report STR 95/TK
DOI: 10.2312/GFZ.b103-95tk7

tsunamigenic earthquakes. It may never be possible to warn those who are within about ten minutes travel time of the tsunami source, but a regional warning center is best positioned to educate the populace in their region of what measures to take should they sense a very large earthquake and are located in a tsunami vulnerable area.

A regional tsunami warning center should have as a minimum an alarm system that can alert center operators of a regional earthquake that may cause a tsunami, an automated computer program that locates and determines the size of the earthquake, or at least a procedure that can produce this information within a few minutes, a real-time telemetered network of water level measurement devices, both in sea water at sites exposed to the maximum expected tsunamis and possibly on land in areas of expected inundation, and direct, full-time communications with emergency managers who can rapidly mobilize evacuation procedures.

Perhaps the greatest obstacle to increasing the number of regional tsunami warning centers in the Pacific basin is staffing. The two centers in the United States, PTWC and ATWC, have a total of eleven staff members who respond to alarms. At each site two of the staff must remain within minutes of the center, outside of office hours, to be able to effect tsunami warning procedures in a minimum amount of time. For this effort the staff receive additional compensation above their regular salaries. To have this done on a voluntary basis, or even a compensatory time basis, over the long term may not be satisfactory with regard to warning reliability. Since tsunamis are relatively rare events, it may be possible to combine a regional warning function with another public service function, such as weather forecasting, where there is staff working on a twenty-four hour basis. This is satisfactory as long as regional warning procedures are exercised with sufficient frequency to ensure that the staff remain capable of swiftly executing warning procedures and keeping the earthquake and water level monitoring systems in operating condition.

6. CONCLUSIONS

The establishment of, and many of the major modifications to, the United States tsunami warning system have been the result of responses to demands for improvements in this area of natural hazard mitigation. Other, more evolutionary, modifications have kept the United States system viable in spite of rapid growth in the use of coastal areas susceptible to tsunamis. The United States, and other countries with warning centers, need to adopt a proactive approach to the fostering of additional regional warning centers in tsunami-prone areas experiencing this rapid growth in commercial and recreational use.

REFERENCE AND BIBLIOGRAPHY

Kanamori, H. and Kikuchi, M. (1993). Mechanism of the 1992 Nicaragua tsunami earthquake. Tsunami '93, Proceed. IUGG/IOC Intern. Symp., August 23-27, Wakayama, Japan, 613-625

Lander, J.F. (1986). THRUST - Final report. U.S. National Geophysical Data Center, Boulder, Colorado

In addition to the proceedings referenced above, the following are two recent compendia of papers

Scientific Technical Report STR 95/TK
DOI: 10.2312/GFZ.b103-95tk7
GeoForschungsZentrum Potsdam

dealing with various aspects of tsunamis:

Bernard, E.N. (Ed.) (1991) Tsunami hazard - A practical guide for tsunami hazard reduction. Kluwer Academic Publishers Group, Dordrecht, Netherlands (in U.S.A., Norwell, Massachusetts), 326 pp.

Tsuchiya, Y. and Shuto, N. (Eds.) (1995) Tsunami: Progress in prediction, disaster prevention and warning. Kluwer Academic Publishers Group, Dordrecht, Netherlands (in U.S.A., Norwell, Massachusetts), 336 pp.

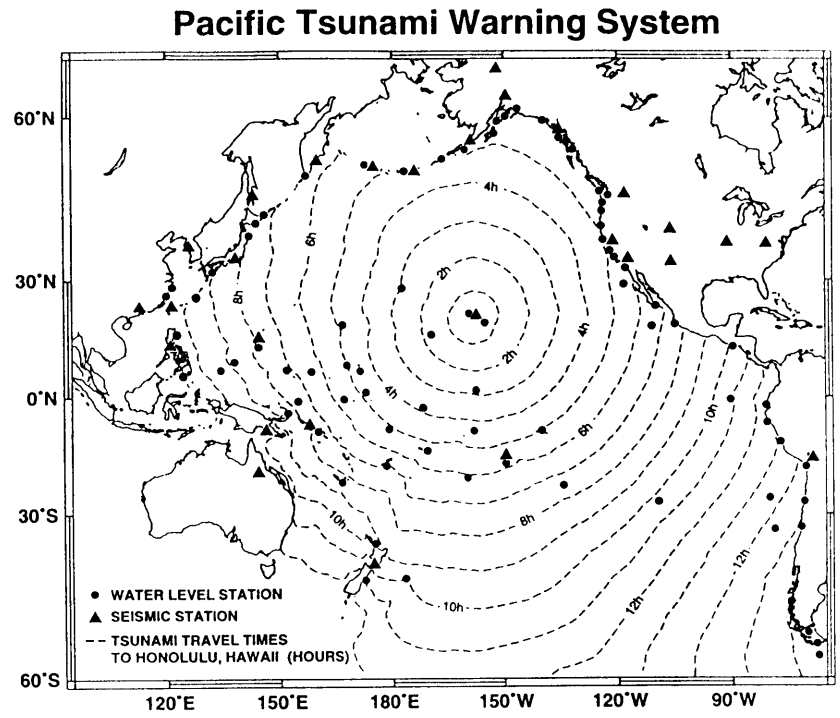

Fig. 1 Current regional distribution of seismic and water-level stations throughout the Pacific Basin which are used by the Pacific Tsunami Warning Center (PTWC) for earthquake location, parameter determination and the assessment of tsunami generation. Additionally, the tsunami travel-time contours to Honolulu, Hawaii, are shown.

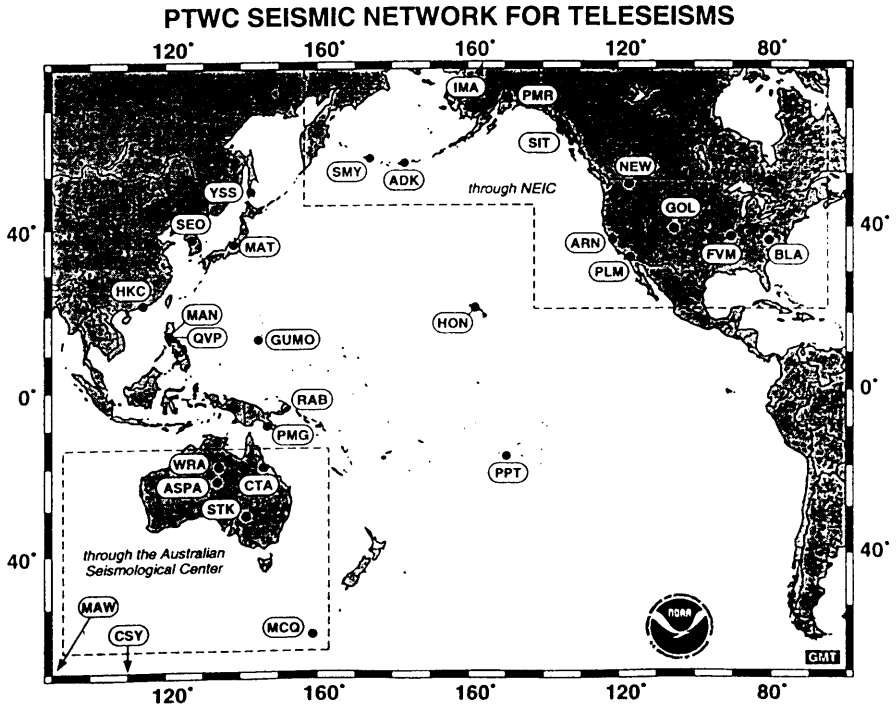

Fig. 2 The PTWC seismic network for teleseismic recordings. Data passed through NEIC are received in Honolulu in real-time over a dedicated telephone circuit while data through the Australian Seismological Center are obtained via Internet. Data from other stations shown in the map are received via telephone, fax or voice through other dedicated circuits.

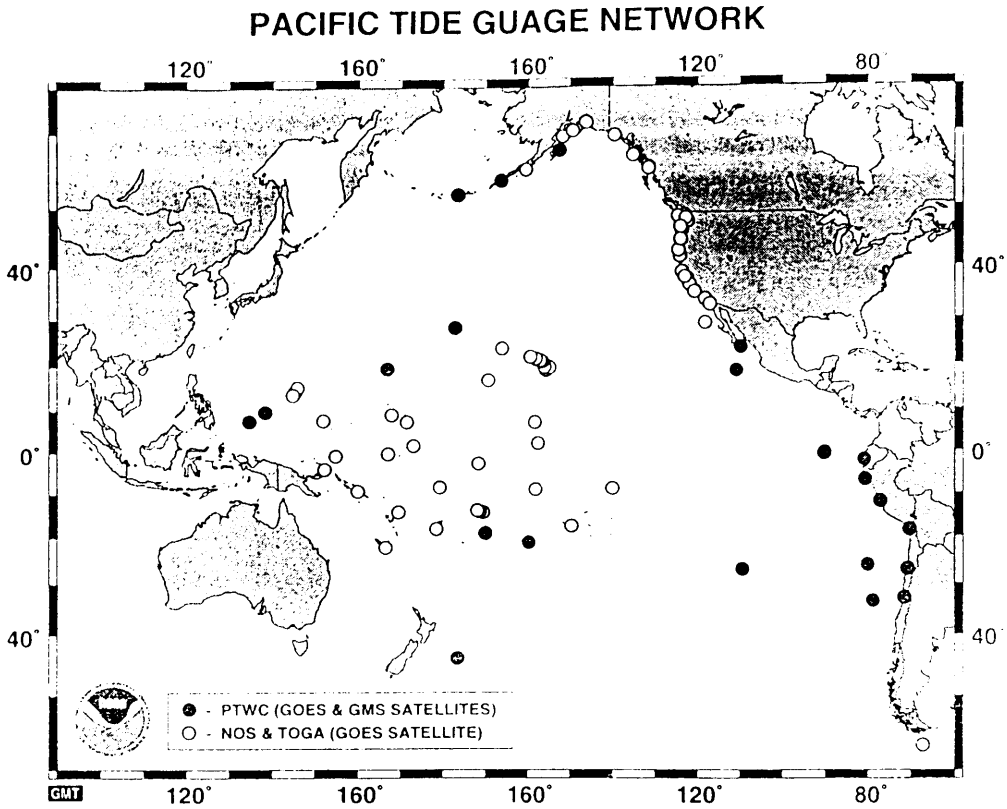

Fig. 3 Water level stations transmitted in near real-time to PTWC via satellite.

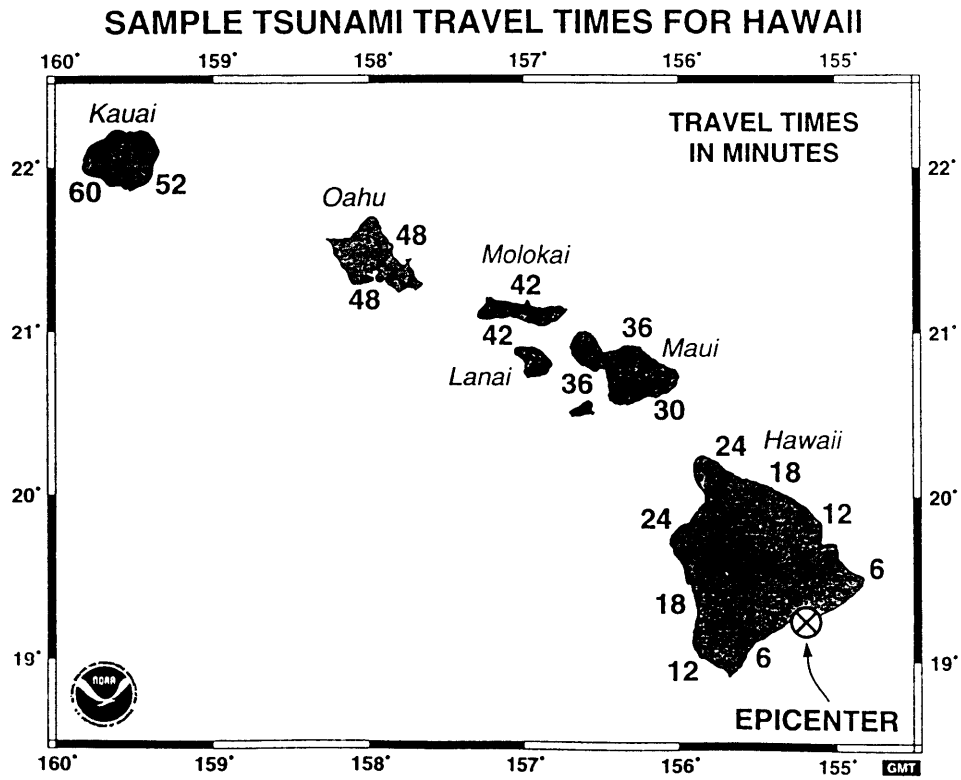

Fig. 4 Example of travel-times for the tsunami generated by the earthquake of November 29, 1975, M_S = 7.2, to different shores of the Hawaiian Islands. It demonstrates the urgent need for rapid response by a regional tsunami warning system.

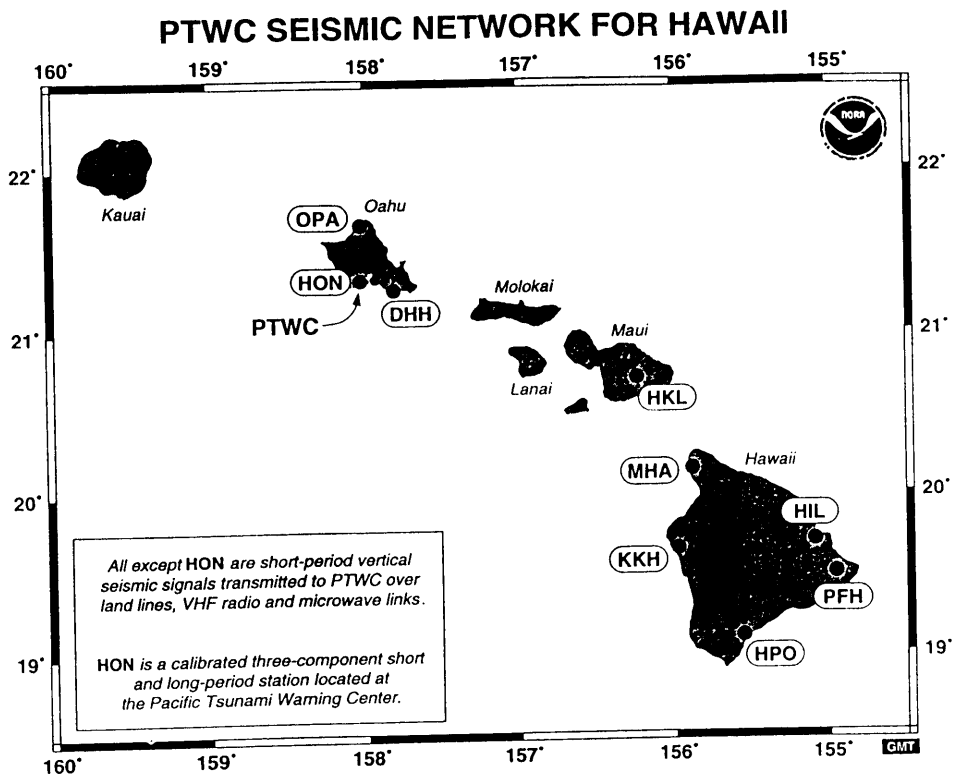

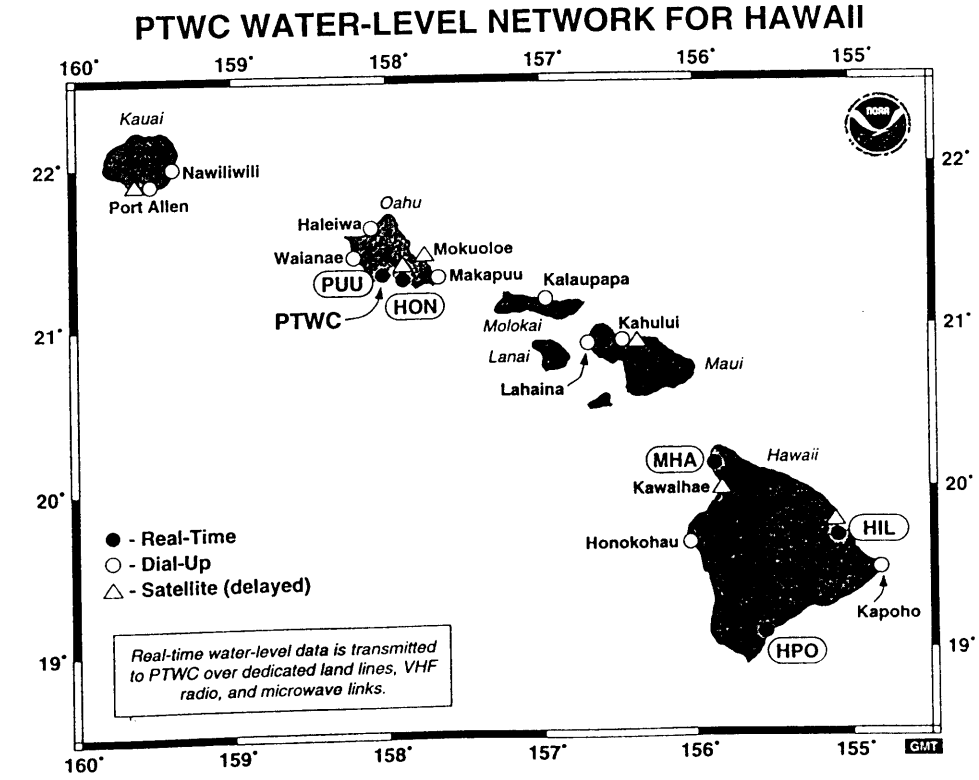

Fig. 5 PTWC seismic (above) and water-level networks (below) for Hawaii.

Scientific Technical Report STR 95/TK
DOI: 10.2312/GFZ.b103-95tk7

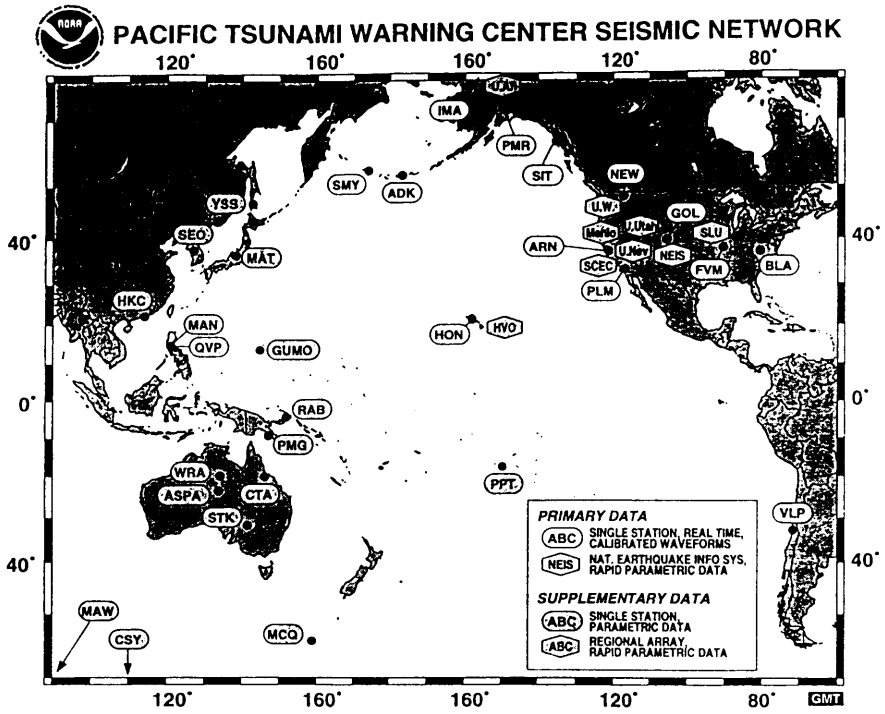

Fig. 6 As for Fig. 2 (primary data) with the addition of regional seismic arrays (supplementary data) providing near-real-time locations and magnitudes.

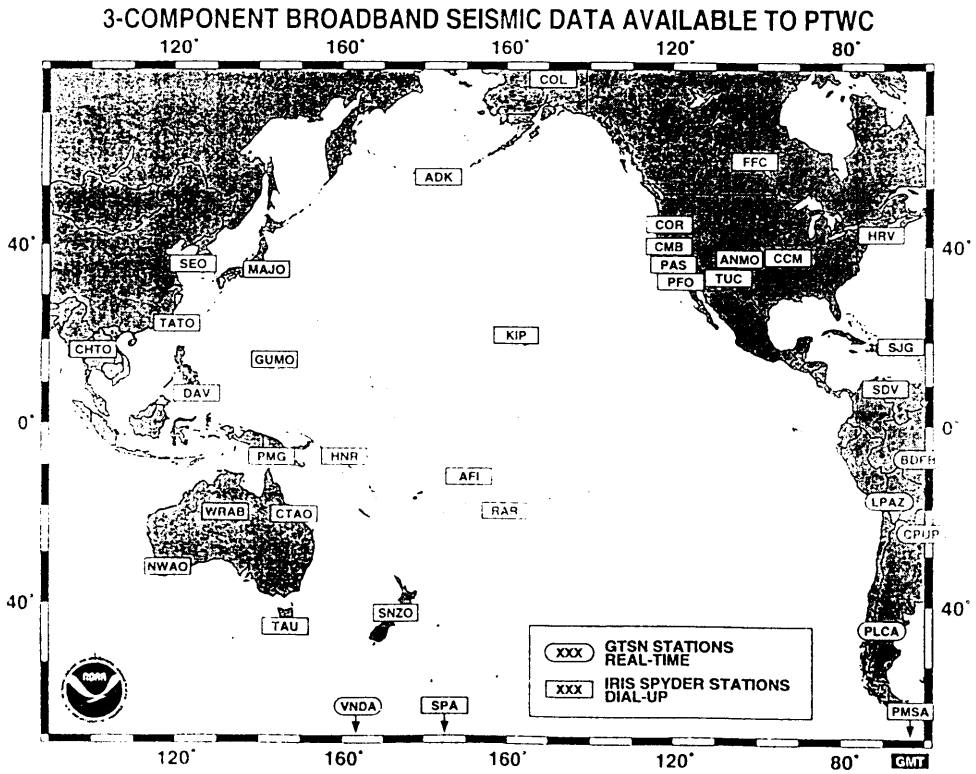

Fig. 7 Shown are all 3-component broadband seismic stations currently (as of November 1995) capable of providing PTWC with data needed to calculate moment magnitudes.

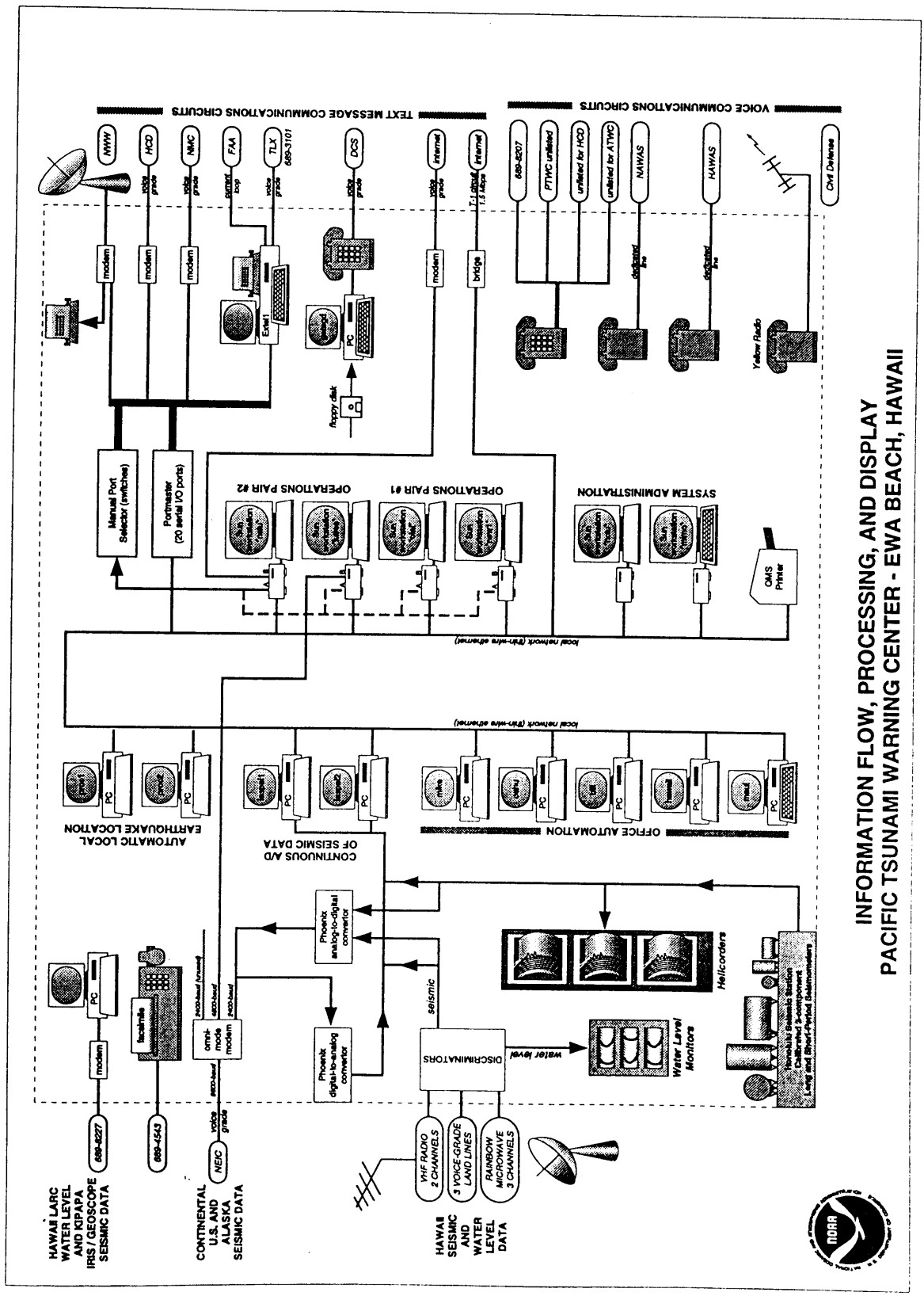

Fig. 8 Schematic data acquisition, processing and display by the PTWC as well as the information flow towards and from PTWC.

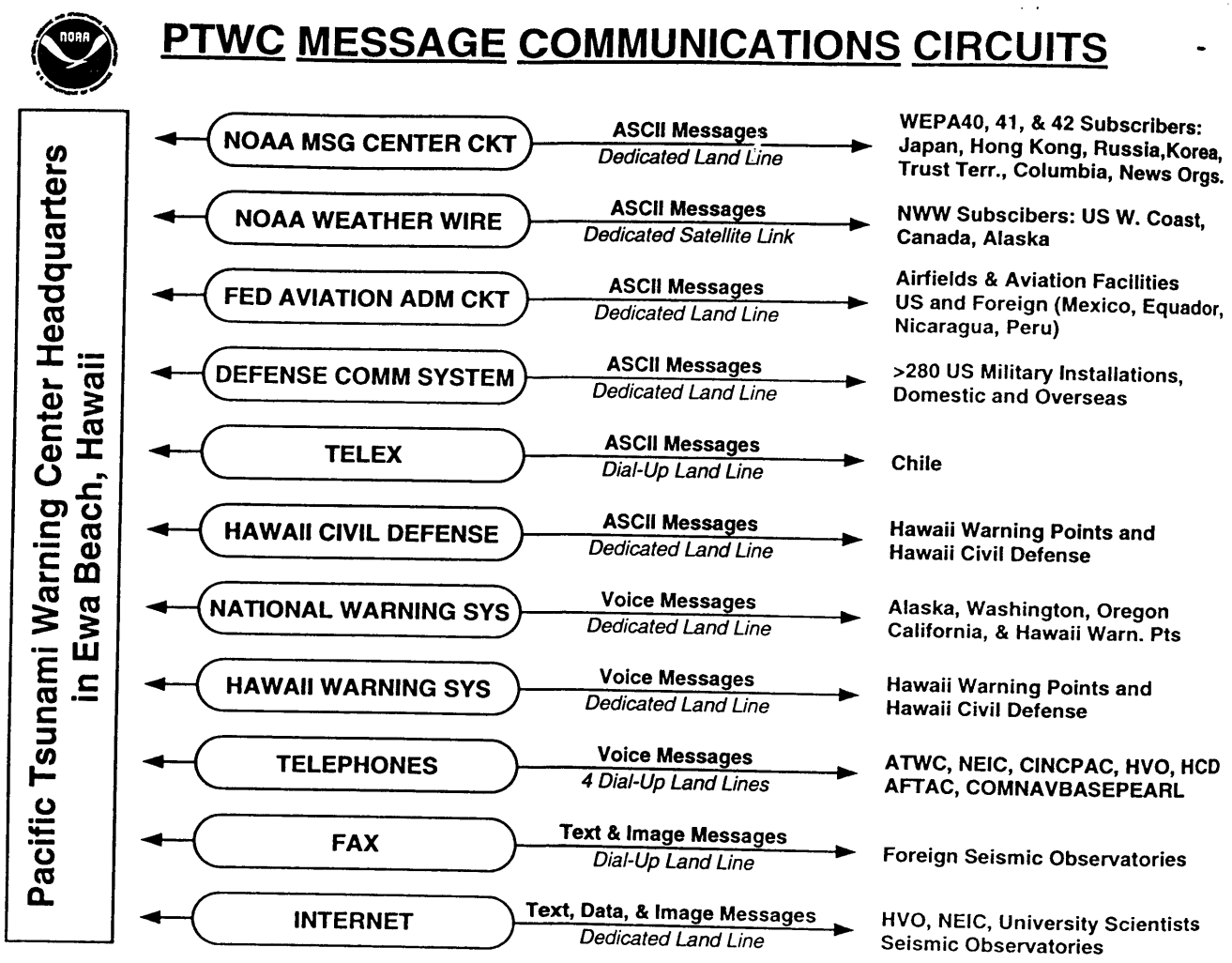

Fig. 9 Details of information flow towards and from the PTWC.

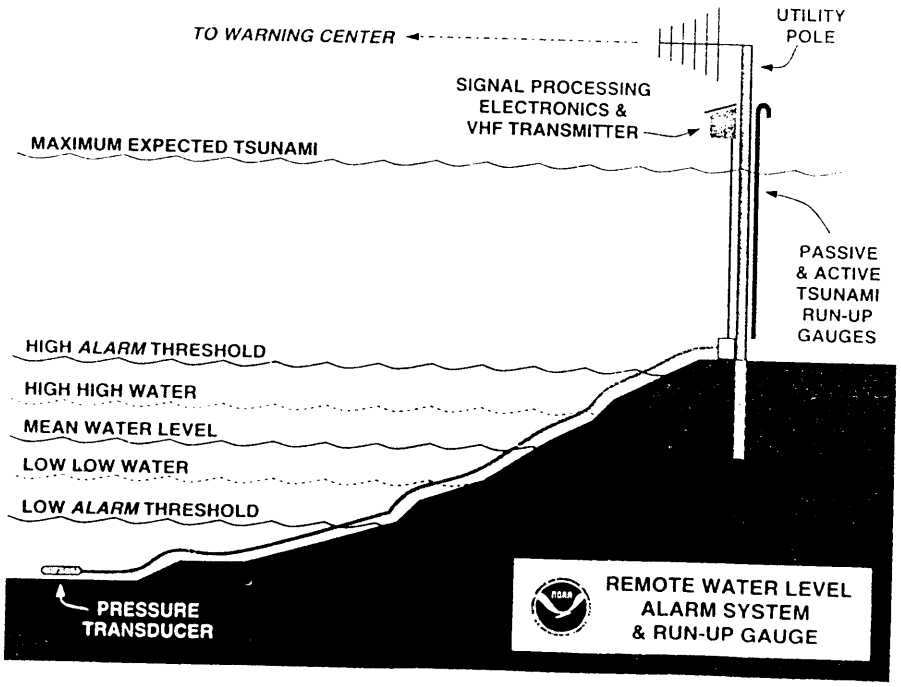

Fig. 10 Conceptual sketch of the remote water level alarm system and run-up gauge currently under development and testing.

TSUNAMI HAZARD IN THE PACIFIC BASIN AND CASE STUDIES FROM JAPAN AND TSUNAMI-PRONE LATIN AMERICAN COUNTRIES

Kuniaki ABE

Niigata Junior College, Nippon Dental University
Hamauracho 1-8, Niigata city, 951, Japan

1. PACIFIC TSUNAMIS

The circum Pacific region is the seismically most active region in the world. Plate tectonics explain how this seismic activity is related to the interaction between adjacent plates. The circum-Pacific seismic region corresponds to plate boundaries. Especially boundaries between oceanic plates and continental plates make up the Pacific coasts of South America, Central America, Alaska, the Aleutian Islands, Kamchatka, the Kuril Islands, Japan, the Philippines and Indonesia, and they are tsunami source areas.

Tsunamis are caused by motions of sea level accompanied by a coseismic vertical displacement of sea bottom, which is understood as an elastic rebound of a continental plate to a subducting oceanic plate. Such a rebound appears at the sea bottom as a thrust fault. Exceptionally, also normal faulting at the basin side of ocean trenches does occur. Big tsunamis of this century in the Pacific Ocean are the 1933 Sanriku tsunami, the 1952 Kamchatka tsunami, the 1960 Chilean tsunami and the 1964 Alaska tsunami. The first one is a normal faulting tsunami while the other ones are thrust faulting tsunamis. All of them caused disasters at the coasts nearest to the sources and even caused tsunamis higher than 2 m as far as the Hawaiian Islands.

2. GENERATION AND PROPAGATION OF THE PACIFIC TSUNAMIS

The tsunami source area, which is a vertical displacement area of sea level, is determined from an integration of source wavefronts. The latter are derived from inverse refraction diagrams based on propagation times observed at various azimuth angles. The size and shape of the tsunami source area depend on fault parameters. For pure dip-slip faults the shape is approximated by an ellipse and the size is represented by a long axis of fault length (L) and a short axis of $W_{\cos \delta}$ with W = fault width and δ = dip angle. As the result the tsunami energy observed at a propagation distance shows a directivity depending on the azimuth angle. That means, along the short axis a large amplitude wave is expected because of the small decay of amplitude with distance. Since the fault is usually formed on a continental slope parallel to the trench, the directivity effect on the amplitudes is further enhanced by the continental slope as shown in Fig. 1. Frequently a maximum level of maximum inundation heights is observed at the coast nearest to the center of the source. The same thing holds for the open sea side. For a distant tsunami an island in the ocean being faced towards the source frequently receives a large amplitude wave.

DOI: 10.2312/GFZ.b103-95tk7

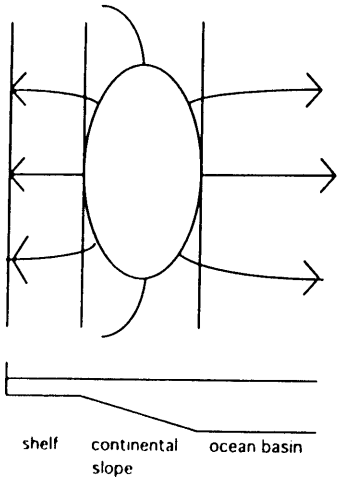

Fig. 1 Schematic representation of wave rays across the continental slope

The directivity is not restricted to the energy. The wave period also depends on the azimuth direction. A tsunami wave is originally impulsive but accompanied by an oscillatory character because of gravitation and inertia. Accordingly, wavelength or period are defined. When a fundamental relation of wave is applied to a tsunami at the source, the period $T_{s,l}$ is approximated by the relation of

$$T_{s,l} = \lambda_{s,l} / v$$

in which $\lambda_{s,l}$ are the wave lengths along short (s) and long (l) axis, respectively, and v the long wave (tsunami) velocity, approximated by $\sqrt{gd}$ in which d is the water depth at the source and g is a gravity acceleration, respectively. During the propagation the period is kept constant. As for the directivity of the period a short-period predominant wave is observed along the short axis and vice versa.

Imamura et al. (1990) studied by means of numerical simulations characteristic properties of tsunami propagating across the Pacific ocean. As the result they verified that Polynesian and Hawaiian islands caused a convergence of wave energy on the shallow regions.

Results about wave motions of tsunamis, without considering the effect of different fault models, were presented in a book written by Murty (1977).

3. TSUNAMIS IN A RIAS COAST AND A STRAIGHT COAST

The Pacific coast of northeast Honshu, Japan, is a Rias coast and coexists with various bays. When the size is expressed as the natural period, it ranges from 8 to 100 minutes. Different bays show a variety of responses to a tsunami. Kato et al. (1961), e.g., noticed different responses of bays to the 1933 Sanriku tsunami and to the 1960 Chilean tsunami. Nakamura and Emura (1961) plotted the maximum height ratio between bay head and the mouth as a function of natural period of bays. Comparing the resonance plot of the 1960 Chilean tsunami with that of the 1933 Sanriku tsunami they found different resonance periods for these events. They explained the resonance curves by assuming periods of 60 and 16 minutes for the 1960 Chilean tsunami and the 1933 Sanriku tsunami, respectively. Characteristic behaviors of tsunami are investigated, therefore, by considering the natural period of bays.

On the other hand, the Pacific coast of the Americas is comparatively straight without pronounced bays. The 1992 Nicaraguan tsunami occurred along such a coast and was recorded by tide gages at Corinto and Pueruto Sandino (Abe et al., 1993). The waveform showed a rapid decrease of

amplitude with time and the following waves with small amplitude in the time history were explained as reflected waves at the margin of the continental shelf. The simple coast prevented the developing of a short period oscillation and made a long period oscillation, excited on the shelf, conspicuous.

4. TSUNAMI HAZARDS

a) The 1993 Hokkaido-Nansei-Oki earthquake tsunami

This tsunami, caused by an earthquake of Ms 7.8, produced waves of 15-30 m in run-up heights at the southern part of Okushiri Island, located at the south western part of Hokkaido, Japan. In all the Japan more than 200 persons were killed and more than 500 houses were totally destroyed by this tsunami. The large destructive potential is due to its deep-sea origin with 2000-3000 m water depth and its early arrival after only about 4 minutes of travel. The deep sea between the source and the island contributed to the increase of the height and to the short travel time. Especially, most part of the residential area of Aonae, having a population of about 1600, was swept by the wave towering 4-15 m high above the mean sea level, and the area saved from the sweeping suffered from the fire. Obstacles, brought by the tsunami and scattered on the roads, prevented fire engines from reaching the fire sites and allowed the fire to spread unhampered.

Shuto (1994) summarized a relation between destruction of houses and tsunami height above the ground level. After his result wooden houses were totally destroyed by waves higher than 2 m, concrete-block houses by waves higher than 3 m while concrete-steel houses were safe up to 5 m wave height at least.
Residents on the island, remembering an earlier tsunami of the 1983 Japan Sea earthquake, supposed a tsunami after the strongly felt ground shaking. This memory helped many residents to evacuate in a short time.

b) The 1992 Nicaraguan earthquake tsunami

A tsunami survey (Abe et al., 1993) clarified characteristic behaviors of the tsunami through interviewing residents along the Pacific coast of Nicaragua. As a result it was shown that most residents did not know tsunamis at all and they perceived the earthquake as a weak oscillation only. They were taken by surprise when the sea level suddenly increased and water covered the residential areas. The maximum run-up heights varied from 1 m above mean sea level along the southern Pacific coast of Nicaragua to 10 m at El Transito in the central part and from there it decreased to 2 m along the northern Pacific coast of Nicaragua. Especially at El Transito, having a population of about 1000, 80 percent of the total residential area was invaded by the tsunami and 20 persons were killed. Some observers told that the tsunami attacked slowly and healthy adults could escape from drowning in the tsunami. The fact was supported by statistics about damages showing that children occupied 90 percent of all the killed persons. Moreover, the number of killed persons in each residential area tended to increase critically for run-up heights of 4 m and more.

This earthquake was a tsunami earthquake (Kanamori and Kikuchi, 1993), defined as an earthquake with a relatively small surface wave magnitude (Ms = 7.2) as compared with the moment magnitude (Mw = 7.6). As the result a large tsunami was accompanying a relatively

small earthquake. The discrepancy was due to a slow rupture velocity.

This tsunami earthquake reminded us of a difficulty in tsunami forecasting based on the surface wave magnitudes of earthquakes. Many tsunami earthquakes are found at a trench side of a continental slope (Pelayo and Wiens, 1992). A slow rupture at the South America trench was the cause of the Nicaragua tsunami. It took a long propagation time of about 50 minutes. The reason for this is found in a shallow continental shelf of only several 10 m water depth. The shallow sea possibly contributed to the slow attack.

Extensive information on recent tsunamis (1992-94), their effects and modelling, is given in a special volume of Pure and Applied Geophysics, edited by Satake and Imamura (1995). It contains 11 papers alone on the two events discussed above and on a magnitude scale for Central America tsunamis.

REFERENCES

Abe, Ku., Ka. Abe, Y. Tsuji, F. Imamura, H. Katao, Y. Iio, K. Satake, J. Bourgeois, E. Noguera, F. Estrada (1993). Field survey of the Nicaragua earthquake and tsunami of September 2, 1992, Bull. Earthq. Res. Inst., Univ. Tokyo, 68, 23-70 (in Japanese with English abstract).

Imamura, F., N. Shuto and C. Goto (1990). Study of numerical simulation of the transoceanic propagation of tsunami, Part 2, Characteristics of tsunami propagating over the Pacific Ocean, Zisin 2, 43, 389-402 (in Japanese with English abstract).

Kato, Y., Z. Suzuki, K. Nakamura, A. Takagi, K. Emura, M. Ito and H. Ishida (1961). The Chile tsunami of 1960 observed along the Sanriku coast of Japan. Science Rep., Tohoku Univ., Ser. 5, Geophysics, 13, 107-125.

Kanamori, H. and M. Kikuchi (1993). The 1992 Nicaragua earthquake, Nature, 361, 714-716.

Murty, T. S. (1977). Seismic sea waves-Tsunamis, Bulletin 198, Fisheries Res. Board of Canada.

Nakamura, K. and K. Emura (1961). Maximum water height at bay head in case of tsunami invasion, Science Rep., Tohoku Univ., Ser. 5, Geophysics, 13, 32-42.

Pelayo, A. M. and D. A. Wiens (1992). Tsunami earthquake: slow thrust-faulting events in accretionary wedge, J. Geophys. Res, 97, 15321-15337.

Satake, K. and F. Imamura (1995) (Eds.). Tsunamis 1992-94. Special issue of Pure and Applied Geophysics, 114, No. 3-4.

Shuto, N. (1994). Damages of houses in Hokkaido nansei-oki earthquake tsunami, Tsunami Engineering, Technical Report, 11, 11-28 (in Japanese).

THE MODELLING OF TSUNAMI HEIGHTS AND POSSIBILITIES FOR IMPROVED ASSESSMENTS OF LOCAL TSUNAMI HAZARD AND TSUNAMI WARNINGS

Kuniaki ABE

Niigata Junior College, Nippon Dental University
Hamauracho 1-8, Niigata city, 951, Japan

1. NUMERICAL SIMULATION

A modern tsunami modelling is a numerical simulation using a computer. To simulate the tsunami generation and propagation we need to know the generation mechanism and equation of motion. The former is approximated by a fault model while the latter is modelled by means of a linear long wave equation with a non-dispersive velocity of $\sqrt{gd}$. In this generation model the rupture velocity, i. e. the velocity of a fault formation, is considered to be large as compared to the

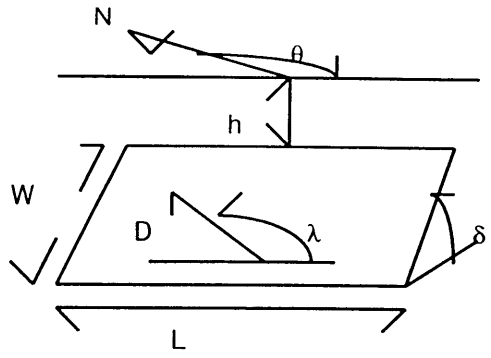

Fig. 1: Fault parameters

tsunami propagation velocity and an instantaneous generation is assumed. Thus the vertical sea level change, equal to the vertical displacement of ground surface derived from the static fault model, is effective as the initial condition (e.g. Aida, 1978). The sources of recent tsunamis have been approximated by the fault models (e.g. Imamura et al., 1993) but the parameters are not always definite.

An analytical expression to represent displacement fields on the fault model was given by Mansinha and Smylie (1971). The fault model is represented by 9 parameters including 3 position parameters, 3 strike direction parameters and 3 size parameters (Fig. 2). The position parameters consist of x-y coordinate of center position including upper depth h, direction parameters are dip angle δ, slip angle λ and strike angle θ, and size parameters are length L, width W and dislocation D. As the direction parameters those obtained from a seismic source mechanism are used and position and size parameters are adjusted to reproduce the observed waveforms or spectra in the numerical simulation. From seismic waves we can obtain a seismic moment $M_0 = \mu DLW$, in which μ is the shear modulus of solid medium. The best model is searched by changing the fault parameters but we have no independent proof of what is the best solution.

The wave propagation in a deep sea can be described by a linear long-wave equation with a continuity equation, i.e.

$$\partial \mathbf{v} / \partial t = - g \, \mathrm{grad} \, \eta$$
$$\partial \eta / \partial t = - \mathrm{div} \, \mathbf{v}$$

in which $\mathbf{v}$, η are particle velocity and water level, respectively. They are transformed into difference equations and solved step by step with a time interval and a grid interval. Goto et al. (1985), repeating the numerical simulation, concluded that the reproduction is guaranteed by using a grid interval smaller than one twentieth of the wavelength. The numerical dispersion is caused by smoothing of the wave profile. The linear equation is applicable for wave amplitudes being small compared to the sea depth.

In running-up we must consider both a non-linearity and bottom friction. Flooding into a dry land is treated under a moving boundary between water and solid. Roughness on the land is represented with a friction constant (Aida, 1977). About the numerical simulation there is a review by Shuto (1991). A more general treatment of numerical modeling is introduced by Mader (1988). Using of an equal grid size is a finite difference method called FDM. On the other hand, using of a variable grid size is a finite element method, called FEM.

Yamashita and Sato (1971) discuss the effect of source models on waveforms based on a spectrum at sea of a constant depth as derived from a fault model. The expression gives us the directivities of amplitude and frequency. The predominant frequency is expressed as velocity ($\sqrt{gd}$)/wave-length of the tsunami. When we can determine the predominant frequency from observations, it can be used as a reference to derive a model.

In making the model of a tsunami the position, direction and size parameters have to be given. Recent results from simulations suggest that direction parameters derived from long-period seismic waves are reliable ones. The position and size are related to the propagation time and the predominant frequency, respectively. After receiving a tsunami we have a data base of, e.g., time histories of sea level, to make a model. If we wish to use the simulation for a tsunami forecasting, we must complete the task before the arrival. High-speed computers can accomplish the task in time. But the problem is how to obtain the exact input parameters for the simulation. There is an approach to solve the problem by Imamura et al. (1991) but there are many problems to obtain reliable fault parameters. One example of practical forecastings are those made by the Japan Meteorological Agency. The generation and height are forecasted from a statistical relation based on the hypocenter and magnitude of the earthquake. But the heights are accurate only within a factor of 2 (Uchiike, 1995). They are improving the system and succeeded in issuing the warning for the 1994 Hokkaido-Toho-Oki earthquake tsunami within 4 minutes (Swinbanks, 1995).

2. LOCAL EFFECTS IN THE PROPAGATION

In this section we will describe topographical effects in the propagation which is difficult to be reproduced in the numerical simulation because of the small scale.

a) Island

A tsunami, passing island regions, refracts toward the center line of the island. The refraction is caused by a sloping sea bottom around the island. As the result it makes the energy concentrate in the direction of the center line.

The energy concentration of the 1960 Chilean tsunami to Polynesian and Hawaiian islands in the Pacific Ocean is verified by numerical simulations as described above. The energy concentration in various islands was quantitatively discussed for the cases of the 1993 Hokkaido Nansei-oki tsunami by Abe (1995a,b). According to his result the amplification ratio of the tsunami at the coast behind the island with respect to that at a coast distant from the island tends to be 2. This is explained by a total constructive superposition of two waves, which were divided by the island. Such a total superposition was completely observed at small islands. The effective width for which the topographic effect can be observed is explained systematically by considering a normalized coast distance from the island, which is a coast-island distance divided by the island size. This effect was also observed for the 1983 Japan Sea tsunami but the amplification ratio was smaller than 2 in the average.

b) Bay

The 1960 Chilean tsunami excited a long-period (60-70 minutes) wave which was amplified in the heads of long period bays as described before. In addition to the period, the incident angle and the number of waves are possibly related to an excitation of the natural oscillation. But still there are many unknown factors about behaviors of tsunami in bays.

c) River

Rivers, discharging into the sea, play a role in the tsunami generation. There were some cases in which tsunamis flooded into towns from river banks. Characteristic behaviors of tsunamis in rivers were studied in conjunction with the 1983 Japan Sea tsunami (Abe, 1985). The maximum propagation distance of a tsunami wave in the river is approximately determined by the upstream water level with respect to the maximum level at the mouth and the maximum level higher than that at the mouth occurring along the way upstream. It corresponds to a resonance curve of the amplitude of sound wave between two fixed boundaries. The maximum propagation point is equivalent to the fixed boundary above the water level. The maximum water level in the river is explained by a superposition of the direct wave and the reflected wave at a margin of continental shelf.

3. AN EXAMPLE OF A NUMERICAL SIMULATION: 1994 HOKKAIDO-TOHO-OKI EARTHQUAKE TSUNAMI

Recently a numerical simulation was carried out on the linear equation for the 1994 Hokkaido-Toho-Oki Earthquake Tsunami by Abe and Okada (1995). Repeating the simulation using various models they found that a geodetic fault model (Hashimoto et al., 1995) can explain tsunami waveforms. The results are shown in Figs. 2 and 3. Time and grid intervals were taken to be 5 s and 3 km, respectively. The vertical displacement field and inverse refraction diagram are shown in Fig. 2 and the comparison of observed waveforms with computed ones from the model is shown in Fig. 3. In making the geodetic model, horizontal displacements observed in Hokkaido played an important role. The observation of reliable coseismic horizontal displacements was made practical with the Geophysical Positioning System (GPS). The model is characterized by a unique fault mechanism. Conventionally it is assumed that a tsunami is generated by a thrust fault on the continental slope. The mechanism of the considered event is a steeply dipping (82°) reverse fault with a horizontal displacement component. The slip angle is 141°and the dislocation is 8 m. The sizes are L = 150 km, W = 50 km and h = 40 km. The moderate depth of 40 km is

also unique for an earthquake-accompanying tsunami.

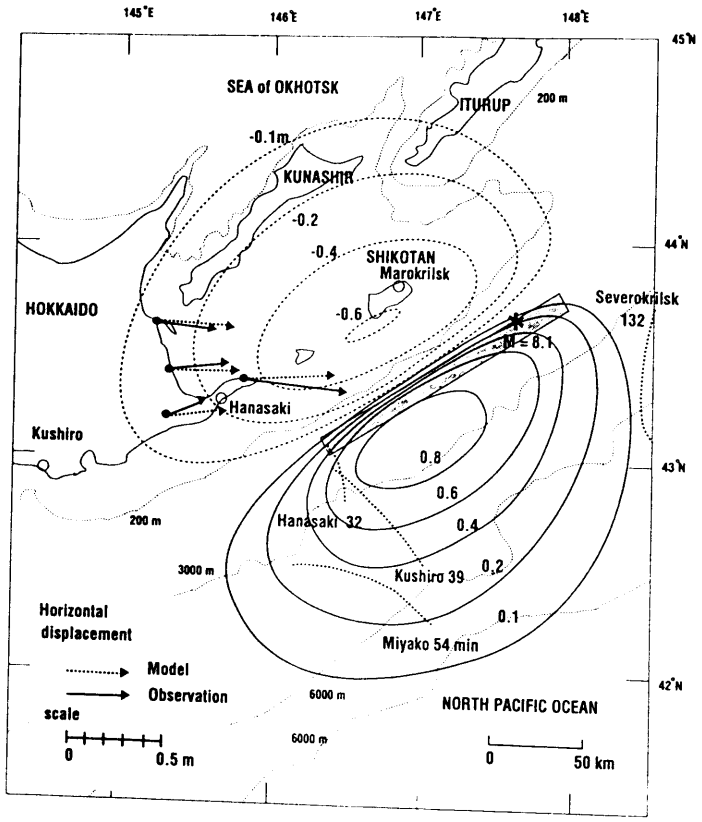

Fig. 2: Fault model, the vertical displacement and the starting wavefronts of tsunami.

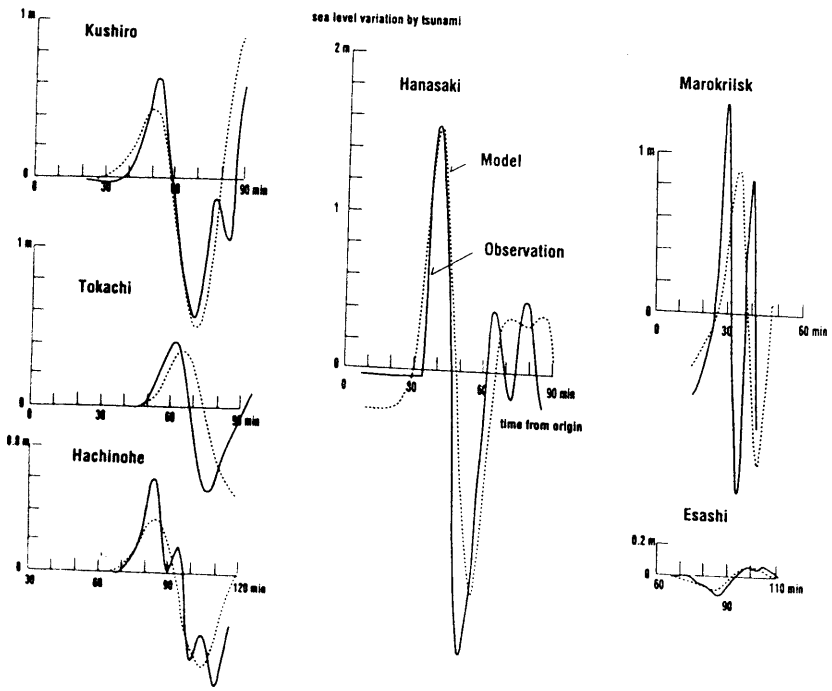

Fig. 3: Comparison of observed waveforms with computed ones.

REFERENCES

Abe, Ku (1985). NOTE: Tsunami propagation in rivers of the Japanese Islands. Continental Shelf Res., 5 , 65-677.

Abe, Ku. (1995a). Focusing effect of tsunami on islands, Part 1, A case of the 1993 Hokkaido nansei-oki earthquake tsunami, in preparation.

Abe, Ku. (1995b). Focusing effect of tsunami on islands, Part 2, A case of the 1983 Nihonkai-chubu earthquake tsunami, in preparation.

Abe, Ku. and M. Okada (1995). Tsunami source model of Hokkaido-Toho-Oki earthquake of 4 October 1994, in preparation.

Aida, I. (1977). Numerical experiment for inundation of tsunami-Susaki and Usa, in Kochi Prefecture. Bull. Earthq. Res. Inst., Univ. Tokyo, 52, 441-460 (in Japanese with English abstract).

Aida, I. (1978). Reliability of a tsunami source model derived from fault parameters, J. Phys. Earth, 26, 57-73.

Goto, C., N. Shuto and F. Imamura (1985). Summary of accuracy and speed of numerical simulation as a means of tsunami warning, Proceeding International Tsunami Symposium 1985, 82-93.

Hashimoto, M., T. Sagiya and T. Tada (1995). Crustal deformation associated with the Hokkaido Toho-oki Earthquake and its fault model. Abstr., Japan Earth and Planet. Sci., Joint Meeting, 151 (in Japanese).

Imamura, F., N. Shuto, S. Ide, Y. Yoshida and Ka. Abe (1993). Estimate of the tsunami source of the 1992 Nicaraguan earthquake from tsunami data, Geophys. Res. Lett, 20, 1515-1518.

Imamura, F., Y. Izutani and N. Shuto (1991). Accuracy of tsunami numerical forecasting with the rapid estimation method of fault parameters - A case of two fault planes with different stress drop of the 1944 Tonankai earthquake, Zisin 2, 44, 211-219 (in Japanese with English abstract).

Mader, C. L. (1988). Numerical modeling of water waves, University of California Press.

Mansinha, L. and D. E. Smylie (1971). The displacement fields of inclined faults, Bull. Seis. Soc. Amer., 61, 1433-1440.

Shuto, N. (1991). Numerical simulation of tsunamis - Its present and near future, Natural Hazards, 4, 171-191.

Swinbanks, D. (1994). Japanese earthquake tests disaster warning networks, Nature, 371, 549.

Uchiike, H. (1995). Tsunami forecasting toward swift warning issuance, Tsunami research and related topics in Japan 1991-1995, Edited by Shuto.

Yamashita, T. and R. Sato (1980). Generation of tsunami by a fault model, J. Phys. Earth, 22, 415-440.

Exercise on tsunami

K. Abe

Niigata Junior College, Nippon Dental University,
Hamaura-cho 1-8, Niigata city, 951, Japan

1. The velocity of tsunami is given as $\sqrt{gd}$. Calculate the velocity for an ocean basin with sea depth d = 5000 m assuming g = 9.8 m/s^2. What is the velocity on the continental shelf with d = 200 m?

2. Calculate the tsunami periods, which are assumed to be

$$T_l = 2\,L/\sqrt{gd}$$

and $$T_s = W/\sqrt{gd}/\cos\,\delta,$$

on the shelf with depth d = 200 m and on the continental slope with depth d = 2000 m by using as the fault parameters the fault length L = 200 km, width W = 100 km and dip angle δ = 30°.

3. In a step structure of sea depth the tsunami refracts according to Snell's law

$$\sin\alpha\,/\sin\beta = \sqrt{gd_1}\,/\,\sqrt{gd_2}.$$

Calculate the emergence angle β for the case of d_1 = 5000 m , d_2 = 200 m, and incident angle of α=60°.

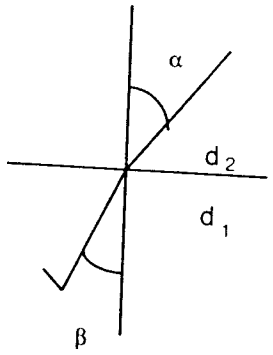

Fig. 1: Refraction at a boundary

4. In a step shelf structure the resonance period of shelf oscillation is given as

$$T = 4\,z/\,\sqrt{gd}$$

in which z is the width of the continental shelf and d is the sea depth.
Prove this formula and calculate the period for a shelf with the width of 34 km and the depth of 20 m. This is an appropriate model of the continental shelf off the Pacific coast of Nicaragua.

MACROSEISMIC AND STRONG-MOTION PARAMETERS

G. Grünthal

Dept. of Kinematics and Dynamics of the Earth
GeoForschungsZentrum Potsdam, Telegrafenberg C3, D-14473 Potsdam

1. INTRODUCTION

The extensive devastations during catastrophic earthquakes require vigorous investigations to reduce losses of life and in economy. Generally, the better the economy and infrastructure is developed in countries of high seismic activity the greater the efforts of the society towards earthquake protection will be. Particular attention should be payed to the assessment and mitigation of earthquake risk in earthquake struck developing countries where major investments and vital lifeline systems are frequently concentrated in seismically dangerous areas. Especially there the economic losses incured by a devastating earthquake may result in serious economic disruptions with all its detrimental social consequences. Therefore, regional as well as detailed urban planning in seismic active areas should rest on proper knowledge of:

- Regional geology and tectonics;
- Regional seismicity, earthquake catalogues (especially investigations of major previous events in the region);
- Characteristics of regional seismic activity and strong ground motion;
- Seismic zoning, both on seismological and tectonical data;
- Faulting and permanent ground deformations, landslides, other geological effects of earlier earthquakes;
- Regional distribution of earthquake effects;
- Microzoning of special local areas;
- Engineering aspects of disastrous earthquakes, damage distribution on different structural types;
- Adequacy of existing building codes and regulations;
- General recommendations for retrofitting of existing housing in the area;
- Social and economic implications of earthquakes in the region.

2. MACROSEISMIC PARAMETERS

The first question arising from the topics stated above is how to scale the earthquake effects in its regional distribution. For engineering design the parameters of primary importance are the recorded amplitudes of ground acceleration, velocity and displacement, the frequency content of such records and the duration of strong ground shakings. In the absence of any dense net of strong motion recording sites the macroseismic intensity as a descriptive quantity provides useful information on the regional distribution of earthquake effects, its dependence on distance, focal depth, local ground conditions etc. Because of the lacking of relevant strong-motion data macroseismic intensity has been used in most cases as scaling parameter for seismic hazard studies.

But the intensity will not fully satisfy the requirements of engineers in charge of designing earthquake resistant structures. Nevertheless, macroseismic investigations have been going

DOI: 10.2312/GFZ.b103-95tk7

through a Renaissance recently because both of their relative simplicity and complexity as well as the necessity of re-evaluation of historical records as a data base for seismic zoning and studies of long term patterns of seismicity. For hazard studies it is necessary to have an as long as possible time span of catalogued earthquake data. These data are macroseismic ones anyhow for times before 1900 and it is not possible to disclaim this part of data, because the better we know the seismic history or past the better we can assess the future process of seismicity.

Macroseismic investigations include the collection of felt perceptions by persons and of damages on structures in a dense net of settlements as well as the compilation of changes in landscape. These non-instrumental macroscopic criteria have to be quantified in grades of intensities according to their definition in an appropriate macroseismic scale. The intensity data depicted in isoseismal maps are analysed with regard to (1) the determination of the epicentre (especially of historical, non-instrumental earthquakes); (2) the attenuation of intensity with distance, (3) peculiarities of isoseismals etc. and their causes.

Problems will arise when comparing the intensity data of different epochs and from different countries owing to the use of different scales and their different versions. Therefore, the knowledge about the used scales since the middle of last century, their relations to each other as well as the underlaying predominant opinions and conceptions in quantifying macroseismic observations is indispensable especially where original descriptions of the observed effects are no longer available. Some of the most important scales are the ROSSI-FORREL scale from 1883 (when dealing with historical data), the scale used in Japan (JMA, 1952), the Modified-Mercalli scale (MM; USA, 1931), and the Medvedev-Sponheuer-Karnik scale (MSK) in its versions from 1964, 1981, and 1992.

The wording of the MSK-92 or EMS-92 scale with its detailed definitions of types of structures, classification of damages and quantities is annxed to the lecture notes "The updated MSK intensity scale EMS-92". Fig. 1 presents the relations between individual intensity range of the above mentioned scales.

Global conversion relations of epicentral intensity I_o, magnitude M and focal depth h[km] as well as for intensity I_n in a hypocentral distance D_n, respectively, are given for shallow earthquakes ($0 < h < 100$) in the nomogram in Fig. 2. But considerable variations of such a "global" relation are known. It is, therefore, essential to apply in a considerer region the relation which is valid for that region or relevant subregions. For Europe, e.g., the following relation after Karnik provides the best results:

$$M = 0.5I_0 + \log h + 0.35 \qquad [h \text{ in km}].$$

It is well known since the beginning of this century that the focal depth has an important influence on the areal distribution of the severity of shakings. This fact can be used to assess the focal depth from macroseismic data. Based on the fundamental work of Kövesligethy (1907), Sponheuer (1960) presented a set of nomograms (Fig. 3) to determine the focal depth h from the mean isoseismal radii D_i of Intensities I_i according to the following relation:

$$I_o - I_i = 3 \log \left(\sqrt{D_i^2 + h^2}\,/h\right) + 3\alpha \log e \left(\sqrt{D_i^2 + h^2} - h\right)$$

Comparison of different macroseismic scales

scale	degrees of intensity										
MSK-64	2	3	4	5	6	7	8	9	10	11	12
MM 1	2	3	4	5	6	7	8	9	10	11	12
RF	2	3	4	5	6	7	8	9	10		
JMA	1	2	3	4	5	6	7				

Fig. 1 Relations of the intensity ranges of the following macroseismic intensity scales: MSK-64, MM, RF, JMA: modified after Shebalin (1975). Between the different versions of the MSK-scale there are no differences in the assessed intensities.

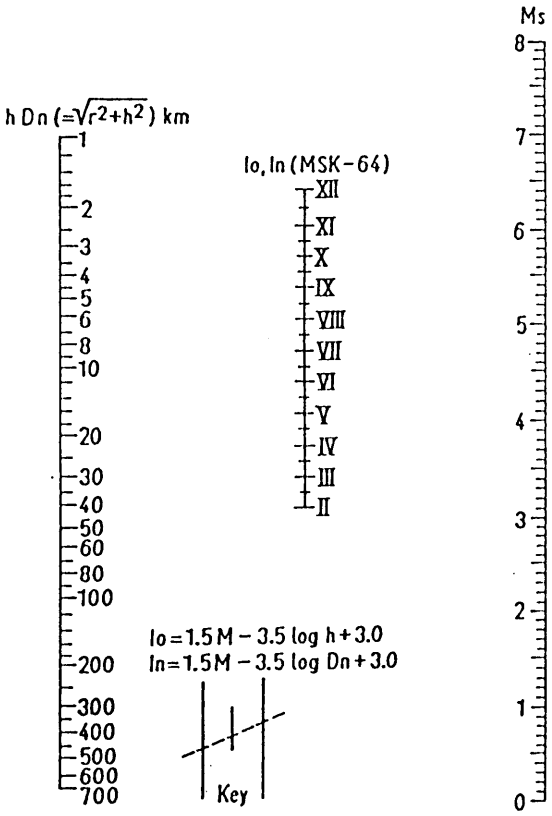

Fig. 2 Nomogram converting M, I_0 and h or M, I_n and D_n (after Shebalin).

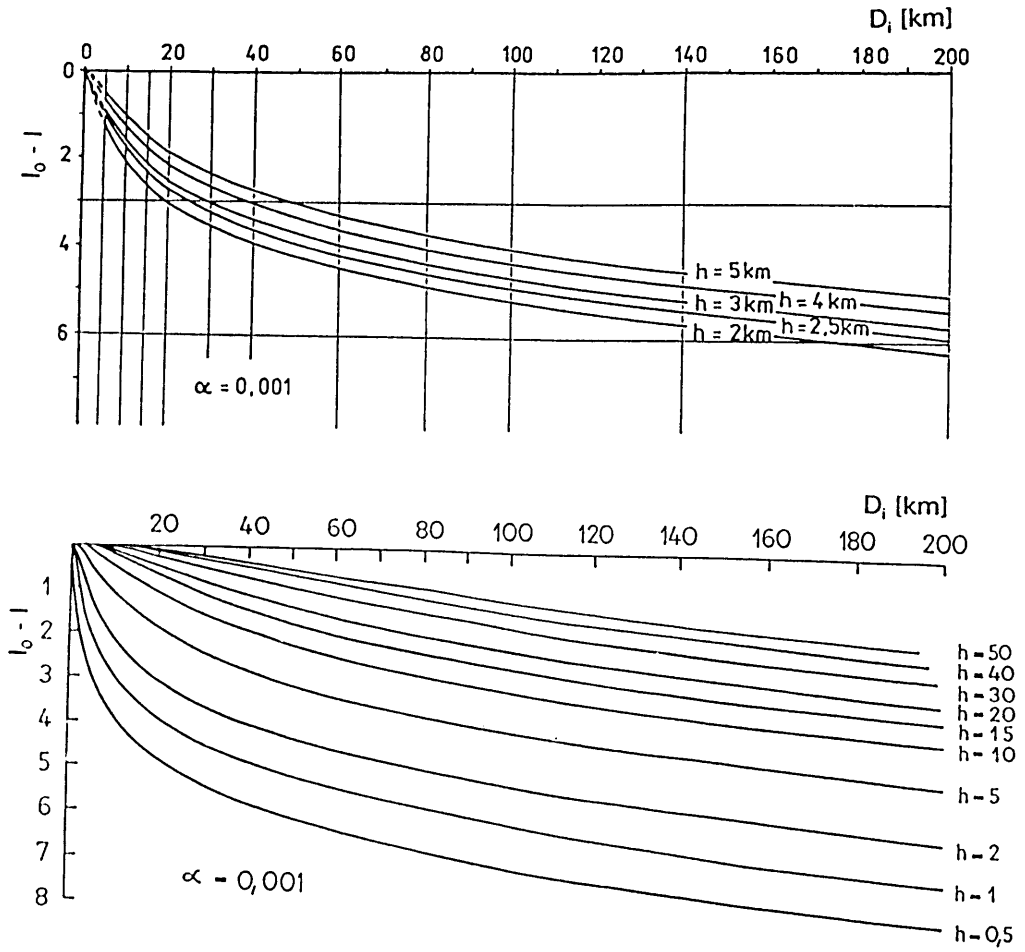

Fig. 3 Diagram for the determination of the focal depth h (in km) from mean isoseismal radii D_i; based on an attenuation coefficient $\alpha = 0.001\ km^{-1}$.

3. STRONG-MOTION PARAMETER

3.1 Strong-motion records and different kind of spectral representations

Damage to engineering structures caused by earthquakes is known to depend both on the ground motion characteristics and on the characteristics of structures. For the purpose of engineering design, the characteristics of ground shaking that are of primary importance, are the amplitude, the frequency distribution and the duration of shaking. These characteristics (see scheme of Fig. 4) depend on various factors such as:

I the earthquake source spectrum depending on the physical source process (the orientation of the site with respect to the source);
II the filter function of the transfer media (influence of distance, structure, attenuation)
III the filter function of the local site conditions (the surface topography, the subsurface configuration and attenuation);
IV the resonance period of structures in relation to the local transfer function of the subsoil
V the soil-structure interaction.

Remarks on the above mentioned characteristics:

to I: The seismic source spectrum determines the spectral content of the strong-motion records in the following way:

- The extent of the source plane F and the amount of dislocation determine the seismic moment M_0 and influences mainly the long-period spectral part which is decisive for far-field effects.
- The dislocation velocity v_B influences especially the short-period spectral part (the higher v_B the shorter the radiated wave lengths); both v_B and F determine the duration of the source process and in particular the shape of the displacement spectrum.
- The stress drop determines the high frequency part and thus the acceleration spectrum which is most decisive for the near-field effects.
- Additionally the orientation of the source to the site can influence the strong-motion characteristics.
- Also the tectonic regime influences the expected peak accelerations. In thrust fault regimes the maximum accelerations can be higher by the factor 4 than in normal faulting regimes.

to II: The filter function of the transfer medium is characterized by:

- the structure and elastic parameters including attenuation of the media through which the waves propagate;
- the length of the travel path.

to III: The filter function of the local soil conditions is also expressed as soil amplification and is the subject of microzoning studies. It is characterized by:

- the local subsoil (3d) structure and its elastic parameters;
- the angle of incident waves;
- the inelastic behaviour for shakings above a certain level.

The earthquake effects on the ground surface and on structures can be considered as follows:

- **Seismic zoning**, i.e. the definition of ground motion parameters on bedrock;
- **Seismic microzoning**, i.e. the consideration of the modification of the ground motion parameters obtained on bedrock due to the influence of the ground surface;
- **Aseismic design** parameters, i.e. the definition of structural design parameters considering the soil-structure interaction.

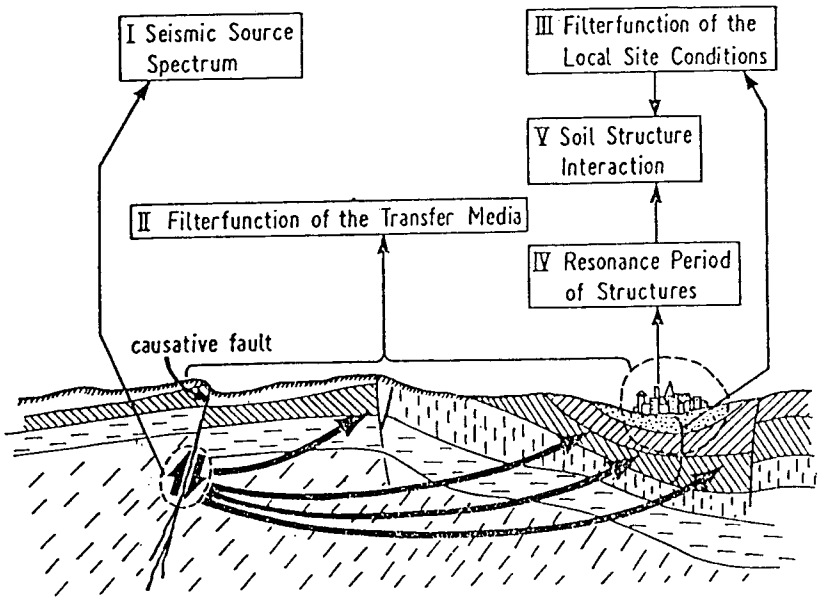

Fig. 4 Schematic illustration of the 5 basic components influencing the damage potential of structures.

The relations between intensity, magnitude and epicentral distance on the one hand and the strong-motion parameters on the other hand (i.e. the absolute peak values or average values of maximum recorded acceleration a, velocity v and displacement d, their frequency spectra, the duration of strong ground motions, the relation between all these parameters and their dependence on the respective soil conditions) are of essential practical importance in hazard assessments. Engineering seismology could be defined as strong-motion seismology which produces results used as input for earthquake engineering, i. e. for earthquake resistant design of structures and appropriate experimental studies.

Fig. 5 shows a typical acceleration record as well as the computed time series of velocity and displacement. The appropriate acceleration response spectra for different structural damping (in percent of the critical damping) is given in Fig. 6. This type of spectra represents the response (maximum amplitude) of a set of single degree of freedom oscillators each characterizing the response of a special natural period excited by the strong-motion record. The principle of the computation of response spectra is shown in Fig. 7.

The velocity response spectrum without damping corresponds with regard to characteristic features with the Fourier acceleration spectrum. The response spectra of acceleration S_a, of velocity (respectively pseudo-velocity) S_{pv} and of displacement S_d are symmetrically according to

$$\frac{T}{2\pi} S_a = S_{pv} = \frac{2\pi}{T} S_d .$$

This distinctive feature leads to the common presentation of smoothed and generalized spectra in special tripartite logarithmic paper (Newmark-spectra or design spectra). Fig. 8 shows such a tripartite spectral presentation in its classical form after Newmark (1973).

The observed strong motion data show a great variation when classified according to intensity, magnitude, distance, type of soil etc. Only a statistical representative data set allows to derive general results.

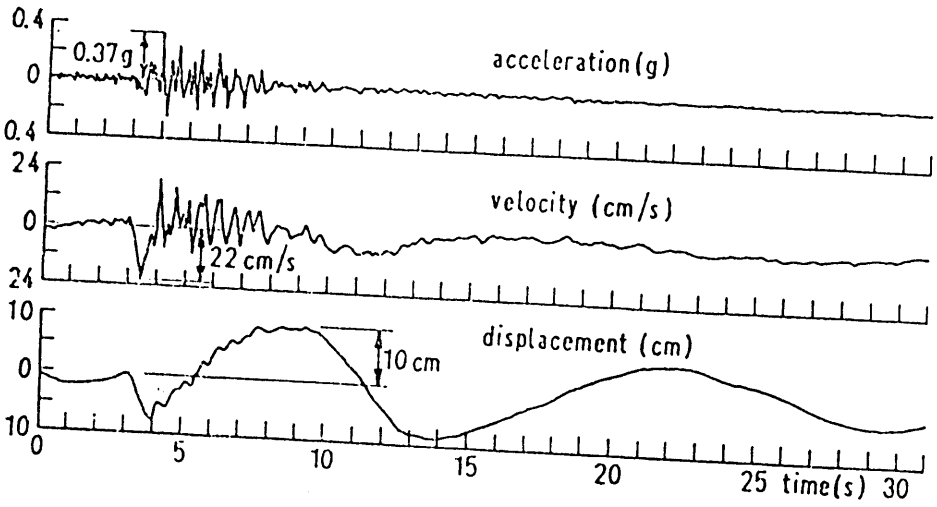

Fig. 5 Acceleration, velocity and displacement (N-S component) recorded at Tolmezzo (N-Italyat 20h 00m 15s on May 6th, 1976 (15 km epicentral distance, M = 6.5, h = 10 km, I_0 = IX - X); CNEL-ENEL (1976).

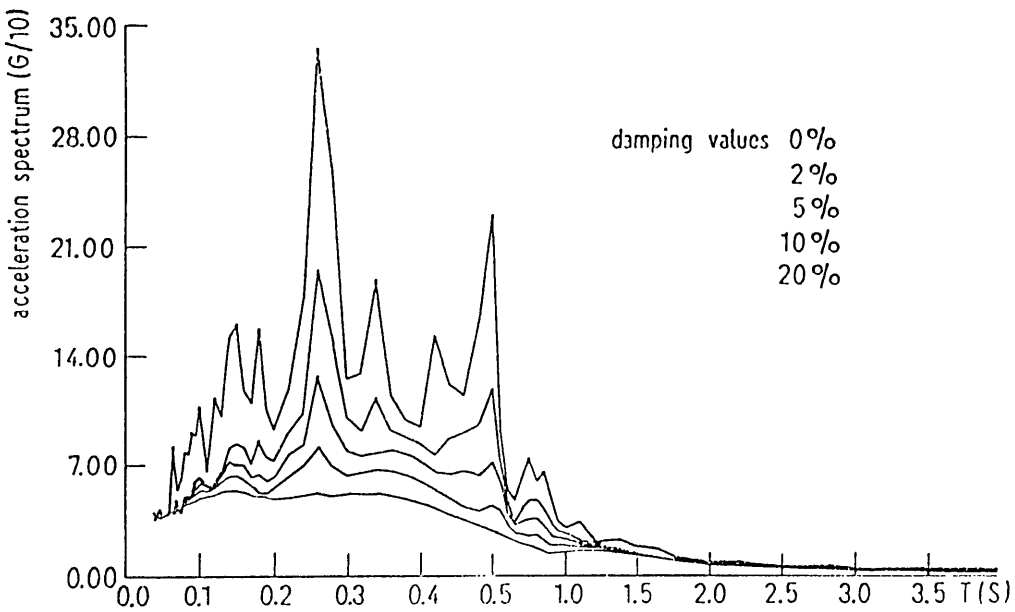

Fig. 6 Acceleration reponse spectrum corresponding to the record shown in Fig. 5 (CNEL-ENEL, 1967).

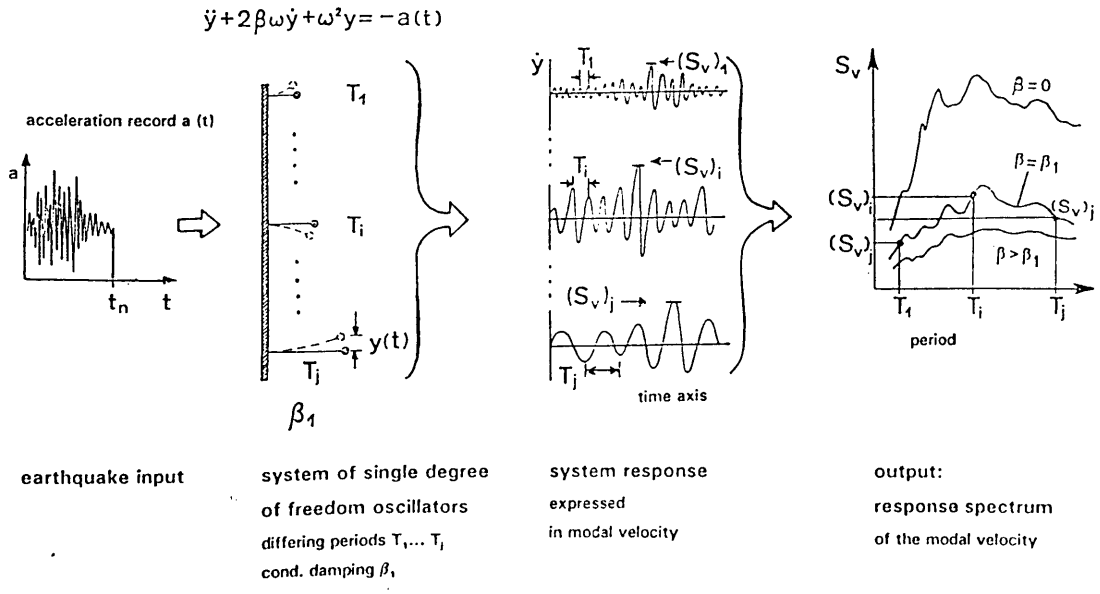

Fig. 7 Schematic presentation of the construction of response spectra.

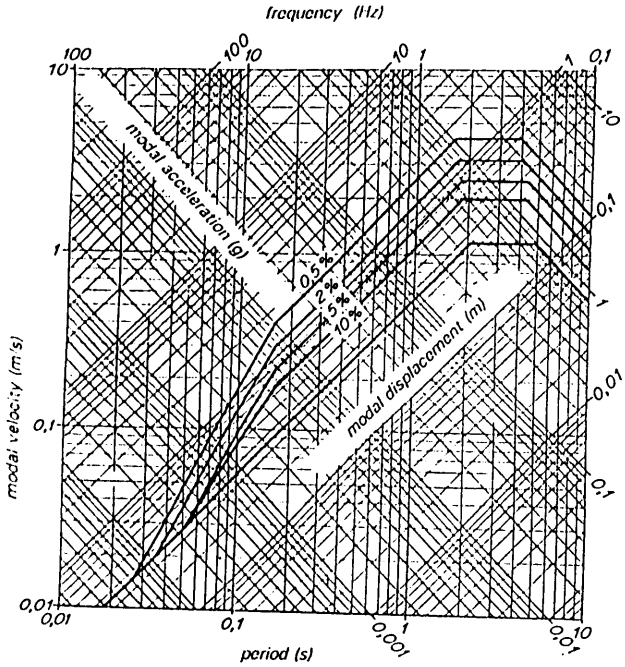

Fig. 8 Tripartite spectral presentation of smoothed design spectra after Newmark (1973) representing intensities of about VII.

3.2 Attempts to correlate intensity with amplitudes of recorded accelerations

From the practical point of view it is often asked to correlate intensity with accelerations. This is a very critical questions and to be answered with caution only.

Fig. 9 shows the observed peak acceleration in relation to intensity for the data from 1933 to 1973. The scatter ranges over two orders in acceleration and illustrates the principal weakness of any correlation attempts of acceleration with intensity. The reasons for this scatter can partly be explained by the various factors influencing the strong-motion characteristics as shown in Fig. 4. But for many practical routine purposes it is sufficient to use a simple intensity-acceleration relation such as the one given by Trifunac and Brady (1975):

$$\log a_{vert.} = 0.30\, I_{MM} - 0.18$$

$$\log a_{hori.} = 0.30\, I_{MM} - 0.14 \qquad IV \leq I_{MM} \leq X$$

with a - acceleration in cm/s^2.

Another frequently used conversion relation is given by Murphy and O'Brien (1977):

$$\log a = 0.25\, I + 0.25;$$

and, when considering especially hypocentral distances smaller than 25km

$$\log a = 0.38\, I - 0.56.$$

A relation which allows to take into account soil categories (s=0 alluvial, s=2 hard rock, s=1 intermediate), the component of recording (v = 0 horizontal, v = 1 vertical), and the chosen confidence interval p ($0 \leq p \leq 1$) has been given by Trifunac (1976):

$$\log \begin{Bmatrix} a_{max}, p \\ v_{max}, p \\ d_{max}, p \end{Bmatrix} = ap + bI_{MM} + c + ds + ev + fI_{MM}^2;$$

	a	b	c	d	e	f
a_{max}	0.942	0.459	-0.047	0.014	-0.270	-0.014
v_{max}	0.883	0.288	-1.411	0.014	-0.286	0.000
d_{max}	0.913	0.006	-0.690	-0.059	-0.186	0.019

More modern relations using the magnitude M and the hypocentral distance R or epicentral distance D in km as parameters, respectively, are those of Abrahamson and Litehiser (1989):

$$\log a(g) = -0.62 + 0.177M - 0.982 \log (R+e^{0.284M}) + 0.132F - 0.0008\,Er$$ with

F - tectonic regime (F=1 thrust faulting, F=0 others than thrust)
Er - type of earthquake (Er = 1 intraplate earthquakes, Er = 0 interplate earthquakes
a(g) - peak ground acceleration as fraction g (Earth's gravity).

Campbell (1989): $\ln a\,(g) = -2.501 + 0.623M - 1.0\ln (D + 7.28)$ for

$2.5 \leq M \leq 5.0$ and $2\ km \leq D \leq 25\ km$.

Joyner and Boore (1981): $\log a\,(g) = 1.02 + 0.249M - \log R - 0.00255\,R$
Ambraseys and Bommer (1992): $\log a\,(g) = -0.87 + 0.217M - \log R - 0.00117\,R$
as well as many others.

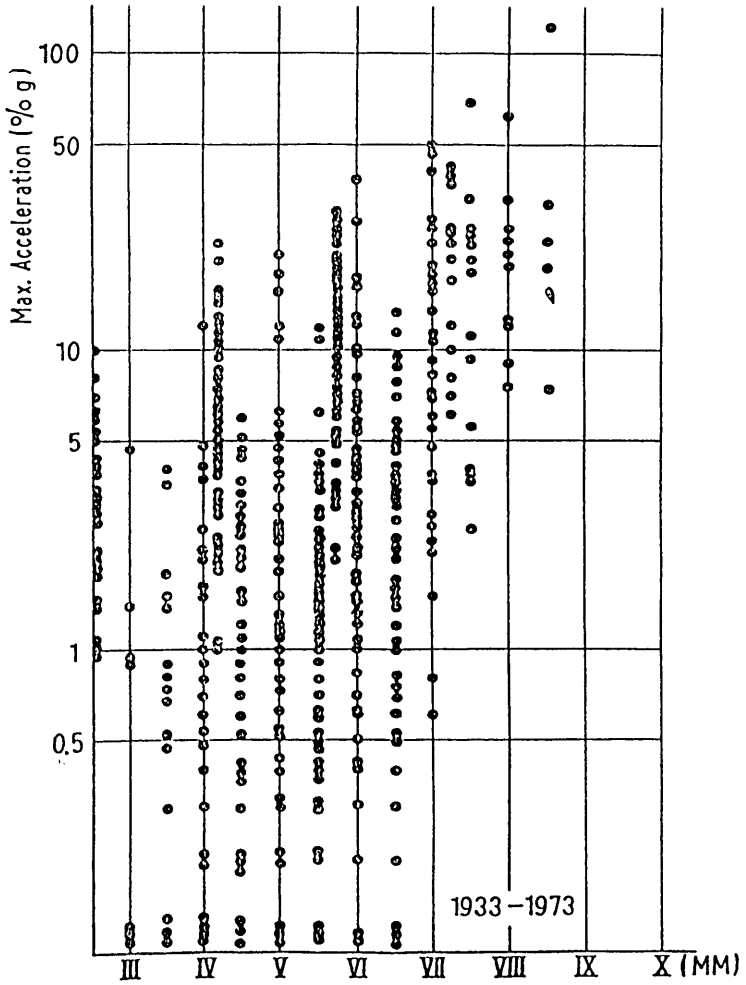

Fig. 9 Recorded maximum acceleration versus reported intensities for the period 1933 - 1973 (Ambraseys, 1974)

Theoretically, the largest possible acceleration in geological media could reach about 2 g (g: Earth's gravity, approx. 981 cm/s^2) (Ambraseys, 1974). The strongest acceleration of 1.49 g shown in Fig. 8 occurred at a site some 2 km from the causative fault during the Oct. 15, 1979, Imperial Valey earthquake (California) with M = 6.4. Relatively small shocks can produce rather strong acceleration peaks as well very close to the causative faulting (e. g. Parkfield earthquake, June 27, 1966, M = 5.6, a_{max} = 0.50 g, distance about 70 m). But the duration of strong shaking is relatively short in such cases so that the intensity which is an integral measure of both acceleration and duration corresponds to the relative small magnitude of these events. A better correlation with intensity shows the velocity (Fig. 10). Here the scatter of data is "only" one order of magnitude. This implies that the velocity is a better measure for intensity and thus for structural damage or human perception, respectively, than acceleration.

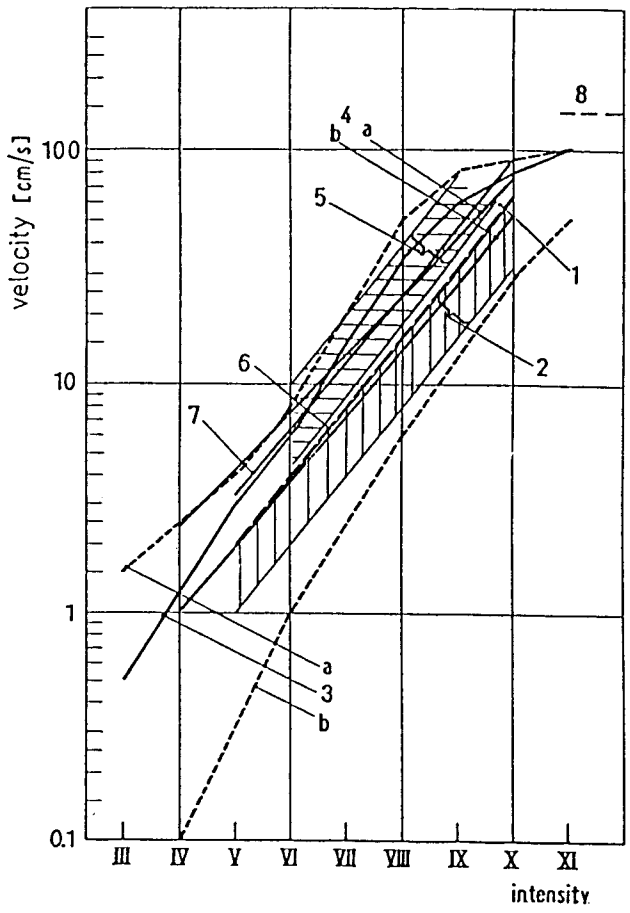

Fig. 10 Relations between recorded maximum soil-velocity and reported intensity: 1 - Neumann (1960); 2 - Medvedev and Sponheuer (1969); 3 - Shebalin (1975) a and b - probable upper and lower bound; 5 - Trifunac and Brady (1975) a - horizontal, b - vertical; 5 - Nazarov and Darbinyan (1975); 6 - Medvedev (1977); 7 - Espinosa (1977); 8 - Ambraseys (1974): expected maximum possible values.

3.3 Generalized spectral presentations

Fig. 11 and 12 show the mean spectral content of acceleration records of horizontal motion for different magnitudes in different epicentral distances for soft soils (s = 0) and hard rock (s=2). The influence of the type of soil at the recording site depends on frequency. Larger amplitudes (by the factor s) are observed on soft soils for periods greater than 0.2 s.

An interesting spectral feature presents Fig. 13 after Devilliers and Mohammadioun (1981). It shows 7 different spectra for the one intensity level I_S = VI - VII. This one intensity level can be produced by different constellations of magnitudes and distances given also in Fig. 13 (i.e. from motions of a M = 4.6 earthquake recorded at a distance of R = 10 km up to an M = 7.5 earthquake recorded at a distance of 200 km, which all yields in the same intensity of I = VI - VII). The different shapes of the spectra reflect both the influence of large discrepancies in the source characteristics of such a wide range of earthquake sizes and the influence of considerable differences of seismic wave attenuations along the wave paths ranging from 10 to 200 km.

The influence of different soil conditions on the spectral shape is shown in Fig. 14a and b after Seed et al. (1974) at the example of the best investigated magnitude 6½ earthquakes in two different distances (5 and 20 miles). For short periods (< 0.6 sec) the largest amplitudes can be expected on stiff soils while for larger periods the effects are largest on soft soil conditions. The prediction of such effects is one of the subjects of microzoning.

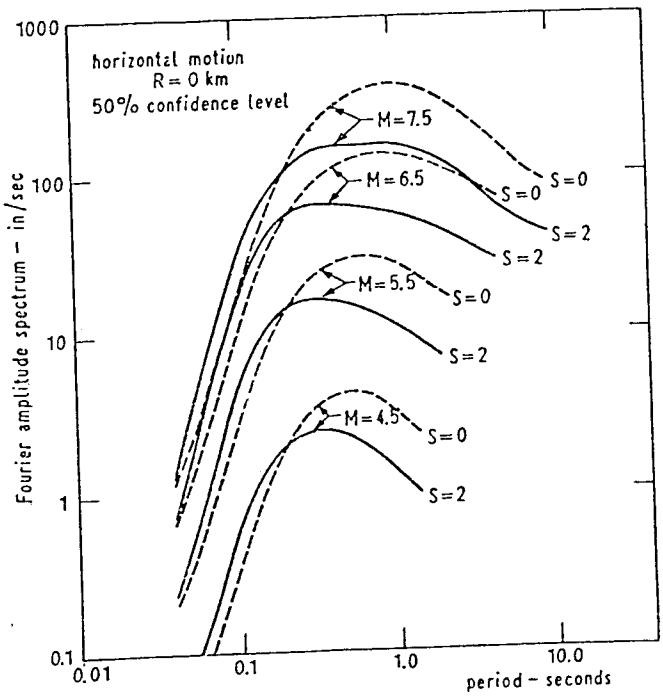

Fig. 11 Mean Fourier amplitude spectra of horizontal acceleration in the epicentre for magnitudes from 4.5 to 7.5 on soft (s = 0) and on hard rock (s = 2); Trifunac (1976).

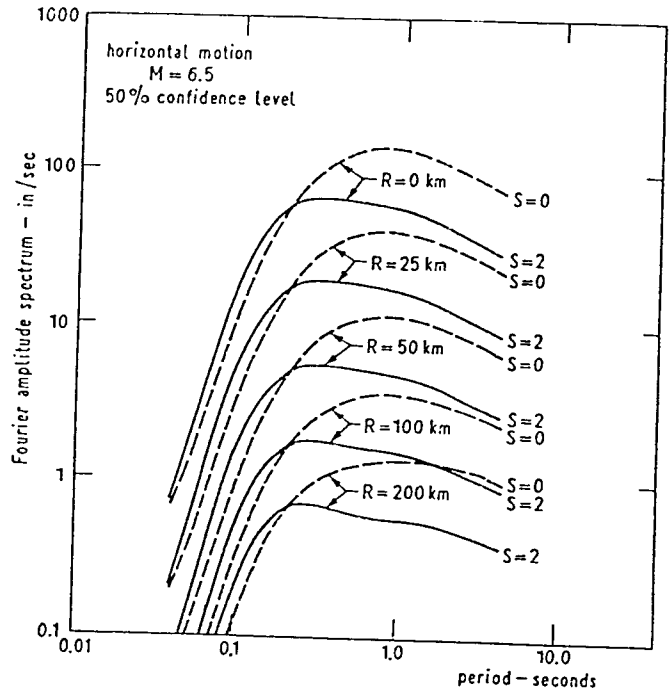

Fig. 12 Mean Fourier amplitude spectra of horizontal acceleration for 6.5 magnitudes in epicentral distances from 0 to 200 km; Trifunac (1976).

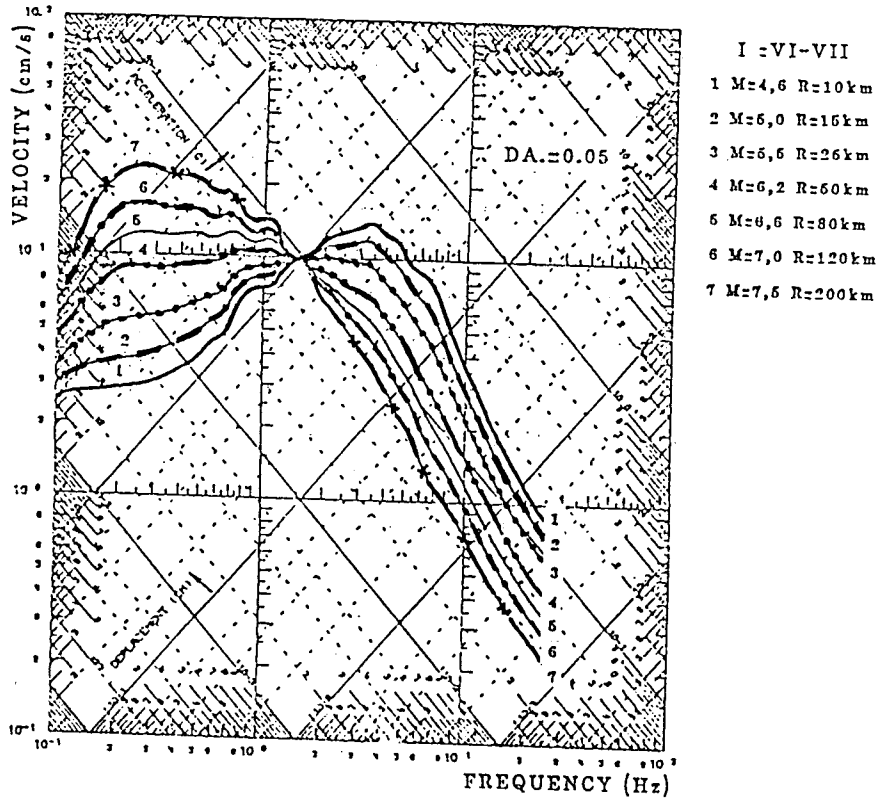

Fig. 13 Variation of spectra corresponding to the intensity VI - VII with magnitude and focal distance.

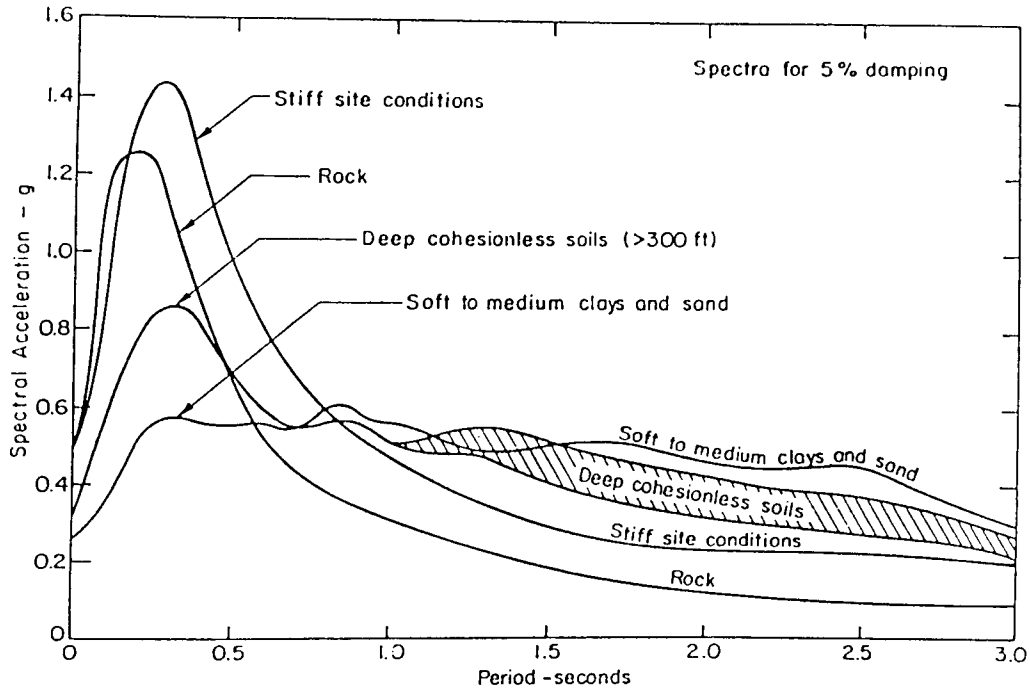

Fig. 14a Anticipated mean spectra for magnitude 6½ earthquakes at a distance of 5 miles (after Seed at al., 1974).

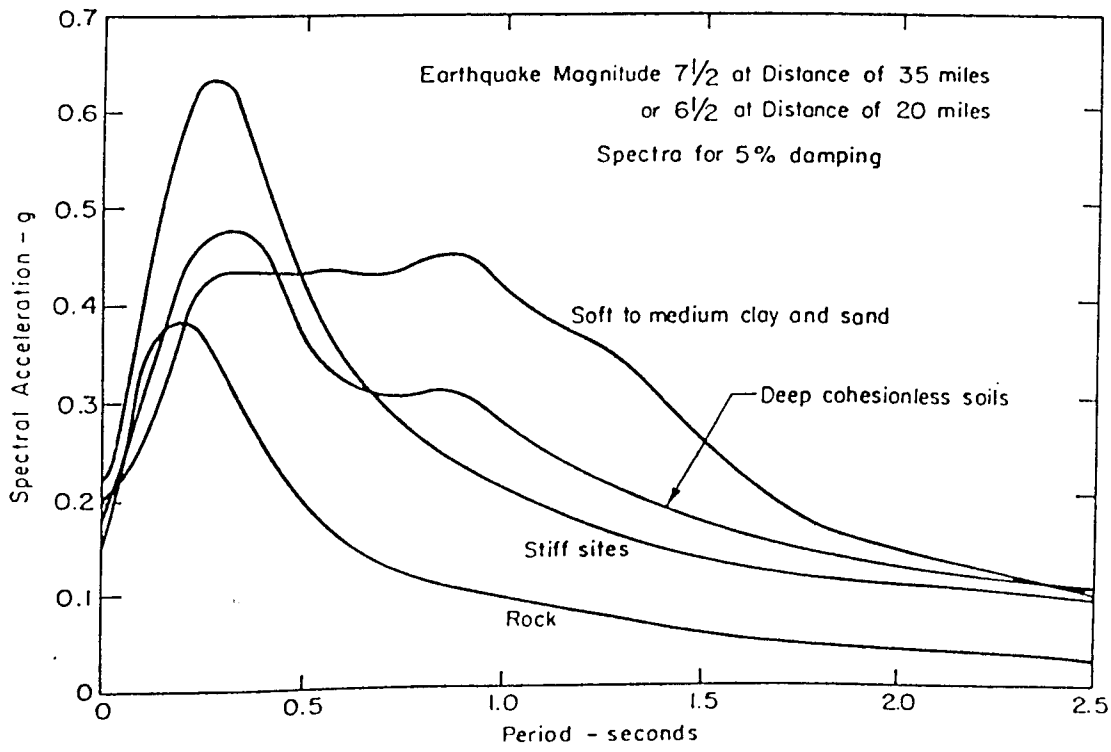

Fig. 14b Anticipated mean spectra for magnitude 6½ earthquakes at a distance of 20 miles (after Seed at al., 1974).

3.4 Attenuation of acceleration with distance and dominating periods of motion

Another important problem concerns the attenuation of acceleration or velocity with distance. The observed peak values with distance show a large variability.

Fig. 15 presents average values of maximum acceleration for different magnitudes as a function of distance in the western United States. It should be noted that the peak acceleration values, e.g. in the Mediterranean region, are in the average by the factor 2 - 3 higher than those in the western United States. This phenomenon can be explained by regional differences in stress drop. Low stress-drop events cause low acceleration records in the epicentral area and vice versa. Further important parameters in engineering seismology are the duration of the strong-motion phase and the dominant periods of motion. The duration increases with magnitude due to the extension of the source process as well as with distance (Tab. 1). The dominant period of strong shaking differs essentially between acceleration, velocity and displacement. Expected mean values for different magnitudes and distances are given for acceleration on rock sites in Tab. 2 and for displacement in Tab. 3.

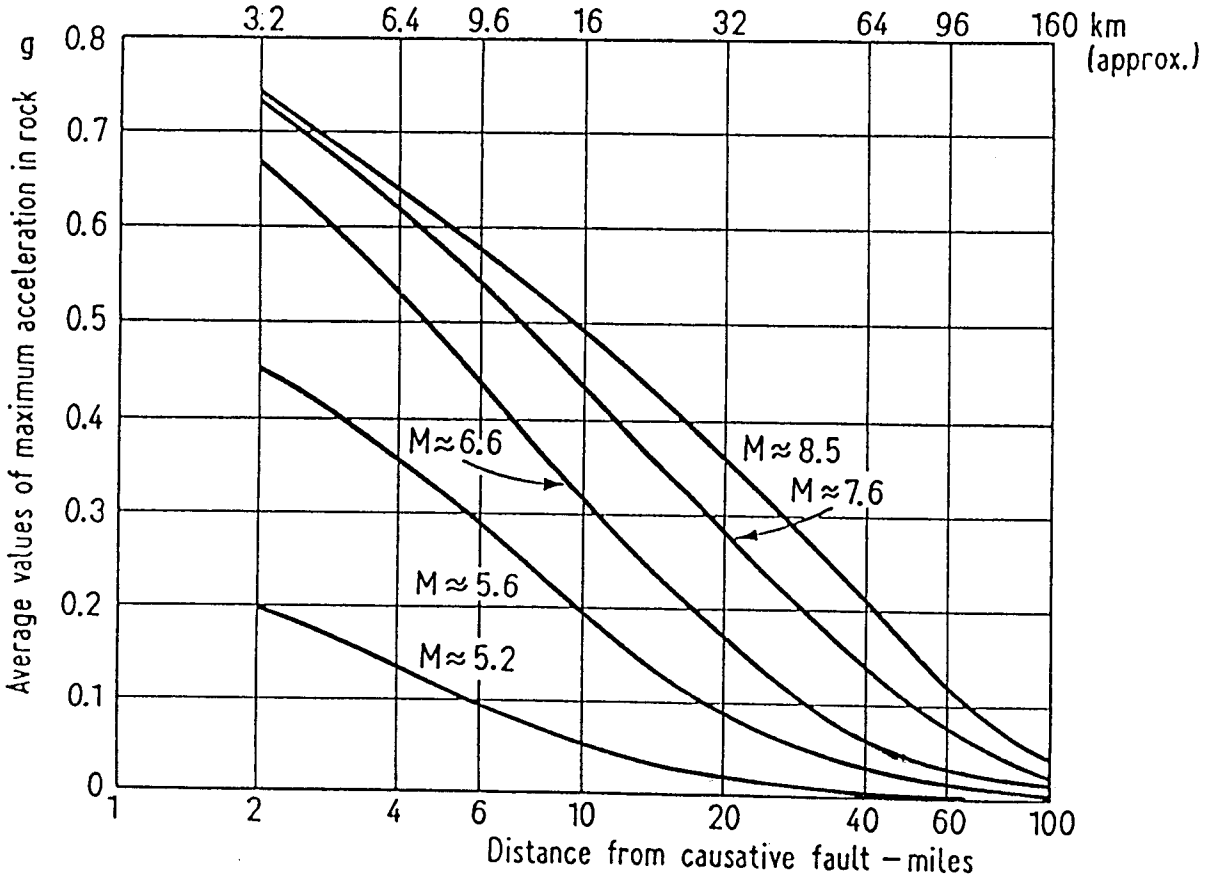

Fig. 15 Average values of maximum acceleration on rock sites versus distance in the western United States (Schnabel and Seed, 1972).

Tab. 1 Duration of strong-motion phase in dependence on magnitude M and distance D in km (Shebalin, 1975).

D \ M	3.3-3.9	4.0-4.6	4.7-5.3	5.4-6.0	6.1-6.7	6.8-7.4	7.5-8.1	8.2
3-7	0.5	1	2	3	5	-	-	-
7-15	0.8	1.5	2	4	7	10	15	-
15-30	1.0	1.5	3	5	9	14	20	30
30-60	1.0	2	3	6	12	20	40	50
60-120	-	2	4	7	14	30	60	100
-250	-	-	4	8	16	40	90	200

Tab. 2: Dominating period of acceleration in dependence on M and D as in Tab. 1 (Shebalin, 1975).

D \ M	3.3-3.9	4.0-4.6	4.7-5.3	5.4-6.0	6.1-6.7	6.8-7.4	7.5-8.1
3-7	0.18	0.21	0.24	0.27	0.29	-	-
7-15	0.20	0.24	0.27	0.30	0.34	0.37	-
15-20	0.22	0.27	0.31	0.35	0.39	0.43	0.43
30-60	0.26	0.31	0.36	0.41	0.45	0.49	0.52
60-120	0.31	0.38	0.42	0.48	0.52	0.57	0.61
250	0.36	0.45	0.50	0.57	0.63	0.70	0.78

Tab. 3: Dominating period of displacement in dependence on M and D as in Tab. 1 (Shebalin, 1975).

D \ M	3.3-3.9	4.0-4.6	4.7-5.3	5.4-6.0	6.1-6.7	6.8-7.4	7.5-8.1	8.2
3-30	0.6	2	3	5	10	-	-	-
30-300	1	2.5	5	9	16	28	40	50

REFERENCES

Ambraseys, N.N.: Dynamics and response of foundation materials in epicentral regions of strong earthquakes.

Abrahamson, N.A.; Litehiser, J.J.: Attenuation of vertical peak acceleration. Bull. Seismol. Soc. Am. 79/3, 549, 1989.

Ambraseys, N.N.: Notes on Engineering seismology. In: Engineering seismology and earthquake engineering, J. Solnes (ed.)

Campbell, K.W.: The dependence of peak horizontal acceletation on magnitude, distance, and site effects for small-magnitude earthquakes in California and Eastern North America. Bull. Seismol. Soc. Am. 79/5, 1311-1346, 1989.

CNEN-ENEL: Contribution of the study of Friuli earthquake of May 1976. CNEN-ENEL Publ., Nov. 1976, Rom.

Devillers, C.; Mohammadioun, B.: 1981. French methodology for determining site adapted SMS (Séisme Majoré de Sécurité) Spectra. Procedings of the 6th International Conference on Structural Mechanics in Reactor Technology, Paris. Vol K, paper 1/9.

Espinosa, A.F.: Practice-velocity attenuations realations: San Fernando earthquake of February 9, 1971.

Joyner, W.B.; Boore, D.M.: Peak horizontal accelerations and velocity from strong-motion recordings including records from the 1979 Imperial Valley, California, earthquake. Bull. Seis. Soc. Am. 71, 2011-2038, 1981.

Kövesligethy, R.V.: Seismischer Stärkegrad und Intensität der Beben. Gerlands Beitr. Geophys. 8 (1907), 22-29.

Medvedev, S.V.: Seismic intensity scale MSK-76. Publ. Inst. Geophys. Pol. Acad. Sc., A-6 (117), 1977, 95-102.

Medvedev, S.V.; Sponheuer, W.: Scale of seismic intensity. Proc. IV World Conf. Earthquake Eng., Santiago, Chile, A-2 (1969), 143-153.

Murphy, J.R.; O'Brien, L.J.: The correlation of peak ground acceleration amplitude with seismic intensities and other physical parameters. Bull. Seism. Soc. Am 67 (1977), 877-915.

Nazarov, A.G.; Darbinyan, S.S.: Škala dlja opredelnija intensivnosti sil'nych zemletrjasenij na količestvennoj osnove. In: Seismičeskaja čkala i metody izmerenija sejsmičeskoj intensivnosti. Nauka (1975), 40-79.

Neumann, F.: A Broad formular for estimating earthquake forces on oscillators. Proc. II World Conf. Earthquake Eng.; 2 (1960), p. 850, Tokyo.

Newmark, N.: A study of vertical and horizontal earthquake spectra. Consulting Engineer Services, Directorate of Licensing, U. S. Atomic Energy Comm. WASH-1255, Wash. D.C. April 1973.

Schnabel, B.; Seed, H.B.: Acceleration in rock for earthquakes in the Western United States. Earthqu. Engin. Research Center Rep. No. 72-2 (1972).

Seed, H.B.; Ugas, C.; Lysmer, J.: Site-dependent spectra for earthquake-resistant design. EERC-Rep. No. 74-12 (1974).

Shebalin, N.V.: Ob ozenke sejsmčeskoj intensivnosti. In: Sejsmičeskaja čkala i metody immerenija sejsmičeskoj intensivnosti (87-109), Nauka 1975.

Sponheuer, W.: Methoden zur Herdtiefenbestimmung in der Makroseismik. Freib. Forschungsh. C88 (1960), 117 pp.

Trifunac, M.D.: A note on the range of peak amplitudes of recorded accelerations, velocities and displacements with respect to the Modified Mercalli Intensity Scale. - Earthquake Notes, Vol. 47/1 (1976), 9-24.

Trifunac, M.D.; Brady, A.G.: On the correlation of seismic intensity scales with the peaks of recorded strong ground motion. Bull. Seis. Soc. Am. 65 (1975), 139-162.

THE UPDATED MSK INTENSITY SCALE EMS-92

G. Grünthal

Dept. of Kinematics and Dynamics of the Earth
GeoForschungsZentrum Potsdam, Telegrafenberg C3, D-14473 Potsdam

An updated version of the MSK macroseismic intensity scale has been prepared by a Working Group of the European Seismological Commission (ESC) and was published in spring 1993 (ed.: Grünthal, G.; European Macroseismic Scale 1992 (updated MSK-scale); Cahier du Centre Europèen de Gèodynamique et de Séismologie, Accord partiel ouvert en matière de prévention, de protection et d'organisation des secours contre les risques naturels et technologiques majeurs du Conseil de l'Europe, Volume 7, Luxembourg 1993). The Working Group "Macroseismic Scales" has operated four years and has organized four meetings in which 19 researchers, including seismologists and engineers, from 9 countries participated. Another 20 sent written contributions.

The following working definition served as a basis: "The macroseismic intensity is a classification of the severity of ground shaking on the basis of observed effects in a limited area". The general rule for the updating was not to introduce substantial changes which would jeopardize the internal consistency and result in intensity evaluations being different from those based on earlier applications of the MSK scale. This would require a reclassification of all earlier intensity assessments and should strictly be avoided otherwise. It would finally result in a complete confusion concerning all studies on seismicity and seismic hazard which are based largely on macroseismic data. Also the classical numbering was adhered so as to avoid any misunderstanding although the twelve-degree macroseismic scales in use are in fact ten-degree scales, i.e., the intensities XI and XII are, quite apart from their very limited practical importance, difficult to distinguish and intensity I means no observation at all besides instrumental recordings.

Other general aspects taken into consideration were: (1) the robustness of the scale, i.e. minor differences in diagnostics should not make large differences in the assessed intensity; (2) the simplicity of use of the scale; (3) the insight that the scale has to be understood and used as a compromise solution, because no intensity scale can hope to encompass all the disagreements between diagnostics for defined intensities. Such disagreements also reflect differences in cultural conditions in the regions where the scale is used; (4) the rejection of any intensity corrections for soil conditions or geomorphological effects, because detailed macroseismic observations should just be a tool for identifying and assessing such amplification effects; (5) the understanding that the derived intensity values should be representative for a whole village, a small town or a part of a larger town instead of being point intensities (for one house, e.g.).

Some of the partial problems to be solved were: (1) the need to include the reference to new types of buildings, especially to those with antiseismic design features, which are not covered by previous versions of the scale; (2) the need to address a perceived problem of non-linearity in the scale arrangement at the junction of the degrees VI and VII (which, after thorough discussion, proved to be a pretended one); (3) the need to improve generally the clarity of wording in the scale; (4) the need to decide what allowance should be made for including high-rise buildings into intensity evaluations; (5) to design a scale which does not

only meet the needs of seismologists, but those of civil engineers as well and which is suitable for the evaluation of historical earthquakes, too; (6) the need for a critical revision of the usage of macroseismic effects visible in the ground.

The updated scale is designed in a modular form consisting of a *Guide to Use of the Scale*, the text of the scale itself (*Core Part*) and a set of Annexes (*Annex A: Examples illustrating Classifications of Vulnerability and Damage used in the Scale; Annex B: Engineered Structures (Buildings); Annex C: Seismogeological Effects; Annex D: Examples of Intensity Assessment).*

The Core Part contains essential innovations like the introduction of the table of vulnerability classes of buildings instead of the former differentiation into building types. Special buildings, being typical outside of Europe, can simply be added in terms of their vulnerability characteristics. The classification of damages could be improved substantially according to broad engineering experiences (i.e. there is a separation into masonry and reinforced concrete buildings and a strict differentiation of the degree of non-structural and structural damage complemented by appropriate illustrations. The new arrangement of the scale follows now more logic constraints.

Serious problems arose with respect to the treatment of antiseismic constructions in intensity evaluations. Therefore the *Annex B* can be understood mainly as an experimental approach in conjunction with the commitment to gather more experience on the subject which will allow to introduce necessary improvements.

It was agreed to use the presented scale for three years (until 1996) in order to check its suitability and internal consistency. The final edition is foreseen for 1996, after the XXXV ESC General Assembly.

Despite of these limitations the EMS-scale presents, even in its current preliminary form, according to evaluations by international experts, the most advanced existing macroseismic scale. Most parts of this new version of the scale are attached here as an annex.

ANNEX

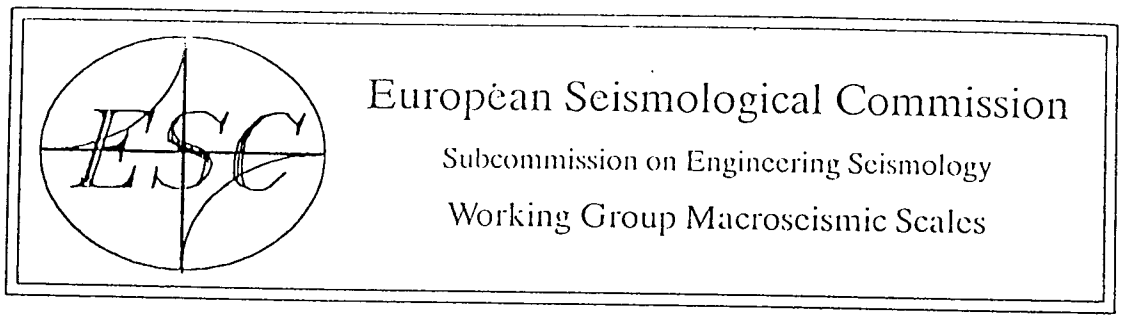

European Macroseismic Scale 1992

(up-dated MSK-scale)

Editor

G. Grünthal

Chairman of the ESC Working Group "Macroseismic Scales"

GeoForschungsZentrum Potsdam, Potsdam, Germany

Associate Editors:

R. M. W. Musson, Britisch Geological Survey, Edinburgh, Great Britain

J. Schwarz, College of Architecture and Civil Engineering, Weimar, Germany

M. Stucchi, Istituto per la Geofisica della Litosfera, C.N.R., Milan, Italy

ACCORD PARTIEL OUVERT
en matière de prévention, de protection et
d'organisation des secours contre les risques naturels et technologiques majeurs
du CONSEIL DE L'EUROPE

LUXEMBOURG 1993

Scientific Technical Report STR 95/TK
DOI: 10.2312/GFZ.b103-95tk7

CONTENTS

Scientific Technical Report STR 95/TK
DOI: 10.2312/GFZ.b103-95tk7

ANNEXES

1 INTRODUCTION

The purpose of this issue of the Cahier du Centre Européen de Géodynamique is to present the new, state-of-the-art, up-dating of the MSK intensity scale by the Working Group on Macroseismic Scales. This Working Group of the European Seismological Commission was reactivated during the XXI. ESC - General Assembly in Sofia in September 1988.
A Call for Proposals for the Up-Dating of the MSK Intensity Scale, together with some general thoughts, which ought to be taken as a basis for up-dating, were distributed as an annexe to the 3rd ESC Bulletin in March 1989. The responses to this appeal for proposals were compiled and distributed in early 1990. Four WG meetings were held: June 7-8, 1990 in Zürich, May 14-16, 1991 in Munich, and March 16-18, 1992 in Walferdange/Luxembourg as well as one with less participants, from June 17-21, 1992 in Potsdam.

It is worthwhile to give briefly some information on the establishment of the original version of the MSK intensity scale by S.V.Medvedev/Moscow, W.Sponheuer/Jena, and V.Kárník/Prague. The introduction of an up-dated scale was initiated by the Institute of Physics of the Earth in Moscow in the early sixties by requesting proposals for improving and completing the scale introduced by Medvedev in 1953 and used in the Soviet Union as the GEOFIAN-scale. In response to this Kárník initiated in 1961 the cooperation of the three fathers of the MSK-scale. A first draft of a new scale, based on the Mercalli-Cancani-Sieberg scale (MCS), the Modified-Mercalli scale (MM), and the Medvedev-scale, was compiled by Sponheuer and Kárník in spring 1962 in Prague. It was revised by Medvedev and Sponheuer in July 1962 and presented as the first draft of the new scale during the 7th Assembly of the ESC in September 1962 in Jena. It was intended at that time to create a unique world-wide scale by combining the experience gathered at that time from the application of the MCS-, the MM-, and the GEOFIAN-scale. The 1962 version of the scale was circulated to all major seismological institutions at that time; not only in Europe but also in Japan, North- and South-America etc. The extensive responses, e.g. from New Zealand, Japan, Spain, Greece, were incorporated by Sponheuer and Medvedev into the second draft in spring 1963 in Moscow. It was presented by Kárník as the "modified scale MSK" during the General Assembly of the IUGG 1963 in Berkeley. According to a recommendation of the UNESCO Working Group on Seismic and Seismotectonic Maps, from December 1963, the process of establishing the new scale as an international standard one should be speeded up in order to present the new scale to the UNESCO Intergovernmental Meeting on Seismology and Earthquake Engineering in Paris in April 1964. Therefore Sponheuer and Medvedev

drafted the third version of the new scale, which was presented as the scale MSK 1964 during the above mentioned meeting in Paris. In the same year it was introduced during the ESC meeting in Budapest. This version of the scale is the one known today as the MSK-64 scale.

Slight, barely noticeably changes to the MSK-64 were proposed by Medvedev in 1976 and 1978. At that time it became evident by many users that the scale needed several improvements, more clarity and adjusting to newly introduced construction techniques. An analysis of the problems arising with the application of the MSK-64 scale was made by an Ad-Hoc Panel of Experts during a meeting in Jena in March 1980. But the recommendations for changes of the scale from this group of experts were also generally of a minor nature.

Other serious attempts for more drastic changes of the scale, or even for its replacement by a completely different version, were made by J.A.Ershov and N.V.Shebalin in 1984 and by J.Drimmel in 1985. Their sophisticated procedures were suitable mainly for special analysis of particular cases, but less suitable for rapid routine intensity evaluations. Such substantial changes to the scale involve the danger of changing the internal consistency of the scale. This may result in intensity evaluations which could be different from earlier applications of the MSK-scale and which would require a reclassification of all earlier intensity assessments. This should be avoided at all costs. It would result in a complete confusion in all studies on seismicity and seismic hazard which draw heavily on macroseismic data. Precisely this problem was explicitly mentioned in the Call for Proposals for Up-Dating from March 1989. It was further emphasised that any changes to the scale should be made carefully so as not to change its internal consistency.

Other general aspects considered to be fundamental to the up-dating were as follows:

- the robustness of the scale, i.e. minor differences in diagnostics should not make large differences in the assessed intensity;
- the simplicity of the scale's use;
- the insight that the scale should be understood and used as a compromise solution, because no intensity scale can hope to encompass all the disagreements between diagnostics for defined intensities - such disagreements may also reflect differences in cultural conditions in the regions where the scale is used;
- the rejection of any intensity corrections for soil conditions or geomorphological effects, because detailed macroseismic observations should just be a tool for finding and elaborating such amplification effects;

- the understanding of intensity values as being representative for any village, a small town or a part of a larger town instead of point intensities (for one house etc.).

The specific problems to be solved by the WG on Macroseismic Scales - on the basis of the above mentioned aspects - were:

- the need to include mention of new types of buildings, especially those including antiseismic design features, which are not covered by existing versions of the scale;
- the need to address a perceived problem of non-linearity in the scale arrangement at the junction of the degrees VI and VII (which, after thorough discussion, proved to be illusory);
- the need to improve generally the clarity of the wording in the scale;
- the need to decide what allowance should be made for including high-rise buildings for intensity evaluations;
- whether guidelines for equating intensities to physical parameters of strong ground motions, including their spectral representations, should be included;
- to design a scale that not only meets the needs of seismologists alone, but which also meets the needs of civil engineers;
- to design a scale which should be also suitable for the evaluation of historical earthquakes;
- the need for a critical revision of the usage of macroseismic effects visible in the ground (like rock falls, fissures in ground) and the exposure of underground structures to shakings.

The members of the WG are aware that the twelve-degree macroseismic scales are in fact ten-degree scales; i.e. intensity I means no observation and the intensities XI and XII are, quite apart from their very limited practical importance, difficult to distinguish. If one takes into account the very rare practical use of the intensities II and XI as well as the fact that intensity XII defines maximum effects, which are not to be expected to occur in reality, the result is even an eight-degree scale. But, as mentioned above, to avoid any confusion, the classical numbering is adhered to.

The basis for elaborating the up-dated scale version was the so-called MSK-81 scale; a version in which the recommendations by the Ad-Hoc Panel of Experts from 1980 (published in Gerlands Beitr. Geophys.,1981) and the earlier proposals by S.V.Medvedev were incorporated. This version was attached to the first Call for Proposals to activate the Working Group.

During the first WG meeting it was discussed, as an introduction, what the term

"macroseismic intensity" actually means. After a long debate as to whether intensity is inherently a measure of ground motion or not, the following working definition was agreed: "The macroseismic intensity is a classification of the severity of ground shaking on the basis of observed effects in a limited area".

Another essential issue of the first meeting was the agreement on the structure of the new scale. It was decided that the new scale should be modular in design and that the scale should include a guideline on its usage. This guide should be illustrated by photographs depicting exactly what is meant by the different defined building types and grades of damage. The modular design means the creation of a so-called *Core Scale*, i.e. the definitions of the single intensity degrees, similar in content to the classical scale version but without all weaker and less essential diagnostics, and also a number of modules addressing particular problems to avoid the possibility of the modules being used separately.

An *Annexe A on Intensity Evaluation of Historical Earthquakes* should deal with the restrictions that need to be borne in mind when evaluating intensities of historical earthquakes. It was intended that it should include also a reduced version of the scale suggested solely for application to historical information. An *Annexe B on Engineered Structures (Buildings)* should enable an extension of the scale to be applied to engineered and antiseismic constructions; i.e. it should consider a greater number of classes of buildings than all previous scales. It should especially meet the needs of engineers. An *Annexe C on Seismogeological Effects* should deal in greater depth with phenomena like landslips, rock falls etc. These diagnostics have been deleted from that part which is now referred to as the Core Scale. It is known that effects of this type are often unreliable as exact intensity diagnostics - especially secondary, triggered effects may have little correspondence with intensity. But when used with caution they can be useful. Therefore, it seemed undesirable to delete them entirely from the scale.

It was agreed also to change the arrangement of the new scale (core part). The previous MSK versions were arranged as:

a) Effects on persons and surroundings
b) Effects on structures (damage)
c) Effects on nature.

The new arrangement is:

a) Effects on humans
b) Effects on objects and on nature (excluding damage to buildings, effects on

ground and ground failure)

c) Damage to buildings.

Further written contributions to several aspects of the scale's updating were prepared for the second and the third WG meeting - not only by the participants of the meeting, but also by other workers, e.g. R. Glavcheva (Sofia). The proposals elaborated by the WG and available to the chairman up to spring 1991 were included into an actual working version of the scale prepared as a basis for the drafting of the Core Scale, which could generally be finished during the second WG meeting. Also proposals for establishing the above mentioned Annexes were thoroughly discussed. But serious problems connected with them became evident. Many details achieved during the WG meetings can be found in the extensive meeting notes taken by R.M.W.Musson.
The WG members met again during the ESC-General Assembly in September 1990 in Barcelona to draft a resolution for the "European Scale" adopted by the ESC-meeting. Activity reports commenting on the results achieved by the WG were presented in Barcelona as well as during the IUGG-General Assembly in Vienna 1991.

During the third meeting one main topic was the discussion of the first version of the Guide on How to Use the Scale prepared by R.M.W.Musson. The Guidelines are certainly an essential, straightforward step in improving the macroseismic practice. The participants recognized that it proved not to be useful, contrary to the intentions after the first meeting, to introduce an Annexe on Historical Earthquakes. This topic is dealt with in a paragraph of the Guideline and in the Annexe D.

Serious problems arose with the treatment of engineered or antiseismic constructions for intensity evaluation. Reasons for this are:

- the up to now limited knowledge and experience on the systematics of earthquake damage patterns for this category of buildings;
- the great variety of systems for classifying engineered constructions in seismic codes;
- disagreements between engineers and seismologists in the use of intensity and related research topics (e.g. a tendency among engineers to overestimate the importance of instrumental data in connection with intensities and therefore the danger to overcharge the concept of intensity);
- the often imprecise seismological approach to intensity assignment with regard to building types previously used in the MSK-scale; i.e. the general neglect of the quality of workmanship, the structural regularity, the strength of material, the state of repair etc., as well as the necessity to consider such features as scaling conditions.

Scientific Technical Report STR 95/TK
DOI: 10.2312/GFZ.b103-95tk7

Seismologists initially expected that a classification of engineered buildings could be devised that would allow their incorporation into the scale in a similar fashion to the original scheme. After long discussions it was accepted that engineered buildings can be used for intensity assignment only on the basis of earthquake resistant design principles. An essential step for overcoming these problems was the introduction of the vulnerability table which enables the possibility to deal in one scheme with different kinds of buildings and the variety of their actual ranges of vulnerability. In former versions of the MSK-scale the building types were defined in a rather strict way. This vulnerability table, as a compromise solution, covering different opinions and incorporating engineered and non-engineered buildings into a single frame was devised during the fourth meeting, at which G.Grünthal, R.M.W.Musson, J.Schwarz, and M.Stucchi participated. It has to be stressed that the adopted compromise, partly included in the Core Scale as well as given as Annexe B, can be understood mainly as an experimental or tentative solution of this problem, connected with the commitment to gathering more information and experiences on this subject, in order to become able to introduce necessary improvements.

Also during the Potsdam meeting, the Guidelines were revised once more. The differentiation of buildings into vulnerability classes (part of the Core Scale) and a first version of a tabulated compilation of seismogeological and hydrological macroseismic effects were drafted. A few days later, J.Vogt and R.M.W.Musson, at Strasbourg, brought that table into a version which was the basis for the lay-out attached here as Annexe C. J. Schwarz compiled Annexe A, the set of photographs provided mainly by H. Tiedemann as well as by E. Kenjebaev and A. Taubaev.

In the course of the XXIII. ESC General Assembly, held in September 1992 in Prague, the outcome of the Working Group was made public first time in form of a poster as well as during a special session dedicated to the presentation of the up-dated MSK-scale. The numerous suggestions for further improvements, being mainly of a minor nature, submitted during or immediately after the Prague symposium, could be considered as a final phase of revision of the scale.

Because of the tentative and experimental nature of parts of the presented version of the up-dated MSK-scale, it has to be considered as a "working version" with the commitment to further revision after several years of practical experience. A period of three years has been stipulated for this, i.e. an improved version, especially regarding the use of engineered construction for intensity evaluation, can be expected for the XXV. ESC General Assembly. Some suggestions for future, not yet elaborated innovations and fields

are kindly requested to submit their comments for further improvements to the chairman of the Working Group "Macroseismic Scale", whose address is attached below.

The XXIII. ESC General Assembly 1992 in Prague adopted the above described proposals of the WG and recommended:" use of the new 'European Macroseismic Scale 1992' (up-dated MSK-scale, MSK-92), proposed by the ESC-Working Group 'Macroseismic Scale' in parallel to the existing scales for a time period of three years, in order to collect experience under realistic conditions, especially on the more experimental parts of the scale on the vulnerability classes and engineered constructions. A final analysis should follow this test period before the scale will officially be recommended by the XXV. ESC General Assembly."

It would extend the scope of the introduction too much to deal with all the "ifs" and "buts" which arose unavoidably during the process of up-dating. It was necessary in each step of the work to find the right balance between the aimed consistency of the up-dated version with the original scale and several obviously excellent ideas for the scale improvement which were going beyond the goal defined for the WG activities. Some of these points are mentioned in the Guideline (e.g. the problem of the correlation of intensities with strong ground motion parameters), or are at least raised in annexes. Others will be subject of further activities. One of them will doubtless be the combination of the descriptive way of defining intensities with formalised procedures of data processing for providing possibilities to exclude (or at least to reduce) the subjective element in the intensity assessment. Several approaches to formalised procedures (or algorithms) for a computerised macroseismic intensity evaluation exist already. It has to be stressed that it was not an aim of the WG to create such algorithms - but to create the basis for them, i.e. to present updated, as clear as possible, qualitative descriptive definitions of what the different intensities should actually stand for. One of the next logical steps would be to establish, based on the defined intensities together with "rules" given in the Guidelines, a strictly defined formalised algorithm for performing as objective as possible intensity assessments. Such computerised methods can be only so good as the basic definitions on which they rely.

The new scale version with all its parts is a product of a cooperative team work - a team of seismologists and engineers. The chairman of the WG is grateful for all the efforts which the participants of the WG have applied to the elaboration of the new version of the scale. The colleagues who have actively contributed to this process of updating, and who were respectively participants in the first three WG meetings, are: G.Grünthal (Potsdam), V.Kárník (Prague), E.Kenjebaev (Alma-Ata), A.Levret (Fontenay-aux

Scientific Technical Report STR 95/TK
DOI: 10.2312/GFZ.b103-95tk7
GeoForschungsZentrum Potsdam

Roses), D.Mayer-Rosa (Zürich), R.M.W.Musson (Edinburgh), O.Novotny (Prague), D.Postpischl (Bologna), A.A.Roman (Kishinev), H.Sandi (Bucharest), V.Schenk (Prague), Z.Schenková (Prague), J.Schwarz (Weimar), V.I.Shumila (Kishinev), M.Stucchi (Milano), H.Tiedemann (Munich), J.Vogt (Strasbourg), J.Zahradník (Prague), T.Zsiros (Budapest).

Thanks are also due to the main authors or compilers of special parts of the results presented by the WG; these are R.M.W.Musson for drafting the Guide on How to Use the Scale as well as the Examples of Intensity Assignment (Annexe D), J.Vogt and R.M.W.Musson for drafting the Table on Seismogeological Effects, H.Tiedemann, J.Schwarz and E. Kenjebaev for introducing essential ideas on using engineered constructions in intensity assessments, for providing the basic information for the Annexe B on Engineered Construction, for providing and compiling the photographs of typical earthquake damages; M.Stucchi for co-ordinating the views and comments of seismologists and engineers in Italy and for finalizing the recommendations concerning the historical data, as well as additionally A.Taubaev (Alma Ata) for drafting the drawings illustrating different damage grades for different building types.
Especially acknowledged is the support of the WG activities by the Swiss Reinsurance Company, the Bavarian Reinsurance Company, and the Council of Europe.
Finally the participants of the WG feel bound to remember to our late WG member Daniele Postpischl and the activities he contributed.

G. Grünthal
Chairman of the Working Group
"Macroseismic Scales"
GeoForschungsZentrum,
Telegrafenberg, D-O-1561 Potsdam

Potsdam, in November 1992

2 GUIDE TO THE USE OF THE INTENSITY SCALE

2.1 General Remarks

2.1.1 The nature of intensity

As stated in the introduction to this scale, intensity is here considered a classification of the severity of the ground shaking on the basis of observed effects in a limited area. Intensity scales, and the concept of intensity itself, have been evolving through the course of this century. From a pure hierarchical classification of effects it has been tried, more and more, to develop a rough instrument for measuring the shaking; at least, it has been used in this sense.

It follows that an intensity scale is in some ways similar to a shorthand system, in that it allows the compression of a verbose description of earthquake effects into a single symbol (usually a number). To describe intensity in this way is useful in representing the limitations of the concept - intensity is descriptive in the manner of a prose account, rather than analytical in the manner of an instrumental measurement. Intensity is capable of analysis and interpretation, is indeed a very useful parameter, and its uses go beyond what could be done with a simple compilation of descriptions. But its basic nature needs to be kept in mind by the user so as not to overload the concept with expectations that it cannot meet.

The development of the scale can be seen most clearly in the consideration of damage and building types. At the purest level of classification, all damage of a particular type would be grouped together irrespective of the strength of the building damaged. At the other extreme, it would be necessary to know the exact strength of a building in order to estimate the amount of shaking required to produce a certain level of damage.

The up-dated version of the MSK scale incorporates a compromise, in which a fairly crude differentiation of the resistance of buildings to earthquake generated shaking (vulnerability) has been employed in order to give a simple and robust way of differentiating the way in which buildings may respond to earthquake shaking. This development is not yet completed; a further trend towards increased formalisation of the scale and of the procedures to be adopted in using it is likely, and desirable, in the future, but at present the amount of observational data that can be used for the construction of these formalised procedures is limited.

Scientific Technical Report STR 95/TK
DOI: 10.2312/GFZ.b103-95tk7

2.1.2 The usage of intensity scales

Traditionally the use of intensity scales has been chiefly through the media of the questionnaire survey and the field visit, applied immediately in the wake of an earthquake. With an increasing interest in past earthquakes since the mid-1970s, there has been a greater usage of intensity scales as tools to be applied to written materials of a very heterogeneous nature. Also, it is increasingly common for engineers and planners to turn to intensity as part of an approach to building predicitive tools for estimating future earthquake losses.

This guideline will concentrate on a discussion of the general use of the scale. It should be stressed that, at present, all material in the scale and annexe dealing with anti-seismic engineered construction is experimental in status, since there is relatively little experience in assessing the effects of earthquakes on this type of building. References to engineered construction in the main body of the scale are printed in italics to emphasise this fact; also the quantitative information is left blank - this will be included in the next revision of the scale when more experience has been gained in observing the behaviour of antiseismically designed buildings in earthquakes.

In the macroseismic study of an earthquake, the following simple stages can be discerned:

i) Data acquisition - by questionnaire survey, field visit, appeals for information, literature search or other means.

ii) Data sorting - organisation of the data into a form in which it can be interpreted by the user - this may be no more than arranging the questionnaires by place of origin.

iii) Intensity assignment - the data are interpreted using the intensity scale and a table of places with intensities is produced.

This is usually then followed by mapping of intensities, which can be followed by contouring to produce isoseismal maps, from which various other analyses may be made. Isoseismal maps are often the basis for seismic zoning and zoning maps introduced into earthquake resistant design regulations (codes). In many European countries engineered structures are designed for seismic loads of a level which directly related an intensity value assigned to the seismic zone in which the building site lies. A discussion of these techniques is, however, beyond the scope of these guidelines. The following discussion concentrates on those matters that are closely related to the use of the intensity scale and the concept of intensity.

2.1.3 The structure and construction of intensity scales

The MSK intensity scale is one of a family of intensity scales which originated with a simple ten-degree scale by Mercalli, which was subsequently expanded by Cancani to twelve degrees, and then defined in a very full way by Sieberg as the Mercalli-Cancani-Sieberg (MCS) scale. It is this scale which forms the starting point not only for the MSK scale, but also for the numerous versions of the "Modified Mercalli" scale. All these twelve degree scales have been shown to be roughly equivalent to one another in actual values. They vary in the degree of sophistication employed in the formulation.

In fact, although these scales have twelve degrees, in practice they tend to function as eight-degree scales. Intensity 1 means in practice "not felt", and intensity 2 is so weak as to be usually not reported and so rarely used. At the other end of the scale, intensity 12 is defined in a manner such that it describes the maximum conceivable effects which can not necessarily be reached in an earthquake. Intensities 10 and 11 are hard to distinguish in practice, so intensity 11 is also rarely used. Thus the "working range" of all these scales tends usually to be from intensity 3 to intensity 10.

The major difference between the MSK scale and other intensity scales is in the detail with which different terms used are defined at the outset, in particular, building types, damage grades, and quantities, and these are now considered individually.

2.1.3.1 Building types and vulnerability classes

The use of letters to stand for various types of building originated with Richter's 1956 version of the Modified Mercalli scale. This subdivision is not made out of architectural interest; it represents, very crudely, different levels of vulnerability. The same degree of shaking that will destroy an adobe hut will have much less effect on a well-constructed modern office block. It is clear, though, that the condition of a building also affects its vulnerability. To account for every last variation in vulnerability according to type and condition would make the scale far too unwieldy to be useful in practice, therefore, a compromise position is necessary.

Previous versions of the MSK scale defined building classes solely by type of construction. In this version, it has been attempted to move closer to classes directly representing vulnerability. Accordingly, six classes of decreasing vulnerability are proposed (A-F) of which the first three represent the strength of a "typical" adobe house, brick building and reinforced concrete (RC) structure, ie they should be compatible with building classes A-C in the MSK-64 and MSK-81 scales. Classes D-F are intended to

Scientific Technical Report STR 95/TK
DOI: 10.2312/GFZ.b103-95tk7
GeoForschungsZentrum Potsdam

represent approximately linear decreases in vulnerability as a result of improved level of anti-seismic design (ASD). Note that no correlation with specialised engineering vulnerability functions are intended in this draft, but this should be considered as an area of further development within the calibration of the scale. (In Annexe B an approach is presented which indicates how results of damage surveys can be transformed and incorporated in the scale.)

Since vulnerability is something which is very difficult to quantify in such a way as to be useful to the user of the scale, it is still necessary to define vulnerability in terms of building type. However, this is done graphically in the Table 1 (part of paragraph 3.1.1) taking into account the fact that vulnerability depends also on other factors such as state of disrepair, quality of construction, irregularity of building shape, etc. For each building type, Table 1 shows the most likely vulnerability class(es) for it, and also the probable range (shown as a dashed line where this is uncertain). To some extent, this table is experimental and may be refined in the final edition of the scale in a light of experience.

Vulnerability of modern engineered buildings, especially those incorporating antiseismic design features, is considered in more detail in Annexe B on Engineered Structures (Buildings). For the purpose of the scale the level of ASD is classified as low (minimal features), medium (improved) and high (meeting all qualifications). It has to be accepted that the level of ASD is mainly ruled by codes/earthquake resistant design regulations and, therefore, is dependent on the seismic zone coefficient of the site and the importance of buildings. It is possible also to classify the level of ASD on the basis of parameters which are directly related to the seismic zone given by national codes, ie on the basis of intensity or base shear.

Commonly the level of ASD should be relatively uniform within one place for which intensity has to be assigned. An investigator commencing a field study of earthquake damage should therefore begin by ascertaining what, if any, building code regulations are in force for the area in question, as this will help to determine the vulnerability level of engineered structures, which should be modified by taking into account the level of regularity, level of quality, serious defects of design and other factors contributing to damage (see Annexe B).

Engineered structures with modern structural systems, not designed against lateral seismic loads, can still provide a certain level of earthquake resistance which can be comparable to the level incorporated in engineered buildings with ASD. Also, structures designed against high levels of wind loading can be regarded as having inherent earthquake resistance. Well-built (non-engineered) wooden or masonry structures can behave in a fashion comparable to buildings with ASD typical for vulnerability classes D, E or F. In the case of these buildings the appropriate selection of vulnerability class should be made on the level of quality (strength of materials and workmanship) and the

regularity. These factors, are, of course, equally important for buildings with ASD (see Annexe B).

2.1.3.2 Damage grades

The damage grades are also something of a compromise - grades 1-5 should ideally represent a linear increase in the strength of shaking. They do this only approximately, and are heavily influenced by the need to describe classes of damage which can be readily distinguished by the operator. A point which has not been made in previous versions of the scale is that different types of building respond and fail in different ways, and this has been addressed in the present draft by giving separate, illustrated accounts of damage to both masonry and reinforced concrete houses.
One should note the difference between structural and non-structural damage. When examining a damaged reinforced concrete building the level of damage to non-structural brick infills should be compared to the actual structural damage to the frame elements of the building.

2.1.3.3 Quantities

The use of quantitative terms ("few", "many", "most") provides an important statistical element in the scale. It is necessary to confine this statistical element to broad terms, since any attempt to present the scale as a series of graphs showing exact percentages would be impossible to apply in practice and would destroy the robustness of the scale. But defining these terms numerically is not very easy. If few-many-most are defined as three contiguous ranges of percentages (e.g. 0-20%, 20-60%, 60-100%), the undesirable effect occurs that a small percentage increase in some observation may in one case cross a threshold value and put the intensity up by one degree, whereas in another case the same increase will not cross a threshold and so not have the same effect. Broadly overlapping definitions (0-35%, 15-65%, 50-100%) cause problems of ambiguity for an observed value (e.g. 25%) and widely separated definitions (0-20%, 40-60%, 80-100%) cause similar problems where a value may be undefined. A compromise solution has been found for this draft of the scale, using narrowly overlapping definitions, but no solution is ideal. The objective here has been to try and maximise the robustness of the scale, and the definitions of quantity presented here should be used with this in mind.

Scientific Technical Report STR 95/TK
DOI: 10.2312/GFZ.b103-95tk7

2.2 Assigning intensity

The descriptions under each degree of the intensity scale are idealised "word-pictures"of the effects to be expected at each level of intensity. Each effect described in the scale may be considered a diagnostic, or test, against which the data can be measured. This cannot be applied too rigorously, though. It is usually not practical to set up rigid formulae to apply to the data, since it is not to be expected that all diagnostics will be satisfied by the data in all cases.

While there is an element of subjectivity in assigning intensity, experienced investigators will rarely find significant disagreements with one another. It is impossible to establish guidelines to cover every eventuality, but the following may be helpful.

In addition, two examples of intensity assignment are presented in Annexe D, one from documentary data and one from questionnaire data. These examples are not intended to be models to be followed rigidly, but rather as illustrations of the processes of evaluation that can be used.

2.2.1 Intensity and place

Intensity is essentially place-related, and normally can only be considered with reference to a specified place, e.g. "the intensity at Pienza was 5" (or more correctly, "the intensity at Pienza was assessed as 5"). To say, "the intensity of the earthquake was 8", with no indication of place, is an improper usage. It should better be formulated as, "the maximum intensity of the earthquake was 8".

The question of how large or small a place may have an intensity assigned to it is important, and not easy to answer definitively. The problem arises because of the well-observed fact that shaking varies considerably, and rather capriciously, over small distances. Thus in two adjacent houses, apparently identical in circumstance, it may be that an earthquake will be felt strongly in one, and not at all in the other, or that one will be severely damaged while the other sustains little or no damage.

The concept of intensity revolves around the idea that some level of severity of shaking is characteristic for a particular place, and this entails, firstly that the settlement is large enough for a statistically significant sample to be obtained, without being unduly affected by small-scale local peculiarities, and secondly, that it is not so large that genuine local variations are not blurred over.

Thus intensity should not be assigned to a single building or street; neither should a single intensity be assigned to a metropolis or a county. In general circumstances, the smallest place should be no smaller than a village, and the largest no larger than a

moderately-sized European town. Thus it is reasonable to assign a single intensity value to, say, Siena, but not to Milan. It would be better to divide Milan up into separate suburbs. No rigid rules will be stated, since individual circumstances will influence the user in the decisions he makes in particular cases.

It is also desirable to assign values to locations which are reasonably homogeneous, especially with regard to soil types, otherwise the range of shaking effects reported may be very large. In this respect, Siena is not such a good example. However, this is not always practicable, depending on the precision in the data and how they were gathered. In the case where a town has areas in which the geotechnical conditions are very different (for instance, one half might be on an alluvial bank but the other on a plateau) then different intensity values should be assessed for the two parts of the town independently.

2.2.2 Establishing the grade

In real life, the data available will often not match the intensity grade descriptions in every aspect. In such cases, the investigator must decide which degree provides the best fit to the data he has. In doing so, it is important to look for an element of coherence in the data overall, rather than to rely on any one diagnostic as a yardstick. It is necessary to be wary of giving too much weight to the occasional extreme observation, which might lead to an overestimation of the intensity at the place in question.

Where the data consist of questionnaires from individuals, or individual field observations, these data should be combined for each place to determine in how many instances a diagnostic was or was not observed.

Where the data consist of other descriptions, the effects may be reported in terms far from the wording of the intensity scale. In such cases, it may be useful to consider whether the overall tenor of the description compares with the general character of a degree of the intensity scale.

2.2.3 Use of negative information

Information that an effect definitely did not occur is often just as valuable as information that it did occur when determining intensity, and such data should not be neglected. However, to assume that an effect did not occur because it was not reported is dangerous and invalid unless there are specific reasons why such an assumption can be justified.

Scientific Technical Report STR 95/TK
DOI: 10.2312/GFZ.b103-95tk7

2.2.4 Reliability and data samples

A point which is important but often neglected, is that the macroseismic data available to the user is never, or very rarely, a complete record of the effects that occurred during an earthquake. When a town with 20,000 buildings in it is shaken by an earthquake, each one of those buildings will be affected in one way or another. The user may have data from only some few tens on which to base his assessment. In other words, his data are a sample from a complete population of observed effects. It is thus valid to ask: is this sample actually representative of the population as a whole or not?

The smaller the number of reports, in absolute numbers, the greater the error there is likely to be in the proportion of observers reporting a certain effect, compared to the true proportion that would be observed over the whole town. If the data have been gathered with proper attention to random sampling techniques, then it is possible to calculate statistically this error in the sample. Unfortunately, this is usually not the case. It is recommended that those who are involved with gathering and studying macroseismic information should make themselves acquainted with the questionnaire and sampling methodologies that have been developed in the social sciences.

The user may not be able to improve the reliability of his data, but he should at least have an idea of what the reliability is, and be able to communicate this; either by qualifying statements, inclusion of sample sizes, or by the use of typographical conventions such as using a smaller font to indicate intensities derived from weak samples.

The problem is likely to be less severe, and may hardly arise at all, in cases where the user has direct control of his data gathering by means of a field investigation. It may be very severe where the data are received second or third hand. A sweeping remark by a journalist about the severity of effects in a town may be based on very little investigation; the report of one observer may be rewritten as if it was typical when in fact it was not. This is often a particular problem with studies of historical earthquakes where the user is dependent on relatively few data which have chanced to survive.

An example may illustrate the point. Suppose the only information from a certain town is that many people found it hard to stand. This is a diagnostic for intensity 7, but without the support of any other diagnostics, is an assignment of intensity 7 justified? It is difficult to lay down precise guidelines as to what is, and what is not, sufficient evidence on which to base intensity assessment. A useful approach when the data are poor is to mark intensity assessment based on potentially unreliable data, using 7? or (7) or some similar form.

2.2.5 Reliability and uncertainty

It will often be the case that no single intensity degree can be decided upon with any confidence. In such cases, it is necessary to decide whether some approximate assessment of intensity can be made, or whether the data are so contradictory that it is better to leave the matter unresolved.

In cases where the data fulfill and exceed the descriptions for intensity 6, but clearly don´t fulfill completely those for intensity 7, the best case is to treat the intensity as being the lower value. The descriptions given in the scale should be viewed as thresholds. If the effects of an earthquake at a particular place can be considered as passing the threshold for intensity 6, it may be considered that that intensity has been reached; if the threshold for intensity 7 is not passed, then the intensity may not be considered to be 7. It is recommended that the user preserves the integer character of the scale, and not uses forms such as "6.5" or "6½" or "6+". It is doubtful if any greater resolution of intensity is either necessary or realisable in practice. If it is felt to be essential for some reason to present more detail then it should be shown in a descriptive manner.

Example: in a village with 100 (masonry) houses, 15 of them, assessed as vulnerability class A, suffer damage of grade 1, 14 other A class houses suffer damage of grade 2; 19 houses, assessed as vulnerability B, suffer damage of grade 1, 9 other B class houses suffer damage grade 2. If damage alone is considered, there is more than enough to justify intensity 6, but not enough to justify intensity 7. The intensity is 6.

There may still be cases where the data can be interpreted equally well as (for example) 6 or 7 (but clearly not 8). In such cases the intensity should be written as 6-7, meaning either 6 or 7; it does not imply some intermediate value. Expressing intensity as a range of values is now quite common practice, especially for historical data which are frequently insufficient to permit better resolution. Wider ranges than spanning two degrees of the scale are possible; it would be possible to write 6-8, and this does *not* mean 7.

Example: a document says, "in our town chimneys fell down but no houses were seriously damaged". In this limited report there is no indication what was the percentage of chimneys that fell, so the intensity might be 6 or 7; the statement that there was definitely no serious damage indicates that the intensity was not 8. The intensity is 6-7.

Vague assignments, such as <6 (less than 6) or >7 (more than 7) are acceptable when no greater accuracy is possible.

Example: a document says, "there was a lot of damage at Cortona". If no other information can be obtained, the intensity is > 6.

A further problem is caused by ambiguity in the data; for example, effects on humans

Scientific Technical Report STR 95/TK
DOI: 10.2312/GFZ.b103-95tk7

may only suggest intensity 6, while effects on structures suggest intensity 8, or vice versa. If this problem occurs consistently, it may indicate some significant regional or cultural factor is at work (people more easily alarmed; very poor local construction techniques) which should be taken into consideration. When applying the scale, when individual cases of this sort of problem occur, if no coherence can be discerned then it is necessary to express intensity as a range, as discussed above.

There will always be cases where the data are so devoid of detail, or so completely contradictory or incredible that no assignment can be made. In such cases, it is necessary to adopt some convention to indicate an observation, for example, a dot, or an F for "felt" and make no assignment. If necessary, an explanatory footnote can be attached. Example: a chronicle states, "this earthquake was also at Ravenna, Ancona and Perugia". No intensity can be assigned to these three places, but it should be recorded that the earthquake was felt there with some appropriate symbol. Note that it is not even known whether there was damage or not on this limited information.

2.2.6 Notation

It used to be regarded as conventional that intensities be notated in Roman numerals, either to distinguish them more clearly from magnitudes or to stress the integer nature of the scale. Since Roman numerals are hard to handle by computer, this convention has to some extent lapsed. The use of Roman or Arabic numerals may now be considered a matter of taste.

There also exists a set of conventional symbols for plotting intensities, based on circles in which an increasing amount is filled in with higher intensity values. These symbols are in routine use in Eastern Europe, but not much elsewhere.

2.3 Assessing intensity from historical records

2.3.1 Historical and documentary data

The term "historical data" is frequently used to mean descriptions of earthquake effects from historical records, that is, written sources prior to the instrumental period (before 1900). It must be stressed, however, that important macroseismic data of the same kind are still available, and used, for earthquakes of the present century, and even for very recent events.

It is therefore practical to consider historical records and modern written evidence together as "documentary data". This term is used here to differentiate descriptions of earthquake effects written for non-seismological purposes from questionnaire data gathered under the guidance of seismologists. These data need to be retrieved and interpreted according to historical methods, irrespective of whether they relate to the 1890s or 1980s.
Retrieving and handling documentary records requires care and expertise, as a large amount of recent literature shows. In particular, the investigator who processes documentary records must be aware that the information has often arrived at him after a long and complicated itinerary. It is of great importance, therefore, to start by considering the context of the data in both historical, geographical and literary terms.

Particular attention should be paid to the following points:
(i) The value of the source, considering the motivation for writing and the context in which it has been produced. What is the sensitivity of the source to earthquakes and other natural events? (For example, at lower intensities a personal diary is much more likely to record an earthquake than the minutes of a town council.)
(ii) The context in which the report appears may contain significant information, and should not be ignored. For instance, a book may contain a short description of earthquake effects in one chapter, but include details that correct this information in some respect elsewhere in the volume. If the earthquake report is extracted in isolation, this qualifying information, which may be vital, will be lost. The nature of the wording is also important, and information should not be precised in such a way as to remove the nuances of the original.
(iii) The spatio-temporal location of the information. This is very important: careless handling here can result in duplication of earthquakes, data on one earthquake being attributed to a different event, or to the right earthquake but in the wrong location. In some cases, data cannot be adequately resolved with regard to place or time or both - in such cases, this has to be clearly indicated when the data are mapped.

2.3.2 Building types (vulnerability classes) in historical records

Historical accounts often report in detail damage to special monumental buildings (castles, churches, palaces, towers, pillars, and so on). Less frequently do they report the effects on ordinary buildings, which are the only ones which can be used within the framework of the scale. The first kind of data will be discussed below in section 2.3.5, as these buildings pose special problems.

Scientific Technical Report STR 95/TK
DOI: 10.2312/GFZ.b103-95tk7
GeoForschungsZentrum Potsdam

With regard to ordinary buildings, the vulnerability classes of traditional houses range in most cases from A to B, even to C and D (wooden structures). Very little is known from the general literature about building typologies in Europe up to the 17th century, except for the obvious facts that people used the materials nearest to hand, and that the richer the owner, the better-built and better-maintained his house was likely to be. But in the Middle Ages, certainly, most houses in many parts of Europe were made of wood, and the transition to brick or stone was long, and sometimes only partial. Without detailed information, it is very difficult to make any reliable pronouncement on the strength of these structures; it is not certain, for instance, if medieval timber structures were as strong as those known today.

Some methods of resolving this problem can be suggested - for instance, if it is believed that the housing type at a particular place and date was either vulnerability class A or B, it is possible to assign intensity assuming A, make a second assignment assuming B, and then use the range of values given by the two assignments. Or it may be possible to consider other cultural factors; if there is evidence that structures were weaker in poor rural areas than in wealthier towns, it may be reasonable to assume vulnerability class A in hamlets and B in towns.

2.3.3 Total numbers of buildings

In order to assign intensity using the percentage of houses damaged, it is necessary to know not only how many houses were damaged, but also how many were not damaged. The sources of data that describe the damage do not systematically (or often) carry this sort of information also. However, information on the total number of buildings in a locality can often be obtained with some success by investigating other kinds of sources, such as demographic studies, topographical works, census data, and so on. In some cases, reliable figures can be found without difficulty. More frequently it is necessary to make use of extrapolations based on population data with various assumptions and correlations. These figures will carry some uncertainties which have to be taken into account when assessing intensity, often leading to uncertain - but still useful - estimates. An additional complication is that the figures available may relate to the territory surrounding a small town, including some villages, hamlets, and isolated houses, although the wording suggests that it is the town itself that is being described. The descriptions of damage can suffer from the same problem. Whether or not this problem can be resolved in individual circumstances, it is as well to recognise that such a situation can lead to misinterpretations of ± 1 degree. In such cases it is probably better to stick to a range of intensities such as 7-8, etc.

2.3.4 Quality of descriptions

Documents reporting earthquake effects, depending on their nature, often concentrate on the most remarkable or newsworthy effects to the exclusion of all other details. The silence of a source with respect to minor effects can be due to a number of factors, and cannot be used as if it was proof that nothing happened other than what is described. Similarly, converse assumptions are also invalid; for instance, there is little sense in making such extrapolations as, "if the bell tower was thrown down, then at least some minor damage should have occurred to most of the other buildings". The only way to improve the data is by further investigation (and this may be simply unsuccessful). Information produced a few days, weeks, or even months after the earthquake, from the same or other sources, can be illuminating, either supplying new damage data or indirect evidence of the effects. For instance, evidence that life in a locality is going on much as usual after an earthquake - people are still living and working in their houses, the town council meets as usual, religous services continue - then this may be considered to be contradictory with a description of damage leading one to believe an intensity of 9.
If the data remain poor after all avenues have been exhausted then one must take it as it is and assess intensity with an uncertainty range that properly represents the poorness of the data. A good procedure is to keep a record of how decisions have been reached.

2.3.5 Damage to monumental buildings

Damage to monumental buildings is usually better represented in documentary sources than damage to ordinary houses, for two good reasons:
(i) These buildings are more important to the writers of such reports because of their social, economic, symbolical or cultural value.
(ii) The structural and non-structural complexity of such buildings is such that they may be more likely to be damaged than ordinary buildings, even though they may be better built. This is the case, for instance, when small architectural decorations are dislodged from churches during earthquake shaking which is generally below the level at which damage occurs. One should be careful not to overestimate intensity as a result of such effects .
Monumental buildings are usually unique, or only a few such buildings occur in one place. Therefore it is impossible to use the data relating to them in a statistical way as the scale requires. Such data must therefore be handled with care, as complementary to other evidence (if available). If only data of this sort are available, intensity ranges

Scientific Technical Report STR 95/TK
DOI: 10.2312/GFZ.b103-95tk7

should be used to indicate the uncertainty in interpretation.
In some cases, where very detailed damage descriptions are given for a building which still stands and can be investigated, or for which there are detailed descriptions, useful conclusions can be drawn about the earthquake shaking by making a specialist analysis.

2.4 Restrictions in the use of intensity

2.4.1 Tall buildings and other special cases

In some cases it may be inadvisable to attempt to use certain data for assigning intensities. A particular case in point relates to observations from high buildings. It is well-known that people in upper stories are likely to observe stronger earthquake vibration than those in lower stories. Various practices, such as reducing the assigned intensity by one degree for every so many floors, have been suggested, but never found general favour. Also, since very tall buildings may behave under earthquake loading in particular ways according to the frequency of the shaking and the design of the building, the increase of severity of shaking with elevation may be irregular. The recommended practice is to discount all reports from observers higher than the fifth floor when assigning intensity; although in practice the actual behaviour of individual buildings will vary considerably, especially dependent on the slenderness of the building. In general, the user should be more concerned with effects observed under normal circumstances rather than in exceptional cases.
As well as the height of buildings, their symmetry and regularity also influences the way they behave in an earthquake. This is particularly true with respect to damage, and affects all types of buildings, not just modern engineered constructions. The more regular and symmetrical the design, the better the building will withstand earthquake shaking. This is considered in more detail in the Annexe on Engineered Structures.
Observations from special structures, such as lighthouses, radio towers, etc, should not be used. Data from observers underground are also not easily comparable with observations made at the surface and should not be used.

2.4.2 Effects of soil conditions

However, in contrast, no attempt should be made to discard or reduce intensity assignments on the grounds that they were influenced by soil conditions. The increase in

shaking due to soil amplification or topographical conditions is part of the hazard to which the built environment is exposed and should not be glossed over. If anomalously strong effects are reported in alluvial areas distant from other areas where strong effects are observed, the correct procedure is to assign high intensities as merited by the effects. It is then possible to interpret these high intensities as due to the soil amplification (although, of course, this may be only one among several contributory causes). Possible exceptions to this generalisation are discussed in the Annexe B on Engineered Structures.

2.4.3 Invalid inferences

A point which follows from the statistical nature of intensity is that no single effect is ever certain. This is important when attempting to infer a negative, rather than a positive conclusion. For example, the existance of a number of ancient slender spires in a particular region might be used to suggest that the overall exposure of the region to past earthquakes was fairly low, but it would be unwise to conclude from a single spire that such-and-such an intensity value had never been exceeded in the locality during the lifetime of the spire.

2.4.4 Observed and extrapolated intensities

Intensity as described in these guidelines refers entirely to a parameter derived from observational data. It is necessary to mention that on occasion intensity values will be encountered which have not been produced from observations at a place, but are extrapolations or interpolations of data from other places. This is most commonly seen in catalogues where compilers have extrapolated from observed values to calculate a presumed intensity exactly at the epicentre of the earthquake.
A discussion of such practices is beyond the scope of these guidelines, but it would be helpful if all intensity values cited which are not derived directly from real observations were distinguished clearly as such.

2.4.5 Correlations with ground motion parameters

Many attempts have been made to correlate intensity to specific physical parameters of ground motion, especially peak ground acceleration, and some early scales actually included equivalent peak ground acceleration values as part of the scale. While it is

Scientific Technical Report STR 95/TK
DOI: 10.2312/GFZ.b103-95tk7

undeniable that the effects observed from which intensity values are deduced are a product of real ground motion parameters, the relationship between them is complex and not amenable to simple correlations; there is also evidence that peak ground acceleration is not the most important single parameter affecting intensity. Correlations between intensity and peak ground acceleration typically show very large scattering, so large as to make the predicted values of limited meaning.
For this reason, no attempt to include a comparative table of intensity and ground motion parameters, such as acceleration, has been made.

2.5 Effects on natural surroundings

Previous versions of the MSK intensity scale, and a number of other intensity scales, include reference to a number of effects on nature which have not been included in this version. It is considered that the evidence is insufficient to establish good correlation between these effects and particular intensity grades. Some general considerations on the limited use which may be made of such effects as well water changes, cracks in ground, landslides, or rockfalls are presented separately as Annexe C.
As a general rule, effects on nature should be used with caution and in conjunction with other effects. Data consisting exclusively of effects on nature normally should not be used for assigning intensities. Such data may be used to confirm intensities suggested by other diagnostics. This means that there is always a problem in estimating intensity in an unpopulated area; at best a range of intensities can be given. This is regrettable, but it is better to admit this restriction than to assign intensities which are too unreliable to be useful.
Care must be taken with the location of effects of this kind; they may occur in the countryside some considerable distance from the nearest town, to which they may be attributed by an imprecise report.

3 MACROSEISMIC INTENSITY SCALE

3.1 Classifications used in the EMS

3.1.1 Differentiation of structures (buildings) into vulnerability classes

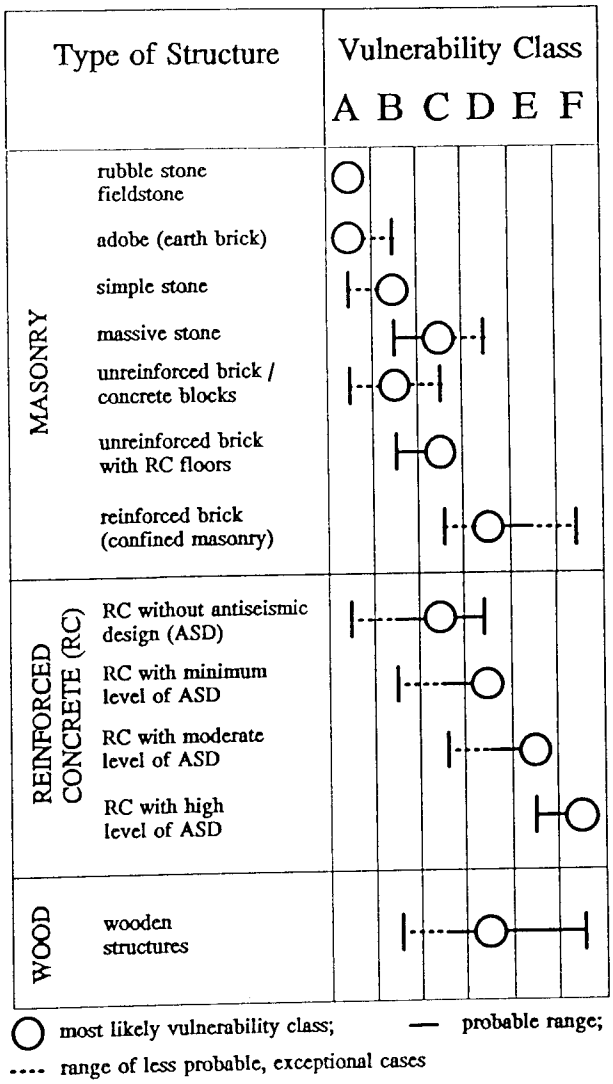

3.1.2 Definition of quantity

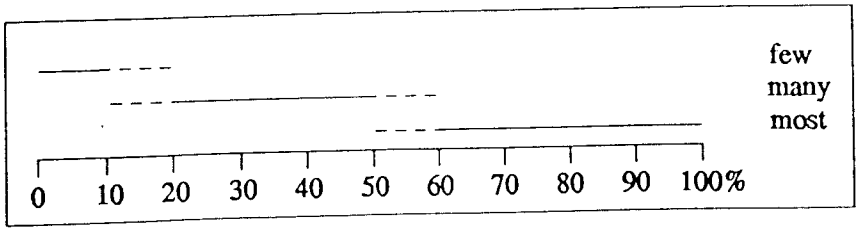

Scientific Technical Report STR 95/TK
DOI: 10.2312/GFZ.b103-95tk7
GeoForschungsZentrum Potsdam

3.1.3 Classification of damage

Note: the way in which a building deforms under earthquake loading depends on the building type. As a broad categorisation one can group together masonry buildings and buildings of reinforced concrete.

Table 2: Classification of damage to masonry buildings	
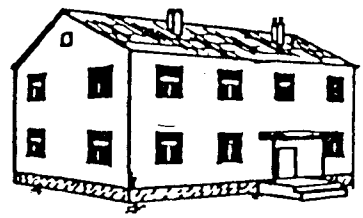	**Grade 1: Negligible to slight damage (no structural damage)** hair-line cracks in very few walls; fall of small pieces of plaster only. Fall of loose stones from upper parts of buildings in very few cases only.
	**Grade 2: Moderate damage (slight structural damage, moderate non-structural damage)** cracks in many walls; fall of fairly large pieces of plaster; parts of chimneys fall down.
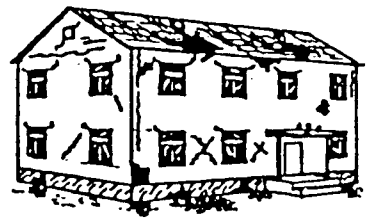	**Grade 3: Substantial to heavy damage (moderate structural damage, heavy non-structural damage)** large and extensive cracks in most walls; pantiles or slates slip off. Chimneys are broken at the roof line; failure of individual non-structural elements.
	**Grade 4: Very heavy damage (heavy structural damage, very heavy non-structural damage).** serious failure of walls; partial structural failure.
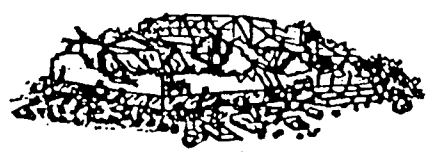	**Grade 5: Destruction (very heavy structural damage)** total or near total collapse.

Table 3: Classification of damage to buildings of reinforced concrete	
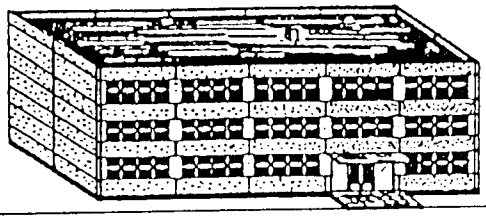	**Grade 1: Negligible to slight damage (no structural damage)** fine cracks in plaster over frame members and in partitions.
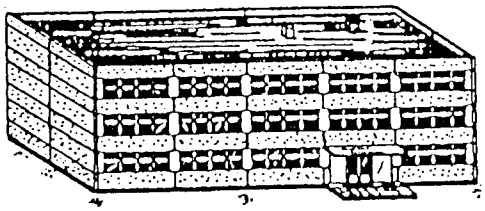	**Grade 2: Moderate damage (slight structural damage, moderate non-structural damage)** hair-line cracks in columns and beams; mortar falls from the joints of suspended wall panels; cracks in partition walls; fall of pieces of brittle cladding and plaster.
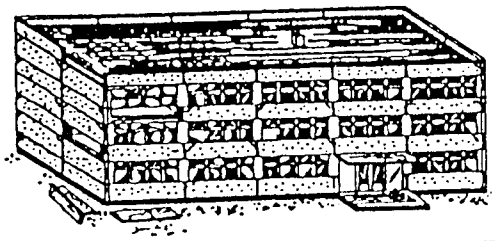	**Grade 3: Substantial to heavy damage (moderate structural damage, heavy non-structural damage)** cracks in columns with detachment of pieces of concrete, cracks in beams.
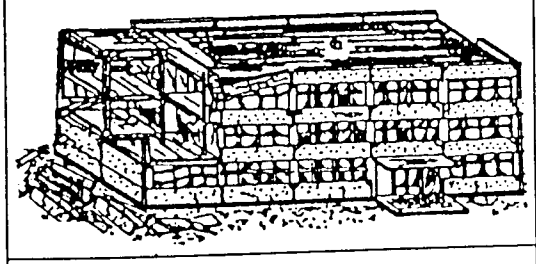	**Grade 4: Very heavy damage (heavy structural damage, very heavy non-structural damage).** severe damage to the joints of the building skeleton with destruction of concrete and protusion of reinforcing rods; partial collapse; tilting of columns.
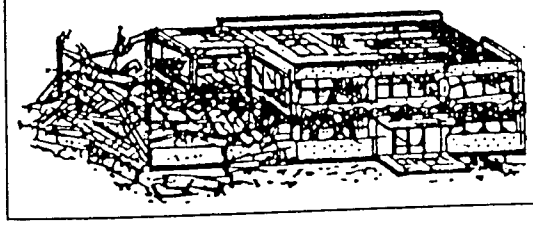	**Grade 5: Destruction (very heavy structural damage)** total or near total collapse.

Scientific Technical Report STR 95/TK
DOI: 10.2312/GFZ.b103-95tk7

3.2 Definitions of intensity degrees

Arrangement of the scale:
a) Effects on humans
b) Effects on objects and on nature
(excluding damage to buildings, effects on ground and ground failure)
c) Damage to buildings

Introductory remark:
The single intensity degrees can include the effects of shaking of the respective lower intensity degree(s), also when these effects are not mentioned explicitly.

I. Not felt

a) Not felt even under the most favourable circumstances.
b) No effect.
c) No damage.

II. Scarcely felt

a) The tremor is felt only by a very few (less than 1 %) individuals at rest and in a specially receptive position indoors.
b) No effect.
c) No damage.

III. Weak

a) The earthquake is felt indoors by a few. People at rest feel a swaying or light trembling.
b) Hanging objects swing slightly.
c) No damage.

IV. Largely observed

a) The earthquake is felt indoors by many and felt outdoors only by very few. A few people are awakened. The level of vibration is not frightening. The vibration is moderate. Observers feel a slight trembling or swaying of the building, room or bed, chair etc.
b) China, glasses, windows and doors rattle. Hanging objects swing. Light furniture shakes visibly in a few cases. Woodwork creaks in a few cases.
c) No damage.

V. Strong

a) The earthquake is felt indoors by most, outdoors by few. A few people are frightened and run outdoors. Many sleeping people awake. Observers feel a strong shaking or rocking of the whole building, room or furniture.
b) Hanging objects swing considerably. China and glasses clatter together. Small, top-heavy and/or precariously supported objects may be shifted or fall down. Doors and windows swing open or shut. In a few cases window panes break. Liquids oscillate and may spill from well-filled containers. Animals indoors may become uneasy.
c) Damage of grade 1 to a few buildings.

VI. Slightly damaging

a) Felt by most indoors and by many outdoors. A few persons lose their balance. Many people are frightened and run outdoors.
b) Small objects of ordinary stability may fall and furniture may be shifted. In few instances dishes and glassware may break. Farm animals (even outdoors) may be frightened.
c) Damage of grade 1 is sustained by many buildings; a few suffer damage of grade 2.

VII. Damaging

a) Most people are frightened and try to run outdoors. Many find it difficult to stand, especially on upper floors.
b) Furniture is shifted and top-heavy furniture may be overturned. Objects fall from shelves in large numbers. Water splashes from containers, tanks and pools.
c) Many buildings of vulnerability class B and a few of class C suffer damage of grade 2. Many buildings of class A and a few of class B suffer damage of grade 3; a few buildings of class A suffer damage of grade 4. Damage is particularly noticeable in the upper parts of buildings.

VIII. Heavily damaging

a) Many people find it difficult to stand, even outdoors.
b) Furniture may be overturned. Objects like TV sets, typewriters etc. fall to the ground. Tombstones may occasionally be displaced, twisted or overturned. Waves may be seen on very soft ground.
c) Many buildings of vulnerability class C suffer damage of grade 2. Many buildings of class B and a few of class C suffer damage of grade 3. Many buildings of class A and a few of class B suffer damage of grade 4; a few buildings of class A suffer damage of grade 5. *A few buildings of class D suffer damage of grade 2.*

Scientific Technical Report STR 95/TK
DOI: 10.2312/GFZ.b103-95tk7

IX. Destructive

a) General panic. People may be forcibly thrown to the ground.
b) Many monuments and columns fall or are twisted. Waves are seen on soft ground.
c) Many buildings of vulnerability class C suffer damage of grade 3. Many buildings of class B and a few of class C suffer damage of grade 4. Many buildings of class A and a few of class B suffer damage of grade 5.
Many buildings of class D suffer damage of grade 2; a few suffer grade 3. A few buildings of class E suffer damage of grade 2.

X. Very destructive

c) Many buildings of vulnerability class C suffer damage of grade 4. Many buildings of class B and a few of class C suffer damage of grade 5, as do most buildings of class A.
Many buildings of class D suffer damage of grade 3; a few suffer grade 4. Many buildings of class E suffer damage of grade 2; a few suffer grade 3. A few buildings of class F suffer damage of grade 2.

XI. Devastating

c) Most buildings of vulnerability class C suffer damage of grade 4. Most buildings of class B and many of class C suffer damage of grade 5.
Many buildings of class D suffer damage of grade 4; a few suffer grade 5. Many buildings of class E suffer damage of grade 3; a few suffer grade 4. Many buildings of class F suffer damage of grade 2, a few suffer grade 3.

XII. Completely devastating

c) Practically all structures above and below ground are destroyed.

ANNEX A

EXAMPLES ILLUSTRATING CLASSIFICATIONS OF VULNERABILITY AND DAMAGE USED IN THE SCALE

The examples of earthquake damage to buildings are classified into the type of structures, their vulnerability classes, and the grade of damage they suffered. The respective vulnerability and damage classes are indicated by a full dot. In cases of unclear relation to a class, an open circle is used to indicate the other possible but less probable class.

It has to be emphasised that it is not intended to demonstrate that the vulnerability class or the grade of damage can be evaluated on the basis of one picture only. Many of the examples were taken from damage inspections. The attached comments to the examples were derived during such inspections and can generally not be recognised from the given examples.

CLASS OF VULNERABILITY						EARTHQUAKE / SITE	GRADE OF DAMAGE				
A	B	C	D	E	F		1	2	3	4	5
●						**Saisan** **East Kazakhstan 1990**		○	●		
TYPE OF STRUCTURE:						**Adobe masonry**					

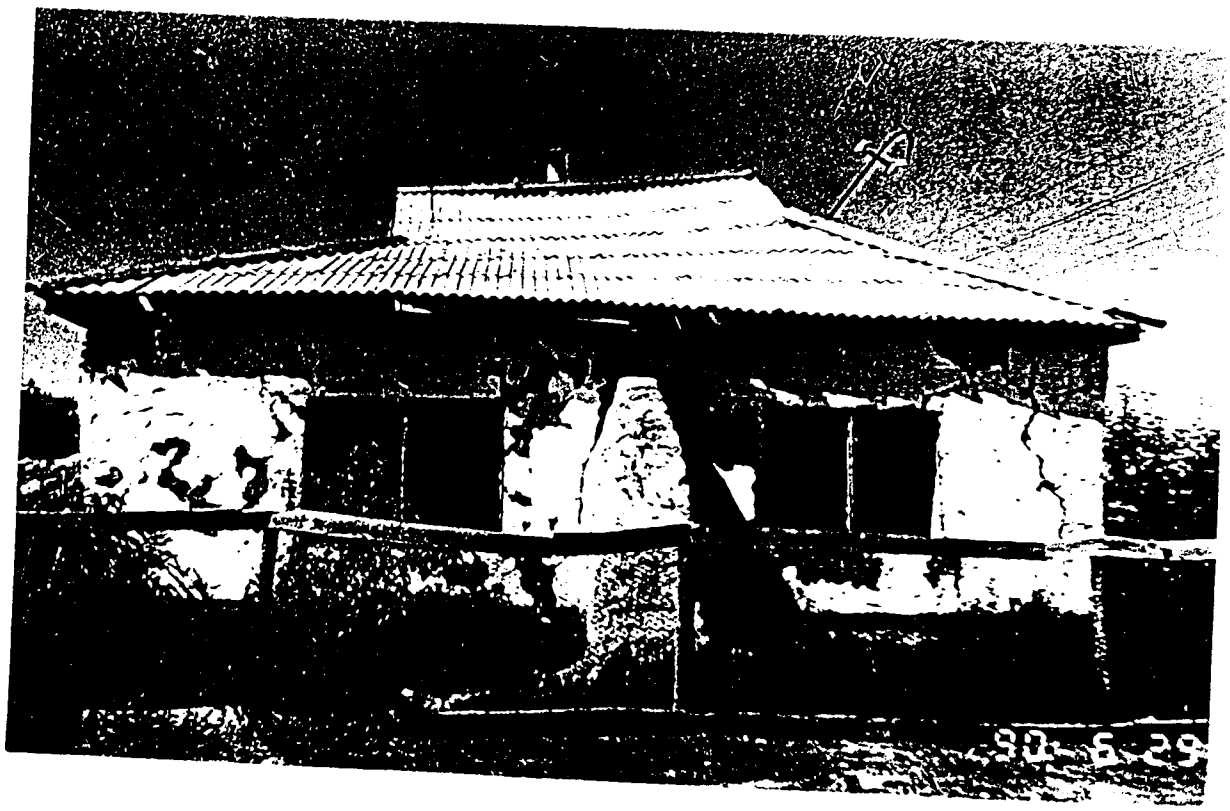

Comment:

Damage of grade 2 to 3; large and extensive cracks in most walls suggest grade of damage 3.

Figure A - 1

CLASS OF VULNERABILITY						EARTHQUAKE / SITE	GRADE OF DAMAGE				
A	B	C	D	E	F		1	2	3	4	5
●						**Moldava, Leovo Carpathia**			○	●	
TYPE OF STRUCTURE:						**Adobe masonry**					

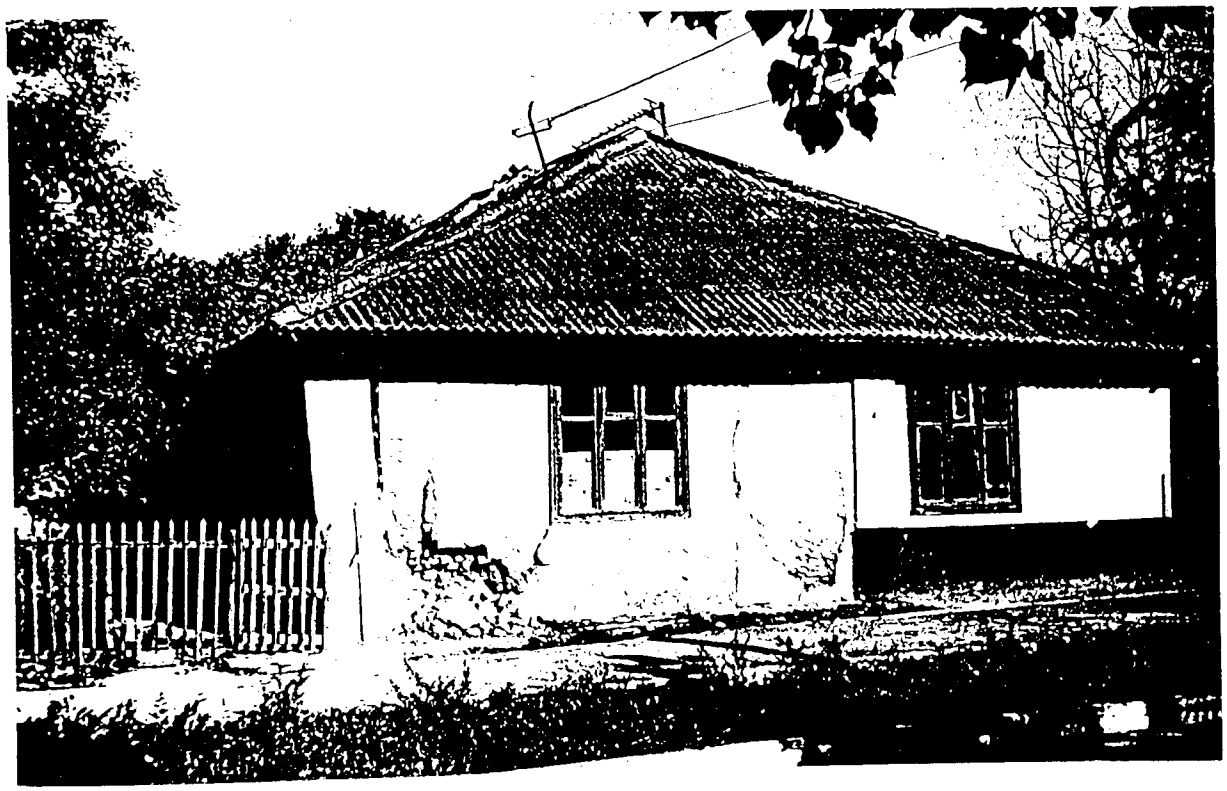

Comment:

Damage of grade 3 to 4; the loss of connection between external walls and the partial failure of the wall at bottom of the corner suggest damage of grade 4 (serious failure of walls).
The right part of the building seems to be without serious damage and is obviously of a better stage of repair. A final classification should consider the reasons for this difference.

Figure A - 2

CLASS OF VULNERABILITY						EARTHQUAKE / SITE	GRADE OF DAMAGE				
A	B	C	D	E	F		1	2	3	4	5
●						**Kairakkoum Tadjikistan 1985**				●	
TYPE OF STRUCTURE:						**Adobe masonry (light roof)**					

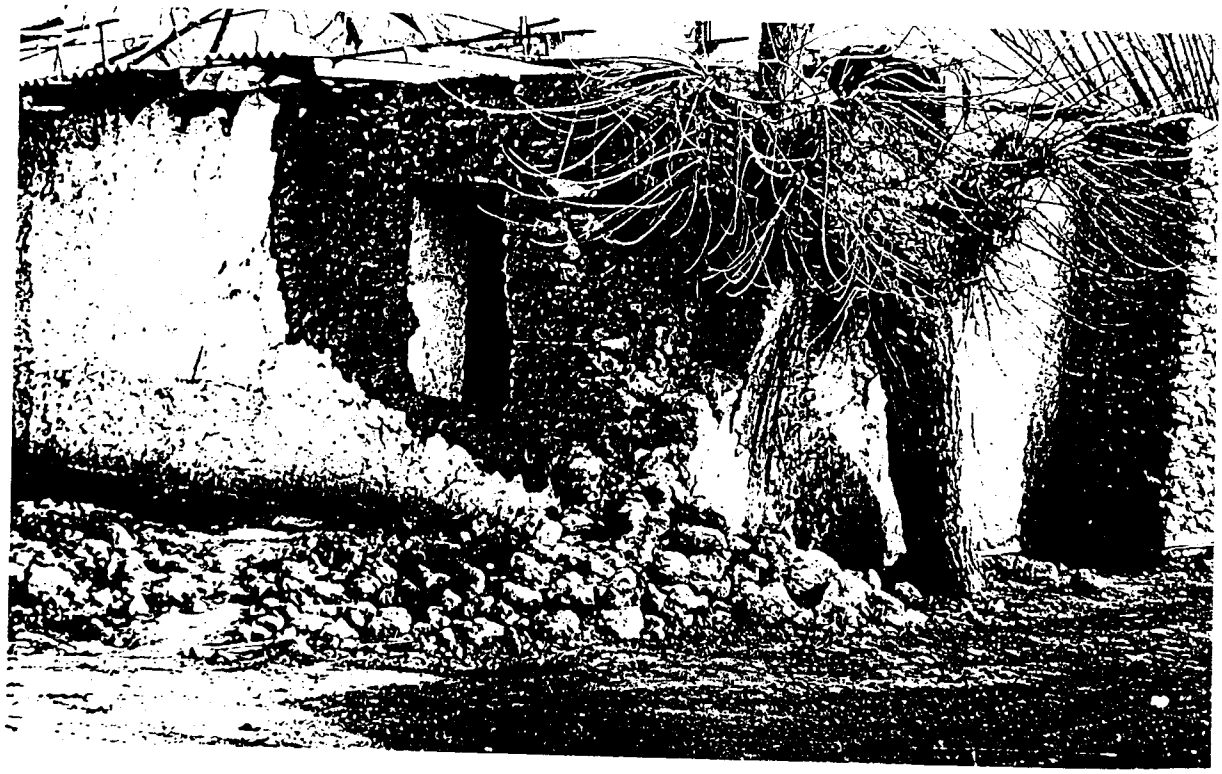

Figure A - 3

CLASS OF VULNERABILITY						EARTHQUAKE / SITE	GRADE OF DAMAGE				
A	B	C	D	E	F		1	2	3	4	5
●						**Balvano Italy 1980**					●
TYPE OF STRUCTURE:						**Fieldstone (in very weak mortar)**					

Figure A - 4

CLASS OF VULNERABILITY						EARTHQUAKE / SITE	GRADE OF DAMAGE				
A	B	C	D	E	F		1	2	3	4	5
●	○					**Kurchum (Saisan) Kazakhstan 1990**			●	○	
TYPE OF STRUCTURE:						**Brick masonry (bad quality)**					

Comment:

Class of vulnerability between A and B; the bad quality of the material, the insufficient strength of primary load-bearing elements (footings) and the lack of sufficient diaphragm action of floor slabs suggest more to vulnerability class A

Figure A - 5

CLASS OF VULNERABILITY						EARTHQUAKE / SITE	GRADE OF DAMAGE				
A	B	C	D	E	F	Kurchum (Saisan) Kazakhstan 1990	1	2	3	4	5
○	●							●			
TYPE OF STRUCTURE:						Brick masonry					

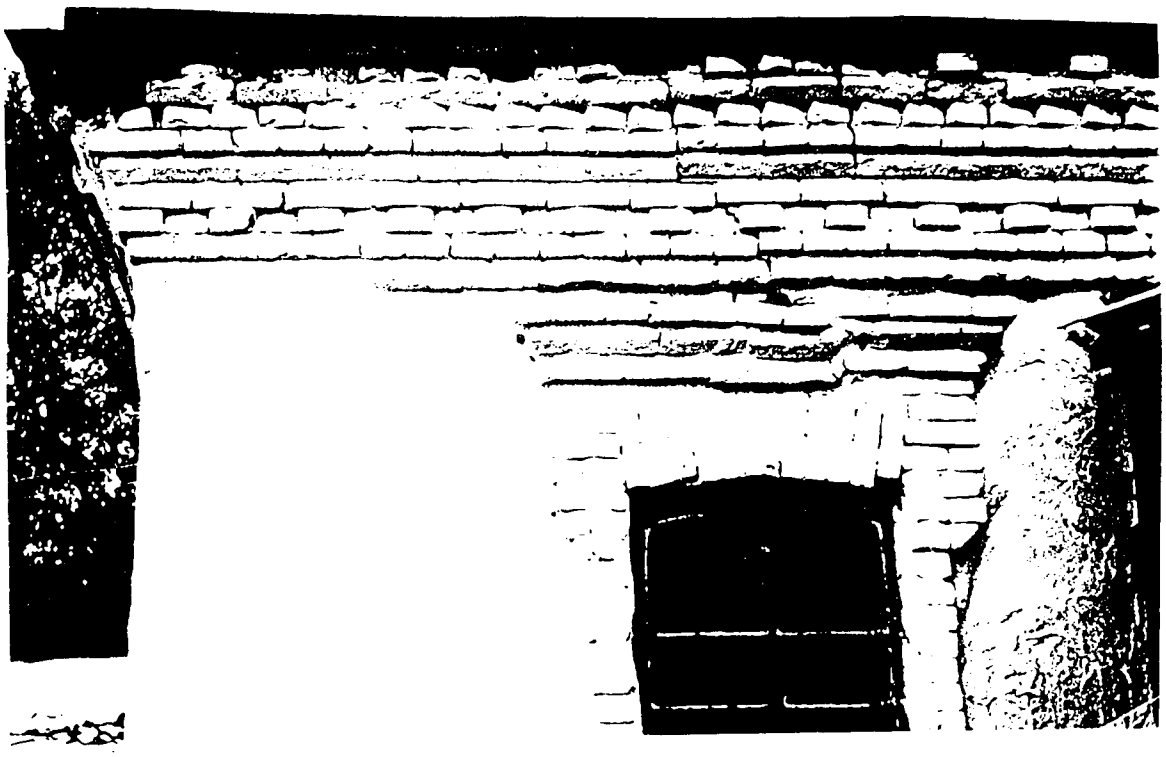

Figure A - 6

CLASS OF VULNERABILITY						EARTHQUAKE / SITE	GRADE OF DAMAGE				
A	B	C	D	E	F		1	2	3	4	5
	●					**Montenegro Yugoslavia 1979**				●	
TYPE OF STRUCTURE:						**Simple stone masonry**					

Figure A - 7

CLASS OF VULNERABILITY						EARTHQUAKE / SITE	GRADE OF DAMAGE				
A	B	C	D	E	F	Montenegro Yugoslavia 1979	1	2	3	4	5
	●	○							●		
TYPE OF STRUCTURE:						Simple stone masonry					

Comment:

Damage of grade 3 (instead of 4): The central wall element at the top which failed is more vulnerable than the whole building. Damage is mainly caused by the transition in the strength of the facing wall, the lack of tie to the two sidewalls and the height above ground. There is no real partial structural failure.

Figure A - 8

CLASS OF VULNERABILITY						EARTHQUAKE / SITE	GRADE OF DAMAGE				
A	B	C	D	E	F	Leninakan Armenia 1988	1	2	3	4	5
	●								○	●	
TYPE OF STRUCTURE:						Stone masonry ("Midis")					

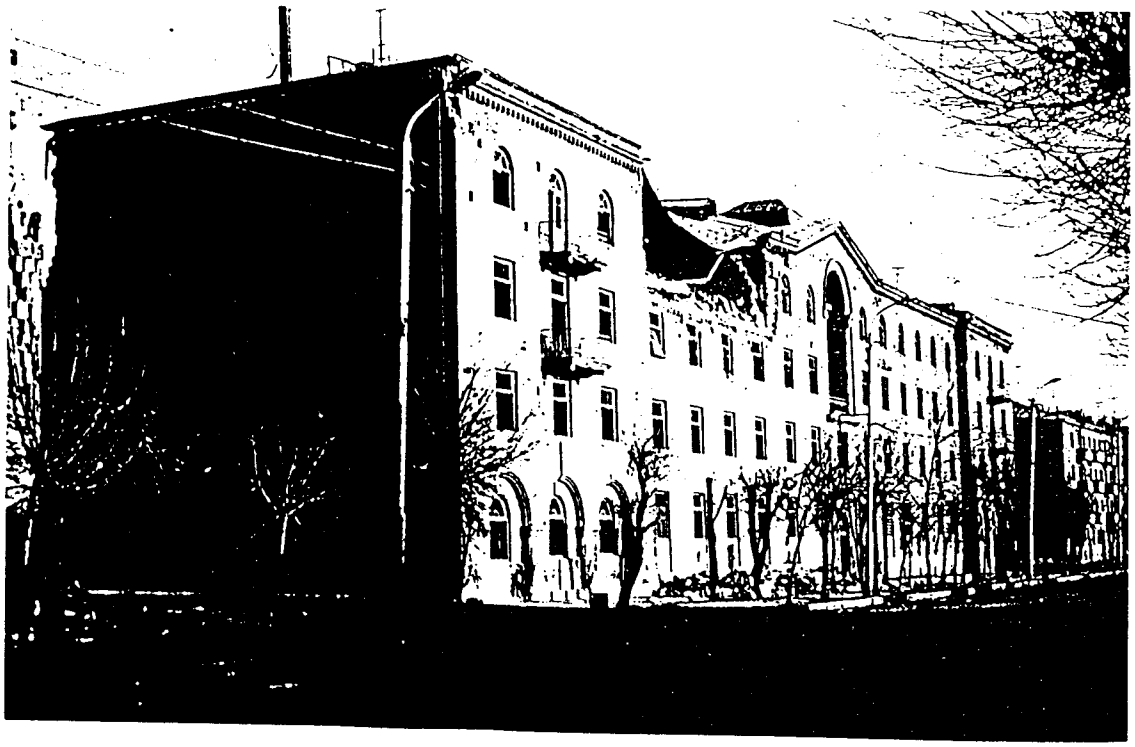

Comment:

Grade of damage between 3 and 4, with tendency to 4: The wall element which failed was more vulnerable than the whole building. Damage is mainly caused by the lack of perpendicular stiffening walls or the length of wall and the height of building.
Damage of grade 4 can be classified: complex failure of external and internal walls and roof, also affecting other parts of the building.

Figure A - 9

CLASS OF VULNERABILITY						EARTHQUAKE / SITE	GRADE OF DAMAGE				
A	B	C	D	E	F	Leninakan Armenia 1988	1	2	3	4	5
	●									●	

TYPE OF STRUCTURE:	Stone masonry ("Midis")

Comment:

Damage is mainly caused by the separation from the outer walls, the absence of ties at the corners and wall connections and the lack of efficient bonding; the longitudinal walls are not affected (see windows) so that an overestimation of intensity should be avoided.

Figure A - 10

CLASS OF VULNERABILITY						EARTHQUAKE / SITE	GRADE OF DAMAGE				
A	B	C	D	E	F		1	2	3	4	5
	●					**Kairakkoum Tadjikistan 1985**		●	○		
TYPE OF STRUCTURE:						**Brick masonry**					

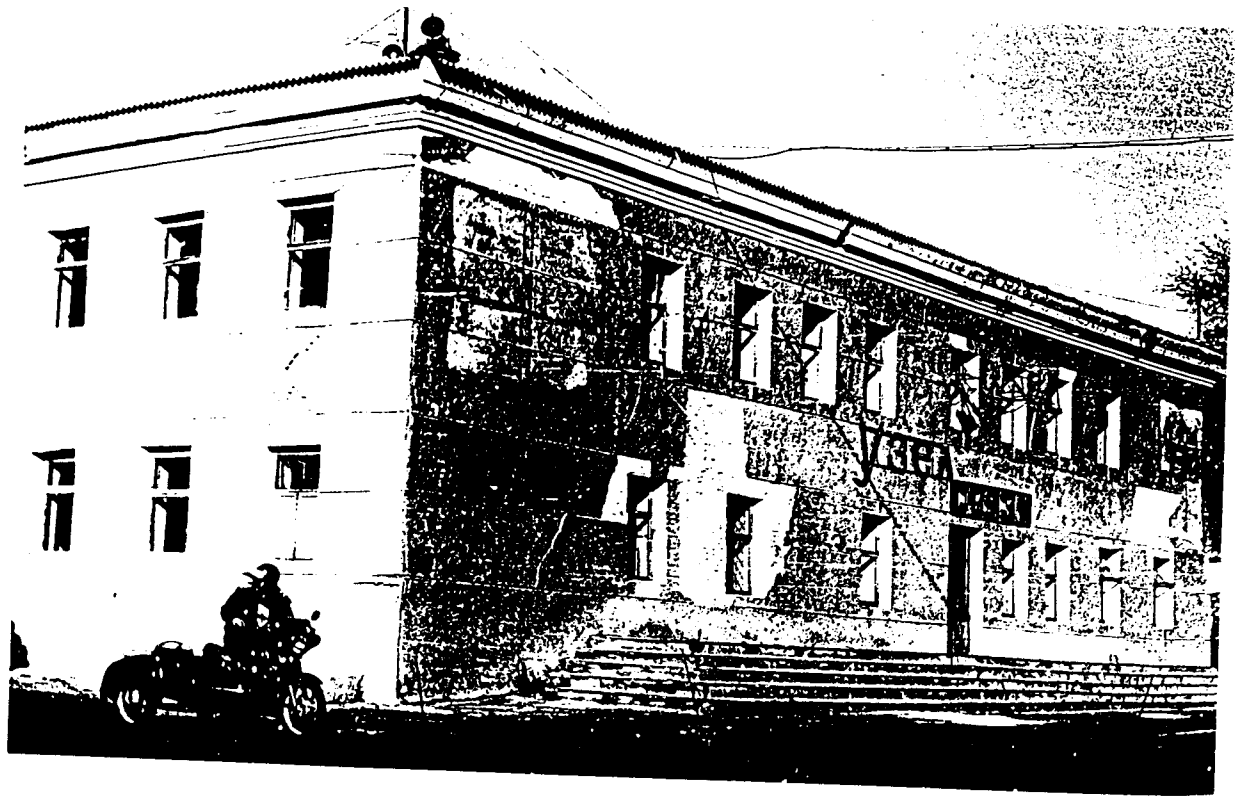

Comment:

Grade of damage between 2 and 3, tending to 2; large and extensive cracks are present, but only in some walls; in regions with falls of fairly large pieces of plaster no significant cracks could be observed; the final decision depends on the entire structure and the damage of inner walls.

Figure A - 11

CLASS OF VULNERABILITY						EARTHQUAKE / SITE	GRADE OF DAMAGE				
A	B	C	D	E	F	Leninakan Armenia 1988	1	2	3	4	5
	●								●	○	

TYPE OF STRUCTURE:	Simple stone masonry ("Midis")

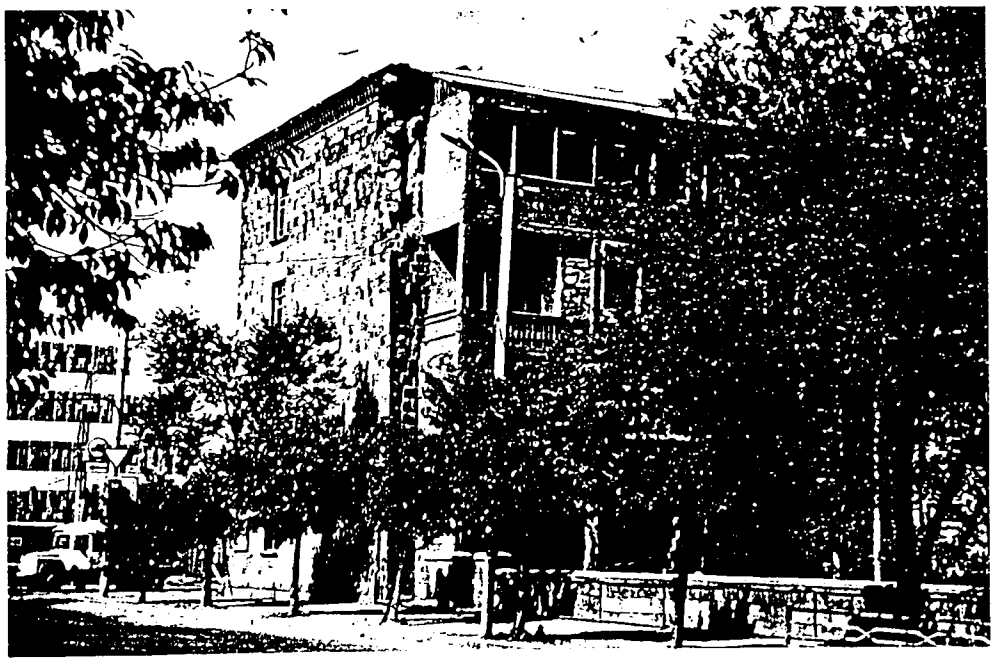

Comment:

System "Midis": partially dressed tuff stone masonry; squared and cut; outer and inner shell; inner surface of stones is uncut to reach better bond (toothing)
(see **Figures A-9, A-10**)

Figure A - 12

CLASS OF VULNERABILITY						EARTHQUAKE / SITE	GRADE OF DAMAGE				
A	B	C	D	E	F		1	2	3	4	5
	●					**Kairakkoum Tadjikistan 1985**			●		
TYPE OF STRUCTURE:						**Brick masonry**					

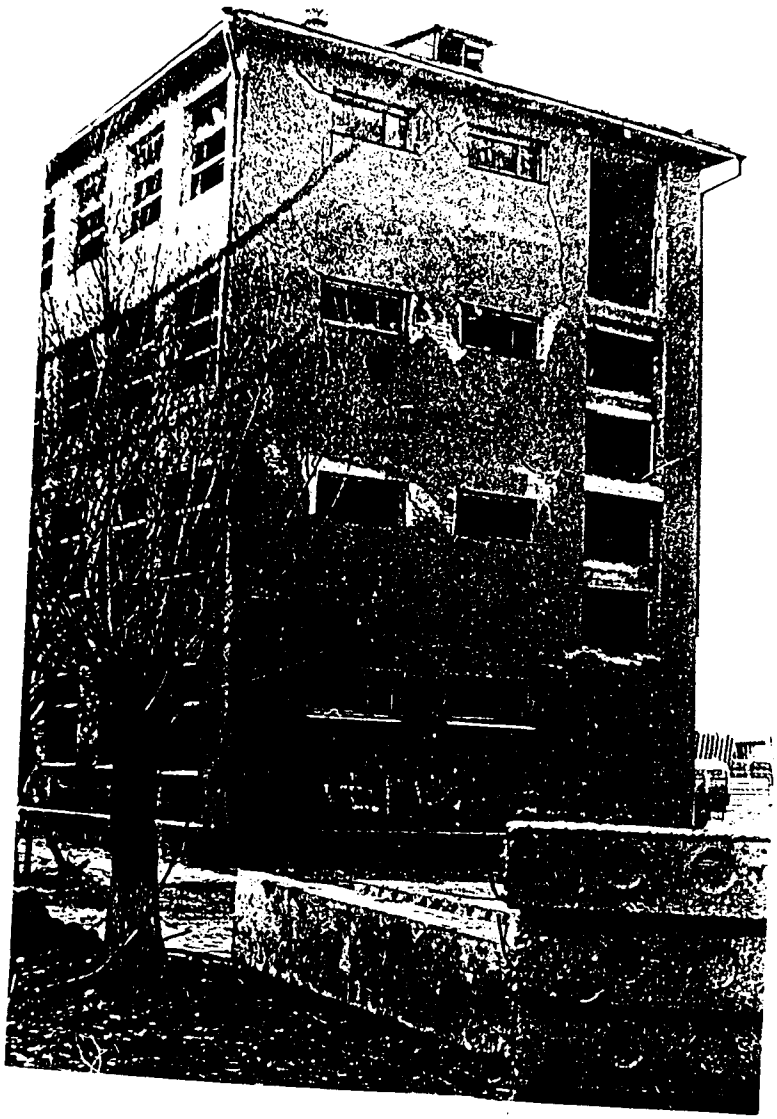

Comment:

Grade of damage 3; large and extensive cracks in most walls

Figure A - 13

CLASS OF VULNERABILITY						EARTHQUAKE / SITE	GRADE OF DAMAGE				
A	B	C	D	E	F	El Asnam Algeria 1980	1	2	3	4	5
		●									●
TYPE OF STRUCTURE:						RC frame and brick infill walls					

Comment:

Clear situation with respect to grade of damage.
The structure was designed against seismic loads (low level of ASD), but there are such serious defects within the design (weak or soft ground floor) that the vulnerability class has to be reduced. Vulnerability class C seems to be appropriate.

Figure A - 14

CLASS OF VULNERABILITY						EARTHQUAKE / SITE	GRADE OF DAMAGE				
A	B	C	D	E	F		1	2	3	4	5
		●	○			**El Asnam Algeria 1980**			●		
TYPE OF STRUCTURE:						**RC frame and brick infill walls**					

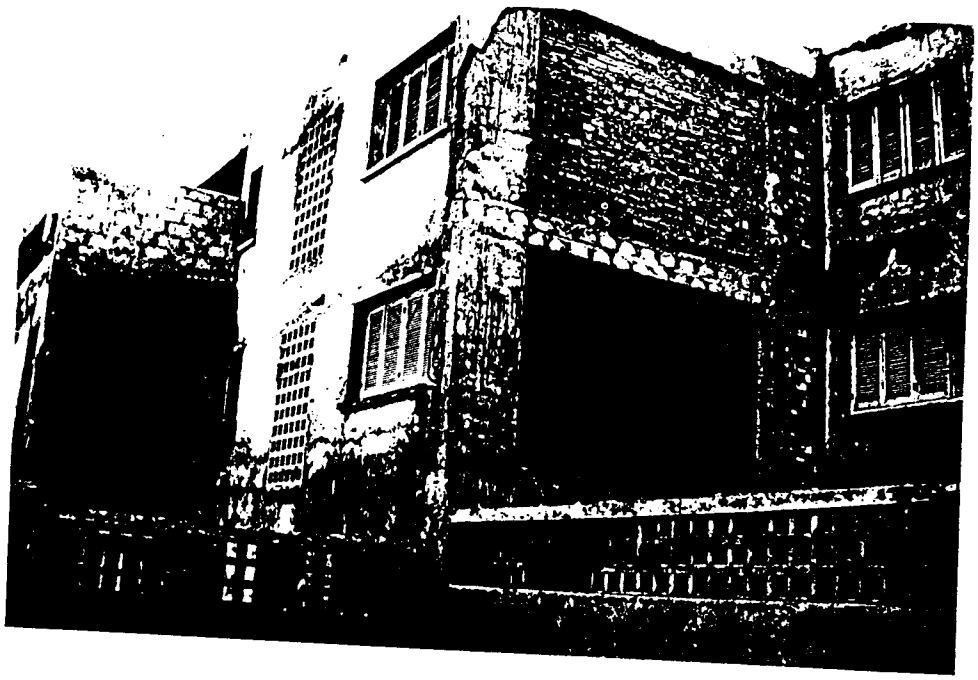

Comment:

Grade of damage 3: The outer shell of the brick wall possesses no intrinsic strength and fell off. The figure indicates the bad quality of bonding and only heavy damage on nonstructural elements; there are no remarkable cracks in the plaster in other walls. The building has a low level of ASD. It is irregular in ground plane. Vulnerability class C seems to be appropriate.

Figure A - 15

CLASS OF VULNERABILITY						EARTHQUAKE / SITE	GRADE OF DAMAGE				
A	B	C	D	E	F	**San Angelo Dei Lombardi Italy 1980**	1	2	3	4	5
			●	○			●				
TYPE OF STRUCTURE:						**RC frame with moderate level of ASD**					

Comment:

Building with good structural properties: strong columns and brick with high strength lead to a less vulnerable building type.

Figure A - 16

CLASS OF VULNERABILITY						EARTHQUAKE / SITE	GRADE OF DAMAGE				
A	B	C	D	E	F		1	2	3	4	5
	○	●				**Artegna (Friuli) Italy 1976**				●	
TYPE OF STRUCTURE:						**RC frame and brick infill walls**					

Comment:

Building incorporating a medium level of antiseismic design, but with many defects (weak ground floor, heavy roof) leading to very vulnerable structure. Vulnerability class should be B or C depending on the regularity and quality of workmanship.

Figure A - 17

CLASS OF VULNERABILITY						EARTHQUAKE / SITE	GRADE OF DAMAGE				
A	B	C	D	E	F	Campania-Basilicata Italy 1980	1	2	3	4	5
		○	●							●	○
TYPE OF STRUCTURE:						RC structure with moderate level of ASD					

Comment:

Unfinished hospital with moderate level of ASD (base shear of 0.07g according to the building code); the L-shaped (irregular) ground plane suggests a lower vulnerability class.

Figure A - 18

CLASS OF VULNERABILITY						EARTHQUAKE / SITE	GRADE OF DAMAGE				
A	B	C	D	E	F	Mexico City 1985	1	2	3	4	5
		○	●							○	●

TYPE OF STRUCTURE:	RC structure with moderate level of ASD

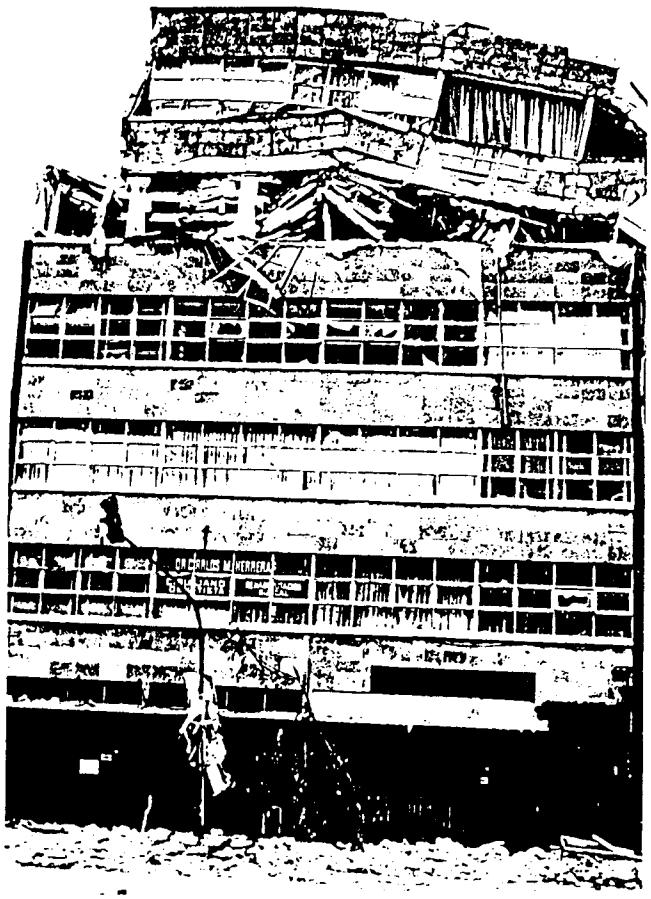

Comment:

RC building incorporating a medium level of ASD, but the vulnerability class is not higher than D: the building is irregular with respect to stiffness distribution (differences in each storey due to the extensive window-bands)

Figure A - 19

CLASS OF VULNERABILITY						EARTHQUAKE / SITE	GRADE OF DAMAGE				
A	B	C	D	E	F		1	2	3	4	5
	●					**Leninakan Armenia 1988**					●
TYPE OF STRUCTURE:						**RC frame with minimum level of ASD**					

Comment:

RC frame structure designed against seismic loads and, therefore, incorporating a medium level of ASD; but a vulnerability class of B has to be taken: insufficient spatial coupling between beams and columns; serious defects in construction, quality of workmanship and strength of material; misinterpretation of seismic hazard and underestimation of seismic loads.

Figure A - 20

CLASS OF VULNERABILITY						EARTHQUAKE / SITE	GRADE OF DAMAGE				
A	B	C	D	E	F	Mexico City 1985	1	2	3	4	5
			●	○					○	●	
TYPE OF STRUCTURE:						RC minimum level of ASD					

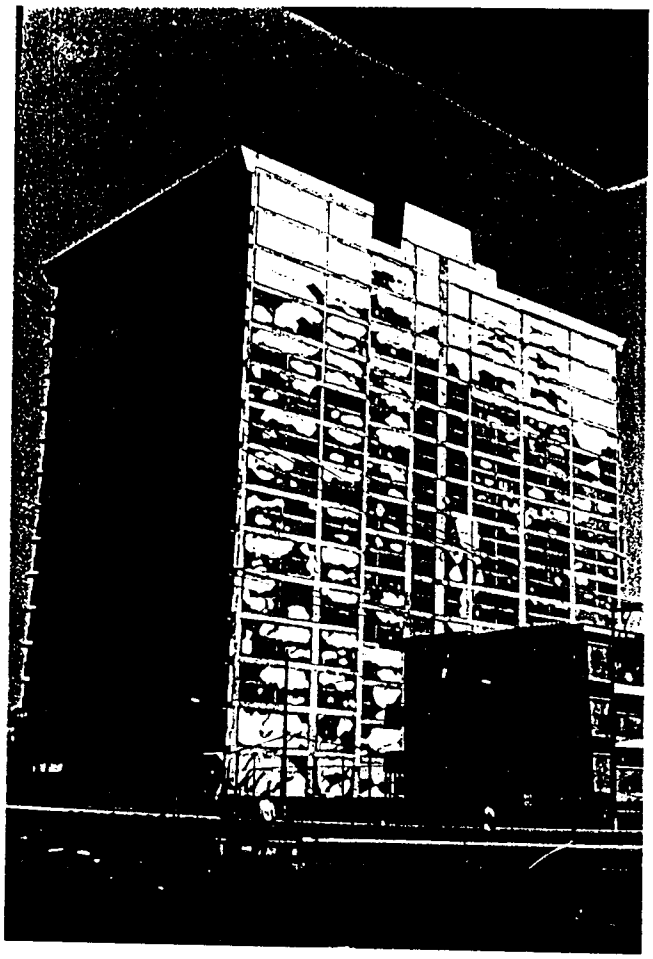

Comment:

RC frame structure incorporating a medium level of ASD, but the system indicates irregularities with respect to the continuity in the line of horizontal beams.
The non-structural damage would suggest a grade of damage between 3 and 4, tending to 3; a detailed internal inspection might increase the damage grade to 4.

Figur A - 21

CLASS OF VULNERABILITY						EARTHQUAKE / SITE	GRADE OF DAMAGE				
A	B	C	D	E	F	San Angelo Dei Lombardi Italy 1980	1	2	3	4	5
			●	○					○	●	
TYPE OF STRUCTURE:						RC frame and brick infill walls					

Comment:

Building with moderate level of antiseismic design. The ground plane is of minor global regularity. The brick infill is not well separated from the load-bearing RC frame, leading to very heavy non-structural damage.

Figure A - 22

CLASS OF VULNERABILITY						EARTHQUAKE / SITE	GRADE OF DAMAGE				
A	B	C	D	E	F	El Asnam Algeria 1980	1	2	3	4	5
				●			●				
TYPE OF STRUCTURE:						RC walls minimum level of ASD					

Comment:

RC wall structure with medium level of ASD. Buildings are under construction. There is only minor damage of grade 1. (The collapsed buildings in front of the photo are from another building type.)

Figure A - 23

CLASS OF VULNERABILITY						EARTHQUAKE / SITE	GRADE OF DAMAGE				
A	B	C	D	E	F	**Kairakkoum Tadjikistan**	1	2	3	4	5
			●	○				●			
TYPE OF STRUCTURE:						**RC (prefabricated) with large panel walls**					

Comment:

RC large panel apartment building with a low level of ASD. The detail shows horizontal cracks in the joint of panels.
During a sequence of different earthquakes in the former U.S.S.R. this type of building suffered only minor damage and justifies denotation of vulnerability class D or higher.

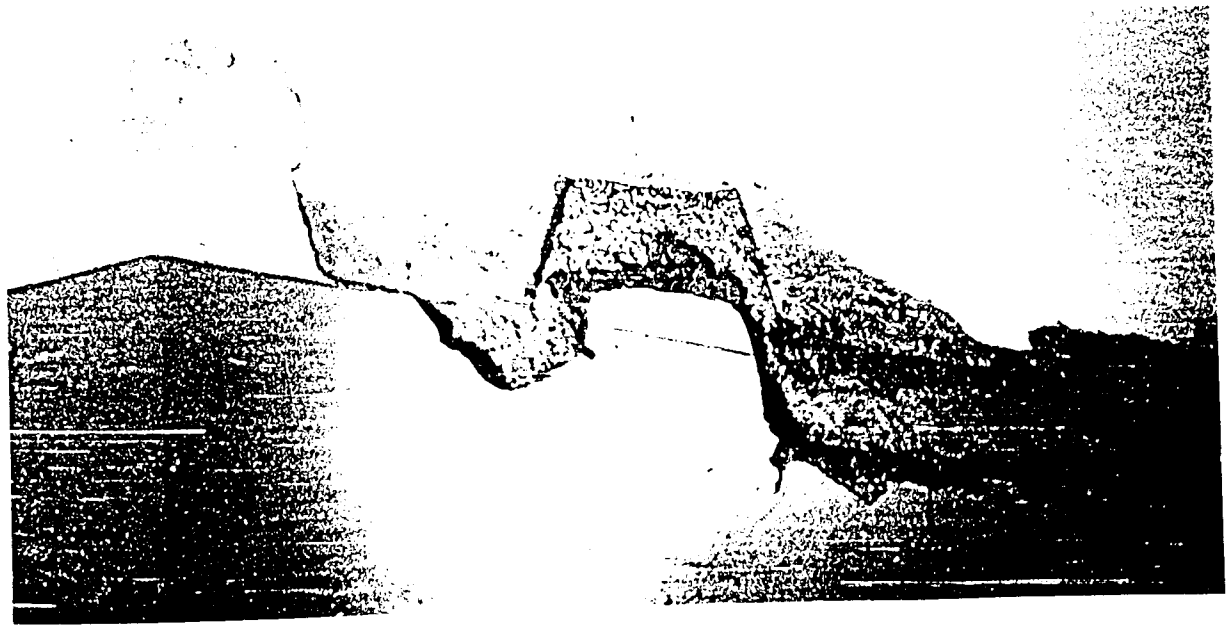

Figure A - 24

References of photographs:

Figures A-1 - 3, A-6, A-9, A-11 - 13, A-24 by E.T. Kenjebaev and A.S. Taubaev (Alma-Ata);

Figures A-4, A-7, A-8, A-10, A-14 - 23 by H. Tiedemann (Swiss Reinsurance Company, Zürich);

Figure A-5 by J. Schwarz (College of Architecture and Cilvil Engineering, Weimar).

ANNEX B
ENGINEERED STRUCTURES (BUILDINGS)

Contents

B.1 Types of engineered structures (buildings)

B.1.1 Introductory remarks (code situation):

The description and classification of engineered buildings can be based on different qualitative parameters.
In seismic codes engineered buildings are subdivided according to
- their **main (primary) structural system** (frame, wall, core or dual systems)
- their **structural material** (steel, reinforced concrete, wooden or masonry) or
- a combination of both (**structural system and structural material**).

Furthermore, engineered buildings are classified according to their
- **importance**
- dynamic characteristics, expressed in terms of **regularity or symmetry**
- ability to withstand seismic loads in the inelastic range, expressed in terms of **ductility**.

For the purpose of scale it is impossible to give a classification of engineered buildings, reflecting differences and refinements within national seismic codes.
Additional types of buildings (structures) are introduced to cover the national differences and to assure direct correlations with intensity scale (see B.1.4).

The performance of buildings is dependent on
- the level of earthquake resistance (quality) and
- the level of regularity of buildings.

and this must be taken into account when evaluating intensity.These parameters should also be considered in the case of buildings that are not antiseismically designed.

B.1.2 Levels of quality

For application of the Annexe B the buildings have to be classified according to their **level of quality.** This means a classification of the level of earthquake resistance has to be introduced, taking into account the quality of workmanship, the strength and quality of material used and the intended level of resistance / protection.

The used **levels of quality** are:
- Q_l : low
- Q_m: medium
- Q_h : high

These levels can differ between different countries. They are also non-uniform with respect to the level and the aims of national earthquake regulations.

Level Q_l is still the dominant level of resistance in most of Europe. The classification of intensity degrees (section B.4) is mainly related to this level.
Level Q_h is typically for countries like Japan or New Zealand and will seldom be reached in Europe.

B.1.3 Level of regularity

With respect to current code developments (Eurocode No 8) engineered buildings have to be classified according to their structural regularity.

The used **levels of regularity** are:
- R_l : low
- R_m: medium
- R_h : high

The **level of regularity** can be defined on the basis of
- global parameters (dimensions, ratios of geometry);
- global and local deviations of regular ground plane and vertical shape;
- parameters of the building, determining dynamic characteristics (stiffness and mass distribution); and
- quality of energy transformation and dissipation, ensured by coupling between ground, foundation and structural elements and by avoiding critical local concentrations of damage (plastic hinges).

Regularity should be considered in a global sense, i.e. regularity is more than just external symmetry in plan and elevation. Regularity in the sense used by this draft includes characteristics of a building and also measures within it to ensure a simple or, in a limited extent, controlled behaviour under seismic action. It is intended that regularity corresponds with rules of earthquake resistant design.

The level R_h, commonly not reached in European countries, should be characterised by
- improved ductility of structural system and
- active controlled mechanism of plastification as result of a special antiseismic measures.

B.1.4 Level of antiseismic design

Introductory remarks
With respect to the quality of antiseismic design engineered structures (buildings) can be subdivided into three main groups:
- Group 1: buildings with special antiseismic measures (base isolated buildings or special structures)
- Group 2: buildings with antiseismic design,i.e. buildings designed and built according to the scope of codes (design philosophy); the seismic hazard assessment and elaborated zoning map (different zones) and the parameters describing seismic action for different seismic zones
- Group 3: buildings without antiseismic design, i.e. buildings designed and built according to modern design principles and codes (concrete, masonry etc.)

Observations from buildings of group 1 should not be used (see also sect. 2.4.1).
Observations from buildings of group 2 can be expected in earthquake regions where the design of buildings has to take into account earthquake resistant regulations.

Observations from buildings of group 3 can be expected in regions with negligible or low seismicity where earthquake resistant regulations are not existent or are present in a still recommendatory manner.

For assigning intensity engineered buildings of group 2 and 3 are considered and further specified.

Definition of type ASD_i

Assuming that buildings in an earthquake zone i are designed and built for a **design earthquake** of the intensity (or ground motion), matching site and subsoil conditions of the zone i, engineered buildings are classified according to the incorporated level of antiseismic design (ASD). The antiseismic design is ruled by national seismic codes.
The level of antiseismic design can be distinguished on the basis of intensity or other design parameters (peak ground motion, base shear) which are directly related to the seismic zone i.
Buildings of type ASD_i are specified for i= 7, 8 and 9; i is an expression for the intensity of the design earthquake.

As an example, a structure of type ASD_7 can be considered to be a structure designed according to seismic code provisions for an intensity of 7, or designed according to seismic code provisions for a design level which is comparable to the level of type ASD_7. In zones of intensity 6 no or only constructional demands will be established.

The types ASD_i can be classified as follows:

Type ASD_7: Engineered buildings incorporating a **minimum level** of antiseismic design.
This level is characterized by the limitation of structural parameters and a simplified method of calculation. Depending on the importance of building it may be permitted to ignore additional seismic loads. Special measures of detailing (to improve ductility) are not typical for this building type. This type is widespread in areas of low or moderate seismicity. (Commonly, buildings of this type are designed for an intensity of 7 or a base shear coefficient of *3 - 4 % g*.)

Type ASD_8: Engineered buildings incorporating a **moderate (improved) level** of antiseismic design.
This level is characterized by the realisation of design rules. Special measures of detailing (to improve ductility) are partially implemented. This type is to be expected in areas of moderate to high seismicity. (Commonly, buildings of this type are designed for an intensity of 8 or a base shear of about *5 - 6 % g*.)

Type ASD_9: Engineered buildings incorporating a **high (qualified) level** of antiseismic design.
Seismic loads are calculated by dynamic methods. Special measures of detailing are provided to ensure a ductile system where the seismic energy is distributed all over the structure and is mainly dissipated in plastic hinges without structural failure. This type should be expected in areas of high seismicity. (Commonly, buildings of this type are designed for an intensity of 9 or a base shear of about *8 - 12 % g*)

Definition of type EASD:
Assuming that engineered buildings of modern structural system and material (reinforced masonry, steel and reinforced concrete frames) and well-built wooden structures, not designed against lateral seismic loads, can provide a certain level of earthquake resistance and assuming that this level can be comparable to the level incorporated in engineered buildings with antiseismic design (ASD_i), buildings of this type are classified according to their level of regularity (sect. B.1.3.) and their level of quality (sect. B.1.2).

Type EASD: Engineered buildings incorporating a **limited or equivalent level** of antiseismic design.

The level of antiseismic design is relatively uniform within an earthquake region for which intensity has to be assigned. The level can be non-uniform when buildings within an earthquake region are designed for different codes (old, up-dated, new).

B.1.5 Importance of buildings

The importance of engineered buildings has to be taken into account for the different levels of antiseismic design (ASD). The importance of a building is determined by the number of occupants or visitors, the use of the building (or the consequences of interruption of the use) or the danger for public and environment in the case of the building's failure.

The classification of importance is not harmonized and also quite different in different European earthquake regulations, and is connected with the definition of seismic load amplifying factors.

In special cases buildings of higher importance are designed for loads which are typical for a higher intensity class. Buildings of high importance or higher risk potential should be carefully considered with respect to the final level of design loads.

B.2 Definition of quantity

Figure B-1 shows the typical frequency distributions of damage grades for damaging intensity degrees without specifying the different types of buildings. The description of intensity is limited to special intersecting points (between the higher grades of damage and the values of damage probability function) of this frequency distribution. In effect, the severity of damage and the probability of its occurrence form a continuum from which sample points (expressed as quantities such as "few", "many" and "most") are used to describe intensity (sect. 3.2).

In the right column of Figure B-1 symbols describing quantities of the probability of

occurrence of damage are introduced (see sect. B.4, **Table B-1**.). As it is illustrated in Figure B-1, intersecting points between the lower grades of damage and the values of damage probability functions are used for assigning intensity degrees.

B.3 Classification of damage

Damage Grades 1 to 5 correspond to those in the core scale (sect. 3.1.3), as given for modern (reinforced concrete) buildings. Locations of damage and damage patterns are different for engineered and non-engineered structures.

One should carefully distinguish between
- damage to the primary (load- bearing/ structural) system;
- damage to secondary (non- structural) elements (like infills, curtain walls);
- damage in special (therefore provided) plastification zones (coupling beams in wall structures, joints in buldings of prefabricated wall elements or beams in joints of frame structures).

The classification of structural damage should be evaluated in the most severely damaged storey of a building. Damage caused by mutual pounding of adjacent building with insufficient separation should not be taken into account.

B.4 Intensity degrees

Note:
The description of intensities is based on the analysis of engineered buildings with earthquake damage (damage surveys) under the following scaling conditions:
- buildings of type ASD_i: a level of regularity of R_m and a level of quality of Q_l
- buildings of type EASD: a level of regularity of R_m and a level of quality of Q_m

The classification of intensities can be based on two approaches.
The **first** approach is consistent with definitions of intensity degrees in 3.2. Therefore, on the basis of the idealised characteristics of ASD_i type structure (B.1.4) the actual level of ASD has to be predicted and has to be expressed in terms of vulnerability classes.

For the assumed scaling conditions it can be stated that:
- type ASD_7 is comparable with the vulnerability class C,
- type ASD_8 is comparable with the vulnerability classes C and D,
- type ASD_9 is comparable with the vulnerability classes D and E,
- type EASD is comparable with the vulnerability class C.

The **second** approach is related to available results of damage surveys. Such results are transformed in Table B-1 for engineered structures (buildings) with a level of regularity

R_m and a level of quality Q_l. Appropriate descriptions for other scaling conditions (i.e. other levels of regularity and/or quality) can be introduced following the scheme given in Table B-1.
Table B-1 provides information about quantities of damage grades for intensity degrees. These, or similar, more representative descriptions can be inserted in 3.2 and could replace the tentative definitions (in italics). The second approach can be regarded as an attempt to calibrate vulnerability classes on the basis of observations for their typical representatives.

B.5 Comments on the assignment of intensity from engineered structures

B.5.1 Definition of regularity

The classification of regularity should follow principles stated in national earthquake resistant regulations. The restriction on the height of buildings to be used for intensity assessment is not required in the case of engineered structures. The height of buildings is of importance when the regularity of a building has to be evaluated.

The height of buildings is considered in seismic codes
- directly, by defining limits of height or of storeys, and/ or
- indirectly, by defining limits of slenderness (ratio of height to plane dimensions).

In European earthquake codes the height of regular buildings is limited to 30 - 40 metres; the slenderness ratio (height to width) should not exceed 4.0 - 6.0. Special design methods and detailing have to ensure earthquake resistance in the case of irregular structures.

B.5.2 Factors contributing to damage

When assessing intensity using non-engineered structures and modern engineered structures (buildings), one should consider the essential factors contributing to damage or to an increase of damage. Otherwise, a misleading interpretation of the actual situation can occur resulting in an overestimation of intensity.

Some of the most important damage contributing factors are (besides the regularity, the quality of materials/ workmanship, which are already implemented through the classification of levels Q and R):
(a) the quality of subsoil and hardness of foundation material, and the potential for soil liquefaction;
(b) the dynamic characteristic of building, the predominant frequency content of ground motion, mainly determined by subsoil conditions, distance and depth of the earthquake source and the type and amount of energy release (magnitude);
(c) resonance conditions between the building and the ground motion and its agreement or relation with the amplification effects considered and expressed in code design

coefficients;

(d) the ability of the building to dissipate seismic energy and to react in postelastic range without collapsing (this factor is commonly quantified in terms of ductility or structural behaviour factor);

(e) the stiffness of the building to limit deformations and damage to nonstructural elements;

(f) the orientational sensivity of buildings with different dimensions and stiffness in the perpendicular axis of ground plane;

(g) **soil behaviour**
The influence of subsoil conditions should be taken into account with respect to design assumptions, i.e. when the frequency content of the actual earthquake differs significantly from that of the design earthquake in the range of dominating building periods (or equivalent terms) when the demands are greater than the resistance capacity provided by antiseismic design (ASD).

B.5.3 Special remarks to the classification of damage and intensity degrees

The progression of damage with intensity degrees does not increase linearly in the case of engineered structures (buildings), introduced as types ASD_i. This can be justified with respect to modern design principles which are related to the performance of engineered stuctures under different levels of design earthquake (intensity):

- Structures designed against an earthquake of low intensity to be expected with high probability of occurrence, should sustain such an event without structural damage and with no damage, or only minor damage, that could affect the serviceability.
- Structures designed against an earthquake of medium intensity to be expected with low probability of occurrence, are explicitly allowed to react under the design earthquake with slight non-structural damage, but should survive without loss of serviceability
- Structures design against an earthquake of high intensity, have to sustain structural damage without loss of structural integrity and stability.

This means that structures in zone i, designed for intensity I, will show higher grades of damage in seismically more active regions. On the other hand, one may postulate that there are no differences in the aim of protection for structures of different structural systems when these buildings are classified into the same importance category (of the national seismic code).

B.5.4 Relation between intensity and other earthquake zone related design coefficients

The definition of ASD_i types of engineered structures is based on intensity and and on other earthquake zone related design parameters (e.g. the base shear coefficient).
It is necessary to establish relations between ASD_i type structures (buildings) of this draft and antiseismic buildings designed

- according to the different seimic codes
- for different (classified and subdivided) seismic zones and
- for quite different design loads and protection levels.

Furthermore, it is necessary to compare design levels of antiseismic structures in each country with the idealized characteristics of ASD_i types expressed in terms of design intensity or other zone related design coefficient. The relation between intensity and other earthquake zone related design coefficients should be considered as a matter of further discussion. Therefore, the base shear in B.1.4 is given in italics to indicate the tentative character.

B.6 Brief examples for application

B.6.1 Non-engineered structures

In a town, damaged after an earthquake, 40% of unreinforced brick buildings with reinforced concrete floors suffered grade 3 damage.
The first question to be answered is, to what class of vulnerability the buildings used for intensity assignment belong. The buildings are of good quality, regularity, and workmanship. So, they can be regarded as vulnerability class C.
Following the definition of intensity degrees in 3.2, an intensity of IX can be assessed.

B.6.2 Engineered structures

General procedure

(1) It is possible to predict the *code-consistent level* of ASD and with this to evaluate the ASD_i type(s) of engineered buildings in the study area on the basis of the seismic zone defined within the national seismic building code. Commonly, each region or town is characterized by one ASD_i type only; but for the assignment of intensity it is necessary that information is available which indicate the distribution or individual sites of those buildings. A region or town can be characterized by different ASDi types when buildings are present which were built according to different seismic codes.

(2) It is necessary to predict the *actual* level of ASD and to qualify the level of regularity as well as of the quality or workmanship of engineered buildings in the study area. Furthermore, it is necessary to compare design levels of antiseismic structures in the earthquake region with the idealized characteristics of ASD_i types of this draft expressed in terms of design intensity or other zone related design coefficients.

(3) The present draft of Annexe B offers two approaches to assign intensity.
- The first approach is directly related to the classification of intensity in the Core part of the scale. For this it is necessary to predict the typical or representative vulnerability class(es) for the actual ASD_i type(s) of the engineered buildings in the study area. The intensity can be classified on the basis of the predicted vulnerability class(es) and the definitions of intensity degrees (see 3.2).
- The second approach is related to available results of damage surveys, which are incorporated in Table B-1 (derived for engineered structures with medium level of regularity and low level of quality). This table alone would be sufficient for establishing of the scaling conditions of intensity. (In the framework of the present version of the EMS, Table B-1 should provide background information for the determination of vulnerability classes of ASD_i types; i.e. this Table contains the basic information for the intensity definitions using vulnerability classes D - F given in *italics* in 3.2).

Both approaches require the classification of the level of regularity and of the quality of the ASD_i type structures.

Example

In a town, damaged after an earthquake, 30% of the engineered buildings suffered damage of grade 2; 5% suffered damage of grade 3.
According to the zoning map of the seismic code the town lies in a zone of design intensity 8 (zone with medium seismic hazard; base shear of 6%g). Earthquake forces were incorporated into the design using calculations by simplified dynamic methods. The zone-consistent ASD_i type of the engineered buildings is type ASD_8.
The buildings have a medium level of regularity, a low level of workmanship but no other design deficits ("defects"). There are no essential differences between design loads and the characteristics of strong ground motion of the actual earthquake. The actual ASD_i type is ASD_8.
According to B.5.1 type ASD_8 is comparable to vulnerability classes C and D (for the level of regularity R_m and the quality level Q_l).
Following the intensity degrees in 3.2, the intensity is VIII for vulnerability class C and IX for vulnerability class D. It can be concluded that the intensity was VIII - IX. (In reality not only damage to enginered buildings should be taken into account but also the other diagnostics arranged under a) and b) of the intensity definitions.) According to the damage surveys incorporated in Table B-1 one can conclude that the intensity tends to be more VIII than IX, because a higher percentage of buildings with damage grade 3 would be expected for intensity IX.

B.7 Suggestions for improvements

For the application and improvement of this Annexe it is suggested to introduce the following tables:
- ***Table B-2**, within which European countries and their seismic codes should be evaluated according to the levels of earthquake resistance provided*
  (necessary to select the appropriate **level of quality** (sect. B.1.2));

- ***Table B-3**, within which qualitative indicators and criteria for the classification of regularity should be illustrated according to modern design principles, proposed in the actual/final edition of the Eurocode 8*

  (necessary to select the appropriate **level of regularity** (sect. B.1.3));

- ***Table B-4**, within which simple illustrations should be given with respect to different behaviour and damage pattern of regular and irregular structures*

  (have to be completed by figures of damaged buildings and should also illustrate typical structural types and systems in various earthquake regions. It seems to be useful to add these tables, as a second part, to the Annexe A: "Examples illustrating classification of vulnerability and damage used in the scale").

***Tables B-2, B-3 and B-4** are not included in the present draft of the EMS (MSK-92).*

Tables B-2 - B-4 have to be developed and introduced according to the results of discussion among national specialists and their proposals. **Table B-1** has to be compared with results from engineering analysis of structural damage in European and other earthquake regions. Tables have to be introduced for other levels of quality and/or regularity. Vulnerability functions for different types of structures (similar to the idealized ones in **Figure B-1**) should be evaluated for engineered structures in dependence on the proposed levels of antiseismic design.

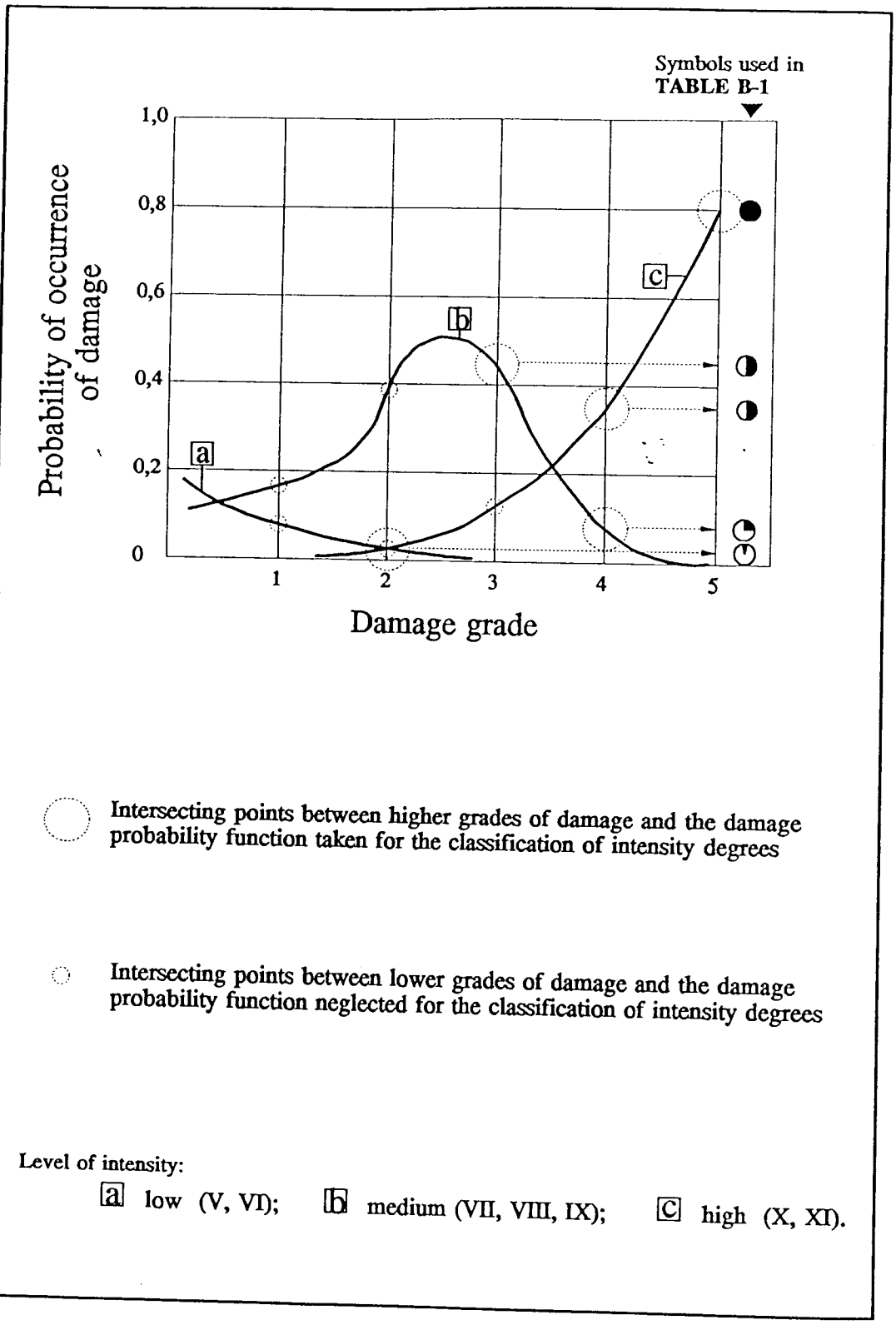

Figure B-1 Relation between typical frequency distributions of damage grades for different intensity degrees and definitions used in the presented intensity scale.

INTENSITY	TYPE	LEVEL Q_i Damage Grade				
		1	2	3	4	5
VI	ASD_7	very few	very few			
	ASD_8	few				
	ASD_9	very few				
VII	ASD_7	many	few			
	ASD_8	many	very few			
	ASD_9	few				
VIII	ASD_7	few	many	few		
	ASD_8	many	many	very few		
	ASD_9	many	few			
IX	ASD_7				few	
	ASD_8		many	many	very few	
	ASD_9		many	few		
X	ASD_7				many	few
	ASD_8		few	many	many	very few
	ASD_9			many	few	
XI	ASD_7					many
	ASD_8				most	many
	ASD_9				many	few
XII						

very few few many most

Table B-1 Relation of damage grades to intensity degrees for ASD_i type buildings of low level of quality Q_i and medium level of regularity R_m.

ANNEX C
SEISMOGEOLOGICAL EFFECTS

The effects of earthquakes on the ground, here summed up as "seismogeological" effects, have often been included in intensity scales but are in practice quite hard to use to advantage. This is because these phenomena are complex, and are often influenced by various factors such as inherent slope instability, level of water table, etc, which may not be readily apparent to the observer. The result is that most of these effects can be seen at a wide range of intensities.

For the purposes of this up-dated scale version, these effects are presented as a table; for each effect, three different signatures are drawn to show:

lines - the possible observation range;

open circles - the range of intensities that are typical for this effect;

full dots - the range of intensities for which this effect is most usefully used as a diagnostic.

These lines are terminated in arrows to show a potential for extreme observations even beyond the limits shown in exceptional cases, different geological settings, or special sensitivity. For some effects, not all three categories are plotted where there is thought to be inadequate experience to formulate an opinion.

It should be remembered that for most of these effects, the severity of the observation will increase with higher intensity. Thus for "flow of springs affected", at intensity 5 one might expect slight change in spring flow, while at higher intensities the change may be very much greater. It was decided that attempting to discriminate between "slight change in flow of springs" and "great change in flow of springs" within the scale was not practical owing to the difficulties in quantifying such expressions.

Care must be taken, especially when dealing with ground breaks, to discriminate between geotechnical observations, ie those caused by shaking, and neotectonic observations, ie those caused directly by fault rupture.

The effects listed in the table are grouped in four categories: hydrological, slope failure, horizontal ground processes and convergent processes (complex cases). This latter group covers instances where more than one type of process is involved in producing the effect. It will be noted that landslides appear both as slope failure effects and convergent processes effects. This is because some landslides are straightforwardly the result of shaking dislodging rocks, whereas others only occur because slope instability is compounded with certain hydrological conditions. Discriminating between these may not be easy; this is an illustration of the problems that arise in dealing with this sort of effect.

Table C-1: Relation of Seismogeological Effects to Intensity Degrees

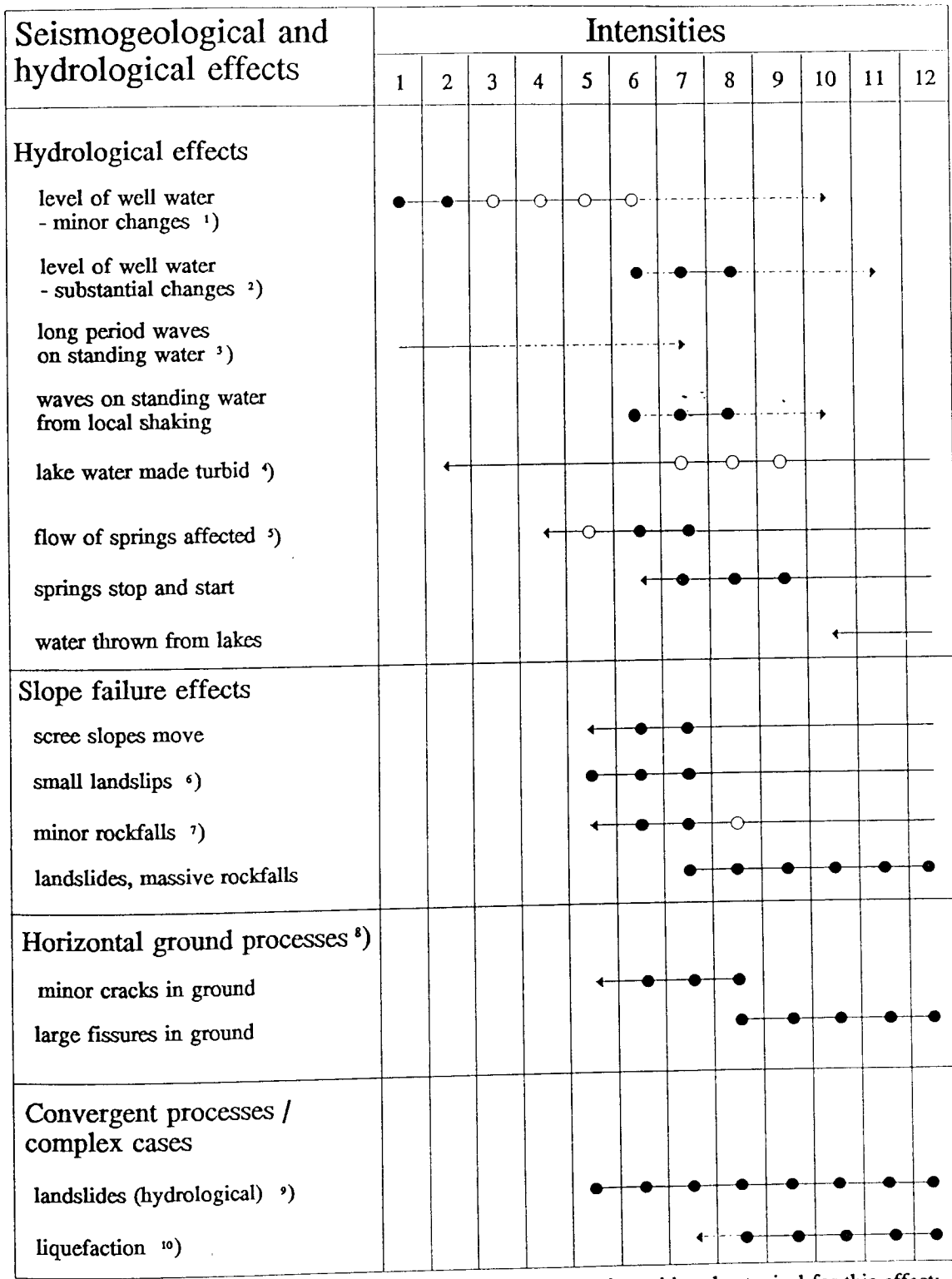

Legend: —●——● most useful range as intensity diagnostic; ○ intensities also typical for this effect; ——·····—— possible observation range; ——→ potential for extreme observations beyond the given limit

Notes to the Table on Seismogeological Effects

[1]) detected by automatic instruments only
[2]) easily observed changes
[3]) resulting from distant earthquakes; possibly with wave-induced turbidity
[4]) from disturbance of bottom sediments
[5]) rate changes or spring water made turbid
[6]) in loose material in natural (river banks etc.) or man-made (road cuttings) sites
[7]) minor rockfalls in natural (cliffs) or man-made (rock cuttings, quarries) sites
[8]) these two categories blur into one another. The warning is repeated about not confusing ground rupture breaks with fissures caused by shaking.
[9]) Landslides with predominant hydrological causes (may be delayed effects)
[10]) Liquefaction (e.g. sand craters, mounds formed, etc.)

METHODOLOGY OF SEISMIC HAZARD ASSESSMENT

G. Grünthal

Dept. of Kinematics and Dynamics of the Earth
GeoForschungsZentrum Potsdam, Telegrafenberg C3, D-14473 Potsdam

1. INTRODUCTION

In seismically active regions, any decision-making for urban or regional planning should be based on probable characteristics of earthquakes to be expected in future. These features are provided by the procedure usually called "seismic hazard assessment".

The term "seismic hazard" (H) means the probability of occurrence of potentially damaging seismic ground motions at a certain site within a certain time interval. The process of determining seismic hazard in a region is also called "seismic zoning". It has to be stated that this term does not involve a special study, how local surface and subsurface conditions can influence the seismic soil or ground motions. This falls into the domain of seismic microzoning. The main outcome of a seismic zoning procedure are seismic hazard or zoning maps displaying a quantity related to the assessed frequency and severity of shaking due to expected future earthquakes.

The term "seismic risk" is derived from the insurance sector with the meaning that there can be no risk due to natural phenomena if there are no values or works of man exposed to natural hazards. But the usage of the term "risk" is not uniform - therefore it is important to define the meaning in which it is used in the following.

Prior to any evaluation of the seismic risk, the "vulnerability" V has to be determined. The vulnerability is the expected degree of loss within a defined area resulting from the occurrence of a certain earthquake (for assessing the seismic risk) on a scale from 0 (no damage) to 1 (total loss). The vulnerability can be reduced by applying antiseismic measures in civil engineering. The seismic specific risk SR_i is then the product of seismic hazard and vulnerability:

$$SR_i = H_i \cdot V$$

The seismic risk R itself is the sum of all products of the value C_i of the different elements at risk multiplied with the seismic specific risks, i.e.:

$$R = \sum_i (SR_i \cdot C_i)$$

According to the recent security philosophy, different levels of earthquake loading have to be considered. The decision on the probability level to be used in practical seismic hazard applications is rather complex and depends on the final risk that the society is willing to accept. The probabilities of exceedance per year (p.a.) currently used in the design of structures are approximately as follows:

standard buildings: $2 \cdot 10^{-2} - 10^{-3}$ p.a.

important structures: $2 \cdot 10^{-3} - 10^{-4}$ p.a.

nuclear power plants: $10^{-4} - 10^{-6}$ p.a.

2. BASIC DATA

2.1 Seismicity studies

The fundamental basis for any seismic zoning is a carefully compiled earthquake catalogue for the study area. The latter is usually a region of some 200-300 km around the site for which the hazard has to be assessed.

The data on earthquakes should be catalogued backward into history so far as possible. A prerequisite for reliable seismic hazard assessments is the determination of the completeness of data backward into history for different classes of event strength. The primary parameters of earthquake catalogues are the date of an event, the location and a parameter classifying the strength, i.e. the epicentral intensity I_0 or the magnitude M. Appropriate relations between I_0, M and the focal depth (h) have to be determined for the study region to express the complete data set in terms of a unique strength parameter.

Plots of the epicentres and sizes of earthquakes provide the primary basis for the recognition and delineation of hazardous regions. Significant earthquakes tend to occur repeatedly in certain regions, whereas other regions have experienced few or no events during long historical periods. But one has to be cautious in interpreting epicentre maps, particularly when the depicted time span is short.

2.2 Delineation of seismic source regions

The next step in the preparation of the basic data for seismic hazard assessment concerns the subdivision of the area under investigation into seismic source regions. Within these regions the character of seismic activity should be uniform and the epicentres of expected future events should be likely fall within them. The character of seismic activity within any region is described by the magnitude-frequency relationship according to Gutenberg and Richter (1944):

$$\log N = a - bM.$$

The parameter a describes the level of **seismic activity**; b indicates the proportion of larger to smaller earthquakes and is also called the **seismic regime parameter** of a certain region. The reliable determination of the parameters a and b is of special importance during the zoning procedure. When regions with different slopes of the magnitude frequency graph are combined, this results in a misleading description of a fictitious source region.

In order to increase the reliability of the delineated features, derived purely from historical or previously observed seismicity, it is advisable to include additional data from geology, tectonics, geophysics and geodesy. Especially useful are seismotectonic maps, indicating provinces with different tectonic regimes (normal-, thrust-, or strike-slip-faulting), and

correlations of epicentres with neotectonic fault activity. In this way, it is sometimes possible to delineate rather narrow source zones.

2.3 Estimates of the upper-bound magnitude M_{max}

For any region there exists a maximum possible magnitude. Its determination, as reliable as possible, is of extreme importance for hazard statements especially for very low occurrence probabilities; i.e. for sites of important structures and nuclear power plant . It has to be stated at the outset that up to now the approaches to determine M_{max} are not yet well established and a considerable portion of personal judgement is still required. Furthermore, the nature of this problem varies from area to area. The best prerequisite for its estimation is in each case a well recorded earthquake history of the study region. Especially useful is the application of different approaches for one region. Some of the existing possibilities to get a reasonable estimate of M_{max} or I_{max}, respectively, are:

- in case of very long and well recorded seismicity observations, simply a certain value should be added to the largest observed intensity;
- to use the GUMBELs type-III extreme value statistics which yields the maximum as an asymptotic value;
- from a cumulative seismic energy release covering at least several centuries, it can be inferred with sufficient reliability;
- to base the estimate on tectonic features, e.g., on the overall length of an active tectonic fault segment.

2.4 Attenuation of ground shaking with distance

The knowledge of attenuation relations - as correct as possible - of that shaking parameter in which the hazard statements will be expressed is also very important for reliable seismic zoning. Appropriate scaling parameters of seismic hazard maps are the macroseismic intensity, the ground acceleration or velocity.

Different versions of algorithms for seismic hazard assessment require either an average attenuation relation for the study region or special relations for the different source regions; additionally, an azimuthal dependence can be introduced.

There are observed large variations in the attenuation pattern - not only on the sub-regional scale due to different subsoil conditions but also from region to region. Therefore, it makes not much sense to transfer any attenuation relation derived for one region to another one without verifying its validity. In order to get reliable seismic hazard maps it is indispensable that the attenuation relations must be based on the detailed analysis of either carefully elaborated macroseismic maps of typical earthquakes or on extensive strong ground-motion recordings in the study region.

3. STATISTICAL BACKGROUND

The tool for the quantitative determination of seismic hazard provides the earthquake statistics. This term means the empirical analysis of the distribution of earthquakes with

regard to their temporal occurrence as well as their energetic classification related to a certain volume of the lithosphere. The necessary assumption for the mostly used approaches on seismic hazard assessment is the random occurrence of earthquakes. But in reality, this assumption has its limitations; i.e. the earthquakes are not fully random - neither in space nor in time.

Seismic hazard assessments are probabilistic. As a numerical value for the statistical probability of the occurrence of an event E, denoted as P(E), the expression

$$P(E) = \frac{\text{number of favourable cases}}{\text{number of possible cases}}$$

can be chosen.

3.1 Temporal occurrence of earthquakes

The frequency of earthquakes above a certain magnitude and within fixed time intervals is fairly good Poissonian when foreshocks and aftershocks are removed from the data set. A random variable N (which can have integer values) is Poissonian with the parameter α if

$$P[N=n] = \frac{\alpha^n}{n!} \exp(-\alpha) \qquad (n = 0,1,2,\ldots)$$

is valid. A suitable estimate for α is the arithmetic mean of the independent realizations of the random variable. This discrete distribution describes many processes in nature (in biology, meteorology, quality control, nuclear physics) and in daily life.

3.2. Frequency distribution of different magnitudes

After Gutenberg and Richter the relation between the number N of earthquakes in a natural sequence, having magnitudes in the interval $m \pm \frac{1}{2} \Delta$, and the magnitude m was given as

$$\log N(m) = a - bm \qquad \text{for } m_{min} < m < m_{max}$$

This is the non-cumulative magnitude-frequency relation. Of special importance in hazard studies is the cumulative magnitude-frequency; i.e. the plot of the number N^* of earthquakes with a magnitude equal to or larger than $m - \frac{1}{2} \Delta$.

$$\log N^*(m) = a^* - b^* m \qquad \text{for } m_{min} < m < m_{max}$$

Here N^* is always non-zero as it can happen with the non-cumulative form which makes problems because logN does not exist for N=0. The parameters of both relations are not substantially different for large event populations (N>4000). But caution must be used in applying the cumulative form in case of poor and too small data sets. Then the cumulative format can introduce a bias and can drive completely unsuitable sets of data to a smoothed a priori established pattern.

Scientific Technical Report STR 95/TK
DOI: 10.2312/GFZ.b103-95tk7

3.3 Cumulative probability distribution function for magnitudes or intensities

For the lowest magnitude class m_1 included in the data set one gets as the cumulative number N* of earthquakes, in the following written as N only for simplicity, having magnitudes or intensities greater than m_1

$$\log N(m_1) = a - bm_1 .$$

Normalizing the cumulative magnitude-frequency by logN (m_1) one gets

$$\frac{N(m)}{N(m_1)} = \exp(-b \cdot \ln 10 \cdot (m-m_1)) .$$

This relation implies the introduction of a probability expression. The probability that the random value M has a value smaller than a real number m, can be denoted as:

$$F_M(m) = P(M<m) = 1 - \exp(-\beta(m-m_1)); \quad \beta = b \cdot \ln 10 .$$

Normalizing this expression by the total number of events in the magnitude range m_n - m_1 yields the truncated exponential distribution function with:

$$F_M^T(m) = \frac{1-\exp(-\beta(m-m_1))}{1-\exp(-\beta(m_n-m_1))} .$$

3.4 Calculation of seismic hazard

The probability that from any point source the random variable in terms of intensity I (or acceleration) at the site of interest can be larger than any realization i, is expressed as the conditional probability, depending on earthquake size m and distance r

$$P[I>i \mid m, r].$$

As a mean intensity-attenuation function a relation of the following type can serve :

$$I_{Site}(m, r) = C_1 + C_2 m + C_3 \ln(r + r_0).$$

Thé total probability theorem is used to express the probability of occurring or exceeding any ground shaking level at any site considering all surrounding source regions:

$$P[I>i] = \int_{r} \int_{m_l}^{m_u} P[I>i \mid m, r] \cdot f_M(m) \cdot f_R(r)\, dm\, dr\,.$$

f_M (m) is the probability-density function of magnitudes, i.e. the first derivative of the cumulative distribution function $F_M(m)$. f_R (r) denotes the probability-density function of the site-to-source distances and is calculated numerically with appropriate algorithms.

Assuming a Poisson process of earthquake occurrence in the study region, then the selected events, fulfilling the condition of the total probability theorem, are also Poissonian. The probability that these events larger than i will not occur in the time interval 0 to t (usually one year) is:

$$P[N_i>i] = 0 = \exp(-vt)\,.$$

The probability of occurring or exceeding any critical i at a site per year - defined as seismic hazard H - is:

$$H = 1 - P[N_{I>i} = 0] = 1 - \exp(-v).$$

The mean return period of any critical event is the reciprocal value of its total annual occurrence rate. The occurrence probability of an event within its mean return period is $1 - e^{-1} = 63\%$.

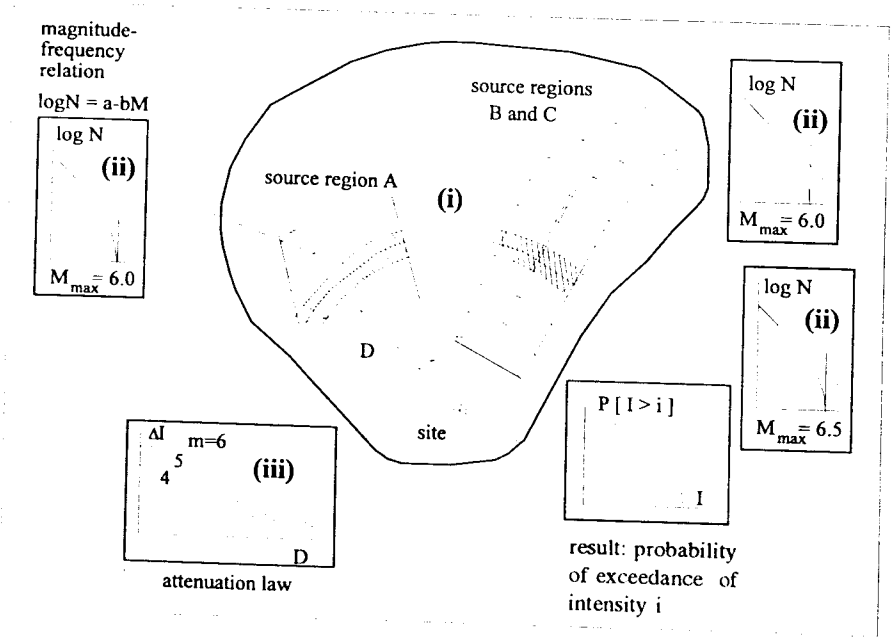

Fig. 1 Scheme illustrating the input data necessary for the process of seismic zoning and the integration procedure over distance and source regions, respectively.

Scientific Technical Report STR 95/TK
DOI: 10.2312/GFZ.b103-95tk7

Exercise on assigning seismic intensities[1)]

G. Grünthal

Dept. of Kinematics and Dynamics of the Earth
GeoForschungsZentrum Potsdam, Telegrafenberg C3, D-14473 Potsdam

1. Intensity assignment based on questionnaire data

The following data are extracted from questionnaires relating to the effects of a magnitude 4.8 earthquake in one town in north-western Europe. The questionnaire was published in local newspapers; readers of the newspaper were invited to fill out the questionnaire and send it in. The questionnaire was not designed with the MSK scale in mind, and therefore not all the questions relate closely to the text of the scale. By way of this this example we show that the scale works well even with data which are not optimal.
For the purposes of this study the city of Carlisle was divided into three areas. The data from the western part of the city will be used in the exercise. The number of questionnaires received was 222.
The time of the earthquake was 03h 57m; almost all observers were indoors and in bed. There were no reports from people outdoors, since the streets were deserted at this time of night.

Question: What did you feel?
87% felt some sort of vibration; 19% described it as strong (though they weren't specifically asked to qualify their description); 1% described it as weak; 11% felt no shaking.
Commentary: the vibration was generally observed and felt as strong by many.

Question: What did others nearby feel or hear?
73% said their neighbours felt or heard the earthquake; 12% said they didn't and the remainder didn't know or didn't answer.
Commentary: the earthquake was felt by... (insert here your conclusion derived from the answers given in the questionnaire with regard to assigning intensity; c.f. commentary given above).

Question: Were you frightened or alarmed?
69% said they were - 18% said they were not. Three people said they ran outdoors, but this information wasn't actually requested by the questionnaire, so more may have done so.
Commentary: ... ... So far the intensity looks to be in the range of ... .

Question: Did doors or windows rattle?
54% said yes; 26% said no.
Question: Did anything else rattle?
54% said yes; 19% said no.
Commentary: the intensity is so far at least ... and probably ... or even more from this evidence.

[1)] These Examples are based on a compilation prepared by R. Musson (Edinburgh)

Question: Did any hanging objects swing?
14% said yes; 26% said no, and the rest had no hanging objects to observe, or couldn't see in the dark, or didn't answer.
Commentary: since the shaking from a relatively small earthquake at close range (as here) is likely to be of high frequency, it is not to be expected that there will be many observations of hanging objects swinging. In these circumstances the ratio of approximately 1:2 yes:no replies suggests quite strong shaking, i.e. at least intensity ....

Question: Did anything fall over or upset?
18% said yes; 72% said no.
Commentary: The intensity was at least ....

Question: Was there any damage?
13% reported damage of some sort; 85% reported no damage. Most of the damage was of cracks to plaster and walls; also fall of slates, fall of chimneys and loose bricks dislodged. In one case it was reported that a gap opened between a garage and a house extension.
Commentary: the type of housing is predominantly brick-built. The damage can be summarised as ... vulnerability class ... buildings suffer damage of grade .... This does not match exactly the descriptions given in the scale, but is closer to that for degree ... than anything else.

Question: Have you any other observations?
A variety of answers were received. Nine people reported that furniture was shifted, an effect first mentioned at degree 6 of the scale.

Question to be answered: What was the intensity in the respective part of the city? Summarize the main reasons for your conclusion.

2. Intensity assignment based on documentary data

The following two descriptions are of the effects of an earthquake on 7 September 1801 at Comrie, in Scotland. Both are taken from contemporary Edinburgh newspapers. Edinburgh was at that time the nearest place at which newspapers were published. The distance from Comrie to Edinburgh is about 75 km. The time of the earthquake was about 6 am.

The following account was written by an observer in Comrie, on 9 September, two days after the earthquake. It was published in the Edinburgh Advertiser (15 September 1801 p174).
1) The ... shock ... was very great, and alarming beyond expression. ... Slates fell from some houses, and many loose bodies tumbled down with great precipitation. Sonorous bodies were dashed on each other, and rang loudly, such as bottles, glasses, &c. Several large stones and fragments of rocks fell down the sides of the mountains. Pieces of stone dykes fell, and one bank of earth slid from its place. If the shock had had a little more impetus, it is probable, several frail houses would have been thrown down; but, in the kindness of Providence, no farther harm has been done than what is above stated.

The second account was also written at Comrie on 9 September, and was published in the Edinburgh Evening Courant (14 September 1801, p3).

2) ... the noise and shock ... were instantaneous; all those persons who were in bed were terrified that their houses were tumbling down about their ears, and many here and in the neighbourhood jumped out as quickly as possible - its duration might be about five or six seconds, and during all that time the floors, beds, and window shutters shook violently, and the roofs creaked and strained at a great rate. The horses that were grazing seemed much frightened and to listen with their ears pricked up; the cows also that were housed appeared, from their lowing, to be very uneasy, and all the dogs and other animals gave signs of fear. A shepherd, a few miles to the westward, had just separated a flock of cattle, but as soon as the earth began to tremble they all crowded together in a moment.

Question to be answered: What was the intensity at Comrie?

Help: A word needs to be said first about local building type, which would have been predominantly stone-built houses (usually single-storey), with timber roofs covered with slates. These can be considered as vulnerability class B structures. The strength of these buildings is likely to have been quite good, where not affected by disrepair.
The "stone dykes" referred to here are boundary walls. This type of structure is not dealt with by the MSK intensity scale as such, but experience shows that this type of damage begins at intensity 5.

Make an extract of all effects reported that have a relation to intensity assessment. Give comments to all these single effects what intensity range could be related to them.
Note that not all of the given effects are explicitly included in the intensity definitions - the appropriate equivalences have to be found out.

Exercise on incompleteness of a catalogue with respect to the determination of the parameters of the Gutenberg - Richter relation

G. Grünthal

Dept. of Kinematics and Dynamics of the Earth
GeoForschungsZentrum Potsdam, Telegrafenberg C3, D-14473 Potsdam

Task: Determination of the annual intensity-frequency relation

$$\log N_y(I_0) = a - b\, I_0$$

Input data: Earthquake catalogue. For simplicity the enclosed Table 1 gives only the origin time of events (in years) and their epicentral macroseismic intensities I_0 (in grades of MSK).

Consider the incompleteness of the earthquake catalogue.

Help:
- Plot a time-chart of earthquake occurrences for each intensity class.
- Estimate the time span for which you assume a completeness of catalogued data.

Make some statements about the problem how the parameters a and b can depend on personal judgement.

Tab. 1

year	I_0	year	I_0	year	I_0	year	I_0	year	I_0
1025	8,5	1526	7,0	1820	5,0	1915	5,0	1957	3,0
1026	7,5	1531	7,0	1827	5,0	1920	4,5	1960	4,0
1030	7,0	1537	8,5	1837	5,5	1922	4,0	1960	3,5
1070	6,5	1550	6,0	1837	4,5	1925	6,0	1961	3,0
1085	7,0	1575	6,5	1838	7,0	1925	5,0	1962	5,0
1100	5,5	1593	7,0	1845	5,5	1932	5,0	1962	3,5
1150	7,0	1600	6,0	1849	6,0	1935	3,0	1964	3,5
1155	6,0	1625	6,5	1850	4,5	1936	4,5	1964	3,0
1250	7,0	1625	5,5	1850	3,5	1937	6,5	1967	3,0
1260	8,5	1638	6,0	1855	8,5	1937	3,5	1968	4,5
1265	7,0	1650	6,0	1859	5,0	1940	4,0	1968	4,0
1280	6,0	1660	7,0	1859	3,5	1940	3,0	1968	3,5
1350	5,5	1675	4,0	1874	6,5	1943	4,5	1969	5,5
1351	7,5	1677	6,0	1875	5,0	1943	3,0	1969	3,0
1376	5,0	1699	6,5	1876	3,0	1944	5,5	1970	3,5
1378	5,0	1701	4,5	1880	5,5	1944	4,0	1973	3,0
1425	6,5	1715	8,0	1887	5,0	1945	3,5	1975	3,5
1438	5,0	1724	6,5	1887	3,0	1947	3,0	1975	3,0
1450	8,0	1725	5,5	1900	6,0	1949	6,5	1976	4,0
1460	7,0	1751	7,5	1905	4,0	1949	4,0	1977	3,0
1470	6,5	1762	6,0	1906	5,0	1949	3,5	1980	3,5
1475	6,0	1775	6,5	1907	7,5	1951	3,0	1980	3,0
1478	6,0	1800	4,0	1910	4,0	1952	3,5		
1500	6,5	1810	7,0	1912	5,5	1955	7,0		
1501	5,5	1812	5,5	1912	4,5	1955	4,5		
1525	5,0	1820	6,5	1915	4,0	1957	3,5		

Exercise on the determination of the parameters of the Gutenberg-Richter relation logN = a - bm

G. Grünthal

Dept. of Kinematics and Dynamics of the Earth
GeoForschungsZentrum Potsdam, Telegrafenberg C3, D-14473 Potsdam

Use the following data and abbreviations:

Data:

m_i	N_i
2.50	(380)
2.75	420
3.00	286
3.25	143
3.50	129
3.75	66
4.00	24
4.25	15
4.50	4
4.75	3

n	-	number of classes
m_0	-	smallest magnitude considered
m_i	-	magnitude of class i events
$\overline{m}$	-	average magnitude in the range of classes i = 1, ... n
N_i	-	non-cumulative number of events

1. Give a graphical presentation of the data given in the table above

2. Make an eye-fit of the data points and determinate the parameters â and $\hat{b}$ from the graph according to

$$\hat{b} = \frac{\log N_2 - \log N_1}{m_1 - m_2}, \qquad \hat{a} = \log N_2 + m_2\hat{b}$$

3. Determinate the parameter b by using the preferable maximum likelihood estimate (MLE) (Utsu, 1965; Aki, 1965):

$$b_{MLE} = \frac{\log e}{\overline{m} - m_o} \qquad \text{with} \qquad \left(\log e = \frac{1}{\ln 10}\right),$$

which yields accurate and unbiased values for $(m_{max} - m_o) \geq 2$ (otherwise use corrections according to Utsu, 1966) or determine the MLE of the parameter β of the exponential distribution $P(M<m) = 1 - \exp(-\beta m)$, respectively:

$$\beta_{MLE} = (\overline{m} - m_o)^{-1}; \qquad \beta_{MLE} = \frac{b_{MLE}}{\log e}.$$

Scientific Technical Report STR 95/TK
DOI: 10.2312/GFZ.b103-95tk7

4. Determine the slope parameter b by least-square estimate (LSE) for logN = a+bm:

$$b_{LSE} = \frac{\sum_{i=1}^{n} (m_i - \overline{m})\ (\log N_i - \overline{\log N})}{\sum_{i=1}^{n} (m_i - \overline{m})^2}, \qquad \overline{m} = \frac{1}{N}\sum_{i=1}^{n} m_i N_i ,$$

$$\overline{\log N} = \frac{1}{N}\sum_{i=1}^{n} N_i \log N_i .$$

Hint: To perform the LSE use the following table:

m_i	N_i	$N_i\ m_i$	$\log N_i$	$N_i \log N_i$	$m_i - \overline{m}$	$(m_i - \overline{m})^2$	$\log N_i - \overline{\log N_i}$

Aki, K., 1965: Maximum likelihood estimation of b in the formula logN = a - bM and its confidence limits. Bull. of the Earthquake Research Inst. of the Univ. of Tokyo 43, p. 237-239.

Utsu, T., 1965: A method for determining the value of b in a formula logN = a-bM showing the magnitude-frequency relation for earthquakes. Geophys. Bull., Hokkaido Univ. 13, p. 99-103.

Utsu, T., 1966: A statistical significance test on the difference in b-value between two earthquake groups. Journal of Physics of the Earth 14(2), p. 37-40.

DOI: 10.2312/GFZ.b103-95tk7

Exercises on earthquake occurrence in time (Poisson distribution)

G. Grünthal

Dept. of Kinematics and Dynamics of the Earth
GeoForschungsZentrum Potsdam, Telegrafenberg C3, D-14473 Potsdam

Check if the data set given below is Poissonean.
Make a plot of the observed numbers N of frequency classes having 0, 1, 2, ... , n earthquakes per time interval t and compare it with the poisson random distribution P. t should be one year.

n = 0, 1, 2, ... ;
α - mean occurrence rate per t

$$P(N = n, t) = \frac{(\alpha \cdot t)^n}{n!} \exp(-\alpha \cdot t)$$

For better comparison of the Poisson distribution with the observed numbers plot:

$$K[N = n, t] = k \cdot P[N = n, t]$$

with k - number of time intervals used.

Data: yearly number of shallow earthquakes with $M \geq 7.5$ from 1904 up to 1980 after Abe (1981): Magnitudes of large shallow earthquakes from 1904 to 1980. Phys. Earth Planet. Int. 27, 72-92.

year	No.	year	No.	year	No.	year	No.	year	No.	year	No.
1904	9	1917	4	1930	1	1943	8	1956	2	1969	3
1905	6	1918	6	1931	9	1944	2	1957	5	1970	1
1906	7	1919	3	1932	4	1945	2	1958	2	1971	5
1907	7	1920	4	1933	3	1946	6	1959	2	1972	1
1908	1	1921	2	1934	5	1947	3	1960	3	1973	1
1909	2	1922	2	1935	4	1948	3	1961	1	1974	1
1910	1	1923	3	1936	1	1949	4	1962	-	1975	6
1911	6	1924	2	1937	4	1950	2	1963	1	1976	5
1912	5	1925	-	1938	9	1951	1	1964	2	1977	2
1913	3	1926	2	1939	4	1952	5	1965	3	1978	3
1914	3	1927	2	1940	2	1953	2	1966	5	1979	2
1915	4	1928	6	1941	5	1954	-	1967	1	1980	1
1916	4	1929	4	1942	5	1955	2	1968	5		

Recommendation: Use the following table.

frequency classes n	number of occurring classes N	total number of events within n	K
0	3	0	2.73
1			
2			

(In textbooks on statistics you will find procedures on possibilities about tests of the goodness of fit between observed distribution and theoretical distribution.)

Exercise on the application of extreme value statistics

G. Grünthal

Dept. of Kinematics and Dynamics of the Earth
GeoForschungsZentrum Potsdam, Telegrafenberg C3, D-14473 Potsdam

Make a graph for the data according to the plotting rule given below. Make statements on the expected extremal intensities of mean return periods of 10, 50, 100 and 200 years.

Data: Maximum earthquakes of an area of low seismic activity within 10 year intervals (t):

interval	data	I_0
1800-1809	-	-
10-	1811 Dec. 12	5.5
20-	1821 Oct. 28	5
30-	1831 Nov. 29	4.5
40-	1847 Apr. 7	6.5
50-	1857 Jun. 7	5.5
60-	1862 Jan. 9	5
70-	1872 Mar. 6	7.5
80-	1883 Oct. 20	5.5
90-	1897 Nov. 7	6.5
1900-1909	1908 Nov. 3	6.5
10-	1914 Jun. 27	6
20-	1926 Jan. 28	6
30-	1936 Dec. 2	4.5
40-	1943 Jun. 20	4
50-	1956 Sep. 19	3.5
60-	1962 Sep. 18	5
70-	1979 Sep. 25	5

N - number of intervals; j - rank; P_j - plotting position of the j th observation

Procedure

j	I_O	$P_j = j/(N+1)$	$-1n(-1nP_j)$	$T= (1-P^{1/t})^{-1}$ [years]
1	-	0.0526	-1.080	3.92
2	3.5	0.1053	-0.812	
.				
18	7.5	0.9474	2.918	185.6

Plot I_0 over P_j and use special extreme value paper. If this paper is not available use $-ln(-lnP_j)$ as abscissa with values in units of 3 cm; I_0 as ordinate with values in units of 2 cm.

Exercise on seismic hazard assessment (a simplified approach)

G. Grünthal and Ch. Bosse

Dept. of Kinematics and Dynamics of the Earth
GeoForschungsZentrum Potsdam, Telegrafenberg C3, D-14473 Potsdam

Task: Estimation of site design earthquake (SDE) and safety shutdown earthquake (SSE) on the basis of the cumulative intensity-frequency relation determined at the site

Input data: Let us assume five seismoactive zones characterized by:

- annual intensity-frequency relations, $\log N_n(I_o) = a - b\, I_o$ which are defined by the coefficients a and b,
- maximum possible epicentral macroseismic intensities I_{max} estimated for each zone separately, and
- attenuation values ΔI of intensities determined for the distance of the seismoactive zone to the site.

Seismoactive zone	a	b	I_{max}	ΔI
1	1.570	0.516	IX-X	1.0
2	0.055	0.335	X	1.3
3	0.387	0.372	XI	2.2
4	-0.394	0.326	IX-X	0.5
5	1.203	0.509	VIII-IX	1.3

Tasks:

1. Compile the cumulative intensity-frequency relation for the site.
2. Estimate the intensity of the SDE and the SSE.
3. What is the maximum possible intensity at the locality?
4. What seismoactive zone is affecting the site most?

Help for answers:

1. $I_{site} = I_{max} - \Delta I$
2. Compare the effects caused by the third and by the fourth seismoactive zones at the site.
3. The return period of the SDE is 100 years and that of the SSE is 10 000 years; compare these periods with the present input data (e.g. take into account the Tab. 1 of exercise "Incompleteness of a catalogue and the parameters of the Gutenberg - Richter relation").

Exercise on PC assisted hazard assessment

Ch. Bosse and G. Grünthal

Dept. of Kinematics and Dynamics of the Earth
GeoForschungsZentrum Potsdam, Telegrafenberg C3, D-14473 Potsdam

Task: Create an input-file for the 1976 McGuire program with help of the "GFZ - toolbox on data preprocessing for seismic hazard assessment".

Input data: You will find an earthquake catalogue and its format description at the PC.

1. Start the toolbox program. (The catalogue should be read in automatically.)

2. In order to estimate the completeness of the catalogue do the following:
   a) delineate a region including the whole catalogue area;
   b) click into the region area with the left mouse button;
   c) click "No vs. time" button (number versus time);
   d) estimate completeness times for the different intensity ranges, note them and remove the region.

3. Define a new completeness table using the noted completeness times.

4. Delineate seismic source areas on the screen. Use the given geological map (Fig. 1).

5. Estimate a characteristic depth for each source region using depth distribution plot of the toolbox (click into the region area with the left mouse button; click "depth distrib.")

6. Create an input file for the 1976 McGuire program with the help of the toolbox (use Output; McGuire 1976; Get all).

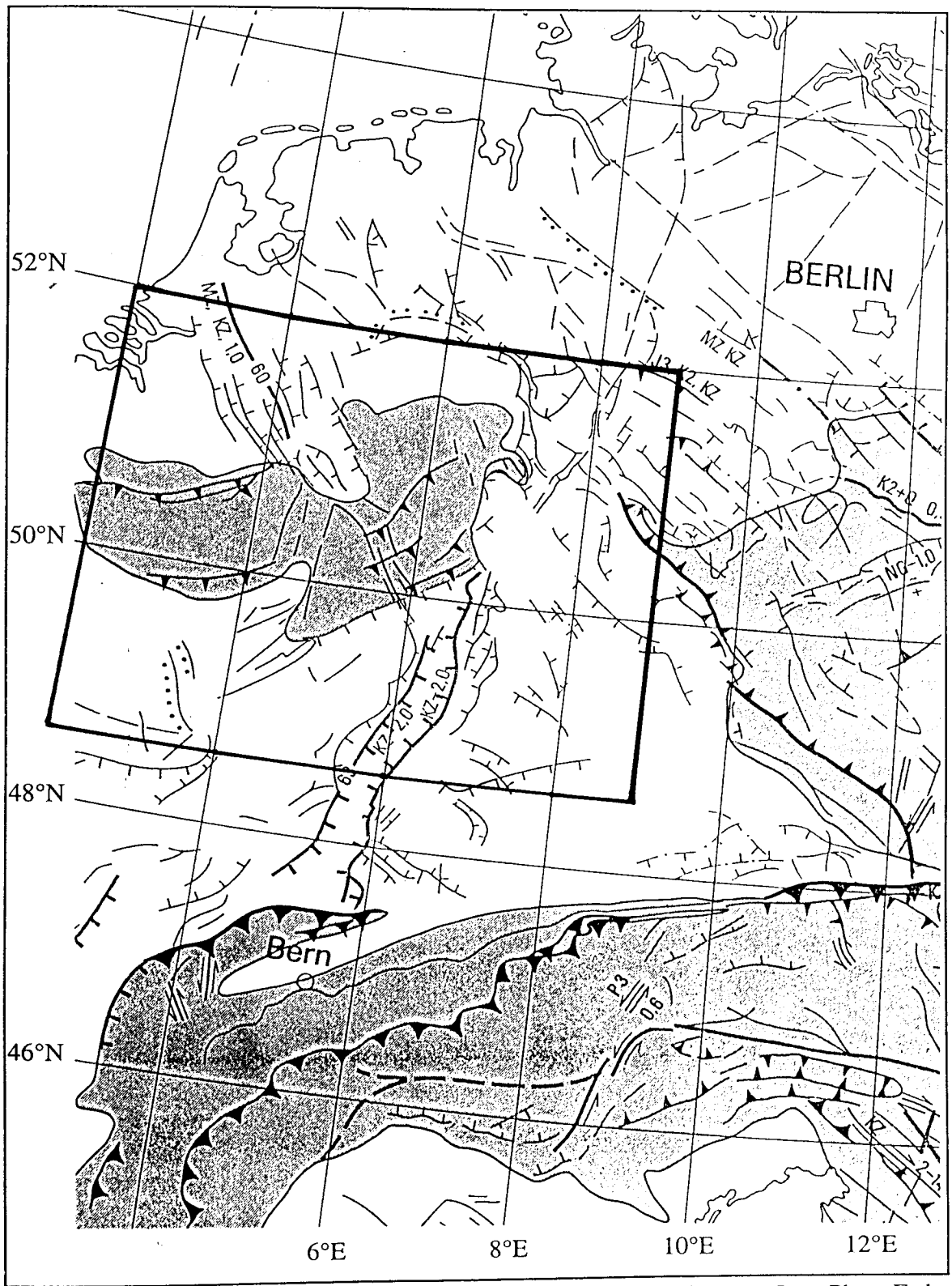

Fig. 1 Map of main tectonic faults (part of Meier, R. et al., Veröff. Zentr.-Inst. Phys. Erde, Potsdam Nr. 47 1976, Materialien zum tekt. Bau von Europa, Tektonische Bruchstörungen Karte 7); conventional signs are made according to the international use

LOCAL EFFECTS ON STRONG GROUND MOTION: BASIC PHYSICAL PHENOMENA AND ESTIMATION METHODS FOR MICROZONING STUDIES

Pierre-Yves Bard

Laboratoire Central des Ponts-et-Chaussées and Observatoire de Grenoble
LGIT/IRIGM - BP 53 X - 38041 Grenoble Cedex - FRANCE
Tel. +33 44 51 44 87, Fax +33 44 51 44 22, Email: bard@lgit.observ-gr.fr

1. INTRODUCTION

It is now well known, and widely accepted amongst the earthquake engineering community, that the effects of surficial geology on seismic motion exist and can be large. Two "famous" examples of such effects are the area of San Francisco, for which local amplifications over unconsolidated sediments have been shown to be responsible for intensity variations as large as two degrees (MM scale) during both the 1906 "big" San Francisco earthquake and the more recent 1989 Loma Prieta event, and the Mexico City valley, in which the surficial very soft lacustrine clay deposits in Mexico City induced dramatically high death toll and economic losses during the distant Guerrero-Michoacan earthquake of 1985 (Figure 1). And almost all recent destructive earthquakes (Armenia 1988, Iran 1990, Philippines 1990, Northridge 1994, Kobe 1995, ...) have brought additional evidence of the dramatic importance of site effects: another example is provided in Figure 2 corresponding to a moderate magnitude event (M = 6.5) near Thessaloniki (Greece) in 1978.

Accounting for such "site effects" in seismic regulations, land use planning or design of critical facilities is therefore a goal of earthquake hazard reduction programs. The question that arises is how to achieve that goal in a way both liable and not too expensive Answering that question is far beyond the scope of the present paper, which is simply intended to give a brief outline of the present state of knowledge regarding these ground shaking site effects, and to figure out the main issues yet to be solved in order to achieve that goal.

In the first section, the main site effects (i.e., amplification effects related with surface topography, amplification effects related with sedimentary sites, and effects connected with strong lateral discontinuities) are briefly presented, together with their main characteristics and some general remarks. Then, the various techniques to estimate these site effects are reviewed: experimental methods, empirical methods, numerical methods, and statistical analysis of existing accelerometric data. Finally, conclusions are drawn as to the most relevant ways to account for such site effects in the practice of microzoning studies.

Although other kinds of site effects such as liquefaction or earthquake triggered landslides have very important consequences for earthquake engineering, too, we consider here only the "ground shaking" site effects, which are basically related to wave propagation phenomena and do not induce large irreversible displacements.

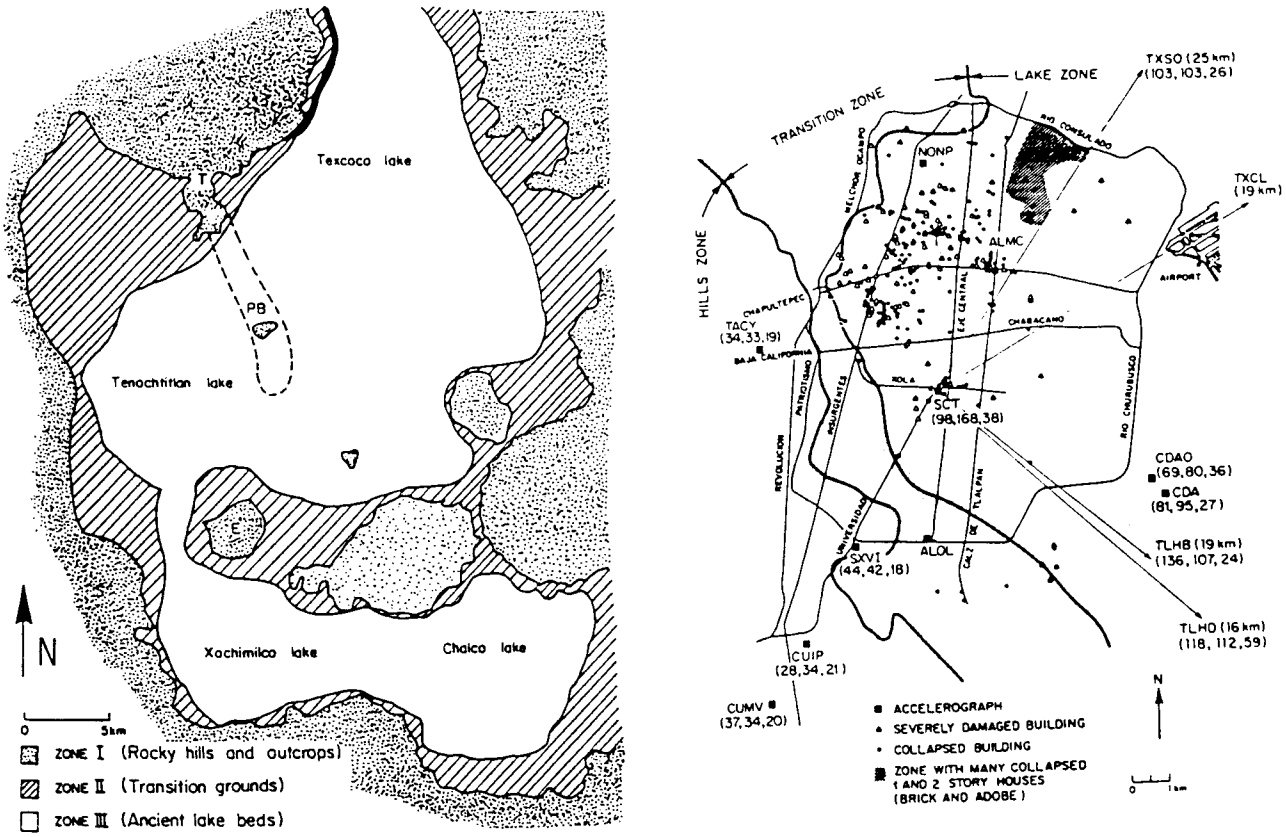

Figure 1 : *An example of dramatic site effects in relation with surface geology: Mexico City.*
a) (left) Simplified geological map of the valley of Mexico City, with three well-defined soil types: rocky hills and volcanoes (zone I), very soft clays of the ancient lake beds (zone III), separated by a transition zone with stiffer and thinner sedimentary deposits (after Seligman et al., 1989).
b) (right) damage distribution in downtown Mexico City during the 1985 Guerrero-Michoacan earthquake:collapsed and severely damaged buildings are concentrated in a limited area of the lake-bed zone.(Also shown are the strong motion sites that recorded the motion (see Figure 8) together with the peak accelerations (in gals) for NS, EW and Z components (after Sigh et al., 1988)

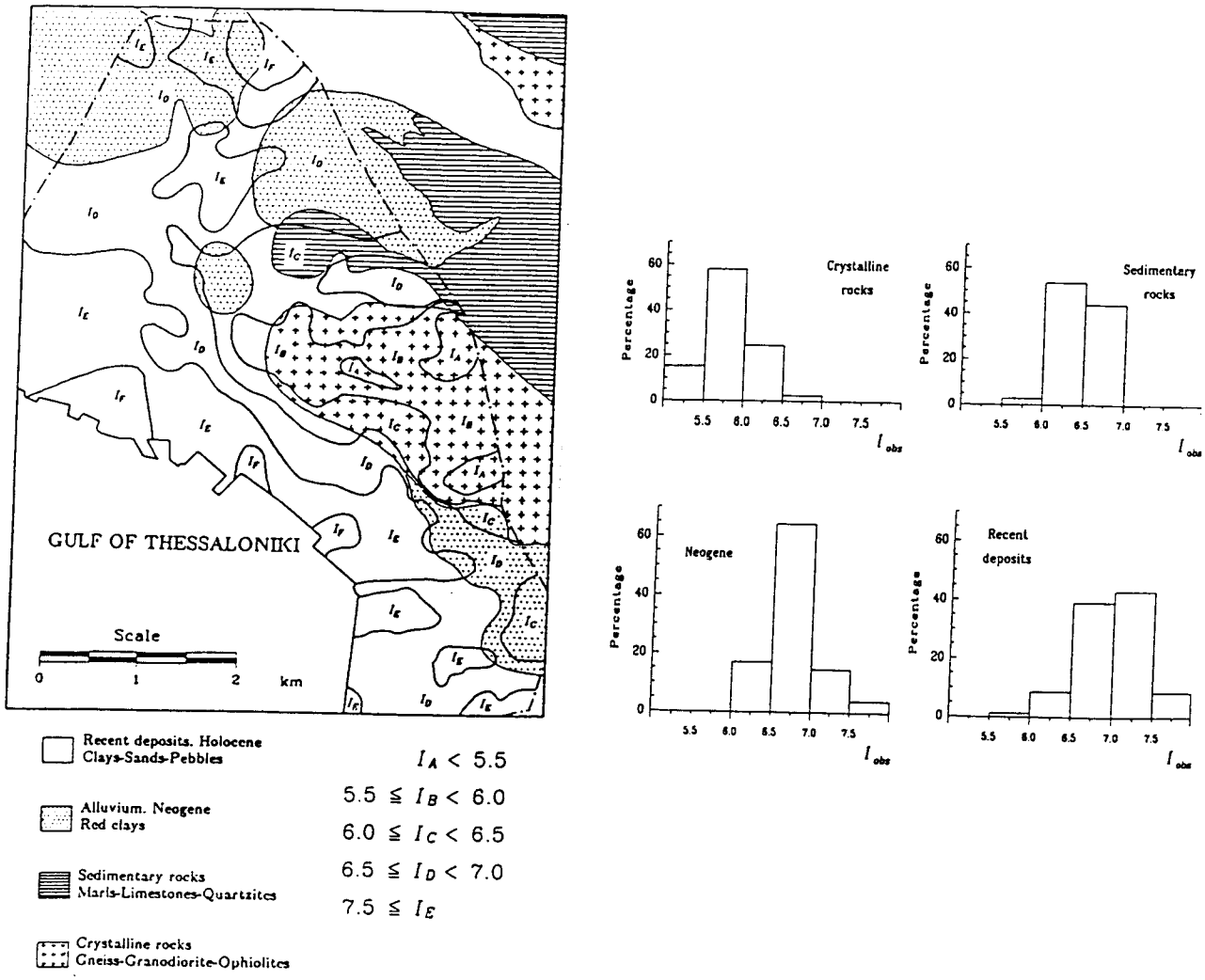

Figure 2 : *Correlation between surface geology and local intensity variations within Thessaloniki (Greece) during the 1978 Volvi-Langhada earthquake sequence (after Chavez-Garcia et al., 1990). Histograms on the right represent the percentage of area comprised in each intensity level for each of the four geological units, and exhibit a mean intensity increment of 1.5 degrees (MSK scale) between crystalline rocks and recent deposits.*

2. GROUND SHAKING SITE EFFECTS: MAIN CHARACTERISTICS

Macroseismic observations, instrumental studies and theoretical or numerical investigations agree on the quasi-systematic occurrence of local effects on a limited number of "typical" geological configurations, characterized by their geometry and their mechanical parameters (S and P velocities, density, damping,...). This section is devoted to a short review of these "typical" effects: for each of them, the basic physical phenomena responsible for the effect are briefly described, the known amplitude range of the effects is given, and what is presently recognized as being unsatisfactorily understood is also briefly mentioned.

2.1 Surface topography effects

2.1.1 Evidence for topographic effects

It has been often reported after destructive earthquakes in hilly areas that buildings located at hill tops suffer much more intensive damage than those located at the base: examples of such observations may be found in Levret et al., 1986 (Lambesc, France, 1909 earthquake), Brambati et al. 1980 (Friuli, Italy, 1976 earthquake), Siro, 1982 (Irpinia, Italy, 1980 earthquake), and Celebi, 1987 (Chile, 1985 earthquake). The recent Kozani (northern Greece) earthquake of May 1995 again brought evidences of severe damage in villages built on hill tops

There are also very strong instrumental evidences that surface topography considerably affects the amplitude and frequency contents of ground motion: a review of such instrumental studies and results may be found in Géli et al. (1988) and more recently in Faccioli (1991) and Finn (1991). To date, the largest recorded topographic effect was presented first in Bard and Mèneroud (1987), and confirmed in Nechtschein et al. (1995) for a very steep site in southern Alps, with a crest/base spectral ratio reaching several tens in a narrow frequency band around 5 Hz, as depicted in Figure 3. The latest example comes from the strong motion recordings made at the Tarzana station during the Northridge, 1994, earthquake, for which the spectral amplification reached a factor of 5 around 3 Hz (Celebi, 1995; Bouchon and Barker, 1995). However, the number of instrumental studies about topographic effects is extremely low compared to studies of soft soil amplification (certainly less than 10 worldwide in the last 4 years, according to international literature), so that it remains impossible to derive any statistics from the existing data.

Finally, theoretical and numerical models also predict a systematic amplification of seismic motion at ridge crests, and, more generally, over "convex" topographies (such as cliff borders), and a correlative deamplification over "concave" parts of surface topography, such as valley and foothills. The amount of those effects have been shown (Pedersen et al., 1994b) to be rather sensitive to the characteristics of the incident wavefield (wave type, incidence and azimuth angles). Theory also predicts complex amplification and deamplification patterns on hill slopes, resulting in significant differential motion.

Basically, these effects are related with three physical phenomena:

i) the sensitivity of the surface motion to the incidence angle - which is especially large for SV waves around the critical angle -, which results in a significant variation of surface motion with slope angle (Figure 4). This kind of effect was advocated by Kawase and Aki (1990) as a possible explanation for the peculiar damage distribution observed during the Whittier Narrows, California, earthquake of 1987.

Scientific Technical Report STR 95/TK
DOI: 10.2312/GFZ.b103-95tk7

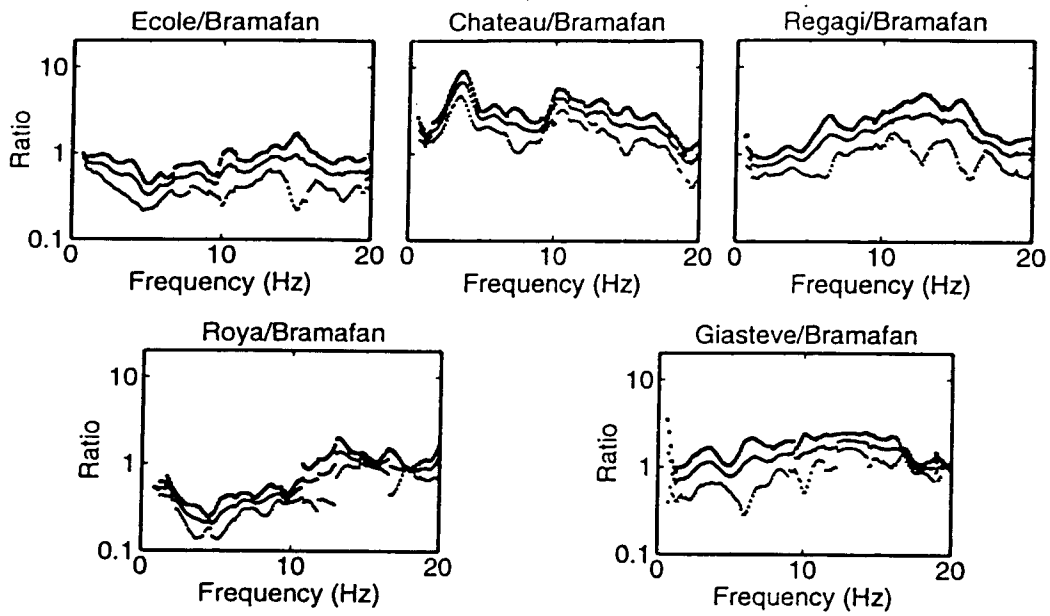

average curves (•), 'average - standard deviation' curves (▲) and 'average + standard deviation' curves (■) of the 5 Piène stations (E-W components only).

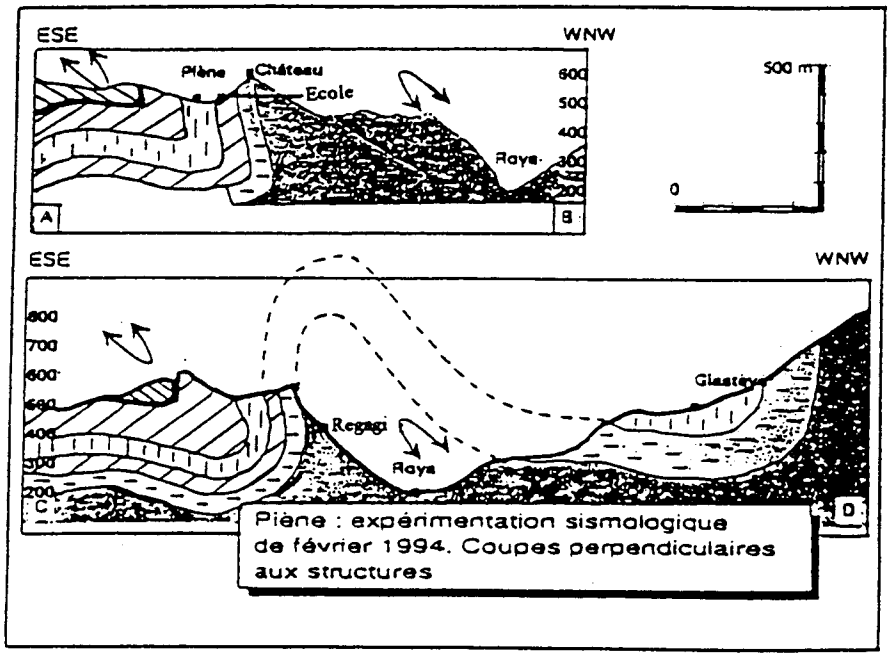

Figure 3 : *An example of a large topographic effect at Piène, France. The 5 top diagrams display the average spectral ratios obtained at 5 surface sites (plus or minus one standard deviations), for the EW (in-plane) component. The reference station is not the base station ("Roya"), but the westernmost, mid-slope station (Bramafan). A cross-section of the investigated topography is shown on bottom. (Reproduced from Nechtschein et al., 1995).*

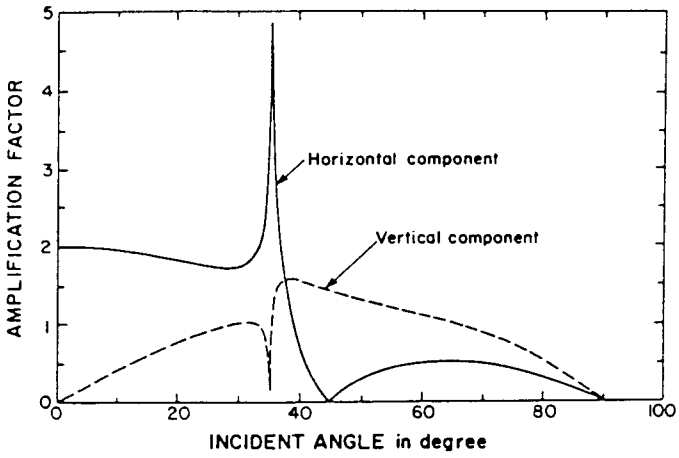

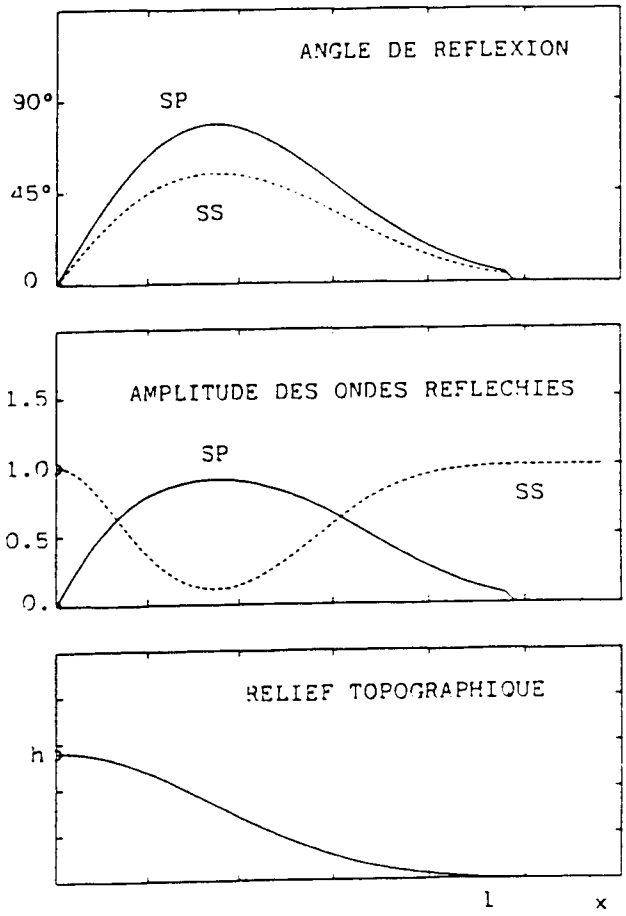

Figure 4 : *Sensitivity of surface motion to incidence angle for obliquely incident plane SV waves. a) (Left) Dependence of in soft soils, for use in linear equivincidence angle for incident SV waves (for a Poisson coefficient of 0.25). b) (Right) Variations of reflection angle and amplitude of locally surface reflected waves for vertical SV waves impinging on the topographic feature illustrated at bottom*

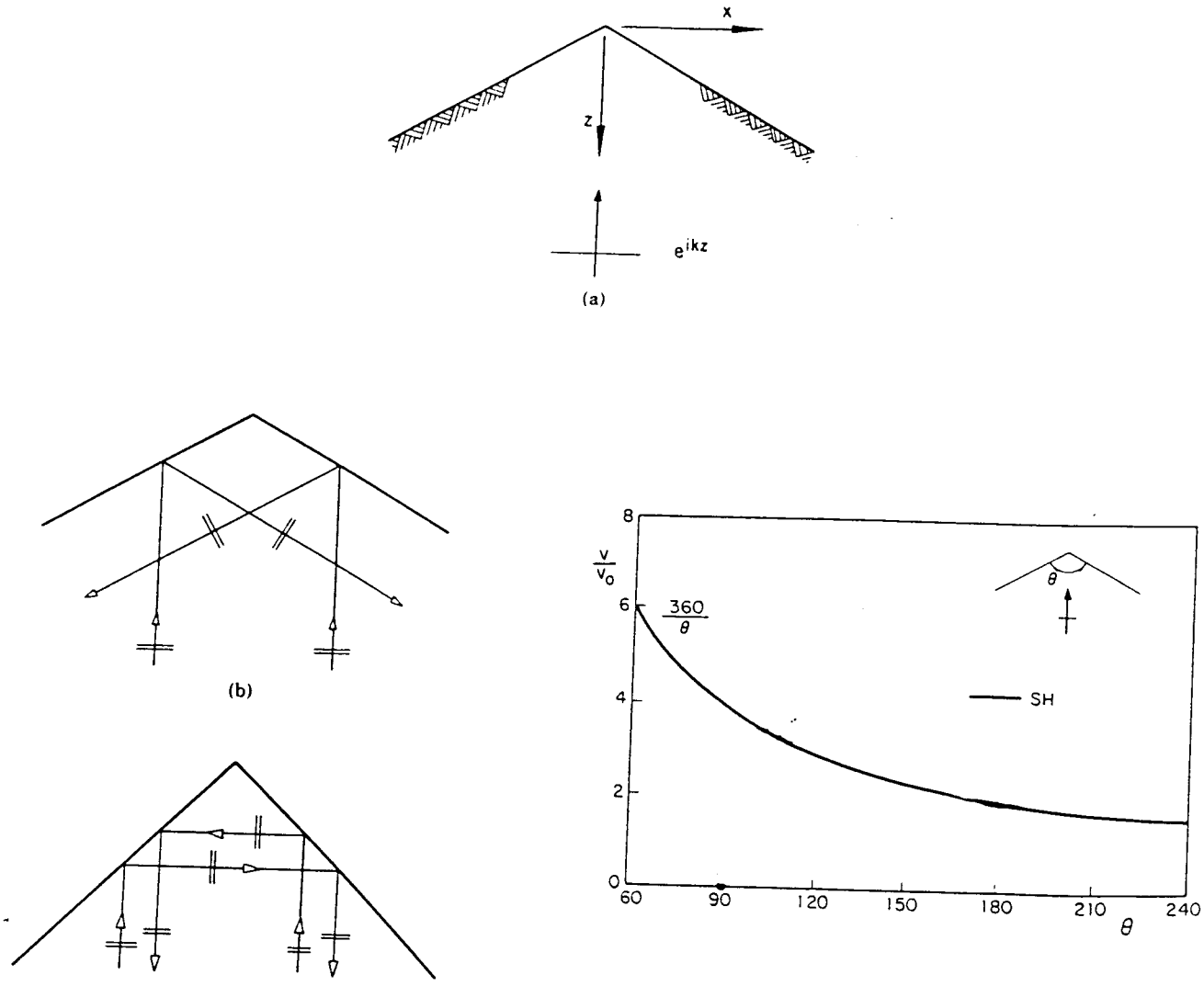

Figure 5 : *Response of a particular class of wedges to vertically incident SH waves (from Sanchez-Sesma, 1990). When the wedge angle is equal to $2\pi/n$, there exist n different waves passing through any point inside the wedge: the direct wave, and the simply and multiply ($n \geq 4$) reflected waves on each side of the wedge. All these waves interfere positively at wedge vertex, since there is no phase lag at this particular location, and the resulting amplitude of motion is n times larger than the incident wave.*
Illustrations of reflected waves are given for $n=3$ and $n=4$, while the resulting vertex motion is shown on right as a function of wedge angle..

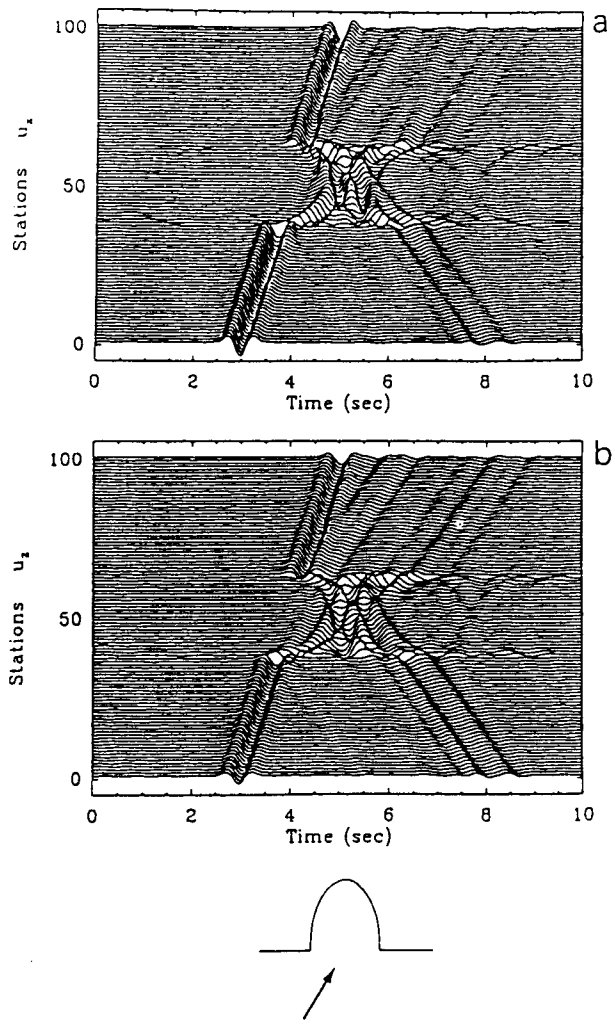

Figure 6 : *Time domain response of a sharp semi-elliptical mountain to incident palne SV waves (θ = 30°). The mountain has a half-width a, a height 2a, and a Poisson coefficient of 0.25. Horizontal (a, top) and vertical (b, bottom) components are computed for 101 surface receivers equally spaced between x=-4a and x=+4a. The incident signal is a Ricker wavelet with central frequency corresponding to a wavelength equal to 1.33 a; it was assumed that 2a/Vs = 1s for the time scale. This topographic feature is an extreme model that shows very clearly all the diffracted waves: diffracted Rayleigh waves, creeping waves along the topography surface, and late emission of Rayleigh waves.*
(After Sanchez-Sesma and Campillo, 1991).

ii) the focusing or defocusing of seismic waves reflected along the topographic surface: Sanchez-Sesma (1990) provided a very intuitive insight of this effect through the simple example of a wedge-shaped medium, the response of which to SH waves may be easily understood and computed when the edge angle is equal to 2p/n: considering the remarkable angles and the resulting number of multiply-reflected waves in such a case (equal to n-1), one may easily derive that the motion amplitude at the vertex is equal to 2n times the incident one, since there is no phase lag between incoming and reflected waves (Figure 5). Up to now, there has not been any instrumental proof of such focusing /defocusing effects, due to the lack of any dense 3D seismological array on a topographic feature.

iii) the diffraction of body and surface waves which propagate downwards and outwards from the topographic feature, and lead to interference patterns between the direct and diffracted waves; however, the amplitude of the waves propagating along the surface generally remain smaller than the direct waves, at least for smooth topographies comparable to those usually met in nature.

iii) the diffraction of body and surface waves which propagate downwards and outwards from the topographic feature, and lead to interference patterns between the direct and diffracted waves. The amplitude of the waves propagating along the surface generally remain smaller than the direct waves, at least for smooth topographies comparable to those usually met in nature (Figure 6). These outward propagating waves consistently predicted by the theory have been reported for the first time (to our knowledge) by Pedersen et al. (1994b) from semi-dense array recordings in Greece, and their amplitude has been shown to be about one fifth of the primary wave.

2.1.2 State of knowledge (and state of ignorance) on surface topography effects

We will reproduce here the conclusions drawn by Géli et al. (1988) at the end of their review section; these conclusions are based on the compilation of instrumental and theoretical results displayed in Figure 7.

i) there is a qualitative agreement between theory and observations about the existence of seismic motion amplification at mountain tops, and correlatively of a deamplification at valley bottoms. This amplification is generally larger on horizontal components (roughly corresponding to S motion) than on the vertical component (~ P motion), and, within the two horizontal components, it seems larger for motion perpendicular to the ridge axis in the case of 2D ridges.

ii) the observed or computed amplification seems very roughly related to the "sharpness" of the topography: the steeper the average slope, the higher the top amplification.

iii) this amplification (deamplification) phenomenon is, very clearly again, frequency dependent, and, more precisely, band-limited. Moreover, there is a satisfactory quantitative agreement between instrumental observations and theoretical results as to the relation between the geometrical and mechanical characteristics of a given topography, and the frequency band where it induces significant effects: the maximum effects correspond to wavelengths comparable to the horizontal dimension of the topographic feature (Figure 7c).

iv) however, from a quantitative viewpoint, the situation is somewhat confusing, as already stressed in Géli et al. (1988). There exist cases where field studies exhibit only very weak amplifications at ridge crests that fit very well the numerical results (Rogers et al., 1974; King et al., 1984), but there also exist numerous cases where the observed amplifications

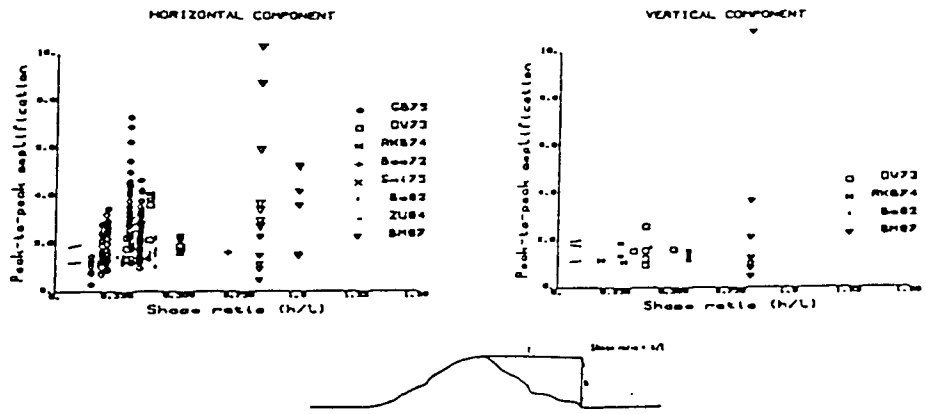

a: Peak-to-peak crest/base amplification as reported in the literature and plotted as a function of the apparent shape ratio h/l. Left: *Horizontal motion;* Right: *Vertical motion. Open symbols (squares, circles, etc...) indicate experimental field studies, while others (crosses, dots, etc.) indicate results of theoretical studies. Each symbol corresponds to a paper as follows: Ba82 – Bard, 1982; Boo72 – Boore, 1972; DW73 – Davis and West, 1973; GB79 – Griffiths and Bollinger, 1979; BM87 – Bard and Mèneroud, 1987; RKB74 – Rogers et al., 1974; Smi75 – Smith, 1975; Si78 – Sills, 1978; TKHN84 – Tucker et al., 1984; ZBY80 – Zhenpeng et al., 1950; ZU84 – Zahradnik and Urban, 1984.*

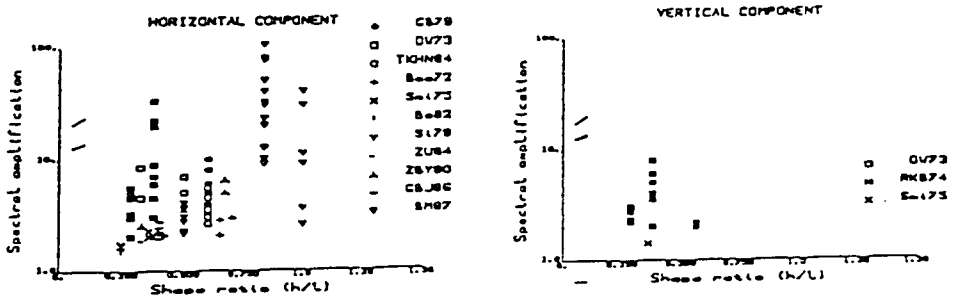

b: Maximum crest to base spectral amplification as reported in the literature and plotted as a function of the shape ratio as in 2a. Left: *Horizontal motion;* Right: *Vertical motion.*

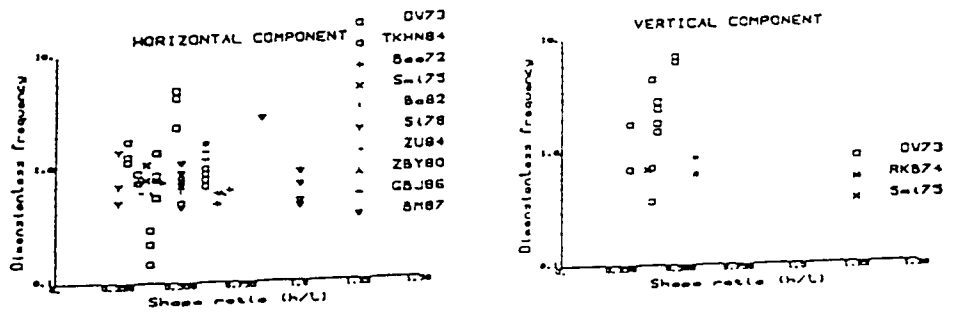

c: Dimensionless frequencies corresponding to the maximum crest to base spectral amplification displayed in Figure 2b, still plotted as a function of shape ratio. Left: *Horizontal motion;* Right: *Vertical motion. The actual frequencies have been, in each case, multiplied by the quantity $2.l/\beta$, where l is the apparent half-width of the topography (measured at its base, see Figure 2a), and β is the S wave velocity. These values were estimated on the basis of the information given in the referenced papers, and are more a guess than a reliable measurement.*

Figure 7 : *Effects of topography on surface motion: a summary of instrumental and theoretical results (after Géli et al., 1988)*

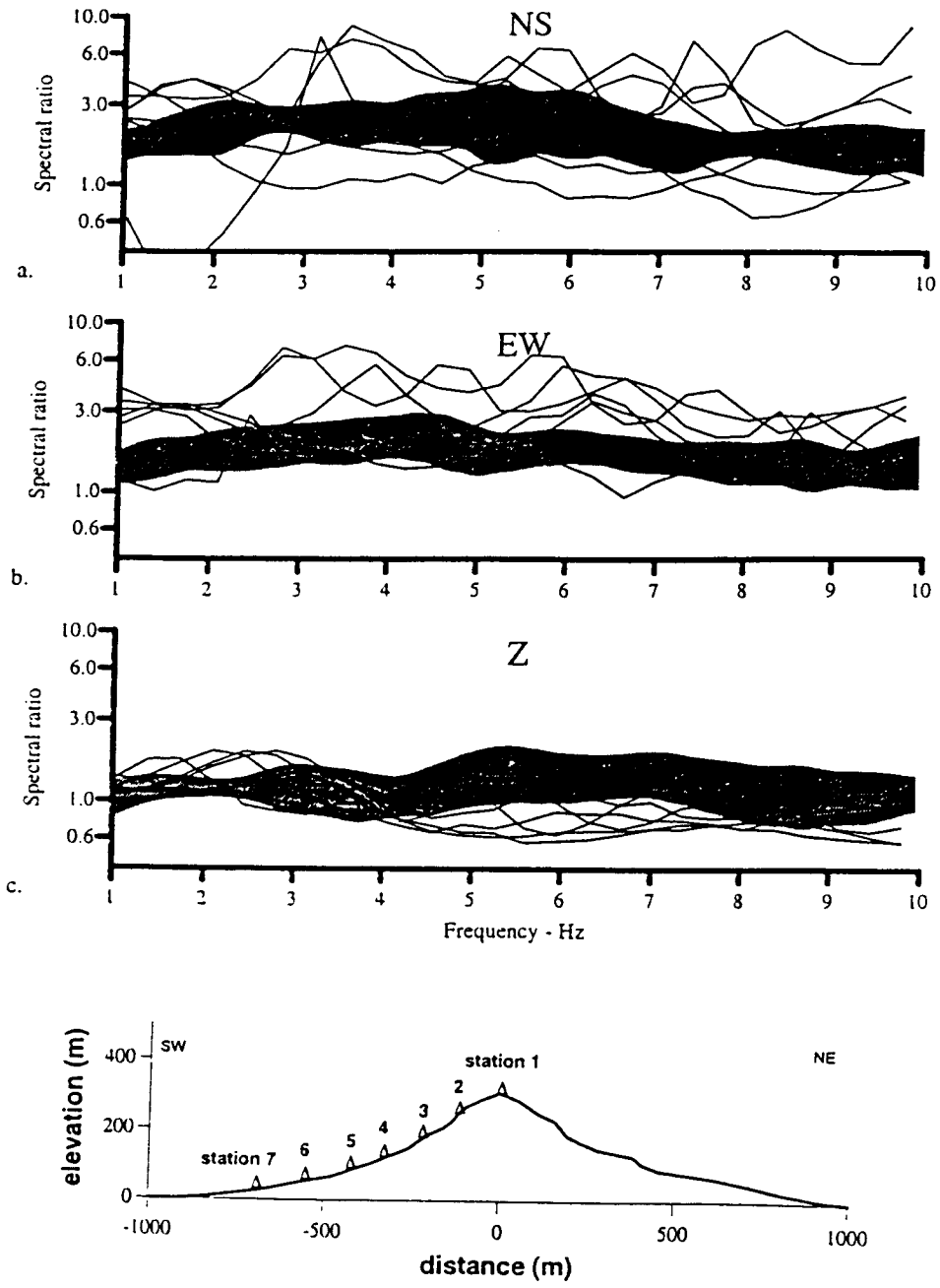

Figure 8: *An example of slight topographic amplification at Sourpi, Greece The 3 top diagrams display, for each component of motion, a comparison between the mean range range of observed crest/base spectral ratios (shaded area), and theoretical estimates using various incidence and azimuth angles (solid lines). A cross-section of the investigated topography is shown on bottom. (Reproduced from Pedersen et al., 1994).*

are significantly larger than the theoretical predictions using sophisticated, two- or three-dimensional models: there are numerous observations of spectral amplifications larger than 10, but only two predictions of such an amplitude by numerical models (Figure 7b). This confusing situation has been confirmed by the two most recent instrumental studies in Greece and French Alps (Pedersen et al., 1994b; Nechtschein et al., 1995). While in the former case only weak amplifications at ridge crest that fit very well the numerical results are reported (Figure 8), in agreement with a few previous observations (Rogers et al., 1974; Tucker et al., 1984), the latter presents two sites with large observed amplifications (as already reported in several other sites, see Géli et al., 1988), and very rapid variations of ground motion amplitude along the slopes: over horizontal distances smaller than 200 m, and altitude differences of a few tens of meters, there may exist a difference about one order of magnitude (Figure 3), which is in agreement with previous damage observations at the same sites. This latter case also provided a good example of motion deamplification at valley bottom, which leads to huge values (several tens) for the crest/base spectral ratio.

The focusing of seismic energy within convex topographies, as predicted by theoretical models, certainly plays a significant role in the observed amplification effects. It does not seem, however, to be the only physical phenomenon involved. Further detailed, tightly controled instrumental studies should be performed with dense arrays and detailed geotechnical surveys, to allow significant advances in the understanding of surface topography effects. These effects have received a surprisingly low attention in recent years; engineers and seismologist should be more concerned about them for basically two reasons: on one hand, earthquake prone areas are, very often, also mountainous areas, and villages, for security reasons, used to be built on hill tops in many places; on the other hand, surface topography effects are certainly closely related to the very often observed dynamic triggering of land- and rock- slides during earthquakes, which may cause severe damage and death toll.

2.2 Effects of soft surface layers

2.2.1 Observational and theoretical evidences

It has been recognized for a very long time that earthquake damage is generally larger over soft surface deposits than on bedrock outcrops. This kind of site effects is especially worth being accounted for, since most of urbanized areas are generally settled along river valleys over such young, soft, surficial deposits. A lot a large cities located in earthquake prone areas may be given as examples: Los Angeles, San Francisco Bay area, San Salvador, Caracas, Lima, Bogota, Tokyo, Osaka and Kobe, Kathmandu, Manilla, Thessaloniki, and, of course, Mexico City (Figure 9)... Such a characteristic may be dramatic for the inhabitants of those cities, but has at least one advantage for engineering seismologists: it has allowed numerous macroseismic observations to be made during the last century, which show very clearly that the damaging effects associated with such soft deposits may lead to local intensity increments as large as 2 to 3 degrees (MM or MSK scale). The amplitude of these effects has therefore stimulated many instrumental studies (comparing seismic records obtained at the sediments surface and in the basement rock underneath or on a nearby bedrock outcrop), as well as a lot of theoretical and numerical investigations based on the theory of wave propagation in more and more complex media, both aiming at a better understanding and quantification of these effects. The extreme engineering importance of such

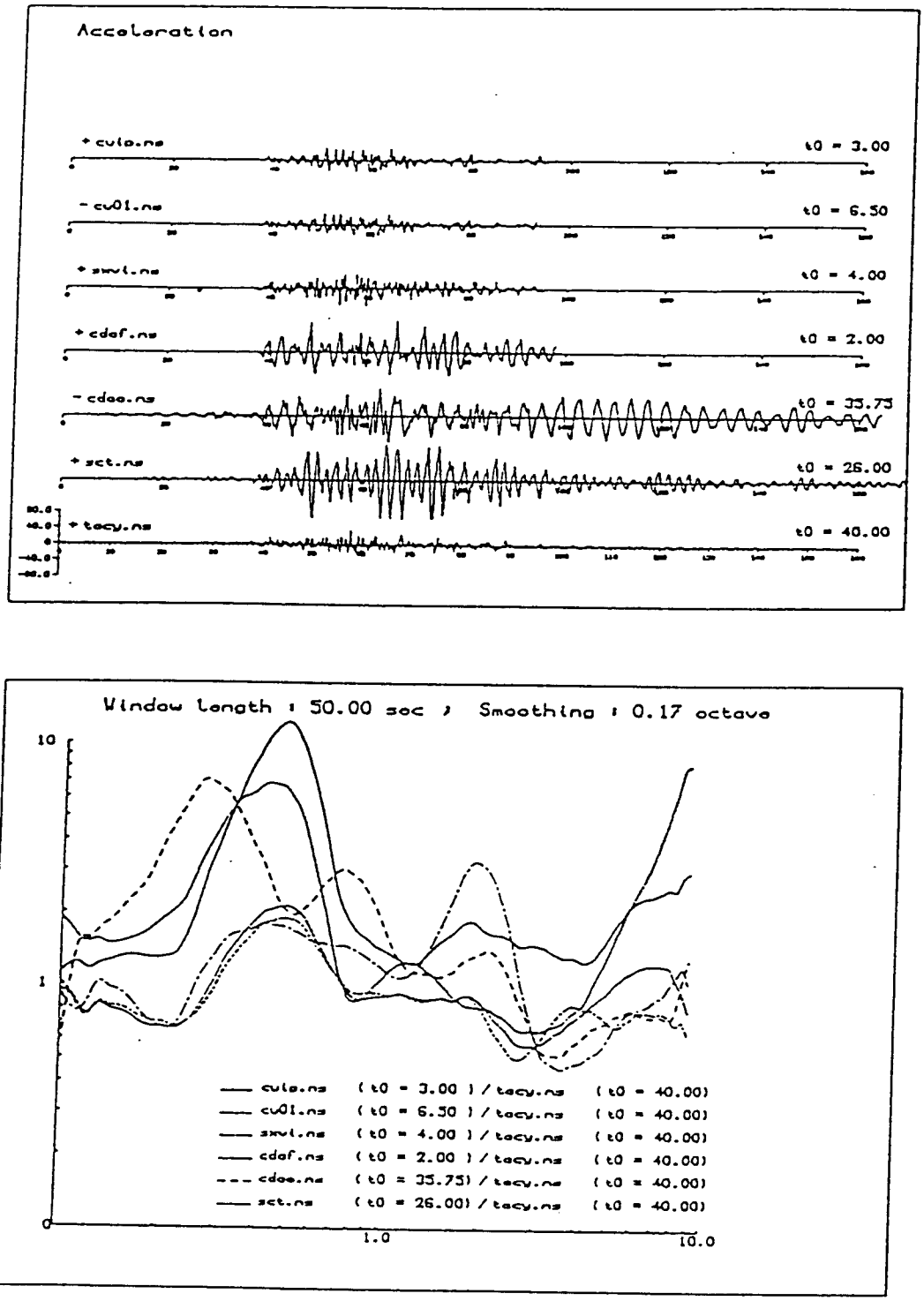

Figure 9 : *Strong motion data recorded in Mexico City during the September 19, 1985 Guerrero-Michoacan earthquake (see Figure 1 for station location)..*
a) (top) acceleration time histories for the NS component;
b) (bottom) smoothed spectral ratios between 6 stations located in the lake-bed zone (SCT, CDAO, CDAF), in the transition zone (SXVI) and in the hills zone (CUIP, CU01) with respect to a station in the hills zone

amplification effects has resulted in several recent review and state-of-the-art papers (Aki, 1988; Aki and Irikura, 1991; Finn, 1991; Faccioli, 1991), which the reader is strongly invited to consult for further information: the present section is a very crude summary of those various papers.

2.2.2 Fundamentals of amplification on soft soils

From all these observations and investigations, the following facts are established:

2.2.2.1 Physical basis

The fundamental phenomenon responsible for the amplification of motion over soft sediments is the trapping of seismic waves due to the impedance contrast between sediments and underlying bedrock. When the structure is horizontally layered (which will be referred to in the following as 1D structures), this trapping affects only body waves, which travel up and down in the surface layers. When the structure is a 2D or 3D structure, i.e., when lateral heterogeneities are present (such as thickness variations in sediment-filled valleys), this trapping also affects the surface waves which develop on these heterogeneities.
The interferences between these trapped waves lead to resonance patterns, the shape and the frequency of which are related with the geometrical and mechanical characteristics of the structure: they are very simple in the case of 1D media (vertical resonance of body waves), and more complex in the case of 2D (and a fortiori 3D) structures, except in the case of embanked valleys as shown by Bard and Bouchon (1985).
An illustration of these 1D and 2D behaviors is given in Figure 10.

2.2.2.2 Spectral characteristics

In the frequency domain, these resonance patterns are, as usual, characterized by various spectral peaks, as illustrated in Figure 11 in the 1D case, and in Figure 12 for a comparison between 1D, 2D and 3D cases.

- the frequency of these peaks is related to the surface layers both thickness and velocities, and also, for embanked 2D or 3D structures, to their width. For one-layer 1D structures, this relation is very simple:

$$f_0 = \beta 1 \ / \ 4\ h \qquad \text{(fundamental)} \qquad (1)$$

$$f_n = (2n+1).\ f_0 \qquad \text{(harmonics)} \qquad (2)$$

(where β_1 is the S wave velocity in the surficial layer, and h its thickness).
The value of fundamental frequency may therefore range between 0.2 Hz (for very thick deposits, such as in Los Angeles or Tokyo; or for extremely soft materials, such as in Mexico City) and 10 Hz or more (for very thin layers such as diluvial deposits or weathered rocks) (Figure 13).

- the amplitude of these peaks is related mainly to the impedance contrast between the very surface and the underlying bedrock and to sediment damping, and, to a somewhat lesser extent, to the characteristics of the incident wavefield (type of waves, incidence angle, near-field or far-field, ...), and for 2D (3D) structures, to their geometry (in case of small damping, this geometrical dependence may become very important). For one-layer 1D structures impinged by vertical plane S waves, this relation is, for the fundamental peak:

$$A_0 = 1. \ / \ (\ 1./C + 0.5\ \pi\zeta 1\ ) \qquad (3)$$

where C is the impedance contrast $\rho_2.\beta_2 \ / \ \rho_1.\beta_1$, ρ_i is the density of medium i (i = 1 for

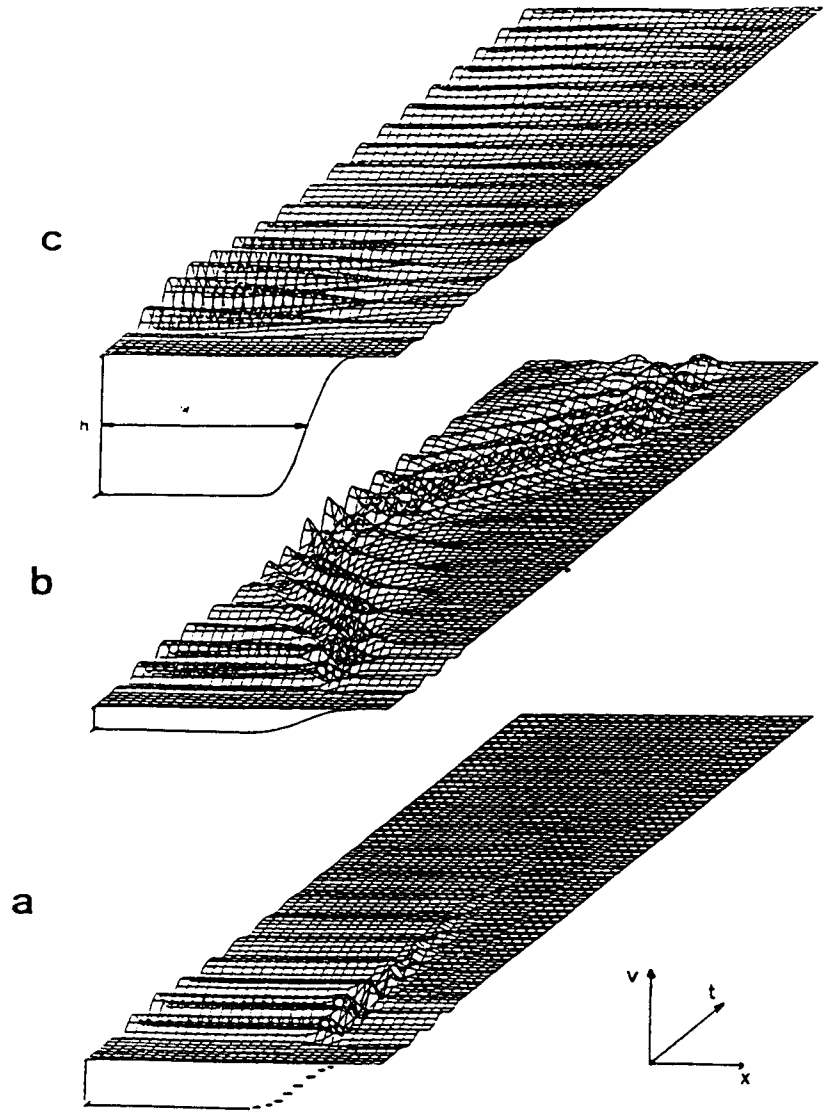

Figure 10 : *Differences between 1D and 2D behaviors for a perfectly elastic (no damping) sediment-filled valley. These diagrams represent the spatial (x) and temporal (t) evolution of the surface motion of a sediment-filled valley impinged by a SH signal with a characteristic frequency $f_p=\beta_1/4h$ (β_1 is the S wave velocity in the sediments, h is the valley thickness).*
a) Results obtained with a 1D approximation (considering only, for each site x, the local sediment thickness)
b) Results obtained a 2D modelling, in the case of a shallow valley: h/w = 0.06
c) Results obtained a 2D modelling, in the case of a thick valley: h/w = 0.70

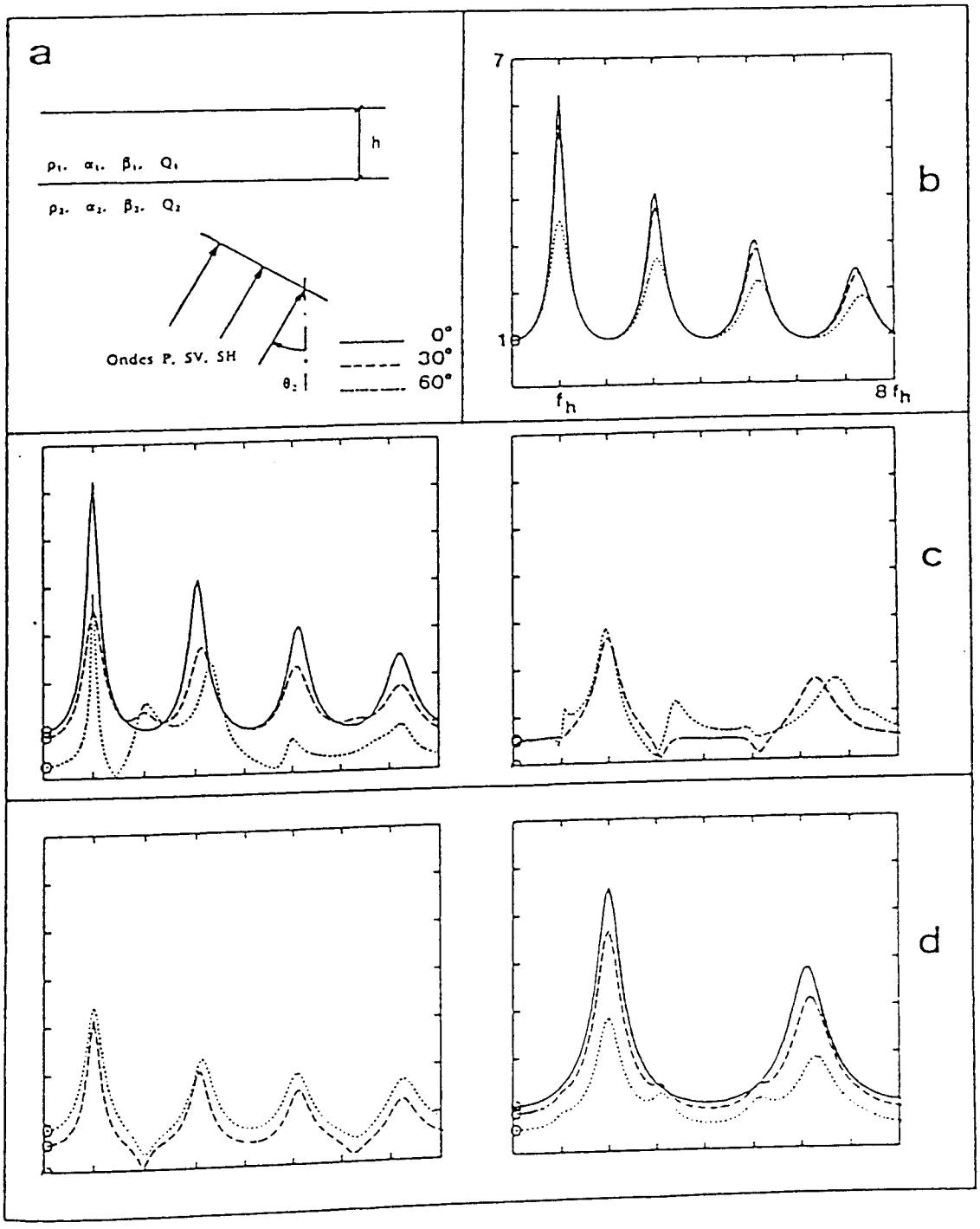

Figure 11 : *Vertical resonance in a plane layer.*
a) Problem geometry: $\alpha_1 = 2\beta_1$; $Q_1 = 20$; $\alpha_2 = 1.732\,\beta_2$; $Q_2 = 10^5$; $\beta_2/\beta_1 = 5$.
b) Fourier transfer functions for the transverse horizontal component in the SH case, and for three incidence angles: 0, 30 and 60°. The frequency unit is the resonance frequency $f_h = \beta_1/4h$.
c) Fourier transfer functions for the radial horizontal (right) and vertical (left) components in the SV case, and for the same three incidence angles.
d) Same as c), but for incident P waves.

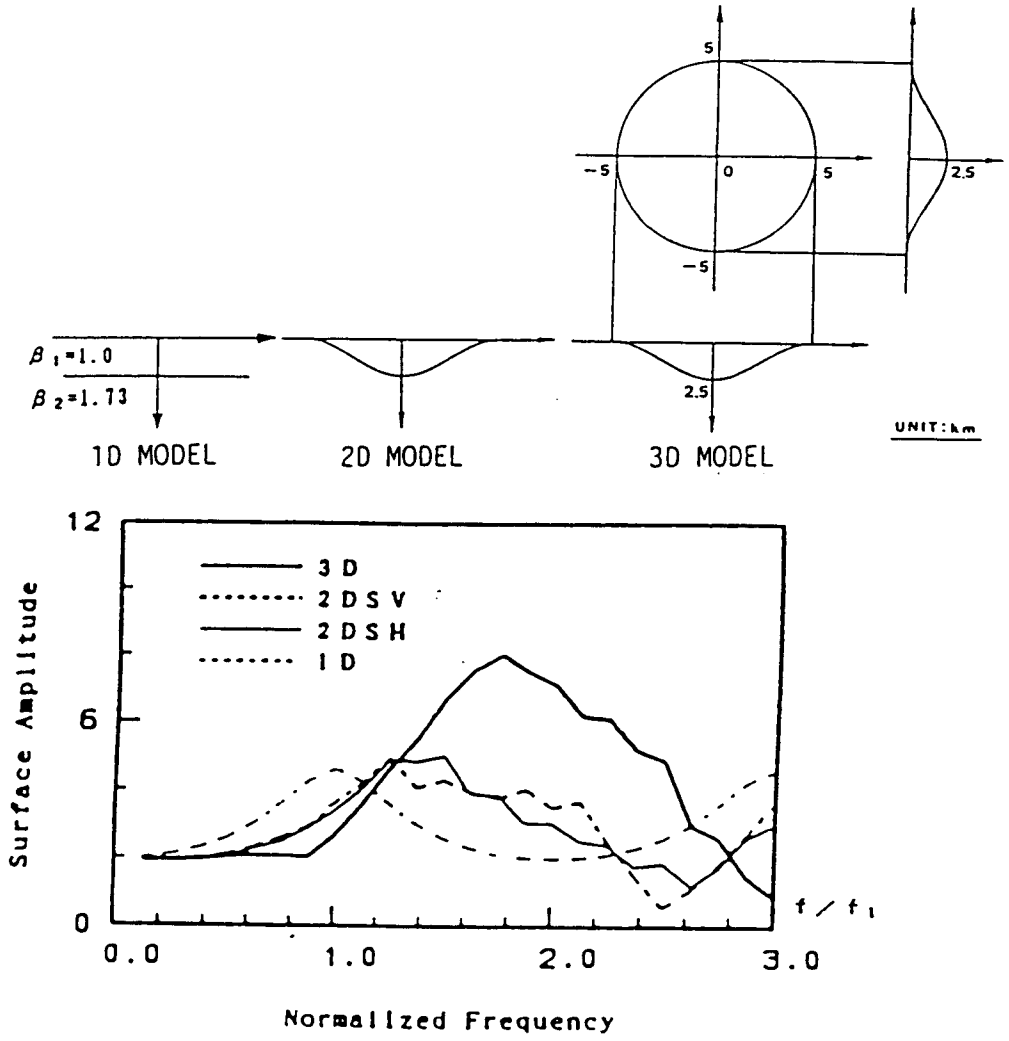

Figure 12 : *Comparison of spectral responses of 1D, 2D and 3D models for an elliptic basin (adapted from Aki and Irikura, 1991). For 2D and 3D models, the motion is computed at basin center.*

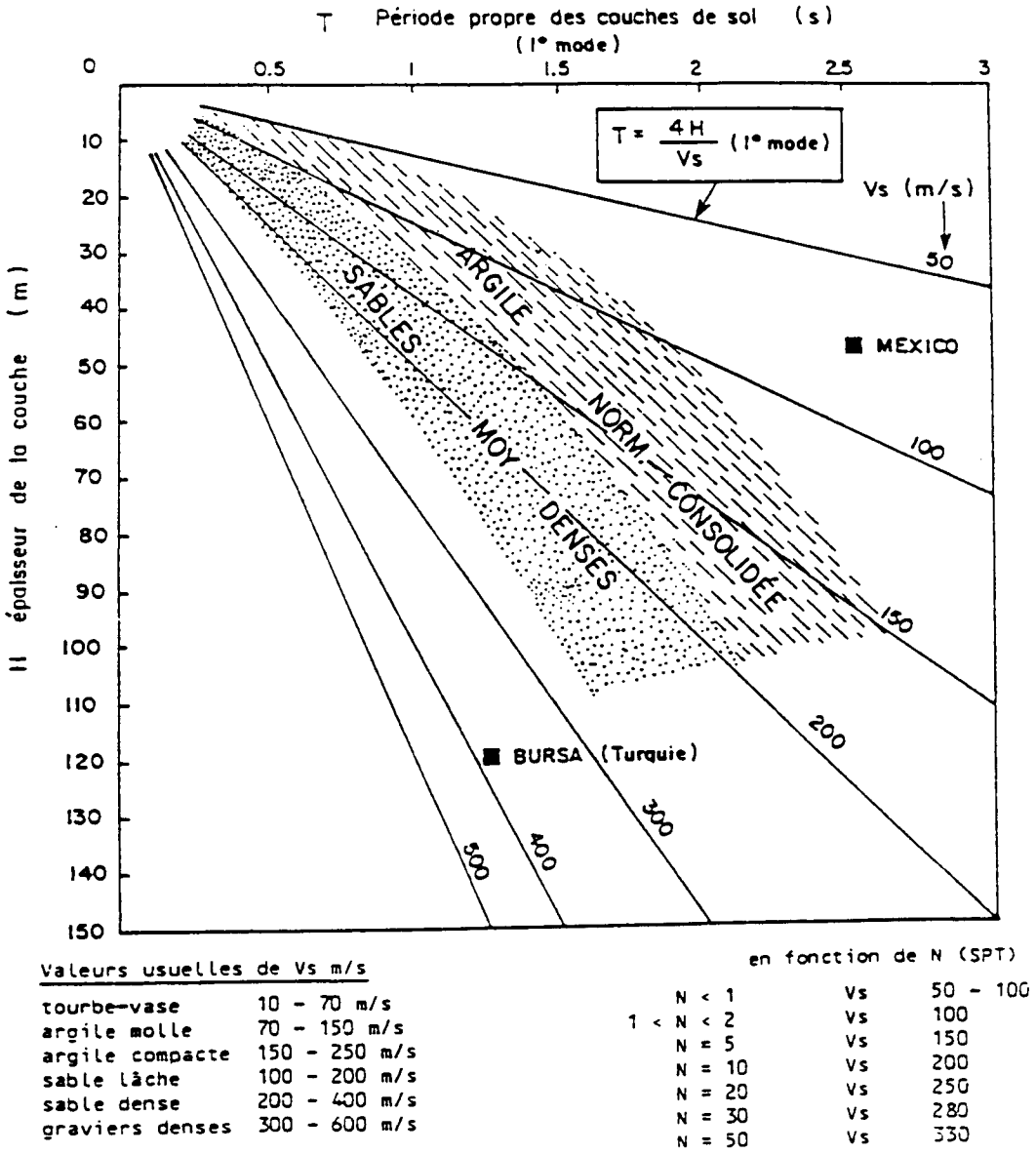

Figure 13 : *Resonance period of a horizontal soil layer, as a function of layer thickness (vertical axis) and S wave velocity (oblique lines). Also indicated are the average range of values of S-wave velocities in various kinds of soils (mud, soft clay, dense clay, loose sand, compact sand, and gravels). From Durville et al., 1985.*

sediments and i = 2 for bedrock), and ζ_1 is the material damping in sediments.
This formula shows that in case of very small damping ($\zeta_1 = 0$), the maximum amplification is simply the impedance contrast. This peak spectral amplitude has been shown, from both experimental and theoretical studies, to reach very often values between 6 and 10, and, in extreme cases (Mexico City, San Francisco Bay mud), to exceed 20.

2.2.2.3 Time domain characteristics

In the time domain, these effects affect the peak amplitudes, the waveforms and the motion duration, especially in the case of 2D structures, as illustrated in Figure 10, and in Figure 9 for the case of Mexico City.

Peak values
Until recently, it was thought, from early statistical analyses performed on a few strong motion data sets, that the peak acceleration is not, in an average, affected by sediments, while peak velocity is generally larger; the Mexico City records (Figure 9) showed, however, that the acceleration level is 4 times higher in the lake-bed zone than in the hills zone. As supported by Campbell (1985), there may be some bias in these statistical analyses, since they use essentially strong motion data recorded on very thick sediments (and especially in the Los Angeles area), and very few (if any) recorded on thin (h < 15 m) deposits, where fundamental frequency exceeds 2-3 Hz, and for which the peak acceleration is therefore likely to be amplified. And such thin deposits are very frequent in earthquake prone mountainous areas.
On the other hand, it was also observed in a few recent earthquakes (among which the Kobe earthquake), that liquefied sandy deposits induce drastic reductions of peak accelerations.
It thus appears that peak acceleration values on sediments cannot be predicted in a straightforward way from pga values on rock. However, an increasing number of engineering seismologists expect an amplification of peak acceleration on soft sediments, at least for moderate acceleration levels (below 0.4 g). This issue is indeed very closely connected to the non-linear issue which is discussed later.

Duration
There exist much fewer statistical analysis of strong motion duration and of its links with site conditions. However, all recent studies (Trifunac & Novikova, 1994; Theodulidis et al., 1995) report a significant increase of duration on sediments, especially at long periods. This issue is indeed very closely connected to effects of lateral heterogeneities and the associated diffraction of surface waves, another topic which is discussed later.

2.2.2.4 Spatial domain

In the space domain, lateral heterogeneities within sediments have been shown, both experimentally and theoretically, to induce significant differential motion, over distances comparable to seismic wavelengths (sometimes as short as a few tens of meters); they therefore have an engineering interest.

2.2.3 Remaining issues

These sediment effects are, without any doubt, the site effects which have been the most

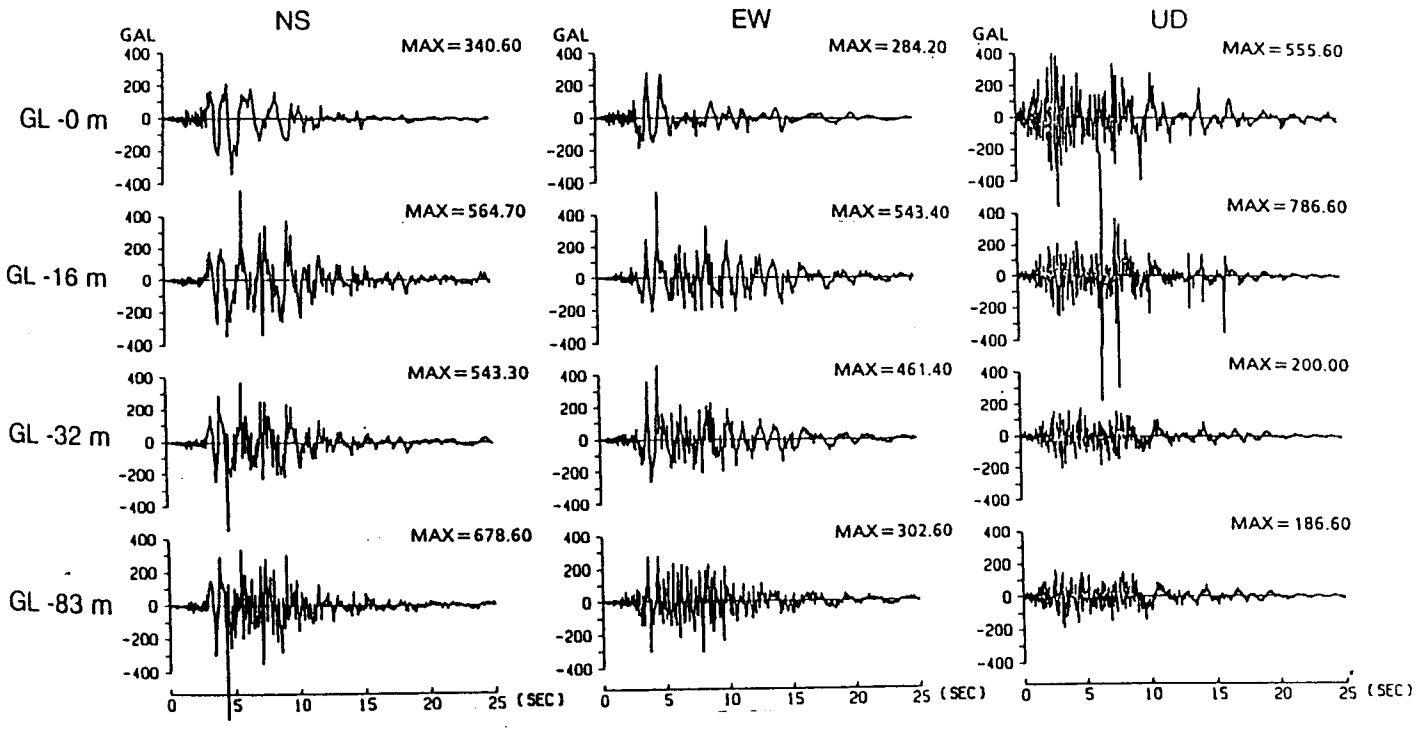

Figure 14 : *An example of the effect of non-linear behaviour of soft soils: acceleration recordings obtained at the Port Island downhole array during the great Hanshin (Kobé) earthquake of January 17, 1995. Note the abrupt reduction of surface horizontal acceleration after a few seconds (due to the liquefaction of the upper sand layer) . Courtesy to Prof. Irikura.*

extensively studied during the last decades. They are therefore much better understood than 50 years ago, and better accounted for in engineering practice. There still exist, however, some unexplored, or at least unsatisfactorily explored, fields:

2.2.3.1 Non-linear behavior of soft soils

Based on the pioneering works of Hardin and Drnevich (1972), geotechnical engineers have been convinced for a long time of strong non-linearities in the seismic behavior of soft soils, characterized by a simultaneous decrease of shear modulus and increase of material damping with increasing shear strain. From numerous laboratory tests performed on soil samples, the strain threshold above which these changes in mechanical properties is generally thought, in the geotechnical engineering community, to be very low: smaller than 10^{-4}. This non-linearity should therefore induce both very significant shifts (decrease) of the fundamental frequency f_0, and decrease of spectral amplification and peak acceleration, especially in the high-frequency range because of the increased damping.

However, many seismologists claim they may interprete strong motion data up to at least a 0.3 to 0.4 g level (and in some cases 1.0 g, see Murphy et al., 1971), with a simple linear viscoelastic behavior. Until recently (i.e., late eighties/early nineties), there was therefore a clear gap between seismologists and geotechnical engineers regarding the importance of such effects.

According to recent studies, this gap is being progressively filled since the observations made in the recent Loma Prieta, California earthquake of 1989: seismologists (see Aki and Irikura, 1991, for further details) do observe some kind of non-linear behaviour in several instances, while on the other hand geotechnical engineers came to the conclusion that non-linear effects are important only for higher acceleration levels than they previously thought.

On the one hand, several seismological studies, using various instrumental techniques described later (chapter 3) and based on weak and strong motion recordings, did provide evidence of non-linear behavior. Caillot and Bard (1990), Chang et al. (1991), Beresnev et al. (1994) report a decrease of amplification factors, and, sometimes, a slight decrease of resonant frequencies at peak accelerations exceeding 0.2 g for the SMART-1 array data in the Lotung valley, Taiwan; a similar amplification reduction was observed by Darragh and Shakal (1991) for the Treasure Island, soft soil site in San Francisco Bay. The latest "seismological" evidence of strong non-linearities comes from Port Island recordings obtained at Port Island during the Kobe earthquake (Figure 14), which show an almost complete filtering of high frequency motion in a liquefied sand layer. Interesting enough is it to notice that all these "non-linear" sites are mainly sandy sites.

On the other hand, the significant amplifications observed in the San Francisco Bay area in 1989, following the Mexico City 1985 recordings (Singh et al., 1988; Ordaz and Faccioli, 1994), lead Idriss (1991) to propose a revised version of the well known Seed and Idriss (1983) relationship between peak accelerations on rock and peak acceleration on soft soils (Figure 15): while in the previous curve the crossover level was about 0.13 g, it is "upgraded" to about 0.4 g in the new one (a value similar to results of previous computations by Mohammadioun and Pecker, 1984). Interesting again is it to notice that those sites correspond mainly to clayey deposits. Along the same line, Darragh and Shakal (1991) also report a quasi-linear behavior for a stiff-soil site in the range 0.006 - 0.43 g, while Borcherdt and Glassmoyer (1992), and Borcherdt and Wentworth (1995) do not see any statistically significant difference between the low-strain response of most of medium stiffness alluvial sites in the San Francisco Bay and Los Angeles area, and their strong motion response during the Loma Prieta event.

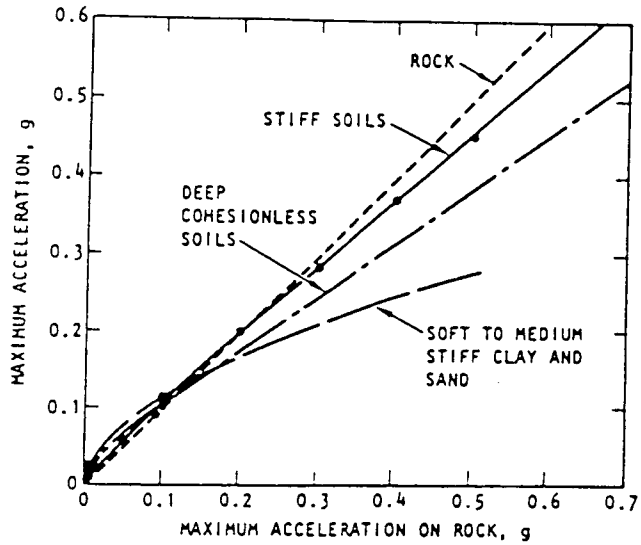

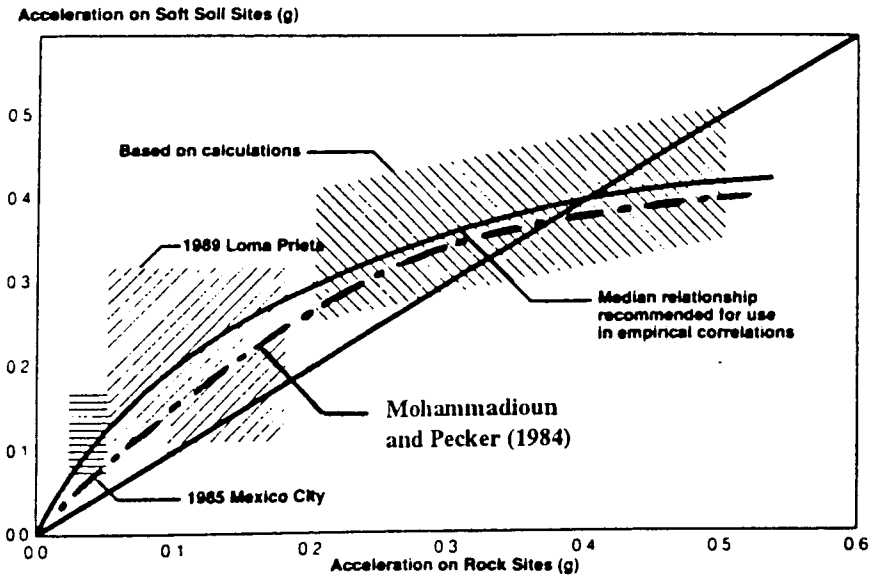

Figure 15 : *Effect of non-linear behaviour of soft soils: approximate relationships between peak accelerations on rock, an peak accelerations in soft soils.*
a) (top) curves published in 1983, exhibiting quasi-systematic reduction of pga on soft soils for destructive earthquakes (pga > 0.1 g). After Seed and Idriss, 1983.
b) (bottom) curves published in 1990 after observations performed during the Mexico (1985) and Loma Prieta (1989) events - compared with curves proposed earlier by Mohammadioun and Pecker (1984), on the basis of numerical modelling - .Pga is amplified on soft sites up to levels of 0.4 g . After Idriss, 1990.

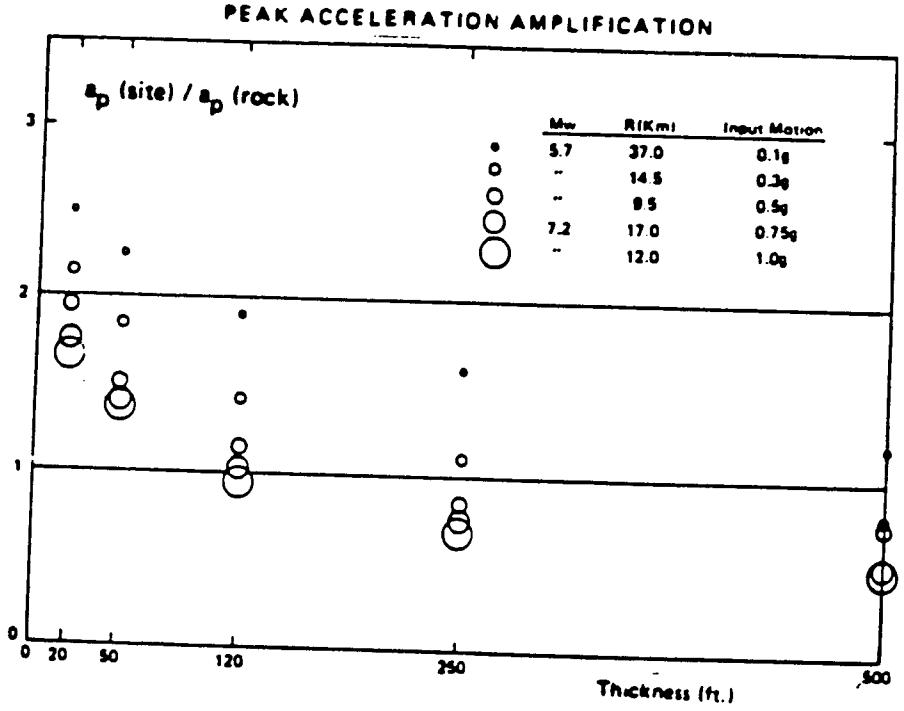

Figure 16 : *Relationship between peak accelerations on soft soils and on hard rocks. Dependency of the soft soil / hard rock acceleration ratio on not only the peak acceleration (various symbols), but also on the soil layer thickness (Reproduced from Silva (1991).*

After these observations and computations, it therefore seems reasonable to expect significant non-linear effects of soft sandy soils when the peak ground acceleration on rock exceeds a threshold level around 0.1 to 0.2 g. However, since this threshold corresponds to the onset of nonlinear effects, one might still expect amplification in the high frequency range up to acceleration levels around 0.3 to 0.5 g. These limits are still very fuzzy, and giving too precise values would be misleading, since they depend on the nature and the thickness of the soft deposits, as well as on the magnitude (and frequency content) of the earthquake: for instance, Silva (1991) predicts a peak acceleration amplification on thin sandy soils for acceleration levels as high as 1.0 g, while much thicker deposits of the same kind of sandy soil give rise to a decrease of peak ground acceleration above threshold values around 0.4 g (Figure 16). Particular caution should be devoted to clayey deposits with high plasticity index, since their non linear behavior is appearing at higher deformations.
Nevertheless, despite their fuzziness, these results may have significant consequences in moderate seismicity countries, where elastic spectra are anchored to peak accelerations in the range 0.1 - 0.3 g, and where the site specific spectral shapes very generally include a significant reduction of the high frequency contents for soft sites (as proposed for instance in Eurocode 8). This assumption, though widely accepted till now by most geotechnical engineers on the basis of early - probably too early and partial - results, should probably be reexamined in detail, as proposed by Borcherdt (1995).
From a very different point of view, but along the same line, Lomnitz (1990, 1991) suggested that non-linear effects could induce "catastrophic" phase transitions in soft soils, moving them in a quasi-fluid phase, where large amplitude gravity waves could develop and play an important role in damage distribution. Although Chavez-Garcia and Bard (1993a and b) showed with numerical modelling that gravity effects were very unlikely in elastic solids, and would require extremely low viscosities in "fluidified" soft soils, the question of phase transition remains open, as well as the explanation of the "progressive" waves reported to have been seen by a number of observators in different earthquakes (see Gilbert, 1967).

2.2.3.2 Diffraction by subsurface topography

In the eighties, many numerical studies have emphasized the possible importance of subsurface topography in alluvial valleys or sedimentary basins, because of the generation of local surface waves and of their subsequent trapping within soft layers, leading to increased amplifications with respect to the classical 1D case. However, there had been very few experimental evidences proving the existence of those surface waves, or showing the failure of 1D models to explain the observed amplifications.
Recent years brought several observations of such locally generated surface waves: in the Santa Clara Valley in California (Frankel et al., 1991), where they induced a long duration of shaking for Loma Prieta aftershocks; in the Osaka plain in Japan (Kagawa et al., 1992), where their excitation is reported to be strongly dependent on the azimuth of the incoming waves; in the Kanto basin around Tokyo (Kinoshita et al., 1992; Phillips et al., 1993; Hisada et al., 1993), where these phases are shown to be generated along the basin edge, and are reported to have often larger amplitudes than the direct S waves (Figure 17); and in the San Bernardino Valley (Frankel, 1994). A common feature for all these observations is that they correspond to large size valleys, whose fundamental period is larger than 1 s (sometimes up to 6 s) and where fundamental surface waves are therefore long period waves, and where the travel times of surface waves between valley edges and valley center may reach several tens of seconds. It is therefore

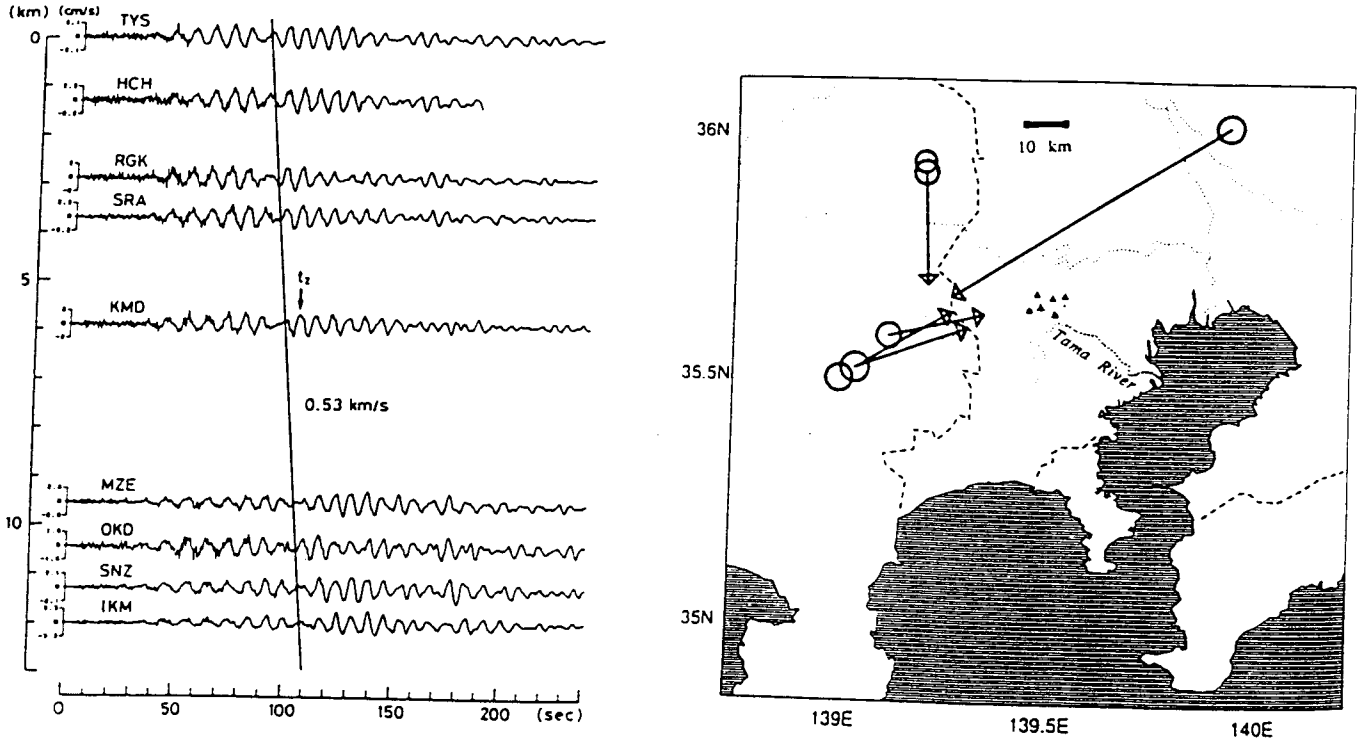

Figure 17 : *An example of local surface waves generated on basin edges in the Kanto basin (Japan). a) (left) Examples of velocity seismograms recorded on an array for one particular event: the late phase has an amplitude comparable to the direct S phase, and propagates through the array with a group velocity about 530 m/s. (Reproduced from Kinoshita et al., 1992) b) (right) S - to Love scattering points calculated using direction and group velocity determined from array recordings. Arrows represent the S-wave path from the earthquake to the surface scattering point. The dashed line is the Kanto basin boundary. (Reproduced from Phillips et al., 1993).*

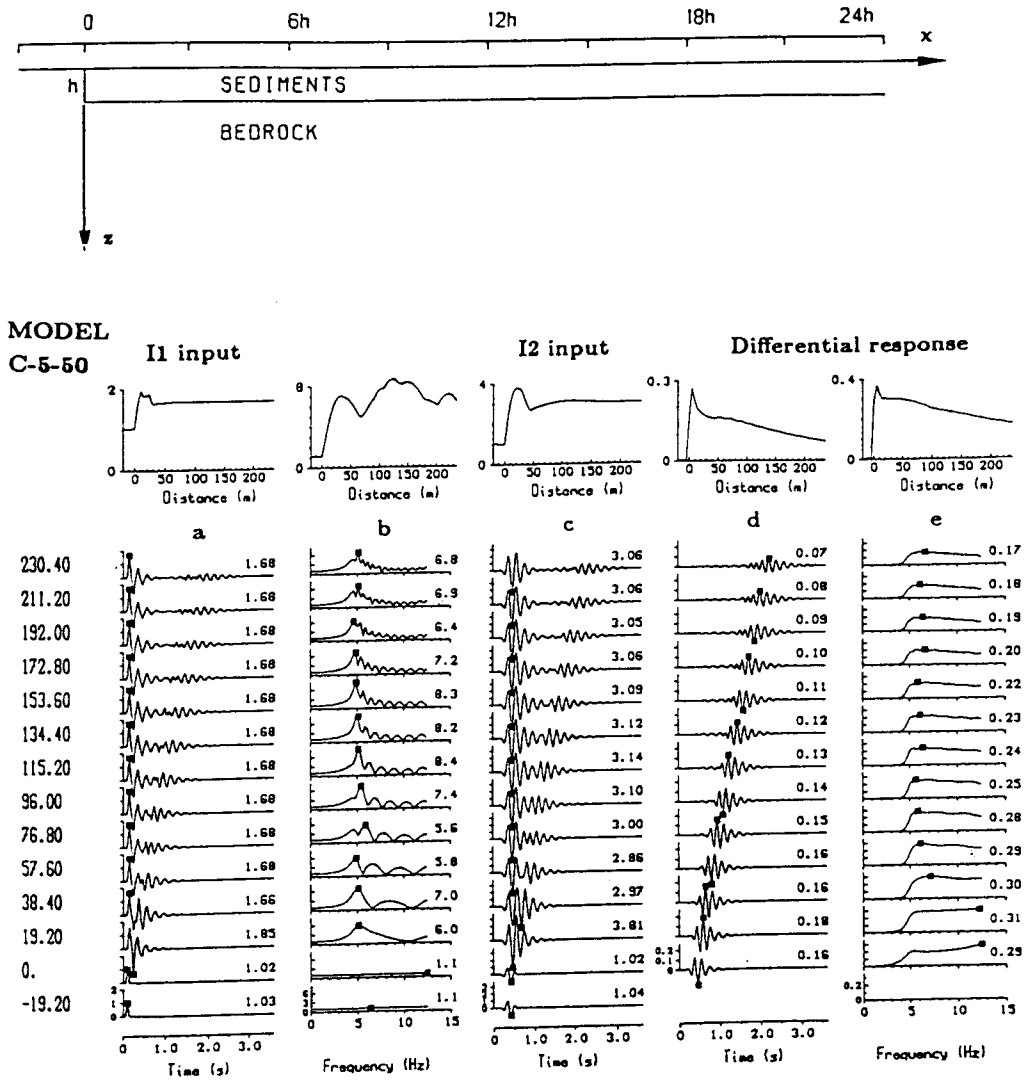

Figure 18 : *Effects of strong lateral discontinuities: response of a semi-infinite horizontal layer near its border. From Moczo and Bard, 1993.*
The model geometry is shown on top (h = 10 m, β_1 = 200 m/s, β_2/β_1 = 5, Q_1=50). Time and frequency domain responses are given in columns a to e for 14 equi-spaced surface sites located between -19.2 m (bottom trace) and +230.40 m (top trace) from the discontinuity.
a) Time domain response to a "pseudo-Dirac" pulse .
b) Fourier transfer functions
c) Time domain response to a transient signal having a characteristic frequency centered on the resonance frequency of the sediment layer (5 Hz).
d) Differential motion (spatial derivative of surface motion) associated with motion shown in c).
e) Spectral contents of differential motion shown in d).
In each column, numbers to the right represent the peak values of the corresponding quantity for the site under consideration. The five curves on top of each column display the spatial variation of these peak values along a cross section of the model.

relatively easy to point out the existence of such late phases with a few stations.
The situation is different in shorter size structures (i.e., with thicknesses smaller than a few hundred meters, and widths smaller than around 10 km): as frequencies are higher and travel times are shorter, locally-generated surface waves are mixed with direct S waves, and are much more difficult to be isolated, since it needs very dense arrays. There had not been, until very recently, any direct evidence of such phases in small-size structures, although the physical phenomena, wave diffraction on heterogeneities, is exactly the same as in large size structures; very clear and energetic diffracted waves were identified at the EUROSEISTEST site near Thessaloniki, in a 5 km wide, 250 m thick graben. In addition, there have been several indirect evidences, through the shown failure of 1D models to explain observed amplifications: that was the case for instance in the Ubaye valley in the French Alps (Jongmans and Campillo, 1993), in the Marina district in San Francisco (Liu et al., 1992; Graves, 1993). On the opposite, no clear evidence for such 2D or 3D effects could be found in the Turkey Flat and Ashigara Valley test sites, since predictions from 1D models were as satisfactory as predictions from 2D or 3D models: this was due to the relatively high material damping which prevents surface waves from developing and travelling. However, in one Ashigara valley site, a clear difference between spectral ratios for NS and EW component was evidenced, which cannot be explained by 1D models.
Results recently obtained about the duration of strong motion signals might also be indirect evidences of diffraction effects: Caillot (1992), and Theodulidis et al. (1994) after a statistical analysis of strong motion recordings from Italy and Greece, consistently found that the duration is significantly longer on alluvial sites than on rock sites, for frequencies smaller than 2-3 Hz. Such an observation might be linked with the diffraction of intermediate to long period waves in deep deposits.

2.2.3.3 Strong lateral discontinuities

In connection with the above mentioned diffraction effects, there are also numerous, consistent macroseismic observations (Lambesc, France, 1909; Irpinia, Italy, 1980; Liege, Belgium, 1983) showing a significant increase in damage intensity in narrow (a few tens of meters) zones located along strong lateral discontinuities, i.e., areas where a softer material lies besides a more rigid one (for instance, ancient faults, abnormal contacts, debris zones,...). Further examples of such effects may be found in Moczo and Bard, 1993.
There have been, however, very few detailed investigations on these effects: the macroseismic observations from different earthquakes have never been compiled in a systematical way, and only very few numerical models have been applied to that particular 2D configuration. Nevertheless, recent simple investigations by Rodriguez et al. (1988) and Moczo and Bard (1993), an example of which is shown in Figure 18, show that such discontinuities generate local surface waves in the softer medium, which have mainly two damaging effects: their amplitude may, under some circumstances (controled by the impedance ratio and the damping), be larger than that of the incident waves, and furthermore, because of their short wavelength, they induce very large differential motions. This latter conclusion suggests that damage level may be related not only to the amplitude of translational motion, but also with its spatial derivative. Such information can be provided only by dense arrays of seismographs, which are still very rare.
Similar observations were made following the Kobe earthquake: the largest damage is concentrated in an elongated zone, which is parallel both to the sediment / rock contact on the Western side of the Osaka basin, and to the causative fault: it is therefore not yet clear whether

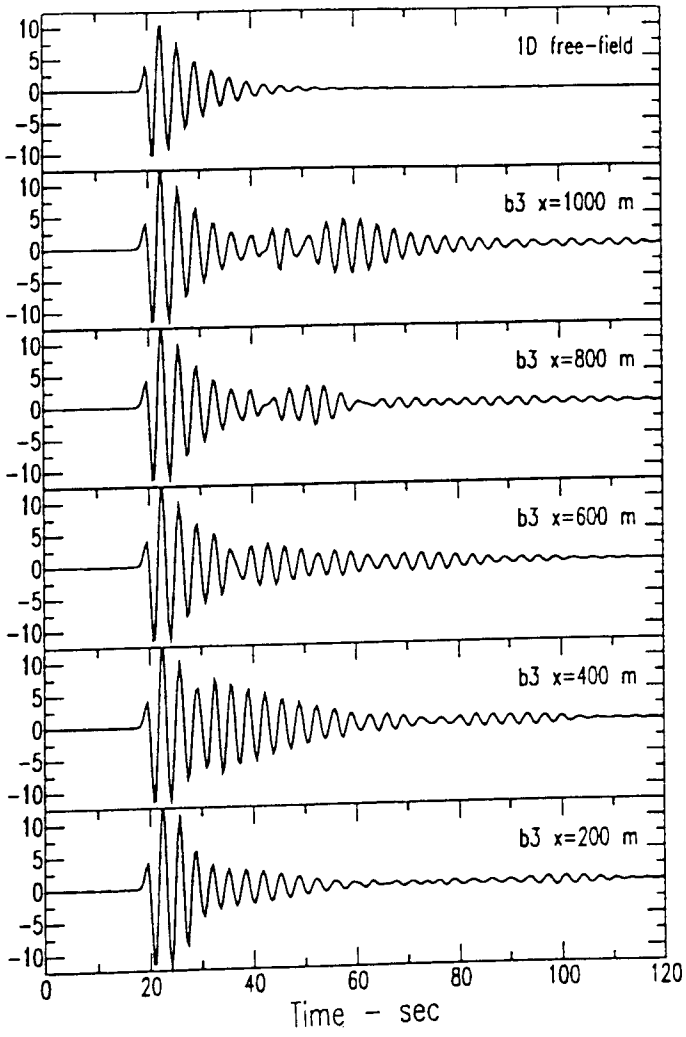

Figure 19 : *An example of possible effects of soil-structure interaction on "free-field" surface motion. Traces 1 through 5 represent the SH motion at the surface of a soft layer, at increasing distances from a "2D building" (i.e., a wall), from 200 m (trace 1) to 1 km (trace 5). The top trace represents the 1D response of the soft layer when no building is present (for reference). The fundamental period of the soft layer is 0.3 Hz, and the fundamental frequency of the building is 0.5 Hz without soil-structure interaction, and 0.28 Hz with soil-structure interaction on this specific soft layer. The incident signal is a Ricker wavelet with a central frequency of 0.33 Hz. (Reproduced from Bard and Wirgin, 1995).*

these damage are due to the existence of the lateral rock/sediment discontinuity, or to the proximity of the causative fault.
There is an urgent need for further investigations about these very poorly documented and understood effects, from both instrumental and theoretical points of view.

2.2.3.4 - Miscellaneous

An interesting and original observation was made at several sites hinting at 2D or 3D effects: the "directional site resonance" reported by Vidale et al. (1991) and Bonamassa and Vidale (1991) at several Californian sites, and corresponding to larger site amplifications along preferential directions (whatever the earthquake epicenter), which was interpreted as related with waves scattered in the immediate vicinity (50 m) of the receiver sites. Similar observations are reported in Mexico City by Chavez-Garcia et al. (1994), which may corroborate some earlier works of Stephenson (see Stephenson, 1991, and Stephenson and Barker, 1991), who also reports some preferential directions of motion in shallow very soft sites, and interprete them as due to peculiar 3D resonance modes ("cells").
Another intriguing result is worth being mentioned in this section, since it might have very important engineering and planning consequences: Bard and Wirgin (1995), based on simple 2D modelling, drew attention on the possible significant modifications induced in "free-field" motion in the vicinity of large-size structures built on very soft sites (such as Mexico City), because of the combined effects of soil-structure interaction and strong impedance contrast (Figure 19). However, their results are preliminary and need to be confirmed by further computations and/or instrumental observations.
Finally, special attention must be paid to sediment response in the very near field, because of possible effects of complex incident wavefield, and of sub- or super-sonic rupture velocities for near-surface faults).

3. METHODS FOR ESTIMATING SITE EFFECTS

The choice of the method to be used in a site effect study depends on the importance of the engineering project for which it has to be done. This section will present the various techniques that may be used: they may be classified according to various criteria. We will use here a "methodological" one, distinguishing between experimental, numerical and empirical approaches. However, these various methods could also be classified according to their cost: some of them are rather expensive methods, which may be used only for "large budget" studies, such as the antiseismic design of critical facilities (nuclear power plants, dams) or the microzoning of big cities, and which provide results that are valid only for one particular site; on the opposite, some other are "cheap", or "general", methods, which are based mainly on a statistical analysis of strong motion data, and which are generally used in seismic regulations.

3.1 Experimental methods

They may be based on different kinds of data: macroseismic observations, microtremor measurements, weak seismicity surveys or strong motion accelerograms.

3.1.1 Macroseismic observations

It sometimes happens that the site of interest has already undergone a destructive earthquake and

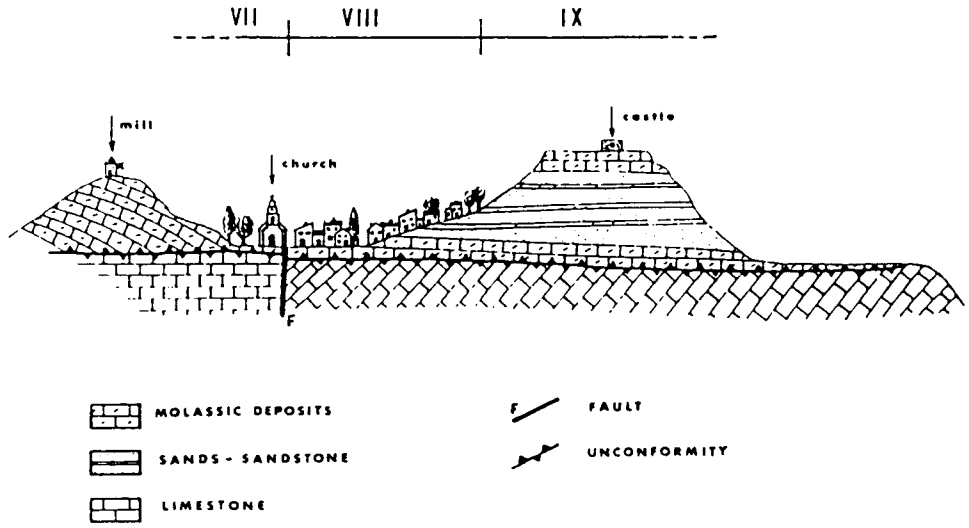

Figure 20 : *An example of detailed post-analysis of macroseismic data for historical earthquakes: evidence for topographic effects in Rognes (France) during the 1909 earthquake. Schematic NS geological cross-section through the village with observed macroseismic intensity (MSK scale, from VII to IX).*

1. When the earthquake occurred, you were
   1 in your town
   2 somewhere else

2. The address where you were located at the time of the earthquake, if known
   street
   city
   state, zip
   If not, approximate location is

3. The place was
   1 flat land
   2 on a top of hill
   3 on a slope
   4 in a valley

4 You were
   1 indoors
   2 outdoors
   3 in a vehicle

5. Check your activity when the earthquake occurred
   1 moving
   2 standing
   3 sitting
   4 lying
   5 other (please specify)

6. If you were inside a building, the type of the building was
   1 house
   2 mobile home
   3 apartment
   4 office
   5 other (please specify)

7. What was the building mainly made of?
   1 brick or block
   2 wood
   3 concrete
   4 steel
   5 other (please specify)

8. How old is the building?
   1 built before 1935
   2 built between 1935 and 1965
   3 built after 1965
   4 don't know

9. How many floors did the building have ?

10. What floor were you on?

11. Did you feel the earthquake
   1 yes
   2 no

12. How manytofethose around you felt the shaking?
   1 nobody
   2 few
   3 many
   4 all
   5 don't know

Figure 21 : *Sample questionnaire sheet for detailed macroseismic intensity survey. From ISSMFE, 1993.*

that detailed macroseismic observations are available: in that case, a detailed analysis of these data in the light of topographical and geotechnical maps may lead to a qualitative appraisal of the most hazardous zones.
This approach was first used for the city of Tokyo as early as 1913 (see ISSMFE report): the damage data of the 1854 Tokyo earthquake allowed to divide the city area in 3 zones with different hazard levels. Despite the growing number of strong motion instruments, the same approach is still followed in many different parts of the world (Mexico, Chile, Peru, Italy, Greece...), for a reinterpretation of historical macroseismic data (see for instance an example of surface topography effects on Figure 20), as well as for recent earthquakes, since building density is still much larger than instrument density (see Figure 2)...
Detailed macroseismic surveys immediately after destructive earthquakes are therefore of primary interest for microzonation purposes, as was again recently shown in Japan (Kagami et al., 1995); moreover, an earthquake need not necessarily to be a very destructive one to provide useful information, as it has been illustrated during the 1983 Liege (Belgium) earthquake, whose magnitude was only slightly above 5: as shown in Jongmans and Campillo (1990), a careful survey of insurance files for post-earthquake reimbursement allowed to draw a detailed damage distribution map, which showed out to be in very strong correlation with the subsoil map. Detailed questionnaires with an adequate format should therefore be carefully prepared: An example of such a questionnaire is given in Figure 21. Such an approach is particularly well suited when there exists some uniformity in construction techniques.
However, one must also remain aware of the difficulty of translating such intensity data into more quantitative design parameters: such macroseismic surveys have therefore to be complemented by the use of some empirical correlations between variations of intensity and variations of a few simple parameters such as peak acceleration, peak velocity, duration, ...: see below section 3.3.

3.1.2 Microtremor data

Microtremors are ambient vibration of ground excited by natural or artificial disturbances such as wind, sea waves, traffic, industrial machinery, ... and may be recorded using high sensitivity seismometers. It has been repeatedly reported that the spectral features of microtremor (= background noise) exhibit a gross correlation with the site geological conditions: for instance a short predominant period of microtremors (< 0.2 s) indicates a rather stiff rock, while a larger period indicates softer and thicker deposits. The microtremor method is very widely used in Japan, but much less in other parts of the world, because of some major questions that are not satisfactorily answered:

- the noise sources are very different from one site to another (even a near-by one), especially in the short period range. There exists therefore a large uncertainty in the relative spectral amplitudes, which do not reflect only the site conditions, but also the source and path effects.

- there are also significant variations in noise level during day and night time. A careful microtremor survey therefore requires repeated measurements (at least when "classical" processing techniques are used, i.e. those presented in 3.1.2.1 and 3.1.2.2), which makes this method less tractable and more expensive.

The use of microtremors in site response estimates is therefore still controversial in Europe and USA: various publications have reported successes as well as failures. Its considerable cheapness,

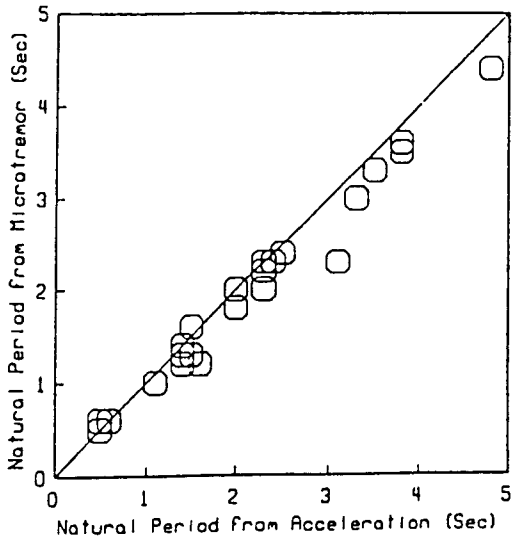

Figure 22 : *Interest of microtremor measurements in Mexico City: Correlation between natural period measured from microtremor spectra, and natural period obtained from strong motion data. From Lermo et al., 1988.*

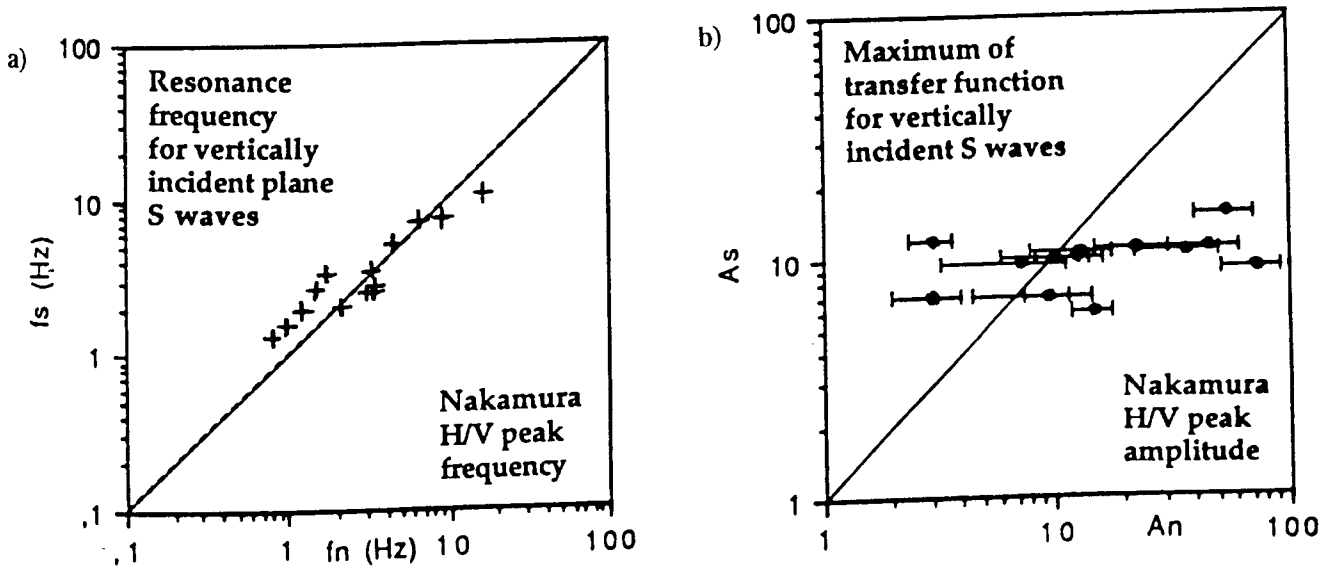

Figure 23 : *Theoretical checks of the Nakamura's technique. Numerical horizontal to vertical spectral ratios were computed from noise models in various (about 15) soil profiles.*
a) Comparison between the S-wave resonance frequency (fs, computed for vertically incident S-waves) and the peak frequency "observed" in theoretical Nakamura's ratios (fn): the agreement is very satisfactory.
b) Same thing for the spectral amplitude at the resonant frequency (As is the amplification for vertically incident S waves, An is the amplitude of the H/V peak obtained from noise modeling): the agreement is very poor... (Reproduced from Lachet and Bard, 1994).

however, justifies any attempt to use them in a qualitative or quantitative way: significant efforts have been done in that direction in recent years in Southern Europe (Italy, Greece, France and Portugal), as well as in latin America (Mexico, San Salvador, Venezuela, Colombia, Chile, ...). Kudo (1995) provides a very interesting historical perspective of the various controversies, that affected the development of the use of microtremors for site response estimates.

Microtremors may be used basically in four different ways:

3.1.2.1 Microtremor spectra:

The crudest way simply consists in determining peak frequencies from average absolute spectra. It has been repeatedly reported (mainly by Japanese scientists) that the spectral features of microtremors exhibit a gross correlation with the site geological conditions: for instance a short predominant period of microtremors (< 0.2 s) indicates a rather stiff rock, while a larger period indicates softer and thicker deposits. The microtremor method used in this way thus provides a qualitative "index" on soil characteristics (see Kanai, 1983 for a review).
These peak frequencies are also interpreted at the fundamental resonance frequencies of the investigated sites. Such an interpretation has received strong experimental evidence in the long period range (T > 1s), in sites such as Mexico City (Figure 22 ; Lermo et al., 1988), Los Angeles (Yamanaka et al., 1993), New York (Field et al., 1990), San Francisco Bay area (Hough et al., 1991) and many sites in Japan. At shorter periods, recent results coincide with previous ones, i.e., they are controversial: Hough et al. (1992) found a good fit in Tiber Valley (Italy) for a resonance frequency around 2.5 Hz, while Yamanaka et al. (1993) report strong perturbations by cultural noise around 3 Hz in the Los Angeles area.

3.1.2.2 Spectral ratios:

They are done for noise recordings in a similar way that what was proposed by Borcherdt for earthquake recordings (see later the section "reference-site" techniques). Recent investigations do confirm the - very logical - outcomes of previous studies. Such ratios are reliable only in the long period range where noise origin is the same for all the studied sites, including the reference site: Yamanaka et al. (1993) find a very good agreement with ratios from strong motion data at periods larger than 5 s. But microtremor spectral ratios are questionable at shorter periods: Guttierez and Singh (1992) obtain qualitative agreement but significant quantitative mismatch with strong motion ratios in the Acapulco area, while Rovelli et al. (1992) report significant differences in the value of resonant frequencies and in the spectral width of the corresponding spectral peaks for various Italian sites.

3.1.2.3 H/V ratio (or "Nakamura's" technique):

The H/V ratio (i.e., the ratio between the Fourier spectra of the horizontal and vertical components of microtremors) has been introduced in the early seventies by several Japanese scientists (Nogoshi and Igashi, 1971; Shiono et al., 1979; Kobayashi, 1980), who investigated its physical meaning and showed its direct relationship with the ellipticity curve of Rayleigh waves, and concluded at its ability to identify the fundamental frequency of soft soils, since the vertical component of Rayleigh wave motion almost systematically vanishes around the fundamental S wave resonance frequency. Their works, however, have been published only in Japanese, and

were not known outside Japan until Kudo's review (Kudo, 1995).
Meanwhile, Nakamura (1989) proposed (in English), on the basis of qualitative arguments, that this ratio is a reliable estimation of the site response to S waves, providing reliable estimates not only of the resonance frequency but also of the corresponding amplification. According to him, dividing by the "reference" vertical component allows to remove source as well as Rayleigh wave effects.
Although his - very qualitative - theoretical explanation looked at least questionable (as indicated in Lachet and Bard, 1994, and again in Kudo, 1995), various sets of experimental data (Ohmachi, 1991; Lermo, 1992; Field and Jacob, 1993b; Duval et al., 1995; Field et al., 1994; Duval et al., 1994) confirmed that these ratios are much more stable than the raw noise spectra, and that, on soft soil sites, they exhibit a clear peak which is well correlated with the fundamental resonance frequency. These observations are supported by several theoretical investigations (Lachet, 1992; Field and Jacob, 1993b; Lachet and Bard, 1994; Lermo and Chavez-Garcia, 1994), showing that synthetics obtained with randomly distributed, near surface sources lead to horizontal to vertical ratios sharply peaked around the fundamental S-wave frequency (Figure 23a). However, the three first studies also conclude that the amplitude of this peak is not well correlated with the S wave amplification at resonance frequency (Figure 23b), since, in particular, it is highly sensitive to some parameters such as the Poisson ratio at the very surface. Lachet and Bard (1994) indeed proposed another explanation for the good match of fundamental frequencies, in main relation with the polarization curves of Rayleigh waves, in perfect agreement with the early Japanese studies (see Kudo, 1995), and according which there should not be a straightforward relation between the H/V peak amplitude and site amplification.
Other examples of estimates obtained with this technique are also shown in Figures 24 and 27, for comparison with other estimates. It shows that Nakamura's technique allows, very simply, to obtain the fundamental resonance frequency, but that it fails in providing higher harmonics, and also that peak amplitude is somewhat different from amplification measured on spectral ratios. However, this Nakamura version of the microtremor method has already proved to be one of the cheapest and most convenient techniques to reliably estimate fundamental frequencies of soft deposits, and it certainly deserves more work to better understand the factors influencing the amplitude of the peak.

3.2.1.4 Array recordings:

There also exists one more, indirect use of microtremor recordings. Aki (1957) showed that noise recordings on small aperture arrays could be used, through an analysis of spatial correlation, to measure phase velocities of surface waves and invert the surface velocity structure, from which it is then possible to compute the site response. Several recent studies in Italy (Hough et al., 1992; Malagnini et al., 1993), and Japan (Kataoka et al., 1994) illustrated the practical interest of this "old" technique, which may favorably compete with other methods used in geotechnical engineering to obtain velocity profiles.

3.2.1.5 Conclusions

As a conclusion to this microtremor section, we think, following Aki (1988), that the microtremor method may provide reliable estimates of both site periods and amplifications in the long period range only (i.e., when source and path effects are the same for all the sites considered), and that its main general outcome (even for short periods) is the measurement of the predominant period

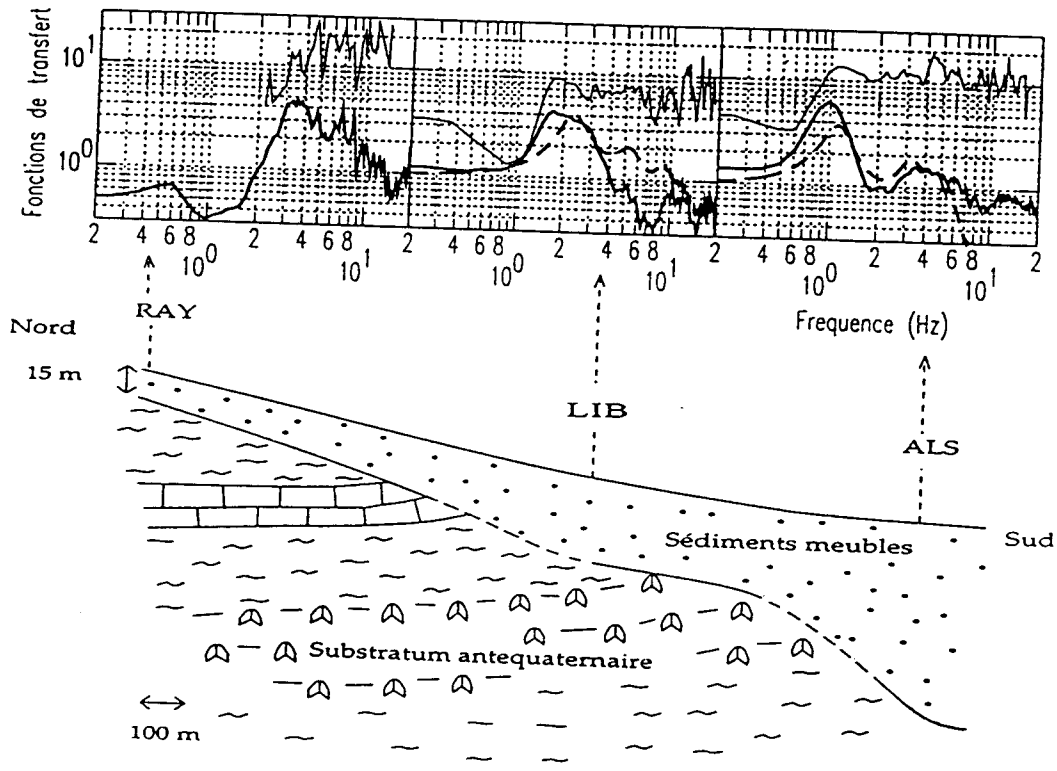

Figure 24 : *An example of use of microtremors through Nakamura's technique. Horizontal to vertical spectral ratios of ambient noise are shown for various locations around an alluvial coastal plain in the city of Nice. The H/V ratios are compared with classical spectral ratios with respect to a rock reference site, and with 1D numerical estimates of the transfer function. From Duval, 1994.*

of the ground: a very good example is the city of Mexico, for which a very good correlation has been observed between the ground periods measured with strong motion recordings, and those obtained from microtremor spectra, as well as with the local thickness of the very soft surficial clay layer (Figure 22, adapted from Lermo et al. (1988).
But we also think - in contradiction with some Japanese scientists - that it cannot generally provide reliable information on the amplification value (except, in some cases, at long periods), at least in the way it is classically used, i.e., through "raw" Fourier spectra or spectral ratios with respect to a reference site. On the other hand, as also emphasized by Aki (1988), short-period microtremor data obtained on small aperture arrays may be very useful in the determination of the local shear velocity structure: microtremors are then used as a tool for in situ geotechnical surveys, which are of great value for microzoning studies (see below sections 3.2 and 3.3).

3.1.3 Weak motion data

Weak motion data are records from small to moderate, natural or artificial seismicity (small magnitude earthquakes, aftershocks of big events, mine or quarry blasts, nuclear tests). Such data are typically recorded by classical digital, high sensitivity instruments exactly similar to those used by seismologists for microseismicity and seismotectonics studies.
As underlined by Field and Jacob (1995), which will be extensively quoted in this section, the greatest challenge in estimating site response from such instrumental recordings is removing the source and path effects. Several methods have been proposed in that aim, which may be divided into two main categories, depending on whether or not they need a reference site, with respect to which the particular effects at other sites are estimated.

3.1.3.1 Reference site techniques

The most common procedure (the principle of which is illustrated in Figure 25, while example results were been already presented in Figure 3.) consists in comparing records at nearby sites (where source and path effects are believed to be identical) through spectral ratios: these spectral ratios constitute a reliable estimate of site response if the "reference site" is free of any site effect, which means that it should fulfill the two following conditions: 1) it should be located near enough to ensure that differences between each site are only due to site conditions, and not to differences in source radiation or travel path, which is generally assumed when epicentral distance is larger than about 5 times the array aperture; and 2) it should also be unaffected by any kind of site effect, which may be in principle secured when it is located on an unweathered, horizontal bedrock. These two conditions prove to be rather restrictive in practice.
This technique, introduced first by Borcherdt (1970), is still widely used; however, since it is applicable only to data from dense, local arrays, it has been generalized by Andrews (1986) who proposed, for large data sets recorded on local or regional networks, to look simultaneously for all source, path, and site effects, through the resolution of a large inverse problem.
Basically, the principle of these methods may be described as follows: for a network of I sites having recorded J events, the amplitude spectrum of the recorded ground motion $R_{ij}(f)$ can be written as:

$$R_{ij}(f) = E_j(f) \cdot P_{ij}(f) \cdot S_i(f)$$

which leads to simple linear equation when written in logarithmic form:

$$\ln (R_{ij}(f)) = \ln (E_j(f)) + \ln (P_{ij}(f)) + \ln (S_i(f))$$

The traditional spectral ratio technique corresponds to the fact where the path term $P_{ij}(f)$ is

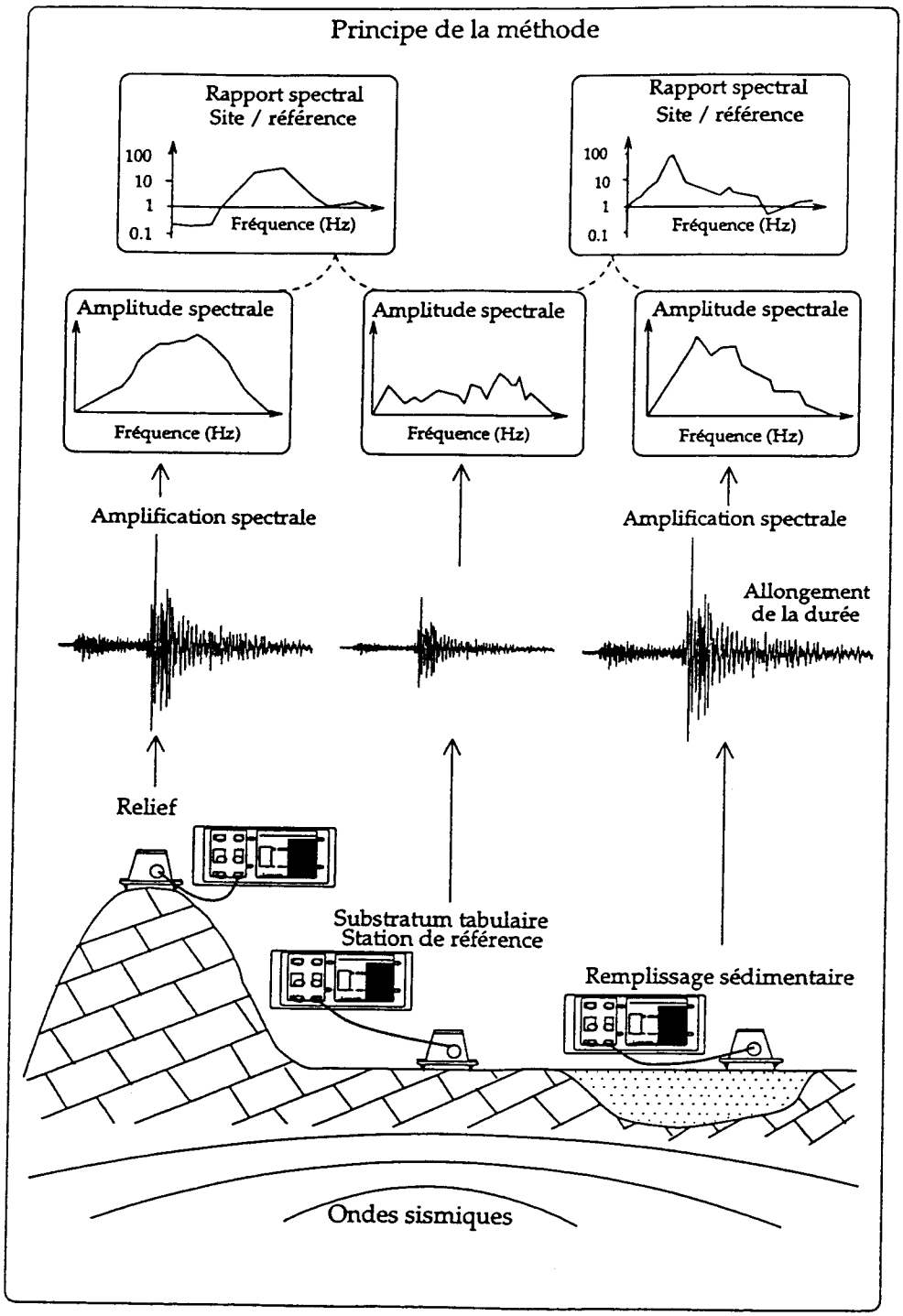

Figure 25 : *Instrumental determination of site effects through transfer function. The reference site (middle) should be on horizontal, unweathered rock.*

assumed to be site independent, i.e., when the distance to the reference site is small compared to the source-to-site distance. Two different techniques have been proposed to obtain the spectral ratio: either through the smoothed Fourier spectra of motion at both sites, or through the normalized cross-spectrum (Figure 26).
In the generalized inversion scheme, the path term is generally assumed to follow an a priori law (for instance $P_{ij}(f) = 1./ r_{ij}$, but any other law may be used, as for instance did Hartzell, 1992), and the (I + J) terms $E_j(f)$ and S_i (f) are estimated from, at most, the I.J observations (if all J events are recorded by all I stations), generally through least square weighted inversion. Since both series of terms are determined only through their product, there is need to have an a priori estimation of one term: generally S_i (f) is taken equal to 1 (or to any given other value) at a reference site i_0. An alternate approach is to determine the site response relative to the network average. Different versions of this method have been proposed by several authors, the main differences coming from a) the choice of the path term formula (including or not material damping, ...), and b) the weighting procedure prior to the inversion. The criteria for assessing the weights are mainly based on the signal to noise ratio (SNR), data with high SNR being affected a larger weight than those with low SNR.
Field et al. (1992), Steidl (1993) and Field and Jacob (1995) performed detailed comparisons of these various techniques; although their studies are based on data from particular (Californian) sites, and particular source - site configurations, their methodological conclusions, are probably more general. They may be summarized as follows:

- for noisy signals (including cases where the signal is noise-generated), cross-spectrum estimates suffer significant downward bias while traditional spectral ratios are relatively unbiased (see Figure 26), but exhibit a large scatter: the main conclusion is that individual spectral ratios (from one or very few events) should be avoided, and that only ensemble averages over many events should be used. For instance, Field and Jacob (1995) propose that, under usual conditions, a 10 % precision on the mean spectral ratio estimate requires the use of about 80 pairs of records.

- on the other hand, it was found (as illustrated in Figure 27), that site amplification factors obtained with traditional spectral ratio technique, or with generalized inversion schemes, were very similar; the uncertainties on the estimates, however, can be significantly different depending on the weighting scheme. After a careful discussion, Field and Jacob (1995) propose a simple "preferred" weighting scheme: it simply consists of eliminating all data for which the signal to noise ratio remains below an a priori threshold value (for instance around 3), and to assign all remaining data a unit weight. This very simple procedure is also to be applied in the traditional spectral ratio technique.

In such conditions, the generalized inversion technique seems generally preferable, mainly because it allows to obtain rather reliable estimates of site effects even at sites where only few recordings are available; however, the traditional spectral ratio technique keeps some advantages when the signal generated noise level varies among the stations, or when the response at some sites is intrinsically more variable than it is at others (for example in case of strong azimuthal sensitivity).

3.1.3.2 Non-Reference site techniques

In the traditional spectral ratio method, as well as in the generalized inversion approach, site and

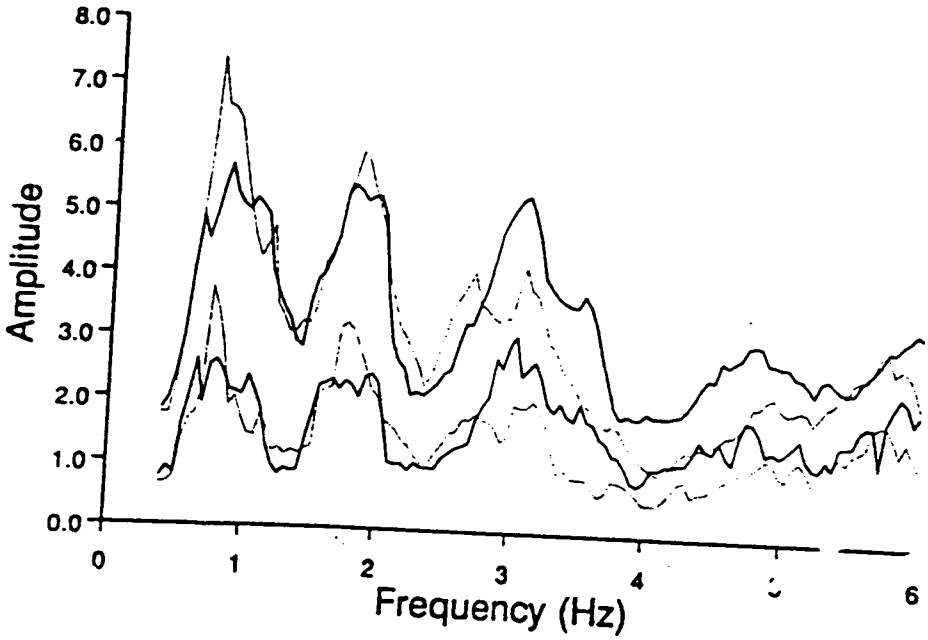

Figure 26 : *Comparison between spectral ratio and cross-spectrum techniques (for an alluvium site in Oakland, California). Each curve corresponds to an average site response estimate for radial (solid line) or transverse (dotted line) component. The higher amplitude pair are the spectral ratio estimates, and the lower amplitude pair are the cross-spectrum estimates. Reproduced from Field et al., 1992.*

source effects are estimated from observations at a reference site. In practice, adequate reference site are not always available: methods have therefore been developed, that do not need reference sites. Basically two kinds of such techniques have been proposed.

On the one hand, the general form of source and path effects may be assumed through formulae providing the spectral shape as a function of a few parameters (corner frequency, seismic moment, Q factor, near site attenuation term or f_{max}, ...), which are estimated together with the site response factors again in a generalized inversion scheme (see for instance Boatwright et al., 1991b): this procedure is called "parameterized source and path inversion" by Field and Jacob (1995). Although these methods have been first proposed to eliminate site effects and improve estimates of source and path characteristics, they may also be used with main emphasis on site effects.

Although the parameterization of source and path effects does remove the need for a reference site, there still exists in this procedure an unconstrained, frequency-independent, degree of freedom: there is a tradeoff between the low frequency spectrum level (seismic moment) and the mean level of site response factors at all sites. This scaling factor can be, in principle, constrained by a priori information, for instance on seismic moment estimates, or on the geotechnical structure at one site: however, the unavoidable uncertainties on those parameters may easily result in a factor of 2 uncertainty in the value of this scaling factor.

The inversion scheme is generally more complex than in the GI approach, since the dependence on some parameters (such as the corner frequency) is non-linear, so that almost every author has his own implementation.

Figure 27 also compares, again on the same example sites in Oakland area, the results obtained with such a parameterized inversion, and those obtained with preferred GI approach. The locations of peaks and troughs, as well as their relative amplitude, are very similar, but the average level is significantly lower: this is simply an illustration of the existence of an unconstrained frequency-independent scaling factor.

A parent, though different, method, has been proposed by Phillips and Aki (1986): it is based on the use of coda waves, and the a priori description of source and path terms is therefore somewhat different. The inversion scheme, however, remains very similar. Recent studies by Mayeda et al. (1991), Su et al. (1992) and Koyanagi et al. (1992) illustrate the interest of such methods in well instrumented areas. However, it is probably of uneasy use in urban areas, where coda records are almost impossible because of noise level.

On the other hand, another technique has been recently proposed that is extremely simple: it just consists in taking the spectral ratio between the horizontal and the vertical components of the shear wave part. This technique is in fact a combination between a seismological method (called the "receiver-function" technique) used by Langston (1979) to determine the velocity structure of the crust from the horizontal to vertical spectral ratio (HVSR) of teleseismic P waves, and the proposal by Nakamura (1989) to use this ratio on ambient noise recordings (see above, section 3.1.2.3 for a discussion of this technique). Its interest is obvious, in relation with its simplicity and cheapness.

It was first applied to the S wave portion of earthquake recordings by Lermo and Chavez-Garcia (1993), who found, for three different sites in Mexico, very encouraging similarities between the classical spectral ratios and these HVSR: both frequencies and amplitudes of resonant peaks agree between both techniques. The same technique has been also checked by Theodulidis and Bard (1994), and Theodulidis et al. (1995), on various sets of weak and strong motion data: they conclude that the HVSR shape exhibits a very good experimental stability, and appears to be well correlated with surface geology, and much less sensitive to source and path effects; however, they

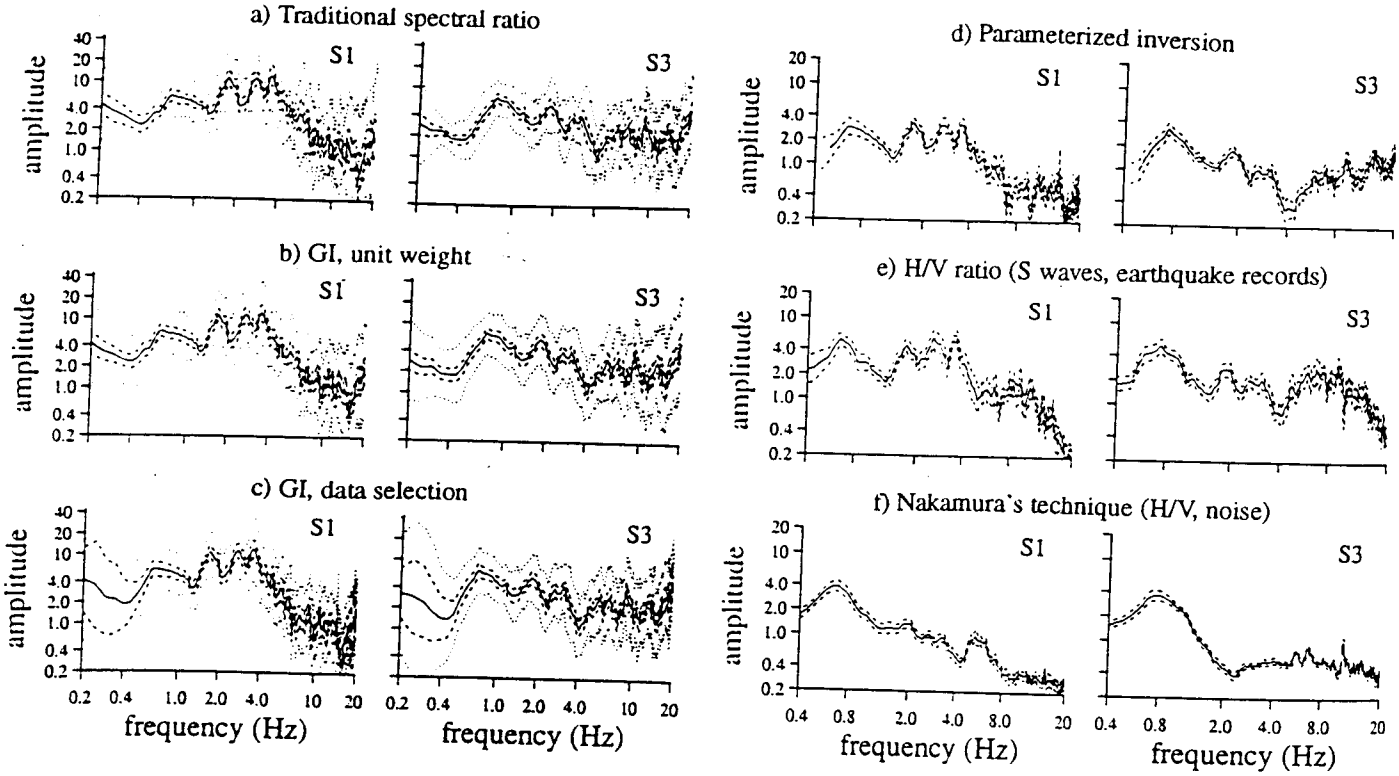

Figure 27 : *Comparison between various techniques for the estimation of site response transfer function. for two sites in Oakland (California).*
a) Traditional spectral ratios ;
b) Generalized Inversion spectral ratios where to noise ratio);
c) Generalized Inversion spectral ratios obtained when only data with signal to noise ratio larger than 3 are kept (and then given an equal weight).
d) Parameterized inversion estimates;
e) Average Horizontal-to-vertical component spectral ratios for S wave part of earthquake records.
f) Nakamura's estimates (average horizontal-to-vertical spectral ratio of ambient noise) Curves a) to c) correspond to site-reference techniques, while curves d) to f) correspond to non-reference site techniques. The dashed-lines represent 95-percent confidence limits of the mean. Adapted from Field and Jacob, 1994.

also conclude, from comparisons with classical spectral ratios (including surface / down-hole recordings), as well as with theoretical 1D computations (see also Lachet and Bard, 1994), that the absolute level of HVSR seems to be dependent on the incident wave-type, so that the determination of the absolute level of amplification from only HVSR is not straightforward.
This technique was also applied by Field and Jacob (1995) in their systematic comparisons, and their results are also displayed in Figure 27e: these estimates clearly reproduce very well the shape of the site response, with, however, a slight underestimation of the amplification level. They also found very different results when applying this technique to the P-wave part of the recordings, and they therefore conclude that HVSR, when applied to the S-wave signals, reveal the overall frequency dependence. Based on our side investigations, we only partly support the same conclusion, since in some cases we did find a good "spectral shape" correlation, but in a few other HVSR were only able to point out the fundamental resonance frequency. One must also bear in mind that this technique has been applied and checked for soft soil sites only, and might not be valid for other kinds of site effects (such as surface topography effects).

3.1.3.3 Concluding comments

Many of the problems raised by the microtremor method no longer exist for these various weak motion techniques, and that is why it has been often used in the last decades, most often under its simplest version of "spectral ratios" with respect to a reference site.
Their main advantage are their relative simplicity and self-sufficiency: using their results does not require any further investigations. This call of methods is amongst the best suited for a reliable estimation of local effects at a given site, especially as the development of digital, telemetered, small-aperture networks, linked with portable microcomputers, will soon allow an almost real-time estimation of site effects. The investment cost of such an equipment is certainly significant, but it may be rapidly "paid off" by numerous studies, and they are needed.
It has, however, some drawbacks. The first one comes from its duration: spectral ratios are not reliable unless they are an average of spectral ratios obtained for at least 10 events (and 20 or 30 is much better than 10), which requires to install, and maintain, the instruments in the field for at least one month (in seismically quiet areas and / or in noisy sites such as urban areas, it may often last for several months...). This requirement of a minimum number of records also stands, of course, when techniques other the spectral ratio technique are used. And it also takes some time to complete a careful analysis of the recorded data, even when the instruments are digital instruments. There is also an important issue in this weak motion method (and a fortiori in the microtremor method), in relation with the expected non-linearity of soils at high strain levels (see section 2.2.3.1): the only way to overcome this difficulty is to use strong motion data instead of weak motion data, as presented in the following paragraph.

3.1.4 Strong motion data

The development of strong motion arrays makes it now possible, in a few big cities such as Los Angeles, Tokyo, Taipei or Mexico City, to apply the above mentioned "weak motion" method on strong motion data. In such a case, there are no longer any questions about the reliability and applicability of the results: even non-linear affects are included in the recordings. For cities such as Mexico City where the strong motion network (Figure 28) is triggered once a year at least in average, several specific techniques have been developed in recent years, allowing to derive both reliable and detailed enough empirical microzoning, which may be used in engineering studies

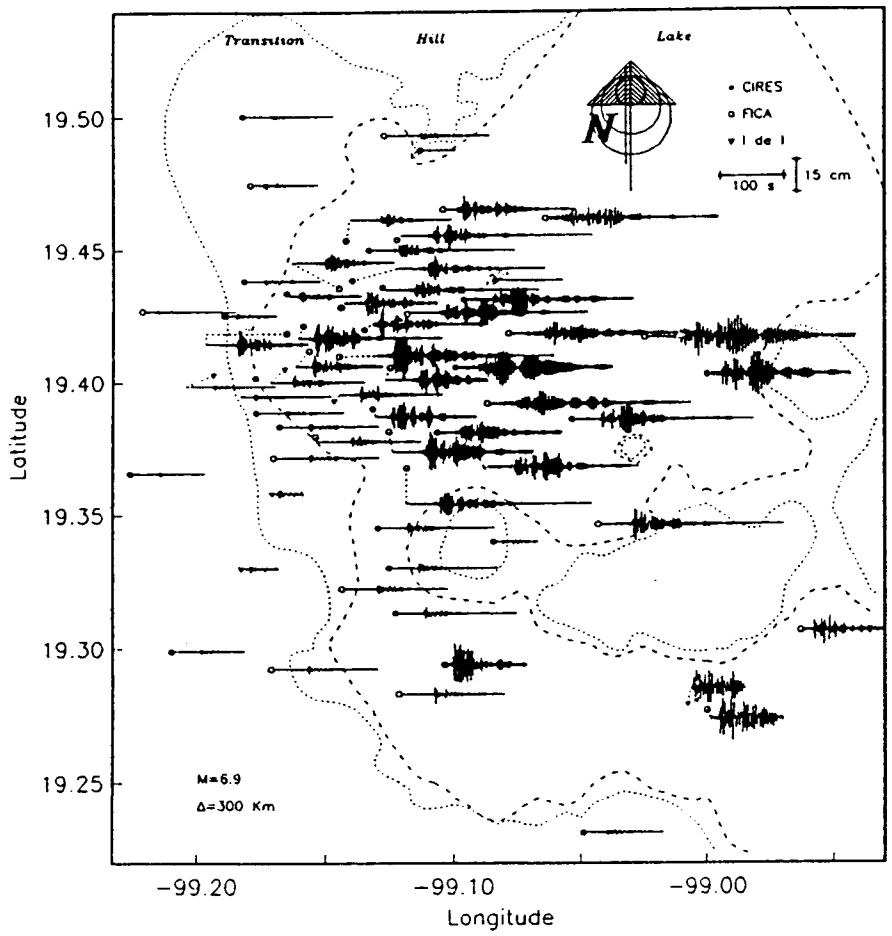

Figure 28 : *An example of strong motion data from a dense accelerometric array: Observed NS displacements within Mexico City for a Pacific coast event on April 25, 1989.*

and or urban panning even though site effects in Mexico City are not yet well understood. The only "problem" is - fortunately - that strong earthquakes at a given site are usually not so frequent. As a consequence, given the investment and maintenance costs of such networks, it will probably take several decades before all the big cities at threat be equipped, so that this method can be applied only in very rare cases.

As a conclusion to this section, recent methodological studies show that there is a fairly good agreement between "old" and "new" techniques, which, except those based on microtremor recordings, all reveal with comparable accuracy the frequency-dependent character of site amplification, at least for soft sites. The recently proposed techniques based on the H/V spectral ratio (using either microtremor or earthquake recordings) provides very cheap and reliable estimates of site fundamental frequency, but further investigations are needed concerning its ability to measure the site amplification factor.

3.2 Numerical methods

When the geotechnical characteristics of the site or of the area are known, site effects can be, in principle, estimated through numerical analysis. The prerequisite of a sufficient geotechnical knowledge generally implies that such ground response analyses be made on a site by site basis, but the density of boreholes and geotechnical information in some large cities may be sufficient to allow a numerically-based zoning. Such an approach, however, requires an in-depth understanding both of the analytical models and of the numerical schemes that are used: as such an expertise is not always met, it may happen that sophisticated numerical analyses lead to less reliable results than simpler and cruder, but more robust, approximations: the present section will therefore mainly emphasize the latter.

3.2.1 Simple methods

Simple methods are available only for the estimation of the amplification on soft soils: the understanding of surface topography effects is not enough satisfactory to justify the use of simple techniques, even though some might be available from parameter studies.

3.2.1.1 Hand calculations

As already mentioned in section 2, amplification on soft soils is related with resonance effects, which show up in the frequency domain by several peaks in the Fourier transfer functions (Figure 11). As the strongest effects generally occur at the fundamental frequency, the most simple numerical methods, which do not require the use of any computer, but only some hand calculations, are just aimed at estimating the fundamental period of the soil T_0 and the corresponding amplification A_0.
Such a simple simultaneous estimation of these 2 parameters is indeed possible only for sites which can be approximated as a one-layer over bedrock structure, for which the formulae given in section 2 may be applied. These formulae show that the estimation of T_0 is relatively easy, since only the S-wave velocity and the thickness of the surface layer are needed, while the estimation of A_0 requires the additional knowledge of the bedrock velocity and of the sediment damping.

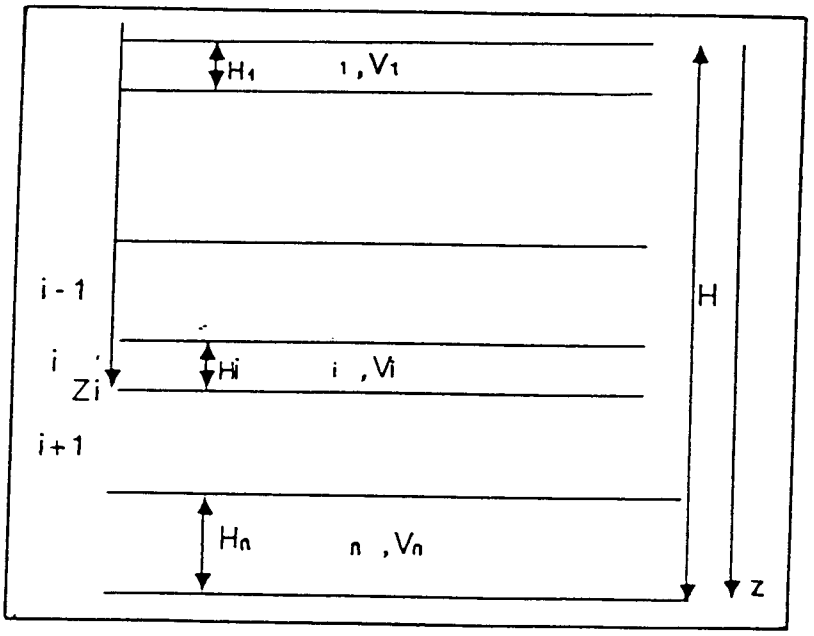

Figure 29 : *Horizontally layered soil structure allowing simple approximate hand calculations of the fundamental period T_0 , and simple 1D computer analysis.*

TABLE I: APPROXIMATE METHODS FOR ESTIMATING THE FUNDAMENTAL PERIOD T_0 OF A HORIZONTALLY LAYERED SOIL

Method	Description	Mathematical Formulation	References	Comments
1	Weighted average of S wave velocities	$\overline{V}=(\sum_{i=1}^{i=n} V_i H_i)/H$ $T_0 \approx T_1=4H/\overline{V}$	Madera (1970) Schnabel *et al.* (1972)	Slight mean overestimating: 10 to 15 % Precision: about 30 % Limitation: No important velocity jump between two contiguous layers ($V_i/V_{i+1}>0.5$ and <1.5)
2	Weighted average of shear moduli and densities	$\overline{G}=(\sum_{i=1}^{i=n} G_i H_i)/H$; $\overline{\rho}=(\sum_{i=1}^{i=n} \rho_i H_i)/H$ $T_0 \approx T_2=4H/\sqrt{\overline{G}/\overline{\rho}}$	Ambraseys (1959) Idriss (1966)	Very slight mean overestimation: 5 % Precision: about 30 %
3	Sum of natural periods of each layer	$T_0 \approx T_3=\sum_{i=1}^{i=n} 4H_i/V_i$	Shima (1962) Zeevaert (1972) Okamoto (1973)	Large mean overestimation : 25 to 30 % Precision: about 40 %
4	Linear approximation of the fundamental modal shape	$\omega_4{}^2=(3\sum_{i=1}^{i=n} V_i{}^2 H_i)/H^3$ $T_0 \approx T_4=2\pi/\omega_4$	Dobry *et al.* (1976)	Very slight underestimation: 5 % Precision: 25 to 30 %
5	Simplified version of Rayleigh approach	$X_{i-1}=X_i+\frac{z_i+z_{i-1}}{V_i{}^2}H_i$; $X_n=0.$ $\omega_5{}^2=\frac{4\sum_{i=1}^{i=n}\frac{(z_i+z_{i-1})^2}{V_i{}^2}H_i}{\sum_{i=1}^{i=n}(X_i+X_{i-1})^2 H_i}$ $T_0 \approx T_5=2\pi/\omega_5$	Dobry *et al.* (1976)	No bias Precision: about 5 % No limitation

For sites with a tabular, multi-layer structure as in Figure 29, hand calculations can provide satisfactory estimates of the fundamental period T_0, using for instance the formulae given by Dobry et al., and summarized in Table I. According to this Table, method n° 3, which is relatively often used and consists in simply summing the "natural periods" of each individual layer considered alone, is a wrong one, since it greatly overestimates the actual periods. The best of these approximate methods is the method n° 5, based on the Rayleigh procedure to estimate the shape of the fundamental mode; however, methods using weighted averages of velocities (n° 1) or rigidities and densities (n° 2) also provide very simple and satisfactory estimates in usual conditions.
However, there do not exist any approximate formulae that provide a reliable estimate of the fundamental amplification A_0 on such horizontally layered sites: as already mentioned for the one-layer model, it depends on many parameters, including the damping, S-wave velocities and thicknesses of each layer. It has been proposed that an upper bound of A_0 may be estimated using formula (2) using the impedance contrast between the softest surficial layers and the most rigid deep formations, and the surficial damping; but this is very crude and may lead to large overestimations.

3.2.1.2 Simple computer analyses: one-dimensional response of soil columns

Apart form the above mentioned hand calculations, there exist a number of still simple analytical methods which allow to compute the seismic response of a given site with the only help of a small personal computer. Amongst them, the most widely used makes use of the multiple reflection theory of S waves in horizontally layered deposits, very often referred to as "1D analysis of soil columns".
Such a soil column is excited by an incoming plane S wave, generally considered as vertically incident, and corresponding to a surface bedrock motion representative of what is likely to occur in the area. The specific parameters required for such an analysis are shear-wave velocity, density, damping factor and thickness of each layer. These parameters may be obtained either through direct in-situ measurement, or drillings and subsequent laboratory measurements, or from known approximate correlations with other, more usual geotechnical parameters such as the SPT number from standard penetration tests.
These analyses may be performed considering either a linear behaviour of soils, or a non-linear behaviour. In that latter case, the non-linearity is very often approximated with a "linear-equivalent" method that uses an iterative procedure to adapt the soil parameters (i.e., rigidity and damping) to the actual strain it undergoes, according to the curves depicted in Figure 30. This kind of non-linear analysis thus requires some quantitative information on the actual strain dependency of rigidity and damping, which in principle require some careful laboratory tests; some generic, average curves have been proposed for different kinds of material (clay, sand, ...), but the actual behaviour of a given deposit may strongly depart from the "average" curves: this was in particular the case for the Mexico City clays which were thought highly non-linear because of their very low rigidity, and which proved indeed to behave almost linearly despite the large strains experienced during the 1985 event.

3.2.2 Sophisticated methods

Although the basis of all numerical methods remains the same: the wave equation, a lot of different models have been proposed to investigate some (never all simultaneously) aspects of site

effects, which involve various kinds of complex phenomena: the incident wave field may be very complex (near-field, far-field, body waves, surface waves,...), the structure geometry may be 1D, 2D or 3D, and the mechanical behavior of earth materials has a very wide range (visco-elasticity, non-linear behaviors, water-saturated media, liquid domains,...). Typically, these methods may be classified into four groups: analytical methods which may be used only for a very limited number of simple geometries; ray methods which are basically high frequency techniques and are uneasy to use when wavelengths are comparable to the size of heterogeneities; boundary based techniques (such as all kinds of boundary integral techniques, or those based on wave function expansions) which are the most efficient when the site of interest consists of a limited number of homogeneous geological units; and domain based techniques (such as finite-difference or finite-element methods) which allow to account for very complex structures and rheologies, but are very heavy from a computational viewpoint. As stressed by Aki and Irikura (1991), "these methods have their advantages and disadvantages, and, in general, those which can deal with more realistic models are less accurate, while those achieving higher accuracies are more time consuming. Most of these methods are still actively developed, because each has its own merit that effectively applies to a certain class of problems." Our aim in this section is not, however, to discuss the intrinsic reliability of each numerical technique, but simply to discuss the interest of numerical methods, considered as a whole, in the estimation of site effects for engineering purposes.

Their main advantage is their flexibility and versatility (combined with their cheapness on standard computers), which allow phenomenological and parameter studies on the one hand (as did for instance Bard and Bouchon, 1985), and also, on the other hand, allow an estimation of the uncertainty in the response of a given site, given the uncertainty in the input geometrical and mechanical parameters. And indeed, these methods did lead to significant breakthroughs in the understanding of site effects during the last two decades. Advances could be achieved along 2 main directions:

- the proper consideration of diffraction effects on complex surface or subsurface topography: there now exist many numerical techniques to account for 2D or even 3D geometries. These latter 3D techniques are, however, very expansive from a computational viewpoint, and moreover limited to rather low frequencies.
- the realistic modelling of strong non-linearities occuring in soft soils, and especially saturated sands, as illustrated in Figure 31.

Nevertheless, their routine use of such methods for the a priori estimation of site effects raises several questions:

- their ability to predict actual effects had, until recently, only very rarely been objectively tested (i.e., comparisons between observations and theoretical computations had always been done a posteriori: the "predictors" knew what they had to find...).
- these methods cannot be used in any case, but only within their validity domain. Unfortunately, in some cases, people who use numerical methods in consulting companies may not be aware of these limits, and that may lead to wrong estimations.
- even if these methods are reliable, their actual cost may be very important - and exceed the cost of instrumental estimates of site effects - as they require as input parameters detailed geotechnical or geophysical information about the site underground and "neighbourhood".

3.2.3 Blind tests

That is why two international experiments have been organized in California and Japan to test

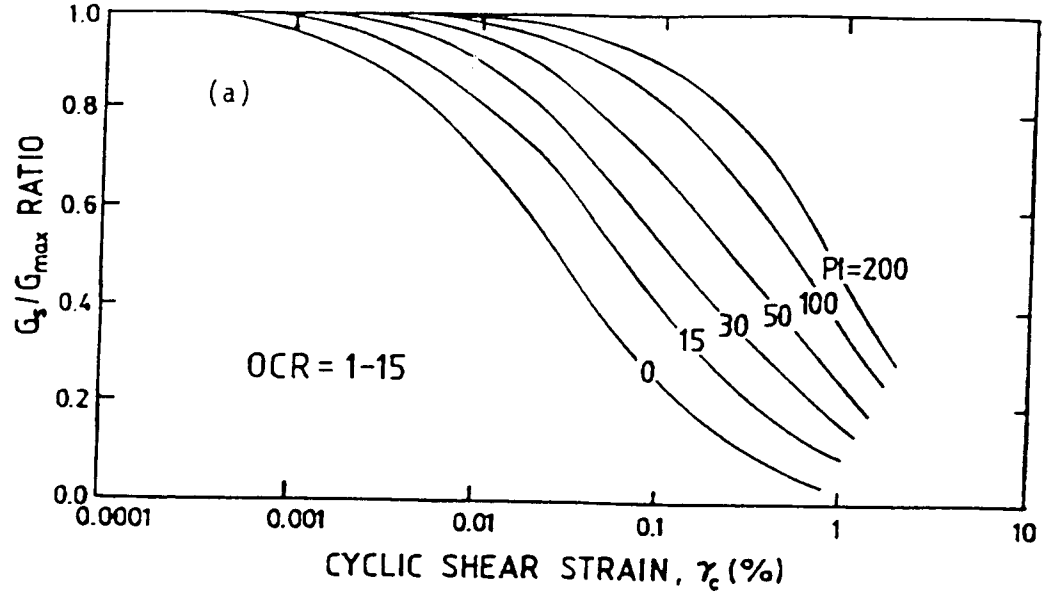

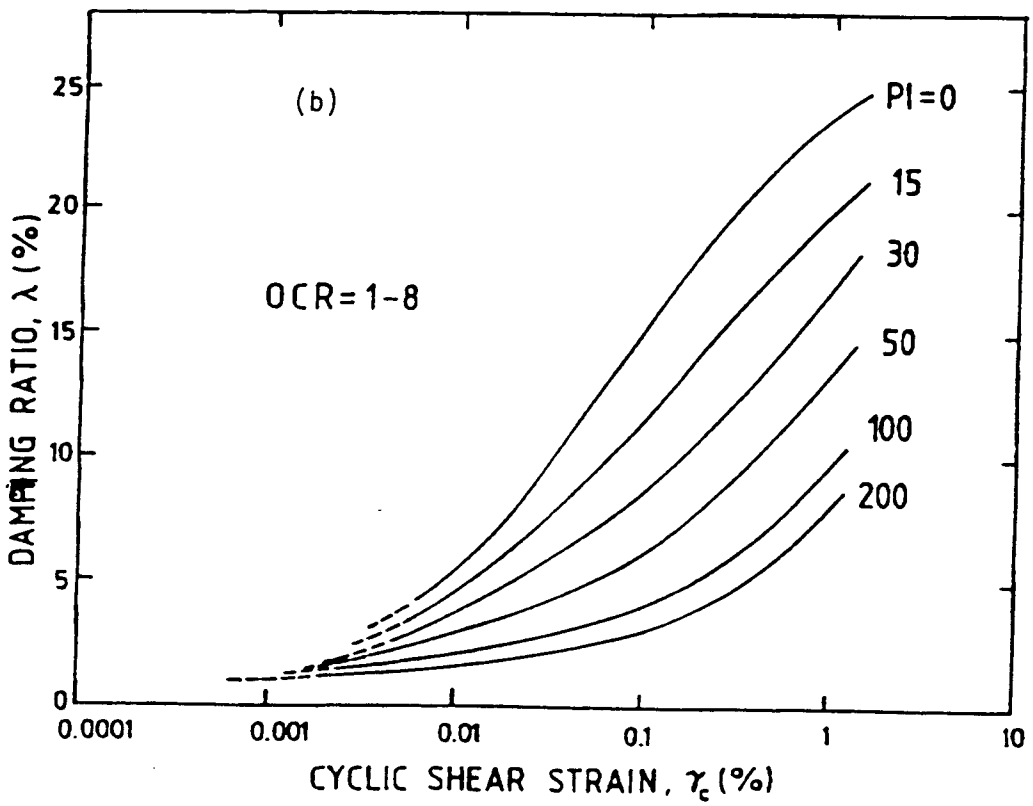

Figure 30 : *An example of strain dependency of normalized shear modulus and damping for soft soils with varying plasticity index (after Dobry and Vucetic, 1991).*

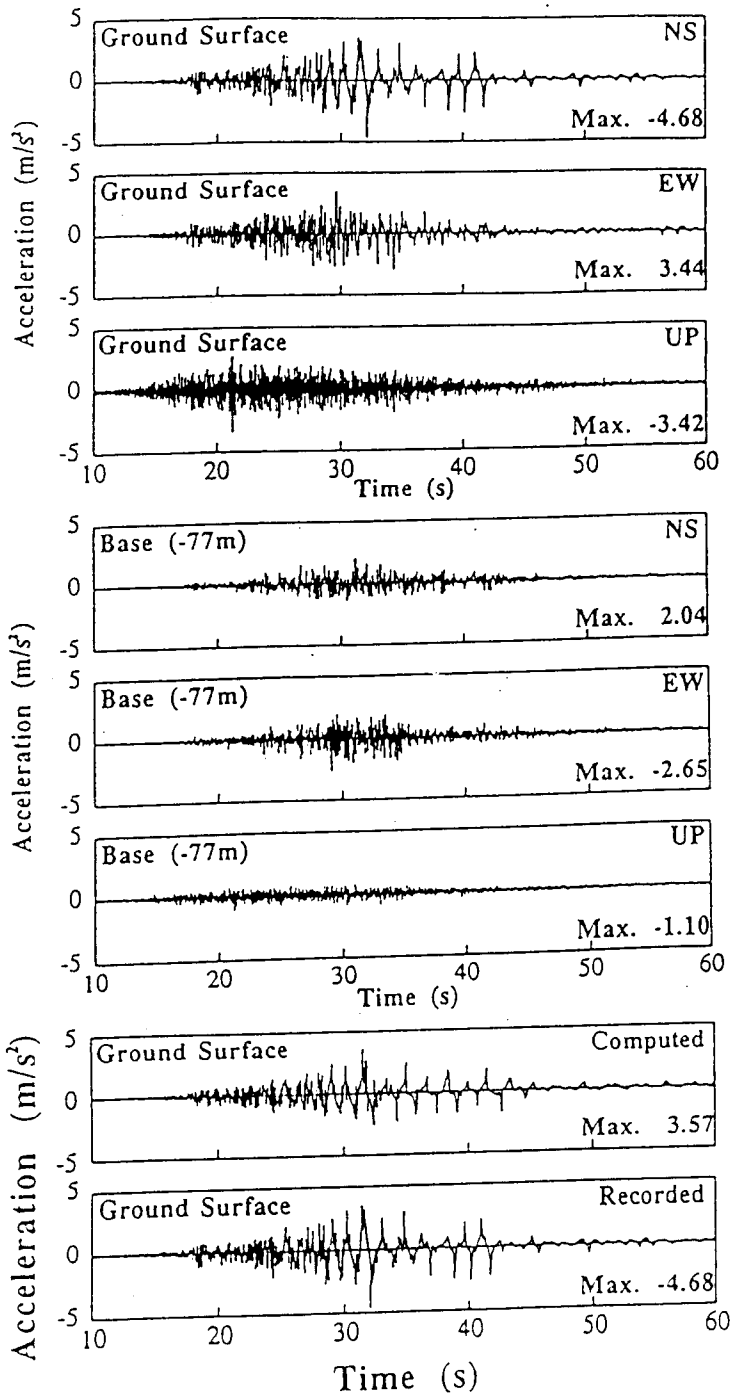

Figure 31 : *Recorded accelerations and synthetics at the 1993 Kushiro-Oki earthquake. (Reproduced from Iai et al., 1995)*

this "a priori" reliability of numerical methods; as their results have already been presented and discussed in several symposia (Cramer and Real, 1991; Midorikawa, 1992; Bard, 1992). Since the corresponding proceedings may not be easily available, the present section briefly summarizes the methodological findings of these experiments, as expressed in those proceedings and in a recent additional paper (Field and Jacob, 1994).
The sites of these experiments were a rather simple, thin, stiff soil in Turkey Flat, California, and a somewhat more complex, softer and ticker site in Ashigara Valley, Japan. In both cases, instrumental recordings confirmed that surface motion undergoes large changes over short distances, and that, although those changes do vary from one event to another, their scatter remains limited enough to justify the attempts to predict such local effects (such a result may appear trivial, but it was not so several years ago in many North American minds).

3.2.3.1 Average performance of predictions

One of the major outcome of the comparison between blind predictions and observed site responses (as measured through the classical spectral ratio technique), has been to point out that presently available methods, in an average, perform "reasonably well". In particular, 1D models, despite their simplicity, proved to provide satisfactory results for both TF and AV sites, despite their different geological conditions, while 2D or 3D models did not lead to a better fit.
However, despite this satisfactory accuracy of the average predictions, a general trend to overestimating the surface motion on sediments was noticed, which may come from some numerical problems in some computations, but also from inaccuracies in the standard geotechnical model as well.

3.2.3.2 Large variability of predictions

Both experiments show that the predictions from different individuals exhibit a significant variability depending not only on the numerical approach, but also on the predictor himself. This should prompt "predictors" to be modest and cautious in drawing detailed quantitative conclusions from their results.
In addition, despite the general "average" agreement between predictors, it was observed that a single method using a single code may provide significantly different results when used by different people; although reasons for that have not yet been analyzed, they probably deal with deconvolution problems and the choice of input motion, as well as with the translation of the geotechnical model into a code-specific computer model. There is therefore a need, in all numerical site response estimates, to specify not only the kind of numerical approach that is adopted, but also the details concerning its specific application to the site under consideration.

3.2.3.3 Importance of geotechnical measurements

These two experiments also showed that the responsibility for the prediction uncertainty or inaccuracy does not lie on the computing side only, but is also tightly linked with the interpretation of geotechnical and geophysical surveys. This point has been especially emphasized by Field and Jacob (1993a) for the Turkey Flat site, who used Monte-Carlo simulation to analyse the uncertainty in theoretical site-response estimates related only to the uncertainties in geotechnical parameters. They took advantage of the redundancy in geotechnical surveys to estimate directly the input-parameter uncertainty. They found that, while the computed results

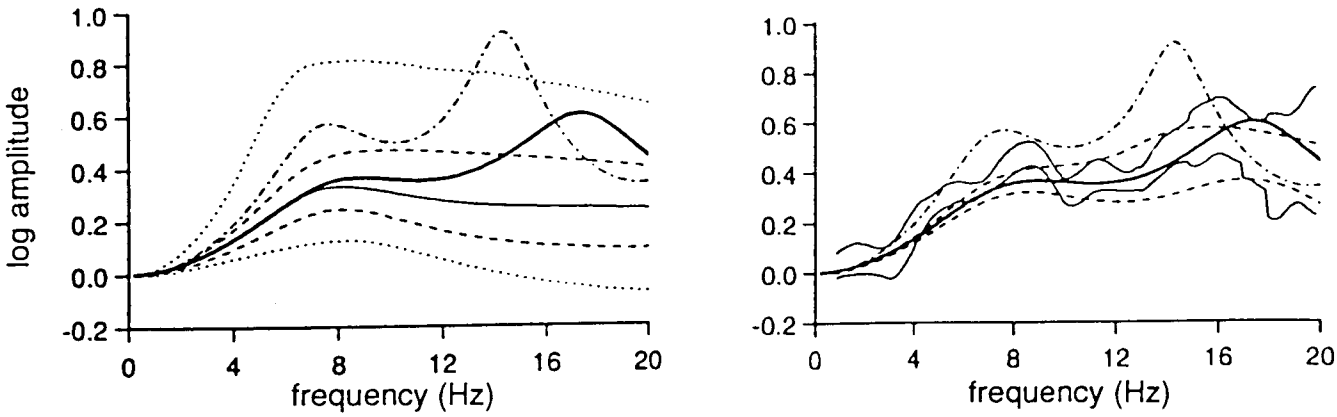

Figure 32 : *An example of the effect of uncertainties in geotechnical parameters on site amplification factor estimates.*
a) (Left) The solid line corresponds to the median estimate after 20000 different 1D computations with different geotechnical parameters, the statistical distribution of which corresponds to the actual distribution of measured values (thicknesses of layers, S-wave velocities, Q values) The dashed lines define the region where the central 50% occurred (first and third quartiles), and the dotted lines represent the area where the central 90% landed. The dot-dashed line represents the response for the "standard" model derived by geotechnical engineers and specified in the blind prediction experiment, while the bold line corresponds to the response computed for the model with median parameter values.
b) (Right) Comparison of median curves with the actual observations, represented by thin solid lines (average +- one standard deviation). (Reproduced from Field and Jacob, 1993a).

generally agree with observed spectral ratios, the input uncertainties lead to a high degree of variability in the theoretical predictions. More precisely, most of the variability is shown to come from poor constraints on the shear wave velocity and thickness of the topmost thin layer (only a few meters thick) - and this result is also valid for Ashigara Valley soft sites, see ESG92 -, and on the attenuation of sediments as well, which appears to be very poorly constrained, and for which there often is disagreement between in-situ measured values and laboratory values (Figure 32).

They conclude that, for "site-response studies which rely exclusively on geotechnically based theoretical predictions, it is important that the variability resulting from input-parameter uncertainties is recognized and accounted for". Which means that several independent geotechnical surveys should be performed, thus considerably raising the actual cost of numerical estimates of site response. (Another possible conclusion might be the need for an improvement in the average quality of geotechnical measurements...) Field and Jacob (1993) also mention, in agreement with other authors, that "average spectral ratios of earthquake recordings" (i.e., the classical instrumental approach) "provide a better estimate of the weak-motion site response than do theoretical predictions". This conclusion may certainly be extrapolated to strong-motion site response, since the measurement of non-linear parameters is an uneasy task adding new uncertainty sources; obtaining direct empirical estimates of site response in the strong-motion range is, however, possible only in very few sites with intense seismic activity, and is out of reach for moderate seismicity areas such as most of Europe.

3.3 Empirical correlations based on surface geology

As emphasized in section 2, the effects of soft sedimentary layers have been observed in many occasions, and the very large number of observations allows several authors to propose some empirical correlations between the surface geology and various measurements of the earthquake motion. These relationships, derived from one particular set of data where both earthquake observations and information on surface geology are available, are then applied at other locations, where only surface geology is known.

3.3.1 Geology / Intensity increment

Various empirical correlations between surface geology and seismic intensity increments, summarized in Table II, have been proposed since the first work of Medvedev (1962), whose relationships have been extensively used for microzoning studies in Eastern European countries. Although each of these relations is based on data from a particular part of the World (California, Chile, Japan, Middle Asia), they are quite consistent to one another (when differences between JMA scale and MM or MSK scales are properly taken into account), and may therefore be thought as general and applicable in any part of the World. Such an approach is relatively currently followed for the establishment of earthquake damage scenarios in California.

3.3.2 Geology / amplification

As intensity is a too qualitative measurement of ground motion, several attempts have also been made to derive some more quantitative relationships between surface geology and local amplification. Several such correlations are summarized in Table III, whose comparison is not straightforward however, since the local amplification is not measured in the same way: average

Geological Unit	Intensity Increments
Medvedev (1962)	(MSK scale)
Granites	0
Limestones, Sandstones, Shales	0.2~1.3
Gypsum, Marl	0.6~1.4
Coarse-material ground	1~1.6
Sandy ground	1.2~1.8
Clayey Ground	1.2~2.1
Fill	2.3~3
Moist ground	1.7~2.8
Moist fill and soil ground	3.3~3.9
Evernden and Thomson(1985)	(MM scale)
Granitic & metamorphic rocks	0
Paleozoic rocks	0.4
Early Mesozoic rocks	0.8
Cretaceous to Eocene rocks	1.2
Undivided Tertiary rocks	1.3
Oligocene to middle Pliocene rocks	1.5
Pliocene-Pleistocene rocks	2.0
Tertiary volcanic rocks	0.3
Quaternary volcanic rocks	0.3
Alluvium (water table < 30ft)	3.0
(100ft < water table)	1.5
(others)	2.0
Kagami et al. (1988)	(JMA scale)
Talus	0
Andesite	0
Gravel	0.2
River deposits	0.4
Volcanic ash	0.5
Sandy silt	0.7
Clayey silt	0.8
Silt	1.0
Peat	0.9
Astroza and Monje (1991)	(MM scale)
Granitic rock	0
Volcanic pumicite ashes	1.5~2.5
Gravel	0.5~1
Colluvium	1~2
Lacustrine deposits	- 2.5

Table II : *Correlations between surface geology and intensity increments, according to various authors. (Reproduced from ISSMFE, 1993)*

Geological unit	Relative amplification factor
Borchert and Gibbs (1976)	
Bay mud	11.2
Alluvium	3.9
Santa Clara Formation	2.7
Great Valley sequence	2.3
Franciscan Formation	1.6
Granite	1.0
Shima (1978)	
Peat	1.6
Humus soil	1.4
Clay	1.3
Loam	1.0
Sand	0.9
Midorikawa (1987)	
Holocene	3.0
Pleistocene	2.1
Quaternary volcanic rocks	1.6
Miocene	1.5
Pre-Tertiary	1.0

Table III : *Correlations between surface geology and relative amplification factor, according to various authors. (Reproduced from ISSMFE, 1993)*

horizontal spectral amplification (AHSA), with respect to granite, in the frequency range 0.5 - 2.5 Hz for Borcherdt and Gibbs (1976), ratio of peak ground motion in the 0.1-10 Hz frequency range with respect to loam ground for Shima (1978), and mean ground amplification in the 0.4 - 5 Hz frequency range with respect to pre-tertiary rocks for Midorikawa (1987).
As some of these relations were derived on sites where detailed intensity data were available (San Francisco), it has been possible (Borcherdt and Gibbs, 1976) to propose relations between the average horizontal spectral amplification (AHSA), and the intensity increment (in Modified Mercalli scale):

$$\Delta I = 0.214 + 2.12 \log (AHSA) \quad (4)$$

Similar relationships should be derived in other parts of the World to allow a more quantitative interpretation of past intensity data.

3.3.3 Geotechnical parameters / amplification

More and more often, especially in large cities or for large development projects, geotechnical information is available in addition to "simple" surface geology. Some authors have thus tried to derive some relations between a few simple but relevant geotechnical parameters, and the local amplification.
The most relevant parameter is the S wave velocity; however, as it is not very easy nor cheap to measure it, another one very often used is the Standard Penetration Test value NSPT, which is much more frequently available, and for which several correlations have been proposed with S velocity and density, at least for soft soils.
Several authors (Midorikawa, 1987; Joyner and Fumal, 1984; and Borcherdt et al., 1991), have thus proposed relations between the "average S velocity of surficial deposits" (i.e., down to a certain depth) and the relative amplification. Those relations are given and compared in Figure 33.
Some studies are also using much more detailed geotechnical descriptions of the soils, including void ratio, grain size, and so on: although they allow a better description of the various deposits, they are probably too complex for being used in a routine environment for which rather few data are available.

3.3.4 Surface geology / response spectra

There exist two ways of relating the surface response spectra to the site geology. The first one is very crude as to the geology and more satisfactory as to the description of ground motion, while the second is slightly better for the former, and more crude for the latter.

3.3.4.1 Empirical attenuation laws

Many empirical attenuation laws have been derived on the basis of existing strong motion records. They all relate one given ground motion parameter (pga, pgv, Sa, duration, ...) to the magnitude and distance of the seismological event, and they also very often take into account a site parameter. Very often this site parameter is simply 0 for rock and 1 for "non-rock"; only very rare are the cases where the description of site geology is more refined (such as in studies based on Italian data, where an interesting distinction is made between thin and thick soft deposits), since detailed information on strong motion recording sites is generally missing.
It is thus possible to modify the ground motion parameters according to the site geology.

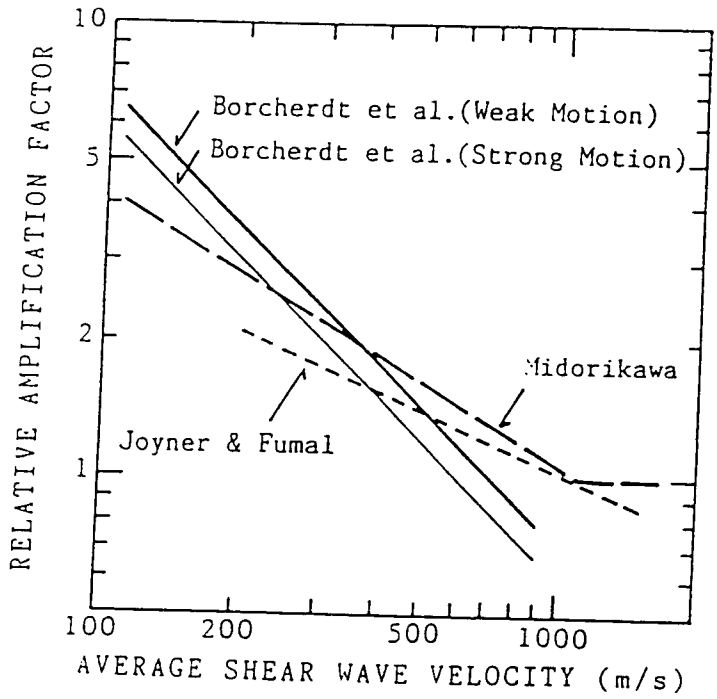

Researchers	Equation
Midorikawa (1987)	$A = 68V_1^{-0.6}$ $(V_1 < 1100\text{m/s})$
	$= 1.$ $(V_1 > 1100\text{m/s})$
Joyner and Fumal (1984)	$A = 23V_2^{-0.45}$
Brochert et al.(1991)	$AHSA = 700/V_1$ (for weak motion)
	$= 600/V_1$ (for strong motion)

A: relative amplification factors for peak ground velocity

$AHSA$: average horizontal spectral amplification in period range of 0.4 to 2.0 sec.

V_1: average shear-wave velocity to a depth of 30 m (in m/sec.)

V_2: average shear-wave velocity to a depth of a one-quarter wavelength of a one-second wave (in m/sec.)

Figure 33 : *Correlations between shear wave velocity and relative amplification factors, according to various authors. (Reproduced from ISSMFE, 1993)..*

However, as it is based on a very crude (generally yes/no) classification of soils, and on statistical studies which in essence smooth out the extreme values, such an approach may lead to a dangerous underestimation of amplifications on some very sensitive sites. (Simultaneously, there is a significant probability for overestimating the motion on usual sites).

3.3.4.2 Building codes

In most of existing building codes, the surface geology is accounted for through a rather broad soil classification, based on both geological and geotechnical information. Usually 3 to 4 site categories are distinguished, such as: rocks; stiff soils; deep cohesionless soils; soft to medium clay and sand (Seed et al. 1976). It can be observed on the three examples of such classifications given in Table IV, that these classifications are generally consistent from one country to another. Such classifications may provide the basis for a mapping of soil conditions, and therefore a subsequent microzoning.
The dependency of the design ground motion on site category is generally defined through a modulation of both the peak acceleration a_{max} and its normalized response spectrum (Sa / a_{max}), leading to what is often called "site specific response spectra". The values of these modulations are mainly based on regression studies made about 10-15 years ago in Japan and USA (see Figure 34), which all showed that response spectra on soil sites have a higher level than those on rock sites at long periods, and that this relation is reversed at short periods. The ratio between design spectra at soil and rock sites never exceeds 3 at long periods, and is never lower than 0.5 at short periods (Figure 34).
The introduction of these site specific response spectra in seismic regulations has certainly greatly helped a wide awareness of the importance of sediment effects in the engineering community. But it also had some pernicious consequences: engineers are now reluctant to admit site amplification factors larger than 3 (even in extreme cases as in Mexico City), and they are also reluctant in admitting that very thin (a few meters) soft deposits may induce large amplifications in the frequency range 4 - 10 Hz. Fortunately, the recent propositions for "up-to-date" response spectra by Borcherdt (1994), and Borcherdt and Wentworth (1995), which are based on strong motion data obtained during the recent Californian earthquakes (Loma Prieta, 1989, and Northridge, 1995), introduce very significant corrections to the "old" shapes, and should greatly improve the next generation of earthquake regulations.

3.3.5 Geometrical effects: surface topography and lateral discontinuities

All the preceding sections consider simply the amplification effects of soft soils, in relation only with their mechanical parameters, and not with their geometry (apart from their local thickness). However, as mentioned in section 2, the geometry of surface (i.e., its topography) and subsurface may have important consequences on the amplitude and spectral characteristics of ground motion. This section is thus devoted to a brief review of the way these "geometrical" effects may, or may not, be accounted for through simple correlations.

3.3.5.1 Surface topography

As emphasized in section 2.1, surface topography effects are not yet fully understood, and existing instrumental or observational data are not numerous enough to justify statistical analyses. That is why there does not exist any empirical relationship, and the consequence is that in most

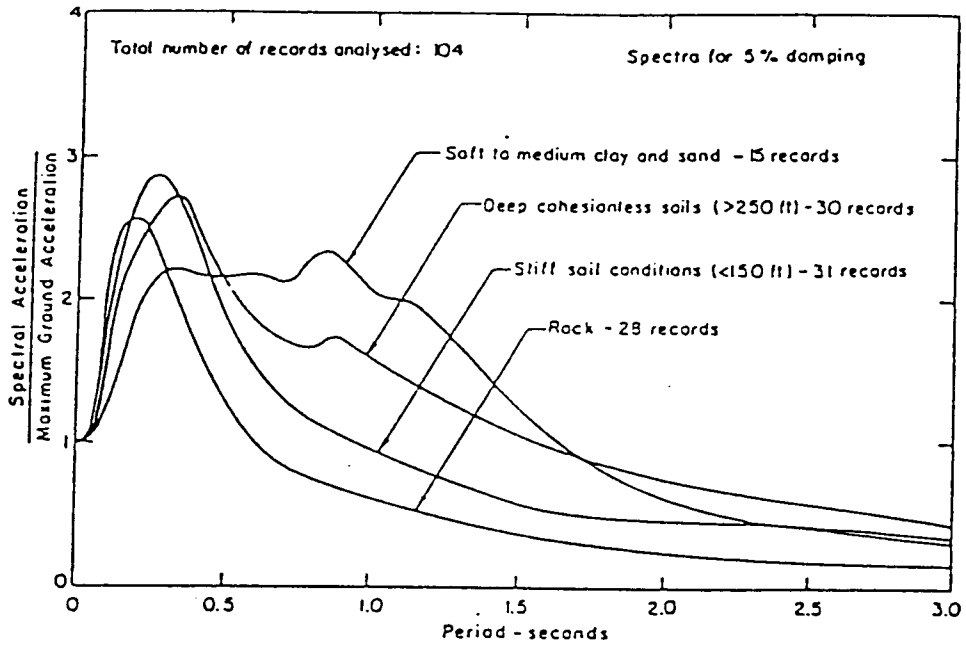

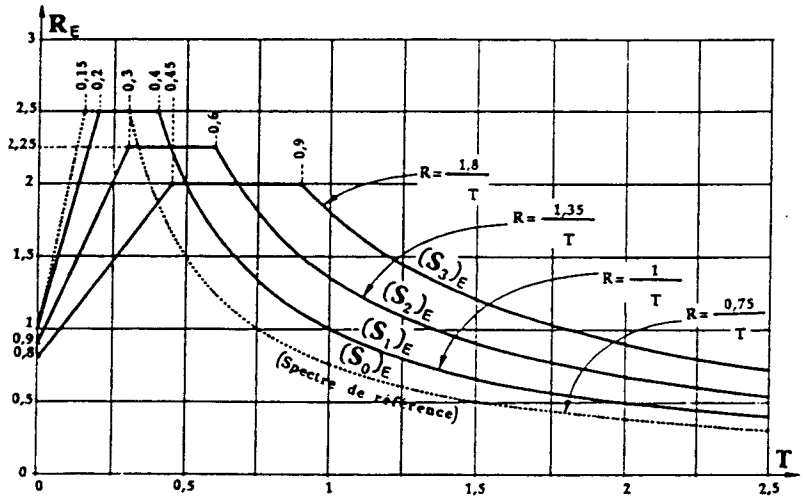

Figure 34 : *Normalized acceleration spectra for different site conditions.*

a) (Top) Average spectra resulting from a statistical analysis of 104 strong motion records (from Seed et al., 1976)

b) (Bottom) Site specific elastic response spectra proposed for the next earthquake regulations in France (AFPS 90). Site category S_0 corresponds to rock sites and thin (h < 15m) "a" soils; site category S_1 corresponds to thick (h > 15m) "a" soils, and to thin (h < 15m) "b" soils; site category S_2 corresponds to moderately thick (15 to 50 m) "b" soils and to thin (h < 10m) "c" soils; site category S_3 corresponds to very thick (h > 50m) "b" soils, and to thick (h > 10m) "c" soils. "a" soils are stiff soils with good to very good mechanical characteristics, "b" soils are soils with intermediate mechanical characteristics, while "c" soils are weak soils (loose sands, soft clays, mud, ...)

TABLE IV: Site classification for UBC, Japanese and European draft building codes		
Code	**Site**	**Description**
UBC	S_1	A soil profile with either: a) a rock-like material characterized by a shear wave velocity greater than 800 m/s or by other suitable means of classification b) stiff or dense soil condition with a soil thickness less than 60 m
	S_2	A soil profile with dense or stiff soil conditions, with a soil thickness exceeding 60 m
	S_3	A soil profile 13 m or more in depth, and containing more than 7 m of soft to medium stiff clay, but not more than 13 m of soft clay
	S_4	A soil profile containing more than 13 m of soft clay
Japanese building code	I	Ground consisting of rocks, hard sandy gravel or the like, classified as tertiary or older strata, over a considerable area around the structure
	II	Ground consisting of sandy gravel, hard sandy clay, loam or the like classified as diluvial, or alluvial gravel about 5 m or more in thickness
	III	Standard ground other than I, II, or IV (sand, sandy clay, clay, classified as alluvium)
	IV	Bad and soft ground falling in one of the following categories: a) alluvium consisting of soft alluvial delta deposits, topsoils, mud or the like about 30 m or more in total thickness b) ground made by the reclamation of marsh, muddy sea-bottom, earth fills or the like about 3 m or more in thickness, where less than 30 years have elapsed since the time of reclamation
EC8 (Draft)	R	Hard rock formations extended considerably both in area and in depth, e.g.: - crystalline massifs consisting mainly of magmatic and metamorphic rocks - massifs consisting mainly of paleozoic and mesozoic sediments
	M	- plateaus covered by mesozoic and cenozoic tertiary sediments - basins filled with cenozoic sediments of relatively low thickness - intensively in-situ eroded rock formations or soils that can be assimilated to them in view of their mechanical characteristics - coarse-grained granular materials of medium relative density - medium stiff clay, slightly overconsolidated
	A	- loose coarse-grained granular materials with low relative dentity - clay/silt soils of reduced stiffness

present day seismic codes and microzoning studies, topographical effects are not accounted for, despite their possible magnitude.
However, since at least part of the observed amplification may be explained by physical phenomena related to wave propagation, some attempts are being made, for instance in the new French recommendations, to introduce a "dissuasive" coefficient simply intended to bring these effects to the attention of engineers and planners. This coefficient is relatively simple (Figure 35): it is frequency independent, and related mainly to the local slope (and to its variations in the immediate vicinity); moreover, it is limited to a maximum value of 1.40 (i.e., much smaller many observed amplifications).

3.3.5.2 Subsurface topography

Are considered here the particular effects related with the lateral thickness variations in soft soil deposits, that may be observed in sediment-filled valleys and/or near to strong lateral discontinuities.
As for the surface topography, there is a lack of experimental data, so that no empirical correlation exists between geometrical shape and observed effect. There have been, however, a few parameter studies based on numerical simulations, which propose some formulae to estimate the amplification in 2D (or even axisymmetric 3D) structures from the 1D amplification and some simple geometrical parameters (basically the shape ratio, related to the thickness over width ratio of the deposit).
These geometrical effects are therefore not considered in current regulations.

4. CONCLUSIONS: RECOMMENDATIONS FOR MICROZONING STUDIES

There exist a lot of different techniques allowing to estimate at least some aspects of the local effects that affect the vibratory characteristics of ground motion. Their cost varies a lot from one to another; the preliminary information they require is not always available; the results they provide are more or less quantitative, not always comparable, and cannot be systematically used in a straightforward manner in a given regulatory context; their use sometimes requires a significant degree of expertise that is not always met. As a consequence, a microzoning study also require at first a methodological choice, depending on the available information, budget, and on the actual risk level of the zone under study.
In both microzoning guides recently issued (AFPS and ISSMFE), three microzoning levels or grades are proposed, corresponding to different levels of coverage, accuracy, and cost. The present section will list the techniques that are recommended for each of these three grades.
In any case, the necessary prerequisite before any microzoning work is the establishment of a geological model for the site under consideration: all the existing geological, seismological and geotechnical information should be compiled, and incorporated in a detailed geological map, the scale of which should be at least 1/25000 and preferably 1/10000 to 1/5000, depending on the available existing information. Such a map should include, in particular, the thicknesses and mechanical properties of surface formations.
Another necessary prerequisite concerns the definition of the "bedrock" microzones, i.e. the areas where the hazard is exactly equal to the regional hazard as derived from regional probabilistic or deterministic studies. It is generally agreed upon that such a "bedrock" may be characterized by a S wave velocity around 800 m/s (+ 200 m/s), and a gentle surface topography: there might

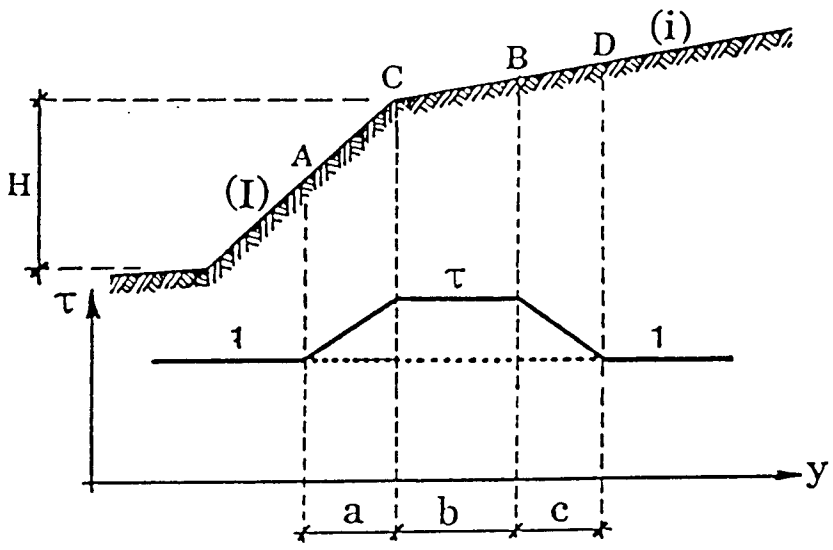

$$\tau = 1 + 0.8\,(I - i - 0.4) \qquad 1.0 \le \tau \le 1.4$$

$$b = \text{Minimum} \begin{cases} 20\ I \\ \dfrac{H + 10}{4} \end{cases}$$

$$a = H/3 \qquad c = H/4.$$

Figure 35 : *An example of topographical coefficient for earthquake regulations (French recommendations AFPS 90).*
This coefficient is related with slope changes: for the topographic profile indicated on top, it is defined as : $\tau = 1. + 0.8\,(I - i - 0.4)$ *with* $1.0 < \tau <$ *where I -i is the change in slope around C point. It is to be applied over a length BC given by the minimum of 20 I and (H+10)/4, with a linear transition over AC (a=H/3) and BD (c=D/4). Its determination for a givent site is based the worst cross-section passing through it.*

therefore exist not only zones with softer material (including sediments and highly or deeply weathered rocks) and increased hazard, but also zones with stiffer rocks (such as unweathered limestone or granite) and decreased hazard.

Level A (Most cursory level):

This is the crudest and lower-cost methodology; it is to be used in case of small funding and/or low risk level (these two aspects should in principle be linked...).
The basic aim of such studies should simply be to map the different site categories that are specified in the local earthquake resistant regulations. It is also recommended to identify the areas that could give rise to particularly important effects, that are not accounted for in the current regulations (such as sharp topographies, strong lateral discontinuities,...), where special investigations should then be required before any important development.
Since site effects are, in such "level A" microzoning, accounted for through site specific spectra, recommended approaches to be used are those presented in sections 3.1.1, 3.3.1 and 3.3.4.

Level B (Intermediate, reliable level):

The reliability of level A microzoning may be significantly improved through the compilation of additional data sets or information (aerial photographs, engineering reports issued for private projects, ...), through some cheap field surveys (in order to refine the geological and geotechnical mapping based on already existing information), and through some more quantitative estimates of ground response.
Geotechnical investigations to be performed, or simply compiled for a careful gathering of engineering reports from governmental agencies and/or private companies, may include bore-hole drilling, penetration tests, P or S wave logging, soil sampling for laboratory tests. One of the most convenient (and also cheapest) ways to identify subsurface soil properties is the use of Standard Penetration Test. Microtremors may also be used to characterize the various site categories found in the zone under study.
Recommended methods for estimating the local ground response are the still simple techniques presented in sections 3.2.1, 3.3.3 and 3.3.5 (in addition to those already recommended for level A microzoning). A specific output of such level B microzoning study might be a mapping of the fundamental period of the soil T_0 and of the estimated corresponding amplification A_0, from which site specific spectral modifications to rock design spectra may be defined.

Level C (Most reliable level, or detailed level):

When the risk is very high and the available funding too (a good example is the case of Mexico City), it is often -always - necessary to look for some more detailed and quantitative information, especially in high hazard areas, and therefore to perform specific geotechnical tests (in situ or in laboratory), to carry seismological experiments aimed at a direct in situ measurement of amplification effects, and to perform detailed computer analysis of ground response for which soil parameters should be measured and not only estimated from empirical correlations.
The basic difference between level B and level C microzoning is that the latter require in-depth understanding of the phenomenology of site effects, as well as of the analytical models and of the numerical procedures that are used. Lack of such in-depth understanding may occasionally result in erroneous zoning, and the results of such analyses should therefore be accompanied with

an evaluation by some recognized experts, and, whenever possible, be validated by confrontation with experience from past earthquakes.
All possible geotechnical investigations are welcome in that microzoning level, in order in particular to measure and map the dynamic characteristics of soils in low and high strain domains: bore-hole drillings, cross-hole and down-hole logging, SASW (seismic analysis of surface waves) are recommended for determination of the S wave velocity 3D structure, as well as for in situ damping estimates (including both scattering and material damping). Lab tests should be performed with care on undisturbed samples; in addition to resonant column tests, cyclic triaxial tests with drained and undrained conditions are often needed for truly nonlinear computations.
Any kind of validated numerical procedure or analytical model (see sections 3.2.1 and 3.2.2) can be used for the computation of surface motion, provided that they are used within their validity limits, and provided that they are fed with accurate input parameters: this, in practice, restrict their use by experienced practitioners.
Finally, direct in-situ measurements of site effects at some selected sites, as presented in sections 3.1.2, 3.1.3 and 3.1.4, are probably the best way to validate computer analyses.

Concluding remarks

The main methodological lesson pointing out of this review concerns probably the greater reliability of the instrumental approach based on the analysis of earthquake recordings. This result should obviously be balanced by the established existence of nonlinear effects, which somewhat limits the validity of amplification factors obtained from weak motion measurements. However, in this latter case too, the reliability of any numerical approach is significantly impaired by the uncertainties in the measurements of non-linear characteristics of soils, which are at least as large as those concerning their linear characteristics.
Numerical approach remains, of course, of primary importance and interest for theoretical investigations on the physics of site effects. But it also keeps interest and advantages for the practical estimate of amplification factors on specific sites, since the instrumental approach described in section 3.1 may not be always used, for instance in urban areas with weak seismicity (gap areas, or intraplate seismicity zones with large return periods). However, the sensitivity study by Field and Jacob (1993a) draws the attention on the need to perform numerous, redundant geotechnical measurements (which increases the actual cost of numerical estimates).
The interest of methods based on microtremors thus appears very clearly because of their considerable cheapness. The recent developments based on the use of the horizontal to vertical spectral ratio (Nakamura's technique), or on the use or array recordings for determining the velocity profile (Aki's technique), together with the shown reliability of "classical" methods in the very long period range, should boost their use in routine studies outside of Japan, as well as further research on their actual limits: for instance, can the Nakamura's technique provide, or not, quantitative estimates of site amplification factors.
The main lessons about the physics of site effects are i) the progressive reconciliation of seismologists and engineers viewpoints about non-linear effects, and ii) the growing experimental evidences for the engineering importance of the 2D or 3D effects (wave diffraction by surface or subsurface topography). A lot of work (regulatory and research work) remains to be done in order to transfer this knowledge in the routine practice: for instance for the determination of the anchoring peak accelerations in regulatory elastic response spectra for soil and rock sites, but also for a simplified accounting of amplification factors due to surface (or sub-surface) topography in routine studies.

In summary, although significant advances have been achieved recently, many issues remain unsatisfactorily solved, regarding the basic phenomenological understanding of site effects as well as the methodology to follow in order to take them into account in a practical way:

- basic research is needed, with both theoretical and experimental approaches, in order to better understand some particular aspects of site effects: surface topography effects, effects of strong lateral discontinuities, actual importance of non-linearity in sediment response, actual level and effects of differential motion on structures,...
- methodological work is to be done to better assess and compare the respective reliability, cost and interests of the various methods used or proposed to predict site effects.
- at last, some regulatory work is also required so as to better account for site effects in seismic codes and microzoning studies, and especially for the effects of surface topography, strong lateral discontinuities and thin, soft alluvial deposits.

On the other hand however, the extreme importance of site effects in recent damaging earthquakes, calls for special efforts for applying right now, without waiting for results of further research, what we already know regarding site effects by performing "present day" microzoning studies. It is certainly not simple, and it does not limit to technical problems, since the results of such microzoning studies are used in fine by local authorities, city planners, land-use specialists and civil engineers, whose background is very different and for whom the recommendations are therefore to be very clear and sound. Various programs recently launched in several countries should help in clarifying the methodology to be followed and the ultimate goals to be pursued.

ACKNOWLEDGEMENTS

This paper has greatly benefitted from two recently issued documents, the drafts which had been made available by their authors: the "Guide méthodologique pour la réalisation d'études de microzonage" issued by the French Association of Earthquake Engineering, provided by A. Pecker, and the draft report of the TC-4 Committee of the International Society of Soil Mechanics and Foundation Engineering (ISSMFE) entitled "Seismic Zonation on Geotechnical Hazards", kindly made available by M.P. Luong.

REFERENCES

AFPS, 1995. Guidelines for seismic microzonation studies. AFPS / DRM, October 1995, 45 pages.

Aki, K. 1988. Local site effects on strong ground motion. "Earthquake Engineering and Soil Dynamics II - Recent Advances in Ground Motion Evaluation", June 27-30, Park City, Utah.

Aki, K. and K. Irikura, 1991. Characterization and mapping of earthquake shaking for seismic zonation, Proceedings of the Fourth International Conference on Seismic Zonation, August 25-29, Stanford, California, 1, 61-110.

Aki, K., 1957. Space and time spectra of stationary stochastic waves with special reference to microtremors, Bull. Earthq. Res. Inst., 35, 415-456.

Archuleta, R.J., S.H. Seale, P.V. Sangas, L.M. Baker and S.T. Swain, 1992. Garner valley downhole array of accelerometers: instrumentation and preliminary data analysis, Bull. seism. Soc. Am., 82, 1592-1621.

Astroza, M. and J. Monge, 1991. Regional seismic zonation in Central Chile, Proceedings of the Fourth International Conference on Seismic Zonation, August 25-29, Stanford, California, 3, 487-494.

Bard, P.-Y., 1982. Diffracted waves and displacement field over two-dimensional elevated topographies. Geophys. J.R. astr. Soc., 71, 731-760.

Bard, P.-Y., 1993. Discussion session: lessons, issues, needs and prospects, Special Theme session on Turkey Flat and Ashigara Valley experiments, Tenth World Conference on Earthquake Engineering, Madrid, July 10-24, 1992, post conference volume.

Bard, P.-Y., and M. Bouchon, 1985. The two-dimensional resonance of sediment-filled valleys. Bull. seism. Soc. Am., 75, 519-541.

Bard, P.-Y., and J.-P. Mèneroud, 1987. Modification du signal sismique par la topographie. Cas de la vallée de la Roya (Alpes-Maritimes). Bull. liaison Laboratoires des Ponts-et-Chaussées, Numéro spécial "Risques Naturels" 150-151, 140-151 (in French).

Bard, P.-Y, M. Campillo, F.J. Chavez-Garcia and F.J. Sanchez-Sesma, 1988. A theoretical investigation of large- and small-scale amplification effect in the Mexico City valley. Earthquake Spectra, 4-3, 609-633.

Bard, P.-Y., and F.J. Chàvez-Garcia, 1993. On the decoupling of surficial sediments from surrounding geology at Mexico City. Bull. seism. Soc. Am., 83, 1979-1991.

Bard, P.-Y., and A. Wirgin, 1995. Effect of built environment on "free-field" motion for very soft, urbanized, sites, Proceedings of the Third International Conference on Recent Advances in Geotechnical Earthquake Engineering and Soil Dynamics, Saint-Louis (Mo), April 2-7, 1995, II, 549-555.

Boore, D.M., 1972. Note on the effect of topography on seismic SH waves. Bull. seism. Soc. Am., 62, 275-284.

Beresnev, I.A., W.-L. Wen and Y.T. Yeh, 1994. Seismological evidence for nonlinear-elastic ground behavior during large earthquakes, Soil Dyn. and Earthq. Engng, submitted.

Boatwright, J., J. B. Fletcher and T.E. Fumal, 1991a. A general inversion scheme for source, site and propagation characteristics using multiply recorded sets of moderate-sized earthquakes, Bull. seism. Soc. Am., 81, 1754-1782.

Boatwright, J., L.C. Seekins, T.E. Fumal, H-P Liu and C.S. Mueller, 1991b. Ground motion amplification in the Marina district, Bull. seism. Soc. Am., 81, 1980-1997.

Bonamassa, O., and J. E. Vidale, 1991. Directional site resonances observed from aftershocks of the 18 October 1989 Loma Prieta earthquake, Bull. seism. Soc. Am., 81, 1945-1957.

Borcherdt, R.D., 1970. Effects of local geology on ground motion near San Francisco Bay. Bull. seism. Soc. Am., 60, 29-61.

Borcherdt, R.D., and J.F. Gibbs, 1976. Effects of local geological conditions in the San Francisco bay region on ground motions and the intensities of the 1906 earthquake. Bull. seism. Soc. Am., 66, 467-500.

Borcherdt, R.D., C.M. Wentworth, A. Janssen, T. Fumal and J.F. Gibbs, 1991. Methodology for predictive GIS mapping of special study zones for strong ground shaking in the San Francisco bay region, Proceedings of the Fourth International Conference on Seismic Zonation, August 25-29, Stanford, California, 3, 545-552.

Borcherdt, R.D., and G. Glassmoyer, 1992. On the characteristics of local geology and their influence on ground motions generated by the Loma Prieta earthquake in the San Francisco Bay region, California, Bull. seism. Soc. Am., 82, 603-641.

Borcherdt, R.D., 1994. Estimates of site-dependent response spectra for design (Methodology and Justification), Earthquake Spectra, 10-4, 617-653.

Borcherdt, R.D., and C.M. Wentworth, 1995. Strong ground motion by the Northridge earthquake of january 17, 1994: Implications for seismic design coefficients and seismic zonation, Proceedings of the Fifth International Conference on Seismic Zonation, October 17-19, 1995, Nice, France, II, 964-971.

Bouchon, M., 1978. The importance of the surface or interface P wave in near earthquake studies. Bull. seism. Soc. Am., 68, 1293-1311.

Bouchon, M., and J.S. Barker, 1995. Seismic response of a hill: the example of Tarzana, California, submitted to Bull. seism. Soc. Am., April 1995.

Bouchon, M., C.A. Schultz and M. N; Toksöz, 1995. Effect of 3D topography on seismic motion, submitted to J. Geophys. Res, March 1995.

Brambati, A., E. Faccioli, E.B. Carulli, F. Culchi, R. Onofri, S. Stefanini, and F. Ulcigrai, 1980. Studio de microzonizzazione sismica dell'area di Tarcento (Friuli), Edito da Regiona Autonoma Friuli-Venezia-Giulia (in Italian).

Caillot, V., and P;-Y. Bard, 1990. Characterizing site effects for earthquake regulations in the French seismicity context: a statistical analysis. Proceedings of the IXth ECEE, Moscow, Vol. 4-B, 27-36.

Caillot, V., 1992. Quantification statistique et étude expérimentale des mouvements sismiques. Application à l'évaluation du risque. Thèse Université Joseph Fourier de Grenoble, Publication LCPC GT51, 192 pages.

Campbell, K., 1985. Strong motion attenuation relations: a ten-year perspective. Earthquake Spectra, 1 , 759-804.

Celebi, M., 1987. Topographical and geological amplifications determined from strong-motion and aftershock records of the 3 March 1985 Chile earthquake. Bull. seism. Soc. Am., 77, 1147-1157.

Celebi, M., 1995. Northridge (California) earthquake: Unique ground motions and resulting spectral and site effects, Proceedings of the Fifth International Conference on Seismic Zonation, October 17-19, 1995, Nice, France, II, 988-995.

Chang, C.Y., C.M. Mok, M.S. Power, Y.K. Tang, H.T. Tang, and J.C. Stepp, 1991.Development of shear modulus curves based on Lotung downhole ground motion data, Proceedings of the Second International Conference on Recent Advances in Geotechnical Earthquake Engineering and Soil Dynamics, March 11-15, St. Louis, Missouri, 1, 111-118..

Chàvez-Garcia, F.J., 1991. Diffraction et amplification des ondes sismiques dans le bassin de Mexico, Thèse de l'Université Joseph Fourier de Grenoble, 331 pages.

Chàvez-Garcia, F.J., and P.-Y. Bard, 1993a. Gravity waves in Mexico City ? I. Gravity perturbed waves in an elastic solid, Bull. seism. Soc. Am., 83, 1637-1655.

Chàvez-Garcia, F.J., and P.-Y. Bard, 1993b. Gravity waves in Mexico City ? II. Coupling between an elastic solid and a fluid layer, Bull. seism. Soc. Am., 83, 1656-1675.

Chàvez-Garcia, F.J., F.J. Sanchez-Sesma, M. Campillo and P.-Y. Bard, 1994. El terremoto de Michoacan de Septiembre de 1985: Effectos de fuente, trayecto y sitio, Fisica de la Tierra., accepted.

Chàvez-Garcia, F.J., D. Hatzfeld, G. Pedotti and P.-Y. Bard, 1990. An experimental study of site effects near Thessaloniki (Northern Greece). Bull. seism. Soc. Am., 80, 784-806.

Clouteau, D., 1990. Propagation d'ondes dans des milieux hétérogènes, application à la tenue des ouvrages sous séismes, Thèse E.C.P., Paris.

Clouteau, D., D. Aubry et B. Tardieu, 1993. Calculs sismiques tridimensionnels d'un barrage voûte: effets de site et interaction sol-fluide-structure, Troisième Colloque National de Génie Parasismique, organisé par l'AFPS á St-Rémy-lès-Chevreuse (France), 24-26 mars 1993, I, FB 62 - 70.

Cramer, C.H. and C.R. Real, 1991. A statistical analysis of submitted site-effects predictions for the weak motion blind prediction test conducted at the Turkey Flat, USA, site effects test area near Parkfield, California, Proceedings of the Fourth International Conference on Seismic Zonation (Stanford, August 1991), II, 467-474.

Darragh, R.B., and A.F. Shakal, 1991. The site response of two rock and soil station pairs to strong and weak ground motion, Bull. seism. Soc. Am., 81, 1885-1899.

Davis, L.L. and R. West, 1973. Observed effects of topography on ground motion. Bull. seism. Soc. Am., 63, 283-298.

Dobry, R., I. Oweis and A. Urzua, 1976. Simplified procedures for estimating the fundamental period of a soil profile, Bull. seism. Soc. Am., 66, 1293-1321.

Durville, J.-L., J.-P. Mèneroud, P. Mouroux and J.-M. Simon, 1985. Evaluation de l'aléa sismique local - Microzonage, in Genie Parasismique, V. Davidovici ed., Presses des Ponts-et-Chaussées, 239-264.

Duval, A.-M., 1994. Détermination de la réponse d'un site aux séismes à l'aide du bruit de fond: Evaluation expérimentale, Thèse de Doctorat, Paris VI, 265 pages (in French).

Duval, A.-M., P.-Y. Bard, J.-P. Mèneroud and S. Vidal, 1995. Mapping site effects with microtremors, Proceedings of the Fifth International Conference on Seismic Zonation, October 17-19, 1995, Nice, France, II, 1522-1529.

Duval, A.-M., P.-Y. Bard, J.-P. Mèneroud and S. Vidal, 1994. Usefulness of microtremor measurements for site effect studies, Proceedings of the 10th European Conference on Earthquake Engineering, Vienna, Austria, Balkema, Duma Ed., I, 521-528.

ESG 1992, Proceedings of the International Symposium on the effects of surface geology on seismic motion, March 25-27, 1992, Odawara, Japan, edited by the Association for Earthquake Disaster Prevention, Tokyo.

Evernden, J.F., and J.M. Thomson, 1985. Predicting seismic intensities, U.S.G.S. Professional Paper 1360, 151-202.

Faccioli, E., 1991. Seismic amplification in the presence of geological and topographic irregularities, Proceedings of the Second International Conference on Recent Advances in Geotechnical Earthquake Engineering and Soil Dynamics, March 11-15, St. Louis, Missouri, 2, 1779-1797.

Fäh, D., C. Iodice, P. Suhadolc and G.F. Panza, 1993. A new method for the realistic estimation of seismic ground motion in megacities: the case of Rome, Earthquake Spectra, Vol. 9-4, 643-648.

Fäh, D., P. Suhadolc, St. Mueller and G.F. Panza, 1994. A hybrid method for the estimation of ground motion in sedimentary basins: quantitative modeling for Mexico City, Bull. seism. Soc. Am., 84, 383-399.

Field, E.H., K. H. Jacob and S.E. Hough, 1992. Earthquake weak motion estimation: a weak motion case study, Bull. seism. Soc. Am., 82-6, 2283-2307.

Field, E.H., and K. Jacob, 1993a. Monte Carlo simulation of the theoretical site response variability at Turkey Flat, California, given the uncertainty in the geotechnically derived input parameters, Earthquake Spectra, Vol. 9-4, 669-702.

Field, E.H., and K. Jacob, 1993b. The theoretical response of sedimentary layers to ambient seismic noise, Geophysical Res. Letters, 20-24, 2925-2928.

Field, E.H., and K. Jacob, 1995. A comparison and test of various site response estimation techniques, including three that are non reference-site dependent, Bull. seism. Soc. Am., 85, 1127-1143.

Field, E.H., A.C. Clement, K.H. Jacob, V. Aharonian, S.E. Hough, P.A. Friberg, T.O. Babaian, S.S. Karapetian, S.M. Hovanessian and H.A. Abramian, 1995. Earthquake site response in Giumri (formerly Leninakan), Armenia using ambient noise observations, Bull. seism. Soc. Am., 85, 349-353.

Finn, W.D. Liam, 1991. Geotechnical engineering aspects of seismic microzonation, Proceedings of the Fourth International Conference on Seismic Zonation, August 25-29, Stanford, California, 1, 199-250.

Frankel, A., 1993. Three-dimensional simulations of ground motions in the San Bernardino valley, California, for hypothetical earthquakes on the San Andreas fault, Bull. seism. Soc. Am., 83, 1020-1041.

Frankel, A., and J. Vidale, 1992. A three-dimensional simulation of seismic waves in the Santa Clara valley, California, from a Loma Prieta aftershock, Bull. seism. Soc. Am., 82, 2045-2074.

Frankel, A., S. Hough, P. Friberg and R. Busby, 1991. Observations of Loma prieta aftershocks from a dense array in Sunnyvale, California, Bull. seism. Soc. Am., 81, 1900-1922.

Géli, L., Bard, P.-Y., and B. Jullien, 1988. The effect of topography on earthquake ground motion: a review and new results. Bull. seism. Soc. Am., 78, 42-63.

Gilbert, F.H., 1967. Gravitationally perturbed elastic waves, Bull. seism. Soc. Am., 57, 783-794.

Griffiths, D.W., and G.A. Bollinger, 1979. The effect of Appalachian mountain topography on seismic waves. Bull. seism. Soc. Am., 69, 1081-1105.

Graves, R.W., and R.W. Clayton, 1992. Modeling path effects in three-dimensional basin structures. Bull. seism. Soc. Am., 82, 81-103.

Graves, R.W., 1993. Modeling three-dimensional site response in the Marina district basin, San Francisco, California. Bull. seism. Soc. Am., 83, 1042-1063.

Guttierez, C., and S. K. Singh, 1992. A site effect study in Acapulco, Guerrero, Mexico: comparison of results of strong-motion and microtremor data. Bull. seism. Soc. Am., 82, 642-659.

Hartzell, S.H., 1992. Site response estimation from earthquake data. Bull. seism. Soc. Am., 82, 2308-2327.

Hisada, Y., K. Aki and T-L Teng, 1993. 3-D simulations of surface-wave propagation in the kanto sedimentary basin, Japan. Part 2: application of the surface wave BEM. Bull. seism. Soc. Am., 83, 1700-1720.

Hough, S.E., L. Seeber, A. Rovelli, L. Malagnini, A. DeCesare, G. Selveggi and A. Lerner-Lam, 1992. Ambient noise and weak motion excitation of sediment resonances: results from the Tiber Valley, Italy. Bull. seism. Soc. Am., 82, 1186-1205.

ISSMFE, 1994, Manual for zonation on seismic geotechnical hazards, TC4 of ISSMFE (Chairmanship: Prof. K. Ishihara), Japanese Society of Soil Mechanics and Foundation Engineering.

Idriss, I.M., 1990. Response of soft soil during soil earthquakes, Proc. H. Bolton Seed Memorial Symposium, 273-290.

Jongmans, D. and M. Campillo, 1990. The 1983 Liège earthquake: Damage distribution and site effects, Earthquake Spectra, 6-4, 713-737.

Jongmans, D. and M. Campillo, 1993. The response of the Ubaye Valley (France) for incident SH and SV waves: comparison between measurements and modeling, Bull. seism. Soc. Am., 83, 907-924.

Joyner, W.B., and T. Fumal, 1984. Use of measured shear wave-velocity for predicting site effects on strong motion, Proceedings of the Eighth World Conference on Earthquake Engineering, San Francisco, 2, 777-783.

Kagawa, T., S. Sawada and Y. Iwasaki, 1992. On the relationship between azimuth dependency of earthquake ground motion and deep basin structure beneath the Osaka plain, J. Phys. Earth, 40, 73-83.

Kagami, H., S. Okada and Y. Ohta, 1988. Versatile application of dense and precision seismic intensity data by an advanced questionnaire survey, Proceedings of the Ninth World Conference on Earthquake Engineering, Tokyo-Kyoto, 8, 937-942.

Kagami, H., S. Okada, N. Takai and H. Murakami, 1995. Seismic zonation maps of Sapporo metropolitan area, Northern Japan, derived from dense questionnaire surveys of seismic intensity, Proceedings of the Fifth International Conference on Seismic Zonation, October 17-19, 1995, Nice, France, II, 1043-1050.

Kanai, K., 1983. Engineering seismology,University of Tokyo Press, Tokyo, 251 pages.

Kataoka, S., M. Matsui and T. Sato, 1994. Using the microtremors to estimate the natural frequency of the site: A case study at Kuno, Ashigara Valley blind prediction site (KS2) in Japan, Proceedings of the 10th European Conference on Earthquake Engineering, Vienna, Austria, Balkema, Duma Ed., I, 83-88.

Kawase, H., and K. Aki, 1990. Topography effect at the critical SV wave incidence: possible explanation of damage pattern by to the Whittier-Narrows, California, earthquake of 1 October 1987, Bull. seism. Soc. Am., 80, 1 - 22.

Kinoshita, S., H. Fujiwara, T. Mikoshiba and T. Hoshino, 1992. Secondary Love waves observed by a strong motion array in the Tokyo Lowlands, Japan, J. Phys. Earth, 40, 99-116.

Kobayashi, K., 1980. A method for presuming deep ground soil structures by means of longer period microtremors, Proc. of the 7th WCEE, Sept. 8-13, Istanbul, Turkey, 1, 237-240.

Koyanagi, S., K. Mayeda, and K. Aki, 1992. Frequency-dependent site amplification factors using the S-wave coda for the island of Hawaii, Bull. seism. Soc. Am., 82, 1151-1185.

Kudo, K., 1995. Practical estimates of site response, Proceedings of the Fifth International Conference on Seismic Zonation, October 17-19, 1995, Nice, France, III, 28 pages.

Lachet, C., and P.-Y. Bard, 1994. Numerical and theoretical investigations on the possibilities and limitations of the "Nakamura's" technique, Journal of Physics of the Earth, 42, 377-397.

Langston, C.A., 1979. Structure under Mount Rainier, Washington, inferred from teleseismic body waves, J. Geophys. Res., 84, 4749-4762.

Lebrun, B., 1993. Effets de site: Etude de deux configurations particulières, Diplôme d'Ingénieur EOPG, Université Louis Pasteur, Strasbourg, 108 pages (in French).

Lermo, J., and F.J. Chavez-Garcia, 1993. Site effect evaluation using spectral ratios with only one station, Bull. seism. Soc. Am., 83, 1574-1594.

Lermo, J., and F.J. Chavez-Garcia, 1994. Are microtremors useful in site response evaluation ?, Bull. seism. Soc. Am., in press.

Lermo, J.,1992. Observaciones de microtremores en Mexico y su aplicacion en la ingenieria sismica. MS Thesis, UNAM, 75 pp.

Lermo, J., M. Rodriguez and S.K. Singh, 1988. Natural periods of sites in the valley of Mexico from microtremor measurements and strong motion data. Earthquake Spectra, 4-4, 805-814.

Levret, A., C. Loup and X. Goula, 1986. The Provence earthquake of June 11th, 1909 (France):

New assessment of near-field effects. Proceedings of the 8th European Conference of Earthquake Engineering, Lisbon, September 1986, Vol. 2, p. 4.2.79.

Liu, H-P, R.E. Warrick, R.E. Westerlund, E.D. Sembera and L. Weinnerberg, 1992. Observation of local site effects at a downhole-and-surface station in the Marina district of San Francisco, Bull. seism. Soc. Am., 82, 1563-1582.

Lomnitz, C., 1990. Mexico 1985: the case for gravity waves, Geophys. J. Int., 102, 569-572.

Lomnitz, C., 1991. On the transition between Rayleigh waves and gravity waves, Bull. seism. Soc. Am., 81, 273-275.

Malagnini, L., A. Rovelli, S.E. Hough and L. Seeber, 1993. Site amplification estimates in the Garigliano valley, central Italy, based on dense array measurements of ambient noise, Bull. seism. Soc. Am., 83, 1744-1744.

Mayeda, K., S. Koyanagi and K. Aki, 1991. Site amplification from S-wave coda in the Long Valley caldera region, California, Bull. seism. Soc. Am., 81, 2194-2213.

Medvedev, J., 1962. Engineering seismology, Science Academy Press, Moscow..

Midorikawa, S., 1992. A statistical analysis of submitted predictions for the Ashigara Valley blind prediction test, ESG 1992, Proceedings of the International Symposium on the effects of surface geology on seismic motion, March 25-27, 1992, Odawara, Japan, II, 65-77.

Moczo, P., and P.-Y. Bard, 1993. Wave diffraction, amplification and differential motion over strong lateral discontinuities, Bull. seism. Soc. Am., 83, 85-106.

Mosessian, T.K., and M. Dravinski, 1990. Amplification of elastic waves by a three-dimensional valley. Part 1: steady-state response, Earthq. Eng. Struct. Dyn., 19, 667-680.

Mosessian, T.K., and M. Dravinski, 1992. A hybrid approach for scattering of elastic waves by three-dimensional irregularities of arbitrary shape, J. Phys. Earth, 40, 241-262.

Murphy, J.R., A.H. Davis and W.L. Weaver, 1971. Amplification of seismic body waves by low-velocity surface layers. Bull. seism. Soc. Am., 61, 109-146.

Nakamura, Y., 1989. A method for dynamic characteristics estimation of subsurface using microtremor on the ground surface. QR of R.T.R., 30-1.

Nechtschein, S., P.-Y. Bard, J.-C. Gariel, J.-P. Mèneroud, P. Dervin, M. Cushing, B. Gaubert, S. Vidal and A.-M. Duval, 1995. A topographic effect study in the Nice region, Proceedings of the Fifth International Conference on Seismic Zonation, October 17-19, 1995, Nice, France, II, 1067-1074.

Nogoshi, M. and T. Igarashi, 1971. On the amplitude characteristics of microtremor (Part 2), Jour. seism. Soc. Japan, 24, 26-40 (in Japanese with English abstract)

Ohmachi, T., Y. Nakamura, and T. Toshinawa, 1991. Ground motion characteristics in the San Francisco Bay area detected by microtremor measurements, Proceedings of the Second International Conference on Recent Advances in Geotechnical Earthquake Engineering and Soil Dynamics, March 11-15, St. Louis, Missouri, 1643-1648.

Ohori, M., K. Koketsu and T. Minami, 1992. Seismic responses of three-dimensionally

sediment-filled valleys due to incident plane waves, J. Phys. Earth, 40, 209-222.

Ordaz, M., and E. Faccioli, 1994. Site response analysis in the Valley of Mexico: selection of input motion and extent of nonlinear soil behavior, Earthq. Eng. and Struct. Dyn., submitted.

Paolucci, R., M.M. Suarez, and F.J. Sanchez-Sesma, 1992. Fast computation of SH seismic response for a class of alluvial valleys, Bull. seism. Soc. Am., 82, 2075-2086.

Pedersen, H., F.J. Sanchez-Sesma and M. Campillo, 1994a. Three-dimensional scattering by two-dimensional topographies, Bull. seism. Soc. Am., in press.

Pedersen, H., B. LeBrun, D. Hatzfeld, M. Campillo and P.-Y. Bard, 1994. Ground motion amplitude across ridges, Bull. seism. Soc. Am., in press.

Pei, D., and A. Papageorgiou, 1994. Study of the response of cylindrical alluvial valleys of arbitrary cross-section to obliquely incident seismic waves using the discrete wavenumber boundary element method, Soil Dyn. and Earthq. Engng, in press.

Phillips, S.W., and K. Aki, 1986. Site amplification of coda waves from local earthquakes in central California. Bull. seism. Soc. Am., 76, 627-648.

Phillips, S.W., S. Kinoshita and H. Fujiwara, 1993. Basin-induced Love waves observed using the strong motion array at Fuchu, Japan. Bull. seism. Soc. Am., 83, 64-84.

Rial, J.A., and H. Ling, 1992. Theoretical estimation of the eigenfrequencies of 2-D resonant basins: numerical computations and analytic approximations to the elastic problem, Bull. seism. Soc. Am., 82, 2350-2367.

Rodriguez, J.L., J. Ramos and G. Macedo, 1988. Respuesta sismica de un estrato limitado por una pared vertical, Sismodinamica (in Spanish).

Rogers, A.M., L.J. Katz and T.J. Bennett, 1974. Topographic effect on ground motion for incident P waves: a model study. Bull. seism. Soc. Am., 64, 437-456.

Rovelli, A., S.K. Singh, L. Malagnini, A. Amato and M. Cocco, 1991.Feasibility of the use of microtremors in estimating site response during earthquakes: some test cases in Italy, Earthquake Spectra, 7-4, 551-561.

Sanchez-Sesma, F.J., 1983. Diffraction of elastic waves by three-dimensional surface irregularities, Bull. seism. Soc. Am., 73, 1621-1636.

Sanchez-Sesma, F.J., 1990. Elementary solutions for the response of a wedge-shaped medium to incident SH and SV waves. Bull. seism. Soc. Am., 80, 737-742.

Sanchez-Sesma, F.J., and M. Campillo, 1990. Diffraction of P, SV and Rayleigh waves by topographic features: a boundary integral formulation. Bull. seism. Soc. Am., 80, 2234-2253.

Seed, H.B., C. Ugas and J. Lysmer, 1976. Site-dependent spectra for earthquake resistant design. Bull. seism. Soc. Am., 66, 221-243.

Seed, H.B., and I.M. Idriss, 1983. Ground motion and soil liquefaction during earthquakes. Earthquake Engineering Research Institute, El Cerrito, California.

Seligman, T.H., J.M. Alvarez-Tostado, J.L. Mateos, J. Flores and O. Novaro, 1989. Resonant

response models for the Valley of Mexico - I: the elastic inclusion approach. Geophys. J. Int., 99, 789-799.

Shiono, K., Y. Ohta and K. Kudo, 1979. Observation of 1 to 5 sec microtremors and their applications to earthquake engineering, Part VI: existence of Rayleigh wave components, Jour. seism. Soc. Japan, 32, 115-124 (in Japanese with English abstract)

Sills, L., 1978. Scattering of horizontally polarized shear waves by surface irregularities. Geophys. J. R. astr. Soc., 54, 319-348.

Silva, W., 1991. Site geometry and global characteristics, in Proceedings of the NSF/EPRI workshop on dynamic soil properties and site characterization, EPRI NP-7337, 1, 6.1-6.80.

Singh, S.K., J. Lermo, T. Dominguez, M. Ordaz, J.M. Espinosa, E. Mena and R. Quaas, 1988. The Mexico earthquake of September 19, 1985 - A study of amplification of seismic waves in the valley of Mexico with respect to a hill zone site, Earthquake Spectra, 4, 653-674.

Siro, L., 1982. Southern Italy November 23, 1980 earthquake. Proceedings of the 7th European Conference on Earthquake Engineering, Athens, Greece, September 20-25, 1982.

Smith, W.D., 1975. The application of finite element analysis to body wave propagation problems. Geophys. J., 42, 747-768.

Steidl, J.H., 1993. Variation of site response estimates at the UCSB dense array of portable accelerometers, Earthquake Spectra, 9-2, 289 - 302.

Stephenson, W.R., 1991, Cellular normal modes: an explanation of alluvium response to earthquakes, Proceedings of the Second International Conference on Recent Advances in Geotechnical Earthquake Engineering and Soil Dynamics, March 11-15, St. Louis, Missouri, 2, 1155-1165.

Stephenson, W.R., and P.R. Barker, 1991, Results from the Pukehou array, Proceedings of the Pacific Conference on Earthquake Engineering,, New-Zealand, 20-23 November, 229-238.

Su, F., K. Aki, T. Teng, Y. Zeng, S. Koyanagi and K. Mayeda, 1992. The relation between site amplification factor and surficial geology in central California, Bull. seism. Soc. Am., 82, 580-602.

Theodulidis, N. and P.-Y. Bard, 1994. Horizontal to vertical spectral ratio and geological conditions: an analysis of strong motion data from Greece and Taiwan (SMART1), Soil Dyn. and Earthq. Engng, in press.

Theodulidis, N., V. Caillot and P.-Y. Bard, 1995a. Band-limited duration and spectral energy in Greece: Empirical dependence on frequency, magnitude, distance, site conditions, and comparison with relevant relations in Italy, submitted to Geophys. J. Int..

Theodulidis, N., R.J. Archuleta, P.-Y. Bard, and M. Bouchon, 1995b. Horizontal to vertical spectral ratio and geological conditions: the case of Garner Valley downhole array in southern California, Bull. seism. Soc. Am., in press.

Trifunac, M.D., and E.I. Novikova, 1994. State of the art review on strong motion duration, Proceedings of the 10th European Conference on Earthquake Engineering, Vienna, Austria, I, 131-140.

Scientific Technical Report STR 95/TK
DOI: 10.2312/GFZ.b103-95tk7

Tucker, B.E., J.L. King, D. Hatzfeld and I.L. Nersesov, 1984. Observations of hard rock site effects, Bull. seism. Soc. Am., 74, 121-136.

Uebayashi, H., M. Horike and Y. Takeuchi, 1992. Seismic motion in a three-dimensional arbitrarily-shaped sedimentary basin due to a rectangular dislocation source, J. Phys. Earth, 40, 223-240.

Vidale, J.E., O. Bonamassa and H. Houston, 1991. Directional site resonances observed from the 1 October 1987 Whittier Narrows, California, earthquake, and the 4 October aftershock, Earthquake Spectra, 7-1, 107-125.

Wen, K.-L., H.-Y. Peng and L.-F. Liu, 1995. Basin effects analysis from a dense strong motion observation network, Earthq. Engng. and Struct. Dyn., 24, 1069-1083.

Yomogida, K., and J.T. Etgen, 1993. 3-D wave propagation in the Los Angeles basin for the Whittier-Narrows earthquake, Bull. seism. Soc. Am., 83, 1325-1344.

Yamanaka, H., M. Dravinski and H. Kagami, 1993. Continuous measurements of microtremors on sediments and basements in Los Angeles, California, Bull. seism. Soc. Am., 83, 1595-1609.

Zahradnik, J., P. Moczo and F. Hron, 1993. Testing four elastic finite-difference schemes for behavior at discontinuities, Bull. seism. Soc. Am., 83, 107-129.

Zahradnik, J. and L. Urban, 1984. Effect of a simple mountain range on underground seismic motion, Geophys. J. R. Astr. Soc., 79, 167-183.

Zhenpeng, L.Y., L. Baipo and Y. Yifan, 1980. Effect of three-dimensional topography on earthquake ground motion. Proceedings of the 7th World Conference on Earthquake Engineering, Vol. 2, Istanbul (Turkey), September 8-13, 1980.

Exercise on ground shaking site effects

Pierre-Yves Bard

Laboratoire Central des Ponts-et-Chaussées and Observatoire de Grenoble
LGIT/IRIGM - BP 53 X - 38041 Grenoble Cedex - FRANCE
Tel. +33 44 51 44 87, Fax +33 44 51 44 22, Email: bard@lgit.observ-gr.fr

San Francisco bay area comprises 3 main geological units, having the following mechanical characteristics:

	ρ (g/cm3)	β(km/s)	Qs
1 - Bay Mud	1.5	0.10	10.
2 - Alluvium	2.0	0.30	25.
3 - Franciscan bedrock	2.4	1.20	200.

1. Use of empirical correlations

1.1 On the basis of the sole geology, estimate the local intensity increments for each of these geological units (use Table II).

1.2 Still on the basis of the sole geology, estimate the relative amplification factor for each of these geological units (use Table III).

2. Estimation of natural periods of the ground

Compute or estimate the natural periods of the ground in the following cases:

2.1 The surficial formation is the alluvium cover, directly underlain by franciscan bedrock; consider 4 different thicknesses for alluvium: h_2 = 15, 25, 50 and 75 m.

2.2 Bay mud is resting directly on alluvium, whose thickness is large enough to be considered as infinite. Consider also three thickness values for bay mud: h_1 = 5 m, 10 m, and 25 m.

2.3 The soil column comprises the three formations, with thicknesses h_1 for bay mud (surficial deposit), and h_2 for alluvium (intermediate deposit); the underlying bedrock is thus made of Franciscan bedrock. Use methods listed in Table I to estimate the natural period of the ground in the following cases: h_1 = 15 m, h_2 = 15 m;
h_1 = 5 m, h_2 = 75 m;
h_1 = 25 m, h_2 = 15 m;
h_1 = 25 m, h_2 = 75 m.

Comment the results.

3. Estimation of surface amplification

3.1 Compute the maximum spectral amplification for the configurations considered in sections 2.1 and 2.2; compute also the maximum spectral amplification for Bay mud lying directly on Franciscan bedrock.

3.2 Use now the average relationships given in Figure 23 to obtain amplification estimates at free surface. Are these estimates consistent with results obtained in 3.1? Comment the differences.

3.3 What kind of technique could you use to obtain estimate of surface amplification for the configurations considered in section 2.3?

4. Discussion

4.1 The enclosed Figure displays several accelerometric recordings obtained at comparable epicentral distances on different kinds of soils, during the Loma Prieta (1989, M = 7.1, D = 80 km) earthquake: are these observations consistent with the estimates obtained in previous sections?

4.2 The San Francisco area had already been shaken in 1957 by a "small" local event (magnitude 5.4), located at an epicentral distance in the range 10-20 km. The recordings obtained during that event displayed exactly the opposite of 1989 observations, i.e., peak acceleration was reduced on soft soils. Can you find an explanation for that apparent inconsistency?

Exercise on the resonance of soft soils

Pierre-Yves Bard

Laboratoire Central des Ponts-et-Chaussées and Observatoire de Grenoble
LGIT/IRIGM - BP 53 X - 38041 Grenoble Cedex - FRANCE
Tel. +33 44 51 44 87, Fax +33 44 51 44 22, Email: bard@lgit.observ-gr.fr

1. Reflection / Transmission: Let us consider two elastic, homogeneous half-spaces (1 on top, and 2 on bottom) separated by an horizontal interface at z = 0. Each of them is characterized by its density ρ_i and its S wave velocity β_i *(i = 1, 2)*. This structure is impinged from below (medium 2) by a stationary, vertically incident plane SH wave, with the associated (unit) displacement

$$v_2^0 = e^{i\omega t}\, e^{i\gamma_2 z}$$

where $\gamma_2 = \omega / \beta_2$ and $\omega = 2\pi f$, f is the frequency of the input plane wave, and the vertical axis z is oriented *downward.*

a) Compute the amplitude T_{21} of the transmitted wave (in medium 1), and the amplitude R_{22} of the reflected wave (in medium 2). What are their range of variations when the impedance contrast C ($C = \rho_2\ \beta_2 / \rho_1\ \beta_1$) varies from 1 to + ∞, then from 1 to 0?

b) Compute in the same way the R_{11} amplitude of the upward reflected wave when the incoming wave is a downgoing vertical plane wave in medium 1 (i.e., when $v_1^0 = e^{i\omega t}\, e^{-i\gamma_1 z}$)

2. Multiples: Let us consider now that medium 1 is indeed a horizontal (elastic, homogeneous) *layer* with a thickness h (surface at *z = -h*). How is the transmitted wave of case 1a affected?

a) Find a formula allowing to compute the amplitude and phase of all the multiples in medium 1, as a function of T_{21} et R_{11}.

b) Compute the surface displacement *(z = -h)* associated with the direct wave and each of these multiples. *[Do not forget i) the free surface effects and ii) the phase terms linked with the wave propagation, i.e., the $e^{\pm i\gamma_1 z}$ dependence]*

c) Compute similarly the displacement at the interface (i.e., at *z = 0*) for the direct wave and each multiple.

3. Resonance: Compute the total displacement resulting from the interferences between all these different waves (the direct one and the multiples), and show they can be written:

$$v_s = v_1(z=-h) = 2\, e^{i\omega t}\, e^{-i\gamma_1 h}\, \frac{2C}{C+1}\, \frac{1}{1-x} \qquad (1)$$

$$v_b = v_1(z=0) = e^{i\omega t}\, \frac{2C}{C+1}\, \frac{1 + e^{-2i\gamma_1 h}}{1-x} \qquad (2)$$

where: $x = e^{-2i\gamma_1 h}\,(1-C)/(1+C)$ and $\gamma_1 = \omega / \beta_1$

4. Amplification: Compute the values of v_s and v_b for different values of the frequency f:
$f = 0$, $f = \beta_1 / 4\ h$, $f = \beta_1 / 2\ h$, $f = 3\ \beta_1 / 4\ h$

5. Damping: Let us now introduce damping in the surface layer (1) through the damping coefficient $\zeta_1 = 1/(2Q_1)$. In this simple case of vertically propagating waves, it may be done by replacing the "elastic" vertical wavenumber $\gamma_1 = \omega / \beta_1$ by an "inelastic" wavenumber

$$\gamma_{1,d} = \omega / \beta_1 \ (1 - i\ \zeta_1).$$

Under such assumptions, derive the following formulae for the moduli of v_s and v_b :

$$| v_s | = 2\ (1 + r)\ [\ \eta / (\ 1 + 2\eta\ r \cos\varphi\ + \eta^2\ r^2\ )\ ]^{1/2} \qquad (3)$$

$$| v_b | = (1 + r)\ [(\ 1 + 2\eta\ \cos\varphi\ + \eta^2\ ) / (\ 1 + 2\eta\ r \cos\varphi\ + \eta^2\ r^2\ )]^{1/2} \qquad (4)$$

with: $r = (C\text{-}1) / (C + 1)$; $\varphi = 2\ \omega\ h\ /\beta_1$; $\eta = e^{-\varphi\zeta 1}$

6. Reference site: Compute $| v_s |$ and $| v_b |$ at the fundamental frequency f_0 ($= \beta_1 / 4\ h$), firstly without attenuation, and secondly with attenuation.
When $\pi\zeta_1$ is small compared with 1, derive the following first order formulae:

$$| v_s (f_0) | \approx 2\ [\ 1 / C\ + 0.5\ \pi\zeta_1\ ]^{-1} \qquad (5)$$

$$| v_b (f_0) | \approx \pi\zeta 1\ .\ C / [\ 1\ + 0.5\ (C\text{-}1)\ \pi\zeta 1\ ] \qquad (6)$$

From these formulae, discuss the respective advantages and shortcomings of the 2 different experimental methods to estimate the surface amplification : comparing the surface motion on soft soils with *i)* the surface motion of a nearby rock outcrop, and *ii)* the motion at depth recorded by a down-hole instrument located just below the surface instrument, near to the rock-sediment interface.

7. Strains: For the particular case $\zeta 1 = 0$ and $f = f_0 = \beta_1 / 4\ h$, derive the *(very simple)* formulae describing the dependence of displacement as a function of depth in the surface layer (between $z = -h$ and $z = 0$).
From this expression, derive

a) the average motion v_{moy} of the whole surface layer, as a function of the surface motion $| v_s |$

b) the strain $\varepsilon = 0.5\ \partial v / \partial z$. For which depth is it maximum?

8. Non-linear effects: The shear modulus G_1 and the damping ζ_1 in the surface layer are now assumed to depend on the strain level ε according to the following relationship:

$$G_1 = G_0\ \ \varepsilon_r / (\ \varepsilon + \varepsilon_r\ ) \quad \text{and} \quad \zeta_1 = \zeta_\alpha\ \varepsilon / (\ \varepsilon + \varepsilon_r\ )$$

where ε_r is the strain level for which the shear modulus is reduced to half its initial, small strain, "elastic" value G_0 (and correlatively, the damping has reached half its final, large strain value ζ_α).
What is the maximum shear stress t_{max} that may be reached in the surface layer ?
Estimate the shear stress at the bottom of the surface layer, as a function of the average acceleration a_{moy} of the whole surface layer.
Denoting α the ratio between the maximum (surface) acceleration a_{max} and the "average" acceleration a_{moy}, derive the following formula showing the existence of an upper acceleration limit:

$$a_{max} \leq \alpha\ \beta_{10}^2\ \varepsilon_r\ / h$$

where β_{10} is the low strain shear velocity in surface layer.
From 7a, do you think that the assumption $\alpha < 2$ is a reasonable one?

9. Numerical applications: Compute the peak surface spectral amplifications for the "linear elastic" case (corresponding to the case $\zeta_1 = 0$ and $\varepsilon \prec \varepsilon_r$), the "linear viscoelastic" case (corresponding to $\zeta_1 \neq 0$ and $\varepsilon \prec \varepsilon_r$), as well as the maximum possible surface accelerations ("non-linear" case) for the corresponding sets of values:

Case	C	β_{10}	ζ_1	γ_r	h
1	2	200	0.02	$5.\ 10^{-4}$	40
2	5	200	0.02	$5.\ 10^{-4}$	40
3	10	200	0.02	$5.\ 10^{-4}$	40
4	10	200	0.05	$5.\ 10^{-4}$	40
5	10	200	0.02	$5.\ 10^{-4}$	10
6	10	80	0.02	$5.\ 10^{-3}$	40
7	10	200	0.02	$5.\ 10^{-3}$	10

INDUCED EFFECTS (LIQUEFACTION AND SLOPE INSTABILITIES): BASIC PHYSICAL PHENOMENA AND ESTIMATION METHODS FOR MICROZONING STUDIES

Pierre-Yves Bard

Laboratoire Central des Ponts-et-Chaussées and Observatoire de Grenoble
LGIT/IRIGM - BP 53 X - 38041 Grenoble Cedex - FRANCE
Tel. +33 44 51 44 87, Fax +33 44 51 44 22, Email: bard@lgit.observ-gr.fr

1. INTRODUCTION

Since the observations made during the Chile (1960), Niigata, Japan (1964) and Alaska (1964) earthquakes, soil liquefaction has been identified as the underlying phenomenon for many ground failures, settlements, and lateral spreads, which are a major cause of damage to soil structures, lifeline facilities and building foundations in many events. It is now recognized as a potential threat to the integrity of structures and facilities during future earthquakes, and the assessment of liquefaction potential has become one of the most important goals of seismic microzonation.

In other respects, failures of natural slopes during earthquakes have been observed since very long ago, and are also recognized as a potential threat for structures built on or in the vicinity of slopes. The scale of those earthquake triggered, natural slope failures may in some cases be huge enough to devastate entire villages or towns, as it was the case in 1970 at Yungay (Peru); but for smaller scale phenomena may also affect man-made slopes, and cause serious problems to the functions of soil structures.

These two different kinds of "geotechnical", earthquake-triggered phenomena are often called "induced effects"; the assessment of the corresponding hazard for a given site involves the combination of two factors: the first one is a geotechnical factor, characterizing the *susceptibility* of the site to the phenomenon, while the second one is simply related to the amplitude of the triggering event, i.e., the seismic hazard, characterizing the *opportunity* for such phenomena to occur. Since the latter is presented in other lectures of the same course, the present text will mainly focus on the former factor; moreover, considering the seismological background of the participants, this presentation will be limited to basic, simple considerations, since further developments would probably require a deeper background in fundamentals of geotechnics.

This presentation is decoupled in two main parts: the first one concerns liquefaction, while the second one concerns slope instabilities. In each case, the underlying physical phenomena are first, briefly, described, together with the main parameters that control them; then are presented some simple methods to estimate first the susceptibility of a given site to liquefaction (section 2) or slope instabilities (section 3), then the actual potential for such hazards given the expected level of earthquake loading. Finally, conclusions are drawn in section 4 as to the most relevant ways to account for such induced effects in the practice of microzoning studies.

2. LIQUEFACTION

2.1 Fundamentals

Soil liquefaction is a physical phenomenon characterized by a complete loss of shear resistance. It is basically a result of a rise in pore pressure caused by cyclic deformation: when a granular, loose material such as sand is shaken, it undergoes a general and rapid compaction; when this material is saturated - in other words located beneath the ground water table -, this compaction results in a quick rise of the pore pressure u; since the shear resistance S is directly and simply related to the effective stress $\sigma' = \sigma - u$, especially in cohesionless materials such as sands (see Figure 1), liquefaction will occur when the rise in pore pressure leads to a vanishing of the effective stress.
As a consequence of this physical process, the main geological formations at risk are young, poorly consolidated deposits such as alluvial or littoral formations, and also man-made land fills. The deformations associated with liquefaction encompass a very wide range of values, from slight settlements when the liquefaction is limited to rather deep, discontinuous sand lenses having a small lateral extent, to huge lateral displacements and vertical disruptions when the shaking is strong and the liquefying layer has a great lateral extent, and/or a large thickness.
The main damaging consequences of liquefaction are essentially two: the loss of soil bearing capacity below foundations (as was the case in Niigata, Japan, in 1964), and the sub-horizontal sliding occuring on quasi-flat surfaces with no lateral abutment (river banks for instance, as was experienced in Chile in 1960) (Figure 2). An additional effect which may cause significant damage to some particular structures is settlement.

Such a phenomenon may be reproduced in laboratory conditions using triaxial cyclic apparatus and cylindrical samples of soils: for a given confining pressure, and a given initial pore pressure, the sample is subjected to cyclic vertical compressions and extensions with a given amplitude, while both the axial deformation and the pore pressure are monitored. After some cycles (the number N of which depends on soil characteristics, initial pore pressure, confining pressure, and cyclic stress), a simultaneous rise in pore pressure and axial deformation is observed, leading to liquefaction (Figure 3). Liquefaction is generally said to occur when this axial deformation reaches a value of 2.5 to 5 %, and characterized by the two parameters N (number of cycles before liquefaction), and the ratio of the cyclic shear stress τ to the effective initial vertical stress σ'_v. Repeating similar experiments with other initial conditions and different cyclic stress amplitude allows to fully characterize the susceptibility of soil to liquefaction (Figure 4). This kind of experimentation, however, is expensive (cyclic triaxial apparatus are sophisticated instruments), and uneasy (it is very difficult to obtain undisturbed samples especially in cohesionless materials, while reconstructing homogeneous samples for given initial conditions requires much time and care). As a consequence, it is necessary to find some other, simpler ways to characterize soil susceptibility to liquefaction, especially for microzoning studies where large areas are to be investigated, and rather few data and small budgets are available.

The occurrence of liquefaction stems from the combination of two factors:
- an intrinsic one, which characterizes the propension of a given soil sample or site to liquefy, and which is called liquefaction *susceptibility*;
- an external one, which characterizes the loading action, in relation with ground motion; it is often referred to as liquefaction *opportunity*, which represents the ability of a given earthquake to cause liquefaction at a given distance from the source. Liquefaction opportunity maps thus consider liquefaction in the most susceptible soils.

LIQUEFACTION

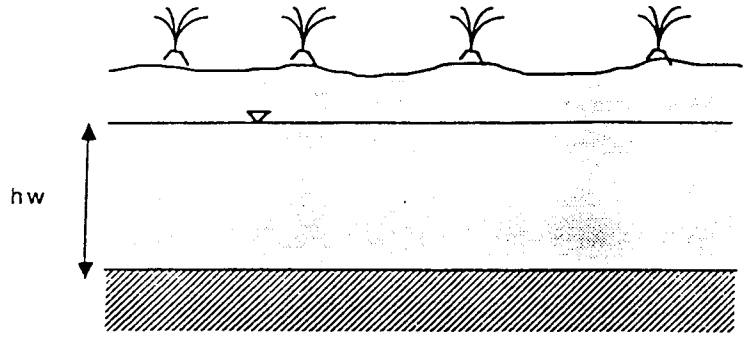

cyclical shear

⇒ compaction of grains

⇒ pore pressure (u) increases

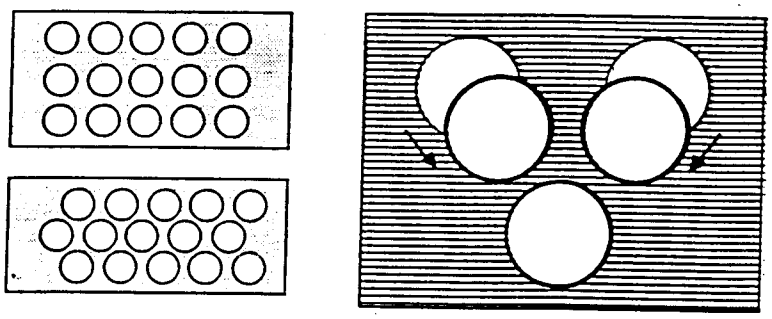

$$S = C + (\sigma - u) \, tg \, \phi$$

si c = 0 ⟶ $S = (\sigma - u) \, tg \, \phi$

si u = σ ⟶ $S = 0$

⇒ effective stress decay

⇒ shear strength decay

($\tau_{max} = \sigma' . tg\phi'$)

Figure 1 : *Principle of soil liquefaction*

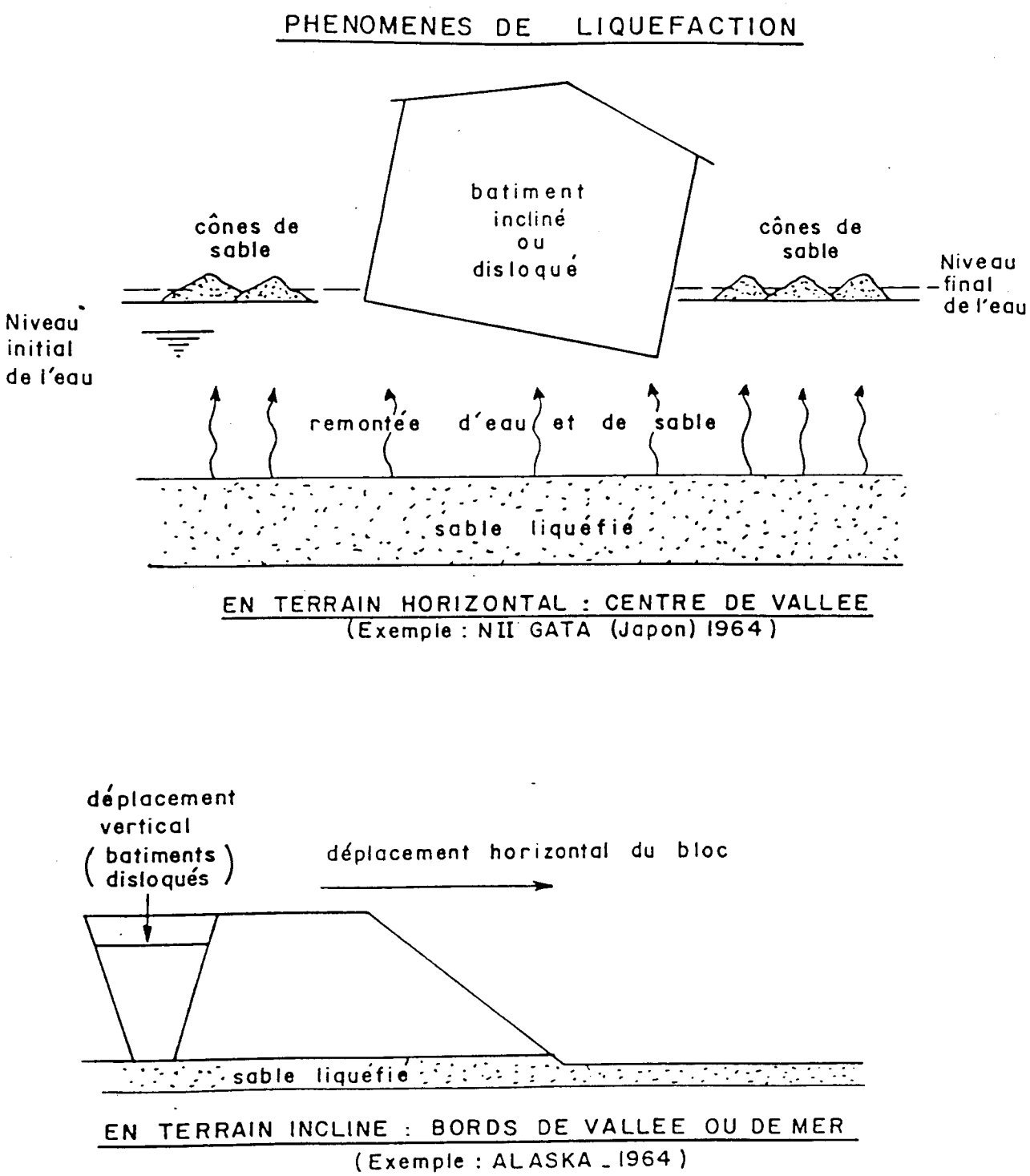

Figure 2 : *Damaging effects of soil liquefaction. a) Loss of bearing capacity of foundations. b) Lateral spread and ground disruption.*

Scientific Technical Report STR 95/TK
DOI: 10.2312/GFZ.b103-95tk7
GeoForschungsZentrum Potsdam

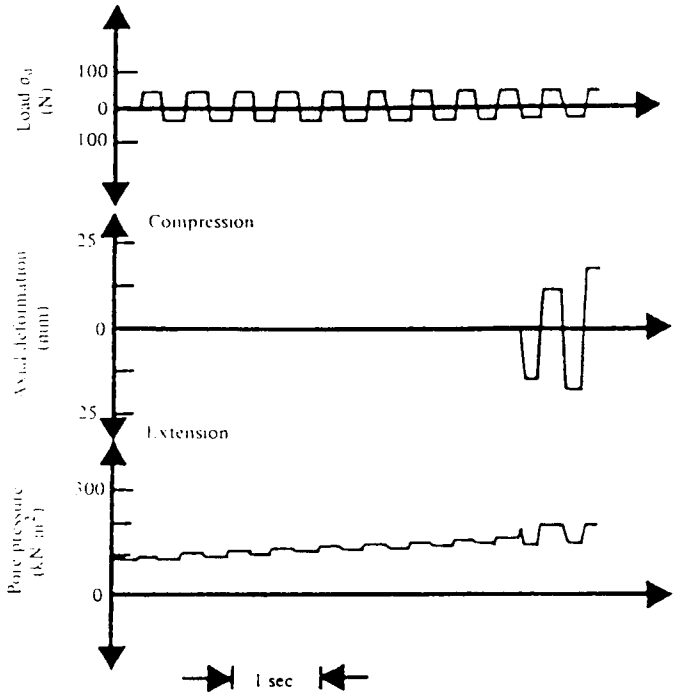

Figure 3 : *Time domain evolution of main soil parameters during a typical cyclic triaxial test for liquefaction studies. a) Cyclic stress as a function of time. b) Axial deformation. c) Pore pressure.*

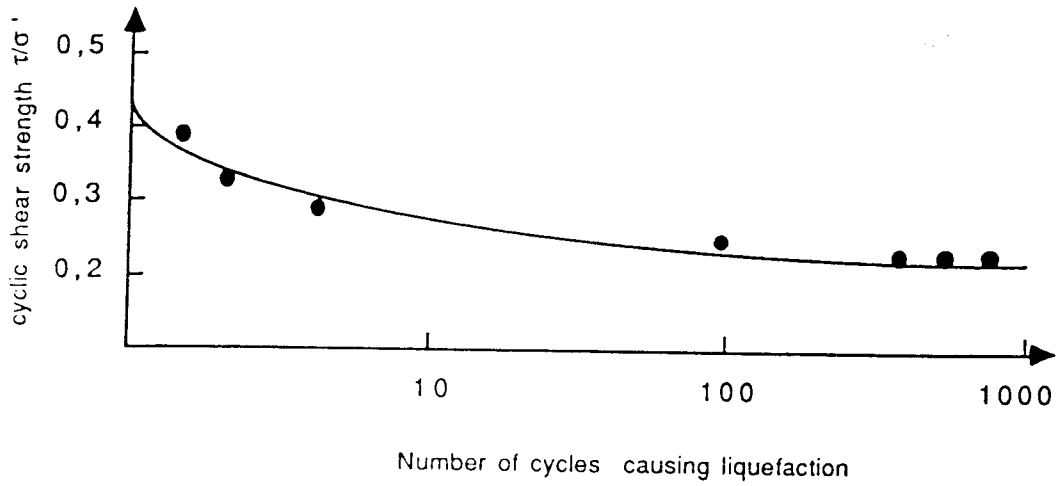

Figure 4 : *An example of results of laboratory tests on liquefaction potential: variations of number of cycles leading to liquefaction (N, abscissa) with cyclic deviatoric stress (τ / σ', ordinate) for a given initial condition.*

The result of the combination of these two factors for a given site, which is the actual liquefaction hazard, is often called the liquefaction *potential.*

2.2 Characterizing liquefaction susceptibility

2.2.1 Main mechanical parameters

From the mechanism briefly described in section 2.1, it follows that the liquefaction susceptibility depends of various soil parameters, the main of which are summarized below.

- *relative density*: the denser the sand, the lower its susceptibility. It is harder to compact an already consolidated granular material, and therefore pore pressure rise is much smaller. This is confirmed in triaxial experiments, as displayed in Figure 5.
- *confining pressure*: the more confined the sand, the lower its susceptibility. A larger pore pressure rise (i.e., a larger number of deformation cycles), is required to balance a larger initial effective stress. In other words, the deeper the sand, the less susceptible it is to liquefaction.
- *overconsolidation ratio*: the more consolidated the soil, the lower its susceptibility. This is just a combination of the two previous factors. This is confirmed in triaxial experiments, as displayed in Figure 6.
- *cohesion / granulometric curve*: the more cohesive the soil, the lower its susceptibility. If the soil has a residual shear strength for zero effective stress, a larger pore pressure rise is required. This results in the fact that only granular material having a low fine contents can liquefy (Figure 7).

2.2.2 Yes / No characterization

It is not always possible to measure the above mentioned mechanical parameters; indeed it is very rare. So more simple characterizations have been looked for, based on routine parameters broadly used in geotechnical engineering: soil granulometry for granular soils (gravels, sands, silts and silty clays), liquidity limits and plasticity index for clayey soils.
Statistical studies on liquefied and non-liquefied soils have led to the following broad yes/no characterization of soil susceptibility, which allows a first, rough screening of soils to be investigated in more detail:

<u>Are susceptible to liquefy:</u>

a) *silty sands and sands* presenting the following characteristics (Figure 7) :
   - saturation degree about 100 %
   - uniform granulometry satisfying the uniformity condition:
   $$C_u = D_{60} / D_{15} < 15 ,$$
   with Di defined as follows: i % of the soil sample has a grain size lower or equal to Di.
   - grain size at 50 %, D_{50}, ranging between 0.05 mm and 1.5 mm

b) *clayey soils* presenting the following characteristics :
   - grain size at 15 %, D_{15}, larger than 0.005 mm
   - liquidity limit w_L lower than 35 %
   - water contents larger than 0.90 w_L
   - plasticity index I_P lower than 0.73 (w_L - 20)

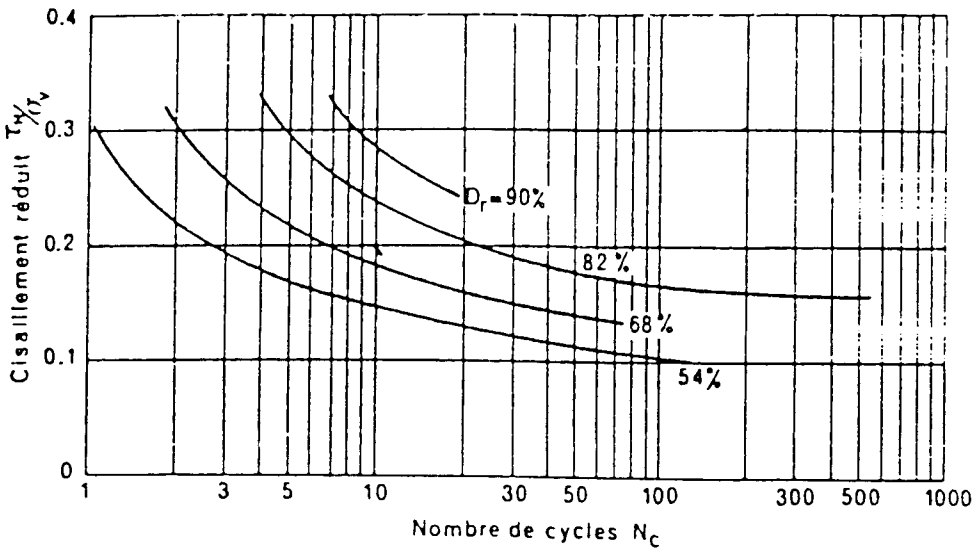

Figure 5 : *Effects of relative density on liquefaction potential.*

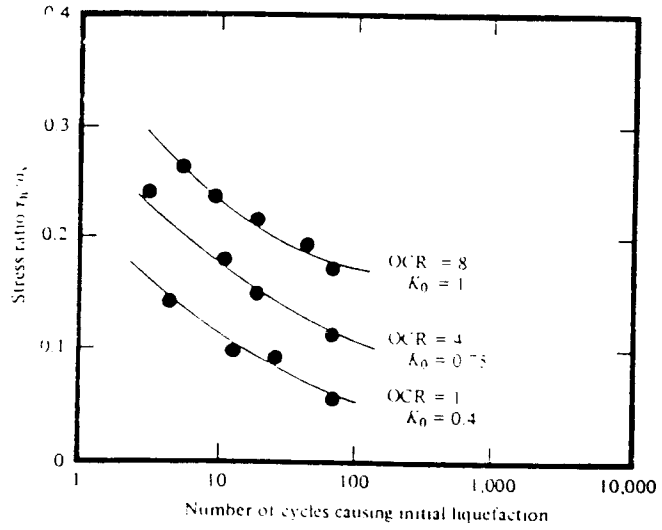

Figure 6 : *Effect of overconsolidation ratio on liquefaction potential*

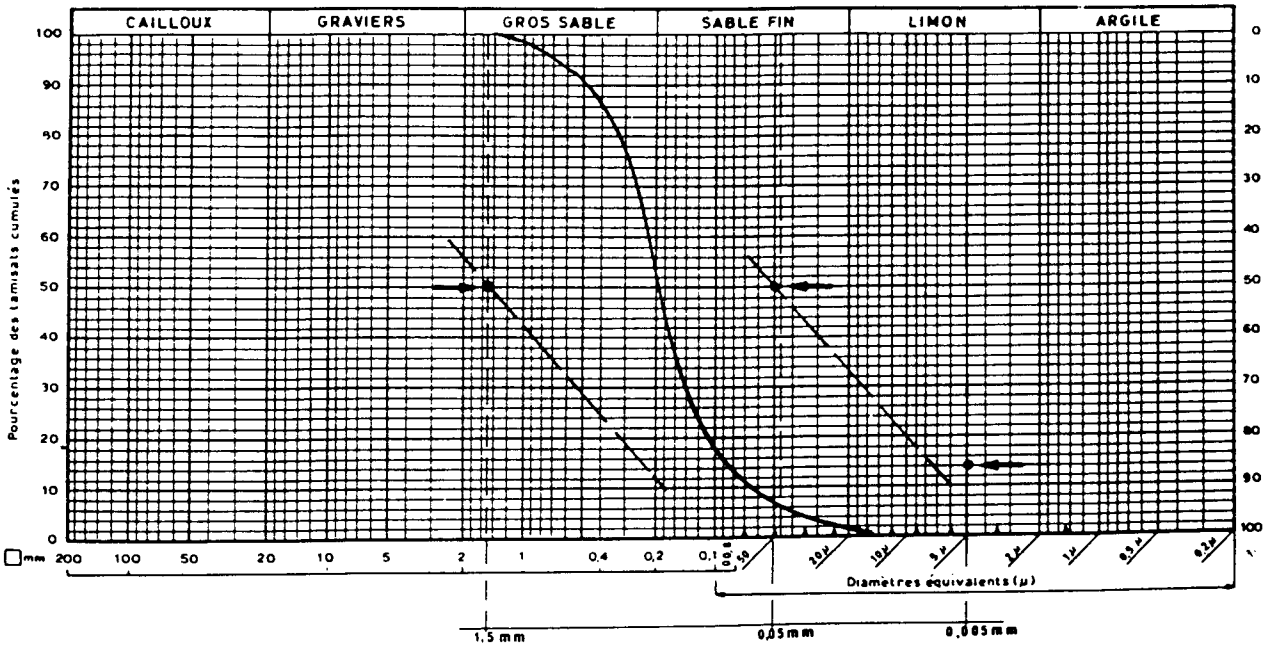

Figure 7 : *Grain size criteria for liquefaction susceptibility of sandy soils. A sandy soil is susceptible to liquefy if its granulometric curve falls in between the limits, as it is the case for the example curve.*

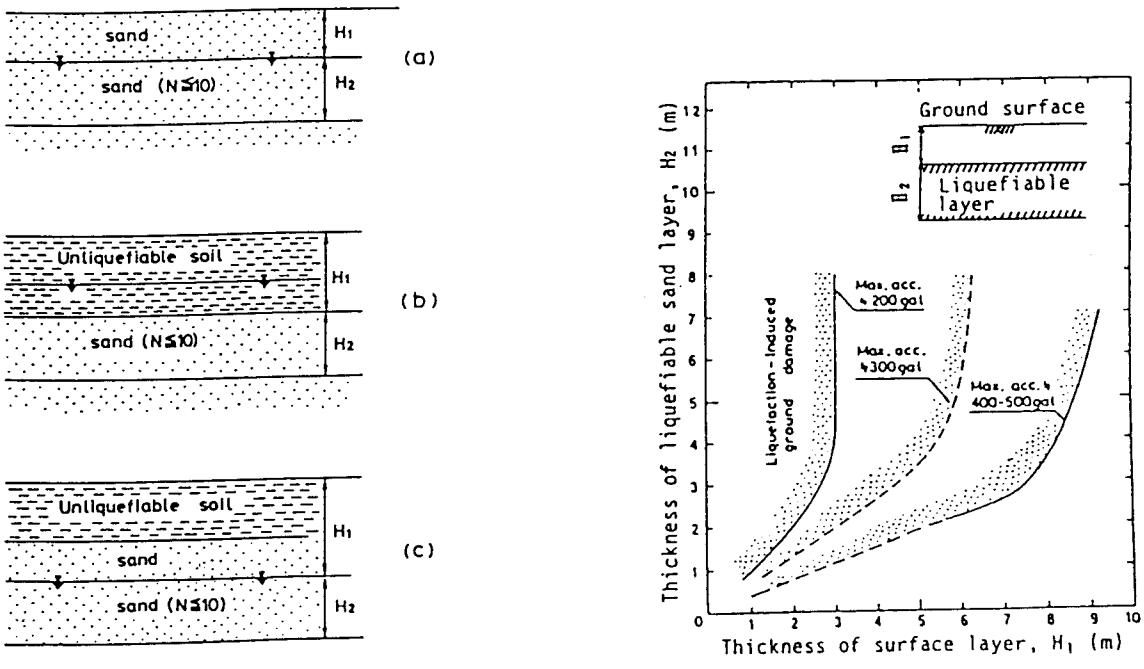

Figure 8 : *Identification of liquefaction induced damage with geological criteria*
a) Top: Geological configurations and definitions of H_1 and H_2; b) Bottom: Proposed boundary curves for various peak acceleration values. (from Ishihara, 1985; Reproduced from ISSMFE, 1993).

Are not susceptible to liquefy in any case:

a) *gravely soils* for which D_{10} is larger than 2 mm
b) *clayey soils* presenting the following characteristics :
   - grain size at 70 %, D_{70}, lower than 74 μm
   - plasticity index larger than 10 %

2.2.3 Correlation with geology

Liquefaction is known to occur repeatedly in the same areas for successive earthquakes, provided that hydrogeological and geological conditions remain unchanged. Thus, when unavailable, maps displaying localities of past liquefaction may be considered as representing likely areas for liquefaction during future earthquakes.
However, such a historical information is not always (not often ...) available. It is nevertheless always possible in those areas to use empirical correlations derived from past observations in many other places, and linking liquefaction occurrences to geological and geomorphological settings. Such qualitative correlations have been established by several authors, which are summarized in Tables I to IV. These 4 tables consistently show that sediments generally have increased resistance to liquefaction with increasing age, and that fluvial and aeolian processes help to sort then sediment granular soils in relatively loose state, thereby generating conditions for high liquefaction susceptibilities. In addition, the depth of the water table is also a very important factor: the deeper it is, the lesser the susceptibility.

From another point of view, the important thing for engineering purposes is not really the occurrence or not of liquefaction, but its deleterious effects on ground (disruptions, failures...). To decide on whether liquefaction will or will not exert damage on ground surface, the thickness H_2 of the liquefiable layer could be checked against the thickness H_1 of the surface, unliquefiable layer, using the criterion shown in Figure 8. If H_1 is greater than the curves displayed in that figure (and corresponding to different peak accelerations), the liquefaction effects will not be damaging.

The use of such correlations require the preliminary establishment of a *very detailed* geological map: usual geological maps are generally not detailed enough, nor focused on quaternary formations, so that it may often be necessary to spend some time in the field to identify and map the actual geomorphological characteristics of the site under consideration. Such field investigations might then also look for paleoliquefaction signs.
These correlations, though qualitative and empirical, are very consistent with the physical mechanism of liquefaction, since the geological and geomorphological conditions control some crucial parameters as granulometry, relative density, water saturation and cementation. However, analyses based only on geological and geomorphological considerations are limited to an assessment of liquefaction susceptibility : estimations of liquefaction potential requires the taking into account, in some way, of the actual mechanical properties of the deposits.

2.3 Liquefaction opportunity

Liquefaction opportunity is related to the loading action; it is intended to tell whether the expected level of loading may give rise to liquefaction for a given class of soil deposits, generally the most unfavorable ones (i.e., those having the highest susceptibility).

Rank	Topography	Liquefaction Potential
A	Present river bed, old river bed, swamp, reclaimed land, interdune lowland	Liquefaction likely
B	Fan, natural levee, sand dune, flood plain, beach, other plains	Liquefaction possible
C	Terrace, hill, mountain	Liquefaction not likely

Table I : *Susceptibility of various geomorphological units to liquefaction (From Iwasaki et al, 1982; reproduced from ISSMFE, 1993).*

Types of Deposit	General Distribution of Cohesionless Sediments in Deposits	Likelihood that Cohesionless Sediments, When Saturated, Would be Susceptible to Liquefy (by Age of Deposit)			
		< 500 yrs	Holocene	Pleistocene	Pre-Pleistocene
Continental Deposits					
River Channel	locally variable	very high	high	low	very low
Flood plain	locally variable	high	moderate	low	very low
Alluvial fan and plain	widespread	moderate	low	low	very low
Marine terraces and plains	widespread	—	low	very low	very low
Delta and fan-delta	widespread	high	moderate	low	very
Lacustrine and playa	variable	high	moderate	low	very low
Colluvium	variable	high	moderate	low	very low
Talus	widespread	low	low	very low	very low
Dunes	widespread	high	moderate	low	very low
Loess	variable	high	high	high	very low
Glacial till	variable	low	low	very low	very low
Tuff	rare	low	low	very low	very low
Tephra	widespread	high	high	?	?
Residual soils	rare	low	low	very low	very low
Sebka	locally variable	high	moderate	low	very low
Coastal Zone					
Delta	widespread	very high	high	low	very low
Estuarine	locally variable	high	moderate	low	very low
Beach: High wave energy	widespread	moderate	low	very low	very low
Beach: Low wave energy	widespread	high	moderate	low	very low
Lagoonal	locally variable	high	moderate	low	very low
Fore shore	locally variable	high	moderate	low	very low
Artificial					
Uncompacted fill	variable	very high	—	—	—
Compacted fill	variable	low	—	—	—

Table II : *Susceptibility of sedimentary deposits to liquefaction according to Youd and Perkins (1978) . (Reproduced from ISSMFE, 1993)*

Geomorphologic Conditions		Liquefaction Potential
Classification	Specific Conditions	
Valley Plain	Valley plain consisted of gravel or cobble	Liquefaction not likely
	Valley plain consisted of sandy soil	Liquefaction possible
Alluvial Fan	Vertical gradient is more than 0.5%	Liquefaction not likely
	Vertical gradient is less than 0.5%	Liquefaction possible
Natural Levee	Top of natural levee	Liquefaction possible
	Edge of natural levee	Liquefaction likely
Back Marsh		Liquefaction possible
Abandoned River Channel		Liquefaction likely
Former pond		Liquefaction likely
Mash/Swamp		Liquefaction possible
Dry River Bed	Dry river bed consisting of gravel	Liquefaction not likely
	Dry river bed consisting of sandy soil	Liquefaction likely
Delta		Liquefaction possible
Bar	Sand bar	Liquefaction possible
	Gravel bar	Liquefaction not likely
Sand Dune	Top of dune	Liquefaction not likely
	Lower slope of dune	Liquefaction likely
Beach	Beach	Liquefaction not likely
	Artificial beach	Liquefaction likely
Interlevee Lowland		Liquefaction likely
Reclaimed Land by Drainage		Liquefaction likely
Spring		Liquefaction likely
Fill	Fill on boundary zone between sand and lowland	Liquefaction likely
	Fill adjourning cliff	Liquefaction likely
	Fill on marsh or swamp	Liquefaction likely
	Fill on reclaimed land by drainage	Liquefaction likely
	Other type fill	Liquefaction possible

Table III : *Susceptibility of specific geomorpholical units to liquefaction in case of a macroseismic intensity VIII MM (JMA V) (From Wakamatsu, 1992; reproduced from ISSMFE, 1993)*

Sedimentary Unit	Depth to Ground Water, in Metres			
	0 - 3	3 - 10	10 - 15	> 15
Holocene:				
Latest	Very high to high	Moderate	Low	Very low
Earlier	High	Moderate	Low	Very low
Pleistocene:				
Late	Low	Low	Very low	Very low
Middle and early	Very low	Very low	Very low	Very low
Tertiary and pre-Tertiary	Very low	Very low	Very low	Very low

Table IV : *Susceptibility of sedimentary deposits to liquefaction as a function of their age and of the depth of water table (After AFPS, 1992)*

2.3.1 Magnitude / Distance criteria

If earthquake activities of an area are known from historical data, the maximum extent of liquefaction susceptible area can be estimated from the magnitudes of events expected to occur in the area. Several authors have investigated the occurrence of liquefaction phenomena during past earthquakes, and plotted the "distance" R between the epicentral area and *farthest* liquefied site as a function of the earthquake magnitude, M.
Many different such curves have been proposed; we will present here only the most recent ones, that take into account the most suitable definition of distance, i.e., the closest distance to the rupture area, usually denoted R_f, together with a consistent definition of magnitude, i.e., the surface wave magnitude M_S or the moment magnitude M_W.
Figure 9 represents the two limiting curves proposed by Youd and Perkins (1978) and Ambraseys (1988). The former authors consider only significant liquefaction, which they define as producing a ground displacement of at least 10 cm, and they ignore slight, non-damaging liquefaction. On the opposite, the latter includes observations such as minor fissures in soil, or sand boils. This may be an explanation for the differences between the 2 curves, which also, however, correspond to different data set: western US and Japan for the former, and worldwide for the latter (thus including some areas with lesser attenuation of ground motion with distance).

2.3.2 Intensity criteria

The maximum extent of liquefaction may also be grossly estimated on the basis of the expected macroseismic intensity. Japanese investigators showed, from simultaneous liquefaction and intensity observations, that liquefaction in areas underlain by Holocene sediments can occur only for intensities above or equal to MM degree VIII, corresponding to Japanese degree V. However, minor liquefaction may possibly occur for lower intensities. The intensity degree V (JMA) or VIII (MM) can therefore be used as the intensity threshold for damaging liquefaction; the degrees IV (JMA) or VI-VII (MM) are minimum thresholds for slight liquefaction.

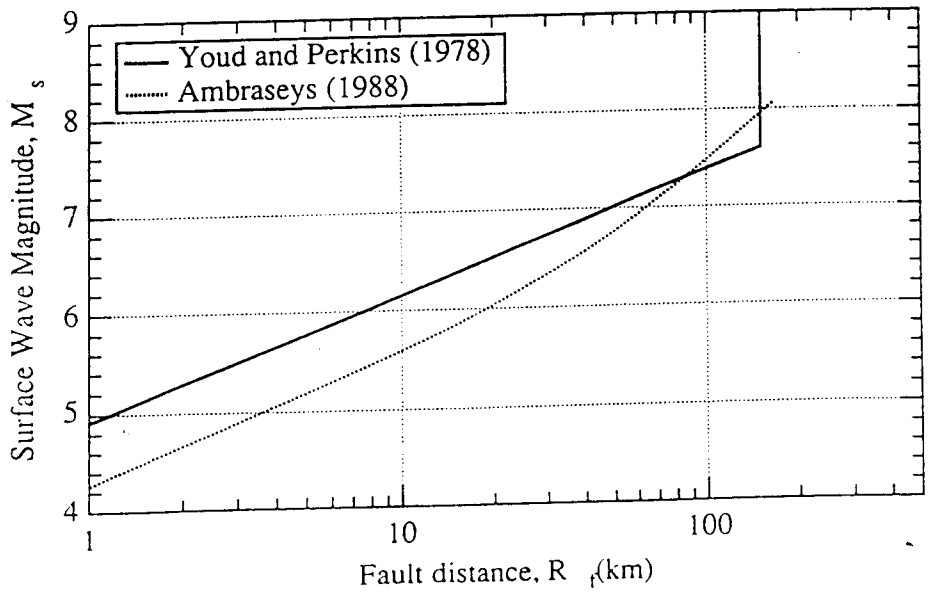

Figure 9 : *Dependency of distance from earthquake fault plane to farthest liquefied sites (R_f in km) on earthquake surface wave magnitude M_S. The Ambraseys curve corresponds to the equation: $M_W = 0.18 + 9.2\ 10^{-8} R_f + 0.90 \log R_f$. (Reproduced from ISSMFE, 1993).*

2.4 Liquefaction potential

Estimating the liquefaction potential of a given site is very generally done through a comparison of the shear forces induced by the loading action, and the soil resistance to liquefaction.
The loading action may be specified in different ways: intensity, peak acceleration, response spectrum, real or artificial accelerogram,...: for sake of simplicity, will be considered here only methods using extremely simple ground motion characterizations: intensity, peak acceleration, "equivalent duration" (see below 2.4.2).
The shear resistance of soil and its sensitivity to ground shaking requires the knowledge of several mechanical parameters; this may be achieved either through in-situ measurements, or through laboratory tests as described in section 2.1. Considering the high degree of sophistication of lab tests, the difficulty to obtain undisturbed samples actually representative of actual field conditions, and their overall cost, only techniques using the simplest in-situ measurements will be presented here. The most widely used in-situ parameter is the SPT number N_{SPT} (Standard Penetration Test); the most widespread technique for estimating liquefaction potential is therefore based on this parameter. New techniques are presently being developed using another rapidly expanding in-situ test, the cone penetration test (CPT); they will not be presented here.
We present here three techniques: the first and simpler one is known as the "Chinese" procedure, the now "classical" procedure originally developed by Seed and Idriss (1971), and well as a slightly more general procedure, based on the Seed and Idriss' one and originally developed in Japan (Iwasaki et al., 1982). The two first techniques allow to determine the liquefaction potential of a given soil unit located at a given depth, while the third one provides a quantitative estimation of liquefaction potential at a given site (i.e., for a whole soil column) through a "liquefaction potential index".

2.4.1 Chinese procedure

In this procedure, ground motion is characterized by its MM macroseismic intensity, while soil conditions are characterized by SPT number ("giving an index of mechanical strength), and the depth of soil with respect to free surface (ds) and with respect to water table (dw); these two latter values characterize the "initial conditions", i.e. the initial effective stress.
Empirical correlations derived from observations of liquefied and non-liquefied sites, lead to the following formula:

$$N_{crit} = N_0 [\ 1 + 0.125\ (ds - 3) - 0.05\ (dw - 2)\ ]$$

where N_0 is a scaling parameter depending on intensity level as specified in Table V. (A rough correspondence between intensity and peak acceleration is also used in this Table to authorize liquefaction potential estimates on the basis of peak acceleration; but the correlation was originally developed for intensity data).
This formula has been recently slightly improved to take into account the influence of fines content in sands, expressed in terms of the clay contents in percent, p_c

$$N_{crit} = N_0 [\ 1 + 0.125\ (ds - 3) - 0.05\ (dw - 2) - 0.07\ p_c\ ]$$

A sandy layer will liquefy at a given intensity level if its SPT number is lower than the value N_{crit}.
This method therefore just provides a "yes/no" information on the liquefaction potential.

Earthquake Intensity	$\bar{N}_0$ in blow/ft	Peak ground acceleration
VIII	6	0.10g
VIII	10	0.20g
IX	16	0.35g

Table V : *N_0 value as a function of macroseismic intensity (and peak acceleration). (Reproduced from ISSMFE, 1993)*

2.4.2 Seed and Idriss procedure

i) Step 1: estimating the equivalent shear stress induced by earthquake shaking
According to these authors, the cyclic stress ratio developed at a particular depth beneath the ground level may be estimated as follows:

$$\tau_{av} / \sigma'_v = 0.65 \cdot (a_{max} / g) \cdot (\sigma_v / \sigma'_v) \cdot r_d(z)$$

where: τ_{av} is the average cyclic shear in irregular time histories of shear stress variations,
σ'_v is the *effective* overburden stress at the depth under study,
σ_v is the *total* overburden stress at the same depth ,
a_{max} is the peak horizontal acceleration, g is the acceleration of gravity,
r_d is a stress reduction factor accounting for the decrease of motion amplitude with increasing depth, in relation with the rigidity of the soil column. Two formulae are proposed for r_d : $r_d = 1. - 0.00075\ z^2$ and $r_d = 1. - 0.015\ z$

ii) Step 2: estimating the resistance of soils to cyclic shear deformation
The cyclic strength is estimated on the basis of empirical correlations with the SPT value (or, more recently, the CPT value) .
The raw SPT number N should first be corrected to account for the actual energy of the hammer, and for the effective overburden pressure, according to the formula:

$$N_1 = C_n \cdot ER_m / 60 \cdot N_{SPT}$$

where C_n may be read off from a chart such as that shown in Figure 10, and ER_m is the actual energy efficiency delivered to the drill rods as shown in Table VI.
This N_1 value may then used in charts such as those illustrated in Figures 11 (sand) and 12 (silty sands), to yield the cyclic stress ratio τ_l / σ'_v required to induce liquefaction *for an earthquake of magnitude 7.5.*
For earthquakes having another magnitude, the corresponding cyclic strength is obtained by multiplying the value obtained for M=7.5, by a magnitude scaling factor, listed in Table VII.

iii) Step 3: safety factor
Once both ratios τ_{av} / σ'_v and τ_l / σ'_v have been obtained in steps i) and ii), a safety factor Fs may be defined as:

$$Fs = \tau_l / \tau_{av}$$

From these results obtained at a variety of depths, one may then define the liquefaction potential of the site under consideration, according to the following classification:

2 < Fs : No liquefaction
1.5 < Fs < 2 : Liquefaction unlikely
1.0 < Fs < 1.5 : Liquefaction likely
Fs < 1.0 : Liquefaction quasi certain

2.4.3 Liquefaction potential index

Iwasaki et al. (1982) proposed to evaluate the liquefaction potential a whole soil column through a new parameter, called "liquefaction potential index" I_L, which is in fact a weighted average of the safety factors obtained at each depth z:

$$I_L = \int_0^{20} (10 - 0.5\ z)\ F_L \cdot dz$$

where: $F_L = 1 - Fs$ when $Fs < 1.0$ and $F_L = 0$ when $Fs > 1.0$

It follows from this definition that the value of I_L will range between 0 for a site where

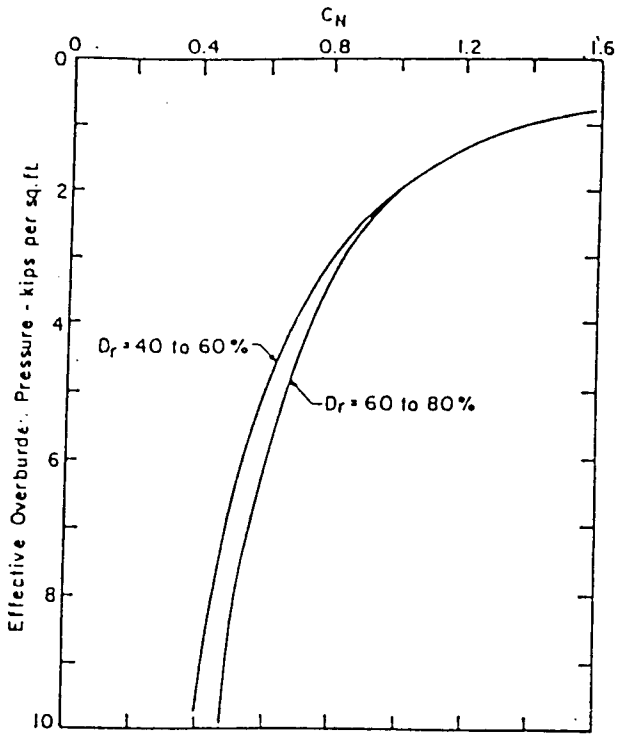

Figure 10 : *Chart values for Cn (After Seed et al., 1985 ; Reproduced from ISSMFE, 1993)*

Country	Hammer type	Hammer release	Estimated rod energy (%)	Correction factor for 60% rod energy
Japan[a]	Donut	Tombi	78	1.30
	Donut[b]	Rope and pulley with special throw release	67	1.12 Average 1.2
U.S.	Safety[b]	Rope and pulley	60	1.00
	Donut	Rope and pulley	45	0.75
Argentina	Donut[b]	Rope and pulley	45	0.75
China	Donut[b]	Free-fall[c]	60	1.00
	Donut	Rope and pulley	50	0.85
UK	Pilcon	Trip	60	1.00
	Old Standart	Rope and pulley	60	1.00

[a] Japanese SPT results have additional corrections for borehole diameter and frequency effects.

[b] Prevalent method in this country today

[c] Pilcon type hammers develop an energy ratio of about 60%

Table VI : *Summary of energy ratios for SPT procedures (After Seed et al., 1985 ; Reproduced from ISSMFE, 1993)*

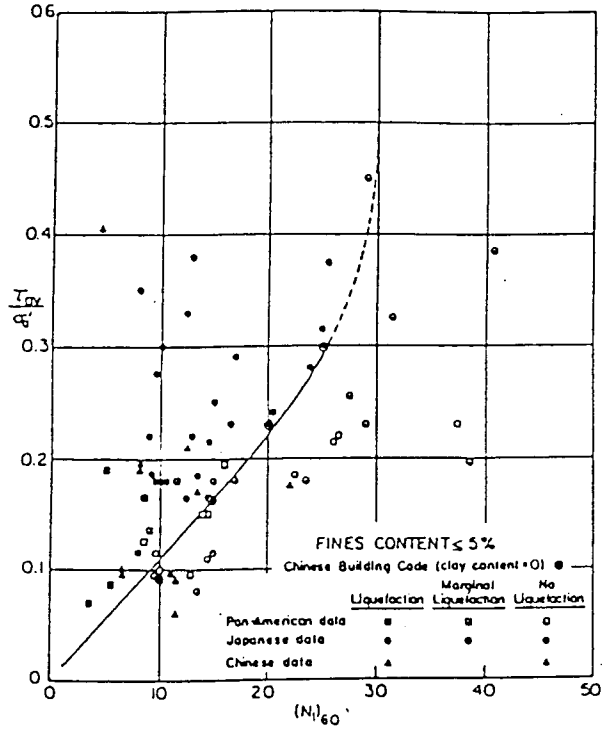

Figure 11 : *Relationship between stress ratios causing liquefaction and N_1 value for clean sands, and for M=7.5 earthquakes.(After Seed et al., 1985 ; Reproduced from ISSMFE, 1993)*

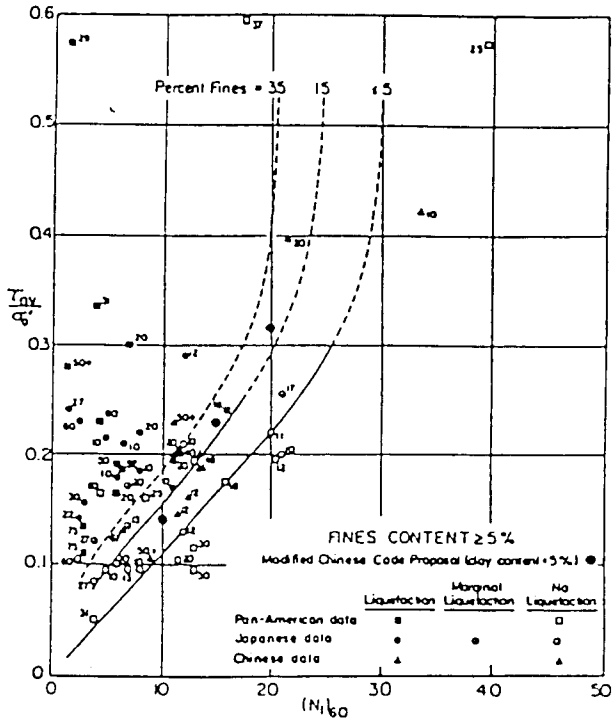

Figure 12 : *Relationship between stress ratios causing liquefaction and N_1 value for silty sands, and for M=7.5 earthquakes.(After Seed et al., 1985 ; Reproduced from ISSMFE, 1993)*

Earthquake magnitude, M	Number of representative cycles at 0.65 τ_{max}	$\frac{\left(\frac{\tau_{av}}{\sigma'_o}\right)_l \text{ for } M = M}{\left(\frac{\tau_{av}}{\sigma'_o}\right)_l \text{ for } M = 7.5}$
8.5	26	0.89
7.5	15	1.0
6.75	10	1.13
6	5~6	1.32
5.25	2~3	1.5

Table VII : *Correction factors for influence of earthquake magnitude on liquefaction resistance (After Seed et al., 1985 ; Reproduced from ISSMFE, 1993)*

liquefaction cannot occur at any depth, and 100 for a site where Fs is zero at any depth. Statistics based on Japanese data (and cyclic strengths computed with a slightly different method) lead to the following site classification:

$I_L = 0$	:	*No liquefaction*
$0 < I_L < 5$	:	*Only slight effects from liquefaction*
$5 < I_L < 15$	:	*Intermediate effects*
$15 < I_L$	:	*Severe damaging effects from liquefaction*

3. SLOPE INSTABILITIES

3.1 Fundamentals

3.1.1 Observations

In the most general terms, earthquake-induced slope instabilities include a variety of phenomena and may be classified, according to Keefer and Wilson (1989) into three main categories:

- *Category I: rock or soil falls, rock or soil slides (i.e., translational sliding along a basal weakened surface), rock and soil avalanches*
  This category corresponds to rapid, sometimes extremely rapid motion, of generally surficial material only. The falling or sliding mass is generally dislodged from steep slopes, and is highly to very highly disrupted, and includes a very large number of separate blocks.
- *Category II: rotational sliding in soils or rock masses, slow earth flows:*
  This category corresponds to relatively coherent slides (except on the edges), which generally affect thick deposits located on moderate to sleep slopes; the motion may be slow to rapid, and may be observed in dry and wet material.
- *Category III: soil lateral spreads, rapid soil flows, subaqueous landslides*
  This category involves a significant component of fluid flow (lateral spreads correspond to translation along a layer with weakened mechanical strength such as liquefied sand layers, or weakened sensitive clay); the motion velocity is moderate to rapid; the thickness of the sliding layer is variable - depending on the depth of the weak layer -; such instabilities may affect deposits with very gentle slopes (for instance flat deposits on river banks).

The motion associated with such slope instabilities may thus be in a number of cases extremely rapid, and therefore catastrophic (in Peru, a rock avalanche coming from Andean glaciers totally swept the entire village of Yungay, and took 20 000 lives); however, slow motion also, although not as dangerous for life, may have very costly consequences when it threatens densely inhabited areas, or industrial sites, or transportation facilities.
The final displacements and deformations induced by such slope instabilities may be extremely large: once triggered, lateral spreads or rock falls may propagate over very large distances.
In this section, we will only consider shallow slides.

3.1.2 Mechanism

Alike liquefaction, the slope instability basically depends on two factors: the external driving force and the material resistance to failure.
The external driving forces are twofold: the static, gravitational force, and the dynamic, seismic action (with its different aspects: amplitude, duration, frequency): unlike in the case of liquefaction, slope instabilities are (for most of them) phenomena that may occur already

in static conditions, and the earthquake action is an additional triggering mechanism.
The resistance to sliding depends on a wide range of factors: geological conditions, hydrogeological conditions, surface and subsurface topography (very often in 3 dimensions), mechanical characteristics of slope material (rock and/or soil), (3D) geometry and rheology of preexisting discontinuities, ...

Given this large number of factors, mechanical analysis of such slope instabilities is very difficult; in addition, it is also very uneasy, and very expensive, to gather detailed enough information on the initial conditions (pore pressure, deep geometry, ...); as a consequence, the few methods that have been developed till now, are either very heavy to use and almost intractable in practice (that is the case for sophisticated numerical codes), or very rough (such as cartographic approach or pseudo static analysis), since they cannot catch the phenomena in their whole complexity. The state of development of hazard assessment methods for slope instabilities is still in its infancy.

3.2 Susceptibility

Since landslide hazard exists even in the absence of seismic action, the first kind of susceptibility analysis consists simply in the assessment of static stability.
The most usual way in that aim is to perform an investigation on the slope instabilities known to have occurred in the area under study. Such an inventory, where events are classified according to their mechanism and the leading triggering action (gravity, water, ...) on the basis of simple criteria (without use of any in-situ or laboratory tests), should allow to generalize the punctual observations to the whole area, and to derive a map of static hazard with three to four levels of hazards: null to weak, moderate, significant, and high.
In such a map, very often, some earthquake-specific instabilities (such as lateral spreads) are not included if no historical event is known. The extrapolation of such a static susceptibility to seismic conditions should therefore include:
- an identification of areas where such specific instabilities are possible (river banks, lake shores, ...)
- an extension of the stopping zones for areas subjected to rock falls.

Such an analysis should be conducted by engineering geologists and/or geotechnical engineers.

3.3 Opportunity

As for liquefaction, landslide opportunity is related mainly to the loading action, and is intended to tell whether the expected level of loading, depending on earthquake magnitude and distance, and/or macroseismic intensity, is likely to induce slope instabilities - *generally in the most unstable slopes* - in the area under consideration.
One must keep in mind that this kind of opportunity analysis does not directly incorporate the geological, geotechnical or hydro meteorological conditions. In order to slightly compensate this pitfall, rain fall conditions in the region are sometimes taken into account.

3.3.1 Magnitude / Distance criteria

Several authors investigated, for various countries, the dependency of the distance between earthquake source and the farthest induced slope instability: the individual results of such studies are strongly connected with the local hydrometeorological context, and can therefore hardly be extrapolated to other, different environments. This is illustrated by the comparison

Earthquake	Magnitude (M)	Maximum distance	
		from an epicenter (km)	from a fault (km)
Loma Prieta	7.1	97	
Manjil	7.3	30	
Luzon	7.8	210	130
Armenia	7.0	15	

Table VIII : *Observed maximum distances of slope failures during four recent earthquakes (Reproduced from ISSMFE, 1993)*

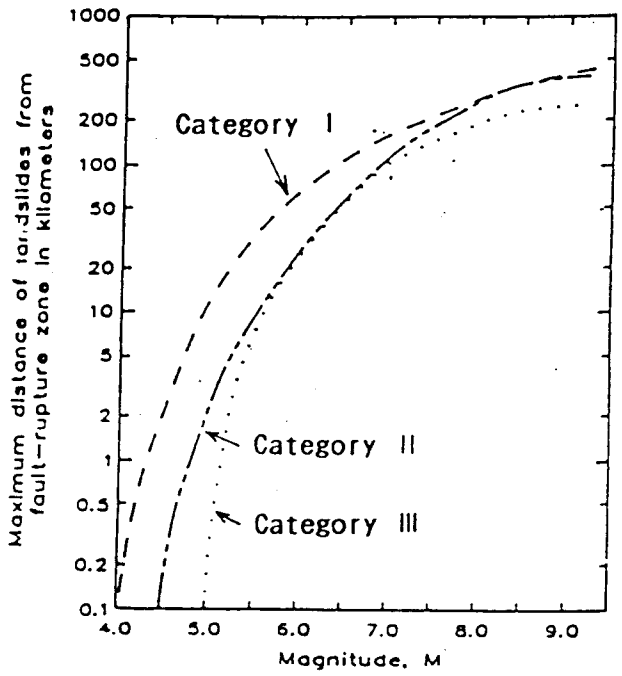

Figure 13 : *Maximum distance from fault rupture zone to slope failure, for three main slope categories (see text), as a function of magnitude (From Keefer and Wilson, 1989; Reproduced from ISSMFE, 1993)*

of observations made in 4 recent earthquakes, as summarized in Table VIII.
Keefer and Wilson (1989) gathered a worldwide sample of observations; they grouped the slope instabilities into the three main categories listed in section 3.1, and derived, for each category, the curves displayed in Figure 13. In this figure, the "distance" is defined as the distance to the fault rupture zone (as in Figure 9 for liquefaction). Category I slides appear to be the most sensitive to earthquakes.
Based on the - still too few - available results, ISSMFE (1993) recommends to use the curves displayed in Figure 14, on the basis of which the following important points are to be noticed:
- the opportunity for earthquake induced sliding is significantly higher in wet environments (which causes the hazard to be different depending not only on the geographical area, but also on the temporal occurence of seismic events within or outside the dry season).
- when distance to the fault zone is to be used, the curves in this Figure should be shifted to the left by a factor between 1/2 and 1/3.

3.3.2 Intensity criteria

Keefer and Wilson (1989) also investigated the relation between macroseismic intensity (MM scale) and the occurrence (or not) of slope instabilities. Their conclusions are summarized in Figure 15. Despite a significant scatter, it seems reasonable to assume that the minimum intensity causing slope instabilities is about V to VI MM degree; a similar study based on Japanese data led to the value of about IV in the JMA scale, which is slightly higher (VI-VII on MM scale).

3.4 Quantitative estimations of slope instability potential

Several methods have been proposed for estimating such a potential for wide areas. Some of them are based on a statistical analysis combining several "geomorphological" and seismic criteria; an example of such a method is presented in section 3.4.1. Some other techniques are based of extremely simple failure (sliding) mechanisms, which allow simple computations with very few parameters, and allow a rather simple extrapolation from static conditions to seismic conditions: an example of such a technique is given in section 3.4.2. Finally, the principle of a more sophisticated analytical approach is presented in section 3.4.3, which may be applied, however, only when the geotechnical and seismic conditions are known in great detail.

3.4.1 Statistical correlations

An example of such technique was used for zoning the slope failure potential in Kanagawa prefecture (Japan), as reported in report TC4 of ISSMFE (1993). It is based on observations made during three recent large earthquakes in Japan.
In this method, mapping of slope failure potential is made on a grid having a 500 m by 500 m mesh size; in each mesh, the potential is estimated with a weighted sum of seven factors W_i, listed below:

- W_1 : maximum surface acceleration in the mesh
- W_2 : length of the contour line corresponding to the average topographic level in the mesh
- W_3 : maximum difference n height within the mesh
- W_4 : hardness of rock for typical slopes in the mesh
- W_5 : length of faults in the mesh
- W_6 : length of artificial cut or filled slopes in a mesh
- W_7 : category of slopes in the mesh (four different categories, based on the convexity of the slope (concave, straight, convex or complex)

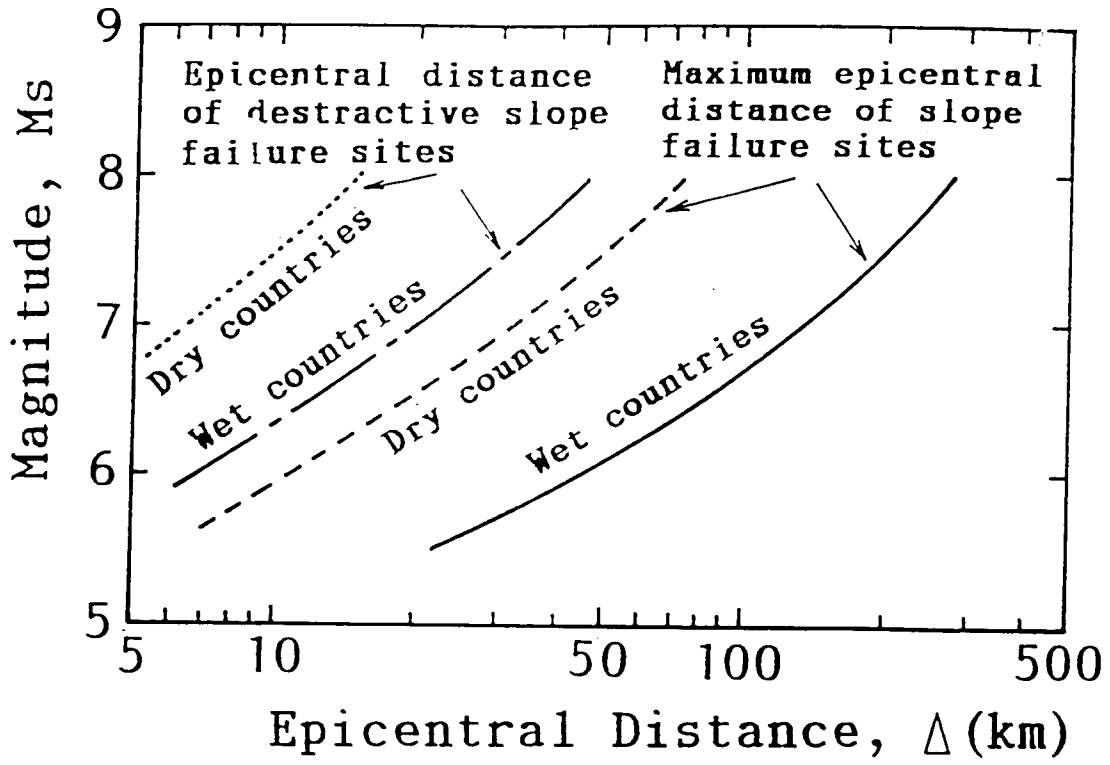

Figure 14 : *Recommended relationships between surface wave magnitude and the farthest epicentral distance a) for slope failures of any kind, and b) for damaging slope failures, in both dry and wet hydrogeological environments (Reproduced from ISSMFE, 1993)*

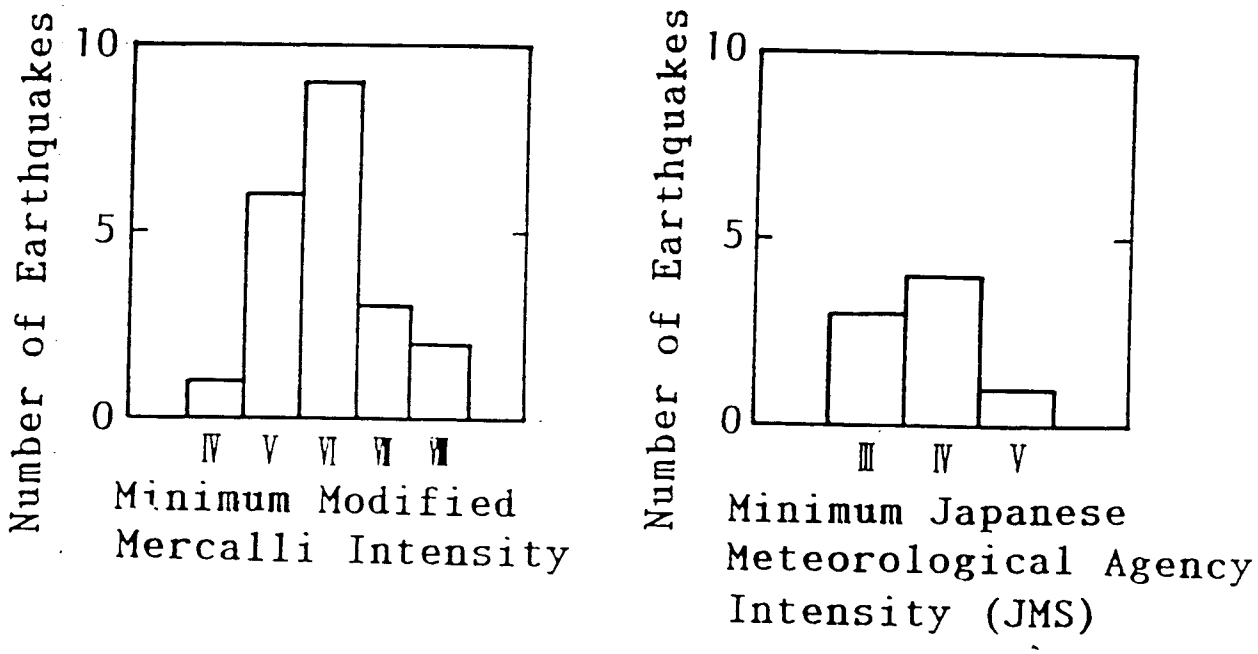

Figure 15 : *Minimum macroseismic intensity causing slope failures . (left) MM scale; (right) JMA scale (From Keefer and Wilson, 1989; Reproduced from ISSMFE, 1993)*

A discriminant analysis of those 7 factors in a total of 4680 meshes led to the weighting factors listed in Table IX. The rate of slope failure potential is thus estimated from the sum of those 7 weighting factors:

$$W = W_1 + W_2 + W_3 + W_4 + W_5 + W_6 + W_7$$

An analysis of the weights listed in this table, shows that the most important factors are 1) the peak acceleration, 2) the maximum altitude change, and 3) the length of natural faults and artificial cuts.

The potential is ranked in four categories according to the values of W indicated in Table X; the same table also provides an estimate of the expected number of slope failures in the mesh, for the given acceleration level.

Similar methods have been proposed by a few other authors, as presented in ISSMFE (1993). It should be kept in mind that each of these methods are based on regional data, the extrapolation of which to other environments is not straightforward. One should therefore, preferably, use similar statistical approach, but fit the weighting factors to the local observations.

3.4.2 Simple pseudo-static analysis

These simple methods generally consider the sliding of plane layers on slopes, according to the geometry illustrated in Figures 16 and 17. However, some other techniques widely spread in soil mechanics for static analysis may also be used (for instance those based on a circular rupture geometry). Only plane rupture is considered here for sake of simplicity.

For the single block displayed in Figure 17, the *static* safety factor, which is the ratio between the maximum resistant force and the driving force, is given by:

$$F_S = \text{tg } \phi \ / \ \text{tg } \beta \ ,$$

where ϕ is the angle of friction between the block and the underlying slope, and β is the slope angle.

When a seismic action is added, it is -very simply - modelled as an additional horizontal acceleration, whose value is given by a coefficient k (in g); the initial *static* safety factor F_S is then modified into a *"dynamic"* (in fact, *pseudo-static*) safety factor F_d, whose value is:

$$F_d = \text{tg } \phi \ \ (1. - k \ . \ \text{tg } \beta \ ) \ / \ (k + \text{tg } \beta \ ) \ .$$

For the plane sliding of soil masses as illustrated in Figure 18, two cases have to be considered: cohesionless soils, having only an internal friction angle parameter ϕ; and purely cohesive soils, characterized by their cohesion Cu: in those cases, the pseudo-static safety factors are given by the formulae:

Cohesionless soils : $F_d = \text{tg } \phi \ \ (1. - k \ . \ \text{tg } \beta \ ) \ / \ (k + \text{tg } \beta \ ) \ .$

Purely cohesive soils : $F_d = Cu \ / \ \gamma \ H \ \times 1. / \ (k \ \cos \beta \ + \ \sin \beta \ ) \ .$

where γ is the specific mass of the sliding layer, and H its thickness.

From these formulae, it is therefore possible to estimate the landslide potential in two ways: either from the knowledge of k, β, and ϕ or Cu, or on the sole basis of the static safety factor F_S, the slope angle, and the seismic coefficient k, since the above mentioned formulae also allow to shift from static factors to pseudo-static factors:

Cohesionless soils: $F_d \ / \ F_S \ = \ \text{tg } \beta \ \ (1. - k \ . \ \text{tg } \beta \ ) \ / \ (k + \text{tg } \beta \ ) \ .$

Purely cohesive soils : $F_d \ / \ F_S \ = \ \text{tg } \beta \ / \ (k + \text{tg } \beta \ ) \ .$

A very important parameter in these formulae is the seismic coefficient k. A pessimistic assumption would be to take k equal to the peak horizontal acceleration (expressed in g). In practice, since acceleration is not constant during an earthquake, and moreover is altered, it is generally assumed that $k = 0.5 \ a_{max} \ / \ g$ is a reasonable value.

Factor	Category	Weight
a)Maximum surface acceleration (Gal), W1	0~200	0.0
	200~300	1.004
	300~400	2.306
	400~	2.754
b)Length of a contour line (m), W2	0~1000	0.0
	1000~1500	0.071
	1500~2000	0.320
	2000~	0.696
c)Difference between the highest site and the lowest site (m), W3	0~50	0.0
	50~100	0.550
	100~200	0.591
	200~300	0.814
	300~	1.431
d)Hardness of a rock, W4	Soil	0.0
	Soft rock	0.169
	Hard rock	0.191
e)Length of faults (m), W5	No fault	0.0
	0~200	0.238
	200~	0.710
f)Length of artificial slopes (m), W6	0~100	0.0
	100~200	0.539
	200~	0.845
g)Topography of slope, W7 (Fig. 2.10)	(1)	0.0
	(2)	0.151
	(3)	0.184
	(4)	0.207

Table IX : *Respective weight of the seven factors accounted for estimating the slope failure potential in Kanagawa prefecture (Reproduced from ISSMFE, 1993)*

W	2.93	3.53	3.68	
Rank	A	B	C	D
Number of slides within one mesh	0	1~3	4~8	9~

Table X : *Ranking of slope failure potential according the value of W, and corresponding number of expected slope failures in every mesh of the Kanagawa prefecture area (Reproduced from ISSMFE, 1993)*

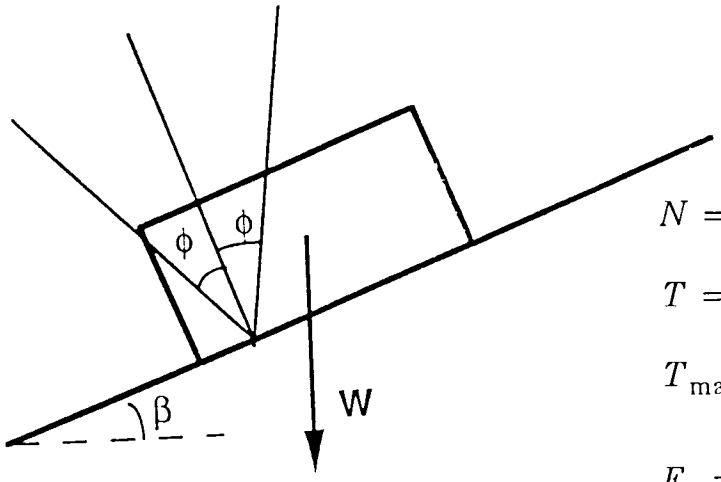

$$N = W \cdot \cos\beta$$

$$T = W \cdot \sin\beta$$

$$T_{max} = N \cdot tg\,\phi = W \cdot tg\,\phi \cdot \cos\beta$$

$$F_s = \frac{T_{max}}{T} = \frac{tg\,\phi}{tg\,\beta}$$

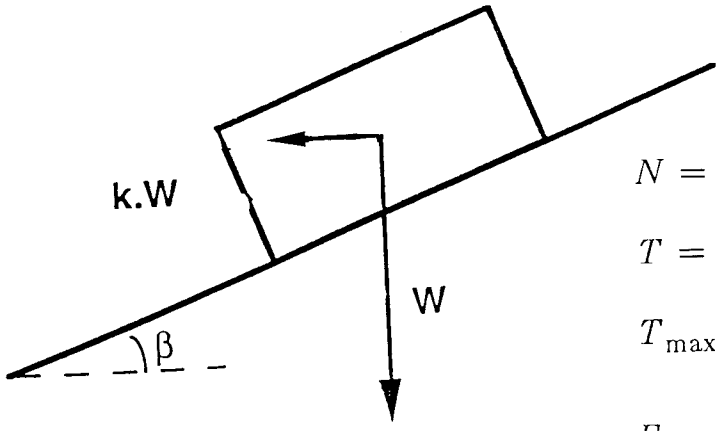

$$N = W \cdot \cos\beta - kW \cdot \sin\beta$$

$$T = W \cdot \sin\beta + kW \cdot \cos\beta$$

$$T_{max} = N \cdot tg\,\phi = W \cdot tg\,\phi \cdot (\cos\beta - k\sin\beta)$$

$$F_d = \frac{T_{max}}{T} = tg\,\phi \cdot \frac{1 - ktg\,\beta}{k + tg\,\beta}$$

Figure 16 : *Sliding of a block on a slope: static (top) and pseudo-static (bottom) cases (Adapted from Mèneroud, 1993)*

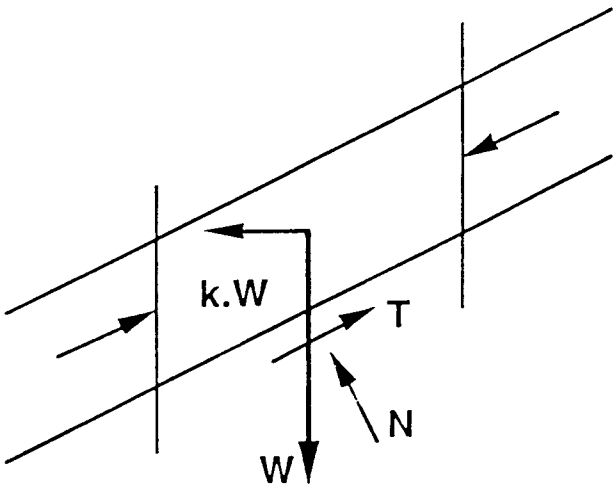

$$N = W \cdot \cos\beta - kW \cdot \sin\beta$$

$$T = W \cdot \sin\beta + kW \cdot \cos\beta$$

$$T_{max} = N \cdot tg\,\phi = W \cdot tg\,\phi \cdot (\cos\beta - k\sin\beta)$$

$$F_d = \frac{T_{max}}{T} = tg\,\phi \cdot \frac{1 - ktg\,\beta}{k + tg\,\beta}$$

Purely frictional soil (tgϕ)

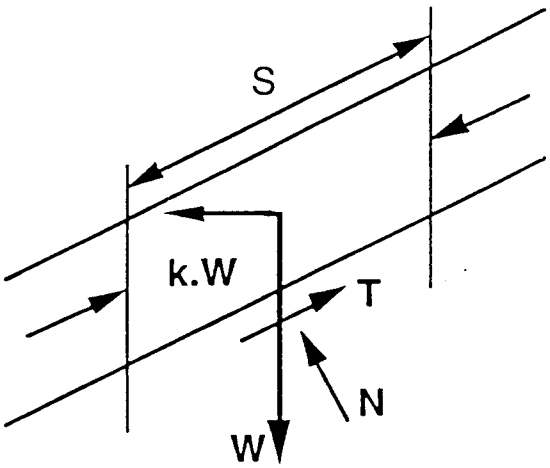

$$N = W \cdot \cos\beta - kW \cdot \sin\beta$$

$$T = W \cdot \sin\beta + kW \cdot \cos\beta$$

$$T_{max} = C_u \cdot S$$

$$F_d = \frac{T_{max}}{T} = \frac{C_u}{\gamma h} \cdot \frac{1}{\sin\beta + k\cos\beta}$$

Purely coherent soil (Cu)

Figure 17 : *Sliding of a plane soil layer along a slope in the pseudo-static case: cases of a cohesionless, frictional soil (top) and of a purely cohesive soil (bottom) (Adapted from Mèneroud, 1993)*

From single slope analysis to microzoning map:

The starting point should always be a landslide hazard map for static conditions, based on three main factors: geology, topography, and hydrogeological conditions. In such maps, the various slope failure hazards are classified according to their type, and according to the hazard level. Such a mapping presently requires a lot of "engineering judgement", most often based on a thorough regional work and experience. The hazard in usually ranked in several categories, depending on the value of the static safety factor F_S. For instance in France, four categories are identified, corresponding to the following ranges for F_S :

$2.0 < F_S$: negligible hazard
$1.5 < F_S < 2.0$: moderate hazard
$1.25 < F_S < 1.5$: significant hazard
$F_S < 1.25$: high hazard

Accounting for additional seismic actions may then be done through the computation of ratios F_d / F_S , which allows to obtain simply the new, pseudo-static safety factor F_d, on the sole basis of the slope angle and of seismic coefficient. Then the ranking of the hazard is made according to the values of F_d. However, the bounds between the different hazard levels are not the same as in the static conditions: since seismic loading is only an accidental loading, the bounds may be slightly reduced; for instance in France, the reduction with respect to static conditions is 15 %, which leads to the following ranking:

$1.70 < F_d$: negligible hazard
$1.30 < F_d < 1.70$: moderate hazard
$1.10 < F_d < 1.30$: significant hazard
$F_d < 1.10$: high hazard

For fixed mechanical parameters (ϕ for instance for cohesionless soils, or Cu for purely cohesive soils), the various bounds given for F_S and F_d for the different categories of hazard, correspond to various slope angles, β_S and β_d respectively. Then, it is possible to construct abacus allowing to simply shift from static bounds β_S to pseudo-static bounds β_d, depending on the value of the seismic coefficient k.

3.4.3 Newmark method

When the loading action is specified as a time history accelerogram, and when the soil parameters are known well enough, a widely known method is the Newmark method, which is intended to provide estimates of final residual displacements of the moving mass along the slope. Its principle is the following:

- a given instable mass loaded by a given accelerogram will start moving only when the acceleration exceeds a critical level. For the geometries displayed in Figures 16 and 17, this critical acceleration level a_C may be easily computed since it corresponds to a pseudo-static safety factor equal to 1.
- each time the acceleration exceeds a_C, the motion is accelerated; inversely, each time the acceleration falls below a_C, the motion is decelerated and possibly stopped because of resisting forces.
- Newmark analysis thus simply consists in computing and adding the total displacements produced by all the discrete time periods where acceleration exceeds that threshold value a_C, according to the schematic procedure displayed in Figure 18.
- the final outcome of such an analysis is the total residual displacement X_f at the end of the accelerogram, and to compare it to some a priori values to decide whether the hazard is significant or not. It is often admitted that threshold values of 10 cm in soils and of 2 cm

in rocks are reasonable criteria.

The final displacement X_f obviously depends on the characteristics of the accelerogram (frequency contents, duration, ...): it is therefore wiser to perform that kind of analysis with several different accelerograms.
The same kind of analysis may be applied with much more sophisticated numerical codes, including pore pressure, non-linearities, 3D geometry, etc...; one must always keep in mind, however, that the reliability of the final results is basically related with the reliability and precision of the input parameters.

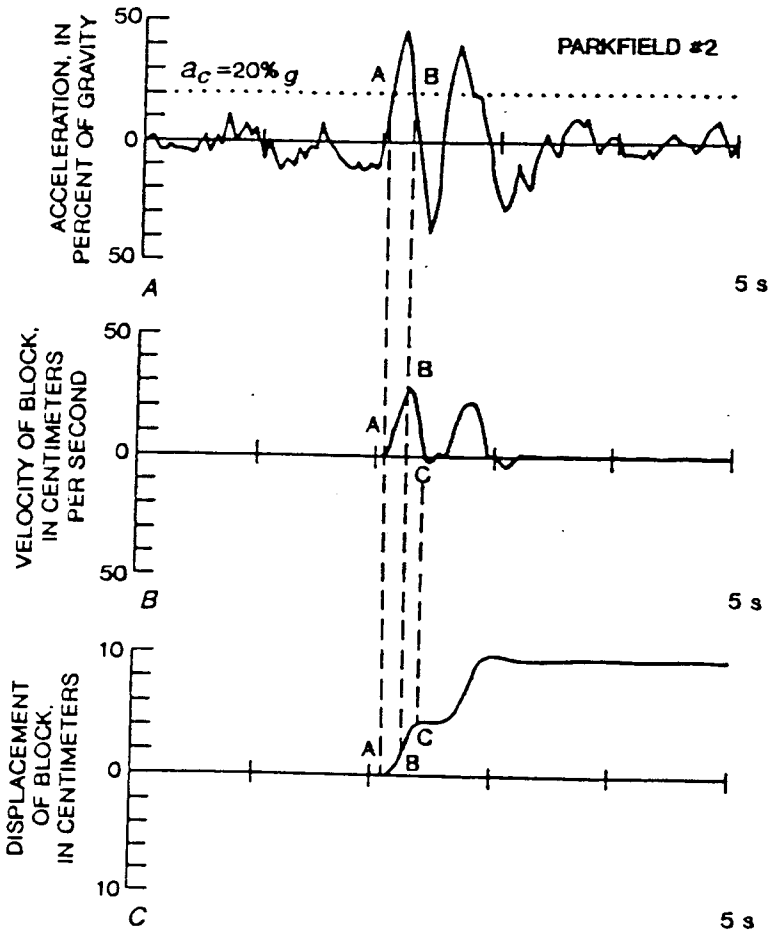

Figure 18 : *Newmark analysis . a) (top) strong motion record used for the analysis, on which a critical acceleration level of 0.2 g for a hypothetical slope has been superimposed. b) (medium) velocity of the sliding block versus time. c) (bottom) displacement of block versus time: at point A, ground acceleration first exceeds the critical acceleration; at point B, block reaches its first maximum velocity; at point C, the first motion ceases and block comes to rest (After Keefer and Wilson, 1989).*

4. CONCLUSIONS: RECOMMENDATIONS FOR MICROZONING STUDIES

As illustrated in this text - *which is by no means a comprehensive review of all proposed methods* - , there exist a lot of different techniques allowing to predict the occurrence of liquefaction or slope instability, and to obtain estimates of their damaging consequences. Their cost varies a lot from one to another; the preliminary information they require is not always available; the results they provide are more or less quantitative, not always comparable, and cannot be systematically used in a straightforward manner in a given regulatory context; their use sometimes requires a significant degree of expertise that is not always met. As a consequence, a microzoning study also require at first a methodological choice, depending on the available information, budget, and on the actual risk level of the zone under study.
In both draft microzoning guides presently under discussion (AFPS and ISSMFE), three microzoning levels or grades are proposed, corresponding to different levels of coverage, accuracy, and cost. The present section will list the techniques that are recommended for each of these three grades.
In any case, as for ground shaking site effects, the necessary prerequisite before any microzoning work is the establishment of a detailed geological map for the site under consideration: all the *existing, and readily available*, geological, seismological and geotechnical information should be compiled, and incorporated in a detailed geological map, the scale of which should be at least 1/25000 and preferably 1/10000 to 1/5000, depending on the available existing information. Such a map should include, in particular, information on slope angles (from topographical maps), some rough characterization of the mechanical strength of surface formations, and should pay particular attention to quaternary deposits, which were shown to be of primary importance for liquefaction hazard.

Level A (Most cursory level):

This is the crudest and lower-cost methodology; it is to be used in case of small funding and/or low risk level (these two aspects should in principle be linked...). The main goal, at such a low level, is simply to screen potential areas for slope instabilities or liquefaction.
The methods used at that level will therefore be limited to the simple empirical relationships listed in sections 2.2.2 (if information on grain-size distribution is available), 2.2.3, 2.3, 3.2 and 3.3 concerning susceptibility and opportunity of both hazards.
The result of such a screening should consist of two maps, one for liquefaction, the other for slope instabilities, where the hazard is ranked in a limited (3 to 4) number of categories: very low to low, weak to moderate, high to very high.
It is also recommended to identify the areas that could give rise to particularly important effects, where special investigations should then be required before any important development.

Level B (Intermediate, reliable level):

The reliability of level A microzoning may be significantly improved through the compilation of additional data sets or information. Because of the lack of uniqueness in the relationship between geological and/or geomorphological criteria, and geotechnical properties, susceptibility maps based only on those criteria generally do not provide definitive information of site specific evaluations, which thus require additional information. This information may come from aerial photographs (refined definition of geomorphological and geological units, flooding areas and sediment accumulation, landslide inventory, detailed topography,...), cheap field studies to better identify and classify the relevant attributes of geological formations, historical

Scientific Technical Report STR 95/TK
DOI: 10.2312/GFZ.b103-95tk7

documents or field interviews for past events, engineering reports issued for private projects ...

The major difference between level A and level B methods is that level A relies on existing, *readily available* (generally published) information, whereas level B incorporates the additional gathering of also existing, *but unpublished*, data from the files of government agencies, private industry, etc. (bore-hole logs, geotechnical reports, ...). Although this distinction between levels A and B may appear minor, the amount of effort - and expense - required for collection of data may be sometimes many times greater in level B.

Such a refined, more reliable information allows, at least, a better use of the Tables II and III, as well as of Figure 8, for liquefaction hazard, and a use of empirical statistical estimates as presented in section 3.4.1 for slope instabilities.

Where sufficient data are available, some simple computations may then be performed, such as the pseudo-static analysis presented in section 3.4.2, and the Chinese and/or Seed and Idriss procedures (sections 2.4.1 and 2.4.2).

Level C (Most reliable level, or detailed level):

When the risk is very high and the available funding too, the improvement of the reliability and precision of results obtained at levels A and B requires to perform specific geotechnical tests. The basic difference between level B and level C microzoning is that the latter require additional geotechnical investigations such as new drillings and *adhoc* testing of rock and soils (in situ or in laboratory). For liquefaction hazard, in-situ tests (SPT, CPT) are generally preferred, since they can circumvent the difficulties in obtaining *undisturbed* samples for lab tests.

Following these additional investigations, refined analyses may be carried to estimate the hazard potential: Any kind of *validated* numerical procedure or analytical model (not only those few mentioned in sections 2.4 and 3.4) can be used to obtain quantitative estimates of hazard potential, provided that they are used within their validity limits, and provided that they are fed with accurate input parameters: this, in practice, restrict their use by experienced practitioners.

Such analyses are usually performed on a site specific basis; however, if sufficient holes are drilled, tests conducted, and analyses made, reliable microzonation maps could be compiled. When such maps are established, and areas of high hazard identified, such microzoning may also include some indication on the possible remedial measures either to stabilize the slopes (retaining walls, drainage, nailing, ...), or to lower the liquefaction potential (pumping, drainage, compaction ...).

The amount of effort and expense required for level C methods are therefore many times greater than for the Grade 2 mapping.

Concluding remarks

As outlined throughout this presentation, and more particularly for landslide hazard, the available methods to obtain quantitative hazard estimates are still very rough, and undergo many uncertainties and scatter; they are very often much nearer to recipes than to rational approaches. They should therefore be constantly discussed and confronted with each other, in order to be improved.

However, the extreme importance of those induced effects in recent damaging earthquakes, calls for special efforts for applying right now, without waiting for results of further research, what we already know by performing "present day" microzoning studies. It is certainly not simple, and it is not limited to technical problems, since the results of such microzoning

studies are used *in fine* by local authorities, city planners, land-use specialists and civil engineers, whose background is very different and for whom the recommendations are therefore to be very clear and sound. Various programs recently launched in several countries should help in clarifying the methodology to be followed and the ultimate goals to be pursued.

ACKNOWLEDGEMENTS

This paper has greatly benefitted from two draft reports, not yet published, which have been made available by their authors: the "Guide méthodologique pour la réalisation d'études de microzonage" issued by the French Association of Earthquake Engineering, provided by A. Pecker, and the draft report of the TC-4 Committee of the International Society of Soil Mechanics and Foundation Engineering (ISSMFE) entitled "Seismic Zonation on Geotechnical Hazards", kindly made available by M.P. Luong.

REFERENCES

AFPS, 1992. Guide méthodlogique pour la réalisation d'études de microzonage. Draft report for the "Délégation aux Risques Majeurs", 60 pages (in French).

Finn, W.D. Liam, 1991. Geotechnical engineering aspects of seismic microzonation, Proceedings of the Fourth International Conference on Seismic Zonation, August 25-29, Stanford, California, 1, 199-250.

Ishihara, K., 1985. Stability of natural deposits during earthquakes, Proceedings, 11th Int. Conf. on Soil Mechanics and Foundation Engineering, San Francisco, Vol. 1, 321-376.

Iwasaki, T., K. Tokida, F. Tatsuoka, S. Watanabe, S. Yasuda and H. Sato, 1982. Microzonation for soil liquefaction potential using simplified methods, Proceedings, Third Int. Conf. on Microzonation, Seattle, Vol. 3, 1319-1330.

Keefer, D.K., 1984. Landslides caused by earthquakes, Bulletin of the Geological Society of America, 95, 406-421.

Keefer, D.K., and R.C. Wilson, 1989. Predicting earthquake-induced landslides with emphasis on arid and semi-arid environments, Publications of the Inland Geological Society, Vol. 2, 118-149.

Mèneroud, J.-P., 1991. Induced effects: liquefaction and slope instabilities, Université Européenne d'Eté sur les Risques Naturels, Session 1991: Les Tremblements de Terre, Udine-Frioul, 15-27 Septembre 1991, Edited by Pole Grenoblois d'Etudes et de Recherches pour la Prévention des Risques Naturels.

Seed, H.B., and I. M. Idriss, 1971. Simplified procedure for evaluating soil liquefaction potential, J. SMFD, ASCE, Vol. 111-3, 1249-1273.

Seed, H.B., and I. M. Idriss, 1982. Ground motions and soil liquefaction during earthquakes, Earthquake Engineering Research Institute, Monograph series, 134 pages.

Seed, H.B., K. Tokimatsu, L.F. Harder, and R.M. Chung, 1985. Influence of SPT procedures in soil liquefaction resistance evaluation, J. GED, ASCE, Vol. 111-12, 1425-1445.

Wakamatsu, K., 1992. Evaluation of liquefaction susceptibility based on detailed geomorphological classification, Proceedings, Technical papers of annual meeting of the architectural institute of Japan, Vol. B, 1443-1444.

Youd, T.L., and D.M. Perkins, 1978. Mapping of liquefaction induced ground failure potential, J. GED, ASCE, Vol. 104, n° 4, 433-446.

Exercise on liquefaction

Pierre-Yves Bard

Laboratoire Central des Ponts-et-Chaussées and Observatoire de Grenoble
LGIT/IRIGM - BP 53 X - 38041 Grenoble Cedex - FRANCE
Tel. +33 44 51 44 87, Fax +33 44 51 44 22, Email: bard@lgit.observ-gr.fr

The SPT (Standard Penetration Test) data obtained from two nearby locations are summarized in the following Table:

	Site A		Site B	
Depth (m)	**N**	**N1** (normalized)	**N**	**N1** (normalized)
3	15	23	13	20
4.5	21	26	13	16
6	25	29	13	15
7.5	30	33	13	14
9	34	34	13	13

At both sites, the water table is found at a depth of 1.5 m. The density of soils is 2 (while water density is, of course, 1).

1. Liquefaction susceptibility

Both sites are made of about 10 m of man-made fill placed over 7 to 10 m of soft clay underlain by stiffer soils. What is the expected susceptibility of that kind of sites, according to Tables I to IV?

2. "Chinese" procedure

2.1 For which intensity level liquefaction is expected to occur at sites A and B ? (Use the formula given in section 2.4.1 and parameters listed in Table V)

2.2 Combining the Chinese procedure and Figure 7, for which intensity would you expect large damage from liquefaction at sites A and B?

3. Seed and Idriss procedure

The peak ground acceleration expected to occur at both sites is about 0.30 g.

3.1 Estimate the average cyclic stress ratio τ_{av} / σ'_v expected to occur at each site and at all depths. (Compute the depth dependent coefficient r_d with the approximate formula $r_d = 1. - 0.015\ z$).

3.2 Put the corresponding values on Figure 1 below, showing the boundary between liquefiable and non-liquefiable areas for different magnitudes. Comment your results.

3.3 Estimate the safety factor at sites A and B for a magnitude 8 earthquake.

4. Liquefaction potential index

From the safety factors found in 3.3, and from the definition of liquefaction potential index (see section 2.4.3 and remember the nature of soils beneath 10 m), do you expect large damage at sites A and B for a magnitude 8 event?

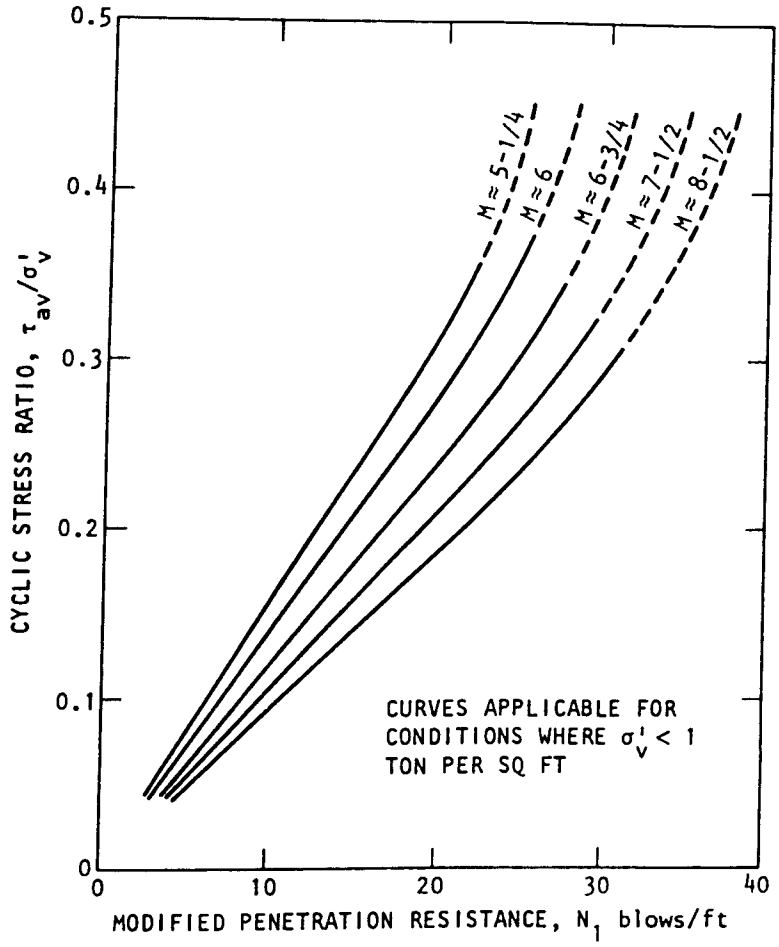
0.5
0.4
0.3
0.2
0.1
0
CYCLIC STRESS RATIO, τ_{av}/σ'_v
M≈5-1/4
M≈6
M≈6-3/4
M≈7-1/2
M≈8-1/2
CURVES APPLICABLE FOR CONDITIONS WHERE $\sigma'_v < 1$ TON PER SQ FT
0
10
20
30
40
MODIFIED PENETRATION RESISTANCE, N_1 blows/ft

Exercise on slope stability

Pierre-Yves Bard

Laboratoire Central des Ponts-et-Chaussées and Observatoire de Grenoble
LGIT/IRIGM - BP 53 X - 38041 Grenoble Cedex - FRANCE
Tel. +33 44 51 44 87, Fax +33 44 51 44 22, Email: bard@lgit.observ-gr.fr

Construction of simple curves to extrapolate from static to pseudo-static conditions

1. Static case

Recall the expression of static safety factors Fs for slides in slopes made of a) cohesionless soils and b) purely cohesive soils.

Let us denote as β_S the slope angle corresponding to the boundary between two zones, characterized by a given value of safety factor Fs .

2. Pseudo-static case

Recall the expression of pseudo-static safety factors Fd for slides in slopes made of a) cohesionless soils and b) purely cohesive soils, when the seismic loading is characterized by an additional horizontal acceleration equal to kg (where is gravity acceleration).

Let us denote as β_d the slope angle corresponding to the boundary between two zones, characterized by a given value of safety factor Fd. Compute, in both cases (a and b) the ratio Fd (β_d) / Fs (β_S). Is it depending on soil properties (frictional angle ϕ or undrained cohesion Cu)?

3. Shifting from case 1 to case 2

It is estimated that lower safety factors are acceptable for seismic loading, corresponding to an "accidental" situation. Therefore, for a static zoning corresponding to boundary values F^j_s, one generally admits that the corresponding pseudo-static zoning should correspond to boundary values F^j_d equal to 85 % of F^j_s.

Derive the relationship between β_S and β_d , in a) the purely frictional case and b) the purely cohesive case.

Construct abacus allowing to read directly β_d from β_S in the two cases.

Case studies of earthquake damage: Lessons to be learned

by

Peter BORMANN and Ingo KAPP

1. Earthquake effects

Earthquakes continue to be a scorge of mankind. The cause death or injury to millions of people each century, rubble thousands of villages and twons to ground, devastate landscapes and cause disrupting effect to many developing economies in particular. On the average 10 000 people die each year due to earthquakes and hundreds of thousands are left homeless.

A UNESCO study gives 350 000 deaths between 1926 and 1950 and damage losses amounting to $ 10 billion. But single strong events such as the 1976 Tangshan earthquake in China may cause human as well as material losses of the same magnitude. A repeat today of the San Francisco, California, earthquake (magnitude 8.3) which in 1906 destroyed buildings with cost translated in 1976 dollars of almost $ 170 million and took 700 lives probably would cause $ 24 billion in damage and about 10 000 death and 40 000 hospitalized injuries /1/.

Rapid population growth, urbanization and industrialization have increased earthquake risk in many parts of the world. Previously unknown kinds of seismic events such as earthquake induced by the construction of large dams and water reservoir (e. g. Koyna high dam in India) or due to the excavation of mines have locally increased seismic hazard in regions which have traditionally been considered aseismic. And only very recently a number of devastating earthquakes in countries which were thought to be low-risk areas or not seismically active at all, have alarmed the public. The major earthquake which struck the highlands of Yeman around Dhamar on 13 December 1982, e. g., was the worst earthquake for 16 centuries leaving about 400 000 people homeless /2/. And the Guinea earthquake of 22 December 1983 which killed some 300 persons, injured at least some 1 500 people and destroyed 16 villages /3/ occurred in an area with no reported seismicity. Both events have made clear that long repeat times between major earthquakes and insufficient or even missing historic records of such events may result in erroneous evaluations of the seismic hazard and complete neglectance even of most simple and cheap precautionary building measures or land use regulations.

Even in some permanently earthquake prone countries the wide-spread lack of public awareness of primary and secondary causes of destructive earthquake effects and their perseverance to traditional building and settlement habits causes many avoidable physical devastation and loss of life. As an example, the destruction of the village Lice in Turkey following an earthquake in September 1975 was greatly increased because of its location. It was built on the site of a former landslide and leaning against a cliff. A large number of rocks tumbled down from the top of the cliff, crushing houses and killing their occupants /4/. Even in highly developed countries such as the United States proper land use planning is some times grossly neglected. In San Francisco, e. g., newly developed suburbs have been placed directly over the active San Andreas Fault and in Anchorage, Alaska, extendes communities with private houses had been build on completely unstable grounds close to the ocean. During the large 1964 Alaska earthquake hundreds of these houses have been tumbled and crashed due to ground failure.

From these and other detailed case studies of earthquake effect conclusion can be drawn with regard to the main causes of seismic hazards, appropriate, land use regulations and suitable building measures.

Seismic hazards may be classified into four types:

1. Fault rupture
2. Ground shaking
3. Trunamies and seiches
4. Secondary hazards such as land slides, soil liquifaction and ground failures, floods from dam failures and fires

Most of these hazards man cannot influence directly. But he can significantly reduce the risk connected with them through appropriate physical land-use planning and regulation as well as engineering measures and building codes.

2. Land-use regulations

Along seismically active faults land-uses should of - as a general guide - be confined to open space, low density functions such as parks and agriculture. Where such fault cross populated areas, zoning regulations should establish building line set-backs from fault lines and specify permissible building types through appropriate building codes. The regulated set-back should be larger for more ciritical structures such as power plants, hospitals, schools, etc. Never a construction should be placed accross active faults.

Damage from ground shaking is probably the most widespread of all categories of damage caused by earthquakes. It is also the most difficult to predict and quantify. As already outlined in previous lectures seismic zoning and microzoning provide qualitative guidelines for damage probability due to ground shaking. It does not, however, provide exact quantitative estimates for complex engineering programmes although the very generalized approach of characterizing ground firmness to assess the gross probable effects of shaking appears be adequate for land-use-planning purposes. As compared with average ground conditions the intensity of ground shaking is amplified up to one degree over loose soils and reduced up to one degree over outeropping formations of well consolidated (hard) rocks with an emphasis of low-frequent vibrations in the first case and more high-frequent vibrations in the latter case. Zoning regulations should, therefore, be extremely strict in preventing in particular the erection of high-rise buildings with long resonance periods on loose, and especially deep, unconsolidated soils. If it is not possible to restrict development on such ground completely only low density, low rise development should be allowed and adequate reinforcement be required even for modest structures.

During earthquakes loose uncompacted materials may also cause landslides or soil liquifaction. Highly water-saturated soils or with low ground-water table, respectively, are particularly risky in this context. They should be avoided as building sites in earthquake-prone countries where ever possible and economically feasible.

There are also areas particularly vulnarable to tsunamies such as shallow concavely shaped beaches, v-shaped coastal inlets etc. In case of existing tsunami potential, development should be restricted or regulated for such areas or at least rational evacuation schemes should be designed and enforced in connexion with an existing tsunami warning system.

3. Building regulations and engineering measures

Although most of the global disaster losses occur in developed countries, the proportional losses in terms of percentage of GNP are much higher in developing countries. In particular the death toll claimed by disaster in the least developed countries is (after /5/), perhaps a hundredfold higher than in the industrialized countries. Insufficient housing conditions and the lack of appropriate building materials and techniques are a major reason for this. By far the most seriously affected structures are non-reinforced adobe and masoury dwellings. They are the most common type of housing in

developing countries. They frequently collapse completely even in case of relatively modest ground shaking as in the case of the Dhamar earthquake burrying their inhabitants under a heap of rubble and dust. Houses in the Dhamar area, e. g., are of simple construction: stone bricks laid one on top of the other, without using metal or concrete strengthening materials. They are mostly built on loose soil on mountain slopes without any deep foundations. Ceilings and flat roof tops are normally supported by girders which are laid on the stone walls without anchoring, tie-bands, shear and torsion resisting braces. Simple struts between girders and supporting columns may already greatly enhance the structure's resistance against ground shaking and prevent its total collapsing. Adequatic tie-bands and braces framing the sections of masoury, solid or hollow brick or concrete slabs convert them into units which react jointly to the ground shaking and absorb the shear energy more effectively. In case of the Argentine earthquake of 23 November 1977, e. g., almost all one- or two-storey dwellings reinforced this way survived virtually undamaged despite of significant ground acceleration ($\leqq$ 0,17 g) while the non-reinforced adobe and masoury dwellings were heavily affected /6/. In another lecture elementary techniques of earthquake resistant design of rural houses in developing countries will, therefore, be dealt with in more detail. Some general recommendations that may be helpful in reducing earthquake hazard in typical single-family houses are (after /7/):

- Basements and open first-floor levels should be adequately braced. Plywood sheathing is valuable for interior bracing of wood frame houses.
- Foundations and studs must be watched for dry rot and termite damage.
- Roofs and ceilings should be as light a construction as the climate allows.
- Foundation ties should be provided for all types of foundations.
- At least one fire extinguisher should be provided in the house.
- Closets, lighting fixtures and heavy furnitur should be fastened to wallstuds.
- Gas heaters in basements and elsewhere should be strapped to walls.
- Flexible joints should be provided between the utility lines (particulary water) and outside mains.

Even in industrialized countries where modern building materials and techniques are easily available the non-proper execution or inappropriate design of structures such as precast concrete panels which are not properly tied together or heavy concrete roofs and ceilings may have disastrous consequences and result in a total collapse of large structures. On the other hand, well-framed structures may not collapse even under strong shaking but turn-over as a whole due to insufficient foundation and ground failure. Also the shape of a building (or its structural elements) and its aspect ratio (basement width as to height) may adversely affect its resistance against ground shaking. Buildings of circular shape are highly resistant. Window and door openings of trapeziform are more suitable than restangular ones. On the other hand buildings with regular outline (groundplan) and the center of mass falling together with the axis of inertia do resist better to earthquake forces than irregularly shaped structures where these two deviate from each other.

After all what was said above it is obvious that engineering precautions in construction of buildings vary greatly from country to country. They depend on climate, ground conditions, building style, size, avaible materials and techniques. One UNESCO study estimates that the additional cost to a one-family house in a medium intensity earthquake region is about 4 per cent while in areas of major earthquakes the seismic resistant design may add 10 to 15 per cent. From the point of view of earthquake resistance

building structures can be classified into the following basic groups (after /8/):

a) Masonry structures:

- Heterogeneous materials of widely varying strength (mud, adobe, stones, bricks, wood or steel beams);
- Weak and ineffective joints between the different materials;
- Main characteristics:
  - high rigidity
  - low tensile and shear strength
  - small ductility
  - low capacity for bearning reversed load

The earthquake resistance of this type of structure can be improved by more rational structural solutions with further use of cement, wood and/or steel for increasing the shear and tensile strength and for reinforcement of weak points.

b) Framed structures:

- Beams and columns linked together by moment resisting joints with walls in the space between the frames;
- The weak points are the joints and connexions between the members of the frame, especially between columns and girders;
- Main characteristics:
  - stress concentrations at joints
  - high rigidity of the infilling walls
  - instabilities can occur by buckling of columns and by lateral deformation causing an eccentricity

c) Framed structures with shear walls or braces in modern constructions:

- Lateral forces are carried by the shearing resistance of beams or shear walls extending over the height the building (shear walls, i. e. stairwell towers, vertical reinforced concrete, masonry-framed diaphragms e. g.);
- Problems: interaction and interconnexions between shear walls and frame elements

d) Box system structures:

- Shear walls along both axes of the building;
- Reinforced concrete, monolitic (tunnel form, creeping form, etc.), precast (large blocks, panels)
- Main characteristics:
  - high rigidity
  - resistance against shear deformation
  - produce torsion in case of long buildings
- Problems: bearing capacity of the panel joints under reverse horizontal loading and admissible deformations of seperate structural elements

e) Other types of structures:

- Suspended buildings (a core bears the total vertical and horizontal loads);
- Buildings with major discontinuities (flexible first story, change of stiffness at some elevation);
- Problems: The earthquake resistance of these structures is greatly influenced by their planning design

4. Recommendations with regard to the execution of utility systems

Additional damage, economic losses, human suffering and loss of life in connexion with earthquakes may not be caused primerily by building failures but rather by a breakdown of public utility systems. Since modern cities usually rely heavily on utility systems for their day to day activities, their disruption may lead to extreme disorder even in cases, when no direct loss of life or property is connected with it. This may, in turn, increase the potential for various secondary disasters and seriously hinder rescue operations, reconstruction and rehabilitation. Utilities such as energy transmission, transportation, communication, water supply etc. are networks comparing sources, transmission lines and distribution systems. Damage at certain points will affect large sections of the whole system.
Shorts in electric circuits or mains or leaks in gas or oil pipelines, e. g., may lead to the outbreak of fire and devastating conflagration as it was the case in the 1923 Tokyo earthquake (although there mainly due to the break of individual fire places). The break of water supply systems may not only cause water damage and reduce the water needed for eventual fire fighting but could also result in a breakdown of public supply and local industrial activities. The blockade of roads and streets by fallen trees or rubble of damaged houses as well as roads or railroads damaged due to ground failure may prevent rescue or fire fighting teams to reach the places where they are most badly needed in time.

The importance of earthquake-proof design and completion of utility systems increases with the level of industrialization and urbanization. CIBOROWSKI /9/ recommends, therefore, to consider the following rules in urban planning:

- Every urban district or part of an urbanized zone should have no less than two access roads;
- Major roads and streets should be integrated into a system offering alternative thoroughfares, alternative accesses to the major focal points in the city and alternative junctions with regional or national roads;
- Major roads should be wide enough to avoid blockage of traffic lanes by collapsed buildings;
- Major thoroughfares should avoid crossing areas of high risk, when feasible;
- Evacuation and emergency routes should be specially marked and protected against any incidental blockage;
- All potential bottlenecks should be supplemented by emergency by-passes and alternative routes;
- The distance of the buildings from the traffic lane should be equal to or greater than the height of the buildings;
- Two seperate traffic lanes are recommended;
- The width of the median green belt between traffic lanes should be, when feasible, equal to that of one traffic lane or even broader and usable, in an emergency, as an additional traffic lane, for pedestrian traffic (evacuation) or as an emergency storage area;
- Water pipelines and other infractructure elements/life lines should be placed under the median strip and not under traffic lanes;
- Trees along main roads should be planted at a distance from the traffic lanes to avoid blockage in case they fall.

To make the water supply and the energy transmission facilities earthquake-resistant the following may be recommended:

- To base the supply of water on more than one source, located if possible at a distance from one another;
- To develop additional emergency supply sources, i. e. deep wells, which may be regularly used as water supply sources for industrial purposes;
- To design the system as a number of closed circuits of mains and supply pipelines for each subdivision of the urbanized area. The closed circuit system, as opposed to the 'dead end' one, offers a chance that supply may continue from another direction when one particular pipeline is broken;
- To safeguard emergency water supply for fire extinguishing is important in all high risk areas, whether equipped with a water supply system or not. Important industrial plants and the most vulnerable public buildings should have, when ever possible, their own emergency source. In residual areas the problem may be partially solved by building open-air reservoirs;
- The local power-supply system should, when possible, be incorporated into a broader system of regional or national scale. If not, more than one supply source should be at service of the system;
- High-voltage power supply lines should have a safeguarded right of way in the form of an open belt of terrain, without any buildings;
- Public buildings, hospitals and other sensitive elements of the city should have their own emergency power supply sources. Major thoroughfares and evacuation roads should have emergency illumination systems supplied from an independent source;
- Within seismic active zones a district central-heating system is not recommended.

Selected references

/1/ OAKESHOTT, G. B.: Volcanoes and earthquakes.- Geologic violence, Mc Graw-Hill, Inc., USA, 1976.

/2/ UNDRO Newsletter, Geneva, March/April 1983.

/3/ UNDRO News, Geneva, January/February 1984.

/4/ UNDRO Newsletter, Geneva, Vol. 1, No. 1, August 1976.

/5/ United Nations Conference on Human Settlements. Vancouver, Canada (1976). Conference background paper A/Conf. 70/B/7. 24 February 1976.

/6/ UNDRO News, No. 6, May 1978, p. 5.

/7/ BOLT, E. A. et al.: Geological hazards.- Springer Verlag Berlin, Heidelberg, New York, 1975.

/8/ SACHANSKI, S.: Buildings: codes, materials, design. In: The assessment and mitigation of earthquake risk; UNESCO, 1978.

/9/ CIBOROWSKI, A.: Some aspects of physical planning for human settlements in earthquake-prone regions.- In: The assessment and mitigation of earthquake risk; UNESCO, 1978.

ASSESSMENT OF EARTHQUAKE LOADS FROM SEISMOLOGICAL PARAMETERS: DIFFICULTIES AND SOLUTIONS

Götz Schneider

Universität Stuttgart, Institut für Geophysik
Richard-Wagner-Straße 44, D-70184 Stuttgart

1. Requirements.

Actual earthquake regulations require response spectra considering the following aspects:

-- the regional seismotectonic situation,
-- the influence of geological underground, and
-- the statistical properties of seismic activity (Fig.1).

Relations have to be found between the different parameters describing the response spectrum - as given in Fig.1 - on one hand and characteristics of the earthquake source (as focal moment, magnitudes etc.) and the geological underground as shear wave velocity, density on the other hand. The macroseismic intensity is regarded as an integral description of earthquake effects. For analysis and synthesis it is useful to develop a system "earthquake effects" which allows to combine different source, medium and receiver effects (Fig.2).

In the frequency domaine it is common to describe "earthquake effects" as the output of a three unit system:

$$\underline{a^*(f)} = \underline{a_o(f)} \cdot \underline{Tr1(f)} \cdot \underline{Tr2(f)}$$

= Source spectrum . transfer f. (underground) . transfer f. (receiver)

f = frequency (Hz)

$\underline{a^*}$ = spectral density of the acceleration inside a building ($m/s^2/Hz \equiv m/s$);

2. Source effects.

Geometric parameters of the source as focal area and dislocation on the fault-plane determine together with the focal depth the basic level of the earthquake spectrum at lower frequencies (Fig.3). Focal depth ho or hypocentral distance s are used to describe the attenuation of the moment with distance from the

source. The focal spectrum can be described as acceleration by the following expression:

$$\underline{ao} = \frac{Mo.Ro(\vartheta, \delta, \lambda)\left[1 + \left(\frac{f}{fc}\right)^2\right]^{-1}}{4\pi\varrho(s,ho)\,cs^3} \cdot \omega^2 \qquad (m/s)$$

Mo = amount of the focal moment (Nm)
Ro = radiation pattern (strike,dip, rake angles)
fc = corner frequency (Hz), depending on geometric parameters of the source (e.g. source radius ro (km)) and the fracture velocity on the fault-plane (vFo = = K.cs (m/s); K = 0,8: fc ≈ vFo/ro (Hz);
ϱ = density (kg/m³);
s = hypocentral distance (m);
ho = focal depth (m);
cs = shear-wave velocity (m/s).

If the moment and the focal distance are assumed as constant the radiation pattern together with the fracture velocity will have an important influence on the seismic time function and its spectrum (Fig.4). The concentrated and strong effects of near surface thrust motions in comparison with the smaller, but more extended macroseismic effects in the case of strike slip motions are well observed facts.

Heterogeneities in stress and strength influence by their space and time distribution on the fault surface the high-frequency segment of the acceleration spectra (Fig.4 + 5). These phenomena have to be considered by statistical variations of the source time function (Boore, 1983; Kunze et al., 1986).

3. Transfer effects.

The radiated source spectrum is changed by different effects having their origin in the medium as well as in the receiver:

-- layering and other geological structures: interference phenomena depending on the geometric parameters, density and elastic parameters deform different parts of the source spectrum. Near-surface layersof small thickness and a high impedance contrast to the underlaying material have e strong influence on the spectrum between 1 and 10 Hz (medium frequency domaine, Fig.3);
-- absorptivity: the different aspects of absorption determine the high-frequency cut-off of the regarded spectra (Fig.3: HF; Boore, 1986).
-- linear damping as well as non-linear reactions of the building (as plastic deformation) change the shape of the receiver transfer function.

The transfer function contains the following elements:

$$\underline{Tr} = \underline{Tr1} + \underline{Tr2} \qquad \text{(d.l.)}$$

$$\underline{Tr1} = e^{-\alpha_s s} \cdot e^{-\pi \kappa f} \cdot f(J2/J1)$$

$$\alpha_s = \frac{\pi . f . s}{Qs . cs} \qquad (m^{-1})$$

Qs = "quality" factor (d.l.)

s = hypocentral distance (m)

κ = attenuation factor (not on distance depending) (Hz^{-1})

J = impedance of an underground unit

= cs. ρ

Tr2 = building seen as a filter response (d.l.)

ao.Tr1 = free field ground spectrum (m/s)

$$Ra = ao . Tr1 . Tr2 . \Delta\omega \qquad (m/s^2)$$

Tr2 = f(D*, γ)

D* = linear damping (%)

γ = ductility ratio

ω = angular frequency (s^{-1})

$\Delta\omega$ = bandwidth of the filter

4. Statistical problems.

Regarding the focal process it is known since Gutenberg & Richter (1944) and Lomnitz (1974), that magnitude distributions for a larger region containing different seismotectonic sources can be described by exponential distributions. Considering only a limited segment of a shear-zone the lower magnitudes follow such a distribution as well whereas the largest shocks at the same fault-system are separated from the smaller events by a hierarchical gap (Wesnous ky et al., 1983).

The main difficulty in forecasting the time function or the response spectrum of a future strong event consists in the changing internal structure of earthquake sequences, i.e. that the magnitude distribution changes significantly from series to series separated by differing recurrance intervals. This is demonstrated by Scholz (1990) for long time span observations collected for earthquake areas in Japan. The same kind of irreversible change has to be assumed considering the distribution of heterogeneities on a fault-surface. These irregularities in strength and stress drop control the acceleration content in the frequency interval above 1 Hz.

5. References

Boore, D.M., 1983:

Stochastic simulation of high frequency ground motions based on seismological models of radiated spectra.
Bull.Seism.Soc.Am. 73, p.1865-1894.

Boore, D.M., 1986:

The effect of finite bandwidth on seismic scaling relationships.
in: S.Das et al., eds.: Earthquake Source Mechanics, Geophys. Monogr. No.37, AGU, p.275-283.

Gutenberg, B., Richter , C.F., 1944:

Frequency of earthquakes in California.
Bull.Seism.Soc.Am. 47, p.185-188.

Kunze, Th., Langer, H., Scherbaum, F., Schneider, G., 1986:

Site dependent strong ground motion simulation.
in: Vogel, A., Brandes, K. (Eds.): Earthquake Prognostics, Vieweg, Braunschweig, p.157-177.

Lomnitz, C., 1974:

Global tectonics and earthquake risk.
Elsevier, Amsterdam-London-New York, 320 pp.

Scholz, Ch.H., 1990:

The mechanics of earthquakes and faulting.
Cambridge Univ. Press, Cambridge etc., 439 pp

Wesnousky, S.G., Scholz,Ch.H., Shimazaki, K., Matsuda, T., 1983:

Earthquake frequency distribution and the mechanics of faulting.
J. Geophys. res.88, p.9331-9340.

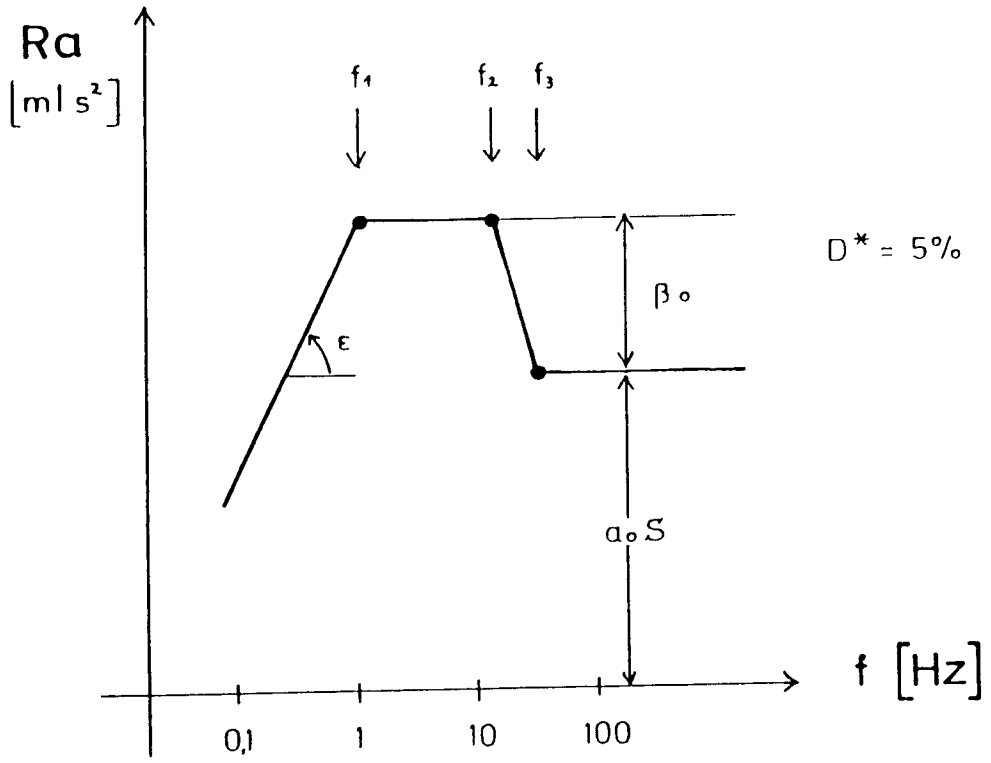

f	frequency (Hz)
Ra	acceleration response (m/s^2)
ao	peak ground acceleration (m/s^2)
S	soil amplification factor (d.l.)
βo	response factor (d.l.)
D*	damping (%)
ε	slope of low frequency branch of the spectrum
f_1 etc	corner frequencies (Hz)

Fig.1 Acceleration response spectrum and its parameters

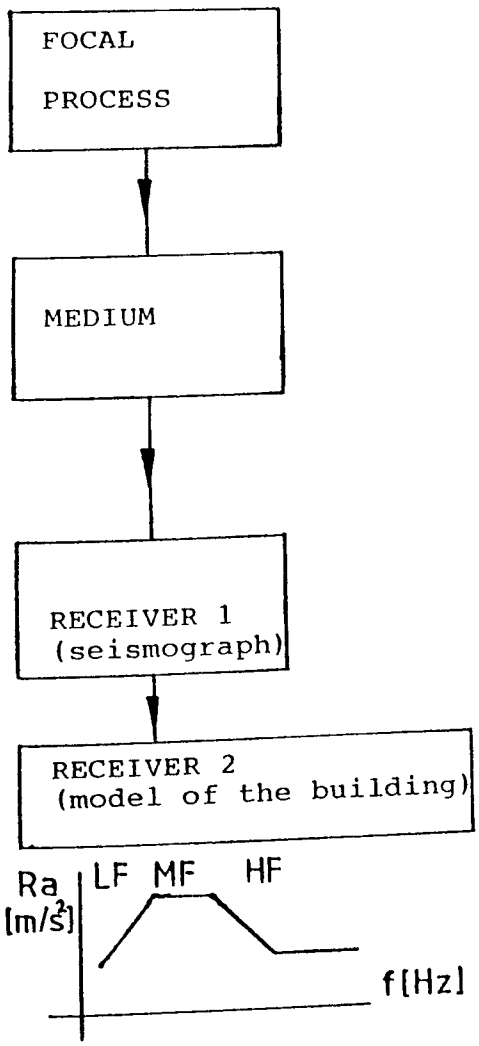

Moment Mo (Nm)
Stress drop $\Delta\tau_o$ (Pa)
Fracture veolicity $\overline{vFo}$ (m/s)

"Stick-slip": do(t) = dislocation-time function

Source signal: uo(t) displacement
vo(t) velocity
ao(t) acceleration

Layer thickness hi(m)
Shear wave velocity csi (m/s)
Density ϱ_i (kg/m³)
Absorptivity Qs_i^{-1} (d.l.)

Interference, absorption

Transfer function of the medium

Free-field signal uo(t)*Tr(t)

Seismogram: ah(t) (m/s²)

Transformation: ah(t) → ah(f)

Transformation by filtering

RESPONSE Spektrum

Fig.2 The system "Earthquake Effects".

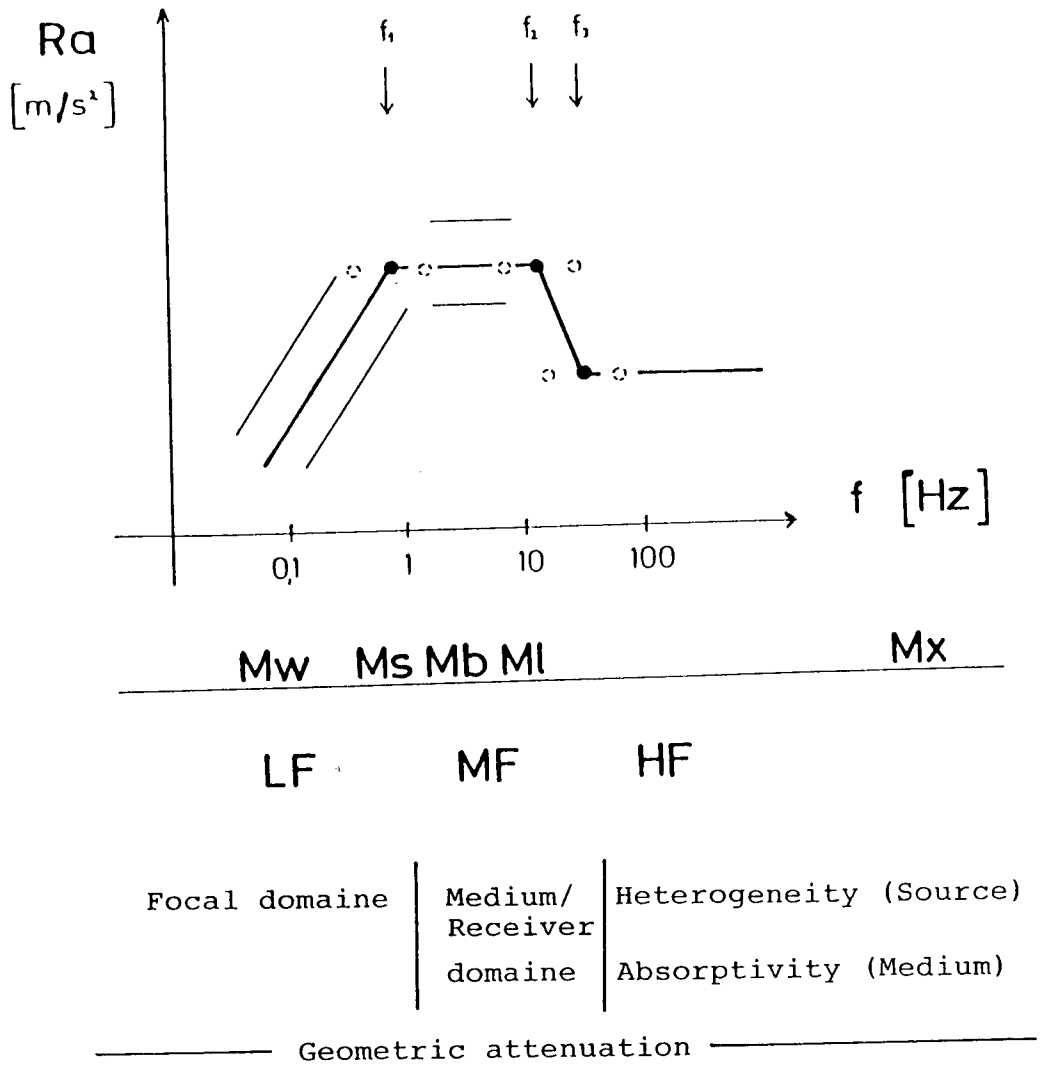

Fig.3 Important factors influencing the level of the acceleration spectrum.

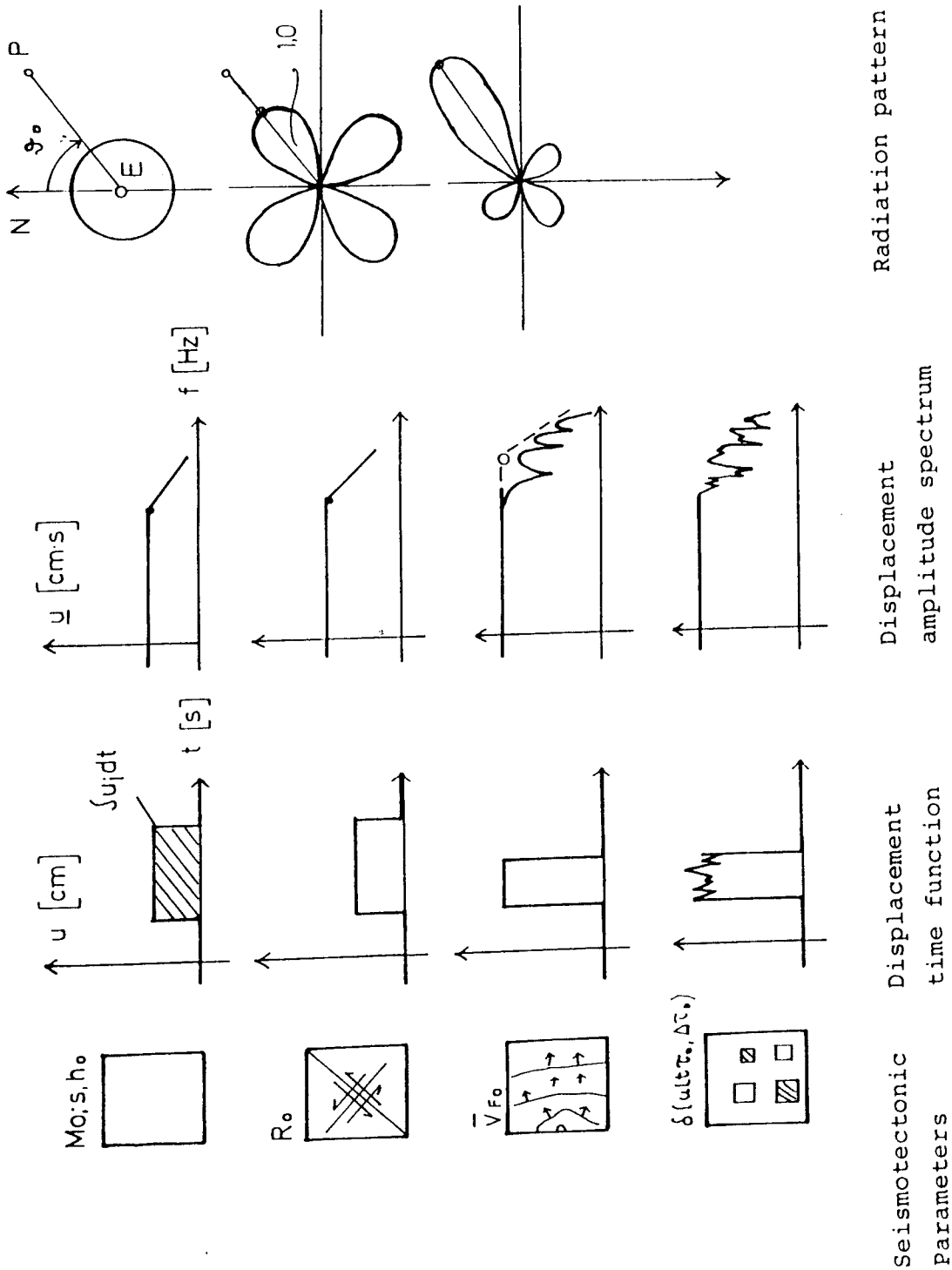

Fig.4 Influence of different seismotectonic parameters on the displacement source spectrum (Fourier amplitude density).

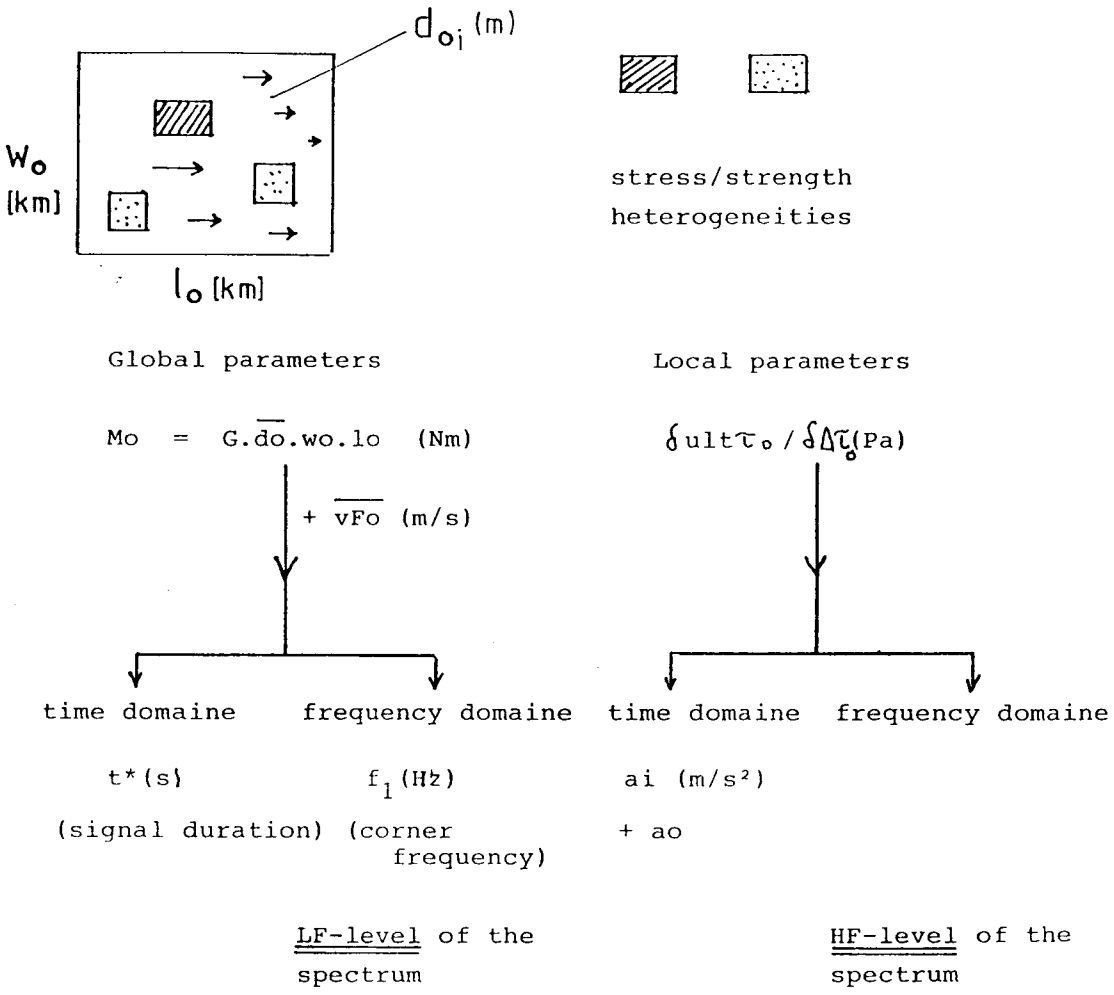

Fig.5 Low- and high frequency effects on seismic signals.

Earthquake Resistance of Traditional Buildings in Developing Countries

H. Schroeder and J. Schwarz
Hochschule für Architektur und Bauwesen Weimar - Universität, D-99425 Weimar

1. Importance of natural disaster reduction in Developing countries

Of all natural disasters, earthquakes cause the greatest amount of death and destruction. Generally they occur without any warning. Depending on their intensity, within a few seconds they can turn thousands of houses into a pile of rubble.

The greatest casualties occur where the population is poorest and the houses are built with cheap, sub-standard methods and materials, on dangerous sites such as slopes, sea shores, valleys below dams etc. Earthquakes of comparable intensities cause far less destruction and death in industrialized countries and rich areas of Third World cities, than in poor rural areas and slums of Developing countries.

An adequate housing is one of the basic needs of the mankind. After estimates of the UN today about one billion of people in the whole world cannot realize this right. Especially the living conditions in the large towns of most Developing countries are characterized by a very critical situation: there is a rapid growing of slums and spontaneous settlements. In such metropolis like Calcutta, Mexico City, Caracas about 50 % of the population live in squatter regions, in houses constructed in a very bad quality by accidentally available, often waste materials. Therefore in the case of natural disasters this part of population will belong to the first victims.

As a reason of this situation in Developing countries there is an enormous need of building materials for housing. Therefore the economy of the most Developing countries is characterized by a higher rate of growth in the building industry and the production of building materials than the whole rate of their gross domestic product. The construction sector has a great absorptive capacity especially for unskilled workers, particularly when labour-intensive methods are adopted. In several countries the construction sector plays the most important role of any sector in absorbing farm labours migrating from rural areas into the large cities. The construction serves as a bridge between unskilled workers of the informal labour market and the skilled labourers of the formal sector.

The great demand for building materials will be satisfied by a broad offer of the mostly informal sector. These small-scale production units work with negligible investments and without a business legal state on the base of self-acquired or trained skills. The part of this informal sector of the building material industry is estimated by 25 - 50 % of the whole production [1].

The building structures dominantly are erected by local-appropriated traditional techniques based on wood, bamboo, clay, brick, stone and concrete as the most appropriated building materials. Adequate to the character of the labour processes the building materials usually are unclassified, produced without regulations and with a broad variation of their parameters.
The main fields of using are one- and two-storied houses of about 30...70 m^2 area. From the viewpoint of the construction for these purposes the parameters of the building materials are

sufficient, if there are not special influences on the structures like storms, earthquakes, slope failures etc.

About 90...95 % of all construction activities in Developing countries are provided in self-help or neighbourhood organisation without any planning or state authorization. Only in the urban areas exist some building regulations. These regulations mostly are not realistic and often they date from the colonial time. But the skilled builder without professional education knows his traditional technologies and material parameters perfectly. He is convinced, that he doesn't need any state regulations. What is the character of these traditional building techniques, also traditional or indigenous architecture?

2. Types of traditional buildings and evaluation of their earthquake resistance

Traditional or indigenous builders are above all pragmatic. They design for economy in using materials and labour with appropriate space for work and domestic life, preservation of warmth in the cold, protection from the heat in the hot season.

Analyzing the essentially factors of indigenous architecture there is a division between "physical" and "cultural" determinists. Every structure exists as a cultural creation within a physical environment. On the other hand, culture - in this context popular architecture - is influenced by the environment. Physical determinants are such as climate, soils, ground surface etc. The indigenous builders considered, that in humid tropical climate constructions must allow a maximum of air circulation through all surfaces of the structure. This is possible by using light materials like bamboo, grass, wood etc. Conversely, in arid tropical areas with patterns of day-time heat and night-time cold structures need massive heat-conserving walls. So the physical constraints set the parameters in which cultural traditions or indigenous architecture can evolve or maintain themselves. This is evident in the wide variety of types and their variants which people choose to build [2].

Building traditions are not static phenomenons. If basic designs remain stable, growing wealth and changing standards of taste or prestige may lead to the substitution of materials. So old traditional techniques can disappear in urban areas and retain in the countryside: for instance more expensive baked bricks replace sun-dried bricks in wall construction. Also whole varieties of structures may disappear: with the sedentariness of pastoral nomads in central Asia till the middle of our century tents and yurts disappeared in this region.

2.1. Classification according to structural type and material

The main topic of the lecture is the earthquake resistance of traditional and indigenous buildings in Developing countries. Regarding this special type of damage influence buildings of the traditional indigenous architecturecan be classified into two main groups describing the load supporting character of the walls:

- *Massive wall constructions*: The heavy wall building material like stone, rammed or pressed earth, adobe, brick, has load bearing function;

- *Skeleton wall constructions*: A timber framework supports the loads of the roof and the ceilings, other materials like wood and wooden materials, stone, adobe, bricks have filling character. The skeleton also may be constructed of reinforced concrete.

2.1.1. Massive wall constructions

2.1.1.1. Massive stone walls

Massive stone constructions are found in all over the world in mountainous regions. The walls consist of one-side stratified stone and rubble laid in an uncoursed random pattern. They may be 60 - 80 cm thick depending on their height. The stones are laid dry or with a simple clay mortar. The inner surface almost is plastered with clay mortar to protect against the wind. To stabilize the corners stone quoins or long pieces of wood, often about the whole length of the wall are used.

The roof and floors of the one- or multistoried houses often are constructed by heavy materials. They are supported by wooden beams (in Central Asia popular) spanning the space between the stone walls and resting on poles recessed in the top of the walls. The space between the wooden poles is spanned by wood brush laid in right angle to the beams. These are topped with layers of reed and sealed with layers of clay, gravelistic clay at the bottom, fine-grained clay at the top. These flat roofs are provided with a slight slope so that the rain and snow-melting water channels to the roof edges.

In wood rich mountainous areas also walls constructed of alternating layers of squared timber and stone are found. The space between the timber is filled with stone and then packed with clay to produce an even, weather tight surface. The timbers are notched and cross-lapped so that they interlock at the corners. This "reinforcement" gives to the buildings the character of semi-framed structures.

Often in two storied houses the first floor completely or partly consisting of massive stone walls is combined with the second floor of other lighter materials.

2.1.1.2. Massive earth wall constructions

Vertical load- bearing elements: walls

Clay as wall building material is found in all regions of the world. For this purpose clay is used in hot dry and temperate climates. According to the different local technical experiences several indigenous techniques have evolved. The most important of them are [3]:

- shaped earth and cob
- rammed earth
- adobe and compressed earth blocks
- straw clay

In all these techniques the soil materials are unfired and air-dried. In the case of contact with water for a longer time the soil material is soaked, will become plastic again and loose its load-bearing capacity. Therefore water protective measures are necessary.

Shaped earth and cob (Usb.:gualjak)

The earth, often improved by addition of straw, other organic fibres or fine-grained rubbish of burnt bricks is shaped by hands into a wall using the same technique as that for pottery. If the earth material is shaped by hands into big balls and piled on top of one another and lightly packed by hand or foot, the technique is called cob. In both cases the result is a shaped monolithic wall. The cob also can be incorporated into a timber framework as filling material. This ancient technique is spread all over the world and still today widely used (Fig. 1).

Rammed earth (Span.: tapial or pise; Usb.: pachsa)

The prepared earth is filled in layers of about 15 cm height into form works and compacted by a rammer layer by layer. The height of the form works is about 1 m. After the first filling with compacted earth the form works are moved on along the foundation size till the first course of rammed earth is complete. Then the form works are put on the top of the first course and the compaction of the second course is providing in the same way (Fig. 2).

Adobe and compressed earth blocks (Russ.: saman)

The prepared earth of a plastic consistence, often improved by organic fibres or other additives, is moulded by hand into a (mostly wooden) brick form and dried at the air. The air-dried bricks are signified by the Spanish word adobe (Fig 3).

As an improvement of the adobe technique instead of being moulded by hand in a wooden frame, blocks are formed by compressing slightly moistened earth in a steel press and dried at the air. This technique has been developed in the fifties in the frame of a research program concerning rural housing in Colombia. In connection with this program the first and most famous portable low-cost soil block press (CINVA-ram) was developed [4] (Fig. 4). Compared to the hand-moulded block, the compressed earth block is very regular in size and shape and much denser. Meanwhile exists a broad variety of different soil presses. Also it is possible to produce soil blocks by powerful extruding machines similar to those used for the manufacturing of fired bricks.
In order to improve the stability and stiffness of the walls the adobes are laid with different bonding techniques.

Straw clay

The fine-grained earth is mixed with water until a homogeneous thick liquid consistence is attained. This muddy liquid is mixed with straw in order to form a clay film on every wisp. The building material conserves its straw like appearance. Now it is piled-up by forks along the building size to tiers of about 50 - 80 cm height till the course is complete. The first course must dry about one week till the next one can piled up (Fig. 5). Straw clay also can used as filling material for timber framed constructions.

Often the above mentioned wall building techniques are mixed in one construction without any constructive protective measures against seismic damages (Fig. 6).

Horizontal stiffening elements: roofs

Regarding the roof construction, for walls of earth materials generally all construction types are used and possible:

- In moist regions sloped roofs with overhangs the roof line to protect the upper parts of the walls against rain are to prefer.
- In hot dry regions two main construction types of roofs are used in the field of traditional architecture: flat roofs and curved roofs.

The flat roofs were described in connection with massive stone walls (see 2.1.1.1.)

Domed and vaulted (curved) roof constructions generally are employed where wood is scarce or the use of untreated wood can suffer from wood-destroying insects like termites. Domed and vaulted roofs are more labour- and material-intensive than flat roofs. This technique also requires skilled craftsmen. Domes are constructed on thick walls of square buildings, vaults serve the same structural purpose as domes but best they are built on rectangular plans. When completed, both domes and vaults are covered with a finish coat of mud plaster containing straw bits (fresh cow dung).

2.1.1.3. Fired bricks

The technique of firing clay to produce bricks for building construction is based on the princi-ple, that clayey soils undergo irreversible reactions, when fired at 850 - 1000 C. At these temperatures the soil particles are bonded together by a glassy ceramic material. In comparison with unburned air dried adobes and compressed earth blocks consisting of the same soil materials fired bricks are of higher compressive strength and irreversible against water and therefore weather-resistant.

Burnt brick production has reached a high level of mechanization and automation in many countries, but traditional small-scale production methods are still very widespread in most Developing countries. The wall building techniques are the same of those of unburned materials. In earthquake zones of lower intensity it is useful to stabilize the corners, crosses and junctions by reinforcing. In earthquake zones of higher intensity framed structures of reinforced concrete with brick filling are necessary.

2.1.1.4. Concrete hollow blocks

Concrete block construction is gaining importance in Developing countries, even in low-cost housing. It has become a valid alternative to fired clay bricks, stabilized soil, stone, timber and other common construction materials, providing that the ingredients are locally available, of good quality and economically [5].

The essential ingredients of concrete are cement, aggregates (sand or gravel) and water. The physical characteristics of the materials can be extremely diverse depending on the type and the relative proportions of these ingredients, the addition of other ingredients and components and also the production method. Concrete is thus a very versatile material which can satisfy a large variety of requirements, whether it is used for foundations, floor slabs, monolithic walls cast in-situ or prefabricating concrete blocks. The main characteristics of the most common types of concrete are:

- high compressive strength, resistance to weathering, impact and abrasion,
- low tensile (and bending) strength which can be overcome with steel reinforcement,
- capability of being moulded into components of any shape and size.

Concrete blocks are produced in a large variety of shapes and sizes, either solid, cellular or hollow, dense or lightweight, air-cured or steam-cured, load-bearing or non-load-bearing. Concrete blocks can be produced manually or with the help of machines. The wall building techniques are similar to those of brick walls.

2.1.2. Framework wall constructions

Framework structures are combined structures with a load bearing skeleton or frame (reinforced concrete, timber) and fillings (concrete hollow blocks, bricks, adobe, textiles etc.). The vulnerability of framed structures against earthquakes generally is lower than that of massive wall structures.

2.1.2.1. Lightweight structures

Lightweight structures like tents, huts, yurts are the typical housing structures of non- or semi-sedentary people like pastoral nomads in all regions of the world. According to the specific climatic and topographic conditions and the available materials there are very different and specific construction types. The most important demands to these structures are easy fitting and minimal weight to be able to transport them by animals if the food or climate conditions became bad and the people must move on.

The basic construction elements are a bearing timber skeleton of stakes and bars in different forms: vertical, T-shaped, bowed or vaulted and walls of light materials. These "wall building" materials in mountainous regions are of textile materials like woven goat hair, felt, cotton, woven reed and ropes. In even grasslands also bundled grass or reed is used..

A special type of lightweight structural housing-types is the yurt. It is an portable dwelling with a maximal amount of usable space within the structure by employing round walls with a domed roof. It is found in a zone stretching from Mongolia and Manchuria across the steppes and mountains into Central Asia to the south Russian steppe. The yurt is designed to withstand the most severe conditions encountered by pastoral nomads: Its framework and form provide exceptional stability against the wind. It is also earthquake-resistant.

2.1.2.2. Timber-frame constructions

Timber-frame constructions are a structural system in which all loads are carried by a wooden skeleton. The sections or truss bays shaped by the vertical and horizontal elements are filled by different materials.

The history of development of wood as building material goes back thousands of years into prehistoric times. Depending on the climatic situation today there are different types of timber-frame constructions:

- Cold and temperate wood rich zones: *log cabin construction*

The walls consist of straight trimmed or squared logs, junctioning by round scarving or saddle notch joints at the wall corners. The vertical door and window posts are connected with the log wall by groove and tenon joints [6].

- Temperate zones: *wattle and daub* (Fr.: torchis, Span.: bajareque)

Into the truss bays shaped by the vertical studs and the horizontal truss members are fixed vertical timber (oak) staves. Than a wickerwork of willers is woven around the oak staves to which is applied a plastic daub consisting a part of straw. Also possible is a closing of the truss bays by vertical or horizontal oak staves with daub infilling. A third method to close the truss bays is to turn long straw to a braid and roll it simultaneously around the staves by adding plastic clay. The staves now are fixed vertically or horizontally into the truss bays (Fig. 7 and 8). The vertical, horizontal and inclined timber elements of the load-bearing skeleton are connected by special traditional joints combined by wooden pegs. These joints and pegs give stiffness to the construction.

The filling of the truss bays also can be made of adobes or fired bricks, which are laid in a masonry bonding pattern. Often this technique is used as the second floor in combination with a massive wall construction in the first floor (stone, fired brick, adobe, rammed earth, straw clay; Fig. 9).

- Humid tropical zones: *timber / bamboo pole or frame buildings*

Timber / bamboo pole or frame houses are traditional in humid tropical zones, especially in Southeast Asia. Timber poles or whole bamboo culms are used as frame. The poles or culms are rammed into the ground or set into boreholes. In humid tropical zone the annual amount of rain is very high. Therefore a floor raised above the ground level at least 50 cm is useful. The frame consists of the vertical load bearing columns (poles or culms), connected with the horizontal floor beams and the trusses and purlins of the roof. Poles can be nailed. Bamboo joints usually are held together with lashes of sisal, rattan, coconut fibre etc., bolts or wooden pins.

The traditional houses are stiffened in both horizontal directions with diagonals between the columns and beams, so that the constructions can withstand to earthquakes or strong winds [7].

2.1.3. Prefabricated panel wall constructions

Generally, the construction of prefabricated panel houses requires the presence of a certain amount of skilled labour, capital, building regulations. Timber and concrete are the most important panel wall materials. The prefabricated wall elements are joined to stiff room cells or units. In this position they can support the loads of the roof and the ceiling.

2.1.3.1. Prefabricated timber panel wall constructions

A certain low degree of prefabrication also in traditional timber framed constructions is possible. There are two main systems of prefabricated timber houses:

- modular panel systems
- large size panel systems.

The modular panel system involves in-plant production of modular panels for floors, ceilings, walls and roof trusses. The large-size panel system is based on the producing of complete wall and floor systems. This system requires a heavy lifting and moving machinery and more skilled manpower. Also a certain degree of plywood industry like sawmills is necessary and therefore it has only a limited suitability for developing countries.

2.1.3.2. Prefabricated concrete wall constructions

Also there are numerous panel systems based on concrete as panel material. Fig.10 shows one of the type "Sandino" which is wide spreaded in Latin America.

2.2. Building types and vulnerability classes (EMS-92)

2.2.1. Classification of buildings in macroseismology

The behaviour of buildings (structures) under seismic conditions is mainly determined by the type of construction or, taking into account architectural and engineering items, by the structural system. The classification of buildings into different building types is of special importance when the severity of ground shaking has to be described in the case of damage inducing earthquakes or when historical earthquakes have to be interpreted to gain insight in the hazard of a certain region. Both tasks can be fulfilled with the help of intensity and their classification according to the different macroseismic scales (MM, MSK etc).

Macroseismic scales incorporate a simple and robust way of differentiating the earthquake resistance (vulnerability) and the response of buildings to earthquakes depending on the level of generated shaking. As it is stated in the introduction of EMS-92 (ed. Grünthal, 1993) "the macroseismic intensity is a classification of the severity of ground shaking on the basis of observed effects in a limited area", allowing the compression of verbal description of effects into a single symbol (number).

Previous versions of the MSK scale are restricted to so-called non-engineered buildings, classified into types A, B and C with the practical consequence that engineered buildings as well as monumental (massive stone) building (like churches, castles) have to be excluded from intensity assessment. With this crude definition different levels of vulnerability are subdivided, neglecting the condition of a building, e.g. the quality of workmanship, the structural regularity, the strength of material, the state of repair. It is clear that these conditions affect vulnerability of buildings and their ability to withstand seismic loads and thus it is necessary to consider these features as scaling conditions. In the case of damaging earthquakes intensity can only be assigned successfully, if the user is able to determine the probable vulnerability or earthquake resistance of building types in the study area.

With regard to engineering problems the basic assumptions of modern macroseismic scales is that for a certain building type there is a representative vulnerability class.
A vulnerability class itself can be interpreted as a crude definition of damage probability functions for a given number of damage grades in dependence on intensity.

One of the main innovations of the up-dated MSK scale, the European Macroseismic Scale EMS-92, is related to the new arrangement of building types in a generalized form by introducing vulnerability classes of different building types.

2.2.2 Resistance of traditional buildings to earthquake generated shaking

Regarding the vertical structural system, traditional (non-engineered) buildings can be classified as wall constructions. A further classification of the different types of these wall constructions (massive, framework, prefabricated panel) considering earthquake resistance as well as classifications of the macroseismic scales MSK and EMS-92 is given in Table 1. It can be concluded that macroseismic scales cannot represent the variety of existing structural systems. Obviously, previous scales (MM, MSK) define only major building types. But it has to be stressed that such a refinement could complicate the intended simple and robust nature of a scale, and thus more sophisticated classification of building types would require a basic knowledge of earthquake engineering from users.

The proposed vulnerability classes according to EMS-92 can be regarded as an attempt to recognize the scatter of vulnerability of one (global described) building type indicating the most probable class as well as the range to be expected under extreme conditions.
Traditional (non-engineered) buildings are falling into the range of vulnerability classes A to D. Therefore, the level of earthquake resistance is "naturally" limited. The level of earthquake resistance compared to engineered structures should be - with the exception of wooden structures - very low (bad), low (medium) and moderate (good). This becomes also evident considering statistically elaborated correlations between building type, the severity of ground shaking, and the observed damages (intensity).
Furthermore, it has to be accepted that earthquake resistance is significantly depending on:

- the kind of horizontal structural elements, particularly of its strength, stiffness and spatial stabilizing effect and
- the kind of non-structural elements and its effect on or interaction with elements of the structural system, resisting activated inertia forces.

Table 1 provides also an evaluation of earthquake resistance of roofs and ceilings.

Construction Element	Type of Building/ Material	Earthquake Resistance			BuildingType/ Vulnerability Class	
		good	medium	bad	MSK 81	EMS 92
Wall	*Massive wall constructions*					
	- massive stone walls			●	B	BCD
	- massive earth walls				A	
	- shaped earth/cob			●		
	- rammed earth		●			
	- adobe			●		AB
	- straw clay			●		
	- fired bricks			●	B	ABC
	- concrete hollow blocks			●	B	ABC
	Framework wall constructions					
	- lightweight structures	●				
	- timber frame constructions				B-C	
	- log cabin constructions	●				
	- wattle and daub		●			
	- adobe/ bricks infill			●		
	- timber/ bamboo pole or frame constructions	●				BC DEF
	Prefabricated panel wall constructions				B-C	
	- timber panel walls		●			
	- concrete panel walls		●			
Ceiling	- lightweight materials	●				
	- heavy materials			●		
Roof	- lightweight materials	●				
	- heavy materials (earth)					
	- flat roofs			●		
	- domes and vaults			●		

D - most likely vulnerability class EF - probable range BC less probable, exceptional case

Table 1 Evaluation of earthquake resistance of traditional (non-engineered) buildings - a comparison with classifications in modern macroseismic scales

2.2.3 Correlation between damage, intensity and building type

It is a convenient way to define the vulnerability of building types in terms of vulnerability functions, i.e. the severity of ground shaking (intensity) depending on damage-describing parameters (mean damage, mean damage ratio). The concept of damage probability distributions provides the logical link between statistical models of damage, buildings, and the macroseismic scales; but future research work is necessary to harmonize procedures of damage surveying and to adapt available results in order to generalize them in intensity scale-related definitions.
The macroseismic scale itself is finally a semi-quantitative representation of the probability distribution of damage where the scatter of results is covered by the verbal definition of quantities (few, many, most) and introducing an overlapping of quantifications.

The probability of damage occurrence can be illustrated either:

- by a set of probability distributions of mean damage or mean damage ratio versus earthquake intensities depending on building type (see Figs. 11 and 12), suitable mainly for insurance purposes;
- by typical frequency distributions of damage grades for different intensities or
- by distributions of mean damage grade or probabilities of a certain damage grade versus intensity, being closely related to the concept of macroseismic intensity (Fig. 13).

As it is known from the limited number of statistical investigations (damage surveys), damage probability functions of different building types show similar tendency (increase of damage with intensity) but they are different in respect of the shape of function (slope of damage progression or saturation versus intensity). A comparison of vulnerability functions in Fig. 11 (after [9]) indicates clearly the insufficient seismic behaviour of traditional non-engineered structures as weel as the improved earthquake resistance of structures incorporating a certain level of antiseismic design.

Recently published vulnerability curves considering basic material type and in general terms the load carrying system are given in Fig. 12 (after [10]). According to this report curves represent regularity conditions between regular and moderately irregular (i.e. conditions correspond to regularity level R_m according to EMS-92, Annexe B). Vulnerability curves for masonry (three types) and wooden buildings (two types), i.e. for traditional building types are shown in Fig. 12. They can be compared with those for modern/ engineered buildings types (reinforced concrete and steel structures) as in Fig. 11. Regarding the evaluation of earthquake resistance again it becomes evident that *framework wall* as well as *prefabricated panel wall constructions* can withstand higher seismic loads than *massive wall constructions*.

The probability of damage grade 4 (partial destruction) for the building types: dressed stone masonry, unreinforced brick masonry, non-seismic R.C. frame and ring-beam reinforced brick masonry is illustrated in Fig. 13 (after [11]) using results of damage surveys [12]. It can be concluded that buildings of the same basic material would suffer much less damage, if antiseismic measures (ring-beam or R.C. lintels etc.) are provided. This becomes much more evident by considering the definitions of intensity degrees according to EMS-92 [8] and by assuming that in many cases well-built adobe or stone buildings can be classified into vulnerability class B.

The following damage (as statistical means) can be expected:

- Intensity VIII: A few buildings suffer very heavy damage (damage grade 4).
- Intensity IX: Many buildings suffer very heavy damage; a few are destructed (grade 5).

Traditional buildings can withstand earthquakes of higher intensities, only, if antiseismic design principles and measures of strengthening are incorporated into the construction. This statement is especially true for buildings in high seismicity areas like Central Asia (Figs. 1, 6, and 9; Usbekistan) where seismic hazard maps and microzoning maps of major cities with highest population density have intensities even higher than 9 grade (MSK).

3. Strategies for improving the earthquake resistance of traditional buildings

Strategies for improving earthquake resistance contains technical, administratory and a to lesser extent scientific aspects. Experience and the recognition of earthquake lessons are the most valuable sources for the improvement of traditional buildings as well as modern ones.

3.1. Wall structures under horizontal (cyclic) loading

The basic strategies for improving the earthquake-resistance of wall structure can be explained by considering their behaviour under horizontal and cyclic loading. Tables 2a and 2b describe the failure mechanism and damage pattern depending on the type of structure and the direction of seismic action.

Nr.	Type of Structure/ *Seismic Action*	Failure Mechanism	Description of Damage Pattern
1	**Freestanding wall** *Perpendicular forces*	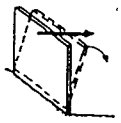	Overturning; resistance is depending on gravity loads (weight; mass distribution) and on tensile strength of mortar
2a	**Freestanding (unreinforced) wall:** small length-to-width ratio *In-plane force (shear)*	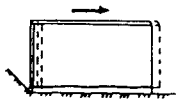	Sliding; horizontal cracking
2b	**Freestanding framed (unreinforced) wall:** moderate length-to-width ratio *In-plane force (shear)*	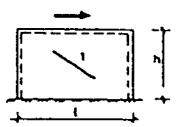	Diagonal cracking (1) in dependence on wall slenderness
2c	**Freestanding (unreinforced) wall:** larger length-to-width ratio *In-plane force (shear)*	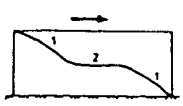	Diagonal cracking (1); horizontal cracking (2) in middle parts of wall

Table 2a Failure mechanism and damage pattern of freestanding walls

Nr.	Type of Structure/ *Seismic Action*	Failure Mechanism	Description of Damage Pattern
3a	**Wall enclosure without roof** ("open box") *Horizontal forces (perpendicular to wall B)*	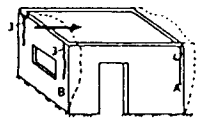	Bending of walls B and vertical cracking (3) Drift away from walls A (4)
3b	**Wall enclosure with roof** ("box") *Horizontal forces (perpendicular to wall B)*	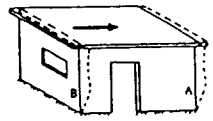	Bending deformations are limited Floor is acting as a slab; distributing horizontal forces into vertical wall elements (A) in dependence on span direction
3c	**Shear wall with openings:** *Horizontal cyclic forces*		Diagonal crossing cracks (5) in piers (critical section for shear cracks) Horizontal (6) or diagonal cracking in the jambs of openings and at the corners of wall
4	**Building** *Horizontal cyclic forces*	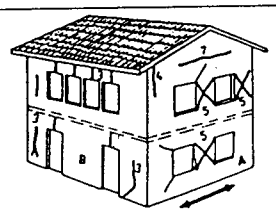	Diagonal cossing cracks (5); Vertical bending cracks (3) Horizontal cracking in gables (7) or partial collapse of unstiffened slender wall sections

Table 2b Failure mechanism and damage pattern of wall enclosures and building

The following types of structures are considered:

- the freestanding and framed unreinforced wall (Table 2a),
- the wall enclosure with and without roof, the shear wall with openings, and
- the building (Table 2b).

The wall structure can withstand horizontal inertia loads much more effective, if the building reacts as a box-like system. Deformations, especially the critical bending deformations can be reduced drastically, if the horizontal forces are distributed by floors or connected floor elements acting as one unit (rigid diaphragm) to the vertical wall elements.

3.2. Strategy 1: Antiseismic design principles (regularity)

The regularity is the basic property of an earthquake resistant construction independently of the type of material and structural system. Regularity should be considered in a global sense, i.e. regularity is more than just external symmetry in plan and elevation.
Regularity includes geometrical characteristics of a building (dimensions, height, number of storeys), mass and stiffness distribution as well as architectural (size of openings) and engineering aspects (measures within a structure to ensure a simple or, to a limited extent, controlled behaviour). Regularity means to transform experience and lessons from earthquakes into design and construction; it means to avoid design errors leading to an increase of vulnerability.

Basic rules for antiseismic design of traditional buildings (earth, stone, masonry) and potential design errors are summarized in Fig. 14 and Fig. 15, respectively.

Sketches of Fig. 16 should provide an idea of consequences which could be caused by unfavourable plan and openings:

- It is quite important to reduce the free length of walls to minimize deformations and bending cracks (see Table 2a). This can be realized by providing vertical elements: inner stiffening walls, cross walls or outer buttresses (Fig. 17).
  If the centre of gravity (mass) is far from the centre of stiffness, structure will vibrate in torsional modes which are critical for outer wall joints (Fig. 16).
  The creation of a compact uniformly stiffened wall system can also be regarded as a simple but very efficient method of strengthening.
- It is necessary to minimize the size and the ratio of opening area versus entire wall area. The distance of openings to the corners (joints) and between openings) should be as large as possible. Note that the pillars between the openings are the main energy dissipating zones a brittle structures having an extremely limited ability of collaps-free energy absorbtion.

3.3. Strategy 2: Repair and strengthening

Special strengthening techniques are related to the creation of a box-like structure independently of the building type (material, technology or load-carrying system).

Massive wall constructions

- In high seismicity regions it is recommendable to increase the strength of walls by different kinds of reinforcing (mesh of canes or bamboo). Large canes have to be tied together, vertical canes should be tied to horizontal elmenents (collar beams, roof beam and horizontal canes, Fig. 18.
- Vertical elements have to be joined together by ring-beam, floors, roofs and foundation. It is recommended to improve the intersection between walls by continuous horizontal reinforcement (collar beams or rough cut lumbers; Fig. 19) [13]. Therefore the natural conditions (wooden) are of importance. If timber elements are not available, pilasters have to be provided. These measures decrease the danger of drift, separation or partial collapse.
- Horizontal elements (floor slab) have to be rigidly connected with vertical ones to limit deformations by activating walls perpendicular to and also in direction of shaking. Roof of floor beams have to be bonded into the walls in a such manner that, between adjacent supports, stress concentrations are avoided. Often, the neglect of this support conditions leads to vertical bending cracks resulting in a failure of beam-bearing wall segments. Finally, such cracks can initiate the failure of the whole floor or roof.

Framework wall constructions

Earth structures can be strengthened very efficiently by framework techniques.

It is important to note that a such method is a practically mean to replace a brittle massive system by a more flexible, to some extent by a ductile construction. By this way, advantages of both systems are combined. Fig. 20 shows structural framework of wood and cane. In some cases prefabricated panels are added and filled with cane, bamboo or some kind of reed matting plastered over both sides with mud [13].

Earthquake resistance can be improved taking into account following simple rules:

- All elements should be well connected. In humid regions galvanised nails should be used preventing loss of connections due to rust; earth filling containing quantities of human acid should be avoided, otherwise, nails have to be replaced from time to time. The resistance of such structure is strongly dependent upon its age.
  Wood has to be protected against rot and termites or weather conditions. Wood or cane elements should preserved by painting or coal tar, especially those parts embedding in the foundation.
- The timber frame should be braced by diagonal members in the plane as well as horizontally in the corners at the top levels. Walls, corners, ribs and diaphragms have to increase global strength and to assure a proper load distribution.

The process of strengthening is often started after earthquake events as a consequence of damage and, therefore, associated with repair work. Often massive earth buildings of low seismic resistance are replaced by framework structures.

An example is given in Fig. 21 illustrating the the proposed construction type after 1990 earthquakes in East Kazakhstan; applied methods of repair are explained in more detail in [14]. A comprehensive damage analysis considering geological, seismological, hydrogeological as well as engineering features will be published under the title *Damage Catalogue of the 1990 Saisan Earthquake* by the German Society of Earthquake Engineering and Structural Dynamics [15].

The structural system shown in Fig. 21 consists of a wooden frame (horizontal, vertical elements with moderate sections), which is diagonally braced by a rib of timber bars. Straw clay is used as infill material.

4. Case Study: Central Asian Republics

In the fourth chapter of the lecture

- results of the engineering analysis of damage caused by the two main shocks of Eastern Kazakh Earthquakes in 1990, elaborated by a Kazakh-German specialist group [14, 15] and
- results of a IDNDR - mission to Usbekistan and Kyrghystan in 1993

are presented and used in the sense of a case study for discussion.

References

[1] UNIDO: The Building Material Industry in Developing Countries: an Analytical Appraisal Sectoral Studies No. 16, Vol. I, Vienna 1985.

[2] Szabo, A.; Barfield, T.: Afghanistan: an Atlas of Indigenous Domestic Architecture University of Texas Press, Austin 1991

[3] Houben, H.; Guillaud, H.: Traité de Construction en Terre. CRATerre; Marseille: Editions Parenthéses 1989.

[4] German Appropriate Technology Exchange (GATE). Soil Block Presses. Product Information. Eschborn 1988.

[5] German Appropriate Technology Exchange (GATE). Concrete Block Producing Equipment. Product Information, Eschborn 1991.

[6] Schreckenbach, H.; Abankwa, J.G.K. Construction Technology for a Tropical Developing Country. GTZ Eschborn, 1983.

[7] Janssen, J.J.A.: Building with Bamboo. Intermediate Technology Publ., London 1988.

[8] Grünthal, G. (ed.): European Macroseismic Scale 1992. Cahiers du Centre Européen et de Géodynamique et de Séismologie, Vol. 7, Luxembourg 1993.

[9] Sauter, F.; Shah., H.C.: Estudio de Seguro contra terremoto. Franz Sauter y Asociados LTDA, San José, Costa Rica, 1978.

[10] Cochrane, S.W.; Schaad, W.H.: Assessment of earthquake vulnerability of buildings. Proceed. of 10th WCEE Madrid 1992, Balkema Rotterdam, Vol. I, 497 - 502.

[11] Schwarz, J.; Grünthal, G.: The European Macroseismic Scale and its engineering aspects. Proceed. of 10th ECEE Vienna 1994.

[12] Spence, R.J.S. et al.: Correlation of ground motion with building damage: The definitions of a new damage-based seismic intensity scale. Proceed. of 10th WCEE Madrid 1992, Balkema Rotterdam, Vol. I, 551 - 556.

[13] Guidelines for earthquake-resistant non-engineered construction. IAEA, Tokyo, 1986.

[14] Taubajev, A.S.et al.: Engineering analysis of earthquake damage in catalogue-like form: Case-study of Eastern Kazakh earthquakes of 1990. Proceed. of 10th WCEE Madrid 1992, Balkema Rotterdam, Vol. I, 39 - 48.

[15] Taubajev A.S; Schwarz, J. (ed.): Damage Catalogue of the 1990 Saisan Earthquake. Schriftenreihe der DGEB (in prep).

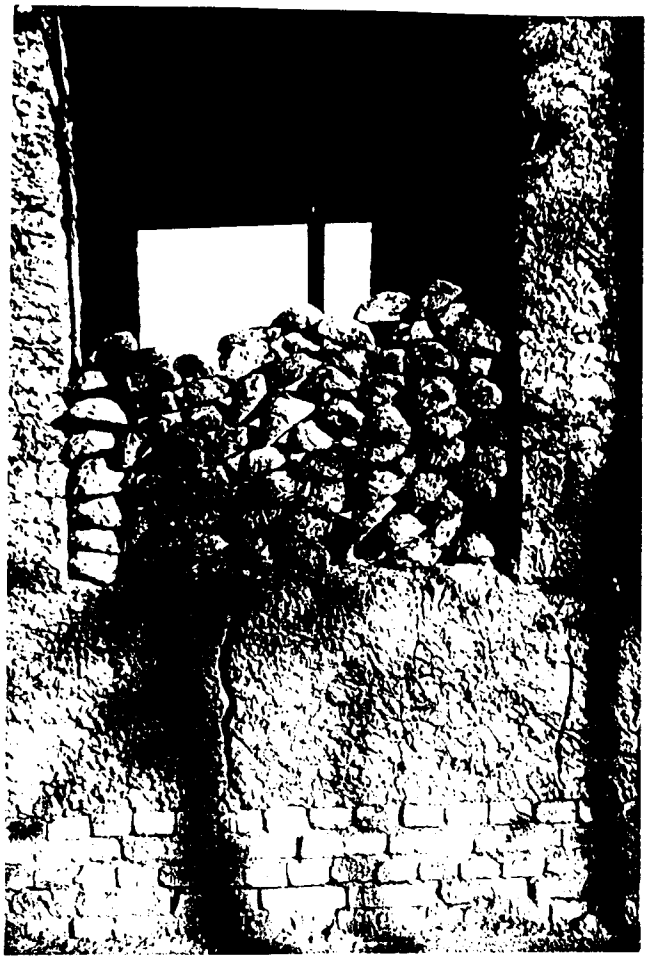

Fig. 1 Gualjak in Usbekistan

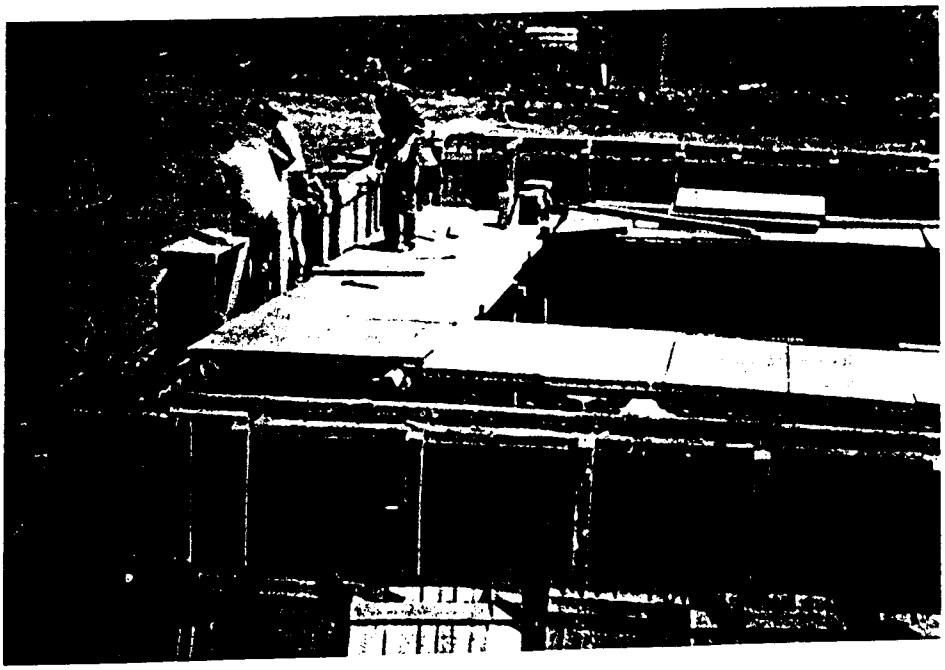

Fig. 2 Rammed earth Herbsleben/ Thuringia Germany

Scientific Technical Report STR 95/TK
DOI: 10.2312/GFZ.b103-95tk7

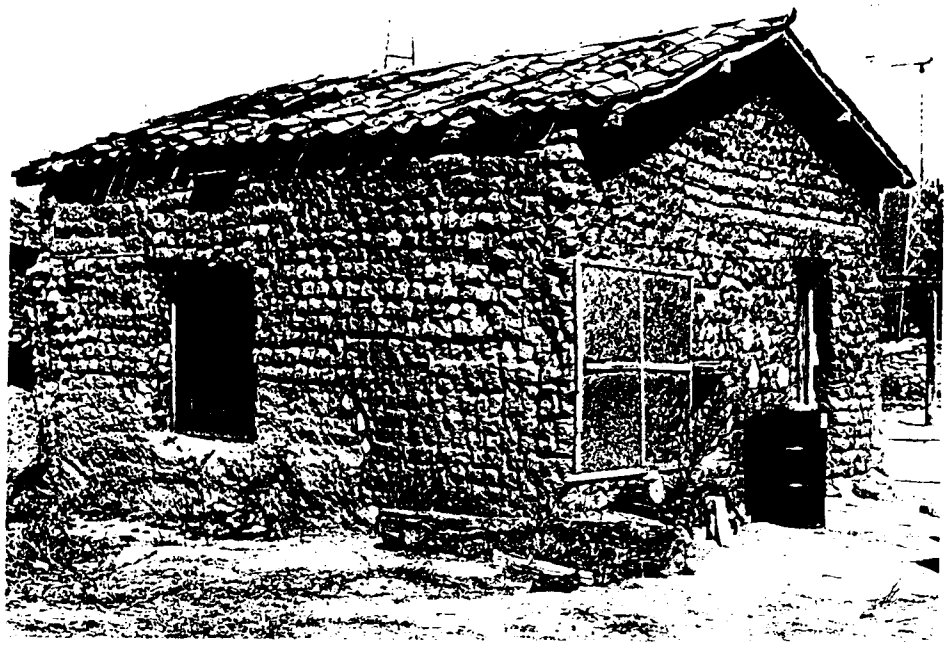

Fig. 3 Adobe Navapalos/ Spain

Fig. 4 CINVA-ram Havana coco solo

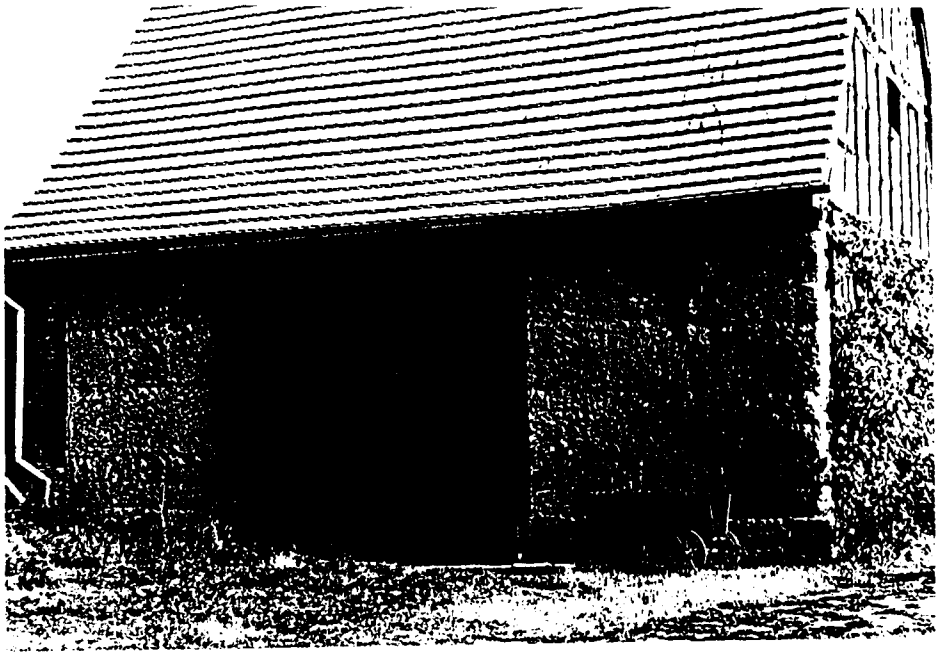

Fig. 5 Straw clay "Wellerbau" Niedertrebra / Thuringia Germany

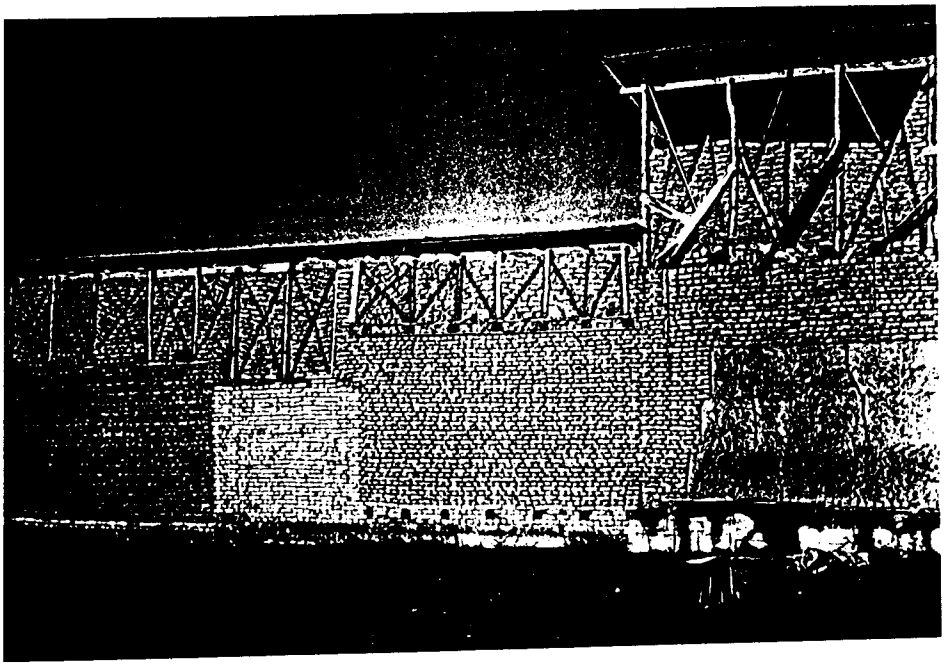

Fig. 6 Combination of adobe, burnt brick and rammed earth at the first floor, timber frames with adobe infill in the second floor; Tashkent / Usbekistan

Scientific Technical Report STR 95/TK
DOI: 10.2312/GFZ.b103-95tk7

Fig. 7 Oak staves with wickerwork as an infill of a truss

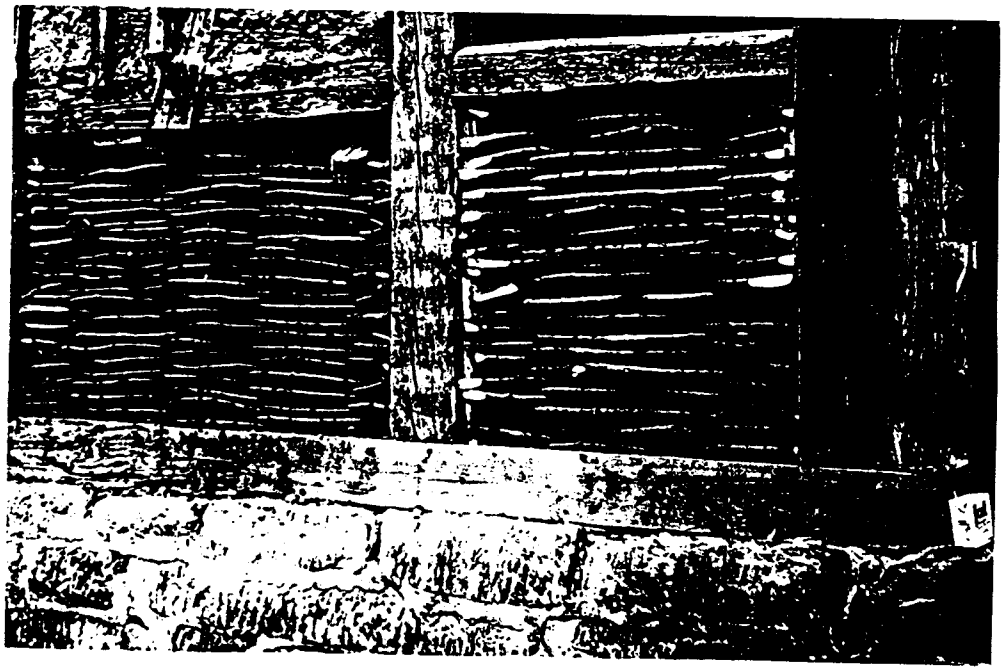

Fig. 8 Oak staves with wickerwork as an infill of a truss

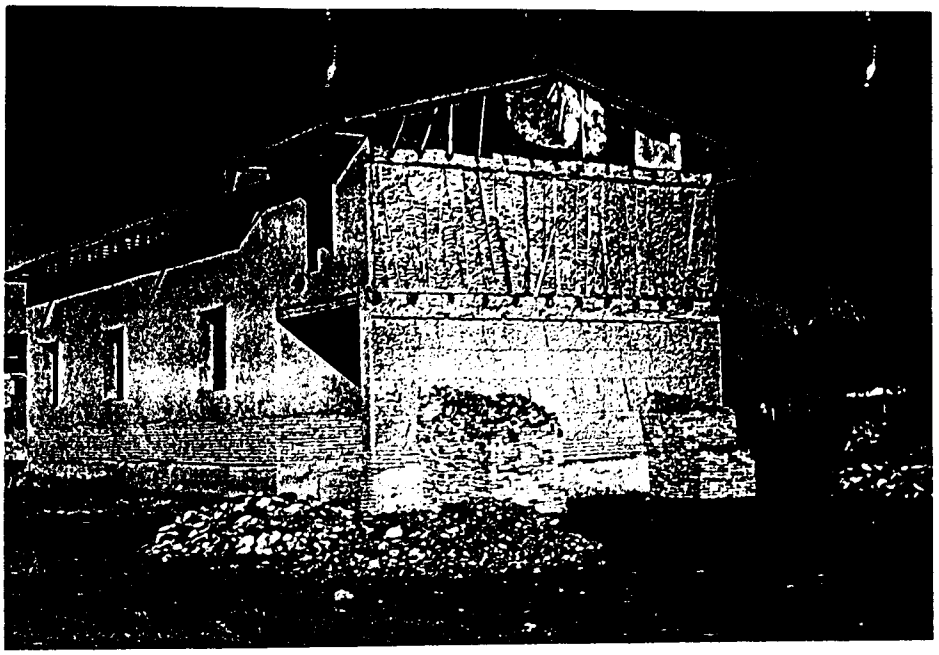

Fig. 9 First floor: pachsa; second floor: timber framed construction with adobe infill; Tashkent / Usbekistan

Fig. 10
Prefabricated concrete panel system type "Sandino"

Scientific Technical Report STR 95/TK
DOI: 10.2312/GFZ.b103-95tk7

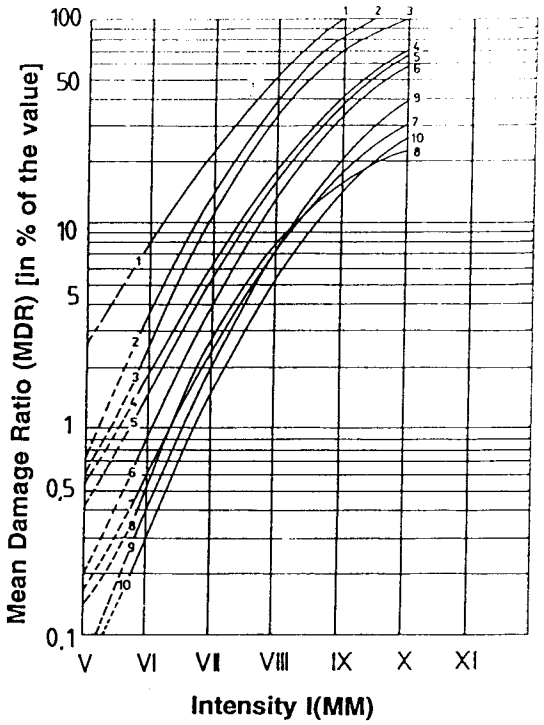

1 Adobe
2 Unreinforced masonry, non-seismic design
3 Reinforced concrete frames, non-seismic design
4 Steel frames, non-seismic design
5 Reinforced masonry, non-seismic design (medium quality)
6 Reinforced concrete frames, seismic design
7 Shear wall structures, seismic design
8 Wooden structures, seismic design
9 Steel frames, seismic design
10 Reinforced masonry, seismic design (high quality)

Fig. 11 Vulnerability functions (after Sauter and Shah [9])

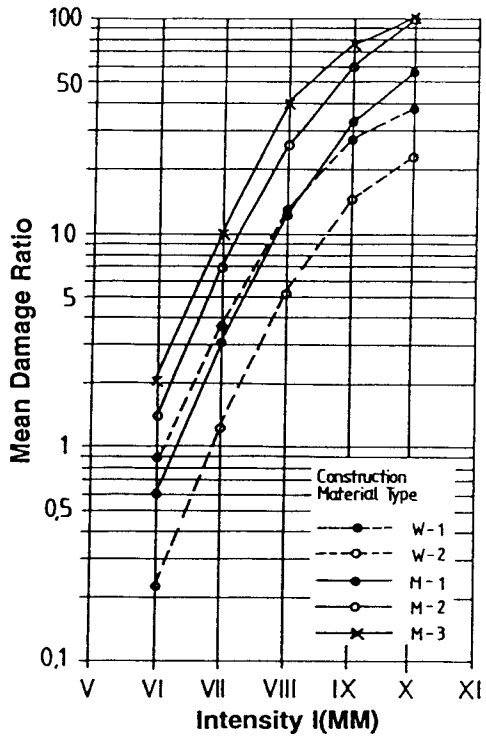

W-1 Wood frame with light exterior wall finish
W-2 Wood frame with brick veneer finish (e.g. plaster, stucco, weatherboard)

M-1 Reinforced masonry, reinforced concrete, precast tilt-up or reinforced hollow block bearing (or non-bearing with pilasters) walls
M-2 Unreinforced brick or solid block bearing walls
M-3 Unreinforced hollow block bearing walls

Fig. 12 Vulnerability functions considering basic building material and load carrying system (after Cochrane and Schaad [10])

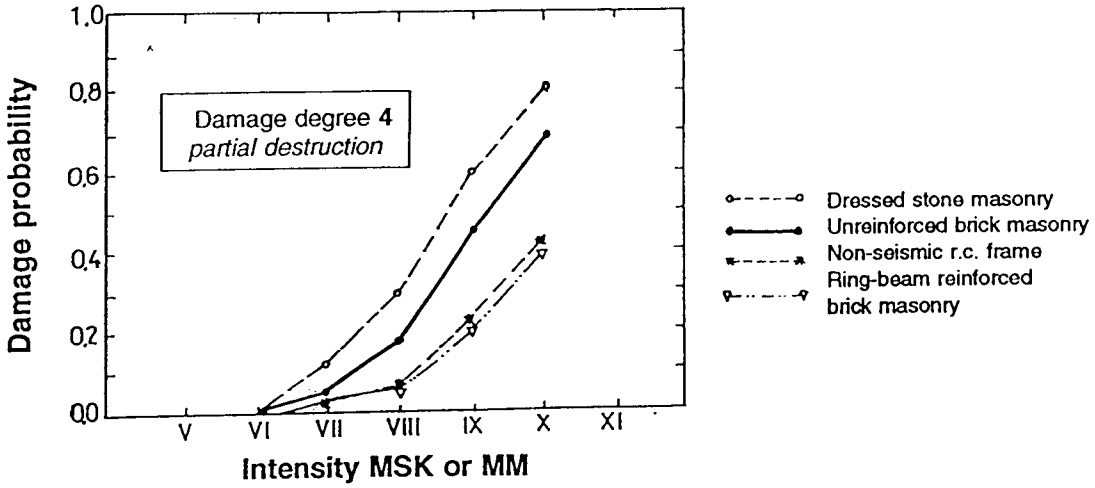

Fig. 13 Probability distributions of damage grade 4 for different buildings types (after Schwarz and Grünthal [11], using results of damage surveys in [12])

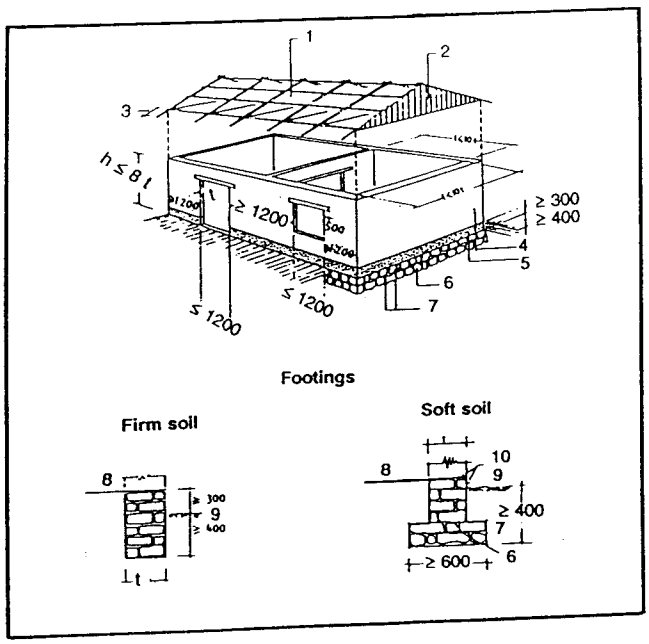

General recommandations (basic rules):

1	Light roof
2	Light gable wall (matting or boarding)
3	Rain protection overhang (about 500 mm)
4	Stable plaster
5	Plinth height for flood protection
6	Stable foundation
7	Good mortar, preferably non-clay

wall thickness t:
$t > h/8$ and $t > L/10$

Levels:

8	Floor level
9	Ground level
10	Water proof level

Fig. 14 Basic rules for antiseismic wall structures (after [13])

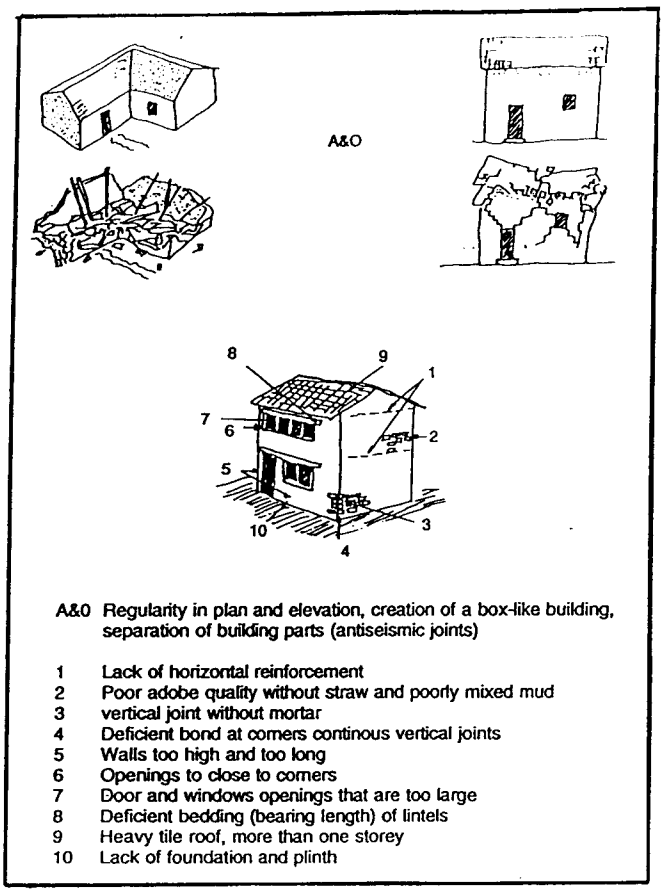

A&0 Regularity in plan and elevation, creation of a box-like building, separation of building parts (antiseismic joints)

1 Lack of horizontal reinforcement
2 Poor adobe quality without straw and poorly mixed mud
3 vertical joint without mortar
4 Deficient bond at corners continous vertical joints
5 Walls too high and too long
6 Openings to close to corners
7 Door and windows openings that are too large
8 Deficient bedding (bearing length) of lintels
9 Heavy tile roof, more than one storey
10 Lack of foundation and plinth

Fig. 15
Typical design errors (after [13])

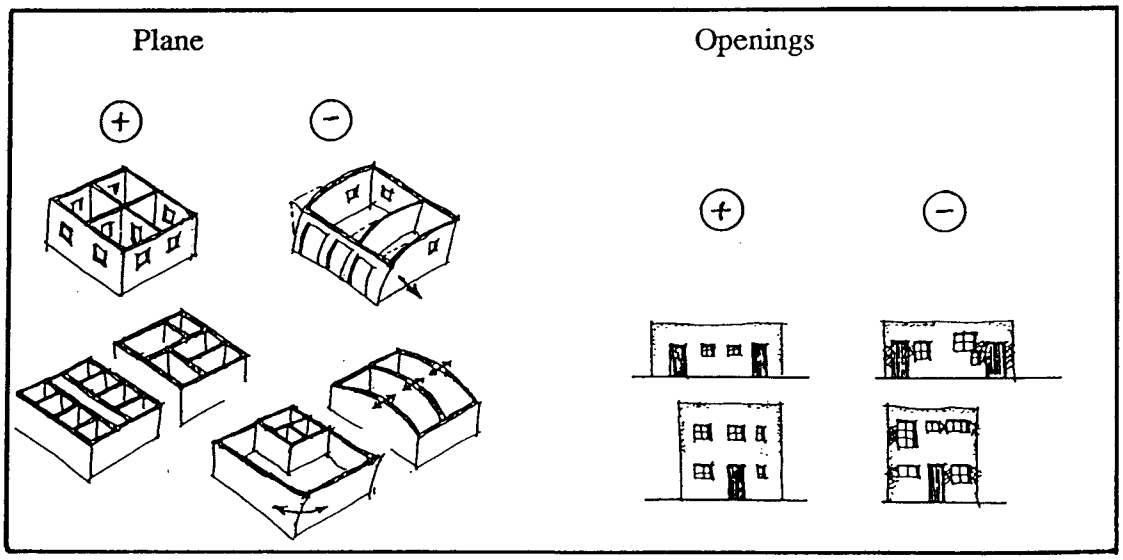

Fig. 16 Favourable and non-favourable design

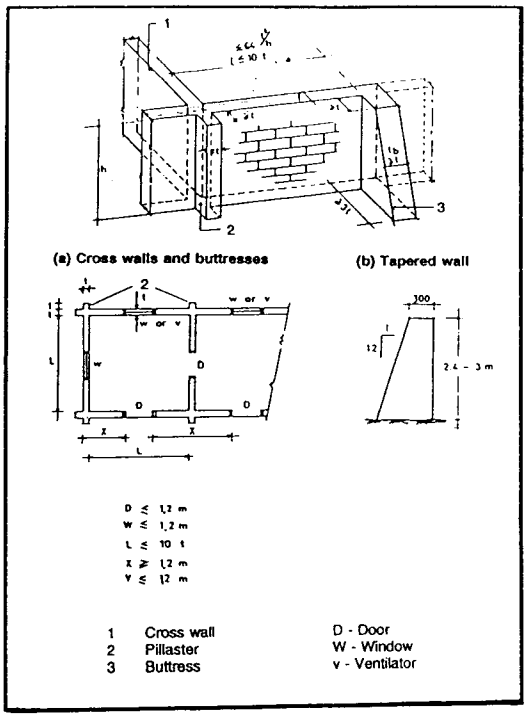

Fig. 17 Vertical stiffening elements [13]

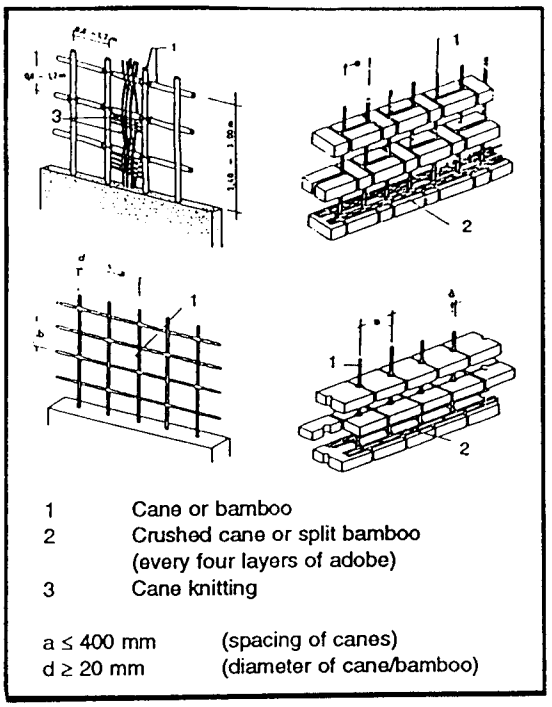

Fig. 18 Different kinds of vertical reinforcing of walls [13]

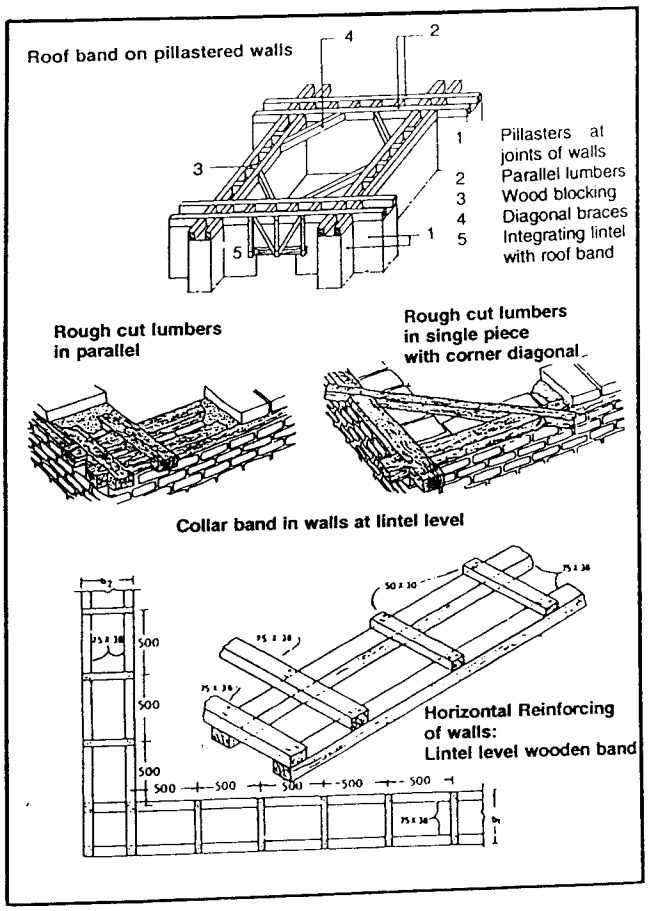

Fig. 19
Horizontal stiffening elements

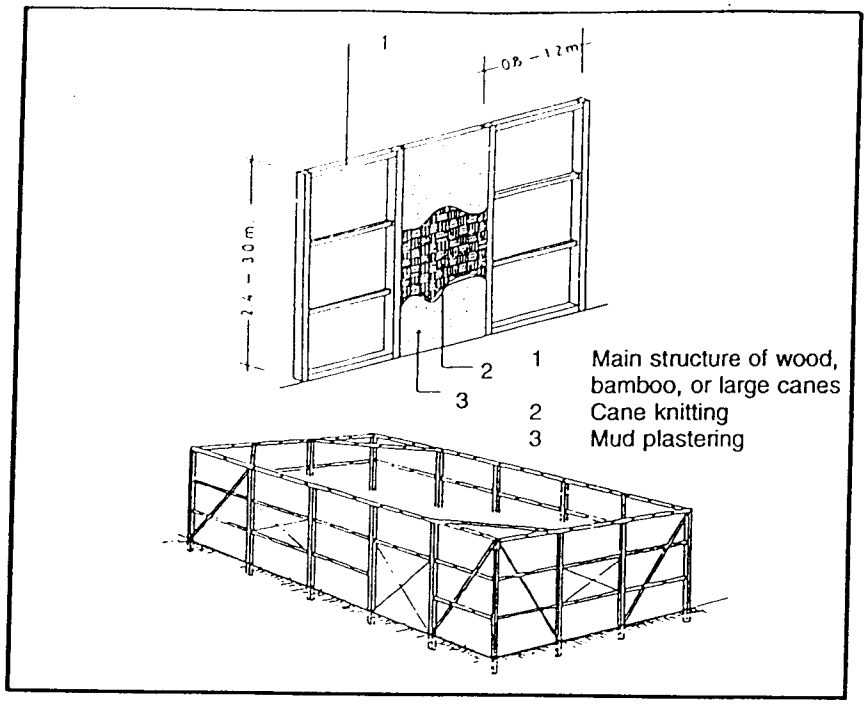

Fig. 20 Strengthening of framework wall structures (wood, cane and earth infill) [13]

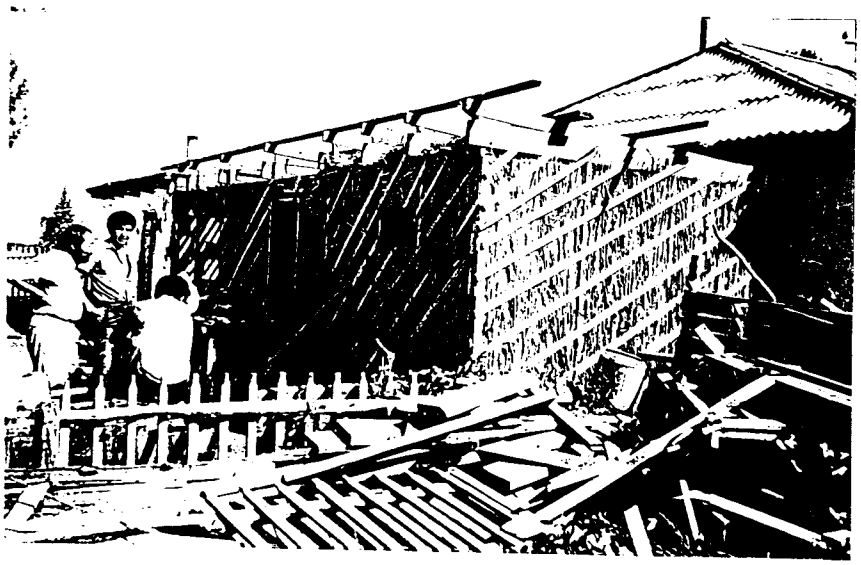

Fig. 21 Replacement of partially damaged or collapsed adobe buildings by timber frame construction (Kurtchum; Saisan earthquake 1990, East Kazakhstan)

Seismic Hazard Related Design Philosophies and Representations of Seismic Action

Jochen Schwarz
Hochschule für Architektur und Bauwesen Weimar - Universität, D-99425 Weimar

1 Engineering aspects of seismic hazard assessment

1.1 Definitions of design earthquakes and needs for harmonization

A real progress in the intended unification and harmonization of seismic input data is depending on the solution of the following problems [1, 2]:

- assessment of seismic hazard and subdivision of seismic zones
- site-dependent and zoning-map consistent description of seismic action
- smoothing of spectra and deviation of norm-like design spectra or parameters

From an engineering point of view it is, furthermore, of special importance to harmonize the description of seismic action for structures of different risk potential or importance.
Practically, it means that concepts, procedures and parameters are required to ensure the elaboration or adaption of design earthquakes in accordance with the importance or the risk-potential of a structure. Four tasks can be established and are still in need of practical proposals (Table 1) [3]:

According to modern design principles (task 1) structures have to be designed against earthquakes

- of *lower* intensity and *higher* probability of occurrence: design earthquake DE*.
  They should sustain such an event without any structural damage and with no or only minor damage which should not effect the serviceability (damage: grade 1);
- of *higher* intensity and *lower* probability of occurrence: design earthquake DE**.
  They are explicitly allowed to react under such an event with non-structural damage, but should survive without a loss of serviceability (damage: grade 2)
- of *maximum* intensity and *low* probability of occurrence: design earthquake DE***.
  They have to sustain structural damage without loss of structural integrity and stability (damage: grades **2, 3,** 4).

(The tolerated damage which one can assume according to the definitions of macroseismic scale EMS-92 [4] is indicated within the brackets.)

As it can be concluded from Table 1 the different design earthquakes are partially correlated and also comparable. Practically, design is only based on the stronger earthquake. Thus, codes for conventional/common buildings are based on events DE*** (DE_{uls} or E_1) according to the above mentioned philosophy. The earthquake for the serviceability limit state (DE_{slk}) can be interpreted as an earthquake that could occur within the intended life-time of the structure. This event is of importance when deflections have to be calculated.

Table 1. Definitions of design earthquake in earthquake engineering and task for engineering seismology [3]

No	Task	Design Earthquakes	Return Period T_R [a]
1	Harmonization of procedures and rules for describing the different earthquakes which are indirectly required according to modern design philosophies	DE^* DE^{**} DE^{***}	20-50 50-150 450-1000[1]
2	Harmonization of procedures and rules for describing the different earthquakes within earthquake resistant regulations for conventional (common) buildings; they are related to the non collapse requirement (the ultimate limit state) and the minimisation of damage (serviceability-limit-state)	DE_{uls} DE_{als} $DE_{uls}=DE^{***}$ $DE_{als}\approx DE^{**}$	450-1000[1] 50-150
3	Harmonization of procedures (factors) which are incorporated in earthquake resistant regulations (codes) to adapt the safety level of structures with different importance by defining factors γ_i (or others) for building classes or categories i (conventional/common buildings).	DE_i $DE_i=DE_{uls}\cdot\gamma_i$ $DE_1(\gamma_1=1)$	450-1000[1]
4	Harmonization of procedures for describing design earthquakes for structures of different risk-potential, i.e. of conventional (common) buildings ruled by codes and of structures with increased secondary risk like nuclear or chemical facilities, dams.	E_1 E_2 $E_1=DE_{uls}$	450-1000[1] ≥ 10 000[2]

[1] Lower and higher values (e.g. 150 or 2250 years) are proposed
[2] Lower values for chemical plants, dams, embankments are proposed in dependence on seismic activity.

Several codes are proposing that differences between these two design earthquakes have to be reflected by a modification factor (ν), i.e. building deflections calculated with forces due to the stronger event have to be scaled-down to the level of the less severe event.

As it will be shown subsequently, essential elements for the required harmonization of seismic impact data can be delivered by the results of hazard assessment and by describing sites on the basis of seismic hazard curves.

1.2 Seismic hazard curves and definition of design earthquakes

Fig. 1 shows an idealized hazard curve. Different kinds of data which are suitable for elaborating hazard curves are related to the ranges of the annual probability of occurrence of the macro-seismic parameter (here: intensity). The quality and peculiarities of hazard curves are explained with the help of different parameters (1-5). From an engineering point of view it is noteworthy to mention that, only in a limited range, definitions could be based on measurements or observations. Especially in the case of events with lower probability of occurrence (or higher return periods) definitions have to be based on extrapolations.

Events of low probability of occurrence are relevant for the design of structures of higher risk-potential, and have be determined on the basis site-dependent ground motions, microzoning studies and/or on an analysis of site effects (transfer functions of subsoils profile).

Coming back to the description of design earthquakes and their definition by different hazard levels (see Table 1), it has to be emphasized that hazard curves can provide the primary information for a new approach which should be consistent with modern design philosophies. If the hazard levels for two different design earthquakes are denoted by E_1 and E_2, the relevant macroseismic parameters for both events can be determined (intensity I_{E1} and I_{E2}). For both intensities (hazard-related) ground motion parameters can be evaluated. As it is explained in Fig. 2, such a procedure can also provide useful information about the "remaining risk", which can be defined according to a proposal by Grünthal and Schwarz [5] as the area between the hazard curve, the hazard level and the assumed maximum event I_{max} (the "upper bound earthquake" having a probability of occurrence "0").

1.3 Seismic zoning on the basis of hazard curves

For assessing the seismic hazard, different methods are available, providing information about similar parameters. In fact, the results are of different quality and seldom comparable.
Considering current research work and recently published codes, two methods for the subdivision of seismic zones based on a probabilistic hazard assessment can be distinguished (Fig. 3):
According to the *first group* of methods, a certain hazard level is defined and zones are classified according to this (reference) hazard level. (For European earthquake regions a hazard level within a range of return periods between 500 to 1000 years is recommended.)
According to the *second group* of methods, seismic zones are subdivided using idealized hazard curves, or only that part (branch) of the hazard curve which is of importance for building design. Each zone is characterized as the area between two of these "model curves". It can be demonstrated that these methods will cause problems when the actual hazard curve of a site will intersect different "model curves". This problem is discussed by the author in [3].
Before subdividing a region into seismic zones, it has to be decided which level of refinement is intended or really necessary. A final decision should be in agreement with seismic activity and the historical periods of observations as well as their completeness, avoiding any sophistication that cannot be justified by an adequate description of seismic action.

2 Hazard-related design parameters in earthquake engineering

2.1 Description of seismic action in dependence on the quality of seismic hazard assessment

It is necessary to introduce into seismic codes a description of seismic action that is consistent with the kind of zoning parameter which is provided for design purposes. To realize this aim, elastic free-field design spectra have to be predicted, and should be representative for different intensity levels (determined by earthquake zones) and different classes of subsoil conditions. Subseqeuntly, intensity- and subsoil-related design spectra are considered due to their direct relation to the definition of design earthquakes (see 1.1).

(Existing concepts are discussed within the lecture, while explaining the difference between *zone-related* and *hazard-consistent* design parameters.)

For elaborating site-dependent design spectra data have to be taken from earthquakes representing typical source, magnitude and distance parameters or conditions. When the remaining earthquake records are classified into different intensity and subsoil classes, statistical investigations of these data groups can be carried out.
It is clear, that the quality of such statistical investigations is strongly depending on the quality of samples and the number of records within the groups. With respect to this "natural limitation" a further improvement of the data base has to be regarded as a permanent task. Results of such investigations for Central Europe, i.e. for regions of low or moderate seismic activity are available [7, 8].
Proposals for intensity- and subsoil- related design spectra for two intensity classes are compared in Fig. 4 (after [2]). The results differ with respect to the composition and the mean intensities of samples.
The great scatter of spectral amplitudes can be expressed in terms of "spectra of standard deviation" [11] or in terms of envelopes of maximum and minimum spectral accelerations.
In Fig. 6 the mean spectra of statistical investigations [8] are compared, representing the whole data for medium dense sediments (class 2) and sedimentary rock for the intensity class 6.5 - 7.4 while indicating the inherent statistical uncertainty of results. Additionally, spectra of single records, mostly differing from the mean spectra, and 84,1 - fractile spectra are given. It can be concluded that often single events (bolters) alone can be responsible for the great scatter of upper and lower limits (dashed lines).

2.2 New concepts for evaluating site-dependent and hazard-related design response spectra

Intensity- and subsoil-related design spectra
Intensity- and subsoil-related design spectra can be regarded as a first concept for a hazard-consistent description of seismic design action. For interpreting and understanding the results amplification factors can be introduced [9, 10, 11]: Intensity-related amplification factors r_I give the ratio of spectral acceleration between spectra of intensity (I+1) and intensity (I) within one subsoil class. They could be interpreted as spectra of amplification factors and are comparable to the ratio of (frequency-independent) zoning or seismicity coefficients, commonly used in seismic codes. Examples of those amplification factors are given in Fig. 6. after [12].

For practical application it seems to be necessary to smooth the irregular curves of statistical investigation. It is common practice to smooth spectra as tetra-logarithmic coordinates so that branches of spectra with constant amplification factors of ground motion are created. It is one of the underlying assumptions of the here presented intensity-related design spectra that correlations with ground motion should be avoided and that the acceleration should not serve as scaling parameter. On the basis of smoothed variants of spectra the code-like representation can be predicted.
(A code-like representation means: decimal coordinates of the period of vibration T and the dynamic (spectral) coefficient, definition of parameters, determining subsoil-dependent branches and decay of amplification effects between control periods.)

Magnitude- and distance-dependent design spectra (uniform risk spectra)

In the last years a new kind of design spectra was developed. Proposed spectra are correlating magnitude, distance, and spectral amplitudes, and, therefore, are restricted to regions of high seismicity with a sufficient data-base and well-defined (active) sources. One of the first practical proposals by Katayama [13] is illustrated by design spectra in Fig. 7. At all frequency points the spectral accelerations have the same probability level (here: 63.2 % probability of exceedence within a life-time of 75 a, leading to a return period of T_R = 75 a).

A further step to a code-like representation is achieved by scaling spectra of different sites to an uniform hazard level. Fig. 8 shows spectra of different sites having a return period of T_R = 475 years and spectral shapes normalized on 1.0 g with a scaling period of T^* = 0,2 s (after [14]). Basic ideas, necessary and available tools for practical realization of this kind of design spectra are presented within the paper (see also [2, 14, 15]).

3 Seismic action for structures of different risk potential

Due to the different design philosophies and the non-comparable level of intended protection or seismic resistance, seismic codes for conventional buildings are to be distinguished from guidelines for high risk structures (nuclear or chemical plants, dams, special structures).

Questions arise, how it could logically be explained that for the same site, structures are designed for quantitatively and also qualitatively different events. It is to be stated that there should be only differences between the levels of hazard, that structures should be designed for, and between the demands relating to the quality of structural behaviour (see Table 1).

3.1 Importance and risk or hazard factors

It is interesting to note that in most codes the importance of standard buildings is taken into account without any relation to the seismic hazard or the intended behaviour under design earthquake, by amplifying seismic action with the so called importance factor (see Table 1, task 3). Rationally, the importance factor can only be explained and interpreted as a substitution of not indicated, but intended differentiation of design earthquakes, i.e of seismic hazard levels. In this sense, importance factors are comparable to risk factors, which are related to a reference hazard level (say of 150 years) and which indirectly express the difference of seismic action when higher or lower hazard levels should come into consideration.

The concept of risk factors was practically applied within different version of seismic code NZS 4203 (New Zealand). Three proposals are given in Fig. 9 (after [3]). It should be emphasized that the risk factor is non-uniformly distributed within an earthquake region. Thus, the variety of proposed risk factors can be explained by the regionally deviating hazard curves. Alternatively, it is possible to develop maps of risk factors [1, 3]. Because of the direct relation to the seismic hazard curves it seems to be appropriate to introduce these kind of parameters as *hazard* factors. On the basis of hazard curves (see Fig. 1), hazard factors can be evaluated and compared with importance factors of seismic codes. With regard to future code development it would be desirable, if decisions on the determination of importance factors would follow the real background of site-specific hazard estimates.

The concept of importance factor γ, hazard (or risk) factor and its presentation in a map-like form are schematically summarized in Fig. 10. These parameters should provide the base for solving tasks 1 to 4 (see Table 1). Concerning task 2, a factor ν (ν=1/R) can be defined. This factor should quantify the deamplification of forces of the stronger design earthquake (ultimate limit state) to the level of the event for the serviceability limit-state, i.e. the design earthquake of lower intensity and higher probability of occurrence.

These parameters have one practical limitation: they are frequency-independent. Especially for task 4, it could be necessary to modify seismic action depending on the impact of earthquake intensity on the amplitude characteristics of design ground motion.

3.2 Determination of seismic action for structures of different risk potential

Practically, various methods can be applied to cover the lack of harmonization in the field of design earthquakes for structures of different risk potential (Table 1, task 4). Fig. 11 shall transmit an impression of some basic ideas. Schemes of spectra and the frequency-dependent ratio between spectra of the stronger design earthquake E_2 (for structures of higher risk) and a weaker earthquake E_1 (for structures of normal risk) are indicated.

The simplest distinction of both earthquakes should follow risk estimates of ground motion or intensity. If a standard spectrum is taken, the ratio between events agrees with the ratio of deviating ground motion. If risk estimates are available for all types of ground motion (acceleration, velocity and displacement) the ratio of spectra is linearly smoothed, but is varying in the ground motion controlled frequency ranges.

The "double-earthquake design philosophy" coming from the design practice of US Nuclear facilities is illustrated as method 1 in Fig. 11. The structural resistance is taken into account, while defining design earthquakes (E_1, E_2) for elastic and elasto-plastic damping values. Differences in spectra are caused by differences in damping-related amplification factors and ground motion, referring to different levels of seismic hazard (return periods).

The other methods are characterized either by modifications of the design action (hazard levels, levels of non-exceedence of spectral values; method 2) or by adaption of the resistance capacity (ductility, inelastic deamplification; method 3), and, as it is practically often preferred, by modifications of both aspects. In Fig. 11 methods 2 and 3 are represented by an unique return period of intensity. The distinction between seismic action is reached by the definition of different probabilities of exceedence (p_1,p_2) of spectral amplitudes or by different inelastic deamplification factors r_μ.
It seems to be more appropriate to modify seismic action with parameters relating to the resistance side, when structures should sustain earthquakes with different grades of damage. Otherwise, it seems to be preferable to modify the impact side, when different damage pattern are specified for different design earthquakes. If intensity-related design spectra are used, the ratio of seismic action types reflects also the different quality of earthquakes and seismological parameters, caused by high intensity ground motion (method 4). The predicted intensity- and subsoil-related spectra can be used for this method (Figs. 4, 5).

In Fig. 11 the differences between seismic action for structures of different risk-potential are expressed by coefficients r_i, indicating the relevant parameter for classification of seismic action (i=a-acceleration, p-hazard level or probability of exceedence, I-intensity, u-ductility, D-damping).

These coefficients are described as frequency-dependent ratios between proposed spectra for the design earthquakes E_2 and E_1 (see Table 1, task 4, and Fig. 2).

Using results of statistical investigations it is possible to quantify the differences of seismic action, which could be expected, when the same sample of earthquake data is used and seismic action has to be evaluated for structures of different importance or risk. Examples are presented in the paper.

References

[1] Schwarz, J.; Grünthal, G.: Harmonization of codes with respect to seismic hazard and seismic action for structures of different risk potential. Proceed. 10th WCEE Madrid 1992, Vol. 10, S. 5789-5795 Balkema, Rotterdam 1992.

[2] Schwarz, J.; Grünthal, G.; Schöbel, B.: Aktuelle Probleme der Beschreibung und Harmonisierung der seismischen Einwirkungen in Erdbebennormen. *Schriftenreihe der DGEB* Heft 2: IDNDR 1992, 73-90.

[3] Schwarz, J.: Harmonisierung von seismischer Gefährdung und seismischen Einwirkungen in Erdbebenbaunormen: Gefährdungsbezogene Einwirkungsgrößen und Parameter DGEB Publikation Nr. 7. D-A-CH Tagung 1993. Seismische Einwirkungen auf Bauwerke unterschiedlichen Risikopotentials. Europäische Regelwerke, Weimar 1994.

[4] Grünthal, G. (ed.): European Macroseismic Scale 1992. Cahiers du Centre Européen et de Géodynamique et de Séismologie, Vol. 7, Luxembourg 1993.

[5] Grünthal, G.; Schwarz, J.: Bauwirtschaft und Naturkatastrophen. Bauen in Erdbebengebieten. Teil 1. *Bauwirtschaft* (1993) 8, 39- 45; Teil 2 (1994) 2.

[6] Schwarz, J.; Grünthal, G.: Aktuelle Probleme der Beschreibung und Harmonisierung von seismischen Einwirkungen in Erdbebenbaunormen. *Bautechnik* (1993) 11,

[7] Hosser, D. et al. 1986: Realistische seismische Lastannahmen für Bauwerke II. Abschlußbericht. Institut für Bautechnik für Bautechnik. Berlin.

[8] Schöbel, B. 1989. Ableitung standortspezifischer Strong-Motion-Aussagen für das Territorium der DDR. Zwischen- und Abschlußbericht 1989; Aktualisierung 1991. Zentralinstitut für Physik der Erde Potsdam.

[9] Schwarz, J. 1991. Probleme bei der Einführung intensitätsbezogener Erregungsdaten. DGEB-Publikation 5, Zentralinstitut Physik der Erde: 69- 84. Potsdam.

[10] Schwarz, J.; G. Grünthal. 1991. Beschreibung der seismischen Einwirkungen in den Vorschriften allgemeiner Hochbauten. Teil 2. Ableitung einer neuartigen Vorgehensweise für das Erdbebengebiet im Osten Deutschlands. Bauplan., Bautech. 45, 10: 443- 459.

[11] Schwarz, J., Goldbach, R., Grünthal, G. & B. Schöbel 1990. Development of Earthquake Resistant Regulations-The New Seismic Code of the GDR. Proc. 9th ECEE, Vol. I: 74- 83. Moscow.

[12] Devilliers, C.; Mohammadioun, B.: French methodology for determinating site adopted SMS (Seisme Majore de Securite). Proc. 6th SMiRt Paris 1981

[13] Katyama, T.: An engineering prediction model of acceleration response spectra and its application to seismic hazard mapping. Earthquake Engineering and Structural Dynamics 10 (1982) 149-163

[14] Donovan, N.: Uniform risk zoning- a simplified approach. Proceed. 9th WCEE, Vol. V, 1063-1068, Tokyo 1988 Earthquake Resistant Regulations. A World List. Tokyo u.a. (a) 1984, (b) 1988, (c) 1992.

[15] Algermissen, S.T.; Leyendecker, E.V.: A technique for uniform hazard spectra estimation. Proceed. 10th WCEE Madrid, Vol. 1, 391-397, Balkema, Rotterdam 1992

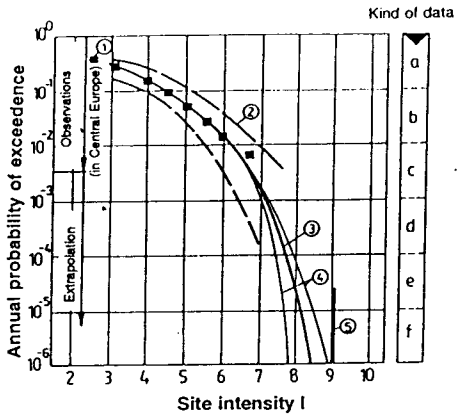

1 Observed numbers N (>I)
2 Statistical uncertainties
3 Hazard curve (from seismicity model)
4 Possible extrapolations
5 Estimation of maximum (upper bound earthquake)

a Microearthquakes
b Intrumental seismicty
c Historical seismicity
d Archaelogical evidence
e Paleoseismicity
f Neotectonics

Figure 1. Quality and peculiarities of seismic hazard curves [after [5])

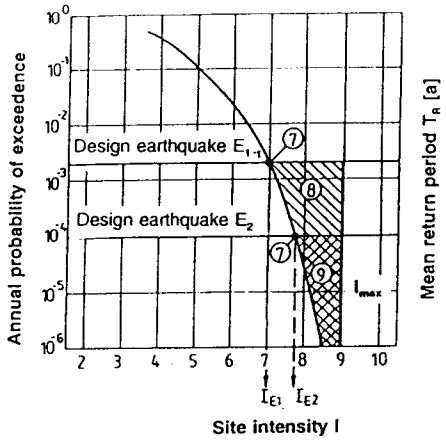

7 Intersecting point between site hazard curve and hazard level of design earthquake (in dependence on risk and importance of structure)

8 , 9 Estimation of remaining risk according to a definition by *Grünthal and Schwarz (1994)*

Figure 2. Definition of design earthquakes on the basis of hazard curves [5]

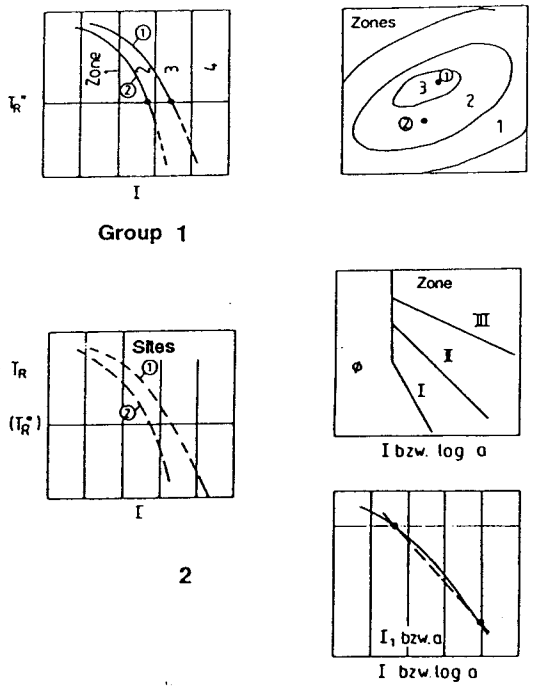

Figure 3. Methods of seismic zoning on the basis of seismic hazard curves [3]

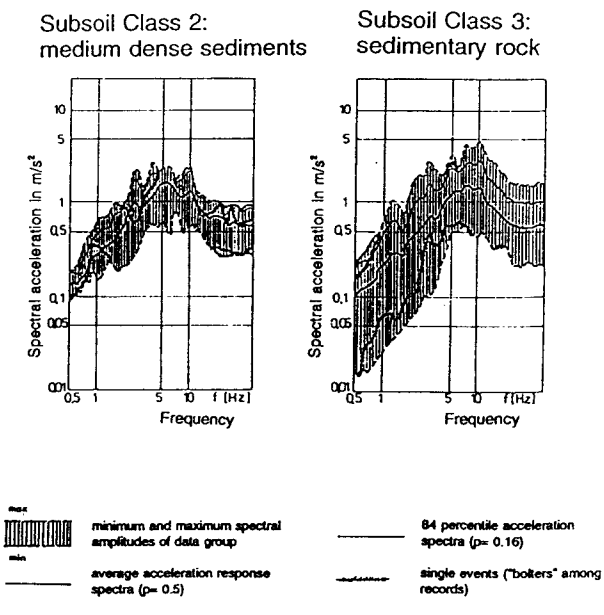

Figure 4. Intensity-related design spectra: intensity class I = 6.5-7.4° [2]

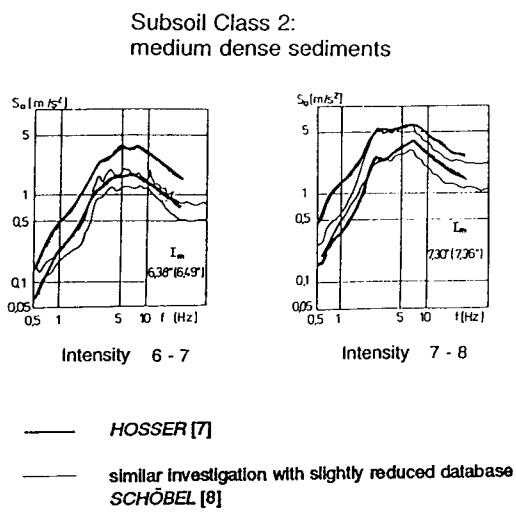

Figure 5. Results of statistical investigations: intensity class: I = 6.5- 7.4°: subsoil class: medium dense sediments [2]

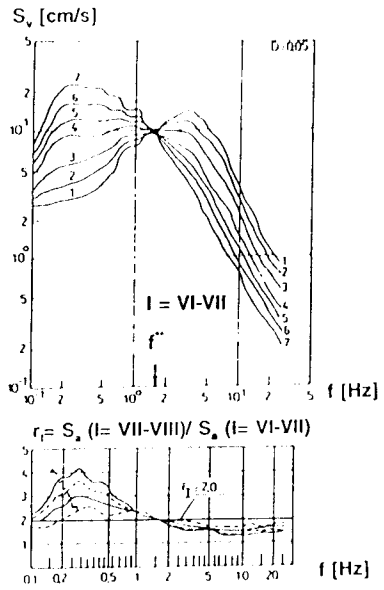

Figure 6. Intensity-related amplification factors r_I ($r_I = S_{a,I+1}/ S_{a,I}$) : I = VI - VII (after [12])

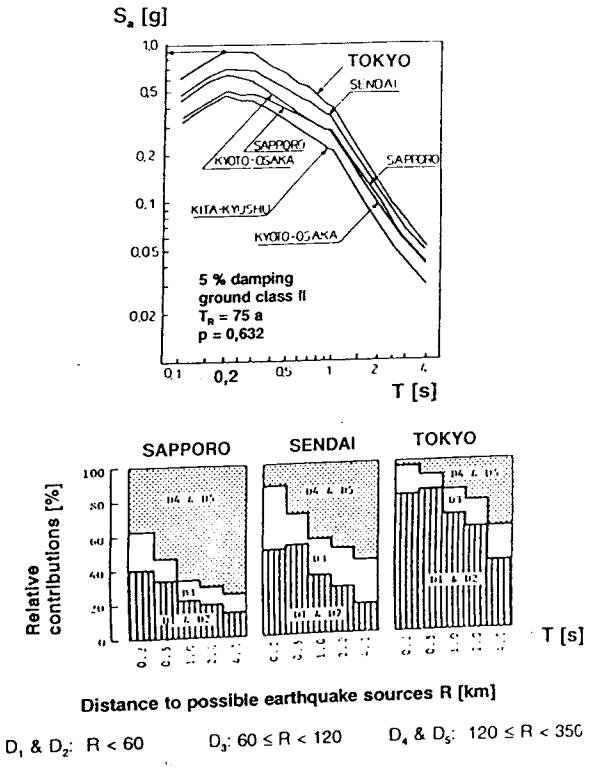

Figure 7. Design spectra for different cities in Japan on the basis of the relative contributions of magnitude and distance to earthquake source (after Katayama [13])

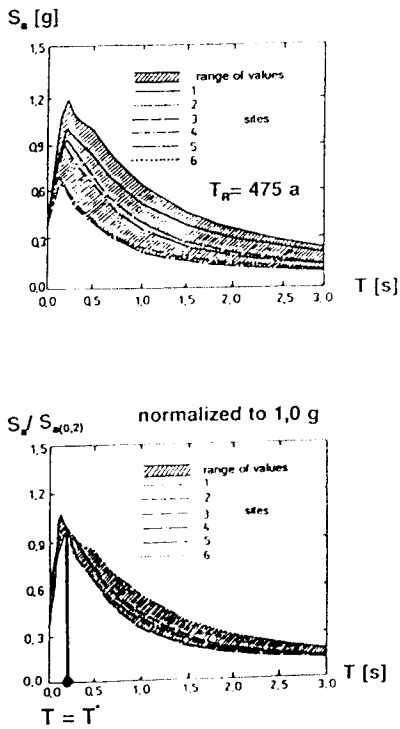

Figure 8. Uniform risk spectra scaled on period T^* T^* = 0,2 s (after [14])

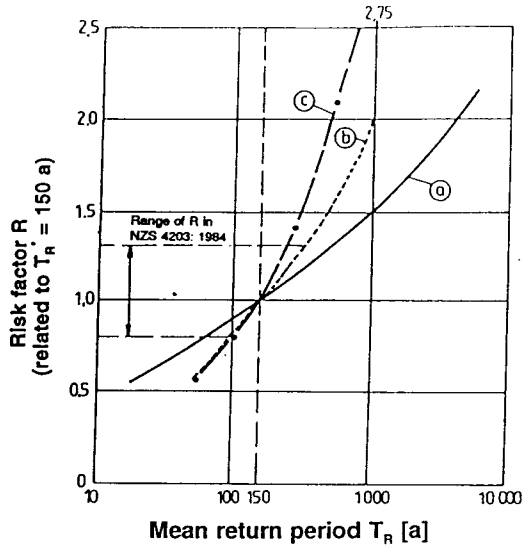

(a) Norton, Gillies and Edmonds (1982) for petrochemical plants on the basis of NZS 4203: 1976

(b) Park et al. (1986); NZS 4203: 1984

(c) Hutchison et al.; revision of NZS 4203: 1984

Figure 9. Proposed risk factors (after [3])

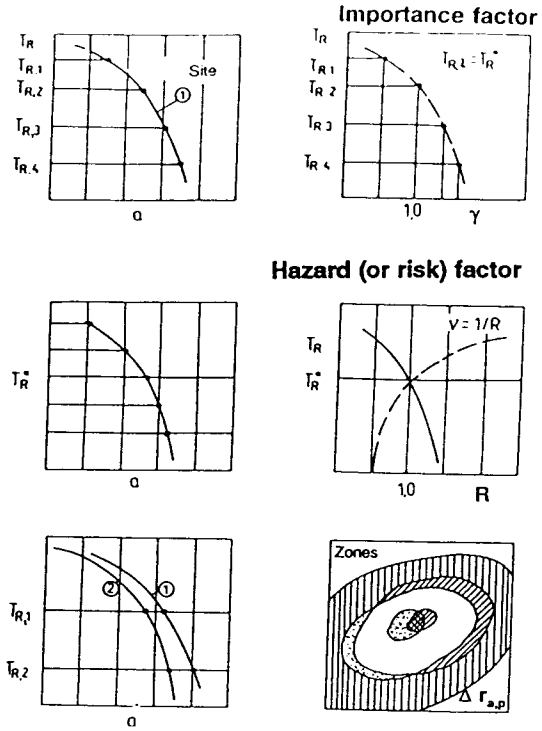

Figure 10. The concept of importance and hazard (or risk) factors [3]

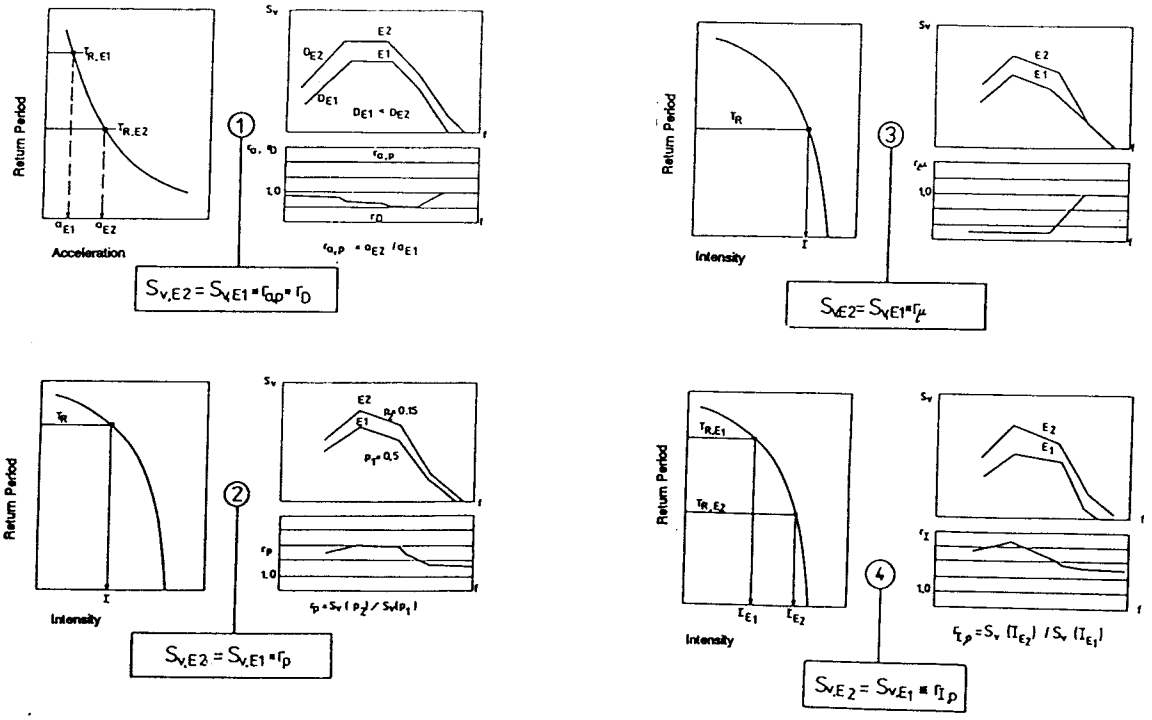

Figure 11. Definition of seismic action for structures of different risk potential - a schematic representation of methods (after [1])